Rec.
21.3.79

This Issue: 1979 ARRS Comprehensive Meeting Information

CUA - H02926-10-P024437

AJR

(10)

American
Journal of
Roentgenology

October 1978

Liquid Polibar with Super XL

A Total System

For double-contrast examination of the colon.

Satisfactory results in the double-contrast examination of the colon require special attention to two aspects of the procedure.

First, the barium sulfate formulation. Our Liquid Polibar (56% w/w) is a bubble-free, non-precipitating uniform suspension formulation ... with proper flow and coating characteristics. No blending required and once routines are established, you can rely on its consistency.

The second concern is with the proper apparatus. The E-Z-EM system is unique in that 1/2" lumen tubing attached to the enema bag is utilized — for freer, more uniform flow. Miller Air Retention Tip, with or without optional cuff completes the system.

A total system for ease of administration and consistently reliable radiological results. For additional literature, write:

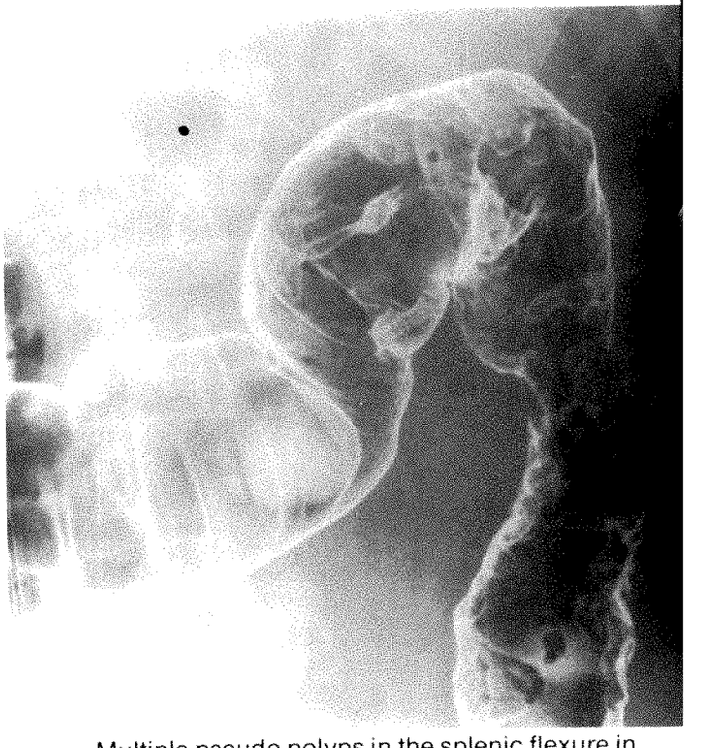

Multiple pseudo polyps in the splenic flexure in longstanding ulcerative colitis.
Film courtesy of Richard Palmer Gold M.D. Columbia Presb. Medical Center N.Y.

E-Z-EM

7 Portland Ave.
Westbury, New York 11590
(516) 333-8230

7/78

International Affiliates: E-Z-EM Rooster B. V., Infirmeriestraat 6-8, Rotterdam 16, Netherlands
E-Z-EM De Mexico, S. A. de C. V., Calz. Azcapotzalco La Villa No 882, Zona Industrial Vallejo, Mexico 16 D. F.

Official Journal
American Roentgen Ray Society
American Radium Society

P24,437
P 24,437

AJR

Including Diagnostic Radiology • Radiation Oncology • Nuclear Medicine Ultrasonography • Related Sciences

Editor Melvin M. Figley

Associate Editor Rosalind H. Troupin

Assistant Editor John D. Harley

Contributing Editor E. Frederick Lang

Consulting Editorial Board Luther W. Brady • Kent Ellis E. Robert Heitzman • Donald L. King • N. Thorne Griscom Eugene C. Klatte • Kenneth Krabbenhoft • John G. McAfee Russell H. Morgan • Thomas H. Newton • Robert G. Parker Stewart R. Reuter • William B. Seaman • Robert J. Shalek John Storer • Michel M. Ter-Pogossian • Joseph P. Whalen David M. Witten

Editorial Staff K. A. Murray, manager • M. B. Wieckowicz, M. J. Leonard, manuscript editors • C. P. Kaiser, secretary J. Anderson

Published monthly by Charles C Thomas, 301-327 East Lawrence Avenue, Springfield, Illinois 62717. All correspondence, except editorial office business, should be addressed to the publisher. Annual subscription rates: $40 ($20 for residents with letter of verification) plus appropriate mailing surcharge (see note next page). Single copies, $5. Undelivered or damaged copies replaced within 60 days of publication; 90 days for foreign subscribers. Allow 90 days for address changes. © 1978 by American Roentgen Ray Society. Second-class postage paid at Springfield, Illinois, and at additional mailing offices. Printed in U.S.A. ISSN 0361-803X

American Roentgen Ray Society

President: Harry Z. Mellins
President Elect: Paul A. Riemenschneider
1st Vice-president: Joseph D. Calhoun
2d Vice-president: Charles E. Bickham, Jr.
Secretary: James F. Martin
Treasurer: Harley C. Carlson

COMMITTEES 1977–1978

Executive Council: H. Z. Mellins, P. A. Riemenschneider, J. D. Calhoun, C. E. Bickham, Jr., J. F. Martin, H. C. Carlson, M. M. Figley, R. G. Evens, B. G. Brogdon, R. A. Gagliardi, E. Gedgaudas, G. A. Kling, T. F. Leigh, S. F. Ochsner, J. F. Wiot, R. E. Buenger, E. C. Klatte, J. P. Tampas, J. L. Gwinn, chairman

Finance and Budget: A. E. James, E. C. Klatte, R. McLelland, J. P. Tampas, R. G. Evens, chairman

Publications: M. P. Capp, K. Ellis, F. F. Ruzicka, Jr., E. R. Heitzman, R. A. Gagliardi, chairman

Editorial Policy: M. M. Figley, E. F. Lang, R. H. Troupin, E. R. Heitzman, K. Ellis, F. F. Ruzicka, Jr., M. P. Capp, R. A. Gagliardi, chairman

Advisory Committee on Education and Research: J. E. Youker, G. Wilson, G. W. Hartman, L. F. Rogers, E. Gedgaudas, chairman

Scientific Exhibits: T. C. Beneventano, G. Dodd, B. G. Brogdon, chairman

Constitution and Bylaws: J. H. Walker, W. M. Whitehouse, J. P. Tampas, chairman

American Board of Radiology Representatives: J. F. Roach, R. W. McConnell, S. W. Nelson

Program Committee: H. Z. Mellins, J. F. Martin, J. L. Gwinn, M. M. Figley, R. A. Gagliardi, B. G. Brogdon, E. Gedgaudas, G. A. Kling, P. Riemenschneider, chairman

Instruction Courses: E. Gedgaudas, director; G. W. Hartman, associate director

American College of Radiology Board of Chancellors Representative: W. B. Seaman

Annual Meeting: March 25–30, 1979, Sheraton Centre, Toronto, Canada

Scientific Program: P. A. Riemenschneider, president elect, Cottage Hospital, Santa Barbara, California 93105

Manager Annual Meeting: George A. Kling, Harper Hospital, Detroit, Michigan 48201

Membership: John L. Gwinn, 4650 Sunset Blvd., Los Angeles, California 90027

Business Office: Keith W. Gundlach, comptroller, American College of Radiology, 20 North Wacker Drive, Chicago, Illinois 60606

American Radium Society

President: Frederick W. George, III
President Elect: Alfred S. Ketcham
1st Vice-president: Julian P. Smith
2d Vice-president: Edwin M. Jacobs
Secretary: Norah duV. Tapley
Treasurer: Simon Kramer

COMMITTEES 1978–1979

Executive: A. S. Ketcham, J. P. Smith, E. M. Jacobs, N. duV. Tapley, S. Kramer, L. W. Brady, R. H. Jesse, F. W. George, F. Rutledge, chairman

Public Relations: V. Marcial, J. Vaeth, C. Honaker, ex-officio, and F. George, chairman

Publication: K. L. Krabbenhoft, D. Hussey, A. Raventos, I. Fix, L. W. Brady, chairman

Scientific Program: R. Parker, J. Durant, A. S. Ketcham, M. S. Mitchell, G. Murphy, F. Rutledge, M. Griem, W. E. Powers, M. Apuzzo, F. George, chairman

Local Arrangements: L. Davis, J. Vaeth, J. Nolan, R. McKenna, J. Slater, J. Stein, J. Scallon, S. Kramer, J. Helsper, chairman

Constitution and Bylaws: A. S. Glicksman, P. J. DiSaia, K. L. Krabbenhoft, chairman

Audiovisual: C. R. Bogardus, J. Helsper, R. Schweitzer, R. H. Jesse, C. Perez, J. Glassburn, A. M. Nisar Syed, R. Young B. Herrington, F. George, chairman

American Board of Radiology Representatives: J. J. Stein, R. E. King, N. duV. Tapley

American College of Radiology Board of Chancellors Representative: L. W. Brady

American College of Radiology Council Representative: J. del Regato

Editorial Board of AFCOS Newsletter Representative: J. Vaeth

National Council on Radiation Protection and Measurements Liaison Representative: L. W. Davis

Annual Meeting: March 4–8, Los Angeles, California

Scientific Program: F. W. George, III, University of Southern California School of Medicine, Los Angeles, California 90033

Local Arrangements: James Helsper, Pasadena, California

Membership: Norah duV. Tapley, secretary, M. D. Anderson Hospital, 6723 Bertner Avenue, Houston, Texas 77030

Business Office: N. V. Jordan, c/o R. H. Jesse, M. D. Anderson Hospital and Tumor Institute, 6723 Bertner Avenue, Houston, Texas 77030

Mailing note.—Mailing surcharges: U.S. and possessions, none; European countries, $25; Japan, $45; other, $10. European rates apply to Algeria, Austria, Belgium, Czechoslovakia, Denmark, Finland, France, Germany, Great Britain, Greece, Hungary, India, Iran, Ireland, Israel, Italy, Kenya, Luxembourg, Netherlands, Nigeria, Norway, Portugal, Romania, South Africa, Spain, Sweden, Switzerland, Turkey, Uganda, Yugoslavia. All subscriptions to Japan and European countries are delivered by air freight; there is no option for surface mail.

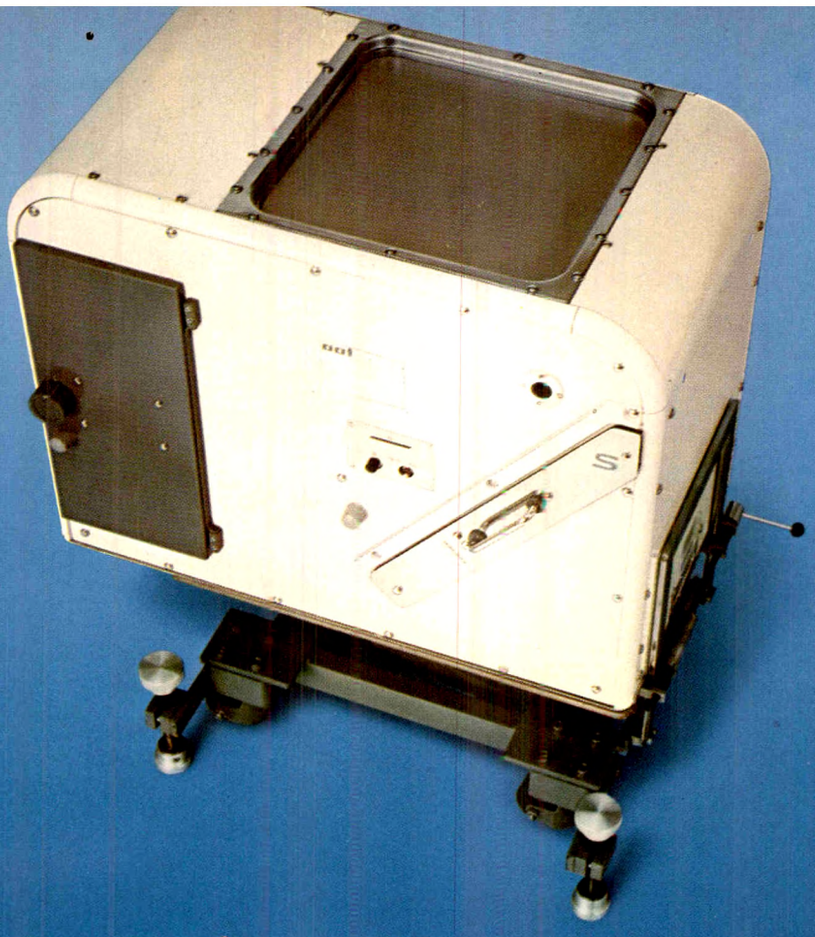

The AOT cutfilm changer— It has worked a long time.

The history of the AOT cutfilm changer is closely tied to the history of angiography. Three decades ago, when radiographic exploration of the vascular system began to advance, Schonander gave the pioneers the tools they needed to obtain full size radiographs at short intervals. We went from regular metal cassettes to lightweight cardboard cassettes to metal frames to roll film... until we reached the ultimate solution: the AOT cutfilm changer using naked standard film sheets.

That was more than 25 years ago. And that's the way it's been ever since: radiographic demands met through engineering ingenuity in a unique interaction between medical and technical expertise. AOT—the workhorse of the special procedures department—built by professionals, with professionals, for professionals.

For more information about the AOT, call (312) 593-6770. Or write Elema-Schonander, Inc., 699 Lively Boulevard, Elk Grove Village, Illinois 60007

elema-schonander, inc.

When a better idea in filmchangers comes along, it will come from us.

THE WORKHORSE

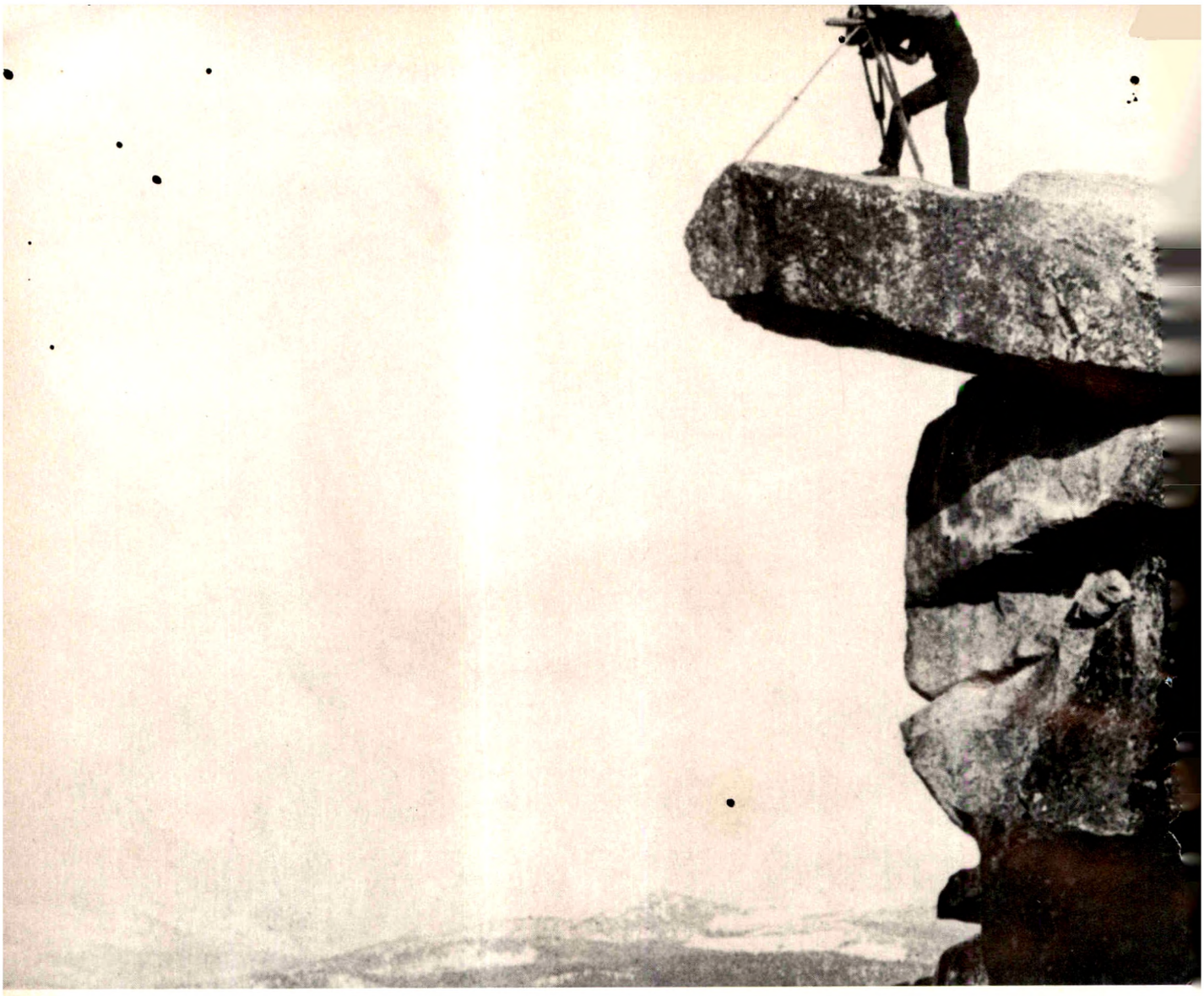

ern History Dept.,
ver Public Library

When the subject can't be moved, it helps to have a camera that can.

With the introduction of lighter photographic cam that ena man to s new persp tives from which to take pictures, new h zons in realism were made possi Searle Radiographics simila influences technology in the fi of nuclear medicine with its extensive line of syste that extend the clinical utility of nuclear cardi throughout the hospital.

The Pho/Gamma® L.E.M. Low-energy Mobile Sc tillation Camera.

The Scintistore™ Time-compression Data Stora Retrieval System.

The Gamma/Cor™ RCG Cardiac Probe.

The Scintiview™ Image Control Station.

Versatility and great images. They're the reasons w this is the most complete and efficient nuclear card ogy line available. Find out how our product technol can serve your needs in nuclear cardiology by conta ing Searle Radiographics.

Searle nuclear cardiology systems move where they're needed to make GREAT IMAGES

ARLE

e Radiographics
on of Searle Diagnostics Inc.
Nuclear Drive

SL 8 8429 1007CMO1

clear, clean colon

X-Prep® Liquid

(standardized extract of senna fruit)

versatile bowel evacuant for diagnostic procedures

Versatile in indications

May be used prior to:

G.I. radiography
Urologic radiography
Colonoscopy
Sigmoidoscopy
Other diagnostic bowel procedures

Versatile in administration

May be used:

Alone, in a single dose
Alone, in divided doses, particularly in elderly or debilitated patients
With adjunctive use of citrate of magnesia, laxative suppositories and enemas, as required
As part of other regimens, such as hydration

X-PREP Liquid is formulated specifically for effective bowel evacuation prior to diagnostic procedures. It induces peristalsis through virtually colon-specific action. X-PREP Liquid has been found effective in cleansing the colon for diagnostic evaluation in 95% of 749 patients prepared for barium enemas, intravenous pyelography, or colonoscopy.* Its pleasant taste meets with high patient acceptance, and its ease of administration is appreciated by the patient and nursing staff.

Supplied: X-PREP Liquid (standardized extract of senna fruit) in 2½ fl. oz. bottles (alcohol 7% by volume). X-PREP Powder (standardized senna concentrate) in ¾ oz. containers. **Now Available:** X-PREP™ Bowel Evacuant Kit. Each kit contains: two SENOKOT® S Tablets (standardized senna concentrate and dioctyl sodium sulfosuccinate), one bottle of X-PREP® Liquid 2½ fl. oz., and one RECTOLAX™ Suppository (bisacodyl 10 mg), plus easy-to-follow patient instructions for hydration, clear liquid diet, and the correct time sequence of administering the above laxatives.

Colonoscope, courtesy of Olympus

*Bibliography available upon request.

Gray Pharmaceutical Co., Affiliate
The Purdue Frederick Company

© Copyright 1978, Gray Pharmaceutical Co. Norwalk, CT 06856

A9047 194578

Fleet® Barium Enema Prep Kits: Make us your first choice for fewer retakes.

The greatest defect in colon examinations is in the preparation of the colon.[1]

Fleet® Barium Enema Prep Kits systematize and improve colon prepping because they conform to the recommended method which provides a combination of diet, hydration and proven laxation which stimulates the large and small intestines.[2] The result? Cleaner colons, clearer x-rays and fewer retakes.

All Fleet Prep Kits offer three laxative steps: 1½ oz. of Fleet® Phospho-Soda® followed by four Fleet® Bisacodyl tablets, plus a final cleansing step. Prep Kit 1 offers Fleet® Bisacodyl suppository. Prep Kit 2 offers a large-volume disposable Fleet® Bagenema. And Prep Kit 3 offers our new Fleet® Bisacodyl enema. And all three Prep Kits have easy-to-follow instructions with a choice of flexible time-tables to fit your schedule.

With Fleet Barium Enema Prep Kits, you'll be sure of convenient, dependable, effective colon prepping every time. And that's reason enough to make Fleet Prep Kits your first choice for fewer retakes.

Fleet Barium Enema Prep Kits
for cleaner colons, clearer x-rays and fewer retakes.

Fleet pharmaceuticals
C.B. Fleet Co., Inc.
Lynchburg, Va. 24505

[1]Dr. R.E. Miller, Ad Hoc Committee on Detection of Cancer of the Colon, Detection of Colon Lesions, American College of Radiology, (Chicago, Ill., 1973) p. 76.
[2]Dr. W.R. Eyler, Ibid. pp. 203, 204.

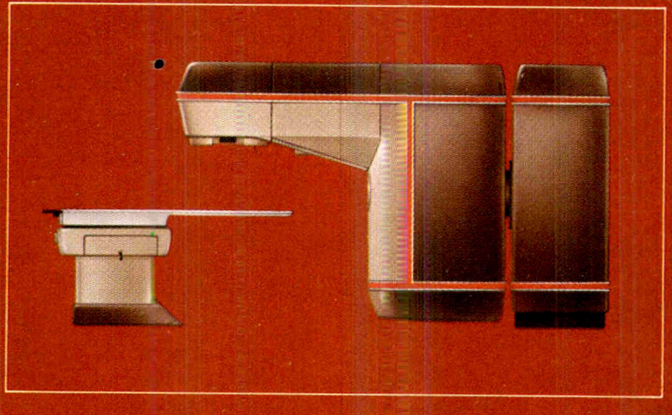

Therac 20

More energy in less space.
20 MeV electrons. 18 MeV photons.

Its space requirements are surprisingly modest.
Yet, the Therac 20 Linear Accelerator from AECL has a high energy output in both electron and photon modes.
Standard among its many features are constant electron beam scanning for optimum dose distribution and record and verify control for added safety.
Therac 20 is more energy in less space.
For complete information, contact AECL.

Atomic Energy of Canada Limited
Commercial Products

P.O. Box 6300, Ottawa, Canada K2A 3V3 Tel: (613) 592-2790

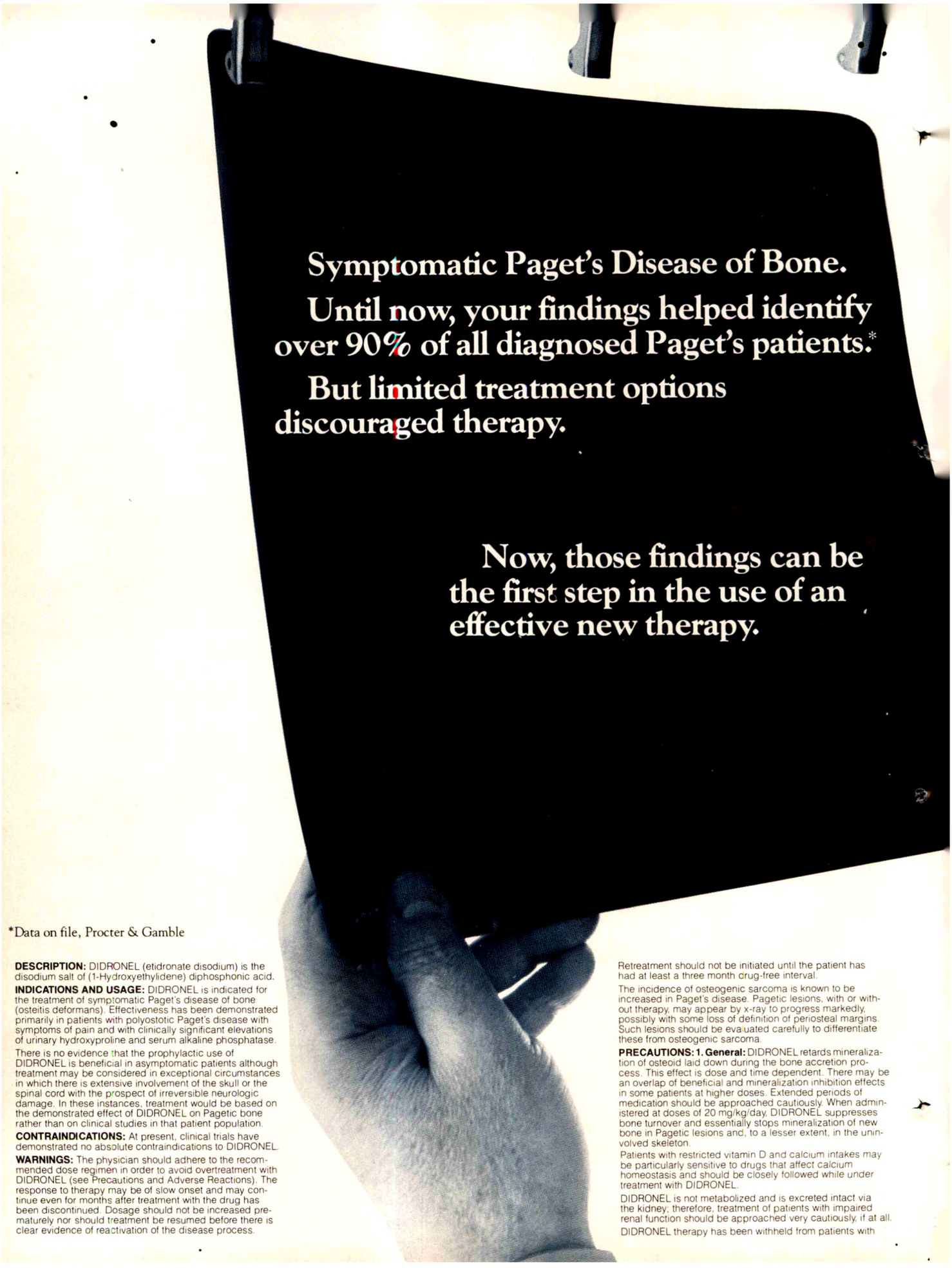

*Data on file, Procter & Gamble

DESCRIPTION: DIDRONEL (etidronate disodium) is the disodium salt of (1-Hydroxyethylidene) diphosphonic acid.

INDICATIONS AND USAGE: DIDRONEL is indicated for the treatment of symptomatic Paget's disease of bone (osteitis deformans). Effectiveness has been demonstrated primarily in patients with polyostotic Paget's disease with symptoms of pain and with clinically significant elevations of urinary hydroxyproline and serum alkaline phosphatase.

There is no evidence that the prophylactic use of DIDRONEL is beneficial in asymptomatic patients although treatment may be considered in exceptional circumstances in which there is extensive involvement of the skull or the spinal cord with the prospect of irreversible neurologic damage. In these instances, treatment would be based on the demonstrated effect of DIDRONEL on Pagetic bone rather than on clinical studies in that patient population.

CONTRAINDICATIONS: At present, clinical trials have demonstrated no absolute contraindications to DIDRONEL.

WARNINGS: The physician should adhere to the recommended dose regimen in order to avoid overtreatment with DIDRONEL (see Precautions and Adverse Reactions). The response to therapy may be of slow onset and may continue even for months after treatment with the drug has been discontinued. Dosage should not be increased prematurely nor should treatment be resumed before there is clear evidence of reactivation of the disease process.

Retreatment should not be initiated until the patient has had at least a three month drug-free interval.

The incidence of osteogenic sarcoma is known to be increased in Paget's disease. Pagetic lesions, with or without therapy, may appear by x-ray to progress markedly, possibly with some loss of definition of periosteal margins. Such lesions should be evaluated carefully to differentiate these from osteogenic sarcoma.

PRECAUTIONS: 1. General: DIDRONEL retards mineralization of osteoid laid down during the bone accretion process. This effect is dose and time dependent. There may be an overlap of beneficial and mineralization inhibition effects in some patients at higher doses. Extended periods of medication should be approached cautiously. When administered at doses of 20 mg/kg/day, DIDRONEL suppresses bone turnover and essentially stops mineralization of new bone in Pagetic lesions and, to a lesser extent, in the uninvolved skeleton.

Patients with restricted vitamin D and calcium intakes may be particularly sensitive to drugs that affect calcium homeostasis and should be closely followed while under treatment with DIDRONEL.

DIDRONEL is not metabolized and is excreted intact via the kidney; therefore, treatment of patients with impaired renal function should be approached very cautiously, if at all.

DIDRONEL therapy has been withheld from patients with

New from Procter & Gamble

200 MG TABLETS

DIDRONEL®

ETIDRONATE DISODIUM

The first oral agent that suppresses symptomatic Paget's disease of bone

...Retards the disease

...Relieves signs and symptoms in many patients

...Promotes sustained posttherapy remission

...Bone-specific pharmacologic action

enterocolitis because increased frequency of bowel movements and diarrhea is seen in some patients when DIDRONEL is administered at a dose of 20 mg/kg/day and may be increased occasionally at lower doses.

2. Pregnancy: There is no experience in pregnant women given DIDRONEL. DIDRONEL should be used only when clearly needed in women who are or may become pregnant.

3. Nursing Mothers: It is not known whether this drug is excreted in human milk. As a general rule, nursing should not be undertaken while the patient is on a drug since many drugs are excreted in human milk.

4. Pediatric Use: No data support the use of DIDRONEL in children.

ADVERSE REACTIONS: Increased or recurrent bone pain at existing Pagetic sites and/or the appearance of pain at sites previously asymptomatic has been reported. At the recommended dose (5 mg/kg/day) 1 out of 10 patients reported the phenomena; at higher doses the figure rose to 2 out of 10. In placebo-treated patients, the occurrence was 1 out of 15. In DIDRONEL-treated patients, the pain resolved while therapy was continued in some patients but persisted for several months in others.

Fractures are recognized as a common feature in patients with Paget's disease. The risk of fracture may be increased when DIDRONEL is taken at a dose level of 20 mg/kg/day in excess of 3 months. This risk may be greater in patients with extensive and severe disease, a history of multiple fractures, and/or rapidly advancing osteolytic lesions. It is recommended that the drug be discontinued when fractures occur and that therapy not be reinstated until fracture healing is complete.

Gastrointestinal complaints such as diarrhea, loose bowel movement, and nausea are increased in some patients when DIDRONEL is administered at doses greater than 5 mg/kg/day. The incidence is about 1 out of 15 in both placebo-treated patients and in patients on DIDRONEL, 5 mg/kg/day. The incidence rises to approximately 2 out of 10 in patients treated with DIDRONEL at the dose of 20 mg/kg/day.

DOSAGE AND ADMINISTRATION: Initial Treatment Guidelines: The recommended initial dose of DIDRONEL for most patients is 5 mg/kg/body weight/day, not to exceed a period of six months. Doses above 10 mg/kg should be reserved for use when there is an overriding requirement for suppression of increased bone turnover associated with Paget's disease or when the patient requires more prompt reduction of elevated cardiac output. Treatment with doses above 10 mg/kg/day should be approached cautiously and should not exceed three months duration. Doses in excess of 20 mg/kg/day are not recommended.

DIDRONEL should be administered as a single, oral dose, two hours before eating. It may be given with fruit juice or water. Food, particularly materials high in calcium content such as milk, in the stomach or upper portions of the small intestine may reduce absorption. Therefore, eating should be avoided for two hours before and after drug administration.

Serum phosphate elevations have been observed when DIDRONEL is administered at daily doses of 10 mg/kg body weight/day or above and occasionally at 5 mg/kg/day. This has not been found to be an indication for discontinuing therapy.

Retreatment Guidelines: Retreatment should be undertaken only after a drug-free period of at least three months and after it is evident that reactivation of the disease has occurred. In no case should duration of retreatment exceed the maximum duration of the initial treatment.

How Supplied: DIDRONEL is supplied as a rectangular white tablet containing 200 mg of etidronate disodium. The tablets are packaged in bottles of 250.

For additional information, write Procter & Gamble, Professional Services, P.O. Box 85507, Cincinnati, Ohio 45201, or call (513) 977-5547.

A Product of Procter & Gamble Research

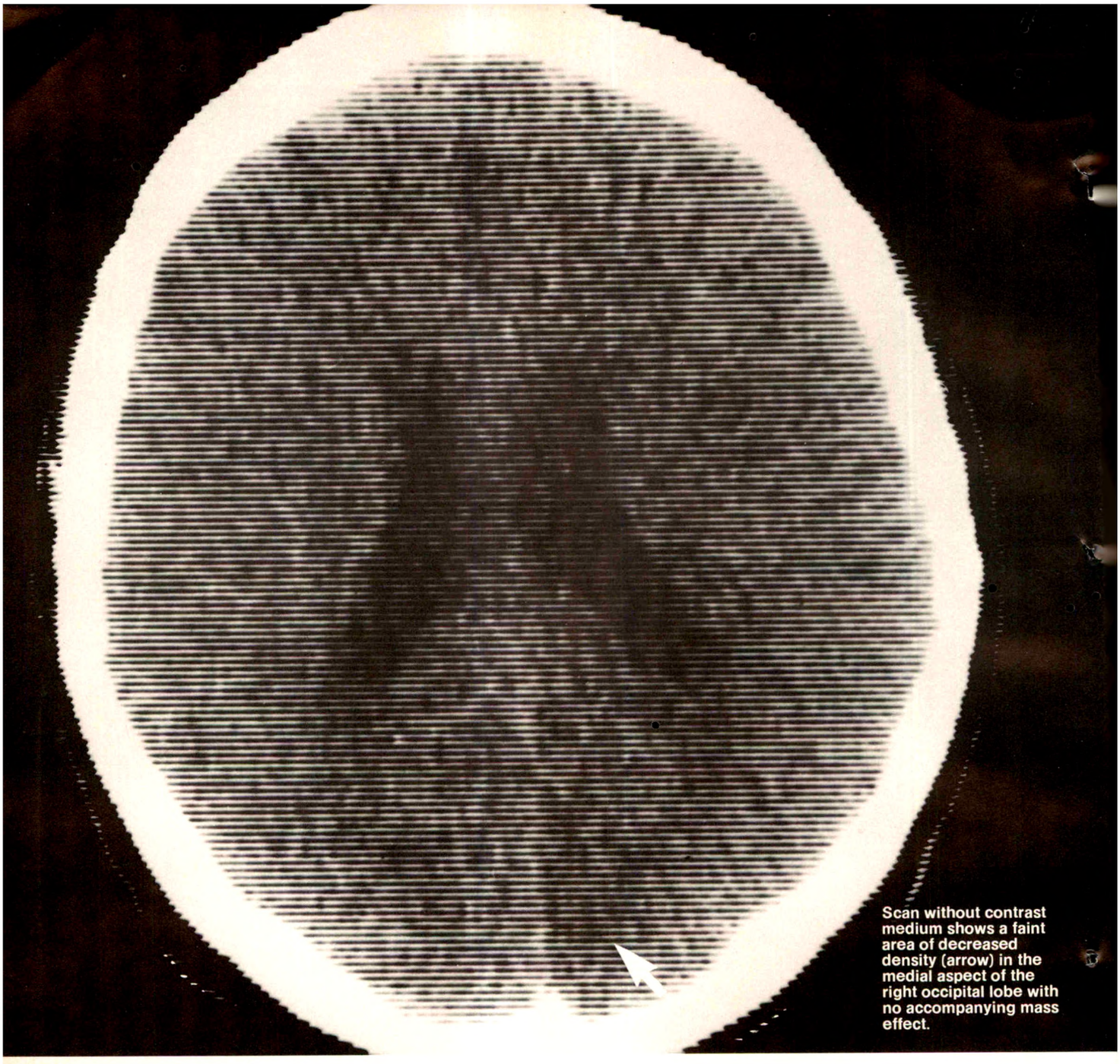

Scan without contrast medium shows a faint area of decreased density (arrow) in the medial aspect of the right occipital lobe with no accompanying mass effect.

Use of this contrast medium to enhance CT brain scans "revealed both an increased detectability and an improved pathologic differentiation of many lesions."*

—**Identifies** lesions not seen on plain CT scans.

—**More specifically defines** nature, size and behavior of wide variety of lesions visualized on plain CT scans.

—**Aids in detection** of aneurysms, arteriovenous malformations, sites of active infection, and in diagnosis of other intracranial pathology.

—**Rules out** the presence of tumor in suspicious areas which may otherwise not have been satisfactorily visualized.

*Davis KR: Massachusetts General Hospital, Boston, MA. Personal communication.

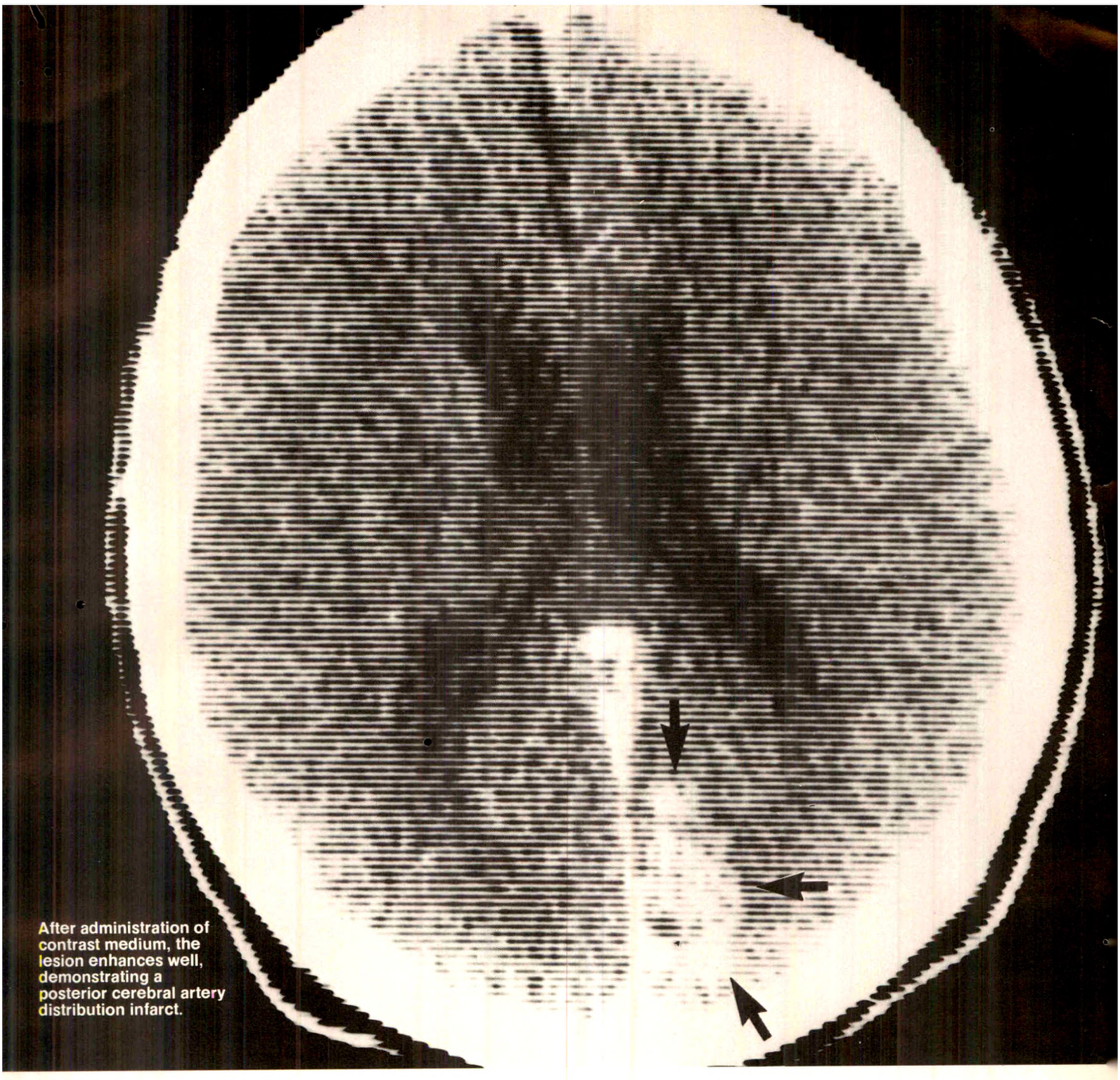

After administration of contrast medium, the lesion enhances well, demonstrating a posterior cerebral artery distribution infarct.

Reno-M-DIP®

Diatrizoate Meglumine Injection USP 30%

for enhanced CT scanning of the brain

The leader in radiologic diagnostics

SQUIBB® contrast media™

See next page for brief summary.

Reno-M-DIP®
Diatrizoate Meglumine Injection USP 30%
for enhanced CT scanning of the brain

Reno-M-DIP (Diatrizoate Meglumine Injection USP) for drip infusion provides a sterile, aqueous solution of 30% diatrizoate meglumine which contains approximately 14% (42.3 g per 300 ml) bound iodine and 0.04% edetate disodium (sequestering agent). *The solution contains approximately 0.054 mg (0.002 mEq) sodium per ml (16.2 mg/300 ml).*

CONTRAINDICATIONS: Contraindicated in patients hypersensitive to salts of diatrizoic acid and in patients with anuria.

WARNINGS: A definite risk exists in the use of I.V. contrast agents in patients with multiple myeloma. There has been anuria with progressive uremia, renal failure and death. This risk of the procedure in these patients is not a contraindication; however, partial dehydration in preparation for study is not recommended since it may predispose to precipitation of myeloma protein in renal tubules. No therapy, including dialysis, has been successful in reversing this effect. Myeloma should be considered in persons over 40 before I.V. administration of a contrast agent.

In cases of known or suspected pheochromocytoma, if the physician feels that the possible benefits outweigh the considered risks, radiopaque materials should be administered with extreme caution; however, an absolute minimum of material should be injected, the blood pressure should be assessed throughout the procedure, and measures for treating a hypertensive crisis should be available.

Contrast media may promote sickling in homozygous individuals when injected I.V. or intra-arterially. Use diatrizoate meglumine with extreme caution in persons with severe concomitant hepatic and renal disease. Perform thyroid function tests prior to administration of diatrizoate meglumine since iodine-containing contrast agents may alter the test results. Although a history of sensitivity to iodine *per se* or to other contrast media is not an absolute contraindication, administration of diatrizoate meglumine requires extreme caution in such cases.

PRECAUTIONS: Diagnostic procedures involving use of contrast agents should be performed under the direction of personnel with prerequisite training and a thorough knowledge of the particular procedure (see ADVERSE REACTIONS). Severe life-threatening reactions suggest hypersensitivity to the contrast agent. A personal or family history of asthma or allergy or a history of a previous reaction to a contrast agent warrants special attention and may predict more accurately than pretesting the likelihood of a reaction although not the type nor severity of the reaction in the individual. The value of any pretest is questionable. The pretest most performed is the slow I.V. injection of 0.5 to 1.0 ml of the preparation prior to injection of the full dose; however, the absence of a reaction to the test dose does not preclude the possibility of reaction to the full diagnostic dose. Should the test dose produce an untoward response, the necessity for continuing the examination should be carefully re-evaluated; if deemed essential, examination should proceed with all possible caution. In rare instances, reaction to the test dose may be extremely severe; therefore, close observation and facilities for emergency treatment appear indicated.

Do not exceed recommended rate of infusion. Renal toxicity has been reported in a few patients with liver dysfunction who were given oral cholecystographic agents followed by urographic agents; therefore, if known or suspected hepatic or biliary disorder exists, diagnostic infusion studies should be postponed following the recent ingestion of cholecystographic agents. The diuretic effect of the drip infusion procedure may hinder an assessment of residual urine in the bladder. Consider the functional ability of the kidneys before injecting diatrizoate meglumine. Adequate visualization may be difficult or impossible in uremic patients or others with severely impaired renal function. Contrast agents may interfere with some chemical determinations made on urine specimens; therefore, collect urine before or two or more days after administration of the contrast medium.

Usage in Pregnancy: This preparation should be used in pregnant patients only when the physician deems its use essential to the welfare of the patient since safe use during pregnancy has not been established.

ADVERSE REACTIONS: Adverse reactions accompanying I.V. use of iodine-containing contrast agents are usually mild and transient although severe and life-threatening reactions (including fatalities) have occurred. Because severe reactions to the procedure and/or to the contrast agent are possible, appropriate emergency facilities and well-trained personnel should be available and should remain available for 30 to 60 minutes following the procedure to treat the reaction since severe delayed reactions have been known to occur.

Reactions most frequently encountered with contrast agents by drip infusion are nausea and urticaria. Chills, metallic taste, vomiting, dizziness, a rise or fall in blood pressure, itching, flushing, or generalized feeling of warmth, sneezing, etc. may occur and, rarely, may be severe enough to require discontinuation of dosage. Severe reactions which may require emergency measures include cardiovascular reaction characterized by peripheral vasodilatation with hypotension and reflex tachycardia, dyspnea, confusion, and cyanosis progressing to unconsciousness. An allergic-like reaction ranging from rhinitis or angioneurotic edema to laryngeal or bronchial spasm or anaphylactoid shock may occur. Temporary renal shutdown or other nephropathy may occur. Although local tissue tolerance to diatrizoate meglumine is usually good, I.V. injection of the medium in a more concentrated formulation has produced a few instances of a burning or stinging sensation and of venospasm or venous pain.

For full prescribing information, consult package insert.

HOW SUPPLIED: Available in single-dose bottles of 300 ml.

The leader in radiologic diagnostics

SQUIBB® contrast media™

©1977 E. R. Squibb & Sons, Inc. H657-503

Significant

Continuing Medical Education Programs

for the Radiologist

on Audio Cassette!

Program 1:

"Nuclear Medicine!"

. . . with James L. Quinn, 3rd, M.D.
and George P. Backer, M.D.
5, one-hour Audio Cassettes

ONLY $35.00!

Program 2:

"New Developments in Nuclear Medicine!"

. . . a supplement to the above program
With James L. Quinn, 3rd, M.D.
and George P. Backer, M.D.
4, one-hour Audio Cassettes

ONLY $28.00!

Program 3:

"Gastrointestinal Radiology!"

. . . with Roscoe E. Miller, M.D.
and George P. Backer, M.D.
6, one-hour Audio Cassettes

ONLY $42.00!

Program 4:

"Neuroradiology!"

. . . with Michael S. Huckman, M.D.
and George P. Backer, M.D.
6, one-hour Audio Cassettes

ONLY $42.00!

Program 5:

"Computers in Medicine!"

. . . with Laurens Ackerman, M.D., Ph.D.
and Daniel K. Harris.
6, one-hour Audio Cassettes

ONLY $42.00!

10 per cent discount on all orders over $100.00!

the institute of continuing education
Sawyer, Michigan 49125 - Phone: 616-426-3433

Please bill me for the following program(s) when shipped:

1 2 3 4 5

10 per cent discount on orders over $100.00
All orders shipped same day received, postpaid

Name _____

Address _____

City _____ State _____ Zip _____

Isn't it time you asked their first name?

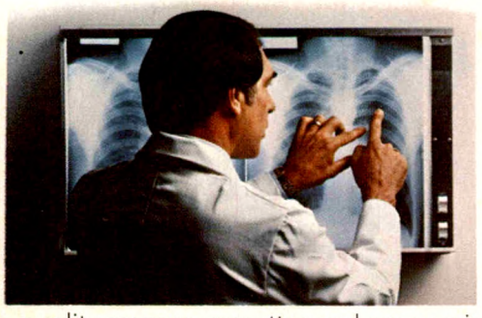

Get familiar with GAFMED.®

GAF® makes it easy to be the first name you think of when ordering quality x-ray films, chemicals, screens and cassettes. We call all our medical x-ray products GAFMED.® Our first-name, only name basis of identity.

It's called GAFMED for one good reason. It's one consistent x-ray system with the confidence to meet a variety of your radiographic needs.

GAF's solid experience and foresight are behind its contemporary x-ray products. This enables GAFMED to respond to any radiographic requirement—be it consistency in your x-ray film, fail-safe chemicals or quality screens, cassettes and accessories. We know you develop favorites in this business and GAF wants to be one of them by measuring up to your toughest standards.

GAFMED®Film and Chemicals: Quality through consistency. To help you manage x-ray imaging, such as getting excellent radiographic contrast and detail, GAF offers a superb line of film that gives you the kind of stability you need in whatever mode you work.

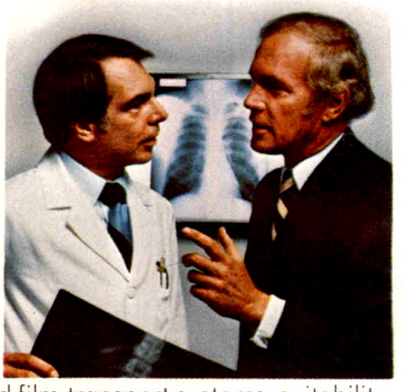

GAFMED®SR/1 When you need an expanded useful density range, wide-latitude SR/1 is your diagnostic radiographic film. It provides high contrast in those low density areas where most radiographic detail is visualized. In addition, SR/1 simultaneously delivers low contrast in high density regions to increase soft tissue detail with maximum exposure latitude. GAFMED SR/1 is designed for use with all blue and blue-green emitting intensifying screens and is fully compatible with all conventional processing methods.

GAFMED®SR/2 SR/2 is a general-purpose medical radiographic film with medium speed, low fog, high contrast and blue spectral sensitivity. Features that make this widely accepted film outstanding are its ideal performance in automated film transport systems, suitability for all automatic and manual processing modes and its high definition image quality. SR/2 renders a wide variety of system speeds when used in combination with GAFMED calcium tungstate and Rarex® rare earth intensifying screens.

GAFMED®SR/S GAFMED SR/S Photofluorography film is designed for use with image intensifiers employing 70mm and 105mm roll film cameras. SR/S features high speed, high contrast and a low base fog for superb optical clarity. GAFMED SR/S is also designed for all 90-second short cycle and extended cycle automatic processing systems.

GAFMED®SC/90 You'd expect the company responsible for the first color-coded chemistry to be equally as innovative with the new GAFMED SC/90 chemical system. **SC/90 DEVELOPER,** color coded red requires no starter solution and cannot be over-replenished. The red pH sensitive quality control feature enables you to quickly determine chemical processing energy through visual check. **SC/90 FIXER,** color-coded blue for easy identity and fail-safe mixing, is designed for use in all short cycle automatic processors and provides excellent archival activity.

for medical x-ray products by

SC/90 chemistry is also a clean-working solution for consistent quality assurance that's part of the GAFMED system.

GAFMED® Screens and Cassettes. The right film and chemicals is just the start.

For optimum radiographic performance the winning GAFMED combination is: a high quality film, superior screens and dependable cassettes.

GAF manufactures two premium GAFMED cassettes to meet your specific requirements: the lightweight Comp-I-Sette™ and the durable Titan.™

The Comp-I-Sette design insures superior screen-film contact for optimum definition. Its lightweight metal construction and special epoxy coating are geared to provide long cassette wear.

The Titan cassette, known for its excellent screen-film contact, is ruggedly constructed to guarantee long lasting service. Its positive-locking feature makes it resistant to sudden jars and jolts. Well recognized as a standard of the industry, Titan cassettes are available in regular and phototiming models.

The GAFMED system also features a wide variety of intensifying screens to meet your particular imaging needs. Our GAFMED Calcium Tungstate screens have an abrasion resistant surface making them ideal for automated film transport systems. Of the four types available, TF-3 with a fast exposure rating, is the most popular for general radiographic applications.

- GAFMED Rare Earth Intensifying Screens allow you to significantly reduce the exposure without requiring a special film or a change in safe-light illumination. Our popular BG High Speed screens allow a 4 time exposure reduction compared to a typical par speed calcium tungstate system.

All GAFMED screens minimize static related artifacts by incorporating an aluminized backing.

GAFMED Product Service: You can't beat the system.

GAFMED is more than a name for our quality line of medical x-ray products. It stands for the GAF people who safeguard your operations with a comprehensive field support program called Radiographic Engineering Services.

Our skilled GAF technical representatives and x-ray engineering consultants will help you get the most efficiency from your radiology department. They provide expert product consultation and high impact training programs to assure consistent radiographic image quality while reinforcing your expertise.

Now is the time to get familiar with GAFMED by contacting your local GAF technical sales representative...GAF x-ray dealer... or GAF Corporation, Medical X-Ray Products, 140 West 51st Street, New York, N.Y. 10020.

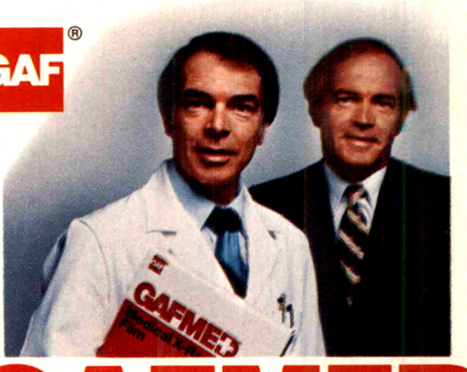

GAFMED®

Medical X-Ray Products.

The image of confidence.

When you're making this kind of commitment, you should know what kind of commitment the manufacturer is making.

Is making...not *will* make. That's the difference between a commitment and a claim. And that's why Pfizer encourages questions about our CT scanner. We think that when it's time to compare answers, you'll see the difference for yourself.

Prestigious installations.
Pfizer has over 150 working CT sites in the United States and 13 foreign countries. Our list includes installations at University of Colorado Medical Center, Columbia-Presbyterian Medical Center Hospital, Johns Hopkins Hospital, Michigan State University Hospital, University of Minnesota Hospital, and Yale-New Haven Hospital.

Near-perfect service.
A worldwide network of dedicated, experienced service engineers, each capable of total system maintenance. They've provided a documented average uptime record of 96% for installations in the U.S. And that's a remarkable service record in the CT industry.

Complete product line.
A full family of scanning equipment. From the industry's first total-body scanner to our benchmark 0200FS whole-body unit, up to the recently announced Pfizer/AS&E CT scanner — the first high resolution fourth-generation scanner. Pfizer now offers one of the most complete lines of CT scanning equipment in the world. Featuring CT images of outstanding clarity, mobile patient handling systems, diagnostic flexibility and advanced software capability every step of the way.

Pfizer and AS&E.® Together.
Early this year, Pfizer Medical Systems, Inc. signed an agreement with American Science and Engineering, Inc. Pfizer and AS&E, both pioneers in the industry, will continue to develop new radiological products, including a revolutionary cardiac scanner. It was Pfizer who developed the first whole-body scanning system. It was AS&E who first introduced fourth-generation geometry, acknowledged as the most advanced CT technology in the world. And together we will continue to practice our commitment. Not just promise it.

For more information, write Pfizer Medical Systems, Inc., Dept. JR, 10 Old Annapolis Road, Columbia, Maryland 21045.

Pfizer

PFIZER MEDICAL SYSTEMS, INC.

We're leaders. And we can show you why.

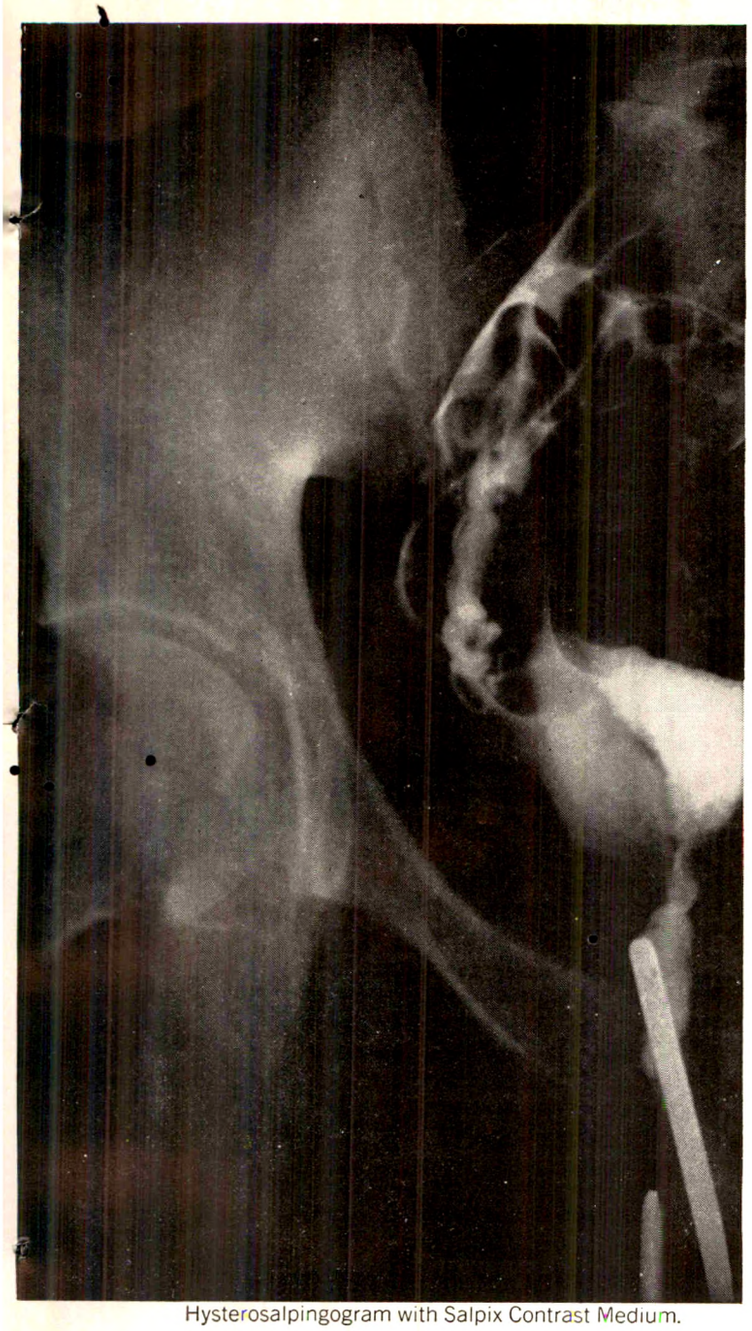

Hysterosalpingogram with Salpix Contrast Medium.

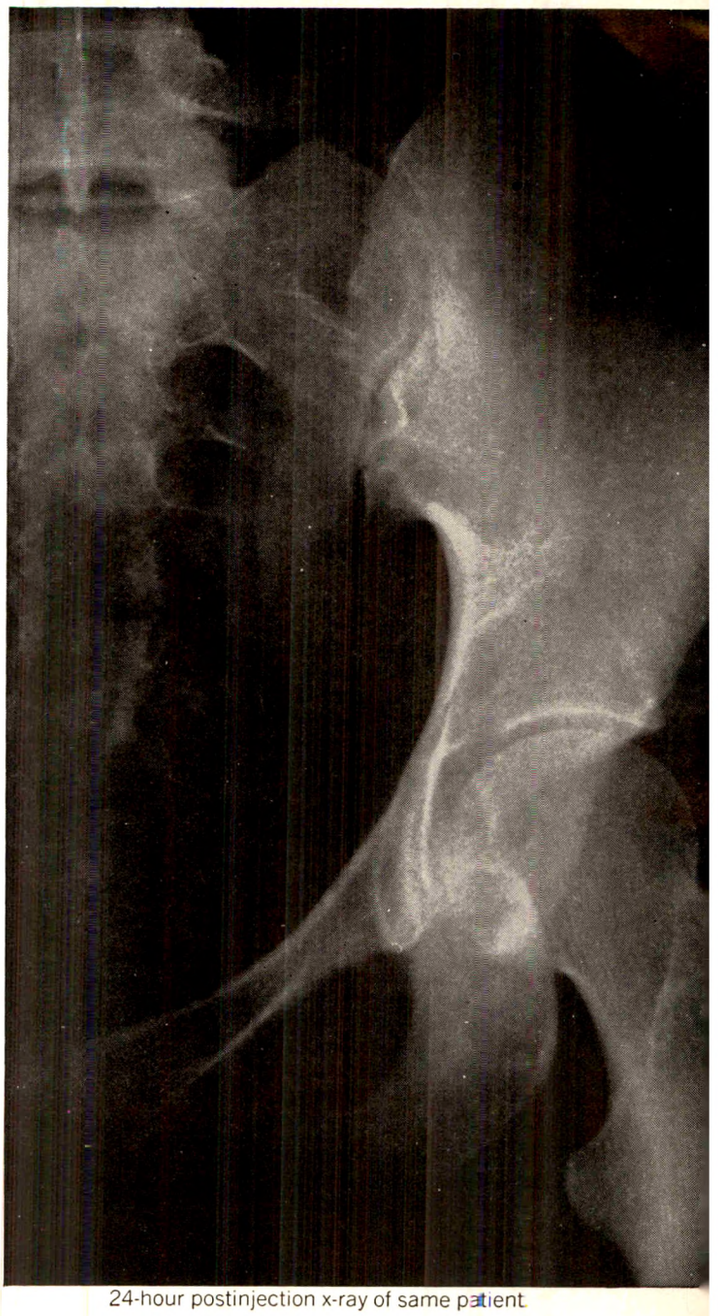

24-hour postinjection x-ray of same patient

now you see it

now you don't

With Salpix as your contrast medium, your gynecologic patient needn't undergo the 24-hour postinjection x-ray usually required with iodized oils. Water-soluble Salpix leaves virtually no irritating radiopaque residue to produce foreign-body reactions, yet it provides the viscosity needed for adequate visualization.

Contraindications: Contraindications to hysterosalpingography include the presence of severe vaginal or cervical infections, existing or recent pelvic infection, marked cervical erosion or endocervicitis, and pregnancy. The procedure is contraindicated during the immediate pre- or post-menstrual phase.

Sensitivity Test: If indicated in the patient's history, an intracutaneous skin test or sublingual absorption observation may be done with 0.1 cc Salpix.

Warning: Not for intravenous use.

© ORTHO PHARMACEUTICAL CORPORATION 1970

CONTRAST MEDIUM

Salpix

TRADEMARK

EACH CC CONTAINS:
sodium acetrizoate 0.53 g and
polyvinylpyrrolidone 0.23 g

Ortho

ORTHO PHARMACEUTICAL CORPORATION • RARITAN, NEW JERSEY 08869

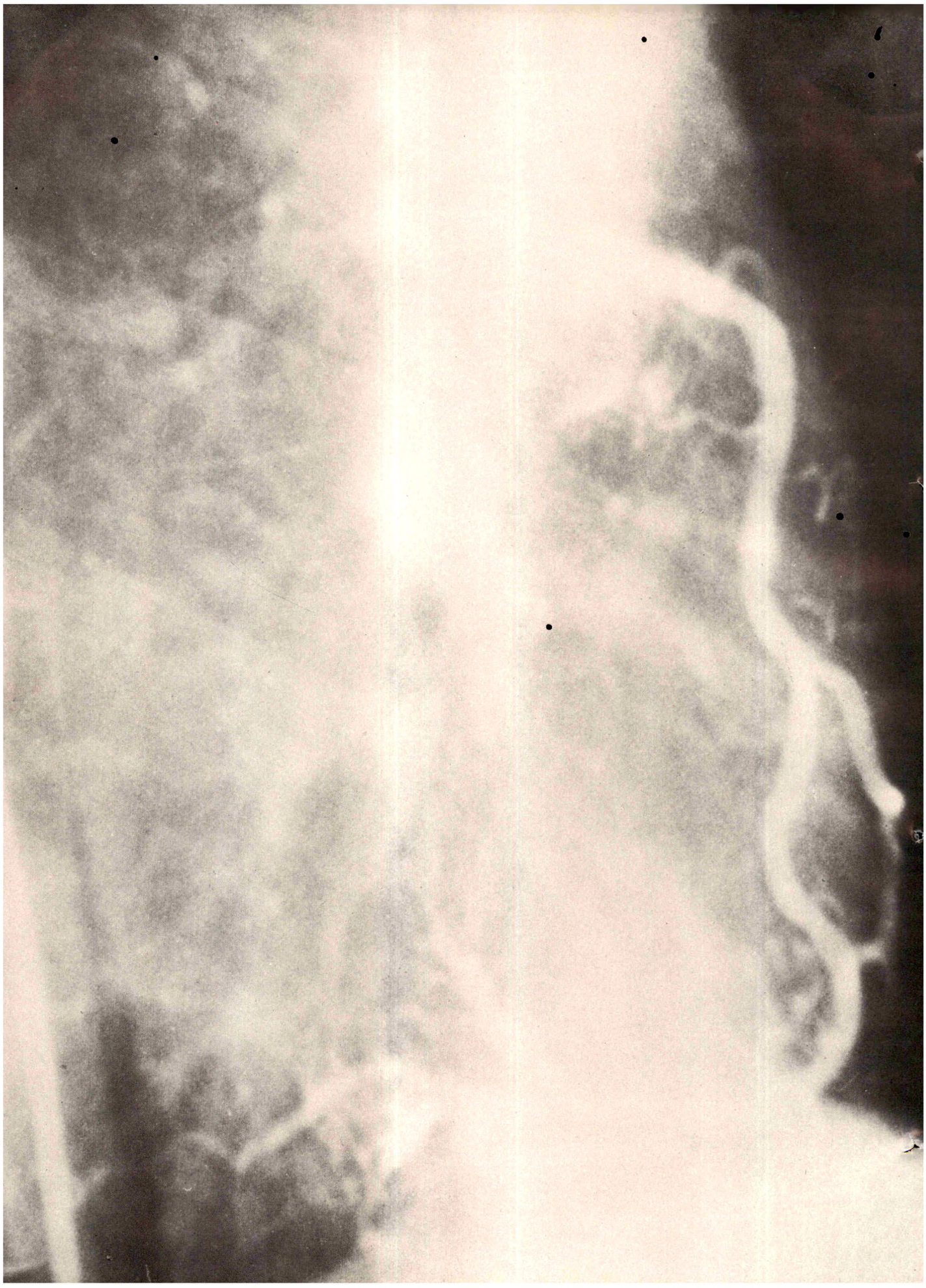

in selective coronary arteriography

the reason is clear™

— excellent image quality

— "minimal myocardial toxicity"

". . . Renografin-76 is eminently suitable as a radiopaque agent for coronary angiography. The film quality was good in every instance, while serious adverse effects were absent in this series of 723 patients." There was a 1% incidence of complications due to the contrast agent (cardiac arrest in 3 and ventricular fibrillation in 5 cases) and a 4% incidence of cardiac complications due to catheterization in this series of patients.*

*Gensini, GG, Kelly, AE. Reassessment of contrast agent for coronary angiography. Current Therapeutic Research 19: 631-636, 1976.

See next page for brief summary.

aortography

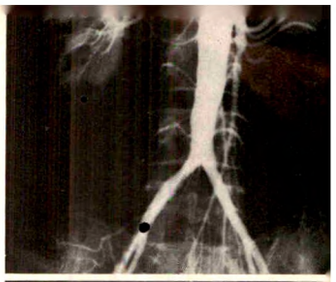

selective renal arteriography

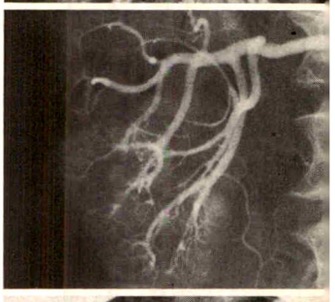

pediatric angiocardiography

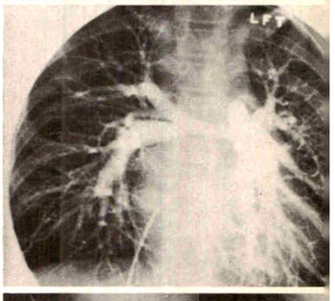

left ventriculography performed following coronary arteriography

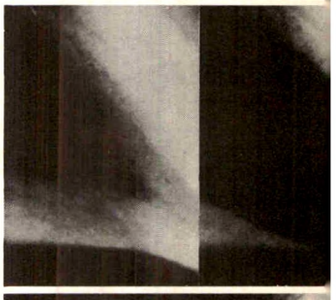

selective visceral arteriography

peripheral arteriography

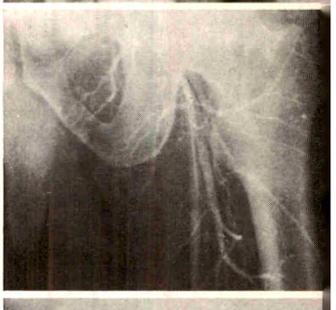

excretion urography

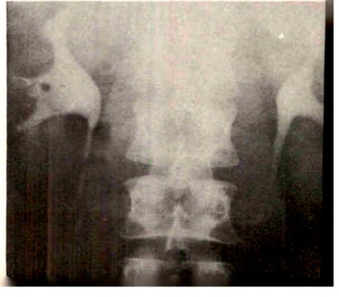

Renografin®-76

Diatrizoate Meglumine and Diatrizoate Sodium Injection USP

SQUIBB®

contrast media™ The leader in radiologic diagnostics

NOW INDICATED FOR CT SCANNING OF THE BRAIN

RENOGRAFIN®-76
Diatrizoate Meglumine and Diatrizoate Sodium Injection USP

Renografin-76 (Diatrizoate Meglumine and Diatrizoate Sodium Injection USP) is supplied as a sterile, aqueous solution providing 66% diatrizoate meglumine and 10% diatrizoate sodium with 0.32% sodium citrate as a buffer and 0.04% edetate disodium as a sequestering agent. The solution contains approximately 37% (370 mg/ml) bound iodine and *approximately 4.48 mg (0.19 mEq) sodium per ml (89.6 mg/20 ml).*

CONTRAINDICATIONS: In patients with a hypersensitivity to salts of diatrizoic acid. Urography contraindicated in patients with anuria.

WARNINGS: A definite risk exists in the use of intravascular contrast agents in patients with multiple myeloma. There has been anuria with progressive uremia, renal failure and death. This risk of the procedure in these patients is not a contraindication; however, partial dehydration in preparation for study is not recommended since it may predispose to precipitation of myeloma protein in renal tubules. No therapy, including dialysis, has been successful in reversing this effect. Myeloma should be considered in persons over 40 before intravascular administration of a contrast agent.

In cases of known or suspected pheochromocytoma, if the physician feels that the possible benefits outweigh the considered risks, radiopaque materials should be administered with extreme caution; however, an absolute minimum of material should be injected, the blood pressure should be assessed throughout the procedure, and measures for treating a hypertensive crisis should be available.

Contrast media may promote sickling in homozygous individuals when injected I.V. or intra-arterially. Although a history of sensitivity to iodine *per se* or to other contrast media is not an absolute contraindication, administration of diatrizoate requires extreme caution in such cases. Perform thyroid function tests prior to administration of this preparation since iodine-containing contrast agents may alter the test results.

Weigh the inherent risks against necessity for performing *angiocardiography* in cyanotic infants and patients with chronic pulmonary emphysema. In *pediatric angiocardiography,* a dose of 10 to 20 ml may be particularly hazardous in infants weighing less than 7 kg; this risk is probably significantly increased if these infants have pre-existing right heart "strain," right heart failure, and effectively decreased or obliterated pulmonary vascular beds. Perform *urography* with extreme caution in persons with severe concomitant hepatic and renal disease. Perform *selective coronary arteriography* only in selected patients and those in whom expected benefits outweigh the procedural risk. Perform *selective visceral arteriography* with extreme caution in presence of severe generalized atherosclerosis, specifically with plaques or aneurysms at level of iliac or femoral arteries.

PRECAUTIONS: Diagnostic procedures involving use of contrast agents should be performed under the direction of personnel with prerequisite training and a thorough knowledge of the particular procedure (see ADVERSE REACTIONS). Severe life-threatening reactions suggest hypersensitivity to the contrast agent. A personal or family history of asthma or allergy or a history of a previous reaction to a contrast agent warrants special attention and may predict more accurately than pretesting the likelihood of a reaction although not the type nor severity of the reaction in the individual. The value of any pretest is questionable. The pretest most performed is the slow I.V. injection of 0.5 to 1.0 ml of the preparation prior to injection of the full dose; however, the absence of a reaction to the test dose does not preclude the possibility of reaction to the full diagnostic dose. Should the test dose produce an untoward response, the necessity for continuing the examination should be carefully re-evaluated; if deemed essential, examination should proceed with all possible caution. In rare instances, reaction to the test dose may be extremely severe; therefore, close observation and facilities for emergency treatment appear indicated.

Renal toxicity has been reported in a few patients with liver dysfunction who were given oral cholecystographic agents followed by urographic agents; therefore, if known or suspected hepatic or biliary disorder exists, administration of Renografin-76 (Diatrizoate Meglumine and Diatrizoate Sodium Injection USP) should be postponed following the ingestion of cholecystographic agents. Use cautiously in severely debilitated patients and in those with marked hypertension. Bear in mind the possibility of thrombosis when using percutaneous techniques. Consider the functional ability of the kidneys before injecting the contrast agent. Since contrast agents may interfere with some chemical determinations made on urine specimens, collect urine before or two or more days after administration of the contrast agent.

In *excretion urography,* adequate visualization may be difficult or impossible in uremic patients or others with severely impaired renal function (see CONTRAINDICATIONS). In *aortography* repeated intra-aortic injections may be hazardous; this also applies to *pediatric angiocardiography* particularly in infants weighing less than 7 kg (see WARNINGS). In *peripheral arteriography,* hypotension or moderate decreases in blood pressure seem to occur frequently with intra-arterial (brachial) injections; this is transient and usually requires no treatment. Monitor blood pressure during the immediate 30 minutes after injection. It is recommended that *selective coronary arteriography* not be performed for about 4 weeks after diagnosis of myocardial infarction; mandatory prerequisites to this procedure are experienced personnel, ECG monitoring apparatus, and adequate facilities for immediate resuscitation and cardioversion.

Usage in Pregnancy: Use Renografin-76 (Diatrizoate Meglumine and Diatrizoate Sodium Injection USP) in pregnant patients only when the physician deems its use essential to the welfare of the patient since safe use during pregnancy has not been established.

ADVERSE REACTIONS: Adverse reactions accompanying intravascular use of iodine-containing contrast agents are usually mild and transient although severe and life-threatening reactions (including fatalities) have occurred. Because severe reactions to the procedure and/or to the contrast agent are possible, appropriate emergency facilities and well-trained personnel should be available and should remain available for 30 to 60 minutes following the procedure to treat the reaction since severe delayed reactions have been known to occur.

Nausea, vomiting, flushing, or a generalized feeling of warmth are the reactions seen most frequently with intravascular injection. Symptoms which may occur are chills, fever, sweating, headache, dizziness, pallor, weakness, severe retching and choking, wheezing, a rise or fall in blood pressure, facial or conjunctival petechiae, urticaria, pruritus, rash and other eruptions, edema, cramps, tremors, itching, sneezing, lacrimation, etc. Antihistaminic agents may be of benefit; rarely, such reactions may be severe enough to require discontinuation of dosage. There have been a few reports of a burning or stinging sensation or numbness, of venospasm or venous pain, and of partial collapse of the injected vein. Neutropenia or thrombophlebitis may occur. Severe reactions which may require emergency measures are a possibility and include cardiovascular reaction characterized by peripheral vasodilatation with hypotension and reflex tachycardia, dyspnea, agitation, confusion, and cyanosis progressing to unconsciousness. An allergic-like reaction ranging from rhinitis or angioneurotic edema to laryngeal or bronchial spasm or anaphylactoid shock may occur. Temporary renal shutdown or other nephropathy may occur.

Adverse reactions as a consequence of *excretion urography* include cardiac arrest, ventricular fibrillation, anaphylaxis with severe asthmatic reaction, and flushing due to generalized vasodilatation. Risks of *aortography* procedures include injury to aorta and neighboring organs, pleural puncture, renal damage (including infarction and acute tubular necrosis with oliguria and anuria), accidental selective filling of right renal artery during translumbar procedure in presence of pre-existent renal disease, retroperitoneal hemorrhage from translumbar approach, spinal cord injury and pathology associated with syndrome of transverse myelitis, generalized petechiae, and death following hypotension, arrhythmia, and anaphylactoid reactions. In *pediatric angiocardiography,* arrhythmia and death have occurred. During *peripheral arteriography,* hemorrhage from puncture site, thrombosis of the vessel, and brachial plexus palsy (following axillary artery injection) have occurred. During *selective coronary arteriography* and *selective coronary arteriography combined with left ventriculography,* transient ECG changes (most patients); transient arrhythmias (infrequent); ventricular fibrillation (from manipulation of catheter or administration of medium); hypotension; chest pain; myocardial infarction; transient elevation of creatinine phosphokinase (occurred in about 30% of patients tested); fatalities have been reported. Complications due to the procedure include hemorrhage, thrombosis, pseudoaneurysms at puncture site, dislodgment of arteriosclerotic plaques; dissection of coronary vessels and transient sinus arrest have occurred rarely. Adverse reactions in *selective renal arteriography* include nausea, vomiting, hypotension, hypertension, and post-arteriographic transient elevations in BUN, serum creatinine and glucose. Complications of *selective visceral arteriography* include hematomas, thrombosis, pseudoaneurysms at injection site, dislodgment of arteriosclerotic plaques; other reactions may include urticaria, hypotension, hypertension, and insignificant changes in renal function and liver chemistry tests.

For full prescribing information, consult package insert.

HOW SUPPLIED: Available in 20 ml and 50 ml single-dose vials and in 100 ml and 200 ml single-dose bottles.

©1977 E. R. Squibb & Sons, Inc. H627-503

SQUIBB®
contrast media™

E.R. Squibb & Sons, Inc.
P.O. Box 4000 Princeton, N.J. 08540

Machlett
For neuroradiography

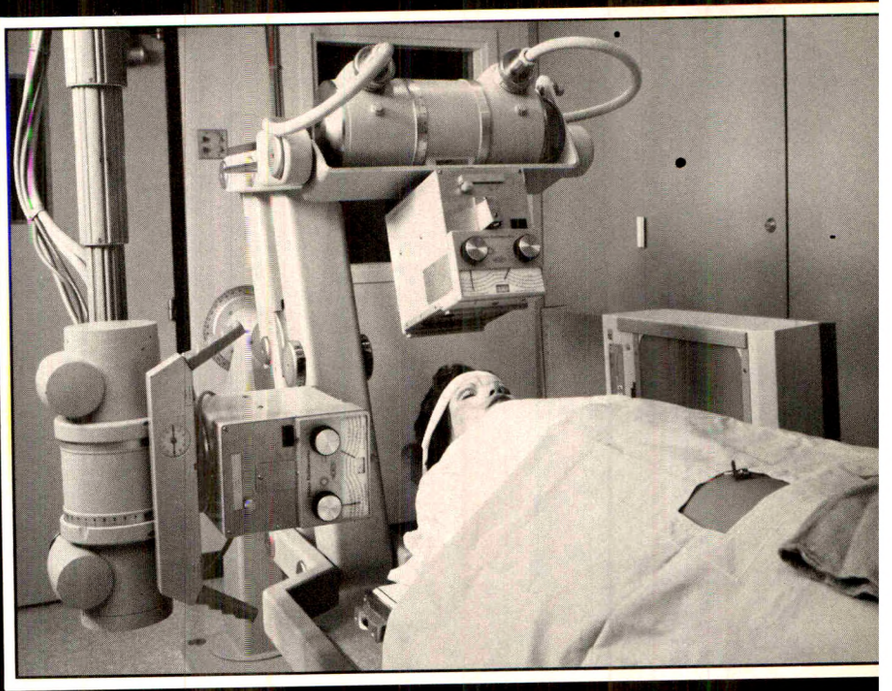

dynamax 68E
dynamax 78E
procedure-designed
x-ray tubes

Designed for the exacting techniques of neuroradiography Machlett's Dynamax 78E and Dynamax 68E inserts feature a large focus to permit the use of heavy-duty angiographic procedures with conventional films and screens.

Dynamax 78E 10/57 inserts biased for small focus will resolve 7 1/2 lines per millimeter at 3-power magnification at 100 mA and 70 kVp.

Dynamax 68E 13/87 inserts biased for small focus will resolve 5 lines per millimeter at 2-power magnification at 140 mA and 70 kVp.

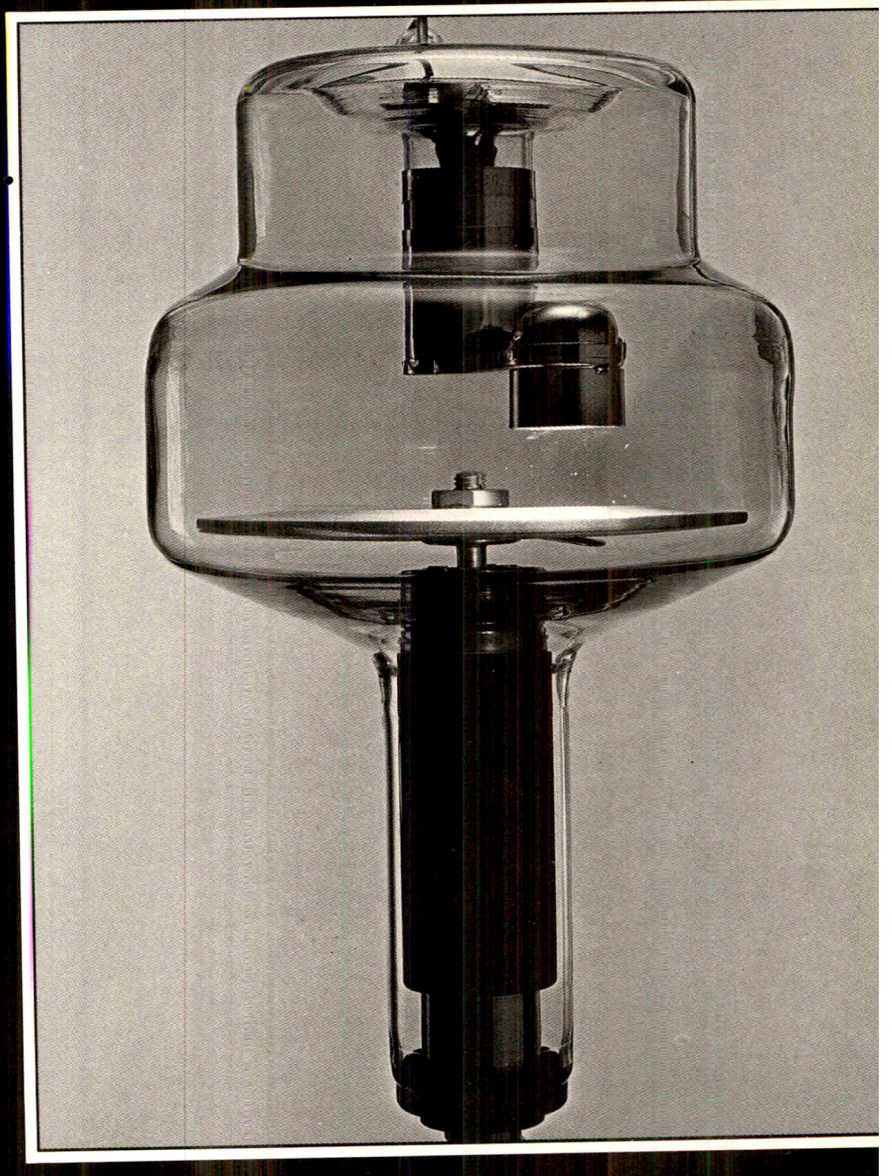

For complete information contact your x-ray dealer or

MACHLETT

The Machlett Laboratories, Incorporated

1063 Hope Street
Stamford, Connecticut 06907
(203) 348-7511

A Raytheon Company

American Journal of Roentgenology Guidelines

Address manuscripts and correspondence to the Editorial Office, 403 Pacific National Bank Building, 4545 15th Avenue N.E., Seattle, Washington 98105; telephone (206) 633-2754.

Publication Policy

The Journal publishes original and timely contributions to the advancement of radiologic diagnosis and treatment. Although the content is predominantly clinical, laboratory investigations are accepted when their relevance to clinical practice is demonstrable. Decisions on manuscripts are based on the opinions of at least two outside reviewers. Statements within an article are the responsibility of the authors and not the Journal or its publisher.

It is understood that material submitted has not been published and is not currrently submitted elsewhere. Portions of the data or illustrations from previously published works may be included if permission release forms accompany the manuscript and such material is clearly credited in the text. Prior publication of abstracts will not prejudice publication of the complete study.

Copyright Information

In accordance with Journal implementation of the new U.S. Copyright Law, authors must release first and subsidiary rights to their manuscript at submission. A dated cover letter, containing signatures of all authors, should state: "We, the authors, assign first and subsidiary rights to the American Roentgen Ray Society in the event that our manuscript (title) is published by AJR." The Journal, in turn, grants authors the right to use portions of their manuscript, without charge, in books or articles of which they are authors or editors.

Manuscript Form

Manuscripts should be typed double-spaced throughout, including references, tables, and figure legends. Tables, footnotes, and figure legends should be on separate sheets, and a separate title page should be provided. In addition to the original typewritten copy, a duplicate copy complete with figures, tables, and references is required. Authors' names should be on title page only and should not be on figures so that author anonymity can be maintained during the review process.

Figures should be submitted as 13 × 18 cm glossy prints, untrimmed and unmounted. Labels and arrows must be of professional quality and should be removable from the prints. Each figure should be numbered to correspond with figure legends, and the top should be indicated. Specific permission for publication of facial photographs of patients is required. Line illustrations and graphs should be drawn in black ink on white background.

References should be cited in the text by number (e.g., [3, 4]). The bibliography should be arranged in the numerical order that references are cited in the text and typed double-spaced throughout. Data for each reference should be arranged according to the uniform style on bibliographic citations adopted by many biomedical journals. Provide all authors' names and inclusive pages. Abbreviations for titles of medical periodicals should conform to those published in *Index Medicus*. Examples:

1. Miller RE, Chernish SM, Skucas J, Rosenak BD, Rodda BE: Hypotonic roentgenography with glucagon. *Am J Roentgenol* 121:264–274, 1974
2. Boijsen E: Superior mesenteric angiography, in *Angiography*, edited by Abrams H, Boston, Little, Brown, 1971, pp 1091–1119

Organization

Title page. Titles should be brief and specific. Include addresses for each author and acknowledgment of grant support when appropriate.

Abstract. A description of the purpose, methods, results and conclusions of the study is required.

Introduction. Clearly state the purpose of the investigation including necessary background facts.

Materials and methods. Describe the protocol clearly. Use standard abbreviations as presented in the *Council of Biology Editors Style Manual*, 3d ed. Metric measurements should be used throughout.

Results. Present results in logical sequence.

Discussion. Interpret the results to lend meaning and importance to the observations. If hypotheses and speculation are included, they must be labeled as such. When results differ from those of previous investigators, an attempt should be made to explain the discrepancy.

References. Only include references which provide adequate background and present fairly any opposing evidence and concepts. Accuracy of reference data is the responsibility of the author.

Legends. Legends should be brief but should provide sufficient description to interpret the figure.

Special Communications

Case Reports. Concise case reports are accepted if they present unusual experiences that are medically important and educational. Clarity and brevity are essential. After preliminary screening by an editor to determine whether the requirement of medical significance has been met, qualifying papers will undergo the same peer review as major papers.

Technical notes. Brief descriptions of new techniques or significant modifications of older ones which are directly applicable to clinical practice will be accepted.

Letters to the Editor. Letters are subject to editing and condensation. Criticism of published articles should be objective and constructive. Letters may also discuss matters of general interest to radiologists.

P 24,437

Coronary, Ventricular, and Pulmonary Abnormalities Associated with Rupture of the Interventricular Septum Complicating Myocardial Infarction

STEPHEN W. MILLER,[1] ROBERT E. DINSMORE,[1] REGINALD E. GREENE,[1] AND WILLARD M. DAGGETT[2]

Left ventricular wall motion abnormalities, the extent and location of coronary artery stenoses, and the radiographic evidence of pulmonary venous hypertension were analyzed in a retrospective study of 40 patients who had surgically proven rupture of the interventricular septum after myocardial infarction. In 33 patients in whom chest films were available, interstitial or alveolar pulmonary edema was present in 78%, while left ventricular enlargement was present in 82%. Of 26 patients who had coronary angiography, complete occlusion of the right coronary artery, left anterior descending artery, or left circumflex artery was present in 92%, with few, if any, collateral vessels around the occlusion. The location of the rupture in the muscular septum was always in the region of akinesis or dyskinesis. Posterior defects were associated with posterobasal and diaphragmatic akinesis, and anterior defects with apical akinesis. Left ventricular aneurysms were adjacent to the septal rupture in 68%, and 74% had mitral regurgitation. The right ventricular diaphragmatic wall in posterior rupture was always akinetic, indicating right ventricular infarction. Thus ventricular septal defect after myocardial infarction (1) tends to occur with multiple coronary occlusions about which little collateral flow develops; (2) can accurately be localized anteriorly or posteriorly in the muscular septum by the location of the akinetic left ventricular wall segment; and (3) has an associated right ventricular infarct when rupture is posterior.

Rupture of the interventricular septum is an uncommon complication of myocardial infarction. It occurs in about 1% of patients with myocardial infarcts [1, 2], and has a mortality of 24% within 1 day, and over 90% at 1 year [3, 4]. The diagnosis of a ruptured septum is suggested clinically with the appearance of a new systolic murmur, concomitant with biventricular failure or cardiogenic shock occurring within hours to weeks after myocardial infarction. Pulmonary edema is usually present on chest radiography. Recently, surgical repair has been successfully accomplished within days [5–7] as well as months [8, 9] after acute septal rupture.

Since improved hemodynamic support [10], in addition to new surgical techniques, is now available for these patients, early and correct diagnosis is necessary for proper clinical management. This paper describes the radiologic abnormalities of ruptured interventricular septum in the chest radiograph and correlates these findings with hemodynamic parameters. In addition, since many of these patients may undergo coronary arterial revascularization, coronary and left ventricular angiograms have been analyzed to determine the extent and location of coronary stenoses and associated ventricular abnormalities.

Subjects and Methods

Forty patients were selected retrospectively with postinfarction rupture of the interventricular septum documented by surgical inspection. This group was evaluated during the years 1969–1977. The 25 men and 15 women ranged in age from 44 to 74 years. Myocardial infarction had occurred from 1 day to several months before surgery. This wide time span reflects the difficulty in making the clinical diagnosis as well as selection bias that permitted these patients to survive long enough to undergo catheterization and surgery. The time between infarct and the septal rupture (i.e., the interval between chest pain and the appearance of a new systolic murmur) was ascertained in 31 patients, and ranged from hours to 1 month, with an approximate mean of 4 days.

Electrocardiograms were available for review in 39 patients: 19 showed anterior myocardial infarcts, 17 had inferior myocardial infarcts, one patient had both an anterior and inferior infarct, one had nonspecific ST-T wave changes, and one had right bundle branch block with left anterior hemiblock. In 38 patients in whom pressures were measured, the mean pulmonary capillary wedge or left ventricular end diastolic pressure was 20 ± 6 mm Hg (mean ± SD) with a range from 8 to 33 mm Hg. In 31 patients, the ratio of pulmonary to systemic blood flow was 3.5 ± 1.2 with a range from 1.3 to 6.

Frontal chest films taken near the time of surgery were available for 33 patients and are summarized in table 1. Five of the 33 patients had standard teleoradiographs, while the remainder were bedside films. Their films were of good quality and are typical of those obtained in clinical practice on critically ill and hemodynamically unstable patients. Of the 33, 32 had hemodynamic data available for correlation with radiographic abnormalities (table 2). Twenty-three patients had films within 1 day of catheterization, nine had films within 3 days, and one went directly to surgery without catheterization.

Each of the radiographs was analyzed by three radiologists without knowledge of hemodynamic data; differences in interpretation were resolved by consensus. Radiologic assessment of heart chamber enlargement was undertaken according to the criteria of Dinsmore [11]. Definite enlargement could be determined only with respect to the left ventricle. Enlargement of other chambers was suspected but not certain. Ventricular and atrial enlargement were coded none, mild, moderate, or severe.

Received January 31, 1978; accepted after revision June 15, 1978.
This work was supported in part by U.S. Public Health Service Grant HL-17665 (Ischemic Heart Disease Specialized Center of Research). S. W. Miller is a James Picker Foundation Scholar.

[1] Department of Radiology, Massachusetts General Hospital and Harvard Medical School, Boston, Massachusetts 02114. Address reprint requests to S. W. Miller.
[2] Department of Surgery, Massachusetts General Hospital and Harvard Medical School, Boston, Massachusetts 02114.

© 1978 American Roentgen Ray Society

0361–803X/78/1000–0571 $00.00
P 24,438

TABLE 1

Chest Radiographic Abnormalities in 33 Patients with Rupture of Interventricular Septum

Abnormality	No.	%
Pulmonary abnormality:		
Normal	4	12
Pulmonary venous hypertension	3	9
Interstitial pulmonary edema	14	42
Alveolar pulmonary edema	12	36
Pleural effusion:		
None	12	36
Right side	1	3
Left side	10	30
Both sides	10	30
Pulmonary artery enlargement	13	39
Cardiac enlargement:		
Left ventricle:		
None	6	18
Mild	13	39
Moderate	12	36
Severe	2	6
Right ventricle:		
None	32	97
Mild	1	3
Left atrium:		
None	31	94
Mild	2	6
Right atrium:		
None	29	88
Mild	4	12

The pulmonary vasculature was coded as pulmonary venous hypertension if upper lobe vessels were enlarged or lower lobe vessels were either small or invisible. Interstitial pulmonary edema was defined as perivascular edema, a diffuse reticular pattern, or septal lines. Alveolar edema was defined as confluent acinar shadows. Pleural fluid and enlargement of the pulmonary arteries were also coded.

Bilateral coronary angiography was performed in 26 patients and left ventriculography in 25. A significant coronary artery lesion was defined as 50% or greater reduction in diameter. The maximum diameter narrowing seen in all projections of a coronary artery was recorded, with the exception that lesions less than 50% were coded 0. The left main coronary artery was defined as that portion between the left coronary ostium and the bifurcation of the left anterior descending and the left circumflex coronary arteries. The proximal left anterior descending artery extends from the origin of that artery to and including the first septal branch. The distal portion was defined as that part after the first septal branch (fig. 1*A*). The right coronary or left circumflex artery was called dominant if it supplied the posterior descending artery. The left ventriculogram was divided into five segments in the right anterior oblique projection (fig. 1*B*). Systolic wall motion was classified as normal, moderate, and severe hypokinesis. Absent systolic contraction of a ventricular segment was classified as akinesis, while a paradoxical systolic bulging was dyskinesis. An aneurysm was defined as an abnormal bulge at end diastole, and was usually associated with dyskinesis. All angiograms were reviewed twice, either by different observers or by the same observer 2 months later without knowledge of the previous classification. Coronary and ventriculographic variability were resolved by consensus.

The location of the septal rupture was ascertained by inspection at surgery. Infarctectomy provided direct exposure of the adjacent septal defect, which was invariably contiguous to the infarct.

Results

The most common abnormality of the cardiac silhouette was left ventricular enlargement (table 1). Elongation of the left ventricular apex to the left and inferiorly was present in 82% of these 33 patients. Enlargement of other cardiac chambers was inconstant, occurring in less than 12% of chest films.

Ventricular aneurysms were not recognized on chest films with one exception. Figure 2 demonstrates a saccular aneurysm in the anterior left ventricular wall in a patient with radiographic evidence of pulmonary venous hypertension. This low sensitivity for the detection of left ventricular aneurysm in a population known to have a high incidence of aneurysm is not surprising, since aneurysms may be difficult to recognize on chest films, and since our patients were selected with abnormalities of the interventricular septum, a region which is not visible on plain radiographs of the heart.

Most patients had evidence of pulmonary venous hypertension with or without pulmonary edema (fig. 3). Chest films demonstrated interstitial or alveolar pulmonary edema in 78%, and pulmonary venous hypertension without demonstrable edema in 9%. Pleural effusions were common, occurring in 64%. While no quantitative measurements of pulmonary artery size were made, the pulmonary arteries were deemed enlarged in 39%, a finding consistent with a hemodynamic status of both pressure and volume overload.

Whether the chest film could distinguish between patients with congestive heart failure after myocardial infarction and those who developed congestive heart failure after rupture could not be determined. Many of the patients were referred, so that serial films were not available. The difficulty of timing the onset of a septal rupture clinically is also compounded in a retrospective survey.

Table 2 compares the interpretation of the pulmonary vasculature with the left atrial pressure and the size of the left-to-right shunt. In general, patients whose chest films were interpreted as showing normal pulmonary vasculature tended to have slightly lower left atrial pressures, although there was no significant difference between their pressures and those judged to have pulmonary venous hypertension or pulmonary edema. In a similar fashion, the size of the left-to-right shunt had no correlation with the development of pulmonary edema. The nearly uniform elevation of the left ventricular end diastolic pressure had the large size of shunt both appeared to contribute to the development of the pulmonary edema.

Extent of Coronary Artery Disease

In 26 patients, bilateral coronary angiography was performed (table 3). Only one patient had a significant stenosis in the left main coronary artery. Seven patients (27%) had left anterior descending artery stenoses be-

TABLE 2

Comparison of Hemodynamic Data with Radiographic Analysis of Pulmonary Vasculature

Pulmonary Vasculature Interpretation	LVED OR PCW (mm Hg)				Qp/Qs			
	No. Patients	Range	Mean	SD	No. Patients	Range	Mean	SD
Normal	2	11–20	16	4.5	3	2.4–3.9	3.1	0.6
Pulmonary venous hypertension without edema	3	20–25	22	2.4	3	1.3–3.5	2.5	0.9
Interstitial pulmonary edema	12	8–33	20	7.3	10	2.9–5	3.6	0.7
Alveolar pulmonary edema	12	15–28	22	4.3	10	1.3–6	3.7	1.6

Note.—LVED = left ventricular end diastolic pressure, PCW = mean pulmonary capillary wedge pressure, Qp/Qs = pulmonary to systemic flow ratio.

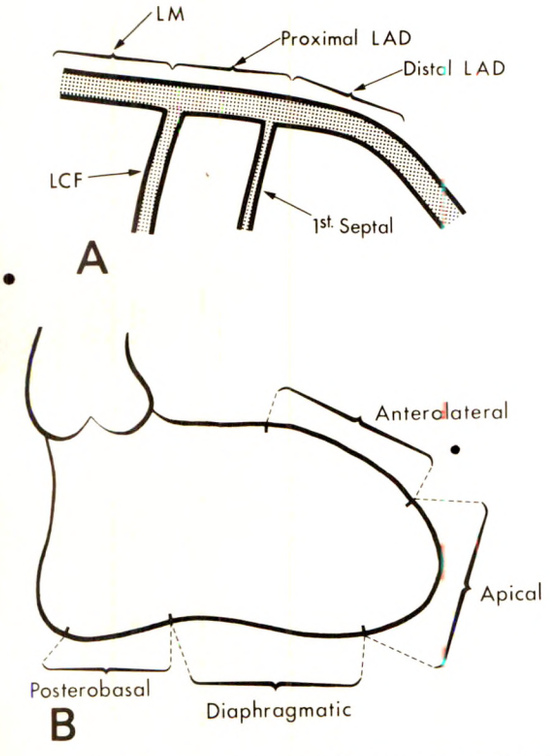

Fig. 1.—Schematic drawing of left coronary artery segments (*A*) and left ventricular wall segments (*B*) used in angiographic analysis. LM = left main coronary artery, LAD = left anterior descending artery, LCF = left circumflex artery.

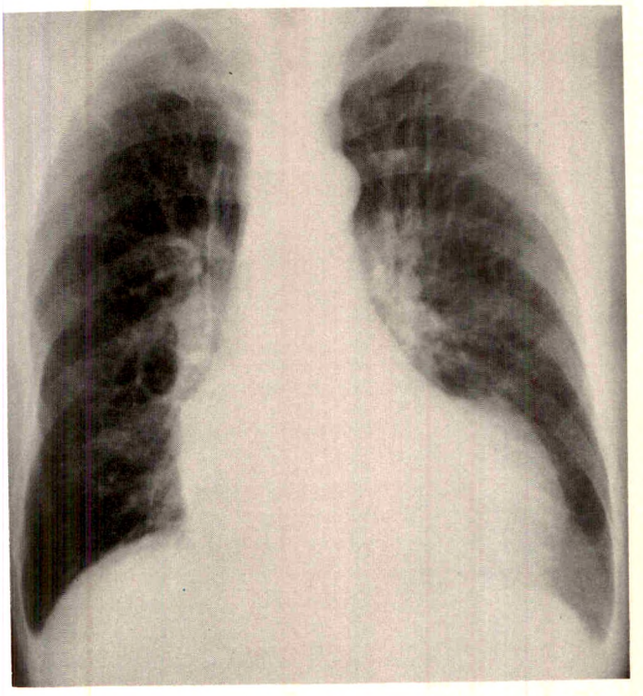

Fig. 2.—Chest film of anterolateral and apical left ventricular aneurysm in patient with septal rupture. Large upper lobe vessels and nearly invisible lower lobe vessels indicate pulmonary venous hypertension.

fore the first septal branch, while 13 patients had stenoses after the first septal branch. Of 25 patients in whom the right coronary artery was dominant, 19 patients had a severe right coronary stenosis, and 15 of those were complete occlusions.

All seven patients who had stenosis of the right coronary artery, but not the left anterior descending, had posterior septal rupture. Similarly, the four patients with severe stenoses in the left anterior descending but not the right coronary artery all had anterior septal rupture near the apex.

A severe stenosis in the left circumflex artery was associated with an anterior defect in three patients and a posterior defect in four; the location of septal rupture in these patients appears to be determined by right coronary and left anterior descending disease with little influence by the nondominant circumflex artery. Of patients who had severe disease in both the dominant right coronary and in the left anterior descending artery, four had anterior ventricular septal defects and four had posterior defects.

Ventriculographic Abnormalities

Left ventriculograms performed in 25 patients were analyzed for segmental wall motion abnormalities, aneurysms, and mitral regurgitation. Right anterior oblique ventriculograms were performed initially to evaluate left ventricular motion and the possibility of mitral regurgitation. Although left anterior oblique ventriculograms are optimal for showing a ventricular septal defect, they were not performed in all cases because the certain diagnosis of ventricular septal rupture had already been established by determination of oxygen saturations, and many of these patients were too unstable hemodynamically to warrant a second left ventriculogram. Table 4

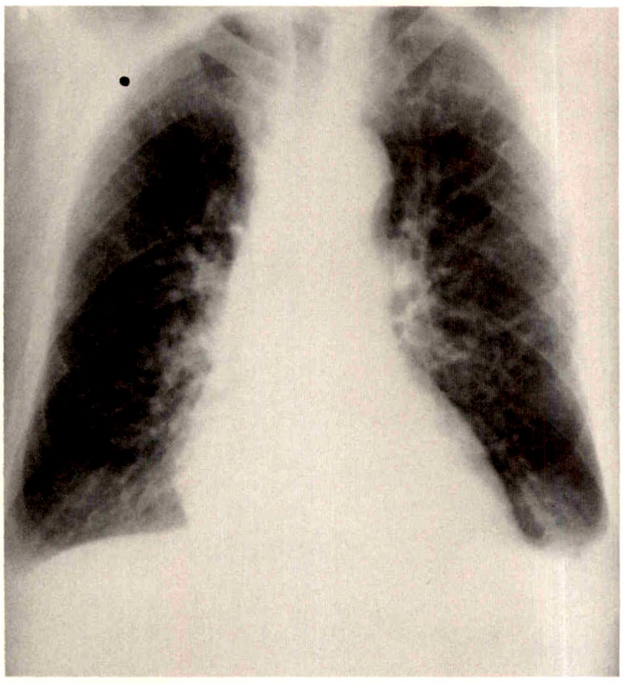

Fig. 3.—Typical chest film of ventricular septal defect complicating myocardial infarction. Left ventricle is slightly enlarged, and interstitial pulmonary edema and bilateral pleural effusions are present.

shows right anterior oblique projection abnormalities. Only two patients did not have at least one segment with akinesis or dyskinesis. In patients in whom a left anterior oblique injection was made, the posterolateral left ventricular wall always had normal motion. In some patients it was hyperkinetic, suggesting that the posterolateral wall was responsible for the maintenance of cardiac output. The septum was always akinetic or dyskinetic.

Seventeen patients (68%) had left ventricular aneurysms by left ventriculography. Since aneurysm of the septum may not be visible except on the left anterior oblique view, this figure could be low. In one of 11 patients in this series who did have left oblique injections, a septal aneurysm was clearly seen, bulging toward the right ventricle. In 19 patients in whom the mitral valve could adequately be assessed, mitral regurgitation occurred in 14.

In most patients, the opacification of the right ventricle was faint so that its wall motion could not be analyzed. In general, when the left ventricular diaphragmatic or posterobasal wall was akinetic, the right ventricular diaphragmatic wall behaved similarly. In patient 25, who had relatively good left ventricular wall motion compared to others in this series, the right ventricular diaphragmatic and anterior wall were akinetic from a right ventricular infarct identified at surgery. In a similar fashion, septal rupture anteriorly at the apex was associated with right ventricular anterior and septal akinesis.

The ventricular septal defects were in the muscular septum either anteriorly near the apex or posteriorly adjacent to the mitral annulus. Contrast material passed through the septal defect opacifying the entire inferior aspect of the right ventricle (fig. 4), but the margins of the rupture were not regularly identified. The location of the rupture could be determined indirectly because it was always in a region of severe segmental wall motion abnormality. Anterior rupture corresponded uniformly with anterolateral and apical akinesis, while posterior rupture occurred with posterobasal and diaphragmatic akinesis.

Discussion

The appearance of interstitial or alveolar pulmonary edema on the chest film in these patients with elevated left atrial pressures is consistent with numerous previous reports [12–16] correlating the appearance of interstitial edema with a left atrial pressure of more than 20 mm Hg. Lesser elevations of left atrial pressure can usually be detected radiologically by observing an increase in size of upper lobe vessels along with disappearance or diminished size of lower lobe vessels. Since most of the patients in this series had elevated left atrial pressures above 20 mm Hg, this correlation of chest film with left atrial pressure was quite reliable. Interstitial edema was not present in four patients with left atrial pressures over 20 mm Hg. However, three of these patients did have an abnormal vascular pattern indicating pulmonary venous hypertension.

Congenital left-to-right shunts greater than 2:1 can usually be recognized radiologically by an increase in size in the main and central branches of the pulmonary arteries in both upper and lower lobes. This type of pulmonary artery enlargement is an inconstant finding in acquired shunts, particularly in the elderly patient. In the present series, only 39% had large central pulmonary arteries, and most of them also had elevated left atrial pressures, so that both a pressure and a volume overload were present in the pulmonary system.

Multiple stenoses in the coronary circulation have been found pathologically in septal and other types of cardiac rupture [17–19]. Combined narrowings of either the anterior descending and the right coronary artery, or right coronary artery and left circumflex artery, or all three arteries, were necessary in those series to produce septal rupture. The present series of patients studied hours to a few months after septal rupture is at variance with those observations. Seven of our patients had only a right coronary occlusion with no stenoses in the left coronary artery, and six patients had occlusions in the left anterior descending artery with a normal right coronary artery. This finding is less surprising when the paucity of collateral vessels in the entire series is taken into account. The coronary artery distal to an occlusion generally was not visualized, indicating that it was completely occluded or that bridging collateral vessels either had not formed or were not currently functioning. The absence of collaterals and the lack of visualization of the coronary artery distal to a proximal occlusion in a patient with septal rupture presumably is associated with a sizable area of muscle infarction that probably is present before the septum ruptures.

Abrams and Adams [20] found that the coronary artery

TABLE 3

Distribution and Percentage Severity of Coronary Stenoses

Patient No.	Left Anterior Descending Artery		Left Circumflex Artery	Dominant Right Coronary Artery	Surgical Location of Ventricular Septal Defect*
	Before First Septal Branch	After First Septal Branch			
1	0	100	0	0	A
2	90	0	90	100	P
3	0	70	0	100	P
4	100	. . .	0	100	A
5	100	. . .	0	0	A
6	80	100	100	100	P
7	0	0	0	100	P
8	0	100	0	90	A
9	0	100	100	50	A
10	80	90	90	100	P
11	0	0	0	100	P
12	0	100	0	90	A
13	0	0	90†	70	P
14	70	0	0	90	P
15	0	0	0	100	P
16	0	100	50	0	A
17	0	0	0	100	P
18	0	100	0	100	A
19	100	. . .	50	0	A
20	0	100	0	0	A
21	0	0	100	100	P
22	0	60	70	100	P
23	0	100	100	100	A
24	0	0	0	100	P
25	0	0	0	100	P
26	0	100	0	0	A

Note.—Stenoses less than 50% are coded as 0. All patients except case 6 (70%) had left main artery stenosis less than 50%.
* A = anterior, P = posterior.
† Dominant left circumflex artery.

TABLE 4

Comparison of Left Ventricular Motion Abnormalities with Wall Segment Location in Right Anterior Oblique Left Ventriculogram

	No. Wall Segments			
	Anterolateral	Apical	Diaphragmatic	Posterobasal
Anterior septal rupture (N = 13):				
Moderate or severe hypokinesis	. . .	2	1	. . .
Akinesis	5	3	. . .	. . .
Dyskinesis	6	8	3	. . .
Aneurysm	9	7	3	. . .
Posterior septal rupture (N = 12):				
Moderate or severe hypokinesis	2	1	5	1
Akinesis	. . .	3	3	6
Dyskinesis	. . .	. . .	1	3
Aneurysm	. . .	. . .	1	4

Note.—Septum in left oblique projection was invariably akinetic or dyskinetic.

segment distal to a proximal occlusion almost always was visualized by some collateralization, while Gensini and Buonanno [21] observed that 75% of occluded coronary arteries have some distal opacification through collaterals. In contrast to these two series, most of our patients were studied acutely, possibly before collaterals developed. It is possible that edema in the ischemic zone around the infarct did not allow existing collateral vessels to be perfused with contrast material, and that these small vessels would be visible if and when the edema regressed.

That 68% of our patients had concomitant left ventricular aneurysms coincides with earlier observations [8, 22, 23] and underscores the extensive wall motion abnormalities in this disease. In spite of the fact that a sizable portion of the left ventricle is at least hypokinetic, the location of the septal rupture could always be located on the left ventriculogram, even though the actual defect was not always visible. Anterior rupture invariably produced apical akinesis or dyskinesis which usually extended to involve the anterior wall. With the exception of patients 3 and 25, posterior defects always produced

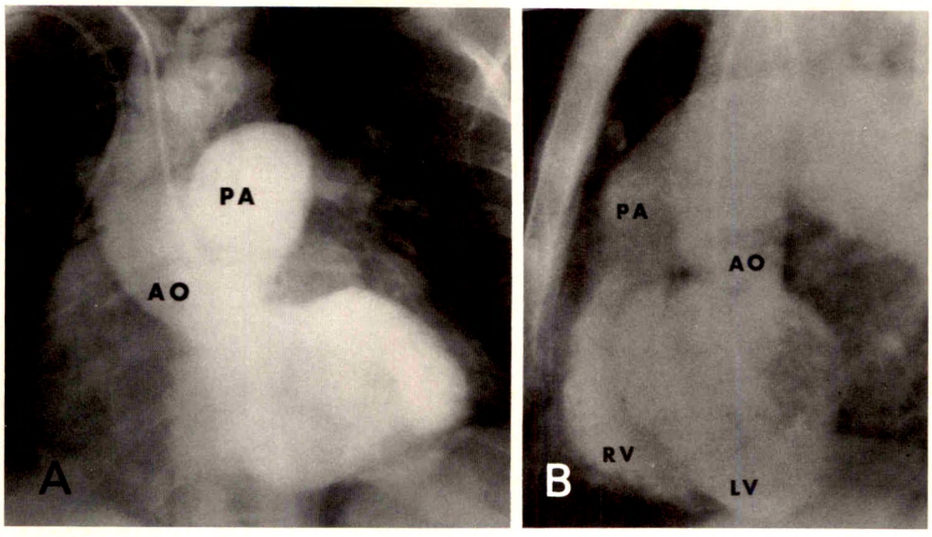

Fig. 4.—Simultaneous posteroanterior (*A*) and lateral (*B*) views of left ventriculogram demonstrating rupture of septum. Right ventricle is opacified, but margins of ventricular septal defect are not seen. RV = right ventricle, LV = left ventricle, PA = pulmonary artery, AO = aorta.

akinesis or dyskinesis in the posterobasal and diaphragmatic walls. In these two patients, the right coronary artery was completely occluded, producing posterior rupture.

In those ventriculographic studies in which the diaphragmatic wall of the right ventricle was opacified sufficiently for wall motion analysis, the right ventricle frequently had large regions of akinesis. In most of these patients, the myocardium was usually pale or blue at surgery, indicating right ventricular infarction. In all cases of posterior rupture, the right ventricular diaphragmatic wall was akinetic, and occasionally the inferior half of the anterior right ventricular wall. Thus the presence of right ventricular infarction is frequently recognized during left ventriculography when a septal defect has occurred.

In the setting of acute myocardial infarction and pulmonary edema, the chest film cannot distinguish between the major complications of cardiogenic shock (left ventricular power failure), rupture of a papillary muscle, and rupture of the ventricular septum. Clinically, it may be impossible to separate the systolic murmur of mitral regurgitation caused by papillary muscle dysfunction from that originating from a ventricular septal defect. The precise diagnosis requires a heart catheterization to obtain the information necessary for planning the surgical approach or medical care. Critical data include: (1) the presence or absence of a left-to-right shunt, (2) the degree of mitral regurgitation, (3) the performance of the left ventricle as manifested by adequate wall motion and by peak systolic and mean diastolic pressure, and (4) coronary anatomy.

A portion of this information could be obtained by noninvasive methods such as nuclear angiography [24] or ultrasound [25]. Tracer techniques are useful for documenting a left-to-right shunt, and ventricular wall motion disorders can be detected with electrocardiographically gated blood pool studies. In the future, B-scan real-time ultrasound potentially may be useful for identifying a septal rupture and ventricular wall motion abnormalities. However, the majority of patients with septal rupture have a changing clinical status and unstable hemodynamics and require a rapid and specific diagnosis, which presently is best provided by cardiac catheterization with angiography. In the future, angiography with cephalocaudad angulation may improve our ability to define and localize the septal rupture.

ACKNOWLEDGMENTS

We thank Linda Gralenski, Betty Boujoukos, and Corinne Bordonaro for expert assistance in preparing the manuscript.

REFERENCES

1. London RE, London SB: Rupture of the heart. A critical analysis of 47 consecutive autopsy cases. *Circulation* 31:202–208, 1965
2. Ross RM, Young JA: Clinical and necropsy findings in rupture of the myocardium. A review of 43 cases. *Scot Med J* 8:222–226, 1963
3. Sanders RJ, Kern WH, Blount SG: Perforation of the interventricular septum complicating myocardial infarction. *Am Heart J* 51:736–748, 1956
4. Swithinbank JM: Perforation of the interventricular septum in myocardial infarction. *Br Heart J* 21:562–566, 1959
5. Daggett WM, Burwell LR, Lawson DW, Austen WG: Resection of acute ventricular aneurysm and ruptured interventricular septum after myocardial infarction. *N Engl J Med* 283:1507–1508, 1970
6. Daggett WM, Guyton MD, Mundth ED, Buckley MJ, McEnany MT, Gold HK, Leinbach RC, Austen WG: Surgery for post-myocardial infarct ventricular septal defect. *Ann Surg* 186:260–270, 1977
7. Buckley MJ, Mundth ED, Daggett WM, Gold HK, Leinbach RC, Austen WG: Surgical management of ventricular septal defects and mitral regurgitation complicating acute myocardial infarction. *Ann Thorac Surg* 16:598–609, 1973
8. Selzer A, Gerbode F, Kerth WJ: Clinical hemodynamic and surgical considerations of rupture of the ventricular septum after myocardial infarction. *Am Heart J* 78:598–607, 1969
9. Kitamura S, Mendez H, Kay JH: Ventricular septal defect following myocardial infarction. *J Thorac Cardiovasc Surg* 61:186–199, 1971

10. Gold HK, Leinbach RC, Sanders CA, Buckley MJ, Mundth ED, Austen WG: Intra-aortic balloon pumping for ventricular septal defect or mitral regurgitation complicating acute myocardial infarction. *Circulation* 47:1191–1196, 1973
11. Dinsmore RE: Roentgenographic examination of the heart, in *Clinical Cardiology*, edited by Willerson JT, Sanders CA, New York, Grune & Stratton, 1977, pp 175–191
12. Simon M: The pulmonary veins in mitral stenosis. *J Fac Radiol* 9:25–32, 1958
13. Harley HRS: The radiological changes in pulmonary venous hypertension, with special references to the root shadows and lobular pattern. *Br Heart J* 23:75–87, 1961
14. Simon M: The pulmonary vessels in incipient left ventricular decompensation: radiologic observations. *Circulation* 24:185–190, 1961
15. Lavender JP, Doppman J, Shawdon H, Steiner RE: Pulmonary veins in left ventricular failure and mitral stenosis. *Br J Radiol* 35:293–302, 1962
16. Lieber A, Rosenbaum HD, Hanson DJ, Kwaan HM: Accuracy of predicting pulmonary blood flow, pulmonary arteriolar resistance and pulmonary venous pressure from chest roentgenograms. *Am J Roentgenol* 103:577–582, 1968
17. James TN: Ruptured interventricular septum and heart block. *Circulation* 55:934–946, 1977
18. Sager RV: Coronary thrombosis. *Arch Intern Med* 53:140, 1934
19. Wessler S, Zoll PM, Schlesinger MJ: The pathogenesis of spontaneous cardiac rupture. *Circulation* 6:334–351, 1952
20. Abrams HL, Adams DF: The coronary arteriogram. Structural and functional aspects. *N Engl J Med* 281:1276–1285, 1336–1342, 1969
21. Gensini GG, Buonanno C: Coronary arteriography. A study of 100 cases with angiographically proven coronary artery disease. *Dis Chest* 54:90–99, 1968
22. Malone RGS, Parkes WE: Rupture of the interventricular septum. *Br Heart J* 17:448–452, 1955
23. Davison T, Degenshein GA, Yuceoglu YZ, Reyes AL Jr, Levovitz B, Dresdale DT, Kantrowitz A: Repair of ventricular septal defect following myocardial infarction. *Ann Surg* 160:33–41, 1964
24. Strauss HW, Pitt B: Evaluation of cardiac function and structure with radioactive tracer techniques. *Circulation* 57:645–653, 1978
25. Corya BC, Rasmussen S, Knoebel SB, Feigenbaum H, Black MJ: Echocardiography in acute myocardial infarction. *Am J Cardiol* 36:1–10, 1975

Bilateral Pleural Thickening: A Manifestation of Asbestos Dust Exposure

E. NICHOLAS SARGENT,[1] JAY GORDONSON, GEORGE JACOBSON, WILLIAM BIRNBAUM, AND MICHAEL SHAUB

Bilateral pleural thickening in a relatively asymptomatic patient without evidence of pulmonary disease is frequently a manifestation of asbestos dust exposure, particularly when it is localized or in the form of a noncalcified pleural plaque. Bilateral pleural thickening will be discovered with increasing frequency if specifically searched for on every radiograph. This radiographic finding is suggested as a more realistic indication of asbestos dust exposure, particularly when correlated with a complete occupational history.

While pleural plaques are generally acknowledged as the most common radiographic manifestation of asbestos exposure, the radiographic finding of pleural thickening has not been specifically correlated with asbestos dust exposure. Since pleural thickening due to asbestos dust inhalation is rarely unilateral, we hypothesized that bilateral pleural thickening of unknown cause might commonly be due to such exposure. A preliminary study to test this theory was undertaken; this report describes the results of this study, the distinctive radiographic characteristics, and the differential diagnosis.

Materials and Methods

While studying the radiographic detection of pleural thickening, we found 36 cases of clinically unsuspected asbestos dust exposure. These were discovered in a single year at our institution, while in the preceding 4 years only 10 cases were diagnosed. All cases were later substantiated by a positive occupational history. No effort was made in this study to determine the prevalence of asbestosis seen at the medical center, which serves a predominately working class population

Although oblique views facilitate the detection and measurement of costal pleural thickening, these additional views were not utilized in this study, since they were not obtained routinely and were not available in all cases. For purpose of analysis, all measurements of pleural thickening were made on the posteroanterior radiograph, adjacent to the medial aspect of the ribs. The maximum pleural thickness was divided into three grades, in keeping with the latest International Labor Organization 1971 classification [1]: grade A, up to 5 mm in width; grade B, 5–10 mm in width; and grade C, over 10 mm in width.

Results

The radiographic findings in 36 patients who were subsequently proven to have been occupationally exposed to asbestos dust are summarized in table 1. The source of the exposure was rather evenly divided between shipyard workers and miscellaneous occupations related to the building trades. The interrelationships of pleural thickening, pleural calcification, and interstitial pulmonary disease are analyzed in this table.

Pleural thickening most frequently involved the fifth through eighth ribs and interspaces (fig. 1). It was detected in the second rib interspace only three times and never at the levels of the first, eleventh, or twelfth ribs or interspaces. There was no associated involvement of the apices of the lung or the costophrenic angles. Total extent of pleural thickening varied from minimal involvement at one rib or interspace to a maximum length of eight ribs or interspaces. When individual pleural plaques occurred, they were usually no greater than four interspaces. When pleural thickening was more extensive, it often reflected a series of multifocal nonconfluent or confluent plaques. There was no uniform progression in the number of interspaces involved.

Grade A pleural thickening occurred most commonly (67%) and involved both hemithoraces with equal frequency. Grade B pleural thickening occurred in 24% of cases and was almost three times as frequent on the right as on the left side.

Maximum pleural thickness was located, with only six exceptions, at the level of the fifth, sixth, seventh, and eighth ribs and interspaces (fig. 2) and was most frequently at the seventh interspace. The extent and severity of the pleural thickening did not correlate with the total duration of or time elapsed since asbestos exposure.

Discussion

Epidemiologic studies have confirmed the association between asbestos dust exposure and bronchial carcinoma, occurring some 24–52 years after exposure. The risk is intensified if there is also a history of heavy smoking. A recent pilot study showed that bronchial carcinoma was 2.5 times more frequent in men with pleural plaques [2]. There is also an increased incidence of primary malignant mesotheliomas of the pleura, pericardium and peritoneum, as well as carcinomas of the gastrointestinal tract.

Although asbestos dust inhalation is not the sole cause of pleural plaques, it is certainly the most common, and the association between pleural plaques and asbestos dust exposure has been amply confirmed [3]. The prevalence of pleural changes on the radiograph has been shown to increase in relation to the estimated dose of asbestos, patient age, and the length of time after the initial exposure [4–6] (I. J. Selikoff, personal communication). This is further confirmed by a fairly strong correlation between pleural plaques found in postmortem studies [7] and previous exposure to all commercial types of asbestos [4, 9].

To date, no satisfactory explanation has been developed to explain how pleural reactions, which almost

Received May 31, 1977; accepted after revision May 31, 1978.

[1] All authors: Department of Radiology, Los Angeles County–University of Southern California Medical Center, 1200 North State Street, Los Angeles, California 90033. Address reprint requests to E. N. Sargent.

© 1978 American Roentgen Ray Society

0361–803X/78/1000–0579 $00.00

TABLE 1

Radiologic Findings in Asbestosis

Finding	No. Cases
Bilateral pleural thickening:	
Alone	13
With pleural calcification	11
With interstitial disease	4
With pleural calcification and interstitial disease	4
Pleural calcification, alone	1
Interstitial disease, alone	3
Total	36

Note.—No patient had unilateral pleural thickening.

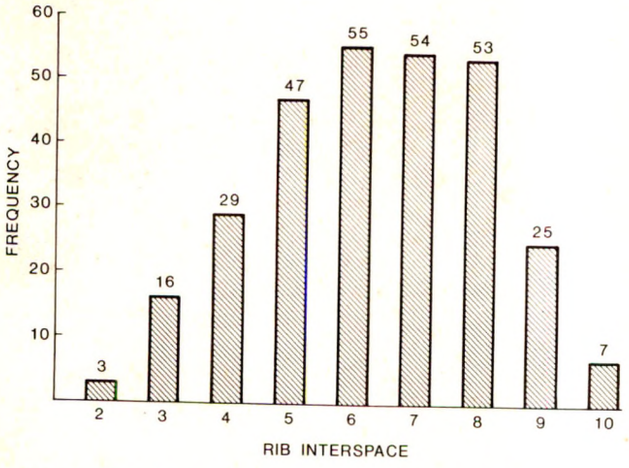

Fig. 1.—Rib interspace involvement in 32 cases of pleural asbestosis with bilateral pleural thickening.

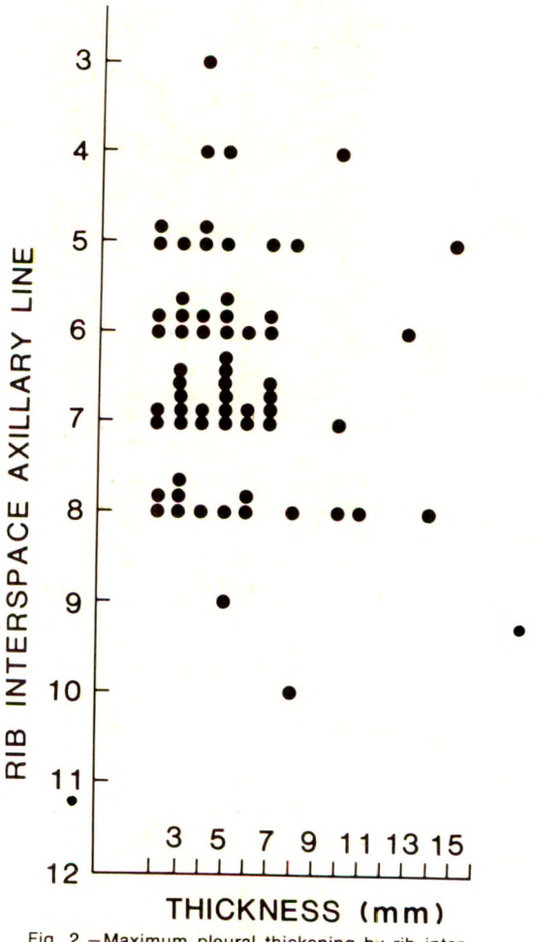

Fig. 2.—Maximum pleural thickening by rib interspace in 32 cases of pleural asbestosis with bilateral pleural thickening.

exclusively involve the parietal pleura, develop in response to inhalation of asbestos fibers. Furthermore these fibers, which are also deposited in the same lung, often cause no reaction to the dust. Asbestos bodies have rarely been found in plaques [7] and, although asbestos fibers may be present in small amounts, the paucity of fibers is out of proportion to the marked fibrotic response [10]. Although asbestos fibers are commonly observed in the lung tissue of patients with plaques [7, 11], the lack of findings of asbestos fibers in plaques by previous investigators has largely been due to inadequate techniques. Recently developed techniques [12] (I. J. Selikoff, personal communication) using transmission electron microscopy, selective electron diffraction, and microchemical analysis of particles now provide morphologic, structural, and chemical data in which many small submicroscopic asbestos fibers have been unequivocally identified in the pleural plaques. These are more concentrated in the calcified zones than in the fibrous zones [13].

Pathologically, asbestos dust causes a submesothelial pleural reaction which results in a characteristic localized hyaline plaque; less commonly a diffuse and extensive pleural thickening occurs. On the routine posteroanterior radiograph, hyalinized pleural plaques are not visualized until they have developed substantial thickness. The plaques are often overlooked, their prevalence is underestimated during life, and only a comparatively small number of plaques identified by postmortem examination are detected on conventional radiographs [11].

Pleural plaques on radiographs appear as limited plateaulike smooth or nodular areas seen either in profile or en face. Seen in profile, there is a localized area of widening of the pleural shadow roughly paralleling the inner surface of the lateral thoracic wall. This results from the x-ray beam striking the surface of the thickened pleura tangentially, causing a sharply marginated band of water density. The very early plaque is seen only as a thin white line of increased density adjacent to the rib, which has been likened to a flange [4], and is easily overlooked (fig. 3). It is often discovered in retrospect, particularly when it resembles the normal bony inner rib surface, or even a vessel running parallel to the rib. As it develops, the plaque becomes somewhat oval or moderately protuberant, with tapering superior and inferior margins typical of an extrapleural lesion (fig. 4). A typical plaque rarely extends more than four interspaces [4], and an important characteristic is that involvement of

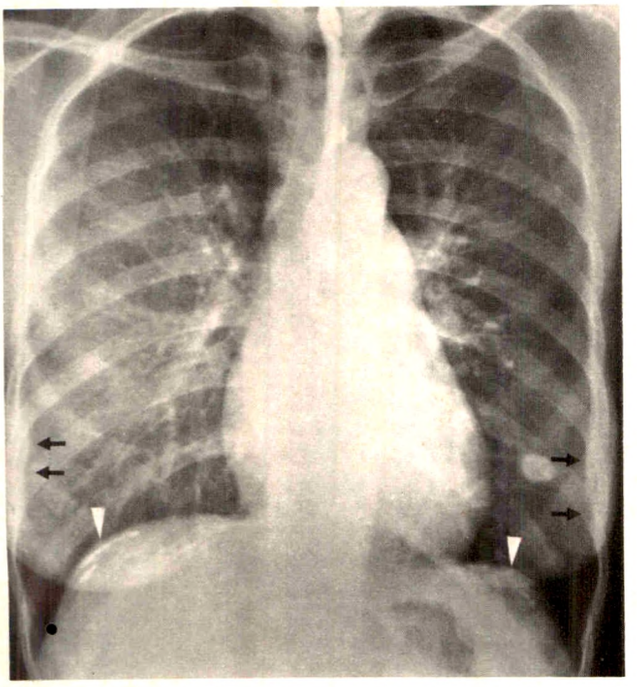

Fig. 3.—Early costal pleural plaque formation (*arrows*). Bilateral calcified diaphragmatic pleural plaques (*arrowheads*) are rarely found without associated costal pleural plaques. Note calcified granuloma in left lower lobe.

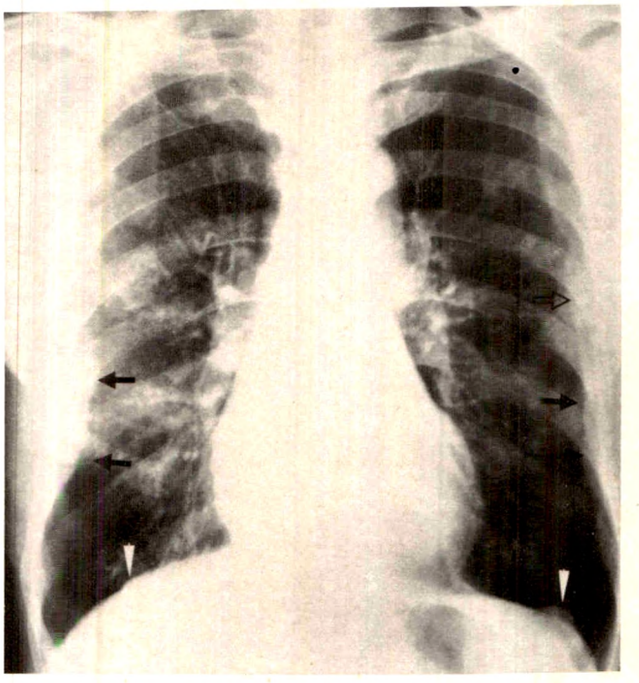

Fig. 4.—Bilateral, well developed pleural plaques crossing intercostal spaces. Note sharp margin adjacent to ribs where plaques are seen in profile (*arrows*). Margins taper superiorly and inferiorly. Outline of plaque in profile on left is not obscured, even by overlying scapula (*open arrow*). Localized, well developed diaphragmatic pleural plaque (*white arrows*) alters contour of left and to lesser extent right diaphragm.

the apices or costophrenic angles is rare. Although single plaques are common, multiple nonconfluent or confluent plaques may also occur, particularly along the posterior aspects of the thoracic cage. Diffuse nonspecific pleural thickening, characterized by obliteration of the costophrenic angle and a more uniform homogeneous density, is a much less frequent occurrence. Evidence of interstitial disease is commonly lacking in patients with pleural plaques.

Plaques in profile are found less commonly on the diaphragm and are rare on the pericardium. They appear as a localized additional convexity to the normal convex surface of these structures. In the region of the diaphragm, they are found at some distance from the angles (i.e., close to the central tendon); when uncalcified, they must be differentiated from normal (scalloping) or abnormal variations in diaphragmatic contour (figs. 4 and 5).

Seen en face, a pleural plaque is a poorly defined, veillike opacity [15] resulting from the x-ray beam striking the pleural surface perpendicularly. These noncalcified opacities are more obvious towards the lateral aspects of the lungs, where they are most oblique to the x-ray beam and hence absorb more radiation. The poorly marginated shadows show a peripheral irregularity of contour which is similar to a map or holly leaf, and they are rarely uniformly rounded. Because of their faint outline, they are often dismissed as artifacts on a single radiograph, but their consistency and increased size or density on repeat examinations will prevent this error (fig. 6). When noncalcified, they are generally of lower radiopacity than an intrapulmonary nodule of the same transverse diameter.

Oblique views (fig. 7) are of great value not only to confirm suspected plaques, but also to detect additional plaques or pleural thickening not seen in the posteroanterior projection. Often the en face appearance will change to a profile presentation when the x-ray beam strikes the surface of the plaque tangentially. Fluoroscopy and spot filming to determine the proper obliquity for demonstrating a plaque is also of value. Oblique views confirm that plaques spare the apices and the costophrenic angles. They are most frequently found along the posterior reflections of the costal pleura but may extend anteriorly as far as the costal cartilages.

Calcifications in the thickened parietal pleura usually occur 20 or more years after exposure to asbestos; the greater the time interval, the greater the incidence [16]. Pleural calcification without radiographically demonstrable evidence of interstitial disease or fibrosis has been reported in only one-third of patients exposed to asbestos dust, but more than 50% of patients with extensive pulmonary fibrosis who survive long enough eventually develop pleural calcifications [10]. Calcified plaques are more obvious and more striking than uncalcified plaques, but in many cases the calcifications are small and easily overlooked (especially in films of poor quality) unless they are sought after systematically (fig. 5). Although calcification is relatively uncommon on conven-

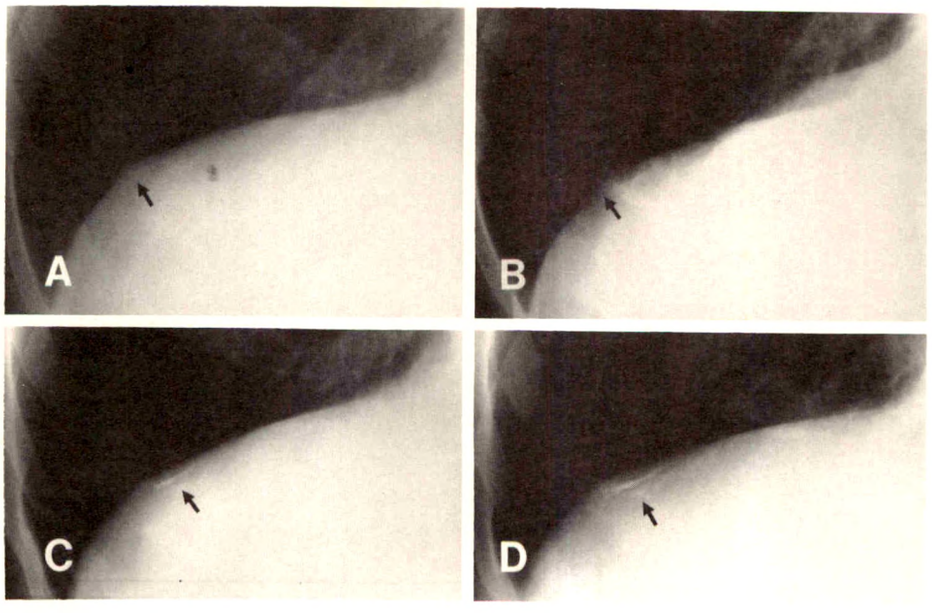

Fig. 5.—Radiographs showing development of calcifications in pleural plaque. Note easily overlooked irregularity of right diaphragm (*A*), with progressive calcification of diaphragmatic pleura 2 (*B*), 6 (*C*), and 8 (*D*) years later (*arrows*).

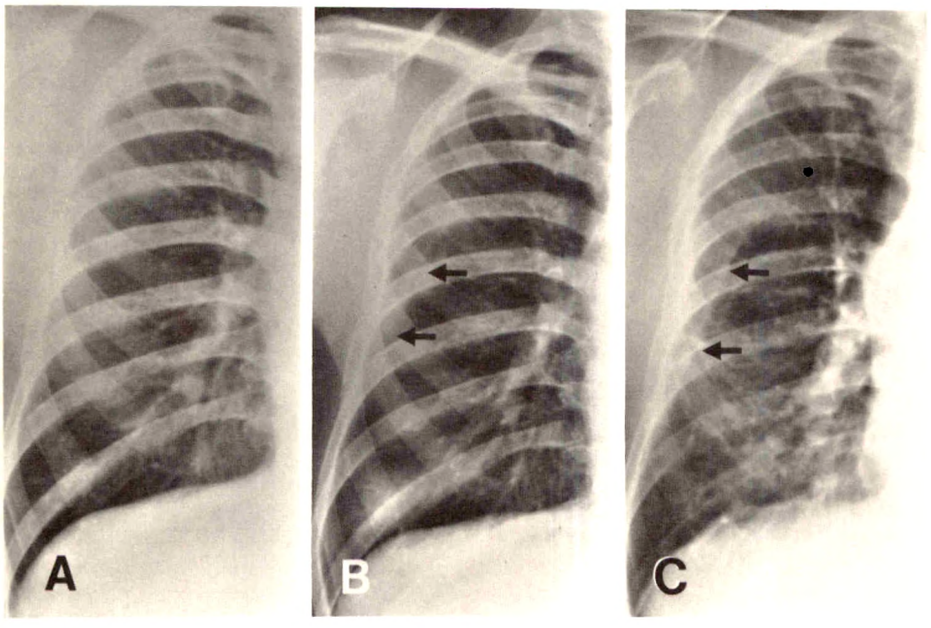

Fig. 6.—Radiographs showing development of pleural plaque on right. *A*, No evidence of pleural thickening. *B*, 8 years later, faint shadow of early en face pleural plaque (*arrows*). *C*, Well developed en face pleural plaque 18 years after *A* (*arrows*). Note progressive interstitial disease at base. (Patient was not included in this series.)

tional films, it is detected histologically in approximately 87% [7].

Differential Diagnosis

The normal pleural shadow is a combination of muscles (subcostal and internal intercostal) [17], the areolar tissue of the endothoracic fascia, fat deposits [18], and the actual pleura. The thickness of the tissue comprising the normal pleural shadow is best measured when the x-ray beam is tangential to the surface; oblique views are particularly helpful. Oblique projections of normal subjects have shown that the normal shadow can vary in thickness from 0–10 mm in males; it is usually somewhat less in females. It is generally widest in the area of the first two or three interspaces (fig. 8). However, in the posteroanterior projection, the thickness of the normal shadow is considerably less (i.e., up to about 5 mm) along the first two or three interspaces. In either projection, the normal shadow is virtually invisible below the fourth interspace, although occasionally a very thin, barely perceptible line may be seen paralleling the inner margin of the ribs, more or less continuing as far as the costodiaphragmatic angle. In our study, 1 mm was arbitrarily designated as the maximum acceptable thickness of the normal pleural shadow below the level of the fourth intercostal interspace.

Pleural thickening should not be confused with extrapleural depositions of fat. In the oblique position, fat

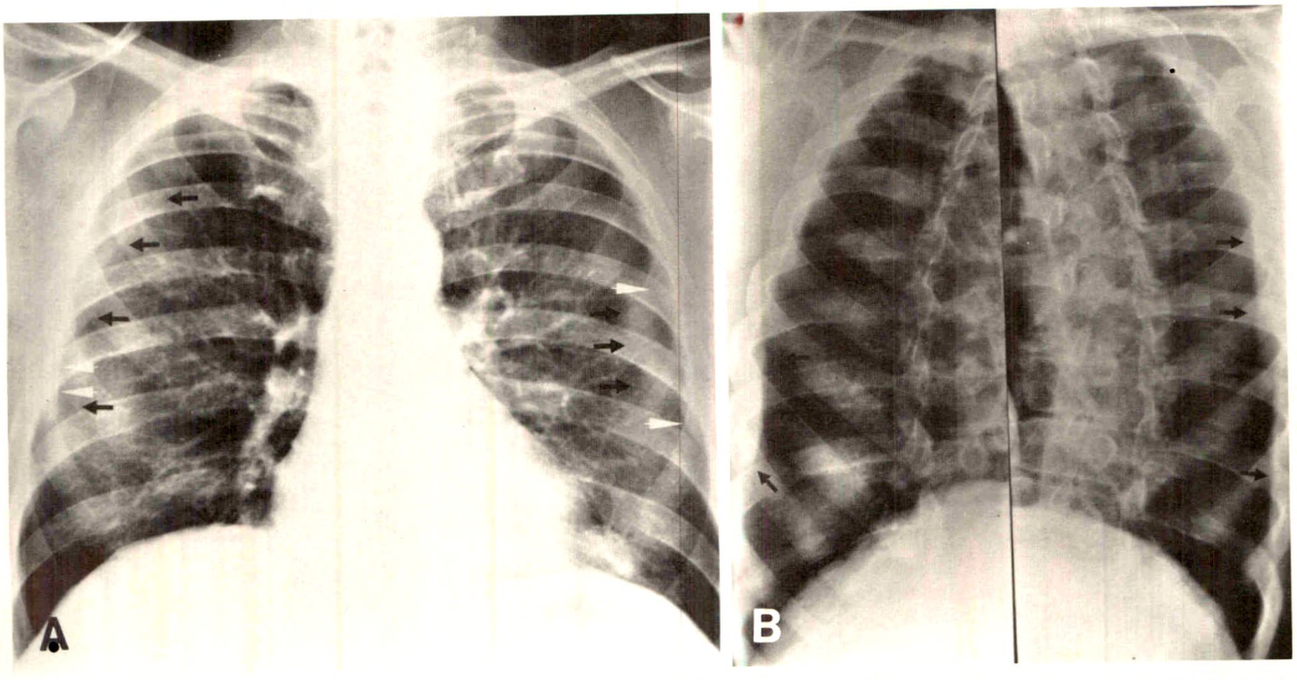

Fig. 7.—*A*, Bilateral noncalcified en face pleural plaques. Faint veillike opacities along lateral halves of lung fields spare apices and costophrenic angles (*arrows*). Additional plaques are in profile (*white arrows*). *B*, Composite of oblique views projects and confirms suspected plaques in profile (*arrows*).

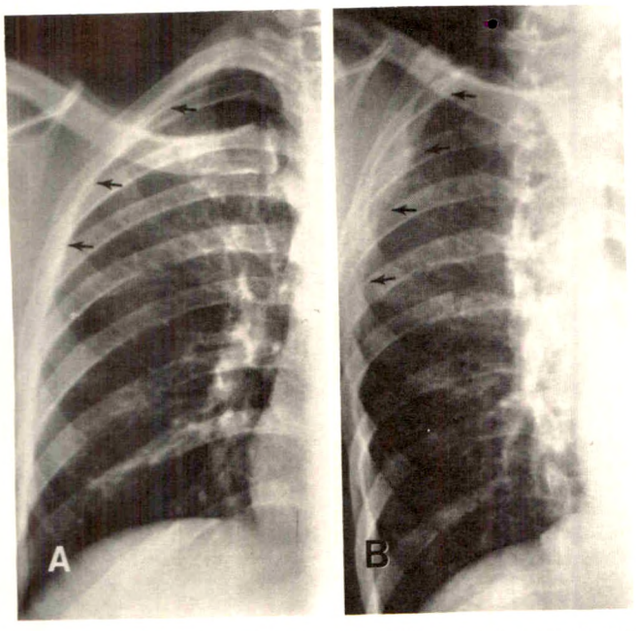

Fig. 8.—Normal pleural shadow (*arrows*) in posteroanterior (*A*) and oblique views (*B*). Shadow is widest superiorly and tapers rapidly inferiorly. In oblique projections normal shadow is wider.

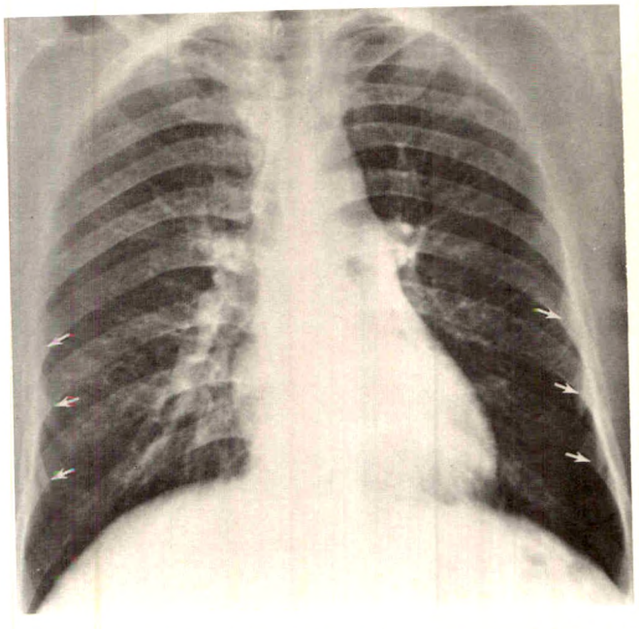

Fig. 9.—Normal shadows of slips of origin of serratus anterior and external oblique abdominal muscles (*arrows*) not to be confused with pleural thickening. Note multiple bilateral shadows which do not project beyond rib margins.

produces a wavy margin which is most prominent on the surface of the ribs near the posterior portions of the lateral chest wall [18]. Fat is not commonly seen on the rib surface of the immediate paravertebral regions or on the surface of the anterior portions of the ribs. Computed tomography is also helpful in this differentiation.

The shadows of the costal slips of origin of the serratus anterior and external abdominal muscles should not be confused with multifocal pleural plaques. They have a characteristic pattern: a rhythmic sequence of uniformly sized bilateral shadows along successive ribs (fig 9).

They are found along the fifth to ninth ribs and consist of one or two distinct triangular shadows or a combination of the two superimposed, which disappear on slightly oblique views.

Occasionally a basilar pleural effusion may occur following asbestos dust exposure. It resolves slowly, leaving signs of diffuse pleural thickening. This, as well as thickening due to infection or hemorrhage, usually is characterized by a smooth, uniform shadow which particularly involves the costophrenic angle.

Discrete, localized, noncalcified pleural thickening in the region of the parietal pleura can occur with localized mesotheliomas, metastatic disease, lymphomas, or myeloma. These are usually unilateral but may mimic pleural plaques. Localized pleural thickening due to asbestos rarely simulates multiple neoplastic pulmonary nodules but differentiation is made by oblique views which confirm the pleural location of the plaques [19].

Localized pleural thickening with calcification due to rib injuries, irradiation, scleroderma [20], and chronic mineral oil aspiration [21] are unusual occurrences which must be differentiated from pleural changes due to asbestos dust inhalation. Rarely, barium in the peritoneal cavity can simulate diaphragmatic pleural calcifications. Calcification of the pleura which occurs secondary to hemorrhage or infection is usually unilateral and lies closely applied to the visceral pleura. The use of fluoroscopy or cineradiography during respiration demonstrates that the calcification is not in the parietal pleura, because calcification in parietal pleural plaques moves synchronously with the chest wall [16]. Induction of a pneumothorax confirms the extrapleural location of a plaque and demonstrates the lack of adhesions between the visceral and parietal pleura. When adhesions are present, they do not occur in areas of plaque formation. Computed tomography will demonstrate plaques and show calcifications not suspected with conventional radiographic techniques [22]. Ultrasonic examination has also been offered as a more sensitive modality for detection of plaques [23].

Conclusions

The radiographic diagnosis of pulmonary asbestosis is usually suggested when there are obvious interstitial changes, large pleural plaques with calcifications, and an appropriate history of asbestos dust exposure. However, on routine posteroanterior radiographs, the unexpected observation of bilateral noncalcified localized pleural thickening or plaques, with no other evidence of disease in a relatively asymptomatic patient, is a signal that the patient may have been exposed to asbestos dust. If bilateral pleural thickening is specifically searched for on every chest radiograph, it will be discovered with increasing frequency, and when retrospectively correlated with a lifetime occupational history, a more realistic indicator of the prevalence of asbestos dust exposure in the general population might be possible. Further, the frequency of bilateral pleural plaques in nonoccupationally exposed populations is unknown. Using the chest radiograph as an epidemiologic tool, the prevalence of bilateral pleural plaques in the general population remains to be established.

ACKNOWLEDGMENTS

We thank Marie Andrianos and Eileen de la Vega for secretarial assistance and Andrew Gero for photography.

REFERENCES

1. Working Group on Definition of Pneumoconiosis: *IV International Pneumoconiosis Conference, Bucharest, September 27–October 2, 1971*. Geneva, International Labor Organization, 1971
2. Edge JF: Asbestos related lung disease in a British ship building population with particular regard to the incidence of bronchial carcinoma in men with pleural plaques. A mortality study (abstr.) *Am Rev Respir Dis* 115:211, 1977
3. Becklake MR: Asbestos related disease of the lung and other organs. Their epidemiology and implication for clinical practice. *Am Rev Respir Dis* 114:187–227, 1976
4. Sheers G, Templeton AR: Effects of asbestos in dockyard workers. *Br Med J* 3:574–579, 1968
5. Harries PG, MacKenzie FAF, Sheers G, Kemp JH, Oliver TP, Wright DS: Radiological survey of men exposed to asbestos naval dockyards. *Br J Ind Med* 29:274–279, 1972
6. Rossiter LE, Bristol LJ, Cartier PH, Gilson JG, Grainger TR, Sluis-Cremer CK, McDonald JC: Radiographic changes in chrysotile asbestos mine and mill workers of Quebec. *Arch Environ Health* 24:388–400, 1972
7. Meurman L: Asbestos bodies and pleural plaques in a Finnish series of autopsy cases. *Acta Pathol Microbiol Scand* [*Suppl*] 181:1–107, 1966
8. Jones JSP, Sheers G: Pleural plaques, in *Biological Effects of Asbestos,* Proceedings of a Working Conference, edited by Bogovski P, Gilson JG, Timbrell V, Wagner JC, Lyon, France, International Agency for Research on Cancer, 1973, pp 243–248
9. Langlands JHM, Wallace WFM, Simpson MJC: Insulation workers in Belfast, morbidity of men still at work. *Br J Ind Med* 28:217–225, 1971
10. Thompson JG: The pathogenesis of pleural plaques, in *Proceedings of the International Conference of Pneumoconiosis,* Johannesburg, South Africa, 1969, edited by Shapiro HA, Capetown, Oxford University Press, 1970, pp 71–74
11. Hourihane D'OB, Lessof L, Richardson PC: Hyaline and calcified pleural plaques as an index to exposure to asbestos. A study of radiological and pathological features of 100 cases with a consideration of epidemiology. *Br Med J* 1:1069–1074, 1966
12. Ochs CW, Smith JP: Chronic pleural thickening; some observations on cause and pathogenesis. *Milit Med* 141:77–81, 1976
13. Le Bouffant L, Martin JC, Durif S, Daniel H: Structure and composition of pleural plaques, in *Biological Effects of Asbestos,* Proceedings of a Working Conference, edited by Bogovski P, Gilson JG, Timbrell V, Wagner JC, Lyon, France, International Agency for Research on Cancer, 1973, pp 249–257
14. Fletcher DE, Edge JR: The early radiological changes in pulmonary and pleural asbestosis. *Clin Radiol* 21:355–365, 1970
15. Anton HC: Multiple pleural plaques. II. *Br J Radiol* 41:341–348, 1968
16. Selikoff IJ: The occurrence of pleural calcification among

asbestos insulation workers. *Ann NY Acad Sci* 132:351–367, 1965
17. Knutsson F: Zur Kenntnis der normalen Roentgenologie der Pleura Parietalis. *Acta Radiol* 13:638–677, 1932
18. Vix VA: Extrapleural costal fat. *Radiology* 12:563–565, 1974
19. Sciammas FD, Shetty S, Navani S: Multiple pleural nodules. *Chest* 59:673–674, 1971
20. Romey MD, Moskowitz M: Scleroderma, pleural calcification and reticulum sarcoma of the lungs. *Chest* 64:371–373, 1973
21. Felson B: Thoracic calcifications, in *Chest Roentgenology*, edited by Felson B, Philadelphia, Saunders, 1973, pp 489–492
22. Kreel L: Computerized tomography using the EMI general purpose scanner. *Br J Radiol* 50:2–14, 1977
23. Viikeri M: Ultrasound examination of pleural plaques. *Acta Radiol [Suppl]* (Stockh) 301:1–62, 1970

Pulmonary Manifestations of Acute Aspiration of Gastric Contents

MICHAEL J. LANDAY,[1] EDWARD E. CHRISTENSEN,[1] AND LINCOLN J. BYNUM[2]

Radiographic manifestations of aspiration of gastric contents were reviewed in 60 patients. The findings were extremely variable, and there was no typical or characteristic appearance. Confluent and acinar infiltrates, as well as infiltrates composed of small irregular shadows, occurred singly or in a variety of combinations; the third pattern predominated in the majority of cases. Distribution was most commonly bilateral and multicentric and usually favored perihilar or basal regions, but localized or atypical densities were also observed. Patients with the most extensive radiographic abnormalities on initial studies tended to have the worst prognosis; however, mild early pulmonary infiltrates occasionally progressed to life-threatening abnormalities, and extensive initial involvement was frequently followed by a benign clinical and radiographic course. Radiographic changes often worsened for several days in uncomplicated cases, but improvement was generally manifested within the first week after aspiration. Worsening of infiltrates after initial improvement was associated with the development of bacterial pneumonia, the adult respiratory distress syndrome, and pulmonary embolism. In the appropriate clinical setting, aspiration of gastric contents should be an important diagnostic consideration in the presence of a wide variety of radiographic changes.

Since the initial descriptions by Hall [1] and Mendelson [2], aspiration of gastric contents has been recognized as an important cause of morbidity and mortality in obtunded patients. The effects of aspirated gastric contents depend on the pH and volume of the aspirate [2–4]. Above a pH of 2.4, liquid instilled into the lungs of experimental animals produces results identical to the instillation of water. Radiographic infiltrates, if produced, clear rapidly. More acidic fluid produces a severe tracheobronchitis, as well as necrosis of alveolar linings with subsequent filling of alveoli by edema, hemorrhage, and inflammatory cells.

Obtundation is considered an almost universal prerequisite for aspiration [1, 2, 5–9]. The initial symptoms are often dramatic [5]. However, a wide spectrum of clinical manifestations may occur [2, 10].

Subjects and Methods

The records of patients admitted to Parkland Memorial Hospital between February 1969 and June 1977 who had a diagnosis of aspiration pneumonia were reviewed. A total of 60 patients had adequate radiographs for this study on the basis of two sets of criteria. In 38 patients, aspiration of gastric contents was witnessed by medical personnel who either saw gastric contents in the airways during intubation or recovered gastric contents by suction from an endotracheal tube. The other 22 patients had clinical courses and radiographic findings typical of aspiration of gastric contents. Of these 22 patients, 10 obtunded young people (nine drug overdoses and one hypoglycemia of unknown etiology) had radiographic infiltrates without another cause; 10 patients vomited during intubation and were thought to have aspirated by the physician involved; and two patients developed postoperative respiratory distress and new infiltrates. Clinical criteria excluded heart failure, bacterial pneumonias, and other causes of infiltrates. Of the 60 patients, 16 were included in an earlier report [5].

Results

Clinical Findings

Of the 60 patients, 26 were 20–40 years of age and another 17 were 40–60. Conditions which predisposed to aspiration included sedative drug overdose (35%), anesthesia (27%), head injury (10%), and alcoholism (10%). In all but one of the 60 patients, an altered state of consciousness played a role in the aspiration. The lone exception was a 63-year-old man with Guillian-Barré syndrome. Three patients aspirated around endotracheal or tracheostomy tubes.

While the clinical onset was often explosive, manifested by tachypnea, dyspnea, cough, cyanosis, wheezing, and fever, six well documented cases had no symptoms except fever. Most patients developed fever, 15 with temperatures to 38.9°C or higher on the first day. In 11 patients, however, the temperature did not rise above 38°C throughout hospitalization.

Forty-one patients had uncomplicated recoveries after aspiration; most were discharged within 2 weeks. Two survivors had prolonged courses complicated by bacterial pneumonia, and one by the adult respiratory distress syndrome, manifested by progressive respiratory insufficiency concomitant with the development of diffuse, bilateral, lingering pulmonary infiltrates.

Sixteen patients died. Postmortem examinations indicated that extensive chemical pneumonias, adult respiratory distress syndrome, superimposed bacterial pneumonias, and pulmonary emboli were important in their demise.

Radiographic Findings

Examinations on the day of aspiration were available in all patients. Of the 60 patients, 54 demonstrated abnormalities on the first radiographs. Of the six originally normal, all of whom had well documented aspiration, only one developed pulmonary infiltrates, and she did so later on the first day. The radiographic findings were often asymmetrical. Therefore we chose to evaluate

Received January 31, 1978; accepted after revision June 29, 1978.

[1] Department of Radiology, Parkland Memorial Hospital, University of Texas Health Science Center, 5201 Harry Hines Boulevard, Dallas, Texas 75235. Address reprint requests to M. J. Landay.

[2] Department of Medicine, Parkland Memorial Hospital, University of Texas Health Science Center, Dallas, Texas 75235.

© 1978 American Roentgen Ray Society

0361–803X/78/1000–0587 $00.00

each of the 119 lungs at risk (one patient had a left pneumonectomy).

Distribution and extent of infiltrates. Two major patterns of distribution were found: one was a radial, or perihilar, pattern of concentric circles emanating from the hilus and the other was a superior or inferior distribution (fig. 1). Forty-two lungs manifested a predominantly radial distribution (fig. 2*A*) and 48 a superior or inferior (fig. 2*B*) pattern; seven lungs demonstrated a mixed pattern. Of 22 initially normal lungs, 10 were in patients with unilateral abnormalities. In lungs demonstrating a radial distribution, perihilar zones were generally most involved; lower lung involvement predominated in those with a superior or inferior pattern (fig. 1). Eight patients demonstrated a predominantly perihilar pattern in one lung and a predominantly superior or inferior distribution in the other.

In all patients, regardless of the predominant distribution pattern, the extent of disease was estimated by the number of superior or inferior zones demonstrating infiltrate on the first films. Six patients were normal and no patient had disease limited to a single zone. More extensive involvement was as follows: two zones, 17%; three zones, 10%; four zones, 25%; five zones, 6%; and six zones, 32%. The frequency of initial involvement of each superior, middle, and inferior zone in the 60 patients is listed in table 1.

Bilateral involvement occurred in 41 patients (68%), and approximately symmetrical infiltrates were present in 25 (42%) (fig. 3). However, there were a number of "atypical" distributions. In nine patients, one lung was affected to a considerably greater degree than the other (fig. 4). Although this more commonly occurred on the right, the left lung was the major target in one third of these instances. Another unusual finding was predominantly upper lung involvement in six patients. One patient (fig. 5) manifested exclusively bilateral upper lung infiltrates. In addition, five patients had a diffuse and homogenous infiltrate extending from apex to base on at least one side (fig. 4). Seven patients had multiple patchy densities with intervening normal parenchyma.

Lateral films were available early in the course of the disease in 11 patients. Posterior and midlung infiltrates were seen most commonly, but two patients had primarily anterior involvement. One of these patients is shown in figure 5. The other had lingular and right middle lobe disease.

Types of infiltrates. We know from pathologic correlations that aspiration of gastric contents produces predominantly air space disease; however, the radiographic picture is quite variable. Three major types of infiltrates occurred: (1) confluent (densities homogeneous enough to support an air bronchogram, fig. 6); (2) acinar (5–6 mm poorly defined nodules as demonstrated in the subapical regions of fig. 3); and (3) small irregular shadows frequently including indistinct vascular margins. Separation into these predominant types of infiltrates was often difficult and sometimes impossible.

The classification of predominant infiltrates per lung on the initial films is presented in table 2. Infiltrates

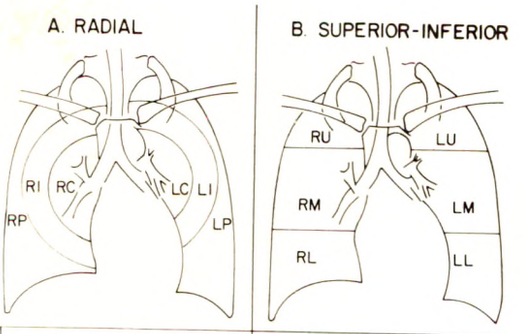

PREDOMINANT PATTERN (By lung)	42			48	
PREDOMINANT ZONE (By lung)	CENTRAL (RC, LC)	37		UPPER (RU, LU)	7
	INTERMEDIATE (RI, LI)	3		MID (RM, LM)	10
	PERIPHERAL (RP, LP)	2		LOWER (RL, LL)	31
		42			48

Fig. 1.—Distribution patterns by lung on first examination.

composed of small irregular shadows were most frequent. Eight patients demonstrated differing types of predominant infiltrates in the two lungs.

Atelectasis was infrequently observed on initial films. Three patients demonstrated segmental volume loss. Ten patients had small linear densities which probably represented minor degrees of platelike atelectasis. No patient had atelectasis without pulmonary infiltrate.

Pleural abnormalities were also infrequent. Eight patients demonstrated thickened fissures on the first film. No free pleural fluid was noted, but the high frequency of portable examinations limited adequacy of evaluation. Cavities were not seen in any patient.

Patient Course

Each patient followed one of two major clinical paths: (1) uncomplicated recovery or (2) complicated recovery or progressive deterioration. Each of these categories was further subdivided (table 3).

Over two-thirds of the patients had uncomplicated clinical courses. One subgroup included five patients whose films were normal initially and remained normal thereafter. In 20 patients, the worst radiographic appearance was on the initial examination and cleared continuously thereafter, with improvement first noted 7 hr to 4 days after aspiration (fig. 7). Another 16 patients (including one who was originally normal but developed small irregular densities later on the first day) had worsening of the infiltrates from 12 hr to 4 days after aspiration, with improvement beginning up to 9 days later (fig. 7). In four of the 16, small irregular shadows progressed to either acinar or confluent densities. Although radiographic abnormalities progressed for variable periods in the last 16 patients, they could not be separated on the basis of clinical criteria from the 20 who cleared continuously after aspiration.

Of the 19 patients with complicated or progressive clinical courses, 13 demonstrated either progressive radiographic deterioration or died with infiltrates unchanged after the first examination. Two of these demonstrated a change from small irregular shadows to

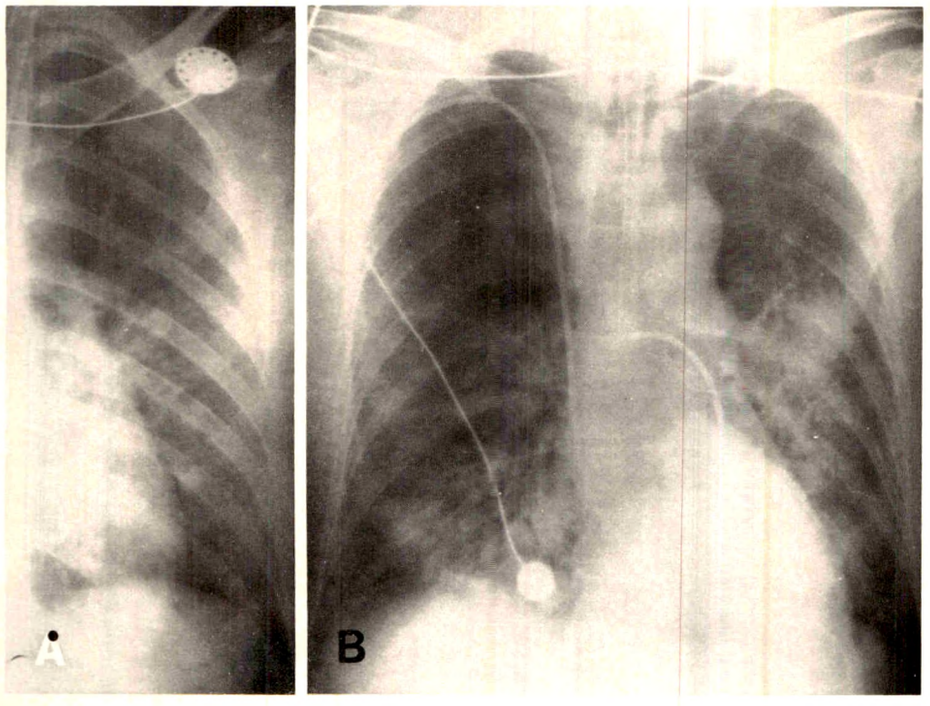

Fig. 2.—*A*, Radial pattern. Predominantly central infiltrate composed of small irregular densities. *B*, Inferior pattern. Confluent infiltrates most marked in both lower lungs.

TABLE 1

Frequency of Involvement of Lung Zones on First Examination

Zone	No. Patients	%
Right:		
Upper	29	43
Middle	47	73
Lower	46	77
Left:		
Upper	20	33
Middle	46	77
Lower	44	73

confluent infiltrates. Two others progressed to a picture consistent with the adult respiratory distress syndrome. There was only one survivor among these 13 patients.

The remaining six patients formed two subgroups whose films deteriorated after a period of improvement. In three, the period of radiographic improvement directly followed the first examination, while in the others initial worsening preceded the improvement. Asice from those differences in the early course, the patients could not be separated and will be dealt with together. Three of these patients, all of whom died, improved both clinically and radiographically before developing the adult respiratory distress syndrome on days 4 to 6. The other three patients developed local infiltrates on days 3–9 and had clinical courses most compatible with superimposed bacterial pneumonias. Two cleared with appropriate antibiotic therapy and the other died.

Of the 15 patients with initial involvement of two zones or fewer, three (20%) had a progressive or complicated course. Six of 23 (26%) with involvement of three or four zones initially and 10 of 22 (45%) with abnormalities of five or six zones had progressive or complicated courses. However, the differences among the three groups are not statistically significant by χ^2 analysis.

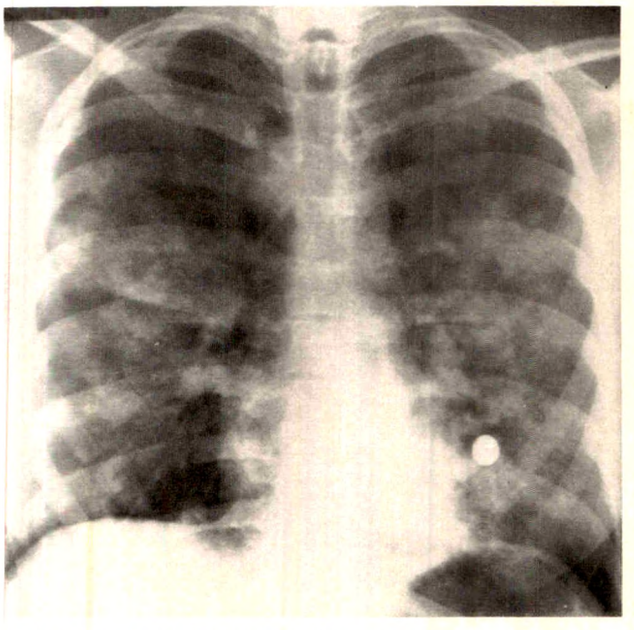

Fig. 3.—Symmetrical infiltrates, mixture of confluent and acinar types. Subapical regions in particular demonstrate latter.

While major atelectasis was not demonstrated on initial films, two patients developed lobar atelectasis in addition to prior infiltrate during their hospitalization. Six other patients developed significant subsegmental or segmental atelectasis. Both of the patients with lobar collapse underwent bronchoscopy, which revealed copious secretions but no obstructing food particles.

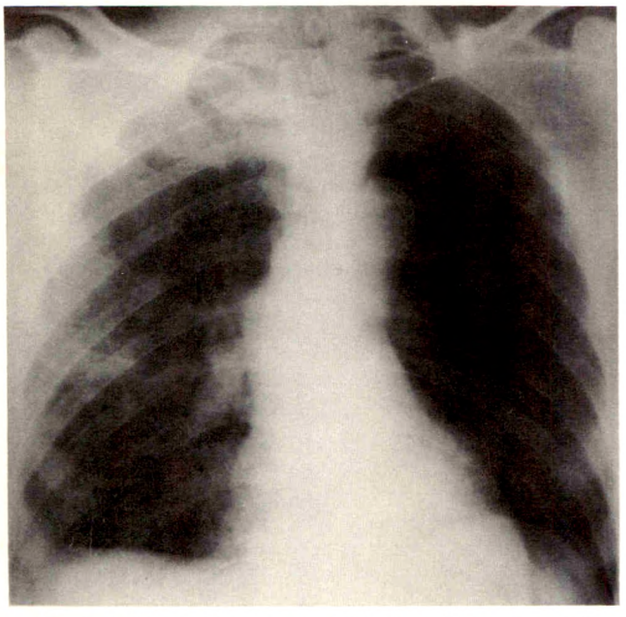

Fig. 4.—Bilateral infiltrates composed of small irregular shadows. Even considering that technical factors contribute to difference in density (see scapulae), right lung is considerably more involved.

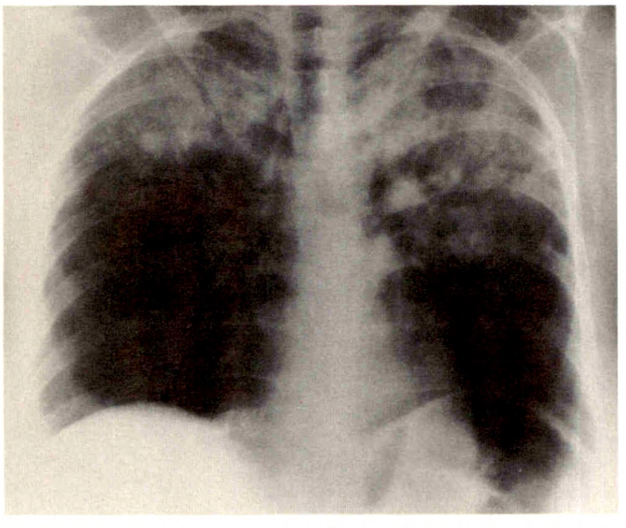

Fig. 5.—Bilateral upper lung infiltrates. Lateral view (not shown) demonstrated primarily anterior involvement.

Small pleural effusions developed in nine patients. Thoracentesis, performed in one case, yielded a sterile transudate. Pneumothorax or pneumomediastinum occurred in eight patients. Six of these had extensive consolidation and required mechanical ventilation. Pneumothorax was controlled by tube drainage and was not instrumental in the demise of any patient. In only one of the four patients in whom recent pulmonary emboli were discovered at autopsy was this process suspected before death.

Discussion

The most remarkable finding of this study is that no typical or characteristic radiographic manifestations can be attributed to the aspiration of gastric contents; that is, variability is the hallmark of this disorder. Radiographic infiltrates may be diffuse or localized, unilateral or bilateral, confluent or composed of small irregular densities, and distribution may be perihilar, lobar, or nondescript. There are virtually no radiographic features which can rule out aspiration; moreover, in an appropriate clinical setting, aspiration of gastric contents should be suspected in the presence of a wide variety of radiographic changes.

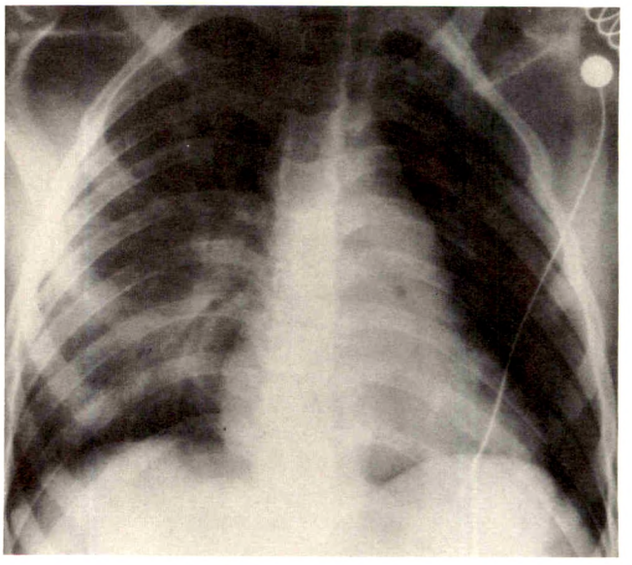

Fig. 6.—Bilateral confluent infiltrates.

TABLE 2

Predominant Infiltrate on First Examination

Type of Infiltrate	No. Lungs	%
Confluent	26	22
Acinar	14	12
Small irregular shadows	49	41
Mixed	8	7
No infiltrate	22	18
Total	119*	100

* One patient had had a pneumonectomy.

Distribution of infiltrate secondary to aspiration may depend on several factors, including patient position, effect of gravity, dynamics of air flow, and characteristics of the aspirate. Distribution and extent of infiltrate varied greatly among patients in this series. Abnormalities in a radial distribution diminishing with distance from the hilus and infiltrate increasing toward the lung bases were the most common patterns (fig. 1). This is in agreement with some earlier findings [5, 8], but contradicts Hartzell and Mininger [11] who found upper lung involvement most common. Bilateral involvement occurred in over two-thirds of our patients, and approximately equal infiltrates were present in both lungs in nearly one-half. A disparity between the two lungs (fig. 6) was not rare, however. Youngberg [12] found aspiration to be a common cause of diffuse unilateral lung

TABLE 3

Clinical Course Correlated with Sequential Radiographic Changes

Course	No. Patients	%
Uncomplicated clinical course:		
Initial film and all follow-up films normal	5	8
Infiltrates worst initially, then improved	20	33
Infiltrates worsened, then improved	16	27
Progressive worsening or complicated clinical course:		
Progressive infiltrate or patient died without change in radiographs	13	22
Infiltrates initially improved, then worsened	3	5
Infiltrates initially worsened, then improved, then worsened	3	5

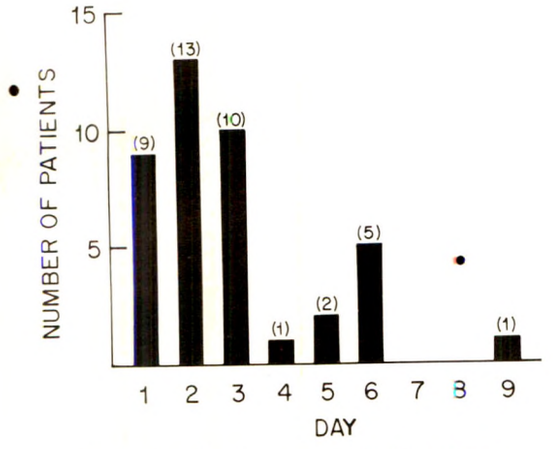

Fig. 7.—Day of earliest radiographic improvement.

opacity. Marked predominance of infiltrate on the left side, while unusual, occurred in three patients.

Just as a wide spectrum of distribution patterns was noted, infiltrates manifested considerable variation in radiographic appearance. Infiltrates composed of small irregular shadows were seen most commonly, but a substantial minority of patients had more extensive consolidation. Moreover, infiltrates frequently exhibited a mixture of patterns in a single patient. Occasionally, one type of infiltrate was superimposed on another at a later point in the course.

Pleural effusions and atelectasis were not major sequelae of aspiration of gastric contents. Cavitation of pulmonary infiltrates was not recognized in our series, and must be infrequent in this entity.

The extent of infiltrate on the first radiograph did not correlate well with outcome. Although there was a trend indicating a higher percentage of complicated or progressive courses in patients with more extensive initial involvement, the differences were small and not statistically significant. It seems more remarkable that patients with minimal early involvement sometimes developed serious complications, and that many patients with widespread abnormalities initially had uncomplicated courses. These observations may in part reflect the timing of initial radiographic studies; films obtained very shortly after aspiration may not reflect the full extent of lung damage, whereas a delay of several hours may result in the initial study appearing much worse. These findings suggest that an insignificant lesion should never be assumed merely on the basis of minimal early abnormalities, and the prediction of a benign course should await the results of serial examinations over several days. On the other hand, extensive radiographic involvement should not alone indicate a need for dramatic therapeutic measures, since subsequent studies may show rapid and uncomplicated resolution.

Because of the great variability in the character of infiltrates with acute aspiration of gastric contents, the occurrence of one type of radiographic abnormality in one area of the lung, while another area has a different type of abnormality, does not necessarily indicate that more than one disease is present. This sort of combined abnormality might lead to the diagnosis of an acute process superimposed on a chronic one, or a complication such as secondary infection superimposed on an acute aspiration injury. However, in the absence of other clinical or radiographic evidence, such interpretations are not warranted, since all the changes could be secondary to uncomplicated aspiration alone.

Although we have emphasized the difficulties in the detection and interpretation of changes secondary to aspiration of gastric contents, certain important clues to the diagnosis also emerge from these observations. In the appropriate clinical setting, any radiographic infiltrates should raise the suspicion of aspiration. The diagnosis is further suggested by the presence of widespread parenchymal densities, a normal cardiac silhouette, the absence of pleural effusions and cavities, and a predominance of involvement of the right side (especially the right lower lung). In addition, features particularly suggestive of aspiration include the rapid development of extensive infiltrates in previously normal lungs and a relatively uncomplicated clinical course with prompt clearing of radiographic abnormalities, as occurred in the majority of our cases.

Of course, these observations are not meant to minimize the importance of complications that may supervene in the setting of aspiration-related lung disease. Progressive worsening of radiographic infiltrates, especially after 3 days or a period of improvement, suggests a variety of prognostically unfavorable developments, such as secondary bacterial pneumonia, the adult respiratory distress syndrome, and pulmonary embolism.

ACKNOWLEDGMENTS

We thank Mary Starling for considerable help in the preparation of this paper, Jan Dolph for the medical illustrations, and Nancy Schrieber for photography.

REFERENCES

1. Hall CC: Aspiration pneumonitis. *JAMA* 114:728–733, 1940
2. Mendelson CL: The aspiration of stomach contents into the lungs during obstetric anesthesia. *Am J Obstet Gynecol*

LIBRARY

52:191–205, 1946
3. Exarhos ND, Logan WD, Abbott OA, Hatcher CR: The importance of pH and volume in tracheobronchial aspiration. *Dis Chest* 47:167–169, 1965
4. Teabeaut JR: Aspiration of gastric contents—an experimental study. *Am J Pathol* 28:51–67, 1952
5. Bynum LJ, Pierce AK: Pulmonary aspiration of gastric contents. *Am Rev Respir Dis* 114:1129–1136, 1976
6. Cameron JL, Mitchell WH, Zuidema GD: Aspiration pneumonia—clinical outcome following documented aspiration. *Arch Surg* 106:49–52, 1973
7. Marshall BM, Gordon RA: Vomiting, regurgitation, and aspiration in anesthesia II. *Can Anaesth Soc J* 5:438–447, 1958
8. Dines DE, Titus JL, Sessle AD: Aspiration pneumonitis. *Mayo Clin Proc* 45:347–360, 1970
9. Leonhardt KO: The late postoperative aspiration syndrome. *Anesth Analg* (Cleve) 42:210–216, 1963
10. Cameron JL, Zuidema GD: Aspiration pneumonia—magnitude and frequency of the problem. *JAMA* 219:1194–1196, 1972
11. Hartzell HC, Mininger EP: Bronchopneumonia following ether anesthesia in obstetrics. *Surg Gynecol Obstet* 82:427–433, 1946
12. Youngberg AS: Unilateral diffuse lung opacity. *Radiology* 123:277–281, 1977

Accuracy of Chest Film Screening by Technologists in the New York Early Lung Cancer Detection Program

BETTY J. FLEHINGER,[1] MYRON R. MELAMED,[2] ROBERT T. HEELAN,[3] CAROLYN M. McGINNIS,[2] MUHAMMAD B. ZAMAN,[2] AND NAEL MARTINI[4]

A study of the feasibility of using specially trained radiologic technologists to screen chest radiographs was undertaken as part of an early lung cancer detection program. In their initial examination, 8,000 men had posteroanterior and lateral chest films which were prepared and evaluated by two specially trained technologists prior to interpretation by a radiologist. The technologists' accuracy in screening was subsequently assessed by comparison with the radiologist's interpretation and with clinical follow-up information. There were differences in the level of suspicion of the two technologists, but both were effective in selecting a subset of the screened population that contained the men with radiologically identifiable lung cancer.

We have reported preliminary results of an ongoing lung cancer detection program in New York City in which cigarette-smoking men over 45 years old are examined annually by posteroanterior and lateral chest radiographs and, for half of the subjects, by sputum cytology at 4 month intervals [1]. One of the questions addressed in the study has been the feasibility of using specially trained radiologic technologists to distinguish radiographs within normal limits from those requiring interpretation by a radiologist. Thus the study design provided for a first screening and interpretation of all routine radiographs by one of two designated radiologic technologists, to be followed by and compared with the interpretation of a radiologist. This paper reports on the accuracy of the technologists.

Study Design

The New York lung cancer detection program is part of a cooperative study supported by the Division of Cancer Biology and Diagnosis of the National Cancer Institute. It has been described in a joint publication by the group [2], and in the preliminary report of prevalence rate data by us [1]. Male volunteers over 45 years old who smoke at least one pack of cigarettes daily are eligible for the study, and over 8,000 have been enrolled since June 1974.

On entering, each man has a standard 35.5 × 43 cm posteroanterior and lateral chest x-ray taken with a General Electric three-phase, 140 kVp, 400 mA phototimed machine with 3 m distance and 15.2 cm air gap. The maximum measured total dose of radiation for the combined posteroanterior and lateral chest x-rays is 70 mrem. A coupled automatic developer processes the films for inspection within 2 min of exposure.

Two radiologic technologists are responsible for operating the equipment and taking the films. As part of the program, they also examine the films as soon as they are developed. If desirable for technical reasons, or if some abnormality is found on preliminary examination, immediate repeat films or additional views are taken at the discretion of the technologist (e.g., with nipple markers, or oblique or lordotic views). Later the same day, the technologist records a screening interpretation of the films on a special x-ray report form, and the data are entered into a computer terminal.

Reporting System

The technologist's screening interpretation is recorded in one of the following three categories:

NEG. Normal; or abnormalities such as emphysema, cardiomegaly, scoliosis, pulmonary inflammatory disease, and pulmonary or pleural fibrosis, not indicative of lung cancer.

SUS. An abnormality thought probably *not* lung cancer but requiring further study to rule out that possibility; findings that require review of old films, tomograms, special views, or early repeat examinations, but not requiring surgical consultation.

CAN. An abnormality raising sufficient suspicion of lung cancer to require thoracic surgical consultation.

As noted, the technologist screens the films on the same day they are taken. On the following day he or she meets with one of five radiologists from the staff of Memorial Hospital, designated by rotation as the "reading radiologist" for that day. With the technologist, the reading radiologist examines all the films taken on the previous day. He dictates his diagnoses to the technologist who codes them on the report forms and, if any significant abnormality is observed, he also dictates a narrative description and diagnosis. The session serves a teaching as well as a diagnostic function, since findings by the radiologist or the technologist are discussed at this time.

If either the technologist or the reading radiologist, or both, classifies an examination as SUS or CAN, the films

Received September 27, 1977; accepted after revision June 19, 1978.
This work was supported by Research Contract no. N-01-CN-45007 from the National Cancer Institute.
[1] Mathematical Sciences Department, IBM T. J. Watson Research Center, Yorktown Heights, New York 10698.
[2] Department of Pathology (Cytology Service), Memorial Sloan-Kettering Cancer Center, 1275 York Avenue, New York, New York 10021. Address reprint requests to M. R. Melamed.
[3] Department of Radiology, Memorial Sloan-Kettering Cancer Center, New York, New York 10021.
[4] Department of Surgery (Thoracic Service), Memorial Sloan-Kettering Cancer Center, New York, New York 10021.

© 1978 American Roentgen Ray Society

0361–803X/78/1000–0593 $00.00

are referred to the "study radiologist." He determines the definitive radiologic diagnosis for the examination and recommends further action. That action is determined by the diagnostic category: for NEG, a return to routine annual examination; for SUS, additional radiologic studies as recommended by the study radiologist; and for CAN, referral to the thoracic surgeon for consultation. Conversely, a decision by the radiologist to request additional radiologic studies, or to recommend thoracic surgical consultation, necessarily entails classification as SUS or CAN, respectively. A flow chart of these procedures appears in figure 1.

Selection and Training of Technologists

The two radiologic technologists chosen for this study were selected because of their technical skill and experience, good judgment, and an interest and ability to undertake additional professional responsibilities. Both have been licensed by the state of New York since 1965, and both have been with the program since its inception. Their training to screen chest radiographs was essentially an apprentice program and informal. In addition to assigned reading in standard texts, they received individual instruction with senior members of the diagnostic radiology staff at Memorial Hospital.

Evaluation

Our purpose in this evaluation was to determine whether these skilled technologists could be used for a first screening of x-rays in a mass program for the early detection of lung cancer. Specifically, for a high risk smoking population we wished to determine whether it is feasible for the technologist to screen all x-rays and to select a subgroup that includes those with sufficient risk of lung cancer to warrant examination by radiologists. With this broad aim in mind, three specific questions were asked: (1) How well does the technologist's interpretation match the diagnosis of the radiologist? (2) Has this match improved with experience in the program? and (3) For an experienced technologist, what proportion of cases ultimately confirmed as lung cancer are correctly detected, and what proportion of cases requiring special studies before lung cancer is ruled out are detected by the technologist?

Results

Comparison of Interpretations

Tables 1 and 2 compare technologist and radiologist interpretations in the first 11 months of the study contrasted to a recent 12 month period. Radiologist opinions are those of the study radiologist in all cases in which he saw the films.

For both technologists, agreement between technologist and radiologist improved in the course of the study. Technologist A functioned at a much higher level of suspicion than did B, with 25% of her films rated SUS or CAN compared to only 8% of his. When reading films with technologist A, the same radiologists reported 12% of cases as SUS or CAN, compared to only 7% when reading with B.

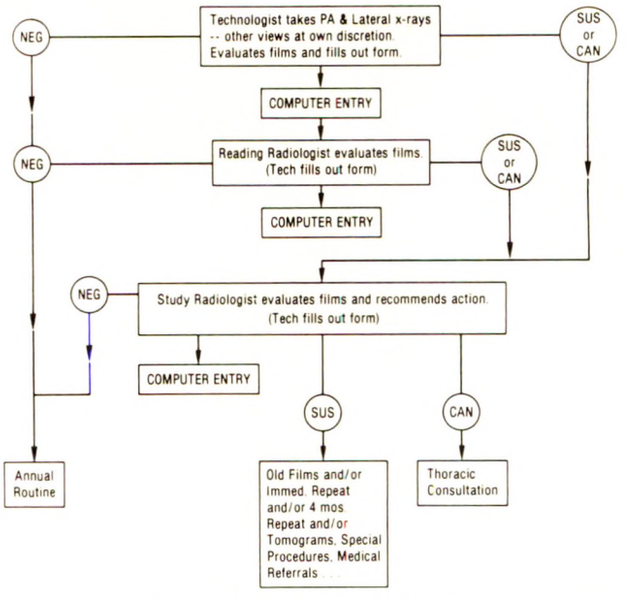

Fig. 1.—Flow diagram showing sequence of procedures for radiologic diagnosis.

TABLE 1

Interpretations of Technologist A and Radiologist

Technologist A	Radiologist		
	NEG	SUS/CAN	Total
Initial period:			
NEG	910 (66.8)	55 (4.0)	965 (70.8)
SUS/CAN	263 (19.3)	135 (9.91)	398 (29.2)
Total	1,173 (86.1)	190 (13.9)	1,361
Subsequent period:			
NEG	1,071 (72.9)	29 (2.0)	1,100 (74.8)
SUS/CAN	222 (15.1)	148 (10.1)	370 (25.2)
Total	1,293 (88.0)	177 (12.0)	1,470

Note.—During initial period (June 1974–April 1975) agreement was 76.7%; during subsequent period (October 1975–September 1976), agreement was 82.9%. Numbers in parentheses are percentages.

TABLE 2

Interpretations of Technologist B and Radiologist

Technologist B	Radiologist		
	NEG	SUS/CAN	Total
Initial period:			
NEG	1,232 (83.1)	82 (5.5)	1,314 (88.5)
SUS/CAN	100 (6.7)	70 (4.7)	170 (11.5)
Total	1,332 (89.8)	152 (10.2)	1,484
Subsequent period:			
NEG	1,339 (88.7)	48 (3.2)	1,387 (91.9)
SUS/CAN	66 (4.4)	57 (3.8)	123 (8.1)
Total	1,405 (93.0)	105 (7.0)	1,510

Note.—During initial period (June 1974–April 1975) agreement was 87.7%; during subsequent period (October 1975–September 1976), agreement was 92.5%. Numbers in parentheses are percentages.

Technologist B had a higher "miss" rate, with 3.2% of examinations reported NEG by him and SUS-CAN by the radiologists, compared to 2.0% for A. Technologist A had a higher "overread" rate; 15.1% of examinations were coded SUS-CAN by her and NEG by the radiologists, compared to 4.4% for B. The terms "miss" and

TABLE 3

Analysis of Outcome of Original Diagnosis by Technologist A

Report By:					
Technologist	1100 Negative			370 Sus/Can	
		Sus/Can			Sus/Can
Reading Radiologist	1071 Negative	29		273 Negative	97
				Sus/Can	
Study Radiologist	No referral of subjects found negative by both Technologist and Reading Radiologist	Sus/Can	29	222 Negative* 51	97
Follow-up of Subjects with suspicion of cancer	Negative: return to routine Annual Examinations				
	a) After review of old films and/or repeat chest x-rays		21	36	61
	b) After special procedures such as Tomography		7	4	11
	Sus—Still being followed		1	9	14
	Open biopsy—No cancer			1	3
	Cancer strongly suspected, not yet confirmed			1	1
	Cancer confirmed				7

*1 Cancer developing later. These films negative on review.

"overread" must be interpreted in a relative sense, since our findings show that the radiologist's opinion may be influenced by the technologist who assists him. Since the radiologist's code may not represent the true data, no estimates of false positive or false negative rates can be made at this time.

Interpretations According to Clinical Outcome

The code SUS may be used in this study when there is no real suspicion of lung cancer (e.g., if the radiologist simply wants to review prior films or to recommend repeat films in less than 1 year). Therefore, the disagreements shown in tables 1 and 2 do not give a complete picture of the ability of the technologists to find lung cancer. To formulate a better picture of that ability, we carried out a detailed study of the course of every man enrolled in the lung cancer detection program from October 1975 to September 1976 who was initially coded SUS or CAN. In addition, we reviewed the records and chest films of every man enrolled in that period in whom lung cancer was subsequently confirmed. Approximately 90% of men coded NEG returned for repeat annual examinations by us, and, including others contacted by telephone or mail, we were able to secure follow-up information on approximately 99%.

The results of this evaluation are displayed in tables 3 and 4 and can be summarized as follows:

Of 2,410 examinations coded NEG by both radiologist and technologist, only one man has subsequently developed cancer. Review of his films showed a small shadow which, in retrospect, may have been an early lesion.

Sixty-six examinations were called SUS or CAN by technologist B, while both reading and study radiologists coded them NEG; A had 222 in that category. In each group cancer was subsequently confirmed in one man. One was visible on review, while the other was considered to have developed at a later date.

There were six cases coded SUS or CAN by technologist B, negative by the reading radiologist, and SUS or CAN by the study radiologist. One has proven cancer. Technologist A had 51 such cases: nine are still SUS, one has had a thoracotomy for a lesion which turned out to be benign, and one is still thought to have cancer, but confirmation is pending.

Of the 148 cases which technologists, reading radiologist, and study radiologist all coded SUS or CAN, 12 have been proven cancers, one has cancer clinically, three had benign lesions diagnosed by open biopsy, and 19 are still being followed.

Finally, 48 cases were coded NEG by technologist B, while both radiologists found them SUS or CAN. These are the cases that might be considered "misses." Three of the 48, called SUS by the radiologists, have subsequently developed cancer, but each at a location unrelated to the original SUS diagnosis; four cases are still being followed. Technologist A had 29 cases in this category. Only one is still being followed; the other 28 have been resolved to negative. Thus the technologists

TABLE 4

Analysis of Outcome of Original Diagnosis by Technologist B

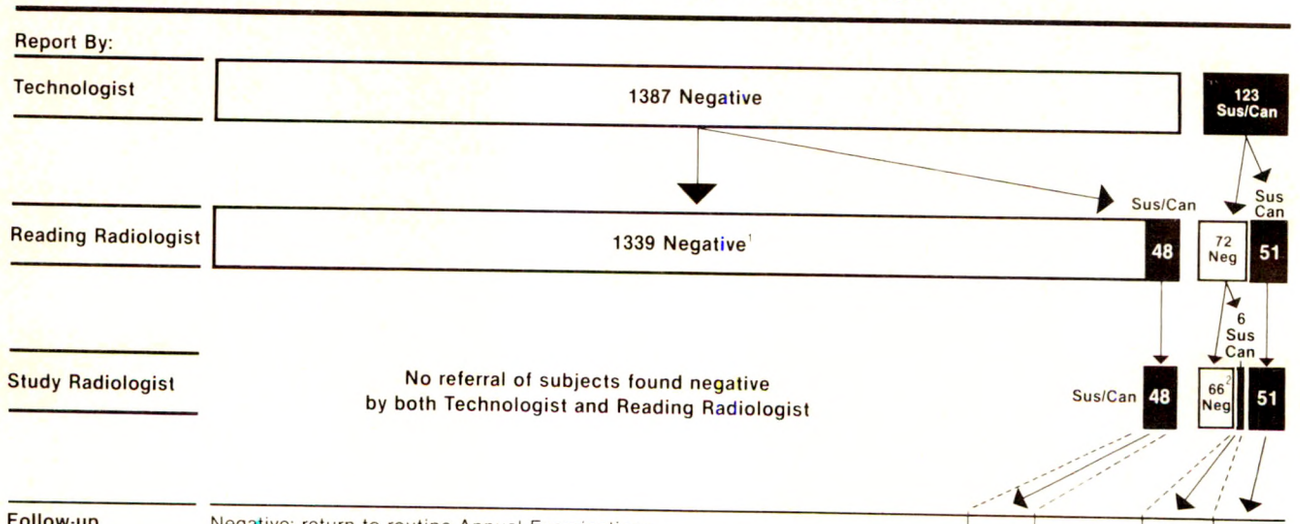

Follow-up of Subjects with suspicion of cancer					
	Negative: return to routine Annual Examinations				
	a) After review of old films and/or repeat chest x-rays	35		4	83
	b) After special procedures such as Tomography	6		1	8
	Sus—Still being followed	4			5
	Open biopsy—No cancer				
	Cancer strongly suspected, not yet confirmed				
	Cancer confirmed	3[3]		1	5

[1] 1 Cancer visible on review.
[2] 1 Cancer visible on review.
[3] Cancers developed later in areas unrelated to the abnormalities responsible for the original "Sus" diagnosis.

did not miss evidences of cancer that were picked up by radiologists.

Discussion

In a prior report of the National Cancer Institute Lung Cancer Detection Program in New York, we drew attention to the complementary roles of sputum cytology and chest radiographs, the former identifying central epidermoid carcinomas and the latter detecting more peripheral bronchiolar or adenocarcinomas [1]. Unlike the Philadelphia Pulmonary Neoplasm Research Project [3] in which screening was conducted with 70 mm frontal photofluorograms, the radiographs in this detection program are full size posteroanterior and lateral films. Because of the higher quality of these films, we believe this is a more adequate test of the radiographic method in this application.

We have two major concerns with the practical application of a screening program requiring interpretation of large numbers of chest films on a clinically well population. One is the need for additional highly trained radiologists, who are unlikely to feel that their skills are used productively in screening mostly normal films; and the second is the possibility of overlooking minimal abnormalities when films are interpreted by a single examiner, particularly when most are expected to be normal.

In a report on the variability of observer perception and description of radiographic pulmonary shadows, Yerushalmy [4] suggested two independent interpretations of chest films whenever possible, with disagreements to be resolved by a third interpretation. That procedure was adopted by the National Cancer Institute early lung cancer cooperative group for this study [2]. However, dual interpretations further increase demands on the time of the radiologist and may limit the feasibility of a widescale screening program.

Sheft et al. [5] suggested that the effectiveness and efficiency of available radiologists could be increased by the use of paramedical personnel. In a pilot study, they reported that the interpretations of 100 test radiographs of the chest by specially trained, advanced radiology technologists compared favorably with those of staff radiologists and senior residents. They felt that technical assistants working under the direction of a radiologist could screen survey chest films in much the same manner as cytologic technologists screen Papanicolaou smears working with pathologists. In other studies, Alcorn and O'Donnell [6] reported on the use of specially trained nonphysicians to screen mammograms, and Campbell et al. [7] reported favorable experience with technicians performing gastrointestinal examinations. Whether a sufficient number of experienced radiology

technologists could be recruited and trained for cancer detection programs on a wide scale, and what the cost of training and monitoring their work would be, still are not known.

In the present study a responsible screening role actually was fulfilled by the radiologic technologist, who performed the initial evaluation of all chest radiographs in our program. Subsequently, all films were examined and reported by a staff radiologist and, where necessary to resolve any discrepancies or confirm abnormalities, they were reexamined by another radiologist. Ultimately, it may be possible to minimize reader error due to visual or perceptual differences between individuals [8] by double screenings, both of which are performed by technologists, and films considered abnormal by either one would then be referred to the radiologist.

Technologists A and B both performed well, yet there was a difference in their approach. Technologist A had a much higher level of suspicion, classifying equivocal abnormalities as SUS, while B limited that classification to films with more definitive findings. Interestingly, and perhaps not surprisingly, their readings influenced the radiologist to some degree. If a field trial actually were initiated using radiologic technologists to screen films and determine which were to be reviewed by the radiologist, it would seem advisable to encourage a high level of suspicion. During the course of the present study, agreement between radiologist and technologist improved as the latter gained more experience, and this experience could influence the optimum level of suspicion. An analogous situation exists between the screening cytotechnologist and pathologist as the former gains experience in practice.

Based on the results of this study, we believe that specially trained radiologic technologists can reliably screen chest radiographs in a cancer detection survey. That is, the technologist can select a group of patients (SUS and CAN) among whom a small number will be found to have cancer. Conversely, the technologist can also identify a larger group (NEG) in whom cancer would not be suspected.

ACKNOWLEDGMENTS

We thank Rena Shore and Yu Fei Wu for help with a detailed review of records of all the men who had abnormal radiographs or who developed lung cancer. We also acknowledge the help of Ron Rosen and Molly Colgan in the computer management of data.

REFERENCES

1. Melamed M, Flehinger B, Miller D, Osborne R, Zaman MB, McGinnis CM, Martini N: Preliminary report of the lung cancer detection program in New York. *Cancer* 39:369–382, 1977
2. National Cancer Institute Cooperative Early Lung Cancer Group: *Manual of Procedures*. Diagnosis Branch, Division of Cancer Biology and Diagnosis, Bethesda, Md., National Cancer Institute, January 1975
3. Boucot K, Weiss W: Is curable lung cancer detected by semi-annual screening? *JAMA* 224:1361–1365, 1973
4. Yerushalmy J: The statistical assessment of roentgenographic pulmonary shadows. *Radiol Clin North Am* 7:381–392, 1969
5. Sheft DJ, Jones MD, Brown RF, Ross SE: Screening of chest roentgenograms by advanced roentgen technologists. *Radiology* 94:427–429, 1970
6. Alcorn FS, O'Donnell E: The training of nonphysician personnel for use in a mammography program. *Cancer* 23:879–883, 1969
7. Campbell JA, Lieberman M, Miller RE, Dreesen RG, Hoover C: Experience with technician performance of gastrointestinal examinations. *Radiology* 92:65–73, 1969
8. Tuddenham WJ: Visual search, image organization and reader error in roentgen diagnosis. *Radiology* 78 694–704, 1959

The Normal and Abnormal Left Superior Intercostal Vein

ARNOLD C. FRIEDMAN,[1] EVAN CHAMBERS, AND SEYMOUR SPRAYREGEN

A study of 500 normal erect posteroanterior chest radiographs was undertaken to determine the incidence of visualization and size of the left superior intercostal vein in normal individuals. The vein produces a small "nipple" lateral to the aortic knob on 1.4% of normal erect posteroanterior chest films; its diameter can be up to 4.5 mm in normal patients. Dilatation of the vein beyond 4.5 mm is a useful sign of a circulatory abnormality warranting further study. Dilatation may be due to absence of the inferior vena cava, hypoplasia of the left innominate vein, congestive failure, portal hypertension, Budd-Chiari syndrome, or superior or inferior vena caval obstruction. The differential diagnosis of an enlarged left superior intercostal vein includes mediastinal mass, especially lymphadenopathy, and aneurysm of the arch of the aorta.

The left superior intercostal vein appears on frontal chest films as a small "nipple" projecting from the lateral aspect of the aortic knob [1] (fig. 1). It is not widely appreciated that this vein may be seen on erect posteroanterior chest radiographs as well as on supine studies. Previous reports [1, 2] emphasize the incidence and size of this vein on supine tomograms (fig. 2), where it has a round configuration. The present study was undertaken to evaluate the incidence of visualization of the left superior intercostal vein and its size on erect chest radiographs. The causes for dilatation of this vein and the differential diagnosis of an enlarged vein are also discussed.

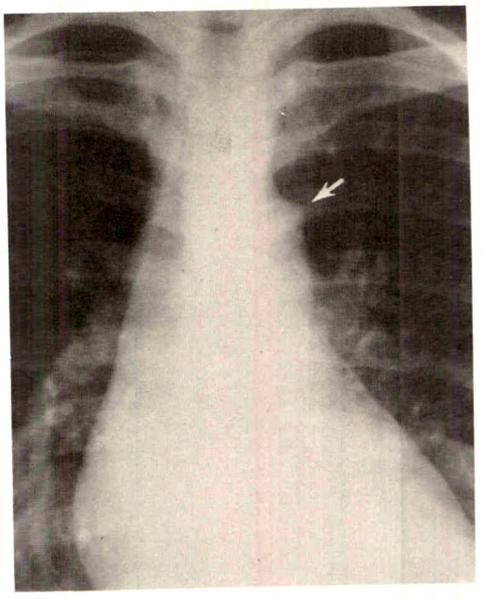

Fig. 1.—Posteroanterior chest film of 19-year-old asymptomatic female demonstrating normal aortic nipple (*arrow*).

Fig. 2.—Anteroposterior supine tomogram of 50-year-old male demonstrating normal appearance of left superior intercostal vein (*arrow*).

Materials and Methods

Five hundred consecutive erect posteroanterior chest radiographs of patients without known cardiovascular or pulmonary disease were examined at Montefiore Hospital and Medical Center for the presence of an aortic nipple. Inpatients and outpatients were included; children under the age of 10 were excluded. In addition to this random sample, nine aortic nipples previously encountered in normal patients were used in calculating the normal diameter. The diameter was measured as the length of a line extending from the lateral wall of the aortic knob to the lateral wall of the nipple, bisecting the nipple.

Results

Seven of the 500 radiographs (1.4%) demonstrated an aortic nipple. The diameter ranged from 1 mm to 4 mm (mean, 2.3 mm; SD, 1.1 mm). Taking the mean plus 2 SD as the upper limit of normal, the diameter of the left superior intercostal vein on erect posteroanterior chest films is therefore normally less than or equal to 4.5 mm. This diameter tends to increase by 1–2 mm when the

Received March 22, 1978; accepted after revision June 6, 1978.

[1] All authors: Department of Radiology, Albert Einstein College of Medicine, Montefiore Hospital and Medical Center, 111 East 210th Street, Bronx, New York 10467. Address reprint requests to A. C. Friedman.

© 1978 American Roentgen Ray Society

0361–803X/78/1000–0599 $00.00

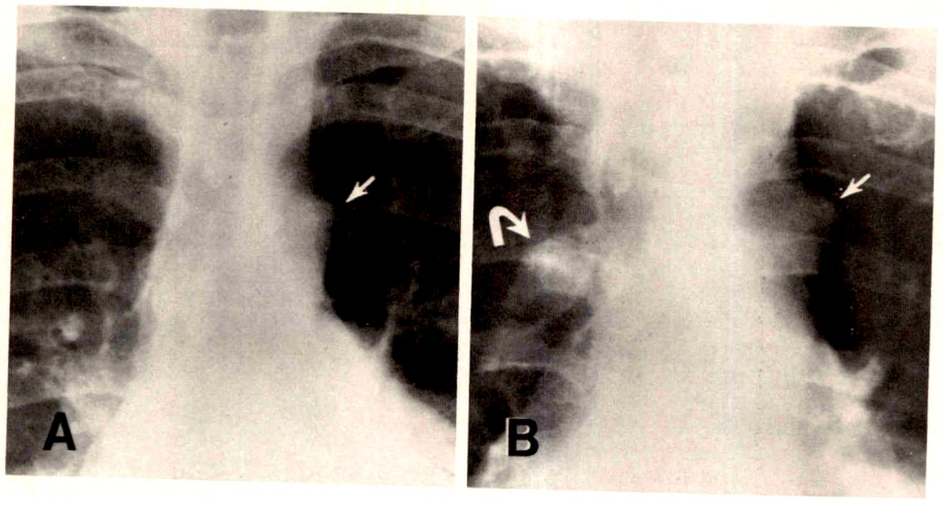

Fig. 3.—*A*, Posteroanterior chest film of 40-year-old asymptomatic male demonstrating normal aortic nipple (*arrow*) 3 mm in diameter. *B*, Supine anteroposterior chest film of same patient showing increased diameter (5.5 mm) of left superior intercostal vein (*straight arrow*). Note dilated azygos vein (*curved arrow*).

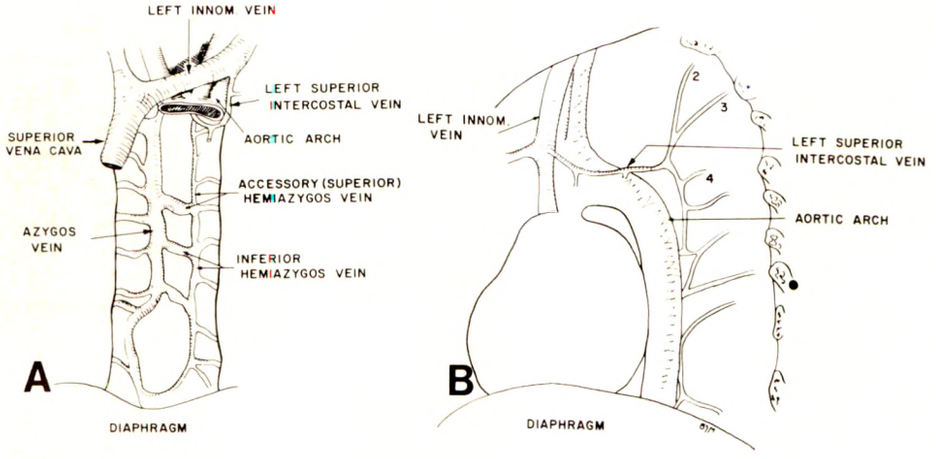

Fig. 4.—Frontal and lateral drawings of anatomy of mediastinal veins showing origin and course of left superior intercostal vein.

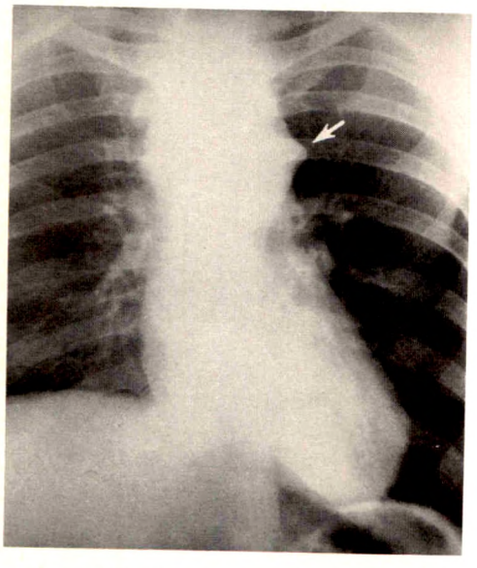

Fig. 5.—Posteroanterior chest film showing markedly dilated left superior intercostal vein (*arrow*) in 54-year-old man with bronchogenic carcinoma and superior vena caval obstruction.

patient assumes a recumbent position (fig. 3) and tends to decrease with the Valsalva maneuver.

Discussion

The left superior intercostal vein arises from the confluence of the left second through fourth intercostal veins, and usually (75%) communicates with the accessory (superior) hemiazygos vein at its lower end [1] (fig. 4). The vein descends vertically in the lateral vertebral gutter, then turns anteriorly adjacent to the aortic arch, to empty into the left innominate vein from behind [1, 3].

An aortic nipple has been reported to be present in 4% of normal individuals on supine tomograms (two of 50 normal adults) and in seven of 100 patients with known or suspected chest disease [1]. Another report found the aortic nipple to be present in 7.1% of anteroposterior tomograms [2]. We found an aortic nipple on 1.4% of normal erect posteroanterior chest films, indicating that the vein is not that uncommon in normal individuals.

Our measurement of the diameter of the normal left superior intercostal vein (2.3 ± 2.2 mm) is at variance with that described by Pagniez et al. [3] who reported a

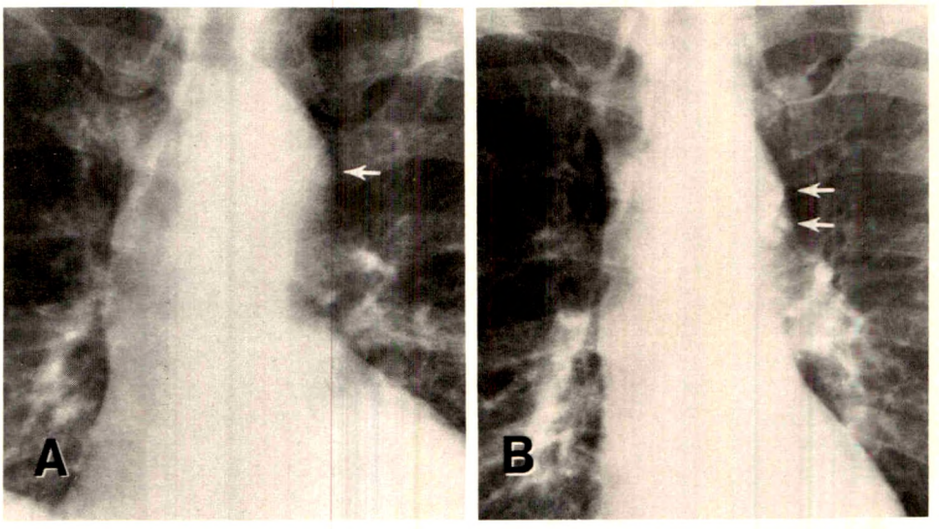

Fig. 6.—25-year-old man with lymphoma. *A*, Small mass in region of aortic nipple (*arrow*). *B*, Film after lymphangiography showing contrast material in region of previously noted mass (*arrows*). Lymphadenopathy, not enlarged left superior intercostal vein, is present.

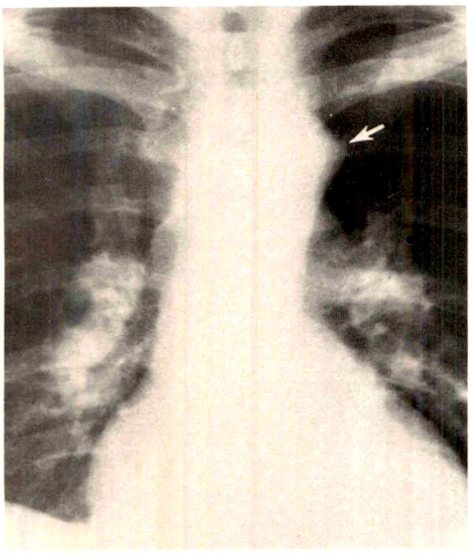

Fig. 7.—Posteroanterior chest film of 38-year-old man with known sarcoidosis demonstrating hilar adenopathy and small mass (*arrow*) in region of aortic nipple. Mass most likely represents lymphadenopathy, as in fig. 6.

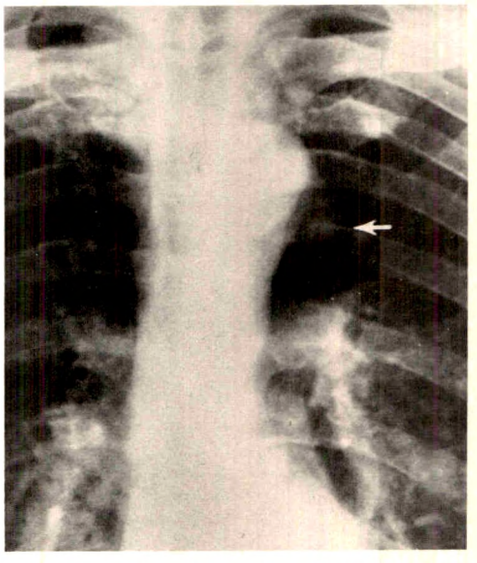

Fig. 8.—Posteroanterior chest film demonstrating mass in region of aortic nipple (*arrow*), which was proven to be small aneurysm of aortic arch.

normal diameter of up to 10 mm. It is unclear from their article how this measurement was obtained.

Dilatation of the left superior intercostal vein can be either congenital or acquired [3]. Congenital causes include absence of the inferior vena cava and hypoplasia of the left innominate vein. Acquired conditions include congestive failure, portal hypertension, Budd-Chiari syndrome, and superior or inferior vena caval obstruction [3–5]. The left superior intercostal vein dilates in these conditions because it is a channel of communication between the superior vena cava and the azygos-hemiazygos system. It is a remnant of the upper left cardinal vein, and drains into a persistent left superior vena cava when this congenital anomaly is present [3]. The vertical vein in anomalous pulmonary venous return is probably the left superior intercostal vein [3].

The differential diagnosis of an enlarged left superior intercostal vein includes mediastinal tumors, lymphadenopathy, and small aneurysms of the arch of the aorta. Figure 5 shows the posteroanterior chest film of a 45-year-old man examined for persistent cough and hoarseness. In addition to the mediastinal mass, narrowing of the left main stem bronchus, and hyperinflation of the left lung, a rounded opacity 8 mm in diameter is noted lateral to the aortic knob and pointing laterally, representing a dilated left superior intercostal vein. These findings suggest the diagnosis of bronchogenic carcinoma with superior vena cava obstruction, which was confirmed clinically.

Lymphadenopathy in a patient with lymphoma (fig. 6)

can cause a bulge lateral to the aortic arch, but it does not often have a discrete rounded appearance with an apex. However, the appearance of lymphadenopathy can very closely mimic that of an enlarged left superior intercostal vein. Figure 7 shows a round, pointed opacity lateral to the aortic knob in a patient with sarcoid and hilar adenopathy that cannot be differentiated from an enlarged left superior intercostal vein on this film. It did not change in size on recumbent films and was therefore felt to represent adenopathy.

A small aneurysm of the aortic arch (fig. 8) can occur lateral to the aortic knob and mimic an enlarged left superior intercostal vein. In this case, the apex of the opacity points downward, whereas the apex of an enlarged left superior intercostal vein tends to point laterally or superolaterally.

In summary, an enlarged left superior intercostal vein can usually be differentiated from small arch aneurysms or lymphadenopathy by the following criteria: the vein tends to maintain its pointed apex and generally ovoid configuration even when dilated, and the apex tends to point laterally or superolaterally. Ancillary findings suggestive of dilatation of the left superior intercostal vein are a lobulated left mediastinal contour (dilated hemiazygos system) and enlargement of the azygos vein.

ACKNOWLEDGMENT

We thank Dr. E. Robert Heitzman for advice and assistance in preparing this manuscript.

REFERENCES

1. McDonald CJ, Castellino RA, Blank N: The aortic "nipple." The left superior intercostal vein. *Radiology* 96:533–536, 1970
2. Hanke R: Lymph nodes or vascular shadows on the aortic knob? *Fortschr Geb Roentgenstr Nuklearmed* 108:197, 1968
3. Pagniez B, Denies JD, Dupus C, Remy J: The left superior intercostal vein. *J Radiol Electrol* 56:285–298, 1975
4. Berk RN: Dilatation of the left superior intercostal vein in the plain film diagnosis of chronic superior vena caval obstruction. *Am J Roentgenol* 83:419–423, 1964
5. Lane EJ, Heitzman ER, Dinn WM: The radiology of the superior intercostal veins. *Radiology* 120:263–267, 1976

Subglottic Edema in Acute Epiglottitis in Children

GARY D. SHACKELFORD,[1] MARILYN J. SIEGEL, AND WILLIAM H. McALISTER

Analysis of airway radiographs of 20 children with proven acute epiglottitis revealed that five (25%) had, in addition to supraglottic edema, localized subglottic edema radiographically indistinguishable from that seen in croup. In all five patients the etiologic organism was *Hemophilus influenzae* type B.

Acute epiglottitis is a cause of rapidly progressive laryngeal obstruction that usually occurs in children, most commonly in the preschool years [1–5]. The etiologic organism in most cases is *Hemophilus influenzae* type B [1, 6, 7]. Although the term epiglottitis has become familiar and is widely used to identify this condition, supraglottitis is probably more appropriate because of the usual involvement of all of the supraglottic structures, including epiglottis, aryepiglottic folds, and false vocal cords. However, it is not generally appreciated that extension of inflammatory edema into the subglottic region can occasionally occur in acute epiglottitis. We report subglottic involvement in five patients with epiglottitis due to *H. influenzae*, documented in all cases with radiographs of the airway.

Subjects and Methods

From 1970 to 1977, 44 children were admitted to St. Louis Children's Hospital with acute epiglottitis. All hospital charts and radiographs were reviewed to analyze the clinical data and determine the presence of subglottic edema. In all cases the diagnosis was confirmed by direct visualization of the inflamed, edematous epiglottis. Twenty patients without airway radiographs and four with radiographs in the lateral projection only were excluded from further analysis. Of the remaining 20 children, all had airway radiographs in the anteroposterior and lateral projections at the time of initial presentation and prior to any type of intubation.

The lateral radiographs were analyzed for the well known signs of epiglottitis, including edema of the epiglottis and aryepiglottic folds, and obliteration of the laryngeal ventricle secondary to involvement of the false vocal cords [8–13]. Subglottic edema was evaluated in the anteroposterior projection, since we feel that the lateral projection is not as sensitive an indicator of mild narrowing. Only localized subglottic narrowing was considered abnormal, since it is known that collapse of the extrathoracic trachea can occur during inspiration in cases of obstruction at or immediately above the level of the glottis [14]. No attempt was made to grade the severity of subglottic narrowing, but cases of questionable narrowing were considered normal. Compared with the shouldered appearance of the upper margins of the normal subglottic trachea (fig. 1), subglottic edema was manifested by symmetric fusiform narrowing localized to the area immediately below the true cords.

Results

All patients with airway radiographs had typical features of epiglottitis in the lateral projection (fig. 2). Of the 20 children with adequate anteroposterior and lateral preintubation airway radiographs, five had localized subglottic edema in addition to the usual signs of epiglottitis (fig. 3). The clinical data in these five patients are summarized in table 1. In all five there was bacteriologic confirmation of *H. influenzae* type B infection. Stridor was described in two patients, but in neither was it the dominant clinical feature. Three patients were managed with nasotracheal intubation and two with tracheostomy. All made uneventful recoveries.

Discussion

Acute epiglottitis as a clinical entity distinct from croup, or laryngotracheobronchitis, has been recognized for nearly 40 years [6]. In croup, which is usually of viral etiology, there is localized subglottic edema with no swelling of the supraglottic structures. In acute epiglot-

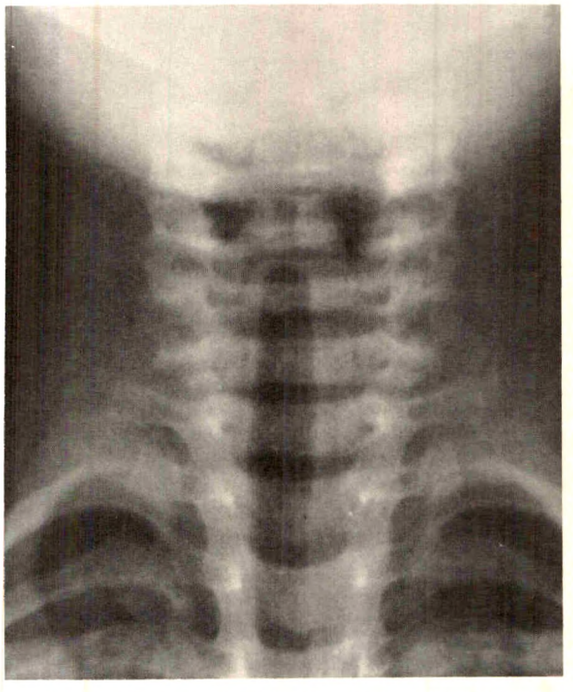

Fig. 1.—Normal anteroposterior airway radiograph in 19-month-old child showing true vocal cords at level of inferior extent of air-filled pyriform sinuses. Subglottic airway has shouldered appearance, with superolateral convexity of upper margins.

Received March 31, 1978; accepted after revision June 9, 1978.

[1] All authors: Department of Radiology, Washington University Medical Center, Mallinckrodt Institute of Radiology, 510 South Kingshighway Boulevard, St. Louis, Missouri 63110. Address reprint requests to G. D. Shackelford.

© 1978 American Roentgen Ray Society

0361–803X/78/1000–0603 $00.00

titis there is marked inflammatory edema of the epiglottis and other supraglottic structures. The subglottic airway is usually uninvolved. It has been postulated that the close adherence of the mucosa to the vocal cords prevents involvement of the cords and extension into the subglottic region [4, 5]. However, microscopic extension of the inflammatory process into the laryngotracheobronchial tree has been described in some autopsied patients [7]. There are also scattered clinical reports that mention the occasional presence of subglottic edema in acute epiglottitis [15, 16].

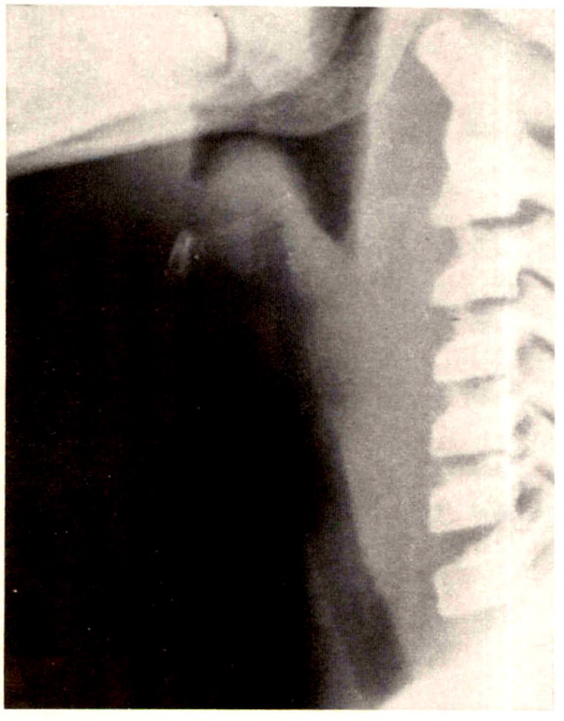

Fig. 2.—Case 5. Lateral airway radiograph showing markedly swollen epiglottis with encroachment on valleculae. Subglottic edema is not as apparent in this projection as in fig. 3*E*.

Our study was performed to determine the frequency of subglottic edema, as determined by airway radiographs. Of the 20 children with radiographs suitable for analysis, five (25%) had subglottic edema, indistinguishable from the type seen in croup. In all five cases the causative organism was *H. influenzae* type B. While the coexistence of croup as a cause for the subglottic edema cannot be excluded, it is very unlikely on the basis of analysis of the case histories (table 1), with the possible exception of case 5. In two of the five children stridor was described, but it was not further characterized.

Except for a single report of subglottic narrowing detectable on a radiograph of a child with acute epiglottitis [15], reports dealing with radiographic findings in this condition have not mentioned the presence of subglottic edema. They have emphasized the lateral projection, and in some institutions this is the only view obtained in cases of possible acute upper airway obstruction. In our study we analyzed subglottic narrowing in the anteroposterior projection, not only because we have found detection of mild narrowing to be unreliable in the lateral projection, but also in order to exclude cases of inspiratory extrathoracic tracheal narrowing due to supraglottic obstruction [14]. It is understandable that subglottic edema would not be readily detectable clinically, due to its obscuration by the striking supraglottic pathology.

The presence of subglottic edema in our patients had no effect on their management or clinical course. We report our findings to document a little known feature of acute epiglottitis and in order to emphasize the importance of the lateral airway projection to differentiate

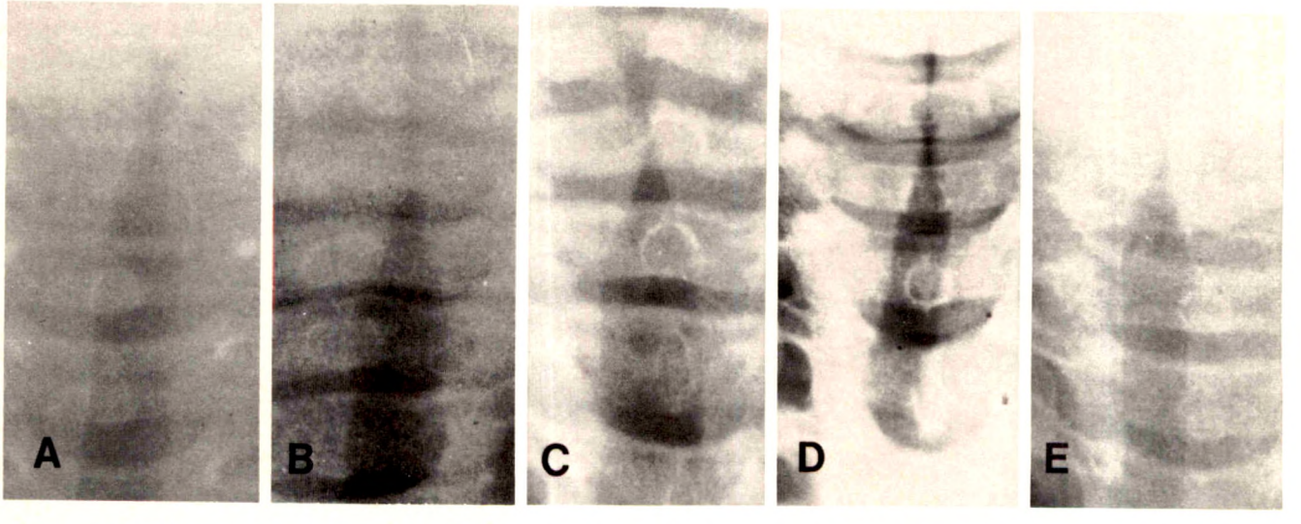

Fig. 3.—Anteroposterior airway radiographs of five patients who exhibited subglottic edema showing in all cases, fusiform narrowing localized to immediate subglottic region, indistinguishable from croup. *A*, Case 1. *B*, Case 2. *C*, Case 3. *D*, Case 4. *E*, Case 5.

TABLE 1

Summary of Clinical Data

Case No.	Sex and Age (years)	Clinical Presentation	Stridor	Bacteriologic Data
1	M, 3	Known seizure disorder; admitted with seizure and 1 day history of fever; respiratory distress developed immediately after admission	No	Blood culture, *H. influenzae* type B
2	M, 1 2/3	Fever for 1 day; acute onset of respiratory distress a few hours before admission	No	Blood culture, no growth; blood countercurrent immunoelectrophoresis, positive for *H. influenzae* type B
3	M, 5	Mild sore throat for 5 days; fever for 1 day; acute onset of difficulty swallowing and worsening sore throat about 12 hr before admission	No	Blood culture, *H. influenzae* type B; tracheal aspirate, normal flora
4	M, 3	Onset of fever and drooling 12 hr before admission; 4 hr history of stridor	Yes	Blood culture, *H. influenzae* type B; epiglottis culture, normal flora
5	M, 3	Sore throat and fever beginning 2 days before admission; stridor for 16 hr	Yes	Blood culture, *H. influenzae* type B; blood countercurrent immunoelectrophoresis, positive for *H. influenzae* type B

epiglottitis from croup. In the anteroposterior projection these two very different conditions may be indistinguishable.

REFERENCES

1. Miller AH: Acute epiglottitis: acute obstructive supraglottic laryngitis in small children caused by *Hemophilus influenzae*, type B. *Trans Am Acad Opthalmol Otolaryngol* 53:519–526, 1949
2. Berenberg W, Kevy S: Acute epiglottitis in childhood: a serious emergency, readily recognized at the bedside. *N Engl J Med* 258:870–874, 1958
3. Baxter JD: Acute epiglottitis in children. *Laryngoscope* 77:1358–1367, 1967
4. Jones HM: Acute epiglottitis and supra-glottitis (acute supra-glottic oedema). *J Laryngol Otol* 72:932–939, 1958
5. Jones HM: Acute epiglottitis: a personal study over twenty years. *Proc R Soc Med* 63:706–712, 1970
6. Sinclair SE: *Haemophilus influenzae* type B in acute laryngitis with bacteremia. *JAMA* 117:170–173, 1941
7. Rabe EF: Infectious croup. III. *Hemophilus influenzae* type B croup. *Pediatrics* 2:559–566, 1948
8. Dunbar JS: Epiglottitis and croup. *J Can Assoc Radiol* 12:86–95, 1961
9. Poole CA, Altman DH: Acute epiglottitis in children. *Radiology* 80:798–805, 1963
10. Capitanio MA, Kirkpatrick JA Jr: Upper respiratory tract obstruction in infants and children. *Radiol Clin North Am* 6:265–277, 1968
11. Dunbar JS: Upper respiratory tract obstruction in infants and children. *Am J Roentgenol* 109:227–246, 1970
12. Rapkin RH: The diagnosis of epiglottitis: simplicity and reliability of radiographs of the neck in the differential diagnosis of the croup syndrome. *J Pediatr* 80:96–98, 1972
13. Swischuk LE, Smith PC, Fagan CJ: Abnormalities of the pharynx and larynx in childhood. *Semin Roentgenol* 9:283–300, 1974
14. Wittenborg MH, Gyepes MT, Crocker D: Tracheal dynamics in infants with respiratory distress, stridor, and collapsing trachea. *Radiology* 88:653–662, 1967
15. Battaglia JD, Lockhart CH: Management of acute epiglottitis by nasotracheal intubation. *Am J Dis Child* 129:334–336, 1975
16. Blanc VF, Weber ML, Leduc C, Laberge R, Desjardins R, Perreault G: Acute epiglottitis in children: management of 27 consecutive cases with nasotracheal intubation, with special emphasis on anaesthetic considerations. *Can Anaesth Soc J* 24:1–11, 1977

Pneumopelvigraphy in Childhood

PATRICK D. LESTER[1, 2] AND WILLIAM H. McALISTER[1]

Pelvic pneumography was performed in 150 children, including those with precocious puberty, suspected pelvic masses, abdominal pain, virilization, ambiguous genitalia, gonadal dysgenesis, Stein-Leventhal syndrome, amenorrhea, and contralateral inguinal hernia detection. Pneumography proved safe, accurate, and easy to perform. However, advances in sonography have limited the use of pneumography primarily to the investigation of infant intersex problems and confirmation of idiopathic precocious puberty in the infant or very young girl.

Pelvic pneumography was first introduced approximately 60 years ago [1]. It has not been widely used in children despite clinical value, low morbidity, and the ease with which the examination is performed. Although ultrasound has replaced pneumography for some problems, other indications for pneumography remain. We report our experience with this procedure in 150 infants and children over a 15 year period.

Subjects and Methods

The procedure was used in 118 girls to evaluate precocious puberty, hirsutism, amenorrhea, Turner syndrome, ambiguous and abnormal genitalia, suspected pelvic masses, mobile pelvic calcifications, and unexplained abdominal pain (table 1). In 32 apparent male children it was performed to evaluate intersex problems and to detect contralateral open peritoneal sacs in patients with clinically unilateral inguinal hernias (table 1).

The method of pelvic pneumography is similar to that described in the literature [2]. All patients except infants were premedicated with Demerol (1 mg/kg) and Phenergan (1 mg/kg) and given a Dulcolax suppository the evening before and 1 hr before examination.

A preliminary film of the pelvis was obtained in the prone position so that the pelvic bones were barely visible. The patient was then placed in a supine position. After sterile cleansing and local anesthesia, a 20–22 gauge plastic sheathed needle was inserted into the peritoneal cavity in the midline between the umbilicus and the pubic symphysis. The intraperitoneal position was confirmed by injection of a small amount of contrast agent (50% Hypaque or Conray-60) under fluoroscopic control. The needle was withdrawn leaving the plastic sheath in place. This allowed more gas to be injected if needed and facilitated gas removal at the termination of the procedure. Nitrous oxide was introduced into the peritoneal cavity utilizing a syringe, tubing, and three-way stopcock. The end point of gas administration was a slightly distended but not a tense abdomen [3]. An alternative approach to calculating an adequate amount of gas is the formula 800 ml/m² [2].

After distention of the abdomen, older children were placed in a prone position on the x-ray table and immobilized with a shoulder harness. Infants and young children were restrained by an octagon board which was placed on the foot board of the x-ray table. The table was tilted to a 45° Trendelenburg position, and five basic radiographs were obtained with the central ray centered on the coccyx and at 1 m distance: (1) the central ray perpendicular to the floor; (2) the central ray angled 10° caudad; (3) the central ray angled 20° caudad; and (4) both 30° oblique positions at 10° caudad angulation. The second and third radiographs can provide a stereoscopic pair.

Results

Complications

In 150 examinations, there were no serious complications. One bladder and two intestinal punctures occurred, but the patients experienced no adverse effects. Prior to the use of contrast agents for needle localization, nine patients had extraperitoneal injection of gas. Radiographs in these patients showed an "empty" or gas-filled pelvis without internal genital structures. Postprocedural pain, especially shoulder pain in older children, was diminished by removing gas at the end of the procedure. While we could not determine the incidence of this pain in this retrospective analysis, it was appreciable enough to warrant premedication of later patients in the series.

Although gas embolism was thought possible, we had no cases and the risk was considered negligible because nitrous oxide is highly soluble in body fluids. Pneumothorax, pneumomediastinum, or pneumopericardium through diaphragmatic defects did not occur nor did vessel lacerations. While not a complication, a full bladder or rectum may distort and obscure the reproductive tract, making interpretation of the examination difficult.

Normal Pneumogynogram

The normal structures identified on female pelvic pneumography are illustrated in figure 1*A*. We were unable to locate any large series describing radiographic measurements of ovarian and uterine sizes in young children. The ovarian and uterine measurements we used were obtained from two sources: (1) five postmortem pneumogynograms on prepubertal girls prior to autopsy to determine magnification factors; and (2) autopsies on 15 girls without pneumogynograms. Ovarian sizes (uncorrected for magnification) were considered abnormally large if they were greater than 22 mm × 11 mm under the age of 5 years and 27 mm × 14 mm from 6 years to puberty. The uterus and ovaries started to enlarge prior to clinical puberty. The pubertal ovaries ranged from 24–45 mm × 15–40 mm. The infantile and prepubertal female uterine diameters were under 15 mm (transverse) × 10 mm (anteroposterior).

Received May 16, 1977; accepted after revision June 20, 1978.

[1] Mallinckrodt Institute of Radiology, Washington University School of Medicine, 510 South Kingshighway Boulevard, St. Louis, Missouri 63110. Address reprint requests to W. H. McAlister.

[2] Present address: Department of Radiology, University of Utah Medical Center, Salt Lake City, Utah 84132.

© 1978 American Roentgen Ray Society

0361–803X/78/1000–0607 $00.00

TABLE 1

Clinical Indications for Pelvic Pneumography

Clinical Problem	No.	Age Range
Girls:		
Precocious puberty	71	6 weeks–7 years
Intersex; gonadal dysgenesis; hypomenorrhea and amenorrhea; vaginal absence	21*	Newborn–16 years
?Stein-Leventhal syndrome and androgen excess	11	11–15 years
Chronic abdominal pain	6	3–14 years
? Pelvic mass; pelvic calcification	9	1 month–14 years
Boys:		
Contralateral inguinal hernia detection	22	1–18 months
Intersex problems	8	Newborn–16 months
Chronic abdominal pain; ?pelvic mass	2	6 years
Total	150	...

* Three of these were true hermaphrodites.

Weigin and Stevens [4] stated that the ovarian area in adults is 3.7–14.6 cm^2 (mean 9 cm^2) and the uterine area is 15–53 cm^2 (mean 33.7 cm^2). Thomas et al. [5] used a formula to help distinguish normal from abnormal adult ovarian sizes. Adult ovaries are generally one-fourth to one-third the size of the uterus.

Isosexual Precocious Puberty

Isosexual precocious puberty was the most common indication for pelvic pneumography (71 girls). Of the 55 girls ultimately diagnosed as having idiopathic isosexual precocious puberty, 45 showed uterine and bilateral ovarian enlargement (fig. 1*B*). Occasionally the ovarian enlargement was mildly asymmetric. Ten had normal ovaries and uteri.

Of five patients with isolated premature breast development, one was normal while four had ovarian and uterine enlargement. The latter four patients developed the full syndrome of precocious puberty. Two girls with only early pubic hair development had normal pelvic gas studies and did not develop other signs of precocious puberty.

Ovarian neoplasms, not a common cause of precocious puberty, were found in two patients and were both granulosa cell tumors. In neither patient was there a palpable pelvic mass, nor did the clinical and biochemical data allow separation of ovarian tumor from idiopathic precocious puberty.

In precocious puberty with obvious central nervous system abnormalities, pelvic pneumography was not done, although there were four patients with uterine and ovarian maturation whose central nervous system lesions were revealed later. Three patients with precocious puberty from subsequently proven exogenuous estrogen administration had normal pelvic pneumograms.

Primary Androgen Excess

In girls with virilization, pneumography for evaluation of an ovarian tumor was employed only if an adrenal etiology was not apparent clinically, biochemically, or radiographically (fig. 2). Of three patients studied for potential ovarian masses only one was shown to have a mass, pathologically a Sertoli-Leydig cell tumor. The other two children had adrenal lesions, one a carcinoma and the other adrenal hyperplasia. Both were diagnosed at surgical exploration.

Stein-Leventhal Syndrome

Pneumogynograms were performed on eight patients to confirm the clinical suspicion of Stein-Leventhal syndrome[4] and to exclude in two of these patients a possible virilizing ovarian tumor. Six patients had bilateral ovarian enlargement compatible with the Stein-Leventhal syndrome (fig. 3). Distinct cysts were identified in two patients. The diagnosis was confirmed by laparotomy and/or laparoscopy in three patients. In three others, the clinical findings and the pneumogynograms were felt to be sufficiently diagnostic to exclude further invasive procedures. Clinical follow-up studies have continued to support the diagnosis of polycystic ovaries in these patients. Two patients had normal pelvic studies, and both were lost to follow-up.

Gonadal Dysgenesis, Teenage Amenorrhea, and Hypomenorrhea

Fourteen of 15 girls in this category had abnormal pelvic gas studies. The pneumogynographic findings of classic gonadal dysgenesis were an infantile uterus and "streak" or tiny longitudinal gonads (fig. 4*A*). Some mosaic Turner syndrome patients had asymmetric ovarian development and a more developed uterus than in the classic Turner syndrome. Pelvic pneumography was a helpful confirmatory study in these nonclassic or questionable gonadal dysgenesis patients. We searched for malignant tumor development in streak gonads when virilization was present or when the karyotype contained a Y chromosome; one nonpalpable malignant tumor was found. Three phenotypically normal patients with amenorrhea were found to have the "unilateral streaked ovary syndrome" with small ovaries on one side, streak ovaries on the other, and infantile uteri (fig. 4*B*). One patient with amenorrhea had normal ovaries but an absent uterus.

Intersexuality

Fourteen patients with abnormal or ambiguous external genitalia were studied to determine the structure of the internal genitalia. In male pseudohermaphroditism and testicular feminization syndrome, pneumogynograms failed to show internal female reproductive organs. However, nonpalpable gonads could be demonstrated in the inguinal canals of patients with testicular feminization when the gas passed into open peritoneal inguinal sacs (fig. 5). Internal female anatomy was found in three patients with abnormal genitalia, subsequently shown to be true hermaphrodites, thus altering clinical management.

Three sex chromatin-negative patients with masculinized genitalia were examined and had a gonad proven to

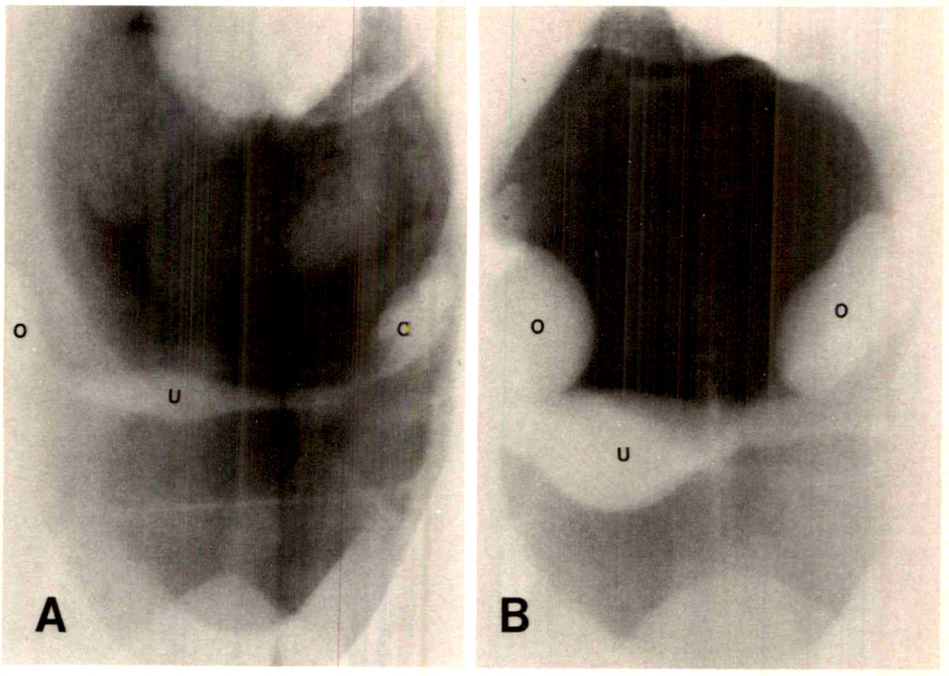

Fig. 1.—*A*, Normal 4-year-old girl. O = ovaries, u = uterus. *B*, 4-year-old girl with idiopathic precocious puberty. Bone age was accelerated to 7 years. Breast development started at 2½ years. Clinical 7 year follow-up confirmed original diagnosis.

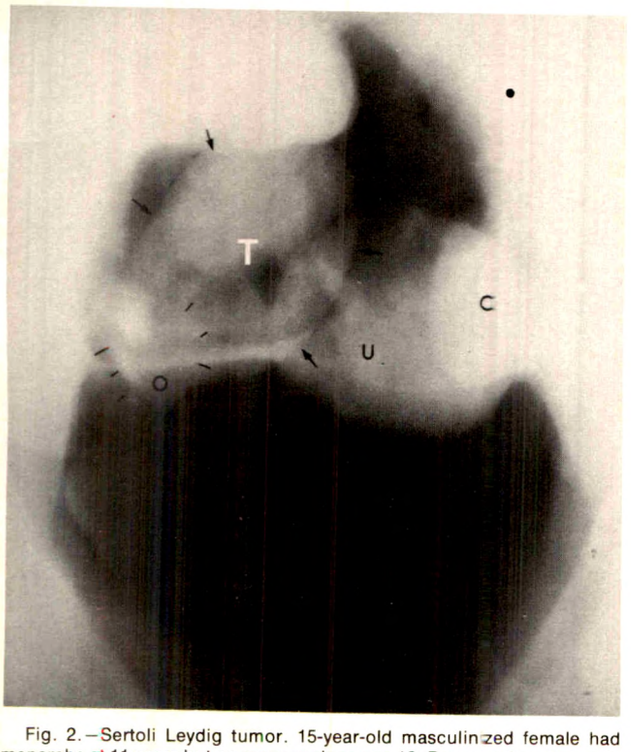

Fig. 2.—Sertoli Leydig tumor. 15-year-old masculinized female had menarche at 11 years but no menses since age 12. Presumptive diagnosis was adrenal hyperplasia, adolescent onset. Pneumogram shows tumor (T) (*arrows*) projecting off right ovary. Tumor was removed surgically. U = uterus, O = ovary.

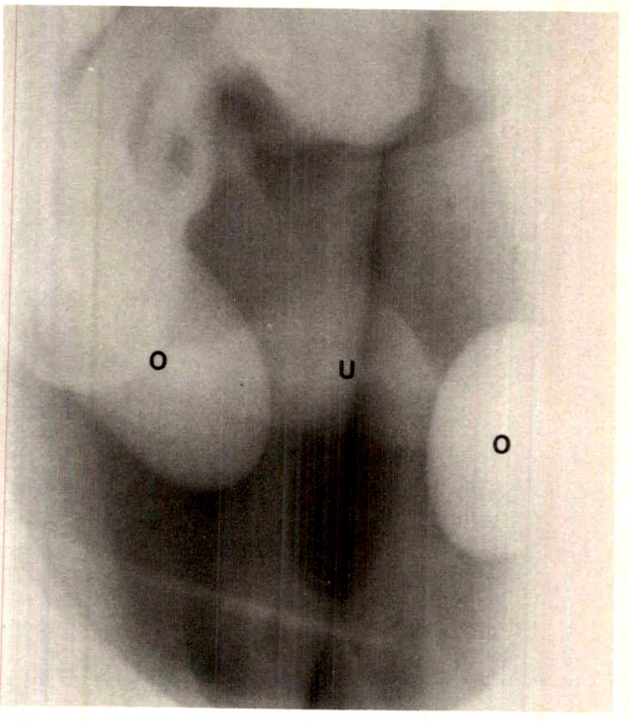

Fig. 3.—Stein-Leventhal syndrome. 11-year-old female with hirsutism and a hoarse voice for 6 months. Both ovaries are moderately enlarged. Diagnosis was confirmed at laparoscopy.

be a testes on one side, a streak gonad on the other, and an infantile uterus. They were diagnosed as mixed gonadal dysgenesis syndrome.

Pneumogynography demonstrated normal-appearing ovaries and uterus in a girl with congenital absence of vagina.

Nonfunctioning Masses and Other Conditions

Pneumogynography was used to evaluate questionable pelvic masses (eight patients), mobile pelvic calcifications (two patients), and chronic pelvic pain (seven patients). Of eight patients with questionable pelvic masses, gas studies were abnormal in four. One had a fluid-filled fallopian tube several years after a lumbar

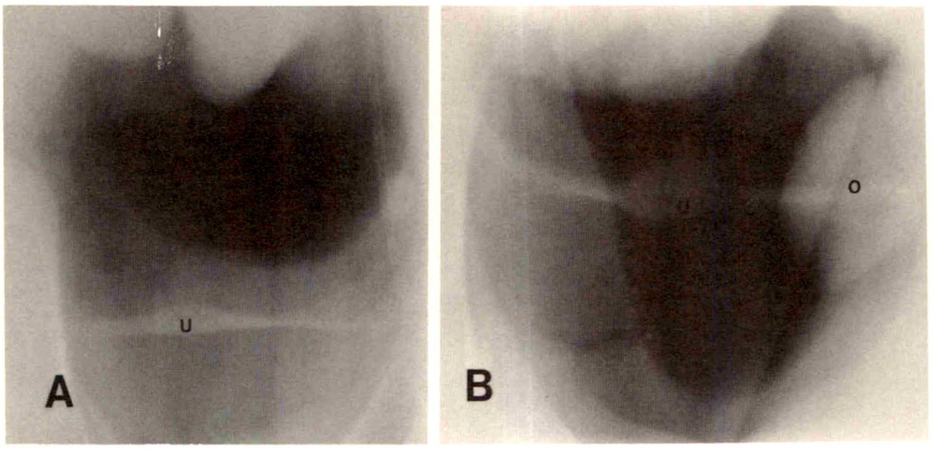

Fig. 4.—Gonadal dysgenesis. *A*, 6-year-old girl with features of Turner syndrome and classical radiographic findings of miniature uterus and streak gonads. *B*, 14-year-old female with mosaic Turner syndrome and oligomenorrhea. Note ovary on left but small hypoplastic right ovary and infantile uterus. Laparotomy confirmed ovary with cysts in left ovary.

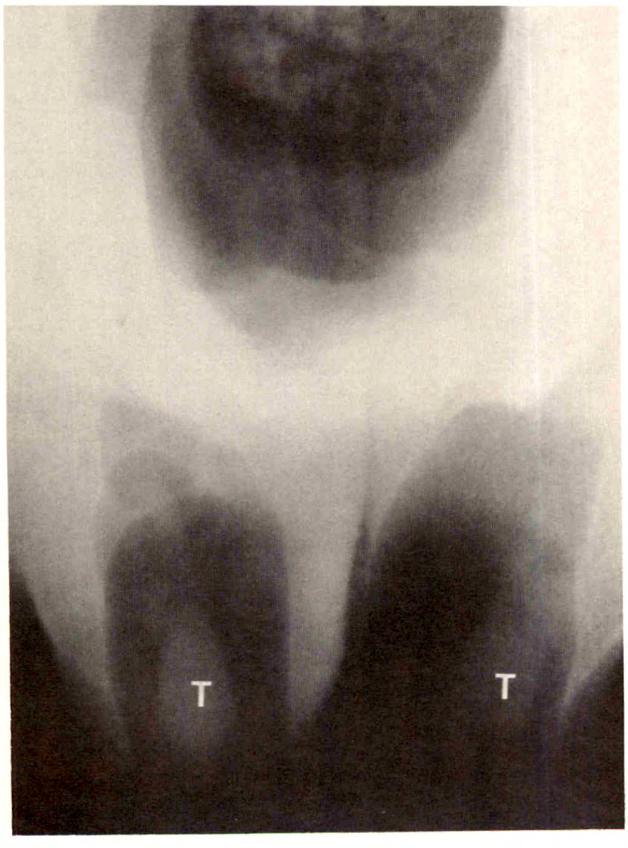

Fig. 5.—Testicular feminization syndrome. 10-month-old "girl" had prominent clitoris. Pneumogynogram did not demonstrate any internal female genital structures. Gonads in scrotal folds were surgically proven to be testes (T).

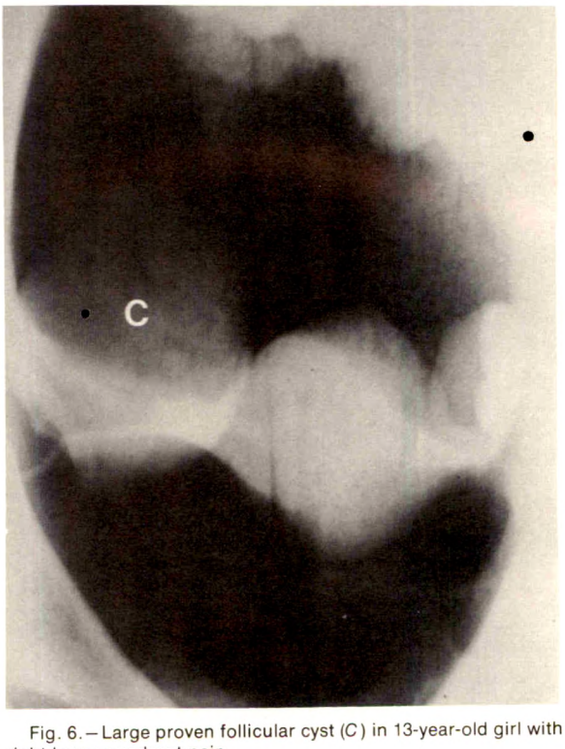

Fig. 6.—Large proven follicular cyst (*C*) in 13-year-old girl with right lower quadrant pain.

subarachnoid-tubal shunt for hydrocephalus. Two dermoids and one follicular cyst (fig. 6) were found and subsequently proven in the other three patients.

Two patients with mobile calcified pelvic masses on plain abdominal radiographs had absence of one ovary on pneumography (fig. 7). Surgery confirmed the free intraperitoneal location of the calcifications and the absence of one ovary. These were thought to represent examples of torsion of the ovary, with subsequent infarction and spontaneous amputation.

Of the seven patients with chronic pain, five were normal. One patient showed pelvic adhesions presumably secondary to earlier abdominal trauma. This latter patient was managed medically and became asymptomatic. One patient with a clinically suspected intermittent ovarian torsion had an enlarged ovary confirmed surgically, giving support to the clinical diagnosis. She was asymptomatic following oophorectomy.

Twenty-two infant boys with clinical unilateral inguinal hernias had pelvic pneumography to detect contralateral open peritoneal inguinal sacs. The condition was shown in 12 patients who underwent bilateral inguinal surgery.

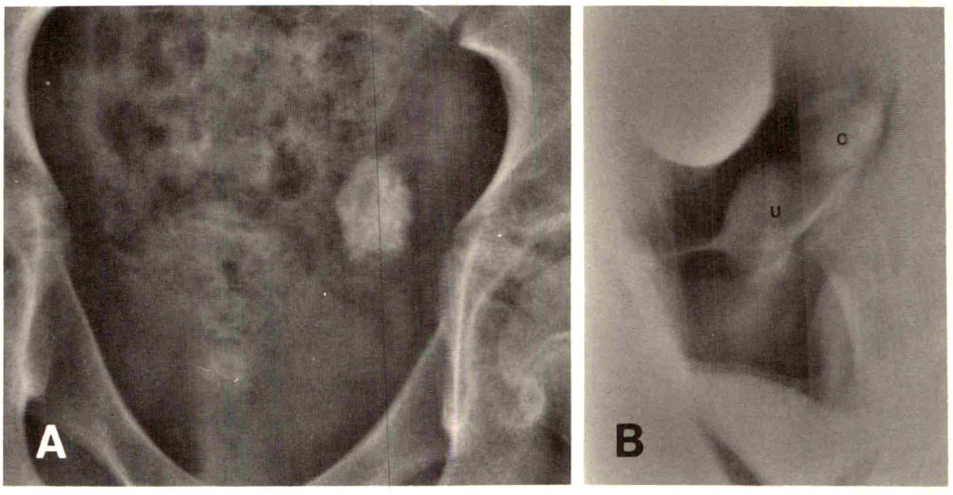

Fig. 7.—Calcified free ovary in 12-year-old girl with abdominal pain [6]. *A*, Plain film shows calcified pelvic mass. *B*, Pneumogynogram failed to demonstrate right ovary. This represented spontaneous torsion of ovary with infarction and amputation. There was surgical confirmation. U = uterus, O = ovary.

To date none of eight patients with a unilateral inguinal hernia sac and a normal contralateral side has developed a hernia on the contralateral side. Four of these patients were lost to follow-up.

Discussion

Physical examination of the internal genitalia is difficult in infants and young children. Pneumography has been a valuable adjunct to the clinical and laboratory findings in evaluating pediatric sex-endocrine disorders. It has been helpful in circumventing laparotomy and laparoscopy, since the radiographic findings correlate well with both the clinical and histopathologic diagnoses. The only contraindications are acute peritonitis or severe chronic pulmonary disease.

In our patients, the most frequent use of pelvic pneumography was to evaluate isosexual precocious puberty in infants and young girls. Unfortunately, there are no clinical or biochemical measurements that can clearly separate the three general causes of precocious puberty in girls, namely cerebral, ovarian, and idiopathic [7–10]. This is in part due to pulsatile gonadotropin release and the estrogen level overlap in each of these situations. Yet it is important to establish a correct diagnosis of precocious puberty to guide and to counsel parents. Precocious puberty of any cause leads to acceleration of maturation and subsequent shortening of stature. Pelvic pneumography aids in establishing the diagnosis, assuring the clinician, and excluding precocious breast or pubic hair development unassociated with precocious puberty. In our series the majority of patients were found to have idiopathic sexual precocity. Nonpalpable ovarian tumors occurred in only two girls [11].

Pelvic pneumography was helpful in patients suspected of having the Stein-Leventhal syndrome. The ovaries were shown to be bilaterally enlarged, and occasionally distinct cysts were identified. A nonpalpable virilizing ovarian tumor was revealed in one patient.

The majority of patients with gonadal dysgenesis or Turner syndrome did not need pelvic pneumography for diagnosis, but it was useful in diagnosing mosaic Turner syndrome, in guiding the use of estrogen therapy, and in detecting gonadal tumors [12–14]. In other patients with amenorrhea, absent or hypoplastic gonads or uteri can be identified [15].

In intersex problems the genital anatomy remains the single most important factor in determining the rearing sex, more important than the gonadal or chromosomal sex. Pelvic pneumography was useful in helping determine the internal anatomy of these patients [16, 17]. For example, absence of internal genital structures supported the diagnosis of male pseudohermaphroditism [18]. Nonpalpable gonads were identified in the inguinal canals in males with testicular feminization syndrome. Ovaries and a uterus were identified in a girl with congenital absence of the vagina [19]. Other abnormal conditions in which pelvic pneumography was helpful included true hermaphroditism and mixed gonadal dysgenesis. However, although pelvic pneumography can identify a gonad, it is limited by its inability to determine function or histology.

Pelvic pneumography was of value to confirm the presence of questionable pelvic masses or an ovarian origin for migratory pelvic calcifications [6]. Pneumography in abdominal pain was useful in our series once in supporting a clinical suspicion of intermittent ovarian torsion. In that patient one ovary was modestly enlarged leading to confirmatory surgery.

Positive contrast herniography is preferred over pelvic gas studies for detection of contralateral inguinal hernia in male infants. However, the latter can be used in patients with a history of sensitivity to iodine-containing contrast agents. After age 2 months, about 40% of males with a clinical unilateral inguinal hernia will have contralateral open peritoneal sacs, and half of these children (20% of the total) eventually develop a clinically evident hernia [20].

Sonography has affected the indications for pelvic pneumography. Currently ultrasonography is preferred for evaluating ovarian tumors and uterine and ovarian enlargement in older girls suspected of having precocious puberty [21]. However, internal genital structures

in infants and young children are frequently below the range of resolution of gray scale sonography. In this age group pneumography is favored over sonography for depicting the uterus and gonads, particularly in patients with precocious puberty or intersex states.

Improved clinical and laboratory diagnoses have resulted in infrequent use of both pneumography and sonography in the evaluation of Turner syndrome. Sonography has a limited role in the workup of intersex problems in the infant age group because of the small size of the internal pelvic organs. However, sonography is preferred for demonstrating ovarian tumors, polycystic ovaries, internal genital structures in amenorrheic patients, and pelvic masses.

Undoubtedly advances in pelvic sonography and possibly computed tomography will progressively narrow the use of pelvic pneumography. At present it remains a valuable tool in the evaluation of internal pelvic structures in children, especially infants and younger children with intersex problems or isosexual precocious puberty.

REFERENCES

1. Stevens GM: Pelvic pneumography. *Semin Roentgenol* 4:252–266, 1969
2. Lippe BM, Gyepes MT, Kaplan SA: Pelvic pneumography in children. *Am J Roentgenol* 123:829–837, 1975
3. Marshall RL, Jebson PJ, Davie IT, Scott DB: Circulatory effects of peritoneal insufflation with nitrous oxide. *Br J Anaesth* 44:1183–1187, 1972
4. Weigin JF, Stevens GM: Pelvic pneumography in the diagnosis of polycystic disease with the normal pelvic pneumogram. *Am J Roentgenol* 100:680–687, 1967
5. Thomas ML, Tonge K, Carty H: Radiographic measurement of ovarian size. *Acta Radiol [Diagn]* (Stockh) 14:251–265, 1973
6. Lester PD, McAlister WH: A mobile calcified spontaneously amputated ovary. *J Can Assoc Radiol* 21:143–145, 1970
7. Reiter EV, Kulin HE: Sexual maturation in the female. *Pediatr Clin North Am* 19:581–603, 1972
8. Baraton J, Ernest C, Poree C, Sauvegrain J: The neuroradiological examination of endocrine disorders of central origin in the child (precocious puberty, hypopituitarism). *Pediatr Radiol* 4:69–78, 1976
9. Romshe CA, Sotos JF: Intracranial human chorionic gonadotropin-secreting tumor with precocious puberty. *J Pediatr* 86:250–252, 1975
10. Grossman H, New M: Precocious sexual development. *Am J Roentgenol* 100:48–62, 1967
11. Eberlein WR, Bongiovanni AM, Jones IT, Yakovac WC: Ovarian tumors and cysts associated with sexual precocity. *J Pediatr* 57:484–497, 1960
12. Simila S, Jukarainen E, Herva R, Heikkinen ES: Gonadoblastoma associated with pure gonadal dysgenesis. *Clin Pediatr* 13:177–180, 1974
13. Swahn G, Lunderquist A, Rafstedt S: Gynecography in diagnosis and treatment evaluation in Turner's syndrome. *Acta Radiol [Diagn]* (Stockh) 4:529–535, 1966
14. McDonough PG, Tho PT: Use of pelvic pneumoperitoneum: critical assessment of 12 years' experience. *South Med J* 67:517–522, 1974
15. Slotnick EA, Goldfarb AF: Unilateral streaked ovary syndrome. *Obstet Gynecol* 39:269–273, 1972
16. Lunderquist A: Pneumopelvigraphy in the early diagnosis of intersexuality. *Am J Roentgenol* 103:202–209, 1968
17. Davidoff F, Federman DD: Mixed gonadal dysgenesis. *Pediatrics* 52:725–742, 1973
18. Prader A: Male pseudohermaphroditism. *Pediatr Annals* 3:57–65, 1974
19. Armstrong MK, Schreiber MH: Pelvic pneumography in congenital absence of the vagina. *Am J Roentgenol* 112:607–609, 1971
20. Kuhn JP: Herniography in perspective. *Am J Dis Child* 131:1206–1208, 1977
21. Zemlyn S: Comparison of pelvic ultrasonography and pneumography for ovarian size. *JCU* 2:331–339, 1974

Radiographic Findings in Ovarian Teratomas in Children

MARILYN J. SIEGEL,[1] WILLIAM H. McALISTER, AND GARY D. SHACKELFORD

Twenty-one infants and children with ovarian teratomas are reported. Calcification or ossification occurred in 68%, a higher figure than quoted in prior series. Teeth were recognized in 29% of these. A lucent fat-containing mass was appreciated in only two patients. In younger children the tumor was more frequently abdominal rather than pelvic. In two patients the tumor was malignant. A patient with an amputated freely mobile teratoma is reported in detail and the differential diagnosis of mobile abdominal calcifications discussed.

Ovarian teratomas are uncommon tumors in infants and children. We have reviewed our experience and summarized the clinical presentations and radiographic findings in 21 patients. One patient with an amputated calcified teratoma that migrated throughout the abdominal cavity is reported in detail.

Clinical Features

Between 1963 and 1977, 23 patients with surgically confirmed ovarian teratomas were seen at St. Louis Children's Hospital. Adequate radiologic studies were available for retrospective review in 21 of these 23 patients, and this group forms the basis of the current study. The age range was 14 months–14 years, with five patients 3 years or under. In 16 symptomatic patients the clinical presentation was as follows: palpable mass, eight; abdominal pain, four (two patients with torsion); abdominal pain and a palpable mass, four. In the remaining five patients the ovarian tumor was an incidental radiographic finding. Two of the teratomas were malignant.

Radiographic Findings

All patients had plain abdominal radiography and a majority underwent excretory urography. Some of the patients had barium studies of the colon and pelvic ultrasonography. Calcification or ossification was seen in 15 patients (68%). In six of 21 patients (29%) there were recognizable teeth. A noncalcified soft tissue mass with the same density as surrounding tissue was noted in four patients (17%). Two of 19 cases showed a relative radiolucency consistent with fat, and in two additional patients radiolucency was detected when the specimens were radiographed in water. There were no bilateral tumors.

In nine patients (43%) the tumor was primarily intraabdominal rather than pelvic in location. In neither of the patients with a malignant teratoma was the primary tumor calcified, although in one patient retroperitoneal metastases contained calcification. Mild reversible hydronephrosis was seen in six patients and was related to the size and location of the mass. One patient with a 3 × 2.5 cm benign teratoma containing a well formed tooth had a normal abdominal radiograph 2½ years earlier. A patient with an unusual irregular mobile abdominal calcification is reported below.

Case Report

A 14-month-old female who 3 months earlier had received a ventriculoperitoneal shunt for communicating hydrocephalus was readmitted for evaluation of a mobile abdominal calcification noted on postoperative shunt radiographs. There was no history suggestive of prior episodes of abdominal pain. Physical examination was normal. Left upper quadrant calcification was an incidental finding on the initial ventriculoperitoneal shunt series (fig. 1*A*). Excretory urography demonstrated migration of the calcific densities to the right lower quadrant as well as absence of the right kidney and compensatory hypertrophy of the left kidney (fig. 1*B*). In view of the mobility of the calcification, a diagnosis of ovarian teratoma on a long stalk was postulated.

At surgery a 7.5 × 4.5 × 1 cm gray free-floating cystic mass was found in the abdominal cavity. The right ovary and fallopian tube were normal; however, the left fallopian tube ended blindly. Pathologically the mass was a cystic structure containing focal calcification in necrotic material that in part resembled squamous epithelium, compatible with an infarcted cystic teratoma (fig. 2).

Discussion

Ovarian teratomas constitute less than 2% of abdominal masses in prepubertal girls, with benign cystic teratoma being most common [1–3]. The vast majority of reported teratomas have been in adolescent girls, with rare occurrences under age 4 [4]. In our series, 11 of 21 patients were 10 years of age or below, and five patients were 3 years or under.

Teratomas of the ovary are usually not discovered until they grow large enough to produce a palpable mass or twist on their pedicle and cause abdominal pain. A smaller number of cases are detected as an incidental finding on abdominal films.

In the patients analyzed we noted a slightly higher incidence of calcification or ossification (68%) than the quoted figures of around 50% [5, 6]. Recognizable teeth were present in 29% of teratomas. This agrees with previous reports in which 22% of ovarian teratomas showed teeth radiographically, permitting a specific diagnosis [6]. Almost one-half of our patients with ovarian teratomas presented with an abdominal rather than a

Received March 10, 1978; accepted after revision June 6, 1978.

[1]All authors: Mallinckrodt Institute of Radiology, Washington University School of Medicine, 510 South Kingshighway Boulevard, St. Louis, Missouri 63110. Address reprint requests to M. J. Siegel.

© 1978 American Roentgen Ray Society

0361–803X/78/1000–0613 $00.00

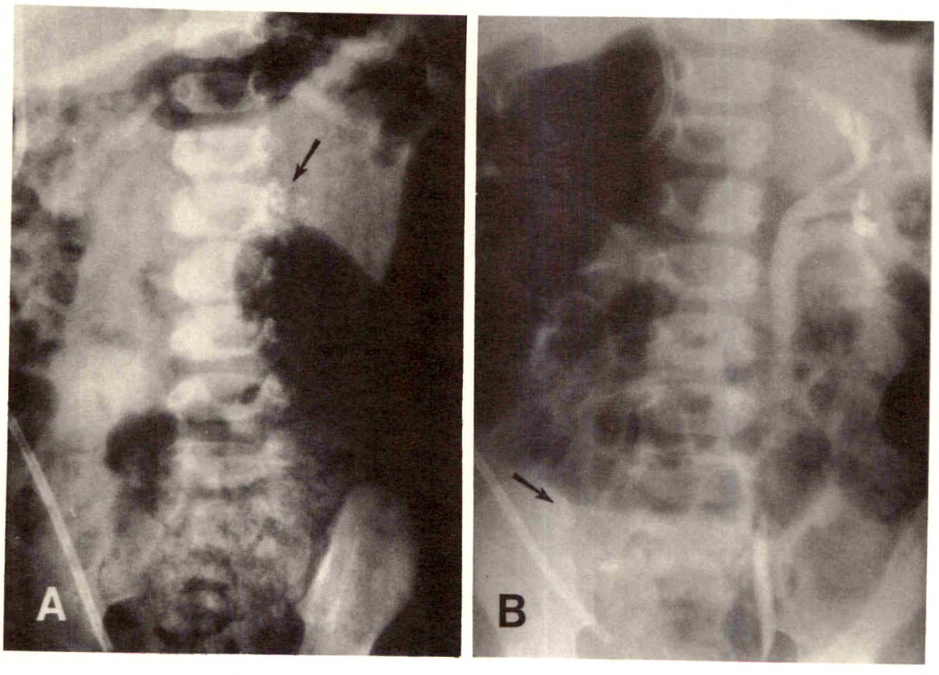

Fig. 1.—*A*, Anteroposterior film from ventriculoperitoneal shunt series showing calcifications (*arrow*) in left upper abdomen. *B*, Anteroposterior film during urography showing migration of calcifications (*arrow*) to right lower abdomen overlying sacroiliac joint. Compensatory hypertrophy of left kidney demonstrated.

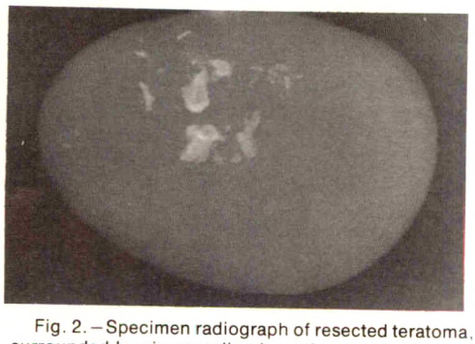

Fig. 2.—Specimen radiograph of resected teratoma, surrounded by air, revealing irregular calcifications.

pelvic mass. This was especially true of younger patients. Only two patients were recognized preoperatively as having fat in the tumor, but radiolucency was noted in two additional cases on specimen radiographs. None of our patients had bilateral tumors, although these have been reported in 10% of cases.

Radiologic differentiation of benign and malignant ovarian teratomas may be difficult, but a useful distinguishing feature is evidence of metastases, such as invasion or ascites. Local or distant extension of malignant teratomas occurs in 30%–50% of cases [7]. Neither of our patients with a malignant teratoma had calcification of the primary tumor, although metastases were calcified in one patient. That patient was still alive after 2 years. The other patient died. Malignancy can occur in ovarian teratomas with calcification or ossification, although it was not noted in our series.

Asymptomatic ovarian infarction and amputation presumably resulting from torsion with ischemia has been reported as an incidental finding in adults at surgery and autopsy [8]. In our asymptomatic patient with migrating calcifications, it is conceivable that there was chronic torsion with insidious amputation of the ovary resulting in a freely mobile abdominal mass.

Differential Diagnosis of Migratory Peritoneal Calcification

Migratory calcification seen within the abdomen in childhood can be due to an autoamputated calcified ovary [9, 10]. A distinguishing feature of five amputated calcified ovaries that we have noted is their ovoid shape. In contrast, the calcification and ossification in the teratomas are somewhat irregular. Radiologic differentiation of the pedunculated ovarian teratoma from an amputated teratoma may be impossible. Other causes of mobile abdominal calcifications include amputated appendices epiploicae [11], deposits in omentum [12], mumified pieces of free small bowel, various enteroliths, liquid calcification in a psoas abscess, gallstones, and omental or mesenteric cysts. Opaque intraperitoneal and intraluminal gastrointestinal foreign bodies are additional considerations. Many of these conditions can be differentiated with plain radiographs in multiple projections and appropriate contrast studies, although the diagnosis may not be made until the patient is surgically explored.

REFERENCES

1. Ein SH, Darte JMM, Stephens CH: Cystic and solid ovarian teratomas in children. *J Pediatr Surg* 5:148–156, 1970
2. Irons GB, Hoge RH, Salzberg AM: Ovarian teratomas in children. *Clin Pediatr* 5:151–153, 1966
3. Moore JG, Schifrin BS, Erez S: Ovarian tumors in infancy, childhood, and adolescence. *Am J Obstet Gynecol* 99:913–922, 1967
4. Norris HJ, Jensen RD: Relative frequency of ovarian neo-

plasms in children and adolescents. *Cancer* 30:713–719, 1972
5. Burfield GA, Kemp FH: The radiological investigation of dermoid cysts of the ovary. *Br J Radiol* 28:199–203, 1955
6. Sloan RD: Cystic teratoma (dermoid) of the ovary. *Radiology* 81:847–853, 1963
7. Dehner LP: *Pediatric Surgical Pathology*. St. Louis, Mosby, 1975
8. Outerbridge GW: Non-teratomatous bone formation in the human ovary. *Am J Med Sci* 151:868–887, 1916
9. Lester PD, McAlister WH: A mobile calcified spontaneously amputated ovary. *J Can Assoc Radiol* 21:143–145, 1970
10. Nixon GW, Condon VA: Amputated ovary: a cause of migratory abdominal calcification. *Am J Roentgenol* 128:1053–1055, 1977
11. Borg SA, Whitehouse GH, Griffiths GJ: A mobile calcified amputated appendix epiploica. *Am J Roentgenol* 127:349–350, 1976
12. Holt JF, MacIntyre RS: Calcified omental fat deposits: their roentgenologic significance. *Am J Roentgenol* 60:612–616, 1958

Mailed Thermoluminescent Dosimeter Determination of Entrance Skin Exposure and Half-Value Layer in Mammography

JOHN F. WOCHOS,[1] GARY D. FULLERTON,[1, 2] AND LARRY A. DeWERD[1]

A method of providing in vivo measurement of entrance skin exposure for mammography using mailed thermoluminescent dosimeters has been developed. The dosimeters are calibrated to ^{137}Cs (662 keV), and a correction is applied to account for energy response. A mailed dosimeter packet which can be used to measure the half-value layer at mammography energies is also described. The results for both systems agree well (to within 10%) with careful ion chamber determinations. These dosimeter measurements provide a simple, inexpensive means to reliably determine exposure and to monitor machine parameters on a periodic basis.

The general consensus in the medical profession at present is that the most specific procedure for early breast cancer detection is mammography. However, accompanying recent increases in numbers of mammograms performed per year is a growing concern for long-term effects of radiation [1–3]. This indicates the importance of measuring the radiation to the breast. The many problems associated with the measurement of dose to the breast include the variation in size and composition of breast tissue and the difficulties associated with measurement of low energy x-rays. The most well defined measurement which can be made is the entrance skin exposure. Special ion chambers, which are expensive and require skilled operators, have been designed to accurately measure the exposure at these low energies. The Midwest Center for Radiological Physics, in association with the University of Wisconsin Medical Physics Laboratories, has developed a less expensive, simple procedure to make in vivo measurements of entrance skin exposure. Lithium fluoride thermoluminescent dosimeters are placed on the breast during the mammography examination and then sent to our laboratory for evaluation.

The center initiated this mailed dosimeter service in 1974 as a supplement to annual ion chamber measurements of skin exposure at the four National Cancer Institute/American Cancer Society Breast Cancer Detection Demonstration Projects in the Midwest region. The service provides a good indication of the stability of both machine and procedural factors involved in patient exposure and a direct measure of the patient's skin exposure. Agreement between these values and calculated skin exposure for ion chamber measurements gives confidence in both techniques.

Materials and Methods

Harshaw TLD-100 ribbons 3.2 × 3.2 mm² and either 0.9 mm or 0.4 mm thick were used. About 1,000 dosimeters were initially annealed at 400°C for 1 hr, cooled to room temperature in about 5 min, and then annealed at 80°C for 24 hr. After this initial annealing procedure, the dosimeters were all exposed to about 1 R with a ^{137}Cs source (662 keV γ-ray). The dosimeters were then read with either an Eberline model TLR5 or a Harshaw model 3000 using a nitrogen purge. They were sorted into groups with a sensitivity range of about 2%. After sorting was completed, we no longer identified individual dosimeters, but identified groups or "calibration sets" of at least 25 dosimeters each.

In preparation for mailing, 17 dosimeters from a calibration set were heat sealed in polyethylene (about 0.1 mm thick) to provide ease of handling while maintaining the necessary cleanliness for accurate dosimetry. The mailed packet consisted of 10 individually packaged dosimeters for patient measurements, one sachet of four dosimeters for x-ray machine consistency check, and one sachet of three to monitor background exposure. Simple instructions are sent with the dosimeters.

Five patients are randomly chosen by the technician for exposure monitoring. For each patient, one dosimeter is taped on the beam entrance side, center of the breast, for the craniocaudad view and then another is placed on the beam entrance side of the other breast for the lateral view. The technician records the kilovoltage, amperage, time, source-receptor distance, and approximate breast thickness for each view. This information is returned to the physics center with the dosimeters.

The output consistency of the mammography unit was monitored by exposure of four dosimeters packaged in a single sachet on top of a Lucite cylinder (10 cm diameter, 5 cm thick). The conditions of irradiation (kilovoltage, amperage, time, and tube-to-skin distance) were selected by the radiologist to best represent typical use. These machine settings were repeated for all subsequent consistency measurements.

For each set sent, four to six dosimeters from the same calibration set were exposed to ^{137}Cs. Since the thermoluminescent exposure response is greater at the lower energies used for mammography, an energy correction factor relative to the ^{137}Cs thermoluminescent calibration has to be applied. The energy correction curves (fig. 1) were derived from comparative measurements with a special mammography chamber on an x-ray unit. Energy correction factors have been determined for both 0.9 mm and 0.4 mm thick ribbons, with and without backscatter in each instance. At low photon energies the exposure response of the dosimeters also depends on their thickness due to self-absorption. We used the energy correction factors determined with backscatter from a breast phantom (Lucite

Received March 7, 1978; accepted after revision June 22, 1978.
The Midwest Center for Radiological Physics is supported by contract no. N01-CN-45153 from the National Cancer Institute.
[1] Midwest Center for Radiological Physics, Sterling Hall, University of Wisconsin, 1300 University Avenue, Madison, Wisconsin 53706. Address reprint requests to J. F. Wochos.
[2] Present address: Department of Radiology, University of Texas Health Science Center, San Antonio, Texas 78284.

© 1978 American Roentgen Ray Society

0361–803X/78/1000–0617 $00.00

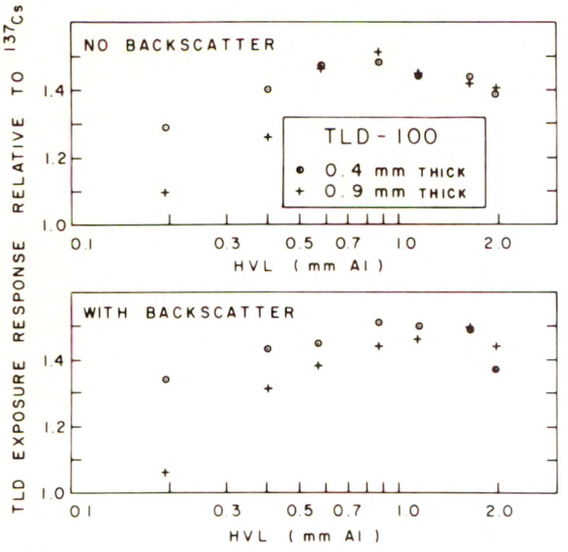

Fig. 1.—Energy correction curves used to correct thermoluminescent reading from mammography exposure to ^{137}Cs calibration exposure. Top curve indicates free in-air measurement; bottom curve indicates measurement with 10 cm diameter backscatter. Uncertainty in these measurements is estimated to be 4%. HVL = half-value layer.

cylinder 10 cm diameter and 5 cm thick) in our calculations. This situation best represents the irradiation conditions during on-patient measurements. The backscatter factors used were obtained from the Northeast Center for Radiological Physics [4]. The extent of the energy dependence variations we determined is in good agreement with those tabulated by several authors, but disagree with the reports of others [5–7]. The energy response of lithium fluoride, especially at these low energies, is not fixed but depends on the history of radiation exposure since the last high temperature anneal (≥ 400°C); this could account for some of the discrepancies [8]. Frequent 400°C annealings were used to avoid this error.

The mailed system was designed to function with minimum time and effort on both ends. The mammography technologist used 10 to 20 min in irradiation of a complete set. About 1 hr is required in our laboratory to read out, anneal, package, and return both the report and new packet to the hospital.

A system to measure beam quality or half-value layer by mail was devised to make dosimeter measurements completely independent of chamber measurements. Measurements were made with three layers of dosimeter chips separated by two 1.0 mm aluminum sheets. The dosimeters were staggered to avoid attenuation by upper layers. This arrangement of dosimeters and aluminum sheets (the half-value layer/thermoluminescent dosimeter package) was selected to give satisfactory results for mammography beam qualities (0.2–1.3 mm Al half-value layers). The dosimeters were indicated as layer 1, 2, or 3, with layer 1 closest to the x-ray source. Calibration exposures for this packet were made on an x-ray unit at various half-value layers. In all calibrations the top layer of dosimeters was exposed to about 2.5 R to provide an adequate signal. The results were analyzed by taking the ratios of layer 2/layer 1 and layer 3/layer 1. These ratios were then plotted against the half-value layer values obtained from good-geometry ion chamber readings (fig. 2). This graph could then be used to determine the half-value layer by mail with minimum time and effort.

On-site measurement of beam quality and exposure in air were made on eight units at four breast cancer detection

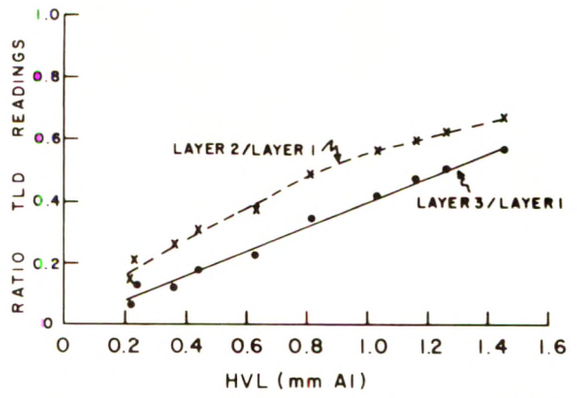

Fig. 2.—Curves used to obtain half-value layer (HVL) from half-value/thermoluminescent dosimeter (TLD) package results.

projects. The ionization chamber used for the measurements was a Memorial Pot Chamber, designed and built especially for mammography at the Department of Medical Physics, Memorial Sloan-Kettering Institute, New York. The sensitivity of the chamber varies less than 2% over the x-ray energy range of 10–30 keV_{eff}. The chamber was calibrated at the New York Regional Calibration Laboratory for beam qualities of 0.22, 1.03, and 1.82 mm Al half-value layers. The same chamber system was used for the dosimeter energy dependence measurements in our laboratory. The procedures used in ion chamber measurements were developed by the Regional Centers for Radiological Physics and are more completely documented in their measurement protocol [9].

Results

The accuracy of the half-value layer/thermoluminescent dosimeter package was about 0.1 mm Al for 18 x-ray units measured subsequent to calibration. This includes molybdenum target and filtered tubes. The best agreement between the ion chamber and the dosimeter measurements for the half-value layer is obtained from the average of the two values from figure 2. The data in figure 1 indicate that an error of 0.1 mm Al in half-value layer determination results in a dosimeter exposure measurement error of less than 10%.

The dosimeter exposure response versus energy correction factor varied from 1.1 to 1.5 with the range of beam qualities observed on the eight mammography units in this study. Thus, using a constant energy correction factor of 1.3, we would have made a maximum error of 20% due to thermoluminescent energy dependence. By using the correction factor for the particular half-value layer, the errors are about 7%. The kilovoltage and filter combination were recorded on a report form returned with the dosimeters each week. The half-value layer for a variety of kilovoltage filter combinations was measured on site with the ion chamber; this half-value layer was used to determine the appropriate energy correction from figure 1.

In each weekly set of on-patient measurements, the results were averaged for each view separately. These exposure averages were plotted as a function of time (fig 3). The exposures and the phantom standard results from some centers were very consistent; from others the

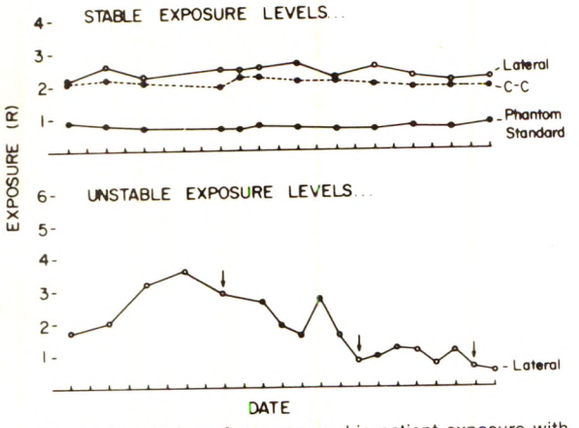

Fig. 3.—Monitoring of mammographic patient exposure with time from two different centers. Upper graph indicates consistent exposures; lower graph indicates inconsistent levels. Each data point is average of five patients.

exposures were high and erratic. The results were very valuable in helping us decide when a particular center should be visited.

A comparison between the on-site chamber measurement and 230 on-patient dosimeter measurements indicated average agreement of 7% for the craniocaudad view and 12% for the lateral view. The ion chamber results were measured with the average kilovoltage and ampere settings used for the dosimeter results.

Discussion

There was some initial concern about making on-patient measurements, since it was felt that the dosimeter might conceal a small grouping of calcifications. As previously mentioned, two dosimeters were used for each patient, one for the lateral and one for the craniocaudad view using opposite breasts to insure that no information was obscured. The dosimeters do appear on the image; however, no radiologist has complained that they interfere with any image in 3½ years of measurements. In addition, we showed that phantom calcifications are visible through the image of a chip.

The reproducibility of mammographic entrance skin exposure measurements, either directly with dosimeter or indirectly with an ionization chamber, is limited by the complexity and variability of irradiation conditions from one patient to the next. We used the following estimates of error to evaluate the accuracy of our measurements: (1) accuracy of ion chamber calibration from Regional Calibration Laboratories, 3.5%; (2) error in dosimeter reading, 2.0%; (3) error in energy correction, 4.0%; and (4) error in reader calibration (roentgen/thermoluminescent reading), 4.0%. When these errors are combined in quadrature, we calculate an overall 7% estimate of error.

The accuracy of ion chamber measurements (3.5%) is much better than dosimeters, but the accuracy of calculated skin exposure is probably worse due to inadequate knowledge of exposure conditions. Therefore, we were pleased to find that dosimeter and ion chamber measurements of entrance breast skin exposure generally agreed within 10%. The dosimeters also have the benefit of being an in vivo measurement. We are able to obtain a measurement of variations in exposure with changes in technique for different patients in both the craniocaudad and lateral projections. For some of the results the dosimeters are a more accurate measure of the surface exposure. For the lateral projection a sponge is often placed under the breast, which results in a different geometry than used for ion chamber measurements. The geometry also changes with the amount of inflation in the compression balloon; thus a single ion chamber measurement will not determine the range of exposures actually encountered. The dosimeters also give the best indication of exposure for phototimed limits.

In conclusion, we have found that mailed dosimeter measurement of patient exposures from mammography is both sufficiently accurate and simple in execution to be a feasible alternative to frequent ion chamber measurements. The system requires effort during the initial stages to insure proper calibration, readout, and handling procedures. Once established, continuing accurate dosimetry is then available via the mailed system.

ACKNOWLEDGMENTS

We thank J. Cameron for his comments; T. Ghilardi-Netto and D. Belden for work on the dosimeter energy calibrations; and M. Piper and M. Van Lysel for dosimeter readings.

REFERENCES

1. Culliton BJ: Breast Cancer: second thoughts about routine mammography. *Science* 193:555, 1976
2. Final reports of National Cancer Institute Ad Hoc Working Groups on Mammography Screening for Breast Cancer and a summary report of their joint findings and recommendations. Department of Health, Education and Welfare publication N(NIH)77-1400, Washington, D.C., Government Printing Office, 1977
3. Lester L G: Risk versus benefit in mammography. *Radiology* 124:1-6, 1977
4. Hammerstein GR, Chen ST, Miller DW: Backscatter factors for mammography (abstr.) *Med Phys* 4:360, 1977
5. Rossiter MJ: Investigation into the use of thermoluminescence measurements for absorbed dose intercomparison in x-ray beams of medium energy. *Radiation Science* report 24, London, National Physical Laboratory, Department of Industry, 1974
6. Attix FH: Basic γ-ray dosimetry. *Health Phys* 15:49–56, 1968
7. Cameron JR, Suntharalingam N, Kenney GN: *Thermoluminescent Dosimetry*. Madison, University of Wisconsin Press, 1968
8. Mayhugh MR, Fullerton GD: Altering the energy dependence of LiF TLDs by pre-irradiation. *Med Phys* 1:275–276, 1974
9. American Association of Physicists in Medicine Coordination Program for the Regional Centers for Radiological Physics, 6900 Wisconsin Avenue, Chevy Chase, Maryland 20015

Benign Multilocal Cystic Nephroma

DAVID H. CARLSON,[1] DESIREE CARLSON,[2] AND HAROLD SIMON[1]

Three cases of multilocular cystic nephroma are described. This entity differs from congenital multicystic kidney and adult polycystic disease in that it involves only a segment of one kidney. While the excretory urogram, nephrotomogram, and arteriogram show the lesion to be primarily avascular, the two cases studied by ultrasound were predominantly solid. This finding is felt to relate to the small size of the cysts as well as the presence of some solid primitive components. Because it is difficult to differentiate this lesion from an avascular renal carcinoma, surgical biopsy should be considered to help avoid a needless nephrectomy.

Segmental cystic disease of the kidney was first described by Edmunds [1] in 1892. He used the term cystadenoma. Since then approximately 70 cases have been reported [2] using a variety of histologic terms. Cystic nephroma [3], multilocular cyst of the kidney [2], polycystic nephroblastoma [4], and differentiated nephroblastoma [5] have all been applied to this lesion, underscoring the controversy over its histogenesis. We feel that the term benign multilocular cystic nephroma applied by Boggs and Kimmelstiel [6] is the most appropriate, since it encompasses both the cystic nature of this tumor and the primitive mesenchymal component frequently found in the intervening septae. If the criteria of Powell et al. [7] are used, only one prior case has been reported in the radiologic literature [8]. Since this tumor is often confused clinically, pathologically, and radiologically with other renal lesions, we feel that these three cases are of great interest.

Case Reports

Case 1

J. H., a 44-year-old female, was hospitalized elsewhere for evaluation of headaches. She was known to have hypertension for 4 years. She was gravida 15, para 11, and aborta four, but her previous medical history was otherwise negative. An excretory urogram and nephrotomogram showed a mass in the lower pole of the left kidney with associated distortion of the adjacent calyx (fig. 1*A*). An abdominal aortogram and left renal arteriogram showed a right renal artery stenosis but no abnormal vascularity in the lower pole of the left kidney (fig. 1*B*). An accessory vessel to the left lower pole could not be catheterized. After signing out against advice, she was subsequently admitted to Newton-Wellesley Hospital with left lower quadrant abdominal pain.

Physical examination was unremarkable. Abdominal gray scale ultrasound showed no evidence of a pelvic mass but again showed an echogenic mass in the lower pole of the left kidney which was felt to be solid (fig. 1*C*). A left lower pole partial nephrectomy was performed after an initial frozen section was interpreted as a hamartoma. In the specimen there was a solid whitish 3 cm mass that was well circumscribed and contained cysts ranging from 0.5–1 cm in diameter. The cysts were filled with clear yellow fluid (fig. 1*D*). The mass impinged on a calyx but did not communicate with it. On histologic examination, the mass was well demarcated and compressed the adjacent normal renal parenchyma. Predominant features were a sparsely cellular fibrous stroma with scattered areas of primitive mesenchyme and abortive small tubules (fig. 1*E*) and large cystically dilated tubules lined by flattened to columnar epithelium. No cartilage, skeletal muscle, or adipose tissue was found.

Case 2

C. B., a 78-year-old female, was admitted because of gross hematuria for 4 weeks with crampy lower abdominal pain. She had been treated for mild hypertension for 10 years. An excretory urogram with nephrotomography done elsewhere showed a large mass in the lower pole of the left kidney with distortion of the lower pole calyces. This was slightly avascular at the lateral margin, suggesting cystic components. Amorphous, flocculent calcifications were seen in the lateral aspect of the lesion (fig. 2*A*). Bistable ultrasound showed echogenic areas, and the mass was felt to be predominantly solid. Abdominal aortography and selective left renal arteriography showed distortion of the vessels of the lower pole but no evidence of tumor vascularity. A preoperative diagnosis of an avascular hypernephroma was made, and a left radical nephrectomy was performed.

At the inferomedial aspect was an encapsulated 8.7 cm predominantly solid multiloculated cystic mass containing clear yellow gel. Larger cysts were present at the lower pole. The remainder of the kidney was normal. The capsule and stroma were sparsely cellular with focal calcification. No metanephric tissue was seen on multiple sections. The cysts were lined by flat to hobnail epithelium and were filled with desquamated cells (fig. 2*B*).

Case 3

K. B., a 63-year-old asymptomatic female, was admitted with a right upper quadrant mass which was palpable on physical examination. Excretory urography showed the mass to occupy most of the lower pole of the right kidney and to distort the calyces (fig. 3*A*). On nephrotomography, the lateral margin appeared to be largely avascular. A right renal arteriogram showed vessels splayed over an avascular lower pole mass (fig. 3*B*). A cyst puncture was attempted but only a few milliliters of serous fluid were obtained.

Laparotomy was performed and again only a few milliliters of fluid could be aspirated on numerous attempts. A right nephrectomy showed the lower pole to be occupied by a 15 × 12 × 6 cm multicystic mass that extended into the hilus with multiple septations. The rest of the kidney was grossly normal. On microscopic examination, multiple cystically dilated tubules in

Received January 4, 1978; accepted after revision June 28, 1978.

[1] Department of Radiology, Tufts University School of Medicine and Newton-Wellesley Hospital, Newton Lower Falls, Massachusetts 02162. Address reprint requests to D. H. Carlson.

[2] Department of Pathology, Newton-Wellesley Hospital, Newton Lower Falls, Massachusetts 02162. Present address: Department of Pathology, Peter Bent Brigham Hospital, Boston, Massachusetts 02115.

© 1978 American Roentgen Ray Society

0361–803X/78/1000—0621 $00.00

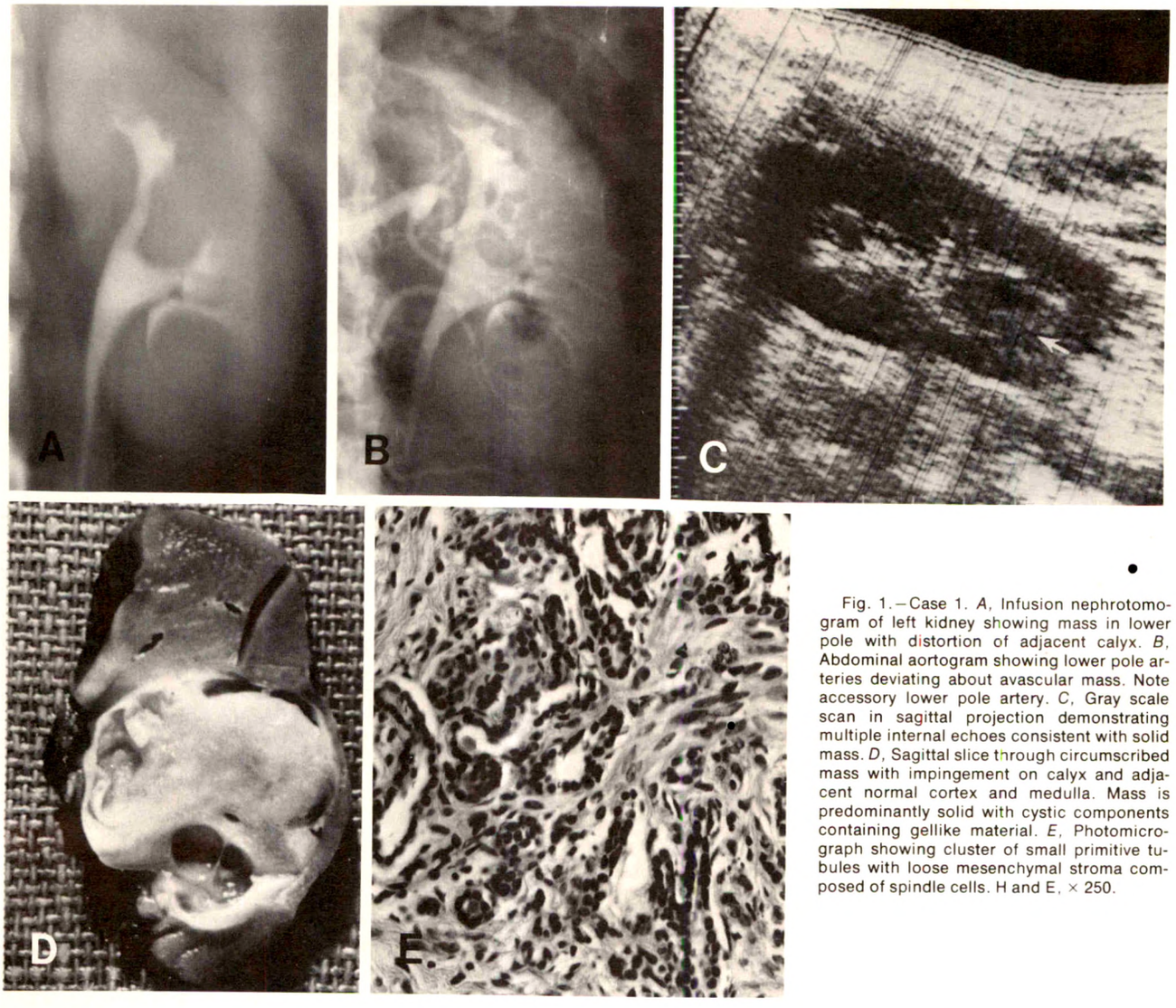

Fig. 1.—Case 1. *A*, Infusion nephrotomogram of left kidney showing mass in lower pole with distortion of adjacent calyx. *B*, Abdominal aortogram showing lower pole arteries deviating about avascular mass. Note accessory lower pole artery. *C*, Gray scale scan in sagittal projection demonstrating multiple internal echoes consistent with solid mass. *D*, Sagittal slice through circumscribed mass with impingement on calyx and adjacent normal cortex and medulla. Mass is predominantly solid with cystic components containing gellike material. *E*, Photomicrograph showing cluster of small primitive tubules with loose mesenchymal stroma composed of spindle cells. H and E, × 250.

a sparsely cellular stroma were found. These were similar in appearance to those in case 2. No metanephric blastema was found in multiple sections.

Discussion

Presentation

While multilocular cystic nephroma is a congenital lesion, in a recent review of the literature only one-half the cases were children [2]. Patients range in age from birth to 71 years. Most of the adults were in the sixth decade. The mean age of presentation in children is 17 months, with an approximately equal sex incidence; a female preponderance is seen in adults. All three of our patients were female. Patients usually present with abdominal mass, pain, hematuria, and rarely hypertension [2].

Diagnosis

Only one of our patients (case 2) showed calcification on plain films. This was of an amorphous, flocculent nature which simulated the calcification seen with renal carcinoma and encouraged the nephrectomy. The only prior case reported, and the only case of multilocular cystic nephroma in the radiologic literature [8], had a similar pattern of calcification. Coincidentally, both patients presented with hematuria, and it could be speculated that intermittent infarction of the cystic mass led to both the calcification and the hematuria.

While all of our cases showed defects in the nephrogram, the presence of thickened capsules in cases 2 and 3 and adjacent areas of solid mass in cases 1 and 2 was atypical for a simple cyst. On occasion, daughter cysts have been found which herniate into the renal pelvis and result in a bizarre configuration [10]. This is shown to a somewhat lesser degree in case 1. All our cases showed calyceal distortion with stretching of the infundibuli in cases 2 and 3.

Arteriography showed deviation and splaying of the vessels about the lesion but no abnormal vasculature. However, in none of these cases could an avascular hypernephroma be excluded.

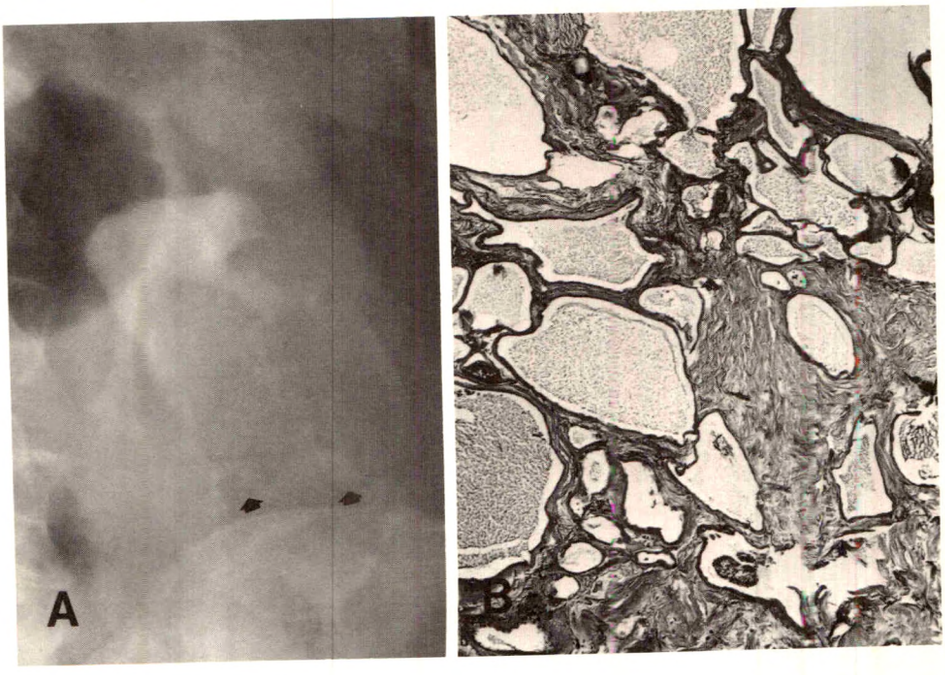

Fig. 2.—Case 2. *A*, Excretory urogram of left kidney demonstrating mass inferomedially. Note somewhat amorphous flocculent calcifications at lower pole (*arrows*). *B*, Photomicrograph showing multiple dilated tubules in predominantly fibrous stroma. H and E, ×40.

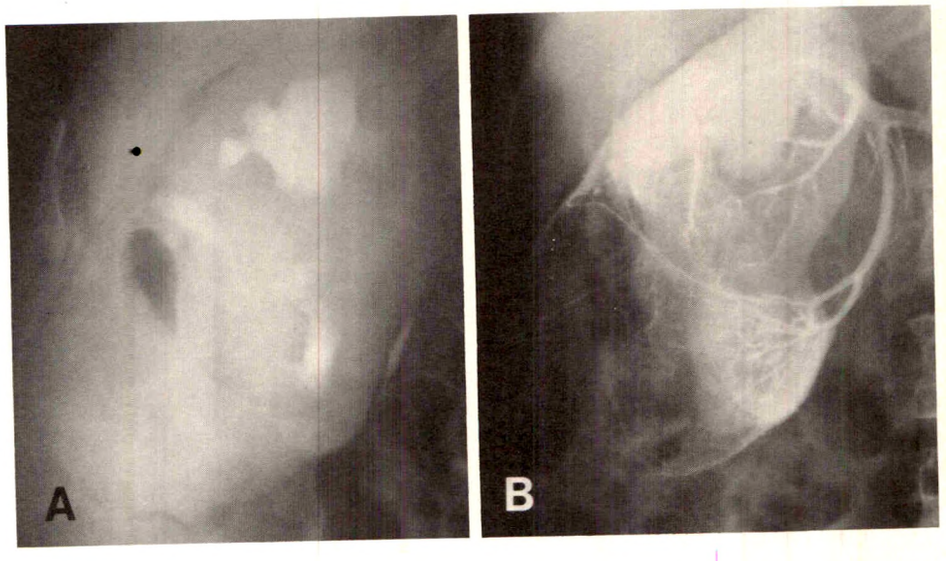

Fig. 3.—Case 3. *A*, Excretory urogram of right kidney showing marked distortion of lower pole calyces with avascular areas inferolaterally. *B*, Right selective renal arteriogram showing lower pole vessels splayed over avascular mass.

Two of our patients (cases 1 and 2) had ultrasonic studies, and in both cases the masses were highly echogenic. This finding increased the likelihood of malignancy and encouraged surgery. The finely cystic structure of these lesions with gellike contents (fig. 2*B*) plus the solid components of embryonic tissue (fig. 1*D* and 1*E*) give these lesions their solid character on ultrasound. The only other case reported with ultrasonic data was primarily sonolucent [9]. Further collection of ultrasonic data on such cases is needed.

In only one patient (case 3) was aspiration of the cyst attempted. This was done both before and during surgery and was unsuccessful. This would corroborate our ultrasonic findings suggesting that the multicystic character of the lesion makes aspiration difficult.

The dilemma of diagnosing these lesions is apparent. Any thick-walled cyst with or without adjacent solid elements with avascularity on arteriogram and an echogenic pattern on ultrasound may represent a multilocular cystic nephroma. Obviously, an avascular hypernephroma cannot be ruled out. Therefore, in cases of this nature we recommend surgical biopsy of the lesion before a potentially unnecessary nephrectomy is performed.

Pathology

In 1951 Powell et al. [7] outlined the criteria for diagnosis of multilocular cystic nephroma. They indicated the cyst should be unilateral, solitary, multilocular, and should not communicate with the pelvis. In addition, the loculi should not communicate with each other and should be lined by epithelium, no renal elements should be present within the main cyst, and remaining renal tissue if present should be normal. Using these criteria,

TABLE 1

Features of Congenital Multicystic Kidney, Multiocular Cystic Nephroma, and Adult Polycystic Disease

	Congenital Multicystic Kidney	Multilocular Cystic Nephroma	Adult Polycystic Disease
Presentation and inheritance	Unilateral; no other congenital anomalies; nonfamilial	Unilateral; no other congenital anomalies; nonfamilial	Bilateral; liver cysts, cerebral aneurysms; familial
Gross pathology	Multiple cysts of varying size which do not communicate with pelvis; entire kidney involved	Multiloculated cyst which does not communicate with pelvis; involves segment of one kidney	Small, uniform cysts communicate with pelvis; entire kidney involved
Microscopic Pathology	Stroma abundant; contains dysplastic tubules, cartilage, and occasional primitive nephrons	Fibrous stroma, some cases may have primitive nephrons in areas of metanephric blastoma	Stroma sparse with interposed normal nephrons
Excretory urography	Nonfunctional kidney	Functioning kidney with segmental mass usually with large or small cystic areas; calyceal and pelvic distortion	Poorly functioning kidney with multiple cysts of varying size; stretching of infundibuli by cysts
Arteriography	Renal artery hypoplastic	Avascular	No increase in vascularity around multiple confluent cysts
Ultrasound	Multiple cysts of varying size	Predominantly solid	Multiple cysts of varying size

multilocular cystic nephroma can be differentiated from multiple simple cysts. This entity is compared with congenital multicystic disease and polycystic kidney disease in table 1.

The gross description of these lesions is classically a well circumscribed mass composed of cysts separated by thin gray-white fibrous septae and filled with clear fluid. Calcification, hemorrhage, and necrosis are not usually found. On microscopic examination, large dilated tubules lined by a flattened to hobnail epithelium are surrounded by a mesenchymal stroma varying in cellularity. There may be scattered clusters of small tubules and undifferentiated metanephric blastema. While these nephroblastomatous areas are most commonly found in infant cases, foci of metanephric blastema were seen in case 1. While in many adult cases only sparse cellular stroma was found, Boggs and Kimmelstiel feel [6] that if multiple sections were taken, more areas of metanephric blastema would be revealed.

Etiology

Several theories have been proposed to explain the pathogenesis of this entity, ranging from a form of unilateral dysplasia [3, 7] to a true neoplasm [4–6, 11]. Osathanondh and Potter [3] placed multilocular cystic nephroma in their type 2 polycystic kidney category as a type of segmental dysplasia. If the kidney is replaced by cystic structures and no normal parenchyma is found, it is called a multicystic kidney. If only a portion is involved, it is called a multilocular cyst. They believe that inhibition of ampullary activity prevents induction of nephrons, causes premature cessation of branching, and is responsible for the conversion of ampullary portions of tubules into cysts. Osathanondh and Potter [3] also described occasional islands of cartilage to help substantiate the dysplastic nature of this lesion. However, other authors who favor a neoplastic theory of origin [6, 11] have not found this dysontogenic cartilage. None of our three cases showed evidence of cartilage.

In comparison, Christ [4] stated that the variability seen may be due to lesions at various stages of development of the embryonic kidney and that the presence of both branched and unbranched tubules is evidence that they arose from the metanephros. He suggested that the well differentiated polycystic form of nephroblastoma is an intermediate or borderline lesion with combined features of nephroblastoma and polycystic kidney disease.

Finally those who believe multilocular cystic nephroma is a neoplasm point to the presence of metanephric blastema forming frustrate glomeruli and tubules and mesenchymal connective tissue found in the cyst septae. Gallo and Penchansky [11] concluded that multilocular cystic nephroma in children is the benign equivalent of nephroblastoma. Boggs and Kimmelstiel [6] pointed out that metanephric elements characteristic of Wilms' tumor but without mitoses make it impossible to explain the cystic portion of the lesion as dilatations of tubules because of nonunion or failure to degenerate in fetal life. Therefore the histogenesis is different from polycystic kidney disease and must be neoplastic, arising from metanephric blastema.

Multilocular cystic nephroma is a childhood disease which is often not detected until adulthood. It should be considered in the differential diagnosis of any renal lesion which appears primarily avascular on the excretory urogram or arteriogram even though it is not sonolucent on ultrasonography or cannot be aspirated. While an avascular hypernephroma cannot be ruled out, multilocular cystic nephroma can easily be diagnosed histologically, and therefore biopsy should be considered to circumvent an unnecessary nephrectomy.

REFERENCES

1. Edmunds W: Cystic adenoma of the kidney. *Trans Pathol Soc* London 43:89–90, 1891–1892

2. Baldauf MC, Shultz DM: Multilocular cyst of the kidney. Report of three cases with review of the literature. *Am J Clin Pathol* 65:93–102, 1976
3. Osathanondh V, Potter EL: Pathogenesis of polycystic kidneys. Type 2 due to inhibition of ampullary activity. *Arch Pathol* 77:474–484, 1964
4. Christ ML: Polycystic nephroblastoma. *J Urol* 98:570–575, 1967
5. Fowler M: Differentiated nephroblastoma: solid, cystic or mixed. *J Pathol* 105:215–218, 1971
6. Boggs LK, Kimmelstiel P: Benign multilocular cystic nephroma: report of two cases of so-called multilocular cyst of the kidney. *J Urol* 76:530–541, 1956
7. Powell T, Shackman R, Johnson HD: Multilocular cysts of the kidney. *Br J Urol* 23:142–152, 1951
8. Brown RC, Cornell SH, Culp DA: Multilocular renal cyst with diffuse calcification simulating renal-cell carcinoma. *Radiology* 95:411–412, 1970
9. Friday RO, Crummy AB, Malek GH: Multilocular renal cyst: angiographic, ultrasonic and cyst puncture findings. *Urology* 3:354–356, 1974
10. Uson AC, Melicow MM: Multilocular cysts of the kidney with intrapelvis herniation of a "daughter" cyst. Report of 4 cases. *J Urol* 89:341–348, 1963
11. Gallo GE, Penchansky L: Cystic nephroma. *Cancer* 39:1322–1327, 1977

Radiographic Features of Ureteral Endometriosis

HOWARD M. POLLACK[1] AND JOHN S. WILLS[2]

The urographic findings in seven patients with ureteral endometriosis were reviewed. These consisted of short strictures (0.5–2.2 cm) located for the most part in that portion of the pelvic ureter projected within 3 cm of the inferior margin of the sacroiliac joint. Although the appearance is judged to be nonspecific, the diagnosis of ureteral endometriosis should be considered in any female patient of child-bearing age who has obstructive uropathy attributable to extrinsic obstruction of the pelvic portion of the ureter.

Endometriosis is a relatively common disease, occurring perhaps in as many as 15% of all women during their menstrual life [1]. Although involvement of the ureters has been said to be rare [2, 3], the growing number of cases reported in the past decade makes that assessment doubtful [4]. There has been little emphasis on the x-ray manifestations of this entity in the radiologic literature, with only one series of patients reported in the past 10 years [5]. We present seven additional cases of this disease, stressing that while the radiographic appearance of the lesion is by itself nonspecific, sufficient suggestive findings exist to permit strong consideration of this diagnosis in the appropriate clinical setting.

Case Material

The seven cases presented in this report were collected over a 9 year period from six different hospitals with a total bed capacity of approximately 2,700. Ages ranged from 31–47 years (average, 41). As far as can be determined, they represent all of the cases of ureteral endometriosis seen at those institutions during this time.

Results

The findings in our seven cases are summarized in table 1. Radiographically, six of the seven showed hydronephrosis and hydroureter on either an excretory urogram or retrograde pyeloureterogram. The degree of dilatation was moderate in two of these and marked in four (fig. 1*A*). In six of the seven cases, an area of narrowing of the ureter was seen; the seventh case showed hydroureter to the SI level, below which the ureter was not well visualized. In these cases, the narrowed segment was located 2–5 cm proximal to the ureterovesical junction (fig. 1*B*). In six patients, it projected below the level of the inferior aspect of the sacroiliac joint, most commonly within 2–3 cm (figs. 2 and 3). In six of the patients, the length of the narrowed segment could be accurately measured (0.5–2.2 cm). In three of the seven patients, medial ureteral angulation was present at the site of the narrowing (fig. 1*B*). The strictures began abruptly and were smooth in five cases (fig. 4); one was gently tapered (fig. 5). No shoulder effect was seen at either end of the lesion in any of the cases. In five cases the lumen of the stenotic area was 1 mm or less in diameter (figs. 1*B* and 4).

Proof of ureteral involvement was obtained at surgery in six of seven patients. The seventh patient, who had bladder endometriosis proved by cystoscopic biopsy, was treated with estrogen-progestin therapy and showed significant decrease in the hydronephrosis and hydroureter over the next 11 months. This phenomenon has been reported previously with ureteral endometriosis [4].

The nature of the involvement (extrinsic versus intrinsic) was specified in the record of six of our patients (table 1). Two patients had endometriosis within the wall of the ureter (cases 1 and 7). Case 1 had extrinsic involvement also. Four patients had only extrinsic involvement. Two of the three patients who had medial angulation of the ureter had extrinsic ureteral involvement; one of these two also had intramural involvement. The third patient did not have surgery.

Discussion

Although involvement of the ureters by endometriosis usually occurs in the presence of widespread pelvic disease, it may also occur without evidence of endometriosis elsewhere [1]. Clues to the presence of ureteral endometriosis include nonspecific flank pain and hematuria present or exaggerated at the time of menstruation [1], pelvic mass [6], previous pelvic or abdominal surgery [6], and nulliparity [6]. At times, however, patients may be asymptomatic. Ages of reported cases have ranged from 25 to 50 years, although one patient was 59 years old [6].

Intrinsic and extrinsic forms of ureteral endometriosis are thought to exist depending on whether the ureter is itself invaded or whether extrinsic pressure alone is present. Stiehm et al. [5] reports a 1:4 ratio of intrinsic to extrinsic involvement. This distinction may be somewhat arbitrary, however, since the depth of involvement in the extrinsic form is seldom corroborated histologically, and the differentiation is rarely apparent clinically [5]. In our experience, we were not able to determine the type of involvement radiologically.

Previous authors have considered the radiologic findings nonspecific. These include hydroureteronephrosis, narrowing of the pelvic ureter [2, 6], and, rarely, an

Received January 24, 1978; accepted after revision June 22, 1978.

[1] Department of Radiology, Hospital of the University of Pennsylvania, 3400 Spruce Street, Philadelphia, Pennsylvania 19104. Address reprint requests to H. M. Pollack.

[2] Department of Radiology, Wilmington Medical Center, Wilmington, Delaware 19899.

© 1978 American Roentgen Ray Society

0361–803X/78/1000–0627 $00.00

TABLE 1

Clinical and Radiological Findings

Case No.	Age (years)	Excretory Urogram	Retrograde Ureterogram	Surgery-Pathology	Diagram
1	42	Marked right hydronephrosis, hydroureter	Severe ureteral stenosis 0.5 cm long 3 cm proximal to ureterovesical junction; medial angulation; mucosa smooth	Endometriosis of ovaries, right fallopian tube, ureteral wall; right ureter enveloped by endometriosis; minimal wall involvement	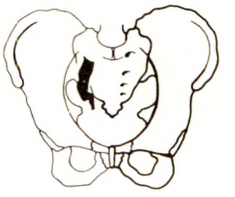
2	31	Marked left hydronephrosis	Abrupt narrowing of ureter with 1.5–2.0 cm long stenosis 5 cm proximal to ureterovesical junction; medial angulation	No surgery; bladder endometriosis by endoscopy; clinical evidence of pelvic endometriosis; significant decrease in hydronephrosis, hydroureter on estrogen-progestin treatment	
3	47	Nonvisualization of right pelvocalyceal system	Severe hydronephrosis and hydroureter; 2 cm long abruptly tapered fusiform stenosis 3 cm proximal to ureterovesical junction; mucosa smooth; lumen 1 mm in diameter	Periureteral endometriosis obstructing ureter	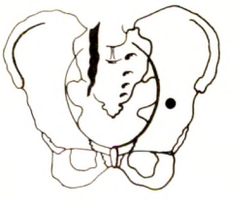
4	40	Severe right hydronephrosis with delayed visualization	Hydroureter to SI level; narrowing 9–10 cm from bladder; mucosa not smooth	Periureteral endometriosis obstructing ureter	
5	37	Moderate left hydronephrosis and hydroureter with abrupt cutoff at level of obstruction	1 cm long ribbonlike flattening of ureter 4–5 cm proximal to ureterovesical junction; medial angulation; mucosa smooth	Periureteral endometriosis obstructing ureter; left ovary and tube involved	
6	43	Nonvisualization of left renal collecting system	Severe left hydronephrosis, hydroureter; 2 cm long abrupt fusiform narrowing 2 cm proximal to ureterovesical junction; mucosa smooth; lumen 1 mm in diameter	Periureteral endometriosis obstructing ureter; diffuse pelvic endometriosis	
7	47	No hydronephrosis; 2.2 cm long area of mild narrowing and poor filling of ureter 4 cm proximal to ureterovesical junction; mucosa smooth	Not done	Endometriosis of rectosigmoid and in wall of ureter	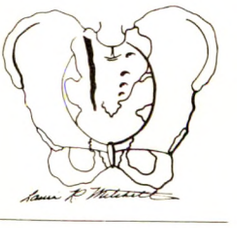

intraluminal ureteral mass [7]. The radiographic appearances in our cases, however, were remarkably similar. With one exception, the involved areas were all located 2–5 cm from the bladder and were short to medium in length (0.5–2.2 cm). The narrowed areas had a predilection for that segment of the pelvic ureter projecting within 3 cm of the inferior aspect of the sacroiliac joint. This corresponds to the approximate location of the

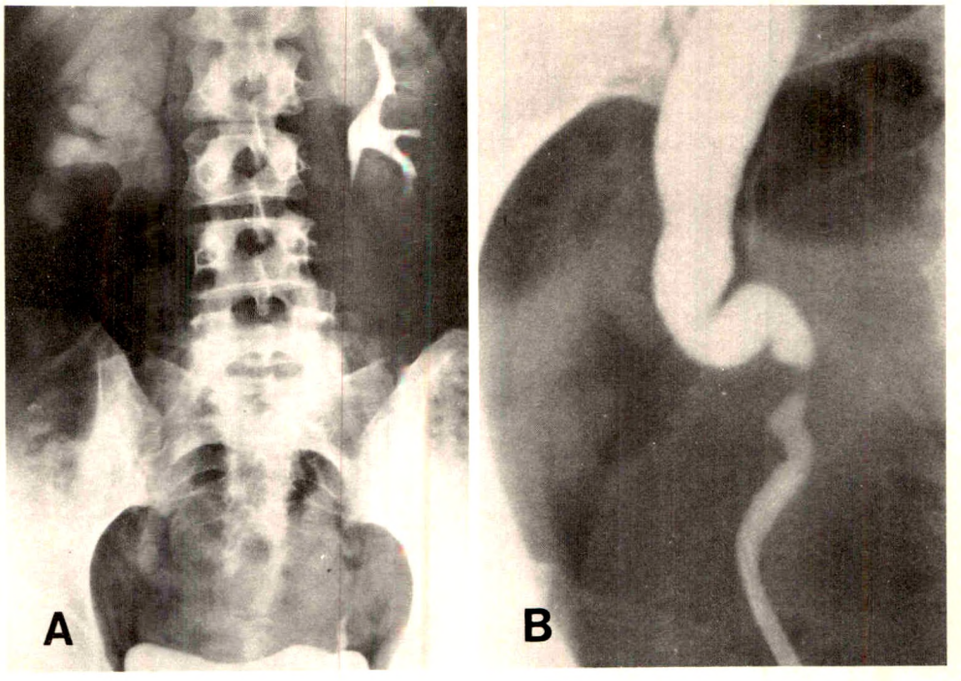

Fig. 1.—Case 1. *A*, Excretory urogram showing severe right hydronephrosis secondary to ureteral obstruction by endometriosis. Detailed visualization of obstructed site not possible. *B*, Retrograde ureterogram by occlusive tip technique revealing short, extremely stenotic stricture 4 cm below and slightly medial to right sacroiliac joint. There is medial displacement. Ureter distal to stenosis is normal. At surgery, ureteral wall was found to be enveloped by endometriosis with little or no mural involvement.

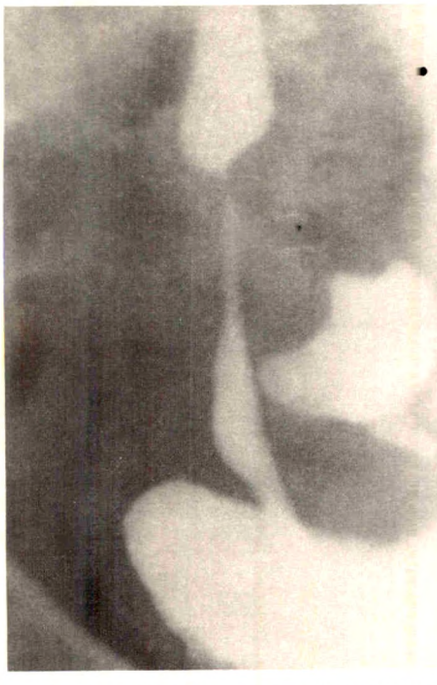

Fig. 2.—Case 3. Retrograde ureterogram showing 2 cm length of ureter constricted by periureteral endometriosis. Stricture is fusiform with tapered margins; mucosa through it is smooth.

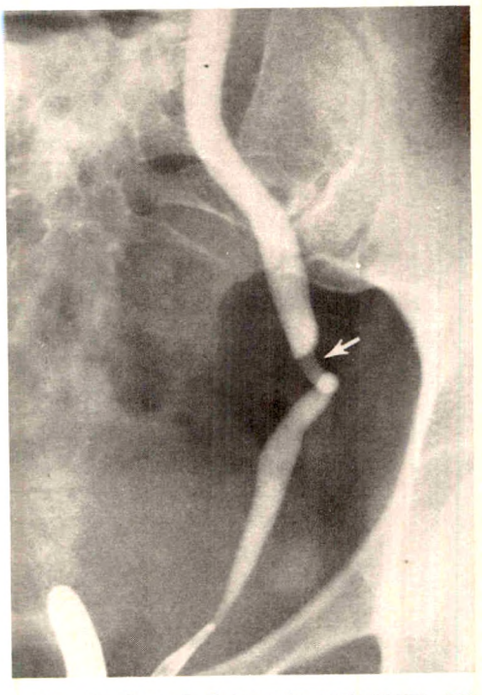

Fig. 3.—Case 5. Retrograde ureterogram performed by occlusive tip technique demonstrating short ribbonlike stenotic area (*arrow*) in left pelvic ureter secondary to periureteral endometriosis. Stricture begins 2 cm below sacroiliac joint and is lined by smooth mucosa. Distal ureter is normal.

posterior attachments of the uterosacral ligaments and correlates well with the known propensity of endometriosis to involve these ligaments both early and extensively (fig. 6). The ureter distal to the diseased segment was normal. Five of the seven strictures were judged to be extremely stenotic, and two were of moderate severity. In keeping with this, the degree of obstructive uropathy was often severe, and one patient had nonvisualization of the pelvocalyceal system on excretory urography. The ureteral strictures characteristically showed smooth, often abrupt tapering but no shoulder effect. The ureteral mucosa was intact in the five cases in which it was clearly demonstrated. Medial angulation of the ureter in

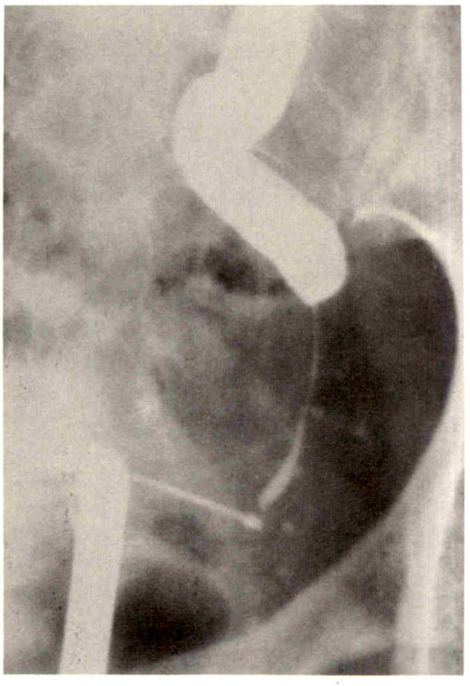

Fig. 4.—Case 6. Retrograde ureterogram with occlusive tip technique revealing 2 cm long filiform stricture of left pelvic ureter with severe proximal obstruction. Mucosa of involved segment is intact. Ureter beyond stricture was normal, its somewhat narrowed appearance attributable to dislodgement of occlusive tip from ureteral orifice. At surgery, periureteral endometriosis was found. This appearance and location are very suggestive of ureteral entrapment by endometriosis.

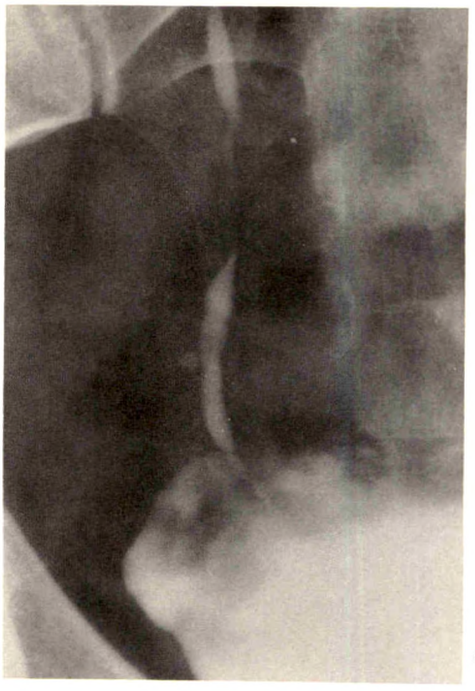

Fig. 5.—Case 7. Excretory urogram showing 2.2 cm long tapered ureteral stricture secondary to mural endometriosis with minimal periureteral involvement. Case 7 was only patient without hydronephrosis.

the region of the narrowed segment in three of our patients has not been described previously and may be due to displacement by an extrinsic mass of endometrial tissue or retraction by fibrosis, which is usually present and often severe in this condition [6, 8].

The excretory urogram was of value in demonstrating the severity of the obstruction, its approximate location, and the laterality of involvement. It also served as a baseline against which posttreatment studies could be compared. Critical assessment of the involved segment of the ureter by urography, however, was possible in only one of these patients. The retrograde pyeloureterogram, on the other hand, was helpful in evaluating the precise location, extent, configuration, and degree of stenosis as well as the appearance of the mucosa in five of the six patients in which it was performed. In the sixth case, it helped localize the area of narrowing. The ability to delineate the above characteristics of the ureteral lesion is of definite value in differential diagnosis, especially in ruling out primary mucosal lesions.

Differential diagnosis includes multiple possibilities; these can be grouped into intrinsic (mucosal or mural) and extrinsic lesions (table 2). Primary carcinomas of the ureter can present as strictures radiologically indistinguishable from endometriosis. However, such tumors are rare in the premenopausal female and, unlike endometriosis, are usually papillary or mucosally destructive.

Tuberculosis may occasionally produce a single short stricture of the ureter, but more commonly the segment of involvement is long and frequently the strictures are multiple. Furthermore, tuberculous changes in the ureter are almost always accompanied by renal or vesical abnormalities. Nonetheless, tuberculosis should be ruled out by the usual microbiologic studies in all cases of otherwise unexplained low ureteral strictures. Nonspecific ureteral strictures can appear similar to endometriosis but are also uncommon. They probably need not be considered seriously in a patient with known endometriosis. The history is valuable in differentiating endometriosis from stricture due to previous surgery, such as ureterolithotomy, or to trauma, such as penetrating injury or stone extraction. If prior hysterectomy has been performed, the possibility of surgical injury to the ureter must, of course, be considered. Since endometriosis often regresses after hysterectomy and iatrogenically produced obstructions do not, a short waiting period may settle this differential point when preoperative urograms are not available for comparison. Amyloidosis may appear as a localized stricture in the distal third of the ureter. However, only six such cases have been reported in females [9], not all of whom were in the premenopausal age group.

Metastatic spread of malignancies of the female pelvic organs, especially the uterine cervix, can be difficult to

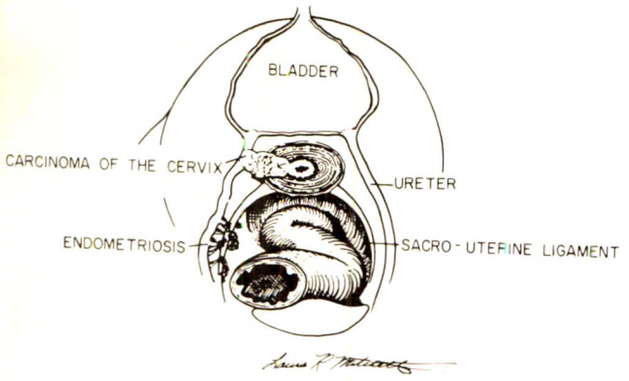

Fig. 6.—Anatomic relationship of ureters to uterosacral ligaments and uterine cervix. Dorsal attachments of uterosacral ligaments are most common site of ureteral involvement by endometriosis. Entrapment of ureters by invasive carcinoma of cervix is frequently confused in differential diagnosis but usually occurs more distally.

TABLE 2

Differential Diagnosis of Ureteral Endometriosis

Intrinsic Lesions	Extrinsic Lesions
Mucosal:	Metastatic spread*
Primary ureteral tumors	Radiation fibrosis
Mural:	Retroperitoneal fibrosis
Stricture:	Tubo-ovarian abscess
Tuberculous	Gastrointestinal inflammatory disease†
Nonspecific	Iliac artery aneurysms
Traumatic	
Amyloidosis	

* Cervix, endometrium, ovary, rectum.
† Appendiceal abscess, granulomatous ileitis, sigmoid diverticulitis.

distinguish from endometriosis on clinical and radiologic grounds. Since the pathway of spread of invasive carcinoma of the cervix is usually directly into the parametria, the ureters tend to become entrapped at a slightly more distal level in this disease than in endometriosis [10] (fig. 6). The picture may be altered if the patient has been previously treated by radiation or surgery. Ureteral strictures following radiation therapy may be attributable to recurrent or residual tumor, radiation fibrosis, or a combination of both. Such strictures may appear either as a localized lesion of the distal ureter or as a long threadlike narrowing of the pelvic ureter [11]. Retroperitoneal fibrosis most commonly produces ureteral obstruction at the level of the lower lumbar spine. The ureter characteristically shows gradual fusiform tapering, and while it is often medially deviated, it may well be in its normal location. A history of methysergide therapy is a helpful differential point. A tubo-ovarian abscess may produce narrowing of the pelvic ureter but is commonly associated with a radiographically visible pelvic soft tissue mass and occasionally by medial displacement of the pelvic ureter [12].

Gastrointestinal inflammation such as an appendiceal abscess, regional enteritis, and colonic diverticulitis can usually be distinguished by the presence of other more typical radiographic manifestations of the disease as well as by the history. Additionally, diverticulitis is uncommon in premenopausal females. Iliac artery aneurysm may produce narrowing of the pelvic ureter, probably partly by compression and partly by an inflammatory fibrous tissue reaction adjacent to the aneurysm. The patient's age and the presence of a pulsatile pelvic mass or bruit are important differential features.

In any patient with suspected endometriosis, it is worthwhile to perform a barium enema examination, since the finding of serosal implants, if present, will provide strong confirmatory evidence of the diagnosis.

ACKNOWLEDGMENT

We thank Dr. Michael Bleshman for permission to use case 7.

REFERENCES

1. Fagan C: Endometriosis: clinical and roentgenographic manifestations. *Radiol Clin North Am* 12:109–125, 1974
2. Berlin L, Waldman I, White FH, McLain CR: Endometriosis of the ureter. *Am J Roentgenol* 92:351–354, 1964
3. Reddy AN, Evans AT: Endometriosis of the ureters. *J Urol* 111:474–480, 1974
4. Lavelle KJ, Melman AW, Cleary RE: Ureteral obstruction owing to endometriosis: reversal with synthetic progestin. *J Urol* 111:665–666, 1976
5. Stiehm WD, Becker JA, Weiss RM: Ureteral endometriosis. *Radiology* 102:563–564, 1972
6. Yates-Bell AJ, Molland EA, Pryor JP: Endometriosis of the ureter. *Br J Urol* 44:58–67, 1972
7. Kaplan JH, Kudish HG: Endometrial obstruction of ureter. *Urology* 3:327–329, 1974
8. Langmade CF: Pelvic endometriosis and ureteral obstruction. *Am J Obstet Gynecol* 122:463–469, 1975
9. Lee KT, Deeths TM: Localized amyloidosis of the ureter. *Radiology* 120:60, 1976
10. Campbell M: *Urology*, 3d ed, vol 2. Philadelphia, Saunders, 1970
11. Aron BS, Schlesinger A: Complications of radiation therapy: the genitourinary tract. *Semin Roentgenol* 9:65–74, 1974
12. Phillips JC: A spectrum of radiologic abnormalities due to tubo-ovarian abscess. *Radiology* 110:307–311, 1974

Inflammatory Cysts of the Pelvic Peritoneum

RICHARD F. LEES,[1,2] PHILIP S. FELDMAN,[3] A. NORMAN A. G. BRENBRIDGE,[1] WILLIE A. ANDERSON,[4] AND ANTHONY J. BUSCHI[1]

Three young women with abdominal distension due to pelvic masses were investigated using ultrasound and conventional radiographic techniques. While the latter revealed masses of soft tissue density arising from the pelvis and displacing bowel, the sonogram indicated the morphologic features of thin-walled multiloculated cysts. They were located entirely within the peritoneal cavity and contained serous to serosanguineous fluid. The mesothelial lined walls were infiltrated with chronic inflammatory cells and were adherent to chronically inflamed fallopian tubes. Although these acquired cysts are familiar to pathologists and gynecologists, the literature contains little information about them.

The investigation of massive abdominal distension is a relatively common clinical and radiological challenge. Recently, at the University of Virginia Hospital, three women presented with steadily increasing abdominal girth due to masses arising from the pelvis. Each mass proved to be a multilocular cyst adherent to chronically inflamed fallopian tubes. The cyst walls consisted of connective tissue stroma infiltrated by chronic inflammatory cells and lined by flattened or cuboidal mesothelial cells. A review of the literature revealed no similar cases. We describe the sonographic and pathologic appearance of the inflammatory cysts of the pelvic peritoneum.

Case Reports

Case 1

A 32-year-old white female, gravida 2, para 2, was investigated for increasing abdominal distension over a 5 month period. During the previous 8 years she had undergone multiple abdominal surgical procedures (cholecystectomy, bilateral ureteral lysis for retroperitoneal fibrosis believed to have been caused by methysergide therapy, bilateral tubal ligation, and exploratory laparotomy). Eight months prior to the present investigation she had been treated for pelvic inflammatory disease.

Abdominal and pelvic examination revealed that the distension was due to a large, soft mass arising from the pelvis to a level slightly above the umbilicus. Radiographs demonstrated a mass of soft tissue density in the lower abdomen and pelvis. Intravenous urography revealed bilateral caliceal dilatation, kinking of the left ureter, and a stricture of the right ureter which were believed to be related to the past ureteral surgery for retroperitoneal fibrosis. The appearances did not suggest retroperitoneal extension of the mass. A barium examination of the upper gastrointestinal tract and small bowel revealed that the mass caused displacement of bowel by extramural pressure but did not appear to involve the wall or lumen. Sonography showed the mass to consist of large, thin-walled cysts arising from the pelvis (fig. 1).

At exploratory laparotomy, multiple thin-walled peritoneal cysts with bilateral hydrosalpinx were found. There were adhesions between the fallopian tubes and the cysts. Total hysterectomy, bilateral salpingo-oophorectomy, and excision of the cysts were performed.

Case 2

A 17-year-old black female, gravida 0, para 0, presented with abdominal distension, discomfort, and a 6 month history of amenorrhea with sporadic vaginal spotting. Prior to being seen at University of Virginia Hospital, she had been treated for gonorrhea and was found to be actively infected again. Physical examination revealed a soft mass arising from the pelvis in the midline and extending above the umbilicus. Radiographic investigation consisted of plain films, intravenous urogram, and barium enema (fig. 2*A*). The soft tissue mass caused neither deviation nor obstruction of the ureters, but displaced the sigmoid colon by extramural pressure; it neither obstructed nor adhered to the bowel itself. A sonogram revealed the mass to consist of a large multiloculated cyst with thin walls (fig. 2*B*).

Laparotomy was performed, and a large, thin-walled, multiloculated, cystic mass was found adherent to the fallopian tubes which were inflamed and clubbed (fig. 2*C*). Total hysterectomy, bilateral salpingo-oophorectomy, and excision of the mass were performed.

Case 3

A 27-year-old white female, gravida 3, para 2, aborta 1, was referred to our institution with a 6 month history of increasing abdominal distension and low back pain. Three years previously she had sustained a gunshot wound to the abdomen which caused multiple perforations of the bowel, requiring a temporary colostomy and ligation of the left external iliac artery. She gave no history of past pelvic inflammatory disease. A large soft mass was found by abdominal and pelvic examination arising from the pelvis and reaching the umbilicus. A plain radiograph revealed a mass of soft tissue density in the lower abdomen, and metallic fragments imbedded in the truncal tissues. Intravenous urography and an upper gastrointestinal and small bowel series indicated no retroperitoneal extension of the mass or pressure effect on the ureter, but did reveal extrinsic displacement of bowel by the mass. A sonogram demonstrated a multiloculated, thin-walled cystic mass (fig. 3).

At laparotomy, a 20 cm diameter multiloculated cystic mass was observed which was densely adherent to the left ovary, fallopian tubes, and sigmoid colon. The fallopian tubes appeared chronically inflamed. A total hysterectomy and bilateral

Received January 27, 1978; accepted after revision May 30, 1978.
[1]Department of Radiology, University of Virginia Medical Center, Charlottesville, Virginia 22901. Address reprints to A.N.A.G. Brenbridge.
[2]Present address: Department of Radiology, Queen Elizabeth Hospital, Woodville, South Australia 5011, Australia.
[3]Department of Pathology, University of Virginia Medical Center, Charlottesville, Virginia 22901.
[4]Department of Obstetrics and Gynecology, University of Virginia Medical Center, Charlottesville, Virginia 22901.

© 1978 American Roentgen Ray Society

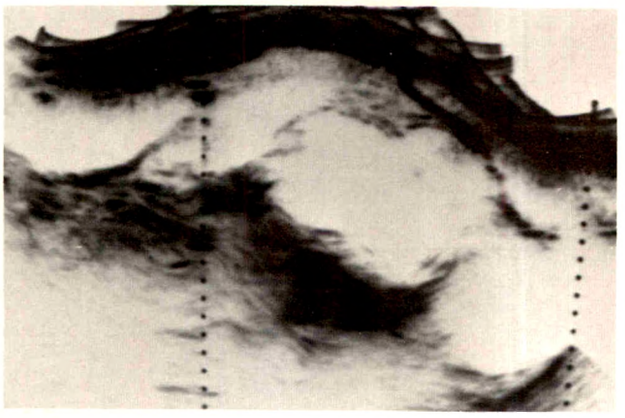

Fig. 1.—Case 1. Sagittal section demonstrating thin-walled cysts extending above umbilicus.

salpingo-oophorectomy were performed, and the cysts were dissected from adherent bowel and removed.

Findings

Pathologic Description

At gross dissection the three cases were characterized by cysts which varied in size, the two largest being 20 and 24 cm and the smallest 5 cm at greatest dimension. Some locules of each specimen were punctured intentionally by the surgeons, and therefore the dimensions of the masses in vivo were larger than when seen postoperatively. They were multiloculated and contained translucent to serosanguineous fluid. No papillary excrescences were found. Adhesions between the cysts and fallopian tubes were present in all three cases, but there was no communication between the lumina of the tubes and the cysts. The lesions were neither paratubal nor paraovarian cystic embryonic remnants of mesonephric origin. The ovaries were unremarkable.

At microscopic examination, the multiloculated cysts were characterized by walls lined by cuboidal to flattened mesothelial cells (fig. 4). Lining cells were absent in focal regions. The cyst walls contained collections of lymphocytes, capillaries, and occasional foam cells within a matrix of loose connective tissue. There was no evidence of granulomatous inflammation or of malignancy. In all three cases, sections of the fallopian tubes demonstrated chronic salpingitis with collections of plasma cells. The ovaries showed no significant microscopic changes.

Radiographic and Sonographic Features

In common with most mass lesions which do not contain calcium, fat, or gas, and do not erode bone, these cysts lacked specific radiographic features. Intravenous urography revealed neither ureteric obstruction nor deviation to indicate retroperitoneal extension of the mass, nor was there evidence of marked extrinsic pressure on the ureters. Contrast studies of the small bowel and colon revealed only an extramural mass causing displacement of the lower intestine. Considerable supplementary anatomic detail was provided by sonography. Each mass was shown to be a thin-walled multiloculated cyst. No mass of solid tissue was identified, and there was no evidence of solid or particulate matter within the locules. The individual locules of each lesion were irregular in shape and varied from 1 to 16 cm in size. In each case the pelvis was occupied by the mass which rose into the abdomen from behind the bladder.

Discussion

Although they have received scant attention in the medical literature, such peritoneal cysts are familiar to both pathologists and gynecologic surgeons. The etiology and pathogenesis of these cysts are uncertain, but the presence of concurrent chronic salpingitis and the similar pathologic features in all three cases suggest an inflammatory origin. These are not hydrosalpinges, as no communications were demonstrated between the cysts and the lumina of the fallopian tubes, and they were located entirely within the peritoneal cavity, originating in the pelvis and extending into the abdomen. These cysts did not appear to be congenital mesonephric cystic remnants, differing from the latter by their size, multiloculated structure, and inflammatory component [1]. It is uncertain, however, whether these cysts originate from embryologic rests.

There are numerous causes for masses of radiographic soft tissue density which lack the natural contrast agents, fat, calcium, and gas. They may be either solid or fluid-filled cysts. By demonstrating the cystic nature and the pelvic and lower abdominal position of the mass by sonography, the diagnostic possibilities are reduced. Among the most difficult to confirm are mesenteric, omental, and retroperitoneal cysts. These masses may all present as abdominal distension of varying rapidity of onset and with such symptoms as pain, nausea, constipation, or diarrhea. Sometimes the only complaint is mild discomfort, and the patient may be totally asymptomatic. Mesenteric and omental cysts are usually found to be soft and mobile on physical examination. Mesenteric cysts are somewhat more common in females than in males and occasionally occur at the extremes of age. Retroperitoneal position may be indicated by ureteric deviation on the intravenous urogram [2–9].

The differential diagnostic consideration of gravest clinical concern is cystic ovarian neoplasms, benign or malignant, which may present with similar radiographic and sonographic features. The sonographic appearance of cystic lymphangiomatosis, recently described by Walsh et al. [10], may be similar and may present clinically with abdominal distension. Neuhauser [11] described a thin-walled peritoneal cyst, probably of lymphatic etiology, which arose from the liver surface in a young child who presented with abdominal distension. Sonography was not performed, but such a cyst may have a similar appearance. Several authors have suggested that duplication of the bowel, hydatid cyst (presumably with many daughter cysts), pancreatic pseudocyst, and congenital pancreatic cysts should also be regarded as alternative diagnoses to mesenteric cyst and therefore may be considered in the differential diagnosis

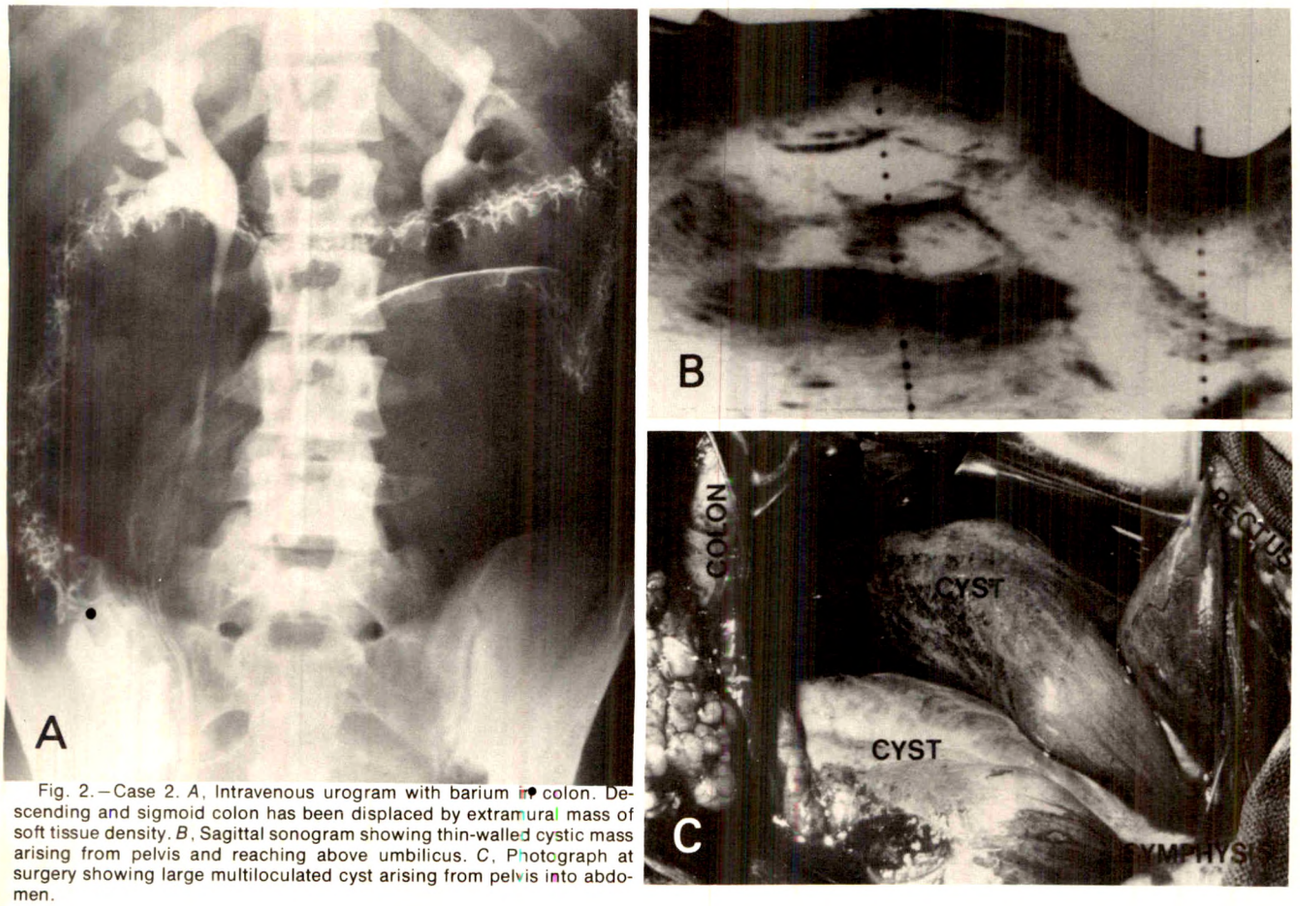

Fig. 2.—Case 2. *A*, Intravenous urogram with barium in colon. Descending and sigmoid colon has been displaced by extramural mass of soft tissue density. *B*, Sagittal sonogram showing thin-walled cystic mass arising from pelvis and reaching above umbilicus. *C*, Photograph at surgery showing large multiloculated cyst arising from pelvis into abdomen.

Fig. 3.—Case 3. Sagittal sonogram. Thin-walled multicystic mass extends from pelvis to umbilicus.

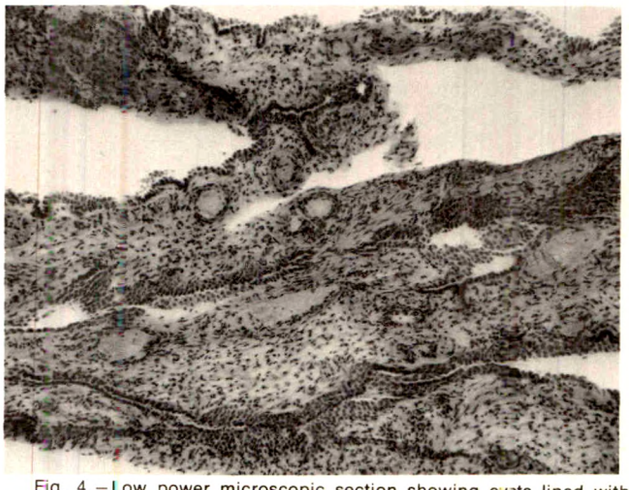

Fig. 4.—Low power microscopic section showing cysts lined with mesothelial cells. Fibrous stroma and inflammatory cells are in cyst walls.

of inflammatory peritoneal cysts [4, 8]. All of these differential considerations may have calcifications in their walls. Apart from ovarian neoplasms, such conditions would most commonly present as abdominal masses, rather than masses entering the abdomen from the pelvis.

The cystic or solid nature of a soft tissue mass within the abdomen and pelvis can be determined using ultrasound. While a multiloculated, thin-walled mass arising from the pelvis cannot be confirmed as neoplastic using sonography, pelvic peritoneal inflammatory cysts must be included among the diagnostic possibilities, especially if the patient has a history of pelvic inflammatory disease.

REFERENCES

1. Krause FT: *Gynecologic Pathology*. St. Louis, Mosby, 1967
2. Shackelford GD, McAlister WH: Cysts of the omentum. *Pediatr Radiol* 3:152–155, 1975
3. Caropreso PR: Mesenteric cysts. *Arch Surg* 108:242–246, 1974
4. Mittelstaedt C: Ultrasonic diagnosis of omental cysts. *Radiology* 117:673–676, 1975
5. Ford JR: Mesenteric cysts: review of the literature with report of an unusual case. *Am J Surg* 90:878–884, 1960
6. Rifkind K, Eng K, Ruoff M: The radiology corner—mesenteric cyst. *Am J Gastroenterol* 62:540–544, 1974
7. Tykka H, Koivuniemi A: Carcinoma arising in a mesenteric cyst. *Am J Surg* 129:709–711, 1975
8. Gordon MJ, Sumner TE: Abdominal ultrasonography in a mesenteric cyst presenting as ascites. *Gastroenterology* 69:761–764, 1975
9. Nordshus T, Lotveit T: Multiple mesenteric cysts diagnosed by ultrasound. *Ann Chir Gynaecol* 65:234–238, 1976
10. Walsh J, Taylor KJW, Rosenfield AT: Gray scale ultrasonography in retroperitoneal lymphangiomyomatosis. *Am J Roentgenol* 129:1101–1102, 1977
11. Neuhauser EBD: Intraperitoneal cyst. *Postgrad Med* 46:65–67, 1969

Pitfalls of Transhepatic Portal Venography and Therapeutic Coronary Vein Occlusion

WARREN C. WIDRICH,[1] ALAN H. ROBBINS,[1] DONALD C. NABSETH,[2] WILLARD C. JOHNSON,[2] AND SUSAN A. GOLDSTEIN[1]

Coronary vein occlusions via transhepatic portography for bleeding esophageal varices was attempted in 24 patients. Problems occurred that either prevented the attempt or resulted in less than adequate occlusion. These included blood flow in the left gastric (coronary) vein toward the liver due to occluded or stenotic splenorenal shunts, spontaneous left gastric vein to inferior vena cava shunts, and failure of powdered Gelfoam and heat-treated autogenous clot to cause permanent occlusion. Of 89 total transhepatic portographies, 65 for diagnosis and 24 for occlusion, major complications occurred in two.

Percutaneous transhepatic portal venography using the right midaxillary approach was first performed by Wiechel [1, 2]. Lunderquist and others, using this technique for coronary vein catheterization and occlusion of bleeding esophageal varices, introduced it into the United States where it has been performed in several medical centers and found to be quite effective [3–5]. In using this approach for coronary vein occlusion in patients bleeding from esophageal varices, we encountered several problems that prevented us either from attempting occlusion of the coronary vein or achieving adequate results. This paper relates these problems so that they may be anticipated.

Subjects and Methods

The technique of percutaneous transhepatic portal venography has been reported [3, 6]. Of 89 transhepatic portal venograms performed on 62 patients since June 1974 at the Boston Veterans Administration Hospital, 65 diagnostic studies were performed on 38 patients who were candidates for or who had undergone distal selective Warren-type splenorenal shunts for elective control of bleeding varices from portal hypertension. Coronary vein (left gastric and short gastric veins) occlusion was attempted in the other 24 patients documented by endoscopy to be bleeding from esophageal varices due to alcoholic cirrhosis and portal hypertension. In 19 of these 24 patients, occlusions were performed using a no. 2 French Fogarty balloon catheter in two, heat-treated autogenous clot and powdered Gelfoam in 10, and Gelfoam strips soaked in 3% sodium tetradecyl sulfate (Sotradecol) in seven.

Results

Problems in Attempting Occlusion

Occlusion of all coronary veins was achieved in 19 of the 24 patients. In five patients, this procedure could not be completely performed. Although the desirability of occluding all the coronary veins has been stated, the problem presented by spontaneous portosystemic anastomoses from these veins directly to the inferior vena cava and the portal vein has not been presented previously [4, 5, 7]. A spontaneous shunt from the coronary vein directly to the inferior vena cava was seen in three of our 62 patients. Selective left gastric venography in three other patients showed direct communication with the left portal vein via a branch going along the lesser curvature of the stomach (fig. 1).

Occluded or stenotic splenorenal shunt occurred in five patients (two had their surgical shunts performed at other hospitals). Because of the change in pressure relationships and the re-reversal of flow in three of these patients, coronary vein occlusion was not attempted.

Effectiveness of Occlusion

Of the 24 patients, 19 had occlusion of all major coronary veins. Nine patients were actively bleeding (bright red blood in the nasogastric aspirate) (table 1). Varices in the distal esophagus had been established at endoscopy. In most of these patients, the blood was seen coming from the varices. These nine patients were failures of Pitressin therapy and Sangstaken-Blakemore tube insertion and were all in Child's class C [8].

Ten patients were not actively bleeding, but had bled usually within 2–3 days prior to the procedure (table 2). Many of these patients had been actively bleeding, but when they reached the angiography suite, their nasogastric aspirate did not contain red blood. In others who were candidates for splenorenal shunt procedure, the surgeons wanted a measure of assurance that they would not rebleed prior to surgery.

Three kinds of occlusive material were used: balloon catheters, Gelfoam and autologous heat-treated clot, and Gelfoam soaked in sodium tetradecyl sulfate. Balloon catheter occlusions of the coronary vein were performed in two patients (tables 1 and 2). One of the patients bled again 11 months later. His left gastric vein was completely patent at that time.

A combination of Gelfoam and heat-treated autogenous clot was used in 10 patients to control variceal bleeding (tables 1 and 2). Embolization with these materials stopped active variceal bleeding in four of five patients (table 1). Of the five recent but inactive bleeders,

Received October 5, 1977; accepted after revision June 20, 1978.
Presented at the annual meeting of the American Roentgen Ray Society, Boston, September 1977.
[1] Department of Radiology, Tufts University School of Medicine and Boston Veterans Administration Hospital, 150 South Huntington Avenue, Boston, Massachusetts 02130. Address reprint requests to W. C. Widrich.
[2] Department of Surgery, Tufts University School of Medicine and Boston Veterans Administration Hospital, Boston, Massachusetts 02130.

© 1978 American Roentgen Ray Society

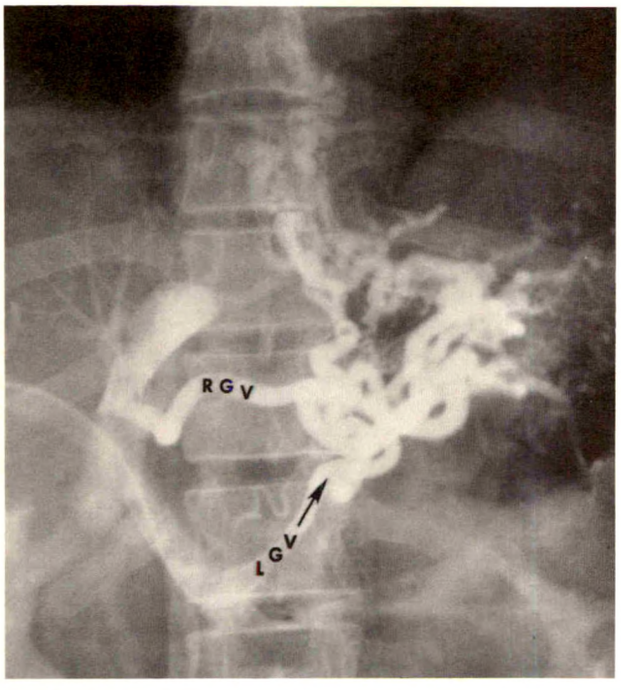

Fig. 1.—Left gastric venogram showing communication to left portal vein via collateral going to lesser curvature of stomach that may represent right gastric vein (RGV).

bleeding recurred in two, 8 days and 4 months, respectively, after embolization.

Gelfoam soaked in 3% sodium tetradecyl sulfate was used in three patients actively bleeding and in four patients not actively bleeding. Bleeding documented by endoscopy to be coming from varices recurred in one patient 2 hr after occlusion; endoscopy was not repeated. Autopsy examination showed a large duodenal ulcer and Gelfoam thrombus in the esophageal varices. None of the other six patients (active or recent bleeders) have had recurrent bleeding.

Complications

Complications of the transhepatic portal vein catheter technique in 89 cases were major in two instances. One patient with severe coagulation factor deficiencies bled profusely from esophageal varices despite Pitressin infusions and the positioning of a Sangstaken-Blakemore tube. He was considered a prohibitive surgical risk. Since no other alternative remained, transhepatic occlusion of the varices was requested. When the catheter was removed from the liver, significant bleeding into the peritoneal space occurred. The other patient had tense ascites. The procedure was uneventful, but right pleural effusion occurred several hours afterward. This was treated with chest tube insertion and decompression of the ascites.

Thrombus in the portal vein occurred in two patients with spontaneous resolution of the thrombus in one. Neither had clinical or hepatic deterioration as a result.

The right colon was entered in three patients and the duodenum in one, all of whom had marked atrophy of the right lobe of the liver. All four patients were treated with antibiotics; two of these developed a fever which disappeared within 24 hr. The biliary system was entered in 30 patients without evidence of bile leakage afterward. The hepatic artery was entered in five patients without adversity.

Illustrative Case Reports

Case 1: Spontaneous Shunt to Inferior Vena Cava

H. O. bled from varices 2 days prior to coronary vein occlusion. A short gastric vein and the smaller of two left gastric veins were occluded with Gelfoam and autogenous clot (fig. 2*A*). However, when the remaining large left gastric vein was catheterized, selective venography showed a large spontaneous shunt directly into the inferior vena cava (fig. 2*B*). This shunt was seen much better on cine than on cut films and was confirmed by Ethiodal injection. The catheter could not be advanced beyond the shunt because of extensive hepatic fibrosis inhibiting catheter maneuverability. Occlusion of this vein was deferred.

Case 2: Occluded Splenorenal Shunt

D. P. had hematemesis 6 weeks after splenorenal shunt surgery. Left renal venography and splenic arteriography showed that the shunt was occluded. A transhepatic occlusion of the coronary vein (which was not ligated at surgery because of ascites) was attempted. However, selective left gastric venography with cine recordings of aqueous contrast and Ethiodol droplet injections showed that the flow in the left gastric vein was toward the liver. Occlusion of this vein was deferred.

Case 3: Stenotic Splenorenal Shunt

H. C. had hematemesis 2 years after a splenorenal shunt had been performed; because of technical difficulties the splenorenal anastomosis had been made end-to-end. A no. 7 French polyethylene catheter was passed up the inferior vena cava into the left renal vein, and then through the stenotic anastomosis. Pressure in the splenic vein measured 44 cm saline. A transhepatic portal vein catheterization was performed and pressure in this vein measured 30 cm saline. Splenic venography showed filling of the gastroesophageal varices through the short gastric veins (fig. 3*A*). The portal vein opacified on this injection via an unligated left gastric vein and collaterals to the surgical stump of the splenic vein. Portal venography showed filling of some of the collaterals from the splenic stump with late wash-out toward the portal vein, indicating a preferential direction of flow from the splenic venous system to the portal vein (fig. 3*B*). The left gastric vein did not visualize. Embolization of the left gastric vein was deferred.

Case 4: Balloon Occlusion

O. F. had recurrent bleeding from esophageal varices 2 weeks after a splenorenal shunt was performed. Because of the desperate clinical situation, a left gastric vein occlusion was requested. Left renal venography suggested that the shunt was occluded. Transhepatic left gastric venography opacified esophageal and gastric varices (fig. 4*A*). A no. 2 French Fogarty balloon catheter was introduced and inflated to 4 mm, its maximum diameter (fig. 4*B*). The catheter was left in place for 16 hr, then withdrawn. Portal venography showed occlusion of the left gastric vein; however, a thrombus in the portal vein incompletely occluded it (fig. 4*C*). The bleeding stopped and no clinical or hepatic deterioration occurred as a result of the portal vein thrombus. The patient was discharged from the

TABLE 1

Coronary Vein Occlusions in Portal Hypertensive Patients Actively Bleeding from Esophageal Varices

Type of Occlusion and Patient	Platelet Count/mm³	Prothrombin Time (sec above control)	Partial Thromboplastin Time (sec above control)	Occlusion Successful	Follow-up
Balloon catheter:					
O.F. (case 4)	88,000	4	7	Yes	Thrombus in portal vein; follow-up study 6 months later showed that thrombus had disappeared; patient underwent splenectomy
Heat-treated clot and Gelfoam:					
W.L.	117,000	2	3	Yes	Has not rebled (26 months)
C.S.	25,000	4	7	Yes	Did not rebleed; died 4 days later due to multiple system failure (liver, kidneys, and lungs)
W.O.	33,000	6	30	Yes	Did not rebleed; died 6 days later due to multiple system failure
M.C.	54,000	4	2	Yes	Did not rebleed; died 2 weeks later due to multiple system failure
N.C.	175,000	5.5	11	No	Failure of treatment; patient died 1 day later
Gelfoam soaked in sodium tetradecyl sulfate:					
J.M.	103,000	7	23	Yes	Did not rebleed; died 11 days later due to multiple system failure; autopsy showed well established thrombus in varices
T.M.	50,000	4	14	Yes	Has not rebled (8 months)
A.C.	80,000	2	10	Yes	Rebled 2 hr later and exsanguinated; autopsy showed large duodenal ulcer and Gelfoam thrombus in varices

Note. – All patients were child's classification C.

TABLE 2

Coronary Vein Occlusions in Portal Hypertensive Patients with Recent Bleeding from Esophageal Varices

Type of Occlusion and patient	Child's Classification	Follow-up
Balloon catheter:		
C.R.	C	Rebled 11 months later; left gastric vein was patent
Heat-treated clot and Gelfoam:		
J.M.	C	Rebled 4 months later; left gastric vein was patent
R.P. (case 5)	C	Did not rebleed; left gastric vein was patent at surgery 2 months later
G.T.	C	Did not rebleed; left gastric vein was patent at surgery 2 months later
E.N.	C	Rebled 8 days later
H.M.	C	Has not rebled (14 months)
Gelfoam soaked in sodium tetradecyl sulfate:		
S.M.	C	Has not rebled (13 months)
W.W.	B	Has not rebled (8 months)
P.L.	C	Has not rebled (7 months)
C.L.	B	Has not rebled (6 months)

Note. – Patients were not actively bleeding.

hospital 3 weeks later. Follow-up transhepatic portography 6 months later showed that the thrombus in the portal vein had totally disappeared (fig. 4*D*). The coronary vein did not opacify. The splenorenal shunt was occluded.

Case 5: Occlusion with Gelfoam and Autologous Heat-treated Clot

R. P. had transhepatic portal venography in preparation for an elective splenorenal shunt (fig. 5*A*). Left gastric vein occlusion was requested by the surgeons to insure that bleeding would not recur before surgery. After the left gastric vein was catheterized, occlusion was achieved by injecting 0.5 ml autogenous heat-treated clot alternately with 0.5 ml Gelfoam at 5 min intervals until the varices no longer opacified with test injections of contrast material. Portal venography after occlusion showed opacification of the coronary vein stump (fig. 5*B*). Because of intermittent hepatic encephalopathy, the patient did not undergo splenorenal shunt until 2 months after occlusion. Surgical portal venography showed that the occlusive material in the left gastric vein had totally disappeared (fig. 5*C*).

Discussion

Before embolization of the coronary veins is undertaken, it is important to perform endoscopy to attempt documentation that the varices are indeed the source of bleeding and that other possible sources of bleeding, such as duodenal or gastric ulcers, are eliminated. Selective left gastric venography is important before embolization. Spontaneous shunts between the left gastric vein directly entering the inferior vena cava occurred in three patients and might have resulted in emboli going directly to the pulmonary arteries had these materials been injected. Additional venous communications from the left gastric vein to the left portal vein along the lesser curvature of the stomach may be venous analogues to the

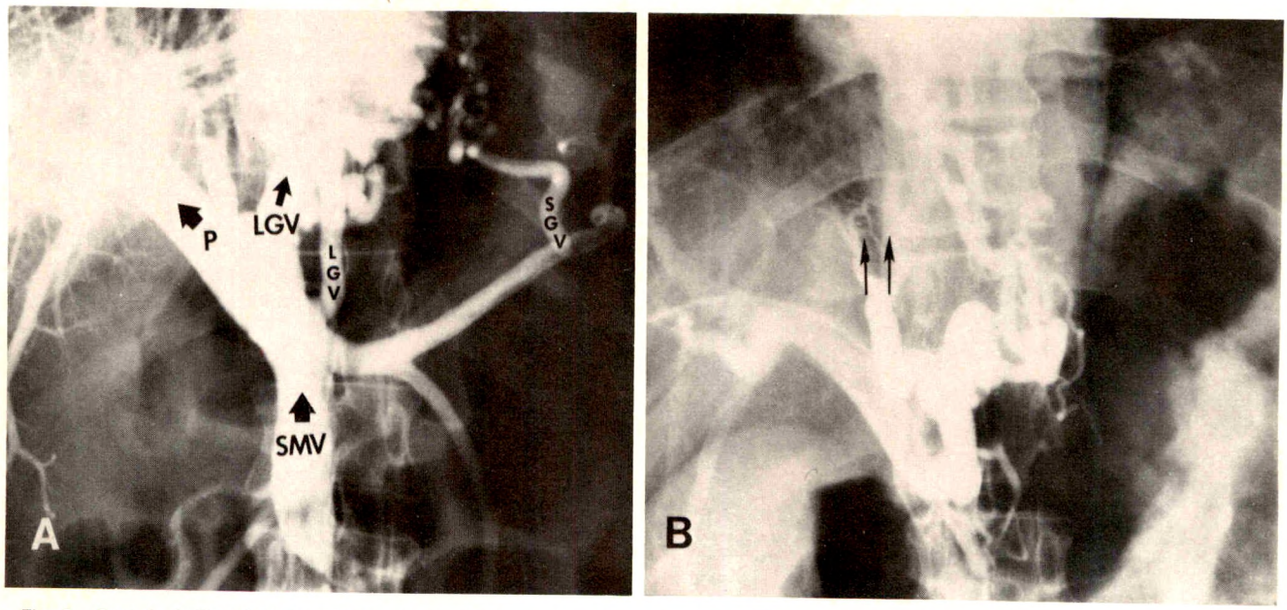

Fig. 2.—Case 1. *A*, Transhepatic splenic venogram showing two left gastric veins (LGV) and short gastric vein (SGV). *B*, Selective left gastric venogram showing direct communication to inferior vena cava (*between arrows*) best demonstrated on cine.

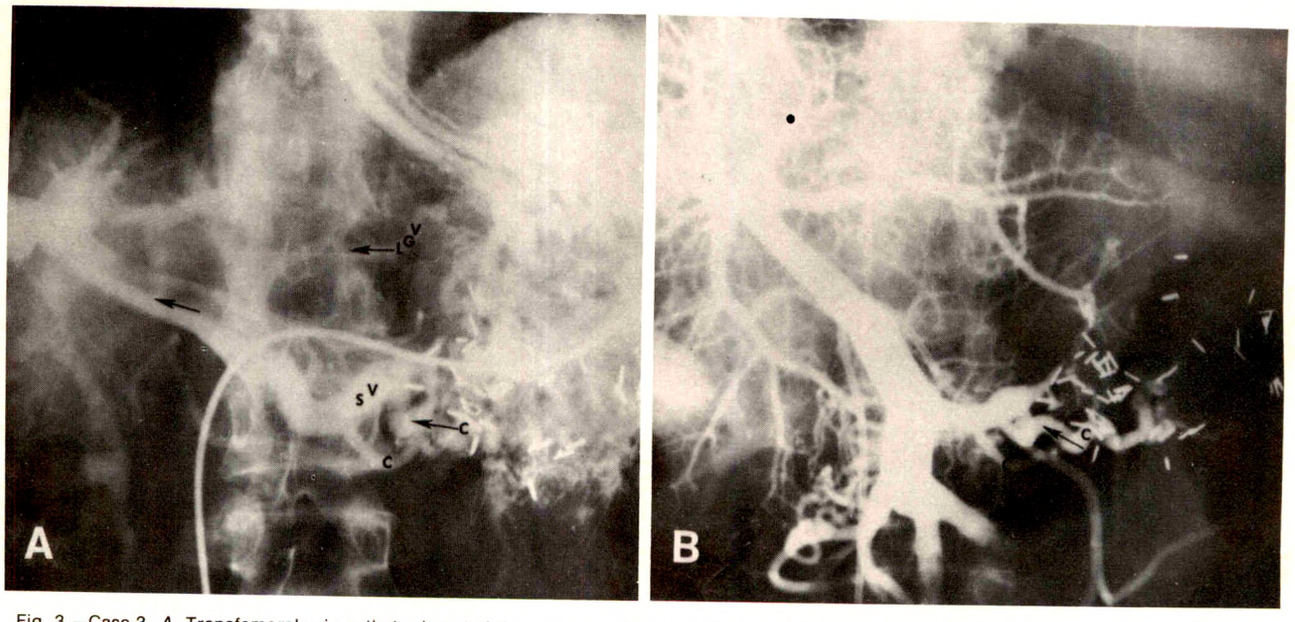

Fig. 3.—Case 3. *A*, Transfemoral vein catheter inserted through stenotic splenorenal shunt showing filling of esophageal varices. Left gastric vein flow is toward liver. Stump of splenic vein (SV) fills via collaterals (C). *B*, Transhepatic portal venogram does not show left gastric vein because it is now filled with non-contrast-laden blood.

right gastric artery. Embolization to the portal vein could be a potential complication. While the above described communications from the left gastric vein have been reported in cadaver specimens, these findings have not been previously demonstrated angiographically in living patients [9, 10].

Blood flow toward the liver occurs in the left gastric vein when the pressure in the splenic venous system considerably exceeds the pressure in the portal vein. This occurs when a splenorenal shunt becomes occluded or severely stenotic. In one patient with the stenotic shunt, we compared the splenic vein pressure with that in the portal vein. When the no. 7 French catheter was passed through the tightly stenotic shunt, it essentially created the situation that occurs when the shunt occludes. Because the splenic vein pressure (44 cm saline) was higher than the portal vein pressure (30 cm saline), there was flow toward the liver through the unligated left gastric vein. The varices, which could be readily demonstrated by splenic venography, were prob-

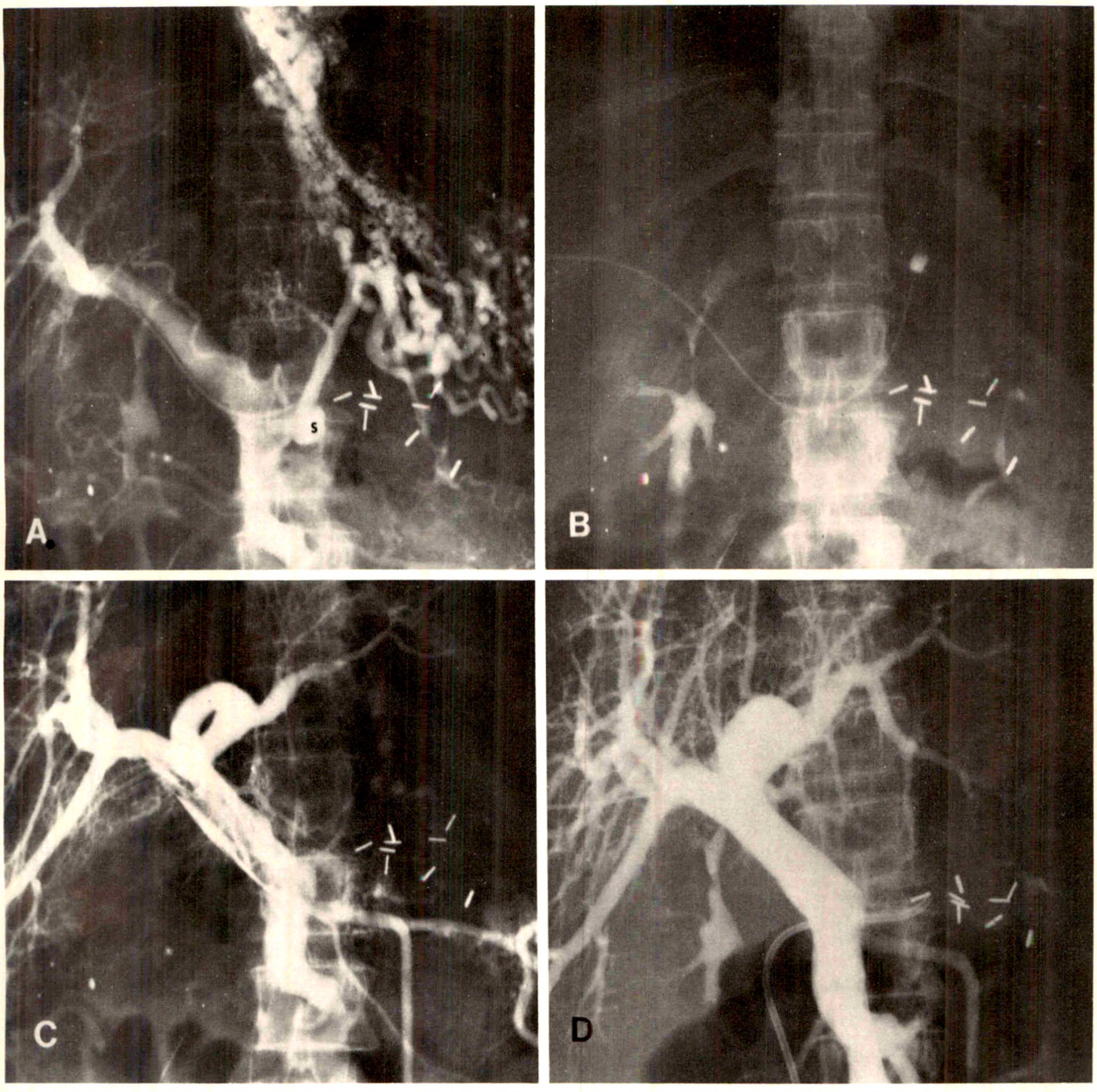

Fig. 4.—Case 4. *A*, Transhepatic left gastric venogram showing extensive filling of gastroesophageal varices. Stump of splenic vein(s) is due to recent surgery. *B*, Fogarty balloon catheter inflated. *C*, Portal venogram 16 hr later showing occlusion of left gastric vein and thrombus in portal vein. *D*, Transhepatic portal venogram 6 months later. Thrombus has disappeared. Left gastric vein does not opacify because it probably flows toward liver and contains non-contrast-laden blood.

ably at a higher pressure than before surgery because the venous blood from the spleen and short gastric veins was driven by the splenic artery pressure. In such a situation, transhepatic injection of emboli into the left gastric vein would result in embolization to the portal vein which could impair hepatic function. Splenectomy or possibly the construction of an alternative portosystemic (mesocaval or portocaval) shunt may be necessary to prevent recurrent variceal bleeding in this situation.

Although balloon catheters can occlude small left gastric veins, portal vein thrombus may occur around the catheter if it is left in place for several hours. Also, the shearing movement between the liver and the right upper abdominal wall that occurs with respiration tends to dislodge the catheter within a short time. For these reasons, use of balloon catheters has been supplanted by selective embolizations of various sorts.

In our experience with 10 patients, the combination of Gelfoam and heat-treated autogenous clot was effective in controlling bleeding from esophageal varices and in allowing time for the surgeon to stabilize the patient. This temporizing tactic has decreased the necessity for

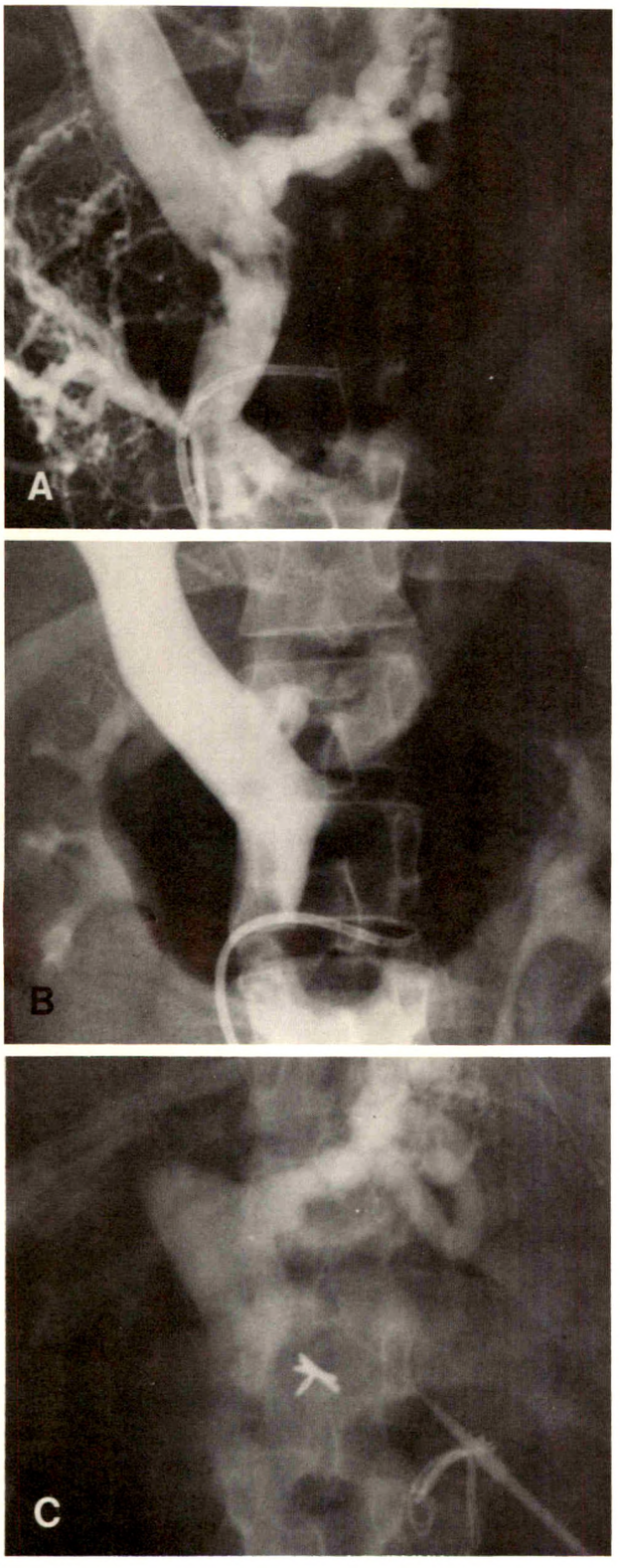

Fig. 5.—Case 5. *A*, Transhepatic venogram showing two left gastric veins. *B*, Portal venogram after occlusion with Gelfoam and autogenous clot showing stump of left gastric vein. *C*, Intraoperative portal venogram 2 months later showing recanalization of left gastric vein.

emergency shunt surgery which has a high mortality and has allowed for an elective well planned operation [11]. However, the clot and Gelfoam disappeared within 8 weeks in three patients restudied in whom these materials were used. Embolization with Gelfoam soaked in 3% sodium tetradecyl sulfate has been reported with long term follow-up and has been found to occlude veins more permanently [4]. We have no experience with N-butyl cyanoacrylate or Ivalon for occlusion [12, 13].

Although a variety of minor complications occurred, only two complications in 89 examinations were significant enough to require medical or surgical management. Most of the patients in whom these procedures were performed were markedly ill and fragile. Yet the vast majority underwent this catheter technique without deterioration. Because the no. 5 French catheter is only 1.6 mm in diameter, the small hole it makes tends to seal over when the catheter is removed.

Conclusions

1. Before embolization of coronary veins is attempted, selective venography should be performed to detect any direct communications to the inferior vena cava or portal vein to prevent embolization to the pulmonary arteries or portal vein, respectively.

2. In patients in whom a distal selective splenorenal shunt has been found to be occluded or severely stenotic by left renal venography and splenic arteriography, transhepatic left gastric vein occlusion is not recommended due to inappropriate direction of flow. Other surgical means may be necessary to control recurrent bleeding.

3. Transhepatic occlusion of the coronary veins using autogenous clot and Gelfoam has been effective in controlling bleeding from esophageal varices, but is only a temporizing tactic and lasts for only a few weeks. Gelfoam soaked in 3% sodium tetradecyl sulfate seems to provide more permanent occlusions.

4. Transhepatic portal venography has been a relatively safe procedure in our experience of 89 cases; only two significant complications occurred.

REFERENCES

1. Wiechel KL: Percutaneous transhepatic cholangiography. *Acta Chir Scand* [*Suppl*] 330:1–99, 1964
2. Wiechel KL: Tekniken vid perkutan transhepatisk portapunkton (PTP) (abstr.). *Nord Med* 86:912, 1971
3. Lunderquist A, Vang J: Transhepatic catheterization and obliteration of the coronary vein in patients with portal hypertension and esophageal varices. *N Eng J Med* 291:646–649, 1974
4. Pereiras R, Viamonte M Jr, Russell E, LePage J, White P, Huston D: New techniques for interruption of gastroesophageal venous blood flow. *Radiology* 124:313–323, 1977
5. Viamonte M Jr, LePage J, Lunderquist A, Pereiras R, Russell E, Viamonte M, Camacho M: Selective catheterization of the portal vein and its tributaries. *Radiology* 114:457–560, 1975
6. Widrich WC, Robbins AH, Nabseth DC, O'Hara ET, Johnson

WC, Laughlin KV: Portal hypertension changes following selective spleno-renal shunt surgery. *Radiology* 121:295–302, 1976
7. Viamonte M Jr, Pereiras R, Russell E, LePage J, Meier WL: Pitfalls in transhepatic portography. *Radiology* 124:325–329, 1977
8. Child CG III: *The Liver and Portal Hypertension*. Philadelphia, Saunders, 1964
9. Calabresi P, Abelmann WH: Porto-caval and porto-pulmonary anastamoses in Laennec's cirrhosis and in heart failure. *J Clin Invest* 36:1257–1265, 1957
10. Doehner GA, Ruzicka FF, Rousselot LM, Hoffman G: The portal venous system: on its pathological roentgen anatomy. *Radiology* 66:206–217, 1956
11. Orloff MJ, Chandler JG, Charters AC III, Condon JK, Gambort DE, Modafferi TR, Levin SE: Emergency portocaval shunt treatment for bleeding esophageal varices. *Arch Surg* 108:293–299, 1974
12. Goldman ML, Fajman W, Galambos J: Transjugular obliteration of the gastric coronary vein. *Radiology* 118:453–455, 1976
13. Tadavarthy SM, Moller JH, Amplatz K: Polyvinyl alcohol (Ivalon): a new embolic material. *Am J Roentgenol* 125:609–616, 1975

Transcatheter Gelfoam Embolization of Posttraumatic Bleeding Pseudoaneurysms

JAMES CHANG,[1] BARRY T. KATZEN,[1, 2] AND KENNETH P. SULLIVAN[1, 3]

Diagnostic angiography combined with transcatheter therapeutic embolization is a simple and effective means of treating complex clinical situations associated with posttraumatic hemorrhage. Bleeding pseudoaneurysms, even when large, can be readily managed by this combined modality with resultant decrease in morbidity and hospital stay. Five patients with posttraumatic pseudoaneurysms are presented. All five were treated by transcatheter therapeutic embolization with Gelfoam. Of these five cases, three involved extremities, one involved the retroperitoneal space, and the last was of renal origin. Two of the five cases still required surgical intervention after initial successful therapeutic embolization, one for recurrent bleeding from collaterals and the other for evacuation of a massive pseudoaneurysm which was causing distraction of fracture fragments. The early use of angiography in suspected cases of posttraumatic hemorrhage, together with careful evaluation of potential collateral supply, is stressed. The use of transcatheter therapeutic embolization in the extremities as presented here is yet another example of the ever-broadening applicability of this technique.

The value of angiography in identifying and localizing the sources of posttraumatic hemorrhage is well established. In contrast to gastrointestinal bleeding, vasopressor therapy is generally of limited value in the posttraumatic bleeding patient. Recently, transcatheter intravascular occlusion has been shown to be an extremely useful means of controlling hemorrhage. Since the first reported visceral application of transcatheter therapeutic embolization by Rosch et al. [1], the technique has gained wide clinical acceptance. Its value and effectiveness has been clearly demonstrated in multiple organ systems and in a broad range of clinical situations. These include treatment of (1) gastrointestinal hemorrhage [1–4]; (2) neoplasms [5–8], both as palliative and preoperative procedures; and (3) vascular malformations [9–11]. In addition, therapeutic embolizations for posttraumatic hemorrhage have been reported in the pelvis [12, 13], kidney [14–16], liver [17–19], and spleen [4, 20, 21].

To the best of our knowledge, the use of this modality in cases of posttraumatic bleeding in the extremities has not been previously reported. We present five cases of posttraumatic bleeding pseudoaneurysms treated by transcatheter embolization. Of these five cases, three involved extremities, one was of renal origin, and the last involved the retroperitoneal space. In three of the five cases, hemorrhage was secondary to stab wounds. The cause of bleeding in the remaining two cases was a direct consequence of fractures and associated surgical procedures.

Technique

The technique is relatively simple but requires the use of superselective catheterization. Many different materials [3, 4] have been used and advocated for transcatheter embolization. However, because of its accessibility, ease of sizing and shaping, and relatively long effective life (weeks to months), we use Gelfoam almost exclusively. From the original 2 × 6 cm pad of Gelfoam, we custom tailor the size and shape of the emboli to the individual case (generally 3 × 12 mm). Gelfoam is difficult to handle when wet. Therefore, it is suggested that all manipulations of this material be in its dry state.

The Gelfoam is placed in a dry 1.5–2.5 ml syringe after removing the plunger. The need to use small volume syringes is stressed. There is usually a sudden decrease in resistance in the catheter system once the embolus is ejected. This sudden decrease in resistance together with the force needed to inject the embolus, can result in the injection of a significant volume of contrast behind the embolus if a large volume syringe is used. This sudden additional volume could cause turbulance and/or reflux, either of which could result in reflux of the embolus from the desired vessel.

Once the Gelfoam is placed in the syringe, the plunger is then replaced and the syringe filled with contrast material. Contrast is preferred to saline because (1) it permits visualization of the embolus as it is being injected; (2) it confirms the position of the catheter and the absence of any significant reflux; and (3) it gives immediate visual feedback on the effectiveness of each embolus. Before connecting to the catheter, the syringe tip is directed upward to expel the air and to permit the Gelfoam, with its lower specific gravity, to rise to the tip of the syringe. At this point, a little gentle tapping and slight pressure on the plunger will result in placing the embolus into the syringe nipple. The syringe is then directly connected to the catheter and the embolus is injected with slow, even pressure.

If necessary, multiple sequential emboli can be injected until the desired vessel is occluded. However, once occlusion is achieved, one must avoid the temptation to inject "just one more embolus." Further injections of embolic material into an already occluded vessel would only result in the dislodgement of the already well

Received February 17, 1978; accepted after revision May 31, 1978.
[1]Department of Radiology, St. Vincent's Hospital and Medical Center of New York, 153 West 11th Street, New York, New York 10011. Address reprint requests to James Chang.
[2]Present address: Alexandria Hospital, 4320 Seminary Road, Alexandria, Virginia 22314.
[3]Present address: St. Francis Hospital, 114 Woodland Street, Hartford, Connecticut 06105.

© 1978 American Roentgen Ray Society

0361–803X/78/1000–0645 $00.00

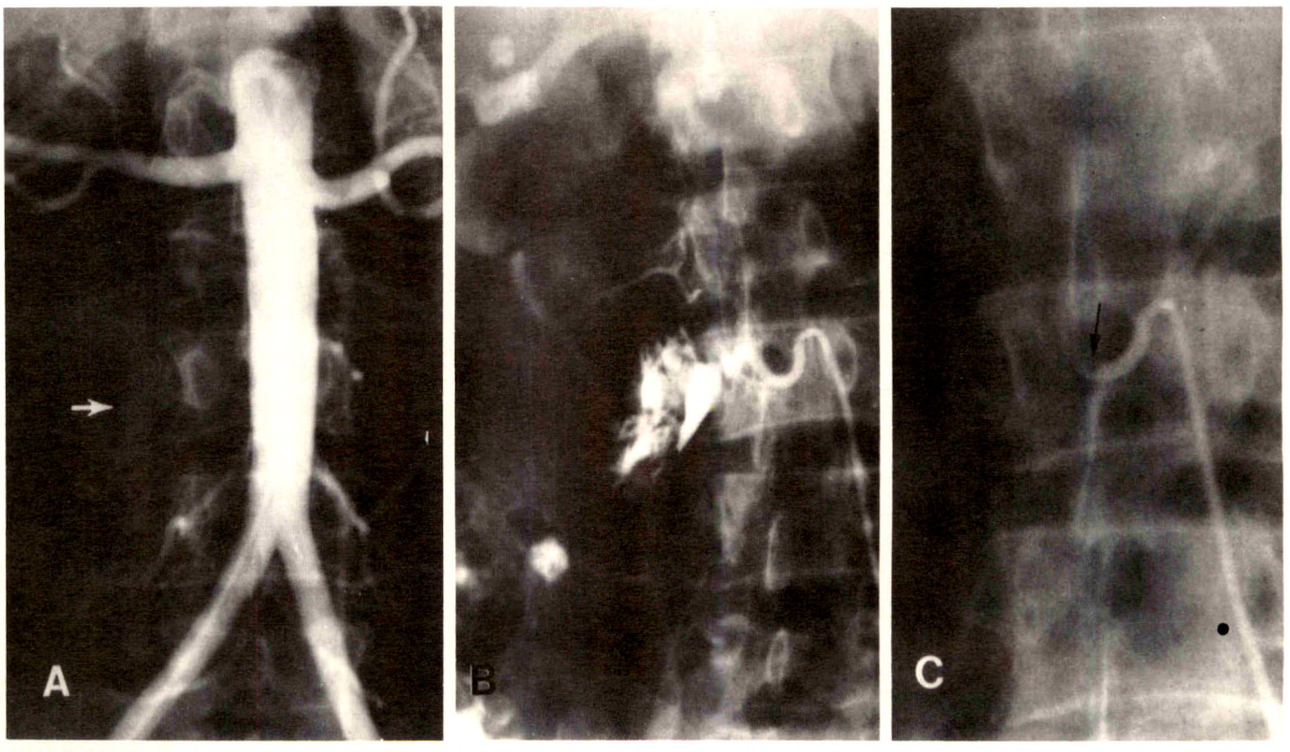

Fig. 1.—*A*, Faintly visualized pseudoaneurysm (*arrow*) filling from poorly defined right third lumbar artery. *B*, Selective injection of right third lumbar artery with partial opacification of pseudoaneurysm. *C*, Occlusion of third lumbar artery following Gelfoam embolization. Note defect caused by embolus (*arrow*).

placed embolus. An even more serious consequence would be reflux of the additional embolic material into undesirable sites.

Case Reports

Case 1

A 39-year-old male was admitted following a stab wound of the back at the level of L2–L3 approximately 4 cm to the right of midline. Emergency excretory urography demonstrated bulging of the lower portion of the right psoas margin and lateral deviation of the lower pole of the normal functioning right kidney. These findings were presumed to be secondary to a retroperitoneal hematoma. The patient was discharged after an uncomplicated course. He was readmitted 2 months later complaining of right costovertebral angle and right lower quadrant pain and tenderness. The hematocrit was 21 and the patient's temperature was 38.3°C. Surgical drainage via a McBurney incision produced 1,000 ml of organizing hematoma, cultures of which were negative. The subsequent hospital course was complicated by purulent drainage from the surgical wound and spiking temperatures to 38.8°C. At surgical reexploration 2 weeks later, purulent material was encountered, cultures of which yielded *Enterobacter* and *Proteus*. The patient was discharged after appropriate antibiotic therapy.

He was readmitted 5 weeks later complaining of right lower quadrant and right thigh pain. He had right costovertebral tenderness, some motor weakness on the right side, and decreased sensation in the right lower extremity. Because of these symptoms, the patient finally came to angiography (6 months after the initial stab wound). The angiogram demonstrated a bleeding pseudoaneurysm arising from the right third lumbar artery which was successfully embolized with Gelfoam (fig. 1). Care was taken to exclude an atypical origin for the artery of Adamkiewiecz and the presence of collateral lumbar feeders to the pseudoaneurysm. The back and thigh pain diminished during the week following the embolization. Repeat aortography 11 days later and again at 6 months demonstrated complete occlusion of the involved lumbar artery with no evidence of bleeding or collateralization.

Case 2

A 45-year-old black male was admitted with gross hematuria and suprapubic pain. Three weeks before admission the patient had sustained a stab wound in the left back. Emergency laparotomy (without prior angiography) at another institution revealed a laceration of the left kidney which was repaired.

Emergency excretory urography on this admission demonstrated nonvisualization of the left collecting system. Selective angiography was then performed and revealed active extravasation of contrast material into a 1.3 cm pseudoaneurysm arising from the superior polar branch of the left renal artery (fig. 2*A*). This was associated with a zone of lucency most likely representing clot within a larger false aneurysm estimated at 3.5 cm in diameter. The bleeding superior polar branch was then selectively catheterized (fig. 2*B*). A single Gelfoam embolus was injected, and obliteration of the neck of the pseudoaneurysm was accomplished (fig. 2*C*). There was cessation of the hematuria 4 days after embolization. The patient was scheduled for repeat excretory urography but signed out against medical advice. The only follow-up available is that the patient is normotensive 8 months after embolization.

Case 3

A 55-year-old female was admitted after sustaining multiple fractures of the extremities following an automobile accident.

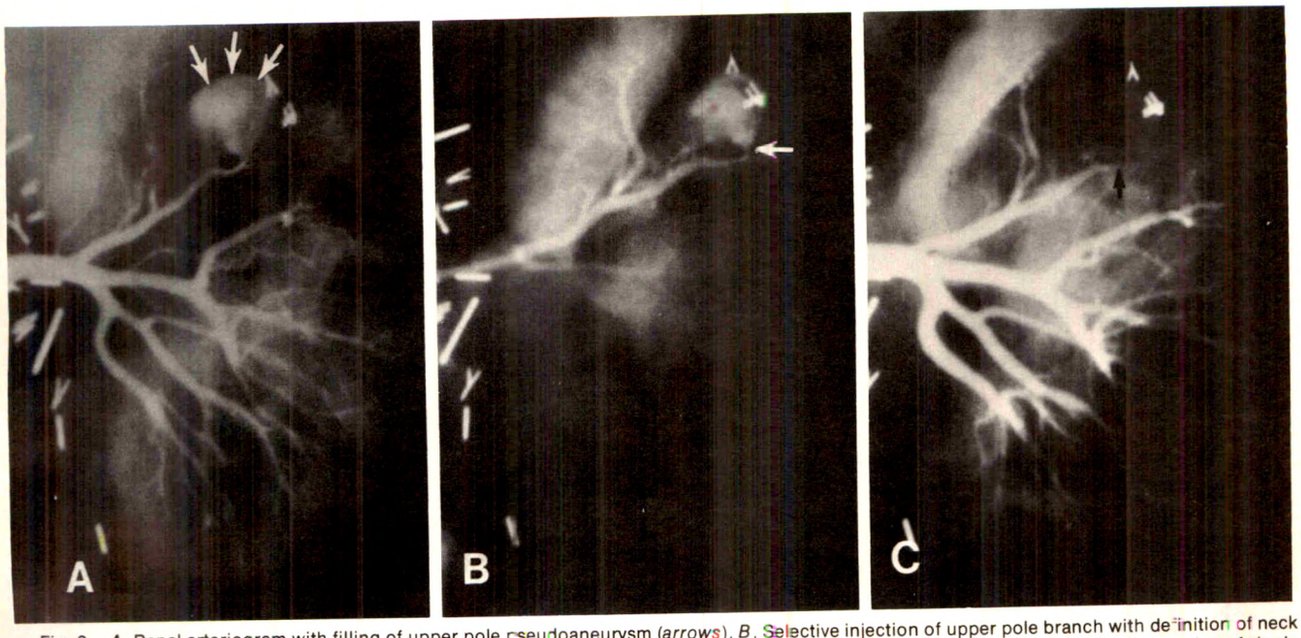

Fig. 2.—*A*, Renal arteriogram with filling of upper pole pseudoaneurysm (*arrows*). *B*, Selective injection of upper pole branch with definition of neck of pseudoaneurysm (*arrow*). *C*, Occlusion of only distal segment of upper pole branch with obliteration of pseudoaneurysm following injection of single embolus.

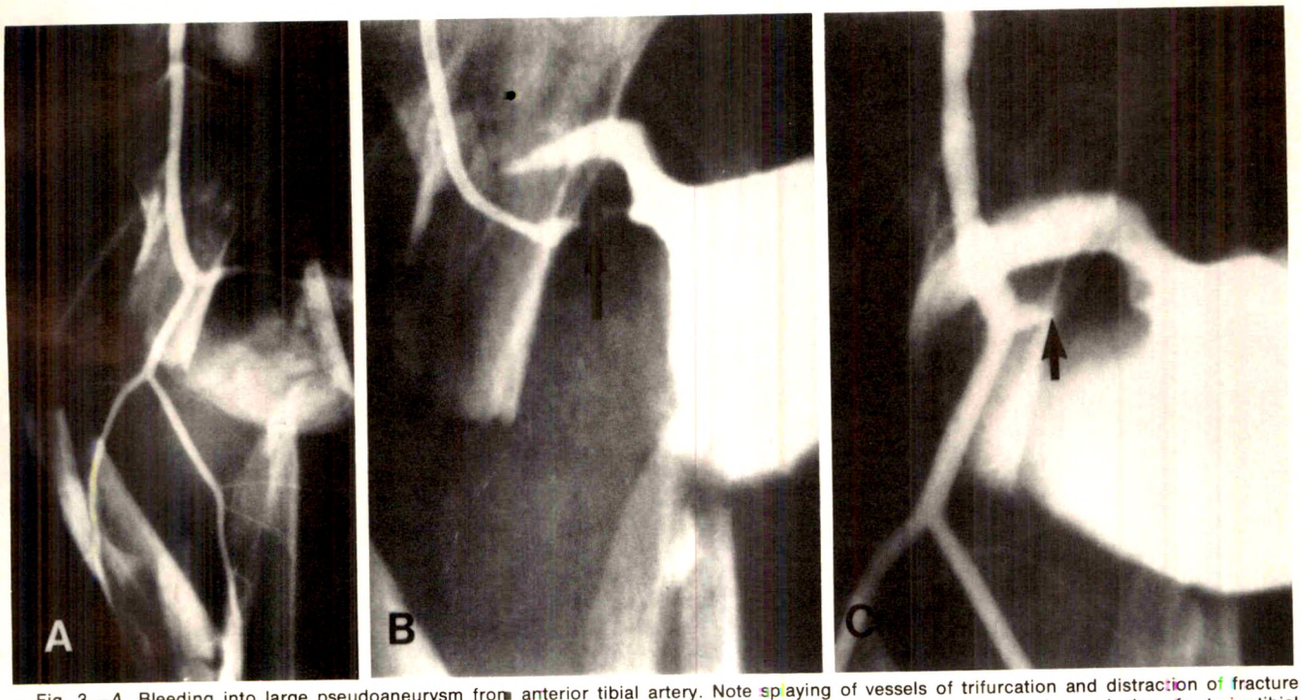

Fig. 3.—*A*, Bleeding into large pseudoaneurysm from anterior tibial artery. Note splaying of vessels of trifurcation and distraction of fracture fragments. *B*, Selective injection of Gelfoam embolus (*arrow*) into anterior tibial artery. *C*, Repeat popliteal injection showing occlusion of anterior tibial artery (*arrow*). Contrast material in pseudoaneurysm is from prior injections.

Hospital course included immediate closed reduction of comminuted fractures of the tibia and fibula. This was followed 12 hr later by fasciotomy of the lower leg for anterior and lateral compartment syndrome. Subsequent procedures included realignment of the tibial fracture at 43 days, and debridement of necrotic bone and removal of pins at 50 days. During this time, there was increasing distraction of the proximal tibial fragments, and the patient experienced persistent pain not relieved by narcotics. In addition, the hematocrit decreased from 41 to 28 over the course of 2 months. On day 67 of hospitalization, skin breakdown over the tibial fracture site along with some bleeding was noted. The patient then had a superficial femoral arteriogram which revealed splaying of the vessels of the trifurcation of the popliteal artery. Bleeding into a large pseudoaneurysm from the proximal anterior tibial artery was also noted (fig. 3*A*). The anterior tibial artery was selectively catheterized, and embolization with Gelfoam was attempted (fig. 3*B*). Because of the large size of the arterial bleeder, it was necessary to inject

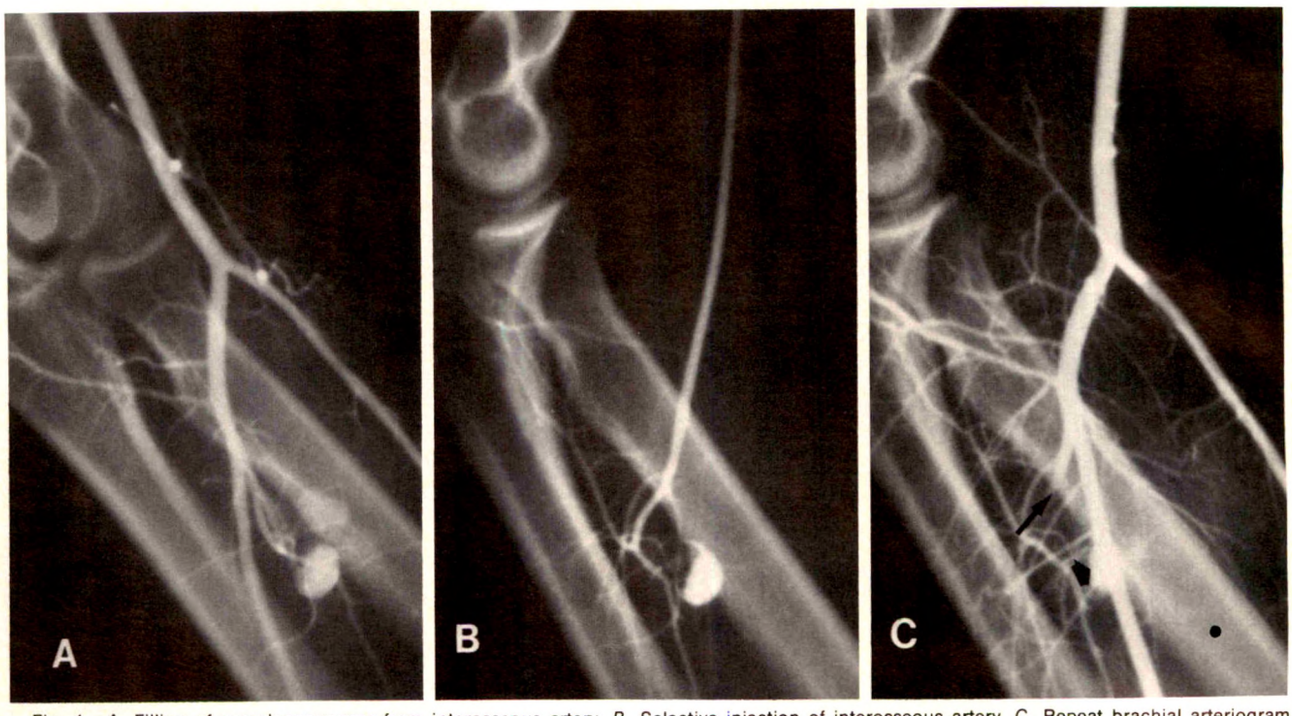

Fig. 4.—*A*, Filling of pseudoaneurysms from interosseous artery. *B*, Selective injection of interosseous artery. *C*, Repeat brachial arteriogram showing occluded interosseous artery (*large arrow*). Residual contrast from prior injection is seen in pseudoaneurysm (*arrowhead*).

multiple Gelfoam emboli of increasing size to achieve total occlusion (fig. 3*C*). Since nonunion at the tibial fracture sites secondary to the large pseudoaneurysm and hematoma had been the patient's major clinical problem, she underwent surgery at which time the false aneurysm was ligated and the hematoma evacuated. The patient's subsequent hospital course was prolonged, but she was discharged with a satisfactory orthopedic result.

Case 4

A 24-year-old male was admitted following accidental stabbing of the left forearm. The entrance wound was on the extensor surface, and the blade extended to, but not through, the flexor surface. After initial emergency treatment consisting of a single suture, he returned to the emergency room 12 hr later with swelling and pain in the forearm. His left hand was held in claw position, and he complained of pain on passive extention of the wrist and fingers. His radial and ulnar pulses were intact. An emergency arteriogram was performed and revealed bleeding into a multilobulated pseudoaneurysm arising from a branch of the interosseous artery (fig. 4*A*). This was selectively catheterized, and a single Gelfoam embolus was injected (figs. 4*B* and 4*C*). There was immediate cessation of bleeding and decreased pain. However, several hours later there was a decrease in the radial pulse and further swelling. The patient was then taken to surgery where a fasciotomy with evacuation of the hematoma was performed. The interosseous artery had to be ligated distally because of retrograde bleeding. No evidence of antegrade bleeding from the occluded branch was seen. The patient's subsequent hospital course was uneventful.

Case 5

An 18-year-old male was admitted with a comminuted compound fracture of the left lower extremity due to a motorcycle accident. The fracture was complicated by infection, delayed healing, and eventual nonunion. Approximately 6 months after the original trauma, the patient again underwent surgery with placement of bone grafts in addition to skin grafting over the surface of the wound. A small pulsatile mass was noted 24 hr later which gradually began increasing in size. The patient was brought immediately to arteriography, where a no. 5 French straight catheter was inserted via an antegrade puncture of the left common femoral artery. Injection of contrast demonstrated extravasation of contrast from the midportion of the anterior tibial artery with displacement of the vessel by the hematoma (fig. 5*A*). The catheter was then placed subselectively in the anterior tibial artery at the mouth of the opening of the false aneurysm. Several Gelfoam emboli were then injected, until complete occlusion of the left anterior tibial artery was accomplished (fig. 5*B*). This result was also monitored visually by the obliteration of pulsations. No surgical intervention was necessary, and healing of both the bone and skin grafts progressed normally.

Discussion

Angiography is a well established diagnostic modality in investigating causes of posttraumatic hemorrhage. In addition, it now has considerable therapeutic potential. The early use of angiography in posttraumatic patients suspected of bleeding from any site is stressed. Early angiography will yield both useful diagnostic information as well as an opportunity to provide immediate nonsurgical therapy if a bleeding site is found. Thus surgery, with its greater morbidity and usually greater associated tissue loss, can be avoided.

Cases 1 and 3 illustrate the types of problems that can arise if angiography is delayed. Case 3 with the increasing distraction of the fracture fragments and the gradu-

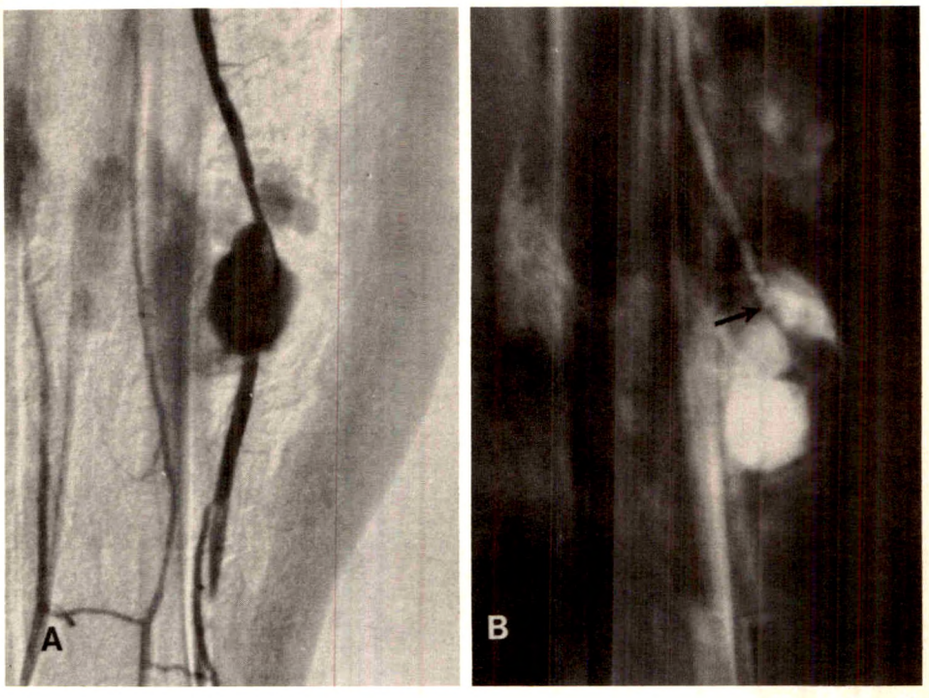

Fig. 5.—*A*, Subtraction film of anterior tibial arteriogram showing filling of pseudoaneurysm and displacement of artery. Note also localized prominence of soft tissue overlying pseudoaneurysm. *B*, Occlusion of anterior tibial artery (*arrow*). Contrast material is from prior injections.

ally decreasing hematocrit secondary to the enlarging pseudoaneurysm did not undergo angiography until after 69 hospital days. The diagnosis could have been made earlier, saving the patient considerable posttraumatic morbidity as well as hospital costs. If the bleeding had been discovered early enough, it is possible that embolic therapy alone might have been sufficient.

Case 1 illustrates the value of both the diagnostic and therapeutic aspects of angiography. Angiography was first performed on his third hospital admission, 6 months after the initial trauma. If the patient had been studied at the time of original trauma, the need for two surgical drainage procedures, multiple costly diagnostic tests, and long complicated hospital courses could have all been avoided. In addition, the successful embolization eliminated the need for potentially difficult surgery in this patient with a history of three prior surgical procedures (including a portacaval shunt) in the involved area, a large and previously infected hematoma, and compromised general medical condition (cirrhosis with ascites).

Similarly, in case 5 therapeutic embolization obviated the need for more complicated surgical intervention which would have likely jeopardized the skin graft and possibly the bone graft as well. Prompt use of angiography in this case permitted early discovery of the bleeding pseudoaneurysm before its size would have necessitated surgical intervention, as in case 3.

One of the most rewarding areas for the application of transcatheter therapeutic embolization is that of posttraumatic renal bleeding. The renal vascular bed is ideally suited for transcatheter occlusive therapy. Because of difficulty in localizing the bleeding site, surgical intervention often results in a hemi- or total nephrectomy. Sometimes (as in case 2) the renal exploration fails to identify the source of hemorrhage. On the other hand, nonsurgical therapeutic embolization can achieve hemostasis with only minimal sacrifice of renal tissue. Even in cases of severe renal trauma, the patient can usually be treated conservatively once active hemorrhage is controlled. Chuang et al. [15] reported successful embolization in six of seven cases of traumatic renal hemorrhage, and nephrectomy was avoided in five of these cases. In the one case where surgery was required after a successful embolization, the kidney was so severely damaged that it was not salvageable. However, even in this case, the use of embolization permitted the transformation of what would normally have been an emergency surgical procedure to an elective one.

Although postembolic development of hypertension is of theoretical concern, thus far it has not proven to be a complication. None of Chuang's seven cases developed hypertension, some having had as long as a 2 year follow-up. This finding would support the experimental data [22–24] that in contrast to a hemodynamically significant stenosis, a complete occlusion or infarct does not appear to activate the renin-angiotensin system. Case 2 has remained normotensive on an 8 month follow-up.

In order to accurately diagnose and effectively treat the sources of hemorrhage, it must be reemphasized that superselective catheterization techniques are essential. Efforts should be directed toward minimizing the amount of tissue sacrificed while still achieving hemostasis. This can only be accomplished by getting as close to the source of bleeding as possible. In general, it is also a good idea to start with relatively small emboli, because it has been our observation that emboli tend to flow to the site of bleeding even though the catheter may

be placed considerably more proximal. We have seen this in a surprising number of our cases, some of which have been previously reported [4]. The exact mechanism is not known but is presumed to be due to a "sump effect" caused by altered vascular resistance and flow dynamics. This finding is well illustrated by case 2. The use of smaller emboli permits a more peripheral occlusion and, therefore, also minimizes tissue loss. In addition, smaller emboli diminish the possibility of rebleeding via local collaterals. If small emboli fail to achieve control, larger emboli can always be used.

Consideration of the local collaterals and potential collaterals is critical prior to any attempt at embolization. This point is particularly well exemplified by case 4. Although hemostasis was achieved after occlusion of a branch of the interosseous artery, several hours later there were symptoms of recurrent bleeding. At surgery, retrograde bleeding from the interosseous artery was noted. It is clear that collaterals from the radial and ulnar artery were responsible for this retrograde bleeding. Collaterals in the extremities are exceedingly good. This, together with the critical nature of the vascular supply, makes successful embolization somewhat less probable than elsewhere in the body. This case demonstrates the need for prolonged film sequences and postembolization studies in order to evaluate the role of collaterals and the possibilities for recurrent bleeding from them. In addition to the extremities, the pelvis and the pancreaticduodenal bed are other areas where the potentially rich collateral supply may be a significant factor in limiting the ultimate success of an attempted therapeutic embolization.

REFERENCES

1. Rosch J, Dotter CT, Brown MJ: Selective arterial embolization. *Radiology* 102:303–306, 1972
2. Gold RE, Grace M: Gelfoam embolization of the left gastric artery for bleeding ulcer. *Radiology* 116:575–580, 1975
3. Grace DM, Pitt DF, Gold RE: Vascular embolization and occlusion by angiographic techniques as an aid or alternative to operations. *Surg Gynecol Obstet* 143:469–482, 1976
4. Katzen BT, Rossi P, Passariello R, Simonetti G: Transcatheter therapeutic arterial embolization. *Radiology* 120:523–531, 1976
5. Goldstein HM, Medellin H, Ben-Menachem Y, Wallace S: Transcatheter arterial embolization in the management of bleeding in the cancer patient. *Radiology* 115:603–608, 1975
6. Goldstein HM, Wallace S, Anderson JH, Bree RL, Gianturco C: Transcatheter occlusion of abdominal tumors. *Radiology* 120:539–545, 1976
7. Bree RL, Goldstein HM, Wallace S.: Transcatheter embolization of the internal iliac artery in the management of neoplasms of the pelvis. *Surg Gynecol Obstet* 143:597–601, 1976
8. Hlava A, Steinhart L, Navratil P: Intraluminal obliteration of the renal arteries in kidney tumors. *Radiology* 121:323–329, 1976
9. Doppman JL, DiChiro G, Ommaya AK: Percutaneous embolization of spinal cord arteriovenous malformations. *J Neurosurg* 34:48–55, 1971
10. Stanley RF, Cubillo E: Nonsurgical treatment of arteriovenous malformations of the trunk and limb by transcatheter arterial embolization. *Radiology* 115:609–612, 1975
11. Wolpert SM, Stein BM: Catheter embolization of intracranial arteriovenous malformations as an aid to surgical excision. *Neuroradiology* 10:73–85, 1975
12. Ring EJ, Athanasoulis C, Waltman AC, Margolies MN, Baum S: Arteriographic management of hemorrhage following pelvic fracture. *Radiology* 109:65–70, 1973
13. Kadish LJ, Stein JM, Kotler S, Meng C-H, Barlow B: Angiographic diagnosis and treatment of bleeding due to pelvic trauma. *J Trauma* 13:1083–1085, 1973
14. Kalish M, Greenbaum L, Silber S, Goldstein H: Traumatic renal hemorrhage treatment by arterial embolization. *J Urol* 112:138–141, 1974
15. Chuang VP, Reuter SR, Walter J, Foley WD, Bookstein JJ: Control of renal hemorrhage by selective arterial embolization. *Am J Roentgenol* 125:300–306, 1975
16. Richman SD, Green WM, Kroll R, Casarella WJ: Superselective transcatheter embolization of traumatic renal hemorrhage. *Am J Roentgenol* 128:843–844, 1977
17. Perlberger RR: Control of hemobilia by angiographic embolization. *Am J Roentgenol* 128:672–673, 1977
18. Jander HP, Laws HL, Kogutt MS, Mihas AA: Emergency embolization in blunt hepatic trauma. *Am J Roentgenol* 129:249–252, 1977
19. Rubin BE, Katzen BT: Selective hepatic artery embolization to control massive hepatic hemorrhage after trauma. *Am J Roentgenol* 129:253–256, 1977
20. Chuang VP, Reuter SR: Selective arterial embolization for the control of traumatic splenic bleeding. *Invest Radiol* 10:18–24, 1975
21. Chuang VP, Reuter SR: Experimental diminution of splenic function by selective embolization of the splenic artery. *Surg Gynecol Obstet* 140:715–720, 1975
22. Almgard LE, Ljungqvist A: Experimental occlusion of the renal circulation in the dog. *Scand J Urol Nephrol* 5:268–272, 1971
23. Chuang VP, Reuter SR, Schmidt RW: Control of experimental traumatic renal hemorrhage by embolization with autogenous blood clot. *Radiology* 117:55–58, 1975
24. Reuter SR, Pomeroy PR, Chuang VP, Cho KJ: Embolic control of hypertension caused by segmental renal artery stenosis. *Am J Roentgenol* 127:389–392, 1976

Transcatheter Embolization: Prevention of Embolic Reflux Using Balloon Catheters

ALAN J. GREENFIELD,[1] CHRISTOS A. ATHANASOULIS, ARTHUR C. WALTMAN, AND EDWARD R. LeMOURE

Reflux of embolic material during therapeutic transcatheter embolization is a potential complication which can result in occlusion of distal vascular beds. The conditions under which reflux was demonstrated in laboratory animals include (1) low flow states, (2) overvigorous flushing, (3) selective contrast injections, and (4) placement of embolic material too proximally. Balloon occlusion of the orifice of the vessel undergoing embolization protects against reflux and allows more homogenous embolization. Because of experience gained in the laboratory, therapeutic transcatheter embolization is now performed in patients with balloon catheter protection. Preliminary clinical experience is described.

Reflux of embolic materials and infarction of distal organs is a potential, yet not well recognized, complication of transcatheter embolization. Published reports describe ischemic infarcts of the spinal cord [1] and the lower extremities [2] as a result of embolic material reflux. In one of our patients, during embolic occlusion of the hypogastric artery for control of bleeding from pelvic trauma, reflux of embolic material produced occlusion of the popliteal artery requiring emergency embolectomy (fig. 1).

We investigated the circumstances under which this complication occurs because of the increasing applications of transcatheter embolization: (1) for control of cerebral [3] and spinal [4] arteriovenous malformations; (2) for treatment of gastrointestinal [5] and posttraumatic bleeding [6] and arteriovenous fistulae [7]; and (3) for renal ablation for tumor [8, 9] and end-stage renal disease [10]. This paper describes our observations as well as methods to prevent embolic reflux.

Materials and Methods

Embolic Material

Pledgets of absorbable gelatin sponge (Gelfoam) approximately 2 × 2 × 2 mm were soaked in liquid iophendylate (Pantopaque) for 30–45 min and gently compressed to remove as much remaining liquid as possible [11]. They were then loaded into tuberculin syringes and suspended in 1 ml of heparinized saline. The pledgets were introduced into the catheter and embolizations were carried out by pressure on the plunger of the syringe. Additional 1 ml increments of saline were introduced as required to flush the catheter and obtained free flow.

Catheters

All embolizations were performed through a new polyethylene balloon-tipped catheter (no. 0B7/2/65, Medi-tech Corp., Watertown, Mass.) (fig. 2). This catheter is heat-formable with good memory retention and torque control. The inner diameter of the catheter is 0.89 mm; outer diameter, 2.3 mm. In animal experimentation the catheter was introduced via a femoral artery cutdown. In subsequent clinical use, it is introduced percutaneously with standard Seldinger [12] technique over a 0.889 cm guide wire. Partial inflation of the balloon during manipulation can impart some flow direction to the catheter and aid in selection of vessels and can increase the seating depth of the catheter tip.

Embolizations

An in vitro series of embolizations was performed by discharging the pledgets of Gelfoam into normal saline. The emboli were radiographed before introduction into the catheter, and then retrieved from the saline solution and reradiographed to determine the degree of retention of contrast medium in the embolized particles, and their size and shape.

An in vivo series of embolizations was performed in six dogs under light sodium pentothal anesthesia. After femoral artery cutdown, selective catheterization and embolization of both renal arteries was performed in each dog, while the procedure was recorded with cinefluorography at 64 frames per second. In each dog, one side was embolized without balloon occlusion, and the opposite side with the balloon inflated. The sides were alternated in each animal. The resulting cine recordings were analyzed with stop-motion viewing equipment.

Results

In the in vitro study, radiographs of the contrast-soaked Gelfoam obtained before embolization showed dense radiopacity of the material (fig. 3*A*). After passage through the catheter, the material broke up into multiple small pieces but remained densely radiopaque (fig. 3*B*). In the in vivo study, radiographs of a representative experimental animal demonstrated the dense radiopacity of the embolic material in the renal vessels and the refluxed material in the lower extremity vessels (fig. 4).

Analysis of the films of the renal arteries embolized without balloon occlusion demonstrated that reflux of embolic material occurred almost immediately after obstruction of segmental vessels (fig. 4). Flushing of the catheter or test injections of contrast material were often responsible for dislodging emboli from the segmental vessels, even though the catheter tip was in the main renal artery. When embolic material was allowed to lodge in the proximal main renal artery, emboli were dislodged while being rocked to and fro by the aortic pulse wave. In addition, repeat arteriography performed after embolization demonstrated very inhomogeneous

Received March 3, 1978; accepted after revision June 5, 1978.
Presented at the annual meeting of the American Roentgen Ray Society, Boston, September 1977.
This work was supported in part by U.S. Public Health Service grants BRSG-0548513 and 1R01 AM 19811-02.
[1] All authors: Department of Radiology, Massachusetts General Hospital, Harvard Medical School, Boston, Massachusetts 02114. Address reprint requests to A. J. Greenfield.

© 1978 American Roentgen Ray Society

0361–803X/78/1000–0651 $00.00

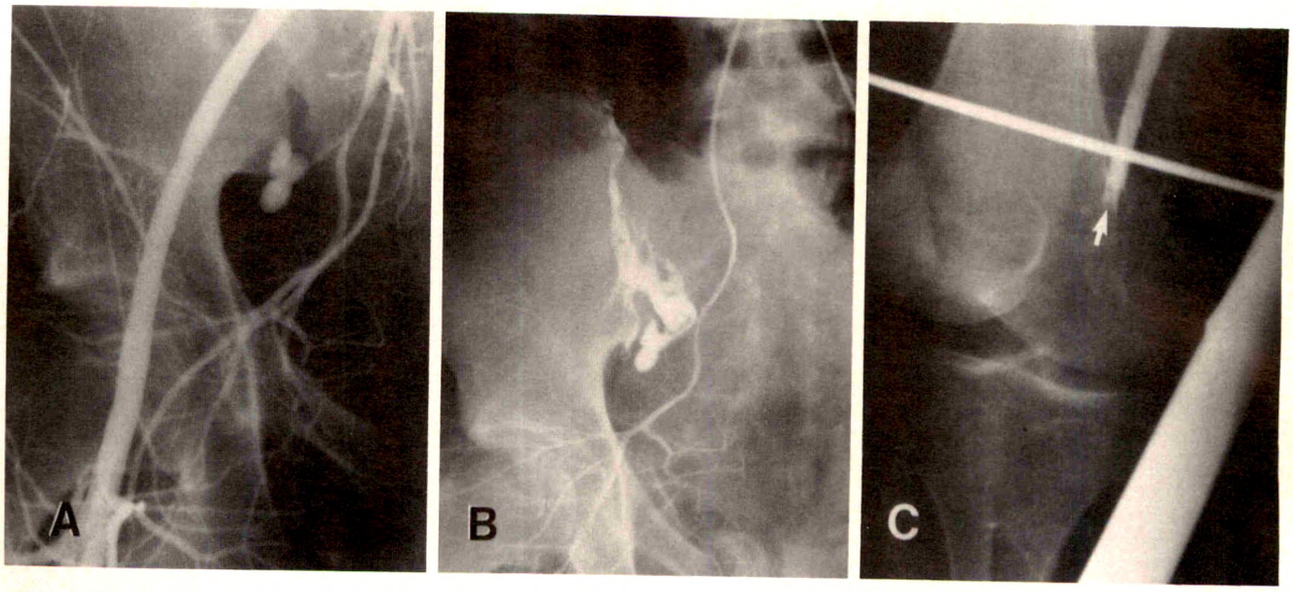

Fig. 1.—Popliteal artery occlusion from embolic reflux during therapeutic embolization. *A*, Selective right common iliac arteriogram demonstrating extravasation of contrast from branch of hypogastric artery. Note extent of pelvic fractures. *B*, Superselective arteriogram demonstrating extravasation from superior gluteal artery. Embolization was carried out from this position. *C*, Arteriogram showing complete obstruction of right popliteal artery, discovered when right dorsalis pedis pulse was lost. Note intravascular filling defect (*arrow*). At surgery (femoral embolectomy), 2 mm Gelfoam pledget was retrieved. Perfusion was successfully restored.

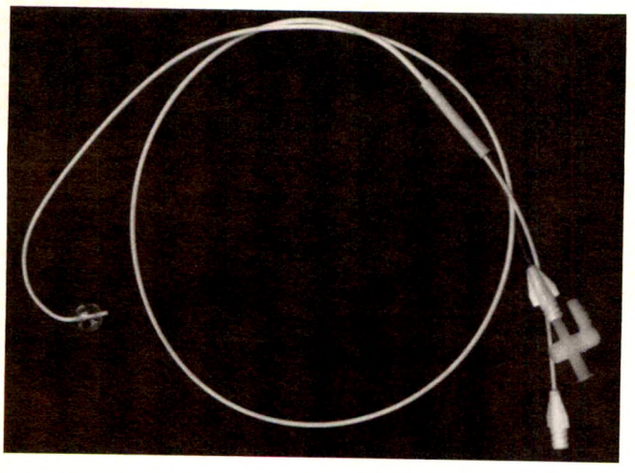

Fig. 2.—Medi-tech balloon catheter. Note curve formed at distal end of catheter.

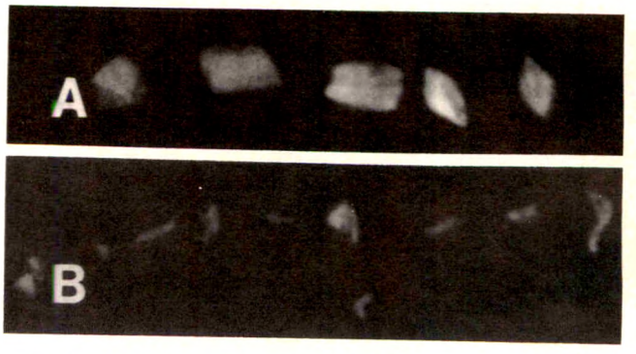

Fig. 3.—Radiographs of Gelfoam pledgets in vitro. *A*, Gelfoam pledgets (original size 2 × 2 × 2 mm) after being soaked for ½ hr in liquid iophendylate (Pantopaque). *B*, Same pledgets of Gelfoam after being extruded through Medi-tech catheter. Gelfoam is now broken up into pieces about size of catheter orifice. They have retained dense radiopacity. (Photograph reproduced to same scale as *A*.)

distribution of vessel occlusion; no further embolic material could be introduced to more completely occlude the renal circulation because all additional material refluxed into the abdominal aorta.

In renal arteries embolized with balloon occlusion, no reflux of material occurred. However, in every case in which emboli were deposited more proximally than the segmental vessels, saline flushing of the catheter or selective injection of contrast medium after balloon deflation produced immediate reflux of most of the embolic material remaining in the main renal artery. Embolic material deposited in the main renal artery with the balloon inflated could be forced distally with repeated saline flushing while balloon occlusion was maintained. Aortography performed at the end of the procedure adequately documented the degree of embolic occlusion of the renal vessels without producing reflux. In addition, embolization was far more homogeneous when balloon occlusion was used.

Discussion

The experimental observation that embolic material refluxed after introduction was originally made by Lalli et al. in 1971 [13]; they were able to prevent reflux with balloon occlusion. More recent reports of embolic com-

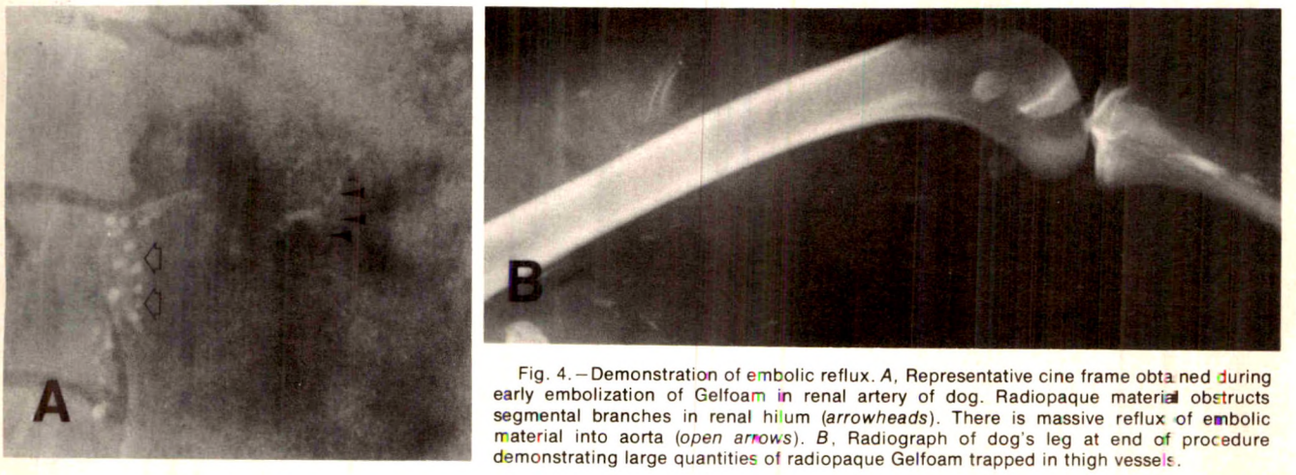

Fig. 4.—Demonstration of embolic reflux. *A*, Representative cine frame obtained during early embolization of Gelfoam in renal artery of dog. Radiopaque material obstructs segmental branches in renal hilum (*arrowheads*). There is massive reflux of embolic material into aorta (*open arrows*). *B*, Radiograph of dog's leg at end of procedure demonstrating large quantities of radiopaque Gelfoam trapped in thigh vessels.

plications of renal embolization have been limited to patients undergoing embolization in end-stage kidney disease. These reports implicate the reduced flow to the kidneys, due to their reduction in volume, along with obliterative intimal fibrosis as the responsible factors [1]. Our investigations confirm that embolic reflux occurs in a low flow state, such as after partial embolization of the renal circulation or during hypotension. In addition, we demonstrated clearly that *spontaneous* reflux of embolic material may occur if material is deposited too close to the orifice of the vessel being occluded.

Kerber [14] suggested that careful fluoroscopic monitoring of the progress of embolization can prevent reflux. However, rather high pressure producing high flow can be required to extrude the embolic material from a partially obstructed catheter, exceeding the flow rate even in high flow vessels. In addition, we observed clinically that Gelfoam particles are rapidly washed free of water soluble contrast material by blood flow or flush solution, and do not reliably remain radiopaque in vitro or in vivo. Finally, an increased load of contrast material is required by his technique, an important consideration in patients with reduced renal function and, especially, prior to nephrectomy.

Levin et al. [16] demonstrated in the laboratory that embolization without balloon protection could be carried out using a special procedure with extremely careful placement of catheters in the center of the arterial lumen "as long as intermittent contrast injections demonstrate continued patency of the catheterized artery and forward flow of contrast material. Once the artery and its major branches become subtotally occluded further embolization is risky." While following their recommendations eliminates the need for additional catheter materials and eliminates use of balloon catheter protection, the degree of vessel occlusion produced, we believe, is suboptimal and may lead to early vessel recanalization. Further, the escape of even one fragment of embolic material has potentially disastrous consequences. Occlusion of the orifice of the embolized vessel with a balloon-tipped catheter followed by embolization through this catheter is a safer, more practical method of preventing complications of embolic reflux, increasing the completeness of embolization, and controlling the proximity of deposition of material to the vessel orifice.

Of equal importance is the demonstration that reflux of embolic material occurs with vigorous flushing of catheters or selective injections of contrast material. As a result of these findings, we have adopted the following protocol for clinical embolization of main aortic branches (fig. 5):

1. Control arteriography is selectively performed through the balloon catheter with the balloon deflated.
2. The balloon is inflated. All further flushing or selective arteriography is carried out prior to deflation.
3. Embolic material is not allowed to lodge proximal to the first major division of the embolized vessel. This can be controlled by flushing the catheter with the balloon inflated, which drives the material peripherally.
4. Hand injections of contrast material with the balloon inflated are performed to determine the completeness of occlusion. These may be documented on film if necessary.
5. For documentation of the embolization, the balloon catheter is exchanged for an aortography catheter, and aortography is performed with the side holes positioned just above origin of the embolized vessels.

On a few occasions, we have used balloon catheter occlusion of the renal artery rather than embolization prior to tumor nephrectomy [15]. However, we feel that is less satisfactory because: (1) the balloon may be dislodged or the femoral artery traumatized during positioning of the patient; (2) prolonged catheterization is necessary under less than ideal conditions; (3) the dislodged balloon could, in theory, be carried by flow into another vessel, with potentially disastrous consequences; and (4) the catheter or balloon may interfere with vessel occlusion during surgery.

Using this technique, no embolic reflux has occurred during preoperative embolization of 11 renal cell carcinomas. With regard to embolization of other vessels, the procedure used depends on the vessel under considera-

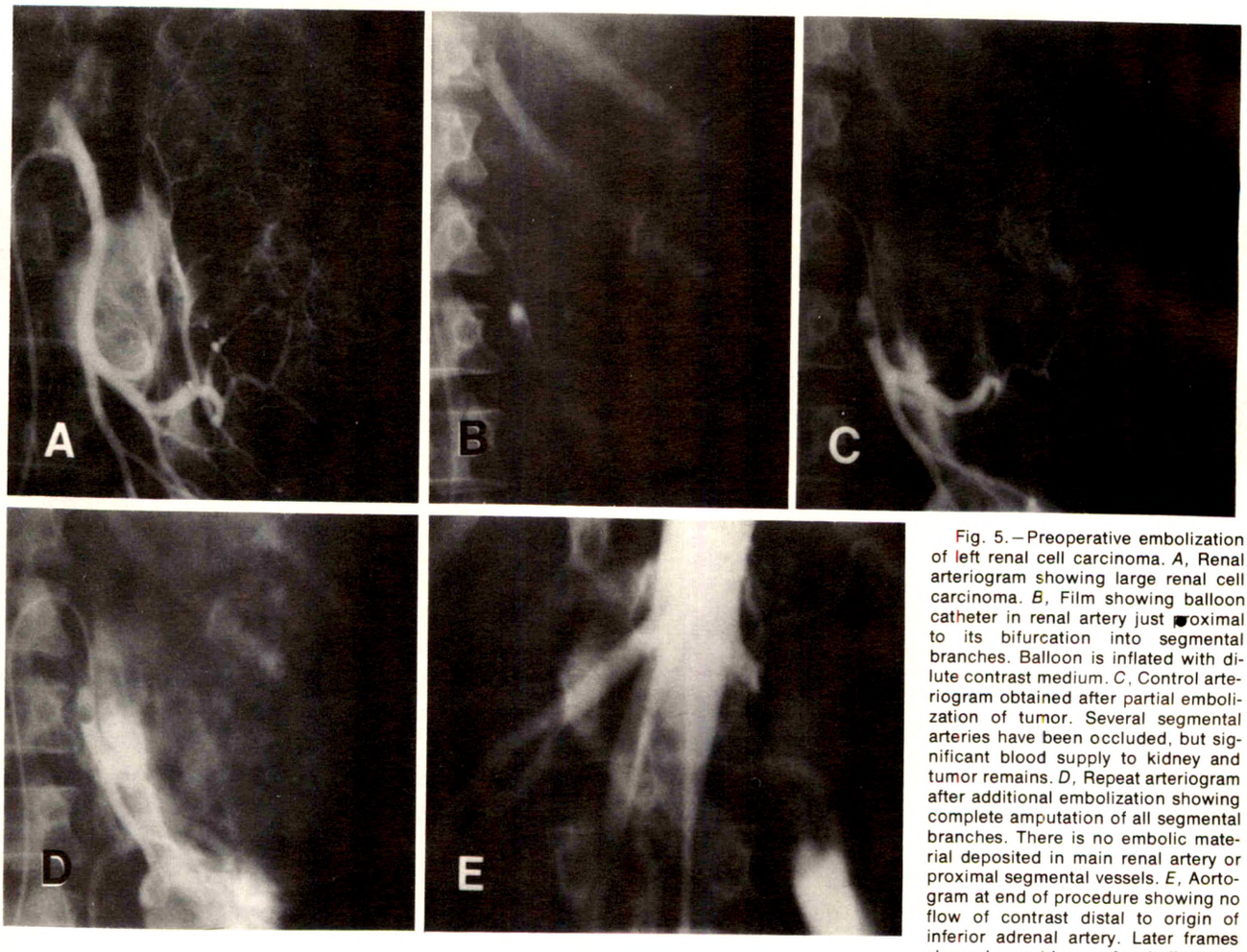

Fig. 5.—Preoperative embolization of left renal cell carcinoma. *A*, Renal arteriogram showing large renal cell carcinoma. *B*, Film showing balloon catheter in renal artery just proximal to its bifurcation into segmental branches. Balloon is inflated with dilute contrast medium. *C*, Control arteriogram obtained after partial embolization of tumor. Several segmental arteries have been occluded, but significant blood supply to kidney and tumor remains. *D*, Repeat arteriogram after additional embolization showing complete amputation of all segmental branches. There is no embolic material deposited in main renal artery or proximal segmental vessels. *E*, Aortogram at end of procedure showing no flow of contrast distal to origin of inferior adrenal artery. Later frames showed no evidence of embolic material in other aortic branches. Nephrectomy was subsequently carried out without incident.

tion. When second- or third-order branches of the aorta are being embolized with superselective catheterization, balloon protection may not be possible with present balloon catheter technology. In these situations, coaxial catheterization allows placement of emboli as peripherally as possible, with the outer catheter occluding the more proximal vessel orifice. Using this method we have safely embolized the left gastric artery on multiple occasions, have selectively embolized a bleeding intralobar renal artery, and have safely embolized a gastrojejunostomy bleeding from the jejunal side with selective occlusion of the single vasa recta supplying the bleeding site. Our experience with embolization will be documented more fully in a subsequent communication.

REFERENCES

1. Gary DL, Dole NB, Adelman LS: Spinal cord infarction following therapeutic renal artery embolization. *JAMA* 237:2841–2842, 1977
2. Woodside J, Schwarz H, Bergreen P: Peripheral embolization complicating bilateral renal infarction with Gelfoam. *Am J Roentgenol* 126:1033–1034, 1976
3. Robbes C, Carrasco-Zanini J: Treatment of cerebral arteriovenous malformation by muscle embolization. *J Neurosurg* 29:603–608, 1968
4. Doppman JL, DiChiro G, Ommaya AK: Percutaneous embolization of spinal cord arterio-venous malformations. *J Neurosurg* 34:48–55, 1971
5. Rösch J, Dotter CT, Brown MJ: Selective artery embolization: a new method for the control of GI bleeding. *Radiology* 102:303–306, 1972
6. Ring EJ, Athanasoulis CA, Waltman AC, Margolies MM: Arteriographic management of hemorrhage following pelvic fracture. *Radiology* 109:65–70, 1973
7. Bookstein JJ, Goldstein HM: Successful management of a posttraumatic AV fisuta with selective arterial embolization. *Radiology* 109:535–536, 1973
8. Almgard LE, Fernstrom I, Haverling M, Ljungqvist A: Treatment of renal adenocarcinoma by embolic occlusion of the renal circulation. *Br J Urol* 45:474–479, 1973
9. Ben-Menachem Y, Crigler CM, Corriere JN Jr: Elective

transcatheter renal artery occlusion prior to nephrectomy. *J Urol* 114:355–359, 1975
10. McCarron DA, Rubin RJ, Barnes B, Harrington JT, Millan VG: Therapeutic bilateral renal infarction in end stage renal disease. *N Engl J Med* 294:652, 1976
11. Kasdon DL, Altemus LR, Stein BM: Embolization of a traumatic arteriovenous fistula of the scalp with radiopaque Gelfoam pledgets: case report and technical note. *J Neurosurg* 44:753–756, 1976
12. Seldinger SI: Catheter replacement of the needle in percutaneous arteriography: a new technique. *Acta Radiol* (Stockh) 39:368–370, 1953
13. Lalli AF, Bookstein JJ, Lapidus J: Experimental renal infarctions in dogs. *Invest Urol* 8:516–520, 1971
14. Kerber CG: Catheter therapy: fluoroscopic monitoring of deliberate embolic occlusion. *Radiology* 125:538–540, 1977
15. Marberg M, Georgi M: Balloon occlusion of the renal artery in tumor nephrectomy. *J Urol* 114:360–362, 1975
16. Levin DC, Beckmann CF, Hillman B: Experimental determination of flow patterns of Gelfoam emboli selectively injected into visceral arteries: safety implications for therapeutic embolization procedures. Paper presented at the annual meeting of the Association of University Radiologists, San Antonio, Texas, April 1978

Bleeding Simulated by the Distal Internal Pudendal Artery Stain

JOHN D. SCHRUMPF,[1] GRAHAM SOMMER, AND RICHARD P. JACOBS

A capillary and venous phase blush in the region of the distal branches of the internal pudendal artery that simulates bleeding can sometimes be seen on arteriograms of male patients who are not bleeding. We describe five such cases. Correct identification of this pooling of contrast material is important to avoid unnecesary treatment by transcatheter embolization or by infusion of vasoactive drugs.

The angiographic catheter has become a useful therapeutic tool. In pelvic trauma in which approximately 60% of deaths are due to massive extraperitoneal hemorrhage and surgery is technically difficult [1–3], angiography can allow for accurate detection of the bleeding site and enable effective control by selective embolization or by infusion of vasoactive drugs [4–8]. We report an angiographic finding that may lead to a false positive diagnosis of pelvic bleeding. A blush in the distal branches of the internal pudendal artery may be seen in the capillary or venous phases, or both, in patients who are not bleeding. Recognition of this may prevent possible morbidity from unnecessary infusion or therapeutic embolization.

Materials and Methods

In the last 2 years, we evaluated the distal abdominal aortograms or run-off arteriograms of 130 patients; five of these patients demonstrated a stain in the region of the distal internal pudendal artery (table 1). All 130 patients were studied by means of percutaneous arterial catheterization. Although the femoral approach was most often used in these patients, we also employed the left axillary approach because we have found it allows excellent and direct access to the descending aorta, the common iliac arteries, and the internal iliac arteries and their distal branches; it is therefore the preferable route when undertaking assessment and therapy of suspected pelvic hemorrhage.

Case Reports

Case 1

Run-off arteriography was performed on a 25-year-old man being evaluated for Buerger's disease. Stenosis of a popliteal artery was demonstrated. A prominent stain was noted (fig. 1) incidentally at the base of the penis during the aortic injection.

Case 2

While riding his motorcycle, a 29-year-old man was struck by a car and suffered diastasis of the symphysis pubis and right sacroiliac joint. Exploratory laparotomy disclosed a ruptured bladder and bowel injury that required a left colostomy. To assess the continued bleeding, a no. 6 French catheter was introduced via the left axillary approach. Contrast material was injected into the lower abdominal aorta, and the arteriogram showed active bleeding from the lateral sacral branch of the left internal iliac artery. Selective embolization of the left internal iliac artery with Gelfoam halted the bleeding. Injections before the embolization demonstrated a symmetrical capillary and venous phase stain in the region of the base of the penis. Washout of contrast material was normal, that is, without continued pooling.

Case 3

A 44-year-old man underwent run-off arteriography because of a gunshot wound in a leg 3 years previously. Incidentally noted on the capillary and venous phase was a bilateral stain in the region of the distal branches of the internal pudendal artery (fig. 2). A second stain extended superior to the base of the penis and appeared to be in the rectal mucosa. No rectal inflammatory process could be found.

Case 4

A 53-year-old man had run-off arteriography performed because of pain in the left calf. A left popliteal artery occlusion was found. Incidentally noted was a bilaterally symmetric stain in the region of the corpus cavernosum.

Case 5

A 30-year-old man was shot in the right buttock, and the bullet exited from the soft tissue lateral to the greater trochanter. A lower abdominal aortogram and run-off arteriogram showed normal vessels; however, a prominent blush was seen at the base of the penis during the capillary and venous phases. Exploration of the buttock wound and laparotomy confirmed that there was no injury to abdomen, pelvis, or perineum.

Discussion

The distal internal pudendal artery supplies the external genitalia, the lower anal canal, and the skin of the perineum. From the internal iliac artery, the internal pudendal artery runs through the buttock and then anteriorly along the lateral wall of the ischiorectal fossa in the pudendal canal. At the posterior end of the canal, the inferior rectal branches of the internal pudendal artery arise, and at the anterior end of the canal the perineal branch arises. The perineal branch gives off a transverse branch to the anal region and a branch to the scrotum. After small branches to the urogenital diaphragm, the internal pudendal artery gives off four named branches: artery of the penile bulb, the urethral artery, the deep penile artery (the central artery of the corpus cavernosum), and the dorsal penile artery. The branches of the internal pudendal vein correspond in location with those of the internal pudendal artery, except the dorsal penile vein drains primarily into the prostatic venous plexus.

Received February 14, 1978; accepted after revision June 16, 1978.

[1]All authors: Department of Radiology, University of California School of Medicine and San Francisco General Hospital, San Francisco, California 94143. Address reprint requests to J. D. Schrumpf.

© 1978 American Roentgen Ray Society

0361–803X/78/1000–0657 $00.00

TABLE 1
Summary of Cases

Case	Age (years)	History	Arteriographic Findings
1	25	Buerger's disease	Stenosis of popliteal artery; stain at corpus cavernosum; otherwise normal findings
2	29	Motorcycle accident	Pelvic fracture; bladder rupture; branch left internal iliac artery bleeding (successfully embolized); stain at corpus cavernosum
3	44	Remote gunshot wound to leg	Stain in region of rectum and corpus cavernosum; otherwise normal findings
4	53	Pain in calf	Stain at corpus cavernosum; otherwise normal findings
5	33	Gunshot wound in right buttock	Stain at corpus cavernosum; otherwise normal findings

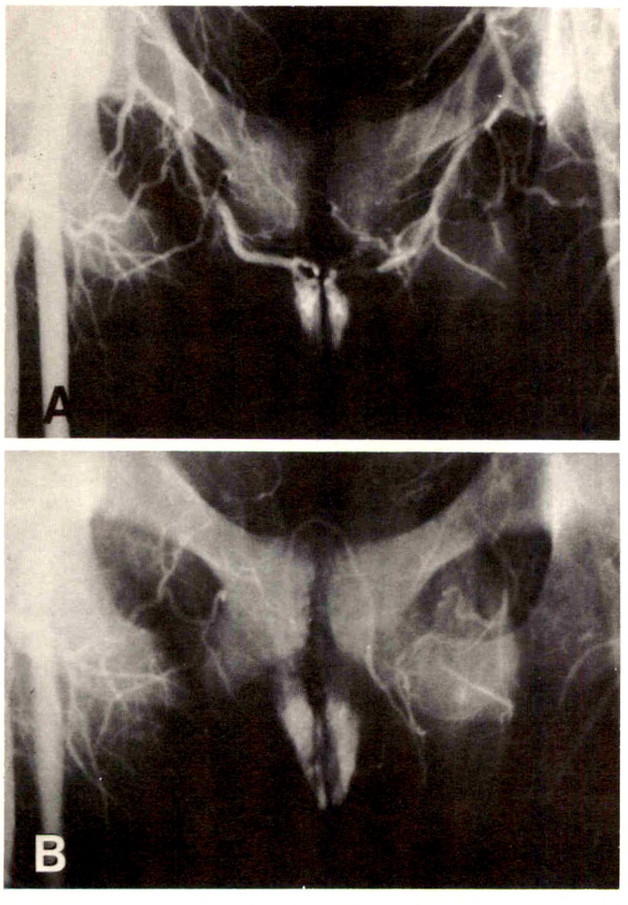

Fig. 1.—Case 1. Early (*A*) and late (*B*) arterial phase aortogram showing normal finding of bilateral symmetric blush in corpus cavernosum.

Fig. 2.—Case 3. Lower abdominal aortogram, late arterial phase, showing dense stain in region of corpus cavernosum. Second, more superior stain is in region of rectum and prostate.

Several explanations, other than that of active bleeding, are possible for the stain visualized arteriographically in the region of the internal pudendal artery.

1. It may represent stasis in the penis secondary to venous occlusion, such as by thrombosis or a pelvic hematoma.

2. Wheeler and Simmons [9] reported a case of posttraumatic priapism with pooling of contrast medium from the distal internal pudendal artery; they believed this pooling was due to a local arteriovenous fistula in the corpus cavernosum.

3. The stain may also simply be a normal capillary phase stain or blush in the corpus cavernosum, as appeared in cases 2, 4, and 5. Since we have not seen this stain in females, it seems likely the stain lies within the penis.

4. In case 3, the stain was more extensive superiorly, suggesting hypervascularity of the anal canal, although there was no history of rectal inflammation.

5. The skin of the perineum might blush if inflamed.

6. Prostatic venous plexus pooling is also a possibility.

Neither autopsy nor surgical proof was available for all of our cases. However, when the distal internal pudendal artery stain is noted incidentally on an arteriogram of a patient without recent trauma (Cases 1, 3, and 4), the overwhelming likelihood is that the stain does not represent bleeding; surgery or autopsy is not likely to be performed on such a patient. In Case 5, the bullet track was in the muscles outside the pelvis; surgery did confirm absence of bleeding in the pelvis and perineum, although the prostate and penis were not incised. In Case 2, surgery did not disclose a site of bleeding. Arteriography showed bleeding was from the lateral sacral branch of the left internal iliac artery which was successfully embolized. This active, continuous extravasation which did not wash out contrasted with the symmetric stain at the base of the penis which did wash out, and which we believe is a normal finding.

Our interest in distinguishing an area of bleeding from a stain not due to bleeding in the region of the distal internal pudendal artery was aroused by a case of a 36-year-old man who jumped from the fourth floor of his residence incurring multiple pelvic fractures. He underwent arteriography to determine if active pelvic bleeding was present and for possible therapy. A large pelvic mass, presumably hematoma, was seen displacing the bladder and vessels. Staining seen at the base of the penis was initially interpreted as extravasation. Four 2 × 3 mm Gelfoam emboli were therefore flushed through the catheter; however, they lodged in small gluteal branches. Reinterpretation of late phase arteriograms showed slowed washout of the contrast material from the corpus cavernosum region but no persistent pooling. This appearance suggested that the stain was actually secondary to venous obstruction due to the hematoma. The study was terminated without complication. Pathologic proof is not available.

This case illustrates that it can be difficult to determine whether a stain in the corpus cavernosum region is caused by bleeding. We believe that a bilaterally symmetric, homogeneous stain at the base of the penis that washes out is a variation of normal, especially if there is no history of pelvic trauma. If the area of contrast extravasation is not bilaterally symmetric, pools, and does not wash out, and the patient has sustained recent pelvic trauma, bleeding is the most likely cause.

Although some instances of stain in the region of the internal pudendal artery, such as those reported by Katzen et al. [8] and Kadish and coworkers [7], probably do represent active bleeding, the possibility of either a normal capillary-venous stain or stasis secondary to venous occlusion should be considered before undertaking embolization or vasoconstrictor therapy.

ADDENDUM

After preparing this manuscript, a corroborative example was brought to our attention by Arthur Gronner of Highland General Hospital, Oakland, California. His patient was a 22-year-old man who was shot in the left thigh. Initial reports indicated that the wound was inflicted with a shotgun. Left femoral arteriography showed no direct arterial injury (fig. 3*A*), but a bright stain was noted inferior to the symphysis pubis (fig. 3*B*). The stain was initially interpreted as contrast extravasation. However, further questioning, police reports, and additional physical examination indicated only a single entrance and exit wound in the midthigh. The patient was hospitalized and his wound debrided. No hematuria or other significant bleeding occurred. The patient recovered without event and was discharged. As in our patients, recognition of this staining phenomenon may avoid initial misinterpretation and perhaps prevent inappropriate therapy.

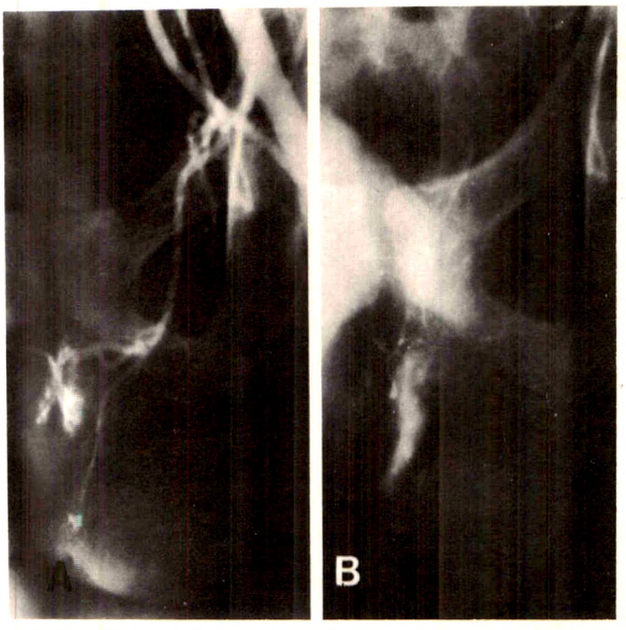

Fig. 3.—*A*, Left femoral arteriogram showing normal arterial anatomy and early staining near terminal branches of internal pudendal artery. *B*, Capillary phase showing contrast accumulation at base of penile shaft.

REFERENCES

1. Hawkins L, Pomerantz M, Eiseman B: Laparotomy at the time of pelvic fracture. *J Trauma* 10:619–622, 1970
2. Ravitch MM: Hypogastric artery ligation in acute pelvic trauma. *Surgery* 56:601–602, 1964
3. Seavers R, Lynch J, Ballard R, Jernigan S Johnson J: Hypogastric artery ligation for uncontrollable hemorrhage in acute pelvic trauma. *Surgery* 55:516–519, 1964
4. Ring EJ, Athanasoulis C, Waltman AC, Margolies MN, Baum S: Arteriographic management of hemorrhage following pelvic fracture. *Radiology* 109:65–70, 1973
5. Margolies MN, Ring EJ, Waltman AC, Kerr WS Jr, Baum S: Arteriography in the management of hemorrhage from pelvic fractures. *N Engl J Med* 287:317–321, 1972
6. Ring EJ, Waltman AC, Athanasoulis C, Smith JC Jr, Baum S: Angiography in pelvic trauma. *Surg Gynecol Obstet* 139:375–380, 1974
7. Kadish LJ, Stein JM, Kotler S, Meng C-H, Barlow B: Angiographic diagnosis and treatment of bleeding due to pelvic trauma. *J Trauma* 13:1083–1085, 1973
8. Katzen BT, Rossi P, Passariello R, Simonetti G: Transcatheter therapeutic arterial embolization. *Radiology* 120:523–531, 1976
9. Wheeler GW, Simmons CR: Angiography in posttraumatic priapism: a case report. *Am J Roentgenol* 119:519–620, 1973

Gas in the Bile Ducts (Pneumobilia) in Emphysematous Cholecystitis

WILLIAM D. HARLEY,[1] ROBERT H. KIRKPATRICK, AND JOSEPH T. FERRUCCI, JR.

Gas in the biliary ducts (pneumobilia) was demonstrated in three cases of emphysematous cholecystitis. Pneumobilia is usually secondary to a spontaneous internal biliary fistula or incompetent sphincter of Oddi, and is rarely considered a manifestation of emphysematous cholecystitis. The presence of gas in the billary ducts in these cases suggests that the cystic duct is patent, allowing gas to escape from the gallbladder lumen. The pathophysiology of emphysematous cholecystitis is discussed and an ischemic etiology considered.

Gas in the biliary ducts (pneumobilia) is an infrequent occurrence in emphysematous cholecystitis. If gas is not simultaneously identified in the wall of the gallbladder, emphysematous cholecystitis might not be considered in the differential diagnosis. More common etiologies for pneumobilia, such as spontaneous internal biliary fistula, incompetent sphincter of Oddi, or biliary enteric surgical anastomosis, would be the prime considerations. We report three cases in which gas in the biliary ducts was a prominent radiographic feature of emphysematous cholecystitis and discuss possible pathophysiologic mechanisms.

The three patients had acute abdominal symptoms, and gas in the biliary ducts was demonstrated on initial plain radiography of the abdomen. Contrast studies of the upper gastrointestinal tract were obtained when appropriate to exclude a communication between the gastrointestinal tract and the biliary system. The diagnosis of emphysematous cholecystitis was confirmed at surgery in each patient within 48 hr of admission. No further examples of gas in the biliary ducts were discovered on review of 11 additional cases of emphysematous cholecystitis gathered from the teaching collections of six area medical centers.

Case Reports

Case 1

A 71-year-old woman with adult onset diabetes mellitus had a 2 week history of intermittent right upper quadrant pain which increased in intensity during the 24 hr prior to admission. Physical examination revealed marked right upper quadrant tenderness. Supine abdominal radiography on admission demonstrated extensive gas in the major intrahepatic bile ducts, as well as gas in the wall and lumen of the gallbladder (fig. 1). At laparotomy the day after admission, the gallbladder appeared crepitant with evidence of early necrosis. Frank intraluminal gas was encountered on opening the gallbladder, and several hundred tiny stones were found. A cholecystostomy was performed. Cultures from the gallbladder wall and bile yielded *Clostridium perfringens*. An elective cholecystectomy was performed after a 3 month interval without complication.

Case 2

An 84-year-old diabetic female was admitted with a 24 hr history of abdominal pain on the right side and vomiting. Physical examination revealed a distended abdomen with diffuse tenderness and a rectal temperature of 38.3°C. Laboratory values included a white blood cell count of 13,000 and a total bilirubin of 1.0 mg/100 ml. Supine radiography disclosed gas in the common hepatic duct (fig. 2*A*). An air-fluid level was evident in the gallbladder on an upright view (fig. 2*B*). An upper gastrointestinal examination was normal, and there was no reflux of barium into the biliary tract. At exploratory surgery on the second day, the gallbladder was gangrenous and contained gas within the wall. Several calculi were present within the lumen. A cholecystectomy was performed. Culture of the bile was not obtained.

Case 3

A 50-year-old male had vague abdominal discomfort for 3 hr, followed by vomiting and severe abdominal pain on the right side. He had undergone a partial gastrectomy and Billroth II anastomosis for carcinoma of the stomach 2 years earlier. No

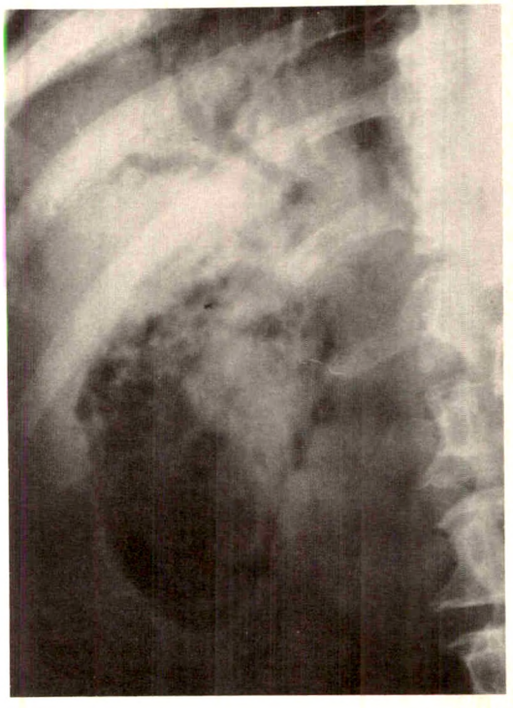

Fig. 1.—Case 1. Extensive gas in intrahepatic ducts. Linear and mottled gas accumulation is evident in wall of gallbladder. Gas in gallbladder lumen identified by air-fluid level on decubitus view (not shown).

Received February 21, 1978; accepted after revision June 23, 1978.

[1] All authors: Department of Radiology, Harvard Medical School and Massachusetts General Hospital, Boston, Massachusetts 02114. Address reprint requests to J. T. Ferrucci, Jr.

© 1978 American Roentgen Ray Society

0361–803X/78/1000–0661 $00.00

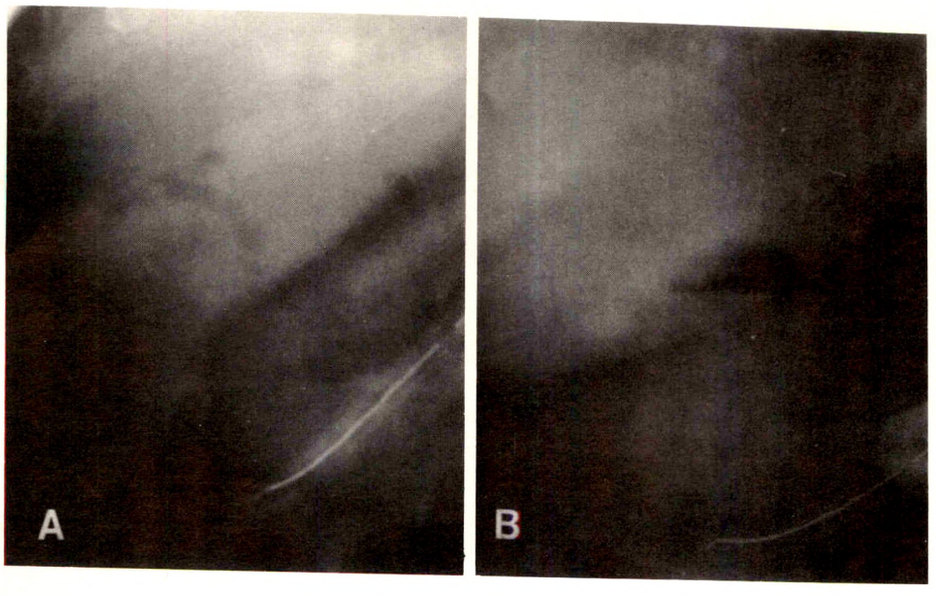

Fig. 2.—Case 2. *A*, Gas in main right and left hepatic and common hepatic ducts. *B*, Upright view demonstrating air-fluid level within gallbladder.

Fig. 3.—Case 3. Gas in lumen of gallbladder and common bile duct. No gas identified in wall of gallbladder.

history of gallbladder disease or diabetes mellitus was elicited. Physical examination revealed right upper and lower quadrant abdominal tenderness and guarding. Laboratory values included a white blood cell count of 17,800 and a total bilirubin of 0.8%. Supine abdominal radiography demonstrated gas in the common bile duct and gallbladder lumen (fig. 3). Oral cholecystography revealed no opacification of the gallbladder, and an upper gastrointestinal examination disclosed no reflux of barium into the biliary tract.

At laparotomy, the gallbladder was tense and gangrenous. Decompression of the gallbladder with a trocar yielded abundant gas with a small amount of bile, but no calculi. No evidence of recurrent gastric carcinoma or biliary enteric fistula was found. A cholecystectomy was performed. The pathology report confirmed acute necrotizing cholecystitis, and culture of the bile yielded *Clostridium perfringens*.

Discussion

Since Hegner [1] made the first radiographic diagnosis of emphysematous cholecystitis in 1931, about 164 cases have been reported [2], and the entity is now considered relatively commonplace. Gas in the wall of the gallbladder is diagnostic of emphysematous cholecystitis. Frequently, both the wall and lumen of the gallbladder contain substantial amounts of gas. Pneumobilia is an unusual occurrence in this disorder. In only seven previously reported cases has gas in the bile ducts been associated with emphysematous cholecystitis [2–7]. Mentzer et al. [2] reported a case of emphysematous cholecystitis in which gas within the biliary ducts was the only radiographic abnormality. Similarly, in two of our three cases, the abnormal gas was confined to the lumen of the bile ducts and gallbladder. Under these circumstances, the correct diagnosis would usually not be considered, and an internal biliary fistula or incompetent sphincter of Oddi would be expected.

The pathophysiology of pneumobilia in association with emphysematous cholecystitis remains an enigma. Obstruction of the cystic duct has been thought to be the precipitating cause of acute cholecystitis, with or without associated gas formation. Several clinical features found in emphysematous cholecystitis tend to distinguish it from acute cholecystitis, including male predominance, lower incidence of gallstones, greater frequency of positive anaerobic bacterial cultures, and associated diabetes mellitus [2, 8]. In addition to these features, the occurrence of pneumobilia in some cases of emphysematous cholecystitis suggests that the cystic duct is patent, allowing gas to escape from the gallbladder into the biliary ducts.

In acute cholecystitis, obstruction of the cystic duct causes the gallbladder to distend, resulting in ischemia of the mucosa secondary to compression of the blood vessels in the gallbladder wall [9]. The same mechanism occurs in emphysematous cholecystitis, although primary ischemia of the gallbladder without cystic duct obstruction is probably the precipitating event in some cases [2, 10]. This hypothesis is supported by the findings of May and Strong [11], in which the blood vessels of three gallbladders removed in cases of emphysematous cholecystitis were narrowed or occluded compared to 60 control gallbladders with recurrent cholecystitis.

Schowengerdt and Wiot [7] reported a case of emphysematous cholecystitis associated with gas in the bile ducts which developed 12 hr after abdominal aortography in a gallbladder previously normal on oral cholecystography. Pathologic examination showed occlusion of the cystic artery branches, probably by atheromatous emboli, leading to necrosis of the gallbladder and gas formation. The prominent association of emphysematous cholecystitis and diabetes mellitus is an additional factor which supports the role of ischemia secondary to primary vascular disease. Ischemia allows bacterial invasion by gas-forming organisms, most frequently *Clostridia perfringens* or *E. coli* [2].

Heifetz and Wyloge [12] proposed an experimental model of emphysematous cholecystitis based on obstruction of the cystic duct, in which gas under pressure dissects into the wall of the gallbladder from the lumen. This model would not explain the occasional occurrence of pneumobilia, unless the gas in the wall of the gallbladder reentered the lumen of the cystic duct distal to the obstruction, or gas-forming cholangitis existed distal to the obstruction. A pathogenetic mechanism in which the cystic duct remains patent, such as primary ischemia of the gallbladder, would more likely explain the presence of pneumobilia in the cases reported.

The differential diagnosis of pneumobilia involves several considerations. When gas is observed in the lumen of the biliary ducts or gallbladder, it is necessary to distinguish emphysematous cholecystitis from a biliary enteric communication or an incompetent sphincter of Oddi. The demonstration of gas in the wall of the gallbladder confirms the diagnosis of emphysematous cholecystitis, while reflux of barium into the biliary tree would indicate a biliary enteric communication. The presence of pneumobilia in association with emphysematous cholecystitis suggests that the cystic duct is patent in these cases.

REFERENCES

1. Hegner CF: Gaseous pericholecystitis with cholecystitis and cholelithiasis. *Arch Surg* 22:993–1000, 1931
2. Mentzer RM, Golden GT, Chandler JG, Horsley JS: A comparative appraisal of emphysematous cholecystitis. *Am J Surg* 129:10–15, 1975
3. Sarmiento RV: Emphysematous cholecystitis *Arch Surg* 93:1009–1014, 1966
4. Friedman J, Aurelius JR, Rigler LB: Emphysematous cholecystitis. *Am J Roentgenol* 62:814–822, 1949
5. Culver GJ, Kline R: Acute gaseous cholecystitis: a report of a case. *Radiology* 50:536–538, 1948
6. Rosoff L, Meyers H: Acute emphysematous cholecystitis. An analysis of 10 cases. *Am J Surg* 111:410–423, 1966
7. Schowengerdt CG, Wiot JF: Emphysematous cholecystitis following aortography. *Am Surg* 38:274–277, 1972
8. Way LW, Sleisinger MH: Acute cholecystitis, in *Gastrointestinal Disease*, edited by Sleisinger MH, Fordtran JS, Philadelphia, Saunders, 1973, pp 1120–1128
9. Berk JE, Monroe LS: Acute cholecystitis, in *Gastroenterology*, vol 3, edited by Bockus HL, Philadelphia, Saunders, 1976, pp 792–793
10. Nelson SW: Extraluminal gas collections due to diseases of the gastrointestinal tract. *Am J Roentgenol* 115:225–248, 1972
11. May RE, Strong R: Acute emphysematous cholecystitis. *Br J Surg* 58:453–458, 1971
12. Heifetz CJ, Wyloge EI: Effect of distension of the gallbladder with air and its relationship to acute pneumocholecystitis. *Ann Surg* 142:283–288, 1955

Rheumatoid Arthritis and Its Variants: Analysis of Scintiphotographic, Radiographic, and Clinical Examinations

D. L. WEISSBERG,[1] D. RESNICK,[2] A. TAYLOR,[3] M. BECKER,[4] AND N. ALAZRAKI[3]

^{99m}Tc pyrophosphate radionuclide scans of the axial and appendicular skeletons in 23 patients with rheumatoid arthritis and 15 patients with systemic arthritic conditions were compared to clinical and radiographic examinations. The nuclear scan was the most sensitive indicator of active disease and correlated extremely well with the other methods. A pattern of abnormal radionuclide activity in rheumatoid arthritis consisting of a symmetric peripheral joint process can be distinguished from that of the rheumatoid variants which tend to have more central skeletal involvement and asymmetric peripheral articular involvement. The nuclear scan is less specific than the radiograph in its ability to distinguish among the clinical entities. However, documentation of scintigraphic activity often antedated radiographic or clinical abnormalities.

Although many bone-seeking radiopharmaceuticals have been used in the evaluation of rheumatoid arthritis [1–6], the recently developed ^{99m}Tc "phosphate" compounds have proved to be the most sensitive [7–9]. These agents have the advantage of low patient radiation exposure and high target-to-background ratios. Axial skeletal joint imaging is also readily performed with these newer pharmaceuticals.

Therefore we decided to reevaluate the potential role of nuclear scanning, using ^{99m}Tc pyrophosphate, in the diagnosis and management of patients with rheumatoid arthritis. The triple-blind prospective study included comprehensive scintiphotographic, radiographic, and clinical examinations. This study compared and correlated the sensitivities of the various methods. The specificity of the nuclear scan in identifying patterns of joint involvement in rheumatoid arthritis was also determined.

Subjects and Methods

Twenty-three patients with clinical and laboratory evidence of rheumatoid arthritis and 15 patients with systemic arthritic conditions (table 1) were randomly selected from the Rheumatology Clinic at the Veterans Administration Hospital in San Diego. Age range of patients with rheumatoid arthritis was 40–84 years (average, 59), they had symptomatology which varied from a few months to greater than 30 years (average, about 15 years). Age range of the other 15 patients was 26–81 years (average, 48). That these patients were all males reflects the patient population at our hospital. This fact should be emphasized because the bias in patient selection may be apparent when our results are compared with those of other investigators. All evaluations were usually performed within 10 days of each other.

Clinical Examination

The patients had complete joint examinations by a rheumatologist (M. Becker). Objective signs of active involvement included periarticular swelling, tenderness, effusion, bursitis, tendinitis, and subcutaneous nodule formation. Deformities, decreased range of motion, and subjective complaints of pain were not used as indicators of active disease. Gradation of individual joint involvement was related to the number of positive findings.

Scintiphotography

Patients were examined with an Anger scintillation camera 4 hr after intravenous injection of 15 mCi of ^{99m}Tc pyrophosphate. Diverging collimators were used for the axial skeleton and shoulders, with time control determined by counting over the posterior thoracic spine. For the peripheral joints, converging collimation with 100,000 counts was used. The survey of the axial skeleton included posterior views of the complete spine and pelvis, and anterior views of the shoulders and pelvis. Appendicular skeletal evaluation included views of the hands, wrists, elbows (lateral), knees (anterior), ankles (lateral), and feet. A complete examination required about 45 min. Two of us (D. Weissberg and A. Taylor) independently graded the degree of activity in relation to normal.

Without knowledge of the clinical diagnosis, one of us (A. Taylor) made presumptive diagnoses based on the pattern of radionuclide uptake. For rheumatoid arthritis, the distinguishing features were: (1) a symmetric process with peripheral joint activity greater than axial activity; (2) uniform involvement of the wrists and proximal joints of the hands and feet; (3) typical deformities; and (4) soft tissue changes such as periarticular swelling, bursal enlargement, and subcutaneous nodules (fig. 1). For the rheumatoid variant disorders the following features on nuclear scan were considered important: (1) an asymmetric process; (2) increased central activity, especially at the sacroiliac joints; (3) distal interphalangeal joint abnormalities; (4) soft tissue involvement, such as tendinitis and bursitis; and (5) plantar calcaneal uptake (fig. 2). In osteoarthritis the criteria included: (1) an asymmetric process; (2) radionuclide activity distributed in weight-bearing joints and the distal joints of the hands and feet; and (3) irregular central skeletal involvement.

Radiography

The radiographic survey included multiple views of the hands, wrists, elbows, knees, ankles, and feet for the appendic-

Received February 7, 1978; accepted after revision June 15, 1978.
Presented in part at the annual meeting of the American Roentgen Ray Society, Boston, September 1977.
D. Resnick is a James Picker Foundation Scholar.

[1]Department of Radiology, University of California Medical Center and University Hospital, San Diego, California 92103. Present address: St. Joseph's Hospital, Orange, California 92668.
[2]Department of Radiology, University of California Medical Center and Veterans Administration Hospital, 3350 La Jolla Village Drive, San Diego, California 92161. Address reprint requests to D. Resnick.
[3]Department of Nuclear Medicine, University of California Medical Center and Veterans Administration Hospital, San Diego, California 92161.
[4]Department of Internal Medicine, University of California Medical Center and Veterans Administration Hospital, San Diego, California 92161.

© 1978 American Roentgen Ray Society

0361–803X/78/1000–0665 $00.00

TABLE 1

Summary of Cases

Diagnosis	No. Patients
Rheumatoid arthritis:	
Seropositive	21
Seronegative	2
Rheumatoid variant disorders:	
Ankylosing spondylitis	4
Psoriasis	4
Reiter's disease	1
Indeterminate	2
Miscellaneous arthritides:	
Gout	1
Calcium pyrophosphate deposition disease	1
Osteoarthritis	1
Reflex sympathetic dystrophy syndrome	1
Total	38

ular skeleton. Two views of the cervical, thoracic, and lumbar spine and shoulders with an anteroposterior view of the pelvis were used for the axial skeleton.

Radiographic parameters of involvement included evidence of soft tissue swelling, effusion, periarticular osteoporosis, joint space narrowing, erosions, cysts, periosteal reaction, and deformities. Without knowledge of the clinical findings or diagnosis, one of us (D. Resnick) estimated the degree of involvement. Standard radiographic criteria for skeletal and soft tissue abnormalities were used to differentiate among the various disorders.

Results

Sensitivity Determination

Rheumatoid arthritis. The percentage of involvement of specific articulations in rheumatoid arthritis as determined by each method is presented in table 2. Nuclear

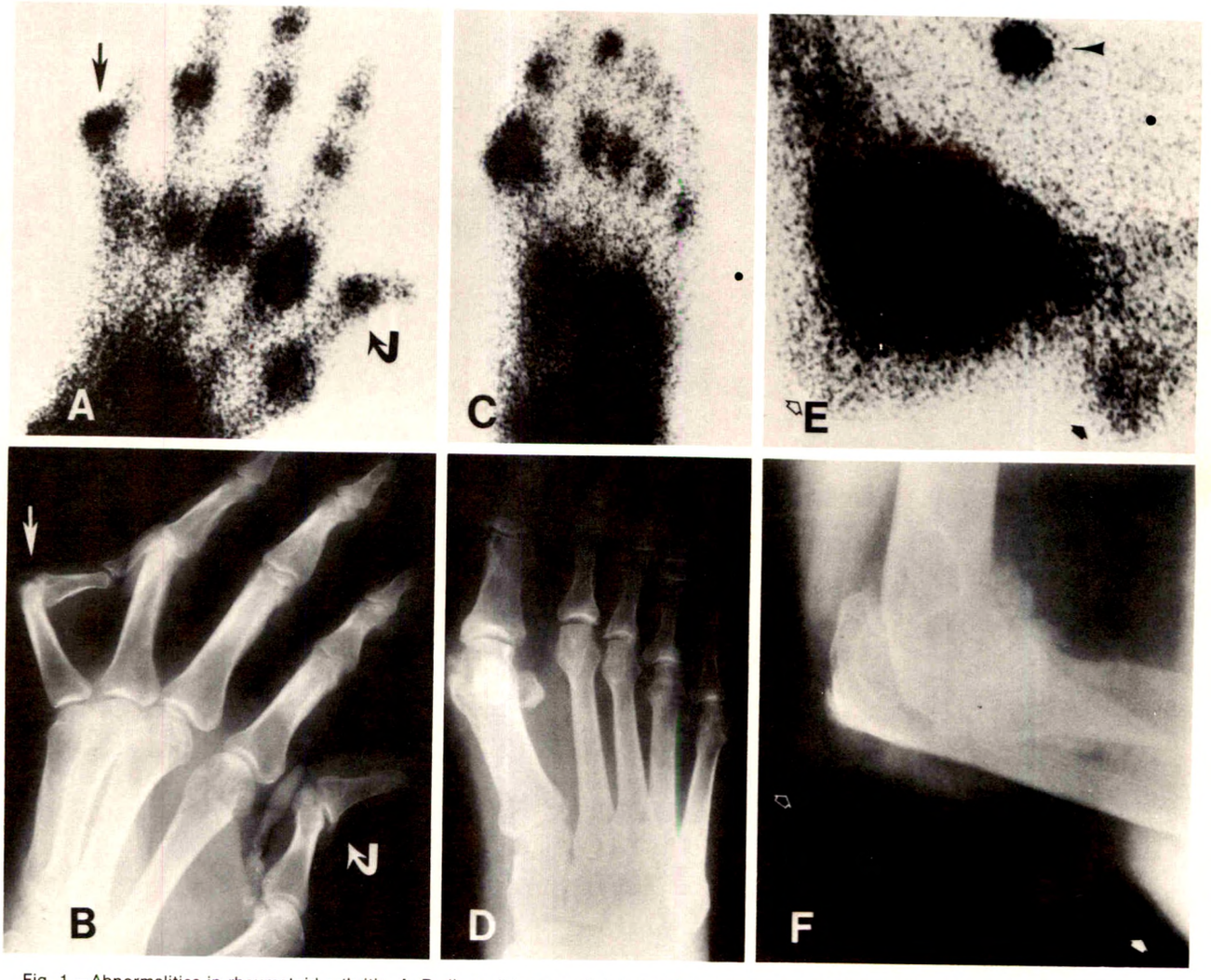

Fig. 1.—Abnormalities in rheumatoid arthritis. *A*, Radionuclide scan of right hand demonstrating uniform wrist activity and greater proximal than distal joint involvement. Note deformities of first (*curved arrow*) and fifth (*arrow*) digits. *B*, Radiograph of hand in *A* showing typical deformities. Areas of greatest radionuclide activity correlate well with radiographic changes. *C*, Radionuclide scan of left foot showing typical distribution of activity, greatest in proximal joints. Corresponding symmetric abnormalities were seen in this patient's right foot. *D*, Radiograph of foot in *C* showing extensive erosive disease corresponding to radionuclide scan. Again, marked radionuclide uptake is seen in areas of greatest radiographic change. *E*, Lateral radionuclide scan of right elbow showing uptake in region of joint. Enlarged olecranon bursa (*open arrow*) and subcutaneous nodule are seen (*closed arrow*). Note uptake at injection site (*arrowhead*). *F*, Radiograph of elbow in *E* showing soft tissue changes of olecranon bursitis (*open arrow*) and subcutaneous nodule (*closed arrow*).

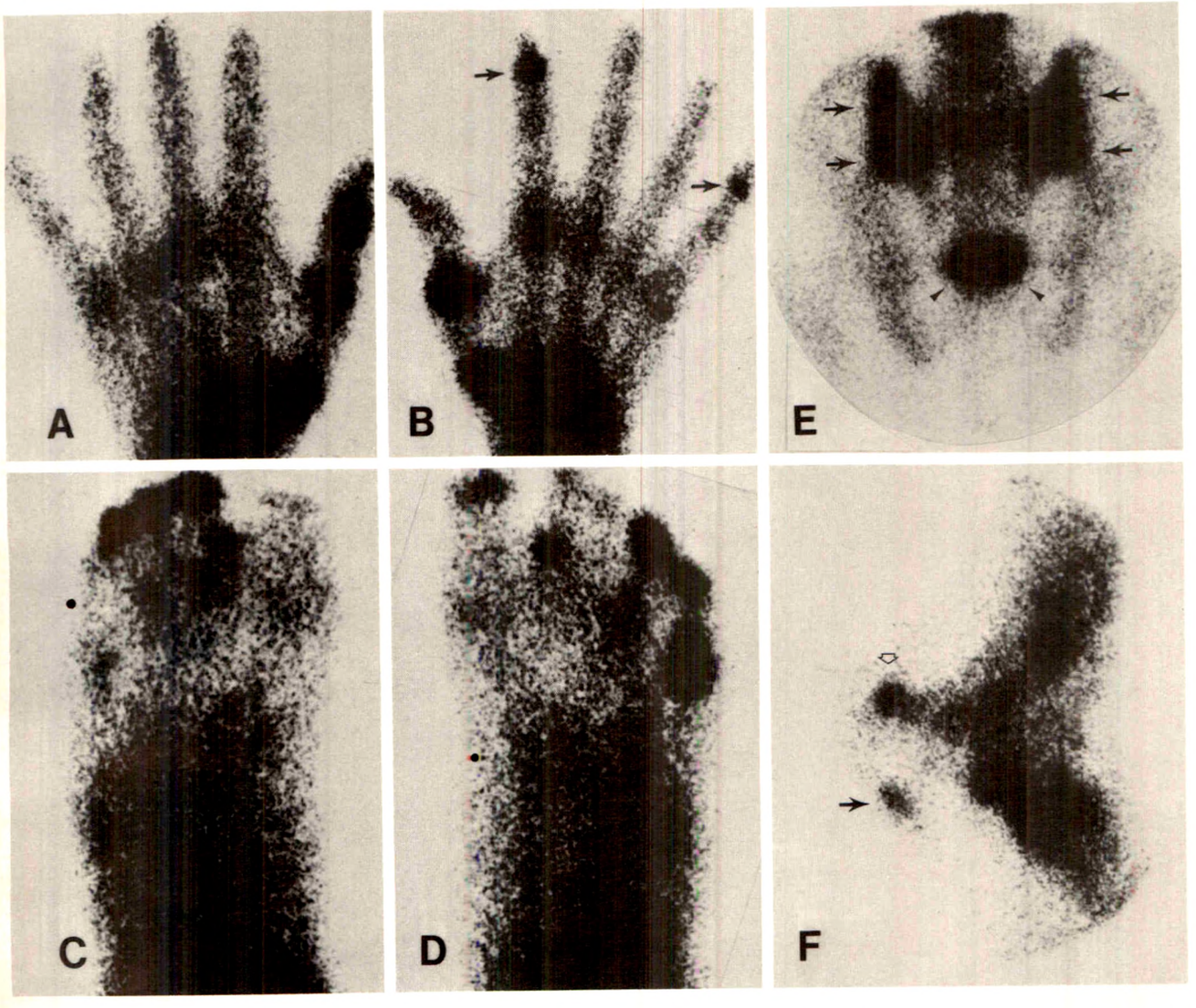

Fig. 2.—Abnormalities in rheumatoid variant disorders. *A and B*, Radionuclide scans of right (*A*) and left (*B*) hands in patient with psoriasis showing asymmetric pattern of uptake and involvement of distal interphalangeal joints (*arows*). *C and D*, Scintiphotographs of same patient showing similar pattern of involvement in peripheral joints of right (*C*) and left (*D*) feet. *E*, Scan of posterior pelvis of different patient with psoriasis demonstrating symmetric uptake in sacroiliac joints (*arrows*). Much greater activity is seen over these joints compared to over sacrum. Radiotracer is present in bladder (*arrowheads*). *F*, Radionuclide scan of right foot of patient with ankylosing spondylitis showing uptake in plantar calcaneal region (*arrow*). Activity is also seen in foot and in region of retrocalcaneal bursa (*open arrow*).

scanning showed involvement was highest in the appendicular joints, greatest in the wrist (98%) (fig. 1*A*). The incidence of joint involvement detected by radiography was generally lower than that recorded by scintigraphy, especially when the changes of osteoarthritis are excluded. For clinical activity, a pattern of involvement which closely follows that of radionuclide activity was seen.

Rheumatoid variants. The results of examination in 11 patients with rheumatoid variant disorders are presented in table 2. The incidence of detection of abnormal joints was greatest on scintigraphy except in the spine, distal interphalangeal joints, and hip. Radiographic studies showed significant abnormalities in the axial skeleton, especially at the sacroiliac joints (63%). However, the incidence of radiographic abnormalities exceeded that detected by the other methods only in the spine, hips, and distal interphalangeal articulations.

On clinical examinations, axial skeletal abnormalities were particularly frequent (table 2). Good correlation between frequency of radiographic and clinical findings was seen in the spine. The degree of clincial involvement in the rest of the skeleton was variable in relation to that detected on radiography, but generally more extensive.

Correlation of Sensitivities

Rheumatoid arthritis. The sensitivity of nuclear scanning was compared to that of radiography in the 23 patients with rheumatoid arthritis (table 3). Of 1,262 joints examined which did not have radiographic changes of osteoarthritis, concordance was seen in 67% of articulations; both methods were negative in 38% and both were positive in 29%. Abnormal nuclear scan activity was seen in 20% of joints which had no radiographic abnormalities. On the other hand, 13% of joints were involved on radiography and uninvolved on scintigraphy.

Nuclear scanning was compared to the clinical evaluation in 1,293 joints (table 4). In one set of joints, the metatarsophalangeal articulation, difficulty in determining clinically active disease was encountered because of associated osseous deformity. This resulted in an increased incidence of clinically detectable active disease

TABLE 2

Percentage of Involvement of Specific Articulations

Joint	Rheumatoid Arthritis			Rheumatoid Variant Diseases		
	Nuclear Scanning	Radiography	Clinical Examination	Nuclear Scanning	Radiography	Clinical Examination
Distal interphalangeal	17	10 (22)	8	9	14	7
Proximal interphalangeal	48	51 (54)	40	30	20	23
Metacarpophalangeal	70	54	70	47	13	35
Wrist	98	65	92	64	17	50
Elbow	78	39	66	45	9	41
Shoulder	46	26	46	41	21	9
Cervical spine	20	23 (45)	20	9	33	27
Thoracolumbar spine	28	5 (41)	12	36	50	60
Sacroiliac	34	7 (17)	0	73	63	59
Hip	2	15	12	5	17	9
Knee	78	41 (50)	82	36	8	23
Ankle	74	22	54	59	8	36
Tarsal	68	39	34	55	8	14
Tarsometatarsal	66	36	26	50	13	9
Metatarsophalangeal	41	49	70	33	18	25
Interphalangeal	16	8	2	4	11	10

Note.—Numbers in parentheses are combined percentages of rheumatoid and osteoarthritic abnormalities.

TABLE 3

Correlation of Nuclear Scanning and Radiography

Joint	Rheumatoid Arthritis				Rheumatoid Variant Diseases			
	Both Negative	Both Positive	Positive Nuclear Scan, Negative Radiograph	Negative Nuclear Scan, Positive Radiograph	Both Negative	Both Positive	Positive Nuclear Scan, Negative Radiograph	Negative Nuclear Scan, Positive Radiograph
Distal interphalangeal	141	0	15	17	67	1	6	5
Proximal interphalangeal	64	78	41	52	68	6	21	10
Metacarpophalangeal	57	112	45	17	54	14	38	1
Wrist	1	32	12	1	6	4	12	0
Elbow	10	18	16	. . .	10	2	9	0
Shoulder	20	5	15	3	11	3	6	2
Cervical spine	12	2	0	3	6	0	1	2
Thoracolumbar spine	11	1	1	0	4	2	1	3
Sacroiliac	21	1	14	2	2	10	6	4
Hip	34	1	0	5	18	1	0	3
Knee	5	19	18	4	13	1	7	1
Ankle	10	8	19	9	9	2	11	0
Tarsal	12	14	13	7	10	2	10	0
Tarsometatarsal	10	9	18	5	11	3	7	0
Subtotal	408 (39)	300 (28)	227 (21)	125 (12)	289 (57)	51 (10)	136 (27)	31 (6)
Metatarsophalangeal	76	62	25	39	68	12	23	7
Total	484 (38)	362* (29)	252 (20)	164† (13)	357 (58)	63‡ (10)	159 (26)	38§ (6)

Note.—Data excluding patients with osteoarthritis. Numbers in parentheses are percentages.

* 18 additional joints had osteoarthritis: distal interphalangeal (10), proximal interphalangeal (two), thoracolumbar spine (four), and sacroilliac (two).

† 16 additional joints had osteoarthritis: distal interphalangeal (four), cervical spine (five), thoracolumbar spine (five), and sacroiliac (two).

‡ Two additional joints had osteoarthritis: thoracolumbar spine.

§ 21 additional joints had osteoarthritis: distal interphalangeal (eight), proximal interphalangeal (one), cervical spine (11), and thoracolumbar spine (one).

TABLE 4

Correlation of Nuclear Scanning and Clinical Examination

	Rheumatoid Arthritis				Rheumatoid Variant Diseases			
	Both Negative	Both Positive	Positive Nuclear Scan, Negative Clinical Tests	Negative Nuclear Scan, Positive Clinical Tests	Both Negative	Both Positive	Positive Nuclear Scan, Negative Clinical Tests	Negative Nuclear Scan, Positive Clinical Tests
Distal interphalangeal	153	0	11	4	74	1	6	5
Proximal interphalangeal	77	48	62	41	69	13	19	10
Metacarpophalangeal	36	126	36	29	50	31	22	8
Wrist	0	42	3	1	5	10	6	1
Elbow	5	27	9	5	9	6	4	3
Shoulder	16	13	11	6	11	. . .	9	2
Cervical spine	18	2	1	2	8	1	. . .	2
Thoracolumbar spine	17	2	4	0	4	2	1	4
Sacroiliac	27	0	19	0	4	11	5	2
Hip	40	1	0	5	20	1	. . .	1
Knee	5	31	6	4	12	3	5	2
Ankle	8	22	12	4	5	5	9	3
Tarsal	12	11	19	4	10	3	9	. . .
Tarsometatarsal	8	4	27	7	11	2	9	. . .
Subtotal	422 (39)	329 (30)	220 (20)	112 (10)	292 (56)	89 (17)	104 (20)	43 (8)
Metatarsophalangeal	38	82	14	76	55	16	19	11
Total	460 (36)	411 (32)	234 (18)	188 (15)	347 (55)	105 (17)	123 (20)	54 (9)

Note.—Numbers in parentheses are percentages.

and marked clinical-scintigraphic dissociation. In fact, 76 of 210 joints (36%) were positive by clinical examination and negative by scintigraphy. If these articulations were excluded from the analysis, evaluation of the remaining 1,083 joints yielded concordance in 69%, while 20% were positive solely by scanning and 10% were positive solely by clinical examination.

Rheumatoid variant diseases. The incidence of abnormality on nuclear scanning in the 11 patients with rheumatoid variant disorders was compared to that seen on radiography in 640 joints (table 3). After exclusion of 23 joints identified by radiography as degenerative disease, 68% of joints had concordant results, 26% were positive by scanning alone, and 6% were positive by radiography alone. It was of interest that 21 of the 23 joints with radiographic evidence of osteoarthritis had no evidence of radionuclide activity.

In correlating nuclear scanning with clinical examination in 629 joints (table 4), concordance of activity was seen in 72% of joints. Discordance was seen in 20% which were positive by nuclear scanning alone and 9% which were positive by clincal examination alone.

Specificity

Diagnostic specificity is outlined in table 5. Of the 23 patients with rheumatoid arthritis, nuclear scanning correctly identified 19. Three cases were diagnosed as variant disorders and the fourth was listed as a variant or rheumatoid with sacroiliac joint involvement. Radiography correctly identified 16 of the 23 cases. The remaining diagnoses were degenerative disease (four patients), osteoporosis (one), rheumatoid variant disease (one), and normal (one).

TABLE 5

Diagnostic Specificity

	Clinical Examination	Nuclear Scanning	Radiography
Rheumatoid arthritis	23	19*	16†
Rheumatoid variants:			
Specific diagnosis	9	5	8
Indeterminate	2	2	2
Other	4	1	2

* Includes two probable.
† Includes three probable.

Of nine patients with specific rheumatoid variant disorders (i.e., ankylosing spondylitis, psoriasis, or Reiter's disease), five were appropriately placed in this general category by nuclear scanning, although distinguishing features could not be discerned to allow a specific diagnosis to be made.

Of the miscellaneous diseases, only the case with osteoarthritis was diagnosed by nuclear scanning. Radiography correctly diagnosed the patient with calcium pyrophosphate deposition disease and reflex sympathetic dystrophy syndrome.

Follow-up Studies

Six patients had complete follow-up examinations, and additional patients had limited follow-up evaluation using the three diagnostic methods. In this small number of patients, certain results were noted. Radionuclide activity often antedated clinical or radiographic changes. This was best demonstrated in the peripheral joints of two patients with psoriasis (fig. 3). Also, areas of greatest

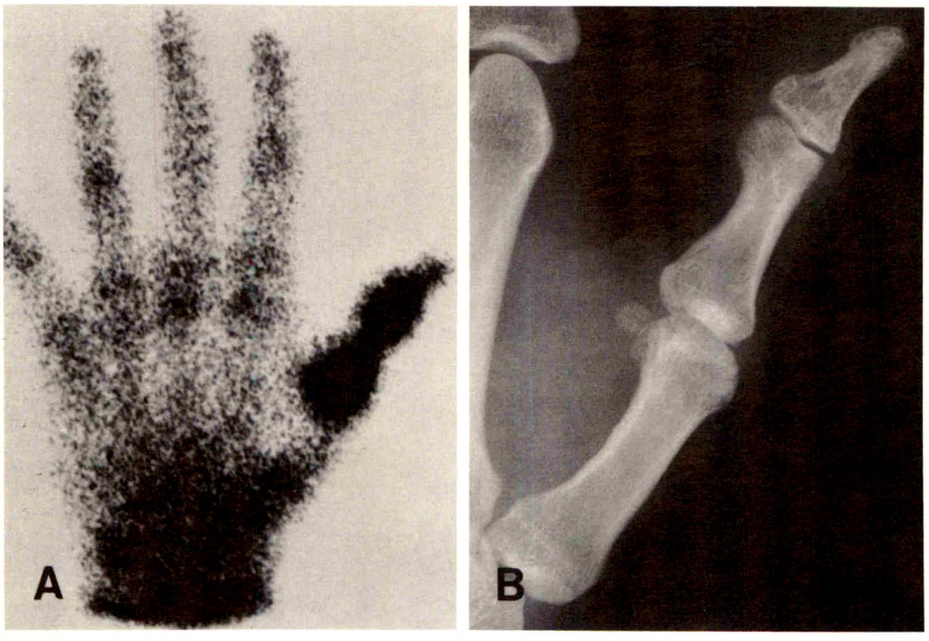

Fig. 3.—Patient with asymptomatic psoriasis. *A*, Radionuclide scan of right hand showing extensive uptake in interphalangeal and metacarpophalangeal joints of thumb. Remainder of joints are normal. *B*, Radiograph of *A* revealing only minimal periarticular soft tissue swelling. Subsequent clinical and progressive radiographic abnormalities developed in these joints.

clinical activity often were predicted by marked radionuclide uptake. In three patients with rheumatoid arthritis with subjective improvement after therapy, there was no documentation of change in nuclear scanning.

Discussion

Since ^{99m}Tc was first used in 1967 for joint scintigraphy [10], many authors have used technetium-labeled pertechnetate to study patients with rheumatoid arthritis [1, 4, 5, 6, 11]. Pertechnetate scans have proved to be very sensitive indicators of peripheral joint disease [4, 11, 12], occasionally antedating clinical activity, and have shown promise as a means of monitoring response to therapy [1, 4, 6, 11]. Subsequent introduction of ^{99m}Tc "phosphate" compounds has provided a means to study both the axial and peripheral skeleton, and has increased the sensitivity of scintigraphy as an indicator of joint disease [7–9].

No comprehensive study of rheumatoid arthritis has been undertaken using one of these newer radiopharmaceuticals. However, Desaulniers et al. [8] compared the distribution of ^{99m}Tc polyphosphate and ^{99m}Tc pertechnetate in the peripheral skeleton to the distribution of radiographic and clinical findings in 27 patients, 17 of whom had rheumatoid arthritis. In our study we performed complete axial and peripheral examinations in all 23 patients with rheumatoid arthritis. Our purpose was threefold: (1) to compare and correlate the sensitivity of ^{99m}Tc pyrophosphate nuclear scanning in the evaluation of rheumatoid arthritis and related diseases to the sensitivity of clinical and radiographic examinations; (2) to note the specificity of radionuclide examination to identify patterns of involvement; and (3) to determine through follow-up examinations if nuclear scanning provided a means of identifying progression of disease and/or response to therapy.

Our study had certain limitations. Because evaluation was visual, interpretation of data had to be qualitative rather than quantitative. For example, the assessment of sacroiliac joint activity on nuclear scanning was accomplished by visually comparing sacral to sacroiliac joint uptake (fig. 2*E*), rather than recording activity for computerized readout. It was difficult at times to separate active from inactive disease on clinical examination, although we did not consider subjective complaints and deformities signs of disease activity. The possible superimposition of one disease process upon another (i.e., osteoarthritis and rheumatoid arthritis) made evaluation of some results more difficult. Rarely, delays in obtaining radiographs or nuclear scans resulted in separation of examinations by more than a few days. Modification of the techique of nuclear scanning evolved during the initial period of our study so that the first examinations were of lesser quality than the majority of studies. Finally, a small number of patients was used as a control group, and an even smaller group had full follow-up examinations. Despite these shortcomings, some general comments can be made.

Sensitivity and Correlation

Our results are consistent with those of previous studies which used pertechnetate [4, 5, 12, 13]. Nuclear scanning was the most sensitive indicator of active disease in rheumatoid arthritis and correlated well with the clinical examination. Abnormal joints were seen with much greater frequency on scanning (with the exception of the spine) than on radiography. Greatest sensitivity was seen in the smaller peripheral joints. For the large peripheral joints, the incidence of clinical activity was equal to or slightly greater than that on scanning in the shoulder, hip, and knee. In the axial skeleton of patients with rheumatoid arthritis, our results were less conclusive. It was surprising that abnormalities of the sacroiliac

joints as determined by increased radionuclide activity (34%) were significantly more common than abnormalities noted by clinical and radiographic examinations. This observation of significant radionuclide activity in the sacroiliac joints was also noted by Lentle et al. [14, 15] using a computerized profile scan technique which compared sacroiliac joint to sacral activity. In the spine, we noted variation of sensitivities manifest by specific methods. Difficulty in discerning active versus inactive disease and the presence of coincident disorders such as degenerative disease probably contributed to this variation.

Superior sensitivity of nuclear scanning was documented when abnormalities in individual joints were correlated. Marked discordance was only noted in two sites. In the first, the metatarsophalangeal joints, 36% of articulations were positive clinically and negative scintiphotographically. The probable explanation for this discordance is in the method of clinical examination. In this location the clinician considered all metatarsophalangeal joints as a single group and often was unable to differentiate deformity from synovial inflammation. Rather than ascribe the lack of radionuclide uptake in this group of joints to insensitivity of the nuclear scan, it seems more likely that there was a failure of the clinical examination to differentiate inactive or "burned out" disease from active disease. McCarty et al. [4], noting that certain joints failed to manifest increased radionuclide uptake, presumed this was evidence of quiescent disease. The second area of significant discordance was the spine, in which a large number of radiographic abnormalities was due to degenerative disease. These also could represent areas of inactive disease.

Our results in patients with rheumatoid variant disorders also showed that nuclear scanning was the most sensitive indicator of active disease. Good correlation of results for each method was documented.

Specificity

When patterns of radionuclide activity were used to make specific diagnoses, 83% of the patients with rheumatoid arthritis were correctly identified. This compares favorably with the 70% who were correctly diagnosed by radiography. On scintiphotography in patients with rheumatoid variant disorders, a pattern of involvement was identified in 56% of cases which was definitely separable from that seen in the patients with rheumatoid arthritis. (Only three of 23 patients with rheumatoid arthritis were misdiagnosed as having rheumatoid variant disorders.) However, nuclear scanning could not distinguish among the specific variants in our small number of patients. In this respect, radiography had higher sensitivity in detecting rheumatoid variant disease and in providing a specific diagnosis of which variant disorder was present. So, although nuclear scanning is quite sensitive as a diagnostic tool in patients with rheumatoid arthritis and related disorders, it is less specific than radiography. Again, this lack of specificity is probably due to the fact that scanning records active bone processes and not inactive states, whereas radiography is a record of prior events.

Of significance in this regard is the known phenomenon of negative radionuclide uptake when there are osteoarthritic changes [3, 4]. In our study, 23 joints were noted to have radiographic changes of osteoarthritis in the patients with rheumatoid variant disorders, and 21 of these manifested no activity by nuclear scanning. Also, 10 of 14 patients with rheumatoid arthritis who had osteoarthritic changes in the spine had negative nuclear scans. Another example of this phenomenon was seen in a patient with classic ankylosing spondylitis, in which there was inactivity on scintiphotography over ankylosed sacroiliac joints, since these were sites of inactive disease (fig. 4).

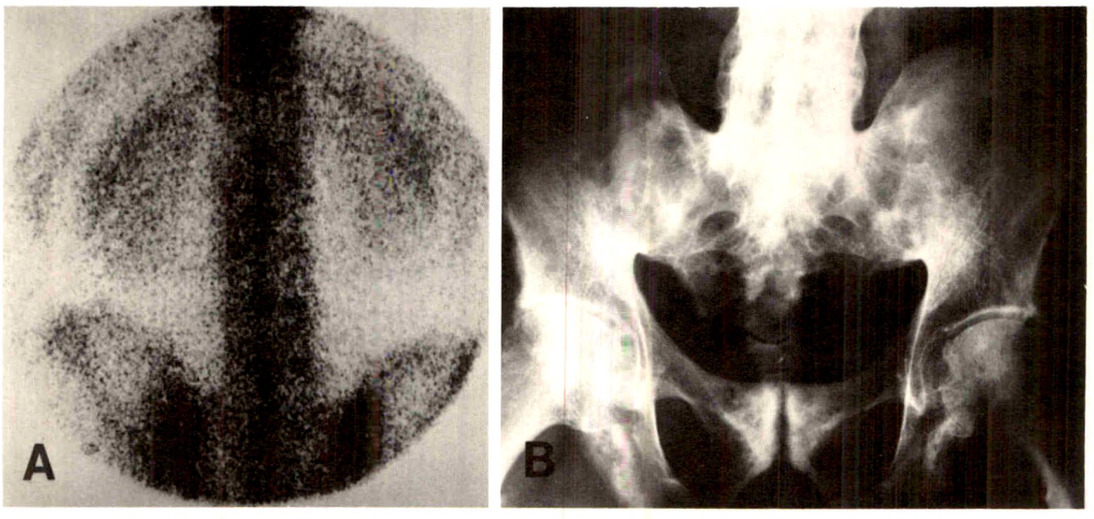

Fig. 4.—Patient with ankylosing spondylitis. Radionuclide scan of posterior lumbosacral spine showing no abnormal uptake within spine. No significant increase in uptake is seen at sacroiliac joints. *B*, Radiograph of lumbosacral spine in *A* showing classic changes of ankylosing spondylitis. Lack of radionuclide uptake is thought to indicate "burned out" disease.

Fig. 5.—50-year-old man with rheumatoid arthritis. Radionuclide scan of left hand showing extensive radiotracer uptake. Bands of activity at epiphyseal-metaphyseal area (*arrows*) may normally be seen in young individuals. In middle-aged patient, it is abnormal.

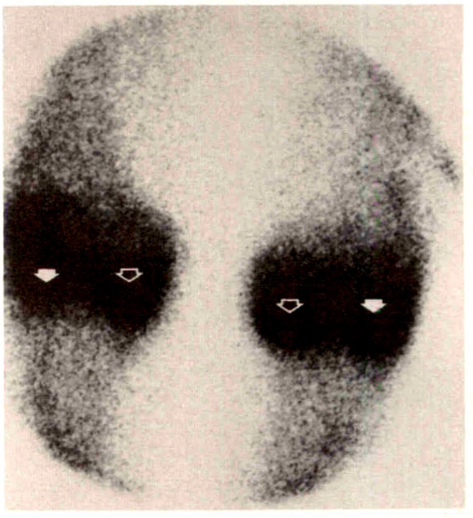

Fig. 6.—Patient with rheumatoid arthritis. Radionuclide scan of knees showing symmetric compartmental distribution of activity in all femorotibial compartments, medial (*open arrows*) and lateral (*closed arrows*).

Certain interesting patterns of uptake were occasionally noted on scans. Some patients had dense bands of activity at the epiphyseal-metaphyseal areas in the small joints of the hand and feet (fig. 5). This pattern is often seen in young individuals, but in our patients this reflected areas of clinical inflammation, confirming the results of other investigators [16]. The typical scan of the knees of patients with rheumatoid arthritis is that of symmetric, medial, and lateral compartment uptake (fig. 6). However, in a few patients with classical rheumatoid arthritis, asymmetric involvement was observed. McCarty et al. [4] also noted this asymmetric involvement in the early cases of rheumatoid arthritis. Possibly this reflects the distribution of stress forces and remodeling within bone which is also seen in osteoarthritis [17].

Follow-up Examinations

Marked radiotracer activity best correlated with specific areas of active clinical disease. Abnormalities were often noted scintiphotographically prior to change in the other methods (fig. 3), and most activity was seen in regions of greatest inflammation. However, concordant progression was not always seen in our follow-up studies, especially in long-standing disease which supposedly had improved clinically. In fact, some joints actually manifested increased activity in the face of clinical improvement. The same findings were noted by Desaulniers et al. [8]. They studied 16 patients who were undergoing therapy and found concordant clinical and nuclear scan progression in 50%. Other investigators have reported better results when nuclear scanning was used to follow response to therapy [1, 2, 6, 11]. Obviously more work must be done to resolve these inconsistencies if nuclear scanning is ever to be used to monitor therapeutic results.

Conclusions

Our data show that the radionuclide scan is an extremely sensitive indicator of activity in rheumatoid arthritis and that nuclear scanning correlates extremely well with radiographic and clinical examinations. A pattern of abnormal radionuclide activity in rheumatoid arthritis consisting of a symmetric peripheral joint process can be distinguished from that of the rheumatoid variants which tend to have more central skeletal involvement and asymmetric peripheral articular involvement. However, nuclear scanning is less specific than radiography in distinguishing among the clinical entities.

What then is the role of nuclear scanning in the evaluation of patients with rheumatoid arthritis? Although the radionuclide scan is a very sensitive indicator of active disease, in routine cases it seems to add little information to help in proper patient management. Clinical parameters of disease activity are well outlined and easily used to monitor progression of the disease. Follow-up radionuclide studies have been inconclusive in relation to these findings. In some patients with rheumatoid arthritis, scintigraphy may be helpful because of its sensitivity. Whether the increased sensitivity of radionuclide examination compared to that of clinical examination in these patients reflects a limitation of the clinical examination or rather reparative and/or potentially active sites which can be detected solely by the radiopharmaceutical cannot be discerned in our limited study. Scanning definitely predicted areas of involvement and was the first method which was positive in some patients with equivocal physical examinations and normal radiographs. Documentation of scintigraphic activity can be helpful in the latter situation as an indicator of "real" disease.

ACKNOWLEDGMENTS

We thank Sue Brown and Robert Turner for photography and Janet Zatlokowicz for preparation of the manuscript.

REFERENCES

1. Dick WC, Neufeld RR, Prentice AG, Woodburn A, Whaley K, Nuki G, Buchanan WW: Measurement of joint inflammation: a radioisotopic method. *Ann Rheum Dis* 29:135–137, 1970
2. Dick C, Whaley K, St. Onge RA, Downie WW, Boyle JA, Nuki G, Gillespie FC, Buchanan WW: Clinical studies on inflammation in human knee joints: Xenon (^{133}Xe) clearances correlated with clinical assessment in various arthritides and studies on the effect of intra-articularly administered hydrocortisone in rheumatoid arthritis. *Clin Sci* 38:123–133, 1970
3. Hoffer PB, Genant HK: Radionuclide joint imaging. *Semin Nucl Med* 6:121–137, 1976
4. McCarty DJ, Polcyn RE, Collins PA: Technetium scintiphotography in arthritis: its nonspecificity and clinical and roentgenographic correlations in rheumatoid arthritis. *Arthritis Rheum* 13:21–32, 1970
5. Maxfield WS, Weiss TE, Shuler SE: Synovial membrane scanning in arthritic disease. *Semin Nucl Med* 2:50–70, 1972
6. Sturrock D, Nicholson R, Wojtulewski JA: Technetium counting in rheumatoid arthritis: evaluation in the small joints of the hand. *Arthritis Rheum* 17:417–420, 1974
7. Bekerman C, Genant HK, Hoffer PB, Kozin F, Ginsberg M: Radionuclide imaging of the bones and joints of the hand: a definition of normal and a comparison of sensitivity using ^{99m}Tc-pertechnetate and ^{99m}Tc-diphosphonate. *Radiology* 118:653–659, 1975
8. Desaulniers M, Fuks A, Hawkins D, Lacourciers Y, Rosenthal L: Radiotechnetium polyphosphate joint imaging. *J Nucl Med* 15:417–423, 1974
9. Genant HK, Kozin F, Bekerman C, McCarty DJ, Sims J: The reflex sympathetic dystrophy syndrome: a comprehensive analysis using fine-detail radiography, photon absorptiometry, and bone and joint scintigraphy. *Radiology* 117:21–32, 1975
10. Alarcon-Segovia D, Trujeque M, Tovar E, Adame MA: Scintillation scanning of joints with technetium-99m (abstr.). *Arthritis Rheum* 10:262, 1967
11. Whaley K, Pack AI, Boyle JA, Dick WC, Downie WW, Buchanan WW, Gillespie FC: The articular scan in patients with rheumatoid arthritis: a possible method of quantitating joint inflammation using radio-technetium. *Clin Sci* 35:547–552, 1968
12. Green FA, Hays MT: The pertechnetate joint scan. II. Clinical correlations. *Ann Rheum Dis* 31:278–281, 1972
13. Sholkoff SD, Glickman MG: Scintiphotographic evaluation of arthritis activity. *Invest Radiol* 4:207–214, 1969
14. Lentle BC, Russell AS, Percy JS, Jackson FI: Scintigraphic findings in ankylosing spondylitis. *J Nucl Med* 18:524–528, 1977
15. Lentle BC, Russell AS, Percy JS, Jackson FI: The scintigraphic investigation of sacroiliac disease. *J Nucl Med* 18:529–533, 1977
16. Sy WM, Bay R, Camera A: Hand images: normal and abnormal. *J Nucl Med* 18:419–424, 1977
17. Thomas RH, Resnick D, Alazraki NP, Daniel D, Greenfield R: Compartmental evaluation of osteoarthritis of the knee: a comparative study of available diagnostic modalities. *Radiology* 116:585–594, 1975

Accuracy of CT in Detecting Intraabdominal and Pelvic Lymph Node Metastases from Pelvic Cancers

JOSEPH K. T. LEE,[1] ROBERT J. STANLEY, STUART S. SAGEL, AND BRUCE L. McCLENNAN

In 40 patients with pelvic cancers evaluated by computed tomography (CT), CT was less accurate in demonstrating lymph node metastasis compared to its high accuracy in detecting nodal involvement in lymphoma patients. This largely reflects the inability of CT to detect alterations in internal architecture in a normal-sized lymph node. While less sensitive, CT is a more specific method than lymphangiography in detecting nodal involvement by pelvic cancers. The role of CT in the staging of pelvic cancers is discussed.

Introduction

It is known that lymphangiography is less accurate in detecting retroperitoneal lymph node metastasis from pelvic cancer than in detecting lymphoma. This is due to its inability to detect microscopic metastatic deposits and to differentiate between malignant and nonmalignant peripheral filling defects in lymph nodes. The problem is compounded by the fact that lymph nodes which serve as the primary drainage site for various pelvic organs are often not opacified by pedal lymphangiography.

Reports of accuracy of lymphangiography in detecting lymph node metastasis from various pelvic cancers vary a great deal and in general relate to the experience of the observer. Schaffer et al. [1] reported that lymphographic interpretation was correct in 20 of 27 histologically proven cases (accuracy, 74%) in patients with metastatic carcinoma of the unspecified primary site. Spellman et al. [2] reported an overall accuracy rate of 78% in pedal lymphangiography in prostatic carcinoma. Loening et al. [3] reported a much higher false positive (59%) but a slightly lower false negative rate (36%) using lymphangiography in the staging of prostatic carcinoma.

Although it was once reported [4] that the primary nodal drainage of the bladder is not visualized on pedal lymphangiography and thus is of no value in staging bladder carcinoma, recent work by Merrin et al. [5] disproved this concept. Johnson et al. [6] and Wajsman et al. [7] reported an overall accuracy above the 90% range in bladder carcinoma. However, both these studies came from large cancer centers where lymphangiograms are interpreted by experienced lymphologists.

Because radical lymphadenectomy was rarely performed in patients with gynecologic tumors, there are few reports on accuracy of lymphangiography in detecting nodal metastasis from these tumors. Piver et al. [8] from M. D. Anderson Hospital and Tumor Institute reported an overall accuracy of 87% with a 22% false negative rate in cervical carcinoma. However, few can achieve this high degree of accuracy.

Due to lack of more accurate methods, short of radical nodal dissection, lymphangiography is still important in the staging of metastatic pelvic cancer. Since the initial application of computed tomography (CT) to the extracranial structures in early 1975, noninvasive imaging of retroperitoneal and pelvic lymph nodes has been possible. This report analyzes the role of CT in the detection of retroperitoneal and pelvic lymph node metastasis from primary pelvic cancers.

Subjects and Methods

CT was performed on an EMI 5000 prototype or 5005 18 sec body scanner. The slice thickness was 13 mm, with a scanning sequence of 2 cm sections taken from the diaphragm caudad to the symphysis pubis. Some patients early in the study had only body scans taken at 4 cm intervals in the same anatomic region. Oral and intravenous contrast media were administered where indicated to evaluate possible gastrointestinal or urinary structures. Data retrieval was accomplished using the computer system CATBOD [9].

The initial scan interpretations were made without knowledge of the lymphangiographic findings. All scans and lymphangiograms were reviewed prior to the completion of the study to avoid gross interpretive error. The final data analysis was done using the interpretations made by review. The diagnostic accuracy of CT scanning was calculated using only patients who had surgical confirmation. In only one confirmed case was a retrospective interpretation used.

The 40 patients in this study were divided into two groups for purposes of analysis. The first group consisted of 26 patients who had CT and histologic confirmation. In this group, eight patients had prostatic carcinoma, six had bladder carcinoma, six had testicular tumors, five had gynecologic tumors, and one had a spermatic cord sarcoma. Concurrent lymphangiography was performed in 14 patients in the first group. Nine patients had CT before lymphangiography and five had CT after. The second group included 14 patients who had CT and other diagnostic methods, such as lymphangiography, ultrasound, or radionuclide scanning, but no histologic confirmation.

Results

Histologic Confirmation

Of the 26 patients who had both CT and surgical confirmation, 23 had exploratory laparotomy within 2 weeks of a CT study. One patient had surgery 2 months after the initial scan. Two other patients had surgery before the CT scan. Both patients had biopsy-proven metastatic nodal disease; CT was done mainly for delin-

Received January 24, 1978; accepted after revision June 2, 1978.

[1] All authors: Mallinckrodt Institute of Radiology, Washington University School of Medicine, 510 South Kingshighway, St. Louis, Missouri 63310. Address reprint requests to J. K. T. Lee.

© 1978 American Roentgen Ray Society

0361–803X/78/1000–0675 $00.00

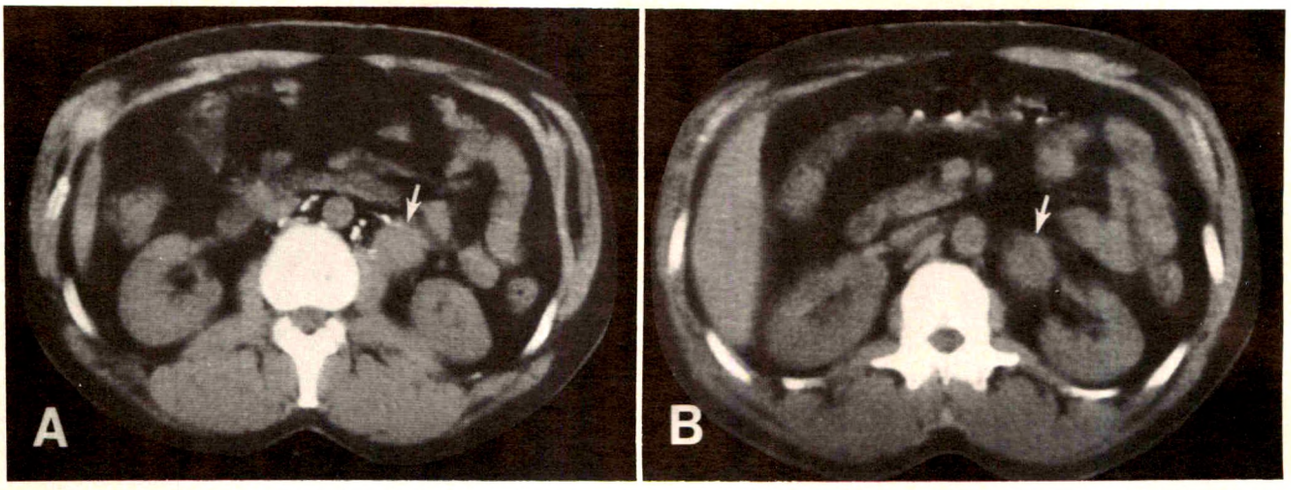

Fig. 1.—Patient with seminoma of left testis. Scans through midportion of both kidneys demonstrating adenopathy (*arrows*) around left renal vein not opacified by preceding lymphangiogram. These lymph nodes are primary drainage system for left testis. *A* 2 cm below *B*. (*A* reprinted with permission from [10])

eating and confirming the extent of involvement before radiation therapy. The CT scans were interpreted without knowledge of the surgical findings in these two cases.

The CT interpretation was correct in nine normal and 10 abnormal cases. CT was incorrect in six cases which were interpreted as normal but proved to be abnormal. One case was interpreted as equivocal. The overall accuracy was 73% (19 of 26) with a false negative rate of 40% (six of 15). No false positive case was encountered. In this group of patients, the CT diagnosis was wrong in six cases. In all six cases the involved nodes contained metastatic deposits but were not enlarged: four had pelvic nodal metastasis only and two had periaortic/pericaval nodal metastasis as well. Two cases were bladder carcinoma; two were prostatic carcinoma; one was spermatic cord sarcoma; and one was ovarian carcinoma.

One case was interpreted as equivocal by CT. This patient had a seminoma of left testicle and a conglomerate of small periaortic lymph nodes medial to the left renal hilum on CT. This was interpreted as suspicious for metastasis, but was not confirmed at surgery. Preoperative lymphangiography was normal in this patient.

Surgical confirmation was available in six cases of testicular tumor: four seminomas, one embryonal cell carcinoma, and one mixed cellular lesion. The CT diagnosis was correct in five cases with one equivocal case described above. Three patients had concurrent lymphangiography, and in one case CT detected enlarged lymph nodes around the left renal vein which were not opacified on the preceding lymphangiogram (fig. 1). The higher success rate in testicular tumors probably is due to the tendency for metastatic testicular tumors to enlarge lymph nodes rather than simply to replace normal-sized nodes.

Excluding six testicular tumors and one spermatic cord sarcoma, 10 patients had advanced disease clinically at the time of CT study, whereas nine patients had early stage disease. Of the 10 with advanced disease, eight patients had proven nodal metastasis: two with pelvic nodal metastasis only, and six with pelvic and periaortic/pericaval nodal metastasis. Three cases were missed by CT: two had pelvic nodal metastasis and the third had periaortic nodal metastasis as well. Of the nine with early disease, only three patients had proven nodal metastasis and two were missed by CT. Both patients had only pelvic node metastasis.

TABLE 1

Accuracy of CT and Lymphangiography

	Pathology	
	Normal	Abnormal
CT:		
Normal	7	5
Equivocal	1	0
Abnormal	0	1
Lymphangiography:		
Normal	5	3
Equivocal	1	0
Abnormal	2	3

Note.—All 14 cases proved at surgery.

Of these 26 patients, 14 also had lymphangiography as part of the staging procedure. CT and lymphangiography agreed and were correct in five cases; they agreed and were both wrong in three cases. The two studies disagreed in six cases and they were each correct in three cases. In this subgroup, the two studies were each correct in 57% of all cases. The false negative rate for CT was 41%; the false negative rate for lymphangiography was 37% with a 40% false positive rate (table 1).

Of six patients in whom CT and lymphangiography differed in interpretation, careful analysis (table 2) shows that the discrepancy was caused by the ability of lymphangiography to show intranodal architecture and collateral lymphatic channels. This certainly helps in detecting metastatic disease missed by CT while increasing the false positive rate of lymphangiography, because it is often difficult, if not impossible, to differentiate between

TABLE 2

Correlation Between Lymphangiography and CT

	No. Cases	Site	Comment
CT and lymphangiography agree:			
Correct:			
Abnormal	1	Testis	...
Normal	4	Bladder, prostate, testis	...
Incorrect, abnormal	3	Bladder, ovary, spermatic cord	Microscopic metastasis missed by both methods
CT and lymphangiography disagree:			
CT correct, normal	3	Prostate, endometrium	Central or peripheral filling defects in normal sized nodes on lymphangiography
Lymphangiography correct:			
Abnormal	2	Prostate, bladder	Replaced but normal-sized nodes on lymphangiography
Normal	1	Testis	Patient thin with suspicious nodes at periaortic area medial to left renal hilus on CT

Note.—All 14 cases proved at surgery.

benign and malignant intranodal architectural changes [2].

No Histologic Confirmation

Of the 14 patients without histologic confirmation, 12 had both CT and lymphangiography, one had CT and ultrasound, and one had CT and carbon-11 putrescine study. (Carbon-11 putrescine is a radioactive polyamine, now under investigation as a possible tumor-localizing agent.)

CT and lymphangiography agreed in 10 cases. The studies were both positive in five patients; four of these had expired at the time of this report. The fifth patient who had a seminoma of the left testicle is still alive 10 months after the initial study. Both studies demonstrated abnormally enlarged periaortic lymph nodes causing nonvisualization of the left kidney on excretory urography. A repeat CT study after a month of radiation therapy demonstrated marked interval decrease in the size of left periaortic nodes, with some return of function to the left kidney. The conventional imaging studies (e.g., excretory urography) also lend support to the CT and lymphangiographic interpretations.

Four cases were interpreted as normal by both methods. All four patients were still alive at the time of this report (9–18 months after the initial study). One case was called equivocal by both studies because several lower abdominal lymph nodes were borderline in size. Two subsequent CT studies performed 4 and 12 months afterward demonstrated no interval change in the size of these lymph nodes in this patient who had no interval treatment for his seminoma. In view of the clinical course, these somewhat prominent lower abdominal nodes probably represent hyperplastic changes, although no surgical proof is available.

CT and lymphangiography disagreed on two cases; both patients had cervical carcinoma. CT was negative for nodal metastasis in these two patients, whereas lymphangiography demonstrated several small central as well as peripheral filling defects in the external and common iliac nodes. Neither study showed any adenopathy in the periaortic or pericaval region. These two patients were alive 20 months after the CT study, although both were treated with radiation extending up to the common iliac region (routine for our institution).

There was a slightly higher percentage of agreement between CT and lymphangiography in this group (10 of 12). No obvious explanation can be offered, except that the group is small and the difference may not be statistically significant. In the other two cases, both ultrasound and radionuclide study confirmed the CT findings, with the subsequent clinical course adding supportive data.

Discussion

Although the number of patients in this series is small, our results again demonstrate the high incidence of lymph node metastasis in pelvic cancers. In the group with advanced disease, nodal metastasis occurred in 80%; in the group with early disease, nodal metastasis occurred in 33%. However, in contrast to the high accuracy of CT in the detection of intraabdominal nodal involvement in lymphoma [11], CT is much less successful in certain metastatic diseases. Our results show a high percentage of false negatives (40%) in this group of patients. In six cases missed by CT, all the involved lymph nodes were of normal size regardless of the clinical stage of the disease. This emphasizes the inability of CT to detect intranodal architectural abnormalities. Schaner et al. [12] reported the same experience in their recent study. At present, CT does not seem able to solve the problems associated with lymphangiography in metastatic disease, namely the inability of the latter to detect microscopic metastatic deposits and the differentiation between malignant and nonmalignant peripheral filling defects. On the basis of the inability of the CT to detect subtle intranodal alteration, it is fair to assume that the false negative rate of CT in metastatic carcinoma should be even higher than that of lymphangiography, although they are about the same in this small series.

Despite this limitation, CT is still useful in unequivo-

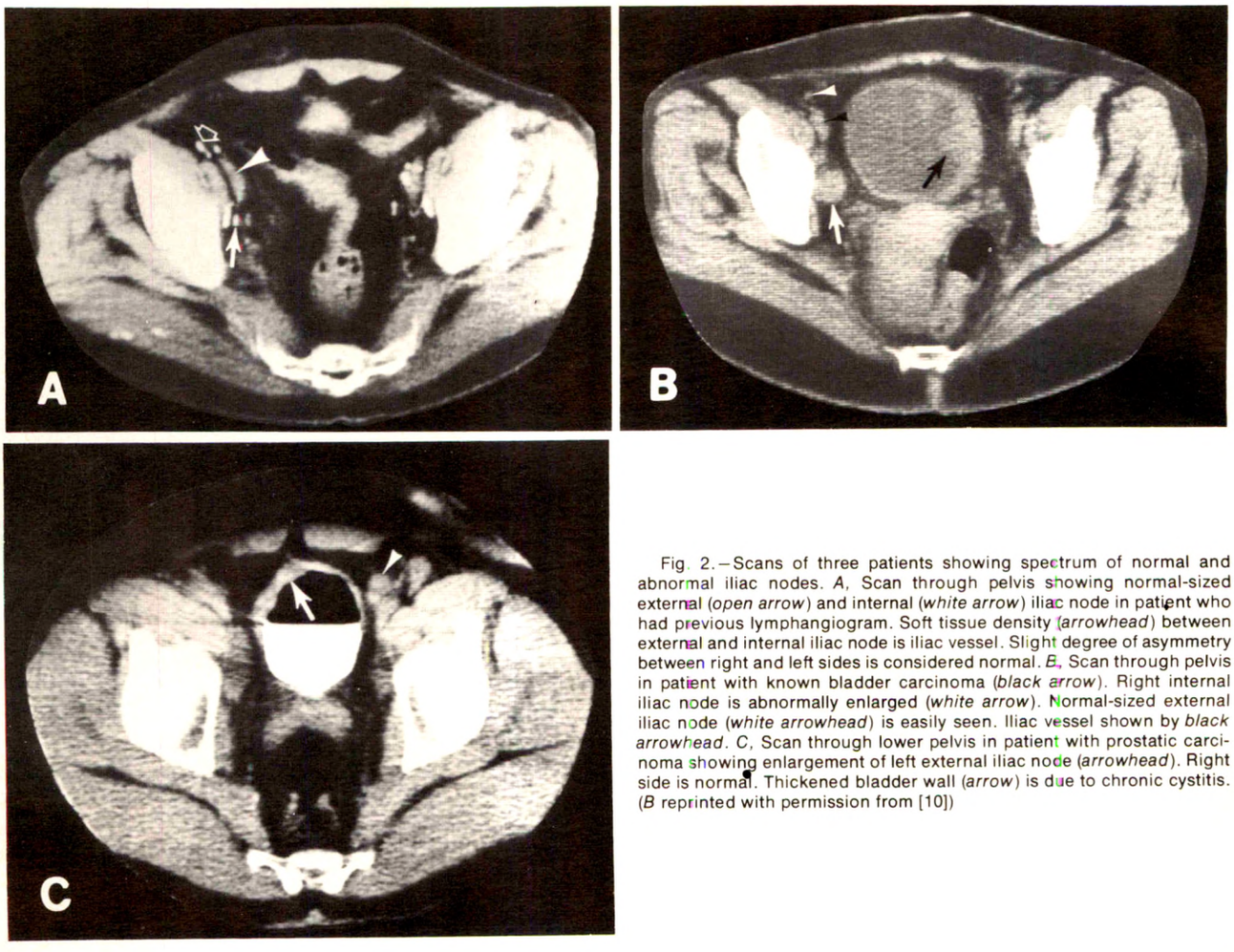

Fig. 2.—Scans of three patients showing spectrum of normal and abnormal iliac nodes. *A*, Scan through pelvis showing normal-sized external (*open arrow*) and internal (*white arrow*) iliac node in patient who had previous lymphangiogram. Soft tissue density (*arrowhead*) between external and internal iliac node is iliac vessel. Slight degree of asymmetry between right and left sides is considered normal. *B*, Scan through pelvis in patient with known bladder carcinoma (*black arrow*). Right internal iliac node is abnormally enlarged (*white arrow*). Normal-sized external iliac node (*white arrowhead*) is easily seen. Iliac vessel shown by *black arrowhead*. *C*, Scan through lower pelvis in patient with prostatic carcinoma showing enlargement of left external iliac node (*arrowhead*). Right side is normal. Thickened bladder wall (*arrow*) is due to chronic cystitis. (*B* reprinted with permission from [10])

cally abnormal cases because of its low false positive rate. A CT diagnosis of abnormality is based on detection of nodal enlargement, sometimes associated with displacement or obliteration of normal anatomic landmarks. Normal-sized pelvic lymph nodes are often not well seen, whereas abnormally enlarged pelvic lymph nodes can usually be detected without any difficulty (fig. 2). Occasionally even the latter may not be as readily identifiable as enlarged periaortic/pericaval lymph nodes because of adjacent bowel loops and smaller vascular structures. In these instances, oral and intravenous contrast media are used to facilitate the differentiation. This has not been a significant problem in our experience.

In the unequivocally abnormal cases, CT is superior to lymphangiography in demonstrating the true extent of tumor involvement, because the abnormality as shown on lymphangiography is often only the "tip of the iceberg." Moreover, CT is also superior in demonstrating abnormal nodes in the retrocrural, renal hilus, splenic hilus, porta hepatis, and mesenteric areas where contrast material from bipedal lymphangiography does not usually reach.

Although experience in testicular tumors is still limited, preliminary data show CT is especially valuable in comparison with the other genitourinary cancers. This is due to the tendency of testicular tumors, especially pure seminomas, to enlarge lymph nodes as well as to replace them. Furthermore, the primary drainage lymph nodes of the testicle at the L1–L3 level are not always opacified by pedal lymphangiography. This unique pathway for lymphatic spread of the testicular tumor certainly would favor the use of CT for evaluation. It enables us to selectively scan around the renal hilar region and thus shorten the examination time. A prospective study of a larger group of patients is underway to evaluate further the role of CT in testicular tumors.

As CT scanning becomes more efficient (rapid scanning and processing), its use as a screening technique will become feasible in terms of cost/benefit and risks/benefit. CT may replace the more invasive and time-consuming lymphangiography in a substantial number of cases, to the benefit of both the patient and physician.

The usefulness of CT in staging of testicular tumors is apparent. Its role in the initial staging of other pelvic tumors is less clear. If CT is to be used as a primary staging test for known pelvic cancers (uterus, cervix, bladder, or prostate), only the unequivocally positive studies will provide diagnostic information. Due to the

expected high false negative rate of CT, a "normal" CT examination should lead to lymphangiography for evaluation of alterations in the internal architecture of normal-sized lymph nodes. Although the number of patients studied is small, theoretically the two tests combined will yield a higher detection rate. In cases where CT is "normal," lymphangiography may detect marginal filling defects in an otherwise "normal" lymph node and thus increase the overall accuracy.

REFERENCES

1. Schaffer B, Koehler PR, Daniel CR, Wohl GT, Rivera E, Meyers WA, Skelley FJ: A critical evaluation of lymphangiography. *Radiology* 80:917–930, 1963
2. Spellman MC, Castellino RA, Ray GR, Pistenna DA, Bagshaw MA: An evaluation of lymphography in localized carcinoma of the prostate. *Radiology* 125:637–644, 1977
3. Loening SA, Schmidt JD, Brown RC, Hawtrey CE, Fallon B, Culp DA: A comparison between lymphangiography and pelvic node dissection in the staging of prostatic cancer. *J Urol* 117:752–756, 1977
4. Lang EL: The roentgenologic assessment of bladder tumors: a comparison of diagnostic accuracy of roentgenologic techniques. *Cancer* 23:717–724, 1969
5. Merrin C, Wajsman Z, Baumgartner G, Jennings E: The clinical value of lymphangiography: are the nodes surrounding the obturator nerve visualized? *J Urol* 117:762–764, 1977
6. Johnson DE, Kaesler KE, Kaminsky S, Jing BS, Wallace S: Lymphangiography as an aid in staging bladder carcinoma. *South Med J* 69:28–30, 1976
7. Wajsman Z, Baumgartner G, Murphy GP, Merrin C: Evaluation of lymphangiography for clinical staging of bladder tumors. *J Urol* 114:712–714, 1975
8. Piver MS, Wallace S, Castro JR: The accuracy of lymphangiography in carcinoma of the uterine cervix. *Am J Roentgenol* 111:278–283, 1971
9. Levitt RG, Jost RG, Trachtman J, Sagel SS, Stanley RJ: A computer-assisted method to determine the diagnostic efficacy of computed tomography of the body. *Radiology* 123:97–101, 1977
10. Stanley RJ, Sagel SS, Fair WR: Computed tomography of the genito-urinary tract. *J Urol* 119:780–782, 1978
11. Lee JKT, Stanley RJ, Sagel SS, Levitt RG: Accuracy of computed tomography in detecting intraabdominal and pelvic adenopathy in lymphoma. *Am J Roentgenol* 131:311–315, 1978
12. Schaner EG, Head GL, Doppman JL, Young RC: Computed tomography in the diagnosis, staging and management of abdominal lymphoma. *J Comput Assist Tomogr* 1:176–180, 1977

Effect of CT Noise on Detectability of Test Objects

EVELYN CHEW,[1] GEORGE H. WEISS,[2] RODNEY A. BROOKS,[1] AND GIOVANNI DI CHIRO[1]

Three types of test objects were superimposed on noisy backgrounds and observed by 58 subjects: large low-contrast disks to simulate tumors, small disks to simulate calcifications, and bars to simulate blood vessels. Three types of noise were used: random noise, CT noise (reconstructed random noise), and an actual water scan taken with an EMI CT1010 scanner. In addition, each image was smoothed by a factor of two, giving six test patterns altogether. Photographic images were presented to 25 lay observers, while 25 other lay observers and eight radiologists used a viewing console. The photographs produced a slightly lower true positive rate than the console, although the degree of confidence in the identifications was slightly greater. The anticorrelation property of CT noise gives it a "lumpy" structure, which aided the identification of bars but impeded the identification of small disks. Smoothing did not significantly affect the detectability with random noise, but with CT noise, smoothing improved the detectability of bars and large disks.

Currently there is much interest in the nature of CT noise and its effect on lesion detectability [1, 2]. There have also been discussions of the effect of smoothing on detectability [2, 3]. To investigate these questions, we conducted an experiment in which test objects were superimposed on noisy backgrounds and observed by 58 people.

The objects were of three types: large low-contrast disks to simulate tumors, small disks to simulate calcifications, and lines or bars to simulate blood vessels. Three types of noise were used: random noise, CT or reconstructed random noise, and an actual water scan taken with an EMI CT1010 scanner. In addition each image was smoothed, giving six noise patterns altogether. The observers were asked to detect and identify as many objects as possible on each image. The results allowed us to make the following comparisons: (1) radiologists versus untrained observers, (2) photographs versus viewing console, (3) three types of noise, and (4) effect of smoothing.

Materials and Methods

Test Objects

Three patterns of test objects were generated on a 160 × 160 matrix using an IBM 370 computer. They were written on magnetic tape in EMI format so that they could be viewed on the EMI diagnostic console. Each pattern contained all three types of objects, distributed in a random manner (fig. 1).

Four small disks (numbered 1–4) had a density of 5 Hounsfield units (H)* and radii of 1, 2, 3, and 4 pixels. Through a programming miscalculation, the smaller ones were elliptical; however, we felt that they were a realistic simulation of calcifications and so were retained. Five large disks (numbered 5–9) all had a radius of 5 pixels and densities of 1, 2, 3, 4, and 5 H. Five bars (numbered 10–14) were each 16 pixels long and 2 pixels wide. They lay horizontally, vertically, or at a 45° angle. The densities were 3, 4, 5, 6, and 7 H.

Noise Backgrounds

Each test pattern was added to a background of pure noise (figs. 2*A*–2*C*). The noise backgrounds were all normalized to a mean value of zero and a standard deviation of 3.5 H, which was the measured value for the water scan. A different test pattern was used for each type of noise so that observers would not remember the positions of the test objects during the examination.

Random (white) noise. Random (white) noise was generated using a random number generating utility on the IBM 370 which produces a Gaussian distribution. The term white refers to the fact that the noise is spatially uncorrelated and hence contains equal power at all frequencies.

Reconstructed noise. Projections were first generated using the random number generator, and an image was then reconstructed from them using filtered back-projection with a ramp filter [4]. No additional high frequency attenuation was used, as is often done in commercial scanners. The reconstruction program was that of Brooks and Di Chiro [5]. Riederer et al. [1] showed that reconstructed noise is rich in high frequencies and is anticorrelated. This means that if the noise value in a given pixel is positive, the noise values nearby will probably be negative. The result is a lumpy appearance which should lend itself well to smoothing techniques, as compared with random noise.

Water scan. To obtain a more realistic example of CT noise, a water scan was taken with an EMI CT1010 scanner. We believe that the primary difference between this noise and the previous reconstructed noise is that some smoothing is incorporated into the reconstruction algorithm of the CT1010.

Smoothing

An additional three images were obtained by smoothing each pattern using a sliding square average. That is, each pixel value was replaced by the average of itself and its neighbors to the right, below, and lower right. Note that both the noise and the test objects were smoothed by this method (figs. 2*D*–2*F*).

Testing Procedure

The images were presented to a total of 58 observers, including eight radiologists. In each case a standard instruction was read describing the nature (but not the number) of the test objects and asking the person to locate and identify them. If an object was misidentified (e.g., if a bar was called a circle), the

Received February 14, 1978; accepted after revision June 2, 1978.

[1] Section on Neuroradiology and Computed Tomography, National Institute of Neurological and Communicative Disorders and Stroke, National Institutes of Health, Clinical Center, Bethesda, Maryland 20014. Address reprint requests to G. Di Chiro.

[2] Division of Computer Research and Technology, Physical Sciences Laboratory, National Institutes of Health, Bethesda, Maryland 20014.

* All density units are reported on the Hounsfield scale (water = 0, air = −1,000). The units are arbitrary in that the only significant quantity is the ratio of object contrast to standard deviation of the noise.

 0361–803X/78/1000–0681 $00.00

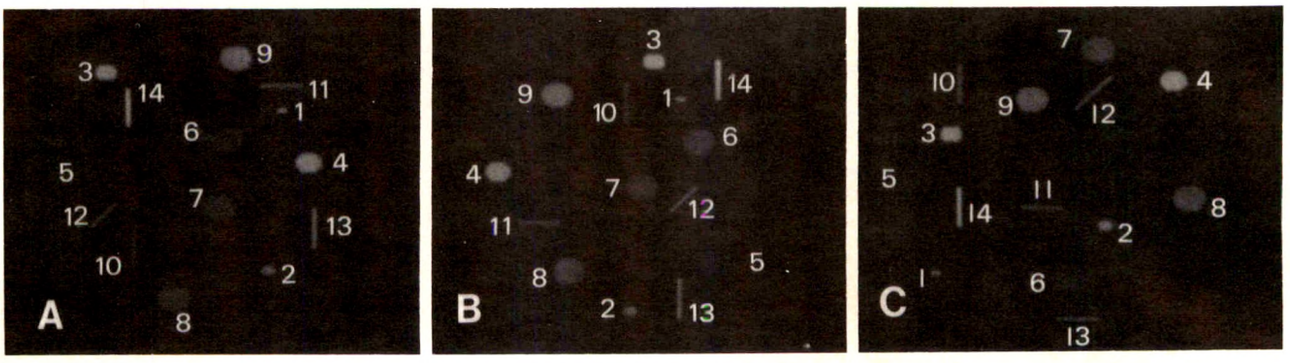

Fig. 1.—Photographs of three noise-free test patterns (window level, 1; window width, 30). Object numbers are shown.

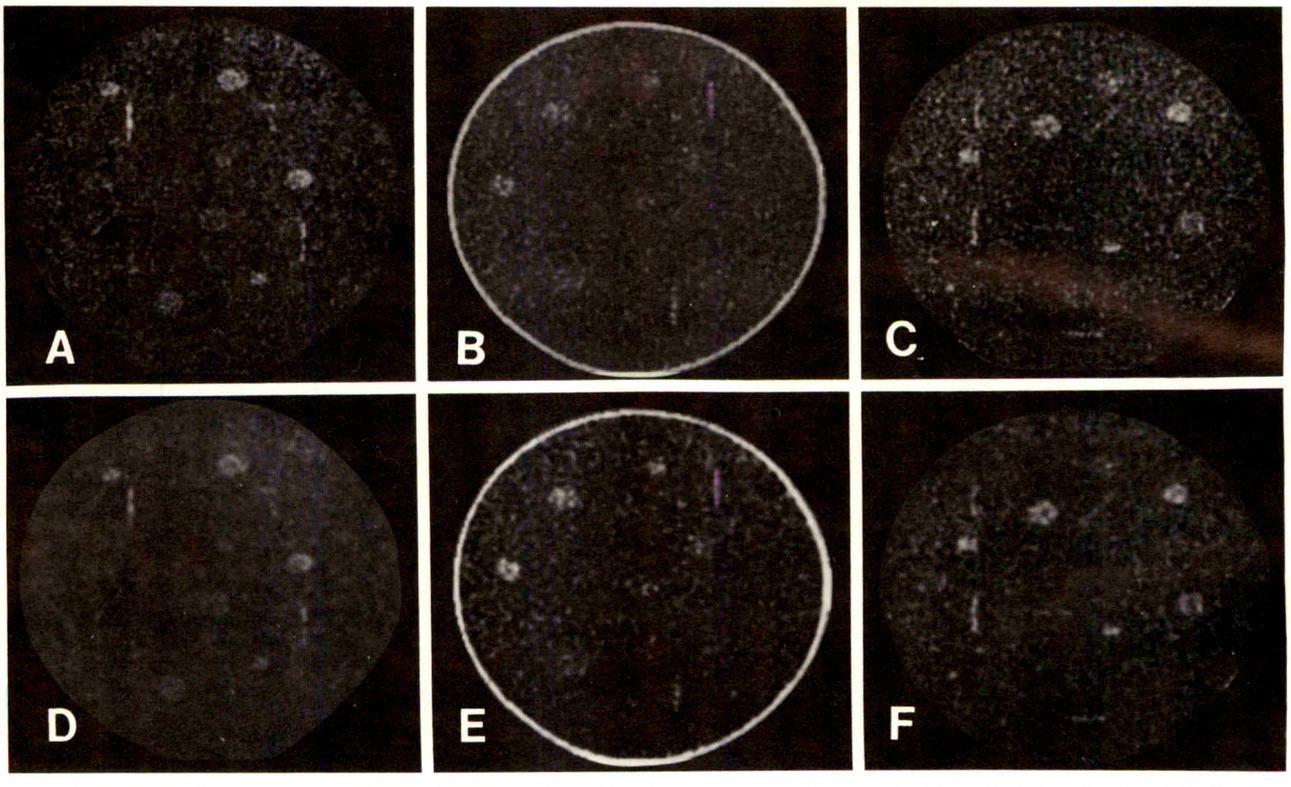

Fig. 2.—*A–C*, Test patterns superimposed on noisy backgrounds: random noise (*A*), reconstructed noise (*B*), and water scan noise (*C*). *D–F*, Same patterns as *A–C* except smoothed with sliding square average (see text).

response was considered incorrect. The images were presented in the following sequence: (1) water scan; (2) random noise; (3) reconstructed noise; (4) water scan, smoothed; (5) random noise, smoothed; and (6) reconstructed noise, smoothed.

Besides identifying each object, the observer was asked to give his degree of confidence according to the following: 1 = 50% chance of being present, 2 = probably present, or 3 = almost definitely present. A record was kept of all responses, including false positives (i.e., identifications given for a location where there was no test object). Scores were computed by weighing each true identification by the degree of confidence values given above. Note that with this method of scoring, "overconfident" observers get higher scores.

The images were displayed either on a console or as Polaroid photographs. A group of 25 untrained observers (x-ray technicians, secretaries, students, etc.) was shown the console images and allowed to set the window level L (brightness) and width W (contrast). Each observer started with the same initial settings (L = 8; W = 30). Some observers changed settings frequently, while others tended to leave them undisturbed. Another group of 25 untrained observers was shown two Polaroid photographs of each image, taken at settings of L = 1, W = 20 and 30 (settings frequently used on the console). Finally, eight radiologists at the National Institutes of Health were shown images on the console under the same conditions as the first group of 25 observers.

Results and Discussion

Radiologists versus Untrained Observers

The radiologists as a group performed better than the untrained observers using consoles. The scores of the radiologists and the untrained console observers were

broken down into 12 comparisons for different types of noise and test objects (table 1). On the hypothesis that untrained observers are equal to radiologists in their ability to detect images, an average of six comparisons should favor the untrained observers, whereas only two comparisons actually did. On the assumption of equality this would occur with a probability $P = .02$, so that it is safe to reject the hypothesis. Looked at another way, the average score for the radiologists is 180 for all test objects, compared with 165 for the untrained observers.

The average number of false positives reported by the members of each group for each type of noise are shown in table 2. The false positives were classified as strong (degree of confidence 3) or weak (degree of confidence 1 or 2). The radiologists reported more false positives (average, 11.0 for all types) than the untrained console observers (average, 7.3). Thus the better record of positive identification is coupled with a tendency to overread.

TABLE 1

Average Scores for Radiologists and Untrained Observers Using Consoles

	Unsmoothed		Smoothed	
	Radiologists	Untrained Observers	Radiologists	Untrained Observers
Random noise:				
Disks	21.4	18.4	21.0	19.4
Bars	8.9	8.5	8.7	8.8
Reconstructed noise:				
Disks	19.6	17.4	20.0	17.4
Bars	10.7	10.9	13.1	12.1
Water scan noise:				
Disks	18.3	16.8	19.7	17.8
Bars	8.9	8.6	9.9	9.2

Note.—Scoring described under Testing Procedure.

TABLE 2

Incidence of False Positives

Group	Degree of Confidence = 3		Degree of Confidence = 1 or 2		Total
	Unsmoothed	Smoothed	Unsmoothed	Smoothed	
Random noise:					
Radiologists	2	3	7	15	27
Console	0	2	23	29	54
Photographs	2	6	25	43	76
Reconstructed noise:					
Radiologists	1	2	10	20	33
Console	1	1	29	28	59
Photographs	3	0	25	26	54
Water scan noise:					
Radiologists	4	8	6	10	28
Console	0	1	42	26	69
Photographs	4	11	28	28	71

Note.—Degrees of confidence: 1 = 50% chance of being present; 2 = probably present; 3 = almost definitely present.

Console versus Photographs

In a comparison of observers using the console and those using photographs (table 3), the total scores showed no clear advantage for either presentation. This somewhat surprising result may be due to the fact that most observers who used the console were not trained in its use. Neither was there a significant improvement in the false positive rate for either method (table 2).

However, if the results are regarded as a function of degree of confidence (table 3), not as many objects were identified with the photographs but a somewhat higher degree of confidence was achieved. Specifically, for all six types of noise more objects were identified in every case with the console ($P = .016$), while in five of the six cases the photographs yielded a larger number of firm identifications ($P = .11$). Because no major difference between console and photographs was found, the results for all 50 untrained observers are combined in the following analyses.

Comparison of Three Types of Noise

The three types of noise were compared for each type of test object (fig. 3). The success rate (i.e., percentage of true positives) was plotted as a function of degree of confidence. These curves are similar to receiver operating characteristic curves [6], except that the abscissa is not scaled to represent the false positive rate. This could not be done because all test objects were combined in one image, rather than being presented separately, as was done by Goodenough et al. [6].

In comparing only random (white) noise and reconstructed noise, the bars were detected better with reconstructed noise, the small disks better with random noise, while for the large disks the detectabilities were about equal. These results are consistent with those of Hanson [2] and may be explained by the anticorrelation property of reconstructed noise [1], which gives it a "lumpy" texture. This is clearly a bad background for picking out very small disks, which tend to blend with the lumps; a bar, because of its linear continuity, stands out more clearly. Large disk detectability depends on ability to average out noise, which should be better for anticorrelated noise. In fact, the equal detectability of large disks with random and reconstructed noise indicates that the eye is not particularly effective at averaging anticorrelations. This was noted by Hanson [2].

The detectability of the water scan noise was always somewhat lower than that for the reconstructed noise. This can perhaps be explained by noting that the water scan has already been somewhat smoothed by the EMI reconstruction algorithm, so there is not as much further averaging available to the eye.

The differences among the various noises can also be studied by focusing on those particular objects at the margin of detectability: the two smallest disks (objects 1 and 2), large disks with density 2 and 3 H (objects 6 and 7), and bars with density 3, 4, and 5 H (objects 10–12). All other objects were either seen by almost everyone or not seen by anyone. Table 4 shows the number of probable or definite identifications and the total score for those seven objects. The smallest disk (object 1) was not detectable with a high degree of confidence on the reconstructed noise and the water scan, while random

TABLE 3

Comparison of Polaroids versus Consoles for Untrained Observers

	Average Score		% Firm Identifications*		% Total Identifications†	
	Polaroid	Console	Polaroid	Console	Polaroid	Console
Unsmoothed:						
Random noise	27.4	26.9	57	55	73	74
Reconstructed noise	28.7	28.2	57	54	75	80
Water scan noise	24.6	25.4	47	42	66	72
Smoothed:						
Random noise	26.8	28.4	57	58	70	76
Reconstructed noise	28.7	28.2	61	59	78	81
Water scan noise	27.0	27.0	56	54	71	73
Average of all noises	27.2	27.3	55.8	53.7	72.3	75.8

* Degree of confidence 3.
† Any degree of confidence.

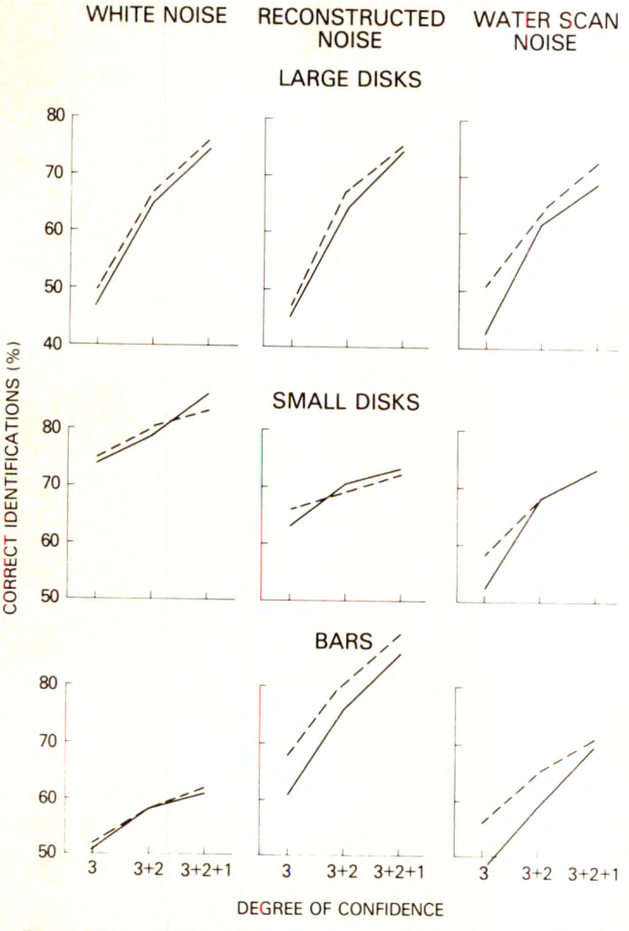

Fig. 3.—True positive rate versus degree of confidence for 50 untrained observers. Ordinate is percentage of objects identified; abscissa is cumulative degree of confidence in identification. Solid lines denote unsmoothed patterns; dashed lines, smoothed ones. White noise = random noise.

noise allowed more definite detection. The faintest bar (object 10) was not positively detected with random noise, but was partially so with reconstructed noise. For all objects, random noise and reconstructed noise produced about the same number of false positives, while the water scan produced somewhat more (table 2).

TABLE 4

Comparison of Results for Specific Objects of Marginal Detectability for Untrained Observers Using Console

Type of Object and Object No.	Score		No. Probable or Definite Identifications*	
	Unsmoothed	Smoothed	Unsmoothed	Smoothed
Water scan noise:				
Small disks:				
1 (R = 1)	1	1	0	0
2 (R = 2)	49	53	18	19
Large disks:				
6 (D = 2)	33	42	12	14
7 (D = 3)	48	55	19	19
Bars:				
10 (D = 3)	1	1	0	0
11 (D = 4)	11	14	3	5
12 (D = 5)	63	64	20	23
Random noise:				
Small disks:				
1 (R = 1)	17	30	4	11
2 (R = 2)	68	62	23	21
Large disks:				
6 (D = 2)	27	37	8	13
7 (D = 3)	54	62	19	24
Bars:				
10 (D = 3)	0	0	0	0
11 (D = 4)	3	10	0	2
12 (D = 5)	60	65	22	24
Reconstructed noise:				
Small disks:				
1 (R = 1)	0	5	0	1
2 (R = 2)	59	48	20	16
Large disks:				
6 (D = 2)	37	42	12	16
7 (D = 3)	42	42	14	15
Bars:				
10 (D = 3)	26	30	8	10
11 (D = 4)	58	71	21	25
12 (D = 5)	38	52	13	19

Note.—R = radius in pixels; D = density in Hounsfield units.
* Degree of confidence = 2 or 3.

Effect of Smoothing

A comparison of the smoothed and unsmoothed results is also shown in figure 3 and table 4. Smoothing made little difference with random noise, but with the water scan and reconstructed noise, detectability was

improved for bars and, to a lesser extent, for large disks. The improvement consisted primarily of an increased confidence level rather than an increased number of identifications, and is clearly related to the ant correlated nature of these two noise types (see above). The lack of improvement for small objects is understandable because (1) the areas of interest in this case are not big enough for effective averaging of anticorrelations, and (2) the objects themselves are degraded by the smoothing. In fact, Hanson [2] found that smoothing of random noise made small disks even less detectable.

There was a slight tendency for smoothing to increase the number of false positives. This is most pronounced for random noise, where in every case (table 2) the smoothed noise led to an increase in the number of false positives for all scores.

Detectable Contrast

If detectable contrast is defined as the minimum contrast that can be detected by 50% of the observers, some limited observations can be made. For the large disks ($R = 5$), the detectable contrast is about 2 H for all noises, which is 57% of the standard deviation. For the small disks ($R = 2$), a contrast of almost 5 H, or 1.4 times standard deviation, is required.

Conclusions

The radiologists in our sample identified more objects, but also had more false positives. Detectability with photographs was comparable to that with consoles, at least for untrained observers. While the photographs produced a slightly lower true positive rate, the degree of confidence was greater.

The anticorrelation property of reconstructed noise causes a "lumpy" structure which, when compared with random noise, aided the identification of bars but impeded the identification of small disks. For large-area objects the detectabilities were approximately equal. The detectability with the water scan noise was generally lower than with reconstructed noise.

Smoothing did not significantly affect detectability with random noise, indicating that the eye alone does an adequate job of spatial averaging. However with reconstructed and water scan noise, smoothing generally improved detectability of bars and large disks, particularly by increasing the confidence of identifications. This seems to indicate that the computer can handle anticorrelations better than the naked eye. Smoothing also caused a slight increase in the false positive rate.

REFERENCES

1. Riederer SJ, Pelc NJ, Chesler DA: The noise power spectrum in computed x-ray tomography. *Phys Med Biol* 23:446–454, 1978
2. Hanson K: Detectability in the presence of computed tomographic reconstruction noise. *Proc Soc Photo-Optical Instrumentation Engineers* 127:304–312, 1977
3. Joseph PM: Trade-off between resolution and density discrimination in CT scanners. Paper presented at the annual meeting of the American Society for Neuroradiology, Bermuda, March 1977
4. Bracewell RN, Riddle AC: Inversion of fan-beam scans in radio astronomy. *Astrophys J* 150:427–434, 1967
5. Brooks RA, Di Chiro G: Theory of image reconstruction in computed tomography. *Radiology* 117:561–572, 1975
6. Goodenough DJ, Rossman K, Lusted LB: Radiographic applications of receiver operating characteristic (ROC) curves. *Radiology* 110:89–95, 1974
7. Chesler DA, Riederer SJ: Ripple supression during reconstruction in transverse tomography. *Phys Med Biol* 20:632–636, 1975
8. Shepp LA, Logan BF: The Fourier reconstruction of a head section. *IEEE Trans Nucl Sci* NS21:21–43, 1974

Optimal Contrast Dosage in Cranial Computed Tomography

DAVID NORMAN,[1] DIETER R. ENZMANN,[2] AND THOMAS H. NEWTON[1]

Comparison of different contrast dosages in adult patients with malignant gliomas studied by computed tomography indicates that 28–42 g of iodine is required for clinically diagnostic results. This can be translated into a 10 min iodine blood level of 100 mg/100 ml. Contrast doses in the range of 14 g of iodine are not satisfactory.

The efficacy of intravenous contrast material for cranial computed tomography is well established [1–3]. However, no objective studies comparing the efficacy of various doses of contrast material in the same patient have been performed. The purpose of this study is to determine minimal dose requirements for clinically diagnostic scans.

Materials and Methods

Three patients with malignant gliomas previously shown to enhance after intravenous contrast injection were studied on successive days following the intravenous administration of 42 g of iodine (300 ml meglumine iothalamate; Conray 30, Mallinckrodt Pharmaceuticals, St. Louis, Mo.) on the first day and following the intravenous injection of 28 g of iodine (200 ml meglumine iothalamate) on the second day. A second group of five patients with malignant gliomas previously shown to enhance after intravenous contrast injection was scanned on successive days following the administration of 42 g of iodine (300 ml meglumine iothalamate) on the first day and 14 g of iodine (100 ml meglumine iothalamate) on the second day. In both groups the contrast medium was injected over a 5–10 min period. The patients were scanned using an EMI Mark 1 (160 × 160 matrix) at the level of maximum tumor size immediately following the completion of contrast injection and again at 20 and 40 min. To insure that the same level would be scanned at each time interval, the patients were not removed from the scanner. Blood samples for blood iodine determination were drawn from two patients in each group during the course of the low dose examination.

In both groups, CT scans were analyzed using the Polaroid image and digital printout. Peak tumor intensity with time [4], area of enhancement, and, if present, changes over time of the low density center were evaluated. Graphs relating tumor intensity were constructed.

Results

In the first group (42 g–28g), peak tumor intensity was achieved on the initial scan in two patients and at 20 min in the third patient for both the 28 g and 42 g iodine injection (fig. 1). Following the 28 g iodine injection, there was a tumor density increase of 9–17.5 EMI units (36%–159%) above the precontrast level. This represents a mean increase of 12 EMI units, or 68%. Enhancement was readily perceived on the polaroid image (fig. 2). Following the 42 g iodine injection, an increase in tumor density of 10–24 EMI units (40%–181%) was seen. This represents a mean increase of 16 EMI units, or 94%. The 28 g dose resulted in 1–7 (3%–20%) EMI units less enhancement than the 42 g iodine dosage. In any individual patient, graphs of tumor CT absorption values were parallel over time for the two doses. Peak blood iodine levels for the 28 g dose in the two patients studied were 170 and 230 mg/100 ml or 85 and 105 mg/100 ml/m².

Three patients in the second group (42–14 g) achieved peak tumor intensity on the initial scan, and the remaining two achieved peak tumor intensity at 20 min for both the 14 g and 42 g doses (fig. 3). Following the 14 g iodine injection, there was a density increase of 2–8 EMI units (15%–80%) above the precontrast level. This represents a mean increase of 5 EMI units, or 39%. It was difficult to visually perceive the phenomenon of contrast enhancement at this dosage level (fig. 4). The increase following the 42 g dosage was 13–20 EMI units (80%–200%). This represents a mean increase of 16 EMI units, or 125%. The 14 g dosage resulted in 11–12 (30%–42%) EMI units less enhancement than the 42 g dosage. Intensity values over time for both doses were parallel in any given patient. Peak blood iodine levels for the 14 g iodine dosage in the two patients studied were 150 and 90 mg/100 ml or 72 and 42 mg/100 ml/m².

Discussion

These studies show a quantitative difference in the degree of contrast enhancement with varying doses of

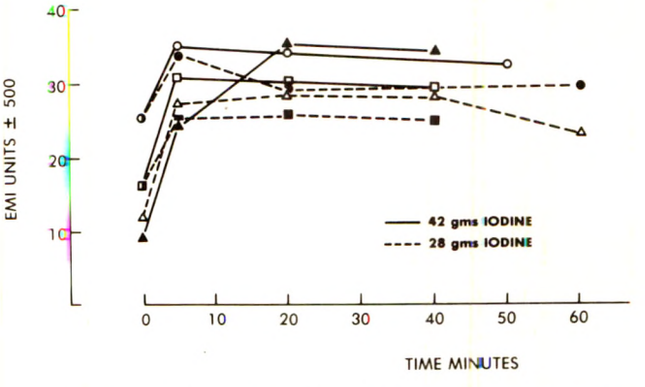

Fig. 1.—Density values of malignant gliomas over time following contrast injection in three patients. Each patient was administered 42 g iodine (*solid line*) and 28 g iodine (*dashed line*) on two successive days.

Received February 28, 1978; accepted after revision June 1, 1978.
This work was supported by Mallinckrodt Pharmaceuticals, St. Louis, Missouri.
[1] Department of Radiology, University of California School of Medicine, San Francisco, California 94143. Address reprint requests to D. Norman.
[2] Department of Radiology, Stanford University Medical Center, Stanford, California 94305.

© 1978 American Roentgen Ray Society

0361–803X/78/1000–0687 $00.00

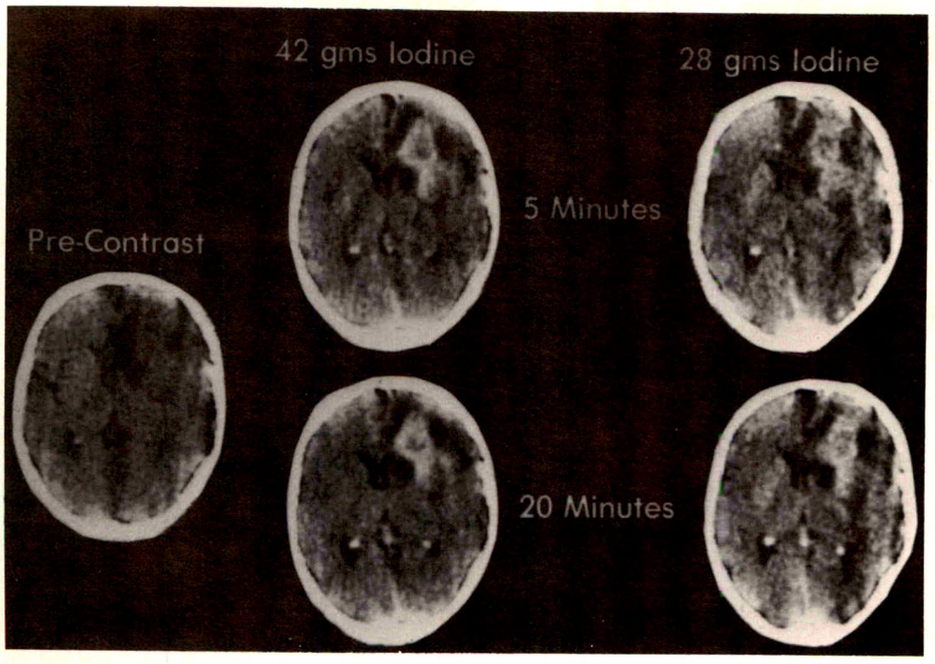

Fig. 2.—CT scans of patient with malignant glioma after bolus injection of 42 and 28 g iodine on two successive days. Note difference in intensity of enhancement. Area of enhancement is increased on 20 min scan and there is slight increase in enhancement density at both dosage levels.

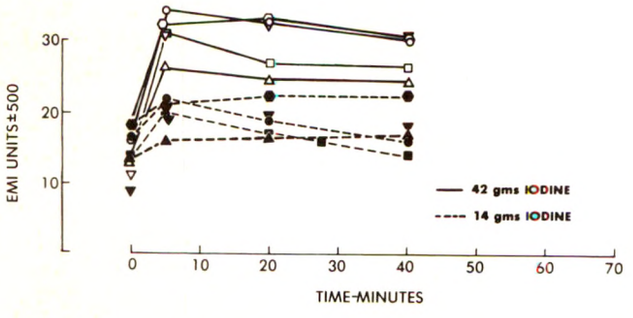

Fig. 3.—Density values of malignant gliomas over time following contrast injection in five patients. Each patient was administered 42 g iodine (*solid line*) and 14 g iodine (*dashed line*) on two successive days.

iodine. The absorption values of any given tumor were parallel over time with various iodine doses. Contrast enhancement was easily discerned in the patients in whom 28 g of iodine was used. There was a 3%–20% difference in the degree of enhancement between the 42 and 28 g dosages, but in both cases the images were diagnostic. In the patients studied with 14 g of iodine, the degree of enhancement was significantly less (30%–42%) than with the 42 g dose. The degree of enhancement was not easily discernible in comparison with the baseline precontrast study. In this series, therefore, both 42 and 28 g iodine contrast doses appeared to produce clinically acceptable results in the detection of malignant gliomas. The 14 g dose was less reliable. In the future, less contrast may be needed with improved density resolution.

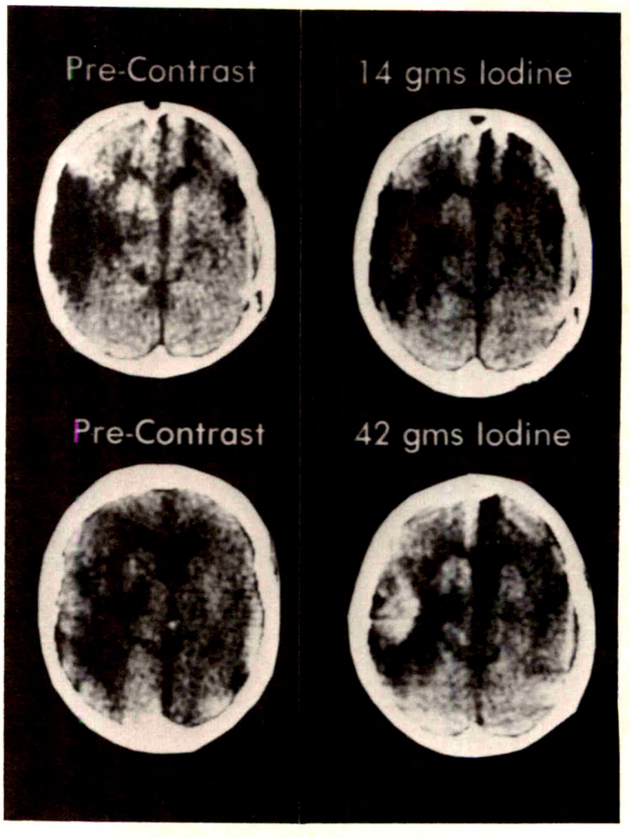

Fig. 4.—CT scans of patient with malignant glioma after bolus injection of 42 and 14 g iodine on two successive days. Note minimal enhancement effect with 14 g dose.

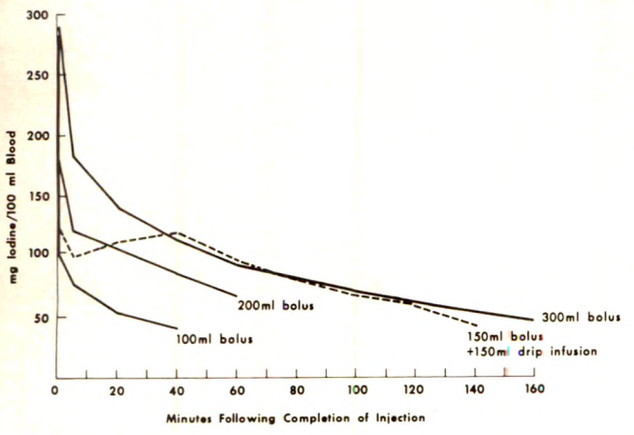

Fig. 5.—Composite curve from grouped data corrected for body surface area to fit mean blood iodine level following injection of 14 g iodine (100 ml bolus), 28 g (200 ml bolus), and 42 g iodine (300 ml bolus) as well as biphasic 42 g iodine injection (150 ml bolus plus 150 ml drip infusion). Blood iodine level rapidly declines during first 10 min reflecting equilibration with extravascular pool.

The mean iodine blood levels, corrected for body surface area, of patients who were administered 42 g [4], 28 g, and 14 g of iodine show a parallel course over time (fig. 5). Iodine levels in the blood during the first 10 min following injection are highly dependent on both speed of injection and quantity of iodine administered [4, 5]. After 10 min, when equilibration is complete, iodine levels in the blood more accurately reflect the combination of total quantity administered and renal excretion rates, and are independent of injection speed [4]. If one accepts that 28–42 g of iodine produces clinically diagnostic results, and that 14 g of iodine may not, an examination of figure 5 suggests that a 10 min iodine blood level of 100 mg/100 ml is required for adequate tumor contrast enhancement.

REFERENCES

1. Gado MH: Contrast enhancement, in *Proceedings of the Conference on Computerized Tomography in Radiology*, St. Louis, Mo., American College of Radiology, 1976, pp 99–102
2. Huckman MS: Clinical experience with the intravenous infusion of iodinated contrast material as an adjunct to computed tomography. *Surg Neurol* 4:297–313, 1975
3. Kramer RA, Janetos GP, Perlstein G: An approach to contrast enhancement in computed tomography of the brain. *Radiology* 16:641–647, 1975
4. Norman D, Stevens EA, Wing SD, Levin V, Newton TH: Quantitative aspects of contrast enhancement in cranial computed tomography. *Radiology*. In press, 1978
5. Cattell WR, Fry K, Spencer AG, Purkiss P: Excretion urography. I. Factors determining the excretion of Hypaque. *Br J Radiol* 40:561–571, 1967

Progress in Radiology:

Colorectal Tumors: Pathology and Detection

DAVID J. OTT[1] AND DAVID W. GELFAND[1]

The prognosis in colorectal neoplasia has not improved in the past 20 years despite improved diagnostic techniques. The greatest promise lies in wider screening and earlier radiographic and endoscopic detection. To clarify the radiologist's role in finding large bowel tumors, the clinical, pathologic, and radiologic literature is reviewed. Since individuals over 40 years of age harbor the bulk of colon neoplasms, the most diligent efforts to detect these lesions should be made in this group. Controlled studies comparing single and double contrast barium enema techniques are lacking, but available data suggest that the double contrast examination is more sensitive for detection of the numerous small, but potentially malignant colon tumors. Careful radiographic technique, including a thoroughly clean colon, is critical for accurate detection regardless of which technique is used.

Carcinoma of the colon and rectum is the most common internal malignancy in the United States today, responsible for 100,000 new cases and 50,000 deaths each year [1]. The prognosis has not changed significantly over the past several decades, the overall 5 year survival remaining less than 50% [2–4]. Despite this apparent lack of progress in curing colorectal cancer, there is evidence that early detection will improve survival statistics [5–8]. As shown recently [2], the 5 year survival rates of patients with invasive colon carcinoma and lymph node involvement compared to those with localized superficial carcinoma were 13% and 71.6%, respectively. Thus earlier and more accurate detection of colonic neoplasms is obviously needed.

This paper reviews the pathologic, clinical, and radiologic literature related to neoplasia of the large intestine with the intent of clarifying the radiologist's role in finding these tumors. The basic pathology of epithelial polyps of the colon is defined, along with an expanded discussion of adenomatous polyps and their relationship to carcinoma. To ascertain the incidence of colonic polyps and their age and site distribution, a thorough review of autopsy-based publications was undertaken. Reports on the sensitivity and accuracy of radiographic examinations of the colon have also been reviewed. The collected data provide a foundation upon which specific comments and recommendations can be formulated to guide the radiologist in detecting large bowel neoplasms by barium enema examination.

Pathology

The term polyp has no histologic implication, and simply indicates a protuberance projecting into the lumen of the colon. Most polyps of the large intestine are of epithelial origin, usually falling into one of two major categories: (1) hyperplastic (metaplastic) polyps, and (2) neoplastic polyps [9–12]. The hyperplastic polyp is typically a smooth and sessile mucosal elevation nearly always less than 5 mm in diameter. More important, these lesions are considered to be nonneoplastic growths with no malignant potential. Approximately 90%–95% of all colon polyps under 0.5 cm in size are of the hyperplastic variety [12, 13]. Neoplastic polyps have been variously classified and include adenoma, adenoma with carcinoma in situ, adenoma with invasive carcinoma, and polypoid adenocarcinoma. Furthermore, Morson [14, 15] has subclassified the adenomas into the polypoid, intermediate, and villous types, although the latter would be placed into a separate category by others [16]. The pathologic criteria for intramucosal carcinoma in colonic adenomas are not universally defined or accepted; however, the entity appears to represent a transition in the adenoma-carcinoma sequence. Invasive carcinoma is defined as penetration through the muscularis mucosae [15]. Juvenile (hamartomatous) and inflammatory polyps of the colon will not be considered.

Adenoma-Carcinoma Sequence

Although debated for years, the controversy related to the adenoma-carcinoma sequence warrants review. In 1964, Ackerman et al. [17] stated that the simple adenomatous polyp of the colon practically never progressed to an invasive carcinoma, a belief supported by others, notably Castleman and Krickstein [18, 19] and Spjut and Spratt [20]. However, Morson and others [21–24] have maintained the opposite viewpoint, stating that the adenoma-carcinoma sequence is indeed a biologic fact of life. There is convincing evidence substantiating the adenoma as a precursor to carcinoma: (1) the coexistence of invasive carcinoma in benign-appearing adenomas [21, 24]; (2) the virtual absence of documented de novo carcinomas less than 5 mm in size in otherwise normal colons [21]; (3) the certainty that nearly all patients with familial polyposis not having surgery will succumb to colon cancer [25, 26]; (4) the increasing evidence that carcinoma in situ represents a preinvasive stage of adenocarcinoma of the large bowel [27]; and (5) the results of the University of Minnesota Cancer Detection Center demonstrating an 85% reduction in the anticipated incidence of carcinoma of the rectosigmoid colon in patients undergoing annual proctosigmoidos-

Received March 22, 1978; accepted after revision June 20, 1978.

[1] Department of Radiology, Bowman Gray School of Medicine and North Carolina Baptist Hospital, 300 South Hawthorne Road, Winston-Salem, North Carolina 27103. Address reprint requests to D. J. Ott.

© 1978 American Roentgen Ray Society

0361–803X/78/1000–0691 $00.00

copy and polyp removal [28]. Ample additional circumstantial information supports the concept of malignant transformation of large bowel adenomas [16]. The apparent conclusion, until proven differently, is confirmation of an adenoma-carcinoma sequence in the colon. Although speculated upon by Morson and colleagues [15, 22–24], several incompletely answered questions remain, including the frequency of progression from adenoma to carcinoma, the average time span for malignant transformation, and whether all carcinomas of the colon arise from adenomas.

Relationship of Adenoma Size to Carcinoma

A correlation between the size of adenomatous polyps of the large intestine and the incidence of invasive carcinoma in such lesions is well documented (table 1). As shown, adenomas 5–9 mm in size have a 1% probability of harboring invasive malignancy, while those under 5 mm in diameter have less than a 0.5% incidence. Since the majority of colon polyps under 5 mm are hyperplastic, with adenomas comprising 10% or less, the overall incidence of invasive cancer in lesions under 0.5 cm must be no more than 0.05%. Consequently, the possibility of infiltrative malignancy in colon polyps less than 1 cm in size applies almost solely to lesions in the 5–10 mm range.

Incidence, Distribution, and Age Factors

The reported incidence of colon polyps has varied greatly depending on the detection method employed, the age group investigated, and the types of lesions included in the studies. In reviewing reports of autopsy series from 1931–1974 (table 2), the reported incidence of polyps was 2.4%–69.0%, with a weighted average of 12.4%. Multiple polyps were present in 50.4% of patients. Interestingly, the excellent autopsy study of Arminski and McLean [38] arrived at a figure of 8% for the incidence of colon polyps greater than 0.5 cm in the general population.

Conflicting data exist as to the distribution of adenomatous polyps within the colon. In many necropsy series, a fairly uniform occurrence of polyps from rectum to cecum is noted [31, 32, 34, 38, 39]. However, other studies document the more widely accepted view of a left-sided predominance of these lesions [30, 33, 35]. Additionally, an increasing proportion of colon carcinomas arising above the rectosigmoid junction has been observed over the past 30 years [41, 42]. In fact, Snyder et al. [41] state that only 50% of colorectal cancers can now be identified with the rigid sigmoidoscope. This would indicate that the traditional means of discovering colon neoplasms by rectal examination and proctosigmoidoscopy are now less effective, and that more emphasis must be placed on other techniques, including testing of stools for occult blood, radiography, and colonoscopy.

The frequency of adenomatous polyps and carcinoma of the large bowel rises with increasing age (fig. 1). Most colonic neoplasms do not appear until after the fourth

TABLE 1

Relationship of Adenoma Size to Incidence of Malignancy

Reference	Incidence of Malignancy (%)			
	<5 mm	5–9 mm	1–2 cm	>2 cm
Grinnell and Lane [21] . . .	0.3	0.9	4.7	10.5
Muto et al. [24]	1.3*	1.3*	9.5	46.0
Welch and Hedberg [16]	0.5	1.0	3.9	20.7
Average	0.4	1.0	6.0	25.7

Note.—Adenomas of all histologic types are included. Malignancy is strictly defined in only those adenomas demonstrating carcinomatous invasion through the muscularis mucosae.

* 1.3% incidence applies to all tumors under 1 cm.

TABLE 2

Incidence of Colon Polyps in Selected Autopsy Studies

Reference	No. Examined	Incidence (%)
Lawrence [29]	7,000	2.4*
Swinton and Haug [30]	1,843	7.0
Helwig [31]	1,460	9.5
Sato [32]	1,000	9.5
Edwards and Jackman [33]	802	9.6
Winblad and Friberg [34]	671	11
Ekelund [35]	3,398	12.5
Feyrter [36]	1,800	21.5
Blatt [37]	556	38.8
Arminski and McLean [38]	1,000	41.3
Chapman [39]	443	51.0
Atwalter and Bargen [40])†	241	69.0
Weighted average	. . .	12.4

Note.—Data on more than 20,000 autopsy examinations.

* Low incidence at least in part reflects inclusion of significant proportion (25%) of patients less than 10 years old.

† Study conducted with a hand lens.

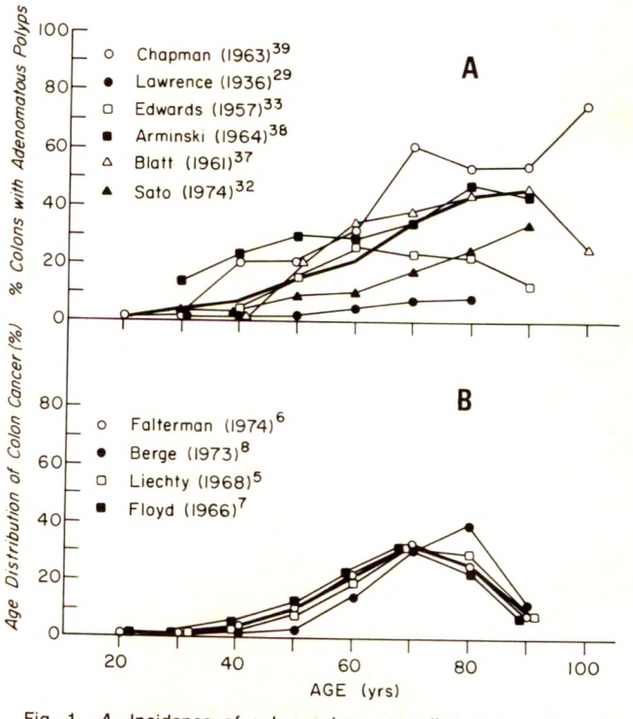

Fig. 1.—*A*, Incidence of colon polyps according to age from six autopsy series. Heavy line is composite average of four necropsy reports [32, 37–39]. *B*, Distribution of colorectal cancer in population according to age. Heavy line is average of four series.

TABLE 3

Detection of Colon Polyps by Barium Enema

Single Contrast		Double Contrast	
Reference	Incidence (%)	Reference	Incidence (%)
Christie et al. [43]	1.0	Laufer et al. [48]	9.8
Brown [44]	1.9	Maruyama et al. [49]	10.5
	3.2	Brown [44]	11.9
Gianturco and Miller [45]	2.7		13.1
		Andrén et al. [50]	12.5
Wietersen [46]	3.1	Welin [51]	12.5
Figiel [47]	7.8		
Mean ± SD	3.3 ± 2.2	Mean ± SD	11.7 ± 1.2

Note.—Most of the single contrast studies were published over 20 years ago, emphasizing the need for a current evaluation of this technique.

decade of life, with only 5% of all colon cancers occurring below the age of 40. Although a 5% incidence of adenomas exists between the ages of 20 and 39 years, the ratio of carcinomas to benign polyps in that group is only 0.2% [17]. The implication is that polypoid lesions of the colon in younger individuals have a reduced likelihood of being malignant.

Radiologic Detection

The detection rate of colonic polyps by barium enema also varies considerably depending on the series studied and the methods utilized. The frequency of polyps seen with the single contrast barium enema ranges from 1.0% to 7.8% [43–47] but increases with the double contrast barium enema to 9.8%–13.1% [44, 48–51] (table 3). The latter figures compare favorably with the average autopsy incidence (12.4%) of colon polyps and seem to indicate that the double contrast barium enema is a more sensitive method for detecting these lesions. Up to 60% of polyps detected by the double contrast examination were less than 5 mm [44, 50, 51], confirming the ability of this technique to find small lesions in the colon. Although available figures favor the double contrast examination for the detection of colon polyps, an adequately controlled study comparing the sensitivity and accuracy of the two barium enema techniques has not been done [52, 53]. Furthermore, there has been no large series in recent years truly using the high kilovoltage, compression spot film single contrast technique described by Figiel and others [45, 46, 54].

Discussion

Colorectal neoplasia remains a major health problem in the United States, with a prognosis unaltered over the past 20 years despite improved diagnostic techniques. More widely applied patient screening methods along with earlier radiographic and endoscopic detection are the most promising areas for improved survival. Evaluation of the stool for occult blood and sigmoidoscopy are the predominate screening procedures currently available and will presumably continue in that role [55, 56]. However, since many large bowel adenomas and carcinomas occur beyond the reach of the rigic sigmoidoscope, the radiologist and colonoscopist must assume a greater responsibility for their detection.

From the data presented above, certain facts relevant to radiologic detection should be emphasized:

1. Polyps smaller than 5 mm are of no practical significance since the huge majority are hyperplastic. Of lesions of this size found to be adenomas, the incidence of malignancy is almost negligible (less than 0.5%).

2. Polyps 5–10 mm in size are predominately adenomas, with a small but not insignificant (1%) incidence of cancer. Detection of these lesions is readily accomplished with current radiographic techniques, primarily the double contrast barium enema. With present endoscopic capabilities, these tumors can be easily removed, resulting in elimination of malignancies in this group.

3. Polyps larger than 1 cm have a significant chance of harboring carcinoma, necessitating accurate radiographic detection and endoscopic or surgical removal.

To accurately detect small polypoid lesions, the radiologist must be continuously critical of his method of colon preparation and examination. For example, it has been shown that 10%–20% of carcinomas of the colon are missed on the initial barium examination [57, 58], primarily because of poor preparation resulting in the tumor being overlooked or confused with fecal material [59]. Therefore, a thoroughly clean colon is the first requirement for obtaining an accurate examination, regardless of the specific radiographic techniques used [60, 61]. Many methods for bowel cleansing have been described [50, 51, 61, 62], but for consistently superior results, the minimum needed is a combination of dietary manipulation, two sequentially administered laxatives, and cleansing enemas, preferably given in the radiology department.

Our current regimen for colon cleansing, used for both single and double contrast examinations includes a clear liquid diet for 24 hr before the examination; an hourly glass of water from noon to midnight; 295 ml (10 oz) of magnesium citrate at 4 P.M.; 118 ml (4 oz) of Neoloid® (Lederle) at 8 P.M.; and nothing orally after midnight. On the morning of the examination, a 1,500 ml cleansing enema is performed in the radiology department.

On the basis of available reports [63–65] the double contrast barium enema must be advocated for the detection of polypoid tumors of the colon. The evidence to date supports its greater sensitivity compared to the single contrast technique, especially in discovering small polyps. In general, any double contrast technique will suffice that produces at least three views in double contrast of every part of the colon, each one of the views taken in a different position [66]. Excellent descriptions of various methods for performing this study have been published [48, 50, 67–70].

Our routine for performing the examination is a primary single-stage technique using a barium suspension specifically formulated for double contrast colon examination, a disposable enema bag with 1.3 cm tubing and Miller air tip, and 1 mg glucagon administered intramus-

cularly at the start of the procedure. With the patient in the prone position, the barium suspension is allowed to reach the distal transverse colon after which air is instilled forcing barium into the right colon. Rectal drainage is employed, and both fluoroscopic and overhead filming are obtained.

Conclusions

1. Only by finding large bowel cancers early and in a potentially curable stage will the prognosis for patient survival increase.

2. Colorectal polyps as small as 5 mm may be malignant, but can be detected with present radiographic techniques if properly applied.

3. Individuals over 40 years of age harbor the bulk of colon neoplasms. The most diligent efforts to detect these lesions should be made in this group.

4. An estimated 8% of the adult population have colon polyps larger than 0.5 cm. Radiologists should endeavor to find these tumors, and if detection rates do not approach or exceed this figure, the technique of barium enema examination needs to be reevaluated or altered.

5. Although well controlled studies comparing single and double contrast barium enema techniques are needed, the literature to date strongly suggests that the double contrast examination is more sensitive for detection of the numerous small, but potentially malignant colon tumors.

6. The colon must be thoroughly clean so that detection of small neoplasms is not hampered by retained stool. Although the regimens required for thorough colon cleansing are strenuous, they must be adhered to for the best results, regardless of the radiographic technique used.

REFERENCES

1. Cancer statistics, 1977. *CA* 27:26-41, 1977
2. Franklin R, McSwain B: Carcinoma of the colon, rectum, and anus. *Ann Surg* 171:811-817, 1970
3. Welch JP, Donaldson GA: Recent experiences in the management of cancer of the colon and rectum. *Am J Surg* 127:258-266, 1974
4. Silverberg E, Holleb AI: Major trends in cancer: 25 year survey. *CA* 25:2-7, 1975
5. Liechty RD, Ziffren SE, Miller FE, DenBesten DL: Adenocarcinoma of the colon and rectum: review of 2,261 cases over a 20-year period. *Dis Colon Rectum* 11:201-208, 1968
6. Falterman KW, Hill CB, Markey JC, Fox JW, Cohn I Jr: Cancer of the colon, rectum and anus: a review of 2,313 cases. *Cancer* 34:951-959, 1974
7. Floyd CE, Stirling CT, Cohn I Jr: Cancer of the colon, rectum and anus: review of 1687 cases. *Ann Surg* 163:829-837, 1966
8. Berge T, Ekelund G, Mellner C, Pihl B, Wenckert A: Carcinoma of the colon and rectum in a defined population. *Acta Chir Scand* [*Suppl*] 438:45-76, 1973
9. Morson BC: Some peculiarities in the histology of intestinal polyps. *Dis Colon Rectum* 5:337-344, 1962
10. Lane N, Kaplan H, Pascal RR: Minute adenomatous and hyperplastic polyps of the colon: divergent patterns of epithelial growth with specific associated mesenchymal changes. *Gastroenterology* 60:537-551, 1971
11. Fenoglio CM, Lane N: The anatomical precursor of colorectal carcinoma. *Cancer* 34:819-823, 1974
12. Lane N, Fenoglio CM: Observations on the adenoma as precursor to ordinary large bowel carcinoma. *Gastrointest Radiol* 1:111-119, 1976
13. Lane N: The precursor tissue of ordinary large bowel cancer: implications for cancer prevention, in *The Gastrointestinal Tract*, edited by Yardley JH, Morson BC, Abell MR, Baltimore, Williams & Wilkins, 1977, pp 95-100
14. Morson BC: Precancerous and early malignant lesions of the large intestine. *Br J Surg* 55:725-731, 1968
15. Morson BC: Genesis of colorectal cancer. *Clin Gastroenterol* 5:505-525, 1976
16. Welch CE, Hedberg SE: *Polypoid Lesions of the Gastrointestinal Tract*, 2d ed. Philadelphia, Saunders, 1975
17. Ackerman LV, Spjut HJ, Spratt JS Jr: The biological characteristics of colonic and rectal neoplasms with refutation of the concept that adenomatous polyps are highly premalignant tumors. *Acta Unio Internationalis Contra Cancrum* 20:716-723, 1964
18. Castleman B, Krickstein HI: Do adenomatous polyps of the colon become malignant? *N Engl J Med* 267:469-475, 1962
19. Castleman B, Krickstein H: Current approach to the polyp-cancer controversy. *Gastroenterology* 51:108-112, 1966
20. Spjut HJ, Spratt JS Jr: Endemic and morphologic similarities existing between spontaneous colonic neoplasms in man and 3:2'-dimethyl-4-aminobiphenyl induced colonic neoplasms in rats. *Ann Surg* 161:309-324, 1965
21. Grinnell RS, Lane N: Benign and malignant adenomatous polyps and papillary adenomas of the colon and rectum. An analysis of 1,856 tumors in 1,335 patients. *Int Abstr Surg* 106:519-538, 1958
22. Morson B: The polyp-cancer sequence in the large bowel. *Proc R Soc Med* 67:451-457, 1974
23. Morson BC: Evolution of cancer of the colon and rectum. *Cancer* 34:845-849, 1974
24. Muto T, Bussey HJR, Morson BC: The evolution of cancer of the colon and rectum. *Cancer* 36:2251-2270, 1975
25. Lockhart-Mummery HE: Diffuse conditions of the large bowel which are premalignant. *Br J Surg* 55:735-738, 1968
26. Bussey HJR: Gastrointestinal polyposis. *Gut* 11:970-978, 1970
27. Maruyama M: Theoretical aspects in radiological diagnosis of early carcinoma of the colon and rectum. *Nippon Acta Radiol* 33:799-810, 1973
28. Gilbertsen VA: Proctosigmoidoscopy and polypectomy in reducing the incidence of rectal cancer. *Cancer* 34:936-939, 1974
29. Lawrence JC: Gastrointestinal polyps: statistical study of malignancy incidence. *Am J Surg* 31:499-505, 1936
30. Swinton NW, Haug AD: The frequency of precancerous lesions in the rectum and colon. *Lahey Clin Bull* 5:84-88, 1947
31. Helwig EB: Benign tumors of the large intestine—incidence and distribution. *Surg Gynecol Obstet* 76:419-426, 1943
32. Sato E: Adenomatous polyps of the large intestine in autopsy and surgical material. *Gann* 65:295-306, 1974
33. Edwards CC, Jackman RJ: Unsuspected and subclinical lesions of the large intestine found at necropsy. *Surg Gynecol Obstet* 105:754-758, 1957
34. Winblad S, Friberg S: Observations on the pathology of polyps of the colon. *Acta Pathol Microbiol Scand* [*Suppl*] 111:89-92, 1956
35. Ekelund G: On cancer and polyps of colon and rectum.

Acta Pathol Microbiol Scand 59:165–170, 1963
36. Feyrter F: Zur Geschwulstlehre (mach Untersuchungen am menschlichen Darm): Polypen und Krebs. *Beitr Pathol* 86:663–760, 1931
37. Blatt LJ: Polyps of the colon and rectum: incidence and distribution. *Dis Colon Rectum* 4:277–282, 1961
38. Arminski TC, McLean DW: Incidence and distribution of adenomatous polyps of the colon and rectum based on 1,000 autopsy examinations. *Dis Colon Rectum* 7:249–261, 1964
39. Chapman I: Adenomatous polypi of large intestine: incidence and distribution. *Ann Surg* 157:223–226, 1963
40. Atwalter JS, Bargen JA: The pathogenesis of intestinal polyps. *Gastroenterology* 4:395–408, 1945
41. Snyder DN, Heston JF, Meigs JW, Flannery JT: Changes in site distribution of colorectal carcinoma in Connecticut, 1940–1973. *Am J Dig Dis* 22:791–797, 1977
42. Rhodes JB, Holmes FF, Clark GM: Changing distribution of primary cancers in the large bowel. *JAMA* 238:1641–1643, 1977
43. Christie AC, Coe FO, Hampton AO, Wyatt GM: The value of tannic acid enema and post-evacuation roentgenograms in examination of the colon. *Am J Roentgenol* 63:657–663, 1950
44. Brown GR: The direct air contrast colon examination: a rapid, simplified, highly diagnostic procedure. Paper presented at the annual meeting of the Radiological Society of North America, Chicago, December 1968
45. Gianturco C, Miller GA: Routine search for colonic polyps by high-voltage radiography. *Radiology* 60:496–499, 1953
46. Wietersen FK: High kilovoltage method of investigation of the colon as a routine roentgenological procedure. *Am J Roentgenol* 77:690–699, 1957
47. Figiel SJ: Colon examination technique, in *Detection of Colon Lesions, First Standardization Conference–1969*, Chicago, American College of Radiology, 1973, pp 132–145
48. Laufer I, Smith NCW, Mullens JE: The radiological demonstration of colorectal polyps undetected by endoscopy. *Gastroenterology* 70:167–170, 1976
49. Maruyama M, Sugiyama N, Funada A, Sasaki T, Takekoshi T, Ujiie K, Kumakura YBK, Kurohawa T: Double contrast radiography of the colon and rectum by means of the universal gyroscopic x-ray television apparatus. *Nippon Acta Radiol* 33:786–798, 1973
50. Andrén L, Frieberg S, Welin S: Roentgen diagnosis of small polyps in the colon and rectum. *Acta Radiol* 43:201–208, 1955
51. Welin S: Results of the Malmö technique of colon examination. *JAMA* 199:119–121, 1967
52. Amberg JR, Berk RN, Burhenne HJ, Clemett AR, Dodds WJ, Friedland GW, Goldberg HI, Goldstein HM, Laufer I, Lawson TL, Margulis AR, Marshak RH, Miller RE, Short WF, Steward ET, Youker JE, Zboralske FF: Colonic polyp detection: role of roentgenography and colonoscopy. *Radiology* 125:255–257, 1977
53. Margulis AR: Is double-contrast examination of the colon the only acceptable radiographic examination? *Radiology* 119:741–742, 1976
54. Figiel SJ, Figiel LS, Rush DK: Study of colon by use of high-kilovoltage spot-compression technique. *JAMA* 166:1269–1275, 1958
55. Sherlock P, Winawer SJ: The role of early diagnosis in controlling large bowel cancer. *Cancer* 40:2609–2615, 1977
56. Miller SF: Colorectal cancer: Are the goals of early detection achieved? *CA* 27:338–343, 1977
57. Saunders CG, MacEwen DW: Delay in diagnosis of colonic cancer—a continuing challenge. *Radiology* 101:207–208, 1971
58. Clarke AM, Jones ISC: Diagnostic accuracy and diagnostic delay in carcinoma of the large bowel. *NZ Med J* 71:341–347, 1970
59. Eyler W: Colon preparation, in *Detection of colon lesions, First Standardization Conference–1969*. Chicago, American College of Radiology, 1973, p 108
60. Miller RE: Detection of colon carcinoma and the barium enema. *JAMA* 230:1195–1198, 1974
61. Miller RE: The clean colon. *Gastroenterology* 70:289–290, 1976
62. Dodds WJ, Scanlon GT, Shaw DK, Stewart ET, Youker JE, Metter GE: An evaluation of colon cleansing regimens. *Am J Roentgenol* 128:57–59, 1977
63. Williams CB, Hunt RH, Loose H, Riddell RH, Sakai Y, Swarbrick ET: Colonoscopy in the management of colon polyps. *Br J Surg* 61:673–682, 1974
64. Laufer I: The double-contrast enema: myths and misconceptions. *Gastrointest Radiol* 1:19–31, 1976
65. Thoeni RF, Menuck L: Comparison of barium enema and colonoscopy in the detection of small colonic polyps. *Radiology* 124:631–635, 1977
66. Shirakabe H: Diagnosis of small colon cancers in Japan. Paper presented at the Society of Gastrointestinal Radiologists, Hilton Head, S.C., September 1977
67. Hamelin L, Hurtubise M: Remote control technique in double contrast study of the colon. *Am J Roentgenol* 119:382–392, 1973
68. Welin S, Welin G: *The Double Contrast Examination of the Colon: Experiences with the Welin Modification*, Thieme ed. Stuttgart, Publishing Sciences Group, 1976
69. Rogers CW: Method for double-contrast study of the colon. *Med Radiogr Photogr* 51:30–42, 1975
70. Miller RE: Examination of the colon. *Curr Probl Radiol* 5:3–40, 1975

Diagnostic Oncology Case Studies

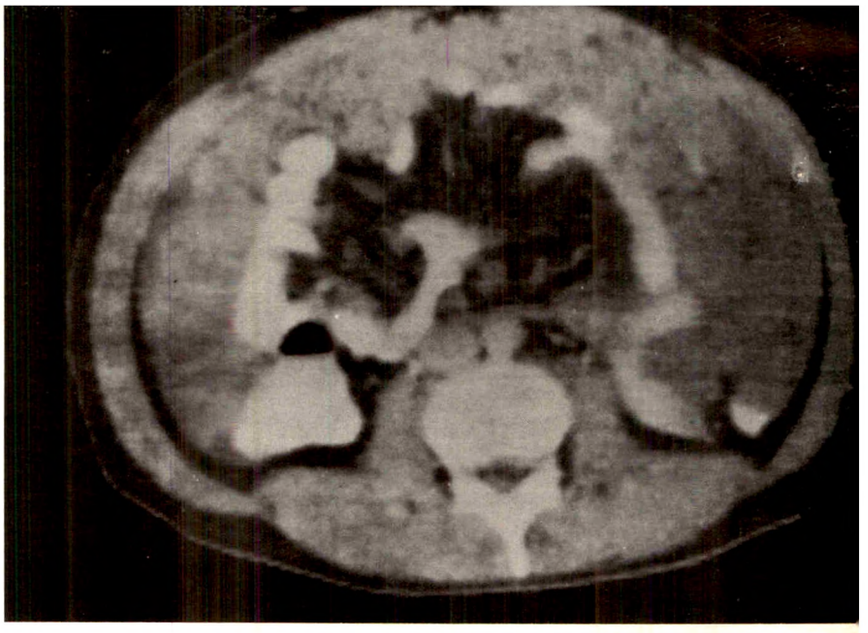

Radiologic Investigation of Bloody Ascites

A 30-year-old Lebanese male was admitted with a history of change in bowel habits and generalized abdominal pain for 6 days. In the past 6 days, his stools had become more frequent and unformed. They were normal in color, and the patient was not jaundiced. There was no history of nausea, vomiting, genitourinary symptoms, fever, or night sweats, and there was no documented weight loss. Physical examination revealed abdominal distension with a positive fluid wave, decreased bowel sounds, and absence of tenderness, rebound, rigidity, or defined masses. A supine radiograph of the abdomen revealed abundant fecal material in the colon but no evidence of obstruction.

Liver function tests including serum bilirubin, alkaline phosphatase, total protein, and albumin/globulin ratio were within normal limits, as were serum amylase, blood urea nitrogen, and creatinine. Serum uric acid and blood glucose were slightly elevated. Chest x-ray, excretory urography, barium enema, upper gastrointestinal series, and liver-spleen scan were all within normal limits. Ultrasound revealed a large echogenic mass adherent to the anterior abdominal wall (fig. 1). Superior mesenteric, celiac, gastroduodenal, and internal and external iliac arteriograms revealed a moderately vascular tumor of the omentum fed by the epiploic branches of the celiac artery (fig. 2). CT scans revealed a large mantlelike mass in the anterior portion of the abdomen and pelvis (lead picture and fig. 3).

Exploratory laparotomy revealed bloody ascitic fluid with multiple friable cystic nodules studding the small bowel, the parietal peritoneal surfaces, and the serosal surfaces of the colon and stomach. There were no palpable lesions within the stomach, bowel, or pancreas, and the liver appeared normal. The main tumor mass appeared to arise in the greater omentum, which was resected. A preliminary histopathologic examination of the 3,200 g omental specimen revealed a cellular malignant neoplasm, type unclassified. Cell block of the ascitic fluid was negative for malignant cells. The final histopathologic diagnosis, after electron microscopy, was mesothelioma, and the patient was placed on multiple-agent chemotherapy. The malignant ascites has continued to reaccumulate, and the anterior abdominal mass has recurred.

Discussion

The causes of ascites are many. If a transudate, it may result from congestive cardiac failure, hepatic venous obstruction, or a hypoalbuminemic syndrome. Chylous ascites occurs rarely and may be associated with lymphosarcoma, diffuse abdominal carcinomatosis, or, in endemic areas of the world, filaria Bancroftii. An exudate or blood ascites, as in this patient, is usually associated today in the United States with carcinomatosis. Tuberculous peritonitis is less frequent. *Echinococcus* cysts can cause ascites, but this is usually secondary to

---

This is another in a bimonthly series of case reports prepared by A. Robert Kagan and Richard J. Steckel (Southern California Permanente Medical Group, 1510 North Edgemont, Los Angeles, California 90027, and UCLA Jonsson Comprehensive Cancer Center, 924 Westwood Boulevard, Suite 650, Los Angeles, California 90024, respectively) to present and discuss contemporary problems and procedures in the identification and staging of neoplasms. Case contributed by R. J. Steckel.

© 1978 American Roentgen Ray Society

hydatid disease within the liver. Weber-Christian disease, "retractile mesenteritis," and Crohn's disease can all lead to mesenteric thickening, but ascites is not a feature unless an acute abdominal complication supervenes. Omental strangulation and infarction usually cause acute abdominal pain and nausea, and are often accompanied by physical signs of peritoneal irritation.

CT scan and ultrasound demonstrated an anterior abdominal mass which was compatible with metastatic carcinoma to the omentum. This occurs most commonly in males from primary adenocarcinoma of the stomach [1], colon [2], or pancreas [3], and in females from ovarian carcinomatosis [4] (or breast carcinoma, in the later stages of disease). These malignancies occur predominantly in the over-40 age group. Because the present patient's tumor appeared to affect the peritoneal lining and omentum without involving lymph nodes or the gastrointestinal tract intrinsically, the most likely diagnosis, in the presence of compatible histopathology, was mesothelioma. Primary sarcomas of the omentum have also been reported [5].

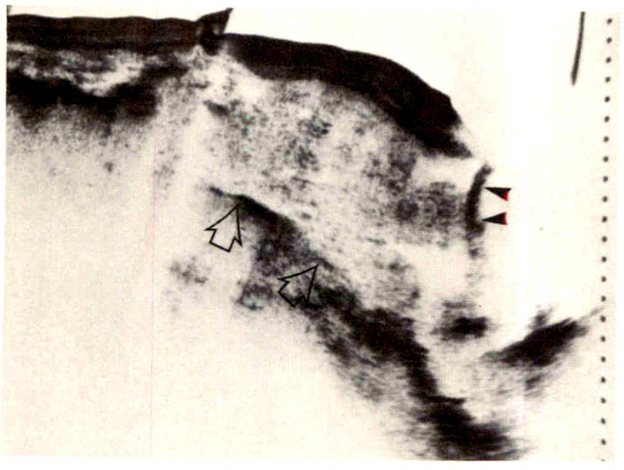

Fig. 1.—Sagittal ultrasound scan at midline showing echogenic anterior abdominal mass (*large arrows*) beneath anterior abdominal wall. Superior wall of bladder is indicated by arrowheads.

It is of interest that the most definitive studies in this patient were the CT scans and ultrasound. In a patient with bloody ascites or a peritoneal exudate, and in the absence of a history or clinical findings pointing toward a specific primary cancer site which could lead to abdominal carcinomatosis, cross-sectional imaging studies (ultrasound, and CT if available) may now be the best starting points for a diagnostic workup. Preoperative excretory urography, gastrointestinal series, and multiple abdominal angiography, while perhaps justified as later studies in certain patients to provide complementary diagnostic or staging information, did not provide additional data affecting therapy or prognosis for this patient [6–8]. Although it was the most helpful study preoperatively after diagnostic pericentesis, the abdominopelvic CT scan was the last to be ordered in the course of a prolonged (and expensive) hospital workup.

While in some instances the CT scan may not be useful in the diagnosis and staging of abdominal cancer, certainly in this patient it would have been much more "cost-effective" to order it early. Once the omentum is massively involved with metastatic carcinomatosis, it makes little difference (prior to exploration) whether the primary tumor is in the stomach or bowel, pancreas, or the gynecologic tract. In fact, a percutaneous needle biopsy of the anterior abdominal mass would probably have yielded the diagnosis of an undifferentiated malignant tumor and eliminated the need for laparotomy in this patient. If a primary gastrointestinal, ovarian, or breast tumor were already known to be present, even the need for biopsy of an abdominal mass would be questionable.

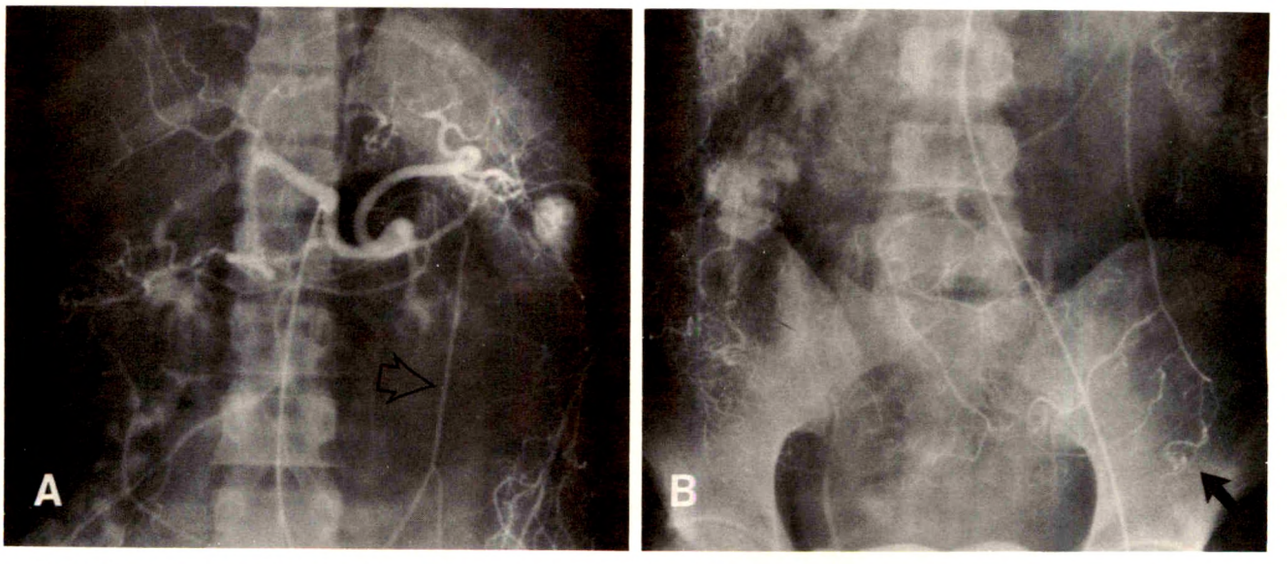

Fig. 2.—Celiac arteriogram showing enlarged left gastroepiploic artery (*A*, *arrow*) supplying tumor vessels within greater omentum (*B*, *arrow*).

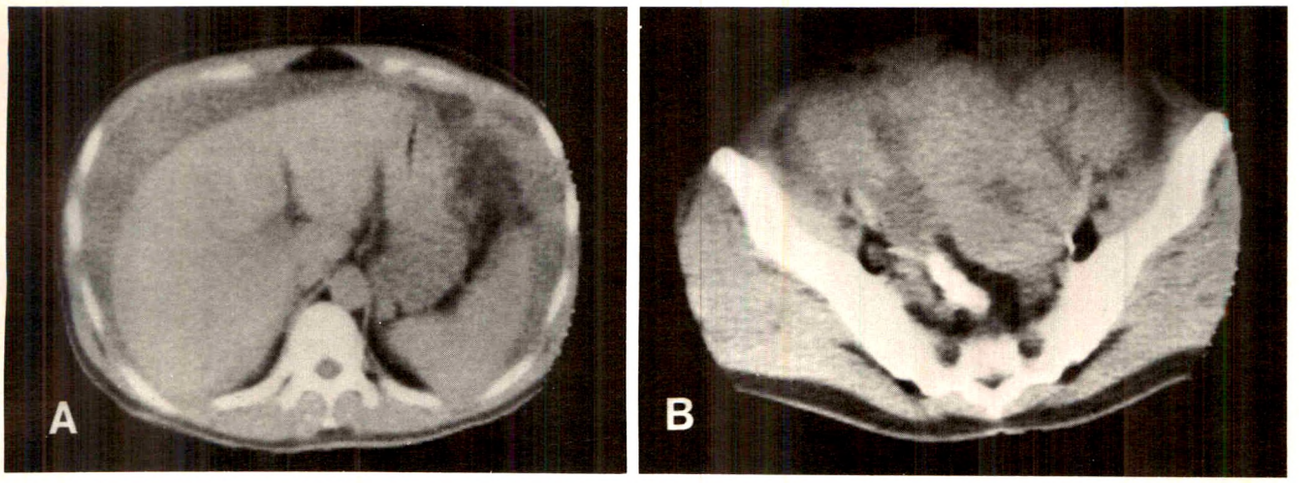

Fig. 3.—*A*, Upper abdominal scan showing central displacement of liver and spleen by ascitic fluid. CT number of fluid was considerably higher than water or peritoneal transudate, suggesting presence of bloody ascites. CT scan of midabdomen (lead picture) shows central displacement of Gastrografin-containing bowel loops by solid tumor which infiltrates greater omentum and forms shieldlike anterior and lateral abdominal mass. *B*, Pelvic scan demonstrating continuity with mass of varying internal density filling pelvis.

In summary, when a patient presents with bloody ascites, CT scan and/or ultrasound should now be among the first radiologic imaging procedures. If one or more solid peritoneal masses were demonstrated in the absence of an acute abdominal condition, a needle biopsy with appropriate histopathologic study, fluid cytology, and cultures could be carried out immediately. A treatment plan could be formulated without further exhaustive search for an intraabdominal primary site, once abdominal carcinomatosis has been proved and lymphoma excluded. If doubt as to the diagnosis persists, laparotomy could be performed. While benign omental masses and cysts can often be resected (the most common is a leiomyoma) [9, 10], primary malignant tumors of the omentum have usually invaded other vital abdominal structures by the time they first reach clinical attention.

REFERENCES

1. Reuter SR, Redman HC: *Gastrointestinal Angiography*. Philadelphia, Saunders, 1972
2. Rösch J: Liver, gallbladder, biliary ducts, in *Diagnosis and Staging of Cancer: A Radiologic Approach*, edited by Kagan AR, Steckel RJ, Philadelphia, Saunders, 1976, pp 176–199
3. Stout AP, Hendry J, Purdie J: Primary solid tumors of greater omentum. *Cancer* 16:231–243, 1963
4. Youker JE, Dodds WJ: Colon and rectum, in *Diagnosis and Staging of Cancer: A Radiologic Approach*, edited by Kagan AR, Steckel RJ, Philadelphia, Saunders, 1976, pp 200–214
5. Friedland GW: Stomach; small bowel, in *Diagnosis and Staging of Cancer: A Radiologic Approach*, edited by Kagan AR, Steckel RJ, Philadelphia, Saunders, 1976, pp 129–175
6. Carbalona P, Vernhet J, Bonnel F: Les leiomyomes du petit epiploon. *Chirurgie* 102:495–499, 1976
7. Caresano A, Del Favero C, Donnini M, Gaizze G, Travi L: L'angiografia del grande omento: rilievi nel normale e nel patologico. *Radiol Med* 61:797–802, 1975
8. Deutsch V, Adar R, Mozes M: Angiography of the greater omentum. *Am J Roentgenol* 113:174–180, 1971
9. Gilbert HA: Female genital tract, in *Diagnosis and Staging of Cancer: A Radiologic Approach*, edited by Kagan AR, Steckel RJ, Philadelphia, Saunders, 1976, pp 244–262
10. Nafissi A, Vakili K: Lymphangiome kystique du grand epiploon. *Chirurgie* 102:198–200, 1976

Case Reports

Sonographic Appearance of Duodenal Atresia in Utero

RICHARD F. LEES,[1, 2] BENNETT A. ALFORD,[1] A. NORMAN A. G. BRENBRIDGE,[1] ANTHONY J. BUSCHI,[1] AND BRIAN R. J. WILLIAMSON[1]

Anomalies of the fetus are being recognized more often as ultrasonic equipment improves and medical experience increases [1–4]. While examining a patient with polyhydramnios by sonography, duodenal atresia of the fetus was recognized. The bistable appearance of fetal duodenal atresia has been previously reported in the obstetric literature [5, 6]; we report the gray scale appearance of this anomaly.

Case Report

A white 25-year-old gravida 3, para 1, aborta 1 developed polyhydramnios during pregnancy. A sonogram confirmed the presence of polyhydramnios and also demonstrated a single term-size fetus within the uterine cavity. Two round fluid-containing masses were seen within the fetal abdomen (fig. 1*A*). No other abnormality was detected. Duodenal obstruction was suspected, and the patient was therefore hospitalized. Spontaneous normal labor resulted in the delivery of a viable term male infant weighing 2,530 g with Apgar scores of 9 and 10. Physical examination of the neonate demonstrated palpable abdominal masses, and a plain abdominal radiograph was consistent with the diagnosis of duodenal obstruction (fig. 1*B*). The diagnosis was confirmed at surgery and the atresia was corrected. The infant was discharged from the hospital 14 days after birth and has subsequently thrived.

Discussion

Polyhydramnios is known to be associated with certain fetal anomalies, such as anencephaly, high and midgastrointestinal obstruction, abnormalities of the swallowing mechanism [2], as well as Rh incompatibility and maternal diabetes. Whereas clinical assessment of the fetus is at best limited and the plain radiograph can show little other than the calcified skeleton, sonography can also demonstrate fetal soft tissues [1, 4]. The appearance of the stomach and proximal duodenum distended with air and the absence of air elsewhere in the bowel of a newborn infant is the characteristic radiographic appearance of duodenal obstruction. The cause is most commonly duodenal atresia, and the appearance has been named the "double bubble" sign [7, 8]. In utero, the bowel is filled with fluid and devoid of air. With complete obstruction of the second portion of the duodenum, dilatation of duodenum and stomach proximal to that

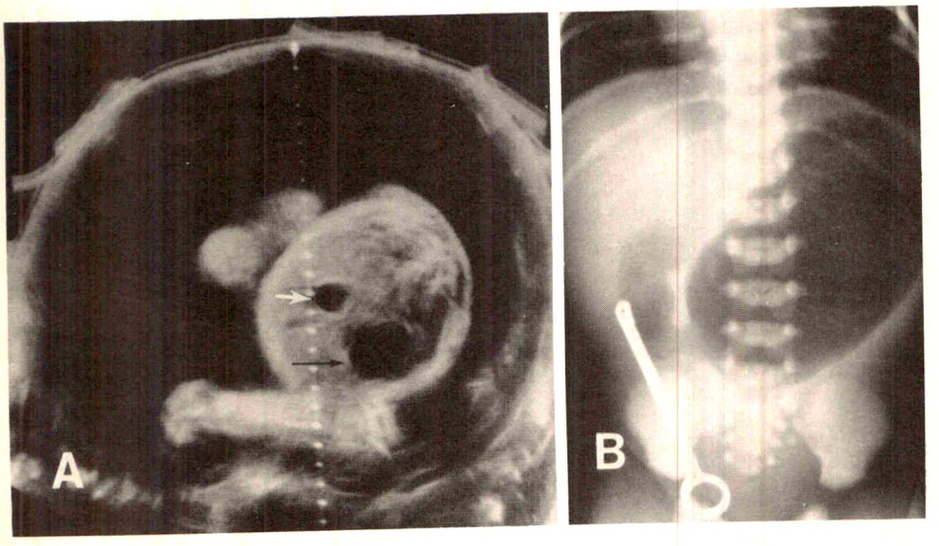

Fig. 1.—*A*, Transverse sonogram demonstrating midabdomen of fetus in cross section. Note distended fluid-filled stomach (*black arrow*) and duodenum (*white arrow*). Marked polyhydramnios is present. *B*, Supine radiograph of infant several hours after birth. Stomach and duodenum are distended by air. There is no air in mid or distal bowel.

Received February 10, 1978; accepted after revision May 23, 1978.
[1]Department of Radiology, University of Virginia Medical Center, Charlottesville, Virginia 22901. Address reprint requests to A. N. Brenbridge.
[2]Present address: Department of Radiology, Queen Elizabeth Hospital, Woodville, South Australia 5011, Australia.

© 1978 American Roentgen Ray Society

0361–803X/78/1000–0701 $00.00

point will occur, resulting in a "double bubble" of fluid visualized sonographically in the fetal abdomen.

The development of polyhydramnios is an indication for investigation of the pregnancy. Sonography can provide sufficient anatomic details to detect cases associated with duodenal obstruction, expediting surgical correction.

REFERENCES

1. Kossoff G, Garrett WJ, Radovanovich G: Grey scale echography in obstetrics and gynaecology. *Australas Radiol* 18:62–111, 1974
2. Santos-Ramos R, Duenhoelter JH: Diagnosis of congenital fetal abnormalities by sonography. *Obstet Gynecol* 45:279–283, 1975
3. Scholl HW Jr: In utero diagnosis of agnathia, microstomia, and synotia. *Obstet Gynecol* 49:81s–83s, 1977
4. Lee TG, Warren BH: Antenatal ultrasonic demonstration of fetal bowel. *Radiology* 124:471–474, 1977
5. Houlton MCC, Sutton M, Aitken J: Antenatal diagnosis of duodenal atresia. *J Obstet Gynaecol Br Commonwealth* 81:818–821, 1974
6. Duenhoelter JH, Santos-Ramos R, Rosenfeld CR, Colin CD: Prenatal diagnosis of gastrointestinal tract obstruction. *Obstet Gynecol* 47:618–620, 1976
7. Caffey J: *Pediatric X-ray Diagnosis*. Chicago, Year Book Medical Publishers, 1972
8. Franken EA Jr: *Gastrointestinal Radiology in Pediatrics*. Hagerstown, Md., Harper & Row, 1975

Pulmonary Uptake of ^{99m}Tc Diphosphonate in Alveolar Microlithiasis

MANUEL L. BROWN,[1, 2] RONALD G. SWEE,[1] ROBERT J. OLSON,[1] AND CLAIR E. BENDER[1]

Rosenthal et al. [1] recently reported a series of patients with pulmonary uptake of bone imaging tracer. All patients in that series had evidence of renal failure, and the majority had hypercalcemia as factors relating to their metastatic pulmonary calcification. We recently studied a patient with pulmonary alveolar microlithiasis without abnormal laboratory values who also demonstrated diffuse intense uptake of bone tracer in the lung.

Case Report

A 67-year-old male was seen for evaluation of low back pain and a several month history of bloody stools. Past medical history included hypertension and alveolar microlithiasis. The patient denied any pulmonary symptoms. Sputum cytology 4 years before admission was negative for pulmonary malignant cells, but positive for spherical concentric calcific structures. At that time serum calcium and phosphorous were normal. An intermediate purified protein derivative test 1 year later was negative, and serum calcium, phosphorous, uric acid, and creatinine levels were normal.

On this admission, laboratory values were again normal. Pulmonary function tests and arterial blood gases were also normal. Chest radiography (fig. 1) demonstrated the characteristic diffuse, fine, calcific micronodulation of alveolar microlithiasis. This finding had first been noted 23 years earlier and remained unchanged. A bone scan was performed 2 hours after injection of 15 mCi of ^{99m}Tc diphosphonate on a tomoscanner (Searle Pho-Con). The bone scan, done for the evaluation of low back pain, demonstrated diffuse intense uptake of the tracer throughout both lungs (fig. 2). Computed tomography of the chest showed a diffuse pulmonary infiltrative pattern with tiny bullae (fig. 3*A*). There was a difference of 196 EMI numbers between the lung field and a normal comparison (fig. 3*B*).

Discussion

Pulmonary alveolar microlithiasis is a relatively rare disorder of unknown etiology. It is characterized by innumerable tiny calcispherytes within the alveoli of the lung. A familial incidence has been reported among siblings, and environmental and metabolic factors have also been implicated as etiologic agents. The calcispherytes range from 0.01 to 0.3 mm in diameter and are composed chiefly of calcium and phosphorus, with the major chemical state being apatite [2]. The diagnosis is almost always made by the classic radiographic findings and the radiologic clinical dissociation. The spectrum of

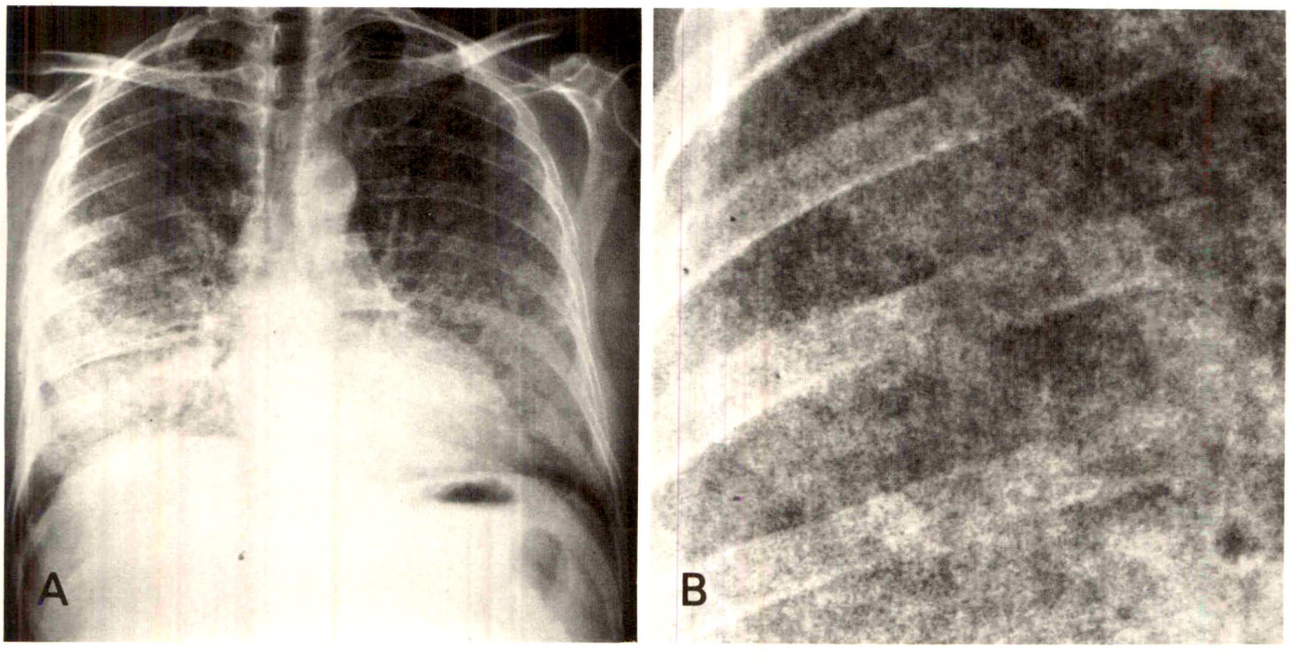

Fig. 1.—*A*, Posteroanterior chest film showing diffuse pattern of sharply defined microliths. Increased density at bases reflects greater volume of lung in this area. *B*, Close-up of portion of right lung.

Received January 13, 1978; accepted after revision June 2, 1978.
[1] Department of Diagnostic Radiology, Mayo Clinic, Rochester, Minnesota 55901. Address reprint requests to M. L. Brown.
[2] Section of Diagnostic Nuclear Medicine, Mayo Clinic, Rochester, Minnesota 55901.

© 1978 American Roentgen Ray Society

0361–803X/78/1000–0703 $00.00

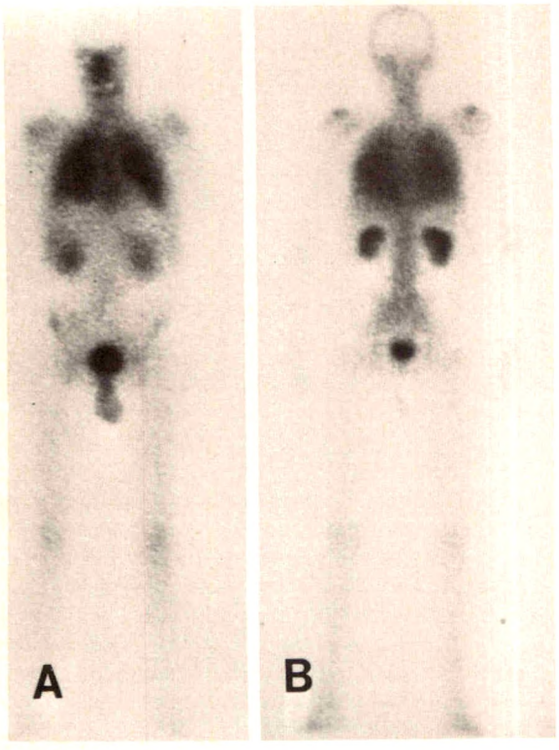

Fig. 2.—Bone scan performed on tomoscanner. Anterior (*A*) and posterior (*B*) sections are normal except for diffuse intense uptake of tracer in lungs.

this disease ranges from normal-appearing lungs and alveolar walls early in the course, with progression to interstitial fibrosis and thickened alveolar walls and often blebs and bullae later.

In view of the chemical composition of the microliths, the intense uptake of the bone tracer is not an unexpected finding. Also as expected, the lung CT examination revealed a pattern resembling a diffuse pulmonary infiltrative process with an overall increase in the EMI number.

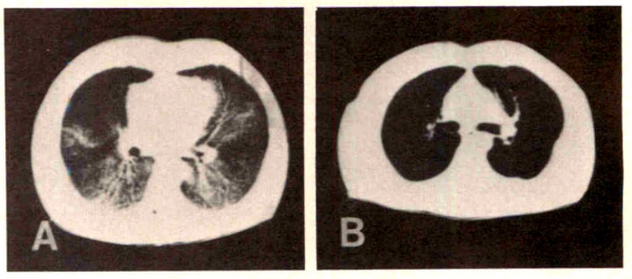

Fig. 3.—CT of lungs. *A*, Diffuse pattern of increased density in patient with alveolar microlithiasis. *B*, Comparison scan with identical window settings in normal patient.

The hypothesis of Rosenthal et al. [1] that the bone scan may yield information about occult pulmonary calcification seems reasonable in view of the sensitivity of bone scanning. Firooznia et al. [3] reported a case of diffuse interstitial pulmonary calcification mimicking pulmonary edema. A bone scan or chest CT scan may have been helpful in making a premortem diagnosis. Our case demonstrates that other causes of deposition of bone tracer in the lungs can occur, and that scintigraphic radiographic correlation is important.

ACKNOWLEDGMENTS

We thank Dr. L. R. Brown and J. K. Crowe for help with the CT images and Nadine Spatz for editorial and secretarial assistance.

REFERENCES

1. Rosenthal DI, Chandler HL, Azizi F, Schneider PB: Uptake of bone imaging agents by diffuse pulmonary metastatic calcification. *Am J Roentgenol* 129:871–874, 1977
2. Fraser RG, Paré JAP: *Diagnosis of Diseases of the Chest*. Philadelphia, Saunders, 1970
3. Firooznia H, Pudlowski R, Golimbu C, Rafii M, McCauley D: Diffuse interstitial calcification of the lungs in chronic renal failure mimicking pulmonary edema. *Am J Roentgenol* 129:1103–1105, 1977

Nonfatal Pulmonary Air Embolism: Radiographic Demonstration

MICHAEL J. FAER[1] AND GERALD L. MESSERSCHMIDT[2]

The use of central catheters for long-term parenteral nutrition and chemotherapy is now standard medical practice. An uncommon complication of central venous catheterization is air embolism, which may occur during insertion [1, 2], during high pressure infusion [3], from inadvertent disconnection or disruption of the catheter [4, 5], or with failure to use an occlusive dressing over the venipuncture site after catheter removal [6]. Although air embolism is potentially fatal, prompt recognition and appropriate supportive and positional therapy can be lifesaving [3, 5, 7]. We report a case of nonfatal pulmonary air embolism via a central venous catheter to illustrate the radiographic findings and to promote increased awareness and earlier diagnosis of this condition.

Case Report

A 53-year-old white female with diffuse histiocytic lymphoma received long-term chemotherapy via a nonopaque, Silastic, central venous catheter. When the patient sat up in bed, she inadvertently disconnected her catheter, grabbed her chest, and became unresponsive. A nurse in attendance immediately started cardiopulmonary resuscitation, and respiratory and cardiac functions returned. Although the patient's sensorium was confused, she was judged to be stable enough to undergo semierect bedside chest radiography, which was obtained and interpreted within 15 min after her initial cardiovascular collapse. The chest film (fig. 1) revealed bilateral collections of air in the central pulmonary arteries and diminished peripheral pulmonary vascularity.

The patient was placed in the left lateral decubitus position. During the next 20–30 min she regained normal mentation and her clinical course stabilized. Repeat radiography 30 min after the initial film showed normal pulmonary vascularity. The patient suffered a residual mild left hemiparesis that gradually resolved over the next few months.

Discussion

Venous air embolism is a well documented [1–9] and feared complication. Its causes, reviewed by Grace [5] include: (1) venous catheter induced; (2) upright head and neck surgery with induction of air through the dural sinuses or major neck veins; and (3) induced pneumoperitoneum or retroperitoneum.

Unlike arterial air embolism, large amounts of venous air [3, 7, 8] are necessary to produce symptoms and/or demise. Generally, four factors seem to influence fatality from venous air embolism: (1) amount of air; (2) speed of injection; (3) position of catheter tip; and (4) position of the right ventricular outflow tract. Animal experiments [8, 9] demonstrated that 1.0–7.5 ml of air/kg of body weight injected within 5 sec produced symptoms and approximately a 70% mortality rate; whereas, in excess of 1,000 ml of air injected slowly over a prolonged period was tolerated without symptoms. Ordway [7] extrapolated these results to man, estimating that the average lethal rate of injection is 70–100 ml of air/sec and the approximate lethal dose is 200 ml of air.

Peripheral venous catheters usually require active injection; however, central venous catheters are under the influence of negative intrathoracic pressure which can rapidly transmit large volumes of air under atmospheric pressure, especially in upright and vascular volume-depleted patients [5, 7]. Unlike carbon dioxide, a more soluble, less hazardous gas used for diagnostic visualization of the right heart and venous system [10], air will remain as a bolus within the vascular system [3], obstructing blood flow. Outflow obstruction of the right ventricle is the presumed mechanism of death [3, 8]; the left lateral decubitus position redistributes the air above the right ventricular outflow tract, relieving the air lock.

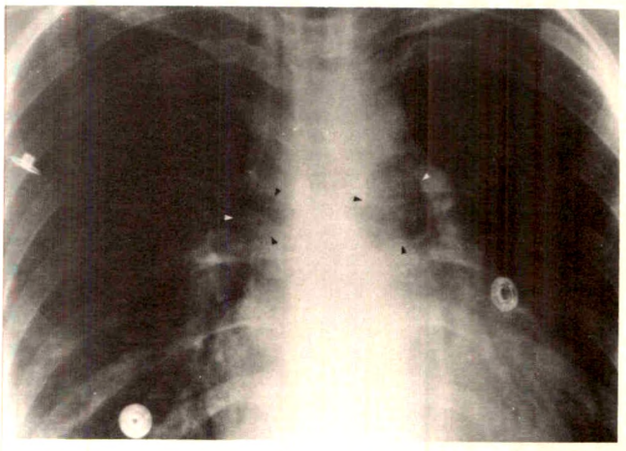

Fig. 1.—Portable sitting anteroposterior chest radiograph demonstrating central bell-shaped collections of air in pulmonary arteries (*arrows*). Pulmonary vascularity is markedly diminished, especially in both upper lung zones.

Received February 28, 1978; accepted after revision May 30, 1978.

The opinions or assertions contained herein are the private views of the authors and are not to be construed as official or as reflecting the views of the Department of the Army or the Department of Defense.

[1]Department of Radiology, Letterman Army Medical Center, Presidio of San Francisco, California 94129. Address reprint requests to Technical Publications Editor, Letterman Army Medical Center.

[2]Department of Medicine, Letterman Army Medical Center, Presidio of San Francisco, California 94129.

© 1978 American Roentgen Ray Society

0361–803X/78/1000–0705 $00.00

Positioning of the patient in the left lateral decubitus position improves cardiorespiratory symptoms and survival [2, 3, 5, 7, 8].

Clinically, the combination of central venous catheter, sudden cardiovascular collapse, and the classic "mill-wheel" murmur strongly suggest the diagnosis of pulmonary air embolism. Neurologic deficit after pulmonary air embolism has been previously reported [5] and may be related to nonembolic stroke from decreased cardiac output and/or direct cerebral air embolism.

To our knowledge, this is the second premortem radiographic illustration of central catheter-induced pulmonary air embolism [6]. The radiographic findings of a bell-shaped collection of air in the central pulmonary outflow tract with bilateral upper lung zone oligemia were present in both cases and are probably pathognomonic. Prevention of catheter induced pulmonary air embolism should be a concern of all hospital personnel. Central venous catheters and venipuncture sites should be airtight, catheter and venous line should be securely connected or locked, and upright positioning during venipuncture, therapy, or surgery should be avoided [5, 7].

ACKNOWLEDGMENTS

We thank Maria Faer, Nina Sanders, and Harry Roberts for assistance in preparation of this manuscript.

REFERENCES

1. Flanagan JP, Gradisar IA, Gross RJ, Kelly TR: Air embolus—a lethal complication of subclavian venipuncture. *N Engl J Med* 281:488–489, 1969
2. Johnson CL, Lazarchick J, Lynn HB: Subclavian venipuncture: preventable complications, report of two cases. *Mayo Clin Proc* 45:712–719, 1970
3. Durant TM, Long J, Oppenheimer MJ: Pulmonary (venous) air embolism. *Am Heart J* 33:269–281, 1947
4. Armstrong RF, Peters JL, Cohen SL: Air embolism caused by a fractured central-venous catheter (letter). *Lancet* 1:954, 1977
5. Grace DM: Air embolism with neurologic complications: a potential hazard of central venous catheters. *Can J Surg* 20:51–53, 1977
6. Tuddenham WJ, Paskin DL: Radiographic demonstration of air embolism. *Med Radiogr Photogr* 50:16–18, 1974
7. Ordway CB: Air embolus via CVP catheter without positive pressure: presentation of case and review. *Ann Surg* 179:479–481, 1974
8. Oppenheimer MJ, Durant TM, Lynch P: Body position in relation to venous air embolism and associated cardiovascular respiratory changes. *Am J Med Sci* 225:362–373, 1953
9. Lucus CE, Frani F: Air embolism via subclavian catheters. *N Engl J Med* 281:966–967, 1969
10. Bendib M, Toumi M, Boudjellab A: A new method of phlebography: carbon dioxide visualization of the venous system, especially for study of the hepatic veins. *Ann Radiol* 16:305–330, 1973

Miliary Aspergillosis Associated with Alcoholism

JEFFREY BLUM,[1] JAMES C. REED,[1] SALVATORIE V. PIZZO,[2] AND WILLIAM M. THOMPSON[1]

Aspergillosis is rarely considered in the initial differential diagnosis of an acute pneumonic illness unless the patient is known to have a chronic debilitating disease or known to have been taking antimicrobial agents or adrenocortical steroid drugs. Chronic alcoholism has not been previously included as one of the predisposing factors. We describe a patient who presented with a miliary pattern on his chest radiograph which rapidly progressed into a diffuse pneumonia attributable to aspergillosis.

Case Report

A 42-year-old black male was admitted after a "falling out spell" with loss of consciousness but no seizure activity. He was reported to have been drinking steadily for the last 4 years, consuming approximately a liter of liquor daily, until about 3 days prior to admission. He had complained previously of vague abdominal pain and had been noted to have a chronic cough productive of yellow sputum for many years. The cough had increased in severity but without fever, night sweats, or weight loss. Recently, an episode of hemoptysis had been noted. The patient had worked as a farmer and was known to have been exposed to persons with tuberculosis.

Physical examination revealed a tremulous, confused, and tachypneic male. His temperature was 40.5°C, pulse 113/min, blood pressure 140/90 mm Hg, and respiration 50/min. Increased breath sounds were heard throughout both lung fields with rhonci at both bases. The liver was tender and slightly enlarged. The spleen was not palpable, and no evidence of adenopathy was detectable. The patient was disoriented with fine tremors, was hallucinating and had poor cerebellar function.

White blood cell count was 13,200/mm^3 with 83% neutrophils. Chest films showed a diffuse miliary nodular pattern (figs. 1*A* and 1*B*). The gram stain of the sputum showed a few polymorphonuclear cells with gram positive diplococci and some gram negative rods. Repeated stains for acid-fast bacilli were negative. Arterial blood gases on room air were Pa_{O_2} of 43 mm Hg, Pa_{CO_2} of 22 mm Hg, with a pH of 7.58. Spinal fluid examination showed no cells or organisms.

The diagnosis of an acute infectious pulmonary process was considered in addition to impending delirium tremens. Medication with cephalothin and gentamicin was started. Sputum cultures produced *Streptococcus* (diplococcus) *pneumoniae* and *Staphylococcus epidermidis*. No blood cultures were obtained. *Candida*, mumps, and PPD skin tests showed no evidence of reaction. The patient's respiratory condition progressively declined, and he required a tracheostomy with ventilatory support. Repeat chest films at 24 hr (figs. 1*C* and 1*D*) showed an increasingly widespread infiltrate in both lung fields. The diagnostic considerations included miliary tuberculosis, a necrotizing pneumonitis, or noncardiac pulmonary edema.

The patient died of respiratory failure 44 hr after admission. Autopsy revealed a severe aspergillus pneumonia of both lungs. The pleural surfaces were studded with tan firm nodules measuring 3 mm in diameter. The cut surface of the lungs revealed similar tan nodules studding the parenchyma diffusely and uniformly in all lobes (fig. 2*A*). The pulmonary vessels were unremarkable. Microscopic examination demonstrated a necrotizing pneumonia consisting of scattered lesions containing a mass of thin, branching, septate hyphae as demonstrated both by routine and fungal stains (fig. 2*B*). Histologically, this is the typical appearance of aspergillus species. The liver showed passive congestion with mild diffuse fatty change.

Other organs appeared unremarkable.

Discussion

A primary infection with aspergillus in a healthy person following occupational exposure to the fungus is now believed to be exceedingly rare [1]. The secondary forms of the disease consist of the well known pulmonary mycetoma, the allergic bronchopulmonary form usually associated with asthmatic patients, and the invasive form found in patients with underlying debilitating disease. The latter group has become increasingly important as we progressively treat more chronic illness. Patients with carcinoma, lymphoma, leukemia, chronic obstructive pulmonary disease, congestive heart failure, sarcoidosis, and numerous other conditions are all susceptible [2–4]. In addition, with increasing use of antibiotics, adrenal cortical hormones, antineoplastic drugs, and immunosuppressive therapy, there has been an increase in aspergillus infection, both pulmonary and disseminated [5]. To our knowledge, invasive aspergillus of the lung in a patient with chronic alcoholism, free from other debilitating diseases and not on long-term steroids or antibiotics, has not previously been reported.

In susceptible persons, the highest infection rate is associated more often with a leukopenia [2, 3]. However, this patient had an adequate leukocyte response in numbers if not function. Alcoholics are known to be more susceptible to infections such as tuberculosis and pneumococcal and *Klebsiella* pneumonias. Therefore, it does not seem unreasonable that some alteration in the effectiveness of their immune systems would result in the development of fungal infections which are normally not found in a healthy host. That such an alteration occurred in this patient is supported by negative skin tests to common antigens.

Another unusual feature of this case is the initial presentation of a diffuse miliary pattern on chest radiographs which resulted in the initial diagnostic impression

Received December 20, 1977; accepted after revision May 3, 1978.
W. M. Thompson is a James Picker Foundation Scholar.
[1]Department of Radiology, Duke Univerity Medical Center, Durham, North Carolina 27710. Address reprint requests to J. C. Reed.
[2]Department of Pathology, Duke University Medical Center, Durham, North Carolina 27710.

© 1978 American Roentgen Ray Society

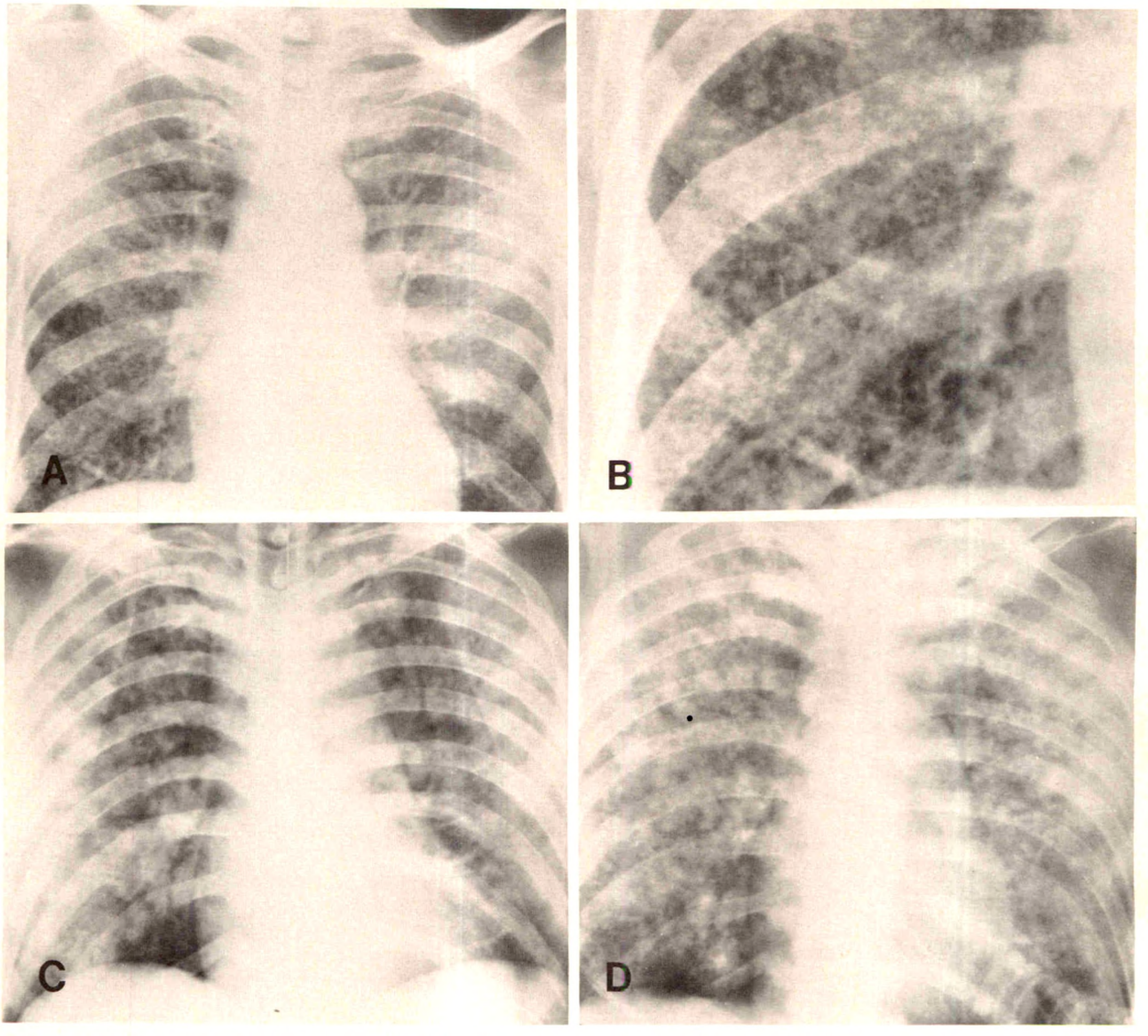

Fig. 1.—*A*, Posteroanterior chest film demonstrating diffuse fine nodular or miliary interstitial pattern. *B*, Close-up of right lower lobe emphasizing nodular appearance. *C*, Follow-up posteroanterior chest radiograph revealing rapid progression of pulmonary infiltrates in 24 hr to large multifocal consolidations. Pattern is commonly associated with invasive aspergillosis. *D*, Subsequent development of densities into even larger areas of confluent consolidations with air bronchograms.

of tuberculosis. The latter diagnosis was questioned with the subsequent rapid development of confluent infiltrates. As in most cases, only a high degree of suspicion leads to an antemortem diagnosis of aspergillus pneumonia since cultures and serological tests are only positive in a small percentage of such patients, and symptoms and physical findings are often attributed to bacterial pneumonias or pulmonary emboli. This case reinforces the protean nature of this fungus and the need to consider it in a patient with an underlying debilitating illness who presents with a chest radiograph compatible with miliary tuberculosis.

REFERENCES

1. Freundlich IM, Israel HL: Pulmonary aspergillosis. *Clin Radiol* 24:248–253, 1973
2. Meyer RD, Young LS, Armstrong D, Bessie Y: Aspergillosis complicating neoplastic disease. *Am J Med* 54:6–15, 1973
3. Young RD, Bennett JE, Vogel CL, Carbone PP, DeVita VT: Aspergillosis: the spectrum of the disease in 98 patients. *Medicine* 49:147–173, 1970
4. Eastridge CE, Young JM, Cole F, Gourley R, Pate JW: Pulmonary aspergillosis. *Ann Thorac Surg* 13:397–403, 1972
5. Feingold FM, Will D, Murray JF: Aspergillosis: a review and report of 12 cases. *Am J Med* 27:463–481, 1959

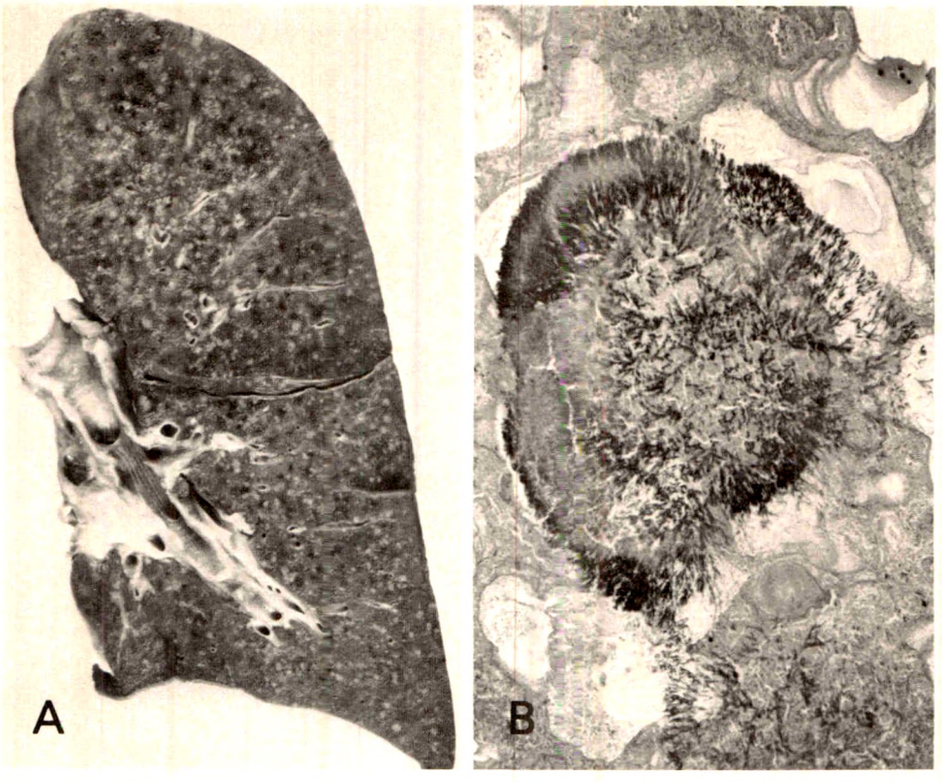

Fig. 2.—*A*, Cut surface of left lung revealing small nodules diffusely studding parenchyma. Right lung had similar appearance. *B*, Microscopic examination of grossly apparent nodule. Typical aspergillus colony is characterized by radiant rounding hyphae (×68). Septations were shown at higher magnification.

Coronary Artery Anomaly in Double-Outlet Right Ventricle

ERIC J. UDOFF,[1] JEAN-MICHEL ROLAND,[2] AND ROBERT I. WHITE, JR.[1]

An anomalous coronary artery distribution exists in 2%–9% of patients with tetralogy of Fallot [1–9] and less commonly with other types of congenital heart disease [3]. This report describes an anomalous origin of the anterior descending coronary artery from the right coronary artery in a child with a double-outlet right ventricle. Prior knowledge of this anomaly may alter the technique of surgical correction. On the basis of this report and our review of the literature, we suggest that preoperative coronary artery visualization be obtained routinely in all such patients.

Case Report

P. A., a 9½-year-old girl, was the product of a normal full-term delivery (3.2 kg at birth). At age 1 month, cyanosis was seen with crying. By 2 months, the child experienced congestive heart failure and was begun on digoxin. Cardiac catheterization at 3 months revealed a ventricular septal defect with a 2.3:1 left-to-right shunt. Digoxin was continued. At age 8 months, the pulmonary artery was banded because of persistent congestive heart failure, and digoxin was stopped. A second cardiac catheterization at age 3½ years revealed a double-outlet right ventricle with the pulmonary and aortic valves at the same level and no aortomitral continuity.

The child was readmitted for evaluation for surgical repair. Physical examination revealed an active precordium without a thrill. A 4/6 harsh systolic ejection murmur was heard all over the chest, maximally at the left sternal border. There was no diastolic component. Electrocardiography demonstrated normal sinus rhythm with right ventricular hypertrophy. Echocardiography suggested overriding of the interventricular septum by the aorta. Angiocardiography demonstrated a classic double-outlet right ventricle with the aortic and pulmonary valves at the same level in both frontal and lateral projections (fig. 1). A bilateral conus was widely patent in diastole, but narrower in systole. The main pulmonary artery was narrowed from the previous banding. Aortography demonstrated the circumflex coronary artery to arise from the left coronary cusp, while the left anterior descending coronary artery originated from the right coronary artery and crossed over the outflow tract leading to the pulmonary artery (fig. 2).

Discussion

Anomalous patterns of coronary artery origin and branching have been seen in many types of congenital heart disease [1–9]. In tetralogy of Fallot, one autopsy study [8] demonstrated a 9% incidence of anomalous coronary arteries. Angiographic and surgical series [4] have revealed incidences of coronary artery anomalies in 2%–5% of patients with tetralogy of Fallot. Other congenital heart lesions associated with coronary artery anomalies include complete and corrected transposition of the great arteries, single ventricle with transposition of great arteries, and double-outlet right ventricle [3].

In our patient, the anterior descending coronary artery branch arose from the right coronary artery, crossed over the right ventricular pulmonary outflow tract, and descended normally in the anterior interventricular groove. In its position on the right ventricular outflow tract, it could be damaged during total surgical repair [7]. High surgical morbidity and mortality have been experienced when an anomalous coronary artery has been injured during cardiac surgery in patients with tetralogy of Fallot and anomalous coronary arteries [1, 4 5, 7]. Our patient also seems at risk since the size of the right ventriculotomy would be limited in order to avoid the left anterior descending coronary artery. In this instance, a Rastelli-type right ventricle-to-pulmonary artery conduit bypassing the right ventricular outflow tract may be preferable to infundibular resection.

In a postmortem study of double-outlet right ventricle, Elliott et al. [3] found two coronary artery anomalies in 14 cases. One patient had two anterior descending coronary branches, one each from the left and right coronary cusps. In another patient, the right coronary artery arose as a branch of the left coronary artery, and an accessory anterior descending artery came from the right coronary cusp.

The incidence of anomalous coronary arteries is well established in tetralogy of Fallot, but the incidence in patients with double-outlet right ventricle has not been described prospectively. If the origin and course of the coronary arteries are not identified at preoperative ventriculography, then aortography is recommended. Aortography with filming in the anteroposterior and lateral projection adds little time to the study; these are the most useful projections for identification of the coronary arteries.

REFERENCES

1. Berry BE, McGoon DC: Total correction for tetralogy of Fallot with anomalous coronary artery. *Surgery* 74:894–898, 1973
2. Edwards JE: Anomalous coronary arteries with special reference to arteriovenous-like communications. *Circulation* 17:1001–1006, 1958
3. Elliott LP, Amplatz K, Edwards JE: Coronary arterial patterns in transposition complexes. *Am J Cardiol* 17:362–378, 1966
4. Fellows KE, Freed MD, Keane JF, Van Praagh R, Bernhard

Received December 6, 1977; accepted after revision May 3, 1978.
[1] Division of Cardiovascular Radiology, Johns Hopkins Medical Institutions, Baltimore, Maryland 21205. Address reprint requests to E. J. Udoff.
[2] Division of Cardiovascular Pediatrics, Johns Hopkins Medical Institutions, Baltimore, Maryland 21205.

© 1978 American Roentgen Ray Society

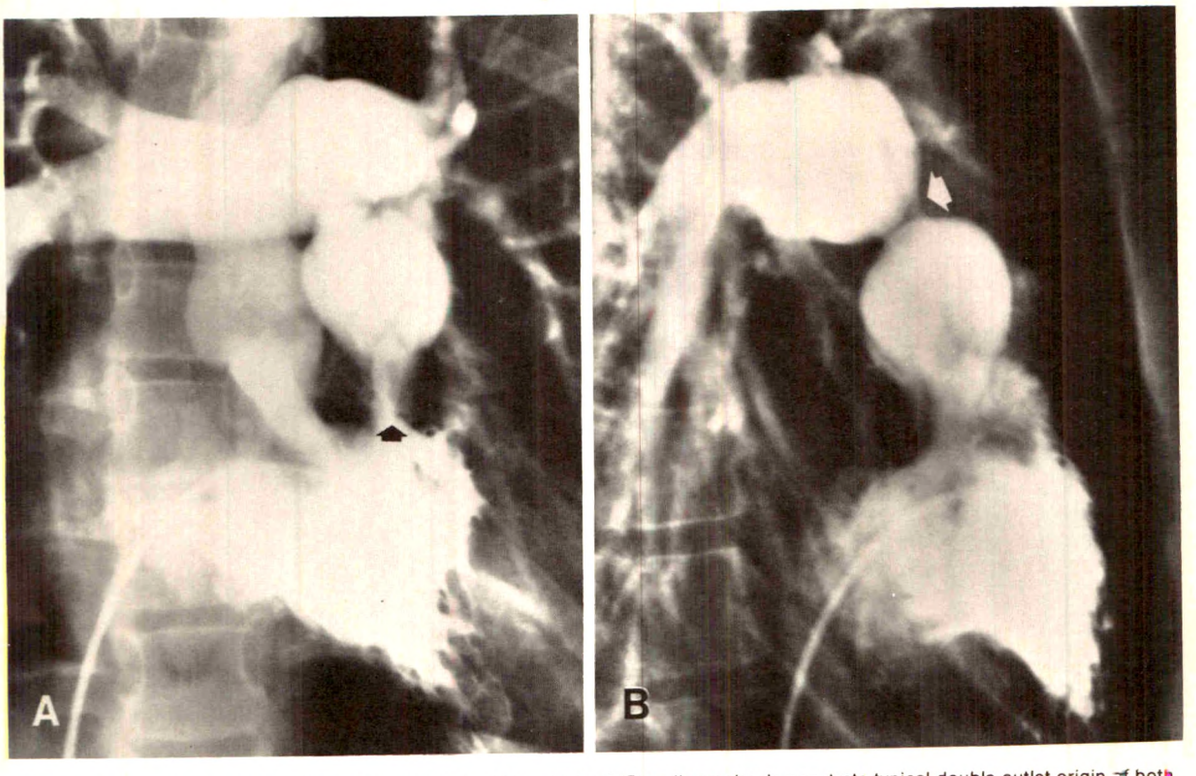

Fig. 1.—Biplane right ventriculogram. Anteroposterior (*A*) and lateral (*B*) radiographs demonstrate typical double-outlet origin of both great arteries from right ventricle. Pulmonary artery band (*white arrow*) and infundibular narrowing (*black arrow*) are present.

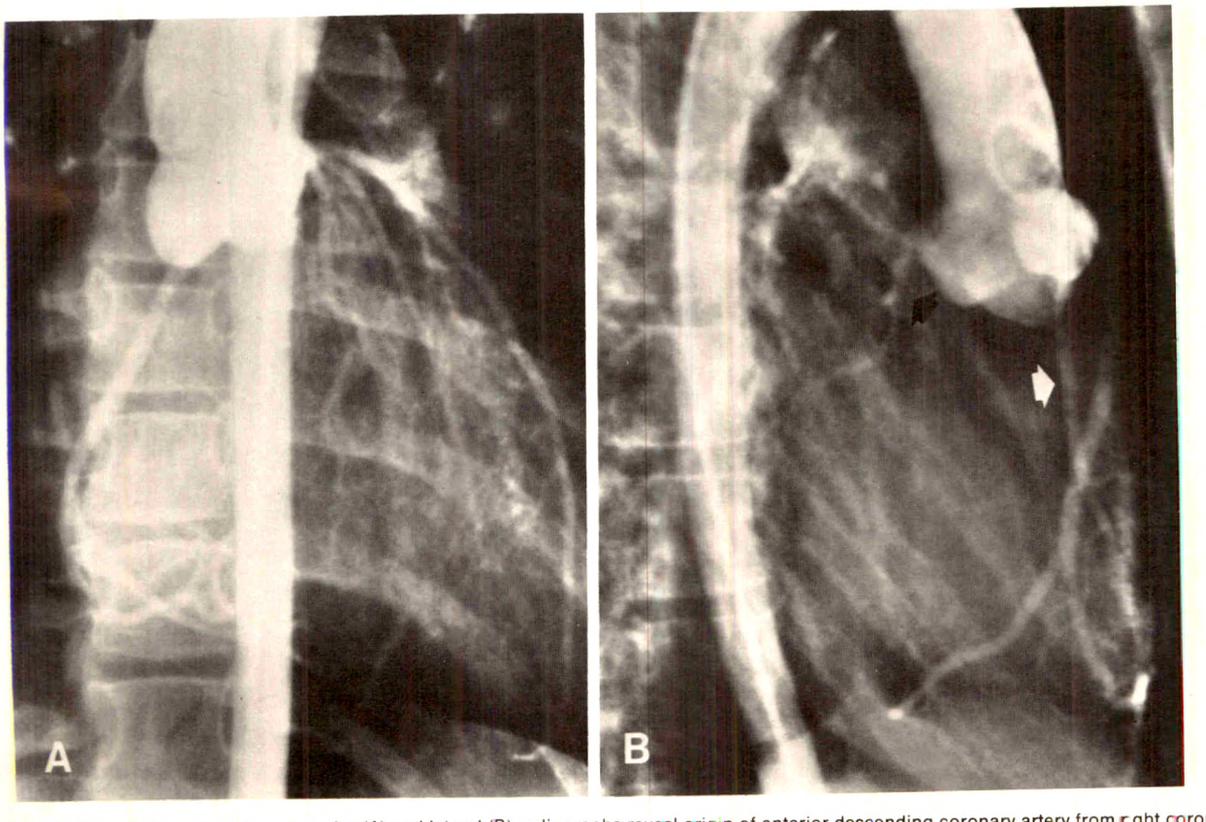

Fig. 2.—Biplane aortogram. Anteroposterior (*A*) and lateral (*B*) radiographs reveal origin of anterior descending coronary artery from right coronary artery (*white arrow*). Separate circumflex coronary artery arises from left coronary cusp (*black arrow*). Anterior descending coronary artery crosses at base of pulmonary valve.

WF, Castaneda AC: Results of routing preoperative coronary angiography in tetralogy of Fallot. *Circulation* 51:561–566, 1975
5. Gadboys HL, Slomin R, Litwak RS: Trecherous anomalous coronary artery. *Am J Cardiol* 8:854–858, 1961
6. Koops B, Kerber RE, Wexler L, Green RA: Congenital coronary artery anomalies. *JAMA* 226:1425–1429, 1973
7. Longnecker LG, Reemtsma K, Creech D Jr: Anomalous coronary artery distribution associated with tetralogy of Fallot: hazard in open cardiac repair. *J Thorac Cardiovasc Surg* 42:258–262, 1961
8. Meng CCL, Eckner FAD, Lev M: Coronary artery distribution in tetralogy of Fallot. *Arch Surg* 90:363–366, 1965
9. White RI Jr, Frech RS, Castaneda A, Amplatz K: The nature and significance of anomalous coronary arteries in tetralogy of Fallot. *Am J Roentgenol* 114:350–354, 1972

Pedunculated Endotracheal Metastasis

HEBER MacMAHON,[1] DENIS J. O'CONNELL,[1] AND GEORGE E. CIMOCHOWSKI[2]

Intraluminal tracheobronchial metastases are unusual lesions; most are secondary to renal, breast, or colorectal carcinoma. The majority are located distal to the carina and may be confused with primary bronchogenic carcinoma. This case is noteworthy in that the patient presented with acute upper respiratory tract obstruction due to a freely mobile, pedunculated endotracheal metastasis from a renal carcinoma. Although this feature has been described at autopsy, it has not been defined radiographically.

Case Report

A 61-year-old man presented to the emergency room with acute respiratory distress and hemoptysis. He had had nephrectomy for renal cell carcinoma 6 years previously and had subsequent radiation therapy for a femoral metastasis.

Admission chest radiographs (fig. 1) showed superior mediastinal widening. A poorly defined mass was visible in the distal trachea. Tomograms showed a lobulated, intraluminal mass above the carina (fig. 2) which was attached by a pedicle to the anterior tracheal wall.

A left supraclavicular node biopsy revealed metastatic adenocarcinoma. Bronchoscopy demonstrated a highly mobile 2.5 x 1.5 cm tumor in the distal trachea that was attached to the anterior tracheal wall by a 2 cm pedicle. At thoracotomy, a mass of tumor tissue was encountered in the anterior mediastinum. The trachea was incised and the endotracheal mass was successfully removed. Sections of both masses showed metastatic renal cell carcinoma. The patient recovered uneventfully and has been subsequently treated with radiation and chemotherapy.

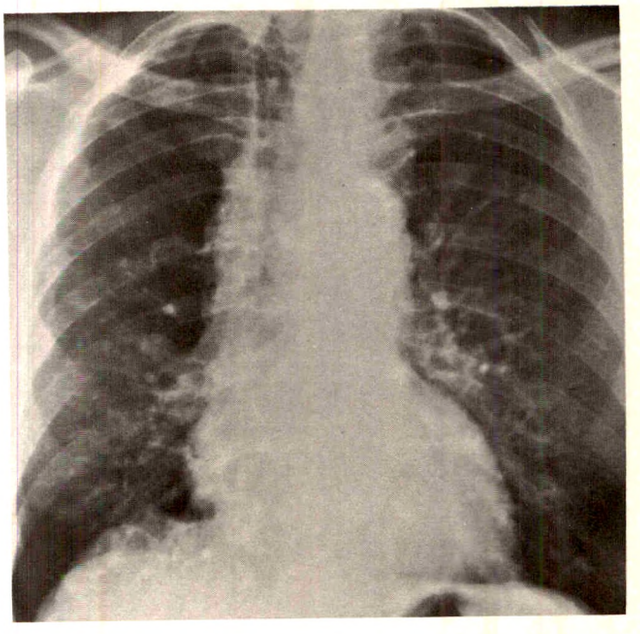

Fig. 1.—Chest radiograph showing diffuse mediastinal widening with deviation of trachea. Poorly defined density obscures tracheal air shadow above carina.

Discussion

Renal cell carcinoma is known to metastasize to the bronchial tree [1]. Carcinomas of the colon, rectum, and breast also have a relatively high incidence of endobronchial metastases. To a lesser extent this is also true of thyroid, ovarian, testicular, and pancreatic tumors as well as malignant melanoma and soft tissue sarcomas [1]. In renal cell carcinoma, average time between nephrectomy and detection of endobronchial metastases is about 4.8 years [1]. Most patients present with hemoptysis, and rarely a tumor mass may be expectorated. These lesions have been heretofore invariably located distal to the carina and are seldom visualized radiographically. Most commonly the patient presents with local atelectasis, and an erroneous diagnosis of primary bronchogenic carcinoma may be made [2]. The correct diagnosis is usually made at bronchoscopy, which demonstrates a polypoid, intraluminal mass.

Pedicles are more typically associated with benign endobronchial tumors, such as lipomas, hamartomas, and inflammatory polyps [3]. Although pedicles have been demonstrated at autopsy in some cases of metastatic endobronchial renal cell carcinoma, pedunculation has not previously been described as a radiologic feature of these lesions.

REFERENCES

1. Gerle R, Felson B: Metastatic endobronchial hypernephroma. *Chest* 44:225–232, 1963
2. Braman SS, Whitcomb ME: Endobronchial metastasis. *Arch Intern Med* 135:543–547, 1975
3. Caldarola VT, Harrison EG, Clagett OT, Schmidt HW: Benign tumors and tumorlike conditions of the trachea and bronchi. *Ann Otol Rhinol Laryngol* 73:1042–1061, 1964

Received December 29, 1977; accepted after revision April 25, 1978.
[1] Department of Radiology, University of Chicago, 950 East 59th Street, Chicago, Illinois 60637. Address reprint requests to H. MacMahon.
[2] Department of Surgery, University of Chicago, Chicago, Illinois 60637.

© 1978 American Roentgen Ray Society

0361–803X/78/1000–0713 $00.00

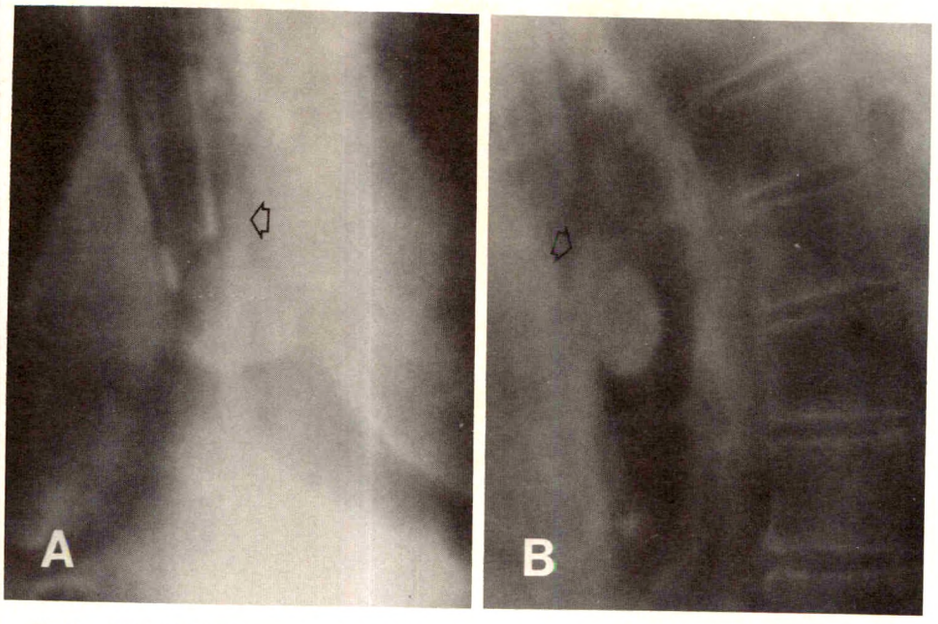

Fig. 2.—*A*, Frontal tomogram showing lobulated mass above carina. Note pedicle (*arrow*). Endotracheal tube is present. *B*, Lateral tomogram redemonstrating mass attached by pedicle (*arrow*) to anterior tracheal wall.

Nonfunctioning Islet Cell Tumors of the Pancreas: Radiographic and Ultrasonographic Appearances in Two Cases

JEROME GOLD,[1] ARTHUR T. ROSENFIELD, DIRK SOSTMAN, MORTON BURRELL, AND KENNETH J. W. TAYLOR

Two patients with nonfunctioning pancreatic islet cell tumors are presented and their ultrasonographic findings discussed. Gray scale ultrasound has proved useful in the identification and characterization of other pancreatic masses [1–8]; however, we are not aware of any published descriptions of the use of ultrasound in nonfunctioning islet cell tumors [3, 4].

Case Reports

Case 1

A 20-year-old black woman was admitted for evaluation of an enlarging asymptomatic left upper quadrant mass. She first noted the mass 18 months earlier, immediately after giving birth. Five months later, she became aware of abdominal asymmetry when lying supine. She sought medical attention at that time but no mass was felt on physical examination. On admission 13 months later, examination revealed a smooth, nontender, left upper quadrant mass.

Ultrasound studies revealed a large predominantly solid 16 cm tumor to the left of the liver (figs. 1*A* and 1*B*). No gross involvement of adjacent organs was demonstrated. Irregular cystic cavities within the mass suggested multiple necrotic areas or cysts. Excretory urography demonstrated posterior superior displacement of the left kidney. Upper gastrointestinal series demonstrated extrinsic mass impression on the greater curvature of the stomach and inferior displacement of the ligament of Treitz. Exploratory laparotomy revealed a 17 × 13 × 10 cm solid mass with squamous epithelium-lined cystic components (fig. 1*C*) which proved to be a benign islet cell tumor of the pancreas.

Case 2

A 49-year-old black female had a 7 month history of anorexia, 18 kg weight loss, and enlarging umbilical mass. Upper gastrointestinal series demonstrated anterior displacement and compression of the gastric antrum, distortion of the duodenal bulb due to an extrinsic mass, anteromedial displacement of the third and fourth portions of the duodenum, and inferior displacement of the proximal jejunum due to an extrinsic mass (fig. 2*A*). These findings were interpreted as pancreatitis. Her complaints persisted and the patient was admitted for further evaluation.

Physical examination disclosed a 10 × 12 cm movable solid mass in the periumbilical region. Abdominal ultrasound examination demonstrated an epigastric mass 13 cm in diameter (fig. 2*B*). The mass was in contact superiorly with the visceral surface of the liver and extended to the region of the inferior vena cava and aorta as far as the anterior abdominal wall. It contained low level echos with attenuation of the ultrasound beam; the findings were considered to be consistent with a homogeneous solid tumor arising from the retroperitoneum.

Excretory urography revealed minimal lateral deviation of the left ureter. Barium enema examination showed a posterior impression on the ascending and transverse colon and mural lesions suggesting invasion of the transverse colon. Celiac and superior mesenteric arteriography demonstrated a large abdominal mass with localized area of neovascularity (fig. 2*C*). At surgery, a tumor was found that arose from the pancreas and invaded the distal stomach, the entire duodenum, the transverse colon, and the mesenteric root. Histologic examination revealed a malignant pancreatic islet cell tumor.

Discussion

Islet cell tumors of the pancreas may be classified according to endocrine function. The more widely described functioning tumors produce a variety of hormones which give rise to characteristic clinical syndromes in most cases [4, 9, 10]. Nonfunctioning islet cell tumors constitute about one-third of all islet cell neoplasms [11]. Malignant islet cell tumors are usually (83%) endocrinologically inert [12]; however, 75% of all nonfunctioning tumors are said to be benign [13]. In general, there is no difference between the patient populations affected by the two types of neoplasm [14], and there is no known predilection for age, race, or sex [13].

Because nonfunctioning islet tumors do not cause specific endocrine or clinical findings, they usually reach a considerably large size prior to detection and patients often have a palpable mass [14]. Gastric, intestinal, or biliary obstruction or gastrointestinal hemorrhage due to local invasion or portal hypertension [11, 14] are directly related to mechanical effects of the mass. Islet cell tumors usually arise from the head of the pancreas [11]. Benign tumors are usually solid, but carcinomas may often contain serous or sanguinous cysts [13], probably resulting from hemorrhage and necrosis [12]. Solid islet tumors are said to be more likely to possess endocrine activity; those which display cystic or necrotic areas tend to be nonfunctioning [13]. Our cases demonstrate exceptions to both these generalizations, in that neither was located in the head of the pancreas and case 1 was benign although it contained cysts.

The findings on barium enema studies, upper gastrointestinal series, and excretory urography are those of a pancreatic mass. Arteriography is more specific and will detect most cases of islet cell tumor because of increased vascularity. A dense parenchymal stain is common in the capillary phase [11, 14] as well as dense, early venous opacification [11]. Vascular displacement is more common in nonfunctioning tumors because of their

Received February 7, 1978; accepted after revision June 2, 1978.
[1]All authors: Department of Diagnostic Radiology, Yale University School of Medicine, 333 Cedar Street, New Haven, Connecticut 06510. Address reprint requests to J. Gold.

© 1978 American Roentgen Ray Society

0361–803X/78/1000–0715 $00.00

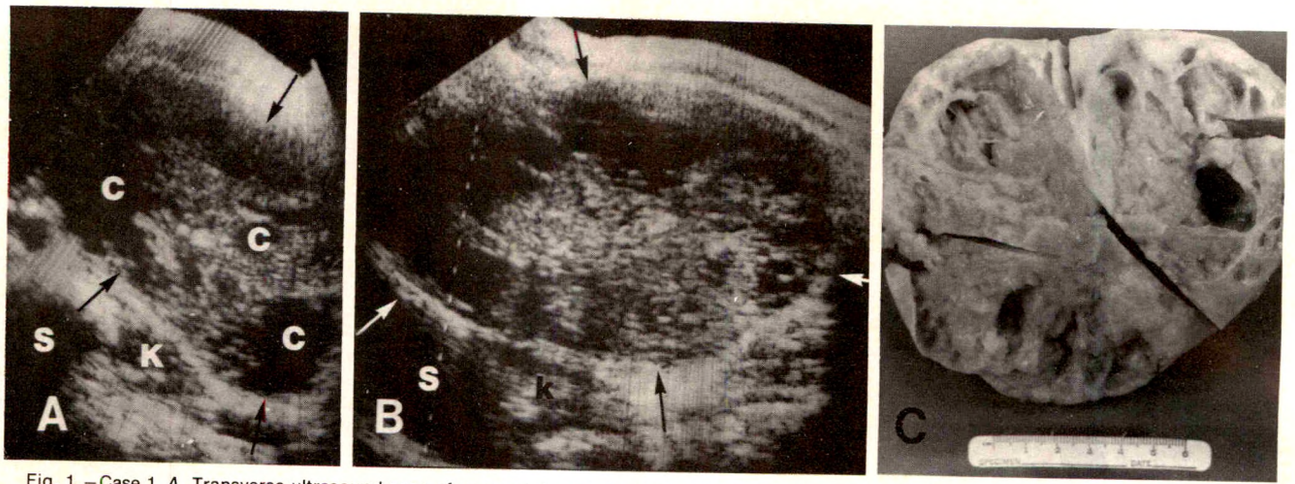

Fig. 1.—Case 1. *A*, Transverse ultrasound scan of upper abdomen demonstrating mass (*arrows*) to left of spine (S) and anterior to left kidney (K). Mass is solid with cystic (C) components. *B*, Longitudinal section through left upper quadrant also demonstrating mass (*arrows*) which is generally solid with some cystic areas. Mass is anterior to left kidney (K) and anterior and inferior to spleen (S). *C*, Section through resected tumor revealing solid mass with cystic areas which on histologic section proved to be benign nonfunctioning islet cell tumor of pancreas.

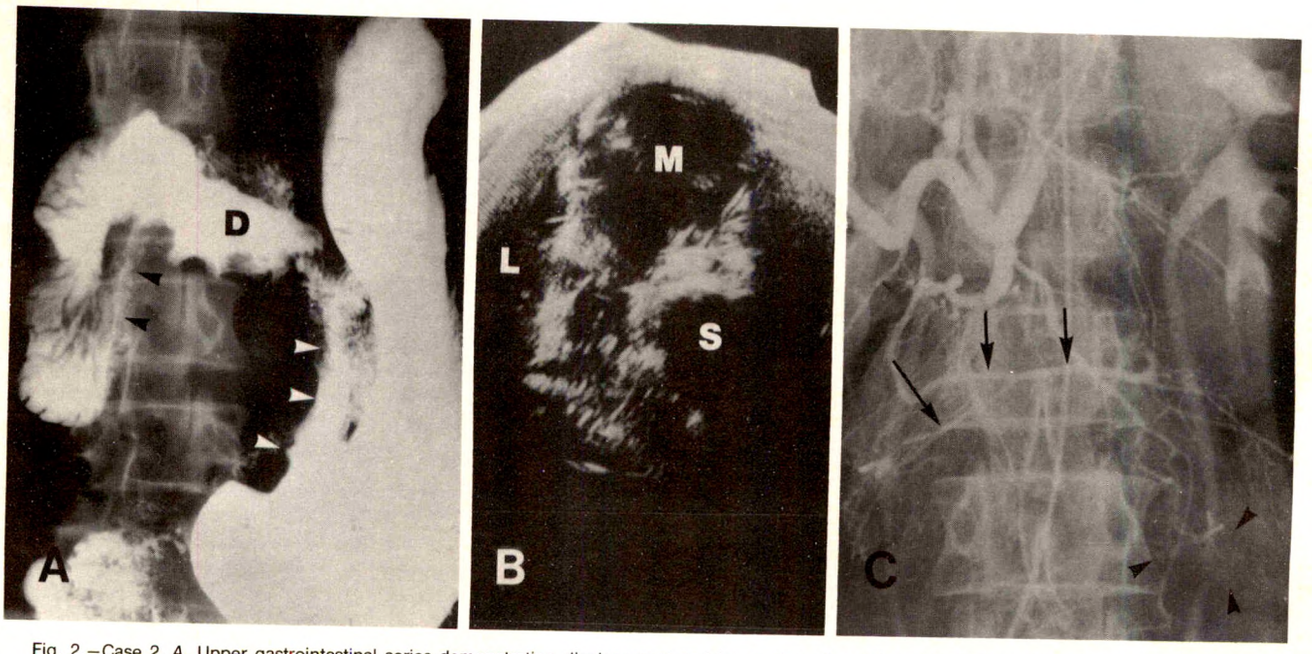

Fig. 2.—Case 2. *A*, Upper gastrointestinal series demonstrating displacement and impression of gastric antrum (*white arrowheads*). Duodenal bulb (D) is distorted due to extrinsic mass invading duodenum. There is medial displacement of third and fourth portions of duodenum (*black arrowheads*). *B*, Transverse ultrasound scan demonstrating mass (M) with low level echos which lies left of liver (L) and anterior to spine (S). *C*, Selective hepatic arteriogram demonstrating encasement of gastroepiploic artery and omental artery (*arrows*). Vessels are rigid and fixed. Area of neovascularity (*arrowheads*) is supplied by pancreatic branch of gastroduodenal artery.

larger size [14]. Neovascularity is more common in nonfunctioning islet cell tumors [14], although this may also be due to tumor size. Differentiation from cystadenoma [15] and other uncommon, highly vascular tumors is difficult [11].

Gray scale ultrasonography was performed on both of our cases of nonfunctioning islet cell tumors [16]. Case 1 had multiple cystic areas, so the differential diagnosis of these ultrasound findings would include cystadenocarcinoma, pancreatic adenocarcinoma, and necrotic lipo- or fibrosarcoma. In case 2, the low attenuation on ultrasound examination of the mass simulated a lymphoma which most commonly produces such an appearance. Vascularity seen on arteriography helps in these

differential diagnoses, since islet tumors are more vascular than pancreatic carcinoma and lymphoma.

REFERENCES

1. Ferrucci JR Jr: Radiology of the pancreas, 1976: sonography and ductography. *Radiol Clin North Am* 14:543–561, 1976
2. Gonzalez AC, Bradley EL, Clements JL Jr: Pseudocyst formation in acute pancreatitis: ultrasonic evaluation of 99 cases. *Am J Roentgenol* 127:315–317, 1976
3. Doust BD: Ultrasonic examination of the pancreas. *Radiol Clin North Am* 13:467–478, 1976
4. Kahn PC: Ultrasonic and radionuclide scanning in pancreatic disease. *Semin Nucl Med* 5:325–338, 1975
5. Walls WJ, Gonzalez G, Martin NL, Templeton AW: B-scan ultrasound evaluation of the pancreas. Advantages and accuracy compared to other techniques. *Radiology* 114:127–134, 1975
6. Walls WJ, Templeton AW: The ultrasonic demonstration of inferior vena caval compression: a guide to pancreatic head enlargement with emphasis on neoplasm. *Radiology* 123:165–167, 1977
7. Wolson AH, Walls WJ: Ultrasonic characteristics of cystadenoma of the pancreas. *Radiology* 117:203–205, 1976
8. Stuber JL, Templeton AW, Bishop K: Sonographic diagnosis of pancreatic lesions. *Am J Roentgenol* 116:406–412, 1972
9. Schein PS, DeLellis PA, Kahn CR, Gordon P, Kraft AR: Islet cell tumors: current concepts and management. *Ann Intern Med* 79:239, 1973
10. Shatney CH, Corage TB: Diagnostic and surgical aspects of insulinoma: A review of 27 cases. *Am J Surg* 127:174–179, 1974
11. Boijsen E: Inactive malignant endocrine tumors of the pancreas. *Radiologe* 15:177–182, 1975
12. Cubilla AL, Hajdu SI: Islet cell carcinoma of the pancreas. *Arch Pathol* 99:204–207, 1975
13. Strasser EJ, DeMarco SJ: Postpartum hemorrhage into a large nonfunctioning islet cell tumor of the pancreas. *Am Surg* 41:444–447, 1975
14. Baghery S, Alfidi RJ, Zelch MG: Angiography of nonfunctioning islet cell tumors of the pancreas. *Radiology* 120:57–59, 1976
15. Pressman BD, Asch T, Casarella WJ: Cystadenoma of the pancreas: a reappraisal of angiographic findings. *Am J Roentgenol* 119:115–120, 1973
16. Yeh HC, Wolf BS: Ultrasonography and computed tomography in the diagnosis of homogeneous masses. *Radiology* 123:425–428, 1977

Abnormal Peripheral Distribution of Thallium-201 due to Arteriosclerosis

EDWIN C. GLASS[1] AND GERALD L. DeNARDO[1]

A diminution of regional blood flow to any part of the body should be demonstrable after the administration of a radionuclide whose distribution is determined by regional blood flow. The distribution of ^{201}Tl in canine myocardium has been found to correlate closely with regional myocardial flow determined by microspheres or with ^{43}K [1]. Additionally, its extracardiac distribution in canine thyroid, kidney, and skeletal muscle has been found to correlate with blood flow to these organs as determined by microspheres [2]. In humans, the agent has been widely used as an effective detector of both stress-induced regional myocardial ischemia [3, 4] and myocardial infarction or scar [4–8].

The utility of ^{201}Tl in the study of blood flow to cardiac muscle is now well established. Its effectiveness for the clinical evaluation of blood flow to skeletal muscles, such as those of the extremities, has not been as thoroughly documented. This report describes an individual with clinical and angiographic evidence of stenosis of the right subclavian artery who demonstrated a corresponding abnormality on a total body image after ^{201}Tl was intravenously injected.

Case Report

A 59-year-old male construction worker was admitted with symptoms of cerebral ischemia and claudication of the legs. He had a history of heavy tobacco use, but there was no history of arm pain or symptoms suggestive of coronary artery disease. Blood pressure was 158/95 in the right arm and 190/88 in the left arm. Carotid pulses were 3+/4 bilaterally, and bilateral carotid bruits were present. The peripheral pulses in the arms were asymetrical: the right brachial pulse was 2+, the right radial pulse was 1+, and the left brachial and radial pulses were 3+. No femoral, popliteal, or pedal pulses could be palpated. There was an absence of hair below the knees.

Contrast angiography of the aortic arch and abdominal aorta demonstrated bilateral carotid stenoses and total occlusion of the abdominal aorta below the level of renal arteries. Severe stenosis of the right subclavian artery just beyond its origin from the aorta was also demonstrated (fig. 1).

Surgical therapy for both the carotid and abdominal aortic disease was considered. Because of the widespread nature of the arteriosclerosis, a preoperative assessment of the extent of disease and of surgical risk was desired, and an exercise myocardial perfusion study using ^{201}Tl was performed. During the treadmill exercise, the patient did not develop angina or electrocardiographic ST changes, but was forced by leg pain to cease exercise. An intravenous injection of 2 mCi of ^{201}Tl was given when he achieved his maximal level of treadmill exercise, which was continued for an additional minute. Myocardial images were obtained immediately after the termination of exercise and again after a 4 hr period of rest. Additionally, a postexercise total body image (fig. 2*A*) was obtained, just after the exercise myocardial imaging was completed. The two postexercise imaging procedures were completed within 40 min of injection.

The myocardial perfusion study (not shown) demonstrated exercise-induced ischemia. The total body image (fig. 2*A*) demonstrated prominent activity in the heart and abdominal viscera and a paucity of activity in the bones, genitalia, elbows, knees, and ankles. The skeletal muscles had substantial activity which made apparent an asymmetry in the appearance of the arms; the entire right arm and shoulder showed diminished activity. When compared to the legs of normal subjects, the legs appeared to have a symmetrical reduction of radioactivity (fig. 2*B*).

Discussion

A variety of radionuclide techniques has been developed to estimate blood flow in the extremities. Early methods were based on measurements of the rate of clearance from an injection site of trace amounts of ^{24}NaCl [9–11], ^{133}Xe in saline [11], or Na ^{131}I [12] and did not allow imaging of regional blood flow.

A second method for studying regional peripheral perfusion used regional intraarterial injections of labeled albumin microspheres or particles of macroaggregated albumin. Subsequent images provided a visual representation of blood flow at the capillary level [13], and results obtained from these studies have correlated well with clinical data [14, 15]. However, the particle perfusion technique has the disadvantages of intraarterial injection and/or catheterization.

There is a rational basis for anticipating that radioactive thallium may be a useful indicator of regional blood flow to skeletal muscle. Sapirstein [16] found that intravenously injected ^{42}K distributes in accordance with regional blood flow, and ^{201}Tl and ^{42}K exhibit similar patterns of uptake and retention in rat skeletal muscle [17] in addition to similarities of biochemical behavior [17, 18]. Furthermore, intravenous ^{201}Tl and intraarterial ^{99m}Tc-labeled microspheres have been found to have similar distributions in canine heart, thyroid, kidney, and skeletal muscle [2].

Assessment of regional blood flow by radioisotopic methods can be enhanced by exercise. Muscle contraction has been reported to augment the uptake of rubidium or potassium in canine skeletal muscle [19, 20], and in man it has been found that ^{201}Tl images after exercise show more activity in skeletal muscle than do images of patients injected at rest [21]. The value of exercise for increasing the sensitivity of imaging techniques in the detection of coronary artery disease is generally appre-

Received February 7, 1978; accepted after revision June 2, 1978.

[1]Department of Nuclear Medicine, University of California School of Medicine, Sacramento Medical Center, Sacramento, California 95817. Address reprint requests to G. L. DeNardo.

© 1978 American Roentgen Ray Society

0361–803X/78/1000–0718 $00.00

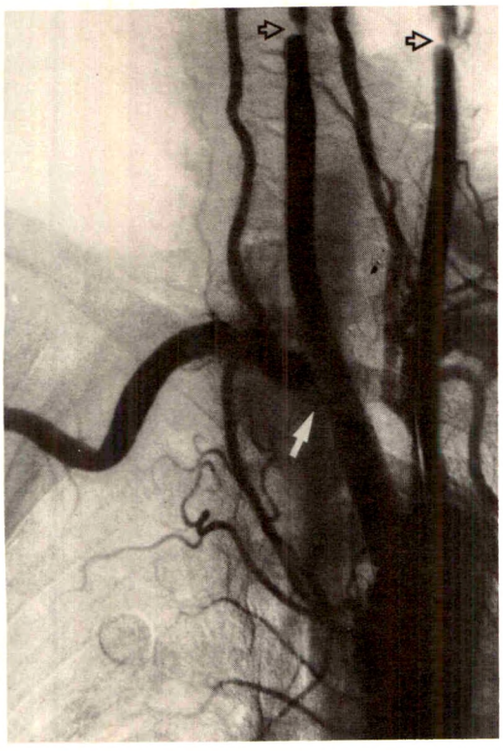

Fig. 1.—Contrast angiogram of thoracic aorta showing severe stenosis of proximal right subclavian artery (*arrow*) as well as bilateral stenoses of carotid arteries (*arrows*).

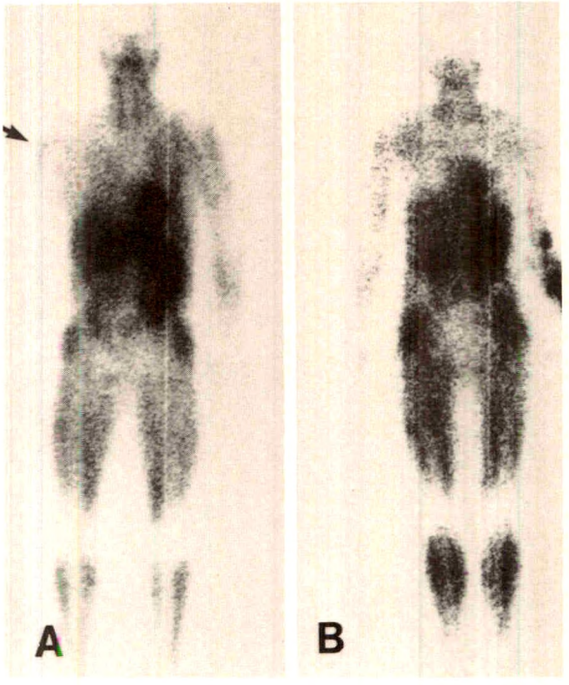

Fig. 2.—Total body ^{201}Tl exercise images of two patients, anterior views, showing prominent activity in myocardium, abdominal viscera, and skeletal muscle with paucity of activity in brain and in predominantly bony structures of extremities, such as knees, ankles, and elbows. *A*, Present case. Note asymmetry in apperance of upper extremities with decreased activity in right arm and shoulder (*arrow*). There is uniform reduction of activity in legs. *B*, Patient without clinical evidence of peripheral vascular disease. Activity in shoulders and arms is symmetrical except for activity at left side injection site.

ciated; this enhancement has also been found for perfusion studies of the legs using ^{99m}Tc-labeled albumin microspheres [14]. Thus the asymmetric distribution of ^{201}Tl in skeletal muscle in our patient may reflect the effects of exercise superimposed on his underlying vascular disease.

A recent report discussed the correlation between thallium uptake patterns in the lower extremities and clinical and angiographic data in patients with arterial insufficiency [22]. Our findings show a similar correspondence of information in an upper extremity. We believe that this information is noteworthy in that it suggests the possible use of imaging with ^{201}Tl as a noninvasive method to study peripheral regional blood flow.

REFERENCES

1. Strauss HW, Harrison K, Langan JK, Lebowitz E, Pitt B: Thallium-201 for myocardial imaging—relation of thallium-201 to regional myocardial perfusion. *Circulation* 51:641–645, 1975
2. Strauss HW, Harrison K, Pitt B: Thallium-201: non-invasive determination of the regional distribution of cardiac output. *J Nucl Med* 18:1167–1170, 1977
3. Lenaers A, Block P, van Thiel E, Lebedelle M, Becquevort P, Erbsmann F, Ermans AM: Segmental analysis of ^{201}Tl stress myocardial scintigraphy. *J Nucl Med* 18:509–516, 1977
4. Bailey IK, Griffith LSC, Rouleau J, Strauss HW, Pitt B: Thallium-201 myocardial perfusion imaging at rest and during exercise. Comparative sensitivity to electrocardiography in coronary artery disease. *Circulation* 55:79–87, 1977
5. Parkey RW, Bonte FJ, Stokely EM, Lewis SE, Graham KD, Buja LM, Willerson JT: Acute myocardial infarction imaged with ^{99m}Tc-stannous pyrophosphate and ^{201}Tl: a clinical evaluation. *J Nucl Med* 17:771–779, 1976
6. Henning H, Schelbert HR, Righetti A, Ashburn WL, O'Rourke RA: Dual myocardial imaging with technetium-99m-pyrophosphate and thallium-201 for detecting, localizing and sizing acute myocardial infarction. *Am J Cardiol* 40:147–155, 1977
7. Wackers FJT, van der Schoot JB, Sokole EB, Samson G, von Niftrik GJC, Lie KI, Durrer D, Wellens HJJ: Noninvasive visualization of acute myocardial infarction in man with thallium-201. *Br Heart J* 37:741–744, 1975
8. Wackers FJT, Sokole EB, Samson G, van der Schoot JB, Lie KI, Liem KL, Wellens HJJ: Value and limitations of thallium-201 scintigraphy in the acute phase of myocardial infarction. *N Engl J Med* 295:1–5, 1976
9. Smith BC, Quimby EH: Use of radioactive sodium as a tracer in study of peripheral vascular diseases. *Radiology* 45:335–346, 1945
10. Kety S: Measurement of regional circulation by the local clearance of radioactive sodium. *Am Heart J* 38:321–328, 1949
11. Lassen NA: Muscle blood flow in normal man and in

patients with intermittent claudication evaluated by simultaneous ^{133}Xe and ^{24}Na clearances. *J Clin Invest* 43:1805–1812, 1964
12. Coffman JD, Mannick JA: A simple objective test for arteriosclerosis obliterans. *N Engl J Med* 273:1297–1301, 1965
13. Wagner HN, Jones E, Tow DE, Langan JK: A method for the study of the peripheral circulation in man. *J Nucl Med* 6:150–154, 1965
14. Siegel ME, Giargiana FA, White RI, Friedman BH, Wagner HN: Peripheral vascular perfusion scanning. Correlation with peripheral vascular disease. *Am J Roentgenol* 125:628–633, 1975
15. Wagner HN, Rhodes BA: Radioactive tracers in diagnosis of cardiovascular disease. *Prog Cardiovasc Dis* 15:1–24, 1972
16. Sapirstein LA: Regional blood flow by fractional distribution of indicators. *Am J Physiol* 193:161–168, 1958
17. Gehring PJ, Hammond PB: The interrelationship between thallium and potassium in animals. *J Pharmacol Exp Ther* 155:187–201, 1967
18. Britten JS, Blank M: Thallium activation of the (Na^+-K^+) activated ATPase of rabbit kidney. *Biochim Biophys Acta* 159:160–166, 1968
19. Mitchell PH, Wilson J, Stanton RE: The selective absorption of potassium by animal cells. *J Gen Physiol* 4:141–148, 1922
20. Renkin EM, Hudlicka O, Sheehan RM: Influence of metabolic vasodilatation on blood-tissue diffusion in skeletal muscle. *Am J Physiol* 211:87–98, 1966
21. Wackers FJT, Busemann E, Samson G, van der Schoot JB: Atlas of ^{201}Tl myocardial scintigraphy. *Clin Nucl Med* 2:64–74, 1977
22. Christenson J, Larsson I, Svensson SE, Wrestling H: Distribution of intravenously injected thallium-201 in the legs during walking. *Eur J Nucl Med* 2:85–88, 1977

Subclavian Artery as the First Branch of the Aortic Arch: A Normal Variant in Two Patients

MARIA INES BOECHAT,[1] VINCENTE GILSANZ, AND KENNETH E. FELLOWS

Although variations in number and arrangement of the great vessels of the aortic arch are not rare, origin of a subclavian artery as the first branch of an aortic arch is extremely uncommon. Two recent books about aortic arch variants fail to mention this anomaly [1–2]. Only four cases of left aortic arch in which the origin of the right subclavian artery preceded the takeoff of a combined common carotid trunk and the left subclavian artery have been described [3]. The mirror image version of this variant, a right aortic arch with the left subclavian artery as the first branch, has not previously been reported.

Case Reports

Case 1

Cardiac catheterization in a 3-year-old boy with multiple congenital anomalies confirmed the presence of D-transposition of the great arteries, a ventricular septal defect, and pulmonic stenosis. In addition, angiocardiography demonstrated a right subclavian artery arising as the first branch of a left aortic arch, followed by a bicarotid trunk and a left subclavian artery (fig. 1).

Case 2

Cardiac catheterization and angiocardiography in a 4-year-old girl demonstrated tetralogy of Fallot with acquired pulmonary atresia and patent left Blalock and Waterston shunts. A right aortic arch was shown in which the left subclavian artery was the first brachiocephalic vessel, followed by a bicarotid trunk and a right subclavian artery (fig. 2). This unusual origin of the left subclavian artery was confirmed surgically at the time of repair of tetralogy of Fallot.

Discussion

The aortic arches of the two children described here were characterized by a subclavian artery arising as the first branch, absence of a brachiocephalic (innominate) artery, and the presence of a combined carotid trunk. This branching pattern has been described in human autopsy studies and is said to occur occasionally in elephants and marsupials [3].

In the usual left aortic arch the brachiocephalic trunk, a derivative of the ventral aorta, gives rise to both the right subclavian and right common carotid arteries. The right

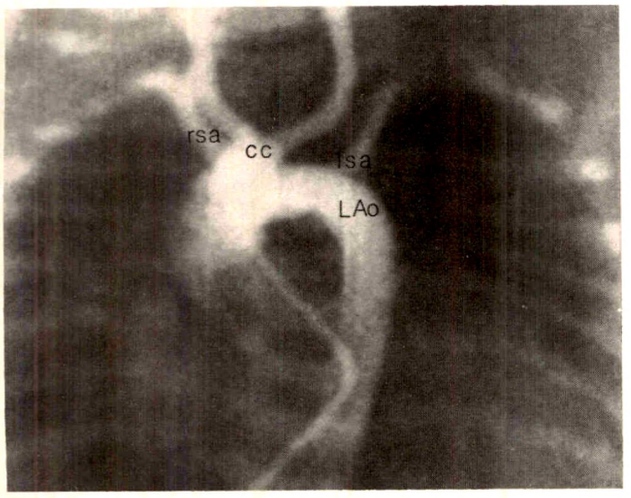

Fig. 1.—Case 1. Cine aortogram showing left aortic arch (LAo) with right subclavian artery (rsa) as first branch. cc = common carotid trunk, lsa = left subclavian artery.

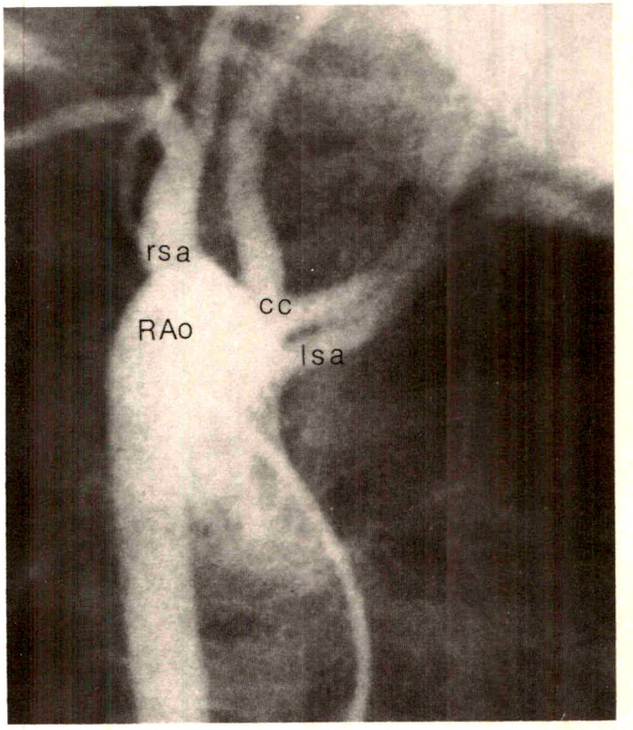

Fig. 2.—Case 2. Cine aortogram showing right aortic arch (RAo) with left subclavian artery (lsa) as first branch. cc = common carotid trunk, rsa = right subclavian artery.

Received December 15, 1977; accepted after revision June 9, 1978.

[1] All authors: Department of Radiology, Children's Hospital Medical Center and Harvard Medical School, 300 Longwood Avenue, Boston, Massachusetts 02115. Address reprint requests to K. E. Fellows.

© 1978 American Roentgen Ray Society

0361–803X/78/1000–0721 $00.00

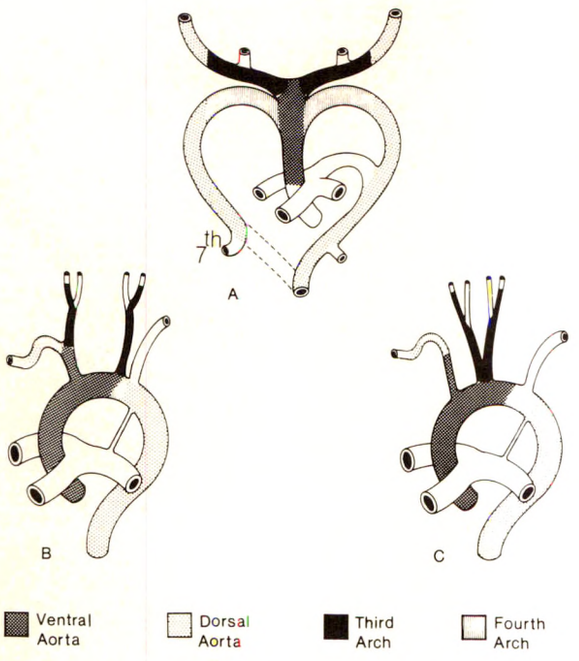

Fig. 3.—*A*, Aortic arches at 6 weeks; at this stage, third arch gives rise to carotid arteries and subclavian arteries arise distally as seventh intersegmental branches of dorsal aorta. *B*, Usual brachiocephalic vessel arrangement, left aortic arch. *C*, Variation in arterial branching, with right subclavian artery arising as first branch, followed by common carotid trunk and left subclavian artery.

subclavian artery is derived from the right fourth aortic arch, the primitive right dorsal aorta, and the seventh intersegmental artery. The right common carotid artery develops from the right third arch [4] (fig. 3, *A* and *B*). It appears that when the right and left third arches are common in their origin from the ventral aorta, the right subclavian artery may originate separately and precede the combined carotid trunk take off (fig. 3*C*), as illustrated by case 1. A similar process would explain the occurrence of this variation with a right arch, illustrated by case 2. Knowledge of this rare and normal variant of brachiocephalic vessel branching will avoid confusion when discovered at angiography, catheterization, or surgical dissection.

REFERENCES

1. Stewart T Jr, Kincaid JE: *An Atlas of Vascular Rings and Related Malformations of the Aortic Arch System*. Springfield, Ill., Thomas, 1964
2. Shufferd WH, Sybers R: *The Aortic Arch and Its Malformations*. Springfield, Ill., Thomas, 1974
3. Poynter CWH: *Arterial Anomalies Pertaining to the Aortic Arch, and the Branches Arising From Them*. Lincoln, University of Nebraska Studies, 1916
4. Hamilton WJ, Mossman HW: *Human Embryology*. Baltimore, Williams & Wilkins, 1972

Polypoid Leukemic Infiltration of the Large Bowel

MICHAEL STANLEY RABIN,[1] ANTHONY GERALD BLEDIN,[1] AND DOROTHY LEWIS[2]

Leukemic infiltration of the gastrointestinal tract, even when extensive, is usually not associated with gastrointestinal symptomatology [1, 2]. Radiologic manifestations have been documented, but reports are sparse. We describe a patient with prolymphocytic leukemia showing unusual polypoid defects on double contrast barium enema.

Case Report

A 69-year-old white female had a 2 week history of mild abdominal pain, diarrhea, and blood and mucus in her stool. Nine months previously, she had been investigated for symptoms of anemia. Bone marrow biopsy revealed prolymphocytic leukemia. White blood cell count at that time was 250,000 with 98% lymphocytes. A splenectomy was performed, and chemotherapy with prednisone and chlorambucil was initiated.

When seen at her most recent admission, her white blood cell count was 378,000. Plain films of the abdomen showed contour defects in the rectum (fig. 1*A*). A barium enema demonstrated diffuse polypoid changes in the sigmoid and rectum (fig. 1*B*). Defects were also noted scattered throughout the remaining colon, but most of these defects had the appearance of feces. At subsequent sigmoidoscopy, a grapelike polypoid appearance was noted throughout the rectum and sigmoid. A mucosal biopsy taken from the rectum showed that much of the lamina propria was occupied by a cellular infiltrate of monomorphic lymphoid cells with scanty cytoplasm. Areas of ulceration were present, and infrequent mitotic figures were observed (figs. 1*C* and 1*D*). The biopsy appearance was consistent with a mucosal leukemic deposit, and morphologically the cells were consistent with the designation of prolymphocytes.

The patient was treated with a course of cobalt therapy: 1,000 rad was administered to a diamond-shaped abdominal field extending from the xiphoid to the symphysis and skirting the costal margins and iliac crests on both sides. At the end of the 10 day course the patient was asymptomatic. She remained well for the next 4 months, then deteriorated rapidly, and died.

Discussion

The incidence of leukemic infiltration of the gastrointestinal tract varies between 13% and 62% in different series [3, 4]. All portions of the gastrointestinal tract may be involved [5–7]. The infiltration is usually asymptomatic [1, 2] but may produce clinical effects which range from nonspecific complaints such as nausea, mild abdominal pain, and diarrhea [5] to severe necrotizing enteritis, bowel hemorrhage, and perforation [6–8]. Other reported complications include intussusception, appendicitis, and protein-losing enteropathy [9, 10].

In lymphocytic leukemia, involvement is usually confined to the mucosa and submucosa [11], a feature noted in our case. In the myelogenous variety the infiltrate may be either localized or diffuse [12], and the infiltrates may form plaques, nodules, or masses [1].

Varying radiologic manifestations secondary to leukemic bowel infiltration have been described. Intraluminal defects have been noted in the esophagus [7]; the appearance in the stomach may be indistinguishable from carcinoma [5, 13]; and in the colon polypoid defects such as noted in our case have been seen [1].

The radiologic appearance in the colon and rectum in our patient was that of diffuse interlacing defects as opposed to the more well defined circular defects in familial polyposis and nodular lymphoid hyperplasia [14, 15]. On plain films they closely simulate the submucosal gas cysts seen in pneumatosis cystoides intestinalis, an entity which has been associated with leukemia [16]. Recognition of localized leukemic deposits in the bowel is of practical importance, since appropriate treatment may result in symptomatic reflief.

REFERENCES

1. Blatt LJ, Chapman I: Multiple colonic polyps of leukemic origin. *Dis Colon Rectum* 3:237–240, 1960
2. Wahl HR, Hill JH: Gastric lesions in Hodgkin's disease and leukemia. *Am J Pathol* 32:235–251, 1956
3. Kirshbaum JD, Preuss FS: Leukemia: a clinical and pathological study of 123 fatal cases in a series of 14,400 necropsies. *Arch Intern Med* 71:777–792, 1943
4. Maher JA: A statistical study of lymphoblastoma in the necropsy series at the University of Michigan Hospital. III. Organs involved. *University of Michigan Med Bull* 24:393–401, 1958
5. Dameshek W, Gunz F: *Leukemia*. New York, Grune & Stratton, 1958
6. Everett CR, Haggard ME, Levin WC: Extensive leukemic infiltration of the gastrointestinal tract during apparent remission in acute leukemia. *Blood* 22:92–98, 1963
7. Stratemeier PH: Massive esophageal hemorrhage in leukemia. *Am J Roentgenol* 129:1106–1107, 1977
8. Wolma FJ, Lynch JB: Leukemic infiltration of the colon. An unusual cause for massive melena. *Arch Surg* 78:74, 1959
9. Winton RR, Gwynn AM, Roberts JC, Thomas L: Leukemia and the bowel. *Med J Aust* 4:89, 1975
10. Cockington RA: Leukemic infiltration of the gastrointestinal tract. An unusual case of protein losing enteropathy. *Med J Aust* 4:103–105, 1975
11. Pearson B, Stasney J, Pizzolato P: Gastrointestinal involvement in lymphatic leukemia. *Arch Pathol* 35:21–28, 1943
12. Boikon WS: Leukemic changes of the gastrointestinal tract. *Arch Intern Med* 47:42–57, 1931
13. Cavins JA, Levin HS, Day HJ: Chronic myelogenous leuke-

Received March 3, 1978; accepted after revision June 20, 1978.

[1]Department of Radiology, Johannesburg Hospital, University of Witwatersrand, Johannesburg, South Africa. Address reprint requests to M. S. Rabin.

[2]Department of Pathology, South African Institute for Medical Research, Johannesburg, South Africa.

© 1978 American Roentgen Ray Society

0361–803X/78/1000–0723 $00.00

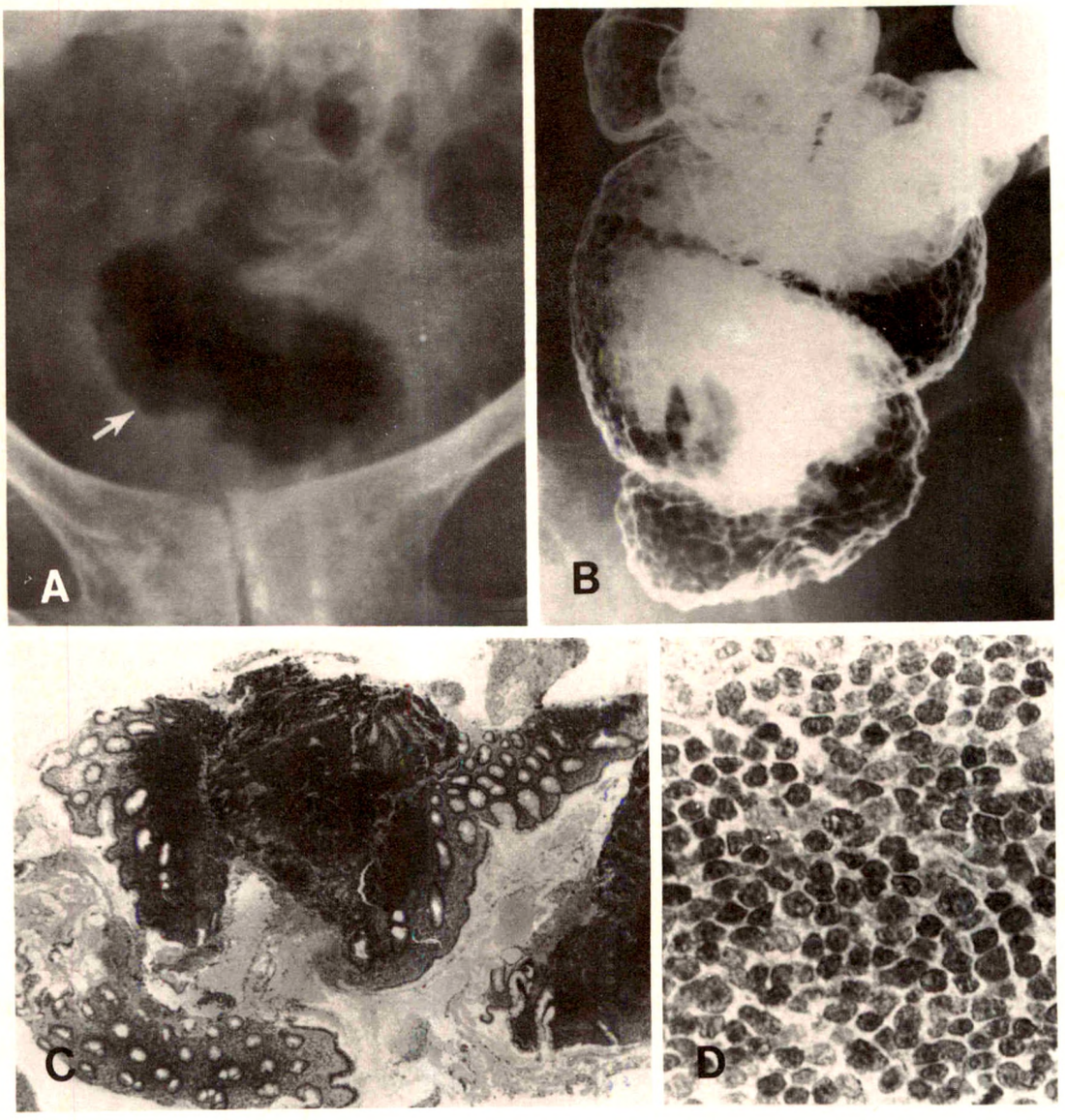

Fig. 1.—*A*, Plain abdominal film showing contour defects in rectal air shadow (*arrow*). *B*, Double contrast barium enema with diffuse polypoid defects in rectum and sigmoid producing latticelike appearance. *C*, Low power view of large bowel biopsy showing area of lamina propria occupied by dense cellular infiltrate. Note central ulceration. *D*, High power view of biopsy showing cellular infiltrate consisting of monomorphic lymphoid cells with irregularity of nuclear outline and scanty cytoplasm. Occasional mitotic figures are present.

mia with gastric infiltration. Report of a case simulating carcinoma of the stomach. *N Engl J Med* 260:1111–1114, 1959

14. Marshak RH, Lindner AE, Maklansky D: Familial Polyposis. *Am J Gastroenterol* 67:177–189, 1977
15. Lo Gerfo FW, Mueller RF: Lymphoid polyposis of the terminal ileum and colon. A source of clinical error. *Am Surg* 41:179–180, 1975
16. Jaffe N, Carlson DH, Vawter GF: Pneumatosis cystoides intestinalis in acute leukemia. *Cancer* 30:239–243, 1972

Leukemic Infiltration of the Colon

ANTHONY J. LIMBERAKIS,[1] JEFFREY A. MOSSLER,[2] LEROY ROBERTS, JR.,[1] DONALD C. JACKSON,[1] AND WILLIAM M. THOMPSON[1]

Leukemia accounts for approximately 4% of all cancer deaths [1]. Numerous gastrointestinal complications are associated with this disorder [2]. As the recent literature suggests [2–12], leukemic lesions of the gastrointestinal tract are increasing in incidence as improvement in treatment prolongs survival. We present the radiographic and pathologic findings in a case of leukemic infiltration of the colon.

Case Report

A 65-year-old white female was seen at her local hospital with a 3 week history of diarrhea. She had been in good health until 6 months earlier when she noted weight loss, fatigue, and anorexia. Diagnostic evaluation revealed pancytopenia and pseudomonas sepsis. Proctosigmoidoscopic examination and rectal biopsy showed a nonspecific colitis. A bone marrow biopsy was interpreted as normal, exploratory laparotomy was negative, and an open liver biopsy demonstrated nonspecific hepatitis. The patient was treated with antibiotics and steroids. She was referred to Duke University Hematology Clinic 2 months later for further diagnostic evaluation. Hematologic workup included bone marrow examination, which showed hypercellularity with many immature monocyloid forms and positive leukemic antigens consistent with a diagnosis of subacute myelomonocytic leukemia [13, 14]. The patient was treated with prednisone, Halotesten, transfusions, and discharged.

Later that month she developed epigastric pain and five to 10 loose bowel movements per day. She was hospitalized locally where she was treated with intravenous fluids, antibiotics, and Lomotil (diphenoxylate hydrochloride and atropine sulfate). Within 2 weeks she was acutely ill and was transferred to Duke University Medical Center. Blood pressure was 130/70 mm Hg; pulse, 100 beats/min and regular; and temperature, 38.3°C. Facial petechiae were present. The abdomen was distended and tympanitic with diminished bowel sounds. A tender, left lower quadrant mobile mass was palpable suggesting sigmoid diverticulitis. Rectal examination was normal. Hematocrit was 26; white blood cell count was 14,488 with a differential of 17 polymorphic cells, one basophil, 40 lymphocytes, and 41 monocytes. Platelet count was approximately 50,000.

Anteroposterior radiographs of the abdomen demonstrated inflammatory and/or ischemic changes in the left transverse colon (fig. 1). A water soluble contrast enema showed a severe ulcerative process extending from the right colon to the rectum (fig. 2). These findings were thought to represent a severe colitis possibly secondary to candidiasis superimposed on leukemic infiltration. Protoscopic examination revealed an edematous and friable mucosa that bled spontaneously. Rectal biopsy showed a nonspecific colitis.

On the ninth hospital day, the patient developed profuse hematochezia. Arteriography was performed to define the cause and possibly treat the lesion. Diffuse colonic bleeding was demonstrated, originating from the inferior mesenteric artery (fig. 3). The patient was started on a vasopressin infusion (0.2 U/min) to control the bleeding. During the next 40 min, she had two cardiac arrests. The second resuscitation was unsuccessful.

Autopsy revealed severe myelomonocytic leukemic infiltration of the transverse and descending colon (fig. 4*A*) extending throughout the submucosa, muscularis propria, and serosal fat with little apparent inflammatory response at sites of ulceration (fig. 4*B*). A necrotizing superficial colitis of the transverse and descending colon was noted with severe hemorrhage from the colonic mucosa. *Escherichia coli* was cultured from ascitic fluid and blood. There was leukemic infiltration of the bone marrow, spleen, and hepatic sinusoids. Death resulted from hypotension caused by acute blood loss from the denuded mucosal surface and possible endotoxins from *E. coli*.

Discussion

The most frequent gastrointestinal lesions of the leukemias are leukemic infiltrates and necrosis of the intestine, hemorrhages, anorectal ulcers, and polypoid masses. Leukemic lesions of the peritoneal cavity, esophagus, stomach, small intestine, appendix, colon, and anorectal region are commonly demonstrated at autopsy [2–12]. The most frequent sites of involvement are the stomach, ileum, and colon [2, 3, 10].

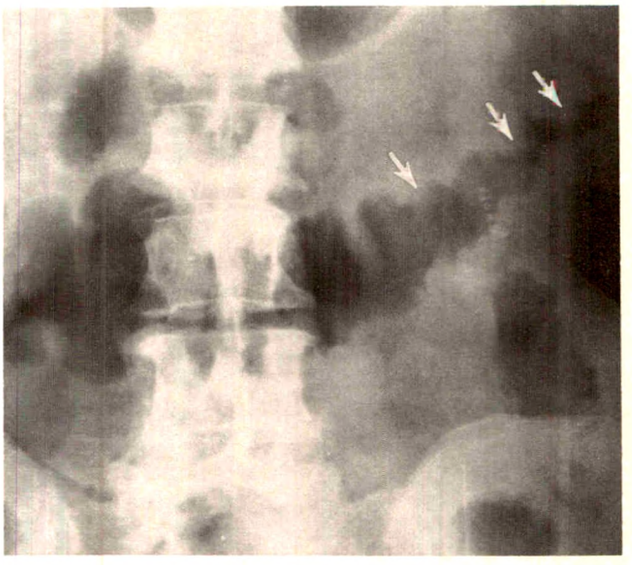

Fig. 1.—Anteroposterior film of abdomen showing thickening of bowel wall in left transverse colon (*arrows*).

Received February 16, 1978; accepted after revision June 6, 1978.
W. M. Thompson is a James Picker Foundation Scholar.
[1] Department of Radiology, Duke University Medical Center, Durham, North Carolina 27710. Address reprint requests to W. M. Thompson.
[2] Department of Pathology, Duke University Medical Center, Durham, North Carolina 27710.

© 1978 American Roentgen Ray Society

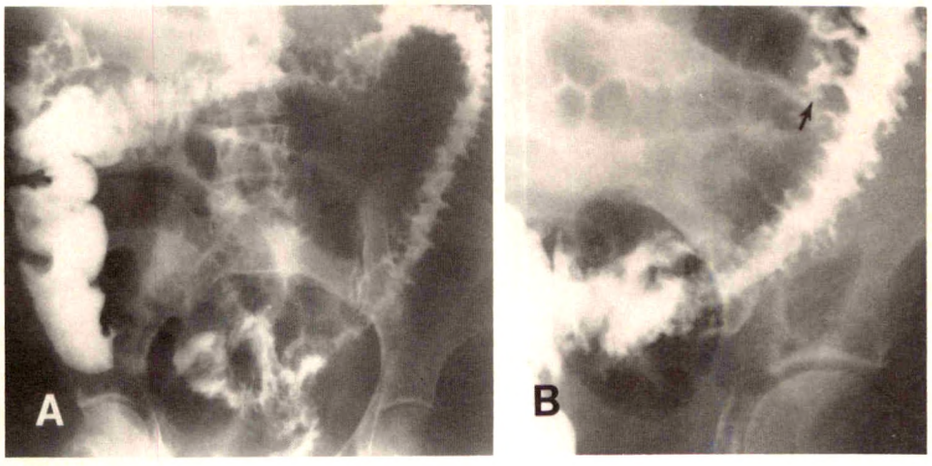

Fig. 2.—*A*, Water soluble contrast enema showing severe ulcerative process extending from right colon to rectum. *B*, Spot film of left colon showing diffuse deep ulceration with submucosal extension (*arrow*).

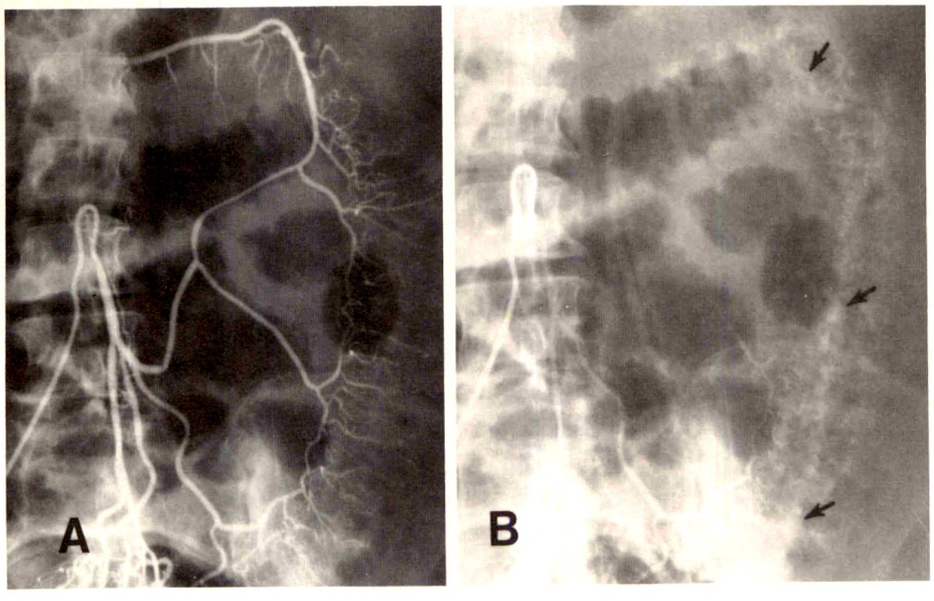

Fig. 3.—Inferior mesenteric angiogram. *A*, Arterial phase. *B*, Venous phase showing multiple diffuse bleeding sites throughout left colon (*arrows*).

Prolla and Kirsner [3] studied the autopsy reports of 148 patients with leukemia and reported that nearly all of the patients had some evidence of leukemic involvement in the gastrointestinal tract; the colon was involved in 20%. Abnormalities were subdivided into leukemic infiltration with or without necrosis, hemorrhagic necrosis, ulcers due to bacterial invasion, and mycotic complications usually secondary to candidiasis. These lesions presented as five macroscopic types: (1) plaquelike thickenings, (2) raised nodular lesions, (3) diffuse infiltrations, (4) leukemic polyposis, and (5) ulceration. The changes in part were due to replacement and enlargement of the lymphatic nodules of the intestinal wall. Ulceration of the colonic mucosa occurred because of fungal and/or bacterial overgrowth in the mucosal as well as leukemic infiltration with necrosis [3].

The plain radiographic findings in our patient of a markedly thickened bowel wall (fig. 1) suggested ischemic colitis or some form of severe enterocolitis. The clinical picture suggested a perforation due to diverticulitis. The water soluble contrast enema was important in this patient's management since it ruled out a perforation of the colon due to diverticulitis and suggested a form of severe inflammatory colitis rather than an ischemic process; the changes were rather diffuse for ischemic colitis.

Leukemic infiltration of the colon demonstrated by a contrast enema has been reported presenting with a polypoid mucosal pattern in the rectosigmoid [4], intussusception and obstruction simulating carcinoma [5], gross mucosal thickening and irregularity suggestive of a prediverticular condition [8], and localized colonic perforations [9]. The contrast enema findings in our case differ from those previously reported. The severe ulcerative process with a markedly distorted mucosal pattern

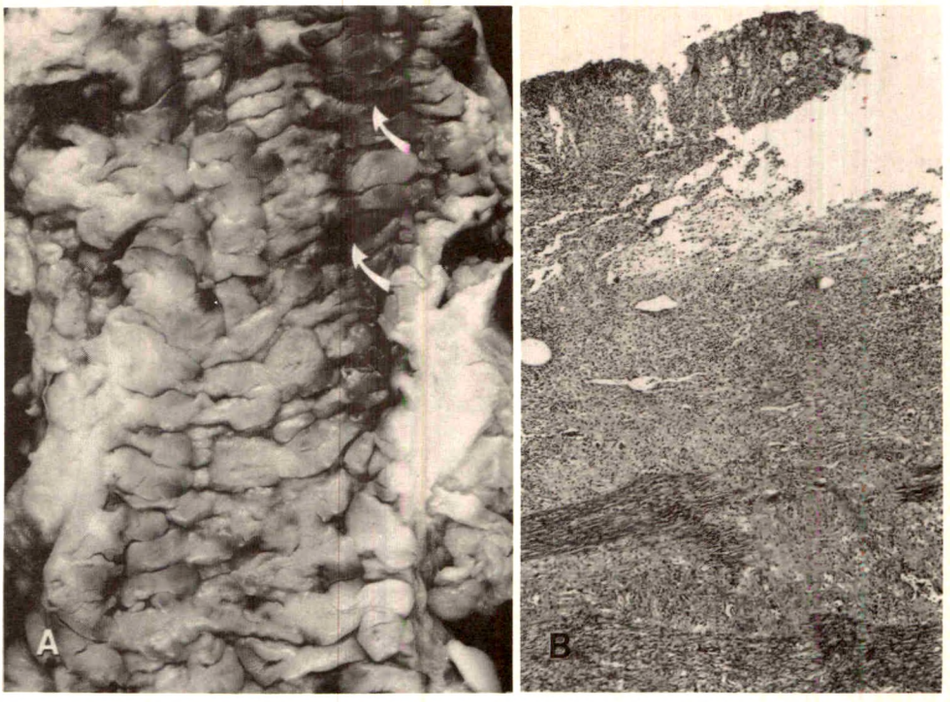

Fig. 4.—*A*, Photograph of 6 cm section of descending colon showing large areas of ulceration throughout. Note hemorrhage with submucosal involvement (*arrows*). *B*, Microscopic section through colon showing extensive submucosal leukemic infiltration with mucosal ulceration (×50).

was most prominent in the left colon and suggested a severe form of ulcerative colitis (fig. 2). This severe inflammatory picture was produced by the diffuse leukemic infiltration with necrosis.

Severe hemorrhage is a common clinical manifestation of patients with leukemia [2, 3, 9, 10], usually caused by the thrombocytopenia. In most cases the hemorrhage occurs from gastric erosions [10]. Wolma and Lynch [9] reported a patient with severe melena secondary to marked leukemic infiltration and ulceration of the colon. The contrast enema showed diffuse diverticulosis of the colon with two localized perforations. There was no evidence of diffuse ulceration as in our case. Our case is the first in which diffuse colonic bleeding in leukemia was demonstrated by angiography. However, previous reports have stressed that leukemic infiltration of the colon with diffuse ulceration and hemorrhage is a common clinical manifestation, and angiography in these patients would be expected to show diffuse sites of bleeding, whether in the stomach, small bowel, or colon [2, 3, 9, 10]. When severe gastrointestinal bleeding occurs in leukemia, angiography as a diagnosis and therapeutic modality may be worthwhile.

Cavaluzzi et al. [15] reported successful control of massive hemorrhage in chronic ulcerative colitis using the standard 0.2 U/min of vasopressin. Others have controlled colon bleeding by interventional angiography [16–19]. In most cases, the hemorrhage was due to diverticular disease, and the bleeding was controlled with the standard vasopressin regimen [16, 17]. Although standard 0.2 U/min infusion of vasopressin was used in our patient, she died before the success or failure of the therapy could be determined. We agree with Cavaluzzi et al. [15] that angiography should not be used in patients with severe hemorrhagic ulcerative fulminating colitis. Angiography was performed in our patient because we believed she might have had a segmental area of bleeding which would respond to vasopressin therapy.

A wide spectrum of radiographic and pathologic features of leukemia of the gastrointestinal tract have been reported, and of the colon in particular. Since this entity may be difficult to prove pathologically by rectal biopsy, it is important for the radiologist to be aware of the spectrum of changes in the leukemic involvement of the colon. When patients with leukemia have gastrointestinal involvement the prognosis is grave. Most of these patients expire within 2–3 weeks [2, 5–9].

REFERENCES

1. Robbins SL: Blood and bone marrow. Disorders of white cells, in *Pathologic Basis of Disease*, edited by Robbins SL, Philadelphia, Saunders, 1971, pp 728–739
2. Cornes JS, Jones TJ: Leukaemic lesions of the gastrointestinal tract. *J Clin Pathol* 15:305–313, 1962
3. Prolla JC, Kirsner JB: The gastrointestinal lesions and complications of the leukemias. *Ann Intern Med* 61:1084–1103, 1964
4. Gildenhorn HL, Springer EB, Amromin GD: Necrotizing enteropathy: roentgenography features. *Am J Roentgenol* 88:942–952, 1962
5. Javett SL, Tefft M, Drummond CP, Levitan R: Leukemic infiltration of the sigmoid colon. Report of a case simulating carcinoma with obstruction. *Am J Dig Dis* 8:299–304, 1963
6. Siegal DL, Bernstein WC: Gastrocomplications of the leukemias. *Dis Colon Rectum* 8:377–381, 1965
7. Blank WA: Anorectal complications in leukemia. *Am J Surg*

90:738–741, 1955
8. Mead CH: Chronic lymphatic leukemia involving the gastrointestinal tract. *Radiology* 21:351–365, 1933
9. Wolma FJ Jr, Lynch JB: Leukemic infiltration of colon, an unusual cause for massive melena. *Arch Surg* 78:71–74, 1959
10. Cornes JS, Jones TG, Fisher GB: Gastrointestinal ulceration and massive hemorrhage in patients with leukemia, multiple myeloma, and malignant tumors of lymphoid tissue. *Gastroenterology* 41:337–344, 1961
11. Aronson AS, Garwicz S, Landberg T, Nelson O: Manifest intestinal involvement during bone marrow remission in a case of acute lymphoblastic leukemia. *Acta Paediatr Scand* 64:369–372, 1975
12. Amromin GD, Solomon RD: Necrotizing enteropathy. A complication of treated leukemia or lymphoma patients. *JAMA* 182:23–29, 1962
13. Saarni MI, Linman JW: Myelomonocytic leukemia: disorderly proliferation of all marrow cells. *Cancer* 27:1221–1230, 1971
14. Bennett JM: Myelomonocytic leukemias: a historical review and perspectives. *Cancer* 27:1218–1220, 1971
15. Calvaluzzi JA, Kaufman SL, White RJ Jr: Vasopressin control of massive hemorrhage in chronic ulcerative colitis. *Am J Roentgenol* 127:672–675, 1976
16. Casarella WJ, Galloway SJ, Taxin RN, Follett DA, Pollock EJ, Segman WB: Lower gastrointestinal tract hemorrhage: new concepts based on arteriography. *Am J Roentgenol* 121:357–368, 1974
17. Baum S, Anthanasoulis C, Waltman A: Angiographic diagnosis and control of large bowel bleeding. *Dis Colon Rectum* 17:419–453, 1974
18. Goldberger LE, Bookstein JJ: Transcatheter embolization for treatment of diverticular hemorrhage. *Radiology* 122:613–617, 1977
19. Naderi MJ, Bookstein JJ: Rectal bleeding secondary to fecal disimpaction: angiographic diagnosis and treatment. *Radiology* 126:387–389, 1978

Fracture of the Occipital Condyle

NICOLE BOLENDER,[1] LAURENCE D. CROMWELL,[1] AND LYLE WENDLING[2]

Fractures of the occipital condyle occur very rarely and were first described by Bell [1] in 1817 in a young patient who had head trauma. The only other reported cases were by Ahlgren and coworkers in 1962 [2] and 1964 [3], and Kissinger in 1900 [4]. We report two additional cases with radiographic manifestations.

Case Reports

Case 1

A 23-year-old male was involved in a motor vehicle accident 12 hr before he was admitted in acute respiratory distress. He was semicomatose and uncooperative. Skull radiography and cervical spine films were normal. After a tracheostomy was performed, the patient was placed on a ventilator. He gradually improved, but when the tracheostomy and nasogastric tubes were removed and an attempt was made to feed him orally, he had difficulty swallowing. Neurologic evaluation revealed atrophy of the right side of the tongue and an absent gag reflex. The patient had a IX, X, XI, and XII cranial nerve palsy on the right. Further workup included computed tomography (CT) which showed a very prominent right jugular tubercle (fig. 1*A*). Anteroposterior linear tomography of the craniovertebral junction (fig. 1*B*) demonstrated avulsion of the right occipital condyle and superior displacement of this bony fragment. A gastrostomy was performed, and at the time of discharge, the patient was alert and in no distress except for being unable to control secretions.

Case 2

A 22-year-old white male was involved in a motor vehicle accident 8 hr before admission. He did not respond appropriately to verbal commands. Anteroposterior and lateral cervical spine films obtained in the emergency room were normal, as were the skull films. The patient developed bilateral VI nerve palsies soon after admission. Over the next several days his level of consciousness improved. However, he then developed a right central VII nerve deficit. Cerebral angiography (fig. 2) demonstrated posterior displacement of the basilar artery from the clivus by an avascular extraaxial mass. Midline angiotomography revealed posterior displacement of the fourth ventricle and the anterior pontomesencephalic vein. In addition, blurred under subtraction technique [5] revealed a bony fragment which was neither part of the dens nor the inferior portion of the clivus (fig. 2*B*).

Anteroposterior hypocycloidal tomography of the craniocervical junction demonstrated medial and anterior displacement of a fragment from the right occipital condyle. The patient was placed on Decadron; however, he developed a IX and X cranial nerve palsy on the right manifested by choking and inability to swallow. A nasogastric tube had to be placed intermittently. The cranial nerve palsies improved substantially; on discharge 16 days after admission, the patient was able to feed himself.

Discussion

Fractures of the occipital condyle are extremely rare; we found only four reported cases [1–4]. However, this entity may be more prevalent than appreciated since these fractures are difficult to diagnose by conventional means. In the two patients we report, both the plain skull films and the cervical spine films were normal, even in retrospect. However, if it is clinically suspected, the diagnosis of fracture of the occipital condyle can be made rather easily with tomography. Although tomography is the procedure of choice, in the clinical setting of progressive cranial nerve dysfunction other examinations such as CT and angiography may be performed first.

Both of our patients sustained head trauma; in case 2, on careful questioning, it was apparent that the patient had been ejected from the automobile headfirst through the windshield. Both patients developed lower cranial nerve palsies. In the one patient on whom CT was performed, there were no intraaxial abnormalities, such as brainstem hemorrhage, to explain the progressive cranial nerve dysfunction. In both cases the occipital condyle was displaced.

With a fracture of the occipital condyle there is great potential for disruption of the hypoglossal canal which is located at the base of the condyle (fig. 3). In addition, the sides of the condylar portions form the jugular process which contains the jugular notch. This notch with the corresponding portion from the temporal bone forms the jugular foramen, which transmits the internal jugular vein and the IX, X, and XI cranial nerves (fig. 3). Thus it is not difficult to imagine how a through-and-through fracture in the region of the condyle can produce lower cranial nerve dysfunction.

We are unable to draw any conclusions on the basis of these two cases regarding the necessity for surgical treatment. Our experience is limited and there is no other information in the literature. Both of our patients recovered spontaneously. However, the diagnosis of an extradural hematoma anterior to the brainstem in case 2 is significant if a surgical approach were contemplated. This extradural collection is more easily approached than a subdural collection.

Why these patients sustained a fracture of the occipital condyle rather than the more common Jefferson fracture is unclear. However, it is important to make the diagnosis of a fracture of this type in order to institute appropriate steroid therapy and to avoid prolonged immobilization.

Received December 6, 1977; accepted after revision June 2, 1978.
[1]Department of Radiology, University of Washington School of Medicine, Seattle, Washington 98195. Address reprint requests to L. D. Cromwell.
[2]Department of Radiology, Sacred Heart Medical Center, Spokane, Washington 99204.

© 1978 American Roentgen Ray Society

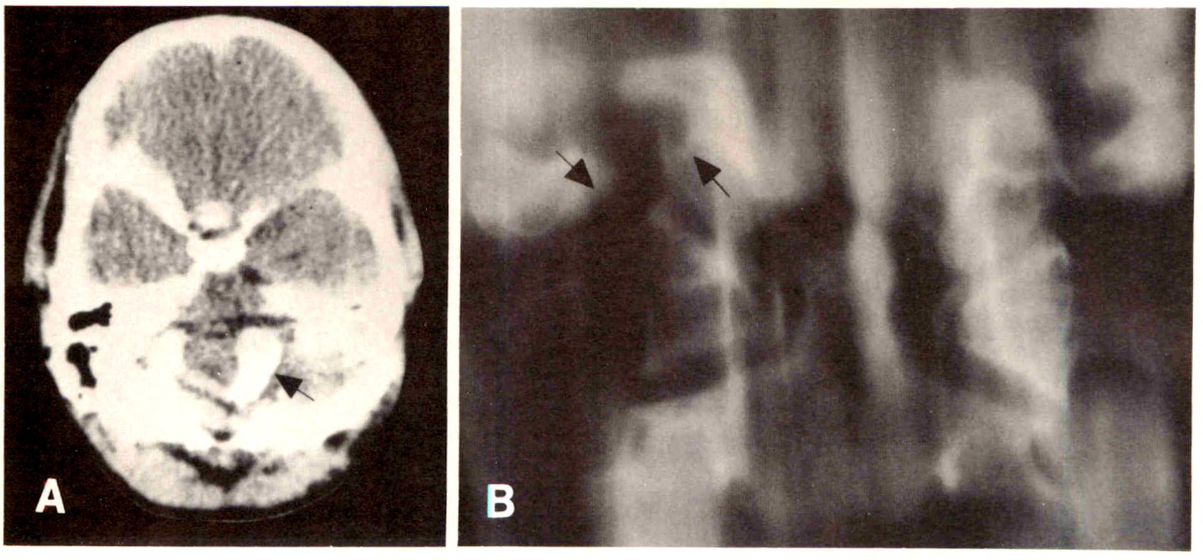

Fig. 1.—Case 1. *A*, CT scan showing right jugular tubercle (*arrow*) displaced medially and superiorly. Asymmetric positioning of head within scanner should have resulted in decreased prominence of right condyle, similar to petrous ridge and sphenoid wing. *B*, Anteroposterior linear tomogram demonstrating fracture dislocation of right occipital condyle (*arrows*).

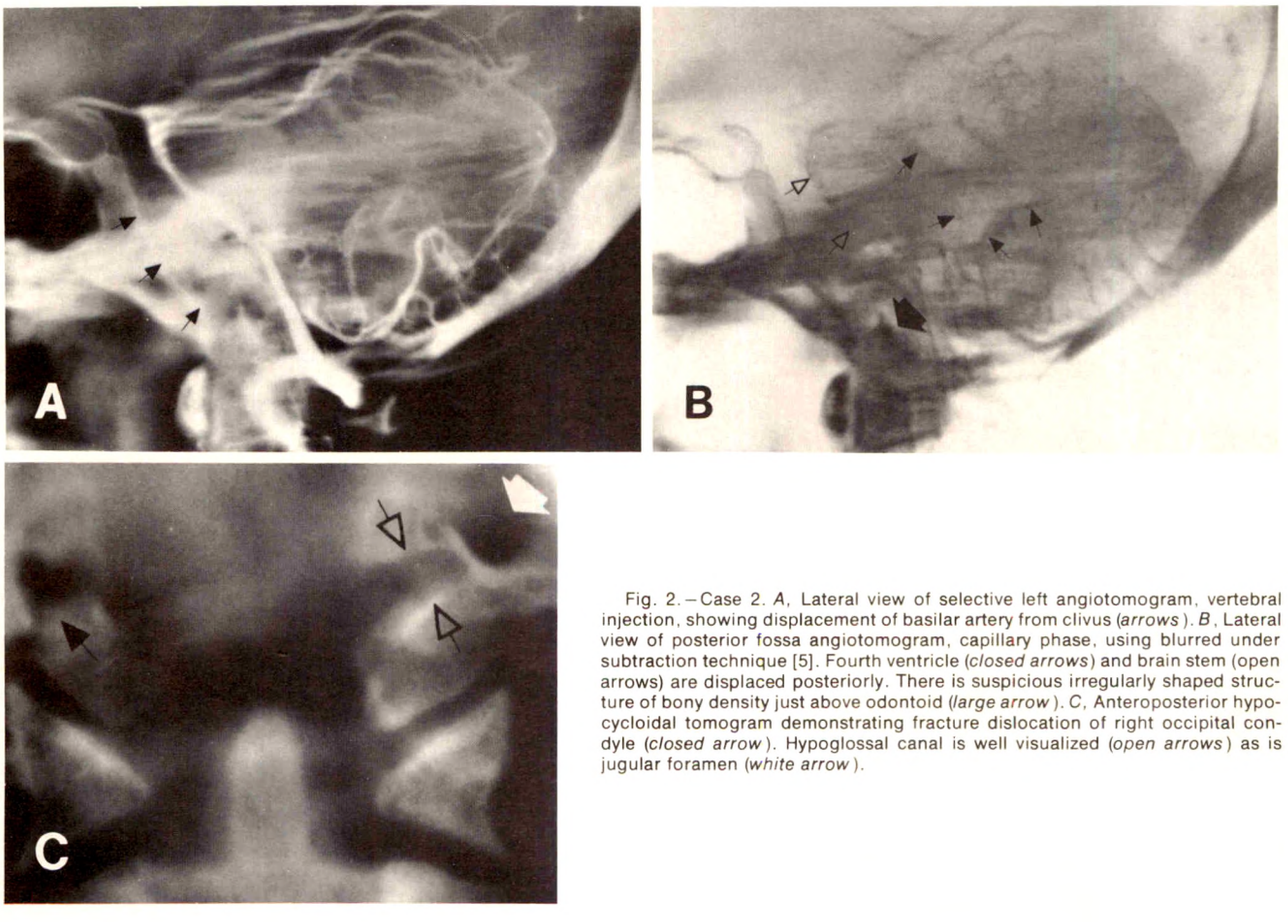

Fig. 2.—Case 2. *A*, Lateral view of selective left angiotomogram, vertebral injection, showing displacement of basilar artery from clivus (*arrows*). *B*, Lateral view of posterior fossa angiotomogram, capillary phase, using blurred under subtraction technique [5]. Fourth ventricle (*closed arrows*) and brain stem (open arrows) are displaced posteriorly. There is suspicious irregularly shaped structure of bony density just above odontoid (*large arrow*). *C*, Anteroposterior hypocycloidal tomogram demonstrating fracture dislocation of right occipital condyle (*closed arrow*). Hypoglossal canal is well visualized (*open arrows*) as is jugular foramen (*white arrow*).

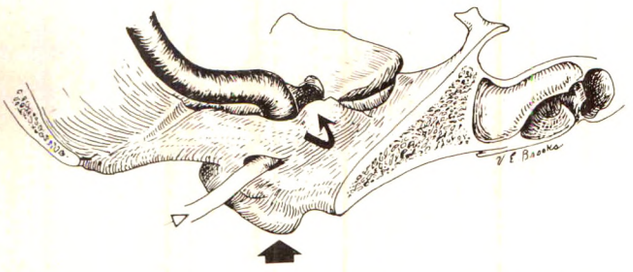

Fig. 3.—Three-quarters view of midsagittal section of dry skull demonstrating relation between occipital condyle (*large arrow*), XII cranial nerve neurovascular bundle (*open arrow*), and jugular tubercle (*curved arrow*).

REFERENCES

1. Bell C: Surgical observations. *Middlesex Hospital* 4:469, 1817
2. Ahlgren P, Mygind T: Eine selten vorkommende Fractura Basis Cranii. *Fortschr Geb Roentgenstr Nuklearmed* 97:388–391, 1962
3. Ahlgren P, Dahlerup JV: Fractura condylus occipitalis. *Fortschr Geb Roentgenstr Nuklearmed* 101:202–204, 1964
4. Kissinger P: Luxationsfraktur im atlantooccip tal Gelenke. *Zentralbl Chirurgie* 37:933–934, 1900
5. Kattan KR, Caplan MC, Felson B: A method for improving roentgenographic illustrations for publications—blurred under subtraction (B.U.S.). *Med Radiogr Photogr* 49:21–22, 1973

Traction Device for Use with Polytome Table

Z. L. DEEB,[1] T. A. MARTIN, AND C. W. KERBER

Patients with suspected cervical spine injuries pose difficult problems for the radiology department. They frequently have traction or other stabilizing apparatus in place, and their injury must not be compounded by head movement during filming. The examination of these patients is complex and lengthy, requiring both patient and table position changes. Plain films, tomography, or even gas myelography may be necessary [1]. We have devised a simple pulley device which allows us to maintain constant traction during performance of these examinations.

Technique

We have previously used a simple portable device [2] for maintaining traction in patients with cervical spine injuries. However, this required frequent adjustment when used with movable and tilting tables such as the Polytome (Phillps Medical Systems, Inc., Shelton, Conn.). We present a solution to this problem. An inexpensive (about $40) and easily constructed pulley assembly was made from a steel bar (fig. 1). This assembly is attached to perpendicular bars that slide into the rails of the Polytome tabletop. The height of the pulley apparatus is adjusted on the perpendicular bars when the patient is placed on the table and is then maintained in that position throughout the examination. There is no need to reposition the traction device when the tabletop is tilted or for any other tabletop adjustments (fig. 2). Although this device was made specifically for the Polytome table, a similar and inexpensive device can be made to fit any other table.

In view of its low cost and utility, we feel this device should be an available accessory for every department using tomography and/or gas myelography for evaluation of patients with cervical trauma.

REFERENCES

1. Rossier AB, Berneuy J, Rosenbaum AE, Hachen J: The value of gas myelography in the early management of acute cervical cord injuries. *J Neurosurg* 42:330–337, 1975
2. Deeb ZL, Drayer BP, Rosenbaum AE: A simple traction device for use in the radiology department. *Radiology* 125:826, 1977

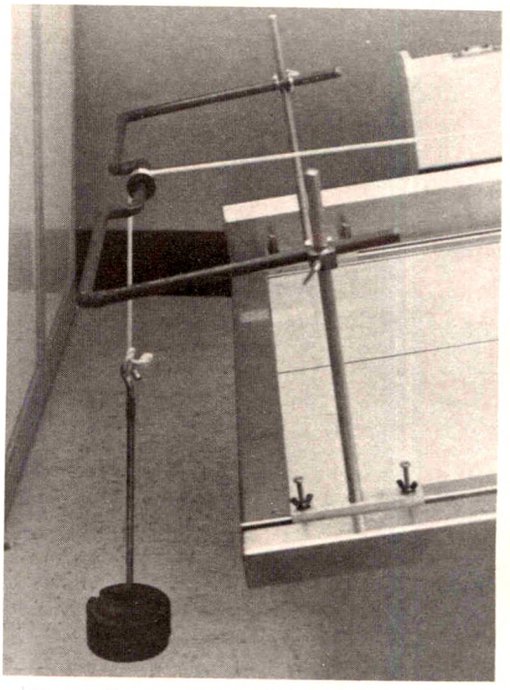

Fig. 2.—Traction device attached to Polytome table with table angulated.

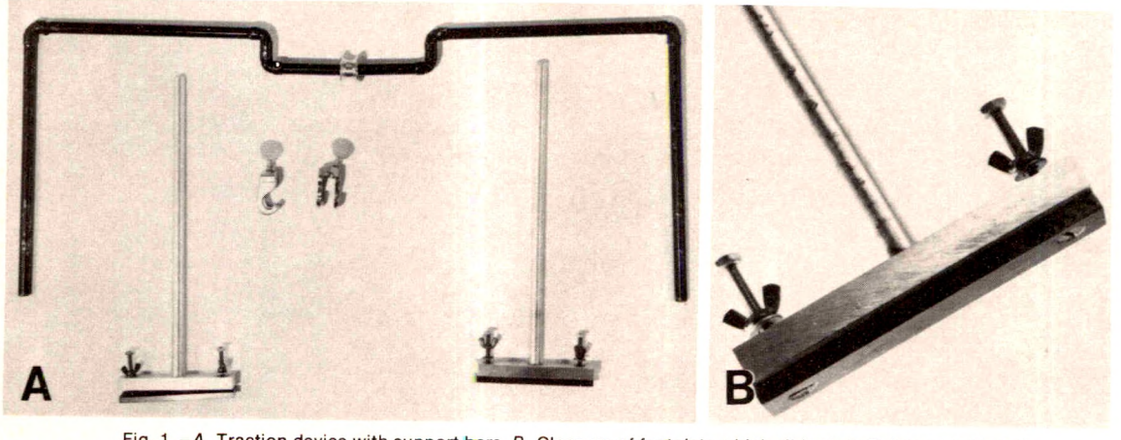

Fig. 1.—*A*, Traction device with support bars. *B*, Close-up of footplate which slides into Polytome table rails.

Received February 21, 1978; accepted after revision June 23, 1978.

[1]All authors: Department of Radiology, University of Pittsburgh School of Medicine, Presbyterian-University Hospital, 230 Lothrop Street, Pittsburgh, Pennsylvania 15261. Address reprint requests to Z. L. Deeb.

© 1978 American Roentgen Ray Society

0361-803X/78/1000-0732 $00.00

Editorial

On Behalf of Translumbar Aortography

Translumbar aortography is a simple, rapid, safe, accurate method for evaluating aortofemoral occlusive disease. Nonetheless, it is a method generally shunned by angiographers and, in my opinion, for reasons that are not valid.

A commonly heard criticism of the translumbar aortography is that it is unsafe. In fact, the number of significant complications with the study, if patients with hypertension and coagulation defects are avoided and the needle is positioned under fluoroscopic control, is about the same as with the transfemoral approach [1]. Other reasons given are that the resulting examinations are of inferior quality and that the needle is not as versatile as the catheter. It is true that translumbar aortography performed by nonradiologists may be of inferior quality, but these are not to be compared with studies produced by angiographers using high dose, controlled injections, oblique or lateral views, and pharmacoangiographic enhancement. The procedure is admittedly not as versatile as a transfemoral approach, but very little versatility is needed if the sole object of the examination is to display the pathologic anatomy of aortofemoral occlusive disease.

I believe the most important reason that radiologists do not use translumbar aortography is historical. A general wave of derision was heaped upon the procedure in the middle 1960s by radiologists attempting to sell the transfemoral approach as a superior method in order to wrest control of angiographic procedures from the surgeons. We so convinced ourselves, that in many institutions today a patient without femoral pulses is approached from the axillary artery rather than by the much simpler and safer translumbar approach.

Translumbar aortography has undergone significant improvement by angiographers who have used it over the past 10 years [2]. The use of a closed-end needle with side holes has significantly decreased the incidence of subintimal dissection of the contrast medium. Many angiographers now use a controlled, mechanized injection of 70–80 ml of contrast medium over 7–10 sec, combined with pharmacoangiography. Although vasodilatory drugs can be used to improve visualization of the tibial arteries, I prefer to inject the contrast medium during the reactive hyperemia that occurs after 7 min of occlusion of the leg circulation by special thigh pressure cuffs. The examinations obtained in this manner are comparable to those achieved with a transfemoral catheter, and visualization of the arterial tree is consistently good through the ankle, even in patients with severe proximal disease. In patients with severe small vessel disease, no technique results in good visualization of the arteries in the distal leg.

Although ultrasound and CT scanning are having a predictable impact on the number of general diagnostic angiographic procedures, these noninvasive techniques have had no impact on the demand for aortofemoral studies. In fact, the number of peripheral vascular studies is increasing in many medical centers, in absolute numbers as well as relative to other angiograms. Since translumbar aortography can be done in less than half the time needed for transfemoral aortography, the time saved becomes an important factor.

Translumbar aortography is, in my opinion, the preferred angiographic approach for lower extremity occlusive arterial disease. Every radiologist doing angiographic procedures should be able to do it and should use it in its proper place alongside the transfemoral and axillary approaches. Try it; you'll like it!

Stewart R. Reuter
University of California
Davis and San Francisco, California 94143

REFERENCES

1. Haut G, Amplatz L: Complication rates of transfemoral and transaortic catheterization. *Surgery* 63:594–596, 1968
2. Thomas ML, Fletcher WL: Large volume translumbar aortography in aortic occlusion. *Am J Roentgenol* 109:541–548, 1970

From Earlier Pages . . .

Although much information about the damaging effects of x-rays was available early in the development of radiology, some workers were severely injured by exposure, while others lived long and productive lives without evidence of deleterious effects from the rays. Still others had only mild changes which did not incapacitate them. The reasons for this variation are not clear. Perhaps personality differences played a part.

Some of the earliest warnings about the dangers of exposure, made in 1896 [1], display lack of unanimity of opinion as to the exact cause of injury. The damaging influence was variously ascribed to ozone, scatter of particles of platinum from the target, electrical effects, or even heat. On the other hand, the biologic effects were also known early, as accounts of epilation by Freund (cited in [1]) and dermatitis indicate. It was also known very early that the effects were cumulative. Epilation without the development of dermatitis was carried out as a planned treatment by Daniel in 1896 (cited in [1]), the year of Roentgen's announcement.

In his presidential address to the Roentgen Society (London) on November 5, 1897 [2], Silvanus Thompson said, "Soon after the invention of the focus tubes had furnished powerful sources of Roentgen rays, it was noticed that exposure to them frequently resulted in severe local inflammation of the skin, accompanied in some cases with destruction. . . ." In 1898 the Roentgen Society went so far as to select a committee to investigate the nature and cause of x-ray injury. In April 1896 in Boston, Elihu Thomson (cited in [3]) irradiated his own finger while a portion of it was protected, to demonstrate that dermatitis developed only in the irradiated part. Thus, knowledge of the damaging effects and even the time intervals involved was readily and widely available.

Information about protection was likewise no problem. Within a few months after Roentgen's discovery, it was known that lead was the most efficient barrier for the new invisible rays, and Roentgen's second communication describes the use of transparent lead glass. As early as 1898, William Rollins of Boston (cited in [3]) used a lead box as a container for the x-ray tube, and he also used a primitive type of collimation.

The germ of the idea of documentation of personal exposure came early: at the eighth annual meeting of the American Roentgen Ray Society in 1907, Rome Wagner, a manufacturer of tubes, reported [4], "I concluded that I would not take chances with any ray that would affect a photographic plate, so I carry one in my pocket, and in the evening, after the day's work, I develop this film to see whether I have been exposed to the ray. Once in a while I find that I have, and then I try to figure out where I have been exposed. Now I often go for a week without any exposure. . . ." In 1903 William Rollins (cited in [3]) stated that his freedom from injury was the result of heeding the advice which had been given in papers he had read earlier.

Despite this wealth of information, exhortation, and example, we read of the serious injuries of the early workers. The first recorded death was that of Edison's assistant, Clarence M. Dally, in 1904 [5]. Percy Brown, in his book *American Martyrs to Science through the Roentgen Rays* [3], records a litany of sorrow, and describes numberless unsuccessful skin grafts and gradual dismemberment. But there were also many who made investigations with the new rays their life's work and who were apparently unscathed: William J. Morton (1845–1920), considered by some the first American radiologist; Gösta Forssell (1876–1950), Swedish pioneer; William S. Newcomet (1872–1960), director of the x-ray department of Philadelphia's Presbyterian Hospital for 50 years; Francis H. Williams (1852–1936), considered by others the first American radiologist; William Rollins (1852–1929), Boston dental radiologist and x-ray engineer. All these men worked with the new discovery, and safely, in contrast to the martyrs whom Brown describes.

Why this vast difference? Interest and work habits may have played a part. Some pioneers were tinkerers with the equipment, others were intellectuals, less interested in the process than in the product, but no one in the early days could work entirely separated from x-ray tubes because of the importance of fluoroscopy at that time.

Could this wide variation in degree of personal damage have expressed more? Could it be a reflection of the personality of the individual? Some people reveal a sense of bravado or machismo by their actions, apparently believing they are relatively immune to risks that are serious to others, that they are braver, stronger. Others, more cautious, perhaps less flamboyant, avoid risks. Impatient, vigorous, enthusiastic individuals might have been deceived by radiation at a distance in both space and time and would pay less heed to warnings from others. Little material is available for a concrete psychological study of these pioneers, but this relation between personality and the disregard for risk is consistent (C. G. Browne, Wayne State Univ., personal communication). A somewhat similar situation exists today in the relation between personality and the putative risk of smoking, and here there is similar action at a distance. Smokers have been described as more extroverted, impulsive, and seeking to be thought of as "tough" [6–8]; and smoking is associated with high risk-taking tendencies [9].

During my training in the 1940s such an active, impatient, self-confident radiologist eschewed lead gloves even at that enlightened period, considering them an interference and a bother. Others could wear lead gloves: he would stay out of the beam; and he used flimsy, single layer cotton gloves for his fluoroscopy "to protect from the scatter." Similar attitudes must have prevailed 80 years ago. With advancing precision of knowledge, and with the horror of the existing examples as a deterrent, fewer and fewer radiologists neglected

protection, and those later users who did suffer injury, such as dentists and dermatologists, more often did so in ignorance.*

This excursion into the epidemiology of radiation injury among the pioneers is in no way a detraction from the contributions of those who suffered. But it was not solely through ignorance that they were martyred. Even Percy Brown [3] suggests apathy or disdain on their part. Attributing to them enthusiasm, a missionary approach, some showmanship, and much impatience would be more generous. It seems possible some combination of personality traits may have led to the distribution of damage among these pioneers. The type of physician who could enter such an exciting, entirely new and untried field frequently had the personality which would lead him into danger. Today radiology is still an exciting field and attracts the same type of person, but fortunately the lessons of the pioneers have been well learned.

* Last month, when I demurred at holding an intraoral film with my index finger, my "brave, impatient, vigorous, young, enthusiastic, self-confident" dentist said he would hold it himself. My subsequent lecture to him may not have breached the personality barrier.

E. Frederick Lang
Harper Hospital
Detroit, Michigan 48201

REFERENCES

1. Hedley WS: Roentgen rays. A survey, present and retrospective. *Arch Roentgen Ray* 2:6–12, 1897
2. Thompson S: Presidential address. *Arch Roentgen Ray* 2:23–31, 1897
3. Brown P: *American Martyrs to Science through the Roentgen Rays*. Springfield, Ill., Thomas, 1936
4. *Transactions of the American Roentgen Ray Society*, 1907
5. Brecher R, Brecher E: *The Rays*. Baltimore, Williams & Wilkins, 1969
6. Rae G: Extraversion, neuroticism and cigarette smoking. *Br J Soc Clin Psychol* 14:429–430, 1975
7. Russell MAH: The smoking habit and its classification. *Practitioner* 212:791–800, 1974
8. Arnold-Krueger M: On the personality of young male smokers. *Z Klin Psychol Psychother* 21:72–80, 1973
9. Williams A: Personality and other characteristics associated with cigarette smoking. *J Health Soc Behav* 14:374–380, 1973

Erratum

In the article "Computed Tomographic Scanning in Children: Comparison of Radiation Dose and Resolving Power of Commercial CT Scanners" by Brasch et al. (*AJR* 131:95–101, July 1978), the equations on page 100 are incorrect. The symbol D should be replaced by D^{-1} and the symbol α by α^{-1}. The final corrected relationship between dose and resolving power should read:

$$D = \frac{\alpha^2 K^2}{[C'(W)]^2 W^3}$$

Letters

Pheochromocytomas in von Hippel–Lindau Disease

Nance et al. [1] reported the occurrence of pheochromocytoma and ipsilateral renal cell carcinoma in a male patient, for whom no information on family history or other diagnostic evaluation was provided. They included von Hippel–Lindau disease in their differential diagnosis of conditions in which these tumors have been found in conjunction [2, 3], but did not establish or rule out that diagnosis in their patient. They implied that the combination of pheochromocytoma and renal cell carcinoma is extremely rare, even in von Hippel–Lindau disease, citing Horton et al. [4] who did not find coexistent tumors in a review of 50 patients with the disease.

However, there are several reports of patients with the disease who manifested both renal tumors and pheochromocytomas. Of a total of 335 patients with von Hippel–Lindau disease from the literature (bibliography available on request) and an additional 11 from my institution, my colleagues and I ascertained 56 patients with renal cell carcinoma, 47 with pheochromocytoma, and six in whom both tumors were found. Lowden and Harris [5] described a 28-year-old woman with bilateral pheochromocytomas and a hypernephroma, site unspecified. Goldberg and Duke [6] discussed a male patient with bilateral pheochromocytomas and hypernephroma on the right side. Rho [7] published another case with similar findings. Mulholland et al. [8] reported a 39-year-old woman with pheochromocytoma on the right and a left renal cortical adenoma. Tishler [9] reported a woman with bilateral pheochromocytomas and hypernephroma on the left. In addition to von Hippel–Lindau disease, that patient had neurofibromatosis. All these patients belonged to families with von Hippel–Lindau disease. Although in the family with von Hippel–Lindau disease discussed by Hagler et al. [10] no one patient had both tumors, the proposita and her maternal aunt both had pheochromocytomas, and the mother and grandmother of the proposita both had renal cell carcinomas.

The problems in estimating the actual frequency of a particular manifestation of von Hippel–Lindau disease lie with (1) the variable age of onset for any of the clinical findings (which makes it difficult to follow patients for an adequate length of time), and (2) the high frequency of asymptomatic organ involvement, often found only at autopsy. Horton et al. [4] noted an incidence of 10% for pheochromocytomas during life and a 17% incidence at autopsy. For hypernephromas, the figures were 28% and 45%, respectively. An example of the difficulties with complete ascertainment over time is the family reported first by Welch [11] and later by Horton et al. [4]. In the same family, Welch noted two cases of pheochromocytoma and one of hypernephroma not mentioned by Horton et al.; Horton et al. listed one family member who developed pheochromocytoma after the Welch study.

In my opinion, the incidence of pheochromocytomas and hypernephromas, both separately and in association, in patients with von Hippel–Lindau disease has been grossly underestimated for several reasons: (1) inadequate information from family histories; (2) unrecognized asymptomatic lesions; (3) failure to follow patients over extended periods of time; and (4) lack of sufficient autopsy information. The same difficulties apply to estimating penetrance of this autosomal dominant gene. Until all members of a family at risk are studied intensively over long periods and until thorough autopsies are performed on as many patients as possible, the incidence of both these tumors will be underestimated.

Virginia P. Sybert
Division of Medical Genetics
University of Washington
Seattle, Washington 98195

REFERENCES

1. Nance EP, Ekelund L, Goncharenko V, Rogers L: Pheochromocytoma and ipsilateral renal carcinoma diagnosed by angiography. *Am J Roentgenol* 130:553–555, 1978
2. Wolf A, Wilens SL: Multiple hemangioblastomas of the spinal cord in syringomyelias: a case of Lindau's disease. *Am J Pathol* 10:545–565, 1934
3. Harbite F: Tumors of the sympathetic nervous system and the medulla of the adrenal glands, especially malignant neuroblastoma. *Arch Intern Med* 16:312–329, 1915
4. Horton WA, Wong V, Eldridge R: Von Hippel–Lindau disease. *Arch Intern Med* 136:769–777, 1976
5. Lowden BA, Harris GS: Pheochromocytoma and von Hippel–Lindau's disease. *Can J Ophthalmol* 11:282–289, 1976
6. Goldberg MF, Duke JR: Von Hippel–Lindau disease. *Am J Ophthalmol* 66:693–705, 1968
7. Rho YM: Von Hippel–Lindau's disease: a report of five cases. *Can Med Assoc J* 101:135–142, 1969
8. Mulholland SG, Nuzhet OA, Walzak MP: Familial pheochromocytoma associated with cellular hemangioblastoma. *JAMA* 207:1709–1711, 1969
9. Tishler PV: A family with coexistent von Recklinghausen's neurofibromatosis and von Hippel–Lindau's disease. *Neurology* 25:840–844, 1975
10. Hagler WS, Hyman BN, Waters WC: Von Hippel's angiomatosis retinal and pheochromocytoma. *Trans Am Acad Ophthalmol Otolaryngol* 75:1022–1034, 1971
11. Welch RB: Von Hippel–Lindau disease: the recognition and treatment of early angiomatosis retinae and the use of cryosurgery as an adjunct to therapy. *Trans Am Ophthalmol Soc UK* 68:367–424, 1970

ARRS Comprehensive Meeting Information

President's Invitation

Dear Colleague:

You are most cordially invited to attend the seventy-ninth annual meeting of the American Roentgen Ray Society March 25–30, 1979, at the Sheraton Centre in Toronto, Ontario. This March meeting date is a departure from the traditional fall meeting of the American Roentgen Ray Society since its first meeting in New York in 1900. It has become increasingly apparent that the close calendar proximity of the annual meetings of the American Roentgen Ray Society and the Radiological Society of North America created intense competition for scientific papers as well as scientific and technical exhibits. This seemed to be working to the detriment of the meetings of both societies. In response to this problem, the members of the American Roentgen Ray Society overwhelmingly voted to support a spring meeting. It is hoped that this new pattern of a major scientific meeting in radiology in the spring and an additional meeting in the fall will provide for an easier distribution of scientific material and of physician attendance.

This is the first visit of the American Roentgen Ray Society to Toronto and the fourth time that the annual meeting has been held outside the United States; previous meetings were held in Montreal in 1927, 1963, and 1973. Our neighbors to the north have done an outstanding job in preparing for this meeting, and I hope we can provide them the support they deserve with an outstanding attendance.

The format for the meeting will be much like that planned for the 1977 meeting in Boston. Scientific programs will be held during the latter half of each morning, Monday through Friday, as well as on Tuesday and Thursday afternoons. Papers will be grouped by topic, and parallel scientific sessions will be held in order to provide a choice depending upon individual interests. The Caldwell Lecture will be presented on Wednesday morning by Joseph Whalen, Cornell University Medical School. This program will also feature outstanding papers from some of the specialty society meetings in radiology. A full scope of refresher courses has been arranged by Eugene Gedgaudas and his committee. These will be Monday and Wednesday afternoons, as well as Tuesday, Thursday, and Friday mornings. A categorical course of 15 hours in neuroradiology has been arranged by Peter Weinberg with outstanding faculty and course content. This will begin Sunday morning, March 25. The scientific exhibits will be open on Sunday, March 25, from 2 p.m. to 11 p.m., 7 a.m. to 11 p.m. Monday through Thursday, and 7 a.m. to 1 p.m. on Friday. The technical exhibits will be open from 9 a.m. to 5:30 p.m. Monday through Thursday and 9 a.m. to 1 p.m. on Friday.

A number of societies have again chosen to hold their meetings in conjunction with the annual meeting of the American Roentgen Ray Society. The Society for Pediatric Radiology will meet Saturday and Sunday, March 24 and 25. A joint program with this group is planned for Monday morning. The Society of Photo-optical Instrumentation Engineers will meet on Sunday evening and Monday, March 25 and 26, and a joint program with this group is anticipated on Tuesday morning. The American Thermographic Society will meet Thursday evening through Sunday March 29–April 1.

There will be a full social program. Because of the time of year and the location of the meeting, the traditional golf tournament has, of necessity, been cancelled. This, in effect, allows an additional day for the meeting. A tennis tournament will be held Wednesday afternoon and evening. A full sightseeing and shopping program is planned for spouses, and an optional evening at Toronto's showplace, Ontario Place, for dinner and movies on Thursday evening.

As president-elect and on behalf of the members of the Program Committee (H. Z. Mellins, J. F. Martin, J. L. Gwinn, M. M. Figley, R. A. Gagliardi, B. G. Brogdon, E. Gedgaudas, G. A. Kling, P. Riemenschneider, chm.) and officers of the American Roentgen Ray Society, it is my great pleasure to invite you to join us at the seventy-ninth annual meeting of the American Roentgen Ray Society. We look forward to an outstanding meeting and assure you that we will do our best to make it a worthwhile event. Meeting, hotel, instruction courses, and local activities registration forms appear elsewhere in this issue and will be repeated in November.

Sincerely,
Paul A. Riemenschneider
President-elect

Local Activities

Plans for activities in conjunction with the 1979 American Roentgen Ray Society meeting in Toronto, March 25–30, 1979, have been finalized by the Local Arrangements Committee. Registration forms listing costs and times appear elsewhere in this issue and will be repeated in November.

Spouses' Program

The Spouses' Committee has arranged three tours in the Toronto area. The first, Monday, March 26, will be backstage at the St. Lawrence Centre for the Arts to see an aspect of the theater that few people have an opportunity to appreciate. The centre houses a summer and winter repertory theater and provides space for numerous public events. Luncheon will be served at the end of the tour in the theater lobby.

On Tuesday, March 27, tour participants have a choice of a walk through a maple woods to see the production of maple syrup, or a bus ride through downtown Toronto. Both groups will meet for lunch at the Board of Trade Country Club. The afternoon will be spent at the "most Canadian gallery in the country," McMichael Canadian Collection in Kleinburg. The gallery, housed in log buildings, is a clear representation of the Group of Seven, the only internationally recognized school of Canadian art. There is also a fine collection of Indian and Eskimo art.

Niagara Falls and Niagara-on-the-Lake are the sites of a day-long tour on Wednesday, March 28. Lunch will be served at a country inn at Niagara-on-the-Lake. Ample time will be provided for photography at the American Falls and the Canadian Horseshoe Falls. After lunch, time will be provided for shopping and a drive around the former colonial capital, now home of the renowned Shaw Festival.

In addition to the three tours, a fashion show and brunch will provide entertainment on Thursday, March 29, in the Aloha Lagoon, Sheraton Centre. The creations of well known Canadian designer Claire Haddad will be shown as well as the best in fur designs by Norman Rogul. Top Canadian models will show the designs.

Tennis Tournament

The tennis tournament is scheduled for Wednesday, March 28, at the Mayfair Racquet Club, Downsview, Ontario. Transportation from the Sheraton Centre will be by bus, following the Caldwell Lecture, at approximately 11:45 a.m., returning to the hotel between 6:30 and 7 p.m. Play will begin at 1 p.m. after a buffet luncheon at the club. Cocktails and trophy presentation follows the conclusion of play.

Social Evening at Ontario Place

On Thursday evening, March 29, there will be a buffet dinner at approximately 7:45 p.m. following a happy hour. Afterward, there will be a 30–40 min film show, starting with the spectacular film North of Superior, at Cinesphere, Ontario Place's triodetic dome theater, a dazzling Toronto waterfront landmark featuring high fidelity and large format motion pictures on one of the world's largest screens. Buses will depart the Sheraton Centre from 6:30 p.m., returning to the hotel at approximately 10 p.m.

Change in President's Award Deadline

Papers to be considered for the President's Award should be submitted by November 30 rather than December 31. They should be submitted to Eugene Gedgaudas, not James Martin.

American Roentgen Ray Society Section on Instruction: Courses Scheduled for 1979 Annual Meeting

EUGENE GEDGAUDAS, DIRECTOR
GLEN W. HARTMAN, ASSOCIATE DIRECTOR

Instruction Courses for the seventy-ninth annual meeting of the American Roentgen Ray Society will be offered afternoons on Monday, March 26, and Wednesday, March 28, and in the mornings on Tuesday, March 27, Thursday, March 29, and Friday, March 30. Each course is scheduled for 90 min. No other activities are scheduled simultaneously. All courses will be at the Four Seasons Sheraton Hotel.

In addition to 58 periods of regular courses, there will be a series of courses dealing entirely with Neuroradiology. This 15 hr categorical course will take place over 5 days. **It will not be possible to take other courses in addition to the categorical neuroradiology program.** The neuroradiology course will begin Sunday, March 25, and will be the only subject presented that day. Eleven other courses will be offered on Monday and Friday, as well as 12 each on Tuesday, Wednesday, and Thursday.

To register for courses, complete the pink registration form in this section and mail promptly. Tickets will be mailed only to those whose forms have been received at the Office of the Director by March 1. Tickets will be mailed in an envelope marked "SECTION ON INSTRUCTION, AMERICAN ROENTGEN RAY SOCIETY—TICKETS ENCLOSED." Ticket requests that arrive after the deadline will not be honored, although tickets will be available at the Instruction Course Registration desk in the hotel for courses that have not been sold out. Tickets will be mailed beginning early in March.

Registration Information

After reviewing the abstracts, select three for each day, then fill out the order form with the course number and instructor's name. For each course, a $3 registration fee is required from nonmembers. The cost for nonmembers if five courses are selected, one each day, will be $15. There is no charge for courses to members of the American Roentgen Ray Society, graduate students or residents in radiology, or nonmembers who are contributing to the program by presenting an instruction course, a paper on the scientific program, or a scientific exhibit. However, everyone must fill out a registration form indicating their choices, and check the proper box opposite their name and address.

All who register for the Neuroradiology Categorical Course must take the entire series and pay the $25 fee, *including members of the American Roentgen Ray Society*. The categorical course totals 15 hr instruction and includes a syllabus.

Promptly mail the registration form to: Eugene Gedgaudas, Director of Instruction Courses, American College of Radiology, 20 North Wacker Drive Chicago, Illinois 60606.

Condensed Schedule of Courses

Sunday, March 25, through Friday, March 30
Categorical Course on Neuroradiology, five sessions, 15 hr. Fee is $25 and must be paid by society members as well as guests. **Registration in this course precludes registration in any other courses.**

Monday, March 26, 3:30–5 p.m.
101. Parkey, Lewis. Nuclear Cardiology Review
102. Greenspan. Intrathoracic Air Trapping
103. Alfidi. Computed Tomography of the Human Body
104. Berk. Radiology of the Gallbladder and Bile Ducts
105. Egan, McSweeney. Correlated Clinical, Radiographic, and Pathologic Approach to Detect Early Breast Cancer
106. Gardiner, Stevenson. Inflammatory Bowel Disease
107. Gehweiler, Charlton. Radiology of Facial Fractures
108. Gilula. Radiology of the Wrist, Part I
109. Meyers. Dynamic Radiology of the Abdomen: Normal and Pathologic Anatomy
110. Hattery. Computed Tomography of the Genitourinary Tract, Retroperitoneum, and Pelvis
111. Carey. CT Scanning—Abdomen and Thorax: Fundamental Considerations

Tuesday, March 27, 8–9:30 a.m.
201. Alazraki, Resnick. Bone and Joint Scanning
202. L'Heureux. The Child with a Flank Mass
203. Chase, Kricheff. Computed Tomography: Nonneoplastic Lesions of the Brain
204. Felson. Some Interesting Patterns of Pulmonary Neoplasms
205. Gehweiler. Cervical Spine Trauma—A Practical Guide to Diagnosis
206. Ackerman. Noninvasive Diagnosis of Carotic Artery Disease
207. Harris. The Radiographic Diagnosis of Acute Injuries of the Lower Cervical Spine
208. Gilula. Radiology of the Wrist, Part II
209. Knight. CT of the Body and Thorax
210. Martel. The Alimentary Tract. Radiologic Vignettes
211. Potter. What Every Radiologist Should Know about the Ear
212. Reilly. Problems of the Immature Infant

Wednesday, March 28, 2–3:30 p.m.
301. Siegel, Koehler, Melson. Comparison of Radionuclide Ultrasound and CT Imaging of the Abdomen

302. Freeny. Algorithmic Approach to Radiologic Diagnosis of Suspected Pancreatic Disease
303. Chase, Kricheff. Computed Tomography: Nonneoplastic Lesions of the Brain
304. Felson. Some Interesting Patterns of Pulmonary Neoplasms
305. Gold. Computed Tomography of the Brain
306. Harwood-Nash. Hydrocephalus in Children: Old Principles, New Philosophies
307. McLelland, Thompson. Inflammatory Diseases of the Colon
308. McLeod. Computed Tomography of the Skeletal System and Soft Tissues
309. Thornbury. Radiologic Diagnosis: A Horse-Sense Approach
310. Kazam, Whalen. Anatomic Approach to Radiology of the Thorax, Part I
311. Wolfe. Mammography, Part I
312. Simon. The Pulmonary Circulation and the Radiologist

Thursday, March 29, 8–9:30 a.m.

401. Christie, Chiu. A Comparison of CT and Radionuclide Imaging in Central Nervous System Disease
402. Goldberg, Cole-Beuglet. An Introduction to Diagnostic Ultrasound
403. Goldman. Interventional Angiography
404. Gray, Muhm, Brown. Radiation Exposure and Risks—In Perspective
405. Heitzman. Computed Tomography of the Thorax
406. Jacobson, Siegelman. Skeletal Radiology—New Concepts and Provocative Challenges, Part I
407. McCallum. Current Concepts in the Anatomy, Pathology, and Radiology of the Male Lower Urinary Tract
408. Payne, McCullough. Basic Principles of Computed Tomography
409. Rosenfield. Renal Ultrasound: Current Concepts
410. Kazam, Whalen. Anatomic Approach to Radiology of the Abdomen, Part II
411. Wolfe. Mammography, Part II
412. Wilkinson. Skeletal Trauma in Infants and Children

Friday, March 30, 8–9:30 a.m.

501. Maynard, Cowan. Radionuclides and the Thyroid Gland
502. MacEwan. Balanced Radiology Services on a Tight Budget
503. Janower. Everything You Ever Wanted to Know about Running a Radiology Department but Were Afraid to Ask
504. Kattan. Tricks and Treats in Tomography
505. King. Cardiac Ultrasound
506. Jacobson, Siegelman. Skeletal Radiology—New Concepts and Provocative Challenges, Part II
507. Marshak. Radiologic-Pathologic Correlation of Interesting Lesions of the Gastrointestinal Tract
508. Singleton. Obstructive Lesions of the Alimentary Tract in the Newborn and Young Infant
509. Stephens. Gastrointestinal Applications of Computed Tomography
510. Swischuk. Neonatal Chest Problems
511. Theros. Exercises in the Analysis of the Unknown Lesion in Bone

Faculty

Robert H. Ackerman, assistant professor, Radiology, Harvard Medical School; assistant radiologist, Massachusetts General Hospital, Boston

Naomi P. Alazraki, chief, Nuclear Medicine, Veteran's Administration Hospital; associate professor, Radiology, University of California, San Diego

Ralph Alfidi, chairman, Radiology, University Hospital, Cleveland, Ohio

R. Thomas Bergeron, professor, Radiology, New York University Medical Center, New York City

Robert N. Berk, professor, chairman, Radiology, University of California Medical Center, San Diego

Eugene Binet, professor, vice chairman, Radiology, University of Arkansas, Little Rock

Manuel L. Brown, assistant professor, Radiology and Laboratory Medicine, Mayo Clinic, Rochester, Minnesota

Lewis S. Carey, professor, chairman, Radiology, University of Western Ontario, London, Canada

Olivier Charlton, assistant professor, Radiology, Duke University Medical Center, Durham, North Carolina

Norman Chase, professor, chairman, Radiology, New York University Medical Center; director, Radiology, Bellevue Hospital, New York City

Lee C. Chiu, associate professor, Radiology, University of Iowa Hospitals and Clinics, Iowa City

James Christie, professor, chairman, Radiology, University of Iowa Hospitals and Clinics, Iowa City

Catherine Cole-Beuglet, associate professor, Radiology, Thomas Jefferson University Hospital, Philadelphia

Robert J. Cowan, associate professor, director, Nuclear Medicine, Bowman Gray School of Medicine, Winston-Salem, North Carolina

David O. Davis, professor, chairman, Radiology, George Washington University Medical Center, Washington, D.C.

Michael Deck, assistant professor, Radiology, Cornell University, New York City

Robert Egan, professor, Radiology, chief, Mammography Section, Emory University School of Medicine, Atlanta, Georgia

Benjamin Felson, professor, Radiology, University of Cincinnati and Cincinnati General Hospital, Cincinnati, Ohio

Patrick C. Freeny, assistant professor, Radiology, University of Washington and the Mason Clinic, Seattle

Mokhtar H. Gado, professor, Radiology, head, Neuroradiology, Mallinckrodt Institute of Radiology, Washington University School of Medicine, St. Louis, Missouri

Richard Gardiner, director, Gastrointestinal Radiology, Presbyterian-St. Luke's Hospital, Chicago.

John A. Gehweiler, associate professor, Radiology, Duke University Medical Center, Durham, North Carolina

Advance Registration: 79th Annual ARRS Meeting
Toronto, Ontario, Canada, March 25–30, 1979

If you plan to attend, please fill out the following form.
Official badges and program booklets will be available at the registration desk in the Four Seasons Sheraton Hotel at the time of the meeting. NO CONFIRMATIONS OF REGISTRATIONS WILL BE FORWARDED PRIOR TO THE MEETING. Preregistration by mail will be accepted only until March 1, 1979. (On site registration will be available.)

MAIL TO: THE AMERICAN ROENTGEN RAY SOCIETY
20 North Wacker Drive, Suite 2920, Chicago, Illinois 60606

Check one box, and include the proper fee in your envelope:
- ☐ Member of the American Roentgen Ray Society (no fee).
- ☐ Nonmember (registration fee $25).
- ☐ Physician in training (registration fee $15). Be sure to include the certification on bottom of this form.

Please print or type:

Name _____

Street _____

City _____

State or Province and zip _____

☐ Check here if you wish a program of events for spouses. Indicate the address to which this is to be sent.

Name _____
(Spouse's name you wish printed on badge)

Street _____

City _____

State or Province and zip _____

FOR PHYSICIANS IN TRAINING:

_____ is in training in my department.

_____
Department Chief

_____
Date

_____
Institution

PLEASE COMPLETE BACK FOR COURSE REGISTRATION.

Section on Instruction Order Sheet

It is important to register early for Instruction Courses since the number admitted to each will be limited. It is also important that first, second, and third choices be listed for each period. All ticket orders will be filled according to postmark.

Nonmembers of the American Roentgen Ray Society will pay $3 for each course period. *Nonmembers' fees must accompany this sheet and will not be returned unless cancellation is received before March 20, 1979.*

Members of ARRS, residents in radiology, and nonmembers who are contributing to the program, either by way of an instruction course, a paper, or a scientific exhibit, are not required to pay for these courses but must submit this form.

Tickets for courses will be mailed to those whose order reaches the office of the director on or before March 1. They will be sent to the address below unless directed otherwise. Tickets for late registrants will be available at the Registration Desk of the Section on Instruction at the Four Seasons Sheraton Hotel on and after Sunday morning, March 25.

Please type or print:

Check one:
☐ Member
☐ Guest
☐ Resident in radiology at: _____
☐ Scientific exhibitor/paper

_____
Last Name First Name or Initials

_____
Street Address

_____
City State Zip Code

I wish to take the Categorical Course on Neuroradiology, five periods, March 25–30. Fee: $25 ☐

Registration in this course precludes registration in any other courses.

Course Registration (for those not taking categorical course). For convenience in selecting your courses consult the condensed schedule of courses. **Be sure to fill out second and third choices for each period.**

Period	First Choice		Second Choice		Third Choice	
	Course No.	Instructor	Course No.	Instructor	Course No.	Instructor
Monday						
Tuesday						
Wednesday						
Thursday						
Friday						

Make checks payable to American Roentgen Ray Society. If mailing late, send to: Dr. Eugene Gedgaudas, Four Seasons Sheraton Hotel, 123 Queen Street West, Toronto, Ontario, Canada.

Application for Hotel Reservations

(DEADLINE: FEBRUARY 25, 1979)

AMERICAN ROENTGEN RAY SOCIETY

MARCH 25–30, 1979

Participating Hotels:	Singles	Doubles	Suites
Four Seasons Sheraton, headquarters hotel	$37, $43, $49	$45, $51, $59	$95–169
Hotel Toronto	$42, $44, $51	$52, $54, $61	$140
Holiday Inn, Downtown Toronto	$34	$42	

(Mail Lower Portion of This Form to Address Listed Below Before FEBRUARY 25, 1979.)

MAIL TO:
ARRS Housing Bureau
Four Seasons Sheraton Hotel
123 Queen Street West
Toronto, Ontario M5H 2M9, Canada

CHOICE OF HOTEL First_____ Second _____ Third _____

ACCOMMODATIONS Single ☐ Double ☐ Twin ☐ 1 Bedroom Suite ☐ Preferred Rate $ _____

Roll-away Bed Requested ☐ 2 Bedroom Suite ☐

Please indicate any special accommodation needs due to a handicap_____

ARRIVAL DATE _____ _____AM _____PM

DEPARTURE DATE_____ _____AM _____PM

Rooms held only until 6:00 PM unless otherwise specified

INDIVIDUAL REQUESTING RESERVATION *(Please type or print)*

Name_____

Mailing Address _____

_____ ZIP_____

Name(s) of other room occupant(s)_____

(SEE REVERSE SIDE FOR MAP AND SPECIAL INSTRUCTIONS)

Important Information:

1. Reservations must be received by the Housing Bureau no later than FEBRUARY 25, 1979 in order to be assured of written confirmed accommodations.
2. Written confirmation of your reservation will be sent to you by the hotel. Please allow 2–3 weeks for confirmation.
3. All changes such as arrival date, departure date, type room and name changes must be made directly with the hotel after confirmation is received.
4. If you plan to share a room, please send in only one housing form. Be sure to list all names of occupants of rooms. Assignment is delayed until complete information is received.
5. Room assignments will be made in order received. If your choices are not available, the Housing Bureau will assign you to a comparable hotel. If rate requested is not available you will be assigned to the next closest rate available.
6. Hotel reservations will be held only until 6:00 P.M. unless otherwise specified.

HOTELS

FOUR SEASONS SHERATON, HEADQUARTERS HOTEL
Hotel Toronto
Holiday Inn-Downtown Toronto

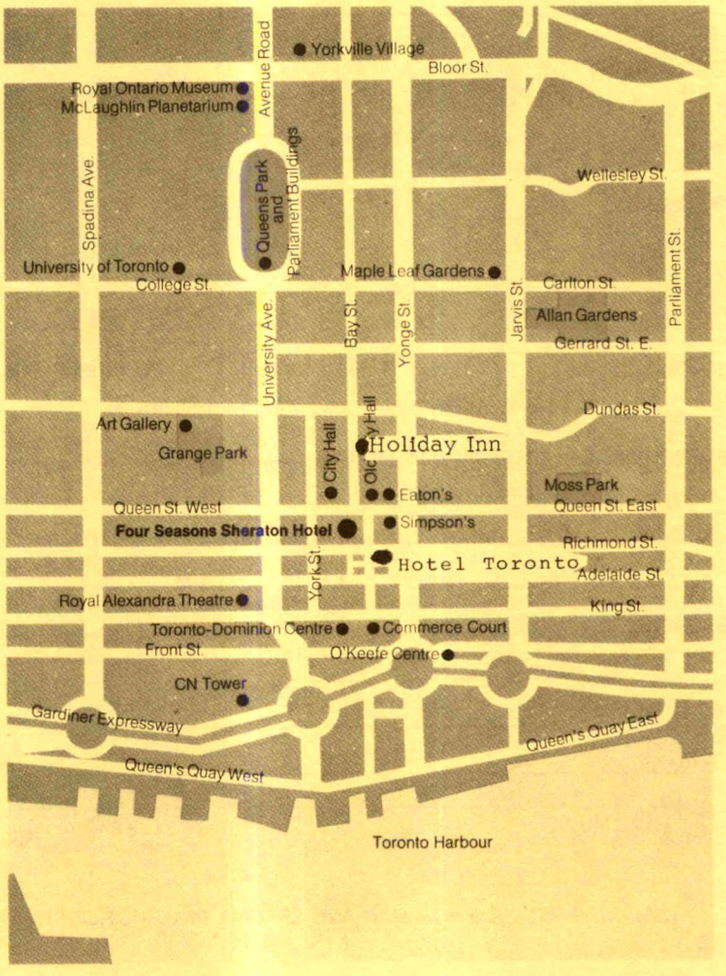

American Roentgen Ray Society Local Activities
Toronto, Canada, March 26–30, 1979

Spouses' Program

Reservations should be made before March 19. Late requests may not be honored. All tickets and badges are to be picked up at the ARRS Spouses' Registration Desk, Sheraton Centre, Toronto. **No receipts or confirmations will be forwarded prior to that time.**

	(Canadian Funds)
Monday, March 26, 10:30 a.m.–2 p.m., St. Lawrence Centre, Backstage at the Theatre, including luncheon	____tickets @ $16.50 $____
Tuesday, March 27, 9:30 a.m.–4 p.m., Maple Sugar Bush and Canadian Art, including luncheon	____tickets @ $16.00 $____
Wednesday, March 28, 9:30 a.m.–4:30 p.m., Niagara Falls and Niagara-on-the-Lake, including luncheon	____tickets @ $22.00 $____
Thursday, March 29, 10:00 a.m.–noon, Fashion, Furs, and Fun, including buffet brunch	____tickets @ $16.00 $____
	Total Enclosed $____

Please detach and mail with your check (payable in Canadian Funds to ARRS-Convention Consultants of Toronto Ltd.) to: ARRS-Convention Consultants of Toronto Ltd., 961 Eglinton Avenue East, Suite 200, Toronto, Canada M4G 4B5.

NAME_____ADDRESS_____

Annual Tennis Tournament, Wednesday, March 28

The tournament will be at the Mayfair Racquet Club, 3855 Chesswood Drive, Downsview, Ontario. Play will be conventional round-robin style (doubles), alternating on six courts, beginning at 1 p.m. A buffet luncheon at the Mayfair Club precedes the tournament. Cocktails and awards will follow. The entire tournament is sponsored by GAF company. Bus transportation will depart the Sheraton Centre at approximately 11:45 a.m. (following the Caldwell Lecture) with return about 6:30 p.m. Taxis will be available. The tournament is limited to 48 players—first come, first served.

To participate, return completed form to: Dr. D. J. Sieniewicz, Department of Radiology, St. Michael's Hospital, 30 Bond Street, Toronto, Canada M5B 1W8.

NAME_____

ADDRESS_____TELEPHONE _____

_____ZIP CODE _____

Social Evening at Ontario Place, Thursday, March 29

A buffet dinner will be served at the Trillium Restaurant of Ontario Place at approximately 7:45 p.m. following a Happy Hour. A 30–40 min film show will follow, starting with the spectacular film North of Superior. Buses will depart the Sheraton Centre from 6:30 p.m. and return at approximately 10 p.m. Tickets are $16.50 (Canadian funds) and are to be picked up at the ARRS Spouses' Registration Desk, Sheraton Centre. **No receipts or confirmations will be forwarded prior to that time.**

To register, please detach and mail before March 19 with your check (payable to ARRS-Dinner) to: Dr. B. J. Reilly, Department of Radiology, The Hospital for Sick Children, 555 University Avenue, Toronto, Canada M5G 1X8.

NAME_____

ADDRESS_____TELEPHONE _____

_____ZIP CODE _____

Ajax E. George, professor, Radiology, New York University Medical Center, New York City

Louis A. Gilula, assistant professor, Radiology, Mallinckrodt Institute of Radiology, St. Louis, Missouri

Lawrence Gold, associate professor, Radiology, University of Minnesota Hospitals, Minneapolis

Barry B. Goldberg, professor, director, Diagnostic Ultrasound, Thomas Jefferson University Hospital, Philadelphia

Herbert I. Goldberg, director, Radiology, University of Pennsylvania Hospital, Philadelphia

Martin L. Goldman, assistant professor, Radiology, Emory University; director, Vascular Radiology, Grady Memorial Hospital, Atlanta, Georgia

Joel Gray, instructor, Radiology, Mayo Clinic, Rochester, Minnesota

Richard Greenspan, professor, chairman, Radiology, Yale University, New Haven, Connecticut

John Harris, chairman, Radiology, Carlisle Hospital; professor, Radiology, Thomas Jefferson Hospital, Carlisle, Pennsylvania

Derek Harwood-Nash, head, Pediatric Neuroradiology, Hospital for Sick Children; professor, Radiology, University of Toronto, Toronto, Canada

Robert Hattery, assistant professor, Radiology, Mayo Clinic, Rochester, Minnesota

E. Robert Heitzman, professor, director, Radiology, State University of New York, Upstate Medical Center, Syracuse

Sadek K. Hilal, professor, director, Radiology, Columbia-Presbyterian Medical Center, New York City

Fred J. Hodges III, professor, Radiology, Johns Hopkins Hospital, Baltimore, Maryland

Wayne O. Houser, assistant professor, Radiology, Mayo Clinic, Rochester, Minnesota

Harold G. Jacobson, professor, chairman, Radiology, Montefiore Hospital and Medical Center, Bronx, New York

M. L. Janower, physician-in-chief, Radiology, St. Vincent Hospital, Worcester, Massachusetts

Kenneth R. Kattan, professor, chief, Radiology, Veterans Administration Center, Dayton, Ohio

Elias Kazam, assistant professor, Radiology, New York Hospital, New York City

Stephen Kieffer, professor, chairman, Radiology, State University of New York, Upstate Medical Center, Syracuse

Donald L. King, associate professor, Radiology, director, Ultrasound, Columbia-Presbyterian Medical Center, New York City

Laura Knight, radiologist, Riverside Methodist Hospital, Columbus, Ohio

Robert E. Koehler, assistant professor, Radiology, Mallinckrodt Institute of Radiology, Washington University School of Medicine, St. Louis, Missouri

Irvin I. Kricheff, professor, Radiology, New York University Medical Center, New York City

Norman E. Leeds, professor, Radiology, Montefiore Hospital and Medical Center, Bronx, New York

Samuel E. Lewis, director, Nuclear Medicine, Southwestern Medical School, Dallas

Philippe L'Heureux, associate professor, Radiology, director, Pediatric Radiology, University of Minnesota, Minneapolis

Douglas MacEwan, professor, chairman, Radiology, University of Manitoba, Winnipeg, Canada

Richard Marshak, clinical professor, Radiology, Mt. Sinai Hospital, New York City

William Martel, professor, Radiology, University of Michigan, Ann Arbor, Michigan

C. Douglas Maynard, professor, chairman, Radiology, Bowman Gray School of Medicine, Winston-Salem, North Carolina

R. W. McCallum, associate professor, Radiology, St. Michael's Hospital, Toronto, Canada

Edwin C. McCullough, assistant professor, Radiology, Mayo Clinic, Rochester, Minnesota

Robert McLelland, associate professor, Radiology, Duke University Medical Center, Durham, North Carolina

Richard McLeod, assistant professor, Radiology, Mayo Clinic, Rochester, Minnesota

Marjorie McSweeney, assistant professor, Radiology, Emory University, Emory University Clinic, Atlanta, Georgia

G. Leland Melson, associate professor, Radiology, Mallinckrodt Institute of Radiology, Washington University School of Medicine, St. Louis, Missouri

Morton Meyers, professor, Radiology, New York Hospital, Cornell Medical Center, New York City

John R. Muhm, assistant professor, Radiology, Mayo Clinic, Rochester, Minnesota

Thomas Naidich, assistant professor, Radiology, Mallinckrodt Institute of Radiology, St. Louis, Missouri

Sidney W. Nelson, radiologist, Swedish Hospital, Seattle, Washington

Robert W. Parkey, professor, chairman, Radiology, Southwestern Medical School, Dallas, Texas

J. Thomas Payne, associate professor, Radiology, University of Minnesota, Minneapolis

Guy D. Potter, professor, Radiology, Columbia-Presbyterian Medical Center, New York City

D. Gordon Potts, professor, Radiology, Cornell University Medical College, New York City

B. J. Reilly, professor, Radiology, University of Toronto, Hospital for Sick Children, Toronto, Canada

Donald L. Resnick, associate professor, chief, Diagnostic Radiology, Veterans Administration Hospital; associate professor, University of California, San Diego

Lee F. Rogers, professor, chairman, Radiology, Northwestern University, Chicago

Arthur Rosenbaum, professor, Radiology, University of Pittsburgh, Pittsburgh, Pennsylvania

Arthur Rosenfield, associate professor, Radiology, Yale University, New Haven, Connecticut

Barry Siegel, associate professor, Radiology, director, Nuclear Medicine, Mallinckrodt Institute of Radiology, Washington University School of Medicine, St. Louis, Missouri

Stanley S. Siegelman, professor, Radiology, Johns Hopkins University, Baltimore, Maryland

Morris Simon, professor, Radiology, Harvard Medical School, Beth Israel Hospital, Boston

Edward Singleton, director, Radiology, St. Luke's Episcopal Hospital, Texas Childrens' Hospital, Texas Heart Institute, Houston

David H. Stephens, assistant professor, Radiology, Mayo Clinic, Rochester, Minnesota

Giles W. Stevenson, associate professor, Radiology, McMaster University Medical Centre, Hamilton, Ontario, Canada

Leonard E. Swischuk, professor, Radiology, director, Pediatric Radiology, Child Health Center, University of Texas, Galveston

Juan M. Taveras, professor, Radiology, Harvard Medical School, Boston

Michael S. Tenner, associate professor, Radiology, State University of New York, Downstate Medical Center, Brooklyn

Elias G. Theros, professor, Radiology, University of California, Los Angeles

William M. Thompson, associate professor, Radiology, Duke University Medical Center, Durham, North Carolina

John R. Thornbury, professor, Radiology, University of Michigan, Ann Arbor

Peter Weinberg, associate professor, Radiology, Northwestern University Medical School, Chicago

Joseph Whalen, chairman, Radiology, New York Hospital, Cornell Medical Center, New York City

Robert H. Wilkinson, associate professor, Radiology, Children's Hospital Medical Center, Boston

John Wolfe, chief, Radiology, Hutzel Hospital, Detroit, Michigan

Samuel M. Wolpert, professor, Radiology, New England Medical Center, Boston

George Wortzman, professor, Radiology, Toronto General Hospital, Toronto, Canada

Categorical Course on Neuroradiology

March 25–30, 1979

Sidney Nelson, general chairman; Peter Weinberg, program cochairman; Stephen Kieffer, program cochairman

Please note: This course extends over 15 hr using all available time for instructional courses. If you select this course, do not register for others. Fee is $25 and must be paid by *everyone*.

Course Outline

Sunday, March 25, 10 a.m.–noon

The abnormal skull. Deck
The temporal bone and cerebello-pontine angle. Bergeron
The orbit and paranasal sinuses. Tenner

Sunday, March 25, 2–4 p.m.

Anatomy of supratentorial region. Rosenbaum
Classification of mass lesions. Leeds
The sella turcica and suprasellar masses. Wolpert

Monday, March 26, 8–10 a.m.

Frontal and parietal masses. Wortzman
Temporal and occipital masses. Davis
Deep and incisural masses. Naidich

Monday, March 26, 2–5 p.m.

Anatomy of posterior fossa. Gado
CT of posterior fossa lesions. Hilal
Angiography of posterior fossa masses. Weinberg
Occlusive vascular disease. Goldberg
Aneurysms and arteriovenous malformations. Kricheff, George

Tuesday, March 27, 8–10 a. m.

Congenital abnormalities of the skull and brain. Harwood-Nash
Radiologic investigation of hydrocephalus. Potts
CT of atrophic and degenerative cerebral processes. Hodges

Thursday, March 29, 8–10 a.m.

CT of intracranial trauma. Taveras
The spine—normal and nontraumatic lesions. Binet
Spinal trauma. Rogers

Friday, March 30, 8–10 a.m.

Myelography: normal and disc disease. Kieffer
Myelography: mass lesions. Houser
Quiz

Description of Courses

101. Nuclear cardiology review. Parkey RW, Lewis SE. An overview of practical Nuclear Cardiology will be presented with discussion of acute infarct imaging, perfusion imaging, and measurement of ventricular function. The role of these techniques in current practice of nuclear medicine will be stressed. Equipment, technique, image interpretation, and clinical diagnosis will be discussed. Finally, future directions of nuclear cardiology will be presented for discussion.

102. Intrathoracic air trapping. Greenspan RH. In this course, the pleura, tension pneumothorax, will be described with underlying lung collapse and without collapse. Air trapping in

"discrete" intrapulmonary structures such as congenital cysts, pneumatoceles, bullae, and the "vanishing lung" will also be described. Partial airway occlusions may result from foreign bodies, tumors, inflammatory disease, or defective airways while total airway occlusion with collateral air drift may be caused by bronchial occlusion with bronchiocele, acquired bronchial occlusion, and the McCloud or Swyer-James syndrome. The course will also cover means of detecting trapping.

103. Computed tomography of the human body. Alfidi RJ. It is safe to say at this time that computed tomography of the body has proven to be a significant diagnostic modality which often supplies information not available by any other means. The indications for study of various portions of the body, use of contrast agents, analysis of accuracy in various organs, and CT biopsies in a variety of neoplastic and inflammatory disorders will be presented. The course will provide time for questions and open discussion.

104. Radiology of the gallbladder and bile ducts. Berk RN. This course includes an update on oral cholecystography: rational selection and most efficient use of oral cholecystopaques, technical aspects, causes and significance of impaired first dose opacification in normal patients and patients with pancreatitis, accuracy, evaluation of cholecystokinin cholecystography, some interesting abnormalities such as the gallbladder in cystic fibrosis, tumors, displacement of the gallbladder, and medical treatment of gallstones. Plain film diagnosis of gallbladder disease will be included. Optimal technique of intravenous cholangiography and infusion nephrotomography with renal contrast agents will be analyzed. The use of ultrasound, percutaneous cholangiography, CT scanning, and stone extraction procedures will be covered if time permits.

105. Correlated clinical, radiographic and pathologic approach to detect early breast cancer. Egan RL, McSweeney M. Illustrative cases will be presented via history, clinical findings, and mammograms. The radiographic findings will be discussed followed by histopathologic studies such as specimen radiography, pathologic preparations, whole organ studies, and histopathology of breast changes. Discussion, including audience participation, will then be carried out regarding diagnosis, treatment, and clinical course.

106. Inflammatory bowel disease. Gardiner R, Stevenson GW. This course will emphasize the most current criteria for early detection, precise localization, and facilitated differential diagnosis of inflammatory bowel diseases. By providing an excellent view of the gut's surface anatomy, double contrast examinations of the entire gastrointestinal tract are especially suited for inflammatory bowel disease evaluation. Radiologic correlation will be made with the endoscopic, gross pathologic, and microscopic appearance and the relative value of full column examinations will be discussed. Specific practical techniques for achieving excellent quality double contrast examinations, including patient preparation and examination materials and methods, will be presented in detail and provided in written form for course registrants.

107. The radiology of facial fractures. Gehweiler JA Jr, Charlton OP. Facial fractures often prove to be a difficult diagnostic problem in the emergency room setting. In this refresher course we emphasize how to examine the acutely injured patient using new modalities currently available, including panoramic zonography and transaxial tomography. The course will be divided into four sections: the anatomy, radiographic techniques, and diagnosis of facial fractures, and the reporting of pertinent information to the maxillofacial surgeon.

108 and 208. Radiology of the wrist, part I. Gilula LA. Carpal abnormalities, especially following trauma, are commonly encountered radiologic entities and are often inadequately understood and misinterpreted. The first part of the course will cover basic normal radiographic carpal bone anatomy, normal intercarpal motion, and basic interpretation of malalignments and fractures. The last part will demonstrate how this easily learned and utilized approach can be applied to more complex carpal bone problems. The basic format will utilize worksheets for self-instruction, with multiple examples shown. Appropriate handouts will be provided.

109. Dynamic radiology of the abdomen: normal and pathologic anatomy. Meyers MA. The new diagnostic imaging of ultrasonography and computed tomography has further underlined the need of the radiologist to understand the detailed anatomic relationships within the abdomen. This course emphasizes the practical application of knowledge of anatomic relationships and the dynamics of spread of disease in the abdomen to precise radiologic diagnosis. This fundamental approach regarding the pathogenesis of disease within the abdomen reinforces and simplifies accurate radiologic analysis. Anatomic sections will provide basic correlation with plain films, conventional contrast studies, ultrasonography, and CT. Features of the intraperitoneal and extraperitoneal spaces will be stressed, leading to specific diagnostic criteria. Clinical applications include abscesses, perforations, traumatic lesions, and malignancies. This information leads to the uncovering of clinically deceptive diseases, the evaluation of the effects of disease, the anticipation of complications, and the determination of the appropriate diagnostic and therapeutic approaches.

110. Computed tomography of the genitourinary tract, retroperitoneum, and pelvis. Hattery R. Computed body tomography is frequently used to evaluate the adrenals, kidneys, other retroperitoneal structures, and pelvis. Computed tomography may be employed as the primary imaging method or used in conjunction with other imaging tests to detect, define, and differentiate disease processes. CT indications, applications, and scanning procedures will be discussed. Pertinent normal cross-sectional anatomy will be reviewed. Computed tomographic scans of various abnormalities will be illustrated and discussed, and the principles of interpretation of abnormal CT findings will be emphasized.

111. CT scanning—abdomen and thorax: fundamental considerations. Carey LS. A basic course in CT scanning of the abdomen and thorax will be presented emphasizing anatomic landmarks and fundamental pathologic processes. Those areas and conditions for which CT is most effective will be dwelt upon, and special attention will be given to the surgical abdomen.

201. Bone and joint scanning. Alazraki N, Resnick D. This refresher course will emphasize the clinical role of bone-joint scanning in the workup of various types of patients including benign and malignant bone diseases and arthritides. Correlations of the radionuclide study with x-ray procedures and computed tomography studies when relevant will be presented. The radionuclide angiographic study of a localized region of bone will be described, with emphasis on the clinical roles that this procedure might play in a variety of diseases, particularly ostiomyelitis versus cellulitis, and benign versus malignant bone tumors.

202. The child with a flank mass. L'Heureux P. The infant or child presenting with a flank mass is a common problem in

pediatrics. Although several new modalities of examination are available, the intravenous urogram remains the most important diagnostic tool in the evaluation of such patients. This course will address itself to the specific, practical aspects of the radiographic investigation of a patient with a flank mass. Contrast dosage, patient immobilization, film sequence and technique, practical methods for improving the diagnostic field, and problems in diagnosis specifically related to infants will be discussed. The diagnosis and differential diagnosis of the more common lesions, and of a few "zebras" will be illustrated. Finally, voiding cystourethrograms, ultrasound, CT scanning, and nuclear medicine will be assessed and compared.

203 and 303. Computed tomography: nonneoplastic lesions of the brain. Chase NE, Kricheff II. This course will include descriptions and relative value of CT in medical and surgical conditions including hemorrhage, trauma, degenerative disease, and hydrocephalus. Some congenital conditions will be included in the discussion. The value of CT in cerebral infarcts at various stages will be included. The relative value of CT and other studies will be discussed.

204 and 304. Some interesting patterns of pulmonary neoplasms. Felson B. It is not only important to diagnose cancer of the lung but also to recognize its absence. In order to do this, it is necessary to call attention to certain of the radiographic signs of this multifaceted disease. For example, the presence of calcium within a pulmonary nodule is strong evidence against a carcinoma, but cavitation, especially if the wall is nodular, is evidence favoring carcinoma. Patients with certain diseases, such as asbestosis and dermatomyositis, are prone to develop carcinoma of the lung. How do you recognize their neoplasm?

Pulmonary collapse secondary to a bronchial lesion may present an atypical radiographic pattern. Tomography or bronchoscopy will usually resolve the dilemma. Multiple lesions generally exclude primary bronchogenic carcinoma, but double primary carcinomas with clearly different histologic patterns are not so rare. Changing concepts related to the histopathology and pathogenesis of alveolar cell carcinoma and bronchial adenoma necessitate a reevaluation of the radiographic criteria for the diagnosis of these conditions.

Other primary benign and malignant neoplasms of the lungs sometimes have their own radiographic characteristics. For example, spindle cell tumors often appear as very large, unusually sharply defined pulmonary masses; irregular calcification is only an occasional feature of hamartoma; tracheobronchial papillomas may present with multiple areas of collapse or multiple large cavitary lesions. Even metastatic lesions may fail to follow expected patterns. Indolence, cavitation, calcification, bronchial mucosal lesions, and arterial deposits lend interest to the radiographic aspects of these common lesions.

205. Cervical spine trauma: a practical guide to diagnosis. Gehweiler JA Jr. The diagnosis of cervical spine trauma is a diagnostic enigma to many radiologists and surgeons. In this refresher course we will cover the following topics: (1) methods of filming the acutely injured patient, (2) significant indirect and direct signs of trauma, and (3) fractures and dislocations including classification, causes and mechanisms of injury, radiographic diagnosis, and differential diagnostic problems.

206. Noninvasive diagnosis of carotid artery disease. Ackerman RH. This course will review current instrumentation and concepts in noninvasive diagnosis of carotid disease. Among the tests to be covered are directional Doppler ultrasonography, thermography, oculoplethysmography, phonoangiography, ultrasonic arteriography, and real-time ultrasound scanning of the carotid. The discussion will include current concepts on the relative efficacy of these tests, the design of a cost-effective battery, and the role of noninvasive diagnosis in the management of patients with cerebrovascular lesions.

207. The radiographic diagnosis of acute injuries of the lower cervical spine. Harris JH Jr. This course will discuss acute traumatic lesions of the lower cervical vertebrae (C2–C7). The presentation will include a description of the appropriate radiographic examination, a review of the radiographic anatomy of the lower cervical segments, and a classification of acute injuries based upon (1) the mechanism of injury and (2) their stability at the time of the acute injury.

208. See 108

209. CT of the body and thorax. Knight L. This course will stress the diagnostic uses of CT in the abdomen and thorax, but a short review of its uses in musculoskeletal problems will also be presented. This will be a review of the state of the art including correlation with the clinical history as well as with other radiologic studies.

210. The alimentary tract: radiologic vignettes. Martel W. A variety of instructive lesions will be presented. Some illustrate conditions which are often misdiagnosed, such as gastric pseudotumors, or missed entirely, such as internal hernias. Conditions which are relatively common will be emphasized, and differential diagnosis and pathologic correlation will be stressed.

211. What every radiologist should know about the ear. Potter GD. The radiographic examination should be keyed to the particular condition of each patient, such as congenital atresia, trauma, inflammatory disease, and neoplasm. The radiographic description of these conditions will be presented in contrast with normal radiographs and tomograms. The information which the radiologist should include in his report to the treating physician will be discussed.

212. Problems of the immature infant. Reilly BJ. An increasing number of very small infants are being admitted to intensive care units, and their chances of survival have improved dramatically over the past few years. There are problems, however. Assisted ventilation, umbilical catheterizations, central venous lines for alimentation, endotracheal, nasogastric, and nasojejunal tubes, a propensity to bleed, and the insidious development of metabolic bone disease are some of the obstacles that have to be overcome by these very small babies. The radiologist must be aware of and monitor the complications likely to arise from these various intrusions and deficiencies.

301. Comparison of radionuclide, ultrasound, and CT imaging of the abdomen. Siegel B, Koehler RE, Melson GL. The availability of three new radiologic techniques for evaluation of abdominal lesions may cause considerable confusion. Each technique has strengths and weaknesses which significantly affect suitability in a particular clinical setting. CT imaging provides excellent anatomical detail. It is, however, a relatively expensive examination which cannot provide much physiologic information. Ultrasound is more readily available, is less expensive, but requires greater technical skill and also lacks physiologic information. Nuclear imaging techniques have poor spatial resolution, may require time delay, but provide physiologic information which may be of critical diagnostic importance. Illustrative cases will be used to emphasize the utility, limitation, and interactive relationship among these modalities.

302. Algorithmic approach to radiologic diagnosis of suspected pancreatic disease. Freeny PC. Once referred to as the hidden organ, the pancreas is now one of the most radiographically visible organs in the body. The wide variety of radiologic procedures available for examination of the patient with suspected pancreatic disease makes it difficult to decide how many and in what order these procedures should be utilized. This course is designed to help answer these questions by presenting algorithmic approaches for the evaluation of patients with suspected pancreatic neoplasm or pancreatitis. Examinations will be discussed in the context of the algorithms with emphasis upon the value, indications, and interpretation of each procedure.

303. See 203

304. See 204

305. Computed tomography of the brain. Gold L. A complete and comprehensive discussion of the principles and techniques of CT scanning will be presented. Neuroanatomy will be dealt with in detail. The course will be amply illustrated with a wide assortment of pathologic material from the University of Minnesota Hospitals.

306. Hydrocephalus in children: old principles, new philosophies. Harwood-Nash DCF. The establishment of the diagnosis of hydrocephalus is basically a clinical one of progressive megalencephaly in the child assisted by an assessment of the skull radiograph, the identification of ventriculomegaly, and the identification of a cause if possible. Unfortunately, large ventricles do not necessarily mean hydrocephalus and, furthermore, most radiographic techniques provide a static image at a specific period in time. This course defines hydrocephalus, outlines a practical classification, and discusses causes, with particular attention to their clinical application rather than merely their identification. The new perspective provided by computed tomography will be compared to other neuroradiologic procedures. Furthermore, the strength of computed tomography is increased with the concomitant use of metrizamide, both in anatomic identification and physiologic evaluation of intracranial structures. Computed tomography has also allowed us to evaluate the presence and causes of hydrocephalus in the very small infant, that is, the premature weighing from 600–2,000 g. Of equal significance is the ease and accuracy by which computed tomography is able to evaluate the possible presence of postshunt complications.

307. Inflammatory diseases of the colon. McLelland R, Thompson WM. The radiologic and pathologic features of ulcerative colitis, granulomatous colitis, and diverticular disease will be presented. Significant anatomic and physiologic considerations will also be discussed. Problem cases, unusual examples, and differential diagnosis will be shown to demonstrate the importance of clinical-pathologic correlation. With this approach, a precise diagnosis can be made in most instances.

308. Computed tomography of the skeletal system and soft tissues. McLeod RA. The difference between the density of bone and soft tissue and the absence of motion artifacts makes the skeletal system well suited for CT examination. It has proven useful in the evaluation of patients with primary bone neoplasm and those with skeletal metastases. It is also helpful in suspected recurrences of previous resected bone tumor, meningoceles, selected joint diseases, fractures, and other skeletal abnormalities. Both routine radiography and xerography have significant limitations as methods for studying soft tissue abnormalities. In our opinion CT has already proved to be superior to these modalities for imaging soft tissues. Our use of CT in this area has been almost exclusively to evaluate the patient with a suspected or known soft tissue mass. CT has also proved valuable in searching for possible pulmonary metastases in a patient with a known malignancy. This course will summarize our clinical experience with CT examination of these areas up to the present time. Emphasis will be on the clinical indications and usefulness.

309. Radiologic diagnosis: a horse-sense approach. Thornbury JR. The aim of this course is to teach radiologists to improve the accuracy of their diagnoses and choice of examinations in solution of clinical problems. Radiologists work in a diagnostic world that involves reliance upon their intuitive subjective probabilities to make diagnoses and patient management recommendations to their referring colleagues. Radiologists' performance has been shown to be improved if they understand better the diagnostic process and if they take into account the consequences of their diagnostic decisions in daily practice. The contents of the course includes the following: (1) the radiologist as a diagnostic consultant; (2) experimental evidence showing that radiologists' performance can be improved; and (3) how to apply large case series experience in the literature to individual cases.

310 and 410. Anatomic approach to radiology of the thorax (part I) and the abdomen (part II). Kazam E, Whalen JP. This course will deal with the anatomy of the thorax and abdomen as displayed by sectional imaging procedures (CT and ultrasound). Sections of cadavers in the horizontal, sagittal, and coronal planes will be correlated with normal and pathologic anatomy as demonstrated by CT, ultrasound, and conventional radiologic techniques. We will then discuss the place of ultrasound and CT in the radiologic workup of patients in different clinical settings. For various disease states flow charts will be presented reflecting our experience with the newer modalities compared to conventional techniques.

311 and 411. Mammography, parts I and II. Wolfe JN. The following subjects will be discussed: (1) the diagnosis of carcinoma with some emphasis on differential diagnosis of various breast abnormalities which can simulate carcinoma; (2) risk for developing breast carcinoma; and (3) selected short subjects (skin abnormalities, axilla, calcifications, circumscribed masses) with emphasis on problems in diagnosis. The subject of the radiographic diagnosis of carcinoma of the breast will be discussed at some length with emphasis on the subtle signs and problems. Some of the recent work done at Hutzel Hospital regarding the prediction of risk for developing breast cancer on the basis of mammography will be presented. Most of the graphic material will be xeroradiographs. We will be discussing morphologic changes, and there should be no problem in the translation of information from the x-rays to conventional film mammography.

312. The pulmonary circulation and the radiologist. Simon M. Radiologic changes involving the pulmonary vessels, the lung parenchyma, the pleura, and the heart reflect abnormalities of the pulmonary blood circulation. As a result of correlative studies these changes can now be translated into a large spectrum of hemodynamic derangements. Not only can the type of derangement be diagnosed, but the severity of any particular derangement can be estimated. It is important for the practicing radiologist to be familiar with these changes. They enable one to identify and quantify the order of magnitude of pulmonary venous hypertension, pulmonary arterial hypertension, and other states of altered blood flow in the lungs. Early recognition

of left ventricular decompensation, its severity, and its response to treatment are proving particularly helpful in everyday clinical practice. The progression or response to treatment of a hemodynamic disturbance can be followed by evaluation of a routine chest radiograph.

Until now the emphasis has been on the evaluation of pulmonary vascular pressures. Currently, we have become more concerned with changes in pulmonary blood flow, and the relationship between pulmonary vessel caliber and flow is now being defined. It is now possible to formulate general biologic principles underlying this aspect of the function/structure response.

The seminar will include the following: (1) a review of the basic physiology of the circulation, focusing upon radiologic aspects; (2) a comparison of the potentials and limitations of clinical and radiologic methods of evaluating the pulmonary circulation; (3) criteria for identifying and quantitating changes in blood flow in the lungs, local, regional, and generalized, as the basic key to understanding the pulmonary circulation; and (4) the current status of radiologic interpretation of pulmonary vascular pressures, resistance, and flow. If time permits, registrants will be invited to apply these concepts to a series of selected "unknown" cases.

401. A comparison of CT and radionuclide imaging in central nervous system disease. Christie JH, Chiu LC. This course will review the present status of CT and radionuclide imaging of pathologic conditions of the brain. Discussion will include correlation of the two techniques with regard to the pathophysiological changes of central nervous system disease. In certain disease states, one method is clearly superior to the other; while in some conditions, both studies are efficacious and each method complements the other. Special emphasis will be on the role and comparative value of each in patient diagnosis.

402. An introduction to diagnostic ultrasound. Goldberg BB, Cole-Beuglet C. Diagnostic ultrasound has assumed ever increasing importance in medicine, particularly as an adjunct to many radiologic procedures. This course will provide information on the diagnostic uses of ultrasound utilizing all four established modes of display, that is, A-mode, M-mode, Doppler, and B-scan including gray scale. The basics of physics and instrumentation will be provided. The established uses of ultrasound in all areas of the body, including the head, chest, abdomen, and pelvis, will be emphasized. A course outline as well as a list of available books will be distributed.

403. Interventional angiography. Goldman ML. Because of the ability of the angiographer to place catheters in close proximity to a site of abnormality, angiography is becoming more and more an interventional method for the delivery of local or regional therapy. A spectrum of the role of therapeutic angiography will be presented. Specific topics to be discussed include (1) massive intestinal bleeding: pitressin and embolization therapy with Gelfoam and tissue adhesives; (2) the transjugular technique: an important adjunctive procedure for liver biopsy, cholangiography, and obliteration of esophageal varices; (3) pancreatic aspiration biopsy; (4) neoplastic therapy: chemoinfusion, embolization, and yttrium-90; (5) transluminal angioplasty; (6) retrieval of foreign bodies; and (7) medical splenectomy.

404. Radiation exposure and risks—in perspective. Gray JE, Muhm JR, Brown ML. A large volume of information in the recent scientific literature and lay press concerns the risks associated with radiation exposure. In many instances this has had a detrimental effect on the ordering of diagnostic radiologic examinations for both the referring physician and the patient. The question of risks associated with diagnostic x-ray procedures will be presented, including discussions of the risks associated with prenatal exposure and with nuclear medicine examinations. Effective and inexpensive methods for reducing radiation exposure will be presented. In addition, the potential risks associated with diagnostic radiologic procedures will be presented in terms of everyday risks which are more easily understood by the referring physician and concerned patient.

405. Computed tomography of the thorax. Heitzman ER. It is becoming evident that computed tomography of the thorax is an important and valuable diagnostic adjunct. Indications for the use of this technique are being formulated and refined, but it is clear that there are certain specific situations in which the study has unique advantages. The following indications in the mediastinum will be illustrated and discussed: (1) evaluation of the mediastinum which is abnormal or questionably abnormal on standard radiographs; (2) evaluation of tumor extent and localization especially as an adjunct to staging of neoplasm; (3) evaluation of the hilum which is abnormal or questionably abnormal on standard radiographs; (4) evaluation of lesions partially hidden or questionably hidden on standard radiographs; (5) evaluation of tissue density of lesions by determination of their attenuation coefficients; (6) identification of the mediastinum which is widened by fatty infiltration or prominent great vessels; and (7) evaluation of the diaphragmatic crura as a means of assessing presence for extent of tumor crossing the thoracoabdominal junction. CT of the lung for the evaluation of the pulmonary nodule will be discussed, as well as study for the evaluation of pleural disease. In addition, comments will be made concerning preliminary observations in the determination of overall lung density by evaluation of the attenuation coefficient.

406. and 506. Skeletal radiology—new concepts and provocative challenges, parts I and II. Jacobson HG, Siegelman SS. These two courses will cover a variety of areas in skeletal radiology. One segment will be devoted to a consideration of three major topics: interesting and unusual manifestations of infective skeletal lesions, pseudomalignancies of the skeleton, and "leave-me-alone" lesions of the skeleton. A number of factors contribute to the changing pattern of pyogenic infective lesions of the skeleton. These include more recent prominence of certain pathogens, narcotic addiction, increasing travel, and effects of antibiotics. Increasingly encountered unusual radiologic features will be illustrated. A variety of skeletal lesions show a radiologic pattern which suggests a malignant neoplasm. The causes include developmental abnormalities, trauma, infection, metabolic and endocrine disorders, and other major categorical groups. The differential diagnosis will be stressed in each instance. A number of skeletal disorders show such definitive radiologic patterns that the radiologic diagnosis is virtually definitive and not subject to challenge. In such instances biopsy is not only unnecessary but costly, time consuming, and subject to complications. Even more important, an unnecessary biopsy is fraught with the possibility of an erroneous histologic interpretation, leading to dire consequences (e.g., amputation). Thus the term "leave-me-alone" lesion is suitably applied. Illustrative material will relate to major etiologic groups (e.g., developmental, traumatic, infective).

Another segment of these courses will demonstrate that the skeleton and soft tissues often exhibit a response or series of characteristic patterns associated with a variety of endocrine and metabolic disorders. A number of radiologic features will be analyzed in terms of their pathophysiologic mechanisms. In this connection infarction of bone, calcification in cartilages and soft tissues, cortical thinning, marrow expansion, metaphy-

seal lucencies, pseudocallus formation, osteoid seams, osteosclerosis, and Wormian bones will be considered. It will be stressed that the diagnosis of the endocrine and metabolic disorders to be considered can be established in most instances by careful evaluation of the radiologic changes. An evaluation of the current status of computed tomography in the demonstration of various lesions of the skeleton will be considered and its efficacy discussed. The role of CT scanning in the detection of soft tissue masses, principally associated with skeletal lesions, will be emphasized.

A sizeable amount of the material illustrated in these courses will be presented against a background of the "test-teach-test" concept. Course registrants will be encouraged to offer diagnostic possibilities for many of the cases in each entity on a completely voluntary and anonymous basis. The concept that the answer is usually on the film, even in the most difficult of cases, will be stressed. Since the learning process is closely related to challenge, it is anticipated that the case material presented in this group of disorders will prove sufficiently stimulating and the gratifications inherent in offering the correct diagnosis sufficiently rewarding to ensure a meaningful learning experience.

407. Current concepts in the anatomy, pathology, and radiology of the male lower urinary tract. McCallum RW. Normal gross and microscopic anatomy of the prostate and urethra will be shown, with particular emphasis on three urinary sphincters (two smooth muscle, one striated muscle) in the posterior urethra. The methods for radiologic examination of the lower urinary tract will be discussed and the important normal radiologic landmarks of the urethra will be emphasized. A presentation of the radiology of urethral pathology will be followed by a short discourse on the radiologist's role in the assessment of lower urinary tract injury in the fractured pelvis. A new radiologic classification of urethral injury in fractured pelvis will be stressed. The radiologic assessment of patients with neurogenic bladder and the radiologist's contribution to the management of such patients will be discussed.

408. Basic principles of computed tomography. Payne JT, McCullough EC. This course will cover the fundamentals of computed tomographic (CT) scanning. Physical principals of obtaining CT images will be discussed. Gantry design from first through fourth generation units plus additional hybrid units will be covered. Various console display characteristics along with their utility will be reviewed. Image quality and performance analysis for CT will be covered. The practical aspects and implementation of a quality control program will be discussed. Radiation dose from CT scanning will be reviewed in light of radiation dose in other areas of diagnostic radiology.

409. Renal ultrasound: current concepts. Rosenfield AT. A logical approach to nephrosonography will be defined. Gray scale ultrasound can define intrarenal structures which could not previously be visualized permitting the identification and characterization of a large number of renal disorders. The normal calyces and infundibula can be appreciated within the renal sinus and evaluated for abnormalities. Optimal techniques to evaluate the renal sinus including proper gain settings and the role of hydration and ureteric compression will be presented. The ultrasonographic demonstration of normal parenchymal anatomy including cortex, medulla, and arcuate vessels will be discussed and the best technique to show this anatomy demonstrated. Criteria and differential diagnoses of type I parenchymal abnormalities, in which the echo intensity within the cortex is increased and corticomedullary definition improved, and type II parenchymal abnormalities, in which there is a focal or diffuse disruption of normal parenchymal anatomy, will be presented. Physical principles and pitfalls in renal ultrasound will be discussed. The application of Doppler and real time ultrasound to the kidney and renal vessels will also be covered.

410. See 310

411. See 311

412. Skeletal trauma in infants and children. Wilkinson RH. Trauma to the immature skeleton may be acute, chronic, and sometimes only physiologic. There is surprising plasticity to the child's skeleton so that bones may bend rather than break. Epiphyseal injuries are common and are often subtle. However, recognition of them is important because of the possibility of subsequent disturbance of normal growth. These and other features of skeletal trauma in infants and children will be discussed.

501. Radionuclides and the thyroid gland. Maynard CD, Cowan RJ. The major radionuclide diagnostic test suitable for evaluation of the patient with suspected thyroid pathology will be discussed in detail. The principles involved and technical aspects of the procedures will be covered, but emphasis will be placed on the interpretation and clinical application of the results. Topics will include thyroid imaging procedures: thyroid uptake studies, including modifications of suppression, stimulation, and perchlorate discharge, and standard serum-assay determination.

502. Balanced radiology services on a tight budget. MacEwan DW. Radiology imaging in the United States and Canada is at another crossroad. Technologic advance to meet vital patient needs must now confront fiscal restraint and demanding questions of quality and efficacy. Cost restraint arrived early in Manitoba. Clinical problems in the breast, colon, biliary system, brain, pregnancy, and vascular abnormality are presented with unique information concerning the incidence of disease, total medical services for the care of these patients, and how radiology facilities were developed. The actions taken by government, hospitals, the medical faculty, and private radiology may indicate the route that others in North America may have to follow to solve such problems.

503. Everything you ever wanted to know about running a radiology department but were afraid to ask. Jarower ML. This course will review the day-to-day operations of a radiology department. Specific subject areas to be discussed include patient scheduling; division of functions between radiologic examination rooms; file room operation; and secretarial functions. The talk will be informal with considerable audience participation.

504. Tricks and treats in tomography. Kattan KR. The course describes the different pitfalls in tomography and how to avoid them. The law of tangent is stressed and its clinical applications are described. Mention is also given to the application of law of tangent to a curved surface. Parasitic and phantom shadow formations are explained in diagrams and clinical examples of each are given. The importance of proper rotation of the patient and the proper direction of the tube in order to decrease distortion of the image is mentioned. This is feasible only if proper examination of the study is initiated. Conventional radiography (and sometimes fluoroscopy) is done before initiation of the tomographic study. The various tube movements, the different thickness of the cut, and the degree of spacing between the cuts in different studies are reviewed.

505. Cardiac ultrasound. King DL. Discussion will include conventional techniques of echocardiography, real-time imaging, and newer advances in technology. Routine clinical applications and clinical reporting of derived diagnostic information will be emphasized.

506. See 406

507. Radiologic-pathologic correlation of interesting lesions of the gastrointestinal tract. Marshak RH. Interesting cases involving the stomach, small intestine, and colon will be presented with their pathologic counterparts. Time permitting, these will include the following entities: polypoid lesions of the stomach, superficial spreading carcinoma, Menetrier's disease, the "narrowed stomach," and the various forms of gastritis. Tumors, immunoglobulin deficiency diseases, retractile mesenteritis and related entities, ischemic disease, and lymphosarcoma of the small bowel will be presented. Colonic lesions will include lymphosarcoma, scirrhous carcinoma of the colon, colitis cystica profunda, Kaposi's sarcoma, amebiasis, colonic polyps, and newer concepts of diverticular disease. The possible etiology and management of some of these difficult cases will be discussed. Differential diagnosis and pathologic features will be stressed.

508. Obstructive lesions of the alimentary tract in the newborn and young infant. Singleton E. The course will describe practical methods for radiologic examination of the intestinal tract of infants and recalcitrant children. Specific anomalies of the esophagus and upper gastrointestinal tract will be discussed plus congenital abnormalities of the colon, anorectal anomalies, and acquired obstructions in the young infant. The section on the esophagus will cover both congenital anomalies and functional problems of deglutition and esophageal motility. The upper gastrointestinal tract portion of the course will include a discussion of congenital gastric and pyloric lesions, and upper small intestinal and lower small bowel obstructions. Congenital abnormalities of the colon include atresia, meconium plug syndrome, meconium ileus, aganglionosis, and the small left colon syndrome. Also detailed will be such acquired obstructions as hypertrophic pyloric stenosis, post necrotizing enterocolitis, and intussusception.

509. Gastrointestinal applications of computed tomography. Stephens DH. The goal of this course is to provide the radiologist with a thorough understanding and practical approach to computed tomography of the gastrointestinal system, especially of the liver and pancreas. The diagnostic accuracy of CT depends on proper performance of the examination and knowledgable interpretation of the results. Useful CT techniques and the various presentations of normal and pathologic anatomy will be discussed and illustrated. The capabilities and limitations of CT will be considered as well as some of the common diagnostic errors and how they might be avoided. Where appropriate, CT will be correlated with other radiologic methods. Specific conditions to be covered are space-occupying lesions of the liver, abnormal biliary tree, diffuse liver disease, pancreatic neoplasms, pancreatitis, abdominal abscesses and effusions, and extraluminal lesions of the alimentary canal.

510. Neonatal chest problems. Swischuk LE. The radiologist plays a key role in the diagnosis of neonatal chest disease. His basic job is to determine whether a surgical or medical condition exists, but many times this can be problematic. It is not so much that one is not familiar with such conditions as hyaline membrane disease, TRDN-wet lung syndrome, congenital diaphragmatic hernia, meconium aspiration, etc., but rather that one is often not able to come up with a useful differential diagnosis for certain abnormal radiographic patterns. For example: What does one think of when one is presented with: (1) a large, opaque hemithorax; (2) a large, hyperlucent hemithorax; (3) a small, densely opaque hemithorax; (4) a small, slightly opaque hemithorax; (5) bilateral fluffy infiltrates; (6) bilateral bubbly lungs, small bubbles, large bubbles; (7) bilateral granular lungs; or (8) bilateral parahilar, streaky, congested appearing lungs? Each disease will be dealt with in enough detail to allow differentiation of one from the other, but grouping according to abnormal pattern is the place to start.

511. Exercises in the analysis of the unknown lesion in bone. Theros EG. Careful evaluation of destructive and reparative processes, including the periosteal reactions, will provide intrinsic data which accurately reflect the nature of the processes acting on the host bone. Once these are appreciated the possibility of specific histologic labels may be entertained. A number of lesions have been selected which will be approached as though they were "unknowns" to this instructor who will verbalize his analytical thought processes in ruling in and ruling out certain possibilities. The evaluation will stress the general morphology as well as the location, size, shape, and general extent of the lesion, since these factors taken together may corroborate to allow further differentiation and often a definitive diagnosis.

Herman C. Sehested, 1901–1978

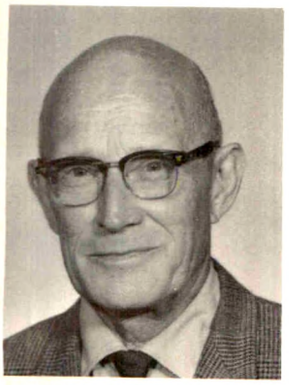

Herman C. Sehested

Herman C. Sehested died in Fort Worth, Texas, on January 3, 1978, at the age of 76. He graduated from the University of Oklahoma College of Medicine in 1931 and did family practice in Tyler, Texas, until 1942 when he joined the Army Air Corps in World War II where he attained the rank of lieutenant colonel. He completed his residency in radiology at the University of Oklahoma in 1946 and came to Fort Worth to practice in 1948, joining Tom B. Bond and myself.

Sehested was an excellent radiologist, especially in the diagnostic field, and a fine and much respected colleague. He was a fellow of the American College of Radiology and served as a counsellor of the College of Radiology in the Texas area. He was a member of the American Roentgen Ray Society and served with distinction as president of the Texas Radiological Society and later also as secretary.

His activities included tracking satellites for the Smithsonian Institute, and he received many awards. He was a member of the University Baptist Church in Fort Worth, Texas. He is survived by his wife, Len, a son, Howard, and four grandchildren.

Maurice C. Archer
Fort Worth, Texas 76104

Percy Douglas Hay, 1899–1977

Percy Douglas Hay died August 5, 1977, at the age of 78, from complications of rheumatoid arthritis. He was born in Beaufort, South Carolina, and graduated from the College of Charleston and the Medical College of South Carolina. After completing his radiologic training at the University of Pennsylvania with Drs. Pancoast and Pendergrass, he organized the Department of Radiology at the McLeod Infirmary, Florence, S. C., and remained as its director until his retirement in 1970. He was on the staffs of the Saunders Memorial and Bruce Hospitals in Florence, and organized a school of radiologic technology.

Hay was a charter member and president of the South Carolina Radiological Society. He organized the State Cancer Clinic and remained its director for many years. He was a member of the county and state medical society as well as the American Medical Association, American Roentgen Ray Society, and the Radiological Society of North America. He was also a fellow of the American College of Radiology.

Hay spent most of his free time rebuilding and improving x-ray equipment. His altered circuits and many unique devices constantly puzzled repairmen. He also invented the Hay periscope used in treatment of intracavitary lesions. He built and used a portable x-ray unit that fit into a small carrying case. Many of his radium applicators and molds were in constant use as he treated cervix, mouth, and skin lesions. Other interests included photography and music. He was a charter member of the Florence Symphony and played violin until he was disabled. He was a lifetime trustee of the Florence Museum and a member of the St. Cecilia Society of Charleston.

Hay wrote the book, *The Neck*, which was volume 9 of the *Annals of Roentgenology*, a series of monographic atlases. He is survived by his wife, Lucille, one son, and a granddaughter.

Tom M. Fullenlove
San Francisco, California 94108

M. Wendell Dietz, 1922–1977

M. Wendell Dietz died at his home in Escondido, California, on July 1, 1977, after a short illness. He was born in Harrisburg, Pennsylvania, on January 15, 1922, and graduated from the University of Pittsburgh School of Medicine in June 1945. He served his residency in radiology at Baltimore City Hospital and John Hopkins Hospital, Baltimore, Maryland.

After being an Instructor in Radiology at John Hopkins University School of Medicine for a year, he became Director of the Department of Radiology at the Burge-Protestant Hospital, Springfield, Missouri, until 1968. In 1969 he became Director of Radiology at the Fallbrook (California) Hospital District, a position he held until his death.

Dietz was a fellow of the American College of Radiology, and a member of the American Roentgen Ray Society, Radiological Society of North America, Missouri State Radiological Society, American Medical Association, and Southern Medical Association. He served in the United States Navy as a lieutenant commander stationed at the Philadelphia Naval Hospital and at the National Naval Medical Center, Bethesda, Maryland. He is survived by four children.

James R. Lash
Fallbrook, California 92028

J. Richards Aurelius, 1897–1977

J. Richards Aurelius

J. Richards Aurelius died on September 4, 1977, at the age of 80. He was born in Saint Paul, Minnesota, and attended the University of Minnesota, receiving his medical degree in 1923. He received postgraduate training in radiology at the Mayo Clinic from 1925 to 1927, where he was one of the last fellows to receive an appointment to the department headed by Russell Carmen.

After his training, Dick joined Ancker, Midway, and Mounds Park hospitals in Saint Paul. This association continued until his retirement in 1970. In 1945, the Radiology Department at Ancker Hospital became associated with the University of Minnesota Radiology Training Program under Leo Rigler. Dick became a clinical professor in the Department of Radiology from which he retired in 1966.

He was a member of many societies including the Radiological Society of North America, American Roentgen Ray Society, and American College of Physicians. He was president of seven societies including the Ramsey County Medical Society and Minnesota Radiological Society. He received numerous awards but was most pleased with receiving the Diehl Award in 1972 given by the University of Minnesota Alumni Association. Survivors include his wife, mother, and three brothers.

Donald H. Peterson
St. Paul, Minnesota

Clarence Peter Truog, 1901–1978

Clarence Peter Truog died in his sleep on May 8, 1978. He was born in Minnesota and never forgot his farm background or his hardworking, thrifty Swiss ancestry. After finishing college and medical school at the University of Minnesota in 1929, he married Catherine Palfrey. She was a woman of rare intelligence, grace and Welsh wit, deceased in 1974.

He interned in Minneapolis and then did general practice at Lindstrom, Minnesota, for 5 years, returning to the University of Minnesota in 1935 for a residency in radiology and later a doctorate in radiology under Leo Rigler. After a brief period of hospital radiology in Miami, he entered the Army Medical Corps in 1942, receiving a medical discharge as a major in 1943. Truog then practiced at Grace Hospital in Detroit and at the Leila Post Hospital in Battle Creek before moving to Grand Rapids, Michigan, where he established a practice which is now a nine man partnership. He retired in 1973 but still filled in when needed and kept up an active interest in diagnostic radiology.

Minnesota knew him as Clarence, but he was Pete in Michigan. The short, vigorous nickname suited his personality. He was not large physically but possessed tremendous energy which poured forth constantly into a very active life. His fishing and hunting trips ranged from Minnesota and western Michigan to Canada, Alaska, India, and Africa. He was long an active member of the National Ski Patrol and skied in Michigan, Colorado, and the Alps.

Troug was a Fellow of the American College of Radiology and a member of the American Roentgen Ray Society, Michigan Radiological Society, the Radiological Society of North America, and the Kent County, Michigan, and American Medical Societies. He is survived by two sons, a daughter, and six grandchildren.

Benjamin R. Van Zwalenburg
Grand Rapids, Michigan

Abstracts of Current Literature

Chest

Bronchial atresia. Meng RL, Jensik RJ, Faber LP, Matthew GR, Kittle CF (Department of Cardiovascular-Thoracic Surgery, Rush-Presbyterian-St. Luke's Medical Center, 1753 West Congress Parkway, Chicago, Illinois 60612). *Ann Thorac Surg* 25:184–192, March 1978

Bronchial atresia is a rare congenital anomaly characterized by bronchial obstruction, mucoid impaction, and hyperinflation of the distal lung. The authors present an excellent example of this lesion, diagnosed both radiographically and pathologically, and review 33 previously reported cases. Bronchial atresia is felt to result from a vascular insult to the developing lung between the fifth and fifteenth gestational week. The bronchial tree distal to the obstruction is normal, but alveoli and respiratory bronchioles are abnormally few. Accumulation of mucous, at the base of the obstructed bronchus, produces a cyst-like mass referred to as a "mucocele." Although the mucocele is isolated from the proximal bronchial tree by the atretic bronchial segment, rudimentary bronchial communications can exist. Distal lung is emphysematous because of collateral ventilation.

This anomaly is most often diagnosed in the second decade, and a majority of patients are asymptomatic. Bronchial atresia most often occurs in the left upper lobe (65%) and the right lower lobe (20%), most commonly with segmental involvement. The mucocele is radiographically visible as an oval, fingerlike, or branching density in the distribution of the bronchial tree. Bronchography best demonstrates the site of bronchial obstruction and fluoroscopy reveals air trapping distal to the mucocele. The differential diagnosis includes mucoid impaction, bronchial adenoma, carcinoma, benign bronchial tumor, sequestration, and bronchogenic cyst. A majority of patients are treated with surgical excision to prevent atresia-related complications such as compression of the adjacent normal lung or mucocele infection.

W. Richard Webb
P. H. Levesque

Chest dimensions in young adults with spontaneous pneumothorax. Peters RM, Peters BA, Benirschke SK, Friedman PJ (Department of Surgery, University Hospital, 225 West Dickinson Street, San Diego, California 92103). *Ann Thorac Surg* 25:193–196, March 1978

It has long been felt that spontaneous pneumothorax is most common in tall and asthenic people with long, narrow chests. This study evaluated the validity of this hypothesis. Forty-six patients with spontaneous pneumothorax were studied; they ranged in age from 17 to 30 years, 34 were men. Six chest dimensions and several height-to-width ratios were measured from standard posteroanterior and lateral chest radiographs in both the patients with pneumothorax and in a group of age and sex-matched controls. In men with pneumothorax, some vertical dimensions of the right lung and the ratio of height to width of the chest were significantly larger than in the male controls ($p < 0.05$). However, it is of note that comparison of vertical dimensions of the left lung did not yield significant differences. The only significant difference found between female groups was a diminished anteroposterior diameter in patients with pneumothorax ($p < 0.05$).

Theoretical studies have related lung height to volume strain at the lung apex. Increased strain on the apical lung parenchyma in patients with long, narrow chests could result in the development of apical blebs and thus explain the increased incidence of pneumothorax thought to occur in asthenic people. Furthermore, the relatively common occurrence of pneumothorax in men could be related to their greater height and, therefore, taller lungs. However, we must emphasize that observed mean differences between study and control groups were small, measuring 1 cm or less, and that standard deviations were relatively large. Although some measurements show significant differences between groups, a good deal of overlapping must exist, and we question whether the observed differences would be radiographically detectable without detailed measurement.

W. Richard Webb
John R. Anderson

Cardiovascular

The clinical course of patients with suspected pulmonary embolism and a negative pulmonary arteriogram. Novelline RA, Baltarowich OH, Athanasoulis CA, Waltman AC, Greenfield AJ, McKusick KA (Massachusetts General Hospital, Boston, Massachusetts 02114). *Radiology* 126:561–567, March 1978

Selective pulmonary arteriography, with superselective magnification views of the lung bases or other areas where abnormalities are shown on perfusion lung scans, performed within 24-48 hours after the onset of symptoms, can effectively rule out clinically significant pulmonary thromboembolism. One hundred and eighty consecutive patients (minimum follow up, six months) with suspected pulmonary embolism and negative pulmonary arteriograms were studied. Not one of the 167 untreated patients died as a result of thromboembolic disease during the acute illness (20 died from unrelated causes), and none of the 147 patients who survived suffered "recurrent embolism" during follow up.

Author Abstract

The origin of the left gastric artery. Naidich JB, Naidich TP, Spraycgen S, Hyman RA, Pudlowski RM, Stein HL (North Shore University Hospital, 300 Community Drive, Manhasset, New York 11030). *Radiology* 126:623–626, March 1978

Five hundred celiac angiograms were reviewed to evaluate the frequency of clinically significant variations in the origin of the left gastric artery. In 13 of 500 cases, the left gastric artery arose anomalously most often as a direct branch of the aorta; in 14 of 500 cases, the left gastric artery primarily supplied the liver with only minor contributions to the stomach. An aberrant origin of the left gastric artery necessarily influences the angiographic diagnosis and therapy of gastrointestinal hemorrhage.

Author Abstract

Gastrointestinal

Trauma to the esophagus. Love L, Berkow AE (Foster G. McGraw Hospital, 2160 South First Avenue, Maywood Illinois 60153). *Gastrointest Radiol* 2:305–321, 1978

This review article classifies esophageal trauma into three categories: (1) iatrogenic; (2) self-induced; and (3) direct. The authors initially outline the anatomy of the esophagus and its relationship to other thoracic structures which assists in interpretation of the roentgen signs associated with esophageal injuries. Plain film, contrast esophageal studies, and angiographic findings are reviewed and illustrated. The statistical information available for the various types of esophageal trauma are presented; the article is well illustrated and adequately referenced.

Charles A. Rohrmann, Jr.

Small-bowel malabsorption and gastrointestinal malignancy. Collins SM, Hamilton JD, Lewis TD, Laufer I (I. Laufer, Department of Gastrointestinal Radiology, Hospital of the University of Pennsylvania, 3400 Spruce Street, Philadelphia, Pennsylvania 19104). *Radiology* 126:603–609, March 1978

In addition to lymphoma, there is an increased incidence of gastrointestinal carcinoma in patients with malabsorption due to celiac disease. This is frequently manifested by a loss of response to gluten withdrawal. Four such cases are described: one patient had lymphoma and the other three had cancer of the esophagus, jejunum, and pancreas, respectively. The literature indicates that carcinoma of the esophagus and small bowel is particularly common in patients with celiac disease. These findings suggest that celiac disease should be considered a premalignant condition and that such patients should undergo a regular radiographic survey to detect early cancer.

Author Abstract

The protean gastrointestinal manifestations of metastatic breast carcinoma. Chang SF, Burrell MI, Brand MH, Garsten JJ (Yale-New Haven Hospital, New Haven, Connecticut 06510). *Radiology* 126:611–617, March 1978

Although the more common sites of breast metastases include lymph nodes, lungs, bones, liver parenchyma, and brain, in one reported series of 337 patients with metastatic breast carcinoma, 16.4% had gut metastases of which 20% were symptomatic. Metastatic breast carcinoma may be silent for long periods subsequent to diagnosis and surgery. Gastrointestinal metastases may simulate specific gastroenterological entities and make diagnosis difficult. An example is achalasia due to infiltrating metastatic carcinoma. Other examples include metastases to the small intestine simulating malignant melanoma, lymphoma, and Kaposi's sarcoma by manifesting as "bull's eye" lesions. Other expressions have been linitis plastica of the stomach caused by metastatic carcinoma and simulating gastric carcinoma, metastases to the terminal ileum and colon simulating both granulomatous colitis and primary colonic carcinoma. The authors suggest a comprehensive history and the missing breast sign as clues to the etiology of such gastrointestinal manifestations and documented lesions.

Asher Nov

***Strongyloides stercoralis* colitis: findings in four cases.** Drasin GF, Moss JP, Cheng SH (Jewish Hospital, 217 Chestnut Street, Louisville, Kentucky 40202). *Radiology* 126:619–621, March 1978

Strongyloides stercoralis is a nematode. Nematodes burrow through the skin and enter the blood stream. In the lungs they mature to adolescence before migrating via the trachea and being swallowed. They are either passed out in the stool or invade small bowel mucosa and lay their eggs. Hatched eggs are either passed out with the stool or via autoinfection the new cycle begins. *Strongyloides stercoralis* infection is usually asymptomatic. Eosinophilia and malabsorption may be present. Reports of hyperinfection have appeared in patients with suppressed immune reaction due to systemic disease or steroid treatment. Barium radiographic findings consist of an ulcerating colitis, with both small and large ulcers, and loss of normal haustral pattern. Abnormality is noted throughout the colon and resembles ulcerative colitis. One of the four cases presented showed focal areas of narrowing. When the small bowel was involved, findings of submucosal edema, fluid, and slow transit time were present. In mild infection, minimal radiographic abnormalities may be present.

Asher Nov

Radiological characteristics of primary intestinal lymphoma of the "Mediterranean" type: observations on twelve cases. Ramos L, Marcos J, Illanas M, Hernandez-Mora M, Perez-Paya F, Picouto JL, Santana P, Chantar C. (Servicio de Radiodiagnostico, Clinica Puerta de Hierro de la Seguridad Social, San Martin de Porres, 4, Madrid-35, Spain). *Radiology* 126:379–385, Feb 1978

Primary intestinal lymphoma of the Mediterranean type as previously described has the following characteristics: (1) younger age group; (2) same rate of presentation in both sexes; (3) preferential location in the duodenojejunal area; (4) lack of alteration of the villi; (5) abnormal immunoglobulin in 15%–20% of cases; (6) histologically characterized by massive infiltration of the lamina propria by plasma cells. Radiologically, two groups were apparent. The first with symmetrical and diffuse thickening of the mucosal folds of the duodenojejunal region. The edges of the folds were irregular, with a "rat-bite" or "postage-stamp edge-like" appearance. The second group was characterized by a marked infiltrative nodular pattern. The folds were distorted and eccentric nodules were noted. In addition, intestinal walls were thickened and loops were separated by mesenteric lymph node masses. This entity should be kept in mind when proximal intestinal thickening and nodularity are noted and other entities such as celiac disease, lymphangiectasia, amyloidosis, eosinophilic enteritis, histoplasmosis, mast-cell disease, giardiasis, Whipple's disease, or Waldenström's disease are considered.

Asher Nov

Antacid titration in the prevention of acute gastrointestinal bleeding. A controlled, randomized trial in 100 critically ill patients. Hastings PR, Skillman JJ, Bushnell LS, Silen W *N Engl J Med* 298:1041–1045, May 11, 1978

This interesting study involved randomization of 100 critically ill patients to receive or not receive antacid prophylaxis to try to prevent gastrointestinal bleeding. Patients had severe respiratory failures, sepsis, peritonitis, and other severe illnesses. Patients with burns, gastrointestinal surgery, or active gastrointestinal bleeding were excluded from study. Antacids were administered by nasogastric tube on an hourly basis to reduce the gastric acidity to a pH above 3.5. Bleeding was measured by guaiac test on the nasogastric aspirates. Overall, there was a highly significant decrease in the frequency of gastrointestinal bleeding in the patients given the antacid treatment. Complications of the therapy were principally those of diarrhea, regurgitation, and elevation of serum magnesium levels in a few patients. For many clinicians it is gratifying to see this control study confirming the utility of a therapy which has become common practice in many medical centers. Because of the emergence of cimetidine as an alternate therapy for preventing ulcer bleeding in these patients, it is not clear which of these two types of therapy is best for the severely stressed acutely ill hospitalized patient.

David C. Dale
Department of Medicine
University of Washington

Prophylactic doxycycline for travelers' diarrhea. Results of a prospective double-blind study of Peace Corps volunteers in Kenya. Sack DA, Kaminsky, DC, Sac RB, Itotia JN, Arthur RR, Kapikian AZ, Ørskov F, Ørskov I *N Engl J Med* 298:758–763, April 6, 1978

Travelers' diarrhea often turns a romantic trip to an exotic locale into a miserable experience. For many years the cause for this misery was unknown. Recent studies, however, indicate that enterotoxigenic *Escherichia coli* are the most common causative agents in many parts of the world. In this study conducted on Peace Corps volunteers in Kenya, the efficacy of doxycycline (100 mg/day) was evaluated in the prevention of travelers' diarrhea in a randomized control study. The Peace Corps volunteers took either doxycycline or an identical placebo and maintained a diarrhea diary. When the code was broken, it was clearly shown that the doxycycline was effective in preventing this illness. Interestingly, the protective effective of the

antibiotics seem to persist for about a week after the drug is discontinued. In this study no problem with the emergence of resistant organisms was observed. The authors conclude that this form of antibiotic treatment is effective but cautioned that their study is a relatively small one from only one geographic area. They also caution that children with growing bones and teeth may be adversely affected by this form of prophylaxis and many other long term effects of chronic doxycycline may be yet unknown.

David C. Dale
Department of Medicine
University of Washington

Dose response to intramuscular glucagon during hypotonic radiography. Miller RE, Chernish SM, Brunelle RL, Rosenak BD (Indiana University, School of Medicine, Indianapolis, Indiana 46202). *Radiology* 127:49–53, April 1978

In a study to determine a dose response to glucagon during hypotonic duodenography, 15 male and female volunteers received placebo and 0.25 mg, 0.5 mg, 1 mg and 2 mg glucagon intramuscularly, double-blind and cross-over. When 0.25 mg glucagon was given, the onset of drug effect was approximately 13–18 min: the mean duration of moderate hypotonicity was approximately 4–7 min. The larger the dose, the greater the duration of drug action. When 2 mg glucagon was given, the onset of drug effect occurred in approximately 4–7 min; the mean duration of moderate hypotonicity was 22–32 min. There were no changes in pulse or blood pressure attributable to the drug with these doses, and reports of nausea and diarrhea did not increase significantly until a dose above 1 mg was given. One mg glucagon given IM is useful in hypotonic upper GI radiographic examinations. The onset of hypotonicity was 8–10 min with a duration of 12–27 min when this dose was given. Few reports of side effects were attributable to this dose.

Author Abstract

Pediatric Radiology

The right paratracheal stripe in children. Savoca CJ, Brasch RC, Gooding CA, Gamsu G (380-M, University of California, San Francisco, California 94143). *Pediatr Radiol* 6:203–207, Feb 1978

On frontal chest radiographs, the thin, soft tissue density between the trachea and adjacent right lung is referred to as the right paratracheal stripe. It is less frequently measurable in children than in adults, particularly if there is slight rotation into the left anterior oblique position. Studies of 150 normal chest films in children 5 months to 15 years found the range of normal to be 0.5 to 3.0 mm. Measurements of 4 mm or greater were found in patients with diseases of the trachea, the mediastinum, or the pleura.

B. J. Wood

Surgical advances in the treatment of lesions of the pediatric airway: the role of the carbon dioxide laser. Healy GB, McGill T, Strong MS (Department of Otolaryngology, Children's Hospital Medical Center, 300 Longwood Avenue, Boston, Massachusetts 02115). *Pediatrics* 61:380–383 1978

The carbon dioxide laser has enabled microsurgery to be accomplished in the pediatric airway transorally and transnasally. Choanal atresia, papillomas, hemangiomas, vocal cord nodules, polyps, and tracheal stenosis are among the lesions amenable to this form of treatment. Postoperative edema is minimal and there is little bleeding and minimal scarring.

B. J. Wood

CT whole-body scanning in pediatric radiology. Pedersen KD, Jensen J, Hertz H (X 2023, Rigshospitalet, Blegdamsvej, DK-2100 Copenhagen, Denmark). *Pediatr Radiol* 6:222–229, Feb 1978

A total of 57 examinations were performed in 28 children, aged 10 months to 14 years. Evaluation of tumor location, spread, and response were the most common uses. Respiratory motion was not found to be a problem, but intestinal peristalsis was, and an antiperistaltic drug was felt to be essential. Scanning of the abdomen produced a skin dose of 3.0 rad, and a gonadal dose of 2.4 rad. For uncooperative patients, sedation or general anesthesia was found necessary.

B. J. Wood

Imperforate anus and colon calcification in association with the prune belly syndrome. Morgan CL, Grossman H, Novak R. (Box 3334, Duke University Medical Center, Durham, North Carolina 27710). *Pediatr Radiol* 7:19–21, April 1978

Two patients with the prune belly syndrome demonstrated colon calcifications and anorectal malformations. Bladder outlet obstruction was present in both cases. Calcifications were also found in the renal collecting system and bladder of one patient. No fistula was demonstrated between the genitourinary tract and bowel in either infant at autopsy. The calcification in the colon and urinary tract is probably secondary to stasis.

Author Abstract

Thoracic and lumbar dural ectasia in a two-year-old boy. Katz SG, Grunebaum M, Strand RD (Children's Hospital Medical Center 300 Longwood Avenue, Boston, Massachusetts 02115). *Pediatr Radiol* 6:238–240, Feb 1978

Multiple paraspinal masses and widening of the interpedicular distance in the thoracic and lumbar spine were noted in a 2-year-old male presenting with failure to thrive and multiple minor anomalies. Metrizamide myelography showed the masses to be due to dural protrusions, and the spinal canal widening to be due to a dilated subarachnoid space. There was no evidence of neurofibromatosis.

B. J. Wood

Intraluminal calcifications in the small bowel of newborn infants with total colonic aganglionosis. Fletcher BD, Yulish BS (Division of Pediatric Radiology, University Hospitals of Cleveland, University Circle, Cleveland, Ohio 44106). *Radiology* 126:451–455, Feb 1978

The authors present four newborn infants who presented with symptoms of small bowel obstruction and abdominal calcifications. These calcifications were mostly noted in the right lower quadrant. They were multiple, punctate, round particles of 4–6 mm diameter. Barium enema demonstrated microcolon. At surgery, calcification was found to be intraluminal and histology showed total colonic aganglionosis. Other reports of intraluminal calcification in the newborn have been associated with intestinal stenosis or atresia, one case of functional ileal obstruction, and in patients with imperforate anus. Intraluminal calcification associated with long segment aganglionosis are assumed to be secondary to stasis. When intraluminal calcification is suspected, the diagnosis of total colonic aganglionosis or small bowel atresia should be considered.

Asher Nov

Renal transplantation in children ages 1 to 5 years. Hodson EM, Najarian JS, Kjellstrand CM, Simmons RL, Mauer SM (Box 491, Department of Pediatrics, University of Minnesota, Minneapolis, Minnesota 55455). *Pediatrics* 61:458–464, 1978

The authors report their experience with 23 renal transplants in 21 children aged 1–5 years. Most of the patients had a one stage bilateral nephrectomy and splenectomy and transplantation. Eighteen children received transplants from a living related donor; 14 received cadaver grafts. Four children died, three of

infection and one of rejection. Rejection caused loss of the graft in five patients, two of whom were retransplanted. Children with normal renal function grew after the transplant and in some, this was accelerated during the first posttransplant year. The authors conclude that transplantation under 1 year of age is usually not successful but that the results in the 1–5 year age group parallel those in older children with accumulative survival 2 and 4 years following living related donor transplantation of 94% and 76%, respectively.

B. J. Wood

Prolonged prostaglandin E_1 infusion in an infant with cyanotic congenital heart disease. Lewis AB, Lurie PR (Division of Cardiology, Childrens Hospital of Los Angeles, 4650 Sunset Boulevard, Los Angeles, California 90027). *Pediatrics* 61:534–536, 1978

Prostaglandin E_1 has been used on a short-term basis in patients with severe or complete right-sided obstructive lesions to increase the pulmonary blood flow and systemic oxygenation. The authors report intravenous infusion of prostaglandin E_1 for 29 days in a 1,010 g infant with a severe tetralogy of Fallot. Patency of the ductus arteriosus was achieved until surgery was performed.

B. J. Wood

Ultrasonics

Ultrasonic detection of nonopaque renal calculi. Pollack HM, Arger PH, Goldberg BB, Mulholland SG (University of Pennsylvania Hospital, Philadelphia, Pennsylvania). *Radiology* 127:233–237, April 1978

Four patients with five nonopaque renal calculi composed of uric acid were examined by ultrasound. The calculi varied in size from a 1.5 × 1.5 cm intrapelvic stone to a staghorn calculus measuring 4 cm. All stones were satisfactorily imaged by ultrasound, allowing a diagnosis of nephrolithiasis to be made with confidence in each case. In two patients with poor excretion on urography, the diagnosis was not suspected prior to the ultrasound examination. The authors feel that ultrasound has great potential value in the investigation of nonopaque filling defects of the renal pelvis and in patients with urographic nonvisualization who have a high risk of uric acid lithiasis.

Author Abstract

Parathyroid ultrasonography. Sample WF, Mitchell SP, Bledsoe RC (UCLA Center for the Health Sciences, Los Angeles, California). *Radiology* 127:485–490, May 1978

Gray scale ultrasound was used to evaluate patients with primary hyperparathyroidism. Twenty-one of the 25 parathyroid glands shown pathologically and anatomically to be greater than 5 mm in diameter were identified and varied between 6 and 15 mm. Although the nosological sensitivity was poor, the false-positive rate was low. Important anatomical limitations and pitfalls are described. The role of ultrasonography is compared to that of other noninvasive diagnostic modalities and related to specific clinical situations and surgical approaches.

Author Abstract

Adrenal ultrasonography. Sample WF (UCLA Center for the Health Sciences, Los Angeles, California). *Radiology* 127:461–466, May 1978

A 95% diagnostic accuracy was obtained in the prospective evaluation of 81 adrenal glands in 59 patients using gray scale ultrasound. Modifications of the scanning technique are described. A coronal plane is used on the left passing through the aorta and left kidney while the longitudinal section on the right side is evaluated scanning perpendicular to the right adrenal gland using the liver as a window. Further modifications and limitations of the technique as well as the role of ultrasound in relation to other noninvasive imaging modalities are discussed.

Stephen J. Carter

Ultrasonic study of the normal and dilated biliary tree. Weill F, Eisencher A, Zeltner F (University Hospital, 2 Place St. Jacques, 25000 Besancon, France). *Radiology* 127:221–224, April 1978

With the advent of real time scanners, segments of the normal biliary tree can now be seen regularly. Normally, the biliary junction is narrower than the portal vein or the portal division. With early dilatation of the bile ducts the diameters of the two systems tend to equalize. Thus, the presence of two parallel ducts with similar diameters is pathologic. As the dilatation of the biliary tree progresses, the portal system may become flattened, thus reversing the initial proportion between the diameter of the biliary junction and that of the biliary tree.

Author Abstract

Ultrasonography in the management of unexplained renal failure. Winston M, Pritchard J, Paulin P (VA Wadsworth Hospital, Los Angeles, California 90073). *JCU* 6:23–27, Feb 1978

The utility of renal echography in the evaluation of the patient with unexplained acute renal failure is illustrated by the authors with four cases of hydronephrosis, one case of previously undiagnosed polycystic kidney disease, one of bilateral renal artery thrombosis (normal appearing kidneys on the echogram), and one of small end stage kidneys secondary to glomerulonephritis. In each case, the excretory urogram was of limited or no value, because of poor or no visualization of the kidneys. The ability of the echogram to accurately demonstrate renal size, anatomy, and especially the presence or absence of a dilated collecting system in the face of renal failure, was extremely helpful in planning further diagnostic procedures or treatment.

John D. Denney

Radiation Oncology

Remineralization of enamel by a saliva substitute designed for use by irradiated patients. Shannon IL, Trodahl JN, Starcke EN (Oral Disease Research Laboratory, Veterans Administration Hospital, 2002 Holcombe Boulevard, Houston, Texas 77211). *Cancer* 41:1746–1750, May 1978

The authors describe the use of a saliva substitute, VA-OraLube in 125 xerostomic patients. The viscosity and electrolyte concentration are adjusted to approximate stimulated whole saliva. Also, microhardness measurements were accomplished on 60 extracted human bicuspids. Clinical acceptance by the xerostomic patients over the 4 month test period was very high. Subjective relief of intraoral soft tissue problems was virtually universal. The capacity of the saliva substitute to reharden enamel could be compared to that of fresh human whole saliva with fresh saliva exerting a 7.3% rehardening affect in two groups of teeth *versus* 5.5% and 5.2% for OraLube rehardened enamel.

Herbert C. Berry

The relation between estrogen receptors and response rate to cytotoxic chemotherapy in metastatic breast cancer. Lippman ME, Allegra JC, Thompson EB, Simon R, Barlock A, Green L, Huff KK, Do HMT, Aitken SC, Warren R (10/6B02, Medicine Branch, National Cancer Institute, National Institutes of Health, Bethesda, Maryland 20014). *N Engl J Med* 298:1223–1228, June 1, 1978

A retrospective study is described in which the authors attempt to define a relationship between lack of estrogen receptors and likelihood of response rate to cytotoxic chemotherapy in 70 patients with metastatic or surgically unresectable primary breast cancer. Of the 45 patients with low or absent

estrogen-receptor values, 34 had objective responses to chemotherapy . Of the remaining 25 patients with positive estrogen-receptors, only three had responses to chemotherapy ($p < 0.0001$). The two groups were compared with regard to several characteristics including age, menopausal status, number of sites involved, prior therapy, and median time from first recurrence to chemotherapy without showing any significant differences. Objective response rate to cytotoxic chemotherapy as a function of visceral disease was also examined. The total of 19 of 25 receptor-positive patients had visceral involvement, as compared with 20 of 45 receptor-negative patients (76 *versus* 44%) ($P < 0.025$). The authors demonstrate that this difference in visceral involvement did not account for the difference in response to chemotherapy between estrogen-negative and positive patients, however, since estrogen receptor-positive patients with visceral disease had response rates in two of 19 patients *versus* 10 of 20 patients in the estrogen negative group with visceral disease. The authors conclude that estrogen receptor values are an important predictor of the response to cytotoxic chemotherapy in patients with metastatic breast cancer.

Herbert C. Berry

Anterior resection and primary anastomosis following high dose preoperative irradiation for adenocarcinoma of the rectosigmoid. Stevens KR, Fletcher WS, Allen CV (Department of Radiation Therapy, University of Oregon Health Sciences Center, 3181 S.W. Sam Jackson Park Road, Portland, Oregon 97201). *Cancer* 41:2065–2071, May 1978

Thirteen patients are described with adenocarcinoma of the rectum and sigmoid who were treated at the University of Oregon Health Sciences Center with 5,000 rads preoperative irradiation of the pelvis followed by anterior resection and primary anastomosis. Anterior resection and primary anastomosis was performed 4 to 8 weeks following completion of irradiation. A temporary colostomy was used in some patients. In no instance was the superior resection line irradiated, however, the inferior surgical resection line was within or very near the edge of the irradiation field in 10 patients. This group of preoperative irradiated patients is compared to a group of 79 patients treated from 1960 to 1976 which serve as a historic control. Eighteen of the 79 surgery only patients had complications, six of these fatal. Six of the group of 13 preoperatively irradiated patients had complications, none of which were fatal. None of the test group of patients had local pelvic recurrence *versus* seven of the control group. The incidence of anastomotic leaks and abdominal wound complications was similar. The authors stress that if the irradiated rectum is considered for forming the anastomosis, a temporary protective colostomy should be strongly considered at the time of surgery.

Herbert C. Berry

The management of clinical stage I endometrial carcinoma. Salazar OM, Feldstein ML, DePapp EW, Bonfiglio TA, Keller BE, Rubin P, Rudolph JH (University of Rochester Cancer Center, 601 Elmwood Avenue, Rochester, New York 14642). *Cancer* 41:1016–1026, March 1978

The authors present a retrospective of analysis of 307 patients with clinical stage I endometrial carcinoma. Treatment was broken down into surgery, surgery followed by irradiation, preoperative irradiation, or x-ray therapy only. The pathologic grade of the tumor was the main prognosticator in this group of patients, the depth of myometrial invasion being directly related to the tumor grade. Uterine size was less significant than tumor grade. The authors found that when irradiation was employed preoperatively, the pelvic failure rate was 7%, being significantly lower ($P < .05$) than when radiation followed surgery (11%). They noted a significantly lower ($P < .05$) rate of pelvic recurrence (3%) in patients treated with preoperative external pelvic irradiation than in those treated with initial surgery (13%), and even with preoperative internal applications (8%). The incidence of pelvic recurrence was 22% when irradiation alone was utilized for treatment. The 5-year survival for the group of patients treated with irradiation alone was 60% and the 5-year survival for those receiving preoperative external irradiation was 87%. Those treated with initial surgery or preoperative intracavitary radiation had 5-year survivals of 80%. Overall, 5-year survivals by grade were 96% (grade I), 87% (grade II), and 70% (grade III). The authors feel that preoperative irradiation should be employed, particularly external pelvic irradiation, for stage I, grades II and III, whereas surgery alone is adequate for stage I, grade I endometrial carcinoma.

Herbert C. Berry

Cushing's disease selective transsphenoidal resection of pituitary microadenomas. Tyrrell JB, Brooks RM, Fitzgerald PA, Cofoid PB, Forsham PH, Wilson CB, (Metabolic Research Unit, 1143 HSW , University of California, San Francisco, California 94143). *N Engl J Med* 298:753–758, April 6, 1978

The authors undertook transsphenoidal microsurgical pituitary exploration in 20 consecutive patients with Cushing's disease, eight of whom had normal sellar polytomography. At transsphenoidal microsurgical exploration of the sella turcica, 17 patients had intrasellar abnormalities; 14 with obvious pituitary microadenomas. An additional eighteenth case had no intrasellar abnormality located but total hypophysectomy was performed as opposed to selective resection in the previous 17. Histologically confirmed pituitary adenomas occurred in 83% of these 18 patients in whom sellar extraction was carried out. The nineteenth and twentieth patients were considered technical failures and no specimens were obtained. Surgical complications were minimal. In the total series of 20 patients, hypercortisolism was corrected in 85%. Seventeen patients who underwent selective tumor removal have all had preservation of anterior pituitary function, except for the induction of ACTH deficiency in one patient. Follow-up was generally 2–6 months postoperative. However, six patients were followed for 1 year or longer. Further follow-up will be required to assess final results. The authors' current concept is that in the great majority of patients, ACTH hypersecretion by a primary pituitary tumor is the initiating event that results in hypercortisolism, suppressing hypothalamic secretion of corticotropin-releasing factor. They feel their results do not support the conclusion that the more radical approach of total hypophysectomy is indicated, since selective adenoma resection rapidly corrected hypercortisolism in the majority of their patients.

Herbert C. Berry

Abnormal CT scans of the brain in asymptomatic children with acute lymphocytic leukemia after prophylactic treatment of the central nervous system with radiation and intrathecal chemotherapy. Peylan-Ramu N, Poplack DG, Pizzo PA, Adornato BT, Di Chiro G (D. G. Poplack, Building 10, Room 3B-03, National Institutes of Health, Bethesda, Maryland 20014). *N Engl J Med* 298:815–818, April 13, 1978

The authors report the results of routine posttreatment CT scanning for all surviving patients in continuous hematologic and central-nervous-system remission following treatment for acute lymphocytic leukemia. Treatment consisted of POMP chemotherapy followed by central nervous system prophylaxis with cranial irradiation and intrathecal chemotherapy. A total of 2,400 rads from a 6 MeV linear accelerator was delivered to the cranial vault in fractions of 200 rads per day. Patients were randomly allocated to receive either intrathecal cytosine arabinoside or intrathecal methotrexate during the period of cranial irradiation and systemic consolidation. A total of 32 patients ranging in age from 1 to 16 years were evaluated with the interval from the initiation of prophylaxis to the time of scanning differing among patients from 19 to 67 months.

Four types of CT abnormalities were noted in the patients who received central-nervous-system prophylaxis i.e. ventricular dilatation, areas of decreased attenuation coefficient, intracerebral calcifications and subarachnoid-space dilatation. However, areas of decreased attenuation coefficient and intracerebral calcification were found only in patients who had received intrathecal methotrexate. Mild central-nervous-system dysfunction was detected in seven patients but did not correlate the presence of tomographic abnormalities. The authors suggest that a reappraisal of current approaches to central nervous system prophylaxis should be considered in view of the finding of CT abnormalities in 53% of this group of asymptomatic patients.

Herbert C. Berry

Radiobiology

A search for an effect of ultrasound alone and in combination with x-rays on chromosomes in vivo. Harkányi Z, Szollár J, Vigvári Z (Radiological Clinic of Semmelweis Medical University, 1082 Budapest, Üllöi út 78/a, Hungary). *Br J Radiol* 51:46–49, Jan 1978

The biological effects of ultrasound depend primarily on the applied frequency, intensity, and duration of exposure. The most important factor amongst these physical parameters is intensity, which is about one hundred times greater in the therapeutic applications of ultrasound than in ultrasonic diagnostic techniques.

Experiments were designed to establish whether ultrasonic doses in the therapeutic range, using 0.1, 0.5 and 1.0 W/cm^2 respectively, would cause demonstrable chromosomal damage in the marrow cells of insonicated mice. Groups of mice were insonicated at these intensities using a therapeutic apparatus at 800 KHz, set for continuous emission, and with a 2 cm diameter probe. All groups were insonicated for 5 min. The mice were killed at 24 hr and chromosome aberrations were assessed partly microscopically and partly using microphotographs of bone marrow. On evaluation chromosome aberrations were not significantly increased after insonication with these three different intensities. In contrast a "control" group receiving 50 R whole body irradiation showed clearly demonstrable chromosomal aberrations. Further groups of mice were insonicated at similar intensities and then received 50 R 2 hr later. Ultrasonic pretreatment did not increase the effects of irradiation significantly.

T. Noel K. Allan

Book Reviews

Emmett's Clinical Urography, 4th ed. Edited by D. M. Witten, G. H. Myers, Jr., and D. E. Utz. Philadelphia: Saunders, 2,250 pp., 1977. $125 (3 vol. set)

The rapidly changing spectrum of medical knowledge is again documented in this fourth edition of the classic of uroradiology which has grown to 2,250 pages during the 6 years since the third edition. New chapters include: Renal Mass Puncture and Percutaneous Translumbar Pyelography; Techniques and Applications of Sonography and Computed Tomography; Renal Failure and Renal Parenchymal Disease. These chapters address areas of new knowledge and are well written with an excellent choice of illustrations. The capabilities of the new techniques are discussed; however, their limitations and how to utilize them practically and efficiently in a urologic workshop remains a quandary for the individual clinician.

The technical aspects of urographic diagnosis are now presented in the first six chapters. Some of the recommended methods described are subsequently contradicted by other authors (e.g., the use of antihistamines in excretory urography and radiographic recording of cinecystourethrograms).

All of the remaining 11 chapters have been thoroughly updated including an emphasis on normal variations as a cause of serious interpretive errors. Throughout all volumes the single most important advance in clinical urography in the past decade, the ability to image and evaluate the renal parenchyma, is given appropriate attention. The chapter on infectious diseases has been greatly improved including discussions of new concepts such as the role of intrarenal reflux.

The editors have achieved their goal of a compendium of useful information and illustrations balancing diagnostic imaging techniques with clinical urology in a manner that will serve both as a textbook and handy reference for the student or an atlas for the busy practitioner. They have succeeded well in making the third edition obsolete.

The number of editorial and publishing errors is surprisingly low for a source of this magnitude. Of the estimated 4,000 or so images portrayed, only two of them are upside down (p. 487).

Leon A. Phillips
University of Washington
Seattle, Washington 98195

S.I. Units in Medicine. An Introduction to the International System of Units with Conversion Tables and Normal Ranges. By H. Lippert and H. P. Lehmann (translated by H. L. Lehmann). Baltimore: Urban & Schwarzenberg, 211 pp., 1978. $14.50

As described in its subtitle, this is an introduction to the International System of Units (Systems Internationale d' Unite's). Quantities and normal ranges referenced are those encountered in clinical chemistry.

The volume is well printed and assembled in ring binder style to stay conveniently flat when open on the laboratory bench or desk. The text begins with a history of the development of units leading to the development of the SI system. This system is composed of seven basic metric units and units coherently derived from them. The resulting numbers may be simplified by designating decimal multiples or fractions of the units with appropriate prefixes. In such a system there is only one unit for pressure and no conversion factors are required. At the moment there are some 14 incoherent units of pressure in use in the United States with an appropriate matrix of conversion factors.

In 1973, Congress passed the Metric Conversion Act which endorsed the setting up of a Metric Board to coordinate and plan the voluntary use of the metric system and thus to provide the legal basis for the voluntary adoption of the SI system in the United States.

The authors reference the concern expressed in American, British, and German literature regarding the difficulties and risks to patients attendant in the conversion. However, they also point out that conversion to the metric system for drug prescriptions in Britain during the 1950s produced no such problem and that trial of SI units in two large Canadian hospitals was achieved without difficulty or gross expense. The effects on the units employed in different branches of medicine are reviewed, and selected resolutions and legislation are reproduced.

Concern among physicians appears to center on the reporting of clinical laboratory results. This book is intended to meet that concern by providing conversion tables from the present incoherent units to those of the coherent SI system for the most commonly reported substances. The tables are of interest for another reason, since their compilation included a review of the published data on normal values. The tables are color coded to indicate if the values are normal to all authors, to some, or definitely not in any reportedly normal range.

The adoption of SI units in American medicine is under active discussion, but without prejudging the outcome a decade or so of familiarization will be necessary for its accomplishment. For some time old and new units may be published together. This book gives an excellent resume of the background, relevant legislation, and discussions that have taken place. It will be a valuable reference for those reading the international literature which will convert to SI units more rapidly.

Peter Wootton
University of Washington
Seattle, Washington 98195

New Methods in Tumor Localization. Edited by Y. Maruyama. Lexington University of Kentucky Press, 333 pp., 1977. $7.95 plus $1.30 postage (available from: Radiation Medicine, University of Kentucky, A. B. Chandler Medical Center, 800 Rose St., Lexington, KY 40506)

This text has been adapted from proceedings of the meeting on New Methods of Tumor Localization in Lexington in October 1976. The text is divided into four sections: Ultrasound in Tumor Localization, Radionuclides in Tumor Localization, New Methods in Radionuclide Tumor Localization, and Computerized Tomography in Tumor Localization. At the beginning of each section, an initial chapter or chapters describes the instrumentation used in each of the imaging procedures and the normal anatomy as visualized by each procedure. The ultrasound section includes an excellent chapter which reviews quality control.

In the Radionuclide Tumor Localization section, a chapter describes basic radiopharmacology. These initial chapters are very informative and provide background information for a thorough understanding of the more detailed chapters in each section.

Each section contains chapters which review the present clinical applicability of these imaging techniques. Also discussed are experimental imaging applications which may eventually become routine. Several important chapters compare the clinical usefulness of ultrasound, nuclear medicine imaging, and computed tomography imaging, especially for the detection of intracranial disease and radiation therapy treatment planning.

Most of the illustrations are of very good quality. There is no index, but a thorough bibliography is provided at the end of each chapter.

This text should be a valuable asset to oncologic surgeons, radiation and medical oncologists, and a wide variety of other specialists because it provides up-to-date information on diagnostic techniques used in the evaluation and management of cancer patients. Clinical cancer researchers may also find this text of value since it may suggest new techniques to assist in tumor localization.

Larry D. Greenfield
City of Hope National Medical Center
Duarte, California 91010

Cross-sectional Anatomy—An Atlas for Computerized Tomography. By R. S. Ledley, H. K. Huang, and J. C. Mazziotta. Baltimore: Williams & Wilkins, 330 pp., 1977. $69.95

Although a reviewer usually does not mention the cover of a book, I must note that the vibrant fuchsia and gold cover of this book will not allow it to be misplaced or overlooked on the library shelf.

The atlas is organized into ten parts: (1) cranium—25° to orbital-meatal line; (2) orbit—15° to orbital-meatal line; (3) lower face and neck to T1; (4) chest—T2–T12; (5) upper abdomen—T12–L4; (6) lower abdomen—L4–sacrum; (7) male pelvis—pelvic brim to upper thigh; (8) female pelvis—pelvic brim to upper thigh; (9) upper extremities; and (10) lower extremities.

The computed tomographic scans were obtained from normal volunteers with an ACTA scanner 0100 for most sections. Some of the head sections were obtained with a 0200 fast scanner. The orientation of the images will make radiologists comfortable (i.e., the right side of the image is on the viewer's left). The black and white and color CT images were photographed directly from the ACTA scanner television monitor, and the television raster lines are sometimes distracting due to the magnification used for publication. However, the adjacent color images save the day in those instances.

The format of the atlas consists of two facing pages for each of the 168 levels illustrated. The right hand side, upper half, is a color CT image; the lower half is the corresponding black and white version. The left page lower half is a line drawing identifying the anatomic structures of the corresponding CT image; the upper left half of the page contains a radiograph of the region with a linear marker indicating the level of the CT cut with an adjacent line drawing frequently at 90° to the radiograph for further aid in orienting the level under study.

The line drawings labeling the anatomy of the CT images are easy to read, clearly delineated, and correctly oriented. This is a marked improvement over many other atlases that have adapted diagrams from Eycleshymer and Shoemaker that require a road map, magnifying glass, and frequently a mirror for orientation to the CT images. In addition to a regular index, there is an anatomic structure index which aids in rapid localization of specific images.

This volume will be a well used asset in the library of radiology residents as well as practicing CT users, especially for the body sections. CT technologists at my institution also have found the atlas to be stimulating educationally, and helpful because it indicates and includes the proper levels for initial CT examinations.

Sidney M. Hechct
2021 S.W. 82nd Place
Miami, Florida 33155

Neuroradiology Case Studies: 110 Case Histories Related to Neuroradiology. By A. E. George, B. Derby, and N. E. Chase. Flushing, N.Y.: Medical Examination Publishing Co., 383 pp., 1977.

According to the authors, facts are remembered and knowledge is gained best at the bedside. The case history quiz format is closest to the bedside technique.

A total of 110 case studies are presented in a ring-bound soft cover volume. A short history with pertinent neurologic findings is given followed by radiographs of generally excellent quality. Multiple-choice questions referable to radiographic detail, a differential diagnosis, and the case diagnosis are followed by the answers, including a concise readable discussion and current references.

The table of contents is organized by case history. The index is organized as to diagnosis and anatomy. The cases are mostly based on cerebral angiography, although many CT scans are included. Also covered are the major neuroradiologic changes seen on myelography, in the skull, and involving the spine. Several examples of tomography and pneumoencephalography are presented.

This volume is relatively free of printing errors. The most serious error is a shifting of the radiographs for cases 18 and 19.

I think the authors' intent has been admirably met. This book would be of most interest and benefit to resident physicians in the neurosciences, although general radiologists, neurologists, and neurosurgeons certainly would find value in it.

Richard A. Flom
St. Joseph's Hospital
Phoenix, Arizona 85013

Atlas of Polytome Pneumography: With Particular Reference to the Midline Ventricles of the Brain. By T. El Gammal and M. B. Allen with assistance of P. Dyken. Springfield, Ill.: Thomas, 386 pp., 1977. $39.50.

This book deals with the normal and abnormal anatomy of the cerebrospinal fluid pathways as studied by polytome pneumography. It is divided into six chapters: Introduction and Technique; Normal CSF Pathways; Atrophy; Hydrocephalus; Intrasellar Subarachnoid Recess—Sellar and Suprasellar Lesions; and Metasellar Mass Lesions—Herniations. Some 114 pages are devoted to normal anatomy of cerebrospinal fluid pathways; 76 pages are assigned to the chapter on hydrocephalus which includes the usual causes. The bibliography consists of only two pages (60 citations).

This atlas clearly establishes the expertise of the authors in polytome pneumography. The illustrations demonstrating the normal and abnormal cerebrospinal fluid pathways change from good to excellent. Legends to the illustrations are sufficiently explanatory. Considering that this is not a textbook, the authors have achieved considerable success in outlining the salient features of disease processes.

In the present era when cranial computed tomography has established itself as a reliable means of detecting central nervous system pathology, sophisticated pneumography may still be needed to detect, among other disease processes, mass lesions in the brain stem, in and around the aqueduct, and in the sellar-parasellar region. To this end, this atlas will be a useful reference.

My minor criticism is that there is some repetition (particularly in the chapter on normal cerebrospinal fluid pathways). This could have been easily avoided, resulting in a somewhat smaller and less costly volume.

Because most of the information can be obtained in textbooks on neuroradiology, I feel that residents and general radiologists need not own a personal copy of this book. Medical libraries may well acquire this volume for use by physicians with particular interest in the neurosciences.

Mohammad Sarwar
University of Texas Medical Branch
Galveston, Texas 77550

Obstetrical Diagnosis by Radiographic, Ultrasonic, and Nuclear Methods. Golden's Diagnostic Radiology, section 10. Edited by J. A. Campbell. Baltimore: Williams & Wilkins, 207 pp. 1977. $29

The radiology of clinical obstetrics is undergoing rapid evolution, with increasing dependence on ultrasonic techniques. This has produced a marked decrease in the reliance on more conventional radiographic techniques, contrast studies, and nuclear medicine, all of which are nicely discussed by Campbell and his contributing editors. Fred Mishkin states in his chapter on nuclear medicine that it serves as a chronicle of the birth, growth, maturity, and senescence of a technique.

The authors of this new section of Golden's Diagnostic Radiology review the general areas of obstetrical radiology, concisely covering the more common problems and giving adequate updated references to those who wish to delve more deeply into a specific area. Campbell has written an informative review on antenatal radiation hazards, and there is an excellent introductory chapter on the use of diagnostic ultrasound by Alan Miyamota.

The quality of some of the radiographic images is suboptimal, but generally quite adequate. I would suggest that the editors give thought to integrating the material in the future to provide the reader with a clearer picture of the value of different diagnostic modalities used to study a particular problem.

The book will serve as a valuable introduction to students of radiology and obstetrics, as well as to the practitioner who wishes to review conventional techniques and gain an introduction to the newer ones, especially now when technology is in such transition.

Chester J. Kay
Park City Hospital
Bridgeport, Connecticut 06604

Advances in Radiation Biology, vol. 7. Edited by J. T. Lett and H. Adler. New York: Academic Press, 442 pp., 1978. $45

This volume is one of a continuing series of reviews aimed at keeping abreast of contemporary developments in the radiation biology field. Special articles, however, also are included to broaden the scope to related nonradiation areas.

Article 1 is the Use of Purified Lesion-recognizing Enzymes to Monitor DNA Repair in Vivo by Malcolm C. Paterson. Topics covered include enzymatic repair mechanisms, conventional repair assays, experimental applications of enzymatic assays, and a compendium of lesion-specific endonucleases. This is an in-depth review of DNA repair mechanisms. The first part of the article will be of interest to nonspecialists because it includes an excellent discussion of the current understanding of types of DNA repair and the steps involved. A clearly written presentation of the various laboratory techniques used also is included. The compendium of lesion-specific endonucleases, however, will be of interest only to those specializing in the field.

Article 2 is The Crucial Role of DNA Double-Strand Breaks in Cellular Radiobiological Effects by H. P. Leenhouts and K. H. Chadwick. These authors bring together their work on a molecular theory aimed at explaining the radiobiologic responses of eukaryotic cells to ionizing radiation. For their basic equation, a linear-quadratic dose model is used to describe the production of double-strand breaks which it is proposed lead to loss of cell reproductive integrity, chromosomal aberations, somatic mutations, and malignancy. A review of the literature shows good agreement between laboratory data and the responses predicted by the model.

This linear-quadratic model is based on the concept that radiation can induce double-strand breaks in DNA by two different modes of action. The double helix can be broken by two simultaneous interactions arising from the passage of one ionizing particle very close to the DNA, resulting in some double-strand breaks, the yield of which will be directly proportional to the radiation dose. The double helix also can be broken by two time-independent interactions arising from the passage of two separate ionizing particles close to the DNA. The number of double-strand breaks produced by this action of radiation will be proportional to the square of the radiation dose. The review will be of considerable interest to those concerned with the molecular biology of radiation effects, since it provides a unifying theory for explaining the mechanism of action of radiation at the cell level.

Article 3 is Evaluating the Effects of Ionizing Radiation on Aquatic Organisms by D. G. Blaylock and J. R. Trabalka. The authors review the aquatic radiation biology literature, mostly from 1960 on. The material will be of interest to those working in the aquatic field and is of particular importance with respect to the environmental impact of uses of nuclear energy. Data from a large number of different experiments and biological systems are covered.

Article 4, Applicability of Bacterial Models of DNA Repair and Recovery to UV-irradiated Mammalian Cells by Roger R. Hewitt and Raymond E. Meyn, evaluates the applicability of bacterial models of repair and recovery in mammalian cells. The authors first discuss repair of UV-induced DNA injury in bacterial cells and then review similar work with mammalian cells. The comparison indicates that the bacterial model is not strictly applicable to repair mechanisms in mammalian cells.

Article 5, Electrophysiological Studies on Radiation-induced Changes in the Adult Nervous System by Makoto Sato, deals for the most part with work published between 1950 and 1969 and covers functional effects of radiation on the brain and the peripheral nervous system. Focus is on acute radiation effects and functional changes that are electrophysiologically demonstrable during exposure to ionizing radiation and will be of particular value to those working in the field of neurophysiology.

Article 6 is The Repair of DNA Modified by Cytotoxic, Mutagenic, and Carcinogenic Chemicals by J. J. Roberts. This last article in the volume is a 286 page review which concentrates on work reported from 1968 through 1977. The review will be of interest not only to those working in the field of nucleic acid biochemistry, but also to those concerned with cancer research since most known carcinogens have been shown to be bound to nucleic acids in receptive animal tissues, either as a consequence of direct chemical reaction or following metabolism of reactive metabolites. The article gives not only an extensive review of chemical modification of DNA and its repair but also interprets these findings in relation to mutagenesis and carcinogenesis.

Kenneth L. Jackson
University of Washington
Seattle, Washington 98195

Books Received

Receipt of books is acknowledged as a courtesy to the sender. Books that appear of sufficient interest will be reviewed as space permits.

Very Early Recognition of Coronary Heart Disease. Edited by L. McDonald, J. Goodwin, L. Resnekov. Amsterdam: Excerpta Medica, 194 pp., 1978. $32.75

Radiation Effects: ESR and ENDOR Analysis. By H. C. Box. New York: Academic Press, 280 pp., 1977. $24.50

An Atlas of Otolaryngologic Radiology. By J. Zizmor and A. M. Noyek. Philadelphia: Saunders, 497 pp., 1978. $ 35

Care of the Patient in Diagnostic Radiography, 5th ed. By D. N. Chesney and M. O. Chesney. Oxford: Blackwell Scientific (U.S. distributor: Lippincott, Philadelphia), 323 pp., 1978. $20

Medical Physics. By J. R. Cameron and J. G. Skofronick. New York: Wiley, 615 pp., 1978. $21.95

The Pacemaker and Valve Identification Guide. By D. Morse and R. M. Steiner. Garden City, N.Y.: Medical Examination Publishing Co., 395 pp., 1978. $40

A Guide for Automatic Radiographic Processing and Film Quality Control. By C. C. Kirby, W. E. J. McKinney, and T. T. Thompson. Chicago: American Society of Radiologic Technologists, 105 pp., 1975. $4

Principles of Chest X-ray Diagnosis, 4th ed. By G. Simon. Boston: Butterworths, 296 pp., 1978. $39.95

Considerations about the Use of Computers in Radiodiagnostic Departments. Special report no. 14. Edited by G. H. duBoulay. London: British Institute of Radiology, 127 pp., 1977. £6.75.

Computed Tomography of Abdominal Abnormalities. Edited by J. Haaga and N. E. Reich. St. Louis: Mosby, 430 pp., 1978. $44.50

Pathology in Computed Tomography of the Brain. By S. D. Henderson. Springfield, Ill.: Thomas, 197 pp., 1978. $17.50

Biological Effects of ^{224}Ra. Benefit and Risk of Therapeutic Application. Edited by W. A. Müller and H. G. Ebert. The Hague: Martinus Nijoff, 236 pp., 1978. 62.50 guilders

Atlas of Radiologic Anatomy. By L. Wicke. Baltimore: Urban & Schwarzenberg, 234 pp., 1978. $15

News

FDA Invites Comments on Proposed Radiation Protection Recommendation

The Bureau of Radiological Health, Food and Drug Administration, has published a proposed recommendation on use of x-ray intensifying screens in the June 2, 1978, *Federal Register* (43 FR 24066). Deadline for receipt of comments on this recommendation is November 29. Copies of the recommendation are available from the Bureau of Radiological Health.

The announcement in the *Federal Register* states, in part, that the Food and Drug Administration "is encouraging the development of a voluntary radiation protection recommendation and related information to encourage the use of x-ray intensifying screens made from recently developed phosphor materials which can result in reduced patient exposure. The recommendation would encourage radiographic facilities to use these new screens when appropriate and would provide guidance and suggestions to assist radiographic facilities in adopting these new screens." Manufacturers "are encouraged to offer improved intensifying screen and x-ray film combinations that do not compromise image quality."

The Food and Drug Administration "acknowledges that the adoption of the newer film-screen systems by facilities with established radiology programs may require the solution of certain clinical and technical problems associated with the different characteristics of the newer systems and the use of multiple imaging systems in a single facility."

Users of rare-earth systems "are invited to submit information on their clinical experience and suggestions concerning the use of currently available systems, together with recommendations for future developments."

Additional information regarding these proposals is available from H. Rudolph, Bureau of Radiological Health (HFX-460), Food and Drug Administration, 5600 Fishers Lane, Rockville, Maryland 20857; telephone (301) 443-3426. Comments on the proposed action should be directed to the same address.

Thoracic Society: Call for Abstracts

The American Thoracic Society is inviting abstracts of papers on all scientific aspects of respiratory disease. All accepted papers will be presented at the society's meeting May 13–16 in Las Vegas. Deadline for submission of abstracts is December 6. Scientific and technical exhibits on all aspects of respiratory disease are also being solicited. Membership in the society is not a prerequisite. Instructions and forms may be obtained from R. H. Winterbauer, Annual Meeting Committee, American Thoracic Society, 1740 Broadway, New York, New York 10019.

International Congress of Radiation Research

The sixth International Congress of Radiation Research will be May 13–19 in Tokyo. Fields covered will include physics, chemistry, biology, and medicine and their corresponding interdisciplinary areas of radiation research including nonionizing radiations. The congress will consist of five plenary sessions and 30 symposia, one workshop, and presentation of contributed papers. Among the topics discussed will be frontiers of radiation oncology, applied radiation research in agriculture and industry, risk assessments of radiation, environmental mutagens and carcinogens, radiation research in fusion powers, global radioecology, and toxicology of radionuclides. Deadline for advance registration and submission of abstracts is November 30. Group flights at reduced rates are planned from various parts of the world. For application forms and travel information, write S. Okada, Secretary-General, Sixth International Congress of Radiation Research, Hongo, P.O. Box 152, Tokyo 113-91, Japan.

Noninvasive Imaging in Medicine

The medical faculty of Lund, Sweden, will host a symposium June 6–9 on Noninvasive Imaging in Medicine: Heart, Liver, and Pancreas. Invited speakers include: H. L. Abrams, R. Alfidi, E. Carlsson, H. Feigenbaum, B. B. Goldberg, D. L. King, H. W. Strauss, A. J. Tajik, all from the United States; M. Collard, Brussels; F. Jensen and H. H. Holm, Copenhagen; P. Gerhardt, Heidelberg, Germany; H. Hundeshagen, Hannover, Germany; L. Kreel, Harrow, United Kingdom; V. R. McCready, Sutton, United Kingdom; and J.-L. Lamarque, Montpellier, France. Additional information is available from E. Boijsen, Department of Diagnostic Radiology, University Hospital, S-221 85 Lund, Sweden.

Conferences on Medical and Biological Engineering and Medical Physics

The XII International Conference on Medical and Biological Engineering and the V International Conference on Medical Physics will meet together August 19–24, 1979, in Jerusalem. For information, contact the Conference Secretariat, P. O. Box 16271, Tel Aviv, Israel.

L. H. Gray Conference

The ninth L. H. Gray Conference will be in Cambridge, England, September 10–14, 1979. Topics are intended to stimulate a critical appraisal of the techniques that are currently in use both experimentally and clinically for assessing tumor response after therapy. Topics will include: in situ measurements of tumor response, including improved methods of tumor detection in clinical studies; factors of prognostic significance; in vitro assays of tumors excised after treatment in vivo; and statistical evaluation of tumor response data. For additional information, contact J. Denekamp, Gray Laboratory, Mount Vernon Hospital, Northwood, Middlesex, England.

Asian Oceanian Congress of Radiology

The third Asian Oceanian Congress of Radiology will be October 28–November 3, 1979, in Singapore. The Singapore Radiological Society is organizing the event. Information may be obtained from the Secretariate, Third AOCR, Department of Diagnostic Radiology, Singapore General Hospital, Singapore 3.

Diagnostic and Therapeutic Angiography

The Society of Cardiovascular Radiology will host a course, Diagnostic and Therapeutic Angiography and Interventional Radiology, March 21–25 in Puerto Rico. Tuition is $295; residents and fellows, $195. Continuing education credits will be available. For information, write A. B. Crummy, Society of Cardiovascular Radiology, 1300 University Avenue, Madison, Wisconsin 53706.

Amipaque Myelography Workshop

Amipaque Myelography and New Techniques in Neuroradiology is the title of a seminar-workshop sponsored by the University of Wisconsin Department of Radiology. Dates are November 15–17, and the event will be in Madison. Fee is $190. For information contact Lyn Apfel, 465B WARF Building, 610 North Walnut Street, Madison, Wisconsin 53706; telephone (608) 263-2856.

Inter-American Congress of Radiology

Radiologists from throughout the western hemisphere will gather in Quito, Ecuador, in late July and early August 1979 for the twelfth Inter-American Congress of Radiology. A preconvention refresher course series will be July 26–28. More than 1,000 radiologists are expected to attend. For additional information, contact Manuel Viamonte, Jr., President, Inter-American College of Radiology, Mount Sinai Medical Center, 4300 Alton Road, Miami Beach, Florida 33140.

Research Training Fellowships

Research Training Fellowships for 1979–1980 are available from the International Agency for Research on Cancer, World Health Organization. Applications should be from junior scientists who wish training in any aspects of clinical and laboratory research. Priority will be given to candidates applying for training in epidemiology, biostatistics, and environmental carcinogenesis, both chemical and viral. In general, fellowships will be awarded to applicants with some postdoctoral research experience related to cancer in medicine or the natural sciences. They must have an adequate knowledge, both written and spoken, of the language of the country in which their fellowship is tenable. Deadline for application is January 31. For application forms and more detailed information, write the Chief of Research Training and Liaison Unit, International Agency for Research on Cancer, 150, cours Albert-Thomas, 69372 Lyon Cedex 02, France.

National Conference on Breast Cancer

The eighteenth annual Conference on Detection and Treatment of Breast Cancer is slated for March 4–9 in Atlanta. Sponsor is the American College of Radiology. In the past, the multidisciplinary conference has drawn physicians from six major specialties. For information, write R. W. Harrington, Plans and Programs, American College of Radiology, 20 North Wacker Drive, Chicago, Illinois 60606.

Diagnostic Ultrasound Preceptor Training Programs

One month programs are offered at the University of California, San Diego, and University Hospital at San Diego to physicians interested in obtaining the beginnings of academic and clinical expertise in ultrasound. Lectures, videotapes, teaching files, and some hands-on experience in scanning techniques are offered. In addition, variable B scan and real-time ultrasound covering approximately 15 to 20 cases daily are studied and reviewed with a staff member. The course is accredited for 140 hr Category I credit by the American College of Radiology, and 10 units through University of California Extension. For further information contact Elizabeth Novak, Division of Diagnostic Ultrasound, University Hospital, 225 Dickinson Street, San Diego, California 92103; telephone (714) 294-6657.

Meeting and Course Review

For reader convenience, a summary of upcoming meetings and courses is provided. Detailed listings of these events appeared in journal issues indicated in parentheses.

CT in Radiotherapy, workshop, March 28–30, Geneva, Switzerland (June).

Courses in Ultrasound, two 8 week postgraduate courses beginning January 8 and April 2, respectively, Winston-Salem, North Carolina (July).

General Diagnostic Radiology, course, February 5–9, Puerto Rico (July).

Diagnosis of Liver Metastases, symposium, November 30–December 2, Brussels (July).

Adjuvant Therapy of Cancer, conference, March 28–31, Tucson (July).

Southeastern Chapter, Nuclear Medicine Meeting, November 1–4, Birmingham, Alabama (August).

Medical Imaging Meeting, December, Hong Kong and People's Republic of China (August).

Nuclear Medicine Meeting, November 10–12, Philadelphia (September).

CT, Ultrasound, Nuclear Medicine in Pediatrics, symposium, January 18–20, Orlando, Florida (September).

Body CT Course, February 26–March 1, San Diego (September).

Current Concepts in Diagnostic Radiology, course, February 12–16, Acapulco, Mexico (September).

Arthrography Course, December 14–16, New York City (September).

Computed Tomography, Ultrasound, and X-ray, course, January 29–February 2, San Francisco (September).

Two Courses: Snowbird and Park City, January 28–February 3, Snowbird, Utah, and February 24–March 3, Park City Ski Resort, Utah (September).

VA Administrative Scholars Program, application deadline November 1 (September).

AJR carries relevant announcements of courses and symposiums if received a minimum of 4 months in advance of the event. There is no charge. Mail announcements to the Editorial Office, American Journal of Roentgenology, 403 Pacific National Bank Building, 4545 15th Avenue N.E., Seattle, Washington 98105. Items will not be acknowledged.

Radiologic Societies

International Societies

Fleischner Society. Secretary K. Ellis, Columbia-Presbyterian Medical Center, 622 West 168th St, New York, NY 10032

Inter-American College of Radiology. Secretary, G. Morillo, Dept Radiology, Jackson Memorial Hospital, 1611 NW 12th Ave, Miami, FL 33136

International Commission on Radiological Protection. Secretariat, F. D. Sowby, Clifton Ave, Sutton, Surrey SM2 5PU, England

International Skeletal Society. Secretary-Treasurer, J. Edeiken, Radiology Dept, Thomas Jefferson University Hospital, 11th and Walnut Sts, Philadelphia, PA 19107

International Society of Radiology. Hon. Secretary-Treasurer, W. A. Fuchs, Dept of Diagnostic Radiology, University Hospital, Inselspital, CH-3010 Bern, Switzerland

World Federation of Nuclear Medicine and Biology. 2d International Congress, Washington Hilton Hotel, Sept 18-21, 1978, Washington, D.C. General chairman, H. N. Wagner, Jr, 1629 K St, NW, Suite 700, Washington, D.C. 20006

U.S. National Societies

American Association of Physicists in Medicine. Secretary, J. Wright, Radiology Dept, Geisinger Medical Center, Danville, PA 17821

American Board of Radiology. Secretary, C. A. Good, Kahler East, Rochester, MN 55901

American College of Radiology. Executive Director, W. C. Stronach, 20 N Wacker Drive, Chicago, IL 60606. Annual meetings: 1979, Sept 16-20, Chicago, IL; 1980, Sept 21-25, New Orleans, LA

American Institute of Ultrasound in Medicine. Executive Secretary, D. LaMaster, PO Box 25065, Oklahoma City, OK 73125. Annual meetings: 1978, Oct 7-13, San Diego; 1979, Aug 23-31, Montreal. Spring educational meetings: 1978, April 4-9, Puerto Rico; 1979, Feb 23-March 3, Lake Tahoe; 1980, March 1-6, Hilton Head

American Nuclear Society. Program Chairman, T. D. Tarr, U.S. Energy Research and Development Administration, Mail Station A-436 Office of Assistant Administrator for Nuclear Energy, Washington, DC 20545

American Radium Society. Business office: N. V. Jordan, Office of the Secretariat, c/o M. D. Anderson Hospital, 6723 Bertner Drive, Houston, TX 77030. Annual meetings: 1979, March 4–8, Los Angeles; 1980, April 27-May 1, Philadelphia

American Roentgen Ray Society. Secretary, J. F. Martin, 300 S Hawthorne Rd, Winston-Salem, NC 27103. Annual meetings: 1979, March 25-30, Toronto; 1980, April 22-25, Las Vegas; 1981, March 24-27, San Francisco

American Society of Neuroradiology. Secretary, T. El Gammel, Medical College of Georgia, Augusta, GA 30902

American Society of Therapeutic Radiologists. Secretary, W. J. Taylor, 1100 9th Ave, Seattle, WA 98101. Annual meetings: 1978, Oct 31-Nov 4, Los Angeles; 1979, Oct 23-27, New Orleans

American Thermographic Society. Executive Director, N. M. Oldfield, PO Box 2055, Gaithersburg, MD 20760.

Association of University Radiologists. Secretary-Treasurer, J. R. Thornbury, University of Michigan, Ann Arbor, MI 48109. Annual meeting: 1979, May 6-10, Rochester, NY

Health Physics Society. Executive Secretary, R. J. Burk Jr, 4720 Montgomery Lane, Bethesda, MD 20014

National Medical Association. Secretary, E. Mapp, Episcopal Hospital, Philadelphia, PA 19148

North American Society of Cardiac Radiology. Secretary-Treasurer, E. Carlsson, University of California, San Francisco, CA 94143

Radiation Research Society. Executive Director, R. J. Burk Jr, 4720 Montgomery Lane, Bethesda, MD 20014

Radiological Society of North America, Inc. Secretary, T. A. Tristan, Fifteenth Floor, One MONY Plaza, Syracuse, NY 13202. Annual meeting: 1978, Nov 26-Dec 1, Chicago; 1979, Nov 25-30, Atlanta, GA; 1980, Nov 16-21, Dallas, TX

Section on Radiology, American Medical Association. Secretary, A. Raventos, Dept Radiology, School of Medicine, University of California, Davis

Society of Cardiovascular Radiology. Secretary-Treasurer, W. J. Casarella, Columbia-Presbyterian Medical Center, New York, NY 10032

Society of Chairmen of Academic Radiology Departments. Secretary-Treasurer, D. Bragg, University of Utah, Salt Lake City, UT 84132

Society of Gastrointestinal Radiologists. Secretary-Treasurer, R. Berk, University Hospital, San Diego, CA 92103

Society of Nuclear Medicine. President, 475 Park Avenue S, New York, NY 10016

Society for Pediatric Radiology. Secretary-Treasurer, N. T. Griscom, 300 Longwood Ave, Boston, MA 02115

Society of Photooptical Instrumentation Engineers. Secretary, A. H. Gott, Aerospace Corp. PO Box 92957, Los Angeles, CA 90009.

Society of Uroradiology. Secretary-Treasurer, R. C. Pfister, Massachusetts General Hospital, Boston, MA 02114

U.S. State and Local Societies

ALABAMA

Alabama Academy of Radiology. Secretary-Treasurer, J. L. Wayland, 401 West College St, Florence, AL 35630

Section of Radiology, National Medical Association. Secretary, I. Brooks, Dept Radiology, Veterans Administration Hospital, PO Box 511, Tuskegee, AL 36083

Southern Radiological Conference. Secretary-Treasurer, J. W. Maxwell, PO Box 2144, Mobile, AL 36601

ALASKA

Alaska Radiological Society. Chapter ACR. Secretary-Treasurer, J. J. Kottra, 3200 Providence Ave, Anchorage, AK 99504

ARKANSAS

Arkansas Chapter of ACR. Secretary-Treasurer, R. Seibold Jr, Wadley Hospital, Texarkana, AR 75501

ARIZONA

Arizona Radiological Society. Chapter of ACR. Secretary, A. Newman, PO Box 5099, Phoenix, AZ 85010

CALIFORNIA

California Radiological Society, California Chapter of ACR. Executive Secretary, J. M. Allen, 1225 8th St, Suite 590, Sacramento, CA 95814

East Bay Radiological Society. Secretary-Treasurer, J. J. Branscom, PO Box 175, Alamo, CA 94507

Los Angeles Radiological Society. Secretary, R. M. Witten, St. Vincent Medical Center, 2131 W. Third St, Los Angeles, CA 90057

Northern California Radiological Society. Secretary-Treasurer, J. C. Buhl, 7733 Bahama Ct, Fair Oaks, CA 95628

Northern California Radiotherapy Association. Secretary-Treasurer, J. D. Earle, Stanford Medical Center, Stanford, CA 94305

Orange County Radiological Society. R. L. Argue, 100 E Valencia Mesa Dr, Fullerton, CA 93632

Radiological Society of Southern California. Secretary-Treasurer, D. E. Blickenstaff, La Jolla Radiology Medical Group, 7849 Fay Ave, La Jolla, CA 92037

Redwood Empire Radiological Society. Secretary, H. B. Peterson, 357 Perkins St, Sonoma, CA 95476

San Diego Radiological Society. President, D J. Fleischli, 7849 Fay Ave, La Jolla, CA 92037

San Francisco Radiological Society. Secretary-Treasurer, P. A. Brodey, Dept Radiology, Mount Zion Hospital, San Francisco, CA 94115

South Bay Radiological Society. Secretary, R. Wirtz, Redwood Medical Clinic, 2900 Whipple Ave, Redwood City, CA 94062

South Coast Radiologic Society Chapter of ACR. Secretary-Treasurer, B. R. Schnier, Dept of Radiology, Cottage Hospital, Pueblo at Bath, Santa Barbara, CA 93105

Southern California Radiation Therapy Society. Secretary-Treasurer, J. Stuhlborg, 514 N Prospect, Redondo Beach, CA 90277

Western Neuroradiological Society. Secretary-Treasurer, A. N. Hasso, Loma Linda University Medical Center, Loma Linda, CA 92354

COLORADO

Colorado Radiological Society. Secretary, P. Danner, St. Anthony Hospital, Denver, CO 80204

Rocky Mountain Radiological Society. Secretary-Treasurer, J. M. Grogan, 4200 E 9th Ave, Denver, CO 80206

CONNECTICUT

Connecticut Valley Radiologic Society. Secretary-Treasurer, G. N. LaPierre, 759 Chestnut St, Springfield, MA 01107

Radiological Society of Connecticut, Inc. Secretary, E. F. Fox, 300 Main St, Eriston, CT 06010

DELAWARE
Delaware Chapter of ACR. Secretary, E. S. Schubert, Wilmington Medical Center, PO Box 1951, Wilmington, DE 19899

DISTRICT OF COLUMBIA
Section on Radiology, Medical Society of the District of Columbia. Secretary-Treasurer, A. M. Zelna, 21 Masters St, Potomac, MD 20854

FLORIDA
The Florida Radiological Society, Chapter of ACR. Secretary, S. H. Sarasohn, PO Box, 610544, North Miami, FL 33161
The Florida West Coast Radiological Society, Inc. Secretary-Treasurer, M. Silbiger, 1 Davis Blvd, Suite 103, Tampa, FL 33606
Greater Miami Radiological Society. Secretary, J. A. Schneider, 1131 N 35 Ave, Hollywood, FL 33021
North Florida Radiological Society. Secretary, C. E. Bender, 1430 16th Ave S, Jacksonville Beach, FL 32250
Northeast Florida Radiological Society. Secretary, O. L. Jeter Jr, Orange Park Community Hospital, Orange Park, FL 32073

GEORGIA
Atlanta Radiological Society. Secretary-Treasurer, J. H. Larose, Dept Nuclear Medicine, South Fulton Hospital, East Point, GA 30344
Georgia Radiological Society. Chapter of ACR. Secretary, T. Vanderzalm, Medical College of Georgia, Augusta, GA 30902

HAWAII
Hawaii Radiological Society, Chapter of ACR. Secretary-Treasurer, M. Meagher, 1301 Punchbowl St, Honolulu, HI 96808

ILLINOIS
Chicago Radiological Society, Division of the Illinois Radiological Society, Chapter of ACR. Secretary-Treasurer, H. J. Lasky, 55 E Washington St, Suite 1735, Chicago, IL 60602

Illinois Radiological Society, Inc, Chapter of ACR. Secretary, R. D. Dooley, Hinsdale Medical Center, Hinsdale, IL 60521

INDIANA
Indiana Roentgen Society of ACR. Secretary, W. S. Tirman, 919 Jefferson Blvd, Sound Bend, IN 46617
Tri-State Radiological Society. Secretary, T. Harmon, St. Mary's Hospital, Evansville, IN 47750

IOWA
Iowa Radiological Society, Chapter of ACR. Secretary-Treasurer, D. L. Roberson, 1948 First Ave NE, Cedar Rapids, IA 52402

KANSAS
Kansas Radiological Society, Chapter of ACR. Secretary-Treasurer, R. H. Baehr, 310 Medical Arts Bldg, Topeka, KA 66604

KENTUCKY
Bluegrass Radiological Society. Secretary-Treasurer, J. King, 3313 Overbrook Dr, Lexington, KY 40504
Kentucky Chapter of ACR. Secretary-Treasurer, A. Lieber, University of Kentucky Medical Center, Lexington, KY 40506

LOUISIANA
Ark-La-Tex Radiological Society. Secretary, E. K. Lang, LSU School of Medicine, Shreveport, LA 71101
Louisiana Radiological Society, Chapter ACR. Secretary-Treasurer, S. L. Smith, 250 Vincent Ave, Metairie, LA 70005
Louisiana-Texas Gulf Coast Radiological Society. Secretary-Treasurer, E. Engert Jr, 618 S. Ryan St, Lake Charles, LA 70601
Section on Radiology, Southern Medical Association. Secretary, M. Sullivan, 1514 Jefferson Highway, New Orleans, LA 70121

MAINE
Maine Radiological Society, Chapter of ACR. Secretary-Treasurer, P. E. Giustra, Penobscot Bay Medical Center, Rockland, ME 04841

MARYLAND
Maryland Radiological Society, Chapter of ACR. Secretary, S. M. Goldman, Sinai Hospital of Baltimore, Belvedere at Greenspring Avenues, Baltimore, MD 21215

MASSACHUSETTS
Massachusetts Radiological Society, Chapter of ACR. Secretary, A. H. Robbins, 150 S Huntington Ave, Boston, MA 02130
New England Roentgen Ray Society. Secretary, H. F. Gramm, 185 Pilgrim Road, Boston, MA 02215.
New England Society for Radiation Oncology. Secretary, S. P. Kadish St. Vincent Hospital, 25 Winthrop St, Worcester, MA 01604
Northeastern Society for Radiation Oncology. Secretary, C. C. Wang, Massachusetts General Hospital, Boston MA 02114

MICHIGAN
Michigan Radiological Society, Chapter of ACR. Secretary-Treasurer, F. P. Shea, Bon Secours Hospital, 468 Cadieux, Grosse Pointe, MI 48230
Michigan Society of Therapeutic Radiologists. Secretary, K. E. Murdock, 302 Kensington Ave, Flint, MI 48502

MINNESOTA
Minnesota Radiological Society, Chapter of ACR. Secretary-Treasurer, J. B. Marta, 125 W College Ave, St. Paul, MN 55102

MISSOURI
Greater Kansas City Radiological Society. President-Secretary, G. D. Dixon, St Luke's Hospital, 44th & Wornall Road, Kansas City, MO 64111
Greater St. Louis Society of Radiologists. Secretary-Treasurer, D. G. Spalding, 621 S New Ballas Rd, St. Louis, MO 63141
Missouri Radiological Society, Chapter of ACR. Secretary-Treasurer, E. M. Herman, 701E 63rd St, Kansas City, MO 64110

MISSISSIPPI
Mississippi Radiological Society, Chapter of ACR. Secretary-Treasurer, J. B. Barlow, 514B E Woodrow Wilson, Jackson, MS 39216

MONTANA
Montana Radiological Society. Secretary-Treasurer, E. Drouillard, St. Patrick Hospital, Missoula, MT 59801

NEBRASKA
Nebraska Chapter of ACR. Secretary-Treasurer, W. H. Northwall, Good Samaritan Hospital, Kearney, NB 68847

NEW HAMPSHIRE
New Hampshire Chapter of ACR. Secretary-Treasurer, E. P. Kane, Claremont General Hospital, Claremont, NH 03743

NEW JERSEY
Radiological Society of New Jersey, Chapter of ACR. Secretary, A. J. Scher, 8 Lord William Penn Dr, Morristown, NJ 07083

NEW MEXICO
New Mexico Society of Radiologists, Chapter of ACR. Secretary, W. M. Jordan, 1100 Central Ave SE, Albuquerque, NM 87106

NEW YORK
Bronx Radiological Society, New York State, Chapter of ACR. Secretary-Treasurer, L. J. Corbin, 1369 Rosendale Ave, Bronx, NY 10472
The Brooklyn Radiological Society. Secretary-Treasurer, E. Arida, 450 4th Ave, Brooklyn, NY 11215
Buffalo Radiological Society. Secretary, A. Favorito, 166 Soldiers Pl, Buffalo, NY 14222
Central New York Radiological Society. Secretary-Treasurer, P. A. Randall, Upstate Medical Center, 750 E Adams St, Syracuse, NY 13210
Kings County Radiological Society. Secretary, M. Moore, 7815 Bay Parkway, Brooklyn, NY 11214
Long Island Radiological Society. Secretary, R. Meisell, 1200 Stewart Ave, Garden City, NY 11533
Mid-Hudson Radiological Society. Secretary-Treasurer, W. D. Stiehm, 37 Flower Hill Rd, Poughkeepsie, NY 12603
New York Roentgen Society. Secretary-Treasurer, N. E. Leeds, Montefiore Hospital, 111 E 210th St., New York, NY 10467. Spring Conference: April 26–28, New York City
New York State Chapter of ACR. Secretary-Treasurer, A. F. Keegan, 6 Secor Dr, Port Washington, NY 11050
Northeastern New York Radiological Society. Secretary, D. R. Morton, Dept Radiology, St. Claire's Hospital, Schenectady, NY 12304
Rochester Roentgen Ray Society. Secretary-Treasurer, R. E. Tobin, 135 Drumlin View Dr, Mendon, NY 14506
Westchester County Radiological Society. Secretary, H. Kessler, Radiological Group, 45 Ludlow St, Yonkers, NY 10705

NEVADA
Nevada Radiological Society, Chapter of ACR. Secretary, C. F. Veverka, Carson Tahoe Hospital, Carson City, NV 89701

NORTH CAROLINA
Catawba Valley Radiological Society. Secretary, J. N. Owsley, 18 13th Ave NE, Hickory, NC 28601
North Carolina Chapter of ACR. Secretary-Treasurer, M. A. Jones, Durham County Hospital, Durham, NC 27705
Southeastern Chapter Society of Nuclear Medicine. Secretary, V. J. Sodd, University of Cincinnati Medical Center, Cincinnati, OH 45267

NORTH DAKOTA
North Dakota Radiological Society, Chapter of ACR. Secretary, H. C. Walker Jr, PO Box 624, Devils Lake, ND 58301

OHIO
Cleveland Radiological Society. Secretary-Treasurer, J. B. McCoy, Elyria Medical Arts Bldg, Suite 12, Elyria, OH 44035
Greater Cincinnati Radiological Society. Secretary-Treasurer, C. D. Eversole, 722 Scott St, Covington, KY 41011

Northwestern Ohio Radiological Society. Secretary, P. C. Chandnani, Medial College of Ohio, C. S. 10008, Toledo, OH 43699

Miami Valley Radiological Society. President, G. W. Bretz, 520 IBM Bldg, 33 W 1st St, Dayton OH 45402

Ohio State Radiological Society, Chapter of ACR. Secretary, W. Howland, Aultman Hospital, 2600 Sixth St SW, Canton, OH 44710

OKLAHOMA

Northwestern Oklahoma Radiological Society. Secretary, W. L. Lavendusky, 100 Center Plaza Suite C, Tulsa, OK 74119

Oklahoma State Radiological Society, Chapter of ACR. Secretary, B. G. Eaton, 2508 Stillmeadow Rd, Edmond, OK 73034

OREGON

Oregon Radiological Society, Chapter of ACR. Secretary-Treasurer, A. I. Kostiner, 8535 SW Bohmann Parkway, Portland, OR 97233

PENNSYLVANIA

Northeastern Pennsylvania Area Radiologists. Secretary-Treasurer, A. S. Haber, 181 Wilson Dr, Hazleton, PA 18201

Pennsylvania Radiological Society. Secretary R. Farrell, 201-6 Medical Arts Bldg, Scranton, PA

Philadelphia Roentgen Ray Society. Secretary, M. E. Haskin, 230 N Broad St, Philadelphia, PA 19102

Pittsburgh Roentgen Society. Secretary, R. J. Clearfield, Citizens General Hospital, 651 Fourth Ave, New Kensington, PA 15068

RHODE ISLAND

Radiological Society of Rhode Island, Chapter of ACR. Secretary, F. H. Scola, Rhode Island Hospital, Providence, RI 02902

SOUTH CAROLINA

South Carolina Radiological Society, Chapter of ACR. Secretary, G. W. Brunson, 4315 Woodleigh Rd, Columbia, SC 29206

TENNESSEE

Memphis Roentgen Society. Secretary-Treasurer, D. R. Ramey, Baptist Memorial Hospital, 899 Madison Ave, Memphis, TN 38140

Middle Tennessee Radiological Society. Secretary-Treasurer, H. P. Pendergrass, Vanderbilt University Hospital, Nashville, TN 37232

Tennessee Radiological Society, Chapter of ACR. Secretary-Treasurer, J. W. Grise, Methodist Hospital, 1265 Union Ave, Memphis TN 38104

TEXAS

Central Texas Radiology Society. Secretary-Treasurer, E. J. Schoolar, Scott and White Clinic, Temple, TX 76501

Dallas-Fort Worth Radiology Society. Secretary-Treasurer, J. T. Telle, 900 W. Randol Mill Road, #120 Arlington, TX 76012

Houston Radiological Society. Secretary, T. S. Harle, 103 Jones Library Bldg, Texas Medical Center, Houston, TX 77030

San Antonio Civilian Military Radiological Society. Secretary, J. M. Chao, Diagnostic Clinic, San Antonio, TX

Texas Radiological Society, Chapter of ACR. Secretary-Treasurer, D. N. Dysart, Scott and White Clinic, Temple, TX 76501

VERMONT

Vermont Radiological Society, Chapter of ACR. Secretary, P. Dietrich, Medical Center Hospital of Vermont, Burlington, VT 05401

VIRGINIA

Mid-Shenandoah Valley Radiological Society. Secretary, K. L. Dwyer, King's Daughters Hospital, Staunton, VA 24401

Richmond Radiological Society. Secretary, M. Vinik, 9504 Carterwood Rd, Richmond, VA 23229

Virginia Chapter of ACR. Secretary-Treasurer, C. P. Winkler, 3500 Kensington Ave, Suite 2-A, Richmond, VA 23221

WASHINGTON

Pacific Northwest Radiological Society. Secretary-Treasurer, K. D. Moores, 1118 9th Ave, Seattle, WA 98101.

Washington State Radiological Society, Chapter of ACR J. F. Sailer, 200 15th Ave E, Seattle, WA 98102. Annual meeting: May 11-13, Portland, OR

WEST VIRGINIA

West Virginia Radiological Society, Chapter of ACR. Secretary-Treasurer, A. W. Goodwin II, 200 Medical Arts Bldg, Charleston, WV 25301

WISCONSIN

Milwaukee Roentgen Ray Society. Vice President, T. C. Lipscomb, 1004 N 10th St, Milwaukee, WI 53233

Society of Nuclear Medicine, Central Chapter. G. J. Weir Jr., Marshfield Clinic, Marshfield, WI 54449

Wisconsin Radiological Society, Chapter of ACR. Secretary-Treasurer, J. Unger, Wood VA Hospital, Wood, WI 53193

Wisconsin Society of Therapeutic Radiologists. Secretary, M. Greenberg, Milwaukee County General Hospital, 8700 W Wisconsin Ave, Milwaukee, WI 53222

WYOMING

Wyoming Radiological Society, Chapter of ACR. Secretary, T. E. Hettinger, 1609 E 19th St, Cheyenne, WY

Canada

Canadian Association of Radiologists. Honorary Secretary, M. J. Palayew, Suite 806, 1440 St. Catherine St W, Montreal, Quebec, Canada H3G 1R8. Annual meetings: 1979, Sept 15-20, Vancouver; 1980, Oct 4-9, Montreal

Edmonton and District Radiological Society. Secretary, B. Caplan, 12320 103rd Ave, Edmonton, Alberta T5N ORZ, Canada

Toronto Radiological Society. Secretary, H. Shulman, Sunnybrook Hospital, 2075 Bayview Avenue, Toronto, Ontario, Canada

Central and South America

Asociacion Costarricense de Radiologia. Secretary, F. A. Arguedas Hauc, Apartado 8-5340, San Jose, Costa Rica

Colegio Brasileiro de Radiologia. Secretary-General L. C. C. Teixeira, 01311 Avenida Paulista, 491, 13th Floor, cj. 132, São Paulo, Brazil

Sociedad Chilena de Radiologia. Secretary, M. Neira, Casilla 13426, Santiago, Chile

Sociedad Colombiana de Radiologia. Secretary-General, G. Sanchez Sanchez, Bogota, Colombia

Sociedad Peruana de Radiologia. Secretary-General, E. de Olazaval Tejada, Colegio Médico del Perú, Casilla de Correo 2306, Lima Perú.

Sociedad de Radiologia del Atlantico. Secretary, R. Fernandez, Calle 40 #41-110, Baranquilla, Colombia

Sociedad de Radiologia, Radioterapéutica y Medicine Nuclear de Rosario. Secretary-General, M. Muñoz, Santa Fe 1798, Rosario, Argentina

Europe

Bavarian-American Radiologic Society. Secretary, S. A. O'Byrne, Radiology Service, Stuttgart, West Germany, 5th General Hospital, APO NY 09154

British Institute of Radiology. Honorary Secretary, D. H. Trapnell, P.N.T. Wells, 32 Welbeck St, London, W1M/7PG, England

Ceskoslovenská Radiologická Spolecnost. Secretary, J. Kolar, Radiological Clinic, Parha 2, Unemocnice 2, Czechoslovakia

Danish Radiological Society. Secretary General, J. Praestholm, Radiological Dept I, Bispebjerg Hospital, DK-2400, Copenhagen NV, Denmark

Deutsch Rontgengesellschaft. President, W. Frik, Dept Radiology, Techn Univ Aachen, D-5100 Aachen, Goethestrasse 27/29, West Germany

European Society of Paediatric Radiology. Permanent Secretary, C. Fauré, Service de Radiologie, Hôpital Trousseau, 8-28, av du Dr. Arnold Netter, 75 571, Paris CEDEX 12, France. Annual meeting and postgraduate course: April 30-May 1, Köln.

Faculty of Radiologists (of Ireland). Honorary Secretary, M. Ryan, Faculty of Radiologists, Royal College of Surgeons in Ireland, Stephen's Green, Dublin 2, Ireland

The Hospital Physicists' Association. Honorary Secretary, R. F. Mould, Westminster Hospital, Physics Dept, Page St Wing, London SW1P2AR, England

Norsk Forening for Medicinsk Radiologi. General Secretary, A. Skjennald, Ullevål sykehus, Oslo, Norway

Nederlandse Vereniging voor Radiologie. Secretary, H. E. Schütte, Dept Radiology, Elizabeth Gasthuis, Haarlem, Netherlands

Royal College of Radiologists. Secretary, P. D. Thomson, 28 Portland Pl, London, W1N4DE, England

Scandinavian Radiological Society. Secretary-General, C-E. Unnérus, Havsvindsv 5C, 02120 Esbo 12 (Hagalund-Tapiola), Finland

Schweizerische Gesellschaft fur Radiologie und Nuklearmedizin. Societe Suisse de Radiologie et de Medecine Nucleaire. Secretary, G. A. Schoch, 7 Gellerstrasse, CH-4052 Basel, Switzerland

Sociedad Española de Radiologia y Electrologia Médicas y de Medicina Nuclear. Secretary-General, P. G. Barberá, Villanueva, Madrid 1, Spain

Società Italiana di Radiologia Medica e Medicina Nucleare. Administrative Secretary, R. Dall'Acqua, Ospedale Mauriziano, 10128, Torino, Italy

Société Française de Radiologie Médicale, Médecine Nucléaire et Electrologie. Secretary-General, J. Sauvegrain, Hôpital des Enfants-Malades, 149 Rue de Sèvres, 75730 Paris Cedex 15, France.

Société Francaise de Neuroradiologie. Secretary-General, R. Djindjian, 16, rue de l'Université 75, Pairs 7°, France

Svensk Forening for Medicinsk Radiologi. Secretary, H. Ringertz, Dept Peciatric Radiology, Karolinska Sjukhuset, S-104 01 Stockholm, Sweden

Africa

Association of Radiologists of West Africa. Honorary Secretary, A. A. Obisen, Dept Radiology, University College Hospital, Ibadan, Nigeria
Radiological Society of South Africa. Secretary, A. Visser, PO Box 8850, Johannesburg, South Africa
South African International Radiological Congress. Director, P. Sneider, PO Box 4878, Johannesburg, South Africa. Durban Annual Congress: Oct 1978

Near East and Asia

Bengal Radiological Association. Honorary Secretary, B. Chatterji, 262 Rash Behari Ave, Calcutta 700019, India
Indian Radiological Association. Honorary General Secretary, S. P. Aggarwal, 10-B Kasturba Ghandi Marg, New Delhi 110001, India
Indonesian Radiological Society. Secretary, G. Sasmitaatmadja, Radiology Dept, University of Indonesia, Salemba 6, Jakarta, Indonesia
Philippine College of Radiology. Secretary-Treasurer, A. Chavez, Box 1284, Commercial Center, Makati, Rizal, D-708, Philippines
Radiological Society of Thailand. Secretary, D. Prabbasawat, Dept Radiology, Siriraj Hospital Faculty of Medicine, Mahidol University, Bangkok 7, Thailand
Royal Australasian College of Radiologists. Honorary Secretary, T. P. Loneragan, 45 Macquarie St, Sydney NSW 2000, Australia

American Journal of Roentgenology

Please enter my subscription as follows:

Beginning with _____, _____.
month *year*

Name _____

Address _____

City and State _____ Zip Code _____

Specialty _____

Amount enclosed $ _____

Annual subscription rates: $40 ($20 for residents with letter of verification) plus appropriate mailing surcharge. Mailing surcharges: U.S. and possessions, none; European countries,* $25; Japan, $45; other, $10. Subscriptions to Japan and European countries are delivered by air freight. There is no option for surface mail.

Send this form and remittance to Charles C Thomas, Publisher, 301-327 East Lawrence Avenue, Springfield, Illinois 62717.

* The European mailing surcharge applies to the following countries. All receive Journal delivery via air freight to Europe. Algeria, Austria, Belgium, Czechoslovakia, Denmark, Finland, France, Germany, Great Britain, Greece, Hungary, India, Iran, Ireland, Israel, Italy, Kenya, Luxembourg, Netherlands, Nigeria, Norway, Portugal, Romania, South Africa, Spain, Sweden, Switzerland, Turkey, Uganda, Yugoslavia.

FISCHER X-RAY

Radiographic/Fluoroscopic Systems

Affordable elegance in x-ray equipment

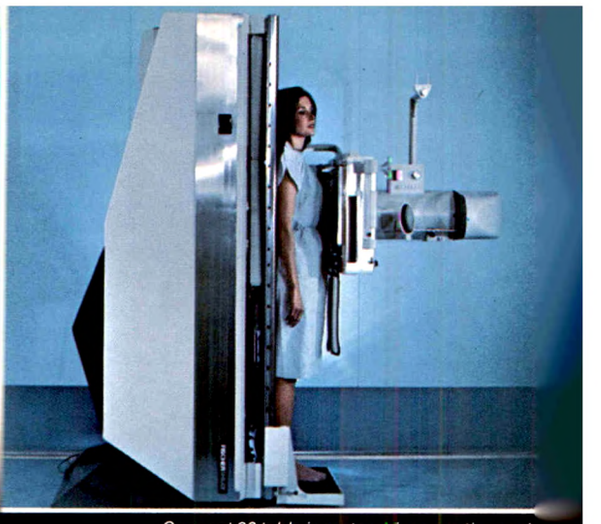

Concept 90 table is motor driven continuously from 15° Trendelenburg to 90° vertical.

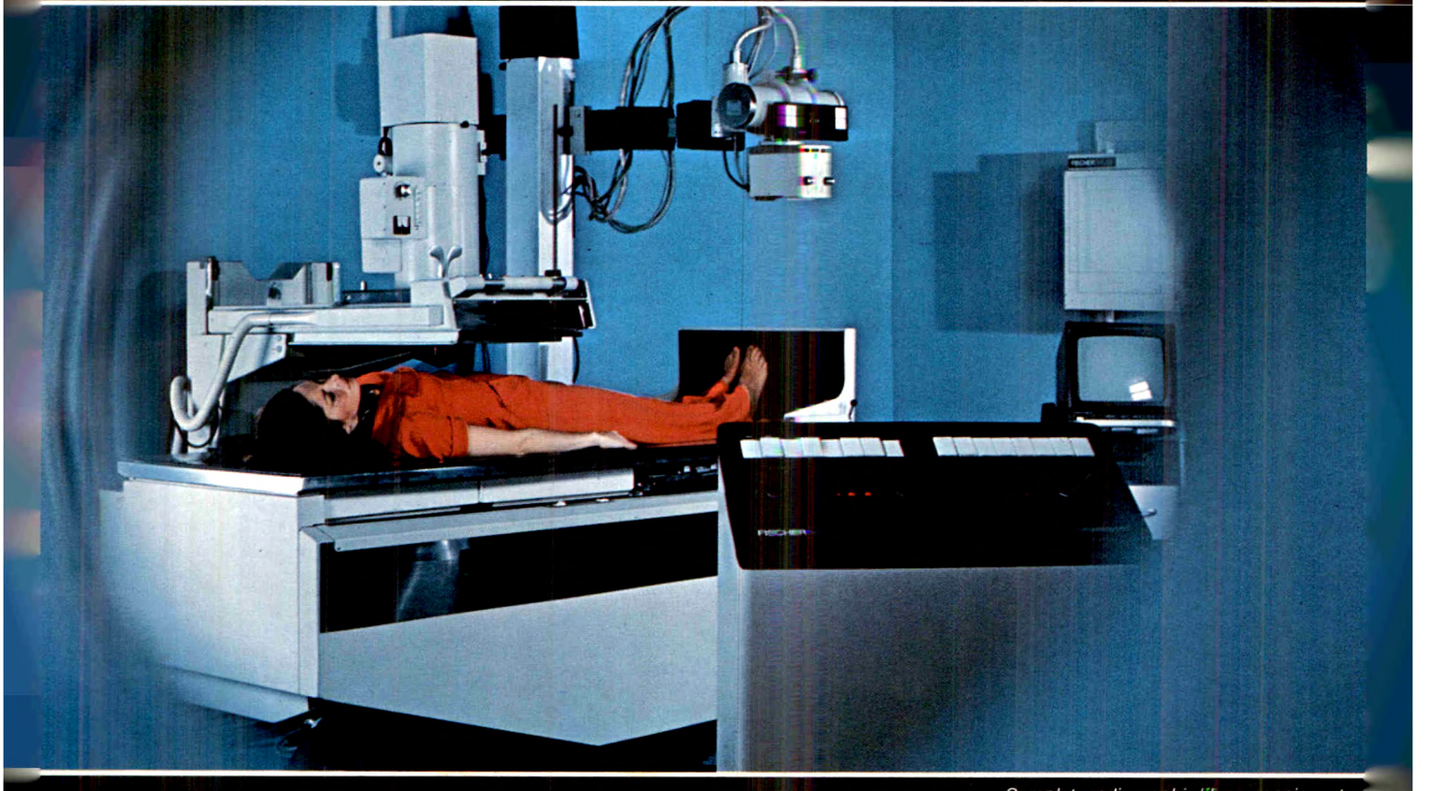

Complete radiographic/fluoroscopic system

- 500mA/125kVp generator
- 90°/15° Concept 90 table
- Remote mA and kVp controls for fluoroscopy

The generator is Fischer's new single phase, solid-state 500mA/125kVp model. The system's modular design allows you to choose just the options you need. The Fischer Concept 90 table is motor driven, and incorporates automatic stops to arrest tilt at 15° Trendelenburg, horizontal and vertical positions. Power assist standard. Fully enclosed design. Incorporates Scholz Spot-O-Matic Spot Film Device with slide-back tower. Remote mA and kVp controls for fluoroscopy may be located on the spot-film device or optical system for table-side work.

Write or call for detailed information, or the name of your local FISCHER X-RAY Representative.

FISCHER X-RAY

An established manufacturer of radiographic equipment, serving the medical profession since 1910.

H.C. FISCHER INC. 2810 N. Carnation Street, Franklin Park, Illinois 60131 • 312/671-5275

CHARLES C THOMAS · PUBLISHER

PATHOLOGY IN COMPUTED TOMOGRAPHY OF THE BRAIN *by* **Scott D. Henderson,** *Rush-Presbyterian-St. Luke's Medical Center, Chicago.* The large number of brain scans included will familiarize the reader with pathology as demonstrated on such scans. The views most representative of pathology from over 400 cases are provided. Analyses are presented in general terms to explain as much pathology as the scans are capable of showing. By reading the explanations and studying the scans, the reader will acquire a feeling for the actual physical nature of the pathology involved. Since several pathological conditions have a similar appearance on the computed tomography scan, the author stresses the importance of correlating clinical data and other diagnostic procedures to arrive at a correct diagnosis. *'78, 216 pp. (6 3/8 x 9 5/8), 839 il., $17.50*

ENDOMETRIAL CARCINOMA AND ITS TREATMENT: The Role of Irradiation, Extent of Surgery, and Approach to Chemotherapy *edited by* **Laman A. Gray, Sr.,** *Univ. of Louisville, Louisville, Kentucky. (27 Contributors)* Outstanding specialists in the fields of radiology, obstetrics, gynecology, pathology, and related disciplines have produced this examination of the treatment of endometrial carcinoma. Analysis of the most progressive treatment modalities of radiotherapy, surgery, and chemotherapy are presented. The reader will encounter documented cases of departures from the standard use of intrauterine radium therapy before surgery. The book examines the roles of radiotherapy, surgery, and chemotherapy in treatment as well, and records reports from cancer centers and universities attesting to recent findings in the field. *'77, 240 pp. (6 3/4 x 9 3/4), 17 il., 138 tables, $22.50*

UROLOGICAL RADIOLOGY OF THE ADULT MALE LOWER URINARY TRACT: Anatomy, Physiology, Pathology and Sequelae, Diagnosis and Management *by* **R. W. McCallum** *and* **V. Colapinto,** *both of St. Michael's Hospital, Toronto, Ontario, Canada.* This monograph outlines the authors' personal experience with fifteen anatomic and microscopic dissections of the urethra, over 1,000 radiological examinations of the urethra and 240 two-stage urethroplasties. Emphasis is made of the presence of three separate sphincter mechanisms below the bladder. Pre- and postoperative radiological urethrographic examinations are detailed. Radiological examinations of the bladder, prostate and urethra are extensively discussed, and numerous original radiographs and illustrations are included. A new method of radiological examination of the lower urinary tract in paraplegics is described. *'76, 376 pp. (6 3/4 x 9 3/4), 248 il., 2 tables, $35.50*

RADIOASSAY IN CLINICAL MEDICINE *edited by* **William T. Newton** *and* **Robert M. Donati,** *both of Washington Univ., St. Louis, Missouri. (9 Contributors)* The text is concerned with the techniques and use of radionuclides in the assay of chemical compounds of biologic interest. Techniques described include: radioimmunoassay, inhibition assays, competitive protein binding assays, and bioassays. Also, individual assays of protein, peptides, steroids, fatty acids (prostaglandins) and a water soluble vitamin are presented. Specific compounds of clinical interest also discussed include: prostaglandins, digitalis, thyroid hormones, vitamin B_{12}, long-acting thyroid stimulator, and erythropoietin. The volume will be of interest to physicians in the growing area of radioassay development, and to nuclear medicine specialists interested in clinical applications. *'74, 200 pp., 41 il., 24 tables, $11.75*

THE PHYSICS OF RADIOLOGY (3rd Ed., 5th Ptg.) Harold Elford Johns *and* **John Robert Cunningham,** *both Univ. of Toronto, Toronto, Ontario, Canada.* This classic radiological physics offers an orderly presentation of mater on a complex subject. The emphasis of the text is on high energy radiation. Computers are finding an ever-increasi application in calculations of dose distributions in radi therapy, therefore numerous sections are devoted to compu techniques as well. A section on the solid state dosimeter lit ium fluoride is included. The concepts of kerma, partic fluence and energy fluence are illustrated with examples, a the chapter, *Clinical Use of Isotopes,* offers considerable d cussion on the use of short-lived isotopes which can be o tained from isotope generators. Final chapters featu diagnostic radiology and television in radiology. A chapter radiobiology provides information concerning the nature radiation damage, repair processes in cells and fractionatic *'78, 816 pp. (6 1/8 x 9 1/4), 398 il., 92 tables, $26.75*

THE CARE AND MANAGEMENT OF THE SICK AND I COMPETENT PHYSICIAN *by* **Robert C. Green, Jr., Geor J. Carroll** *and* **William D. Buxton,** *all of the Virginia St Board of Medicine.* The authors detail the management, p vention and identification of problems which impair t ability of a physician to perform adequately. They unders the medical profession's responsibility to itself and to t public to provide action to correct such situations. Init chapters outline the demand for professional discipline a methods for maintaining professional competence. Speci issues are then discussed, with chapters on the addicted phy cian, psychiatric illness and behavioral problems among ph sicians, senility, physical illness, clinical obsolescence, t legal rights of the physician and the profession's sponsibility toward him. This is a timely book which w provide impetus to better management of a growing proble *'78, 116 pp., 13 tables, $8.50*

THE BASIC PHYSICS OF RADIATION THERAPY (2 Ed.) *by* **Joseph Selman,** *Tyler Junior College, Tyler, Tex* The author states, "The purpose of this book is to explain t fundamental physical principles underlying radiation thera in as comprehensive and comprehensible a manner as possib without sacrificing accuracy for simplicity." Doctor Selm fulfills his purpose by focusing on these specific areas: simp mathematics in radiation therapy, basic physical concepts, diation quality, radiation exposure and dosage, therapy pla ning, newer modalities in radiotherapy, and radium a radionuclide therapy. He includes detailed discussion of radi biology and health physics. Primarily written for the radiolo resident and practicing radiologist, this handbook will useful in training programs and helpful as a comprehensi refresher course. *'76, 768 pp., 356 il., 66 tables, $25.75*

THE BIOLOGICAL AND CLINICAL BASIS OF RADI SENSITIVITY *edited by* **Milton Friedman,** *Instituto Reg Elena, Rome, Italy. (35 Contributors)* To reduce the gap tween laboratory and clinical schools authorities from fields of radiobiology, radiation pathology, preclinical radio ology and experimental clinical radiotherapy relate their inv tigations to the common denominators of radiosensitivity a chemosensitivity. Topics discussed include: changes produ by irradiation at the molecular level, recovery from irradiati factors like DNA strand breaks which can influence radiose tivity, and clinical concepts of radiosensitivity such as tun lethal dose. *'74, 592 pp. (7 x 10), 373 il., 67 tables, $49.5*

Orders with remittance sent, on approval, postpaid

301-327 East Lawrence Avenue • Springfield • Illinois • 62717

Philips Angiography Systems.

TOTAL BODY COVERAGE WITH THE BROADEST RANGE OF EQUIPMENT

. . . from the only company offering all the choices you need!

Poly Diagnost C

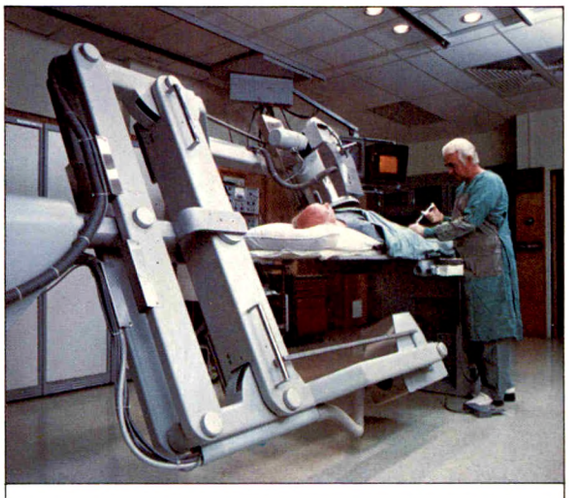

The parallelogram construction of the Poly Diagnost C permits the patient to remain stationary, leaving the physician more relaxed and able to concentrate fully on the procedure. Insuring maximum safety for both patient and operator, the Poly C provides both routine and cranio-caudal views that insure clear, unobstructed views of overlapping vessels. Stenoses which might have been obscured can be detected with a high degree of efficiency and operational ease.

Designed for both the brachial and femoral techniques of cardiac angiography, the Poly C is also successfully used in abdominal and thoracic studies.

Poly Diagnost N

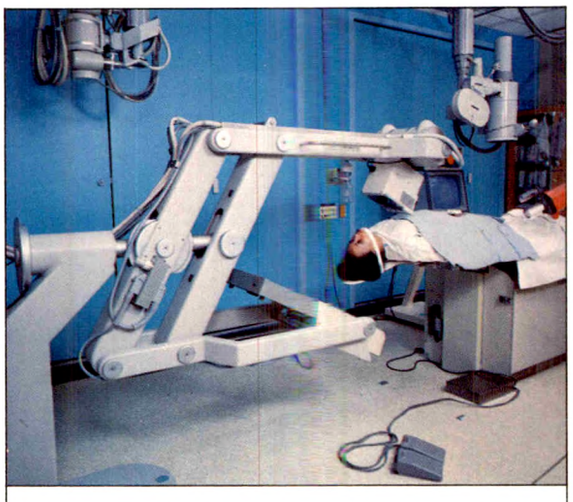

Designed specifically for cerebral angiography at 2:1 magnification, the Poly Diagnost N easily provides views of the patient previously difficult (or impossible) to achieve. The parallelogram construction allows full rotation around the long axis of the body *and* the maximum desirable head-to-foot angulation. The unique construction insures all motions are isocentric and all results are distortion free.

Designed for use in single or bi-plane operation with a Puck rapid film changer, the Poly N lends itself to extensions for more dedicated requirements, such as the latest configuration with a quickly interchangeable image intensifier and a rapid film changer.

PHILIPS MEDICAL SYSTEMS, INC.
710 Bridgeport Avenue, Shelton, Conn. 06484

Philips Angiography Systems.

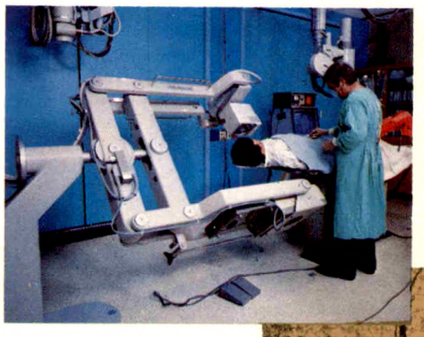

Poly Diagnost N

The first in Philips' family of dedicated cerebral angiography systems with parallelogram construction. For optimum results with isocentric patient positioning for all projections.

Poly Diagnost UPI

Philips' new universal angiography system for the most flexible filming of cerebral, thoracic, abdominal and peripheral angiography, with full provision for occasional cardiovascular examinations.

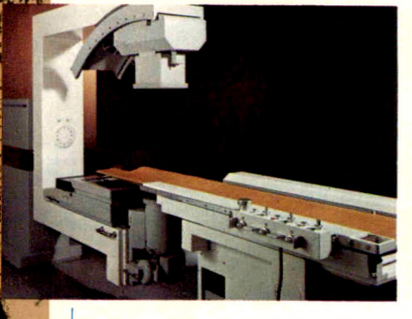

Poly Diagnost C

An extension of the U-arm principle first developed by Philips in the Cardio Diagnost, the Poly C is a dedicated cardiovascular system. Parallelogram construction provides routine and cranio-caudal views without moving the patient, making the Poly C widely used for imaging the thoracic and abdominal areas.

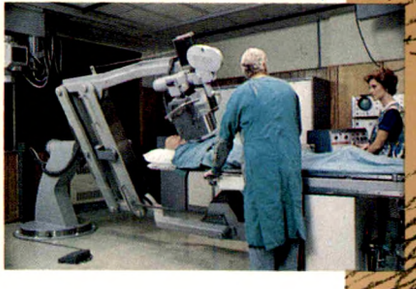

Poly Diagnost UPI

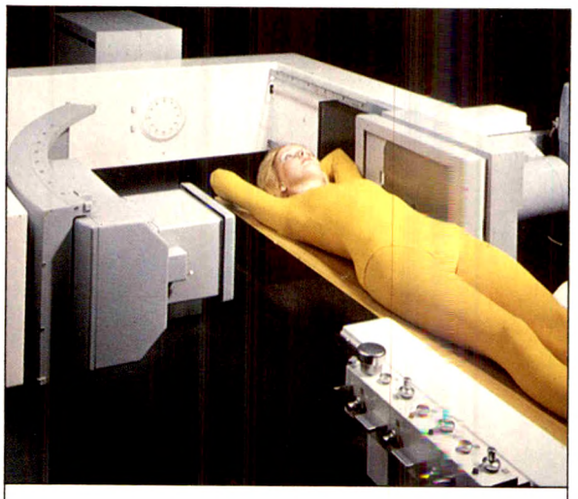

A universal system with revolutionary design, the Poly Diagnost UPI features a rotating U-arm that carries the X-ray tube and an image intensifier and rapid film changer which are quickly interchangeable.

A new experience in examination convenience, the Poly UPI is a masterful combination of system features: free choice of oblique, cranio-caudal and caudo-cranio projections; rapid changeover from fluoroscopy to film changer work; automatic control of object-film distance; motorized height adjustment of both table and U-arm, which provides contact and up to 2:1 geometric enlargement; and a unique boating movement that keeps the object centered in the beam while the object-film distance is automatically controlled in every projection. It's the ideal universal system for angiography.

PHILIPS®

® TM N.V. Philips of Holland

A COMPLETE FAMILY OF IMAGE INTENSIFICATION SYSTEMS, X-RAY TUBES AND GENERATORS FOR PHILIPS ANGIOGRAPHIC EQUIPMENT.

The 14″ Triple-Mode Image Intensifier
Another first from Philips! An amazingly lightweight 14″ image intensifier for highly detailed surveys with outstanding results.

Super Rotalix and Trinodex X-ray Tubes
Preferred for exceptional image quality and reliable performance in sustained operation, Philips' tubes are designed for high loadability and superbly efficient heat dissipation.

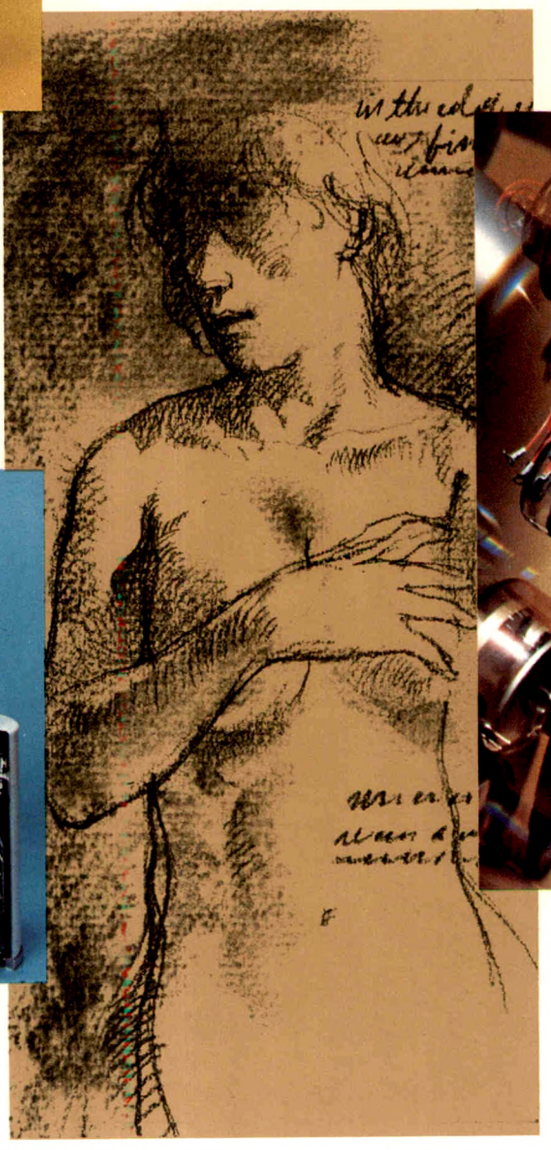

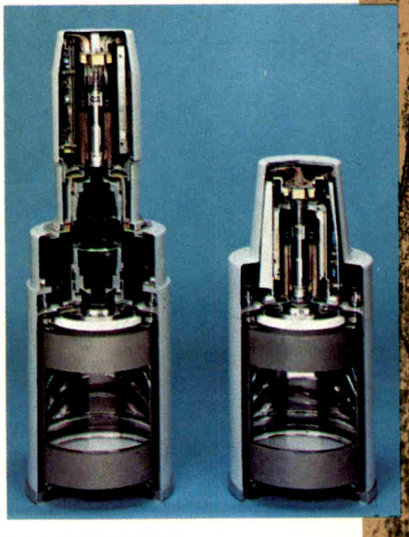

Conventional or Fiber Optic Image Intensifiers
Select from a full range of fields in conventional image intensifiers . . . or Philips' Exclusive Fiber Optic Image Intensification System. Fiber optics provides 30:1 contrast ratio for greater detail, uniform image quality over the entire screen, optimum image transfer and compactness for easy maneuverability.

PHILIPS®
the most reliable family of systems and people in the industry.

A Full Range of Generators
From the very affordable three-phase, high output Classic line, to a full range of Modular Generators, to the computerized Optimus M200, Philips' family of generators combines quality, performance and price for your every examination need.

"IMAGEOLOGY 1979"

February 16-23, 1979
Konover Hotel
Miami Beach, Florida

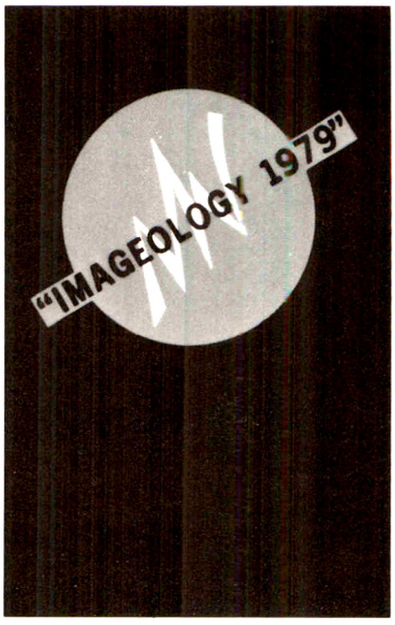

Presented by

The Department of Radiology at Mount Sinai Medical Center in collaboration with the Department of Radiology at the University of Miami School of Medicine/Jackson Memorial Medical Center.

***Program Director:* Manuel Viamonte Jr., M.D.**

GUEST FACULTY

Arthur R. Clemett, M.D., Clinical Professor of Radiology, New York University School of Medicine; Chief, Department of Radiology, St. Vincent's Hospital and Medical Center, New York, New York.

Erich K. Lang, M.D., Professor and Head, Department of Radiology, Louisiana State University Medical Center, New Orleans, Louisiana.

John E. Madewell, M.D., Chief, Registry of Radiologic Pathology, Armed Forces Institute of Pathology, Washington, D.C.

Rogelio Moncada, M.D., Professor of Radiology, Loyola University Medical Center, Maywood, Illinois.

Donald L. Resnick, M.D., Chief, Department of Radiology, Veterans Administration Hospital; Associate Professor of Radiology, University of California, San Diego, California.

And Local Faculty of Mount Sinai Medical Center and the University of Miami School of Medicine/Jackson Memorial Medical Center.

AMA CREDIT HOURS IN CATEGORY 1—36

(with an additional 8.5 Credit Hours for Self-Instruction Materials)

Description of Course: In this course outstanding clinicians will describe various clinical problems; Radiologists (guest and local faculty) will discuss the diagnostic efficacy of different imaging techniques; and expert physicians responsible for treatment will indicate how they use the information provided by the Radiologist for the cure or palliation of the following disease processes: Mediastinal and Cervicomediastinal lesions; Ischemic Myocardial and Cerebral Diseases; Bronchial Carcinoma; Aortopathies; Pulmonary Thrombo-Embolism and other Angiopathies; Liver Masses; Jaundice; Tumors of the Breast, Pancreas, Brain and Genitourinary Tract; Focal and Generalized Osteopathies and Arthropathies.

The attendees will receive summaries of the presentations and a group of diagnostic flow-charts (algorithms). A questionnaire with over 200 questions will be submitted to the registrants which should be answered prior to the meeting. The same questionnaire will be given at the conclusion of the course to assess its educational effectiveness.

REGISTRATION FEES: GENERAL $300—RESIDENTS & FELLOWS $150

I am interested in attending the "Imageology 1979" Seminar in Miami Beach on February 16-23, 1979. Please send more information.

NAME_____

ADDRESS:_____

_____

(City) (State) (Zip Code)

I will_____ will not_____ require hotel reservations.

Accompanied by spouse Yes_____ No_____

Detach and Mail To: **Lucy R. Kelley**
c/o Miami Seminars
Post Office Box 343762
Coral Gables, Florida 33134

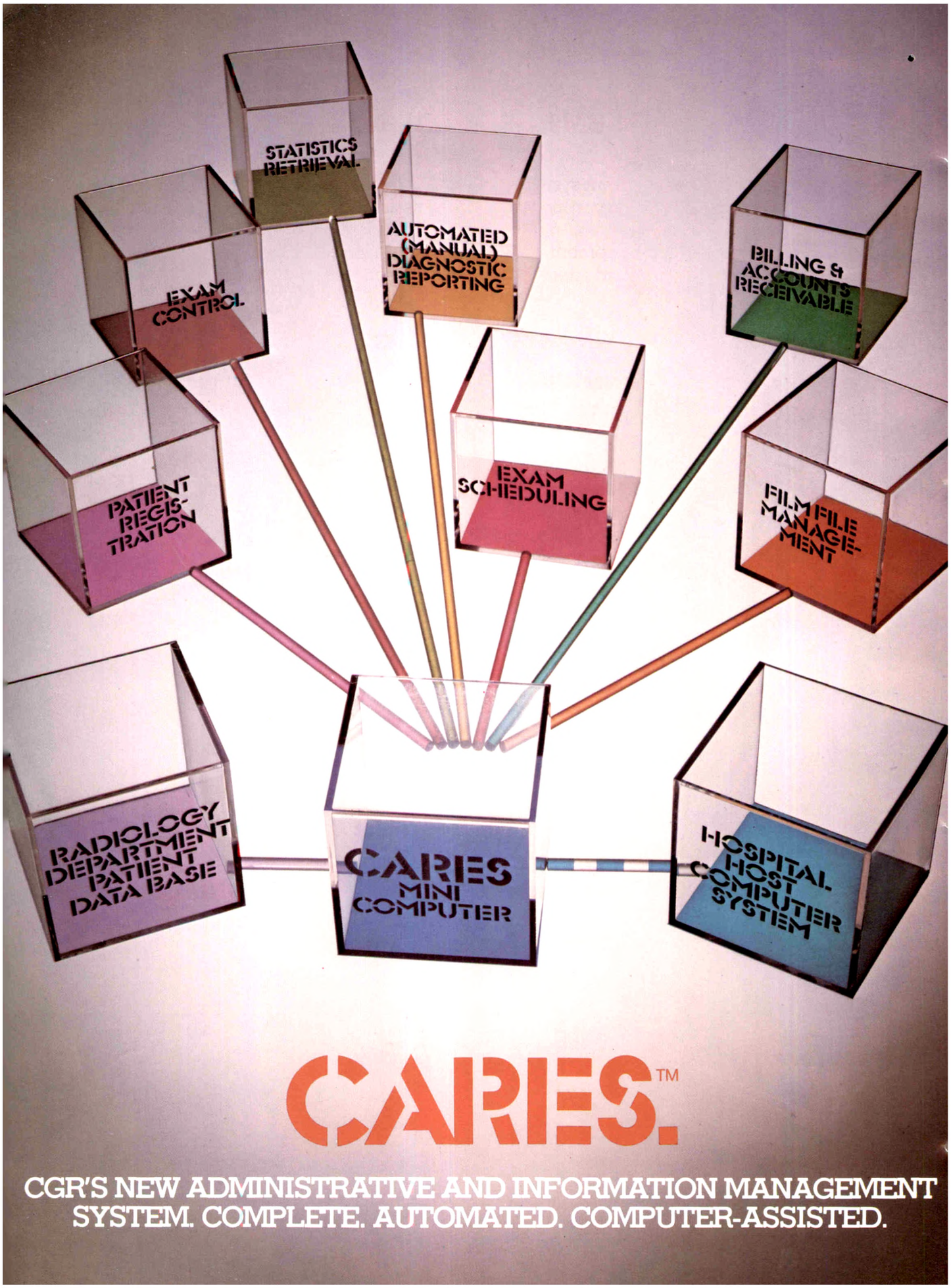

CARES™

CGR'S NEW ADMINISTRATIVE AND INFORMATION MANAGEMENT SYSTEM. COMPLETE. AUTOMATED. COMPUTER-ASSISTED.

A TOTAL SYSTEM FOR TOTAL MANAGEMENT.

CARES is CGR's total management system for today's modern radiology department. A system that extends the advances of your professional technique and equipment by improving information flow and departmental administrative functions.

It's a complete computer system. Hardware and software designed specifically for the radiology department. By radiology professionals.

CARES will speed your patient registration, cut paperwork, control examination scheduling and maximize your filing and record retrieval. It will assist you in diagnostic reporting, typing and distribution and expand your statistical capabilities. CARES will control your accounts receivable, bill accurately and monitor equipment usage and staff/departmental functions. And finally it will improve efficacy for both patient and department staff.

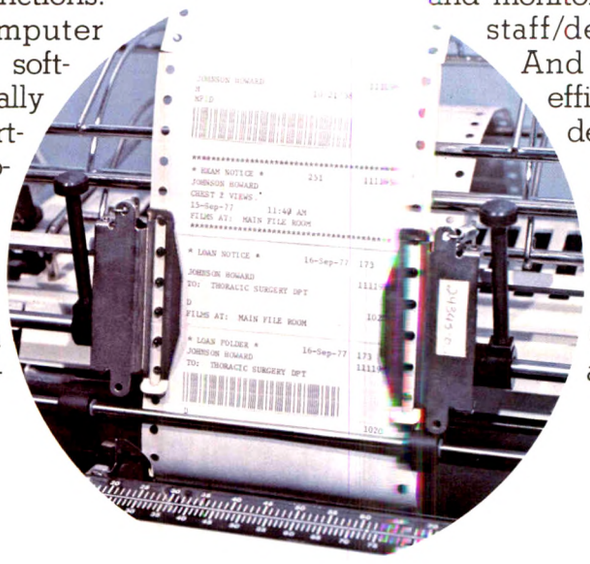

CARES has been designed for you. To keep pace with increased demands and promote cost effectiveness. Your CGR representative has all the details.

CGR

CGR MEDICAL CORPORATION
2519 Wilkens Avenue, Baltimore, Maryland 21223 (301) 233-2300
CGR CANADA LTÉE-LTD.
500 Boulevard de l'Aéroparc, Lachute, Québec, Canada (514) 562-8806

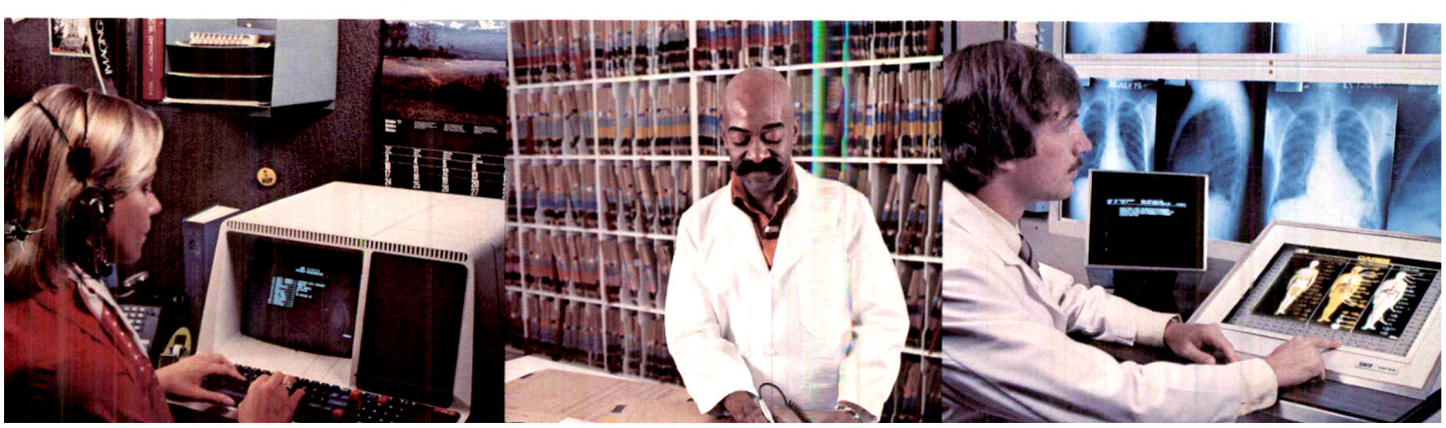

If you had dyslexia it could take you thirty minutes to read this ad.

Some dyslexics might not be able to read it at all.

Instead of a page of words, this ad would appear as a jumble of letters to the severely dyslexic person.

Dyslexia is a learning disability which prevents the brain from receiving correct written messages sent by the eyes. And since dyslexics are often extremely bright, imagine how frustrating it must be to be able to see and yet not read.

Of course, dyslexics, the blind and physically handicapped could attend school along with everyone else if someone read their textbooks to them.

And that's what we do. Recording for the Blind "reads" to thousands of disabled students by lending them tapes of their school books free of charge. Recording for the Blind's Master Tape Library numbers nearly 40,000 recorded titles and is still growing. New texts are recorded all the time.

You can help us keep up with the demand. If you can spare two hours a week, and if you have a technical background, or if you are a professional or a native speaker of a foreign language, please volunteer. If you know of someone in need of our services, let us know. Recording for the Blind is a non-profit organization supported by volunteers and contributions from the public.

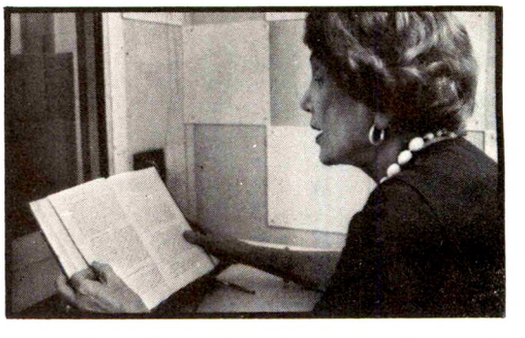

Recording for the Blind has 29 recording studios across the country. To find the one nearest you and for more information, please write us:

Recording for the Blind . . . . . *an educational lifeline*
215 East 58th St., New York, NY 10022

CHARLES C THOMAS • PUBLISHER

BONE TUMORS: General Aspects and Data on 6,221 Cases (3rd Ed.) *by* **David C. Dahlin,** *Mayo Clinic, Rochester, Minnesota.* New features for this edition include chapters on benign and malignant (fibrous) histiocytomas; description and illustration of recognizable types of osteosarcoma and chondrosarcoma; and several novel examples of bone tumor simulators. The text as a whole continues to document the experience of the Mayo Clinic in the diagnosis, management and follow-up of more than six thousand patients with primary tumors of bone. The gross pathologic, histologic and roentgenologic features of these lesions have been correlated. The 97 to 100 per cent complete follow-up studies of the various entities have allowed certain conclusions regarding clinical courses and responses to therapy. The text is amplified by detailed coverage of reactive processes, developmental lesions, traumatic alterations and other conditions that produce skeletal abnormalities. Pathologists, radiologists and surgeons concerned with skeletal disease will find this respected treatise a valuable repository of information. *'78, 464 pp. (8 1/2 x 11), 740 il., 7 tables, $32.75*

A STUDY GUIDE FOR RADIOLOGIC TECHNOLOGISTS *by* **Judith Posner Baron,** *College of Lake County, Grayslake, Illinois.* This text will be ideal for the practicing technologist who wishes to up-date his knowledge. Because it is a programmed text, it will provide optimum comprehension. Emphasis is placed on the development and application of concepts rather than on rote learning. Along with standard radiologic technology topics, the book details such subjects as exposure techniques, solid state rectifiers and exposure switches, rare earth intensifying screens, grid-controlled x-ray tubes, thermoluminescent dosimeters, radiation biology, image intensifier tubes, image storing and retrieval devices, xeroradiography, and electron radiography. The text further features a brief introduction to relevant physics, chemistry and biology, and a review of terminology for the novice. *'78, 560 pp., 200 il., $17.50*

PRINCIPLES OF RADIOGRAPHIC EXPOSURE AND PROCESSING (2nd Ed., 13th Ptg.) *by* **Arthur W. Fuchs,** *Rochester, New York.* An amply illustrated guide for the x-ray technician and radiologist on the accepted procedures for the production of good quality radiographs from properly exposed x-ray film, this book describes a simple though exact exposure system which is based upon proven fundamental theories and practices. Wherever possible, the exposure factors have been reduced to constants, thereby eliminating many sources of possible error. The book discusses in detail the operations necessary for correct handling and chemical treatment of exposed x-ray film to convert it to a radiograph. A fourteen page glossary of terms and techniques adds to this work. *'77, 302 pp. (7 x 10), 600 il., 25 tables, $18.50*

ELEMENTS OF RADIATION PROTECTION *by* **Ronald V. Scheel,** *and* **Jack Wakley,** *both of the Univ. of Virginia School of Medicine, Charlottesville.* Information in this textbook includes atomic structure, ionizing radiation, interaction of radiation with matter, sources of radiation exposure, biological manifestation of radiation exposure, permissible dose limits, principles of radiation protection and monitoring devices. Several chapters of the book deal with federal performance standards and Atomic Energy Commission regulations. The material content and mode of presentation are clear and nonmathematical for those students who have little background in physics and mathematics. *'75, 112 pp., 15 il., 10 tables, $7.95, paper*

Orders with remittance sent, on approval, postpaid

301-327 EAST LAWRENCE
SPRINGFIELD • ILLINOIS • 62717

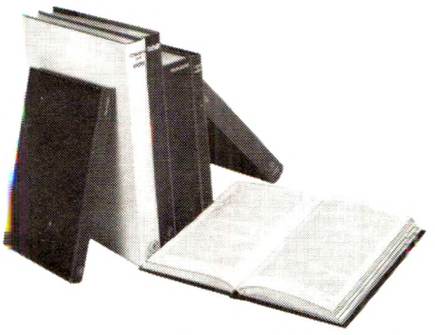

Asbestos-Related Disease

RADIOLOGIC ASPECTS IN DIFFERENTIAL DIAGNOSIS

Edited by LESLIE PREGER, M.D., F.R.C.R., with DONALD T. ARAI, M.D., PAUL KOTIN, M.D., HANS WEILL, M.D., and JACK WERCHICK, J.D.

FROM THE PREFACE:
The purpose of this book is to help identify asbestos-related disease and to provide a guide to physicians who must reassure the "worried well" who have been exposed to asbestos but who are free from asbestos-related disease. Much has been written on asbestos in the past, but such material frequently appears in journals not usually read by general physicians and clinical radiologists. Computer searches of this material have allowed collation of many of these reports.

CONTENTS: *D. T. Arai and H. Weill,* Clinical Problems in Asbestos-Related Diseases. *L. Preger,* Organ Involvement in Asbestos-Related Disease. *L. Preger,* IlO U/C 1971 International Classification of Radiographs of the Pneumoconioses. *P. Kotin,* The Industrial Medical Officer and Corporate Responsibility. *J. Werchick,* Medicolegal Aspects.

1978, 288 pp., $24.50/£15.90 ISBN: 0-8089-1083-5

Roentgenology of Fractures and Dislocations

A Seminars in Roentgenology Reprint

Edited by BENJAMIN FELSON, M.D.

CONTENTS: *B. Felson,* Letter from the Editor. *T. A. Tomsick,* Gamut: Normal Skull Variants that may Simulate a Fracture. *R. Grusd,* Gamut: Pseudofractures and Stress Fractures. *R. R. Renner et al.,* The Radiologist, the Orthopedist, the Lawyer, and the Fracture. *T. E. Keats,* An Atlas of Simulated Fractures. *T. A. Tomsick et al.,* Skull. *K. D. Dolan and C. G. Jacoby,* Face. *J. H Harris, Jr.,* Spine. *K. R. Kattan,* Bony Thorax. *H. Pavlov and R. H. Freiberger,* Shoulder. *L. F. Rogers,* Elbow. *J. J. Kaye,* Hand and Wrist. *A. Thaggard III et al.,* Bony Pelvis and Hip. *J. Edeiken and J. M. Cotler,* Ankle. *L. F. Rogers and R. E. Campbell,* Foot. *F. N. Silverman,* Pediatric Fractures.

1978, 192 pp., $19.50/£12.65 ISBN: 0-8089-1131-7

Send payment with order and save postage and handling charge. *Prices are subject to change without notice.*

GRUNE & STRATTON
A Subsidiary of Harcourt Brace Jovanovich, Publishers
111 FIFTH AVENUE, NEW YORK, N.Y. 10003
24-28 OVAL ROAD, LONDON NW1 7DX

Remote but not removed

With our new Galaxy™ II Remote system, you can perform high-quality R&F examinations with the time-saving accuracy and ease of remote control. And yet, you can change easily to tableside operation when being close to your patient is important. A turn of a key fulfills your choice—either remote or classic operating modes.

Remote operation offers maximum patient throughput with minimum operator fatigue in a minimum radiation environment...while you maintain control over every examination.

Understandably certain examinations such as myelography or those involving the uncooperative patient require close patient contact and suggest tableside operation. Then again, for routine GI work with cooperative patients, why not relax at your remote console? The choice is yours for remote or classical operation.

The Flushmount™ imaging concept maximizes spotfilm results with improved patient geometry. And our "mini-cassetteless" Multispot 100 camera eliminates the need to change spotfilm cassettes during the examination. Also, for those who prefer a spotfilmer, a programmed Multiview filmer is available.

Galaxy II Remote.

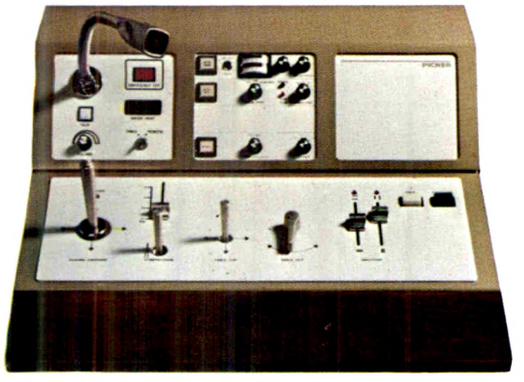

For installation versatility, Picker's Galaxy II Remote console may be desk or pedestal mounted in the control booth. The compact design requires minimal space and features simple operator controls. These are human engineered for quick orientation.

Maximum diagnostic information is achieved with our high-performance, dual-mode televised imaging system. For permanently recorded images, automatic exposure control provides consistent film density...exposure after exposure.

Four-way power top coverage for full patient positioning is provided. The Galaxy II-90 Table is capable of all necessary motions for tableside or remote R&F procedures. The Universal Bucky II features sinusoidal grid drive to give line-free films with X-ray exposures as short as 2 milliseconds.

And like all Picker equipment, this system is backed by our worldwide service organization which has a reputation for top performance.

Galaxy II Remote works hard to make your work easy. For more information contact your local Picker representative, or write Picker Corporation or Picker International, 595 Miner Road, Cleveland, OH 44143.

PICKER®
ONE OF THE CIT COMPANIES

We want you to talk in our library.

Ours is a living library of spoken words. A library of roughly 40,000 textbooks on tape, available free of charge to blind students. Eligible students also include the visually impaired, the learning disabled, and the physically handicapped who cannot handle printed material.

These students continually require new texts. And to fill this need, volunteer readers make tapes in our 29 recording studios across the country.

We urgently need readers with technical or professional backgrounds, and native speakers of foreign languages. If you can spare two hours a week, please volunteer. We are a non-profit organization supported by contributions from the public.

Recording for the Blind . . . . . *an educational lifeline*
215 East 58th St., New York, NY 10022.

Most computer tomograph scanners have excessive lag-time between machine scanning and image reconstruction.

The Siemens Difference: Instantaneous image reconstruction

Immediate clinical evaluation

Delayed processing time is a thing of the past with Siemens computer tomographs, SIRETOM and SOMATOM. A specially designed high-speed computer reconstructs scanned images instantaneously. This permits immediate decisions as to diagnosis and course of treatment while providing for faster and smoother patient processing.

Reduced scan time

Scanning for both SIRETOM (head scanner) and SOMATOM (whole body scanner) is governed by the SCINTILLARC fan-beam solid-state detector array system. The result of this advanced engineering is evidenced by a dramatic reduction in setup and scan time along with unsurpassed quality tomograms achieved under clinical conditions.

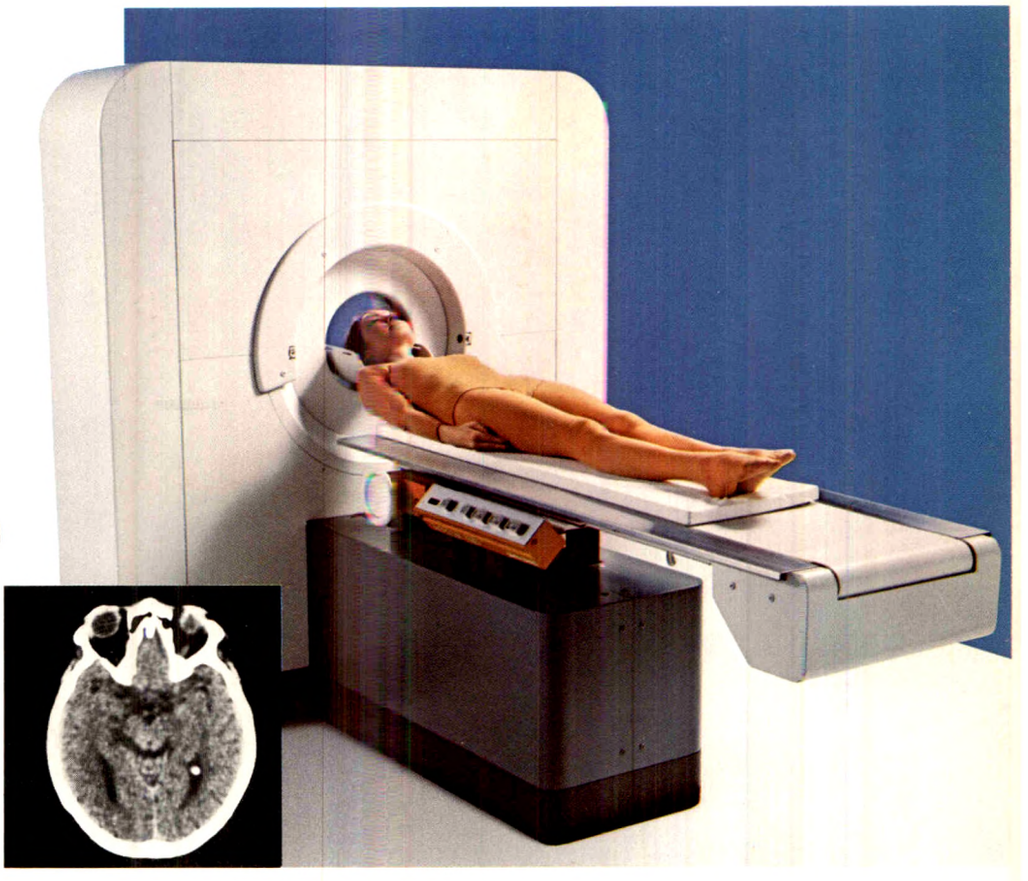

Concepts... engineered to radiologic excellence

SIEMENS

Most high-energy linear accelerators continue to use thick target and thick scattering foil techniques to produce X-ray and electron beams.

The Siemens Difference: Advanced X-ray target and electron scattering foil systems

The MEVATRON-20

Siemens' newest accelerator, the MEVATRON-20, utilizes a multiple element X-ray target and a unique double-foil electron scattering system to produce outstanding beam quality. Additionally, it features an integral verification capability for error-free machine setup. And with the highly flexible "Z" patient table, it forms a truly integrated installation ideally suited for modern radiation therapy technique.

The MEVATRON series

Siemens' product selection also includes the MEVATRON-6 and MEVATRON-12 which, together with MEVATRON-20, cover the full spectrum of energy and modality requirements.

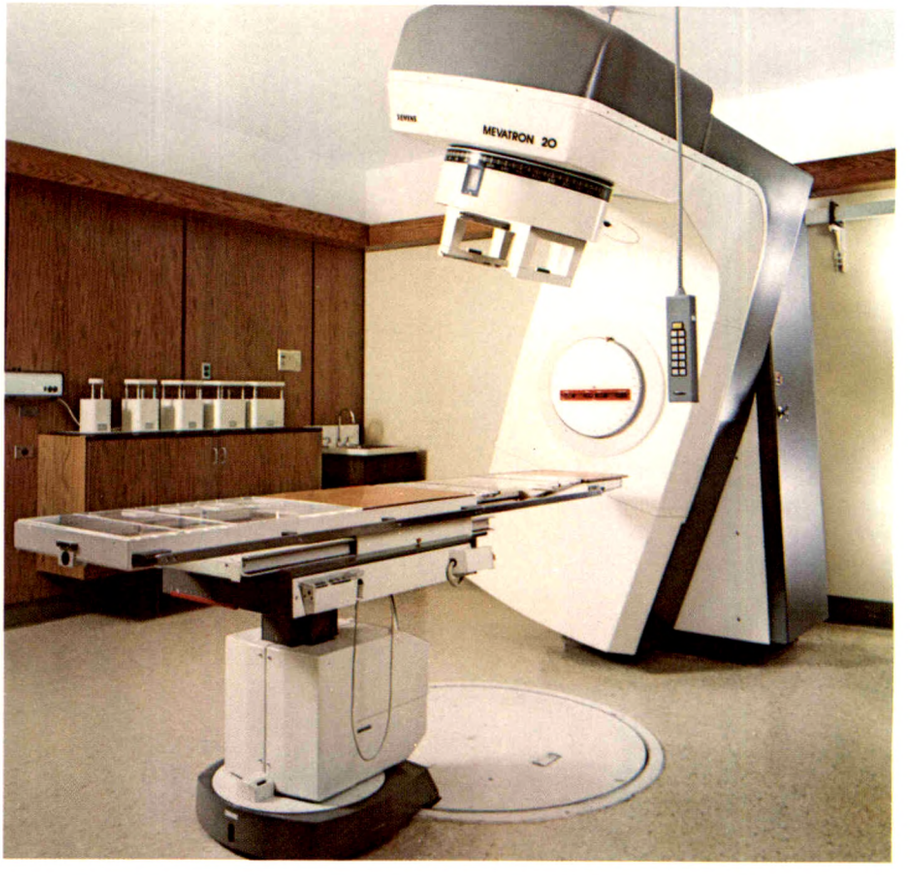

Most remote-controlled examination units are products of alterations to standard radiographic and fluoroscopic units.

The Siemens Difference: Specific systems for specific needs

Versatile applications

Siemens responds to the varying needs of the radiologist with a full line of remote-controlled examination units – SIREGRAPH A, SIREGRAPH B, and SIREGRAPH II. Virtually every radiographic or fluoroscopic examination may be performed on a system from our wide selection of universal procedure or dedicated-purpose remote-controlled diagnostic products.

Individualized systems

Our systems were developed to meet the growing preference for remote examination tables and to meet the need for individual, custom-designed units that would satisfy different levels of requirements for versatility and application.

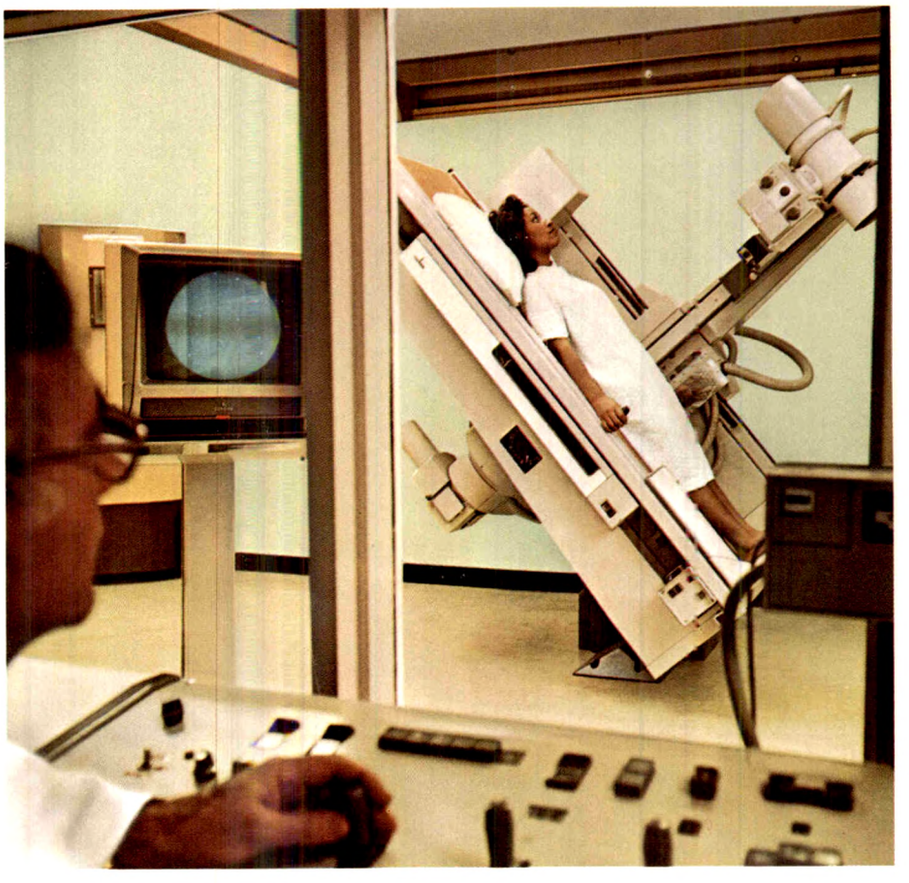

Concepts... engineered to radiologic excellence

SIEMENS

Most of today's diagnostic X-ray generators still require lengthy programming of routines—individual selection of exposure time, focal spot, milliampere, and major and minor kilovoltage settings.

The Siemens Difference: Organ-related push-button programming

Simplicity of operation

Siemens has engineered operator time efficiency into diagnostic X-ray generators. Both OPTIMATIC and ORGANOMATIC generator series feature organ-related techniques which eliminate errors caused by miscalculation of exposure times and settings. One push button selects the examination units, kV, mAs, focal spot, and screen-type. The result is more efficient operational control and improved patient processing.

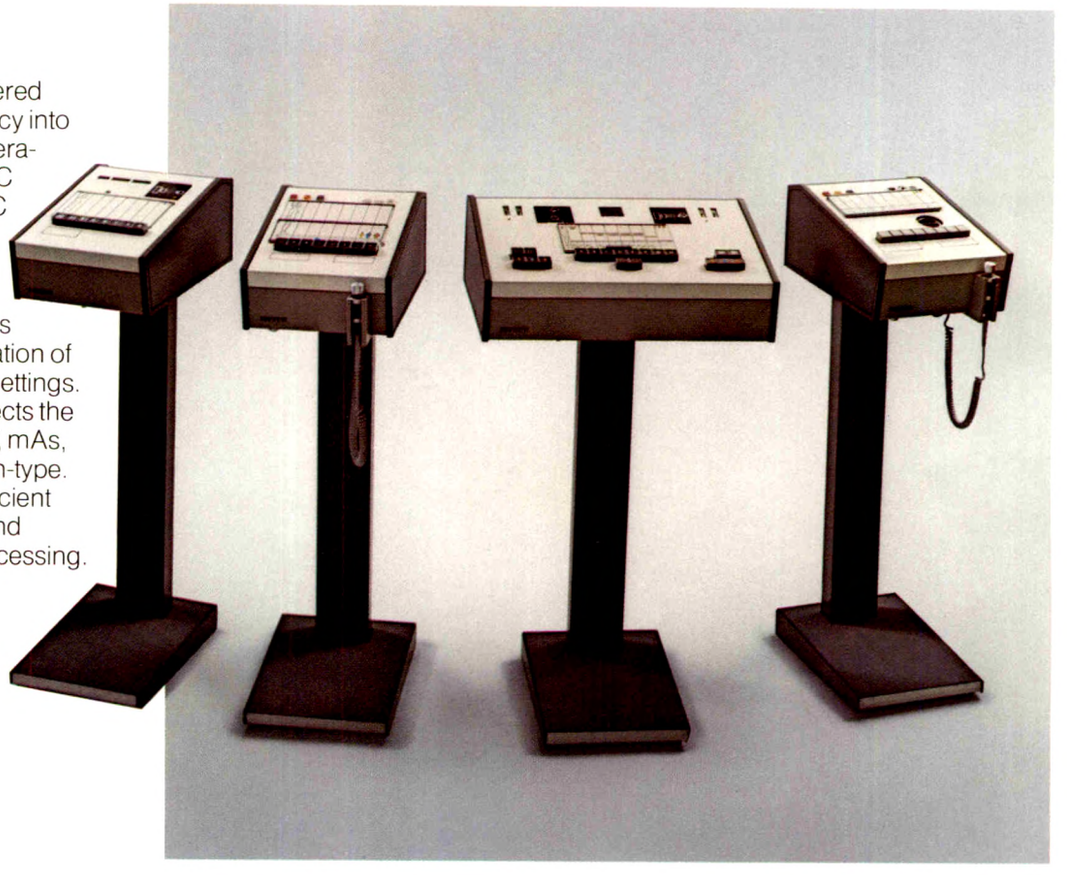

For Double Contrast Stomachs, Use

NEW! E-Z-HD™

High Density with High Fluidity Barium Sulfate for Suspension

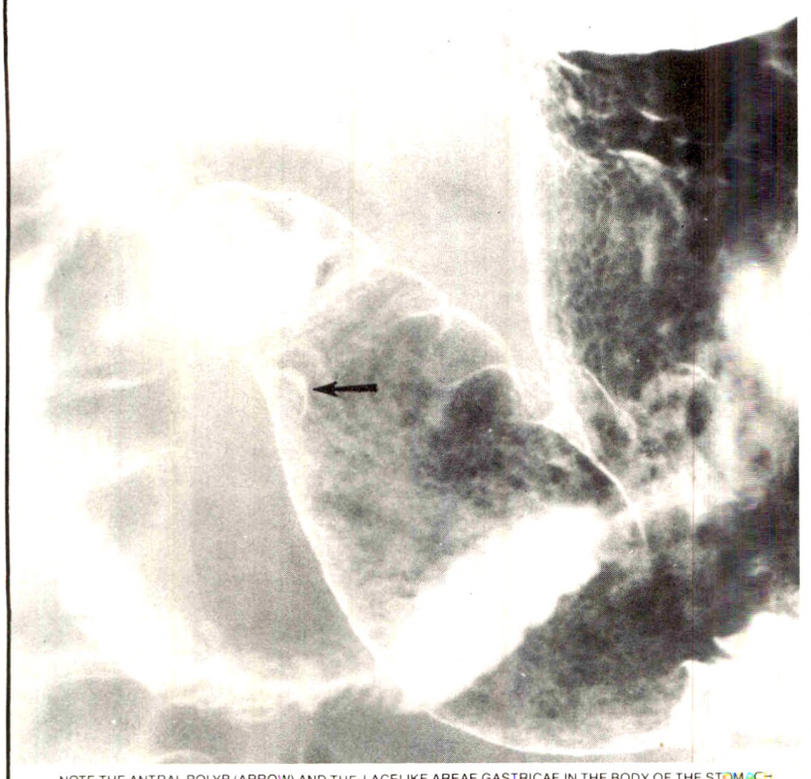

NOTE THE ANTRAL POLYP (ARROW) AND THE LACELIKE AREAE GASTRICAE IN THE BODY OF THE STOMACH
Film, courtesy of Robert E. Koehler, M.D. Washington University, Dept. of Radiology, St. Louis, Missouri

Double contrast radiography appears to offer the potential for significant improvements in diagnostic accuracy.

Double contrast studies of the stomach best demonstrate the surface pattern of the stomach (areae gastricae). This leads to improved detection of superfical erosions and ulcers, malignancies, polyps and other benign tumors, and ulcer scars.

E-Z-HD barium sulfate provides the basic ingredient necessary for good double contrast of the stomach.

The higher the density of the barium suspension, the better the coating. E-Z-HD allows for the highest density suspension of any commercial product on the market today: 85% w/w, 250% w/v. E-Z-HD achieves this density while remaining fluid for ease of administration.

- High density
- High fluidity
- Palatable
- Unit dose convenience.

E-Z-HD – The barium for the double contrast examination of the stomach and duodenum.

Optimal Density & Fluidity for the Modern Double Contrast Examination of the Stomach and Duodenum

Refrences:

David W. Gelfand: The Japanese-Style Double Contrast, Examination of the Stomach, Gastrointest Radiol. 1, 7-17 (1976)

Igor Laufer: The Diagnostic Accuracy of Barium Studies of the Stomach and Duodenum – Correlation with Endoscopy, Radiology 115: 569-573, June 1975

Roscoe E. Miller: The Air Contrast Stomach Examination: an overview. Radiology 117: 743-744 Dec. 1975

E-Z-EM

For Further Information Write:

7 Portland Ave.
Westbury, New York 11590
(516) 333-8230

9/77

Ultra-high resolution.

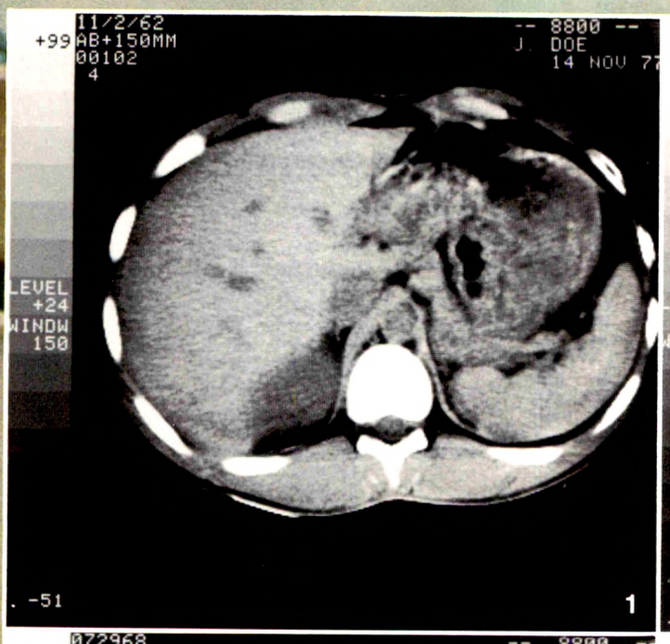

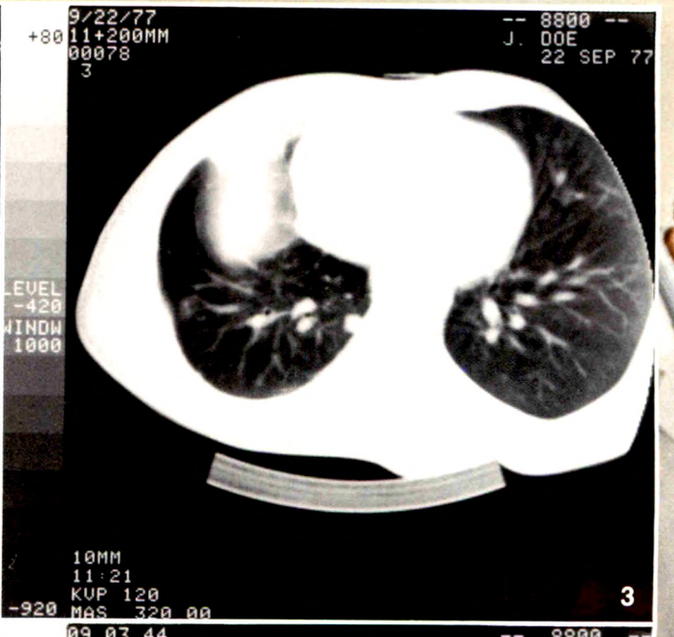

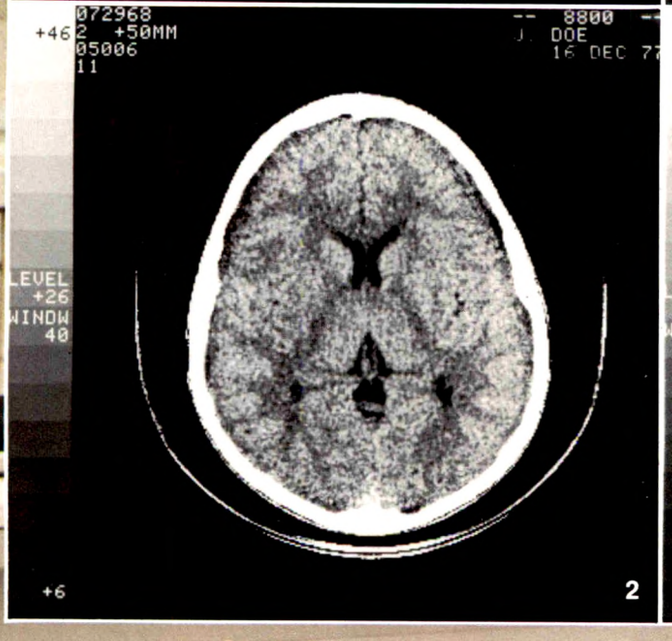

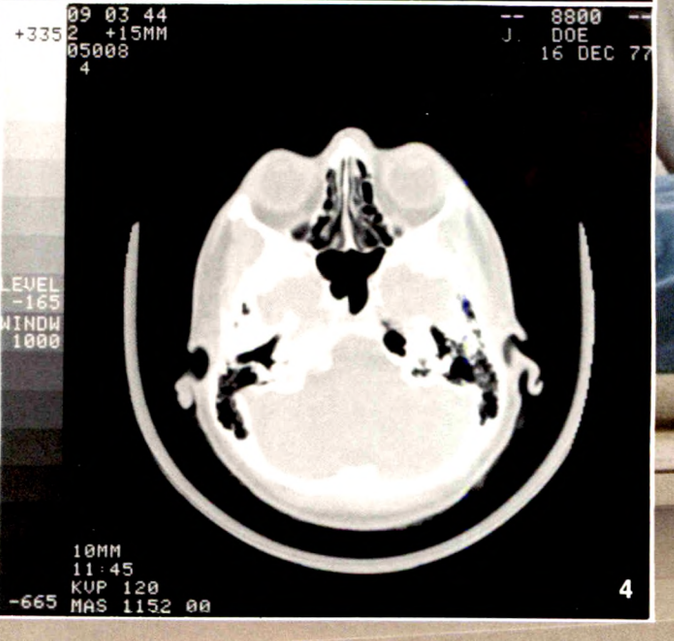

Contrast resolution—The CT/T's ability to resolve very slight differences in tissue densities permits clear visualization of biliary structure within the liver (figure 1) and superb grey matter/white matter differentiation within the brain (figure 2). Although not an example of contrast resolution, note the superb visualization of the neural tube and spinal nerves in figure 1.

Spatial resolution—The CT/T has the ability to resolve very small structure, such as the bronchii cut in cross-section (figure 3) and the lamina papyracea and bony detail within the ethmoid sinus (figure 4).

You'd expect it from GE.

The company that pioneered Fast-Scan CT also gives you the best images.

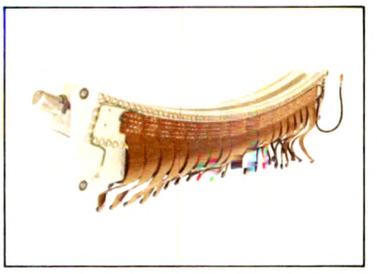

GE started with the right design, right from the beginning: 360°, rotate-only, 4.8 second scanning with a stable xenon detector.

Now, for CT applications requiring ultra-high resolution images, GE offers the X-2 detector package. We've nearly doubled the number of detector elements to 523 in a 30° arc.

The result: resolving power of better than 1.0 mm. With 4.0 mm resolution at 0.4% contrast. These unprecedented images provide clarity and detail unmatched by any other CT system.

The X-2 detector package comes as standard equipment on the CT/T 8800 scanner, or as an option for the CT/T 7800 system. Both detectors (X-1 and X-2) carry GE's straightforward 5-year warranty.

These latest developments in CT are a direct result of GE's continuing commitment to diagnostic imaging. A commitment you can count on—now and in the future.

General Electric Medical Systems, Milwaukee, Toronto, Madrid.

100 Years of Progress for People

GENERAL ELECTRIC

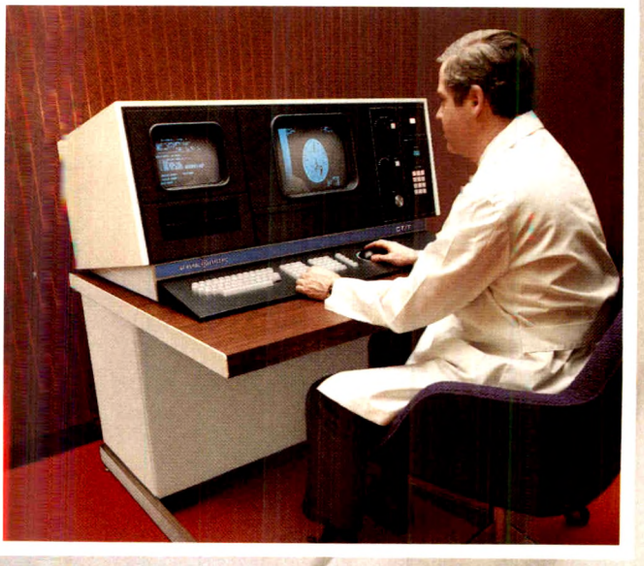

The CT/T Continuum. Best images, best value. Now and in the future.

The UN mea business.

How would you like a new market of two billion customers? The UN is creating it by helping developing nations develop.

Raw materials? The UN Development Program has unearthed mineral deposits worth over $40 billion. Iron. Bauxite. Copper. Manganese. Tin.

You see, the UN is the only place where economic issues are dealt with on a worldwide basis. By helping countries grow, new markets are created. American business benefits from the increased demand for products and services. And these countries often become sources for much needed raw materials.

Eighty percent of American contributions to the United Nations Development Program come back to the United States in the form of new business.

Other things the UN does to help business? A UN commission is codifying laws of international trade so that importers and exporters will know exactly what their rights are and when they should get paid.

The UN protects your work force too. It keeps track of diseases like flu so that in be prepared in ti epidemics and ab those of you who the UN has mad language spoken control towers. A think regulates a postage and telec

The UN mea American busine

Get the whole story. "The You in the U Nations Association- Street, New York, Nev

Name_____

Address_____

City_____

State_____

A Public Service of This Magazine & Th

ND 8000

The quality of a tomodensitometer is defined by four main characteristics.

- Density resolution
- Patient dose
- Spatial resolution
- Linearity of response

The first three parameters are interdependent. Improvement of one cannot occur without sacrificing one or both of the others. And on the other hand, if only a single "best combination" of parameters is available, image quality is most certainly compromised for all cases. CGR recognizes this problem. Depending on the anatomy to be examined, the user may select the most important parameter. Superior image quality is thus always maintained.

ND 8000 unique selection of data acquisition modes permits optimum image quality with minimum radiation to the patient.

DOSE UTILIZATION

Excellent total radiation control by effective primary and secondary collimation. Useful dose always at optimum minimum value due to user-selected modes and high efficiency detectors.

Selective beam filtration and slice thickness depending on level being examined. Excellent density resolution 0.2 % at a spatial resolution of 4.5 cycles/cm. For study of intracerebral abnormalities in the primary stage.

Exceptional spatial resolution. 7 cycles/cm at a density resolution of 1.0 %. For analysis of the orbits, auditory canals and other fine detail structures.

Patient dose:
- 0.23 Rads (skin) 0.1 Rads (orbit) in fast scan high spatial resolution mode.
- 1.45 Rads (skin) in high density resolution mode.

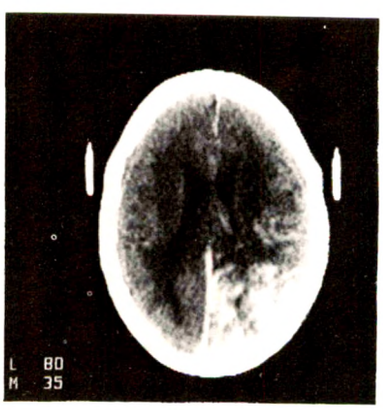

On the left: a CT slice showing the sylvian fissure, the optic canals and the cerebral trunk.

On the right: angioma of the posterior region. Very good distinction between the cortical gray matter and the white matter.

The patient head holder allows angulation of the head in conjunction with gantry angulation to provide the best anatomical orientation of the cerebral level to be examined, as well as the most comfortable position for the patient.

CGR

performance never occurs by accident

ND 8000

Total image display and interpretation capability is immediately available.

Even if data acquisition is excellent, optimum diagnosis is only possible if images are properly processed and presented. A display console with complete image analysis capability is mandatory.

Automatic and multiple processing functions create the most advanced, yet easiest to use, analysis system available.

Three ND 8000 image console versions are available. Depending on application, providing a minimum of 8 basic functions up to 24 more sophisticated capabilities.

Each console includes a dedicated data processor, contributing to even faster patient examination and image diagnosis.

The Department of Radiology, University of Utah College of Medicine, is sponsoring a postgraduate course in Gastrointestinal Radiology, January 27 - February 3, 1979 at the Snowbird Ski Resort, Snowbird, Utah and a second similar meeting at the Park City Ski Resort from February 24 - March 3, 1979.

Registration fee is $230.00 for each meeting and includes breakfasts and coffee breaks. A limited number of residents will be accepted at a registration fee of $150.00 if accompanied by a letter of endorsement from their departmental chairman. Cancellations will be accepted up to January 4, 1979 for the Snowbird course and up to February 4 for the Park City course, subject to a $30.00 handling fee. Rooms have been secured at Snowbird and Park City and will be held until November 28 and December 24, 1978, respectively. After that time, reservations will be accepted on the basis of availability.

The course has been accredited for 20 hours AMA - CME Category I credit.

FACULTY:

David G. Bragg, M.D.
Professor and Chairman, Radiology

R. Edward Coleman, M.D.
Associate Professor, Radiology

Virgil R. Condon, M.D.
Associate Professor, Radiology

William B. Cutcliff, M.D.
Assistant Professor, Radiology

James W. Freston, M.D., Ph.D.
Professor, Medicine and Pharmacology

John R. Haaga, M.D.
Staff Radiologist, Cleveland Clinic

Richard B. Jaffe, M.D.
Associate Professor, Radiology

P. Ruben Koehler, M.D.
Professor, Radiology

Timothy G. Lee, M.D.
Associate Professor, Radiology

Patrick D. Lester, M.D.
Associate Professor, Radiology

William J. McSweeney, M.D.
Professor and Chairman, Radiology
Children's Hospital National Medical Center

Franklin J. Miller, Jr., M.D.
Associate Professor, Radiology

D. Edward Mineau, M.D.
Instructor, Radiology

Frank G. Moody, M.D.
Professor and Chairman, Surgery

James A. Nelson, M.D.
Associate Professor, Radiology

G. William Nixon, M.D.
Associate Professor, Radiology

Patrick F. Sheedy, M.D.
Associate Professor, Radiology
Mayo Clinic

Edward B. Singleton, M.D.
Professor, Radiology
Texas Children's Hospital

Karl T. Wickstrom, M.D.
Assistant Professor, Radiology

Preliminary Program

Sunday Evening
7:00 - 9:00 Film Reading Session

Monday
7:30 - 9:30 a.m. Contrast Examination of the Biliary Tract
Drs. Mineau, Moody, Nelson, Wickstrom

4:30 - 5:30 p.m. CT and Ultrasound of the Biliary Tract
Drs. Haaga*, Lee, Sheedy*

Tuesday
7:30 - 9:30 a.m. Ultrasound and CT of Abscess; Contrast Studies in Oncologic Entities
Drs. Koehler and Bragg

4:30 - 6:30 p.m. Plain Film and Barium Studies Technique
Drs. Freston, Mineau, Nelson, Wickstrom

Wednesday
7:30 - 9:30 a.m. Liver Imaging and Interventional Techniques
Drs. Coleman, Haaga*, Miller, Sheedy*

4:30 - 6:30 p.m. Pediatric Lower GI Tract: Part
Drs. Cutcliff and Jaffe

Thursday
7:30 - 9:30 a.m. Pediatric Upper GI Tract: Part
Drs. Condon, Lester, McSweeney*, Singleton*

4:30 - 6:30 a.m. Pediatric Upper GI Tract: Part I
Drs. Condon, Nixon, McSweeney*, Singleton*

Friday
7:30 - 9:30 a.m. Pediatric Lower GI Tract: Part II
Drs. Condon, Lester, McSweeney*, Singleton*

afternoon Free Time

* Drs. Haaga and McSweeney at Park City Conference, Drs. Sheedy and Singleton at Snowbird Conference.

REGISTRATION FORM

FOURTH ANNUAL SNOWBIRD/PARK CITY RADIOLOGY CONFERENCE
GASTROINTESTINAL RADIOLOGY

Check course(s) desired:

☐ Snowbird Ski Resort January 27 - February 3, 1979
☐ Park City Ski Resort February 24 - March 3, 1979

NAME: _____

ADDRESS: _____

_____

CITY, STATE: _____ ZIP: _____

TELEPHONE: _____

Fee: $230.00

Checks payable to:
Department of Radiology
University of Utah

Return with registration fee to:
Franklin J. Miller, Jr., M.D.
Department of Radiology
University of Utah Medical Center
50 North Medical Drive
Salt Lake City, Utah 84132

(801) 581-8188

Upon receipt of registration, hotel and ski information will be forwarded. Lodging guaranteed until November 28, 1979 for Snowbird course and December 24, 1979 for Park City course. After these dates, lodging on availability basis only.

Benign Antral Ulcers

Benign prepyloric ulcers often are accompanied by perifocal inflammatory "mounds" (masses), easily confused with malignant disease. When reasonable doubt exists concerning the latter, a brief course of intensive medical therapy may resolve the dilemma. The following examples are all proven benign antral ulcers.

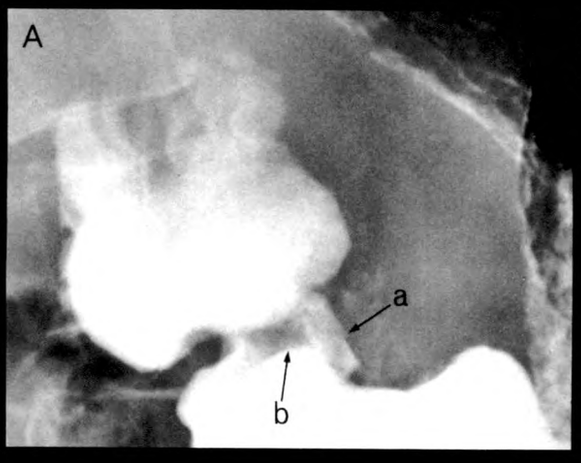

Case I - Fig. A. The barium-filled antrum shows an ulcer crater (a) plus a radiolucent pyloric defect (b).

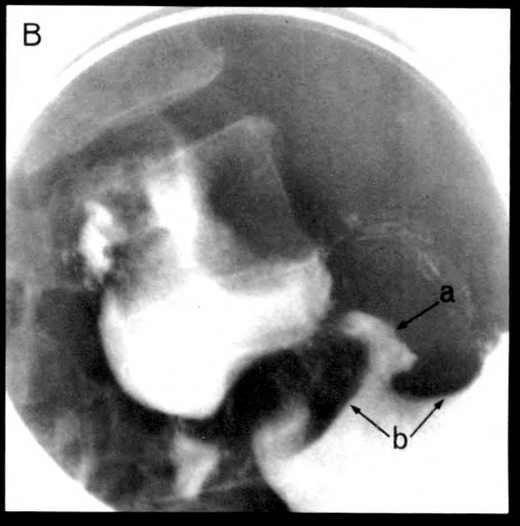

Fig. B. With compression, the ulcer (a) is better demonstrated. Of concern was the perifocal mass (b) which disappeared in 3½ weeks following medical care alone.

Case II - Fig. A. An ulcer (a) is clearly defined, as are its perifocal soft tissue masses (arrows).

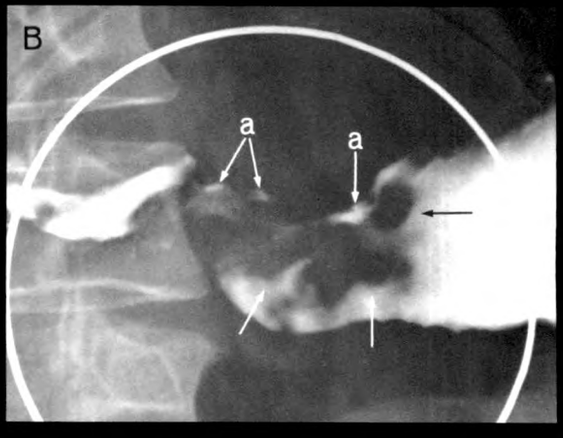

Fig. B. Following gastric lavage, three ulcers (a) plus the perifocal masses (arrows) are clearly demonstrated.

Radiographs and caption material from the American College of Radiology—An Atlas of Tumor Radiology—Yearbook Medical Publishers, Inc. Reprints of this and subsequent reports available upon request. Please write, Eastman Kodak Company, Dept. 740B, Rochester, New York 14650. (M3-309)

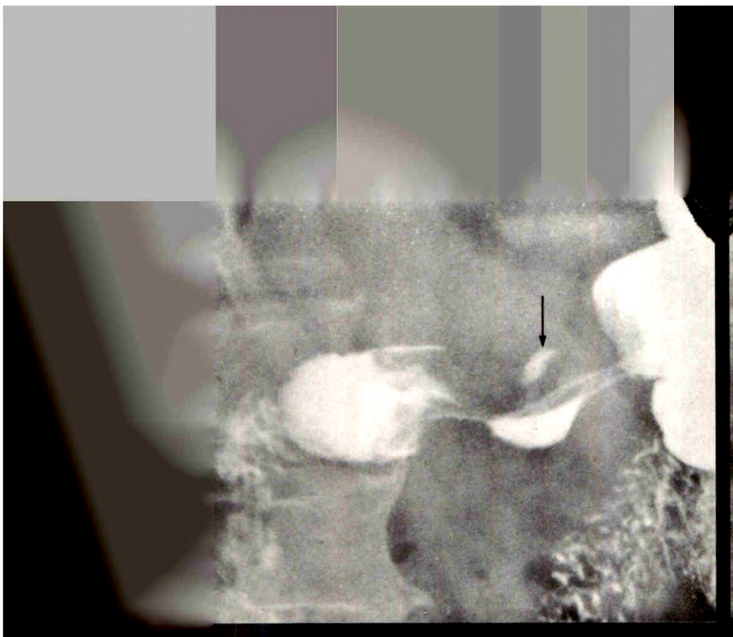

Case III - Fig. A. During antral contraction, an ulcer (arrow) with its perifocal soft tissue "mound" is obvious.

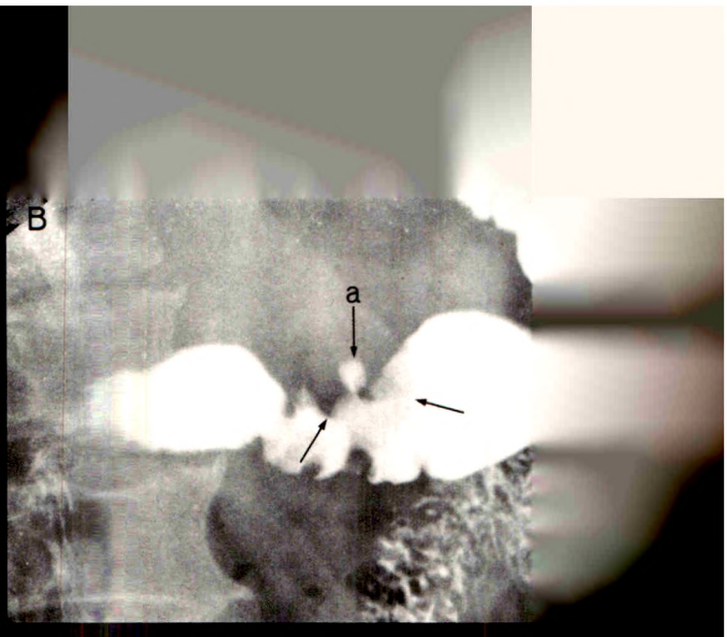

Fig. B. The ulcer (a) and perifocal masses (arrows) persist during relative antral relaxation.

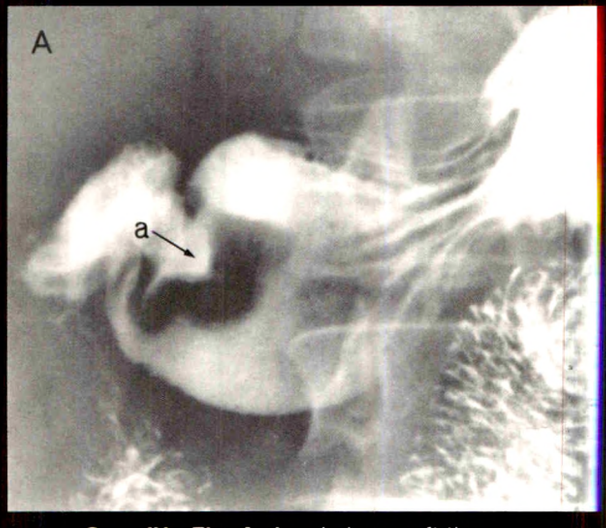

Case IV - Fig. A. An obvious soft tissue mass envelops a large prepyloric ulcer (a).

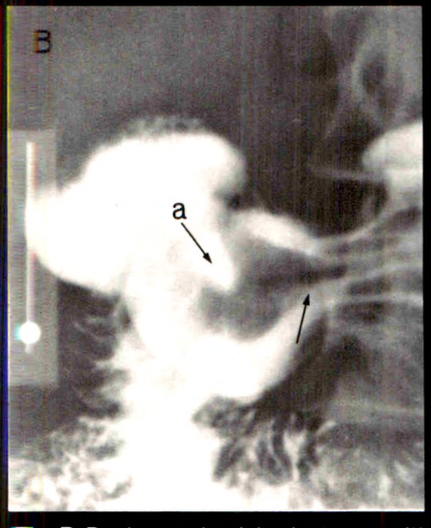

Fig. B. During peristalsis, the "mound" changes in shape (arrow) as would edema or a soft tumor. The configuration of the crater (a) too has changed.

Diagnosis of patient problems are capably supported and strengthened by quality radiography, using your skills and high-quality x-ray products.

At left is the Kodak RP X-Omat processor, model M7A. The processor that's designed for economy, convenience and quick access to quality radiographs.

What's important is: it runs on unheated water. You don't need a hot-water supply or special mixing valve. It helps cut water heating costs, while delivering ready-to-read radiographs in 2½ minutes. Consistently.

Kodak also offers a wide choice of films for your specific needs—automatically processable. The durable Kodak X-Omatic cassette provides intimate film/screen contact.

Ask your Kodak Technical Sales Representative for further information. Or consult your medical x-ray products dealer.

©Eastman Kodak Company, 1973

Kodak

CHARLES C THOMAS • PUBLISHER•

XERORADIOGRAPHY: Breast Calcifications *by* **John N. Wolfe,** *Hutzel Hospital, Detroit, Michigan.* This monograph provides the criteria necessary for diagnosing the cause of breast calcification. Each subject is discussed in text form and is amply illustrated. In addition, each illustration is accompanied by text which includes history, radiographic observations and thoughts of the interpreter at the time the x-ray report was submitted, presentation of the diagnosis, and discussion of the case. Topics include calcifications associated with malignancies, characteristic tumor calcifications of specific forms of malignancies, calcifications associated with benign conditions, calcifications within lymph nodes, calcifications of the skin and areola, arterial calcifications, pseudocalcifications and specimen radiography. *'77, 184 pp. (8 1/2 x 11), 284 il., 3 tables, $22.50*

XERORADIOGRAPHY: Uncalcified Breast Masses *by* **John N. Wolfe,** *Hutzel Hospital, Detroit, Michigan.* The order of presentation in this text proceeds from the obvious malignancies characterized by a mass with a well-developed spiculated margin, through the more subtle circumscribed carcinomas such as the medullary or colloid variety, and finally, to the most difficult, those that do not present a well-defined mass, but merely an area of increased density. The section concludes with a presentation of some less common forms of malignancies. Following the section on malignancies, benign tumors are considered in detail. This section illustrates the classic types of pathology followed by examples of variations. Finally, cases are shown where one simply cannot arrive at a correct diagnosis. *'77, 208 pp. (8 1/2 x 11), 307 il., $28.00*

THE FUNDAMENTALS OF X-RAY AND RADIUM PHYSICS (6th Ed.) *by* **Joseph Selman,** *Tyler Junior College, Tyler, Texas.* This is the text against which all other tomes of similar intent are measured. Now in its Sixth Edition, this classic introduction to x-ray and radium physics has again been revised, rewritten, updated and enlarged to accommodate a constantly changing field. The basic format — proven effective in many classrooms over many years — has been retained. Selected for new or amplified discussions in this edition are such items as focal spot evaluation, modulation transfer function, new types of intensifying screens, the basic phenomena of phosphorous luminescence, direct magnification in small vessel angiography, high kilovoltage radiography, and radiation protection. *'77, 616 pp., 296 il., 29 tables, $18.75*

PUBLIC RELIGIOUS SERVICES IN THE HOSPITAL *by* **S. Denton Bassett,** *Univ. of Texas Medical Branch, Galveston. Foreword by* **Myron C. Madden.** This volume surveys the religious ministry in American hospitals and the feelings of patients desiring this service. The author enlarges on the concept of a relationship between the lasting elements of worship and body function, and emphasizes the primary importance of the patients' need for blessing through worship. Four questions related to public religious services in the hospital are discussed: Is there a need for public religious services in the hospital? What are the general responses patients have who attend public religious services in the hospital? What public religious services are provided in various hospitals in the United States? What kinds of religious services are best suited for hospital patients? *'76, 80 pp., 12 tables, $7.50*

Orders with remittance sent, on approval, postpaid

301-327 East Lawrence Avenue • Springfield • Illinois • 62717

YOU CAN ACQUIRE VALUABLE BACK VOLUMES AND SINGLE ISSUES OF THE PUBLICATIONS OF

The American Roentgen Ray Society

A limited quantity of the issues available are listed below. Orders are subject to the exhaustion of available stock. This offer is subject to withdrawal without notice. **NOTE: For your convenience, the same price—$5.00—applies to all issues—no quantity discount.**

Order *BACK ISSUES* of the Journal from:

CHARLES C THOMAS • PUBLISHER *301-327 East Lawrence Ave.* **SPRINGFIELD • ILLINOIS 62717**

The American Journal of Roentgenology

Vol. 83, Nos. 1-6 (1960)
Vol. 84, Nos. 1-6 (1960)
Vol. 85, Nos. 1-6 (1961)
Vol. 86, Nos. 1-6 (1961)
Vol. 87, Nos. 1-6 (1962)
Vol. 88, Nos. 2-6 (1962)
Vol. 89, Nos. 1-6 (1963)
Vol. 90, Nos. 1-5 (1963)
Vol. 91, Nos. 1,2,4,6 (1964)
Vol. 92, Nos. 1,2,3,5,6 (1964)
Vol. 93, Nos. 1-4 (1965)
Vol. 94, Nos. 1-4 (1965)
Vol. 95, No. 1 (1965)
Vol. 96, No. 3 (1966)
Vol. 97, Nos. 1,4 (1966)
Vol. 98, Nos. 2-4 (1966)
Vol. 99, Nos. 1,3,4 (1967)
Vol. 100, Nos. 1-4 (1967)
Vol. 101, Nos. 1-4 (1967)
Vol. 102, Nos. 2,3 (1968)
Vol. 103, Nos. 1,2,4 (1968)
Vol. 104, Nos. 1-3 (1968)
Vol. 105, No. 2 (1969)
Vol. 107, Nos. 2-4 (1969)
Vol. 109, No. 1 (1970)
Vol. 110, Nos. 2,4 (1970)
Vol. 111, Nos. 1-4 (1971)
Vol. 112, Nos. 1-4 (1971)
Vol. 113, Nos. 1,2,4 (1971)
Vol. 114, Nos. 1,3,4 (1972)
Vol. 115, No. 2 (1972)
Vol. 116, Nos. 2-4 (1972)
Vol. 117, Nos. 1-4 (1973)
Vol. 118, No. 2 (1973)
Vol. 119, Nos. 1-4 (1973)
Vol. 120, Nos. 2-4 (1974)
Vol. 121, Nos. 1-4 (1974)
Vol. 122, Nos. 1-4 (1974)
Vol. 123, Nos. 1,3,4 (1975)
Vol. 124, Nos. 1-4 (1975)
Vol. 125, Nos. 1-4 (1975)
Vol. 126, Nos. 1-6 (1976)
Vol. 127, Nos. 1,2,4,5,6 (1976)
Vol. 128, Nos. 2-5 (1977)
Vol. 129, Nos. 2-6 (1977)
Vol. 130, Nos. 1-3 (1978)

AJR Index to Advertisers

(In Order of Appearance)

E-Z-EM Company
Elema-Schonander, Inc.
G. D. Searle & Company
The Purdue-Frederick Company
C. B. Fleet
Atomic Energy of Canada
Procter & Gamble
E. R. Squibb & Sons, Inc.
Institute of Continuing Education
GAF Corporation
Pfizer Medical Systems
Ortho Pharmaceutical Corporation
E. R. Squibb & Sons, Inc.
Machlett Laboratories

• • •

H. G. Fischer, Inc.
Charles C Thomas · Publisher
Philips Medical Systems
Miami Seminars
CGR Medical Corporation
Grune & Stratton
Charles C Thomas · Publisher
Picker Corporation
Siemens Corporation
E-Z-EM Company
General Electric Company
CGR Medical Corporation (Paris)
University of Utah
Eastman Kodak Company
Charles C Thomas · Publisher
Hanley Medical Equipment Company
Schneeman Electronics, Inc.
Picker Corporation
Gordon Projectors
S & S X-Ray

Hanley Space Saver X-Ray and Medical Record Cabinets are installed in most hospitals in America.

Top quality and low price is the reason. It's #1. Regular 5 compartment with doors open 19½ x 32 x 83. Deluxe Oversize 5 High 23 ¾ x 32 x 88. F.O.B. Factory **In X-Ray rooms it's the oversize.** Extra depth means easier filing.

AMERICA'S LARGEST DISTRIBUTOR OF X-RAY CABINETS.

HANLEY MEDICAL EQUIPMENT CO.
5614 South Grand X-Ray Division St. Louis, Mo. 63111
Phone 314-351-3359

THE AMERICAN JOURNAL OF ROENTGENOLOGY

CONSOLIDATED INDICES

Volume I	*—(1903-1937)—*	*Out of Print*
Volume II	*—(1938-1942)—*	*$10.00*
Volume III	*—(1943-1947)—*	*22.50*
Volume IV	*—(1948-1952)—*	*23.50*
Volume V	*—(1953-1957)—*	*25.00*
Volume VI	*—(1958-1962)—*	*23.50*
Volume VII	*—(1963-1967)—*	*30.00*
Volume VIII	*—(1968-1972)—*	*40.00*

STANFORD
X-RAY STEREOSCOPE
CONSULTATION IN 3-D

International usage
for over 30 years
See Your X-Ray Dealer
Manufactured in U.S.A.

SCHNEEMAN ELECTRONICS, Inc.
Grants Pass, Oregon, 97526

Still using a fulcrum bar?

In Tomolex,™ there is no heavy, cumbersome fulcrum bar. With touch-button controls, just the finger tip is all that is required to set the Tomolex for tomography, erect-chest work or routine horizontal radiography. Being able to switch from tomography to radiography and back again within seconds assures maximum patient throughput.

Faster throughput isn't all that Tomolex offers. The four-way float-top table makes patient positioning faster and easier for the technologist, more comfortable for the patient. And the extra-wide tabletop gives your patient a greater feeling of security. Yet you can still position carts flush against the Tomolex top because tableside controls glide out of the way quickly and effortlessly.

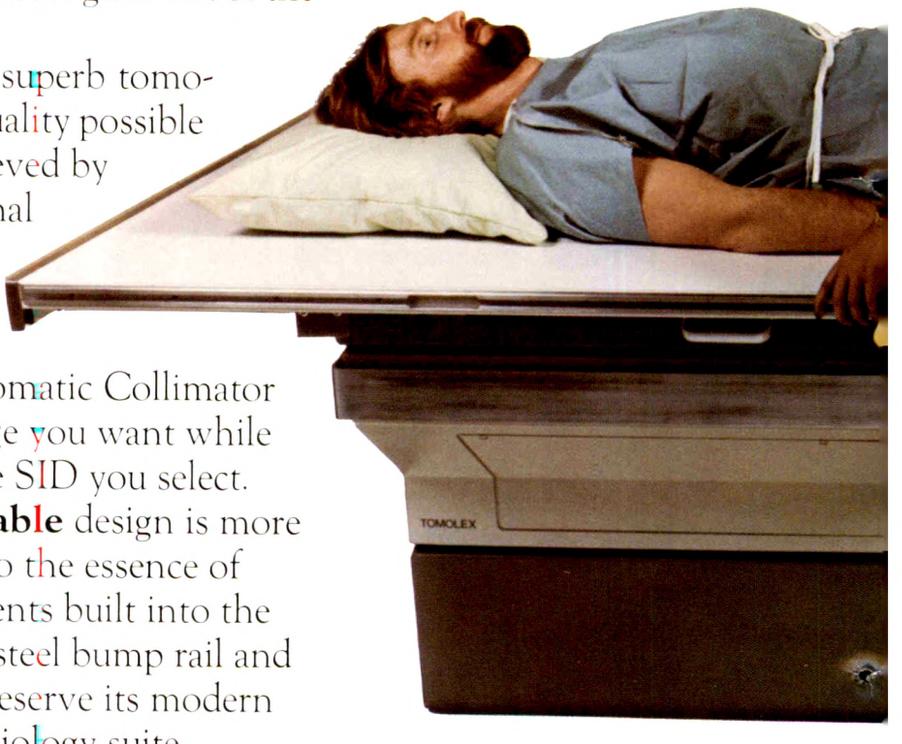

Radiologists appreciate the superb tomographic and radiographic image quality possible with Tomolex. Quality that's achieved by design from inception through final assembly. Further, automatic exposure control assures optimal radiologic film density — consistently. And the Collimatic Automatic Collimator provides the precise beam coverage you want while tracking film size, according to the SID you select.

Tomolex's award-winning table design is more than just visually attractive. It's also the essence of practicality with all table components built into the table base for servicing. Further, a steel bump rail and impact-resistant kick plate help preserve its modern good looks even in the busiest radiology suite.

Tomolex doesn't.

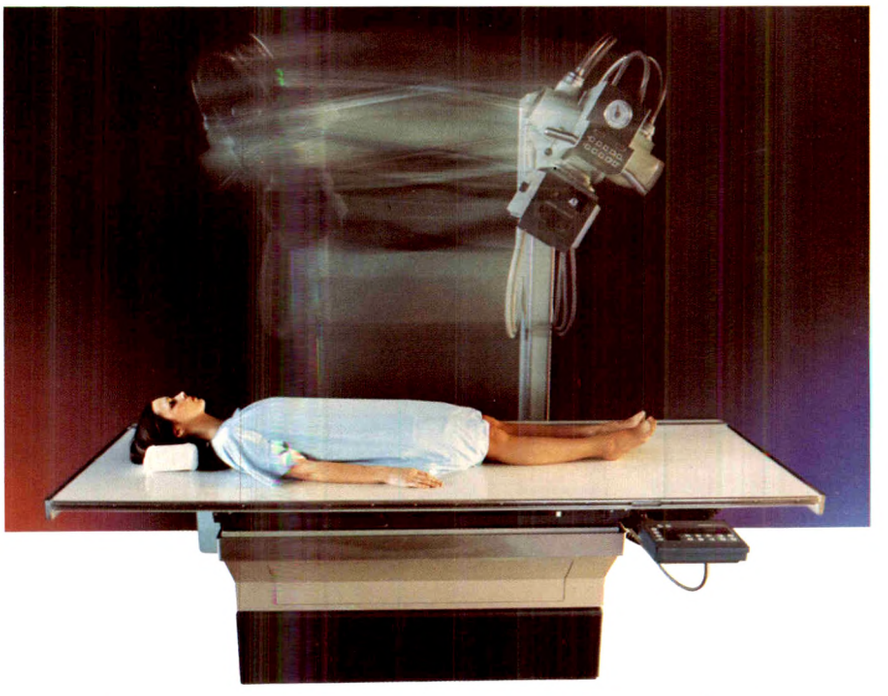

Customized acquisition plans, or leasing can be arranged through your channels or through Picker's parent CIT Financial Corporation.

For ease, speed and quality results, Tomolex is still the paragon in radiographic/linear tomography systems. And like all Picker equipment, it's backed by our worldwide service organization. Contact your local Picker representative, or write Picker Corporation or Picker International, 595 Miner Road, Cleveland, OH 44143.

PICKER®
ONE OF THE CIT COMPANIES

t mp · guard™

temperature stabilizer

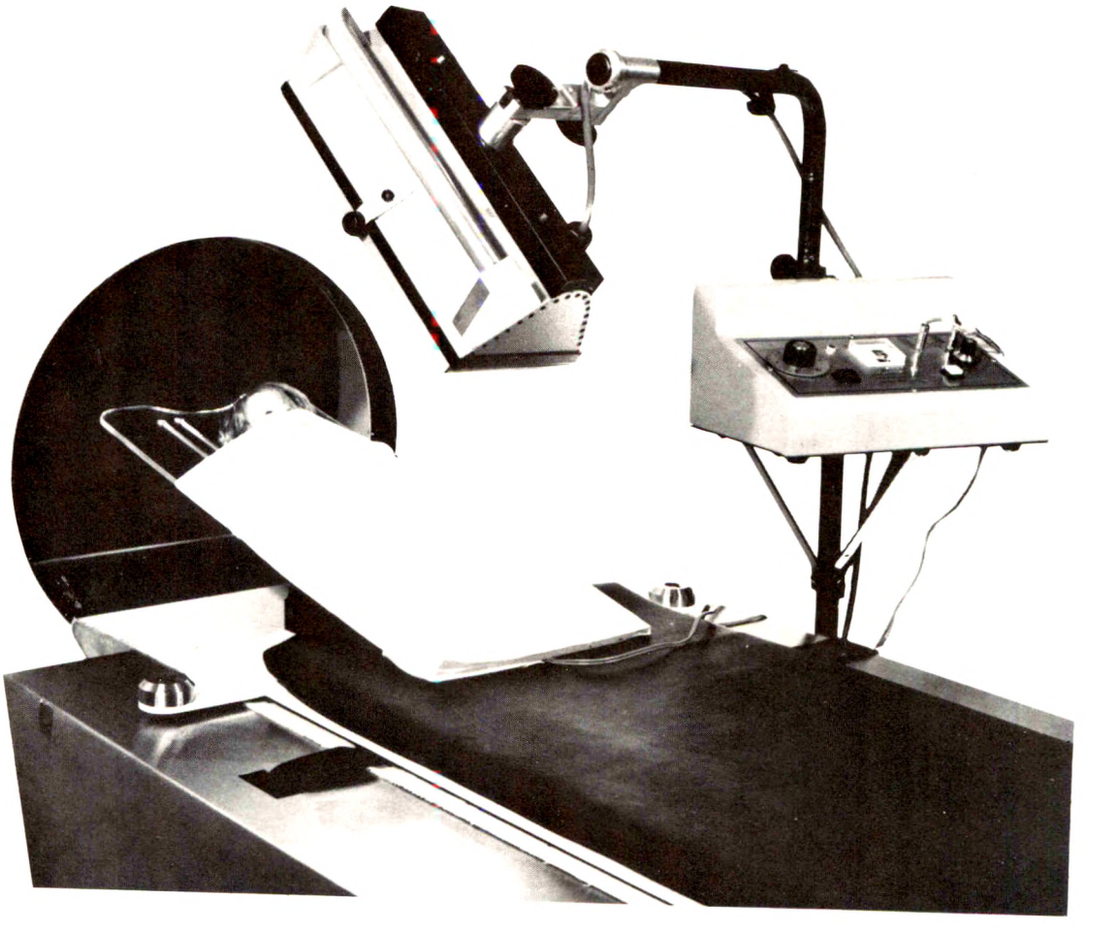

- coverless temperature support system for complete accessibility
- mobile and versatile
- for use in fluroscopy, special procedures, c.t. and ultrasound
- feed back probe which provides accurate temperature control and readout display
- fail safe instrumentation

call direct 716 882-0862

or write

gordon consultants, inc. 361 dewitt st. • buffalo, new york 14213

Introducing "MINI-VIEWER"

SAVES SPACE
SAVES TIME

NEW CONVENIENT MINI-SIZE, MOTORIZED, PORTABLE 48-FILM X-RAY VIEWER IS

- Attractive modern styling for every decor! • Optional shelf or desk available.

SMALL!

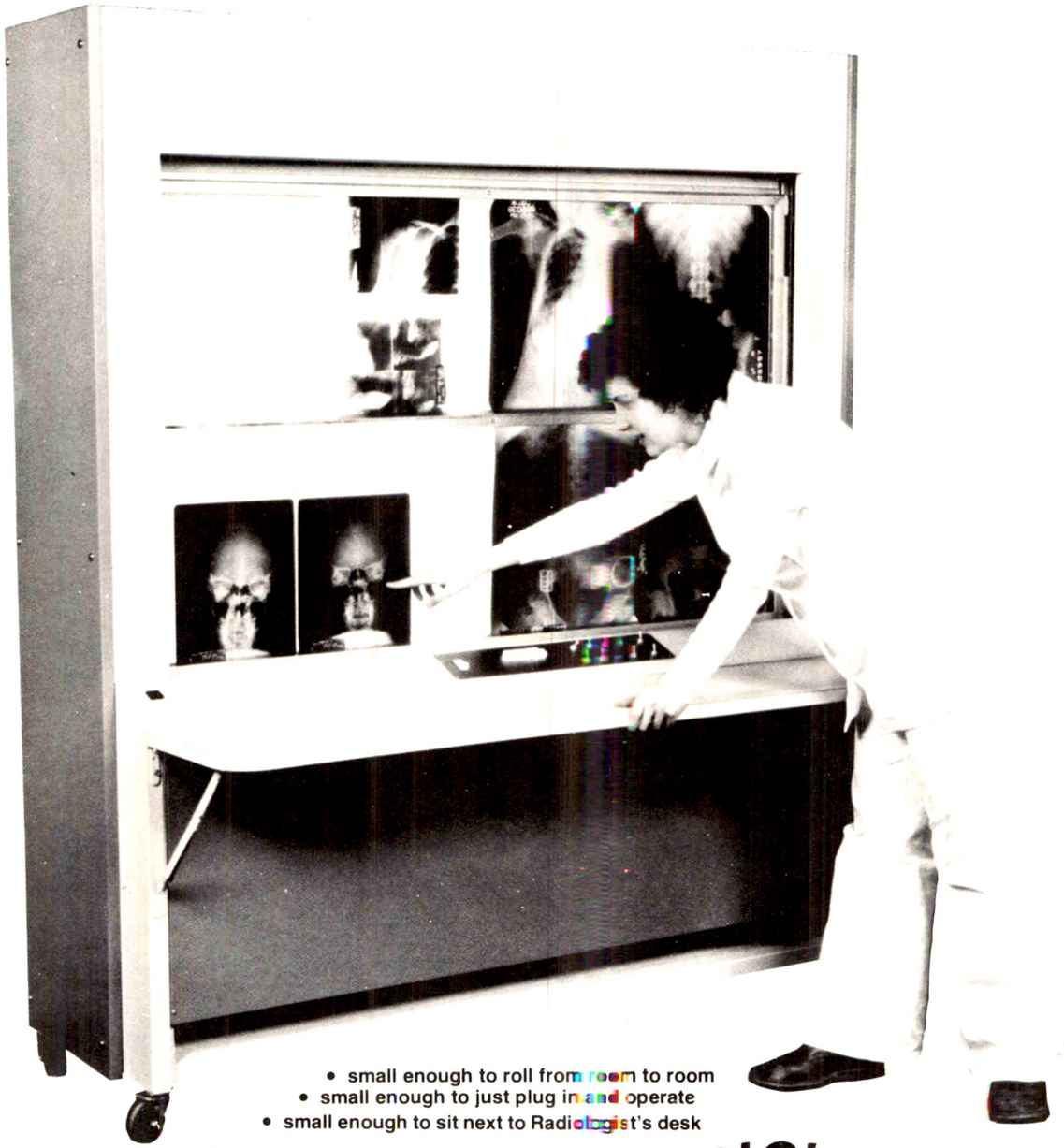

- small enough to roll from room to room
- small enough to just plug in and operate
- small enough to sit next to Radiologist's desk

BUT ... "MINI-VIEWER" IS BIG!

- BIG enough to view & store up to 48 — 14″x17″ (or smaller) films (equivalent of 6-4 over 4 ills)
- BIG enough to illuminate 4 over 4 films
- BIG enough for 7-second random access touch-control viewing
- BIG enough to offer individually-controlled, extra bright lighting — without spillover between sections
- BIG enough to be rugged yet compact — 70″ wide, 79″ high, 22″ deep

MANUFACTURED BY

S. & S. X-RAY PRODUCTS INC.

The Complete Line of X-Ray Accessories

Telephone: 212-852-6900

87-93 JAY STREET, BROOKLYN, N.Y. 11201

Manufactured in USA by **S & S**, who have made more motorized viewers than any one else in the world. Sold by local X-Ray dealers backed up by **S & S** parts inventories and experience.

American Journal of Roentgenology

Vol. 131 October 1978 No. 4

DIAGNOSTIC IMAGING

571 **Coronary, Ventricular, and Pulmonary Abnormalities Associated with Rupture of the Interventricular Septum Complicating Myocardial Infarction.** *Miller SW, Dinsmore RE, Greene RE, Daggett WM*

579 **Bilateral Pleural Thickening: A Manifestation of Asbestos Dust Exposure.** *Sargent EN, Gordonson J, Jacobson G, Birnbaum W, Shaub M*

587 **Pulmonary Manifestations of Acute Aspiration of Gastric Contents.** *Landay MJ, Christensen EE, Bynum LJ*

593 **Accuracy of Chest Film Screening by Technologists in the New York Early Lung Cancer Detection Program.** *Flehinger BJ, Melamed MR, Heelan RT, McGinnis CM, Zaman MB, Martini N*

599 **The Normal and Abnormal Left Superior Intercostal Vein.** *Friedman AC, Chambers E, Sprayregen S*

603 **Subglottic Edema in Acute Epiglottitis in Children.** *Shackelford GD, Siegel MJ, McAlister WH*

607 **Pneumopelvigraphy in Childhood.** *Lester PD, McAlister WH*

613 **Radiographic Findings in Ovarian Teratomas in Children.** *Siegel MJ, McAlister WH, Shackelford GD*

617 **Mailed Thermoluminescent Dosimeter Determination of Entrance Skin Exposure and Half-Value Layer in Mammography.** *Wochos JF, Fullerton GD, DeWerd LA*

621 **Benign Multilocal Cystic Nephroma.** *Carlson DH, Carlson D, Simon H*

627 **Radiographic Features of Ureteral Endometriosis.** *Pollack HM, Wills JS*

633 **Inflammatory Cysts of the Pelvic Peritoneum.** *Lees RF, Feldman PS, Brenbridge ANAG, Anderson WA, Buschi AJ*

637 **Pitfalls of Transhepatic Portal Venography and Therapeutic Coronary Vein Occlusion.** *Widrich WC, Robbins AH, Nabseth DC, Johnson WC, Goldstein SA*

645 **Transcatheter Gelfoam Embolization of Posttraumatic Bleeding Pseudoaneurysms.** *Chang J, Katzen BT, Sullivan KP*

651 **Transcatheter Embolization: Prevention of Embolic Reflux Using Balloon Catheters.** *Greenfield AJ, Athanasoulis CA, Waltman AC, LeMoure ER*

657 **Bleeding Simulated by the Distal Internal Pudendal Artery Stain.** *Schrumpf JD, Sommer G, Jacobs RP*

661 **Gas in the Bile Ducts (Pneumobilia) in Emphysematous Cholecystitis.** *Harley WD, Kirkpatrick RH, Ferrucci JT Jr*

665 **Rheumatoid Arthritis and Its Variants: Analysis of Scintiphotographic, Radiographic, and Clinical Examinations.** *Weissberg DL, Resnick D, Taylor A, Becker M, Alazraki N*

675 **Accuracy of CT in Detecting Intraabdominal and Pelvic Lymph Node Metastases from Pelvic Cancers.** *Lee JKT, Stanley RJ, Sagel SS, McClennan BL*

681 **Effect of CT Noise on Detectability of Test Objects.** *Chew E, Weiss GH, Brooks RA, Di Chiro G*

687 **Optimal Contrast Dosage in Cranial Computed Tomography.** *Norman D, Enzmann DR, Newton TH*

691 **Progress in Radiology: Colorectal Tumors: Pathology and Detection.** *Ott DJ, Gelfand DW*

697 **Diagnostic Oncology Case Studies: Radiologic Investigation of Bloody Ascites.** *Contributed by Steckel RJ*

CASE REPORTS

701 **Sonographic Appearance of Duodenal Atresia in Utero.** *Lees RF, Alford BA, Brenbridge ANAG, Buschi AJ, Williamson BRJ*

703 **Pulmonary Uptake of ^{99m}Tc Diphosphonate in Alveolar Microlithiasis.** *Brown ML, Swee RG, Olson RJ, Bender CE*

705 **Nonfatal Pulmonary Air Embolism: Radiographic Demonstration.** *Faer MJ, Messerschmidt GL*

707 **Miliary Aspergillosis Associated with Alcoholism.** *Blum J, Reed JC, Pizzo SV, Thompson WM*

710 **Coronary Artery Anomaly in Double-Outlet Right Ventricle.** *Udoff EJ, Roland JM, White RI Jr*

713 **Pedunculated Endotracheal Metastasis.** *MacMahon H, O'Connell DJ, Cimochowski GE*

715 **Nonfunctioning Islet Cell Tumors of the Pancreas: Radiographic and Ultrasonographic Appearances in Two Cases.** *Gold J, Rosenfield AT, Sostman D, Burrell M, Taylor KJW*

718 **Abnormal Peripheral Distribution of Thallium-201 due to Arteriosclerosis.** *Glass EC, DeNardo GL*

721 **Subclavian Artery as the First Branch of the Aortic Arch: A Normal Variant in Two Patients.** *Boechat MI, Gilsanz V, Fellows KE*

723 **Polypoid Leukemic Infiltration of the Large Bowel.** *Rabin MS, Bledin AG, Lewis D*

725 **Leukemic Infiltration of the Colon.** *Limberakis AJ, Mossler JA, Roberts L Jr, Jackson DC, Thompson WM*

729 **Fracture of the Occipital Condyle.** *Bolender N, Cromwell LD, Wendling L*

TECHNICAL NOTE

732 **Traction Device for Use with Polytome Table.** *Deeb ZL, Martin TA, Kerber CW*

733 **Editorial: On Behalf of Translumbar Aortography.** *Reuter SR*

734 **From Earlier Pages**

736 **Letters**

737 **1979 ARRS Comprehensive Meeting Information**

755 **Memorials**

757 **Abstracts of Current Literature**

763 **Book Reviews**

767 **News**

769 **Radiologic Societies**

735 **Erratum**

18.9.79

AJR

American
Journal of
Roentgenology

November 1978

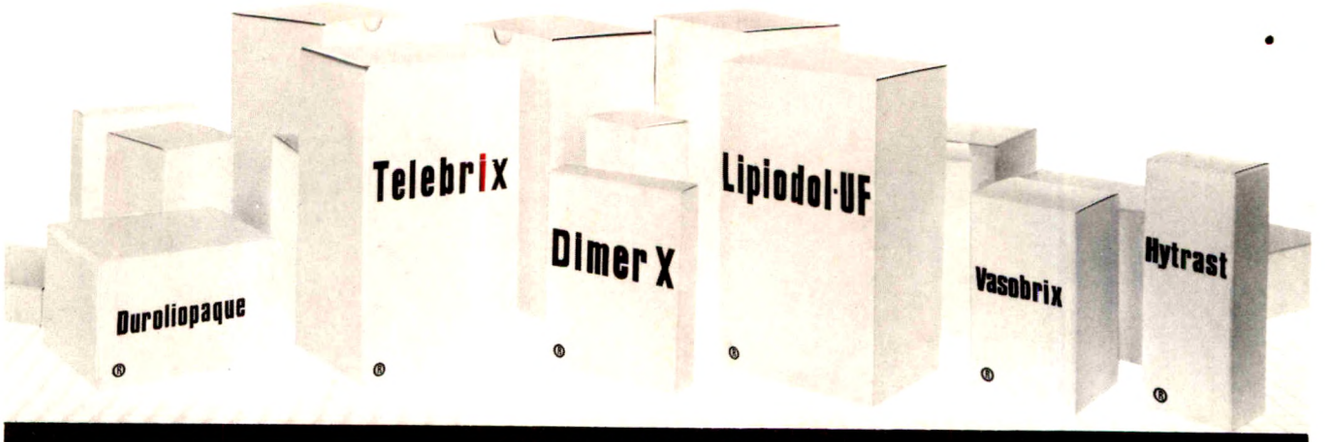

WE MANUFACTURE

contrast

MEDIA

OUR

products

ARE

known

WORLD-WIDE

OUR

name isn't

GUERBET

BETTER CONTRAST MEDIA THROUGH RESEARCH

Laboratoire Guerbet, 16/24, rue Jean-Chaptal
93601 AULNAY-SOUS-BOIS Cedex - FRANCE
Telex : Guerbet 690682

Official Journal
American Roentgen Ray Society
American Radium Society

AJR

Including Diagnostic Radiology • Radiation Oncology • Nuclear Medicine Ultrasonography • Related Sciences

Editor Melvin M. Figley

Associate Editor Rosalind H. Troupin

Assistant Editor John D. Harley

Contributing Editor E. Frederick Lang

Consulting Editorial Board Luther W. Brady • Kent Ellis E. Robert Heitzman • Donald L. King • N. Thorne Griscom Eugene C. Klatte • Kenneth Krabbenhoft • John G. McAfee Russell H. Morgan • Thomas H. Newton • Robert G. Parker Stewart R. Reuter • William B. Seaman • Robert J. Shalek John Storer • Michel M. Ter-Pogossian • Joseph P. Whalen David M. Witten

Editorial Staff K. A. Murray, manager • M. J. Leonard, manuscript editor • J. Anderson, assistant manuscript editor • C. P. Kaiser, secretary

Published monthly by Charles C Thomas, 301-327 East Lawrence Avenue, Springfield, Illinois 62717. All correspondence, except editorial office business, should be addressed to the publisher. Annual subscription rates: $40 ($20 for residents with letter of verification) plus appropriate mailing surcharge (see note next page). Single copies, $5. Undelivered or damaged copies replaced within 60 days of publication; 90 days for foreign subscribers. Allow 90 days for address changes. © 1978 by American Roentgen Ray Society. Second-class postage paid at Springfield, Illinois, and at additional mailing offices. Printed in U.S.A. ISSN 0361-803X

American Roentgen Ray Society

President: Harry Z. Mellins
President Elect: Paul A. Riemenschneider
1st Vice-president: Joseph D. Calhoun
2d Vice-president: Charles E. Bickham, Jr.
Secretary: James F. Martin
Treasurer: Harley C. Carlson

COMMITTEES 1977–1978

Executive Council: H. Z. Mellins, P. A. Riemenschneider, J. D. Calhoun, C. E. Bickham, Jr., J. F. Martin, H. C. Carlson, M. M. Figley, R. G. Evens, B. G. Brogdon, R. A. Gagliardi, E. Gedgaudas, G. A. Kling, T. F. Leigh, S. F. Ochsner, J. F. Wiot, R. E. Buenger, E. C. Klatte, J. P. Tampas, J. L. Gwinn, chairman

Finance and Budget: A. E. James, E. C. Klatte, R. McLelland, J. P. Tampas, R. G. Evens, chairman

Publications: M. P. Capp, K. Ellis, F. F. Ruzicka, Jr., E. R. Heitzman, R. A. Gagliardi, chairman

Editorial Policy: M. M. Figley, E. F. Lang, R. H. Troupin, E. R. Heitzman, K. Ellis, F. F. Ruzicka, Jr., M. P. Capp, R. A. Gagliardi, chairman

Advisory Committee on Education and Research: J. E. Youker, G. Wilson, G. W. Hartman, L. F. Rogers, E. Gedgaudas, chairman

Scientific Exhibits: T. C. Beneventano, G. Dodd, B. G. Brogdon, chairman

Constitution and Bylaws: J. H. Walker, W. M. Whitehouse, J. P. Tampas, chairman

American Board of Radiology Representatives: J. F. Roach, R. W. McConnell, S. W. Nelson

Program Committee: H. Z. Mellins, J. F. Martin, J. L. Gwinn, M. M. Figley, R. A. Gagliardi, B. G. Brogdon, E. Gedgaudas, G. A. Kling, P. Riemenschneider, chairman

Instruction Courses: E. Gedgaudas, director; G. W. Hartman, associate director

American College of Radiology Board of Chancellors Representative: W. B. Seaman

Annual Meeting: March 25–30, 1979, Sheraton Centre, Toronto, Canada

Scientific Program: P. A. Riemenschneider, president elect, Cottage Hospital, Santa Barbara, California 93105

Manager Annual Meeting: George A. Kling, Harper Hospital, Detroit, Michigan 48201

Membership: John L. Gwinn, 4650 Sunset Blvd., Los Angeles, California 90027

Business Office: Keith W. Gundlach, comptroller, American College of Radiology, 20 North Wacker Drive, Chicago, Illinois 60606

American Radium Society

President: Frederick W. George, III
President Elect: Alfred S. Ketcham
1st Vice-president: Julian P. Smith
2d Vice-president: Edwin M. Jacobs
Secretary: Norah duV. Tapley
Treasurer: Simon Kramer

COMMITTEES 1978–1979

Executive: A. S. Ketcham, J. P. Smith, E. M. Jacobs, N. duV. Tapley, S. Kramer, L. W. Brady, R. H. Jesse, F. W. George, F. Rutledge, chairman

Public Relations: V. Marcial, J. Vaeth, C. Honaker, ex-officio, and F. George, chairman

Publication: K. L. Krabbenhoft, D. Hussey, A. Raventos, I. Fix, L. W. Brady, chairman

Scientific Program: R. Parker, J. Durant, A. S. Ketcham, M. S. Mitchell, G. Murphy, F. Rutledge, M. Griem, W. E. Powers, M. Apuzzo, F. George, chairman

Local Arrangements: L. Davis, J. Vaeth, J. Nolan, R. McKenna, J. Slater, J. Stein, J. Scallon, S. Kramer, J. Helsper, chairman

Constitution and Bylaws: A. S. Glicksman, P. J. DiSaia, K. L. Krabbenhoft, chairman

Audiovisual: C. R. Bogardus, J. Helsper, R. Schweitzer, R. H. Jesse, C. Perez, J. Glassburn, A. M. Nisar Syed, R. Young, B. Herrington, F. George, chairman

American Board of Radiology Representatives: J. J. Stein, R. E. King, N. duV. Tapley

American College of Radiology Board of Chancellors Representative: L. W. Brady

American College of Radiology Council Representative: J. del Regato

Editorial Board of AFCOS Newsletter Representative: J. Vaeth

National Council on Radiation Protection and Measurements Liaison Representative: L. W. Davis

Annual Meeting: March 4–8, Los Angeles, California

Scientific Program: F. W. George, III, University of Southern California School of Medicine, Los Angeles, California 90033

Local Arrangements: James Helsper, Pasadena, California

Membership: Norah duV. Tapley, secretary, M. D. Anderson Hospital, 6723 Bertner Avenue, Houston, Texas 77030

Business Office: N. V. Jordan, c/o R. H. Jesse, M. D. Anderson Hospital and Tumor Institute, 6723 Bertner Avenue, Houston, Texas 77030

Mailing note.—Mailing surcharges: U.S. and possessions, none; European countries, $25; Japan, $45; other, $10. European rates apply to Algeria, Austria, Belgium, Czechoslovakia, Denmark, Finland, France, Germany, Great Britain, Greece, Hungary, India, Iran, Ireland, Israel, Italy, Kenya, Luxembourg, Netherlands, Nigeria, Norway, Portugal, Romania, South Africa, Spain, Sweden, Switzerland, Turkey, Uganda, Yugoslavia. All subscriptions to Japan and European countries are delivered by air freight; there is no option for surface mail.

Taking the Pain out of Chest X-rays

Of course, chest x-ray examinations are not normally painful for the patient. However, the heavy patient load this type examination places on radiology departments can create chronic operational PAIN! This PAIN can be in scheduling chest examination patients into various rooms between other studies and the constant trips to and from the darkroom for cassette loading, unloading and film processing. Variable film quality due to different screens, cassettes, x-ray equipment and processor being used, can also contribute to department operation PAIN.

The ULTRARAD Chest System by Liebel-Flarsheim eliminates these operational pains and inefficiencies. When the ULTRARAD Chest System is installed with a dedicated film processor and automatic exposure timing, all your chest radiographs will be of the same high quality because the same screens, grid, x-ray equipment and film processor are used for all chest examinations. In addition, the system will deliver radiographs, ready for diagnosis, in less than 2 minutes[1] from time of exposure.

The 100 supply film capacity[2] of the ULTRARAD reduces the greatest operational pain of all; those time consuming trips to and from the darkroom with cassettes, for loading, unloading and film processing.

Let Liebel-Flarsheim take the PAIN out of your chest x-ray examinations—write for our free brochure on PAINLESS CHEST RADIOLOGY.

See our new compact and economical "DIRECT FEED" adaptation for the Kodak M7 processor at the 1978 RSNA . . . Booth No. 3038

[1]When used with Kodak model M6 processor
[2]The ULTRARAD is furnished with two supply magazines each capable of holding up to 50 films.

Liebel-Flarsheim Company
Division of Sybron Corporation
111 E. Amity Road,
Cincinnati, Ohio 45215, U.S.A.
(513) 761-2700

SYBRON | Liebel-Flarsheim

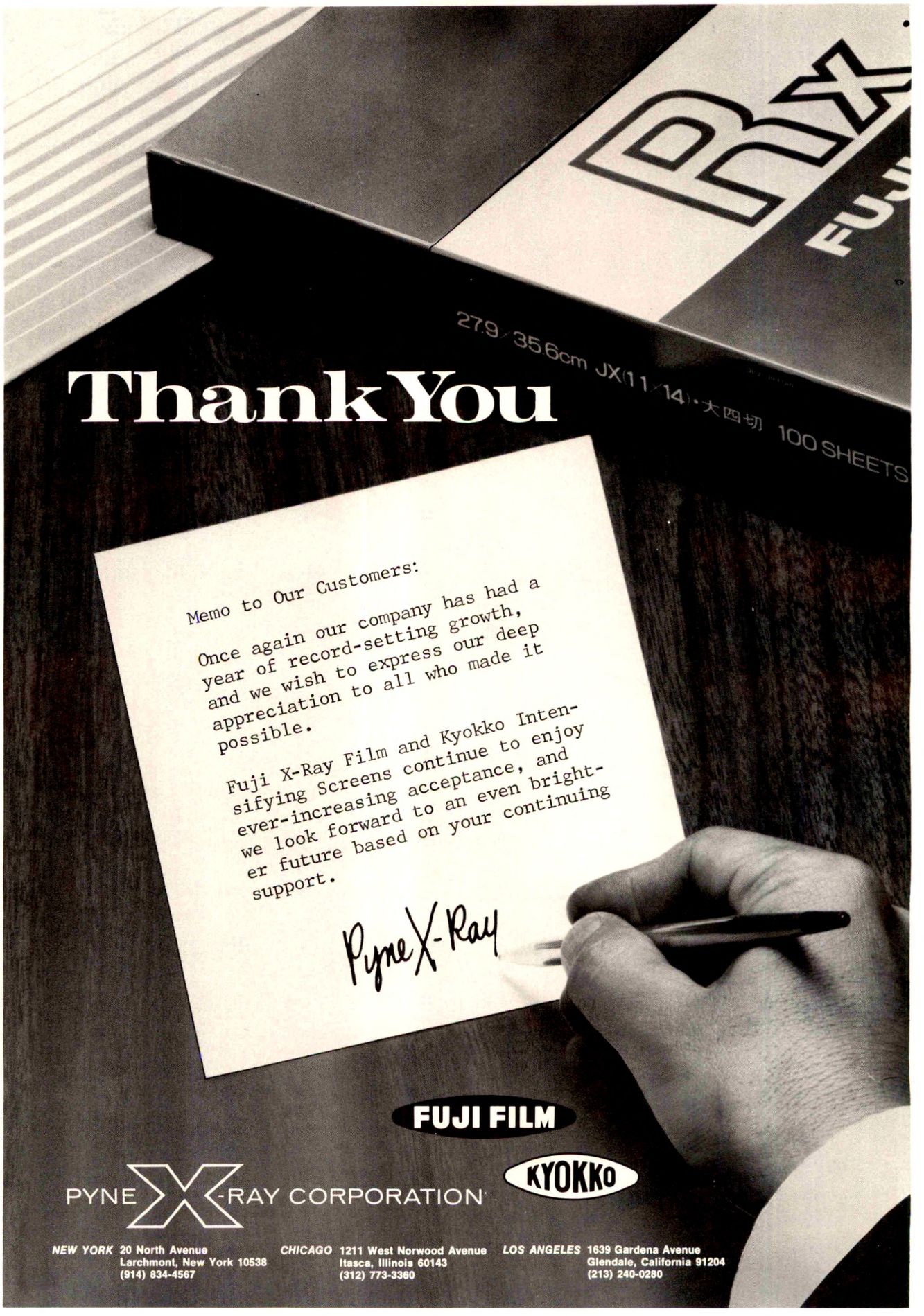
RX
27.9×35.6cm JX(11×14)・大四切 100 SHEETS
Thank You
Memo to Our Customers:
Once again our company has had a year of record-setting growth, and we wish to express our deep appreciation to all who made it possible.
Fuji X-Ray Film and Kyokko Intensifying Screens continue to enjoy ever-increasing acceptance, and we look forward to an even brighter future based on your continuing support.
Pyne X-Ray
FUJI FILM
KYOKKO
PYNE X-RAY CORPORATION
NEW YORK 20 North Avenue Larchmont, New York 10538 (914) 834-4567
CHICAGO 1211 West Norwood Avenue Itasca, Illinois 60143 (312) 773-3360
LOS ANGELES 1639 Gardena Avenue Glendale, California 91204 (213) 240-0280

clear, clean colon

X-Prep® Liquid

(standardized extract of senna fruit)

versatile bowel evacuant for diagnostic procedures

Versatile in indications

May be used prior to:

G.I. radiography
Urologic radiography
Colonoscopy
Sigmoidoscopy
Other diagnostic bowel procedures

Versatile in administration

May be used:

Alone, in a single dose
Alone, in divided doses, particularly in elderly or debilitated patients
With adjunctive use of citrate of magnesia, laxative suppositories and enemas, as required
As part of other regimens, such as hydration

X-PREP Liquid is formulated specifically for effective bowel evacuation prior to diagnostic procedures. It induces peristalsis through virtually colon-specific action. X-PREP Liquid has been found effective in cleansing the colon for diagnostic evaluation in 95% of 749 patients prepared for barium enemas, intravenous pyelography, or colonoscopy.* Its pleasant taste meets with high patient acceptance, and its ease of administration is appreciated by the patient and nursing staff.

Supplied: X-PREP Liquid (standardized extract of senna fruit) in 2½ fl. oz. bottles (alcohol 7% by volume). X-PREP Powder (standardized senna concentrate) in ¾ oz. containers. **Now Available:** X-PREP™ Bowel Evacuant Kit. Each kit contains: two SENOKOT® S Tablets (standardized senna concentrate and dioctyl sodium sulfosuccinate), one bottle of X-PREP® Liquid 2½ fl. oz., and one RECTOLAX™ Suppository (bisacodyl 10 mg), plus easy-to-follow patient instructions for hydration, clear liquid diet, and the correct time sequence of administering the above laxatives.

* Bibliography available upon request.

Colonoscope, courtesy of Olympus

Gray Pharmaceutical Co., Affiliate
The Purdue Frederick Company

© Copyright 1978, Gray Pharmaceutical Co. Norwalk, CT 06856

A9047 194578

Isn't it time you asked their first name?

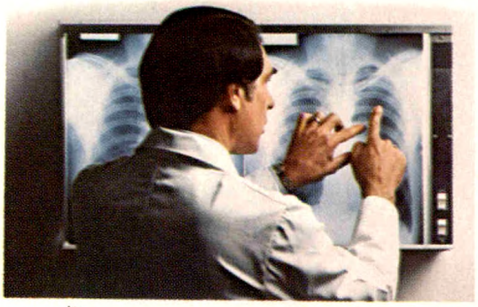

Get familiar with GAFMED.®

GAF® makes it easy to be the first name you think of when ordering quality x-ray films, chemicals, screens and cassettes. We call all our medical x-ray products GAFMED.® Our first-name, only name basis of identity.

It's called GAFMED for one good reason. It's one consistent x-ray system with the confidence to meet a variety of your radiographic needs.

GAF's solid experience and foresight are behind its contemporary x-ray products. This enables GAFMED to respond to any radiographic requirement—be it consistency in your x-ray film, fail-safe chemicals or quality screens, cassettes and accessories. We know you develop favorites in this business and GAF wants to be one of them by measuring up to your toughest standards.

GAFMED® Film and Chemicals: Quality through consistency. To help you manage x-ray imaging, such as getting excellent radiographic contrast and detail, GAF offers a superb line of film that gives you the kind of stability you need in whatever mode you work.

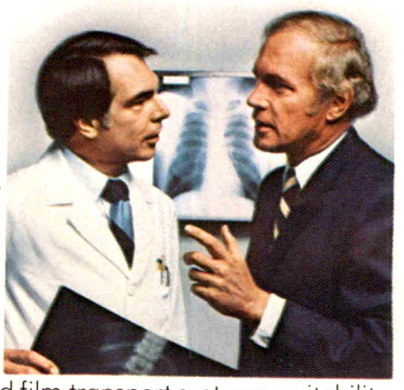

GAFMED® SR/1 When you need an expanded useful density range, wide-latitude SR/1 is your diagnostic radiographic film. It provides high contrast in those low density areas where most radiographic detail is visualized. In addition, SR/1 simultaneously delivers low contrast in high density regions to increase soft tissue detail with maximum exposure latitude. GAFMED SR/1 is designed for use with all blue and blue-green emitting intensifying screens and is fully compatible with all conventional processing methods.

GAFMED® SR/2 SR/2 is a general-purpose medical radiographic film with medium speed, low fog, high contrast and blue spectral sensitivity. Features that make this widely accepted film outstanding are its ideal performance in automated film transport systems, suitability for all automatic and manual processing modes and its high definition image quality. SR/2 renders a wide variety of system speeds when used in combination with GAFMED calcium tungstate and Rarex® rare earth intensifying screens.

GAFMED® SR/S GAFMED SR/S Photofluorography film is designed for use with image intensifiers employing 70mm and 105mm roll film cameras. SR/S features high speed, high contrast and a low base fog for superb optical clarity. GAFMED SR/S is also designed for all 90-second short cycle and extended cycle automatic processing systems.

GAFMED® SC/90 You'd expect the company responsible for the first color-coded chemistry to be equally as innovative with the new GAFMED SC/90 chemical system. **SC/90 DEVELOPER,** color coded red requires no starter solution and cannot be over-replenished. The red pH sensitive quality control feature enables you to quickly determine chemical processing energy through visual check. **SC/90 FIXER,** color-coded blue for easy identity and fail-safe mixing, is designed for use in all short cycle automatic processors and provides excellent archival activity.

or me l--l -r--y pr-- ucts y

E/90 chemistry is also a clean-working solution for consistent uality assurance that's part of the GAFMED system.

-AFMED® Screens and Cassettes. he right film and chemicals is just the start.

or optimum radiographic performance the winning GAFMED combination s: a high quality film, superior screens and dependable cassettes.

GAF manufactures two premium GAFMED cassettes to meet your pecific requirements: the lightweight Comp-I-Sette™ and the durable Titan.™

The Comp-I-Sette design insures superior screen-film contact for ptimum definition. Its lightweight metal construction and special epoxy oating are geared to provide long cassette wear.

The Titan cassette, known for its excellent screen-film contact, is ruggedly constructed to guarantee long lasting ervice. Its positive-locking feature makes it resistant to sudden jars and jolts. Well recognized as a standard of the ndustry, Titan cassettes are available in regular and phototiming models.

The GAFMED system also features a wide variety of intensifying screens to meet your particular imaging needs. Our GAFMED Calcium Tungstate screens have an abrasion resistant surface making them ideal for automated ilm transport systems. Of the four types available, TF-3 with a fast exposure rating, is the most popular for general adiographic applications.

GAFMED Rare Earth Intensifying Screens allow you to significantly reduce the exposure without requiring a special film or a change in safe-light illumination. Our popular BG High Speed screens allow a 4 time exposure eduction compared to a typical par speed calcium tungstate system.

All GAFMED screens minimize static related artifacts by incorporating an aluminized backing.

GAFMED Product Service: You can't beat the system. GAFMED is more than a name for our quality line of medical x-ray products. It stands for the GAF people who safeguard your operations with a comprehensive field support program called Radiographic Engineering Services.

Our skilled GAF technical representatives and x-ray engineering consultants will help you get the most efficiency from your radiology department. They provide expert product consultation and high impact training programs to assure consistent radiographic image quality while reinforcing your expertise.

Now is the time to get familiar with GAFMED by contacting your local GAF technical sales representative...GAF x-ray dealer... or GAF Corporation, Medical X-Ray Products, 140 West 51st Street, New York, N.Y. 10020.

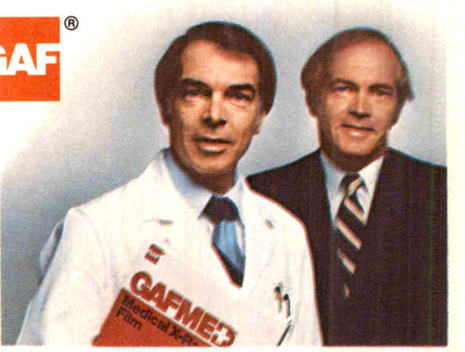

GAFMED®

Medical X-Ray Products.
The image of confidence.

Liquid Polibar with Super XL

A Total System

For double-contrast examination of the colon.

Satisfactory results in the double-contrast examination of the colon require special attention to two aspects of the procedure.

First, the barium sulfate formulation. Our Liquid Polibar (56% w/w) is a bubble-free, non-precipitating uniform suspension formulation ... with proper flow and coating characteristics. No blending required and once routines are established, you can rely on its consistency.

The second concern is with the proper apparatus. The E-Z-EM system is unique in that 1/2" lumen tubing attached to the enema bag is utilized — for freer, more uniform flow. Miller Air Retention Tip, with or without optional cuff completes the system.

A total system for ease of administration and consistently reliable radiological results. For additional literature, write:

Multiple pseudo polyps in the splenic flexure in longstanding ulcerative colitis.
Film courtesy of Richard Palmer Gold M.D. Columbia Presb. Medical Center N.Y.

E-Z-EM

7 Portland Ave.
Westbury, New York 11590
(516) 333-8230

7/78

International Affiliates: E-Z-EM Rooster B. V., Infirmeriestraat 6-8, Rotterdam 16, Netherlands
E-Z-EM De Mexico, S. A. de C. V., Calz. Azcapotzalco La Villa No 882, Zona Industrial Vallejo, Mexico 16 D. F.

When you're making this kind of commitment, you should know what kind of commitment the manufacturer is making.

Is making...not *will* make. That's the difference between a commitment and a claim. And that's why Pfizer encourages questions about our CT scanner. We think that when it's time to compare answers, you'll see the difference for yourself.

Prestigious installations.
Pfizer has over 150 working CT sites in the United States and 13 foreign countries. Our list includes installations at University of Colorado Medical Center, Columbia-Presbyterian Medical Center Hospital, Johns Hopkins Hospital, Michigan State University Hospital, University of Minnesota Hospital, and Yale-New Haven Hospital.

Near-perfect service.
A worldwide network of dedicated, experienced service engineers, each capable of total system maintenance. They've provided a documented average uptime record of 96% for installations in the U.S. And that's a remarkable service record in the CT industry.

Complete product line.
A full family of scanning equipment. From the industry's first total-body scanner to our benchmark 0200FS whole-body unit, up to the recently announced Pfizer/AS&E CT scanner — the first high resolution fourth-generation scanner. Pfizer now offers one of the most complete lines of CT scanning equipment in the world. Featuring CT images of outstanding clarity, mobile patient handling systems, diagnostic flexibility and advanced software capability every step of the way.

Pfizer and AS&E.® Together.
Early this year, Pfizer Medical Systems, Inc. signed an agreement with American Science and Engineering, Inc. Pfizer and AS&E, both pioneers in the industry, will continue to develop new radiological products, including a revolutionary cardiac scanner. It was Pfizer who developed the first whole-body scanning system. It was AS&E who first introduced fourth-generation geometry, acknowledged as the most advanced CT technology in the world. And together we will continue to practice our commitment. Not just promise it.

For more information, write Pfizer Medical Systems, Inc., Dept. JR, 10 Old Annapolis Road, Columbia, Maryland 21045.

Pfizer

PFIZER MEDICAL SYSTEMS, INC.

We're leaders. And we can show you why.

NEW FROM KODAK

90-SECOND

WITH TAP-

PROCESSING

Now you can get the dependability of Kodak's 90-second automatic processor, with the convenience and savings of ambient water wash and reduced water flow.

The KODAK *RP* X-OMAT Processor, Model M6AW, gives you fully processed, dry, ready-to-read radiographs in 90 seconds, and uses tap water from 40° to 90°F (4–32°C). This eliminates the need for hot-water plumbing and a thermostatic mixing valve, and enables you to install the Model M6AW wherever you have a tap-water outlet and drain. Since hot water is not required, you can save on energy costs.

A new air-type heat exchanger helps control developer temperature, making the Model M6AW independent of hot-water availability. The single water service eliminates the possibility of developer temperature fluctuations due to abrupt changes in water pressure or temperature.

This reliable new processor occupies less than five square feet of floor space, but can process an average of 385 sheet films of intermixed sizes per hour. And it can process roll films up to and including 17 inches in width at the rate of 66 inches per minute.

A standby control unit is also available, to turn off water as well as drive and dryer mechanisms when not in use, further reducing power consumption and wear.

Dependability. 90-second processing, energy-saving. That's the KODAK *RP* X-OMAT Processor, Model M6AW. Ask your Kodak Technical Sales Representative or your x-ray products dealer to show you how this new processor can serve your department. Or write: Eastman Kodak Company, Dept. 740-B, Rochester, New York 14650.

TURNING ENERGY INTO IMAGES

Kodak

COMPUTED TOMOGRAPHY • NUCLEAR MEDICINE
ULTRASOUND • RADIOGRAPHY • THERMOGRAPHY

WATER WASH

temp · guard™

temperature stabilizer

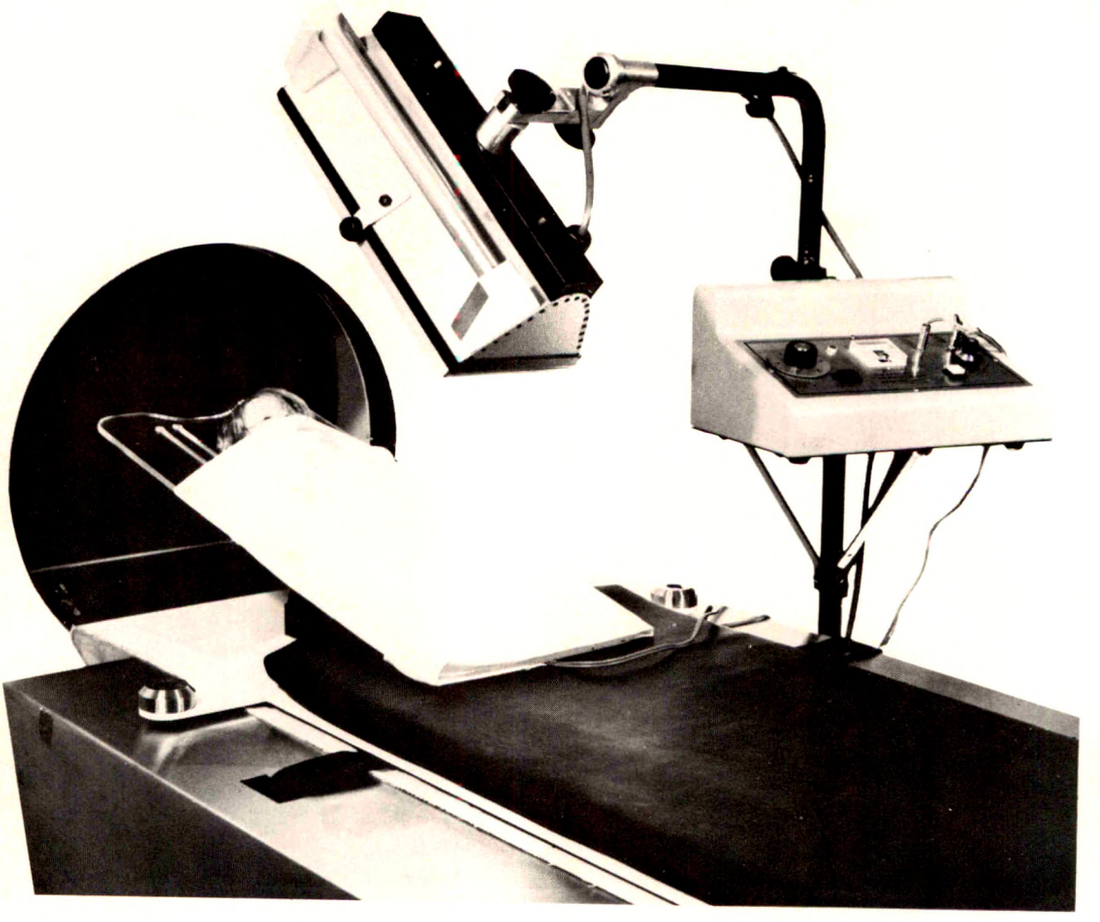

- coverless temperature support system for complete accessibility
- mobile and versatile
- for use in fluroscopy, special procedures, c.t. and ultrasound
- feed back probe which provides accurate temperature control and readout display
- fail safe instrumentation

call direct 716 882-0862

or write

gordon consultants, inc. 361 dewitt st. • buffalo, new york 14213

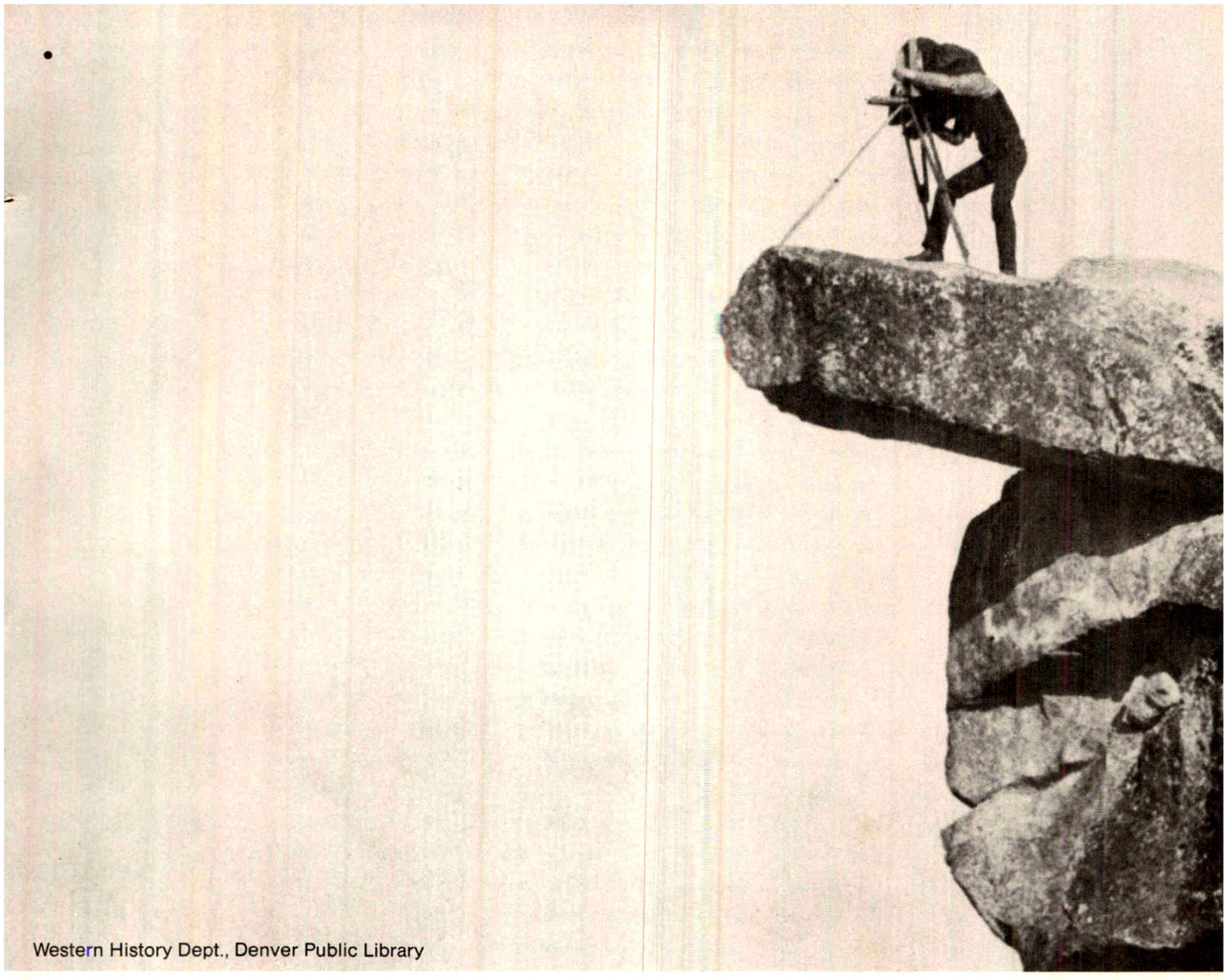

Western History Dept., Denver Public Library

When the subject can't be moved, it helps to have a camera that can.

With the introduction of lighter photographic cameras that enabled man to seek new perspectives from which to take pictures, new horizons in realism were made possible.

Searle Radiographics similarly influences technology in the field of nuclear medicine with its extensive line of systems that extend the clinical utility of nuclear cardiology throughout the hospital.

The Pho/Gamma® L.E.M. Low-energy Mobile Scintillation Camera.

The Scintistore™ Time-compression Data Storage/Retrieval System.

The Gamma/Cor™ RCG Cardiac Probe.

The Scintiview™ Image Control Station.

Versatility and great images. They're the reasons why this is the most complete and efficient nuclear cardiology line available. Find out how our product technology can serve your needs in nuclear cardiology by contacting Searle Radiographics.

Searle nuclear cardiology systems move where they're needed to make GREAT IMAGES.

SEARLE

Searle Radiographics
Division of Searle Diagnostics Inc.
2000 Nuclear Drive
Des Plaines, Illinois 60018

SI-8-8429 R1 1007CMO1990

Introducing "MINI-VIEWER"

SAVES SPACE
SAVES TIME

NEW CONVENIENT MINI-SIZE, MOTORIZED, PORTABLE 48-FILM X-RAY VIEWER IS

- Attractive modern styling for every decor! • Optional shelf or desk available.

SMALL!

- small enough to roll from room to room
- small enough to just plug in and operate
- small enough to sit next to Radiologist's desk

BUT ... "MINI-VIEWER" IS BIG!

- BIG enough to view & store up to 48 — 14″x17″ (or smaller) films (equivalent of 6-4 over 4 ills)
- BIG enough to illuminate 4 over 4 films
- BIG enough for 7-second random access touch-control viewing
- BIG enough to offer individually-controlled, extra bright lighting — without spillover between sections
- BIG enough to be rugged yet compact — 70″ wide, 79″ high, 22″ deep

MANUFACTURED BY

S·S *The Complete Line of X-Ray Accessories*

S. & S. X-RAY PRODUCTS INC.

Telephone: 212-852-6900

87-93 JAY STREET, BROOKLYN, N.Y. 11201

Manufactured in USA by **S & S**, who have made more motorized viewers than any one else in the world. Sold by local X-Ray dealers backed up by **S & S** parts inventories and experience.

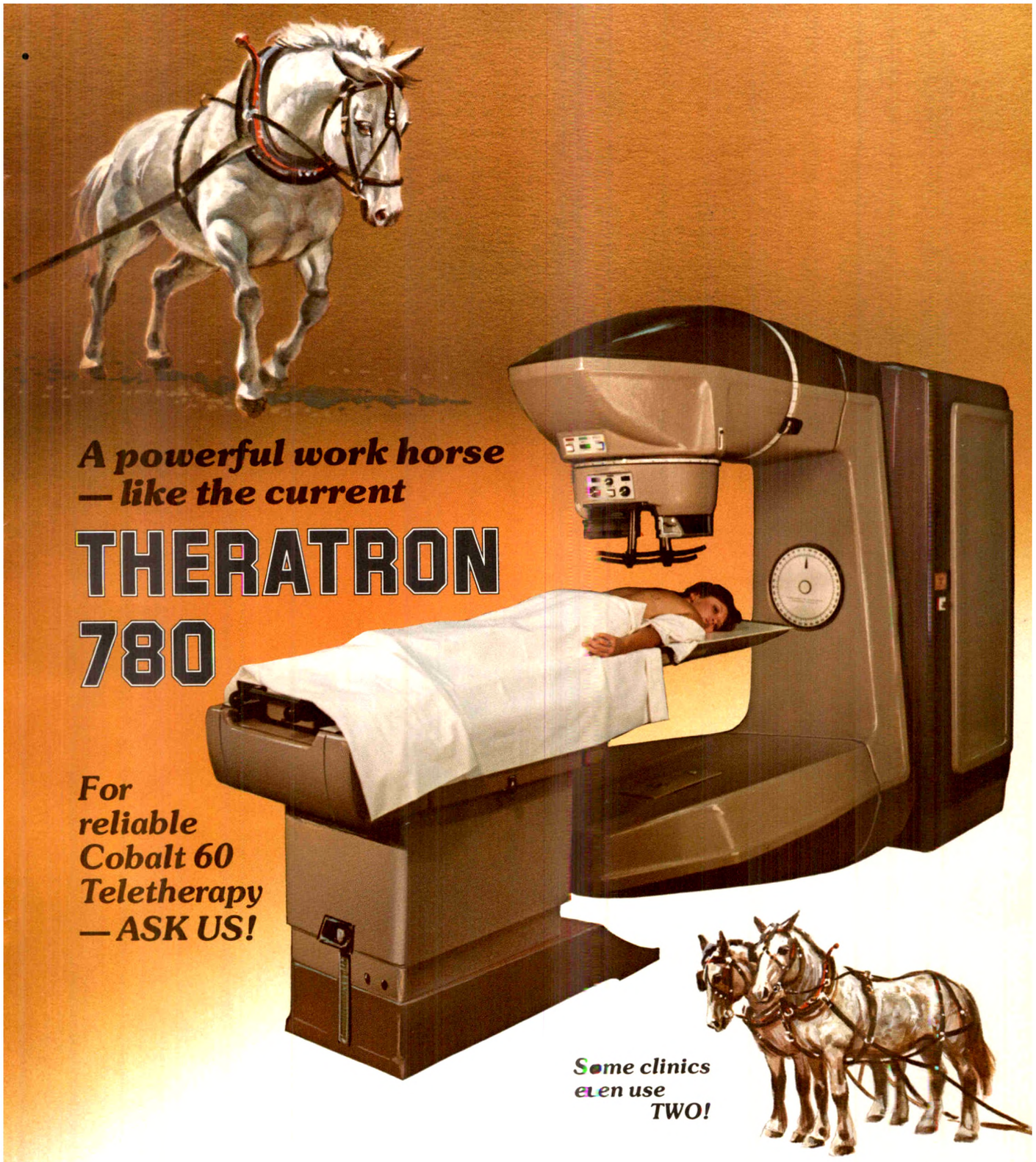

Atomic Energy of Canada Limited

Commercial Products

P.O. Box 6300, Ottawa, Canada, K2A 3W3
Tel. 613/592-2790 • Cable Nemota • Telex 053-4162

77.4M

Introducing the first radiographic table that kneels.

Patent Pending

Amrad's new THV table literally obsoletes every horizontal radiographic table on the market—including, unfortunately, some of our own. "THV," you see, stands for *Top Height Variable*.

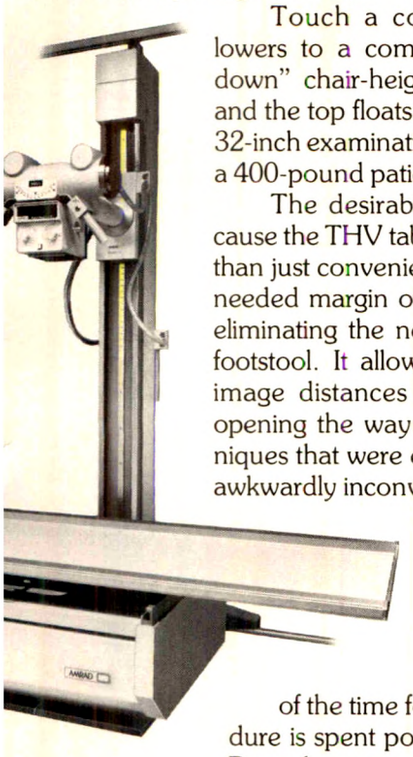

Touch a control and the top lowers to a comfortable, "please-sit-down" chair-height. Touch it again, and the top floats effortlessly back to a 32-inch examination height, even with a 400-pound patient aboard.

The desirability is obvious. Because the THV table offers much more than just convenience. It adds a much needed margin of safety—completely eliminating the need for a hazardous footstool. It allows extended source-image distances of 55″ or more—opening the way to many new techniques that were either not possible or awkwardly inconvenient before.

And with today's spiraling costs, the Amrad THV table offers an important *savings of time*. After all, most of the time for an average procedure is spent positioning the patient. Procedures are often complicated by patient feebleness or incapacity—certainly a common problem in every radiographic facility. Throughout the day, extra people must be available to help the technologist with those instances.

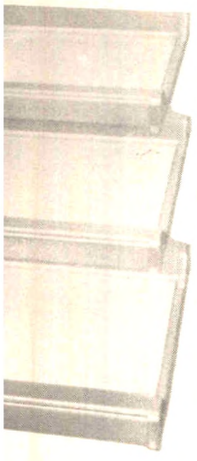

But not with the Amrad THV table. An Amrad THV room allows fewer people to perform more examinations in less time.

That high-volume capacity is augmented by the now-famous Amrad four-way floating top—the one that travels as far or farther in every dimension than that of any other radiographic table—no matter what the price. After initial positioning, there is no possible coverage, head to toe, side to side, that could require scooting or sliding the patient.

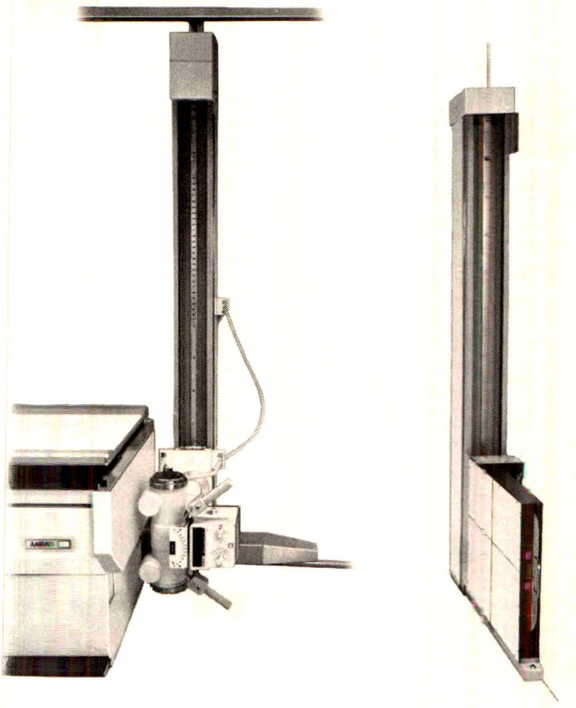

The table is augmented by the Amrad tubestands—the ones where the tube and vertical bucky combination *goes all the way to the floor*—allowing weight-bearing procedures to be handled with a minimum of dangerous and bulky platform accessories. And by the superb Craig-series of 600 MA generators—the ones with the small, remote-control console connected with low-voltage telephone cable. The ones that have earned a near-perfect record of reliability.

And so Amrad's new THV table makes possible the first radiographic room that is designed around people, instead of machines. Surprisingly, it's not expensive—costing little or no more than obsolete tables. Phone collect for the name of your local Amrad dealer.

And go sit down on the first radiographic table that kneels.

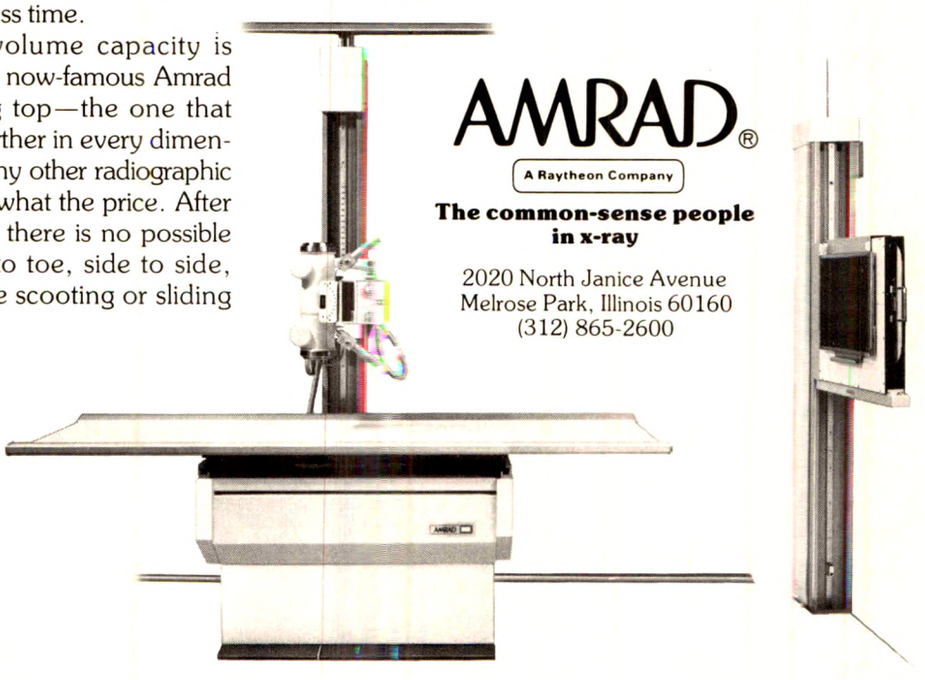

AMRAD®

A Raytheon Company

The common-sense people in x-ray

2020 North Janice Avenue
Melrose Park, Illinois 60160
(312) 865-2600

better

The 600 Beta Series Camera

Nice looking. The camera, we mean.

No need to pout. This camera won't let you make any careless mistakes, like forgetting to pull the dark slide.

Easy access. Takes the pain out of installation and service.

How do you name the heir to a classic?

We needed a way to tell the world that our new generation of 600 Series cameras was part of the original family of multi-format, video display cameras. But different. Totally redesigned for improved performance. But recognizably the same. So we picked the second letter of a classic alphabet – the Greek – and called it the Beta camera. It's second, but not second best. In fact, it's better.

Better than the camera that established the concept of multiple image hard copy on 8"×10" x-ray film? (And has the patent to prove it.) That has sold more units in this country and abroad than any of its numerous imitators? Hard to believe . . . hard to achieve. But true.

Better operating, for one thing. Single-handed front loading. Film cassette and dark slide interlocks that keep you from taking a picture when you shouldn't. Automatic Reset when a new film is loaded so you operate the camera almost without thinking.

We still offer the proven formats. And all the proven features, like flash card data entry, spot meter exposure system and footswitch remote operation. Our components will always be the finest available, including a new, high performance video monitor, Schneider lens and CMOS electronics.

This all pays off where it counts – in image quality. And when you see our images, you'll know for sure that Beta's not only better. It's best

For more information, call collect or write Dunn Instruments, Inc., 544 Second Street, San Francisco, CA 94107, (415) 957-1600

Dunn Instruments

The 600 Beta Series Camera

Single-handed front loading. Lets you install the Beta anywhere you like and load it on the run.

Ho hum. Simplified front panel controls make picture-taking a breeze.

Where Beta's best – superb clinical images in any format, positive or negative.

What you'd expect from
RAYTHEON MEDICAL IMAGING

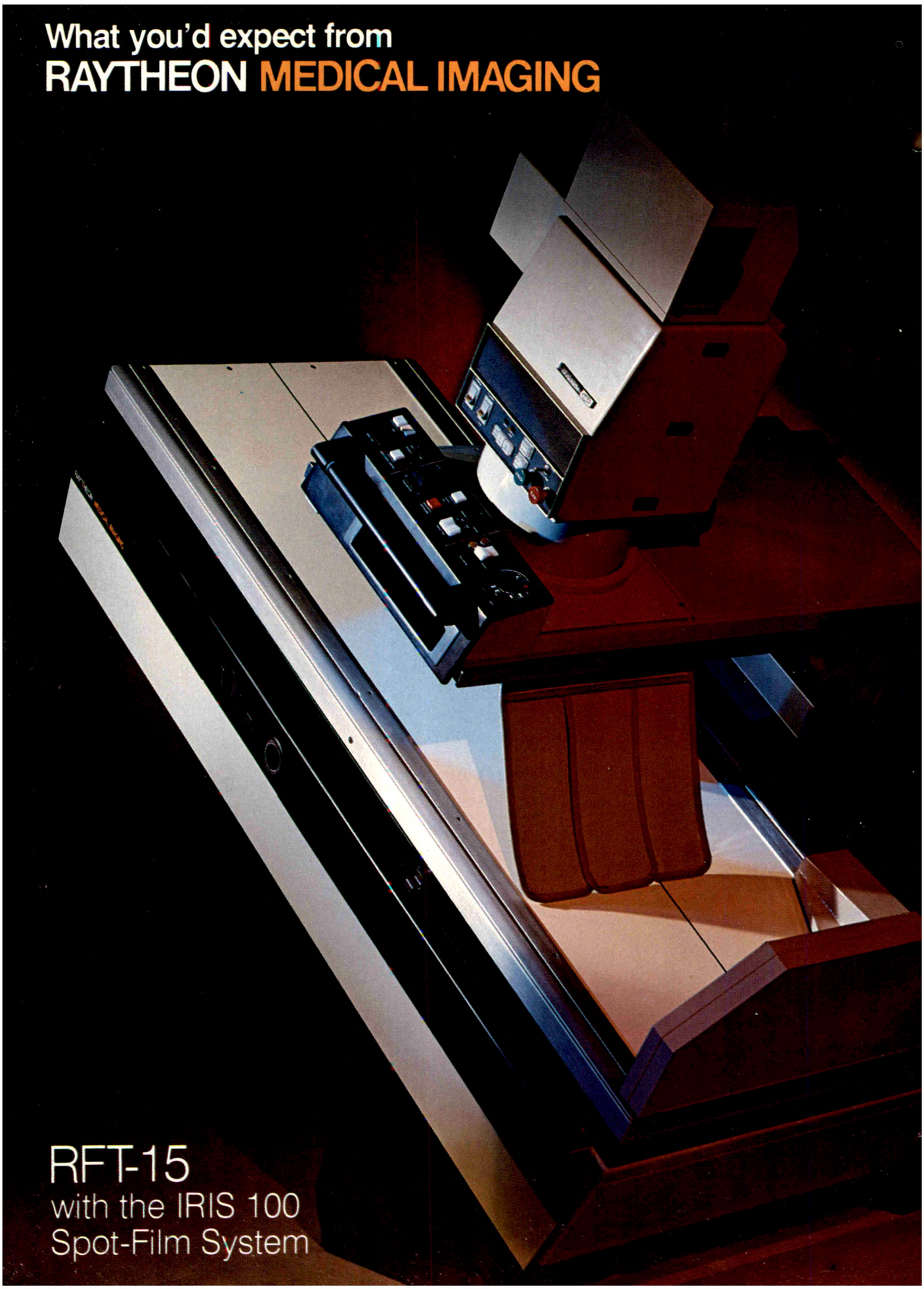

RFT-15
with the IRIS 100
Spot-Film System

FLUORO 1

A cost-effective x-ray system designed to let the radiologist concentrate on diagnosis

RFT-15
90/15 R/F Diagnostic X-Ray Table

Unencumbered by past practices and outmoded equipment, Raytheon Medical Imaging had but one goal in mind in developing its top-of-the-line RFT-15 diagnostic x-ray table —

To perfect a combination of motor-driven tilt table and spot-film console so easy to use that it would focus the skills of the radiologist by allowing him to concentrate on his patient, not his equipment.

The RFT-15 features:

Two-speed power tilt to 90-degree vertical and the full 15-degree Trendelenburg position with programmed stop at horizontal.

Two-way power-driven table top with an exceptional total movement of 61 inches (36 inches toward head, 25 inches toward feet), permitting great flexibility in patient positioning.

Desirable tabletop height of 31½ inches, comfortable for both patient and technologist.

One-handed operation of footrest latch.

Minimum table-top-to-film distance for excellent radiographs in conventional procedures.

Quiet, easily positioned power-driven spot-film tower.

Suspension-free television or mirror-viewing imaging systems. Also accommodates IRIS 100 intensified spot-filming systems.

Human-engineered pushbutton controls on spot-film console arranged for procedure-oriented operation. Patient positioning controls are duplicated on table side.

Available without fluoroscopic carriage for radiography-only rooms (RT-15).

Finally, easy installation is not the least of FLUORO 1's virtues. But this cost-effective system and its components offer so many other features, that you really should ask for our descriptive literature.

Contact your local Raytheon Medical Imaging representative, or

RAYTHEON

RAYTHEON MEDICAL IMAGING
Stamford, Connecticut 06907
(203) 348-2499

And a companion Generator
RMX-625R/F

Designed for heavy-duty service, the RMX 625R/F Radiographic/Fluoroscopic Generator is a fit companion for the RFT-15 Diagnostic Table in the FLUORO 1 System.

Its three-piece design — Remote Operator Console, Power Control Unit and High-Tension Transformer — permits total flexibility in location. Connected by low-voltage cables, the handsome Operator Console can be wall mounted, placed on a table or desk or equipped with its own free-standing pedestal, complete with writing surface.

Controls have been laid out to take advantage of both traditional operating sequences and the latest findings of human-factors engineering to provide the easiest operation available today.

RMX-625R/F Operator Console

Features include:

High power 600 mA at 100 kVp, 500 mA at 125 kVp.

Digital pre-reading of mAs and kVp settings.

Pushbutton switches for all functions.

1/120-second solid-state timer/contactor, for long life and trouble-free accuracy.

Automatic line compensation to eliminate the effects of changing power-line conditions.

4 WAYS TO GET MORE FOR

1 DON'T OVERREPLENISH.

Guidelines for replenishment are based on an assumed average of the number of square metres of film processed. If your intermix of film sizes falls outside the average, you may be overreplenishing. An analysis of your actual needs by a Kodak representative can provide useful data and maybe save you money.

2 BE CONSISTENT.

Follow the manufacturer's recommendations for processing temperature, time, mixing, and storage procedures. By doing this, you'll reduce the chance of variability—no matter whose chemicals you use.

YOUR CHEMICAL DOLLAR

3 RECOVER YOUR SILVER.

It can help pay for your chemicals. Not all silver recovery equipment and procedures are alike. We'll be happy to share our knowledge with you via the mail or your Kodak Technical Sales Representative.

TURNING ENERGY INTO IMAGES

Kodak

COMPUTED TOMOGRAPHY • NUCLEAR MEDICINE

4 USE *KODAK* CHEMICALS.

They are produced and packaged to uncompromising quality. They are formulated to bring out the imaging characteristics of your x-ray film consistently, batch after batch, day after day.

For more information on Kodak chemicals and other products, ask your Kodak representative for a copy of the KODAK Medical X-ray

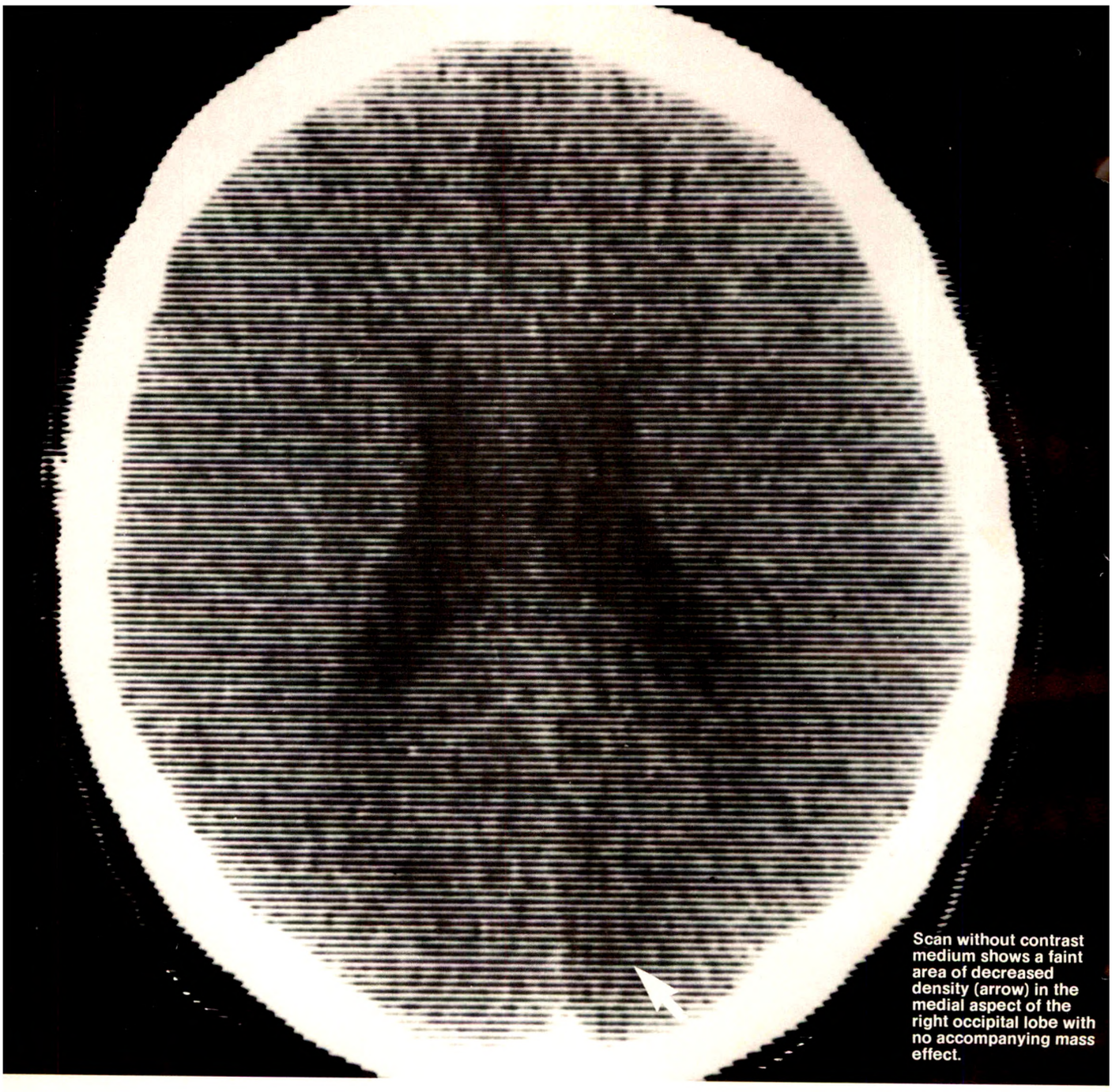

Scan without contrast medium shows a faint area of decreased density (arrow) in the medial aspect of the right occipital lobe with no accompanying mass effect.

Use of this contrast medium to enhance CT brain scans "revealed both an increased detectability and an improved pathologic differentiation of many lesions."*

—**Identifies** lesions not seen on plain CT scans.

—**More specifically defines** nature, size and behavior of wide variety of lesions visualized on plain CT scans.

—**Aids in detection** of aneurysms, arteriovenous malformations, sites of active infection, and in diagnosis of other intracranial pathology.

—**Rules out** the presence of tumor in suspicious areas which may otherwise not have been satisfactorily visualized.

*Davis KR: Massachusetts General Hospital, Boston, MA. Personal communication.

After administration of contrast medium, the lesion enhances well, demonstrating a posterior cerebral artery distribution infarct.

Reno-M-DIP®

Diatrizoate Meglumine Injection USP 30%

for enhanced CT scanning of the brain

The leader in radiologic diagnostics

SQUIBB®

contrast media™

See next page for brief summary.

Reno-M-DIP®
Diatrizoate Meglumine Injection USP 30%
for enhanced CT scanning of the brain

Reno-M-DIP (Diatrizoate Meglumine Injection USP) for drip infusion provides a sterile, aqueous solution of 30% diatrizoate meglumine which contains approximately 14% (42.3 g per 300 ml) bound iodine and 0.04% edetate disodium (sequestering agent). *The solution contains approximately 0.054 mg (0.002 mEq) sodium per ml (16.2 mg/300 ml).*

CONTRAINDICATIONS: Contraindicated in patients hypersensitive to salts of diatrizoic acid and in patients with anuria.

WARNINGS: A definite risk exists in the use of I.V. contrast agents in patients with multiple myeloma. There has been anuria with progressive uremia, renal failure and death. This risk of the procedure in these patients is not a contraindication; however, partial dehydration in preparation for study is not recommended since it may predispose to precipitation of myeloma protein in renal tubules. No therapy, including dialysis, has been successful in reversing this effect. Myeloma should be considered in persons over 40 before I.V. administration of a contrast agent.

In cases of known or suspected pheochromocytoma, if the physician feels that the possible benefits outweigh the considered risks, radiopaque materials should be administered with extreme caution; however, an absolute minimum of material should be injected, the blood pressure should be assessed throughout the procedure, and measures for treating a hypertensive crisis should be available.

Contrast media may promote sickling in homozygous individuals when injected I.V. or intra-arterially. Use diatrizoate meglumine with extreme caution in persons with severe concomitant hepatic and renal disease. Perform thyroid function tests prior to administration of diatrizoate meglumine since iodine-containing contrast agents may alter the test results. Although a history of sensitivity to iodine *per se* or to other contrast media is not an absolute contraindication, administration of diatrizoate meglumine requires extreme caution in such cases.

PRECAUTIONS: Diagnostic procedures involving use of contrast agents should be performed under the direction of personnel with prerequisite training and a thorough knowledge of the particular procedure (see ADVERSE REACTIONS). Severe life-threatening reactions suggest hypersensitivity to the contrast agent. A personal or family history of asthma or allergy or a history of a previous reaction to a contrast agent warrants special attention and may predict more accurately than pretesting the likelihood of a reaction although not the type nor severity of the reaction in the individual. The value of any pretest is questionable. The pretest most performed is the slow I.V. injection of 0.5 to 1.0 ml of the preparation prior to injection of the full dose; however, the absence of a reaction to the test dose does not preclude the possibility of reaction to the full diagnostic dose. Should the test dose produce an untoward response, the necessity for continuing the examination should be carefully re-evaluated; if deemed essential, examination should proceed with all possible caution. In rare instances, reaction to the test dose may be extremely severe; therefore, close observation and facilities for emergency treatment appear indicated.

Do not exceed recommended rate of infusion. Renal toxicity has been reported in a few patients with liver dysfunction who were given oral cholecystographic agents followed by urographic agents; therefore, if known or suspected hepatic or biliary disorder exists, diagnostic infusion studies should be postponed following the recent ingestion of cholecystographic agents. The diuretic effect of the drip infusion procedure may hinder an assessment of residual urine in the bladder. Consider the functional ability of the kidneys before injecting diatrizoate meglumine. Adequate visualization may be difficult or impossible in uremic patients or others with severely impaired renal function. Contrast agents may interfere with some chemical determinations made on urine specimens; therefore, collect urine before or two or more days after administration of the contrast medium.

Usage in Pregnancy: This preparation should be used in pregnant patients only when the physician deems its use essential to the welfare of the patient since safe use during pregnancy has not been established.

ADVERSE REACTIONS: Adverse reactions accompanying I.V. use of iodine-containing contrast agents are usually mild and transient although severe and life-threatening reactions (including fatalities) have occurred. Because severe reactions to the procedure and/or to the contrast agent are possible, appropriate emergency facilities and well-trained personnel should be available and should remain available for 30 to 60 minutes following the procedure to treat the reaction since severe delayed reactions have been known to occur.

Reactions most frequently encountered with contrast agents by drip infusion are nausea and urticaria. Chills, metallic taste, vomiting, dizziness, a rise or fall in blood pressure, itching, flushing, or generalized feeling of warmth, sneezing, etc. may occur and, rarely, may be severe enough to require discontinuation of dosage. Severe reactions which may require emergency measures include cardiovascular reaction characterized by peripheral vasodilatation with hypotension and reflex tachycardia, dyspnea, confusion, and cyanosis progressing to unconsciousness. An allergic-like reaction ranging from rhinitis or angioneurotic edema to laryngeal or bronchial spasm or anaphylactoid shock may occur. Temporary renal shutdown or other nephropathy may occur. Although local tissue tolerance to diatrizoate meglumine is usually good, I.V. injection of the medium in a more concentrated formulation has produced a few instances of a burning or stinging sensation and of venospasm or venous pain.

For full prescribing information, consult package insert.

HOW SUPPLIED: Available in single-dose bottles of 300 ml.

The leader in radiologic diagnostics

SQUIBB® contrast media™

©1977 E. R. Squibb & Sons, Inc. H657-503

Significant

Continuing Medical Education Programs

for the Radiologist

on Audio Cassette!

Program 1:

"Nuclear Medicine!"

. . . with James L. Quinn, 3rd, M.D.
and George P. Backer, M.D.
5, one-hour Audio Cassettes

ONLY $35.00!

Program 2:

"New Developments in Nuclear Medicine!"

. . . a supplement to the above program.
With James L. Quinn, 3rd, M.D.
and George P. Backer, M.D.
4, one-hour Audio Cassettes

ONLY $28.00!

Program 3:

"Gastrointestinal Radiology!"

. . . with Roscoe E. Miller, M.D.
and George P. Backer, M.D.
6, one-hour Audio Cassettes

ONLY $42.00!

Program 4:

"Neuroradiology!"

. . . with Michael S. Huckman, M.D.
and George P. Backer, M.D.
6, one-hour Audio Cassettes

ONLY $42.00!

Program 5:

"Computers in Medicine!"

. . . with Laurens Ackerman, M.D., Ph.D.
and Daniel K. Harris.
6, one-hour Audio Cassettes

ONLY $42.00!

10 per cent discount on all orders over $100.00!

the institute of continuing education
Sawyer, Michigan 49125 - Phone: 616-426-3433

Please bill me for the following program(s) when shipped:

1 2 3 4 5

10 per cent discount on orders over $100.00
All orders shipped same day received, postpaid

Name _____

Address _____

City _____ State _____ Zip _____

American Journal of Roentgenology Guidelines

Address manuscripts and correspondence to the Editorial Office, 403 Pacific National Bank Building, 4545 15th Avenue N.E., Seattle, Washington 98105; telephone (206)633-2754.

Publication Policy

The Journal publishes original and timely contributions to the advancement of radiologic diagnosis and treatment. Although the content is predominantly clinical, laboratory investigations are accepted when their relevance to clinical practice is demonstrable. Authors should indicate if informed consent was obtained. Decisions on manuscripts are based on the opinions of at least two outside reviewers. Statements within an article are the responsibility of the authors and not the Journal or its publisher. Reviewers receive manuscripts without title pages to protect the identity of authors and to ensure an unbiased review; names of reviewers, in turn, are never revealed to authors.

It is understood that material submitted has not been published and is not currently submitted elsewhere. Portions of the data or illustrations from previously published works may be included if permission release forms accompany the manuscript and such material is clearly credited in the text. Prior publication of abstracts will not prejudice publication of the complete study.

Copyright Information

In accordance with Journal implementation of the new U.S. Copyright Law, authors must release first and subsidiary rights to their manuscript at submission. A dated cover letter, containing signatures of all authors, should state: "We, the authors, assign first and subsidiary rights to the American Roentgen Ray Society in the event that our manuscript (title) is published by AJR." The Journal, in turn, grants authors the right to use portions of their manuscript, without charge, in books or articles of which they are authors or editors.

Manuscript Form

Manuscripts should be typed double-spaced throughout, including references, tables, and figure legends. Tables, footnotes, and figure legends should be on separate sheets, and a separate title page should be provided. In addition to the original typewritten copy, a duplicate copy complete with figures, tables, and references is required. Authors' names should be on title page only and should not be on figures so that author anonymity can be maintained during the review process.

Figures should be submitted as 13 × 18 cm glossy prints, untrimmed and unmounted. Labels and arrows must be of professional quality and should be removable from the prints. Each figure should be numbered to correspond with figure legends, and the top should be indicated. Specific permission for publication of facial photographs of patients is required. Line illustrations and graphs should be drawn in black ink on white background.

References should be cited in the text by number (e.g., [3, 4]). The bibliography should be arranged in the numerical order that references are cited in the text and typed double-spaced throughout. Data for each reference should be arranged according to the uniform style on bibliographic citations adopted by many biomedical journals. Provide all authors' names and inclusive pages. Abbreviations for titles of medical periodicals should conform to those published in *Index Medicus*. Examples:

1. Miller RE, Chernish SM, Skucas J, Rosenak BD, Rodda BE: Hypotonic roentgenography with glucagon. *Am J Roentgenol* 121:264–274, 1974
2. Boijsen E: Superior mesenteric angiography, in *Angiography*, edited by Abrams H, Boston, Little, Brown, 1971, pp 1091–1119

Organization

Title page. Titles should be brief and specific. Include addresses for each author and acknowledgment of grant support when appropriate.

Abstract. A description of the purpose, methods, results and conclusions of the study is required.

Introduction. Clearly state the purpose of the investigation including necessary background facts.

Materials and methods. Decribe the protocol clearly. Use standard abbreviations as presented in the *Council of Biology Editors Style Manual*, 3d ed. Metric measurements should be used throughout.

Results. Present results in logical sequence.

Discussion. Interpret the results to lend meaning and importance to the observations. If hypotheses and speculation are included, they must be labeled as such. When results differ from those of previous investigators, an attempt should be made to explain the discrepancy.

References. Only include references which provide adequate background and present fairly any opposing evidence and concepts. Accuracy of reference data is the responsibility of the author.

Legends. Legends should be brief but should provide sufficient description to interpret the figure.

Special Communications

Case Reports. Concise case reports are accepted if they present unusual experiences that are medically important and educational. Clarity and brevity are essential. After preliminary screening by an editor to determine whether the requirement of medical significance has been met, qualifying papers will undergo the same peer review as major papers.

Technical notes. Brief descriptions of new techniques or significant modifications of older ones which are directly applicable to clinical practice will be accepted.

Letters to the Editor. Letters are subject to editing and condensation. Criticism of published articles should be objective and constructive. Letters may also discuss matters of general interest to radiologists.

Radium-induced Malignant Tumors of the Mastoid and Paranasal Sinuses

MARGARET S. LITTMAN,[1] ISRAEL E. KIRSH, AND ALBERT T. KEANE

In the records of 5,058 persons with therapeutic or occupational exposure to radium, 21 patients with carcinoma of the mastoid and 11 with malignant tumors of the paranasal sinuses were identified. Tumor induction times were 21–50 years for mastoid tumors (median, 33) and 19–52 years for paranasal sinus tumors (median, 34). Dosimetric data are given for the patients whose body burdens of radium have been measured. We found a high proportion of mucoepidermoid carcinoma, comprising 38% of the mastoid and 36% of the paranasal sinus tumors. Three patients had antecedent bone sarcoma at 20, 11, and 5 years, respectively, and a bone sarcoma was discovered at autopsy in a fourth patient. Radiographic changes in the mastoid and paranasal sinuses were similar to those seen in nonradium malignant tumors. More than 800 known persons exposed to radium before 1930 and another group of unknown size who received radium water or injections of radium from physicians are still alive and at risk of developing malignant tumors of the mastoid and paranasal sinuses.

The incidence of malignant tumors of the mastoid and paranasal sinuses in persons with skeletal deposits of radium is far in excess of that reported for non-radium-related malignant tumors in the same sites. On the basis of the 1964 Registrar General's figures for all deaths due to carcinoma of the skull for England and Wales, Vaughan [1] estimated that, for the radium patients, the ratio of observed to expected was 100:1. In general malignant tumors of the mastoid and paranasal sinuses are uncommon, comprising about 0.2%–0.3% of all malignancies [2, 3].

From 1970 to 1977, seven mastoid carcinomas appeared among radium patients under study by the Center for Human Radiobiology, Argonne National Laboratory. The records contained 14 additional patients with mastoid carcinoma and 11 with paranasal sinus malignancies, many of whom were reported previously [4–18]. However, the aggregate of the clinical, radiologic, and pathologic features as well as dosimetric aspects of the entire series have not been reported.

The two objectives of this report are to briefly describe all the malignant tumors of the mastoid and paranasal sinuses known to have occurred to date (1978) in 5,058 radium-exposed persons and to alert physicians that a sizable number of these persons are still alive and at risk.

Subjects and Methods

The Center for Human Radiobiology, Argonne National Laboratory, has records of 5,058 persons who were occupationally or therapeutically exposed to radium. This group includes 2,036 persons who were measured for radium body content by whole body gamma ray spectrometry, radon and thoron breath samples, or by radiochemical analysis of bone specimens; 1,526 persons who were located but not measured; and 1,496 persons who were not located. In all but five patients in this report the radium body burden has been measured (tables 1 and 2).

For the 21 cases of mastoid carcinoma, proof of neoplasm was provided by histopathologic tissue slides for 14 cases, copies of surgical pathology reports for four cases, hospital records for one case, and previously published case reports which contained the histologic diagnosis and autopsy reports for two cases. For the 11 cases of paranasal sinus tumors, proof of neoplasm was provided by histopathologic tissue slides for six cases, copies of surgical pathology reports for two cases, hospital records for one case, and previously published case reports for two cases.

Exposure History

Radium acquisition occurred in three ways. One was in the luminous watch-dial industry where dial painters pointed the brush between their lips, thereby ingesting radioactive material. The radium content of the luminous paint mixture varied from about 5–100 μCi/g. The second was during the treatment of various medical problems; patients received intravenous injections of radium or drank radium water. Each injection usually contained 10 μCi of radium; a full course may have consisted of several tenths of a millicurie. The third was in the industrial and research processing of radium and involved chemists, physicists, and laboratory workers.

Dosimetry

The estimates of body content of radium (^{226}Ra) and the ratios of mesothorium (^{228}Ra) to radium body content listed in tables 1 and 2 were determined by one or more of the following methods: whole-body γ-ray spectrometry in vivo; measurement of radon (^{222}Rn) and thoron (^{220}Rn) in samples of breath; γ-ray spectrometry on large amounts of bone; and radiochemical analysis of small sections of bone or of teeth. The methods of measurement and the statistical error associated with each are reported elsewhere [19].

The values of intake listed in tables 1 and 2 were calculated from the measured body content using the expression of Norris et al. [20] ($0.54t^{-0.52}$) for biologic retention of radium as a function of time following a single injection. When radium and mesothorium entered the blood over an extended period of time the intake rate was assumed constant over this period, and an average value of fractional retention was calculated. When body content of radium and mesothorium was measured after death or was estimated from the measurement of an amputation specimen, the ^{226}Ra value was taken as the body content at the time of death or amputation. The corresponding ^{228}Ra value was corrected for radioactive decay between time of

Received October 12, 1977; accepted after revision July 19, 1978.
This work was supported by the United States Energy Research and Development Administration.
[1] Center for Human Radiobiology, Argonne National Laboratory, Argonne, Illinois 60439. Address reprint requests to M. S. Littman.

 0361–803X/78/1100–0773 $00.00

LIBRARY U. S. NAVAL

TABLE 1

Exposure Data for Cases of Mastoid Carcinoma

Case No.	Exposure		Year Last Measured	Body Content*		Calculated Dose Values			
	Type and Year	Age (years) and Sex		^{226}Ra (μCi)	Ratio of ^{228}Ra to ^{226}Ra (μCi/μCi)	Intake ^{226}Ra (μCi)	Intake ^{228}Ra (μCi)	Skeletal Dose†	
								^{226}Ra (rad)	^{228}Ra (rad)
01-014	DP, 1916	15,F	1968	2.24	0.00036	536	89.0	5,471	1,328
01-022	DP, 1917	17,F	1968	0.60	0.0	147	0	1,544	0
01-087	DP, 1921	16,F	1964	0.78	0.0369	213	1,060	2,260	15,860
01-587	DP, 1919	25,F	NM	. . .	. . .	. . .	. . .	. . .	. . .
03-101	P, 1931	22,F	1963	1.58	0.0	380	0	4,448	0
03-141	P, 1933	27,M	1962	0.96	0.0	220	0	1,550	0
03-206	P, 1936	22,M	1973	3.30	0.0	858	0	7,056	0
03-214	P, 1925	30,F	1964	1.38	0.0	370	0	3,964	0
03-232	P/O, 1917	19,F	1956	4.70	0.0	1,260	0	14,736	0
03-240	O, 1930	13,F	1973	4.32	0.0	917	0	7,655	0
03-402	DP, 1923	18,F	1974	1.22	0.00010	370	14.7	4,376	220
03-407	DP, 1923	18,F	1958	1.54	0.00022	382	4.90	4,132	73
03-423	DP, 1923	16,F	1962	0.59	0.0	155	0	2,036	0
03-429	DP, 1923	15,F	1974	1.17	0.0	354	0	4,783	0
03-488	DP, 1922	15,F	1958	0.17	0.0	43.5	0	605	0
03-648	DP, 1922	18,F	1956	5.00	0.00430	1,220	271	12,420	4,043
03-676	DP, 1924	27,F	1963	1.70	0.0	455	0	6,433	0
03-760	DP, 1924	17,F	NM	. . .	. . .	. . .	. . .	. . .	. . .
03-772	DP, 1922	18,F	NM	. . .	. . .	. . .	. . .	. . .	. . .
03-785	DP, 1925	22,F	NM	. . .	. . .	. . .	. . .	. . .	. . .
05-284	DP, 1919	20,F	1969	0.22	0.00080	65.3	18.9	894	284

Note.—DP = dial painter, P = parenteral, O = oral, P/O = parenteral or oral, NM = not measured.
* At time of measurement.
† To year of diagnosis.

TABLE 2

Exposure Data for Cases of Paranasal Sinus Malignant Tumors

Case No.	Exposure		Year Last Measured	Body Content*		Calculated Dose Values			
	Type and Year	Age (years) and Sex		^{226}Ra (μCi)	Ratio of ^{228}Ra to ^{226}Ra (μCi/μCi)	Intake ^{226}Ra (μCi)	Intake ^{228}Ra (μCi)	Skeletal Dose†	
								^{226}Ra (rad)	^{228}Ra (rad)
01-006	DP, 1919	19,F	1970	3.59	0.00144	612	314	4,144	4,361
01-008	DP, 1917	17,F	1960	6.00	0.00067	1,630	186	19,519	2,790
01-145	DP, 1918	17,F	1966	6.33	0.00077	1,680	413	19,506	6,195
01-149	DP, 1919	31,F	1969	1.63	0.00533	440	995	5,140	14,927
01-171	P/O, 1914	19,M	1958	1.50	0.0	427	0	4,311	0
01-179	P/O, 1924	34,F	1959	2.00	0.0	502	0	6,019	0
01-573	DP, 1916	24,F	1970	0.67	0.00195	145	135	1,307	2,000
03-105	P, 1931	27,M	1951	2.60	0.0	490	0	3,143	0
03-126	P, 1931	21,F	1965	1.30	0.0	323	0	3,449	0
03-235	P, 1928	28,F	1965	1.29	0.0	336	0	3,803	0
03-675	DP, 1922	26,F	NM	. . .	. . .	. . .	. . .	. . .	. . .

Note.—DP = dial painter, P = parenteral, O = oral, P/O = parenteral or oral, NM = not measured.
* At time of measurement.
† To year of diagnosis.

death or amputation and time of measurement, using a value of 0.00033 day^{-1} for the radioactive decay constant of ^{228}Ra (half period 5.7 years).

The skeletal α-particle doses listed in tables 1 and 2 were calculated from the intake values, the time integrals of the various retention functions, and the α-energetics of the decay schemes. It was assumed that virtually all radioactive decay in the body occurred in the skeleton (7,000 g mass for male skeleton without marrow, and 5,000 g mass for female skeleton without marrow). The calculations of intake and of skeletal α-particle dose were carried out with the aid of a computer program written by Neal [21], who also developed the computational methods employed.

The lowest skeletal dose associated with a sinus or mastoid malignancy was 605 rad (case 03-488). Sinus or mastoid cancers have appeared in 27 of 250 measured persons with skeletal dose above 500 rad. One of 50 persons with skeletal dose between 500 and 1,000 rad developed a sinus or mastoid cancer. In 200 persons with skeletal dose above 1,000 rad, the frequency of these cancers was relatively constant with dose and averaged 13%.

Virtually all the α-particle energy released in the skeleton is probably absorbed in bone tissue (i.e., virtually all radon not exhaled decays at or near its site of production in mineral bone). A 7 kg skeleton has about 2 kg cartilage and periarticular tissue and 5 kg bone tissue. Therefore, the α-particle dose to

bone tissue is 7/5 skeletal dose. Bone dose is relevant to the dosimetry of endosteal cells, believed to be the cells of origin of bone sarcomas, and to the dosimetry of the sinus and mastoid epithelium. For bone uniformly labeled with an α-particle emitter, the dose to tissues within α-particle range of bone surface is directly proportional to bone dose.

We have not attempted to estimate doses to the sinus and mastoid mucosa of individual radium cases for lack of knowledge of the microdistribution of radioactivity in subjacent bone and mucous membrane, the radon content of sinus air, and the location of target cells in relation to these sources of radioactivity. An additional factor has been the observation that in some cases ^{226}Ra and ^{222}Rn concentrations were up to 50 times the uniform label. However, some generalizations can be made. The average dose to the mucous membrane of the sinuses and mastoid air cells lying within 50 μm of bone surface, due to α particles originating in uniformly labeled subjacent bone, is estimated to be 17% of the ^{226}Ra bone dose and 21% of the ^{228}Ra bone dose, or 24% and 29%, respectively, of the ^{226}Ra and ^{228}Ra skeletal doses (see Appendix).

Radon (^{222}Rn), the gaseous decay product of ^{226}Ra, collecting in poorly ventilated sinus and mastoid cavities, is potentially an additional contributor to epithelial α-particle dose. Postmortem measurements of the radon concentration in air samples of the sinuses and mastoids of several radium cases suggest that the sinuses are sometimes poorly ventilated. Many of the observed radon concentrations in sinus air greatly exceeded the estimated radon concentrations in lung air before death. In one case an in vivo air sample showed a radon concentration 40 times that of the exhaled air. For a well ventilated sinus with a radon concentration equal to that of exhaled air, the α-particle dose to tissues within 50 μm of the air-tissue interface would be about 0.5% of the integral dose to bone from the α particles of the ^{226}Ra series.

Radon in cavity air may be the important source of α-particle dose to the epithelium of the relatively thick mucous membrane of the paranasal sinuses, because the average distance from bone to the epithelial lining is considerably greater than the 50 μm range of the α particles. Radon may be relatively less important in the dosimetry of the mastoid air cells because the epithelium is probably well within range of the α particles originating in bone, and because the air cells are relatively small. A review of pertinent observations reported in the literature and a discussion of their implications for sinus dosimetry are presented in full in the Appendix.

Findings

Clinical Data

There were 28 females and four males in our series of radium-induced cancers. Most of the cases were women employed in the dial-painting industry, and this fact is evident in the high female to male ratio. The four males received radium therapeutically for medical and mental problems.

Carcinoma of the left mastoid was twice as frequent as that of the right. The most frequent clinical findings included blocked ear or discharge, a periauricular mass, and pain (table 3). Tumor induction time, defined as the interval from the first exposure to radium to the first symptom or clinical sign of tumor, ranged from 21 to 50 years (median, 33 years). Two of the 21 patients (01-087 and 03-402) are alive 21 years and 14 years, respectively, following surgical treatment and radiotherapy. Both are free of tumor. Mean survival time from surgical resection to death was 2 years. Of the 19 patients who died, 16 died of their disease, and the remaining three patients died of arteriosclerotic heart disease, chronic brain syndrome, and brain abscess, respectively.

TABLE 3

Clinical Symptoms of Mastoid and Paranasal Sinus Malignant Tumors

Clinical Findings	Mastoid Cases	Paranasal Sinus Cases
Blocked ear or discharge	12	3
Periauricular mass	11	1
Pain	10	6
Hearing loss	8	4
Headache	6	0
Tinnitus	6	1
Cranial nerve palsy	6*	4†
Mass	5‡	2§
Mastoiditis	4	0
Nasal discharge	0	4
Sinusitis (excluding mastoid)	0	2
Ocular	1	10

* Facial.
† Mixed.
‡ Ear canal.
§ One nasal cavity and one ethmoid sinus.

The distribution of the 11 malignant tumors of the paranasal sinuses was as follows: five in the sphenoid, two in the ethmoid, one in the frontal, one in the maxillary, and two in the ethmoid or sphenoid sinuses. Infection, soreness, or pain in the eyes, diplopia, blurred vision, and blindness occurred most frequently (table 3). Tumor induction time ranged from 19 to 52 years (median, 34 years). Mean survival time from surgical resection to death was 2 years. All patients died, ten from their disease and one from a dissecting aortic aneurysm. In the latter patient (01-171) the frontal sinus was free of the tumor resected 9 years before death.

Radiology

Radiographs and/or radiologic reports were available for 13 mastoid and 10 paranasal sinus malignancies. The most reliable radiographic finding in this series was destruction of the bony walls of the mastoid or paranasal sinus. This was present in every mastoid carcinoma and all but one of the paranasal sinus tumors, and often extended into adjacent bones (figs. 1–4). A less frequent alteration consisted of replacement of air by a water-dense tumor mass (figs. 4 and 5). Bony sclerosis of the walls was observed in two sphenoid sinus carcinomas but was not seen in the mastoid carcinomas. A unique finding in one case of sphenoid sinus carcinoma was a spontaneous pneumocephalus associated with cerebrospinal fluid rhinorrhea.

Pathology

Of the 21 mastoid carcinomas, 12 were epidermoid carcinomas, eight were mucoepidermoid carcinomas, and one was of unknown histologic type. The 11 para-

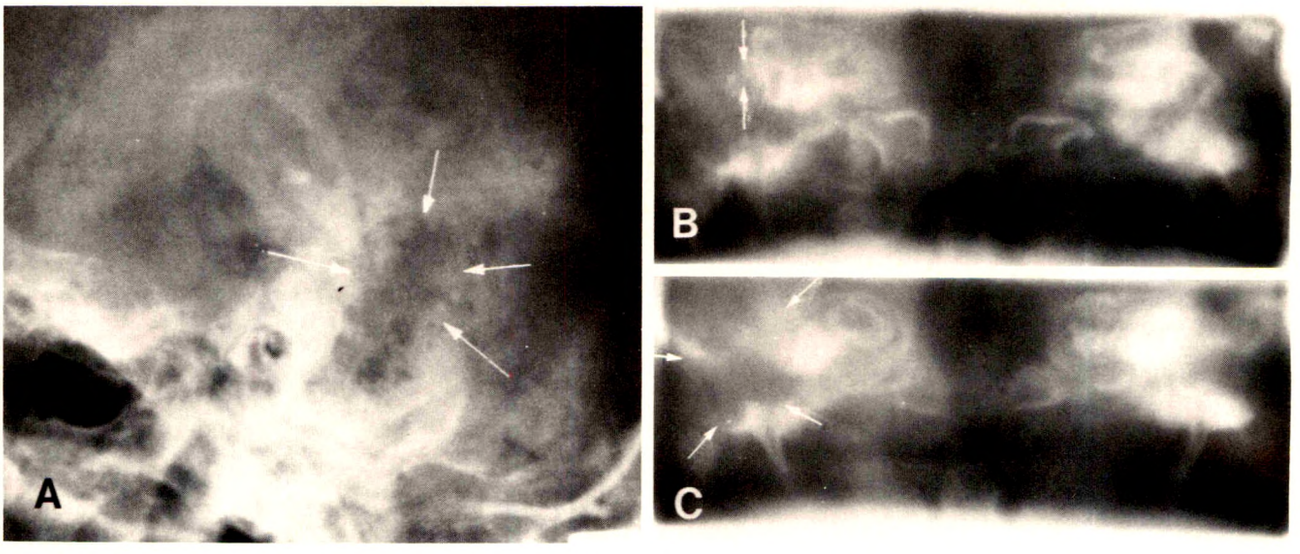

Fig. 1.—Case 03-206. Carcinoma of right mastoid. *A*, Destruction of mastoid bony septa (*arrows*). *B*, Anteroposterior tomography showing erosion of right lateral semicircular canal. *C*, Erosion of right middle ear and mastoid antrum, extending into inner ear.

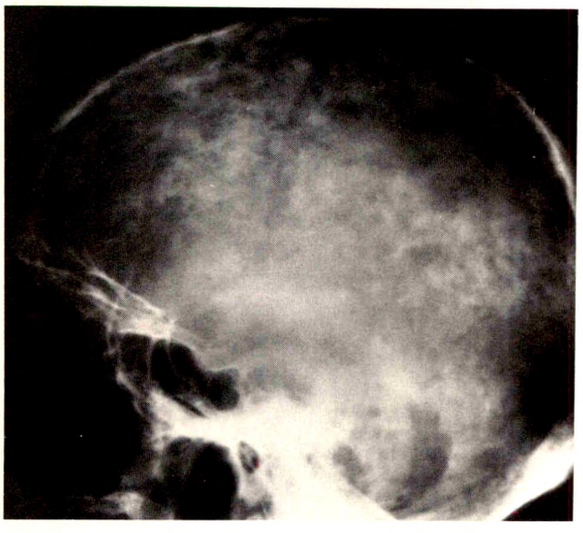

Fig. 2.—Case 05-284. Carcinoma of left mastoid. Large area of destruction extends from mastoid into occipital bone. Many small osteolytic areas in skull vault represent radium osteitis.

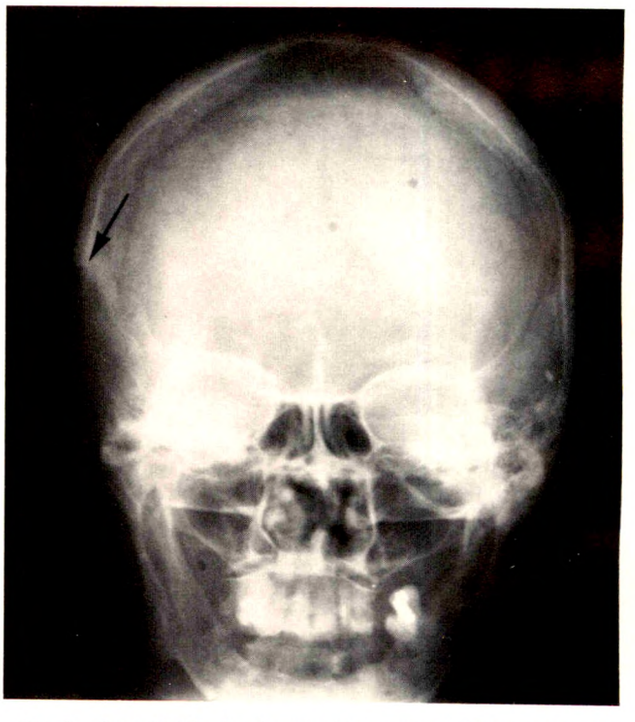

Fig. 3.—Case 03-488. Carcinoma of left mastoid. Bone destruction extends from mastoid into parietal bone (*arrow*).

nasal sinus malignancies consisted of three epidermoid carcinomas, four mucoepidermoid carcinomas, two adenocarcinomas, one rhabdomyosarcoma, and one unknown histologic type.

Epidermoid carcinoma. The epidermoid carcinomas were well or moderately differentiated (fig. 6*A*). A fibroblastic reaction and a cellular infiltrate of a few lymphocytes, plasma cells, and eosinophils were found near the advancing margins of the tumor.

Mucoepidermoid carcinoma. In common with mucoepidermoid carcinomas elsewhere in the body (salivary glands, larynx, bronchus, cervix, etc.), mucin-producing cells, epidermoid cells, and intermediate or basal cells were represented. Glands were the predominant component (fig. 6*B*), and the presence of cysts varied. In two cases the glands were small and compressed by dense fibrous tissue. They were lined by cuboidal cells with dark, irregular, pleomorphic nuclei with distinct nucleoli. Mitoses were infrequent. In the rest of the tumors the glands were moderate in size or large, or a combination,

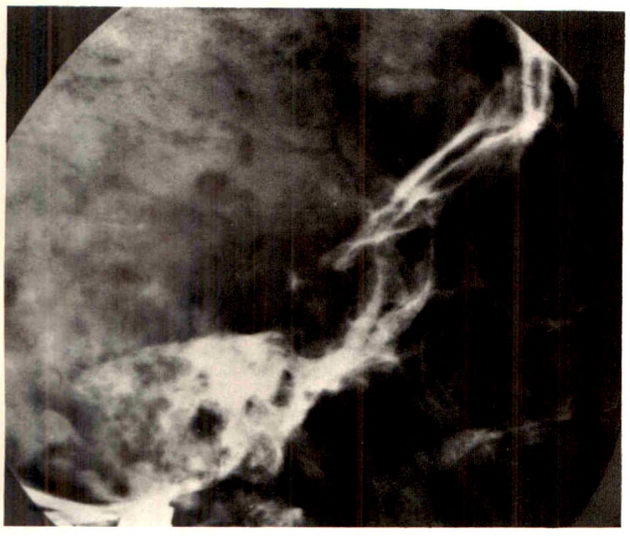

Fig. 4.—Case 01-149. Carcinoma of sphenoid sinus. There is destruction of dorsum and floor of sella. Sphenoid sinus is partly opacified.

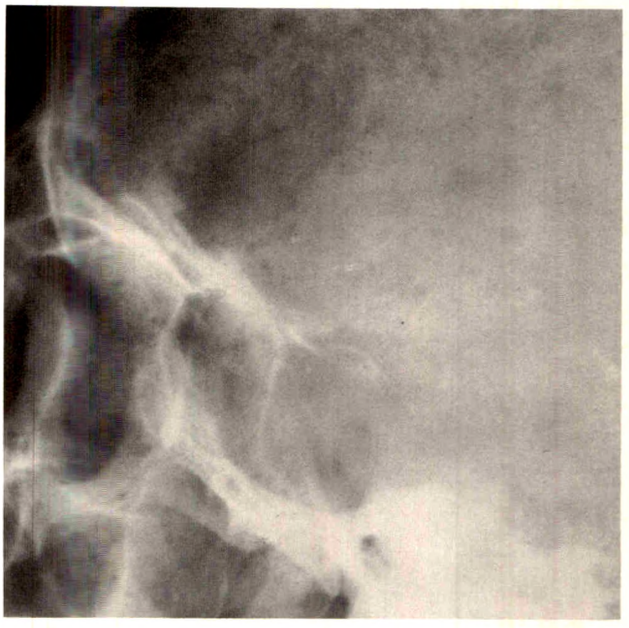

Fig. 5.—Case 03-105. Carcinoma of sphenoid sinus. Tumor density replaces air in sphenoid sinus. Dorsum sellae is destroyed.

occasionally cystic, and lined by single or multilayered columnar cells. Occasional papillary formations were present. Nuclei were vesicular, and nucleoli were large (fig. 6*C*). Mitoses were moderate in number. Intracytoplasmic and intraglandular mucin was positive with PAS and mucicarmine stains. Signet-ring cells were occasionally present (fig. 6*B*). Epidermoid elements were identified with difficulty. Small keratinized cells were interposed between glandular cells, or in groups of one to three cells in the stroma, or as masses of intermediate cells partly lining the glands or cysts and bulging into the lumens or into the stroma (fig. 6*D*). Solid masses contained mucus-secreting cells, intermediate cells, and keratinized cells. Pearl formation, though infrequent, was seen. Basal cells were not conspicuous. In one case, groups of large "balloon" keratinized cells (fig. 6*D*) were most frequently seen around necrotic bone.

Adenocarcinoma. Only one histologic slide was available for review (case 01-145). There were several small glands, sheets of cells, and one papillary tuft. The cells were large with vacuolated cytoplasm and large vesicular nuclei. Mucicarmine stains were positive for mucin.

Rhabdomyosarcoma. We could not obtain tissue slides of this tumor (case 03-675). However, the surgical pathology report and three consultation reports were available. The microscopic description was that of a densely cellular tumor containing fusiform cells, "strap" cells, and multinucleated pleomorphic cells; cross-striations were seen. A diagnosis of rhabdomyosarcoma was made by three pathologists. One pathologist considered it a liposarcoma.

Autopsy Findings

Autopsies were performed on nine patients with mastoid carcinoma and on seven with paranasal sinus malignancy. Intracranial extension of the neoplasm was observed in eight of the mastoid and in six of the paranasal sinus tumors, and was listed as the cause of death in five additional mastoid and three paranasal sinus tumors, either on the death certificate or by the attending physician. Extracranial metastases (lungs, liver, thyroid, cervical and peribronchial lymph nodes, spinal cord, heart, skin of chest, cervical and thoracic vertebrae, femur, and pelvis) were found in one case of epidermoid carcinoma of the mastoid and in three cases of mucoepidermoid carcinoma of the mastoid, in one case of mucoepidermoid carcinoma of the sphenoid sinus, and in one case of rhabdomyosarcoma of the maxillary sinus.

Illustrative Case Reports

Case 03-206

At age 22 years (1936), this white male received an estimated 860 μCi of radium intravenously over a 1 month period for gonococcal urethritis and arthritis. At age 28 a left mastoidectomy for chronic mastoiditis was done. Radium necrosis of the skeleton was noted for the first time at age 41. During the next 4 years he had spontaneous fractures of both femurs, the right humerus, and of many ribs. At age 59 he was seen at our institution because of severe headaches on the right side. Skull radiographs revealed destruction of the septa of the right mastoid; carcinoma was suspected (fig. 1).

Surgical exploration 6 months later revealed a large tumor that filled the right mastoid air cells and antrum and invaded the temporal bone. Frozen section diagnosis was squamous cell carcinoma. The bulk of this tumor was curretted, and postoperative radiation was given. He developed increasing pain at the tumor site, disorientation, and died 10 months after surgery. Autopsy revealed a mucoepidermoid carcinoma of the right mastoid air spaces, antrum, and temporal and occipital bones, and acute suppurative meningoencephalitis.

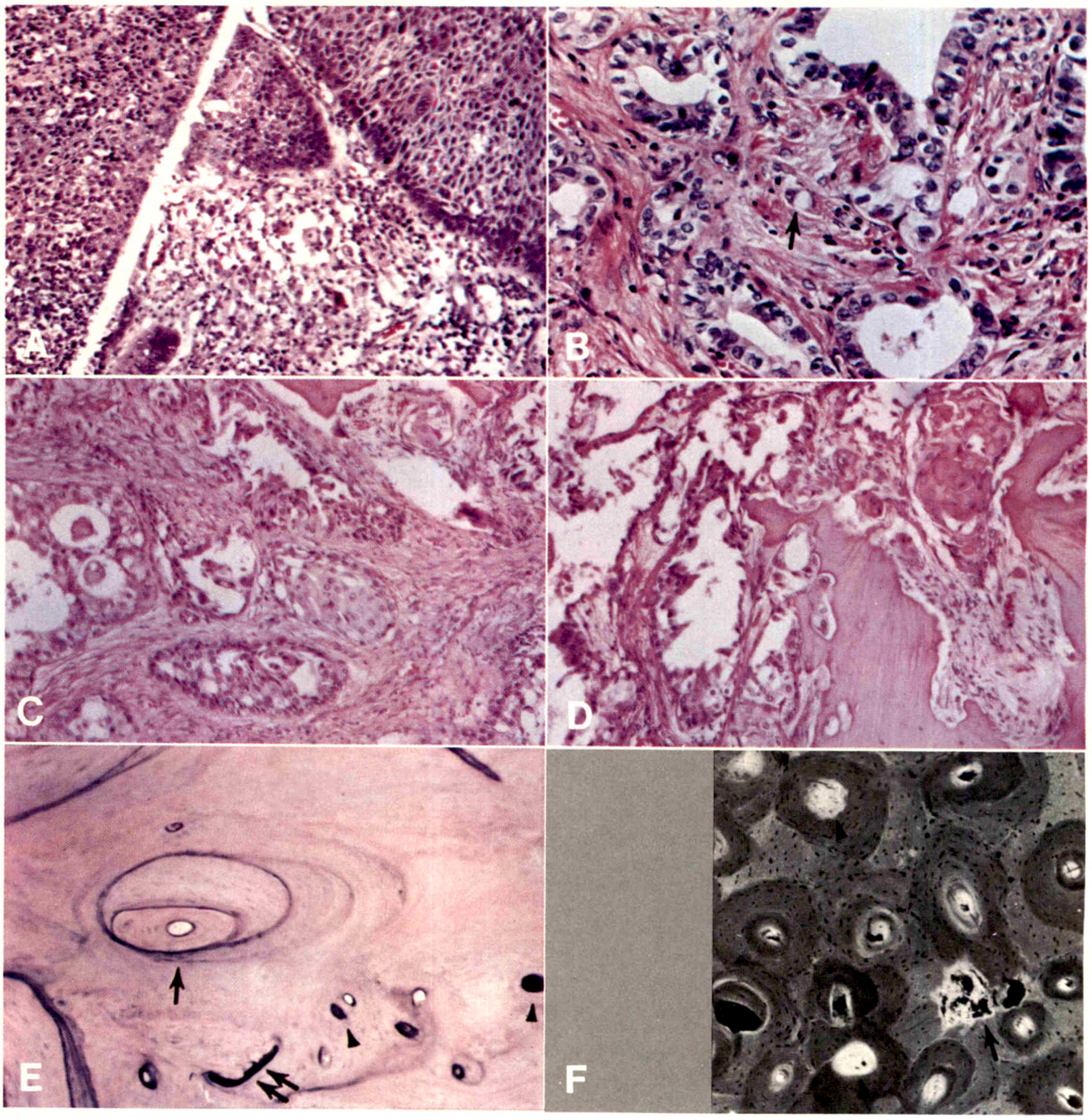

Fig. 6.—Histology (H and E stain; A–D, ×125; *E*, ×63). *A*, Moderately differentiated epidermoid carcinoma of left mastoid. Case 03-676. *B*, Mucoepidermoid carcinoma of left mastoid. Field contains glands only. Signet-ring cell is in center of field (*arrow*). Case 05-284. *C*, Mucoepidermoid carcinoma of right mastoid. Moderately sized glands with occasional papillary tufts lie below necrotic bone. Basal and intermediate cells line some glands. Case 03-407. *D*, Mucoepidermoid carcinoma of right mastoid. Keratinized ballooned cells form large groups in and near glands and bone. Case 03-407. *E*, Radiation osteitis of left mastoid bone adjacent to mucoepidermoid carcinoma. Large osteon contains three arrested growth rings with hypermineralization (*single arrow*). Solid dark and round Haversian canals (*arrowheads*) and one Hering's canal (*double arrows*) are occluded by sclerotic bone, so-called "plugs." Case 03-423. and *F*, Microradiograph of long bone with radiation osteitis. Note resorption cyst (*arrow*). White areas indicate sclerotic plugs in Haversian canals (*arrowheads*).

Case 03-488

This white female watch dial painter worked from 1922 to 1923, beginning at age 15 years, and pointed the brush in her mouth. Skull radiographs at age 52 revealed many small areas of radium necrosis; dental films showed destructive changes in the dentin. At age 66 she entered the hospital because of a painless hard retroauricular mass, and fullness and tinnitus in the left ear. Physical examination revealed left ptosis and exophthalmos, and a hard 3.0 cm mass over the left mastoid bone. Skull radiographs revealed a lytic lesion of the petrosal portion of the left temporal bone extending to the parietal and occipital bones (fig. 3). An arteriogram revealed hypervascular soft tissue masses in the areas of bone destruction and a parasagittal mass.

Surgical exploration disclosed a large tumor involving the temporal bone. Frozen section diagnosis was metastatic adenocarcinoma. However, mucoepidermoid carcinoma was diagnosed on the permanent sections. A large portion of the tumor and temporal bone were resected. Postoperatively she received radiation therapy; she expired 2 years after surgery. Autopsy revealed mucoepidermoid carcinoma of the left mastoid invading the left temporal bone, middle cranial fossa, posterior auricular area, and scalp with metastases to the left lung and heart, and an independent parasagittal meningioma with focal sarcomatous degeneration.

Discussion

Dosimetry

Loutit et al. [22] suggested that cells with the highest proliferative potential were at risk for tumor induction by α-particle radiation from radium. In bone these are the endosteal preosteoblasts or osteoprogenitor cells, and in the air sinuses, unique anatomically because of the close proximity of mucosa to bone, the mucosal stem cells.

Ash and Raum [23] noted that the mucoperiosteum of the paranasal sinuses consisted of mucosal cells and two layers of connective tissue, a loose subepithelial and a compact periosteal layer fixed to bone. They listed normal variations of thickness for the mucous membrane of the paranasal sinuses as 300–1,000 μm for the medial wall and 100–500 μm for the lateral wall of the maxillary sinus, 70–300 μm for the frontal sinus, 80–400 μm for the ethmoid sinus, and 70–500 μm for the sphenoid sinus. For α particles of the ^{226}Ra and ^{228}Ra series, the weighted mean ranges in tissue are about 40 μm and 50 μm, respectively. If the dimensions of the sinus walls [23] are applicable to the radium cases, it would appear that only a relatively sparse population of epithelial cells in the submucosal glands of the paranasal sinuses would receive a significant dose from α particles originating in bone.

Observations and theoretical considerations strongly suggest that radon in the air of sinuses may be an important or perhaps a major factor in the induction of paranasal sinus malignancies in the radium cases. Given the relatively thick paranasal sinus mucosa, we suspect that radium-induced carcinomas probably begin primarily in the mucosa of poorly ventilated sinuses. If a radium-induced carcinoma had arisen in a well ventilated sinus, it would probably have had its origin in the submucosal glands.

On the other hand, the epithelium of the mastoid air cavities is probably sufficiently close to bone to receive an oncogenic dose from radioactivity deposited in bone at the levels found in the cases of this study. Measurements of mastoid mucosal thickness were not available. In case 03-423 the mean bone-to-mucosa thickness of the mastoid air cells, measured with calibrated optics and a 10 power objective lens, was 17 μm. Thus the simple squamous and cuboidal mastoid mucosal cells are within α-particle range of bone.

While the epithelial layer of the paranasal sinuses lies within the range of β particles emitted by radon daughter products in surrounding bone, the β-particle dose would be low (β-particle dose to bone is about 3% of α-particle dose to bone for the radium cases) and would be expected to be less effective than α-particle dose, rad for rad, in inducing tumors.

Several studies are in progress at our institution to improve the microdosimetry of the sinus epithelium so that estimates of risk for mastoid and paranasal sinus malignancies derived from the radium studies can be applied to other bone-seeking α-particle emitters.

Frequency of Mucoepidermoid Carcinoma

The proportion of mucoepidermoid carcinoma in our series was unusually high: 38% of the mastoid carcinomas and 36% of the paranasal sinus tumors. In the reported series of mastoid carcinomas not associated with radium exposure [24–26], mucoepidermoid carcinoma was not mentioned. Buchanan and Slavin [27] found one mucoepidermoid carcinoma in their report of 58 tumors of the nose and paranasal sinuses, while other authors [28–30] did not report any cases. Our study suggests a relationship between α-particle radiation and mucoepidermoid carcinoma.

In identifying mucoepidermoid carcinoma we used the criteria and classification of Healey et al. [31]. Most of our tumors corresponded to their grade II or poorly differentiated mucoepidermoid carcinomas and behaved clinically like aggressive tumors with intracranial extension in all but one of the mastoid carcinomas and in all of the paranasal sinus carcinomas. Extracranial metastases occurred in three mucoepidermoid carcinomas of the mastoid and in one of the sphenoid sinus, as well as in one epidermoid carcinoma of the mastoid and the rhabdomyosarcoma of the maxillary sinus.

Whether the single rhabdomyosarcoma of the maxillary sinus is related to α-particle radiation or whether it represents a spontaneous tumor cannot be answered at this time. Rhabdomyosarcoma of the paranasal sinuses is a rare tumor. Ringertz [30] did not report any cases in his personal series of 391 cases, though he referred to four cases reported by other authors. That it was the only malignancy to involve the maxillary sinus also favors a spontaneous origin.

In three patients with mastoid carcinoma, bone sarcomas also occurred. In two patients, a fibrosarcoma of the

femur and an osteosarcoma of the metacarpal were resected 11 and 5 years, respectively, before the appearance of the mastoid carcinoma; a third patient was found to have fibrosarcoma of the femur and ischium at autopsy. In one patient with sphenoid sinus carcinoma, an osteosarcoma of the tibia was resected 20 years previously.

An extensive literature exists on the pathologic effects of radium on bone [4, 10, 12, 22, 32, 33]. The following changes have been recorded. First, radiation osteitis which includes necrosis, sclerosis, occlusion of the Haversian canals, and replacement of resorbed bone by atypical fibrous tissue (figs. 6*E* and 6*F*); sequelae include pathologic fractures and bone deformities, loss of teeth, and osteomyelitis. Second, osteosarcomas and fibrosarcomas of bone have developed.

Radiography

The radiographic changes observed in our series of mastoid and paranasal sinus tumors were similar to those seen in non-radium-related tumors and consisted of destruction of the bony walls, extension to and destruction of adjacent bones, and replacement of air by a water-dense tumor mass. Bony sclerosis was not noted in any mastoid carcinoma cases and was infrequent in the paranasal sinus series. Correlation of these findings with the presence of radium osteitis of the skeleton and with a history of radium exposure would assist in diagnosis. Radiologists unfamiliar with radium osteitis of the cranium have confused its lesions with those of multiple myeloma, metastatic carcinoma, and malignant lymphoma for which the patients were studied intensively.

Patients Still at Risk

Physicians should be aware that more than 800 persons known to have been exposed to radium before 1930 are still alive, some of whom are at risk of developing malignant tumors of the paranasal sinuses and mastoid air cells. They are mostly in their late sixties and older. Of all exposed persons known to be alive, more than one-half live in Connecticut, Massachusetts, New Jersey, New York, or Pennsylvania; about one-fourth live in Illinois and about one-fifth elsewhere in the United States. Of the last group, about one-third live in California or Florida. A small number live in Canada and elsewhere outside the United States. In addition, many persons who were treated by physicians with injections of radium or with radium water are unknown to us. Based on published reports and on interviews with physicians, these persons probably number in the thousands, and many of them may still be alive and at risk.

APPENDIX

Calculation of Dose Rate in Sinus Tissues

The behavior of α particle dose rate with depth in a layer of soft tissue adjoining a uniformly radioactive plane surface (plane interface geometry) was analyzed by Munson [34] and later by Mays [35], employing the assumption that the rate of energy loss dE/dr (LET, linear energy transfer) of α particles of initial energy E and range R has the constant value E/R over the range. The basic derived result, for the dose rate Q (energy/sec-g) in soft tissue of density ρ at a distance x from a plane surface deposit of an α-particle emitter with a disintegration rate N sec^{-1} per unit area, is

$$Q(x, E_0) = \frac{NE_0}{2R\rho} \ln\left(\frac{R}{x}\right), \qquad x \le R, \tag{1}$$

where E_0 is the initial energy of the α particles and R is the range of the α particles in soft tissue.

From equation (1), Mays [36] derived an expression for the dose rate in soft tissue at a distance x from the surface of a layer (e.g., of bone or air) of thickness d containing a uniform concentration of an α-particle emitter with a disintegration rate N sec^{-1} per unit volume:

$$Q(x, x', E_0) = \frac{NE_0R'}{2R\rho}\left(\frac{x'}{R'} - \left(\frac{x}{R} + \frac{x'}{R'}\right)\ln\left(\frac{x}{R} + \frac{x'}{R'}\right) + \frac{x}{R}\ln\frac{x}{R}\right), \qquad x' \le R', x \le R(1 - x'/R'), \tag{2}$$

where R' is the range of the α particles in the radioactive layer, and x' is the maximum depth in the radioactive layer from which α particles can just reach the soft tissue (i.e., R') or the thickness d of the radioactive layer, whichever is smaller. Under the constant LET assumption, a distance x' in the radioactive layer is equivalent to a distance (Rx'/R') in soft tissue. Equation (2) thus holds for $(x/R + x'/R') \le 1$.

For values of x between $R(1 - x'/R')$ and R,

$$Q(x, x', E_0) = \frac{NE_0R'}{2R\rho}\left(1 - \frac{x}{R} + \frac{x}{R}\ln\frac{x}{R}\right), \qquad R \ge x \ge R\left(1 - \frac{x'}{R'}\right). \tag{3}$$

Note that equation (3) holds for $R \ge x \ge 0$ when the thickness of the radioactive layer is $\ge R'$ [34, 36–38].

The average dose rate $\bar{Q}$ in soft tissue over a distance x from the surface of the radioactive layer, obtained by integration of equation (2) between the limits 0 and x and division by x, is

$$\bar{Q}(x, x', E_0) = \frac{NE_0R'}{2R\rho}\left(\frac{x'}{R'} + \frac{R}{2x}\left\{\left(\frac{x}{R} + \frac{x'}{R'}\right)^2\left[\frac{1}{2} - \ln\left(\frac{x}{R} + \frac{x'}{R'}\right)\right] - \left(\frac{x}{R}\right)^2\left(\frac{1}{2} - \ln\frac{x}{R}\right) - \left(\frac{x'}{R'}\right)^2\left(\frac{1}{2} - \ln\frac{x'}{R'}\right)\right\}\right), \qquad x \le R(1 - x'/R'), \quad x' \le R'. \tag{4}$$

Integration of equation (3) between the limits $x_1 \ge R(1 - x'/R')$ *and* $x_2 \le R$ and division by $(x_2 - x_1)$ gives

$$\bar{Q}(x, x', E_0) = \frac{NE_0R'}{2R\rho(x_2 - x_1)}\left(x_2 - x_1 - \frac{3}{4R}(x_2^2 - x_1^2) + \frac{x_2^2}{2R}\ln\frac{x_2}{R} - \frac{x_1^2}{2R}\ln\frac{x_1}{R}\right), \qquad R \ge x_2 > x_1 \ge R(1 - x'/R'), \quad x' \le R'. \tag{5}$$

Dose to Sinus Tissues from Radioactivity in Bone

In order to estimate doses to sinus tissues from radioactivity in bone for the cases of this study, average relative disintegration rates were calculated for ^{226}Ra and ^{222}Rn and its decay

products from values of the time integrals of the functions of Norris et al. [20] for retention of ^{226}Ra ($0.54t^{-0.52}$) and ^{222}Rn ($0.021t^{-0.28}$) for a mean tumor induction time of 12,800 days. The α particle emitters of the ^{228}Ra series were assumed to have equal disintegration rates, except that the branching ratios of 0.64 and 0.36 were used as relative disintegration rates for ^{212}Po and ^{212}Bi. The relative disintegration rates for the α emitters of the ^{226}Ra series would not have varied appreciably from the average over the range of tumor appearance times found in this study, so that calculated average values of soft-tissue dose rate relative to bone dose rate are good approximations of average integral soft-tissue dose relative to integral bone dose.

Mays and Sears [39] calculated the ranges in bone and in water from ranges in air of the α particles of the ^{226}Ra and ^{228}Ra series, using the Bragg-Kleeman relationship:

$$R = 3.2 \times 10^{-4} \cdot \frac{\sqrt{A}}{\rho} \cdot R_{air}$$

where A is the effective atomic weight and ρ the density of the material, and R_{air} is the α particle range in air (A = 14.6, ρ = 0.001226 g/cm^3). Mays and Sears [39] used A values of 9.00 and 17.9, and ρ values of 1.0 and 2.0 g/cm^3 for water and bone, respectively. Values of R_{air} were based on the data of Bethe and Ashkin [40].

The average relative disintegration rates and α-particle energies and ranges in bone, water, and air of the α-particle emitters of the two radium series are given in table A1.

The average dose rate in the mucous membranes of the air sinuses over a distance x from the surface of underlying bone is given by equation (5). For a thick layer of uniformly radioactive bone, the maximum depth x' from which α particles can just reach the surface is R', the α-particle range in bone. Therefore, the minimum value x_1 in equation (5) is reduced to zero, and

$$\bar{Q}(x,E_0) = \frac{NE_0R'}{2R\rho}\left(1 - \frac{3x}{4R} + \frac{x}{2R}\ln\frac{x}{R}\right), \quad x \le R. \tag{6}$$

This equation was given by Mays and Sears [39] and also by Spiers [38].

The dose rate (energy/sec-g) in bone is given by NE_0/ρ', where ρ' = 2g/cm^3. Therefore, the average dose rate in the mucous membranes over a distance x from the bone surface, relative to the bone dose rate Q_{bone}, is

$$\frac{\bar{Q}(x,E_0)}{Q_{bone}} = \frac{R'}{R}\left(1 - \frac{3x}{4R} + \frac{x}{2R}\ln\frac{x}{R}\right), \quad x \le R. \tag{7}$$

To obtain an expression for average dose rate in soft tissue over a distance $x \ge R$ from the bone surface, $\bar{Q}(R,E_0)/Q_{bone}$ is multiplied by the dosed fraction of the soft tissue mass, R/x, to give

$$\frac{\bar{Q}(x,E_0)}{Q_{bone}} = \frac{R'}{4x}, \quad x \ge R. \tag{8}$$

Values of Q_{bone} were calculated as $fNE_0/2$ and corresponding values of $Q(x,E_0)$ and $\bar{Q}(x,E_0)$ were obtained by evaluating equations (3), (7), and (8) for several values of x for each of the nuclides in table A1. Dose rates for the individual members of each series were summed to obtain $\sum Q(x,E_0)_i$, $\sum \bar{Q}(x,E_0)_i$, and $\sum Q_{bone_i}$. These results are given in table A2.

If α particles originating in subjacent bone induce paranasal sinus malignancies, the target cells would necessarily lie within a distance not much greater than 50 μm from the bone surface. Most likely these would be the submucosal glandular cells. In the mastoid air sinuses, α particles emerging through the thinner mucosa could have sufficient range in air to impart a significant additional dose to the epithelium of the opposite wall of the air cavity.

TABLE A1

Energies and Ranges of α Particles and Average Relative Disintegration Rates in Bones of Radium Cases

Nuclide	f*	E_0 (MeV)	α-Particle Range [39]		
			Bone (μm)	Water (μm)	Air (cm)
^{226}Ra series:					
^{226}Ra	1	4.77	22.3	31.6	3.28
^{222}Rn	0.25	5.49	27.6	39.-	4.06
^{218}Po	0.25	6.00	31.7	44.8	4.66
^{214}Po	0.25	7.68	46.8	66.3	6.89
^{210}Po	0.12	5.30	26.1	36.9	3.84
^{228}Ra series:					
^{228}Ra	0	. . .	. . .	. . .	. . .
^{228}Th	1	5.40	26.9	38.-	3.96
^{224}Ra	1	5.67	29.0	41.-	4.27
^{220}Rn	1	6.28	34.0	48.-	5.00
^{216}Po	1	6.77	38.3	54.3	5.64
^{212}Bi	0.36	6.05	32.1	45.5	4.73
^{212}Po	0.64	8.78	57.9	82.-	8.53

* f = average relative disintegration rate (for ^{226}Ra series, α/dis ^{226}Ra; for ^{228}Ra series, α/dis ^{228}Th).

TABLE A2

Relative Local and Average Dose Rates in Mucous Membranes of Air Sinuses from Radioactivity in Uniformly Labeled Bone

Depth in Tissue (μm)	Relative Local Dose Rate*		Relative Average Dose Rate†	
	^{226}Ra Series (n = 5)	^{228}Ra Series (n = 6)	^{226}Ra Series (n = 5)	^{228}Ra Series (n = 6)
0	0.705	0.705	. . .	. . .
10	0.279	0.336	0.446	0.485
20	0.109	0.167	0.315	0.364
30	0.035	0.073	0.232	0.281
40	0.013	0.028	0.180	0.223
50	0.0044	0.012	0.146	0.182

* $\sum_{i=1}^{i=n} \bar{Q}(x,E_0)_i / \sum_{i=1}^{i=n} Q_{bone_i}$.

† $\sum_{i=1}^{i=n} \bar{Q}(x,E_0)_i / \sum_{i=1}^{i=n} Q_{bone_i}$.

Dose to Sinus Tissues from Radioactivity in Sinus Air

Maitland [10], Evans [41, 42] and others discussed the potential role of radon (^{222}Rn, the gaseous decay product of ^{226}Ra) and its short-lived decay products ^{218}Po and ^{214}Po on the induction of sinus and mastoid malignancies. The blood efficiently transports to the lungs radon that has escaped, by recoil and diffusion, from its site of production in mineral bone. All but a small fraction of the radon produced in bone decays either in bone or outside the body.

In the calculation of dose rates to sinus tissues from the decay of radon in sinus air, the plane-interface geometry is not quite applicable because of the shape and dimensions of the air cavities. However, as noted by Kolenkow [43], such calculations permit some useful provisional estimates of dose rate.

For the air-tissue interface dosimetry, the average dose rate $\bar{Q}(x,d,E_\alpha)$ in soft tissue over a distance x from the surface of a layer of air of thickness d with an α-disintegration rate N sec^{-1} per unit volume is calculated from equations (4) and (5).

If N is expressed in pCi per unit volume of air, $Q(x,d,E_0)$ can be converted from dose rate in energy/sec-g to dose rate in rad/day by multiplying by

$$\frac{(8.64 \times 10^4\ sec/day)\,(3.7 \times 10^4\ \alpha/sec - \mu Ci)}{(6.25 \times 10^7\ MeV/g - rad)\,(10^6\ pCi/\mu Ci)} = 5.12 \times 10^{-5}\ \frac{rad/day}{(MeV/\alpha)(pCi/g)}.$$

Values of $Q(x,d,E_0)$ and $\bar{Q}(x,d,E_0)$ for x = 20 and 50 μm and x' = d (air-layer thickness) = 0.5, 1.0, and 2.0 cm were obtained by appropriate evaluations of equations (2), (3), (4), and (5) with the values of E_0, R' (range in air), and R (range in water) for ^{222}Rn, ^{218}Po, and ^{214}Po taken from table A1. The dose rates for the three members of the ^{222}Rn series were summed and converted to rad/day for N = 1 pCi ^{222}Rn/cm^3 in sinus air to obtain values of $\sum Q(x,d,E_0)$ and $\sum \bar{Q}(x,d,E_0)$. Limits of $Q(x,d,E_0)$ as x approaches zero were obtained by evaluating equation (2) for x = 0. The results of the dose rate calculations are given in table A3.

Two problematic situations are encountered in the application of the plane interface geometry to the air-tissue dosimetry. The first relates to the estimation of the appropriate effective air-layer thickness d for a given irregularly shaped air cavity. In estimating the dose rate in the mucous membrane of a frontal sinus (case 01-171) which was roughly ellipsoidal in shape with major axes of 3, 2, and 1 cm and about 3 cm^3 in volume, Kolenkow [43] took as the air layer thickness the small dimension, 1 cm. For smaller cavities, a choice of air-layer thickness would be more arbitrary. We have not attempted to resolve this problem, but suggest that in the treatment of a more applicable geometry, the constant LET assumption probably yields sufficiently close approximations of average dose rate (as discussed below) to justify its use.

The second problem relates to the distribution of ^{218}Po and ^{214}Po, the solid daughter products of ^{222}Rn, within the air cavity. If these daughters plate out on the walls of the cavity, as might be expected, then two-thirds of the α particles would be emitted on the surface of the mucous membranes. However, we can show that knowledge of the exact distribution of radioactivity within the cavity is not of practical importance.

The dose rate in sinus tissue at a distance x from a plane surface deposit of radioactivity is obtained from equation (1).

The average dose rate over a distance x from the surface, obtained by integrating equation (1) from 0 to x and dividing by x, is

$$\bar{Q}(x,E_0) = \frac{NE_0}{2R\rho}\left(1 + \ln\frac{R}{x}\right),\ x \le R. \qquad (9)$$

The value of N sec^{-1} per cm^2 for ^{218}Po or ^{214}Po for a ^{222}Rn disintegration rate of N sec^{-1} per cm^3 in an air layer of thickness d can be calculated as

$$N(Po)sec^{-1}\ cm^{-2} = \frac{d(cm)}{2}\,N(Rn)sec^{-1}\ cm^{-3},$$

by assuming that the daughter products are deposited uniformly on the plane surfaces at the two air-tissue interfaces. In addition to the dose rates in the sinus tissue calculated from equations (1) and (9), α particles arriving at the opposite interface after traversing the air layer also contribute to the dose rate. This additional contribution, the soft-tissue dose rate at a distance $(x + d)$ from a radioactive plane buried by a thickness d of air, given by Mays [36], is

$$Q(x,d,E_0) = \frac{-NE_0}{2R\rho}\ln\left(\frac{x}{R} + \frac{d}{R'}\right),\quad x \le \left(1 - \frac{d}{R'}\right),\ d \le R', \qquad (10)$$

TABLE A3

Local and Average Dose Rates in Mucous Membranes of Air Sinuses Due to Radioactivity in Cavity Air

Depth (x) in Tissue μm	Local Dose Rate* (rad/day)			Average Dose Rate† (rad/day)		
	d = 0.5 cm	1.0 cm	2.0 cm	0.5 cm	1.0 cm	2.0 cm
→0	0.16	0.26	0.38	...	...	...
20	0.038	0.066	0.10	0.076	0.13	0.20
50	0.0035	0.0057	0.0068	0.040	0.068	0.10

Note.—Sinus air contains 1 pCi ^{222}Rn/cm^3. d = air layer thickness.

* $\sum_{i=1}^{i=3} Q(x,d,E_0)_i$.

† $\sum_{i=1}^{i=3} \bar{Q}(x,d,E_0)_i$.

where N is the disintegration rate of the α-emitter per unit area.

The average dose rate in sinus tissue over a distance x from the air-tissue interface, obtained by integrating equation (10) from 0 to x and dividing by x, is

$$\bar{Q}(x,d,E_0) = \frac{NE_0}{2x\rho}\left\{\left(\frac{x}{R} + \frac{d}{R'}\right)\left[1 - \ln\left(\frac{x}{R} + \frac{d}{R'}\right)\right] - \frac{d}{R'}\left(1 - \ln\frac{d}{R'}\right)\right\},\ x \le R(1 - d/R'). \qquad (11)$$

Equations (1), (9), (10), and (11) were evaluated to obtain dose rates from surface deposits of ^{218}Po and ^{214}Po and converted to rad/day for a concentration of 1 pCi ^{222}Rn per cm^3 in the air layer, and these dose rates were added to the dose rate from ^{222}Rn. The results were close to the values given in table A3 and suggest that calculations can be simplified by assuming that all three radionuclides are deposited on the surfaces of the sinus tissues.

Given an appropriate configuration for the air-tissue interface, the volume-to-surface ratio of the air cavity can be estimated, the value of N sec^{-1} per unit area can be calculated from the observed (or expected) ^{222}Rn concentration in sinus air, and average dose rates obtained by evaluating equation (9) and appropriate modifications of equations (10) and (11).

In estimating integral doses to sinus tissues, we have followed the method of Kolenkow [43] in assuming that the concentration N of ^{222}Rn in sinus air varies according to the time dependence of freely emanating ^{226}Ra in bone:

$$N(t) = N(0)(0.54t^{-0.52} - 0.021t^{-0.28}),\ t \ge 1\ \text{day}. \qquad (12)$$

The average integral dose $\bar{D}$(rad) to the sinus tissues over a distance x from the surface of an air layer of thickness d with a ^{222}Rn concentration $N(T)$ at T days after a systemic intake of ^{226}Ra is given by

$$\bar{D}(x,d,T) = N(T)\sum \bar{Q}(x,d,E_0)\ \frac{1.125T^{0.48} - 0.029T^{0.72}}{0.54T^{-0.52} - 0.021T^{-0.28}}, \qquad (13)$$

where $N(T)$ is in pCi/cm^3 and $\sum \bar{Q}(x,d,E_0)$ is in rad/day−(pCi/cm^3).

From inspection of the photomicrographs presented by Ash and Raum [23], the epithelial layer of the paranasal sinuses varies in thickness from about 20 to 50 μm. Estimates of average dose to tissues within 50 μm of the air-tissue interface from radioactivity in paranasal sinus air probably are not unreasonable estimates of epithelial dose. For the simple squamous and cuboidal cells of the mastoid mucosa, the "true" epithelial dose from radioactivity in cavity air probably lies between the 0–50 μm average dose and the dose at x = 0.

The ^{222}Rn concentration N_{exh} (pCi/cm^3) in exhaled air following an intake of ^{226}Ra (0) μCi can be expressed as

$$N_{exh}(t) = {}^{226}\text{Ra}(0)(\mu\text{Ci})\ (10^6\ \text{pCi}/\mu\text{Ci}) \cdot \lambda_{Rn}\ (\text{min}^{-1})(\text{RMV})^{-1}\ (\text{min}/\text{cm}^3)\ N(t)/N(0), \quad (14)$$

where λ_{Rn} is the radioactive decay constant of ^{222}Rn (1.26×10^{-4} min^{-1}), RMV is the respiratory min volume, and $N(t)/N(0)$ is given by equation (12). For an average RMV of 10^4 cm^3, the expression for $N_{exh}(T)$ (pCi/cm^3) at T days after ^{226}Ra intake is

$$N_{exh}(T) = 0.0126\ {}^{226}Ra(0)\ (0.54T^{-0.52} - 0.021T^{-0.28}). \quad (15)$$

If the concentration of ^{222}Rn in an air cavity is equal to that in exhaled air, the right side of equation (15) can be substituted for $N(T)$ in equation (13) to give an expression for the average integral dose $\bar{D}_v$ to sinus tissue within a distance x of the air-tissue interface of a "well-ventilated" sinus:

$$D_v(x,d,T) = 0.0126\ {}^{226}\text{Ra}(0)[\textstyle\sum \bar{Q}(x,d,E_0)] \cdot (1.125T^{0.48} - 0.029T^{0.72}). \quad (16)$$

For the cases of this study, $\bar{D}_v$ (50 μm,d,T) would have ranged from 2% to 5% of the average integral dose to sinus tissue within 50 μm of the bone surface due to ^{226}Ra and its daughter products in uniformly labeled bone, for values of d from 0.5 to 2 cm.

Comparison with the More Exact Treatment of Kolenkow

Kolenkow [43] found a semiempirical relation for the rate of energy loss with distance of heavy charged particles in matter and applied it to an analysis of the plane-interface geometry. The range-energy relation given by Kolenkow is

$$R = \frac{K_1}{2} E_0^2 + K_2 E_0.$$

Values of K_1 and K_2 for water were obtained by Kolenkow from a least-squares fit of his relation to experimentally determined ranges in water published by other investigators; those for bone were obtained from his analysis of α-particle spectra of compact bone from a radium case; those for air were obtained from his analysis of α-particle spectra taken with air absorbers of accurately known thickness. The α-particle ranges in air for the members of the ^{226}Ra and ^{228}Ra series used by Kolenkow in his analysis of sinus dosimetry averaged 1.01 times those given in table A1, the ranges in bone averaged 0.94 times those of table A1, and the ranges in water averaged 1.2 times those of table A1.

Kolenkow performed his dose-rate integrations with a 20 × 20 point net in Simpson's rule and presented the results in graphic form. By estimating the areas under his curves of unit dose rate versus depth in tissue, we calculated average dose rates in soft tissue over distances of 20 and 50 μm from radioactivity in bone and in sinus air to compare with those obtained with the constant LET assumption. These results are given in table A4.

Comparison with the results in tables A2 and A3 shows that the use of the constant LET assumption, by which numerical integrations are avoided, introduces no serious errors in estimating average doses to sinus tissues. Results of the Kolenkow treatment for relative average dose rate to sinus tissues within 50 μm of the bone-tissue interface due to radioactivity in bone are quoted in the main text of this paper because they are based on an accurate energy-loss relation and on experimentally determined α-particle ranges. However, Kolenkow regarded his values of α-particle range in water and in bone as provisional due to experimental inaccuracies. We would expect that estimates of average dose rates to sinus tissues based on the Kolenkow treatment or on the treatment employing the constant LET assumption are accurate within ± 20% in situations where the plane-interface geometry can reasonably be applied.

TABLE A4

Average Dose Rates to Sinus Tissues due to Radioactivity in Bone and Sinus Air using Kolenkow's Treatment

Depth (x) in Tissue (μm)	Relative Average Dose Rate due to Radioactivity in Bone*		Average Dose Rate due to 1 pCi ^{222}Rn/cm^3 Sinus Air† (rad/day)		
	^{226}Ra Series (n = 5)	^{228}Ra Series (n = 6)	d = 0.5 cm	1.0 cm	2.0 cm
20	0.32	0.35	0.063	0.12	0.19
50	0.17	0.21	0.039	0.071	0.11

Note.—d = air layer thickness.

* $\sum_{i=1}^{i=n} Q(x,E_0)_i / \sum_{i=3}^{i=n} Q_{bone_i}$.

† $\sum_{i=1}^{i=n} Q(x,d,E_0)_i$.

Observations Relevant to Sinus Dosimetry

Estimates of dose to tissues near bone surfaces assume an underlying slab of uniformly labeled bone; however, the bones of the radium cases are not uniformly labeled. Kolenkow [43] reported that in case 01-171, ^{226}Ra and ^{222}Rn concentrations in a layer of bone adjacent to the left frontal sinus were 40 and 55 times greater, respectively, than the average concentrations in the bones of this case. In case 01-022, Schlenker [44] found ^{226}Ra concentrations near the inner surface of several pieces of skull bone that ranged from 1.5 to 40 times the skeletal average. Evans [42] noted that these hot layers are probably associated with osseous growth at the time of radium intake, which occurred at ages 17 and 19 for cases 01-022 and 01-171, respectively.

R. A. Schlenker (personal communication) suggested a calculation that supports the speculation that radon in sinus air is potentially an important contributor to mucosal dose. For a pillbox-shaped sinus with dimensions 2 × 1.5 × 1 cm, the activity of radon in sinus air required to deliver a tissue dose comparable to the tissue dose from radioactivity in bone is equal to the activity of freely emanating ^{226}Ra in 2.6×10^{-3} cm^3 of bone. The surface area of the sinus is 13 cm^2. Therefore, the activity of freely emanating ^{226}Ra that would support the required activity of radon in sinus air would be contained in a surrounding bone layer of minimum thickness 2 μm. This result suggests that significant levels of locally produced radon are readily available to the mucous membranes and probably to the air of the sinuses and mastoid air cells.

Air samples taken from sinuses and mastoid air cells of several radium cases within 24 hr of death at Massachusetts Institute of Technology [45] and at our institution suggest that the sinuses are at least sometimes poorly ventilated. For some of these cases, the observed concentrations of radon greatly exceeded the concentrations of radon in exhaled air given by equation (15).

In the single case (01-171) of a sinus air sample taken in vivo, Kolenkow [43] reported a radon concentration of 0.44 pCi/cm^3 in the air of the right frontal sinus, a value about 40 times that of the exhaled air of this case [eq. (15)]. Interestingly, the ratio of radon concentration in exhaled air to average radon concentration in bone and the ratio of radon concentration in sinus air to local radon concentration in the subjacent bone layer (see above) were both about 5×10^{-5} for case 01-171.

TABLE A5

Average Integral Dose to Sinus Tissues of Case 01-171

Tissue	Method of Calculation	Depth in Tissue (μm)	Average Integral Dose (rad)
Tissue adjoining uniformly labeled bone	$\sum \bar{Q}(x,E_0)/\sum Q_{bone}$ (table A2) $\times D_{bone}$ (6,000 rad)	0–20	1,900
		0–50	880
Mucoperiosteum left frontal sinus adjoining "hot" bone layer	$\sum \bar{Q}(x,E_0)/\sum Q_{bone}$ (table A2) $\times D_{bone}$ (280,000 rad)	0–20	88,000
		0–50	41,000
Mucoperiosteum of "well ventilated" sinus ($N = N_{exh}$) adjoining air-layer 1 cm thick	Eq. (16): ^{226}Ra(0) = 427 μCi; $\sum \bar{Q}(x,d,E_0)$ from table A3; T = 19,000 days	0–20	65
		0–50	34
Mucoperiosteum right frontal sinus (sampled for Rn) adjoining air layer 1 cm thick	Eq. (13): $N(T)$ = 0.44 pCi/cm^3; $\sum \bar{Q}(x,d,E_0)$ from table A3; T = 19,000 days	0–20	2,800
		0–50	1,470

Integral Doses to Sinus Tissues of Case 01-171

To illustrate the application of the results of the foregoing analyses, calculations of integral dose to the sinus tissues of case 01-171, based on the experimental data obtained for this case, were carried out. A carcinoma of the left frontal sinus was surgically treated 52 years after oral and intravenous administration of ^{226}Ra (estimated intake [^{226}Ra(0)] was 427 μCi). The average integral bone dose $\bar{D}_{bone}$ was 4,311 rad (table 2) × 7 kg/5 kg, or 6,000 rad. In a piece of sinus bone removed at surgery, Kolenkow [43] (see above) found a layer near the inner surface that contained 40 to 55 times the average concentration of radioactivity in the bones, and the integral dose to this bone layer was 280,000 rad. The method of calculation and the resulting estimates of average integral dose to various sinus tissues are given in table A5.

The reader is referred to the report of Kolenkow [43] for a detailed analysis of sinus dosimetry for case 01-171 and a case involving body contents of both ^{226}Ra and ^{228}Ra.

Other Sources of Dose to Sinus Tissues

The average integral α-particle dose to soft tissue from ^{226}Ra and ^{228}Ra, based on the soft-tissue retention function for radium given by Marshall et al. [46], would have been about 1% of the integral dose to bone from ^{226}Ra and ^{228}Ra. The average dose to tissues within 50 μm of bone surface from short-term retention of ^{226}Ra and ^{224}Ra (if present in dial paint) on bone surfaces would have been about 2%–4% of the bone dose from ^{226}Ra and ^{228}Ra, based on equation (9) and the bone-surface retention function for radium given by Marshall et al. [46].

External radiation and the inhalation of radium and radon are not considered significant potential sources of dose for the occupational cases. The reported levels of these sources, the observation that the therapeutic cases have an elevated incidence of sinus and mastoid malignancies similar to that of the dial painters, and the relationship between incidence and intake of radium speak against the importance of these sources.

While it is not expected that thoron (^{220}Rn), the gaseous decay product of ^{224}Ra in the ^{228}Ra series, would have attained significant concentrations in the tissues or air spaces of the sinuses because of its 54 sec half-period of radioactive decay, the probable small fraction of thoron atoms that diffuse into the mucous membranes of the paranasal sinuses would have a high probability of decay there. At late times, only about 0.1% of the thoron produced in the body is exhaled, compared to about 60%–70% of the radon.

ACKNOWLEDGMENTS

We are indebted to the following physicians for contributing clinical data, radiographs, and pathologic material: Paul B. Szanto, Charles E. Platz, Phillip Collins, R. Morson, Gregory J. Matz, and Francis L. Archer, all Chicago, Ill.; R. V. Kowalski and James Goodlad, Peoria, Ill.; Robert F. Bettasso, Ottawa, Ill.; Shigeo Kondo, Orange, N.J.; and Robley D. Evans. Without their generous assistance our study could not have been made.

We are grateful to Drs. Austin M. Brues, Elizabeth L. Lloyd, Anthony P. Polednak, Robert E. Rowland, Herta Spencer, and Andrew F. Stehney for reviewing the manuscript; Helen Cummins for preparation of the histologic material; Janet Tutskey for preparation of the manuscript; and Georgia Anast for assistance in reference material. Photographs were prepared by the Graphic Arts Department at Argonne National Laboratory.

REFERENCES

1. Vaughan JM: *The Effects of Irradiation on the Skeleton.* Oxford, Clarendon Press, 1973
2. Rubin P: Cancer of the head and neck, nose and paranasal sinuses. *JAMA* 219:336–337, 1972
3. Tucker NN: Cancer of the middle ear. A review of 89 cases. *Cancer* 18:642–650, 1965
4. Aub JC, Evans RD, Hempelmann LH, Martland HS: The late effects of internally-deposited radioactive materials in man. *Medicine* 31:221–329, 1952
5. Evans RD: *Massachusetts Institute of Technology Radioactivity Center Annual Progress Report,* Contract AT(30-1)-952, May 1960
6. Brues AM, Littman MS: Recent cases of mastoid carcinoma in radium patients, in *Radiological and Environmental Research Division Annual Report,* Argonne National Laboratory, ANL-75-3 II, July 1973–June 1974, pp 2–6
7. Finkel AJ, Miller CE, Hasterlik RJ: Radium-induced malignant tumors in man, in *Delayed Effects of Bone-Seeking Radionuclides,* edited by Mays CW, Jee WSS, Lloyd RD, Salt Lake City, University of Utah Press, 1969, pp 195–225

8. Beal DD, Lindsay JR, Ward PH: Radiation-induced carcinoma of the mastoid. *Arch Otolaryngol* 81:9–16, 1965
9. Miller CE, Hasterlik RJ, Finkel AJ: *The Argonne Radium Studies, Summary of Fundamental Data.* ANL-7531 and ACHR-106, January 1969
10. Martland HS: Occupational tumors. (6) Bones. *International Labor Office: Occupation and Health, Encycl Health and Hygiene,* Geneva, 1939, pp 1–23
11. Baker WH, Bulkley JB, Dudley RA, Evans RD, McCluskey HB, Reeves JD Jr, Ryder RH, Salter LP, Shanahan MM: Late effects of internally deposited mixtures of mesothorium and radium in twelve dial painters. *N Engl J Med* 265:1023–1028, 1961
12. Martland HS: The occurrence of malignancy in radioactive persons. *Am J Cancer* 15:2435–2516, 1931
13. Glenn JA Jr, Galindo J, Lawrence CE: Chronic radium poisoning in a dial painter. *Am J Roentgenol* 83:465–473, 1960
14. Evans RD: *Massachusetts Institute of Technology Annual Progress Report,* Contract AT(30-1)-952, May 1959, pp 86–162
15. Marshak RH, Newburger RA, Eliasoph J: Skeletal lesions following internally administered radium. *JAMA* 160:41–44, 1956
16. Evans RD: *Massachusetts Institute of Technology Radioactivity Center Annual Progress Report*, MIT-952-4, May 1967, p 371
17. Evans RD: *Massachusetts Institute of Technology Radioactivity Center Annual Progress Report,* MIT-952-6, May 1969, pp 294–296
18. Hasterlik RJ, Lawson LJ Jr, Finkel AJ: Ophthalmologic aspects of carcinoma of the sphenoid sinus induced by radium poisoning. *Am J Ophthal* 66:55–58, 1968
19. Center for Human Radiobiology: Appendix A, in *Radiological and Environmental Research Division Annual Report,* ANL-77-65 II, July 1976–June 1977
20. Norris WP, Speckman TW, Gustafson PF: Studies of the metabolism of radium in man. *Am J Roentgenol* 73:785–802, 1955
21. Neal WR: Dose variables and their calculations, in *Massachusetts Institute of Technology, Radioactivity Center Annual Progress Report,* MIT-952-3, May 1966, pp 94–141
22. Loutit JF, Brues AM, Marinelli L, Spiers FW, Vaughan JM: *A Review of the Radiosensitivity of the Tissues in Bone,* International Commission on Radiological Protection Publication II, Oxford, Pergamon Press, 1968
23. Ash JE, Raum M: *An Atlas of Otolaryngic Pathology,* 4th ed. New York, Armed Forces Institute of Pathology, p 112 (undated)
24. Conley J: Cancer of the middle ear. *Ann Otol Rhinol Laryngol* 74:555–572, 1965
25. Goodman ML: Middle ear and mastoid neoplasms. *Ann Otol Rhinol Laryngol* 80:419–424, 1971
26. Sorenson H: Cancer of the middle ear and mastoid. *Acta Radiol* 54:460–468, 1960
27. Buchanan G, Slavin G: Tumors of the nose and sinuses. A clinico-pathological study. *J Laryngol Otol* 86:685–696, 1972
28. Frazell EL, Lewis JS: Cancer of the nasal cavity and accessory sinuses. A report of the management of 416 patients. *Cancer* 16:1293–1301, 1963
29. Gamez-Araujo JJ, Ayala AG, Guillamondegui O: Mucinous and adenocarcinoma of nose and paranasal sinuses. *Cancer* 36:1100–1105, 1975
30. Ringertz N: Pathology of malignant tumors arising in the nasal and paranasal cavities and maxilla. *Acta Otolaryngol [Suppl]* (Stockh) 27:1–405, 1938
31. Healey WV, Perzin KH, Smith L: Mucoepidermoid carcinoma of salivary gland origin. *Cancer* 26:368–388, 1970
32. Looney WB, Hasterlik RJ, Brues AM, Skirmont E: A clinical investigation of the chronic effects of radium salts administered therapeutically (1915–1931). *Am J Roentgenol* 73:1006–1037, 1955
33. Looney WB: Late skeletal, roentgenographic, histopathological, autoradiographic and radiochemical findings following radium detection. *Am J Roentgenol* 75:559–572, 1956
34. Munson RJ: A note on the paper of F. W. Spiers. *Br J Radiol* 23:505, 1950
35. Mays CW: Determination of localized alpha dose I, in *Radiobiology Laboratory,* University of Utah, COO-217, 1958, pp 161–171
36. Mays CW: Determination of localized dose II, in *Research in Radiobiology,* University of Utah, COO-220, 1960, pp 200–207
37. Spiers FW: Alpha-ray dosage in bone containing radium, *Br J Radiol* 26:296–301, 1953
38. Spiers FW: *Radioisotopes in the Human Body.* New York, Academic Press, 1968, pp 191–193
39. Mays CW, Sears KA: Determination of localized alpha dose III, in *Research in Radiobiology,* University of Utah, COO-226, 1962, pp 78–85
40. Bethe HA, Ashkin J: Passage of heavy particles through matter, in *Experimental Nuclear Physics,* vol 1, edited by Segre E, New York, Wiley, 1953, pp 166–251
41. Evans RD: The effect of skeletally deposited alpha-ray emitters in man. *Br J Radiol* 39:881–895, 1966
42. Evans RD: On the carcinogenicity of inhaled radon decay products in man, in *Massachusetts Institute of Technology Radioactivity Center Annual Progress Report,* MIT-952-4, May 1967, pp 76–110
43. Kolenkow RJ: Alpha-ray dosimetry of the bone-tissue interface with application to sinus dosimetry in the radium cases, in *Massachusetts Institute of Technology Radioactivity Center Annual Progress Report,* MIT-952-4, May 1967, pp 163–201
44. Schlenker RA: Thick source alpha-ray spectroscopy of radium-bearing bones, in *Massachusetts Institute of Technology Radioactivity Center Annual Progress Report,* MIT-952-5 II, May 1968, pp S11–S13
45. Keane AT, Gunner DL, Costello MM: Radon concentration in sinus air from radium cases, in *Massachusetts Institute of Technology Radioactivity Center Annual Progress Report,* MIT-952-7, May 1970, pp 61–68
46. Marshall JH, Liniecki J, Lloyd EL, Marotti G, Mays CW, Runco J, Sissons HA, Snyder WS: *Alkaline Earth Metabolism in Adult Man,* International Commission on Radiological Protection Publication 20, Oxford, Pergamon Press, 1973

Radiologic and Clinical Assessment of Broad-Spectrum Antibiotic Therapy in Crohn's Disease

ALBERT A. MOSS,[1] JOHN V. CARBONE,[2] AND HERBERT Y. KRESSEL,[1,3]

Continuous treatment with broad-spectrum antibiotics resulted in symptomatic improvement in 41 of 44 patients (93%) with Crohn's disease who were treated for 6 months or longer. Radiographic follow-up demonstrated evidence of improvement in 20 of 35 patients (57%) for whom posttherapy radiographs were available. Radiography demonstrated resolution of ulcerations, abdominal masses, stenosis, and in some patients restoration of a normal intestinal mucosal pattern. In some patients these changes occurred within weeks; in others, over a period of years. Patients with perianal fistulas and patients who had previously undergone surgery and had recurrence of their disease prior to treatment with antibiotics accounted for the therapy failures.

Crohn's disease of the small and large bowel is the most common chronic, nonmalignant disease of the gastrointestinal tract for which no effective therapy is currently available. Corticosteroids, sulfasalizine, (Azulfidine, Pharmacia Labs., Piscataway, N.J.) azathioprine, and surgery have been tried without convincing success. A nationwide clincial trial of sulfasalizine, azathioprine, and prednisone is currently underway. Reported results indicate azathioprine to be no improvement; prednisone and sulfasalizine therapy were somewhat better than placebo in inducing clinical remission, but neither drug was better than the placebo in preventing flare-up of disease [1].

Broad-spectrum antibiotics which are absorbed into the systemic circulation have not been used for Crohn's disease as therapy because of their reported lack of effectiveness in patients with ulcerative colitis [2]. Although spontaneous remission of clinical symptoms has occurred in patients with Crohn's disease, regression of the lesions has been radiographically documented in only a very few instances [3–5]. We treated a series of 44 patients with granulomatous bowel disease with broad-spectrum antibiotics and observed radiologic improvement in the healing of fistulae, ulcerations, stenosis, and elimination of associated mass lesions. This is the first report documenting long-term radiologic improvement in a series of patients treated for Crohn's disease.

Subjects and Methods

From January 1972 until January 1977, one of us (J. V. Carbone) treated 44 patients with Crohn's disease with broad-spectrum antibiotics. The diagnosis of Crohn's disease was established before antibiotic therapy was started, by surgical resection and pathologic examination of diseased intestine in 16 patients, radiographic findings of Crohn's disease in the terminal ileum and colon in 23, and radiographic abnormalities consistent with Crohn's disease and coexistent fistulae in five patients. The disease had been present for an average of 7.4 years (range, 1–29) before start of antibiotic therapy. Thirty patients had disease of the colon and small bowel, 10 had only small bowel disease, and four patients had disease confined to the colon. There was no predeliction for sex; ages ranged from 13 to 60 years (mean, 30). There were 31 patients younger than 30 years when antibiotic therapy was initiated. No patients similarly treated are excluded from this report.

Table 1 summarizes the treatments that had been used for our 44 patients before antibiotic therapy. All but four patients had extensive therapy previously, including conventional medication and surgery. Almost all had undergone several therapeutic methods without success. When the antibiotic therapy was instituted, all patients were acutely ill with abdominal pain and had experienced exacerbation of their disease while taking conventional medication.

We used a variety of broad-spectrum antibiotics. Table 2 shows the usual dosages and the frequency of use. No combination of antibiotics was given, but five patients received two different antibiotics and three patients received three different antibiotics during the course of therapy. Once antibiotic treatment was instituted, it was continued indefinitely, even after the patient ceased to have clinical symptoms of inflammatory bowel disease. Three patients are still on antibiotics 5 years after initiation of therapy. Four patients experienced allergic reactions to the medications. No patient developed pseudomembranous colitis, and none exhibited any gastrointestinal findings suggestive of colitis associated with long-term antibiotic therapy.

Radiography was performed prior to institution of antibiotic therapy and at varying times from 2 months through 5 years after therapy was begun. The pre- and posttherapy radiographs were coded, randomized, and interpreted by two experienced gastrointestinal radiologists blindly without knowledge of which radiograph was obtained before or after antibiotic therapy. The interpreters indicated whether there was any difference between radiographs and, if so, the difference was scored as small, moderate, or marked.

Clinical improvement was judged by decreased frequency of bowel movements, loss of abdominal pain, weight gain, normalization of temperature, decrease in size or disappearance of palpable abdominal masses, cessation of rectal bleeding, and decrease in prednisone dosage after (as compared to before) antibiotic therapy.

Results

The results of the study are summarized in tables 3 and 4. The follow-up period ranged from 6 months to 5

Received February 28, 1978; accepted after revision July 18, 1978.
H. Y. Kressel is the recipient of National Institutes of Health Training Grant GM 01272 from the National Institute of General Medical Sciences.
[1] Department of Radiology, University of California School of Medicine, San Francisco, California 94143. Address reprint requests to A. A. Moss.
[2] Department of Medicine, University of California School of Medicine, San Francisco, California 94143.
[3] Present address: Department of Radiology, Hospital of the University of Pennsylvania, Philadelphia, Pennsylvania 19104.

© 1978 American Roentgen Ray Society

0361–803X/78/1100–0787 $00.00

TABLE 1

Therapy before Antibiotic Medication

Therapy	No. Patients
Sulfasalizine* and prednisone	23
Sulfasalizine	8
Prednisone	6
Azathioprine	5
Sulfisoxazole† and prednisone	4
Sulfisoxazole	3
Hydrocortisone enema and prednisone	3
Surgery	16

Note.—Some patients had more than one type of treatment.
* Azulfidine.
† Gantrisin, Roche Labs., Nutley, N.J.

TABLE 2

Systemic Antibiotics Used in Treatment of Crohn's Disease

Antibiotic	Dosage (mg)	No. Patients	Allergic Reactions
Ampicillin	500*	28	3
Tetracycline	250†	14	1
Clindamycin	150†	8	0
Cephalothin sodium	500‡	3	0
Erythromycin	250*	1	0

Note.—Some patients had more than one type of treatment.
* Four times a day.
† Three times a day.
‡ Keflin, Lilly, Indianapolis, Ind.

TABLE 3

Antibiotic Therapy: Clinical Summary of Treatment

Symptom	Total Cases	No. Improved
Diarrhea	42	41
Abdominal pain	44	41
Appetite	23	22
Rectal bleeding	11	11
Abdominal mass	11	11*
Fever	11	10
Weight	35	22†

* Eliminated in 10; smaller in one patient.
† Increased more than 5 kg.

years (average, 2 years). All 44 patients have been observed for 6 months or longer; 41 have been clinically well for longer than 6 months, 28 for more than 1 year, and 15 for over 2 years. The improvement observed occurred usually within a week and persisted during antibiotic treatment. Pretreatment steroid dosage was decreased or eliminated in all patients who responded to therapy. Three patients underwent subsequent surgery because of progression of their disease while on antibiotic medication. These three failures all occurred in patients who had prior surgery and extensive fistula and perirectal disease at the time antibiotic therapy was initiated.

TABLE 4

Effect of Antibiotic Therapy on Steroid Dosage

	Average Daily Prednisone Dose (mg)					Total No. Patients
	0	1–5	6–10	11–20	21–50	
Initial	3	1	2	13	10	29
Final	18	10	7	2	0	37

Follow-up radiographs were obtained on 35 of the patients. Improvement was noted in 20 patients while lack of improvement and progression of the disease were found in 10 and five, respectively. In six patients the improvement was scored as small, in eight as moderate, and in six others as marked (figs. 1–3). In five cases the posttherapy radiographs were judged normal. All patients whose radiographs showed regression of disease had also improved symptomatically. Ten patients improved clinically but showed no radiographic change in the extent or degree of involvement. The three patients who were considered to be clinical failures (see above) also showed radiographic progression of the disease; two patients who remain asymptomatic on antibiotic therapy demonstrate progression of abnormalities radiographically.

Discussion

Viruses [6], bacteria [7, 8], constituents of the fecal stream [9], and immunologic mechanisms [10, 11] have been proposed as causes of Crohn's disease, but no consensus has been reached [12]. Recent immunologic studies [10, 11] implicate immune mechanisms in the pathogenesis of inflammatory bowel disease, but a specific antigen-antibody reaction has not been demonstrated in the diseased bowel [12]. Cave et al. [7] produced small bowel granulomas in rabbits by inoculating Crohn's disease tissue obtained from surgical specimens directly into the wall of the ileum. While not conclusive, their investigation suggests a transmissible agent as the cause of Crohn's disease.

Excluding the national study of Crohn's disease, there have been only six double-blind clinical therapeutic trials in patients with this disorder [12–15]. The results of these studies indicate that neither sulfasalizine nor azathioprine is effective in inducing remissions in patients with symptomatic disease, but azathioprine seemed to be of some benefit in maintaining remission once it had been achieved [16–18].

In none of these therapeutic trials were antibiotics investigated as a method of treatment and, except for the national cooperative Crohn's study, radiologic follow-up has not been used as a measure of therapeutic effectiveness. The radiologic follow-up in the national cooperative study was limited to changes occurring within 13 weeks, and the results have not yet been

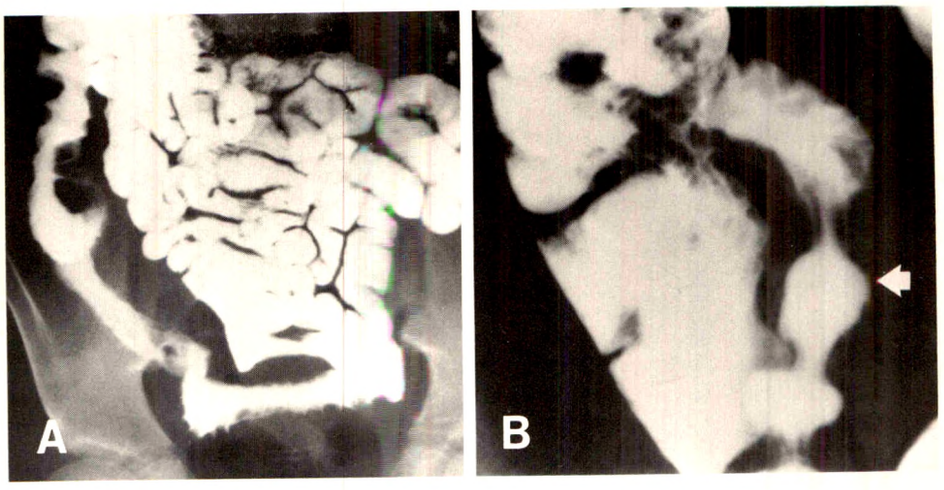

Fig. 1.—16-year-old boy with delayed growth and maturation having six to 10 bowel movements per day. *A*, Extensive ulcerations of terminal ileum and cecum prior to antibiotic therapy, typical of Crohn's disease. *B*, Terminal ileum (*arrow*) and cecum are markedly improved after 23 months of clindamycin therapy. Weight increased to 69 kg, and patient grew 17 cm and was symptom free with normal bowel movements for 2 years.

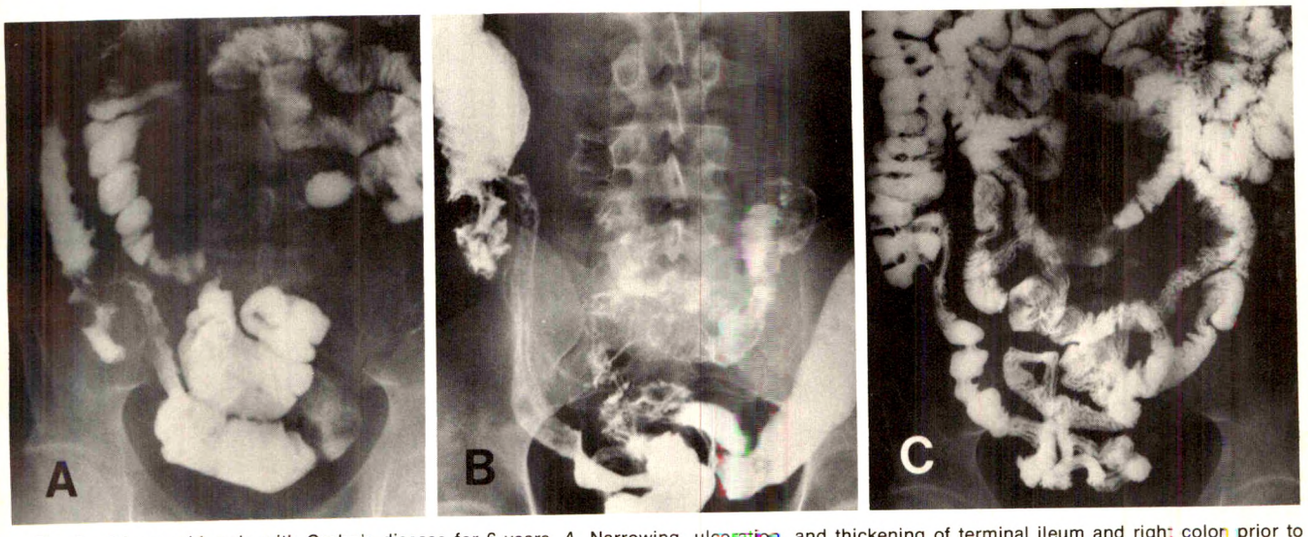

Fig. 2.—24-year-old male with Crohn's disease for 6 years. *A*, Narrowing, ulceration, and thickening of terminal ileum and right colon prior to antibiotic therapy. *B*, Little change in appearance of diseased segments of small bowel and colon after 8 months of high dose steroid and sulfasalizine therapy. *C*, Terminal ileum, cecum, and right colon are radiographically normal after 3 years of ampicillin therapy without steroids. Patient has been symptom free for over 4 years.

published. Thus our study is the only evaluation of antibiotic therapy in Crohn's disease which has correlated long-term radiologic follow-up with therapeutic effectiveness.

While our study does not provide information concerning the mechanism by which broad-spectrum antibiotic therapy produces its effect, the results indicate that systemic antibiotic therapy is a useful method of inducing and maintaining clinical well-being in some patients with Crohn's disease. Further support of the efficacy of antibiotic therapy is found in the reversal of the abnormalities seen radiographically in some patients and in the marked reduction in average daily steroid dosage.

Whenever there was radiographic evidence of improvement (57%), the patients had become free of symptoms. Some patients (29%) improved clinically but failed to demonstrate any definite evidence of healing. Further radiologic follow-up is needed to determine if these patients are exhibiting a slow resolution of their bowel abnormalities or will ultimately prove to have progressive disease.

It is possible that the radiologic improvement was due in part to the elimination of gut bacteria overgrowth or sterilization of abscesses. However, we feel our patient population did not represent a select group of patients with bacterial overgrowth or occult abscesses. The patients placed on antibiotic therapy had clinical and radiographic features indistinguishable from those referred for conventional therapy. It is interesting to speculate that if Crohn's disease is due to a transmissible agent, antibiotic therapy was at least in part treating the etiologic factor. While the results of this study are encouraging, we caution that they are preliminary and must await further confirmation.

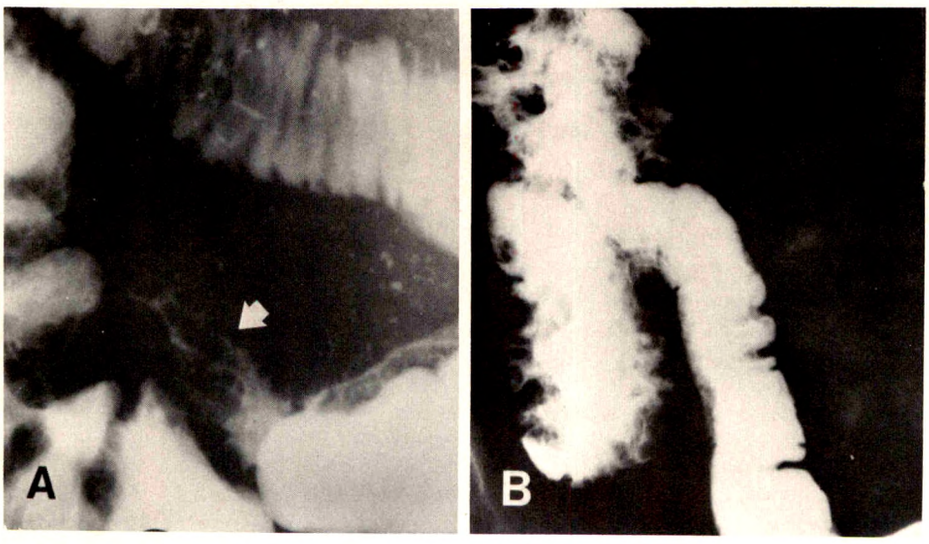

Fig. 3.—16-year-old male with Crohn's disease involving terminal ileum for 2 years. Weight decreased from 70 to 56 kg and patient had eight bowel movements per day. *A*, Spot film shows nodular terminal ileum with several fistula tracts (*arrow*). *B*, Spot film of terminal ileum after 18 months of ampicillin therapy. Ileum is distensible and nonulcerated; no fistulae could be demonstrated. Patient currently weighs 75 kg and is symptom free.

ACKNOWLEDGMENTS

We thank Drs. Alexander R. Margulis and Henry I. Goldberg for reviewing the radiographs.

REFERENCES

1. Singleton JW: National cooperative Crohn's disease study (NCCDS): results of drug treatment (abstr.). *Gastroenterology* 72:1133, 1977
2. Kirsner JB, Palmer WL: Ulcerative colitis: consideration of its etiology and treatment. *JAMA* 155:341–346, 1954
3. Goldstein F, Murdock MG: Clinical and radiologic improvement of regional enteritis and enterocolitis after treatment with salicylazosulfapyridine. *Am J Dig Dis* 16:421–431, 1971
4. Jones JH, Lennard-Jones JE, Young AC: Reversibility of radiological appearances during clinical improvement in colonic Crohn's disease. *Gut* 10:738–743, 1969
5. Marshak RH, Lindner AE: *Radiology of the Small Intestine*, 2d ed. Philadelphia, Saunders, 1976
6. Gitnick GL, Rosen VJ: Viral investigations in inflammatory bowel disease (abstr.). *Gastroenterology* 72:1062, 1977
7. Cave DR, Mitchell DN, Kane SP, Brooke BN: Further animal evidence of a transmissible agent in Crohn's disease. *Lancet* 2:1120–1122, 1973
8. Mitchell DN, Rees RJW: Agent transmissible from Crohn's disease tissue. *Lancet* 2:168–171, 1970
9. Shorter RG, Huizenga KA, Spencer RJ: A working hypothesis for the etiology and pathogenesis of nonspecific inflammatory bowel disease. *Am J Dig Dis* 17:1024–1032, 1972
10. Kraft SC, Kirsner JB: The immunology of ulcerative colitis and Crohn's disease: clinical and humoral aspects, in *Inflammatory Bowel Disease*, edited by Kirsner JB, Shorter RG, Philadelphia, Lea & Febiger, 1975, pp 60–80
11. Watson DW, Shorter RG: The immunology of ulcerative colitis and Crohn's disease: cell-mediated immune responses, in *Inflammatory Bowel Disease*, edited by Kirsner JB, Shorter RG, Philadelphia, Lea & Febiger, 1975, pp 81–98
12. Shorter RG, Shephard DAE (eds): Frontiers in inflammatory bowel disease: the proceedings of a conference sponsored by the McReynolds Foundation, part I. *Am J Dig Dis* 20:540–571, 1975
13. Anthonisen P, Barany F, Folkenborg O, Holtz A, Jarnum S, Kristensen M, Riis P, Walan A, Worning H: The clinical effect of salazosulphapyridine (Salazopyrin®) in Crohn's disease: a controlled double-blind study. *Scand J Gastroenterol* 9:549–554, 1974
14. Klein M, Binder HJ, Mitchell M, Aaronson R, Spiro H: Treatment of Crohn's disease with azathioprine: a controlled evaluation. *Gastroenterology* 66:916–922, 1974
15. Rhodes J, Bainton D, Beck P, Campbell H: Controlled trial of azathioprine in Crohn's disease. *Lancet* 2:1273–1276, 1971
16. Levin B, Rosenberg J, Wall A, Settles R, Kirsner J: A controlled trial of azathioprine in the treatment of Crohn's disease (abstr.). *Clin Res* 21:868, 1973
17. Watson WC, Bukowsky M: Azathioprine in management of Crohn's disease: a randomized cross-over study (abstr.). *Gastroenterology* 66:796, 1974
18. Willoughby JMT, Kumar PJ, Beckett J, Dawson AM: Controlled trial of azathioprine in Crohn's disease. *Lancet* 2:944–947, 1971

Association of Squamous Cell Carcinoma of the Head and Neck with Cancer of the Esophagus

HARVEY M. GOLDSTEIN[1] AND JESUS ZORNOZA[1]

The frequency of esophageal carcinoma in association with squamous cell carcinoma of the head and neck region is dramatically higher than in both the general and cancer population. The esophageal tumor may be discovered synchronously or asynchronously. Alcohol and tobacco are likely causative factors relating these two primary cancer groups. The importance of complete radiologic evaluation of the esophagus in head and neck cancer patients is emphasized.

As life expectancy has increased and as more effective therapy has prolonged survival of cancer patients, multiple primary neoplasms in the same individual are being recognized more frequently. Multiple tumors may arise in the same, related, or different organ systems.

The association of squamous cell carcinomas of the head and neck structures with cancer of the esophagus has received little attention and none in the radiologic literature since it was first suggested approximately 40 years ago [1]. Since radiologic evaluation of the esophagus is frequently not obtained in the initial evaluation of these patients, it is important that the relationship between these two primary tumor groups be recognized.

This communication documents our experience with the association of these two primary tumors. Epidemiologic data and possible causative factors are discussed. The importance of complete radiologic evaluation of the esophagus in head and neck cancer patients is emphasized.

Case Material and Findings

Pertinent data from the Department of Epidemiology files were reviewed for the period March 1944 to August 1976. During this time, approximately 10,000 patients over the age of 40 with squamous cell carcinomas of the head and neck (oral cavity, pharynx, larynx) were evaluated. During this same period, about 850 patients with squamous cell carcinoma of the cervical and thoracic esophagus were seen. Eighty-nine patients were found who had separate primary squamous cell tumors of the head and neck and esophagus. This represents over 10% of all patients with esophageal carcinoma evaluated at this institution.

All 89 patients had at least one primary tumor of the head and neck and one primary tumor of the esophagus, but 18 had more than one primary tumor of the head and neck region. Twenty-two had cancer of the cervical esophagus, and the remainder had a malignancy of the thoracic esophagus. The tumors of the cervical esophagus were considered separate primaries rather than direct extension since they were not anatomically contiguous to the original lesion of the head and neck. In 16 patients, the head and neck and esophageal tumors were discovered synchronously. In the larger asynchronous group, the average time interval between discovery of the first head and neck lesion and the tumor of the esophagus was approximately 46 months (range, 2 months to 16 years).

The expected number of esophageal carcinomas was approximated by applying general population average annual incidence rates [2] for esophageal carcinoma (3.4/100,000) to the estimated person-years at risk in the total M. D. Anderson head and neck cancer population. Even if an estimate of 30 years follow-up per patient is assumed, 10 patients of the 10,000 total would be expected to develop esophageal carcinoma compared to the 89 patients who did. Similar determinations show that the number of second primary tumors arising in the stomach and colon in the head and neck cancer population group is not greater than the anticipated incidence.

Using Department of Epidemiology files, records of concurrent and asynchronous primary tumors were recalled. When esophageal carcinoma was a second primary, in over 60% of the cases a head and neck primary was the other tumor. The only other substantial association of esophageal carcinoma was with patients having skin cancer. Of a total of approximately 4,500 patients with colorectal cancer recorded, only one known patient has had a synchronous or asynchronous esophageal carcinoma.

Illustrative Case Reports

Case 1

A 65-year-old male was treated for squamous cell carcinoma of the right tonsillar area (fig. 1*A*). No dysphagia was present, and an esophageal evaluation was not performed. After 1½ years, the patient presented with weight loss and fullness in the epigastrium after eating. Esophagram demonstrated a large tumor of the distal thoracic esophagus (fig. 1*B*). Endoscopy and biopsy confirmed the diagnosis of squamous cell carcinoma. The patient underwent preoperative radiation and an esophagogastrectomy, but he became progressively emaciated and expired 4 months later.

Case 2

A 73-year-old male had trouble swallowing and a choking sensation for several months. Examination revealed a 3.5 cm

Received April 20, 1978; accepted June 28, 1978.

[1]Department of Diagnostic Radiology, University of Texas System Cancer Center, M. D. Anderson Hospital and Tumor Institute, 6723 Bertner, Houston, Texas 77030. Address reprint requests to J. Zornoza.

© 1978 American Roentgen Ray Society

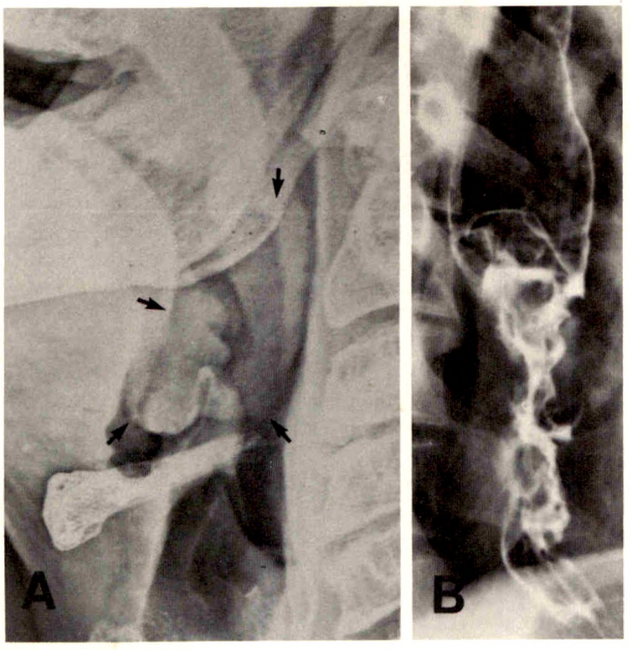

Fig. 1.—Case 1: asynchronous carcinomas of oropharynx and esophagus. *A*, Lateral xerogram demonstrating large nodular soft tissue mass in oropharynx (*arrows*) extending down below epiglottis. *B*, Esophagram 1½ years later demonstrating large irregular carcinoma involving distal third of thoracic esophagus.

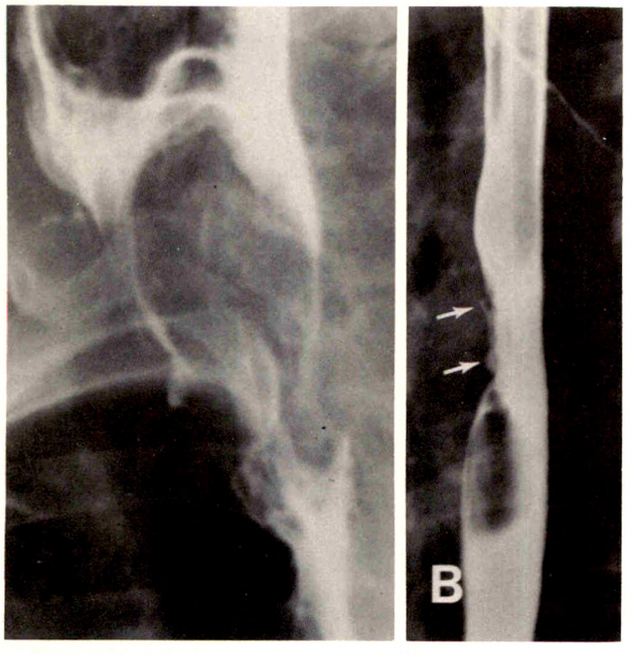

Fig. 2.—Case 2: synchronous carcinomas of oral cavity, hypopharynx, and thoracic esophagus. *A*, Barium swallow demonstrating irregular bulky neoplasm involving hypopharynx and cervical esophagus. *B*, Small ulcerating carcinoma arising from anterior wall of midthoracic esophagus (*arrows*). Small quantity of aspirated barium is present.

squamous carcinoma along the right tongue border and floor of the mouth. Barium swallow at this time demonstrated a large tumor of the hypopharynx and cervical esophagus (fig. 2*A*). Examination of the thoracic esophagus also demonstrated a small ulcerating carcinoma in the midthoracic esophagus (fig. 2*B*). Because of the patient's debilitated condition and mental status, only supportive and symptomatic therapy was elected.

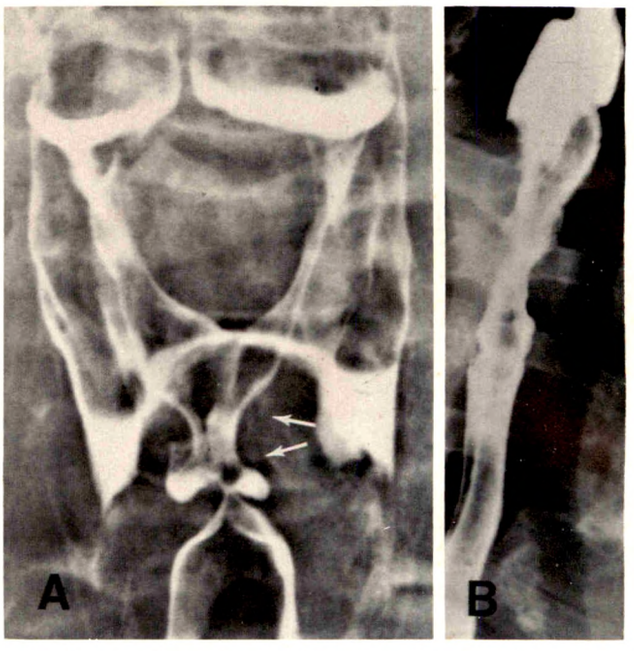

Fig. 3.—Case 3: asynchronous carcinomas of larynx and esophagus. *A*, Laryngogram demonstrating mass involving distal left aryepiglottic fold and false cord (*arrows*). *B*, Esophagram demonstrating elongated annular carcinoma of proximal thoracic esophagus.

Case 3

A 60-year-old white male was treated with radiation in 1973 for a localized squamous cell carcinoma of the left aryepiglottic fold and false cord (fig. 3*A*). No evaluation of the gastrointestinal tract was performed. About 2 years later the patient presented with a short history of dysphagia, and a barium examination demonstrated a 6 cm annular carcinoma of the proximal thoracic esophagus (fig. 3*B*). Endoscopic biopsy confirmed the diagnosis, and the patient was treated with radiotherapy. Some improvement in the dysphagia occurred, and he is presently being followed.

Case 4

A 63-year-old male underwent extensive surgery and radiotherapy for carcinoma of the right retromolar trigone and left anterior tonsillar pillar 2½ years before the present admission. The patient presented with upper abdominal pain, but no esophageal symptoms were present. Upper gastrointestinal series demonstrated a lesser curvature gastric ulcer and a plaquelike lesion arising from the anterior wall of the esophagus (fig. 4). Endoscopy and biopsy documented the diagnoses of squamous cell carcinoma of the esophagus and a benign gastric ulcer. The patient received the first portion of a split radiation course, but he did not return for follow-up. The patient expired about 6 months later.

Case 5

A 72-year-old male was treated 12 years previously for squamous cell carcinoma of the right tonsil. The patient presented with increasing difficulty in swallowing which was felt to be secondary to neuromuscular dysfunction related to the previous

Fig. 4.—Case 4. Double contrast esophagram demonstrating small irregular plaquelike carcinoma along anterior wall of midthoracic esophagus (*arrows*).

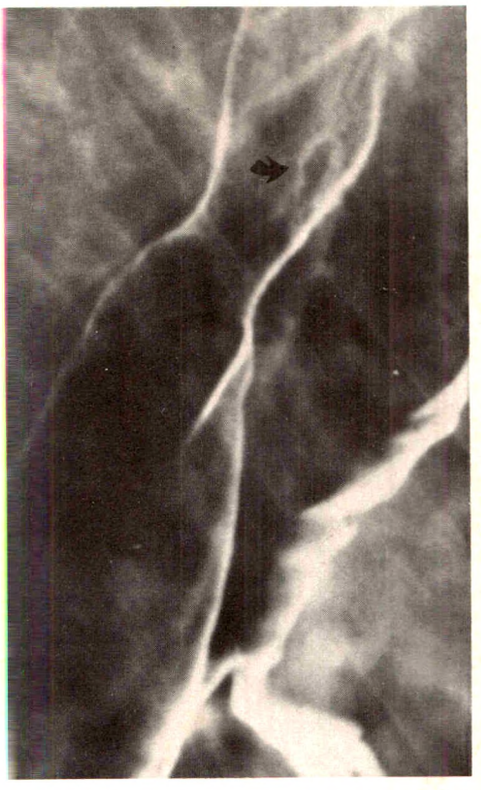

Fig. 5.—Case 5. Double contrast esophagram demonstrating small irregular nodule. (*arrow*) and slight associated narrowing in proximal thoracic esophagus. Aspirated barium in tracheobronchial tree is secondary to previously treated tonsillar carcinoma.

surgery and radiotherapy. Barium studies demonstrated a small amount of aspiration with each swallow. At about the level of the aortic knob, a small nodule and slight narrowing were identified in the esophagus (fig. 5). Endoscopy was recommended but was not performed. Repeat examination 1 year later because of dysphagia demonstrated an annular carcinoma of the esophagus at the location of the previously described finding. The patient received palliative radiotherapy but became progressively cachectic and expired 3 months later.

Discussion

The known occurrence of esophageal carcinoma in our group of head and neck cancer patients presumably represents a minimum incidence. Some cases of cervical esophageal carcinoma were excluded so that the possibility of direct extension from a pharyngeal or laryngeal tumor was eliminated. In addition, some patients with treated head and neck tumors were lost to follow-up and may have developed an esophageal tumor that is unknown to us. Finally, the listings of patients available are based largely on discharge diagnoses and may therefore be incomplete. For example, some patients with esophageal carcinoma may have a past history of a head and neck tumor treated elsewhere which is not recorded.

Comparisons of the risk of esophageal carcinoma developing in the head and neck cancer population at this institution versus the general population are difficult. Our patients originate primarily from the southwestern United States and form a preselected population group in that a malignancy is present or suspected. Therefore, comparisons within the cancer population at this institution probably enable more valid statements. In this regard, the lack of esophageal carcinoma in association with other visceral malignancies within the cancer population further emphasizes the link between squamous cell carcinomas of the head and neck and the esophagus.

Awareness of the increased association between tumors of the head and neck and the esophagus may lead to the detection of small and potentially curable cancers of the esophagus. In fact, this high risk patient population might serve as a model to evaluate whether the discovery of asymptomatic esophageal carcinomas is associated with improved survival. In addition, the search for and discovery of synchronous esophageal cancers in patients with known head and neck tumors will often affect the therapy of the latter tumors. In such instances, it is unlikely that radical surgery of the head and neck lesion would be performed.

Several previous reports discussing the association of separate primary tumors in the head and neck region and esophagus have appeared. Cahan et al. [3] reported 60 patients with primary carcinomas of the head and neck and esophagus over a 23 year period. In their study, approximately 25% were synchronous, and 68% occurred within 2 years of each other. Goodner and Watson

LIBRARY

[4] reported that 126 of 1,315 cases of carcinoma of the esophagus had an associated neoplasm. Fifty-two of these were associated with head and neck tumors. Sugarbaker and Jesse [5] reviewed 371 consecutive patients with squamous carcinoma of the oropharynx seen during a 5 year period; 18% of all patients and 35% of the survivors at 5 years developed at least one new malignancy of foregut structures including head and neck, esophagus, and lung. Of the 65 new tumors, 10 occurred in the esophagus. The magnitude of the problem is illustrated in their series by the fact that the risk of a new carcinoma was as great as the risk for regional and distant metastatic spread from the initial head and neck tumor.

Presumably the same predisposing factors which play a role in the etiology of head and neck carcinomas are also important in the production of carcinoma of the esophagus. Several reports have established that heavy tobacco and alcohol use significantly increases the risk of squamous cell carcinoma of both areas [6–8]. The vast majority of patients reported here had a long-standing history of considerable cigarette and alcohol use. Although the exact mechanism of carcinogenesis is not known, it would appear that exposure of the oral cavity, respiratory tract, and upper alimentary tract to the same potentially cancer-producing agents is the major variable in the increased association between head and neck and esophageal tumors.

In over 80% of the patients in this series, the separate primary tumors were discovered asynchronously. Undoubtedly some of these were present synchronously, but the esophageal primary was overlooked at the time of initial evaluation for the head and neck lesion. As noted in our illustrative cases, radiologic examination of the esophagus was usually not performed.

Careful radiologic examination of the entire esophagus is imperative in all patients with newly discovered squamous cell tumors of the head and neck region. In some patients with laryngeal carcinoma, barium examination of the hypopharynx and cervical esophagus is a standard part of the initial workup in order to assess local invasion, swallowing function, and the presence of aspiration. Evaluation of the thoracic esophagus should be conducted at the same time in these patients. Following surgical and/or radiotherapy of head and neck tumors, some swallowing difficulties may occur. As a result, minor changes in symptomatology also warrant complete examination of the esophagus. When feasible and clinically indicated, serial examinations of the esophagus also might be considered in previously treated head and neck cancer patients.

ACKNOWLEDGMENTS

We gratefully acknowledge the assistance and advice of Bradley Borlase, Ann Murphy, and Dr. Jerry W. McLarty of the Department of Epidemiology; the photographic support of Eugene Szwarc; and manuscript preparation by Janet Schell.

REFERENCES

1. Watson WL: Cancer of the esophagus: some etiological considerations. *Am J Roentgenol* 41:420–424, 1939
2. Cutler SJ, Young JL (eds): Third national cancer survey: incidence data. *Natl Cancer Inst Monogr* 41:1–454, 1975
3. Cahan WB, Castro EB, Rosen PP, Strong EW: Separate primary carcinomas of the esophagus and head and neck region in the same patient. *Cancer* 37:85–89, 1976
4. Goodner JT, Watson WL: Cancer of the esophagus, its association with other primary cancers. *Cancer* 9:1248–1252, 1956
5. Sugarbaker EV, Jesse RH: Second primary carcinoma of the "foregut": high risk of the head and neck patient. Submitted for publication
6. Schottenfeld D, Gantt RC, Wynder EL: The role of alcohol and tobacco in multiple primary cancers of the upper digestive system, larynx and lung: a prospective study. *Prev Med* 3:277–293, 1974
7. Wynder EL, Bross IF: A study of etiological factors in cancer of the esophagus. *Cancer* 14:389–413, 1961
8. Wynder EL, Dodo H, Bloch DA, Gantt RC, Moore OS: Epidemiologic investigation of multiple primary cancer of the upper alimentary and respiratory tracts. *Cancer* 24:730–739, 1969

Cystic Neoplasms of the Pancreas: New Angiographic and Ultrasonographic Findings

PATRICK C. FREENY,[1] CAROL J. WEINSTEIN,[2] DAVID A. TAFT,[3] AND FRANK H. ALLEN[4]

Cystic neoplasms of the pancreas (cystadenoma, cystadenocarcinoma) are rare tumors. Early diagnosis and differentiation from other pancreatic lesions are essential for appropriate management. Pancreatic angiography and gray scale ultrasonography facilitate rapid, accurate diagnosis and proper surgical therapy. In a 7 year period, eight patients were studied (one cystadenoma, seven cystadenocarcinoma); five had selective visceral angiography and six underwent abdominal ultrasonography. The ultrasonographic characteristics of these neoplasms and some new angiographic findings are presented. The sonographic findings for cystadenocarcinoma were similar to those of cystadenoma.

Most cystic lesions of the pancreas are pseudocysts or retention cysts related to trauma or pancreatitis [1, 2]. About 15% are cystic neoplasms: cystadenoma or its malignant counterpart, cystadenocarcinoma [3, 4]. The actual incidence of these tumors is quite low. Only 42 cystadenocarcinomas and 20 cystadenomas were seen at the Mayo Clinic over a 50 year period [4, 5]. In 1965, Becker et al. [3] reviewed 164 reported cases of cystadenoma and 65 cases of cystadenocarcinoma.

This paper describes the radiologic-pathologic features of eight cystic pancreatic neoplasms (one cystadenoma, seven cystadenocarcinomas). The angiographic spectrum of changes and ultrasonographic features of these tumors are described. The combination of routine radiologic examinations plus pancreatic angiography and ultrasonography facilitates accurate preoperative diagnosis and differentiation from the more frequent solid adenocarcinomas and traumatic or postinflammatory cysts.

Case Material

From 1971–1977, eight patients had cystic neoplasms of the pancreas (one cystadenoma, seven cystadenocarcinomas) diagnosed at the Virginia Mason Medical Center or the Good Samaritan Hospital. The two males and six females ranged in age from 35 to 82 years. All patients underwent surgical exploration with pathologic confirmation of the radiologic diagnosis.

Five patients had selective visceral angiography using standard catheterization techniques. Six patients underwent abdominal ultrasonography using commercially available gray scale units. The angiographic and ultrasonographic findings were correlated with surgical findings or gross specimens in each case.

Results

The correct preoperative diagnosis was made in six of eight patients. The diagnosis was correct in each of the three patients who had both ultrasonography and angiography; in two of the three patients who had only ultrasonography; and in one of two patients who had only arteriography. In the latter case, only an aortogram and selective left renal arteriogram were performed, and the lesion was diagnosed incorrectly as a calcified renal mass (fig. 1). In retrospect, the calcification is typical of pancreatic cystadenoma, and a dilated pancreatica magna artery was seen supplying the calcified tumor.

During the same period, two false positive diagnoses of cystic pancreatic neoplasm were made: one was a moderately vascular duodenal leiomyosarcoma; the other was a large nonfunctioning islet cell carcinoma. Ultrasonography demonstrated complex masses in both cases. No pseudocysts were diagnosed as cystic neo-

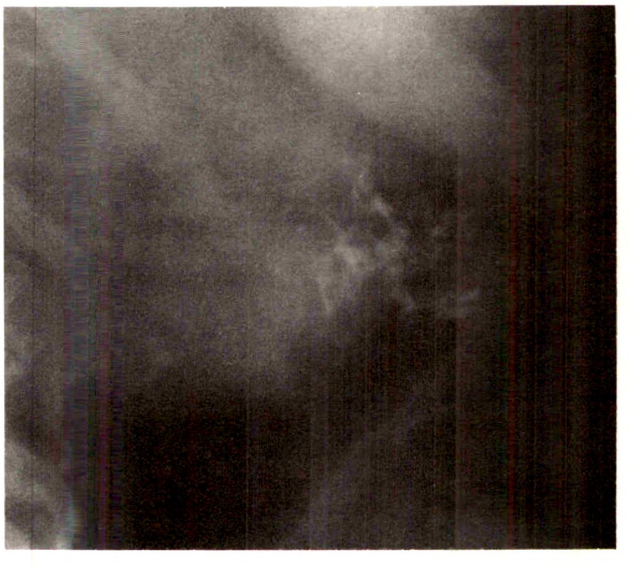

Fig. 1.—Cystadenoma in 75-year-old female. Plain film showing typical sunburst pattern of calcification.

Received February 28, 1978; accepted after revision July 14, 1978.

[1] Department of Diagnostic Radiology, Mason Clinic, 1100 Ninth Avenue, Seattle, Washington 98111. Address reprint requests to P. C. Freeny.
[2] Department of Diagnostic Radiology, Good Samaritan Hospital, Portland, Oregon 97210.
[3] Department of Surgery, Mason Clinic, Seattle, Washington 98111.
[4] Section of Nuclear Medicine and Ultrasound, Mason Clinic, Seattle, Washington 98111.

© 1978 American Roentgen Ray Society

0361–803X/78/1100–0795 $00.00

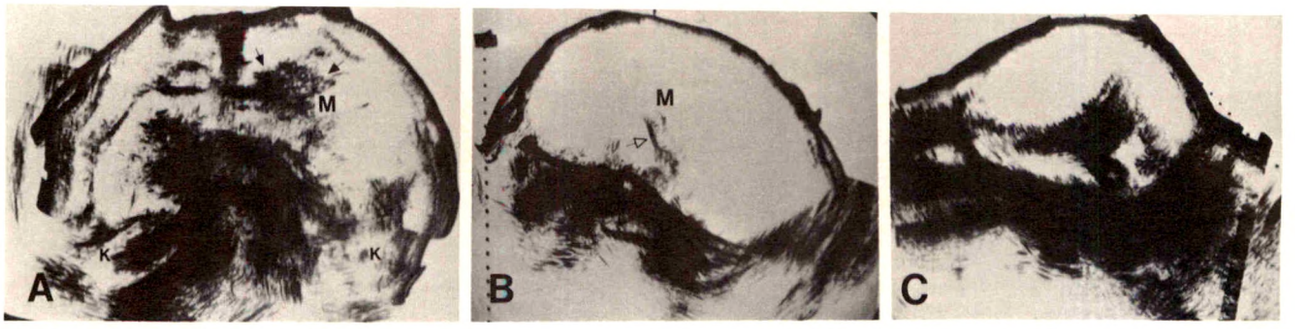

Fig. 2.—Cystadenocarcinoma in 75-year-old female. *A*, Transverse ultrasound scan at level of kidneys (K) showing complex mass (M) filling left side of abdomen. High gain setting emphasizes tumor excrescences (*arrows*). *B*, Longitudinal scan (low gain) 5 cm left of midline showing mass to be anechoic except for minimal echoes arising from septum (*arrow*). *C*, Longitudinal scan (high gain) 2 cm left of midline showing diffuse echoes arising from internal septa.

TABLE 1

Angiographic Findings in Cystic Neoplasms of the Pancreas

	Cystadenoma	Cystadenocarcinoma			
	Case 1	Case 2	Case 3	Case 4	Case 5
Age and sex	75,F	49,F	35,F	42,M	71,F
Arterial changes:					
Displacement	0	+	++	+	++
Dilatation	++	+++	0	0	+++
Neovascularity	++	+	0	+	+++
Venous changes:*					
Obstruction or encasement	0	+	+	+	+
Arteriovenous shunting	0	0	0	0	+
Tumor stain	++	++	0	+	++
Associated areas of lucency	0	+	0	+	+
Overall vascularity	Moderate	Moderate	Hypovascular	Moderate	Moderate

* Contrast puddling not seen.

TABLE 2

Angiographic Findings in Published Cases of Cystic Pancreatic Neoplasms

	Cystadenoma	Cystadeno-carcinoma
Arterial changes:		
Displacement	17 (94)	2
Dilatation	11 (61)	2
Neovascularity	14 (78)	3
Venous changes:		
Obstruction or encasement*	7	2
Arteriovenous shunting†	4	0
Tumor stain	15 (83)	3
Associated areas of lucency	15 (83)	2
Contrast puddling	3 (17)	1
Overall vascularity:		
Hypervascular	10 (56)	2
Moderately vascular	4 (22)	1
Hypovascular	4 (22)	1
Total	18	3

Note.–Data on 21 cases [6–20]. Numbers in parentheses are percentages.
* Information not available in eight cases.
† Information not available in seven cases.

plasms. One patient had a preoperative diagnosis of ovarian cystadenocarcinoma (fig. 2).

Tables 1 and 2 list angiographic findings in our series and in other published cases, respectively. Four of five arteriograms demonstrated moderately vascular pancreatic masses with neovascularity and tumor staining. In three cases, irregular areas of lucency were identified within the masses, giving them a heterogenous appearance. The areas of lucency and tumor stain correlated grossly with the cystic and solid tissue components of the tumor (fig. 3). Puddling of contrast was not seen, and only one case demonstrated arteriovenous shunting (fig. 4). One cystadenocarcinoma was hypovascular with no evidence of tumor stain (fig. 5). Although previous reports have described hypovascular cystadenomas [7, 13], this is only the second report of a hypovascular cystadenocarcinoma [20].

While ultrasonographic characteristics of four cases of cystadenoma have been described [21 ,22], this is the first report of sonographic findings in cystadenocarcinoma. Features were similar for the two types of lesions. Three neoplasms were located in the body of the pancreas, two in the tail, and one in the head. They ranged from 7–23 cm in diameter (average, 14 cm). Each had sharply defined borders with marginal irregularities, correlating with grossly identified tumor lobulation (fig. 3). There was excellent posterior wall visualization and through-transmission in each case (fig. 6). Overall, the neoplasms tended to be relatively anechoic at low gain settings; however, septation was seen in all six cases

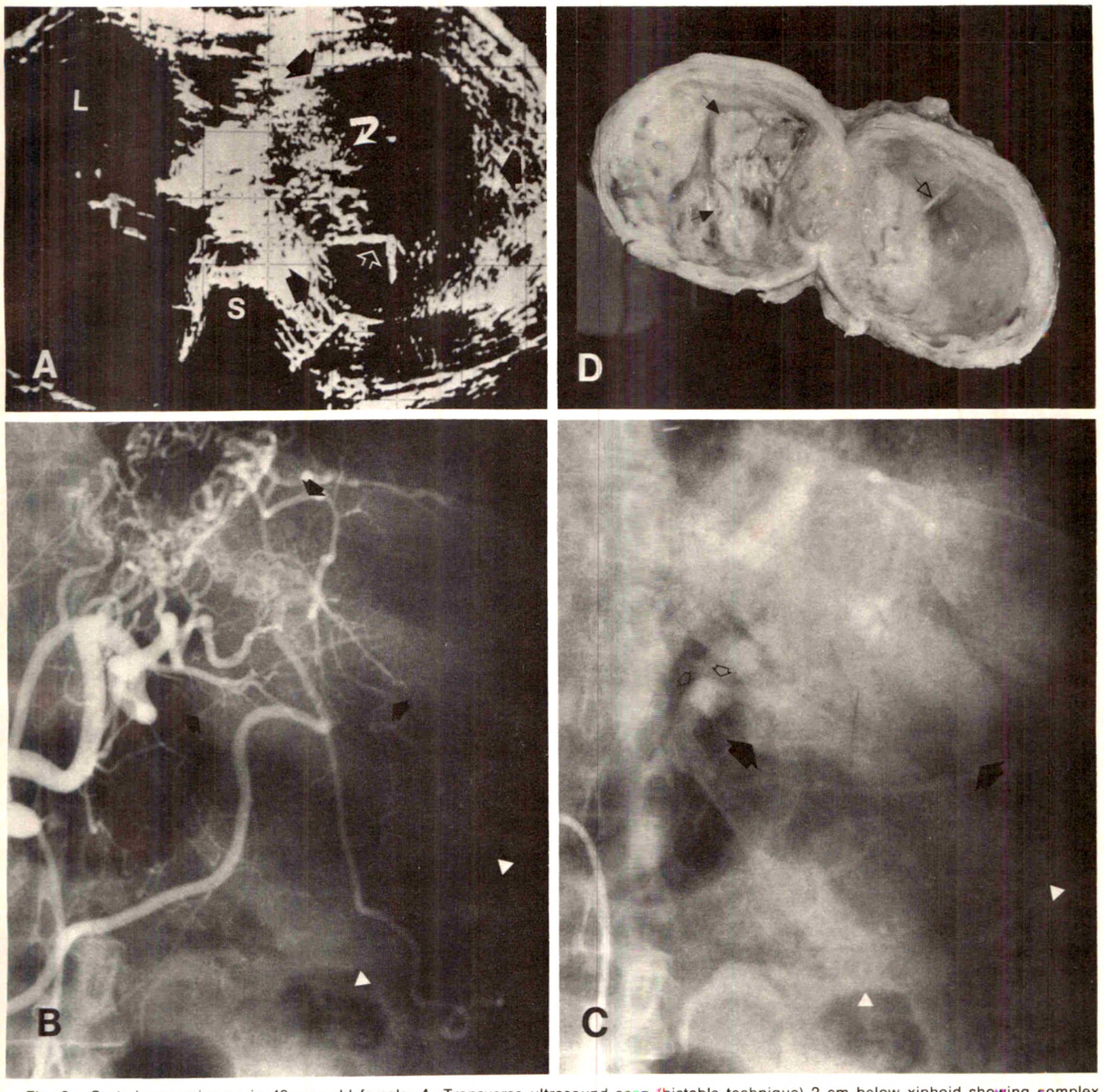

Fig. 3.—Cystadenocarcinoma in 49-year-old female. *A*, Transverse ultrasound scan (bistable technique) 2 cm below xiphoid showing complex pancreatic mass (*black arrows*) with septa (*open arrow*) and nodule of solid tissue medially (*white arrow*). Borders are well defined but irregular. L = liver, S = spine. *B and C*, Celiac arteriogram, arterial phase (*B*) and venous phase (*C*), showing large pancreatic mass with displacement and encasement of splenic artery and obstruction of splenic vein. Inferior portion of mass (*white arrows*) is hypovascular; superior portion is hypervascular with neovascularity and irregular area of tumor stain (*black arrows*). Note large draining vein (*open arrows*). *D*, Bivalved gross specimen showing smooth lining and septation (*open arrow*). Superiomedial area of tumor excrescence (*closed arrows*) corresponds to areas of solid tissue and neovascularity seen on ultrasonogram and arteriogram, respectively.

and produced linear collections of echoes (figs. 2–4). Increasing gain settings resulted in irregular fill-in patterns which seemed to be related to the degree of internal septation and tumor excrescence (figs. 2 and 3). Two of the neoplasms had separate distinct areas of solid and cystic tissue (fig. 4).

Discussion

Cystic neoplasms of the pancreas are rare, comprising only 10%–15% of all pancreatic cysts. They occur more frequently in females and, compared with conventional pancreatic adenocarcinoma, tend to arise at an earlier age [3–5]. In the series of Becker et al. [3], age range was

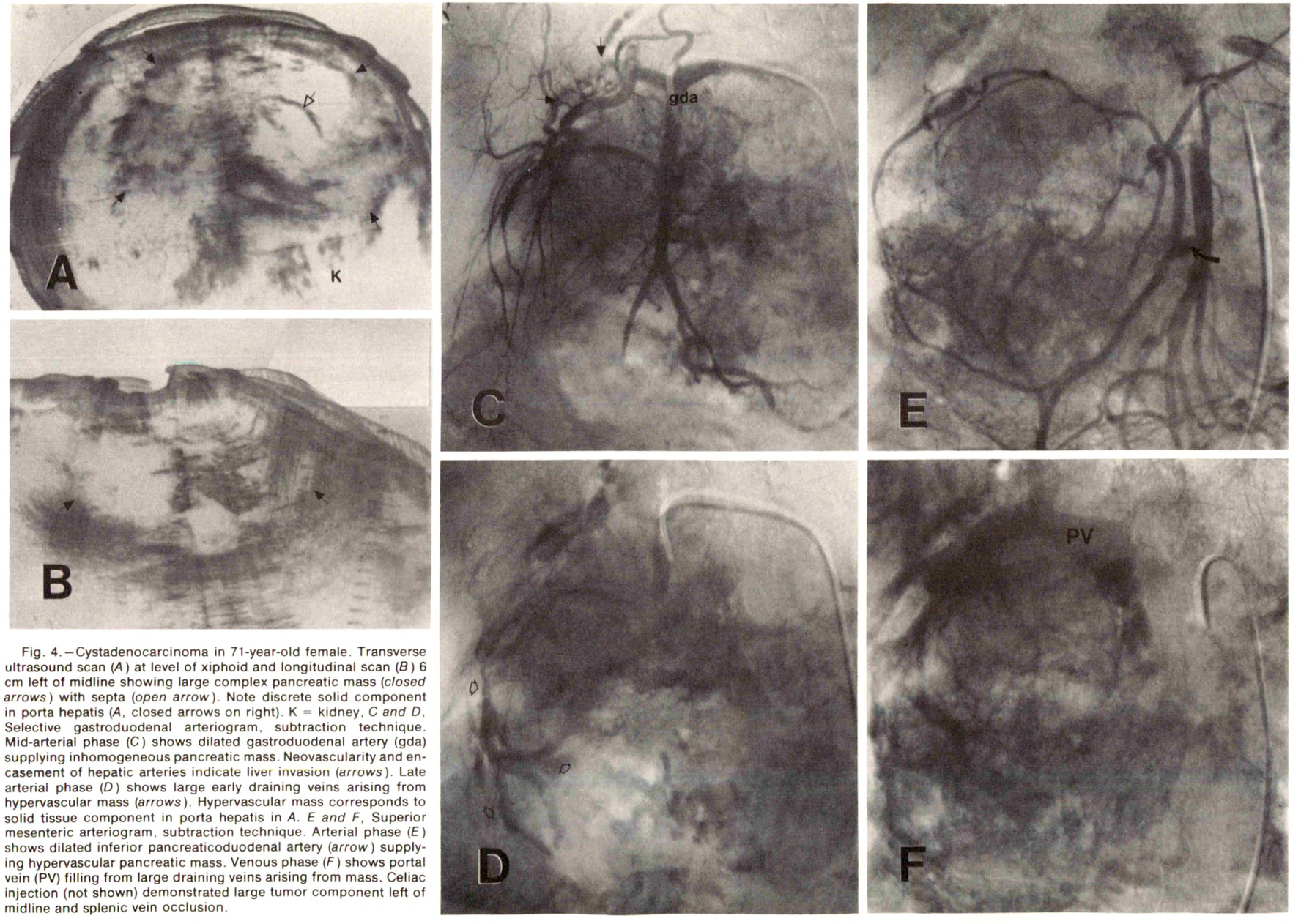

Fig. 4.—Cystadenocarcinoma in 71-year-old female. Transverse ultrasound scan (*A*) at level of xiphoid and longitudinal scan (*B*) 6 cm left of midline showing large complex pancreatic mass (*closed arrows*) with septa (*open arrow*). Note discrete solid component in porta hepatis (*A*, closed arrows on right). K = kidney, *C and D*, Selective gastroduodenal arteriogram, subtraction technique. Mid-arterial phase (*C*) shows dilated gastroduodenal artery (gda) supplying inhomogeneous pancreatic mass. Neovascularity and encasement of hepatic arteries indicate liver invasion (*arrows*). Late arterial phase (*D*) shows large early draining veins arising from hypervascular mass (*arrows*). Hypervascular mass corresponds to solid tissue component in porta hepatis in *A*. *E and F*, Superior mesenteric arteriogram, subtraction technique. Arterial phase (*E*) shows dilated inferior pancreaticoduodenal artery (*arrow*) supplying hypervascular pancreatic mass. Venous phase (*F*) shows portal vein (PV) filling from large draining veins arising from mass. Celiac injection (not shown) demonstrated large tumor component left of midline and splenic vein occlusion.

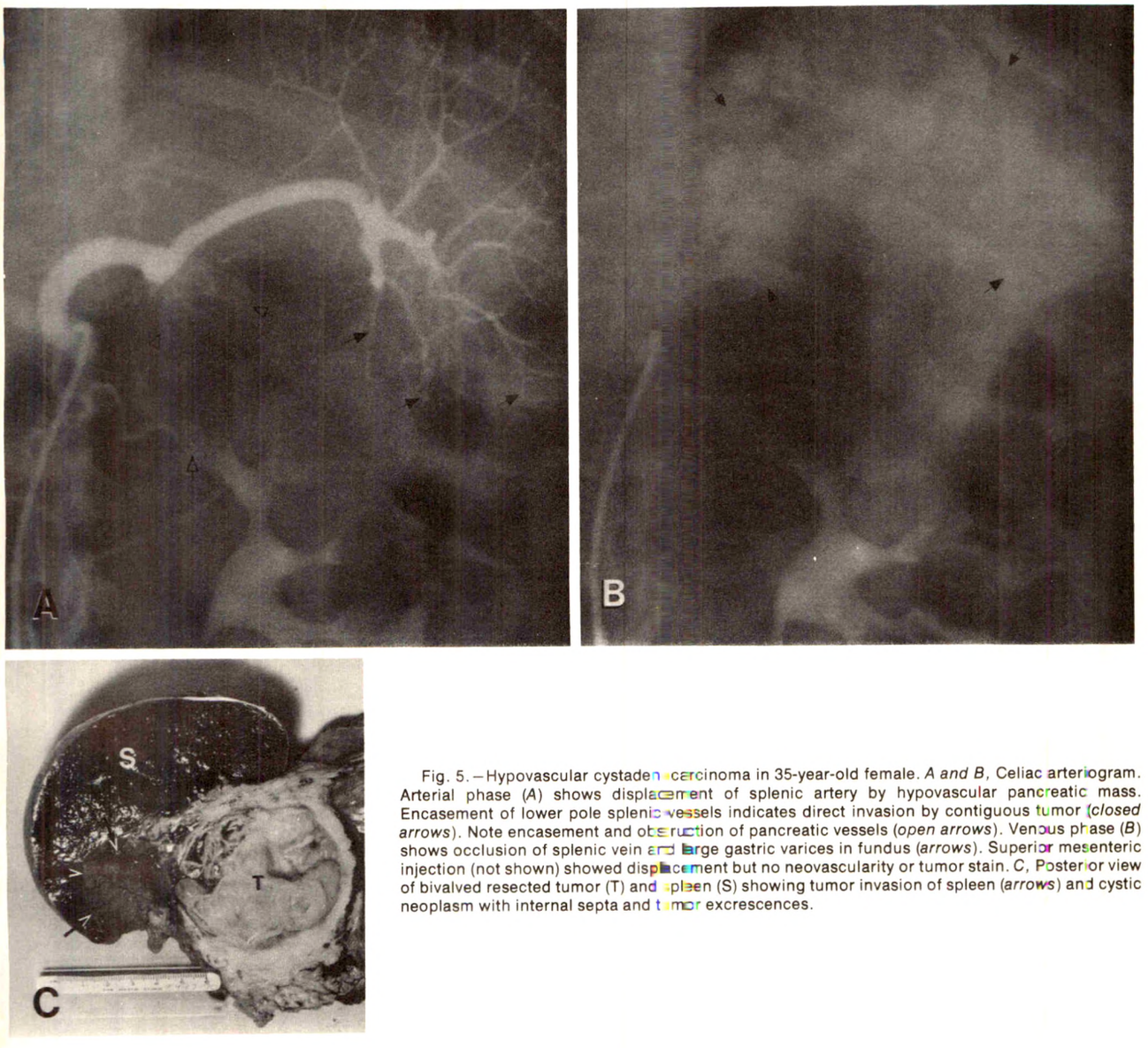

Fig. 5.—Hypovascular cystadenocarcinoma in 35-year-old female. *A and B*, Celiac arteriogram. Arterial phase (*A*) shows displacement of splenic artery by hypovascular pancreatic mass. Encasement of lower pole splenic vessels indicates direct invasion by contiguous tumor (*closed arrows*). Note encasement and obstruction of pancreatic vessels (*open arrows*). Venous phase (*B*) shows occlusion of splenic vein and large gastric varices in fundus (*arrows*). Superior mesenteric injection (not shown) showed displacement but no neovascularity or tumor stain. *C*, Posterior view of bivalved resected tumor (T) and spleen (S) showing tumor invasion of spleen (*arrows*) and cystic neoplasm with internal septa and tumor excrescences.

13–83 years for cystadenoma and 18–76 years for cystadenocarcinoma.

The clinical presentation of cystic neoplasms is nonspecific. A palpable abdominal mass in a patient with long duration of symptoms and no history of traumatic or inflammatory pancreatitis is common [3]. Symptoms are related to pressure on adjacent organs. Associated biliary tract disease was noted in 12% of the cases reported by Becker et al. [3]. However, jaundice was unusual due to the relative infrequency of cyst origin in the pancreatic head. Although hemorrhage is not uncommon in patients with pancreatic pseudocysts, only one case of bleeding has been described with a cystadenoma [23]. Soloway [24] noted an unusually high incidence (40%) of associated malignant tumors in patients with cystadenomas. This had not been described previously and was not mentioned in the extensive review by Becker et al. [3]. Only one of our patients developed a subsequent unrelated neoplasm—a mucinous cystadenocarcinoma of the ovary.

Pathology

Several theories of the origin of cystic pancreatic neoplasms have been described. It has been suggested that the lesions result from (1) displaced embryonic cells of the alimentary canal primordia; (2) neoplastic proliferation of the pancreatic acinar epithelium; and (3) proliferation of the pancreatic ductal epithelium [4]. The most common theory is that they result from neoplastic change of the pancreatic ductal epithelium [25]. Cystadenocarcinomas quite likely are the result of malignant change in a previously benign cystadenoma [26, 27]. This theory is supported by: (1) similarity of sites of origin, sex, and age distribution [27]; (2) coexistence of

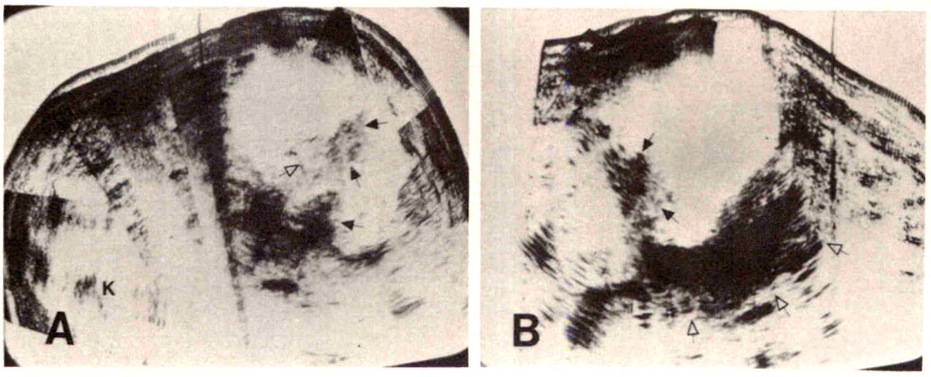

Fig. 6.—Cystadenocarcinoma in 82-year-old male. *A*, Transverse ultrasound scan 2 cm below xiphoid showing sharply marginated complex pancreatic mass with irregular borders. Note central area of tumor excrescence (*closed arrows*) and septum (*open arrow*). K = kidney. *B*, Longitudinal scan 5 cm to left of midline showing enhanced echoes arising from septum at higher gain (*closed arrows*). Note good through-transmission and strong posterior wall echoes (*open arrows*).

benign and malignant areas in the same neoplastic cyst with a definite transition between the two [5]; and (3) development of cystadenocarcinoma in a benign cystadenoma followed for several years [26].

Cystic neoplasms are most common in the body and tail of the pancreas and have a characteristic gross appearance [28]. They are round, lobulated, multiloculated cysts covered by a thin capsule. The cut sections usually have a honeycomb appearance with multiple small and large cysts and a variable amount of solid tumor (figs. 3 and 5). They usually contain serous or mucinous fluid. Diameter varies from a few centimeters up to 20 cm.

The cysts are lined by a single layer of epithelium which may be flat, cuboidal, or columnar. The lining may be smooth or may be thrown into multiple papillary projections [4]. Differentiation between cystadenocarcinoma and multilocular cysts of the pancreas may be difficult or impossible [4]. Malignant change is determined by the presence of invasion of the cyst wall, distant metastases, regional lymph node involvement, or histologic dedifferentiation [27].

Radiologic and Ultrasonographic Features

Prior to the widespread use of angiography, radiologic features of cystic pancreatic neoplasms were nonspecific. Although a sunburst pattern of calcification (fig. 1) has been described as quite characteristic, it is seen in less than 10% of cases [3, 28, 29]. Barium studies of the stomach, small bowel, and colon may show extrinsic displacement or invasion (fig. 3).

The first description of the angiographic appearance of pancreatic cystadenoma was by Pyrah and Cowie in 1957 [14]. Since that time, the arteriographic findings in only 18 cystadenomas and three cystadenocarcinomas have been published (table 2). Initially, both cystadenomas and cystadenocarcinomas were considered hypervascular neoplasms. However, four of the 18 reported cases of cystadenoma are hypovascular [7, 13]. The current case (fig. 5) is only the second reported arteriogram of a hypovascular cystadenocarcinoma. Typically, both lesions tend to be hypervascular with enlargement of feeding arteries, neovascularity, and tumor stain. The degree of vascularity is related to the relative proportion of cystic to solid tumor (figs. 3 and 5). Mixed lesions usually are hypervascular with scattered, irregular lucencies. Venous obstruction or encasement is common. Including the present series, contrast puddling and early venous shunting were seen in only five of the 25 arteriograms. The current cases and a review of the published arteriograms (table 2) indicate that cystadenocarcinoma can be differentiated from cystadenoma only if metastases or invasion of contiguous organs are demonstrated (figs. 4 and 5). Arteriography is the most specific radiologic procedure, and the diagnosis should be suggested in a majority of cases.

In the case of a hypovascular pancreatic mass, confusion with pseudocyst may arise. Gray scale ultrasonography, or perhaps computed tomography [40], plays an important role in subsequent differential diagnosis (fig. 3). A correct preoperative diagnosis was made in all three of our patients who had both ultrasonography and angiography. Wolson and Walls [21] described the ultrasonographic features of three cases of cystadenoma. The lesions were sonolucent with good through-transmission and slightly irregular but well defined margins. Internal echoes frequently arose from septa. The sonographic findings in the present series are the first to be reported for pancreatic cystadenocarcinoma and did not differ from those of cystadenoma [21, 22]. The value of ultrasonography was the identification of septa and the diffusely increasing irregular echo pattern at high gain settings (figs. 2 and 6). Although these findings are fairly specific for cystic neoplasms, a hemorrhagic pseudocyst might have a similar pattern. Although we have not had the opportunity to study a pancreatic adenocarcinoma with an associated pseudocyst, this combination has been reported [30] and probably would be impossible to differentiate from a cystadenocarcinoma.

Most islet cell tumors are suspected clinically due to their hormonal activity. These lesions are usually small (1–3 cm) when studied angiographically and present no difficulty in differential diagnosis. Islet cell tumors which are endocrinologically quiescent frequently are large (6–20 cm) and hypervascular [31, 32]. These lesions may be confused with cystic neoplasms. Dilatation of feeding arteries, tumor blush, neovascularity, venous obstruction, and early draining veins may be seen. Vascular displacement, lobulated contours, and lucencies within the mass (cystic spaces) are helpful differentiating fea-

tures suggesting cystic neoplasm. Gray scale ultrasonography is useful in characterizing the lesion as solid and thus provides important information for preoperative differential diagnosis.

Traumatic or postinflammatory pancreatic pseudocysts are easily differentiated from cystic neoplasms with current radiographic modalities. Plain films may show the typical small calcifications of chronic pancreatitis or curvilinear calcifications in the wall of the pseudocyst. The sunburst pattern seen in cystic neoplasms (fig. 1) has not been described with chronic pancreatitis or pseudocysts. Ultrasound examination of pancreatic pseudocysts usually demonstrates a unilocular, anechoic (cystic) mass with good through-transmission and a strong posterior wall [33]. Although these lesions are usually completely cystic, occasionally they may be multiloculated and contain debris, blood, or pseudoaneurysms which may produce internal echoes; thus they might be confused with a cystic neoplasm. Clinical features are usually helpful. Serial scans are important since pseudocysts are dynamic lesions and frequently demonstrate changes in size and structure.

Endoscopic retrograde cholangiopancreatiography usually demonstrates the typical ductal changes of pancreatitis; about 60% of pseudocysts communicate with the main pancreatic duct and are filled at the time of the study [34]. Although only a few such examinations of cystic pancreatic neoplasms have been described [35], the ductal changes of pancreatitis, with or without associated pseudocyst, and pancreatic carcinoma are well defined and should not present interpretative problems [35, 36].

Pancreatic angiography is accurate in the diagnosis of pseudocysts. Typical findings are an avascular mass with vessel displacement, occasional occlusion or compression of the splenic vein, and associated arteriographic changes of chronic pancreatitis [36, 37]. There is no dilatation of surrounding vessels, neovascularity, tumor blush, or contrast puddling.

Treatment

The importance of preoperative diagnosis and differentiation of cystic pancreatic neoplasms from posttraumatic or inflammatory cystic lesions of the pancreas is manifested by the difference in surgical treatment of neoplastic and nonneoplastic cysts. Inflammatory pseudocysts may be managed medically or treated surgically by internal drainage procedures [1, 38]. The treatment for cystic neoplasms is total surgical excision [3, 4, 39]. Drainage procedures are inadequate and may lead to recurrence or eventually to malignant change and metastasis. Cystadenocarcinomas typically are slowly growing neoplasms which metastasize late. Early diagnosis and resection usually result in cure or excellent survival. Occasionally, drainage procedures may be used for temporary palliation for unresectable cystadenocarcinoma [3, 27]. In one of our patients, a cystojejunostomy was used for temporary palliation, which resulted in reduction of size of the neoplasm and facilitated subsequent surgical resection.

ACKNOWLEDGMENT

We thank Sheila Green for help in preparing the manuscript.

REFERENCES

1. Scharplatz D, White TT: A review of 64 patients with pancreatic cysts. *Ann Surg* 176:638–640, 1972
2. Nardi GL, Lyon DC, Sheiner JH, Bartlett MR: Solitary retention cysts of the pancreas. *N Engl J Med* 280:11–15, 1969
3. Becker WF, Welsh RA, Pratt HS: Cystadenoma and cystadenocarcinoma of pancreas. *Ann Surg* 161:845–863, 1965
4. Piper CE, ReMine WH, Priestley JT: Pancreatic cystadenoma. Report of 20 cases. *JAMA* 180:648–652, 1962
5. Cullen PK, ReMine WH, Dahlin DC: A clinicopathologic study of cystandenocarcinoma of the pancreas. *Surg Gynecol Obstet* 117:189–195, 1963
6. Boijsen E: Pancreatic angiography, in *Angiography*, edited by Abrams HL, Boston, Little, Brown, 1971, pp 967–970
7. Abrams RM, Berenbaum ER, Berenbaum SL, Ngo NL: Angiographic studies of benign and malignant cystadenoma of pancreas. *Radiology* 89:1028–1032, 1967
8. Baum S, Kuroda K, Roy RH: Value of special angiographic techniques in management of patients with abdominal neoplasms. *Radiol Clin North Am* 3:583–599, 1965
9. Bieber WP, Albo RJ: Cystadenoma of the pancreas: its angiographic diagnosis. *Radiology* 80:776–778 1963
10. Cheung L, Matolo N, Maxwell JG: Cystadenoma of the pancreas. Report of a case and its arteriographic diagnosis. *Gastroenterology* 67:155–158, 1974
11. Didolkar MS, Malhotra Y, Holyohe ED: Cystadenoma of the pancreas. *Surg Gynecol Obstet* 140:925–928, 1975
12. Glenn F, Evans JA, Halpern M, Thorbjarnson B: Selective celiac and superior mesenteric arteriography. *Surg Gynecol Obstet* 118:93–100, 1964
13. Pressman BS, Asch T, Casarella WJ: Cystadenoma of the pancreas. A reappraisal of angiographic findings. *Am J Roentgenol* 119:115–120, 1973
14. Pyrah LN, Cowie JW: Two unusual aortograms. *J Faculty Radiol* 8:416–420, 1957
15. Rösch J: Tumors, in *Gastrointestinal Angiography*, edited by Feuter SR, Redman HC, Philadelphia, Saunders, 1972, p 138
16. Rösch J: *Roentgenology of the Spleen and Pancreas*. Springfield, Ill., Thomas, 1967
17. Suzuki T, Kawabe K, Nakayasu An, Takeda H, Kobayashi K, Kubota N, Honjo I: Selective arteriography in cancer of the pancreas at a resectable stage. *Am J Surg* 122:404–407, 1971
18. Swanson GE: A case of cystadenoma of the pancreas. *Radiology* 81:592–595, 1963
19. Van Cangh PJ, Thorlakson RH: Cystadenoma of the pancreas. *Can J Surg* 11:63–68, 1968
20. Hawkins IF Jr, Kaude JV: Angiographic findings in some rare pancreatic tumors. *Fortschr Geb Roentgenstr Nuklearmed* 125:521–526, 1976
21. Wilson AH, Walls WJ: Ultrasonic characteristics of cystadenoma of the pancreas. *Radiology* 119:203–205, 1976
22. Stuber JL, Templeton AW, Bishop K: Sonographic diagnosis of pancreatic lesions. *Am J Roentgenol* 116:406–412, 1972
23. Rosenbaum H, Connolly PJ, Climie AWR, Reveno WS: Pancreatic cystadenoma with intestinal hemorrhage. *Am J Roentgenol* 90:735–739, 1963
24. Snoeway HB: Constitutional abnormalities associated with

pancreatic cystadenomas. *Cancer* 18:1297–1300, 1965
25. Glenner GG, Mallory GK: Cystadenoma and related nonfunctional tumors of the pancreas. Pathogenesis, classification and significance. *Cancer* 9:980–996, 1956
26. Probstein JG, Blumenthal HT: Progressive malignant degeneration of a cystadenoma of the pancreas. *Arch Surg* 81:683–689, 1960
27. Sawyer RB, Sawyer JC, Spencer JR: Proliferative cysts of the pancreas. *Am J Surg* 116:763–767, 1968
28. Barbee CL, DeMello FB, Grage TB: Cystadenoma and cystadenocarcinoma of the pancreas. *J Surg Oncol* 8:1–10, 1976
29. Haukohl RS, Melamed A: Cystadenoma of pancreas: a report of two cases showing calcification. *Am J Roentgenol* 63:234–245, 1950
30. Gambill EE: Pancreatitis associated with pancreatic carcinoma: a study of 26 cases. *Mayo Clin Proc* 46:174–177, 1971
31. Deutsh V, Adar R, Jacob ET, Bank H, Mozes M: Angiographic diagnosis and differential diagnosis of islet-cell tumors. *Am J Roentgenol* 119:121–132, 1973
32. Baghery S, Alfidi RJ, Zelch MG: Angiography of non-functioning islet-cell tumors of the pancreas. *Radiology* 120:57–59, 1976
33. Bradley EL, Clements JL: Implications of diagnostic ultrasound in the surgical management of pancreatic pseudocysts. *Am J Surg* 127:163–173, 1974
34. Silvis SE, Vennes JA, Rohrmann CA: Endoscopic pancreatography in evaluation of patients with suspected pancreatic pseudocysts. *Am J Gastroenterol* 62:452–459, 1974
35. Bilbao MK, Katon RM: Neoplasms of the pancreas, in *Atlas of Endoscopic Retrograde Cholangiopancreatography*, edited by Stewart ET, Vennes JA, Gennen JE, St. Louis, Mosby, 1977, pp 124–235
36. Freeny PC, Ball TJ: Evaluation of endoscopic retrograde cholangiopancreatography (ERCP) and angiography in the diagnosis of pancreatic carcinoma. *Am J Roentgenol* 130:683–691, 1978
37. Reuter SR, Redman HC, Joseph RR: Angiographic findings in pancreatitis. *Am J Roentgenol* 107:56–64, 1969
38. Warren KW, Badosa F: Individualization in treatment of pancreatic cysts. *Am Surg* 39:555–561, 1973
39. Warren KW, Hardy KJ: Cystadenocarcinoma of the pancreas. *Surg Gynecol Obstet* 127:734–736, 1968
40. Carroll B, Sample WF: Pancreatic cystadenocarcinoma: CT body scan and gray scale ultrasound appearance. *Am J Roentgenol* 131:339–341, 1978

Lymphangiographic Changes after Radiation Therapy

KJELL JONSSON,[1, 2] HERMAN I. LIBSHITZ,[1] AND BARBARA M. OSBORNE[3]

Lymphangiographic appearance following radiotherapy is described in 21 patients with pre- and posttherapy lymphangiograms. Following radiotherapy to normal lymphatics, decrease in nodal size and lymph vessel caliber is noted uniformly after 12 months. Before 12 months the development of these changes is variable and may not be seen, especially during the first several months. Following irradiation of abnormal lymph nodes, dilatation of the lymph vessels distal to the abnormal nodes may occur. These lymphangiographic findings can be related to histologic changes seen in lymph nodes after radiation therapy.

Lymphangiography is a useful tool in evaluating the extent of malignant tumors before treatment and possible recurrence of disease following treatment. It is important to appreciate the alterations in the lymphatics caused by radiation therapy. This report reviews our experiences with patients who have had lymphangiograms both before and at variable intervals after radiation therapy.

Materials and Methods

Twenty-one patients were identified who had lymphangiograms both before and after radiation therapy. Three patients had two lymphangiograms after therapy and one had three. Patients who received cytotoxic medication were excluded since the lymph nodes can be affected by these medications. The average age at treatment was 43 years (range, 12–73 years). The length of time from radiation therapy to follow-up lymphangiogram ranged from 3 to 106 months (average, 36 months). Eleven of the patients had lymphoma (eight Hodgkin's disease, three non-Hodgkin's lymphoma). Seven of the patients had squamous cell carcinoma of the cervix, and three had adenocarcinoma of the cervix.

The lowest radiation dose was 2,000 rad in two fractions of 1,000 rad 32 days apart. The next lowest dose was 2,850 rad, given at 200 rad per day in 14 treatments over 19 elapsed days. All other patients received 3,000 rad or more. The highest dose was approximately 6,000 rad in patients with cervical cancer generally delivered in two radium insertions and 4,000 rad external beam therapy.

Findings

Pathologic Changes

The effects of radiation on lymph nodes have been well described both in clinical situations and in carefully designed experimental studies in inbred mice [1]. The effects on lymph vessels in clinical situations have been less well defined.

The fact that radiation in therapeutic doses results in decreased size of lymph nodes is explained by the radiosensitivity of the T and B lymphocytes of the lymph nodes. Experimentally, it has been shown that B cells are more radiosensitive and that B-dependent areas in the lymph node become depleted more rapidly than T-dependent areas. Burge [2] corroborated this in a clinical study; he found that with increasing doses of radiation, the changes in the lymph nodes become more pronounced. At doses less than 1,000 rad, decreased cellularity of the lymphoid follicles, B-dependent areas, was noted. These changes progressed at doses over 2,000 rad to actual disruption of follicles with the appearance of eosinophilic material between cells of germinal centers. Lymph nodes exposed to over 4,000 rad eventually became hyalinized with fibrosis, particularly if radiation therapy preceded the lymphadenectomy by several months. While we did not observe these extreme changes of complete fibrous replacement of nodes, irradiated nodes did show lymphoid depletion and some capsular fibrosis with a plasma cell infiltrate. Many of the irradiated lymph nodes show a decreased size and number of follicles.

Presumably, failure to completely repopulate the lymph node accounts for the smaller size of nodes following irradiation. Experimental studies in mice [1] show that T cell restoration from exogenous sources occurs earlier than B cell restoration, and it is not clear that B cell restoration is ever complete. Therefore, the smaller follicles, B cell–dependent areas, in irradiated nodes may account in part for the smaller size of lymph nodes in postirradiation lymphangiograms. The clinical study of Burge [2] showed the average follicular size was smaller in irradiated notes.

In normal lymph nodes which have been irradiated, the subcapsular sinuses and deeper sinuses remain patent (fig. 1*A*). In tumor-bearing lymph nodes the first area involved with metastasis is the subcapsular sinus into which the afferent lymphatic channels drain. If the radiotherapy has eradicated the metastasis, depending upon the interval following irradiation, there is first tumor necrosis, then a xanthogranulomatous reaction, and finally fibrosis marking the prior site of metastatic tumor. The fibrosis clearly obliterates the subcapsular sinus where the metastasis was located (fig. 1*B*). Occasionally viable tumor will be found in such areas of fibrosis, pointing to the fact that fibrosis follows eradication of the tumor. This obstruction presumably causes dilatation of afferent lymphatics due to increased resistance.

Received April 13, 1978; accepted July 18, 1978.

[1] Department of Diagnostic Radiology, University of Texas System Cancer Center, M. D. Anderson Hospital and Tumor Institute, Houston, Texas 77030. Address reprint requests to H. I. Libshitz.

[2] Present address: Department of Diagnostic Radiology, Allmänna Sjukhuset, 21401 Malmo, Sweden.

[3] Department of Pathology, University of Texas System Cancer Center, M. D. Anderson Hospital and Tumor Institute, Houston, Texas 77030.

© 1978 American Roentgen Ray Society

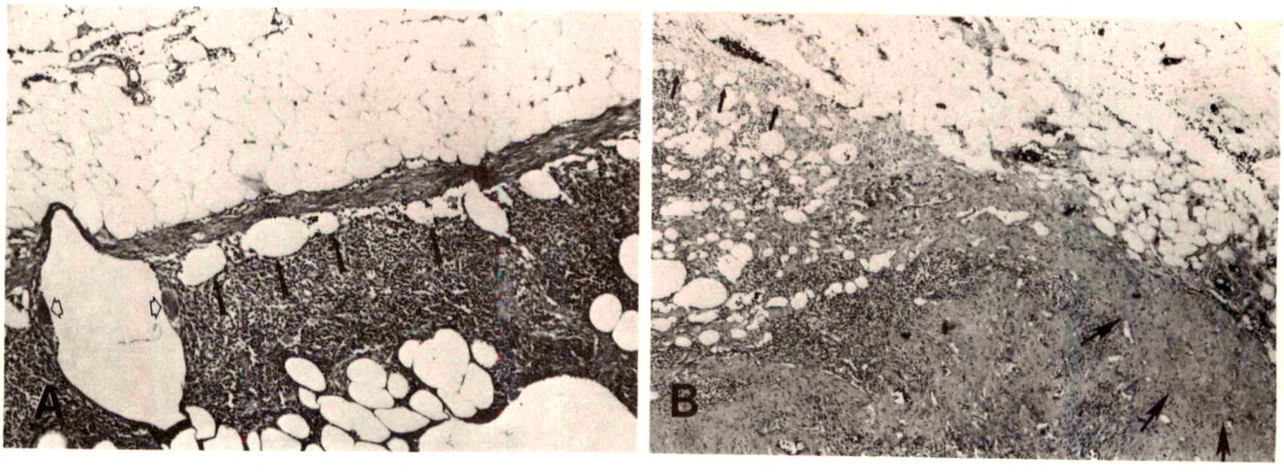

Fig. 1.—*A*, Irradiated lymph node containing no metastatic tumor. Subcapsular sinuses are patent (*black arrows*). Lymphangiogram effect is seen in lower portion of photograph. Note hypocellularity and absence of follicles. Large subcapsular sinus with giant cell on either side (*open arrows*) is seen on left. H and E, ×50. *B*, Lymph node from same patient containing metastatic embryonal carcinoma of testis which has been irradiated. Note residual fibrous tissue with obliteration of subcapsular sinuses (*large arrows*) where metastatic tumor has been eradicated. Subcapsular sinuses are patent (*small arrows*) where there had been no secondary deposits. Lymphangiogram effect is seen below this. H and E, ×30.

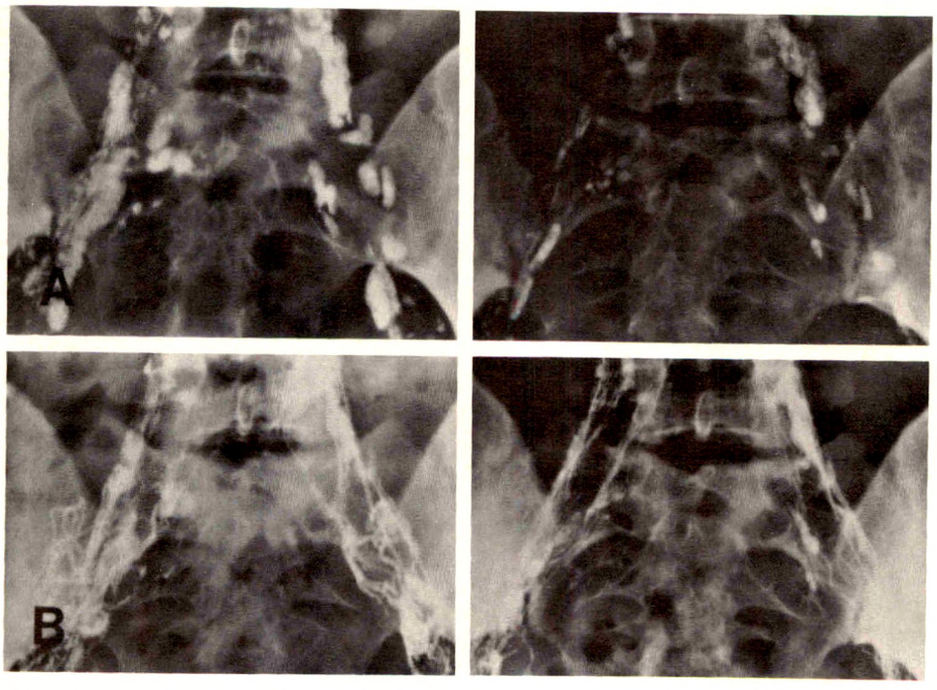

Fig. 2.—30-year-old female with squamous cell carcinoma of cervix treated with two radium applications and 4,000 rad external irradiation. *A*, Nodal phase of normal pretreatment lymphangiogram (*left*) and lymphangiogram 27 months after treatment (*right*). Nodes in irradiated field below lumbosacral junction are smaller after therapy. *B*, Vascular phase of pre- (*left*) and posttreatment (*right*) lymphangiogram. Caliber of channels in irradiated field has diminished.

Radiographic Changes

Patients were divided into three groups: (1) normal pretreatment lymphangiogram and follow-up study at least 12 months after irradiation; (2) follow-up study less than 12 months after therapy (normal or abnormal pretreatment nodes); and (3) abnormal nodes before therapy.

The number of patients in the three groups is greater than 21 because of multiple postirradiation lymphangiograms in three patients and because two patients were in both the second and third groups.

Normal pretreatment nodes and follow-up study at least 12 months after irradiation. Ten of these 11 patients had decrease in the size of lymph nodes and lymph vessels on the follow-up lymphangiogram. The other patient also had decrease in the size of the lymph nodes but showed dilatation of the lymph vessels immediately distal to a paraaortic lymph node biopsy. All of the other lymph channels were diminished in caliber. A typical example is shown in figure 2.

Follow-up lymphangiogram less than 12 months after irradiation. The seven patients in this category were seen at 3, 4, 9 (two patients), and 10 months (three patients). The patient seen 4 months after irradiation is the only one in whom the nodes did not decrease in size. Another nodal area in this patient that was separately irradiated 3 months earlier had decreased in size (7 months postirradiation). In four patients no change was seen in the caliber of lymph channels (patients seen at 3, 4, 9, and 10 months). The other three patients showed diminished caliber of the lymph vessels. A patient in whom the lymph

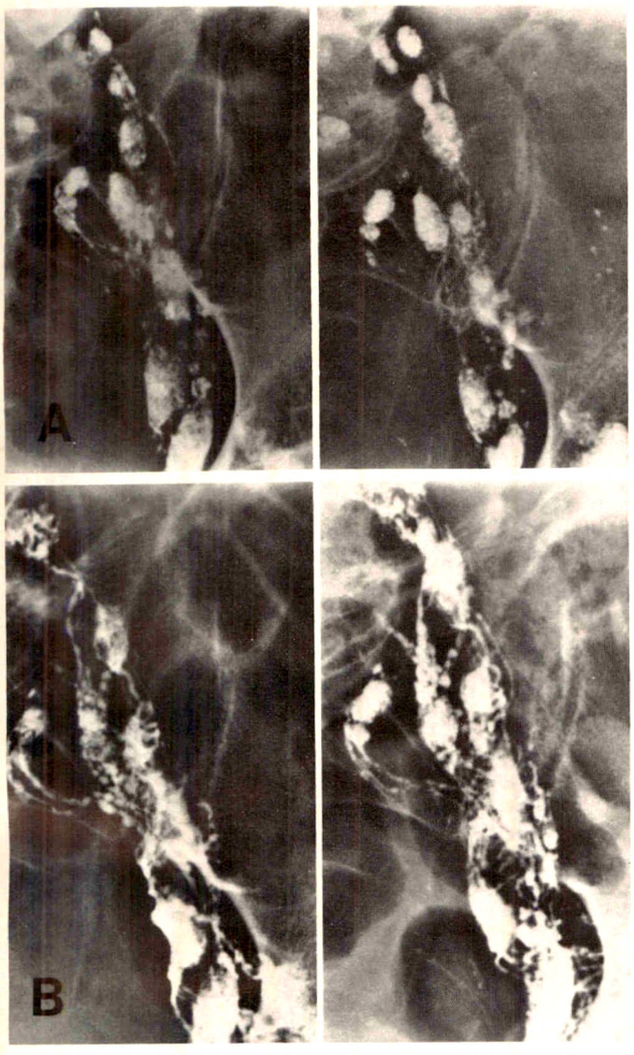

Fig. 3.—73-year-old female with squamous cell carcinoma of cervix treated with 3,000 rad ^{60}Co radiation pelvis. *A*, Nodal phase of pretreatment lymphangiogram (*left*) and lymphangiogram 3 months after therapy (*right*) showing slightly smaller lymph nodes, particularly near pelvic wall, after therapy. *B*, Vascular phase of pre- (*left*) and posttreatment (*right*) lymphangiograms showing no change in lymphatic channels after therapy.

nodes became smaller and the lymph vessels remained unchanged is shown in figure 3.

Abnormal nodes prior to radiation therapy. Abnormal lymph nodes were identified in six patients. Five of these patients had the follow-up lymphangiogram more than 1 year after irradiation. The sixth patient was seen 3 months after irradiation and is the same patient included in the group above at 3 months. Decrease in lymph node size was noted in all six patients. The lymph vessels were not changed in caliber in the patient seen at 3 months. Of the five seen at least 1 year after irradiation, three had increased caliber of vessels distal to the abnormal nodes (fig. 4), no change was seen in one, and the lymph channels could not be evaluated in one.

Discussion

Experimental studies in laboratory animals have been performed to evaluate the response of lymph vessels and nodes to irradiation. These, however, have often been performed utilizing large single doses of radiation or a few fractions in a short period of time. Lenzi and Bassani [3] irradiated the pelvis and paraaortic area of rabbits with 3,000–8,000 R, 500 R per day. One week after completion of irradiation the lymph vessels were injected with latex, and a preparation of the lymphatics was obtained. No alterations of the lymph vessels were noted after 3,000 R. At 6,000 R there was no interruption of the lymph vessels, but some dilatation and varicosities were noted. After 8,000 R the lymph vessels were tortuous and rigid and the varicosities were more evident but no disruption was noted. Uteri were examined in the same way following intracavitary radium treatment, and only with tissue necrosis at a dose of 25,000–30,000 R was disruption of lymph vessels found.

Engeset [4] performed a study in rats giving a single dose of 3,000 R to the right popliteal region; lymphangi-

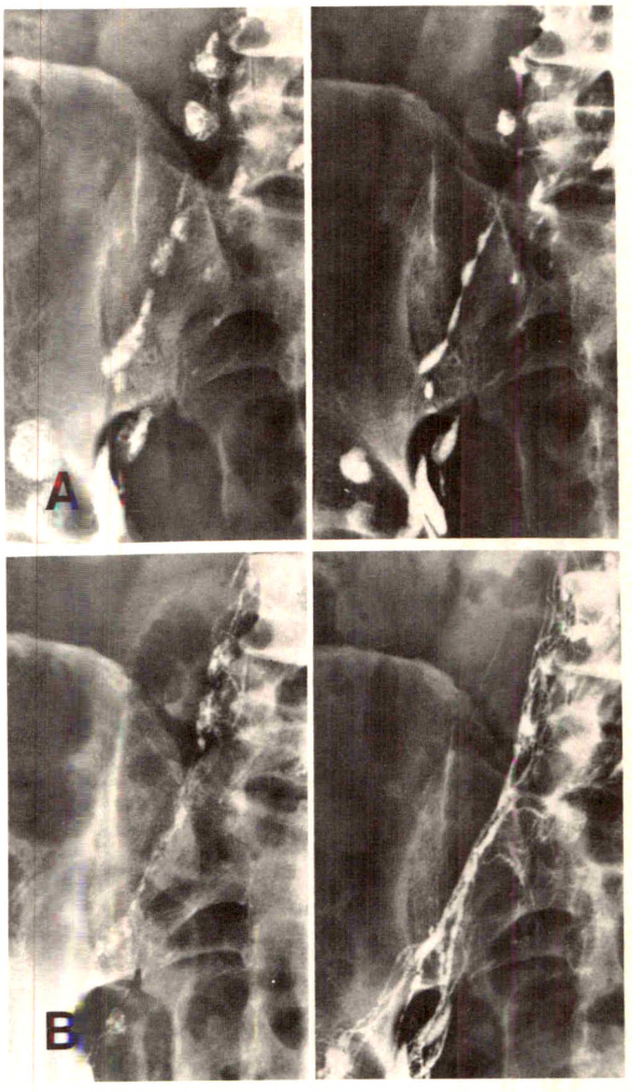

Fig. 4.—53-year-old male with Hodgkin's disease treated with ^{60}Co irradiation, 3,600 rad to paraaortic lymph nodes and 3000 rad to iliac lymph nodes. Paraaortic nodes were treated 24 months before and iliac nodes 27 months before second lymphangiogram. *A*, Nodal phase of pre- (*left*) and posttreatment (*right*) lymphangiogram. Abnormal node overlies transverse process of L5 and another is immediately above it. Other paraaortic nodes on right were also abnormal. Note uniform decrease in lymph node size after therapy. *B*, Vascular phase of pre- (*left*) and posttreatment (*right*) lymphangiogram showing increased caliber of lymphatic channels distal to abnormal nodes after therapy.

ography was then performed at various time intervals. During the first 6–9 months following irradiation the lymph vessels were unaltered, but after 1 year they were constricted by scar formation in the irradiated field. The lymph nodes were smaller on the irradiated side from 2 weeks following treatment when compared to the untreated side. In a smaller group of rats treated with fractionated doses (600 R in five fractions), the results were similar.

Sherman and O'Brien [5] carried out a similar study in 40 dogs. A control group and groups receiving 1,000 R, 2,400 R, 3,000 R, and 3,600 R were studied. The 1,000 R group received a single treatment. The other groups received three equal fractions at weekly intervals. The lymphatic channels remained essentially unchanged in all but four animals. Rupture of the afferent lymphatics was noted at the junction of irradiated and nonirradiated tissue several months after treatment (one at 2,400 R and three at 3,600 R). The lymph nodes in the treated dogs all were smaller after several months. No animal showed evidence of lymphatic obstruction.

Clinical studies describing the effects of radiation on the lymphangiographic appearance of vessels and nodes have in many cases been carried out without pretreatment lymphangiograms. In nearly all reports, decrease in size of the irradiated nodes was noted. No significant alteration in lymphatic flow was observed following radiation therapy in this series. There is general agreement that the usual therapeutic levels of radiation do not generally impede lymphatic flow [6–11]. However, others [11–13] have reported impaired lymphatic circulation, obstruction, and/or extravasation.

We believe that at therapeutic doses, time rather than dose is the prime factor in the development of radiation change. Similar changes are observed at doses given clinically above 2,500 rad. After 12 months there is a generally uniform response, with decrease in the size of nodes and narrowing of the lymph channels. These findings agree closely with those of Sedgenidze and Zyb [14] who considered alterations in the inguinal, external iliac, and common iliac nodes in patients with pelvic malignancy in whom pre- and postirradiation lymphangiograms were available.

Our findings include six of seven patients in whom the lymph nodes were smaller within 12 months of treatment. In our experience, decrease in lymph node size within the first year usually occurs in patients in whom opacified nodes have been followed on postlymphangiogram radiographs. Sedgenidze and Zyb [14] saw change in only 17% of the nodal groups in the first 6 months and in 73% between 6 months and 1 year. They also noted a dose dependency in the first year ranging from no change below 2,500 rad to changes in all nodes and vessels over 6,100 rad. In patients seen from 1 to 10 years after radiation therapy, narrowing of the vessels and decrease in the size of the nodes was seen in all patients receiving over 6,100 rad. Nearly 90% of the patients receiving 2,600–6,000 rad showed the same alterations. Below 2,500 rad only slightly more than half the patients showed these alterations.

In abnormal lymphangiograms (lymphoma or cervical cancer metastases in this series), the pattern of development of postirradiation changes in lymph vessels is different from that in normal lymphangiograms.

The lymph nodes decreased in size in the same time frame as in normal nodes, but the lymph vessel caliber appeared to be maintained or dilated in channels distal to the abnormal nodes when compared to pretreatment examinations. This may account for some observations of altered lymphatic flow previously noted. The explanation for this may in part be a larger volume of contrast in the abnormal lymphomatous nodes leaving vessels with less contrast.

Another factor probably of more importance is that subcapsular lymph sinuses in nodes containing metastatic malignancy become obliterated and/or scarred following irradiation. Obliteration of the subcapsular sinuses is usually seen in lymphoma, so that fibrosis following irradiation would also be expected. This obstruction of the afferent lymphatics would cause dilatation distally. The subcapsular sinus usually remains patent following irradiation of normal nodes.

REFERENCES

1. Anderson RE, Olson GB, Autry JR, Howarth JL, Troup GM, Bartels PH: Radiosensitivity of T and B lymphocytes. IV. Effect of whole body irradiation upon various lymphoid tissues and numbers of recirculating lymphocytes. *J Immunol* 118:1191–1200, 1977
2. Burge AJS: The significance and management of metastatic lymph nodes in the neck. *Proc R Soc Med* 68:77–79, 1975
3. Lenzi M, Bassani G: The effect of radiation on the lymph and on the lymph vessels. *Radiology* 80:814–817, 1963
4. Engeset A: Irradiation of lymph nodes and vessels. *Acta Radiol [Suppl]* (Stockh) 229:10–18, 1964
5. Sherman JO, O'Brien PH: Effect of ionizing irradiation on normal lymphatic vessels and lymph nodes. *Cancer* 20:1851–1858, 1967
6. Ariel IM, Resnick MI, Oropeza R: The effects of irradiation (external and internal) on lymphatic dynamics. *Am J Roentgenol* 99:404–414, 1967
7. Ludvik VW, Wachtler F, Zaunbauer W: Veränderungen am Lymphogramm durch Operation und ionisierende Strahlen. *Fortschr Geb Röentgenstr Nuklearmed* 110:307–321, 1969
8. Malina J, Bruckner L, Beska F, Cerny J, Klega J: Lymphographie nach durchgefuhrter Roentgenbestrahlung der Leisten- und Beckenlymphknoten. *Radiol Clin Biol* 34:357–363, 1965
9. Markovits P, Blache PM, Gasquet C, Charbit A: Les images radiologiques des lymphographies faites apres irradiation. *Ann Radiol* (Paris) 12:845–847, 1969
10. Vuksanovic M, Viamonte M Jr, Martin JE: The place of lymphangioadenography in the diagnosis and during the treatment of malignant diseases. *Am J Roentgenol* 96:205–221, 1966
11. Wiljasalo M, Perttala Y: Lymphographic changes caused by radiotherapy. *Ann Med Int Fenn* 55:57–60, 1966
12. Beltz VL, Thurn P: Diagnose und Differentialdiagnose des Lymphangiogramms bei retroperitonealen Tumormetastasen. *Fortschr Geb Roentgenstr Nuklearmed* 107:1–14, 1967
13. Averette HE, Ferguson JH: Lymphographic alterations of pelvic lymphatics after radiotherapy. *JAMA* 186:554–557, 1963
14. Sedgenidze GA, Zyb AF: Lymphographische darstellung von Veränderungen an normalen Lymphgefässen und Lymphknoten nach Strahlentherapie, in *Lymphographie bei malignen Tumoren,* edited by Luning M, Wiljasalo M, Weissleder H, Stuttgart, Georg Thieme, 1976, pp 292–296

High-Dose Renal Pharmacoangiography in the Assessment of Hypovascular Renal Neoplasms

VINCENT P. CHUANG[1,2] AND ANDREW M. FRIED[1]

From 6% to 25% of primary renal carcinomas are either hypovascular or avascular and are the major source of false negative angiography. High-dose renal pharmacoangiography, a valuable adjunct to conventional angiography, combines a renal vasodilator, acetylcholine, with a high dose of contrast medium. High-dose renal pharmacoangiography improves the diagnosis of hypovascular mass by enhancement of tumor vessels, increase of tumor stain, and better opacification of main and collateral renal veins. During a 4 year period, 20 hypovascular renal neoplasms were studied and successfully diagnosed preoperatively by this method.

Despite the advancement of renal sonography and cyst aspiration, renal angiography remains the most important tool for the preoperative evaluation of renal neoplasms. This is largely due to its ability to demonstrate not only the presence of a neoplasm, but also the vascular anatomy, the presence of renal vein invasion, and the status of opposite kidney and liver. Several publications discussed the difficulties in angiographic diagnosis of avascular or hypovascular renal tumor [1–3]. This paper describes a refined angiographic method using the combination of a renal vasodilator and high-dose contrast medium to improve the diagnosis of the "avascular" mass.

Materials and Methods

A renal mass identified by intravenous urography is first evaluated by renal sonography. If the mass is cystic, a diagnostic cyst puncture under sonographic guidance is performed. If the mass is solid or of equivocal consistency, angiography is recommended.

The angiographic approach to a renal mass used is shown diagrammatically in figure 1. Conventional renal arteriography uses 6–12 ml of 76% Renografin, depending on kidney size and arterial flow. The renal pseudotumors (e.g., column of Bertin, fetal lobulation, and regenerating nodule) which produce calyceal displacement on excretory urography are easily excluded. If a typical renal cyst is identified, the study is terminated; a cyst puncture is done at the request of the referring physician. A hypervascular mass obviously excludes a cyst. If the hypovascular mass is of uncertain nature, high-dose renal pharmacoangiography is performed. The present series includes 20 cases.

Acetylcholine (500 μg) is infused by hand through the renal artery catheter over a 1 min period, followed by a power-injected high dose of contrast medium (20–40 ml 76% Renografin). Tolazoline (25 mg) was used in earlier studies when acetylcholine was not available. The injection rate for conventional renal arteriography is determined by test injection under fluoroscopy. Conventional arteriography then serves as a guide for selection of the injection rate for high-dose pharmacoangiography. The renal arterial flow frequently increases after acetylcholine infusion, necessitating a 1–2 ml/sec increase in the injection rate from the conventional study. A 4 sec injection is routinely used. Thus, a kidney which had a 6 ml/sec estimated renal flow in the conventional study would require 8 ml/sec for 4 sec for high-dose pharmacoangiography, a total of 32 ml. The filming sequences are: two films per second for 3 sec, one film every 2 sec for 4 sec, and one film every 3 sec for an additional 6 sec, a total of 13 sec coverage. Two-fold magnification was routinely used in both conventional angiography and high-dose pharmacoangiography in the latter half of this study (nine patients). Celiac or hepatic angiography is also routinely performed to search for liver metastasis once a renal neoplasm is observed.

Indications

The role of high-dose renal pharmacoangiography is the further evaluation of mass deemed equivocal on conventional studies. Certain signs on routine angiography are taken to be valid indications for the arbitration provided by the high-dose study.

An unusually prominent artery circumscribing (fig. 2*A*) or traversing (fig. 3*A*) the otherwise hypovascular mass is viewed with suspicion. Inordinate crowding of otherwise normal arteries at the junctional zone between normal renal parenchyma and mass (fig. 4*A*) likewise prompts further study. Occasionally, normal renal parenchyma anterior or posterior to the mass may project

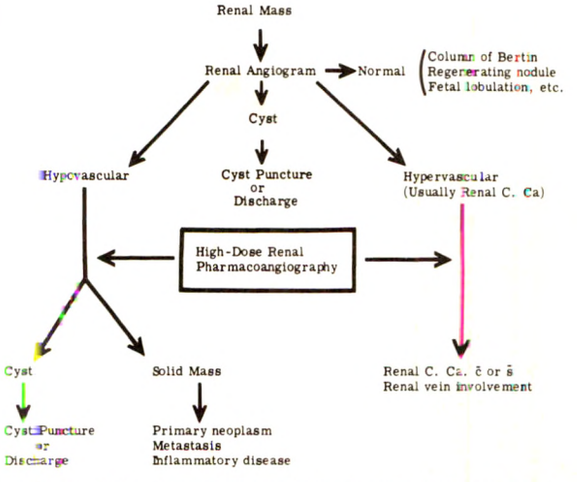

Fig. 1.—Role of high-dose renal pharmacoangiography in renal mass evaluation.

Received October 5, 1977; accepted after revision July 5, 1978.
Presented at the annual meeting of the American Roentgen Ray Society, Boston, September 1977.
[1] Department of Diagnostic Radiology, University of Kentucky Medical Center, Lexington, Kentucky 40506.
[2] Present address: Department of Diagnostic Radiology, M. D. Anderson Hospital and Tumor Institute, Houston, Texas 77030. Address reprint requests to V. P. Chuang.

© 1978 American Roentgen Ray Society

0361–803X/78/1100–0807 $00.00

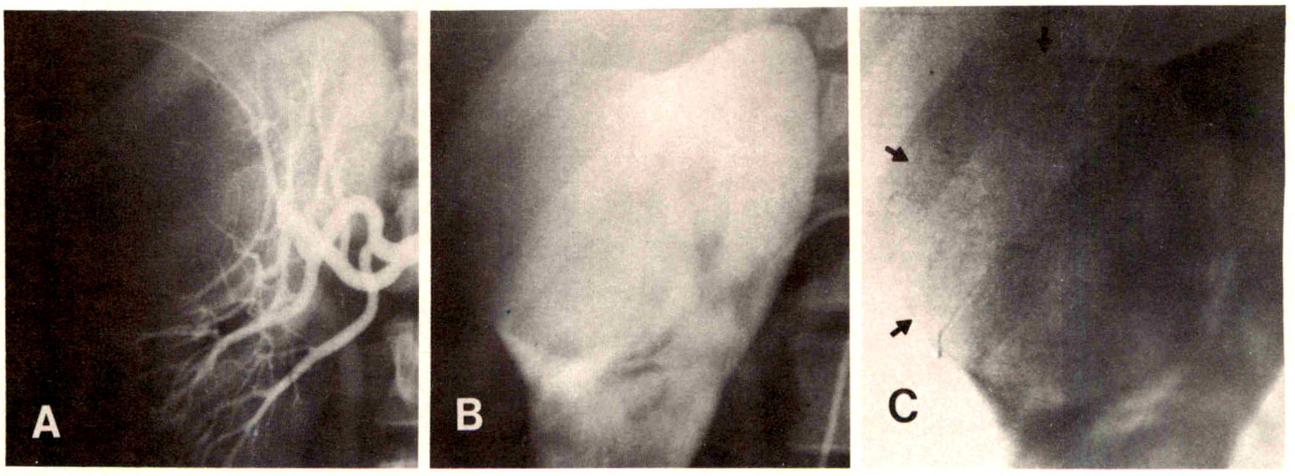

Fig. 2.—35-year-old female with one episode of hematuria. Nonmagnification technique. *A*, Selective conventional right renal arteriogram showing "avascular" mass on lateral aspect of right kidney. Unusually prominent arteries encircling superior and inferior borders of mass suggest this may not be benign cyst. *B*, Nephrogram phase showing excellent superior and inferior beaks. *C*, High-dose pharmacoangiogram showing increased density of entire mass (*arrows*) and subtle neovascularities throughout. Histologic diagnosis was well differentiated papillary adenocarcinoma.

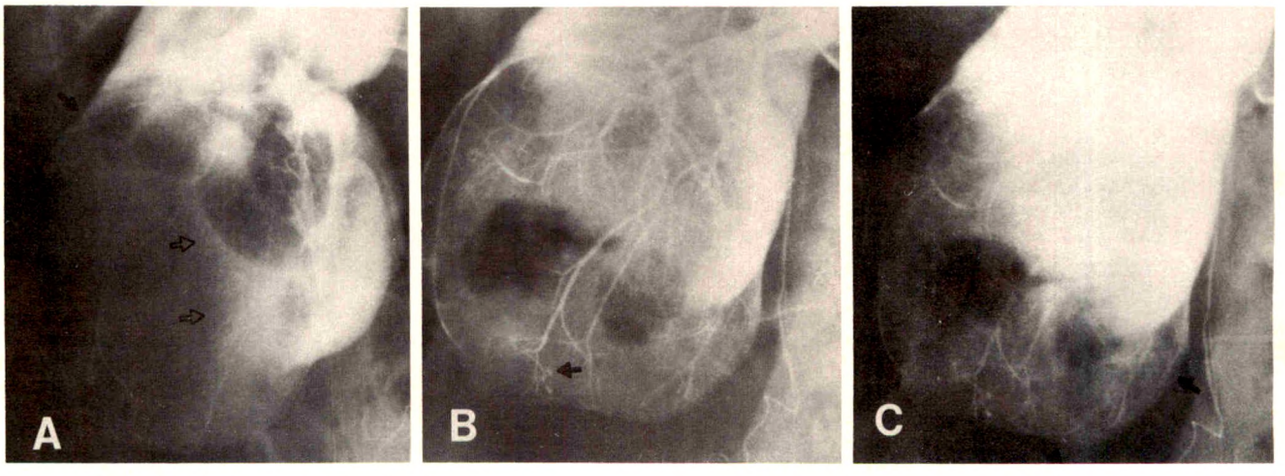

Fig. 3.—52-year-old male evaluated for epigastric discomfort. Intravenous urogram revealed right renal mass. Magnification technique. *A*, Late arterial phase of conventional renal arteriogram showing beak at superior aspect of mass (*closed arrow*). Renal parenchyma (*open arrows*), not to be confused with tumor stain, projects into mass. Extension of several vessels into most distant border suggests that mass is solid tumor rather than cyst. *B*, Arterial phase of high-dose pharmacoangiogram showing enhancement of arteries surrounding and feeding mass. Puddling of contrast medium is seen at inferior aspect of mass (*arrow*). *C*, Late arterial phase showing increased tumor stain of entire mass (*arrows*), indicative of hypovascular renal cell carcinoma. Histological diagnosis was well differentiated renal cell carcinoma with necrosis.

over it mimicking tumor stain or wall irregularity (fig. 3*A*). High-dose pharmacoangiography will then demonstrate the density of this junctional area to be normal and equal to that of the remaining renal cortex (fig. 3*C*). Finally, nonvisualization of the renal vein or the suggestion of collateral venous channels on the conventional study raises questions which require further investigation.

Results

Both qualitative and quantitative changes in the appearance of a mass judged "avascular" on conventional studies may be effected by the use of high-dose renal pharmacoangiography. All are the logical sequellae of the alteration in the hemodynamics of the tumor produced by this method. The high-dose study results in an increase in the number of vessels visible within the mass as well as improvement in the definition of those faintly seen on the standard study (figs. 2*C* and 3*B*). Enhancement in the tumor stain is appreciated as increased density of the mass in the nephrographic phase of the high-dose sequence (figs. 2*C*, 3*C*, and 4*B*). This phenomenon also allows clear definition of a significant cortical defect not identifiable on conventional angiography (figs. 5*A*–5*C*.).

Two grossly different angiographic patterns were encountered in our 20 patients; a solitary mass was seen in 14 and an infiltrative mass in six. Quantitation of the changes in angiographic appearances of the tumors is, of necessity, somewhat subjective; the advantages gained by the use of the high-dose study are summarized

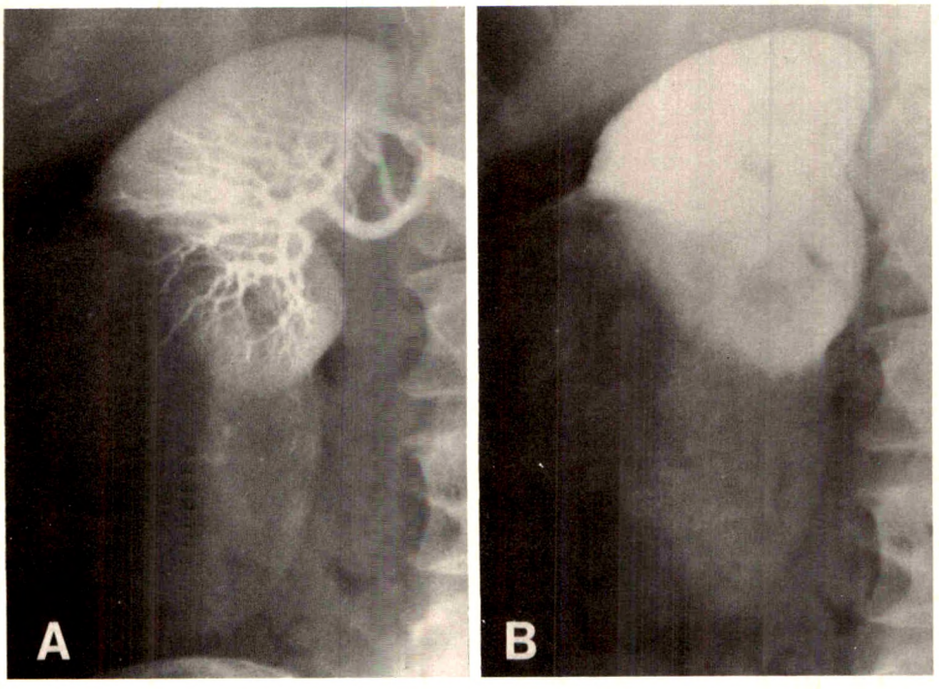

Fig. 4.—63-year-old asymptomatic male. Non-magnification technique. *A*, Renal arteriogram showing "avascular" mass with thin rim. Several fine tortuous vessels are seen at junction between mass and remaining renal parenchyma which can easily be mistaken for interlobar arteries crowded and compressed by huge cyst. *B*, High-dose pharmacoangiogram showing multiple fine tumor vessels and homogeneous faint stain revealing "hypovascular" mass. Histologic diagnosis was well differentiated adenocarcinoma with necrosis and hemorrhage.

in table 1. Of the 14 solitary masses, seven showed substantially better visualization of the tumor vessels in the arterial phase, and eight substantially enhanced density of the tumor stain in the nephrographic phase. Of the six infiltrative masses, only one showed significant improvement of the tumor vessel, but four had improved tumor stain.

A normal renal vein was seen in 12 of the 20 patients, obviating the need for cavography or renal venography. Of the eight patients who had no visualization of the renal vein, five had multiple collateral veins (fig. 5*C*). All five had tumor thrombus in the renal vein confirmed by either venography (fig. 5*D*) or subsequent surgery. Of the remaining three patients in whom neither renal vein nor collateral veins were seen, two had normal renal veins shown by subsequent venography; the other patient had an infiltrative mass involving the entire left kidney and left renal vein. Of the 20 patients, 16 underwent surgical exploration; the remaining four patients did not have surgery due either to distant metastases or unresectable primary lesions. The angiographic prediction of patency or occlusion of renal vein by high-dose study was confirmed in all surgical cases.

Discussion

The incidence of avascular or hypovascular renal neoplasms is 6%–25% [1–5]. The terms "avascular" or "hypovascular" (mass) are not strictly defined in the literature and the criteria probably vary from series to series. In the strictest sense, an "avascular" mass indicates a space-occupying lesion which has neither tumor vessels in the arterial phase nor tumor stain in the nephrogram phase. A truly avascular tumor seldom occurs. Instead, minute tumor vessels and a subtle tumor stain are frequently present, so that "hypovascular" mass is a preferred term. Among these are completely solid renal cancers, neoplasms with central necrosis, cancers growing within the cyst wall, and, rarely, infiltrative tumors. Although nearly 100% diagnostic accuracy of renal angiography has been described [6, 7], a more realistic 8%–10% false negative rate has been reported [3, 8].

Renal angiography using a high dose of contrast medium to opacify the renal vein after demonstration of a neoplasm has been described by many; the recommended dose ranges from 20 to 60 ml [9–11]. However, this method has not been applied to the diagnosis of an avascular or hypovascular neoplasm. The combined use of a renal vasodilator and high-dose contrast medium to convert an avascular mass into a hypovascular mass is the major innovation of this study. With the high-dose technique, varying degrees of improvement in visualization of tumor vessels and tumor stain resulted in the majority of solitary masses. With the infiltrative masses, less enhancement of tumor vessels was achieved in the arterial phase, but the infiltrative nature was better displayed in the nephrogram phase (table 1).

Acetylcholine produced the largest increase in renal flow, best arterial dilatation, and the most marked increase in venous density among a group of renal vasodilators [12]. Its accumulation to toxic levels is prevented in the human by circulation and tissue cholinesterase. Furthermore, a specific competitive antagonist to its

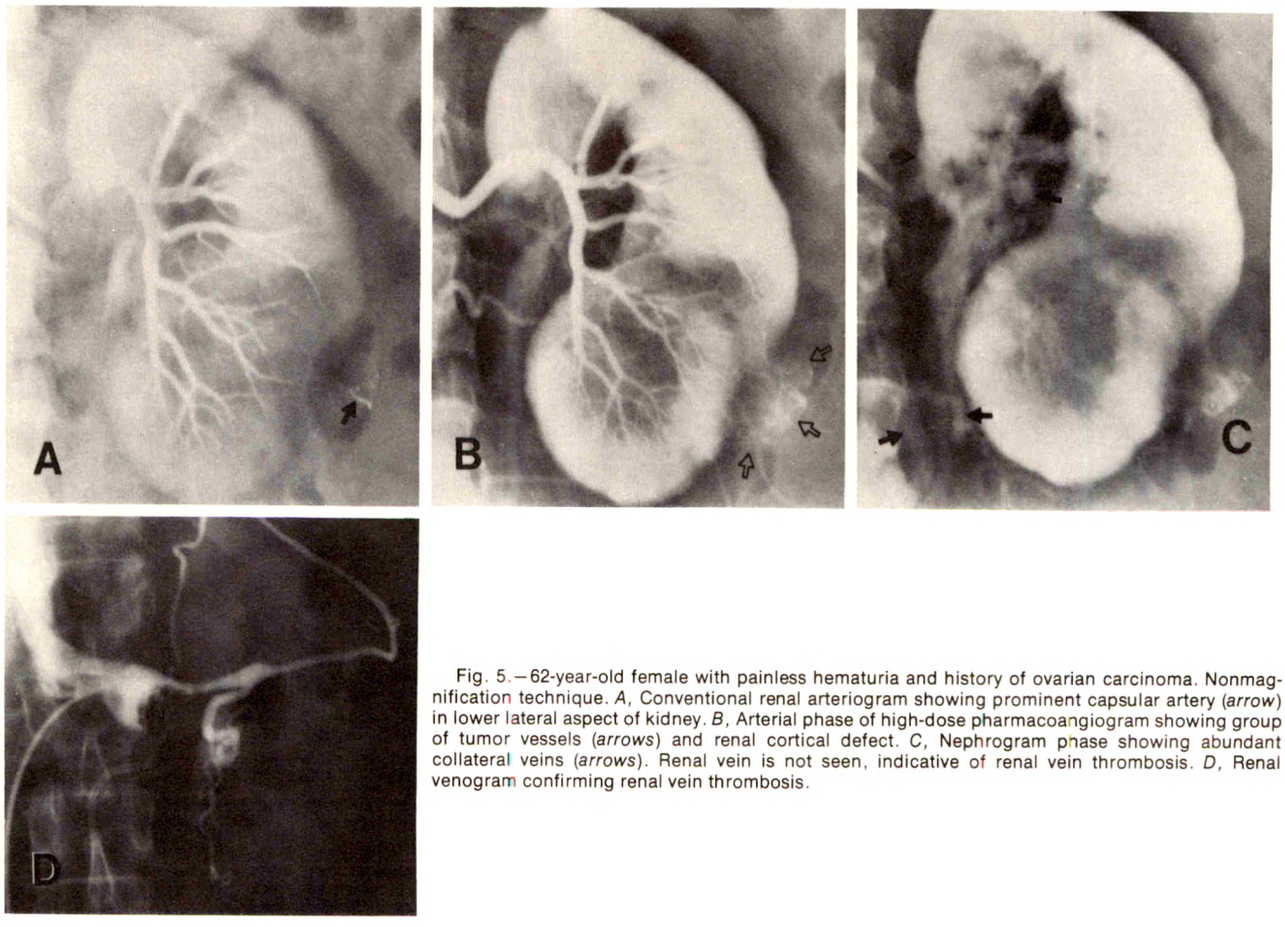

Fig. 5.—62-year-old female with painless hematuria and history of ovarian carcinoma. Nonmagnification technique. *A*, Conventional renal arteriogram showing prominent capsular artery (*arrow*) in lower lateral aspect of kidney. *B*, Arterial phase of high-dose pharmacoangiogram showing group of tumor vessels (*arrows*) and renal cortical defect. *C*, Nephrogram phase showing abundant collateral veins (*arrows*). Renal vein is not seen, indicative of renal vein thrombosis. *D*, Renal venogram confirming renal vein thrombosis.

TABLE 1

Quantitative Evaluation of High-Dose Renal Pharmacoangiography in Hypovascular Renal Masses

Degree of Enhancement	Arterial Enhancement	Nephrographic Enhancement
Solitary masses:		
+++	1	4
++	6	4
+	4	4
0	3	2
Infiltrative masses:		
+++	0	1
++	1	3
+	2	2
0	3	0

Note.—++ and +++ indicate substantially better enhancement.

cardiovascular effects, atropine, is available. Thus, acetylcholine is considered the most effective and safest renal vasodilator [12].

The prognostic significance of clinical, angiographic, and histologic findings in renal carcinoma has been extensively discussed [8, 13–16]. Although renal vein invasion seemed to have minor prognostic values in some studies [15, 17], most showed that it carried an ominous prognosis [8, 13, 18, 19]. Preoperative recognition of renal vein involvement greatly facilitates the planning of surgical approach [20]. Our surgeons request this information routinely whenever surgery is contemplated.

The collateral vein sign has been reported as a reliable indicator of renal vein invasion by a neoplasm, and high-dose contrast medium angiography has been recommended to replace selective renal venography [9–11, 21]. However, the reliability of this sign is questioned by Brindle [22]. In our series, the presence of collateral veins in conjunction with absence of the renal vein was highly significant; all five of such patients had proven renal vein tumor thrombus. High-dose renal pharmacoangiography makes it possible to omit renal venography and cavography.

ACKNOWLEDGMENTS

We thank Nancy Ford for secretarial assistance in the preparation of this manuscript.

REFERENCES

1. Blath RA, Mancilla-Jimeniz R, Stanley RJ: Clinical comparison between vascular and avascular renal cell carcinoma. *J Urol* 115:514–519, 1976

2. McLaughlin AP, Talner LB, Leopold GR, McCullough DL: Avascular primary renal cell carcinoma: varied pathologic and angiographic features. *J Urol* 111:587–593, 1974
3. Meaney TF: Errors in angiographic diagnosis of renal masses. *Radiology* 93:361–366, 1969
4. Talner LB: Radiologic-pathologic correlations in avascular renal masses, in *Diagnostic Radiology,* edited by Magulis AR, Gooding CA, St. Louis, Mosby, 1977 pp 181–195
5. Watson RC, Fleming RJ, Evans JA: Arteriography in the diagnosis of renal carcinoma. *Radiology* 91:888–897, 1968
6. Lang EK: The accuracy of roentgenographic techniques in the diagnosis of renal mass lesions. *Radiology* 98:119–128, 1971
7. Meaney TF, Stewart BH: Selective renal angiography: an integral part of the management of renal mass lesions. *J Urol* 96:644–650, 1966
8. Lang EK: Arteriographic assessment and staging of renal cell carcinoma: an analysis of a series of 120 patients. *Radiology* 101:17–27, 1971
9. Eisenman JI, Finck EJ, O'Loughlin BJ: Collateral vein sign: angiographic demonstration of renal vein invasion in renal carcinoma. *Radiology* 92:1256–1261, 1969
10. Folin J: Angiography in renal tumors. *Acta Radiol [Suppl]* (Stockh) 267:23–96, 1967
11. Henriksson L, Mikaelsson CG: Angiographic diagnosis of renal vein thrombosis in malignant renal tumors. *Acta Radiol* 14:682–688, 1973
12. Ozer H, Hollenberg NK: Renal angiographic and hemodynamic responses to vasodilators: a comparison of five agents in the dog. *Invest Radiol* 9:473–478, 1974
13. Lang EK: Arteriography in the diagnosis and staging of hypernephromas. *Cancer* 32:1043–1052, 1973
14. Cox JE, Lacy SS, Montgomery WG, Boyce WH: Renal adenocarcinoma: 28-year review, with emphasis on rationale and feasibility of preoperative radiotherapy. *J Urol* 104:53–61, 1970
15. Ralla S: Renal cell carcinoma: natural history and results of treatment. *Cancer* 25:26–40, 1975
16. Schreiber MH, Rea VE: The resectability of carcinoma of the kidney: analysis of roentgen signs in 63 histologically verified cases. *Am J Roentgenol* 104:343–349, 1968
17. Grammstedt B, Wahlqvist L: Prognostic significance of clinical, angiographic and histological findings in renal carcinoma. *Scand J Urol Nephrol* 3:117–127, 1969
18. Carter RL: The pathology of renal cancer. *JAMA* 204:221–222, 968
19. Myers JH Jr., Fehrenbaker LG, Kalalis PP: Prognostic significance of renal vein invasion by hypernephroma. *J Urol* 100:420–428, 1968
20. Freed SZ, Caplan LH, Bosniak MA: The role of renal arteriography in the management of renal carcinoma. *Surg Gynecol Obstet* 123:1303–1308, 1966
21. Genereux GP: The collateral vein sign in renal neoplasia. *J Can Assoc Radiol* 19:46–55, 1968
22. Brindle MJ: Alternative vascular channels in renal cell carcinoma. *Clin Radiol* 23:321–330, 1972

Optimal Technique of Renal Arteriography in Living Renal Transplant Donors

GARRY D. STRAUSER,[1] DEREK P. STABLES,[1] AND RICHARD WEIL, III[2]

Sixty consecutive living related renal donors were evaluated retrospectively with regard to the adequacy of their preoperative angiograms. Comparison of the original radiologic reports and the surgical findings revealed no errors in the prediction of the number and length of renal arteries of the transplanted kidneys. The optimal arteriographic technique is defined in the context of the information required by the surgeon: it is concluded that selective renal arteriography, although often advocated, is seldom necessary if the standard anteroposterior view of the abdominal aortic injection is supplemented by oblique and occasionally other views in selected cases.

Definition of renal arterial anatomy before renal transplantation is of broad concern to radiologists, since many potential donors prefer evaluation in their community hospital before referral to a transplantation center for surgery. Earlier authors advocated either transfemoral [1] or translumbar [2] aortography, while more recently the need for selective renal arteriography [3, 4] of the donor has been stressed. Since no data were provided in support of any of these opinions, we reviewed our recent experience.

Subjects and Methods

A consecutive series of 60 prospective renal donors, aged 18–58 years, underwent renal arteriography at the University of Colorado Medical Center or the Denver Veterans Administration Hospital between 1972 and 1977, prior to donation of a kidney. Donors whose arteriographic assessment was performed elsewhere and cadaver donors were excluded from this study. All examinations were performed by transfemoral catheterization; in all but one examination an aortic injection was filmed in the anteroposterior projection, with additional injections as required (table 1). A straight no. 6.3 French polyethylene catheter with four side holes was positioned with its tip at the T12 level and 50 ml of meglumine/sodium diatrizoate was injected at 25 ml/sec for 2 sec. Filming was performed at a rate of three films per second for 2 sec, one per second for 2 sec, and every third second for 6 sec with an injector delay to provide a contrast-free radiograph for subtraction. There were no complications of arteriography.

The original radiologic report of each examination was compared to the surgical findings with respect to number of renal arteries, adequacy of renal arterial length, presence of renal arterial or adjacent aortic disease, and the presence of unsuspected parenchymal disease. Data on the number of injections and other technical variables were obtained from the complete technical record of each examination. In addition, radiographs of 55 of the 60 examinations were retrospectively assessed for adequacy of arteriographic technique, detection of unrecognized renal arterial or parenchymal disease, and measurement of approximate renal artery length.

Results

There were 44 patients (73%) with bilateral single renal arteries, 13 patients (22%) with unilateral double renal artery supply, and three patients (5%) with bilateral double renal arteries. In the 60 arteriography reports only two errors occurred. One plaque of renal artery atheroma was missed, which was not identifiable on retrospective examination of the radiographs but was found at surgery. The other interpretative error was failure to recognize unilateral medial fibroplasia in one patient. While no surgical confirmation was available (contralateral kidney donated), it was identified on retrospective examination of the radiographs. There were no errors in the prediction of the number and length of renal arteries of the transplanted kidneys. Renal artery length from a retrospective review of 55 examinations is shown in table 2, and use of contralateral posterior oblique projections is summarized in table 3.

Discussion

There are four objectives of preoperative arteriography performed on prospective living related renal donors.

Determination of arterial number. The complexity of renal transplantation is increased by arterial multiplicity [5]. The frequency of multiple renal arteries in the general population is 26% unilaterally [6, 7] and 6% [6] to 8% [7] bilaterally, which is reason alone for preoperative arteriography. The slightly lower incidence of multiple renal artery supply in this surgical series reflects the bias introduced by rejection of some prospective donors specifically because of renal arterial multiplicity.

The relative distribution of multiple renal arteries should be noted. Many surgeons will sacrifice a small upper polar artery, but anomalous lower polar arteries should not be ligated because of the risk of ureteral ischemia [8].

Measurement of renal artery length. This important objective is often neglected. The requirements of safe ligation of the renal artery stump in the living donor and anastomosis without stricture in the recipient make a 2 cm length of main renal artery desirable; it is extremely difficult for the surgeon to work with less than 1 cm of renal artery (fig. 1). This measurement is made to the first parenchymal or ureteral branch, since capsular and

Received April 4, 1978; accepted after revision July 28, 1978.

[1] Department of Radiology, University of Colorado Medical Center, 4200 East Ninth Avenue, Denver, Colorado 80262. Address reprint requests to G. D. Strauser.

[2] Department of Surgery, University of Colorado Medical Center, Denver, Colorado 80262.

© 1978 American Roentgen Ray Society

0361–803X/78/1100–0813 $00.00

TABLE 1

Injections Performed

Injection	No.
Single aortic injection in anteroposterior projection	41(68)
Additional aortic injections:	
One contralateral posterior oblique projection	14
Two contralateral posterior oblique projections (different angles)	1
Bilateral posterior oblique projections	0
Repeat anteroposterior projection:	
With altered catheter position	1
With collimated magnification view	1
For machine failure	1
Subtotal	18(30)
Aortic injection and selective renal injection	0
Bilateral selective renal injections alone	1(2)*
Total	60

Note.—Numbers in parentheses are percentages.
* Previous incomplete examination performed elsewhere.

TABLE 2

Angiographic Measurement of Renal Artery Length

Renal Artery Length (cm)	Kidneys Examined	Kidneys Donated
< 1.0	2	0
1.0–2.0	12	4
> 2.0	96	51
Total	110	55

Data from 55 examinations (110 kidneys) reviewed retrospectively. Angiographic measurements are uncorrected.

TABLE 3

Use of Contralateral Posterior Oblique Projections

Oblique Projection Use	No. Examinations
Unilateral oblique projection:	
Performed and desirable	14
Performed but superfluous	2
Desirable but not performed	8
Bilateral oblique projections:	
Performed	0
Desirable but not performed	1
Oblique projections neither performed nor desirable	30
Total	55

Note.—Examinations reviewed retrospectively.

adrenal branches can be ligated safely. The measurements in table 2 are only approximate. Precise measurement requires accurate visualization of the arterial origin, allowance for aortic wall thickness averaging 1–2 mm ([9]; H. W. Toll, personal communication), and corrections both for inherent radiographic magnification and for the usual foreshortening of renal artery course seen in the anteroposterior projection. If there is any doubt of sufficient arterial length, an additional aortic injection in the 45° contralateral posterior oblique posture will project the renal artery roughly parallel to the plane of the film.

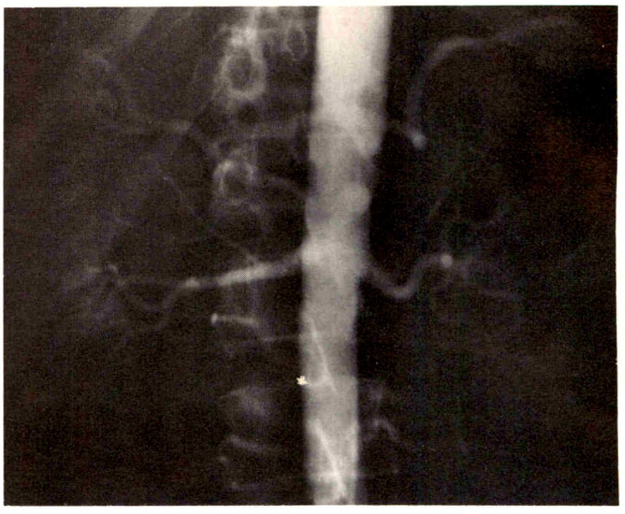

Fig. 1.—Standard single aortic injection in anteroposterior projection adequately displaying bilateral single renal arteries. Since only 5 mm of left main renal artery (after allowance for aortic wall thickness and for radiographic magnification) were available, right kidney was accepted. Length of right main renal artery (9–10 mm) was acceptable, although inferior vena cava had to be retracted for access to artery.

Unsuspected renal arterial or adjacent aortic disease. Particular attention should be paid to atheromatous plaques since their size is often underestimated at arteriography [10–12]. A plaque at the origin of the left renal artery was completely missed in one of our patients examined only in the anteroposterior projection. Fortunately the vessel was of sufficient length to allow transection distal to the plaque, but we advise the routine use of a contralateral oblique projection for optimal visualization of a *short* renal artery in older transplant donors, particularly if there are atheromatous plaques elsewhere in the aorta.

Small renal artery aneurysms [13], arteriovenous fistulas [5], and mild medial fibroplasia [13] do not prevent transplantation, but their presence should be recognized and their extent carefully evaluated. One of the two interpretative errors in this series was a failure to recognize unilateral medial fibroplasia. The subsequent donation of the contralateral kidney violated the principle that the donor should retain a normal kidney. Fortunately, this avoidable error was mitigated by the age of the donor, since medial fibroplasia seldom progresses after the age of 40 [14].

Unsuspected parenchymal disease. This also should be sought, although it is rarely found if the previous urographic study is of good quality. However, renal cell carcinoma is sometimes detected at arteriography performed for other reasons [15]. The consequences of transplanting this tumor into an immunosuppressed patient can be disastrous [16].

Our data show that the arteriographic technique used was adequate to achieve the objectives outlined above. A single high abdominal aortic injection filmed in the anteroposterior projection was sufficient in 68% of this series (table 1). A single 45° contralateral posterior oblique injection was the most helpful additional maneu-

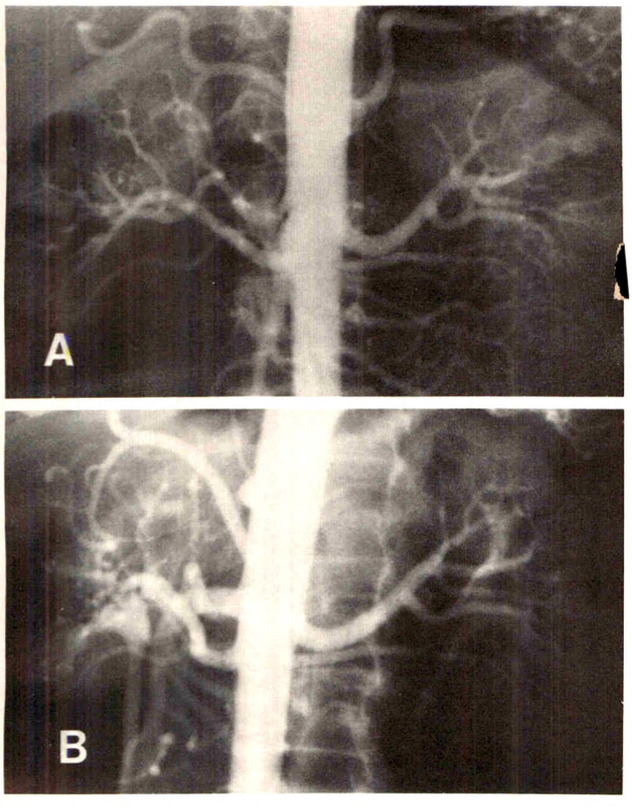

Fig. 2.—*A*, Anteroposterior projection unreliable for assessment of number of left renal arteries. There is either right double artery supply with early bifurcation of lower artery or triple renal artery supply. *B*, 45° right posterior oblique view displaying superior mesenteric artery separate from two left renal arteries, each with adequate length for grafting.

ver used to further study one kidney in another 25% (fig. 2). Even though no errors in prediction of arterial number and length occurred, the retrospective analysis of the radiographs (table 3) showed that an additional oblique projection was not used with sufficient frequency to ensure absolute confidence in every examination. If there is any doubt about renal arterial anatomy, a 45° oblique injection should be added to study one or occasionally both kidneys. In one instance a second contralateral posterior oblique injection was made at a 20° angle to resolve persistent uncertainty about arterial multiplicity.

Other additional injections are seldom required. Repositioning of the aortic catheter with the tip just above the aortic bifurcation is useful to confirm an unusually low anomalous lower polar artery origin (fig. 3). A coned magnification view of an aortic injection performed early in this series yielded no additional information and cannot be recommended for evaluation of arterial number and length; there would be a place for magnification technique in conjunction with selective renal injection if a small arteriovenous malformation or a tumor were detected. Photographic subtraction can provide a clearer view of the proximal renal artery overlying the spine and might be used occasionally in conjunction with an additional injection in the oblique projection.

Our use of selective arteriography in only one examination contrasts with earlier opinions, offered without tabulated data, on the necessity for routine selective technique [3, 4]. Even our one such examination was atypical in that the patient had undergone incomplete arteriography at another hospital; while the use of selective catheterization was logical for the *repeat* study, review of the previous examination gave every reason to believe that additional aortic injections in oblique projections could have provided the necessary information at that time. The routine use of selective arteriography in addition to aortography would prolong catheter time and increase patient irradiation; since there is an association between catheter time and incidence of femoral artery occlusion [17], the risk of the examination would probably be increased. The use of selective renal arteriography *alone* can lead to serious errors in interpretation by inexperienced observers (fig. 4).

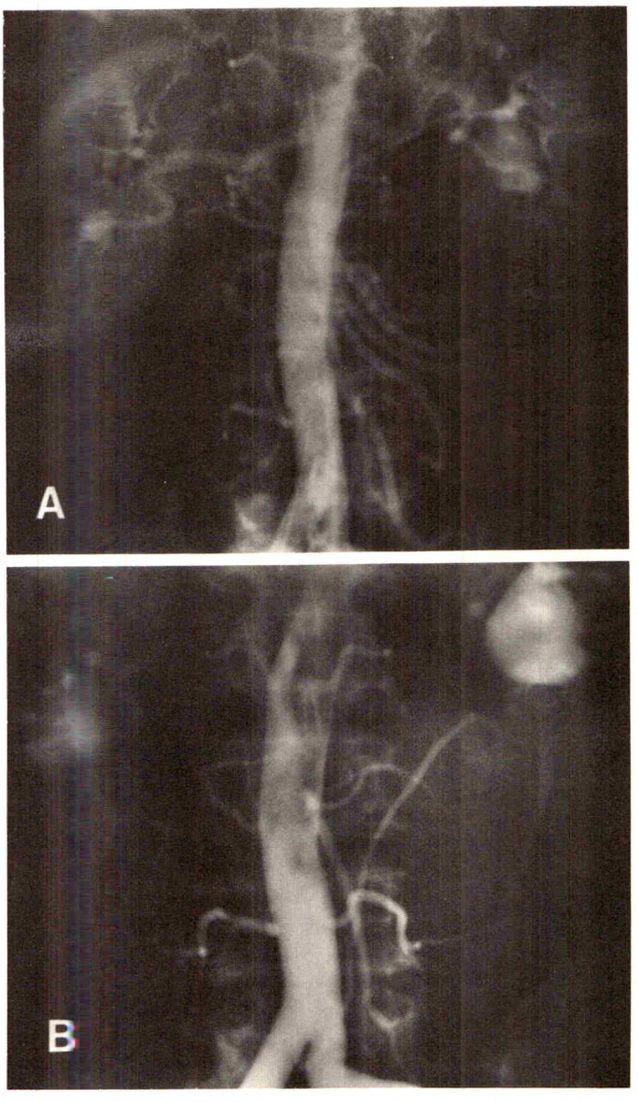

Fig. 3.—*A*, Standard high abdominal aortic injection showing delayed appearance of nephrogram in medial aspect of left lower pole which may be supplied by vessel arising from region of aortic bifurcation. *B*, Second injection with catheter tip just above aortic bifurcation displaying anomalous left lower polar artery originating from right common iliac artery.

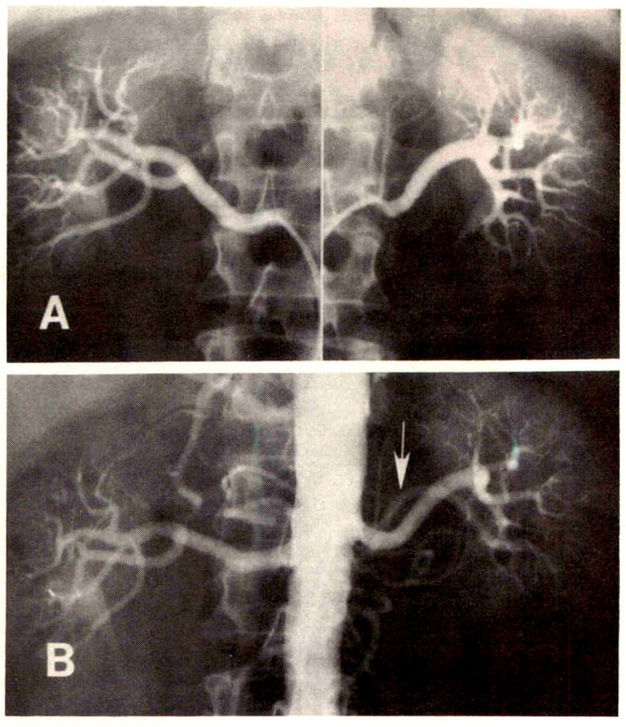

Fig. 4.—*A*, Bilateral selective renal arteriography performed at another hospital without aortography and interpreted as showing bilateral single renal arteries. Incomplete vascularization of left lower pole indicates presence of second left renal artery. Irregularity of upper left renal artery simulates medial fibroplasia. *B*, Subsequent aortography confirming double left renal artery supply (*arrow*). Normal appearance of upper left renal artery indicates that irregularity on previous selective study was due to standing waves rather than medial fibroplasia.

REFERENCES

1. Hamburger J, Crosnier J, Dormont J, Bach JF: *Renal Transplantation: Theory and Practice*. Baltimore, Williams & Wilkins, 1972
2. Trenti A: L'angiografia renale quale premessa al prelievo del rene per trapianto. *Policlinico [Chir]* 75:269–278, 1968
3. Sullivan MJ, Palmer JM: Arterial considerations in renal transplantation. *Urology* 3:297–303, 1974
4. Mendez R, Mendez RG, Payne JE, Silcott GR, Berne TV: Management of multiple renal arteries in renal transplantation. *Urology* 3:409–412, 1974
5. Penn I, Halgrimson CG, Ogden D, Starzl TE: Use of living donors in kidney transplantation in man. *Arch Surg* 101:226–231, 1970
6. Crummy AB, Atkinson RJ, Daves ML: An analysis of the aortorenal angiograms of sixty-six prospective renal donors. *Radiology* 84:683–687, 1965
7. Edsman T: Angionephrography and suprarenal angiography. *Acta Radiol [Suppl]* 155:21, 1957
8. Ehrlich RM, Smith RB: Surgical complications of renal transplantation. *Urology* 10, suppl 1:43–56, 1977
9. Kani I: Systematische Lichtungs—und Dickenmessungen der grossen Arterien und ihre Bedeutung für die Pathologie der Gefässe. *Virchows Arch [Pathol Anat]* 201:45–78, 1910
10. Haimovici H: Patterns of arteriosclerotic lesions of the lower extremity. *Arch Surg* 95:918–933, 1967
11. Beales JSM, Adcock FA, Frawley JS, Nathan BE, McLachlan MSF, Martin P, Steiner RE: The radiological assessment of disease of the profunda femoris artery. *Br J Radiol* 44:854–859, 1971
12. Dyde JA: Aortic bifurcation reconstruction for claudication. *Lancet* 2:326–327, 1968
13. Spanos PK, Simmons RL, Kjellstrand CM, Buselmeier TJ, Najarian JS: Screening potential related transplant donors for renal disease. *Lancet* 1:645–649, 1974
14. Meaney TF, Dustan HP, McCormack LJ: Natural history of renal arterial disease. *Radiology* 91:881–887, 1968
15. Kirchner FK, Braren V, Smith C, Wilson JP, Foster JH, Hollifield JW, Rhamy RK: Renal carcinoma discovered incidentally by arteriography during evaluation for hypertension. *J Urol* 115:643–645, 1976
16. Penn I: Transplantation of kidneys containing primary malignant tumors. *Transplantation* 16:674–675, 1973
17. Siegelman SS, Caplan LH, Annes GP: Complications of catheter angiography. *Radiology* 91:251–253, 1968

Complications in Expanded Polytetrafluoroethylene Arteriovenous Grafts: An Angiographic Study

PAUL LEMAITRE,[1] SEAN O'REGAN,[1,2] MILTON HERBA,[3] AND MICHAEL KAYE[1]

Expanded polytetrafluoroethylene grafts were used for creation of arteriovenous shunts in 35 patients on chronic hemodialysis. When flow studies or mechanical factors indicated abnormal flow in the graft, angiography was performed. Detection of venous backflow or obstruction, arterial stenosis, aneurysm formation, or graft kinking facilitated correction and thus salvage of the grafts.

The repeated access to the circulation required for regular hemodialysis therapy necessitates the creation of an arteriovenous communication. The Brescia-Cimino forearm fistula is generally accepted as the most desirable vascular access. However, alternative means are necessary for patients with inadequate superficial vessels due to constitutional, pathologic, or other reasons. While the Sparks mandrill [1, 2], Dacron velour [3, 4], and saphenous vein grafts [5, 6] have enjoyed limited success, the bovine carotid artery heterograft [7, 8] is more commonly used. Nevertheless, infectious, thrombotic, and vascular complications of the bovine graft have led to the investigation of the use of polytetrafluoroethylene vascular prostheses [9]. This report deals with the angiographic demonstration of the vascular complications observed in a series of polytetrafluoroethylene grafts and of the outcome of surgical repair. Our purpose was to anticipate any possible problems and avoid graft loss.

Materials and Methods

The polytetrafluoroethylene (Impra) had an internal diameter of 6 mm. These were implanted as straight grafts from the radial artery to the antecubital vein in 13 patients or as loop grafts from the brachial artery to an antecubital vein in 22 patients. Angiography was performed in all grafts which appeared clinically abnormal. Abnormal graft hemodynamic measurements (blood flow and intragraft pressure) [10] also led to radiologic investigation.

A 19 gauge scalp vein needle was inserted into the graft, and 10–20 ml of methylglucamine diatrizoate 30% or 60% was injected manually. Either a single spot film or multiple timed-sequence films were obtained. The arterial anastomosis was visualized by the antegrade flow of contrast material drug external compression of the venous outflow from the graft. Moderate burning pain in the arm and hand lasting less than 1 min during retrograde arterial flow was the only complication of the procedure.

Results

Normal Grafts

A normally functioning graft displays no mural or anastomotic irregularities. The straight graft has no angled bends to obstruct blood flow. The loop graft has a generous, gradually looped portion which prevents the kinking that might result from a more narrow, hairpin turn.

Venous Backflow

Four patients developed prolonged forearm edema. This complication occurred only in loop grafts. Angiography revealed retrograde blood flow in forearm veins. These patients' veins were apparently unable to fully accommodate graft blood flow, which led to rapid edema formation. The edema in all cases gradually remitted as venous channels dilated or after arterial banding in one case decreased blood flow.

Venous Obstruction

Postthrombectomy angiography was performed in eight patients with graft thrombosis. In six cases severe stenosis at the venous anastomosis was demonstrated as the primary cause of graft clotting (fig. 1). Two other patients with reduced graft blood flow were found to have extrinsic compression of the distal ends of the polytetrafluoroethylene grafts. In one case, a fibrous band significantly reduced the caliber of the graft. In the other patient, large organizing thrombus resulted in compression of the distal end of a loop graft 2 months after implantation.

Intragraft hypertension and false aneurysm formation prompted angiography of another graft. A segment of basilic vein several centimeters beyond the venous anastomosis was noted to be narrowed (fig. 2). Pressure measurements above (70 mm Hg) and below (100 mm Hg) the stenotic site demonstrated its hemodynamic importance.

Arterial Stenosis

Poor blood flow in a straight graft was evaluated by brachial arteriography after antegrade injection of contrast medium into the graft failed to reveal graft-venous anastomotic stenosis; injection with distal venous compression demonstrated stenosis of the artery graft

Received October 18, 1977; accepted after revision May 12, 1978.

[1] Department of Medicine, Division of Nephrology, Montreal General Hospital, Montreal, Quebec, Canada H3G 1A4.

[2] Present address: Department of Pediatrics (Nephrology), Hôpital Sainte-Justine, 3175 Chemin Sainte-Catherine, Montreal, Quebec, Canada H3T 1C5. Address reprint requests to S. O'Regan.

[3] Department of Radiology, Montreal General Hospital, Montreal, Quebec, Canada H3G 1A4.

© 1978 American Roentgen Ray Society

0361–803X/78/1100–0817 $00.00

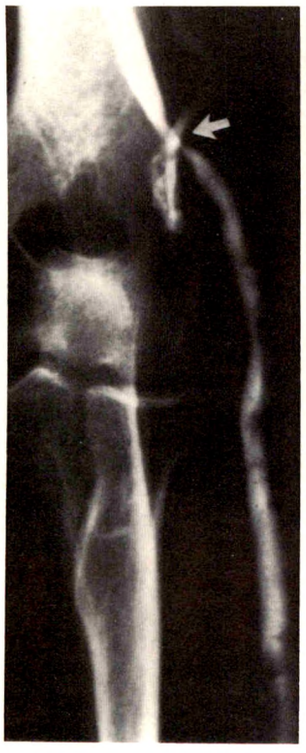

Fig. 1.—Stenosis of graft-vein anastomosis (*arrow*) with retrograde venous flow.

Fig. 2.—Retrograde filling of venous drainage system due to proximal venous stenosis (*arrow*).

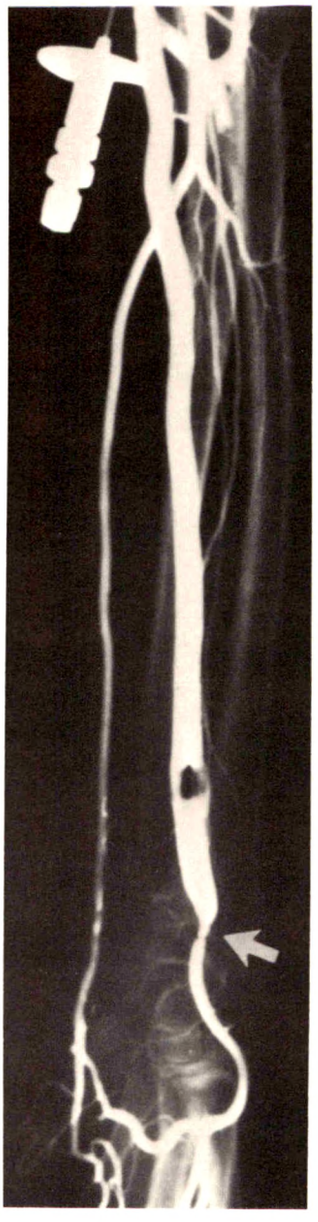

Fig. 3.—Stenosis of arterial-graft anastomosis. Flow is provided by ulnar artery via palmar arch. Lucency in graft may be due to localized thrombus.

anastomosis with failure of opacification of the proximal radial artery (fig. 3). Revision of the arterial anastomosis was rejected because of the probable development of a steal syndrome across the palmar arch. Therefore, the graft was ligated.

Aneurysm

Three patients developed false aneurysms in the grafts. Most were small and were thought to be due either to poor hemostasis at the needle sites following treatment or to repeated punctures at the same site in consecutive dialyses. In addition, two of these three grafts had high intragraft pressures which may have contributed to the formation of the aneurysms. In one graft, the aneurysm enlarged to a precarious size (fig. 4) and the graft was removed. The other two grafts continue to be used as access for hemodialysis with care being taken to avoid the microaneurysms during needle insertion and to insure adequate maintenance of hemostasis after dialysis.

One patient developed a false aneurysm at the venous anastomosis after an infection; it was repaired after antibiotic therapy. However, 6 weeks later the patient had a pulsatile 2 cm mass at the proximal end of the graft. Angiography demonstrated a false aneurysm at the arterial anastomosis (fig. 5) and a stenosis at the venous end of the graft. Presumably the venous stenosis resulted in graft hypertension and in subsequent rapid expansion of a small defect at the proximal end of the graft. After surgical repair, no further problems have been encountered.

Postanastomotic venous dilatation occurred in two straight grafts. The nearly right-angled venous anastomosis in these grafts resulted in a high pressure pulsatile flow against the thin-walled expansile vein, leading to dilatation. The lack of progressive enlargement obviated the need for surgery.

Graft Kink

Graft hypertension and a small pulsatile focal enlargement of the arterial graft limb prompted angiography in one patient. It showed a kink at the bend of the loop (fig. 6) as well as a small false aneurysm on the arterial limb. The kink was responsible for a marked pressure difference between the proximal and distal limbs and probably resulted in the development of the false aneurysm noted.

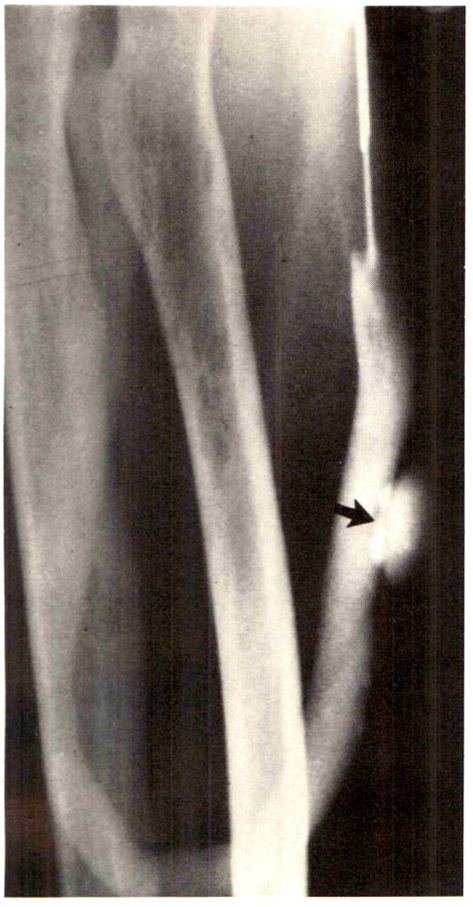

Fig. 4.—False aneurysm (*arrow*) on arterial limb of loop graft.

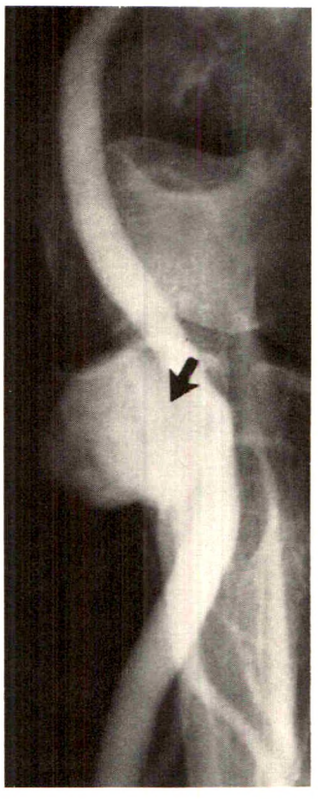

Fig. 5.—False aneurysm (*arrow*) at arterial graft anastomosis.

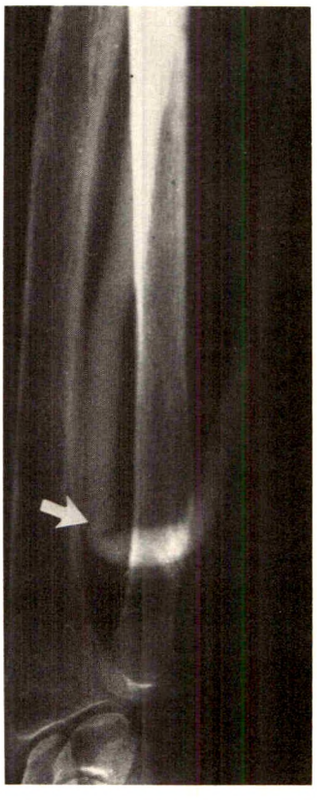

Fig. 6.—Kink (*arrow*) obstructing flow in loop graft.

The graft was not repaired; instead a needle was inserted in the venous limb, since the graft pressure on that side was such that microaneurysm formation could be avoided by careful needle technique. Blood flow was adequate for hemodialysis.

Discussion

The Brescia-Cimino fistula is considered the most suitable form of circulation access in hemodialysis patients. However, with the increasing longevity of these patients, the finite survival of this fistula has led to new methods of circulation access. The loss of superficial veins due to fistula thrombosis and to multiple access site procedures has posed major problems in the development of vascular access with flow sufficiently high to sustain dialysis. Bovine carotid heterografts, though providing useful access, are often associated with thrombosis, infection, aneurysm formation, and steal syndromes [7]. Also, the dense fibrous adhesion of the graft to subcutaneous tissues often causes difficulties when surgical revisions are attempted [11]. Other allo- and autografts have similar disadvantages. However, the limited experience with expanded polytetrafluoroethylene grafts has been more encouraging. The lack of severe perigraft fibrosis has allowed for surgical revision when indicated by angiographic demonstration of correctable abnormalities [12]. Also graft removal when indicated has been easily accomplished, thus allowing for further graft insertion on the same forearm.

When polytetrafluoroethylene grafts became readily available, they were used in patients who would otherwise have had bovine grafts. After slightly more than 1 year, we have gained appreciable experience in the various complications to which this prosthetic material is prone. False aneurysms, stenosis at anastomotic sites, thrombosis, infection, kinks, and venous backflow have been observed. Because of the paucity of available veins in many patients, salvaging defective grafts is of critical importance. When definitive assessment of graft function was not possible by noninvasive means, angiography often identified the causative abnormality. As a result, many grafts have been salvaged and the patient morbidity and mortality associated with circulation access has decreased.

REFERENCES

1. Beemer RK, Hayes JF: Hemodialysis using a mandrill-grown graft. *Trans Am Soc Artif Intern Organs* 19:43–48, 1973
2. Morgan A, Lazarus M: Vascular access for dialysis. Technics and results with newer methods. *Am J Surg* 129:432–438, 1975
3. Flores L, Dunn I, Frumkin E, Forte R, Requena R, Ryan J, Knopf M, Kirschner J, Levowitz BS: Dacron arteriovenous shunts for vascular access in hemodialysis. *Trans Am Soc Artif Intern Organs* 19:33–37, 1973
4. Levowitz BS, Flores L, Dunn I, Frumkin E: Prosthetic arteriovenous fistula for vascular access in hemodialysis. *Am J Surg* 132:368–372, 1976
5. May J, Tiller D, Johnson J, Stewart J, Sheil AGR: Saphenous vein arteriovenous fistula in regular dialysis treatment. *N Engl J Med* 280:770, 1969
6. Izquierdo GF, Vivero RR: Venous autografts for hemodialysis. *Nephron* 8:57–66, 1971
7. Merickel JH, Andersen RC, Knutson R, Lipschultz ML, Hitchcock CR: Bovine carotid artery shunts in vascular access surgery. *Arch Surg* 109:245–250, 1974
8. VanderWerf BA, Rattazzi LC, Katzman HA, Schild AF: Three year experience with bovine graft arteriovenous (A-V) fistulas in 100 patients. *Trans Am Soc Artif Intern Organs* 21:296–298, 1975
9. Baker LD, Jr, Johnson JM, Goldfarb D: Expanded polytetrafluoroethylene (PTFE) subcutaneous arteriovenous conduit: an improved vascular access for chronic hemodialysis. *Trans Am Soc Artif Intern Organs* 22:382–387, 1976
10. O'Regan S, Lemaitre P, Kaye M: Expanded PTFE grafts: hemodynamic studies. *Clin Nephrol*. In press, 1978
11. Tellis VA, Driscoll B, Soberman R, Veith FJ: Comparison of bovine heterografts (BH) and polytetrafluoroethylene grafts (PTFE) for hemodialysis access (abstr.). *Abstr Am Soc Artif Intern Organs* 6:88, 1977
12. Ackman CFD, O'Regan S, Herba M, Laplante MP, Lemaitre P, Kaye M: Experience with P.T.F.E. (polytetrafluoroethylene) grafts in a chronic hemodialysis programme. *Can J Surg*. In press, 1978

Complication Rate with Supine Phlebography

MARC N. COEL[1] AND WINIFRED DODGE[1]

The incidence of complications following supine phlebography was studied in 109 patients (142 legs) retrospectively and 89 patients (106 legs) prospectively. Virtually all patients had some discomfort during the procedure, while three patients had delayed pain for up to 4 days following examination. Three patients developed hives, one of whom also had bronchospasm. There were two cases with subcutaneous extravasation. The shorter endothelial contact time of supine phlebography compared to the semiupright technique might explain the reduced incidence of pain.

The lower limb phlebogram remains the definitive diagnostic procedure for evaluating venous disease of the legs. Few studies [1–3] have documented the incidence of side effects. While most lower limb phlebograms are performed using the upright technique [1, 2, 4, 5] we have been impressed by the low incidence of complications associated with machine-injected supine phlebography [6].

Materials and Methods

All patients were examined at the Veterans Administration Hospital, San Diego, using the supine technique. Scalp vein needles (18–21 gauge) were inserted in a superficial vein in the foot, with tourniquets on the ankles and thighs; 95 ml of 76% meglumine diatrizoate (Renografin-M-76, Squibb) were machine injected at a rate of 1–2 ml/sec. The injection lasted approximately 45–90 sec. Immediately after injection, the contrast media was flushed from the veins by a continuous drip infusion of 250–500 ml 5% dextrose in water. Bilateral examinations were performed simultaneously with two injectors and a total of 180 ml of undiluted contrast medium.

For the retrospective study, the charts of all patients who had undergone phlebography during 1975 and 1976 were reviewed. There were 109 patients and 142 legs examined; 33 patients had both legs injected simultaneously. Notes made by the physicians and nurses were reviewed. It is customary at this institution for nurses to include spontaneous comments from patients about how they feel as well as responses to direct questioning.

All patients studied during 1977 were prospectively followed by the angiographic physicians and nurses. The 89 patients were directly questioned about their sensations during and immediately after the examination and each day for 2–3 days. Objective signs and symptoms were also recorded (i.e., bronchospasm, hives, or swelling). Fifty-four outpatients were excluded from the study because of lack of follow-up. None had immediate reactions.

Results

Of the 109 patients retrospectively studied, two complained of pain for 1 and 2 days, respectively, after the phlebogram. One had deep venous thrombosis shown on the initial study, while the other had severe varicosities. Neither had a repeat venogram, although the patient with varicosities did have multiple other venous and arterial studies without incident. One patient with a normal venogram developed hives and itching at the conclusion of the study and was treated with 50 mg diphenhydramine hydrochloride (Benadryl) with relief of symptoms and signs. Thus three complications were recorded on the 142 legs studied for an incidence of 2.1%.

In the group studied prospectively, there were five complications in the 89 patients (5.6%) and 106 legs examined (4.7%). One patient with deep venous thrombosis developed bronchospasm and hives. He was treated with 0.2 ml subcutaneous 1:1,000 mg epinephrine (0.02 μg) and 50 mg intramuscular Benadryl. One other patient developed hives and was treated with Benadryl. There were two instances of extravasation; one caused an 8 × 15 cm slough of skin. This was healing when the patient died of a myocardial infarction 2 weeks later. The fifth patient had leg pain for 3 days following the initial examination. A repeat venogram on the third day was normal, as was the initial study. The pain receded on the fourth day after the initial study. There was no new symptomatology following the second examination.

Pain response recorded during the study ranged from virtually absent, to mild flushing and warmth, to severe leg pain. Of the prospectively studied patients, 49 (55%) had mild to moderate discomfort during or immediately after the examination, and 40 (45%) had severe discomfort.

Of the 248 legs examined, only 126 were normal (50.8%). Deep vein thrombophlebitis accounted for 98 cases (39.5%), slightly higher than in a previous series [2]. There were 12 cases with varicosities, and 12 with changes compatible with previous thrombophlebitis (postphlebitic syndrome) [7]. One patient had traumatic venous disruption, and one had a venous malformation of the foot.

Discussion

Phlebography has had a resurgence with the recent emphasis on complications of long-term anticoagulation [8]. Venography remains the standard by which other techniques, notably isotope studies, are judged. Many hospitals do not have isotope venography and rely on contrast phlebography.

The risk inherent in phlebography is almost totally related to the contrast media and includes pain, skin

Received April 11, 1978; accepted after revision July 14, 1978.

[1] Department of Radiology, University of California and Veterans Administration Hospital, 3350 La Jolla Village Drive, San Diego, California 92161. Address reprint requests to M. N. Coel.

© 1978 American Roentgen Ray Society

0361–803X/78/1100–0821 $00.00

necrosis, allergic reactions, bronchospasm, and anaphylaxis. Pulmonary embolization is a theoretical risk, but has not been reported in the English literature.

Bettman and Paulin [1] found a direct relationship between the incidence of adverse reactions and the concentration of contrast medium. Although we used a higher concentration of contrast medium, (76% compared to 45%) the incidence of allergic side effects was comparable in the two studies. They reported a 1.5% incidence, while we found a 3.8% incidence (0.9% retrospective group, 2.8% prospective group). The delayed reaction, late pain, was considerably less frequent in our study; it occurred in 1.5% of our patients (1.2% of the legs examined) compared to 7.5% in the series of Bettman and Paulin [1]. We hypothesize that the lower sodium content of the contrast medium (Renografin-M-76) used in this study (0.04 mEq/ml compared to 0.16 mEq/ml) might be a factor in the lower reaction rate.

Differences in examination technique may also contribute to this discrepancy. The contrast medium is in contact with the endothelium for considerably less time using the power-injected supine technique than the more static upright technique. This may prevent the local toxic changes which have been experimentally demonstrated [9]. It is possible that the combination of dilute contrast medium and the supine injection technique may further reduce the rate of adverse reactions to the minimum level of generalized systemic reactions (1/10,000) [10].

Additional technical factors must be taken into account. Extravasation may occur and cause skin necrosis. Gothlin [11] reported extravasation rates of 78% with steel needles and 4.5% with plastic cannulas. In our experience, both rates seem unusually high. Our filming technique almost always shows the feet, but using steel needles (butterfly scalp vein needles) we have had only two documented cases of extravasation (1.8%).

ACKNOWLEDGMENTS

We thank Wayne Amende, Donald Litzenberg, and Loretta Jemmott for technical assistance. We also thank Cathy Nancarrow for assistance in preparation of this manuscript.

REFERENCES

1. Bettman MA, Paulin S: Leg phlebography: the incidence, nature and modification of undesirable side effects. *Radiology* 122:101–104, 1977
2. Albrechtsson U, Olsson CG: Thrombotic side effects of lower limb phlebography. *Lancet* 1:723–724, 1976
3. Lea Thomas M, Andress MR, Browse NL, Fletcher EWL, Philips JD, Pim HP, McAllister V, Stephenson RH, Tonge K: Phlebography in the prevention of recurrent pulmonary embolism: techniques and value. *Am J Roentgenol* 110:725–733, 1970
4. Lea Thomas M: Phlebography. *Arch Surg* 104:145–151, 1972
5. Greitz T: The technique of ascending phlebography of the lower extremity. *Acta Radiol* 42:421–441, 1954
6. O'Dell CW, Coel MN: Ascending lumbar venography in lumbar disc disease. *J Bone Joint Surg [Am]* 59:159–163, 1977
7. Lipchick EO, DeWeese JA, Rogoff SM: Serial long-term phlebography after documented lower leg thrombosis. *Radiology* 120:563–566, 1976
8. Porter J, Jick H: Drug-related deaths among medical inpatients. *JAMA* 237:879–881, 1977
9. Ritchie WGM, Lynch PR, Stewart GH: The effect of contrast media on normal and inflamed canine veins; a scanning and transmission electron microscopic study. *Invest Radiol* 9:444–455, 1974
10. Lasser EC, Lang J, Sovak M, Kolb W, Lyon S, Hamlin AE: Steroids: theoretical and experimental basis for utilization in prevention of contrast media reactions. *Radiology* 125:1–9, 1977
11. Gothlin J: The comparative frequency of extravasal injection at phlebography with steel and plastic cannula. *Clin Radiol* 23:183–184, 1972

Flow-directed Balloon Catheterization for Aortofemoral Arteriography Using the Axillary Artery Approach

EDWARD BUONOCORE[1] AND THOMAS P. LYNCH[1]

An axillary artery approach is occasionally necessary in the evaluation of the abdominal aorta and peripheral arteries in patients with severe and complicated arteriosclerotic disease. Difficulty may be encountered in directing the catheter into the descending aorta in patients with extremely tortuous and elongated aortic arches. Use of flow directed angiographic balloon catheters has made abdominal, pelvic, and lower extremity arteriography readily obtainable using an axillary approach when other methods failed and translumbar aortography was considered hazardous. This might be particularly useful in patients with high abdominal aortic occlusions, in anticoagulated patients, in patients with abdominal aortic grafts, and in some patients with small aortas displaced to the right.

Newer surgical vascular techniques have extended the usefulness of arteriographic examinations in patients with advanced obliterative arteriosclerotic disease. These patients often challenge the angiographer's technique, since distal abdominal aortic and iliac disease often exists and precludes catheterization from the femoral arteries.

Translumbar aortography may be difficult or hazardous in patients with proximal abdominal aortic occlusions, small abdominal aortas displaced to the right, in patients with abdominal aortic grafts, and in patients receiving anticoagulants or in whom bleeding is suspected. Introduction of catheters through axillary or brachial arteries may be necessary for study of the abdominal aorta and its tributaries in these situations.

On occasion, markedly tortuous elongated thoracic aortic arches may render catheterization of the descending thoracic aorta difficult, time consuming, or virtually impossible despite the use of deflectors. This dilemma has lead to the use of flow-directed gas-filled balloon catheters (Berman angiographic balloon catheter, Extracorporeal Medical Specialties, Inc., King of Prussia, Penn. 19406) to facilitate the placement of catheters from the upper extremities into the abdominal aorta.

Technique

Initially the flotation catheter technique was used only in patients in whom it was impossible to position a standard vascular catheter from the upper extremity into the descending aorta because of tortuosity of the aortic arch. Lately we use this technique as the method of choice. If catheterization of the descending thoracic aorta could not be achieved, the arterial catheter was replaced by a sleeve introducer (Cordis Co., Miami, Fla.) using standard Seldinger technique. An angiographic balloon catheter (fig. 1) is introduced into the thoracic aorta through the sheath and directed into the aortic

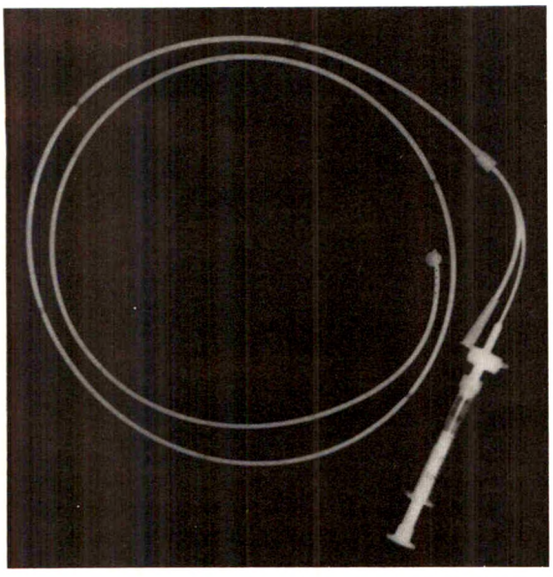

Fig. 1.—Berman double lumen balloon catheter. Balloon is inflated with 1.25 ml of gas (preferably carbon dioxide) to achieve flow direction capability.

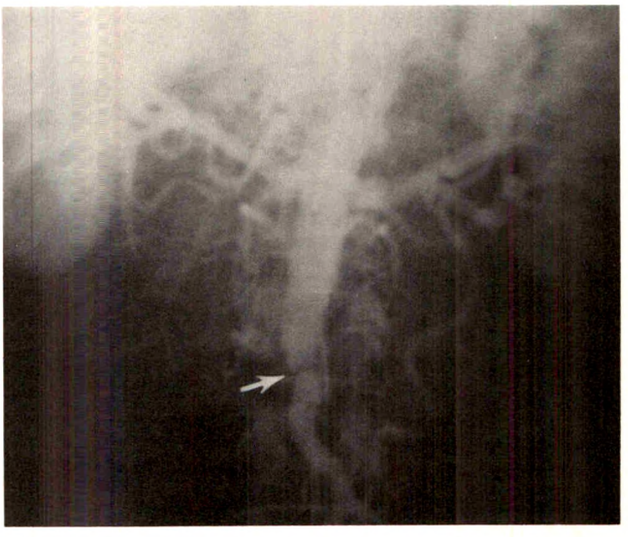

Fig. 2.—Case 1. Aortogram after flotation of catheter into the distal aorta demonstrating complete occlusion of the aorta (*arrow*) below level of inferior mesenteric artery.

Received April 11, 1978; accepted after revision July 14, 1978.

[1] Department of Radiology, University of Tennessee Hospital, 1924 Alcoa Highway, Knoxville, Tennessee 37920. Address reprint requests to E. Buonocore.

© 1978 American Roentgen Ray Society

0361-803X/78/1100-0823 $00.00

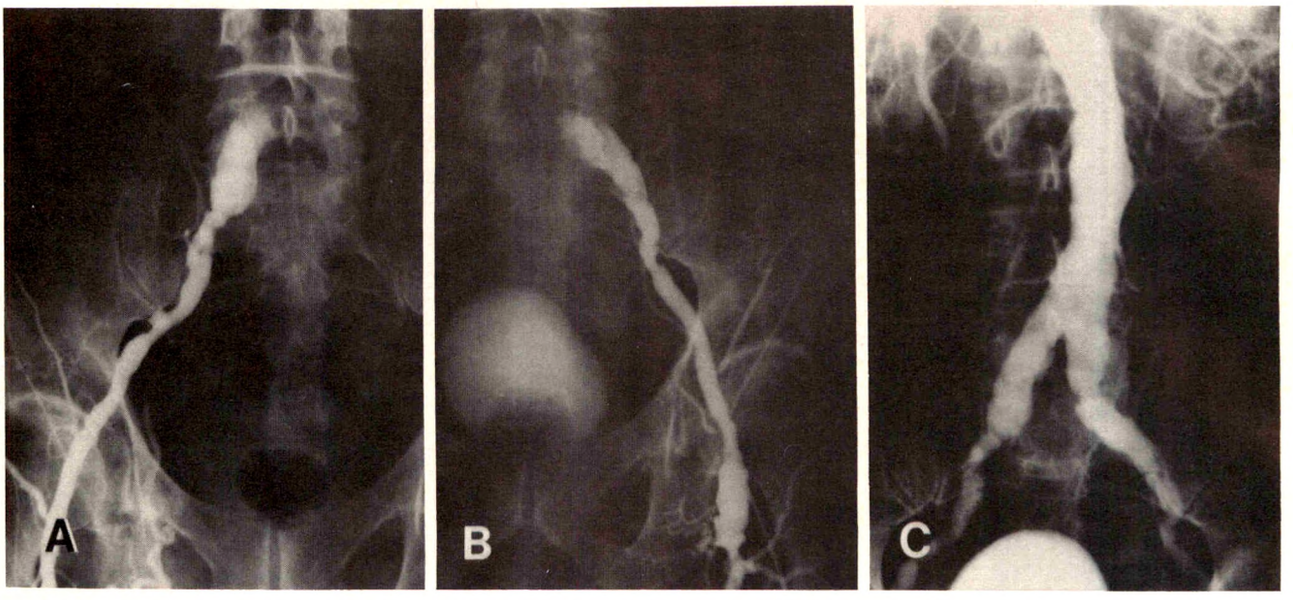

Fig. 3.—Case 2. *A and B*, Retrograde injections of each femoral artery demonstrating severe occlusive disease. Retrograde catheterization was not possible despite extensive manipulation. *C*, Abdominal aortogram through flow-directed balloon catheter. Injection rate was 20 ml/sec for a total of 40 ml. Aorta is patent with severe occlusive disease of common iliac arteries.

arch. The balloon is filled with 1.25 ml of carbon dioxide, using an accompanying syringe which safeguards against overdistention of the balloon. The balloons have never ruptured with only single usage and proper care against overdistention. Even in case of rupture, carbon dioxide escape would not be hazardous because of its solubility.

With easy manipulation, arterial flow directs the catheter tip into the descending thoracic aorta. With further gentle manipulation, the catheter is advanced into the abdominal aorta below the renal arteries. The balloon is deflated, and abdominal angiography is performed using a pressure injector and a seriographic changer.

The no. 8 French catheter 110 cm long allows a maximum injection rate of 27 ml/sec with generated pressure of 56 kg/cm^2. The no. 7 French catheter 90 cm long allows a maximum flow rate of 20 ml/sec with generated pressure of 49 kg/cm^2. The balloon catheters have multiple side holes in two opposing rows. Filling of the balloon with radiographic contrast medium or saline is inadvisable. The flow-directed capabilities are lost with the denser media and the liquid cannot be withdrawn. A Swan-Ganz pulmonary angiogram catheter (Edwards Laboratory Div., American Hospital Supply Corp., Santa Ana, Calif. 92711) may be used. We have found this catheter to be more supple, and the permissible injection rates are slightly lower.

In our patients, only the axillary artery has been used for catheter introduction. Catheter sizes have been restricted to nos. 7 and 8 French. The sleeve introducer has been very effective to allow easy introduction of the catheter into the axillary artery and protected the puncture site from undue trauma caused by catheter manipulation. None of our patients has had an acute thrombosis or late neurologic sequelae.

In one patient with a severely tortuous atherosclerotic right subclavian artery, the balloon catheter could not be negotiated into the thoracic aorta. In all patients careful manipulation is required; however, the blunt closed-end soft tip of the balloon catheter is less likely to damage the arterial intima than standard catheters.

Illustrative Case Reports

Case 1

A 51-year-old male had an aortofemoral graft for treatment of severe occlusive disease of the distal abdominal aorta. On examination, femoral pulses and the left axillary pulses were not palpable. An angiographic catheter was introduced into the ascending thoracic aorta using standard Seldinger technique through the right axillary artery. Despite multiple attempts with various guide wires and catheters, catheterization of the descending thoracic aorta was not achieved. The angiographic catheter was replaced by a sheath introducer system, and a no. 7 French multiholed balloon catheter was inserted into the thoracic aorta. After inflation of the balloon, the catheter was easily directed into the descending aorta with minimal manipulation. Supine angiography was performed after pressure injection of contrast material at the maximum rate of 20 ml/sec for a total of 40 ml. Complete occlusion of the abdominal aorta below the origin of the inferior mesenteric artery at the site of previous graft was identified (fig. 2).

Case 2

A 70-year-old male was admitted for evaluation claudication. Attempts at catheterization of the abdominal aorta through the femoral artery were not successful because of severe arteriosclerotic narrowing of the proximal common iliac arteries (figs. 3*A* and 3*B*). Using the same technique as described for case 1, a balloon catheter was introduced into the abdominal aorta, and serial films were made after pressure injection of contrast material. The iliac arteries were patent; however, there was

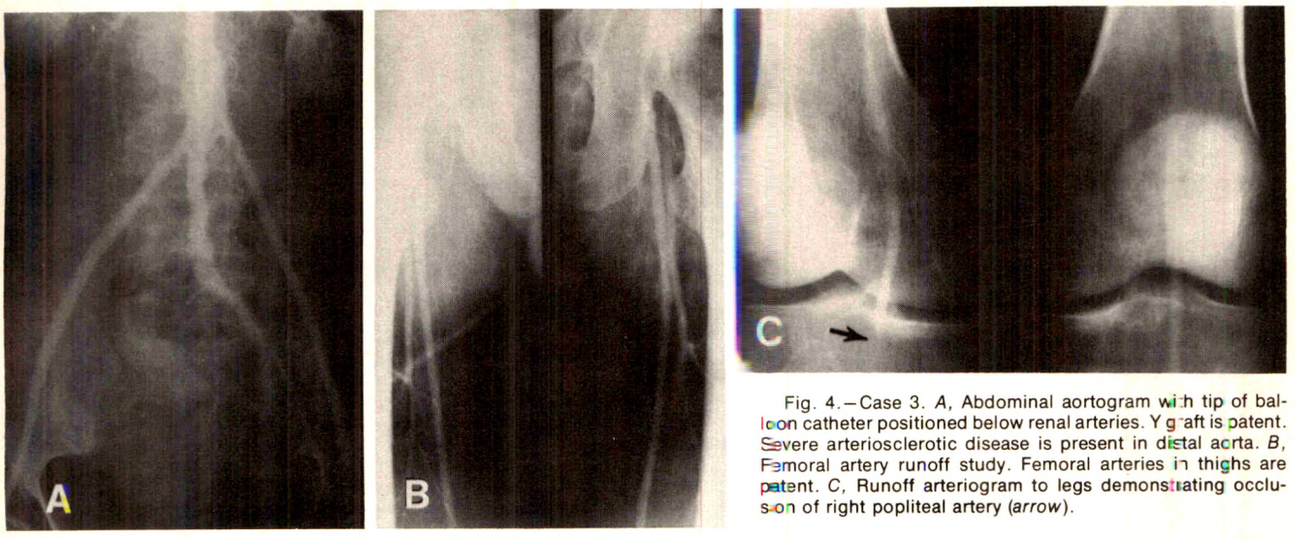

Fig. 4.—Case 3. *A*, Abdominal aortogram with tip of balloon catheter positioned below renal arteries. Y graft is patent. Severe arteriosclerotic disease is present in distal aorta. *B*, Femoral artery runoff study. Femoral arteries in thighs are patent. *C*, Runoff arteriogram to legs demonstrating occlusion of right popliteal artery (*arrow*).

severe atherosclerotic narrowing with irregularity of the mid-common iliac arteries (fig. 3*C*).

Case 3

A 63-year-old male had an abdominal Y graft for severe atherosclerotic disease of the distal abdominal aorta and common iliac arteries. One year later he had signs of occlusion of the right limb of the graft, confirmed by surgical femoral arteriography. Surgical replacement of that portion of the graft was accomplished. Immediately after surgery, right pedal pulses were not palpable and the left pedal pulses were diminished. The patient had been receiving anticoagulants, and bleeding from the graft was suspected.

Because of the presence of the abdominal aorta graft, anticoagulation, and suspected bleeding, translumbar aortography was considered hazardous. An axillary insertion of a catheter for visualization of the abdominal aorta and its branches was considered the best technique to determine graft patency. In this patient, additional assistance of a deflector wire system was necessary. In combination with the inflated balloon catheter, the abdominal aorta was readily entered. An embolus in the right popliteal artery was found, while both limbs of the graft were patent (fig. 4).

Discussion

The use of flow-directed balloon catheters has become a standard technique among cardiologists for catheterization of the right ventricle and pulmonary artery [1, 2]. This technique allows easy recording of physiologic data, including pulmonary venous wedge pressures. The addition of multiple side holes has allowed sufficient injection rates to produce satisfactory pulmonary arteriography. With this technique, catheterization of the pulmonary artery has been possible without fluoroscopy due to the flow characteristics of the inflated balloon.

Use of this technique to float catheters into difficult areas of the "downstream" arterial circulation for peripheral arteriography seems a natural extension. This technique has made angiographic examinations possible after all other attempts in some patients failed and translumbar aortography was considered hazardous. Because of the ease of manipulation and safety of these catheters, this technique may represent a preferable method of catheterization for peripheral studies in all patients requiring an axillary approach. Since there is the possibility of balloon rupture, carbon dioxide gas should be used.

REFERENCES

1. Swan HJC, Ganz JW, Forrester J: Catheterization of the heart in man with the use of flow directed balloon tipped catheter. *N Engl J Med* 283:447–451, 1970
2. Kelly DT, Krovetz LJ, Rowe RD: Double lumen flotation catheter for the use of complex cardiac anomalies. *Circulation* 44:910–913, 1971

A New Noninvasive Approach to Peripheral Vascular Disease: Thallium-201 Leg Scans

MICHAEL E. SIEGEL[1] AND JAN K. SIEMSEN[1]

A new noninvasive technique to evaluate blood flow distribution to the legs is described. Intravenous thallium-201 is used during rest and exercise followed by scanning and point counting of the lower extremities. The normal blood flow distribution recorded in 30 patients with no known peripheral vascular disease was primarily proportional to muscle mass. Using both scans and point counting, normal intra- and interextremity ratios were qualitatively and quantitatively defined, and significant increases in muscular to nonmuscular perfusion with exercise were documented. The symmetry in perfusion in the contralateral muscle groups was verified for the first time.

Anatomic detail offered by contrast angiogram is essential to the presurgical workup of patients with peripheral vascular disease. However, other methods of assessing the physiologic significance and the effect of vascular disease on the distribution of blood flow also frequently yield clinically significant information [1]. Previous work using intraarterial injections of radioactive human serum albumin microspheres has demonstrated effects of vascular disease unresolved by angiography in symptomatic patients and the true perfusion status of so-called ischemic ulcers [2, 3]. Microspheres labeled with various tracers injected at rest and during stress have demonstrated the effectiveness of collateral blood flow. In addition, such methods have localized what appeared to be physiologically significant lesions [4]. However, because of the particulate nature of the tracer, the microsphere perfusion study must be performed via intraarterial injection. To compare blood flow in both lower extremities the tracer must be delivered into the abdominal aorta.

It has been demonstrated that thallium-201 accumulation in heart is related to regional myocardial blood flow [5]. More recently it has been shown that, in skeletal muscle, thallium-201 distribution reflects the fractional distribution of cardiac output and is thus related to regional blood flow [6]. We have chosen to evaluate the nonparticulate, monovalent, cationic tracer, thallium-201, as a method for noninvasively studying the distribution of blood flow perfusion at rest and during stress in the lower extremities. This report accomplishes our initial objective of describing quantitatively and qualitatively the normal perfusion pattern and the effect of exercise on the distribution of blood flow.

Materials and Methods

Thallium-201 peripheral perfusion scans were performed in 30 consenting subjects who clinically showed no peripheral vascular disease and in five additional subjects who had angiographically demonstrable disease. Twenty males and 10 females were given an intravenous injection of 1–2 mCi of thallium-201 (as thallous chloride) while resting.

Approximately 5 min after injection of the tracer, the patients were placed supine on the scanning table of a dual probe 12.7 cm scanner and, using 1:5 minification, anterior and posterior scans of the lower extremities were obtained. A 20% window centered over the abundant mercury x-ray peak (69–80 keV) was used. In addition, point counting over the midthighs, knees, midcalves and ankles was performed and counts per unit area recorded. Points at measured distances from the knee were selected. The counting was performed with both a hand-held 2.54 × 1.27 cm collimated scintillation crystal attached to a pulse height analyzer and digital readout and with the scanning head and electronics of the dual probe scanner. No significant difference in ratios occurred using either method.

One week later the 30 normal subjects and the five subjects with vascular disease without foot ulcers had a second intravenous administration of 1–2 mCi of thallium-201 during peak exercise. A standardized cardiac treadmill exercise program was followed and patients were exercised until 90% of predicted heart rate was reached or until exercise could no longer be tolerated. The dose of tracer was administered during the peak exercise via indwelling intravenous catheter, and exercise was maintained an additional 2 to 3 min to assure the distribution of tracer reflected perfusion during that state. Scanning was begun approximately 5 min later and point counting was then performed as in the rest study.

To quantitatively define the perfusion distribution intra- and interextremity, at rest and during stress, between muscular groups, and between muscular and nonmuscular structures, various perfusion ratios were calculated from the counting data. Intraextremity distribution is described by thigh to calf (T/C), thigh to knee (T/K), and calf to ankle (C/A) ratios, and interextremity distribution is described by thigh to thigh (T/T) and calf to calf (C/C) ratios.

In addition to establishing the normal distribution patterns and to better understand the perfusion dynamics involved in going from rest to stress, each subject's ratios were compared at rest and during exercise to assess the magnitude and type of change in perfusion between the two states. Moreover, the distribution of perfusion and the changes in perfusion were assessed qualitatively by visual inspection of the perfusion scans.

Results

The ratios reflecting the distribution of perfusion in the normal subject in the resting state are summarized in table 1. The perfusion per unit area of the thigh tends to be greater than the calf as expected by its larger underlying bulk; in fact, it can be as much as 50% greater. As demonstrated in microsphere studies [1], the distribution

Received March 14, 1978; accepted after revision August 1, 1978.

[1] Department of Radiology, University of Southern California, 1220 North State Street, Suite 5250, Los Angeles, California 90033. Address reprint requests to M. E. Siegel.

© 1978 American Roentgen Ray Society

0361–803X/78/1100–0827 $00.00

TABLE 1

Perfusion Ratios in Normal Subjects

Ratio	Resting	Exercise
Thigh/calf	1.3 ± 0.2	1.4 ± 0.3
Thigh/knee	2.2 ± 0.3	3.7 ± 0.5
Calf/ankle	2.3 ± 0.5	3.5 ± 0.6
Right thigh/left thigh	1 ± 0.05	1 ± 0.5
Right calf/left calf	1 ± 0.05	1 ± 0.5

Note.—Data on 30 normal subjects. Values shown are mean ± SD.

of perfusion in normal individuals is primarily proportional to muscle mass (documented here by the mean T/K and C/A ratios of 2.2 and 2.3, respectively). The symmetry of perfusion between the muscle masses of the extremities is noted with the side to side, thigh and calf ratios approaching unity. This is especially useful information since even in the nonmuscular patient symmetry is maintained, although the muscular to nonmuscular perfusion ratio may be in the lower end of the normal range. The exercise perfusion ratios summarized in table 1 show symmetry of perfusion, perfusion primarily proportional to muscle mass, and a relative increase in perfusion of the thigh in comparison to the calf.

Fig. 1 graphically illustrates the relationship between the rest and exercise ratios in the 30 normal subjects. The relative distribution of perfusion between muscle masses (T/C ratio) is maintained; the symmetry is maintained (TR/TL, CR/CL ratios), and, as previously reported in the microsphere studies [1], there is a relative increase in perfusion of the muscular structures compared to the nonmuscular regions (T/K and C/A ratios). These changes are better appreciated when the individual ratios are displayed (fig. 2). Quantitatively, the changes indicated a mean increase in thigh to knee perfusion of 85% with a range of 40%–220%, and a mean increase in calf to ankle perfusion of 91% with a range of 45%–260%. These findings are qualitatively illustrated in the rest and exercise scans of a normal patient whose perfusion is symmetric and primarily proportional to muscle mass (fig. 3).

The normal study contrasts with figure 4, which is the rest scan of a 49-year-old female with left common iliac stenosis, bilateral superficial femoral artery occlusions, and ischemic changes of the first, second, and third toes of the left foot. Her left C/A ratio of 1.1 is greater than 2 SD from the mean, as is her left T/C ratio of 2.9. The intraextremity ratios on the right were not significantly different from normal. An ulcer involving the toes of the left foot is hypoperfused. This study suggests adequate collateralization on the right such that an extensive operative procedure may be avoided at this time.

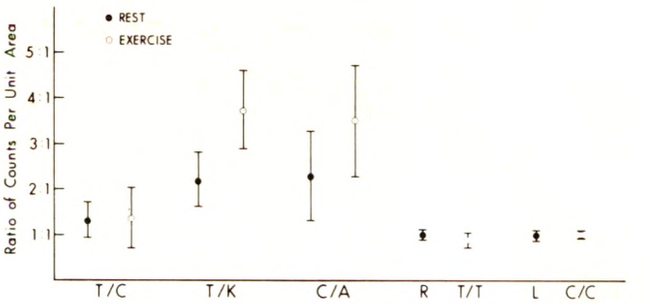

Fig. 1.—Peripheral vascular perfusion ratios defining distribution of perfusion in extremities at rest and during stress (mean ± 2 SD). T = midthigh, K = knee, C = midcalf, RT/T = right thigh to left thigh, and LC/C = left calf to right calf.

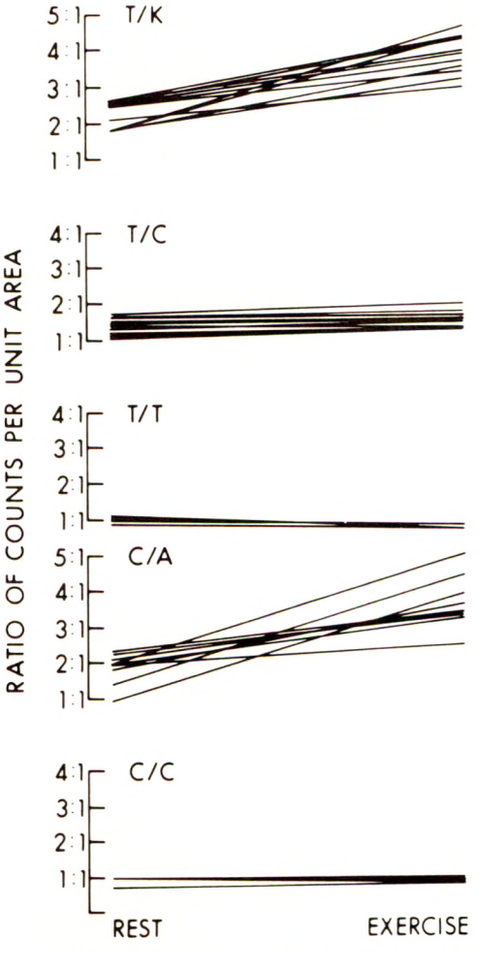

Fig. 2.—Changes in peripheral vascular perfusion ratios between rest and stress of five normal randomly selected subjects (10 extremities). Intraextremity distributions and interextremity symmetries are maintained.

Discussion

Thallium has properties similar to potassium in biologic systems and its distribution is determined by active intracellular transport and perhaps to some extent by tissue permeability. In interpreting our data we assume these factors are similarly operative among the patients such that distribution of the thallium is related to blood flow.

Miyamoto et al. [7] qualitatively assessed lower extremity perfusion using ^{43}K in nine patients and found good correlation between perfusion distribution, symptoms, and angiographic findings. Using microspheres in a larger series of patients, symptoms correlated better with the perfusion study than with the arteriogram, suggesting they reflected the physiologic effect of the disease and not merely the anatomy of larger vessels [8].

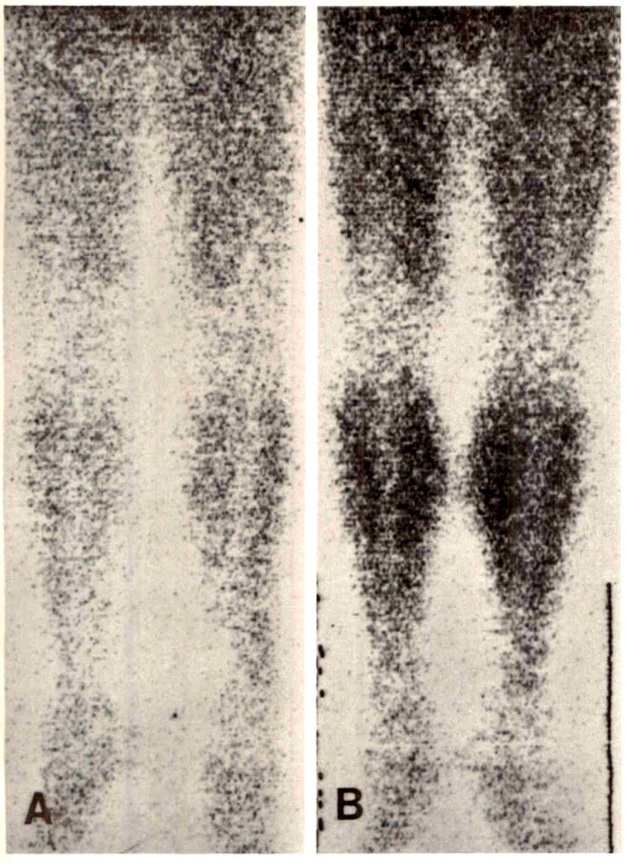

Fig. 3.—Normal distribution of tracer at rest (*A*) and during exercise (*B*). Perfusion to muscular structures increases with exercise.

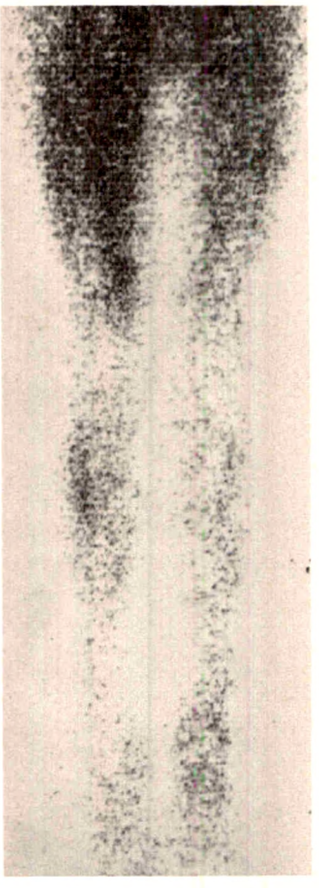

Fig. 4.—Rest scan of patient with left iliac stenosis, bilateral superficial femoral artery stenosis, and ulcer involving first three toes of left foot. Thighs and calves are asymmetric. Ulcer region appears hypoperfused.

The advantage to the microsphere study is that the particle size of 15–30 μm diameter allows essentially total extraction of tracer in one passage through the organ so that the distribution, assuming good mixing, reflects only arterial flow. However the particulate nature of the microsphere is a major disadvantage necessitating intraarterial administration, frequently by translumbar approach. Use of intravenous thallium-201 circumvents this drawback and also eliminates any question of inadequate mixing of the tracer with the blood. Moreover, its distribution appears to be primarily related to blood flow. A correlation coefficient of .93 has been reported in animals between distribution of microspheres and thallium in a group of organs including skeletal muscle [6].

Because of reports suggesting thallium uptake may not be linearly related to blood flow in the myocardium [9], we did not utilize directly the counts per unit area, but rather ratios between muscle and nonmuscular tissues. Although presently undocumented it may be that at higher flow rates where the linearity between thallium deposition and flow is lost, the cellular transport becomes the limiting factor in thallium distribution.

It is anticipated that this noninvasive approach to the study of peripheral vascular disease will offer a simple means of pre- and postoperatively evaluating the physiologic significance of vascular disease and the effects of various surgical interventions. it may also assist in the formulation of effective pharmacologic therapeutic regimens. The pathologic anatomy of the vasculature of the lower extremity can be readily demonstrated angiographically; yet, as already noted in ischemic ulcers [3], functional effects of occlusive disease are equally important in the clinical evaluation. On the basis of the observations in normal subjects reported in this paper, we are continuing our study of the effect of arterial disease on blood flow distribution.

REFERENCES

1. Siegel ME, Wagner HN: Radioactive tracer in peripheral vascular disease. *Semin Nucl Med* 6:253–278, 1976
2. Giargiana FA, Siegel ME, James AE, White RA, Wagner HN: A preliminary report on the complimentary roles of arteriography and perfusion scanning in assessment of peripheral vascular disease. *Radiology* 108:619–624, 1973
3. Siegel ME, Giargiana FA, Rhodes BA, Williams GM, Wagner HN: Perfusion of ischemic ulcers of the extremity. *Arch Surg* 110:265–268, 1975
4. Siegel ME, Giargiana FA, Rhodes BA, White RA, Wagner HN: Effect of reactive hyperemia on the distribution of radioactive micrography in patients with peripheral vascular disease. *Am J Roentgenol* 118:814–821, 1973
5. Strauss HW, Harrison BS, Langan RT, Lebowitz E, Pitt B: Thallium-201 for myocardial imaging. *Circulation* 51:641–645, 1975
6. Strauss HW, Harrison K, Pitt B: Thallium-201: non-invasive

determination of the regional distribution of cardiac output. *J Nucl Med* 18:1167–1170, 1977

7. Miyamoto AT, Mishkin FS, Maxwell TM: Non-invasive study of extremity perfusion by potassium 43 scanning. *Arch Surg* 10:58–63, 1975
8. Siegel ME, Giargiana FA, White RA, Friedman BA, Wagner HN: Peripheral vascular perfusion scanning: correlation with the arteriogram and clinical assessment in patients with peripheral vascular disease. *Am J Roentgenol* 125:628–635, 1975
9. Hamilton GW, Narahara RA, Yee H, Ritchie JL, Willimas DL, Gould KL: Myocardial imaging with thallium-201: effect of cardiac drugs on myocardial images and absolute tissue distribution. *J Nucl Med* 19:10–16, 1978

Computed Tomography in the Detection of Retroperitoneal Hemorrhage after Translumbar Aortography

ALAN B. BERGMAN[1] AND HARVEY L. NEIMAN[1]

Direct imaging of retroperitoneal hemorrhage following translumbar aortography was performed using computed tomography. Seven patients were scanned over the area of aortic entry immediately after undergoing angiographic examination. In five cases, there was definite evidence of periaortic hematoma, most commonly seen as a discrete soft tissue density with absorption coefficients between +20 and +35 EMI units. Other signs of retroperitoneal bleeding were less consistently present (e.g., loss of aortic contour, aortic displacement, and thickening of diaphragmatic crura). The clinical implications of detecting significant hemorrhage following translumbar aortography are also discussed.

The translumbar approach to aortography is frequently used to evaluate patients in whom severe aortoiliac occlusive disease, aneurysm, or previous surgery precludes femoral catheterization. The complications of this procedure have been well documented by several investigators who have performed large numbers of these examinations [1–4]. One of these complications, that of retroperitoneal hemorrhage, frequently accompanies translumbar catheterization, although it does not commonly produce major clinical sequelae. The presence of bleeding around the puncture site has been noted at surgical exploration and can occasionally be detected by conventional radiologic signs (soft tissue mass, psoas shadow obliteration, renal or ureteral displacement). The direct imaging of retroperitoneal hemorrhage following translumbar aortography, however, has not been previously documented. The use of computed tomography (CT) has been helpful in this regard, since this modality provides direct visualization of both acute and chronic hematomas. In this study the aorta was scanned immediately after translumbar aortography in order to identify patterns of bleeding in the retroperitoneal space.

Subjects and Methods

Seven patients were evaluated, all of whom had clinical evidence of advanced aortoiliac atherosclerotic disease. These patients were seen consecutively and all were asymptomatic following the study. Translumbar aortography was performed in five cases with a 17 gauge dos Santos needle (Becton-Dickinson, Rutherford, N.J.) and in two cases with a needle-sheath combination. A "high" suprarenal approach was used in all cases, with aortic puncture performed at the T12 level. In six of the seven patients, the procedure was atraumatic, with entry into the aorta on the first or second pass. In one patient with thoracolumbar scoliosis, three needle passes were attempted before successful aortic puncture was accomplished.

Following contrast injections and filming, the level corresponding to the aortic puncture site was marked on the skin under fluoroscopic control. The patient was then immediately examined by computed tomography, using the EMI 5005 unit. With the patient in the prone position, scans were obtained at 1 cm intervals for a distance of 3 cm above and below the marked level of aortic puncture. Subsequently, the scans were viewed on a 320 × 320 matrix display. Analyses of the resultant images were then made, attempting to delineate the presence and site of retroperitoneal hemorrhage around the area of needle entry.

Results

On the basis of previous reports, the criteria used for CT diagnosis of retroperitoneal hemorrhage include: (1) presence of a medium to high density soft tissue mass in the periaortic region; (2) partial or complete obliteration of aortic countour; (3) displacement of the aorta; and (4) asymmetric thickening of the diaphragmatic crura [5–7]. Table 1 shows the CT findings in our patients. Five patients (71%) had one or more signs of retroperitoneal hemorrhage following translumbar aortography. In two patients, there was no demonstrable evidence of retroperitoneal bleeding using the above criteria. All patients with positive CT examinations were found to have a soft tissue mass surrounding the aorta. Crural thickening and partial contour obliteration were seen in four patients, and aortic displacement was noted in one case.

Examples of these findings are provided in the accompanying illustrations. The scan from case 1, performed at the level of puncture, shows a diamond-shaped soft tissue density marginated laterally by the left diaphragmatic crus and medially by the left aortic wall (fig. 1*A*). This mass had an absorption coefficient of +30 EMI units, placing it within the range of blood. A single film

TABLE 1

CT Findings

Case No.	Periaortic Soft Tissue Mass	Aortic Contour Obliteration	Aortic Displacement	Crural Thickening
1	+	+	–	+
2	+	+	–	+
3	+	+	+	+
4	+	+	–	+
5	+	–	–	–
6	–	–	–	–
7	–	–	–	–
Total	5/7 (71%)	4/7 (57%)	1/7 (14%)	4/7 (57%)

Received April 28, 1978; accepted July 20, 1978.

[1] Department of Radiology, Northwestern Memorial Hospital and Northwestern University School of Medicine, 250 East Superior Street, Chicago, Illinois 60611. Address reprint requests to H. L. Neiman.

© 1978 American Roentgen Ray Society

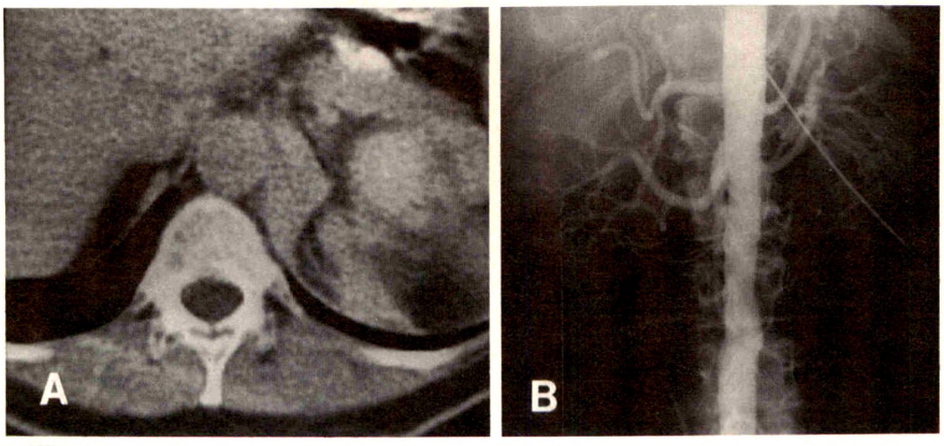

Fig. 1.—Case 1. *A*, Scan at level of aortic puncture showing soft tissue mass between aorta and left diaphragmatic crus. *B*, Aortogram demonstrating intraluminal placement of needle at T12 level.

from the aortogram documents the intraluminal position of the needle at the T12 level (fig. 1*B*).

The scan from case 2 was made 1 cm above the level of the puncture site. Thickening of the retrocrural space is demonstrated bilaterally, as well as obliteration of aortic contour (fig. 2).

Case 3 had a markedly calcified aorta which made puncture somewhat difficult. The scan was performed 1 cm below the level of the puncture site. It demonstrates prominent calcification of the aortic wall, the posterior aspect of which is displaced anteriorly by a small transversely oriented band of soft tissue representing the hematoma (fig. 3). In addition, there is also slight fullness in the left retrocrural space, indicating extension of bleeding into this contiguous compartment.

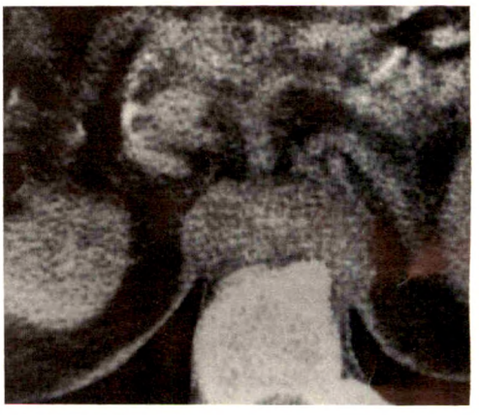

Fig. 2.—Case 2. Scan 2 cm above puncture site showing thickened retrocrural space and obliteration of aortic contour. Celiac, splenic, and common hepatic arteries are well demonstrated.

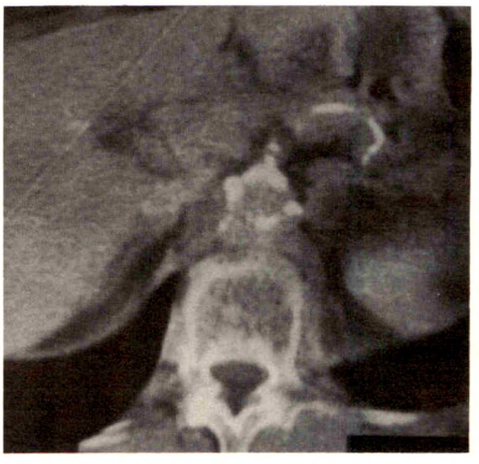

Fig. 3.—Case 3. Scan 1 cm below puncture site showing markedly calcified aorta displaced by posteriorly located hematoma.

Discussion

The translumbar technique has been a valuable adjunct to the clinical evaluation of patients with arterial disease. The overall safety of this method in experienced hands has been well established [1]. However, the occasional complication of severe periaortic hemorrhage is a danger that should be taken into account when evaluating patients for this procedure, especially patients with severe hypertension or hemorrhagic diatheses. Another rare but significant complication is hemothorax secondary to transpleural puncture. Szilagyi et al. [1] described four patients with this complication, one with a fatal outcome. Intrathoracic hemorrhage is obviously more frequent with the use of the high puncture technique at the T12 level. Thus CT can be important in the detection of bleeding following translumbar aortography.

Approximately 50 ml of blood can be noted around the aortic puncture site if surgical exploration is undertaken after translumbar catheterization [8]. Judging from the relatively well confined hematomas in our series, this appears to be true in uncomplicated cases. Because of the anatomic configuration of the retroperitoneum, blood loss of a clinically significant magnitude into this space can occasionally be masked until acute symptoms occur. CT allows for early detection of such bleeding when it may represent a significant clinical problem. In addition, this imaging modality can demonstrate the extension of bleeding beyond the retrocrural space into other areas of the retroperitoneum, such as the pararenal space. Such information may aid in assessing the approach for surgical evacuation of the hematoma, should

this be necessary. CT may also be used in the follow-up of patients who are treated for retroperitoneal hemorrhage by transfusion alone. The documentation of increasing size of a hematoma in the face of continued blood replacement would be helpful in evaluating the patient for possible surgical intervention. In considering the rare but serious transpleural laceration from misdirected punctures, CT may also be an adjunctive procedure in patients with equivocal radiographs.

Our study indicates that most retroperitoneal hematomas following translumbar aortography are small and cause minimal alterations in surrounding structures. The presence of a small but discrete soft tissue mass is the most common CT finding in the positive cases of this series. The other signs of retroperitoneal hemorrhage (i.e., thickened diaphragmatic crura, obliteration of aortic contour, and aortic displacement) were not consistently demonstrated because hematomas have variable size and do not encroach upon surrounding tissue to the same degree.

REFERENCES

1. Szilagyi DE, Smith RF, Elliot JP, Hageman JH: Translumbar aortography: a study of its safety and usefulness. *Arch Surg* 112:399–408, 1977
2. Gammil S: Translumbar aortography updated. *Surg Gynecol Obstet* 140:59–64, 1975
3. Stocks LO, Halpern H, Turner AF: Complete translumbar aortography. *Am J Roentgenol* 107:835–839, 1969
4. Amplatz K: Translumbar catheterization of the abdominal aorta. *Radiology* 81:927–931, 1963
5. Siegel SS, Siegel MJ, Stanley RJ, Jost RG: Detection of retroperitoneal hemorrhage by computed tomography. *Am J Roentgenol* 129:403–407, 1977
6. Axelbaum SP, Schellinger D, Gomes MN, Ferris RA, Hakkal HG: Computed tomographic evaluation of aortic aneurysms. *Am J Roentgenol* 127:75–78, 1976
7. Stephens DN, Williamson BW, Sheedy PF, Hattery RR, Miller WE: Computed tomography of the retroperitoneal space. *Radiol Clin North Am* 15:377–390, 1977
8. White RI: *Fundamentals of Vascular Radiology*. Philadelphia, Lea & Febiger, 1976

Detection of Neoplastic Involvement of the Mesentery and Omentum by Computed Tomography

ROBERT G. LEVITT,[1] STUART S. SAGEL, AND ROBERT J. STANLEY

A total of 39 patients undergoing abdominal computed tomography and subsequent surgical biopsy of the mesentery or omentum were studied to evaluate the sensitivity of CT in detecting metastases to those areas. Twelve patients had negative biopsies; there were no false positive CT interpretations in that group. Of the 27 patients with positive biopsies, 18 showed positive findings on CT scan. Those patterns of involvement are described and illustrated. The nine false negative cases related to very small metastatic foci, contiguity with the primary tumor, or paucity of intraabdominal fat.

The radiologic diagnosis of neoplastic involvement of the mesentery and omentum has heretofore relied on indirect evidence on a barium upper gastrointestinal and small bowel examination. With the advent of CT scanning, the diagnosis of mesenteric or omental masses may be made directly. This report illustrates the various CT presentations of neoplastic involvement of the mesentery and omentum in 18 surgically proven cases. The limitations of the technique and differential diagnostic possibilities are also discussed.

Materials and Methods

CATBOD, a computerized CT data storage and retrieval program [1], was used to identify all patients with a surgical biopsy of mesentery or omentum who had a prior abdominal CT scan. A total of 39 patients were identified: 27 patients had pathologic evidence of neoplastic mesenteric or omental disease and 12 patients had normal mesentery or omentum. All 27 cases of neoplastic disease were metastatic carcinoma or lymphoproliferative disease. Primary mesenteric and omental neoplasms are rare and were not encountered in this series. CT scanning had been performed in the majority of these cases to search for an occult malignancy or to evaluate the extent of disease in a patient with known malignancy.

CT examinations were performed on a prototype EMI model 5000 scanner or the updated model 5005, both with 18 sec scanning times. Oral contrast, consisting of 235–470 ml (8–16 oz) of a 3% solution of Gastrografin, was given 30–60 min prior to scanning to opacify intestinal loops so that fluid-filled intestinal loops would not be mistaken for abnormal masses. Peristaltic motion during scanning was limited with 0.5 mg glucagon given intravenously just before scanning.

Results

Of the 27 cases of neoplastic disease involving the mesentery or omentum, 18 were identified using CT. No false positive diagnoses were made. Each case of neoplastic involvement of the mesentary or omentum presented as a mass(es) of soft tissue density (20–30 EMI units) within the abdomen or pelvis.

Positive CT Findings

Mesentery (12 cases). Clusters of round soft tissue density masses due to enlarged lymph nodes were seen. Individual masses ranged from 1 to 5 cm in diameter (figs. 1 and 2). This pattern was seen in four cases of lymphoma and two cases of chronic lymphocytic leukemia. Single well demarcated soft tissue masses (fig. 3) were seen in five patients: three with lymphoma and two with colonic carcinoma. In such cases the mass probably represented a conglomeration of enlarged mesenteric lymph nodes. Thickened mesenteric leaves radiating from the mesenteric root were seen in a single case of breast carcinoma (fig. 4).

Omentum (six cases). All of these cases were due to ovarian carcinoma and showed soft tissue masses in the anterior portion of the pelvis (fig. 5). In three of these cases, the fat plane between the soft tissue density pelvic mass and anterior abdominal wall could not be discerned (fig. 6). At surgery the omental mass was adherent to the abdominal wall, and the surgeons described all the masses as "omental cakes" (i.e., thickened omentum diffusely infiltrated with tumor nodules).

False Negative CT Findings

Analysis of surgical and pathologic findings in the nine cases in which proven mesenteric or omental metastases were not detected by CT revealed the following:

1. Mesenteric or omental metastases were less than 1 cm at surgery (one case of cervical carcinoma and one case of breast carcinoma).
2. Only microscopic evidence of tumor was present (two cases of lymphoma). There was no evidence of mesenteric or omental metastases at surgical or gross pathologic inspection.
3. Mesenteric or omental metastases were adjacent to the primary tumor and could not be resolved from the primary tumor by CT (one case each of cecal carcinoma, pancreatic carcinoma, gastric leiomyosarcoma, and lymphoma of the ascending colon).
4. Gross mesenteric and retroperitoneal metastases from a spermatic cord carcinoma were seen at surgery in a thin patient who lacked abdominal fat. Only the retroperitoneal metastases were identified on the preoperative CT scan.

Received May 23, 1978; accepted July 28, 1978.
R. G. Levitt is a James Picker Foundation Scholar.

[1] All authors: Mallinckrodt Institute of Radiology, Washington University School of Medicine, 510 South Kingshighway Boulevard, St. Louis, Missouri 63110. Address reprint requests to R. G. Levitt.

© 1978 American Roentgen Ray Society

0361–803X/78/1100–0835 $00.00

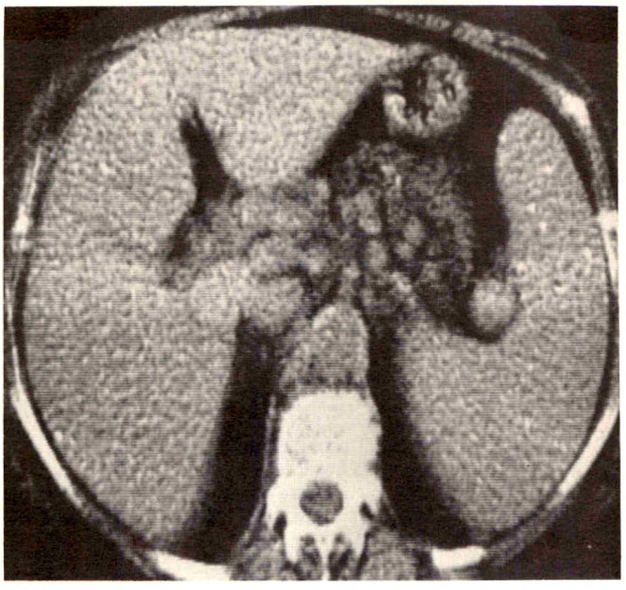

Fig. 1.—68-year-old woman with chronic lymphocytic leukemia and epigastric pain. Upper gastrointestinal series showed retrogastric mass. CT scan shows cluster of small soft tissue density masses in midabdomen around pancreas. At splenectomy, masses were enlarged leukemic mesenteric lymph nodes.

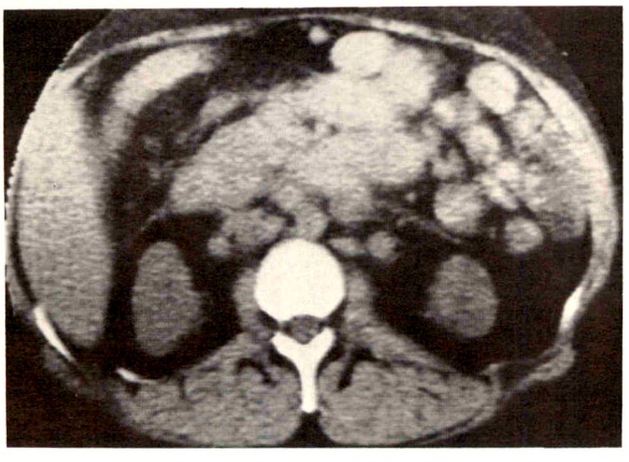

Fig. 2.—31-year-old woman with lymphoma and epigastric pain. CT scan shows large soft tissue density masses in midabdomen due to enlarged lymphomatous mesenteric lymph nodes, as well as retroperitoneal adenopathy.

CT Correlation with Barium Studies

Although only gross evidence of mesenteric or omental neoplastic disease was identified using CT, mesenteric or omental metastases were identified with CT which were not detected on conventional upper gastrointestinal and small bowel barium examinations. Such examinations were performed in seven of 18 cases in which surgically proven mesenteric or omental metastases were detected using CT. In three cases the barium examinations showed displacement of the stomach,

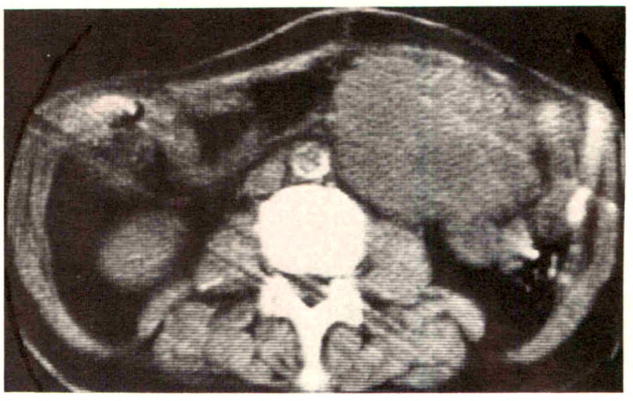

Fig. 3.—68-year-old man with palpable mass in left abdomen. CT scan shows large solitary soft tissue density mass with epicenter in peritoneal cavity. Surgery revealed conglomeration of enlarged mesenteric lymph nodes due to histiocytic lymphoma.

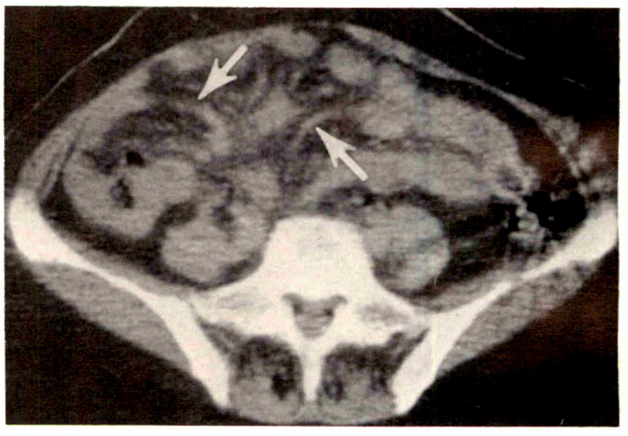

Fig. 4.—72-year-old woman with breast carcinoma and abdominal pain. CT scan shows linear radiating soft tissue densities (*arrows*) along course of normal mesenteric vessels. At surgery, mesentery of small bowel was infiltrated with tumor which thickened the perivascular bundles.

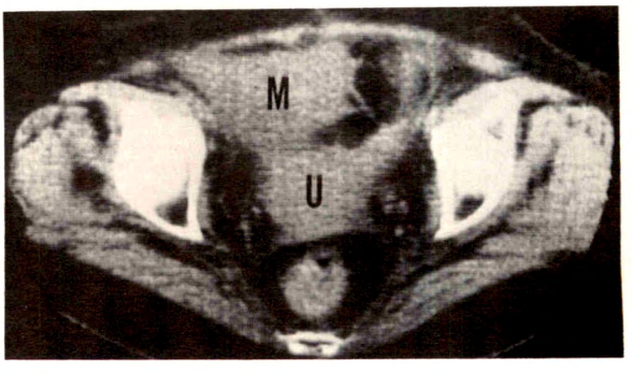

Fig. 5.—66-year-old woman with previously resected carcinoma of right ovary who developed palpable pelvic mass. CT scan shows soft tissue density pelvic mass (M) due to omental metastases anterior to uterus (U).

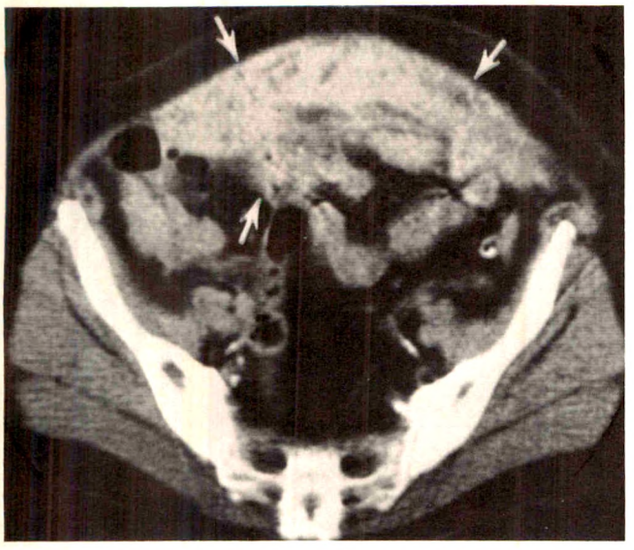

Fig. 6.—80-year-old woman with previous resection of ovarian carcinoma and current symptoms suggesting bowel obstruction. CT scan shows anterior pelvic mass (*arrows*). Normal fat plane posterior to abdominal wall is not defined. Air and fluid in bowel loops are intimately associated with posterior border of mass. At surgery, omentum was infiltrated with tumor and fixed to abdominal wall anteriorly and to bowel loops posteriorly.

duodenum, or small bowel by an extrinsic mass. In the other four cases the barium examinations were normal. Conventional barium examinations were also performed in three of nine cases in which surgically proven mesenteric or omental metastases were not detected using CT. In no case was an extrinsic mass effect detected by the contrast studies.

Discussion

Review of our cases revealed that only gross evidence of mesenteric or omental metastases could be identified using CT. Such identification required patients with some amount of intraabdominal or intrapelvic fat who were able to suspend respiration for the 18 sec scanning period.

The location of omentum anterior to small bowel and colon allowed omental masses to be differentiated from mesenteric masses in this series. However, if a large mesenteric mass extends anteriorly, this differentiation may not be possible. Mesenteric metastases from lymphoproliferative disease and omental metastases from ovarian carcinoma, a common occurrence when these tumors disseminate, were the most frequent metastases detected by CT. Interestingly, only lymphoproliferative disease was seen as a cluster of round soft tissue density masses within the mesentery. No case of metastatic carcinoma producing such a pattern was encountered in our series.

While 18 of 27 cases (66%) of proven mesenteric or omental metastases were detected using CT, this figure probably overestimates the sensitivity of CT in the detection of mesenteric and omental metastases. In many patients with primary abdominal or pelvic malignancy in whom no mesenteric or omental metastases have been detected using CT, the diagnosis of metastatic disease has been made by biopsy of tissue other than mesentery or omentum (e.g., a portal lymph node in pancreatic carcinoma). Many of these patients may have had mesenteric or omental metastases as well, but they are not included in this series because there was no pathologic examination of the mesentery or the omentum.

Some interpretative problems may arise. A "pseudomass" of the mesentery may be observed on CT scans of obese patients (fig. 7). Although abundant fat in the mesentery may create a focal mass effect, the attentua-

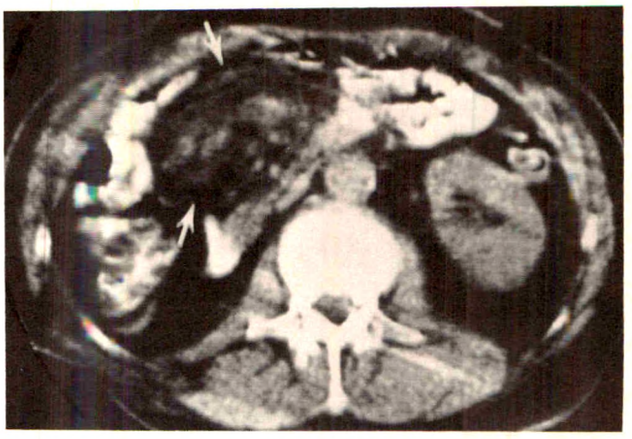

Fig. 7.—66-year-old moderately obese man. CT scan shows "pseudomass" (*arrows*) produced by unopacified bowel loops and vascular structures in abundant mesentery surrounded by opacified bowel loops.

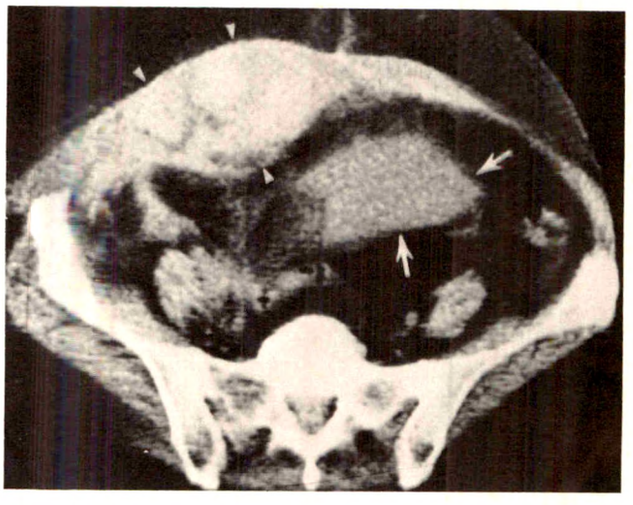

Fig. 8.—61-year-old obese woman on anticoagulants with acute onset of abdominal pain and fall in hematocrit value. CT scan shows soft tissue masses in mesentery (*arrows*), consistent with hematoma. Large mass in right anterior abdominal wall with high density areas (35 EMI units) consistent with acute rectus sheath hematoma (*arrowheads*).

tion value is that of neutral fat, and normal-sized vessels can be seen coursing through the fat. Additionally, the mesentery or omentum about an operative site may become fibrotic and matted from chronic inflammation and produce a pseudomass on CT. Also, the various CT presentations of mesenteric and omental metastases are not specific for malignant disease within these tissues. Any soft tissue density mass within the mesentery or omentum (e.g., hematoma, fig. 8) could produce a similar appearance.

ACKNOWLEDGMENTS

We thank Jack Trachtman for programming assistance, Nancy M. Levitt for collating this data, and Ann Marie Brock for editorial assistance.

REFERENCE

1. Levitt RG, Jost RG, Trachtman J, Sagel SS, Stanley RJ: CATBOD: a computer-assisted method to determine the diagnostic efficacy of computed tomography of the body. *Radiology* 123:97–101, 1977

Computed Tomography of Necrotic Hepatic Metastases

WAYNE B. WOOTEN,[1] MICHAEL E. BERNARDINO,[1] AND HARVEY M. GOLDSTEIN[1, 2]

Seven patients with necrotic liver metastases were evaluated by computed tomography. The metastases demonstrated low attenuation areas varying from a small central portion to the entire lesion. Other findings included mural nodules and fluid-fluid levels. Possible etiologies for necrotic metastases are presented and their differential diagnosis is discussed.

Computed tomography (CT) is useful in evaluating the liver for space-occupying lesions, including cysts, abscesses, and primary or metastatic tumors [1–5]. All of these entities have been described as areas of varying decreased attenuation when compared to adjacent normal parenchyma. Only a few reports have mentioned the CT appearance of necrotic hepatic metastases which may be confused with benign cysts or abscesses. [4, 5]. This communication describes our experience with seven patients who demonstrated very low density hepatic metastases. The evidence that this appearance represents necrosis is discussed, and the CT appearance is correlated with other radiographic studies and pathologic findings. Differential diagnostic considerations are emphasized.

Subjects and Methods

The series included seven patients with metastatic liver disease. The five females and two males ranged in age from 31 to 71 years. Histologic proof of liver metastases was obtained in six cases by laparotomy and/or percutaneous needle biopsy. The primary neoplasm was colon carcinoma in three, gastrointestinal leiomyosarcoma in two, carcinoid tumor in one, and melanoma in one.

Each case had liver enlargement and abnormal liver function tests. All of the patients had positive radionuclide liver scans showing one or more focal defects. All patients but one had an ultrasonographic examination before or just after CT examination. Two patients were examined by hepatic angiography, and one patient had percutaneous needle puncture of a metastatic lesion with fluid analysis and double contrast examination of the cavity. One patient had examination of the liver at autopsy.

All patients were examined with a commercially available EMI 5005 scanner using a 13 mm collimator, a 320 × 320 matrix, and an 18 sec scan time. Most studies were obtained at 2 cm intervals. Six patients had examinations before and after intravenous drip infusion of 300 ml of 30% meglumine diatrozoate; one patient had examination only after contrast infusion. Images were recorded at wide and narrow window widths and attenuation measurements were made of all lesions.

Results

Six patients had multiple liver metastases, some of which had low attenuation areas; one patient had a solitary low density lesion. The size of the lesions ranged from 2 to 10 cm. Their general two-dimensional shape was round to ovoid with contours varying from discrete and smooth to poorly defined and irregular.

The area of low attenuation relative to the entire metastasis varied from only a small central portion (fig. 1) to the entire lesion. In most of the metastases, the low density area constituted the vast majority of the lesion (fig. 2). The remaining peripheral portion of the metastasis often had the appearance of a higher density, thick rim around the low attenuation area. After administration of intravenous contrast material, there was relative enhancement of the peripheral portion of the metastasis which tended to accentuate the rim effect and make the demarcation more discrete. No enhancement of the central low attenuation areas occurred. In three cases a small "mural nodule" of somewhat higher density was observed to project from the periphery into the low attenuation area (fig. 3).

Attenuation measurements of the central portion of the lesions were obtained in all patients (table 1). The measurements ranged from 0 to about 15 EMI units, and all were uniformly lower than other, more typical metastatic lesions seen in the same liver. There was no change in the attenuation measurements after the ad-

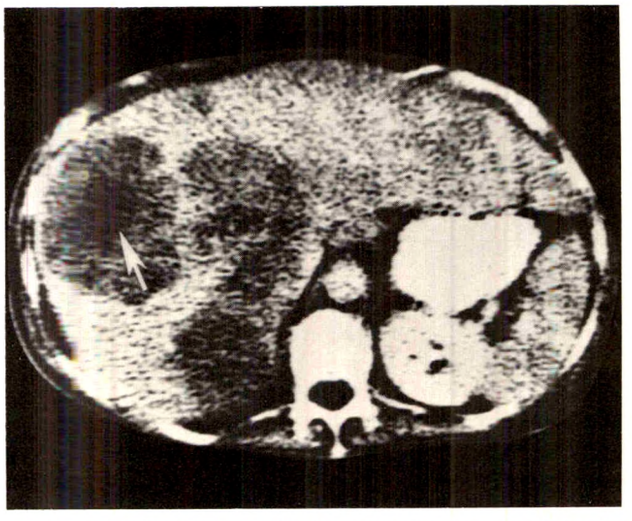

Fig. 1.—Case 1, 57-year-old female with colon carcinoma. Scan after intravenous contrast administration demonstrating liver metastasis with small central area of lower attenuation (*arrow*). Other metastases are also noted in various stages of evolution.

Received April 4, 1978; accepted after revision July 27, 1978.

[1] Department of Diagnostic Radiology, University of Texas System Cancer Center, M. D. Anderson Hospital and Tumor Institute, Houston, Texas 77030. Address reprint requests to M. E. Bernardino.

[2] Present address: 3303 Buckhaven, San Antonio, Texas 78230.

© 1978 American Roentgen Ray Society

0361–803X/78/1100–0839 $00.00

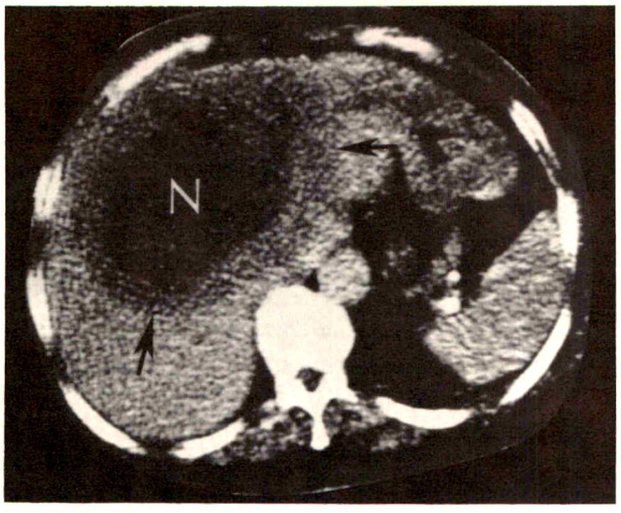

Fig. 2.—Case 2, 71-year-old female with gastric leiomyosarcoma. Scan after intravenous contrast administration showing large area of decreased tissue attenuation (N) constituting almost entire metastatic lesion. Note higher density peripheral rim (*arrows*).

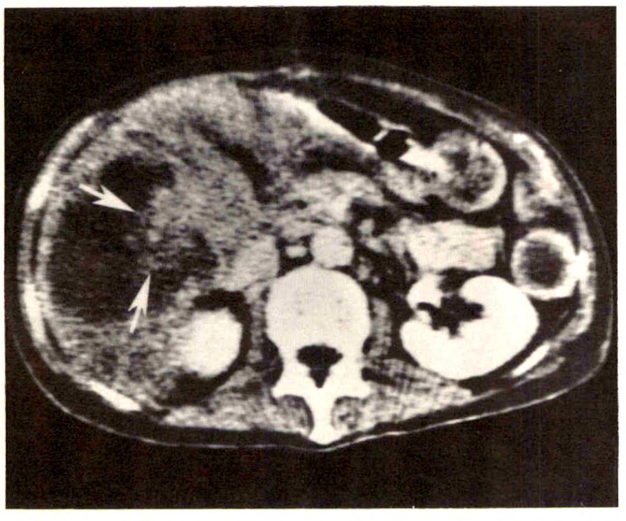

Fig. 3.—Case 3, 66-year-old female with colon carcinoma. Scan with intravenous contrast material showing mural nodule (*arrows*) projecting from periphery of necrotic metastasis.

ministration of intravenous contrast material in six patients.

Two patients had fluid-fluid levels in some of the lesions (fig. 4*A*). In one of these patients, a single metastasis illustrated this finding on the initial examination; in the other case, development of fluid-fluid levels was noted in multiple lesions on a follow-up study (fig. 5). The attenuation measurements of the metastatic contents above the fluid-fluid level was that of water, while the lower layer ranged from 10 to 15 EMI units. Rescanning one patient in the lateral decubitus position demonstrated shifting of the fluid-fluid levels to maintain a horizontal position (fig. 5*B*).

The CT features correlated well with other imaging studies and pathologic findings. In the six patients who

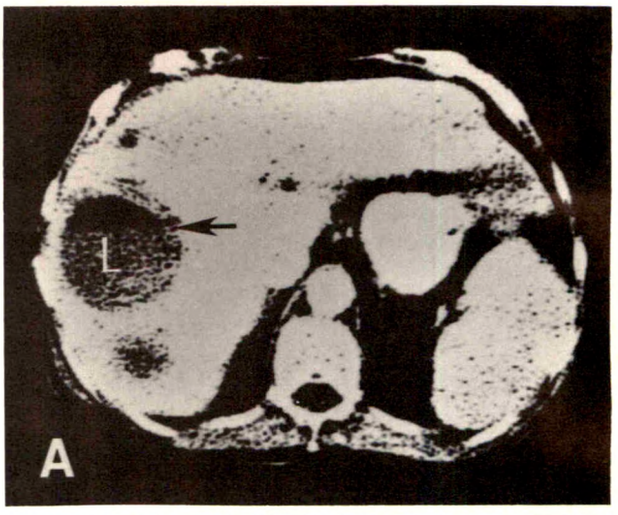

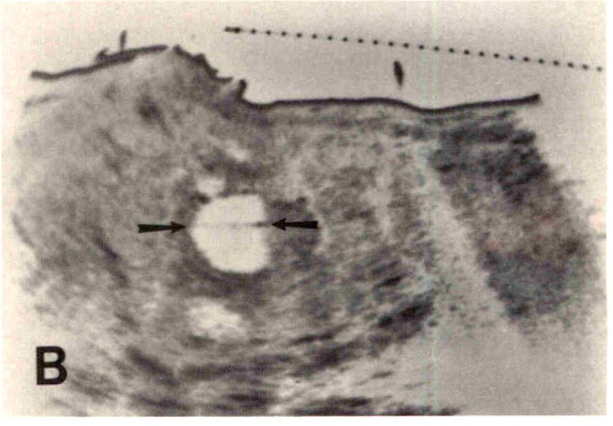

Fig. 4.—Case 4, 61-year-old female with carcinoid tumor of small bowel. *A*, Necrotic metastasis with fluid-fluid level (*arrow*) in right lobe (no contrast enhancement). Upper level has attenuation value near zero, while lower level (L) measured about 15 EMI units. *B*, Sagittal ultrasonogram correlates with CT findings. Anechoic metastasis with fluid-fluid level (*arrows*) is demonstrated.

TABLE 1

Attenuation Measurements of Central Portion of Metastases

Case No.	Precontrast	Postcontrast
1	. . .	0
2	2–4	2–4
3	3–8	3–8
4	2*	2*
	15†	15†
5	0–5	0–5
6	0	0
7	0	0

Note.—Data reported in EMI units. Ranges represent measurements of several similar lesions or several from the same lesion.

* Upper level.

† Lower level.

had ultrasonographic examination, partially or totally anechoic lesions, some closely resembling cysts, were identified (fig. 5*C*). In the two patients with fluid levels, the ultrasonic counterpart was also readily identified (fig. 4*B*). Both patients who underwent hepatic angiog-

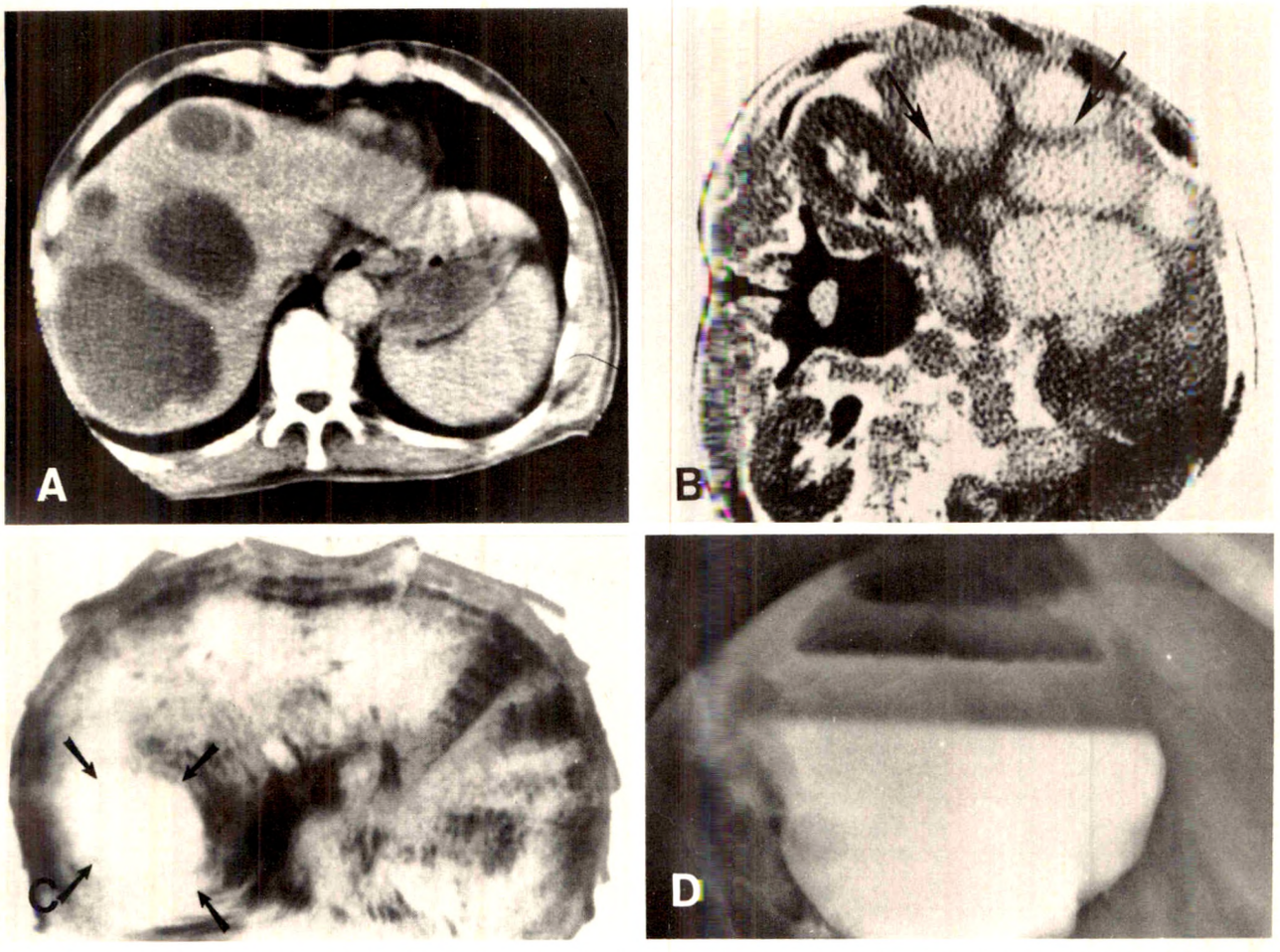

Fig. 5.—Case 5, 64-year-old male with metastatic leiomyosarcoma. *A*, Initial CT examination after contrast infusion demonstrating multiple low attenuation metastatic lesions. *B*, CT examination with contrast 4 months later after further chemotherapy, left lateral decubitus position. Note horizontal layering of fluid-fluid levels (*arrows*) within two necrotic metastases. *C*, Ultrasonographic examination at same time as *A* demonstrating sonolucent metastasis in right lobe (*arrows*). *D*, Upright radiograph after injection of contrast material and air into metastasis further confirming its cavitary nature.

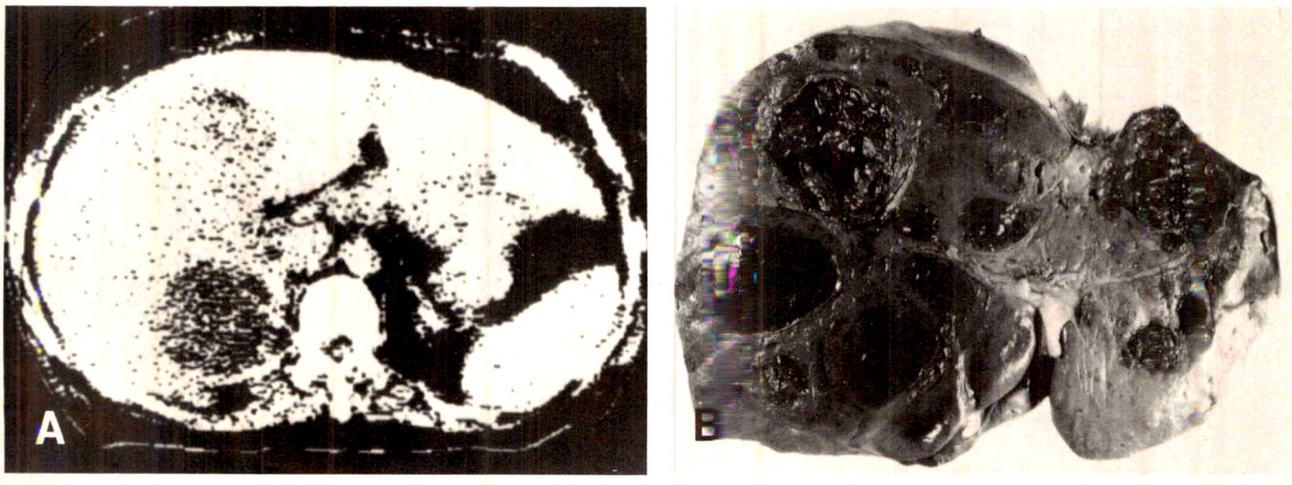

Fig. 6.—Case 6, 58-year-old female with metastatic melanoma. *A*, Measurement mode of non-contrast-enhanced scan demonstrating necrotic metastasis with attenuation value near zero. *B*, Postmortem specimen illustrating multiple metastases in varying stages of necrosis.

raphy demonstrated avascular metastases with thickened hypervascular rims.

In the patient in whom percutaneous aspiration was performed, free-flowing, dark brown fluid which contained considerable hemolyzed blood was obtained. Injection of contrast material confirmed a large cavity (fig. 5*D*). Postmortem examination in another case revealed a large number of excavated metastases filled with dark fluid or reddish brown, semisolid necrotic material (fig. 6).

Discussion

Liver metastases have been described as areas of decreased density within the liver and may be well defined or indistinct [1–5]. Usually the attenuation values are 5–10 EMI units lower than the normal surrounding parenchyma. Low density metastases, as described here, have been illustrated only twice, but the attenuation values in these cases were not indicated [4, 5].

Considering the ultrasonographic appearances in six patients and the pathologic material in two patients, we believe the presence of a low density metastasis signifies necrosis. The range of attenuation measurements seen in our patients may reflect variations in the degree of necrosis. The higher attenuation levels probably indicate an earlier stage of necrosis while attenuation values near that of 0 presumably represent liquefactive necrosis. The extensive degree of excavation with actual liquefaction in some cases is further demonstrated by the two patients in whom fluid-fluid levels were demonstrated.

Necrosis of hepatic metastases is in part due to the natural course of certain metastatic lesions such as sarcomas [6]. As these metastases increase in size, they often begin to degenerate and necrose. In addition, all of our patients were being treated with chemotherapy prior to or at the time of the CT examination. Presumably this also plays a role in the necrotic process.

Major differential considerations include benign hepatic cysts, abscesses, and chronic hematomas. Differentiation of cystic-appearing metastases from benign hepatic cysts may be difficult in some cases using the information solely provided by CT. Cysts are generally sharply demarcated with thin walls having attenuation coefficient values near that of 0 [5]. Liver abscesses also usually appear as low density areas that typically have attenuation values falling between those of cysts and neoplasms [2]. Depending on the stage of their evolution, abscesses may have variable contours. Although abscesses can mimic necrotic metastases, they are usually distinguishable by the clinical history [7]. The presence of a fluid-fluid level within a lesion may be a particularly helpful differential point. Although it is conceivable that a fluid-fluid level might occur secondary to inflammatory debris in an abscess or cyst, it has not been described to date in these entities.

Effective use of the attenuation coefficient values is important to the accurate evaluation of hepatic masses in selected cases. Manipulation of the window width and window level to alter contrast also may be necessary to correctly define the internal characteristics of some hepatic lesions. In our experience, this was especially true in order to optimally demonstrate fluid-fluid levels. Nevertheless, on the basis of CT alone, it may be difficult to differentiate necrotic hepatic metastases from other focal masses. In some cases, the clinical history may be helpful and occasionally percutaneous needle aspiration may be necessary to provide the definitive diagnosis.

REFERENCES

1. Alfidi RJ, Haaga JR, Harvilla TR, Pepe RG, Cook SA: Computed tomography of the liver. *Am J Roentgenol* 127:69–74, 1976
2. Levitt RG, Sagel SS, Stanley RJ, Jost RG: Accuracy of computed tomography of the liver and biliary tract. *Radiology* 124:123–128, 1977
3. Kreel L: Computerized tomography using EMI general purpose scanner. *Br J Radiol* 50:2–14, 1977
4. Stanley RJ, Sagel SS, Levitt RG: Computed tomography of the liver. *Radiol Clin North Am* 3:331–347, 1977
5. Stephens DH, Sheedy PF, Hattery RR, MacCarty RL: Computed tomography of the liver. *Am J Roentgenol* 128:579–590, 1977
6. Ackerman LV, delRegato JA: *Cancer: Diagnosis, Treatment and Prognosis*, 4th ed. St. Louis, Mosby, 1970
7. Stanley RJ, Sagel SS, Levitt RG: Computed tomography of the body: early trends in application and accuracy of the method. *Am J Roentgenol* 127:53–67, 1976

CT Diagnosis of Tumor Thrombosis of the Renal Vein and Inferior Vena Cava

WILLIAM M. MARKS,[1] MELVYN KOROBKIN, PETER W. CALLEN, AND JAY A. KAISER

Four cases of tumor thrombosis of the inferior vena cava and renal veins were diagnosed by computed tomography. In two, the thrombus itself was demonstrated within the vascular lumen after intravenous injection of urographic contrast material. The diagnosis was made in the other two patients by identification of massive enlargement of the vascular diameter.

Extension of renal carcinoma into the renal vein or inferior vena cava significantly alters prognosis [1]. The incidence of intracaval involvement by hypernephroma varies from 9% to 33% [1, 2]. Preoperative knowledge of such venous tumor thrombosis may affect the surgical procedure [3]; some surgeons will resect a tumor thrombus even when it extends into the right atrium.

Although renal vein and intracaval extensions of tumor have been demonstrated by ultrasonography [4], angiography is the conventional radiologic method of preoperative assessment. If a renal carcinoma is demonstrated angiographically, many radiologists go on to perform inferior venacavography and renal venography to determine the venous extent of the lesion. We report the demonstration of tumor thrombosis of the renal vein and inferior vena cava by means of computed tomography (CT).

Case Reports

Case 1

A 35-year-old woman was evaluated for hirsutism, amenorrhea, and hypertension. Serum testosterone and 17-ketosteroids were elevated. Urography demonstrated a left suprarenal mass and delayed excretion of contrast material by the left kidney; the injection of contrast material precipitated an episode of hypotension. A CT scan 24 hr later showed a large left adrenal mass and massive dilatation of the left renal vein and inferior vena cava (figs. 1*A*–1*C*). Cavography showed deviation of the inferior vena cava, but did not demonstrate an intraluminal mass (fig. 1*D*). At surgery a 2 kg left adrenal carcinoma was disclosed, extending into the left renal vein, left kidney, and inferior vena cava. The adrenal tumor and left kidney were resected, but residual tumor was left in the inferior vena cava and stump of the left renal vein. Radiation and chemotherapy were begun.

Case 2

A 96-year-old woman with nausea, vomiting, and weight loss underwent CT scanning to evaluate a suspected pancreatic mass. A large renal mass was demonstrated with massive enlargement of the left renal vein and contiguous portion of the inferior vena cava (fig. 2). Urography confirmed the presence of a left renal mass, but surgery was not performed because of the patient's advanced age and other chronic medical diseases.

Case 3

A 25-year-old man had a right nephrectomy for Wilms' tumor. At surgery, tumor thrombus was seen in the right renal vein. Radiation therapy and chemotherapy were given. CT scanning 6 months later showed a small retroperitoneal mass in the bed of the resected right kidney; after a combined infusion and bolus injection of contrast material into a foot vein, a filling defect in the inferior vena cava was also clearly demonstrated (fig. 3).

Case 4

A 72-year-old man was evaluated for hematuria. Urography showed a large right renal mass, which ultrasonography demonstrated to be solid. Renal arteriography demonstrated a hypervascular mass extending into the inferior vena cava (fig. 4*A*). Shortly thereafter, the patient suffered a myocardial infarction; thus nephrectomy was not performed. A metallic coil was placed in the renal artery to infarct the kidney. Over the next few months, CT scanning (figs. 4*B*–4*D*), using intravenous infusion of contrast material into an antecubital vein, showed the intracaval thrombus but progressive decrease in the size of the inferior vena cava. After 1 year of progesterone therapy, the patient is clinically stable with no evidence of metastasis.

Discussion

CT diagnosis of venous thrombosis was made using the indirect finding of massive enlargement of venous diameter with adjacent neoplasm or the direct finding of an intraluminal filling defect.

The left renal vein can be identified in most CT examinations of the abdomen. It courses transversely and lies anterior to the aorta and posterior to the superior mesenteric artery and vein; its junction with the inferior vena cava is frequently visible. Although the diameter of the left renal vein varies, in our experience the normal diameter has never exceeded 1.5 cm (actual diameter corrected from diameter on scan). In case 1, an adrenal carcinoma had extended into and distended both the left renal vein and inferior vena cava, and had invaded the left kidney via the intrarenal veins. The left renal vein was 4.0 cm in diameter. In case 2, the presumed neoplasm originated in the left kidney rather than the adrenal gland. The left renal vein was 3.5 cm in diameter and

Received May 2, 1978; accepted July 17, 1978.

M. Korobkin is the recipient of Career Development Award GM 00055 from the National Institute of General Medical Sciences, National Institutes of Health, and is a James Picker Foundation Scholar in Radiological Research.

[1] All authors: Department of Radiology, University of California School of Medicine, San Francisco, California 94143. Address reprint requests to M. Korobkin.

© 1978 American Roentgen Ray Society

0361–803X/78/1100–0843 $00.00

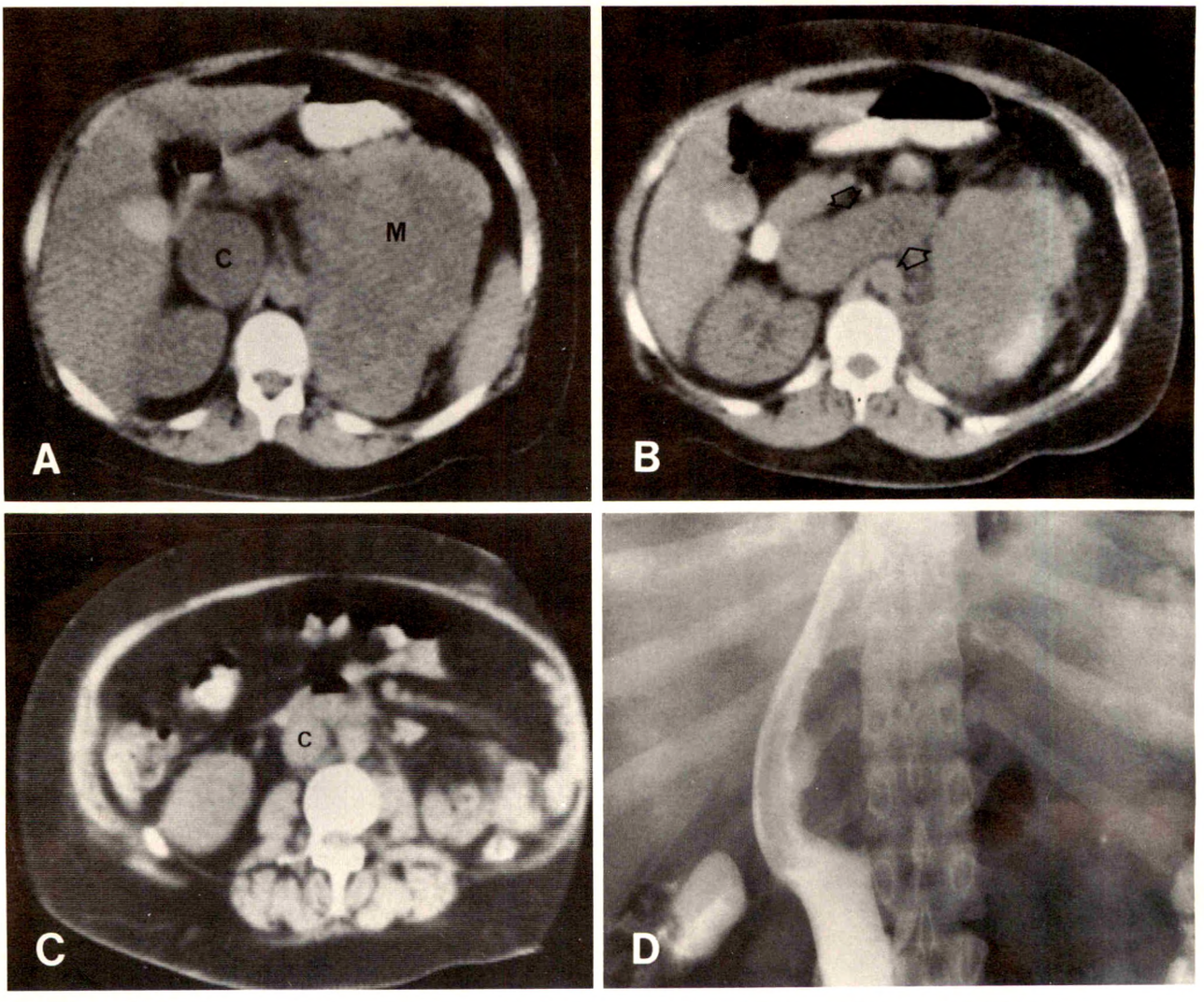

Fig. 1.—Case 1. *A*, CT scan through upper abdomen showing mass (M) inseparable from anterior aspect of upper pole of left kidney. Inferior vena cava (C) is markedly dilated. *B*, Scan 2 cm caudal from *A* showing markedly enlarged left renal vein (*arrows*) entering dilated inferior vena cava. *C*, Scan 4 cm caudal from *B* showing normal diameter of inferior vena cava (C). *D*, Inferior vena cavogram showing displacement and possible invasion of vena cava by mass. Cavogram fails to demonstrate enlarged diameter of vena cava because contrast material does not outline left wall.

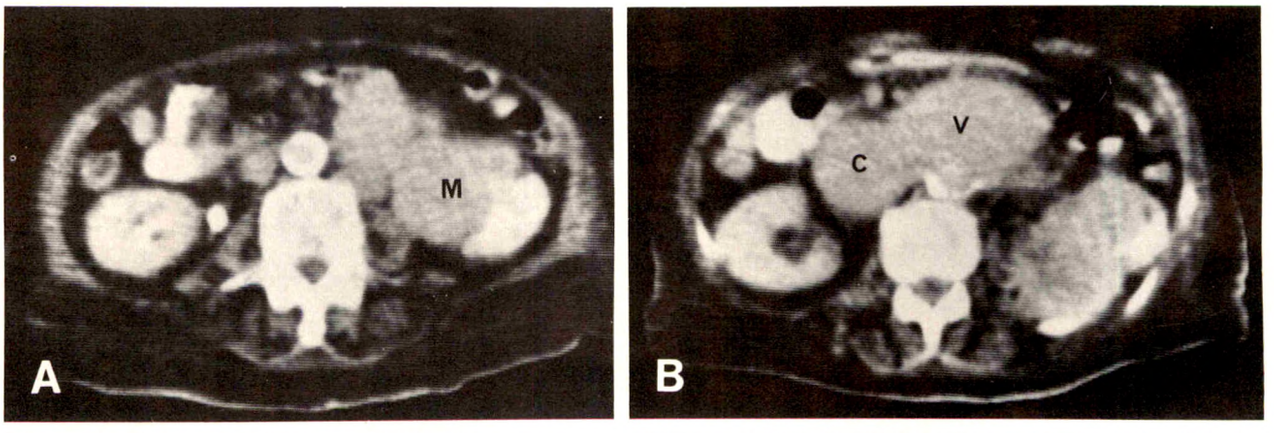

Fig. 2.—Case 2, *A*, CT scan showing mass (M) involving medial aspect of left kidney. *B*, Scan 2 cm caudal from *A* showing massive dilatation of left renal vein (V) and inferior vena cava (C).

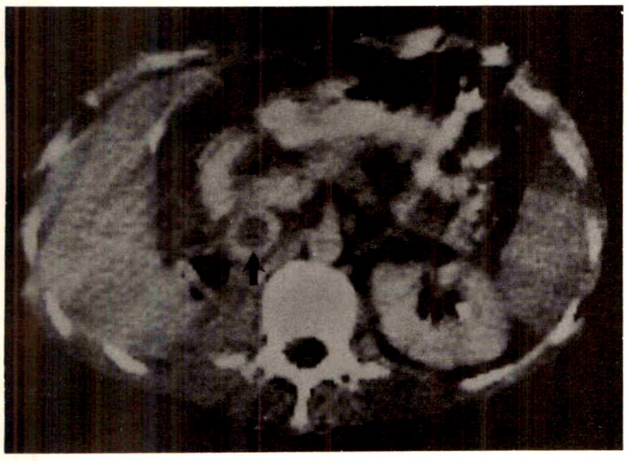

Fig. 3.—Case 3. CT scan showing diameter of inferior vena cava within normal limits, but intraluminal thrombus appears as low density filling defect (*arrow*) surrounded by contrast material. (Reprinted with permission from [5]).

joined a massively enlarged inferior vena cava. Although case 2 was not surgically proved, the similarity to case 1 of the CT appearance of dilated inferior vena cava and left renal vein makes the diagnosis of a tumor thrombus reasonable.

The diameter of the inferior vena cava also varies when seen on CT scans. In some patients it appears oval or slitlike, while in others it is round and can have a diameter about twice that of the adjacent aorta. These variations probably reflect, in part, various degrees of the Valsalva maneuver in patients suspending respiration for the CT scanning. A review by us of CT scans of 50 consecutive adult patients disclosed a mean inferior vena cava diameter of 2.7 cm (actual diameter corrected from diameter on scan) in the upper abdomen (range 1.5–3.7 cm). The diameter of the inferior vena cava in case 1 was 5.0 cm at the level where it was adjacent to the massively enlarged left renal vein; both vessels were found to be filled with tumor at surgery. In case 2 the diameter of the inferior vena cava was 6.0 cm, presumably because it was distended with the renal carcinoma extending from the dilated left renal vein.

Although marked dilatation of the inferior vena cava theoretically can be due to increased vascular resistance at the level of the diaphragm or right atrium, a contiguous dilated renal vein, lack of dilatation of the opposite renal vein, and an abrupt decrease in caliber of the infrarenal vena cava all favor the diagnosis of tumor thrombus. An arteriovenous fistula of the kidney with increased blood flow can also result in the CT appearance of abrupt massive enlargement of the inferior vena cava, but intravenous injection of contrast material in this instance should show marked enhancement of the entire caval lumen.

Definitive diagnosis of inferior vena cava thrombosis can be made by CT scanning using injection of intravenous contrast material [5]. If the lumen of the cava is only partially occluded, the thrombus will be clearly seen as a low density filling defect surrounded by the iodine-containing blood (fig. 3). Bolus injection of a foot vein is helpful because if an upper extremity vein is injected, the contrast material will be considerably diluted by the time it passes through the heart, lungs, and systemic capillary bed on route to the inferior vena cava. However, case 4 demonstrates that an intraluminal thrombus can sometimes be clearly shown when an upper extremity vein is used. Direct demonstration of the intraluminal thrombus in the inferior vena cava is the only method of diagnosis by CT if it does not appear dilated (figs. 3 and 4*D*).

We have found that opacification of the lumina of large vessels is best accomplished by using a combination of intravenous infusion and bolus injection of contrast material. However, sometimes (case 2) infusion alone will be sufficient. Failure to demonstrate a filling defect in the inferior vena cava may indicate either complete luminal obstruction or insufficient concentration of iodine in the patent portion of the lumen. The range of normal attenuation values for the inferior vena cava after intravenous injection of contrast material is unknown.

Although intraluminal thrombi have been identified by CT in the aorta [5] as well as in the inferior vena cava, we do not know if such defects are detectable in vessels, such as the renal vein, imaged in their long rather than short axis. In addition to the dilution of contrast material between point of injection and the renal vein, the partial volume error that results from a renal vein coursing oblique to the transverse CT plane can make diagnosis of thrombosis in a renal vein difficult.

REFERENCES

1. Robson CJ, Churchill BM, Anderson W: The results of radical nephrectomy for renal cell carcinoma. *J Urol* 101:297–301, 1969
2. McCoy RM, Klatte EC, Rhamy RK: Use of inferior venacavography in the evaluation of renal neoplasms. *J Urol* 102:556–559, 1969
3. McCullough DL, Talner LB: Inferior vena caval extension of renal carcinoma: a lost cause? *Am J Roentgenol* 121: 819–826, 1974
4. Greene D, Steinbach HL: Ultrasonic diagnosis of hypernephroma extending into the inferior vena cava. *Radiology* 115:679–680, 1975
5. Korobkin M, Kressel HY, Moss AA, Koehler RE: Computed tomographic angiography of the body. *Radiology* 126:807–811, 1978

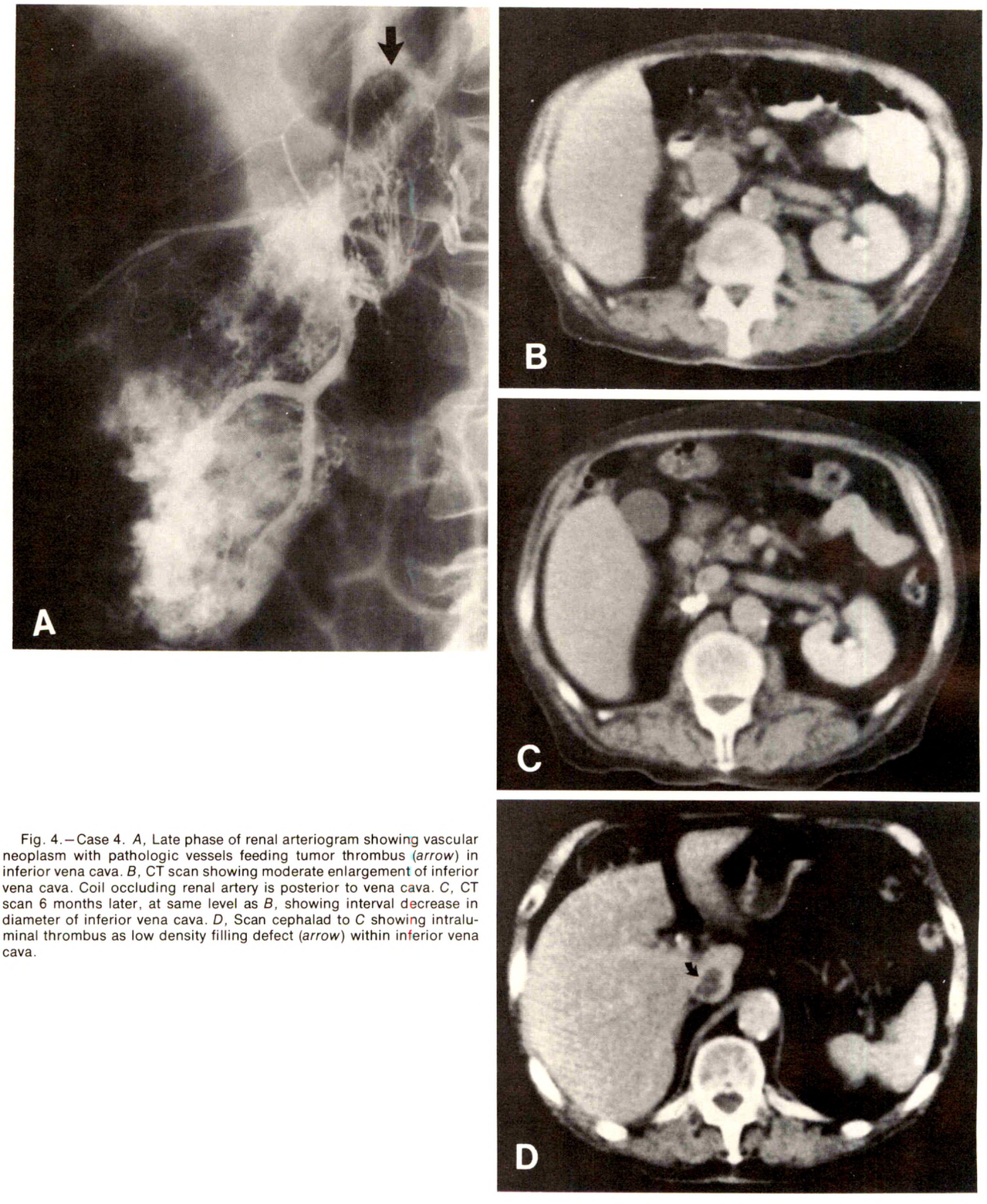

Fig. 4.—Case 4. *A*, Late phase of renal arteriogram showing vascular neoplasm with pathologic vessels feeding tumor thrombus (*arrow*) in inferior vena cava. *B*, CT scan showing moderate enlargement of inferior vena cava. Coil occluding renal artery is posterior to vena cava. *C*, CT scan 6 months later, at same level as *B*, showing interval decrease in diameter of inferior vena cava. *D*, Scan cephalad to *C* showing intraluminal thrombus as low density filling defect (*arrow*) within inferior vena cava.

Diminished Radiopacity of Contrast Material: A Urographic Sign of Ureteral Calculus

MELVYN KOROBKIN,[1] RICHARD P. JACOBS,[2] ROBERT E. CLARK,[3] AND HIDEYO MINAGI[2]

Eleven patients with unilateral ureteral calculus had excretory urography which showed the radiopacity of excreted contrast material to be diminished on the side of the calculus. This finding was of diagnostic importance in nine patients who demonstrated little or no dilatation of the urinary tract proximal to the calculus. Other forms of unilateral renal disease, such as acute pyelonephritis, can produce the same urographic finding.

Acute unilateral ureteral colic due to an obstructing calculus is one of the most common of all medical problems, especially in the hospital emergency room. On plain radiography of the abdomen, a radiopaque structure overlying the expected course of one of the ureters is suggestive of ureteral calculus. If acute ureteral calculus is suspected, excretory urography is usually performed to document the presence, site, and degree of obstruction.

The diagnosis of acute, ureteral obstruction is made when urography demonstrates a prolonged dense nephrogram, a delayed pyelogram, or significant pyeloureterectasis [1]. We have observed that, in the absence of these well recognized urographic findings, diminished radiopacity of contrast material on the side of the suspected calculus can be a useful functional sign of obstruction.

Subjects and Methods

We reviewed the medical records and radiographs of 11 patients diagnosed unequivocally as having acute unilateral ureteral calculus and in whom definite diminution in radiopacity of contrast material on the suspected side was observed during excretory urography. No attempt was made to assess the incidence or prevalence of this urographic finding. All urograms included a radiograph of the renal areas exposed 5 min after intravenous injection of a bolus of a conventional urographic contrast agent. Radiographs were then obtained in the usual manner for 30 min after injection. None of the patients showed a prolonged dense nephrogram or delayed pyelogram.

Results

All 11 patients had unilateral flank pain within the 24 hr before urography. In most the flank pain radiated to the ipsilateral groin. Hematuria was evident macroscopically or microscopically in 10 patients. All 11 patients were treated conservatively, because radiography suggested a calculus was probably present in the distal ureter. All patients for whom adequate follow-up information was available had resolution of the flank pain within a few minutes, hours, or days; five reported passage of a stone or sludge in the urine.

Table 1 shows the principal plain film and urographic features in the 11 patients. Two patients had definite dilatation of the ureter, making the diagnosis of ureteral obstruction easy. Diminished radiopacity of contrast material on the side of the suspected calculus was an important diagnostic sign in nine patients in whom ureteral dilatation was either absent or only slight compared to the opposite side. In these nine patients the diminished radiopacity was evident on every radiograph obtained during urography. Figures 1–3 exemplify this unilateral diminution in contrast agent radiopacity on the side of the ureteral calculus.

Discussion

An obstructing ureteral calculus is not always demonstrated on plain abdominal radiography. It may be only faintly calcified, mistaken for the ubiquitous pelvic phlebolith, or not calcified at all. In only one-third of a large series of patients with acute ureteral calculus obstruction was the calculus demonstrated on plain abdominal radiography [2]. The widely recognized urographic features of acute ureteral obstruction are not present in every case. Even if one ureter or collecting system is slightly dilated in comparison to the opposite side, this dilatation may be the residual effect of a previous obstruction or reflux, or it may simply be a normal variant. Nine of the 11 patients we studied had

TABLE 1

Radiographic Findings

Findings	No. Patients
Calculus (plain radiograph):	
Probable	5
Equivocal	3
Absent	3
Dilated ureter (urogram):	
Definite	2
Slight	5
Absent	4

Received March 14, 1978; accepted after revision July 17, 1978.

Presented in part at the annual meeting of the Radiological Society of North America, Chicago, November 1976.

M. Korobkin is the recipient of Career Development Award GM 00055 from the National Institute of General Medical Sciences, National Institutes of Health, and is a James Picker Foundation Scholar in Radiological Research.

[1] Department of Radiology, University of California School of Medicine, San Francisco, California 94143. Address reprint request to M. Korobkin.

[2] Department of Radiology, San Francisco General Hospital, San Francisco, California 94110.

[3] Department of Radiology, Veterans Administration Hospital, San Francisco, California 94121.

© 1978 American Roentgen Ray Society

0361–803X/78/1100–0847 $00.00

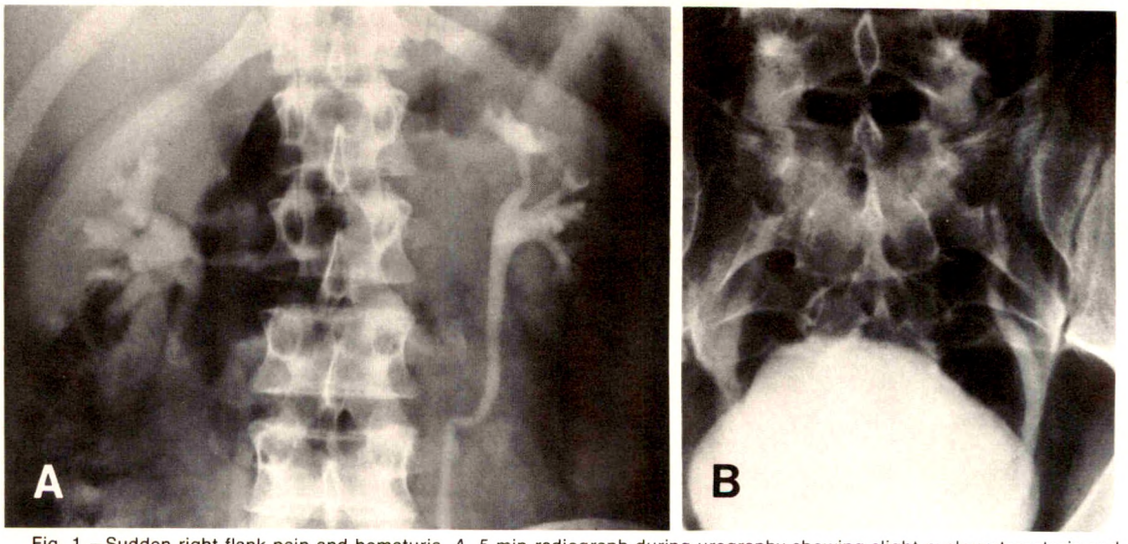

Fig. 1.—Sudden right flank pain and hematuria. *A*, 5 min radiograph during urography showing slight pyeloureterectasis and marked diminution in radiopacity on right side. *B*, Distal ureters showing same discrepancy in density of contrast material.

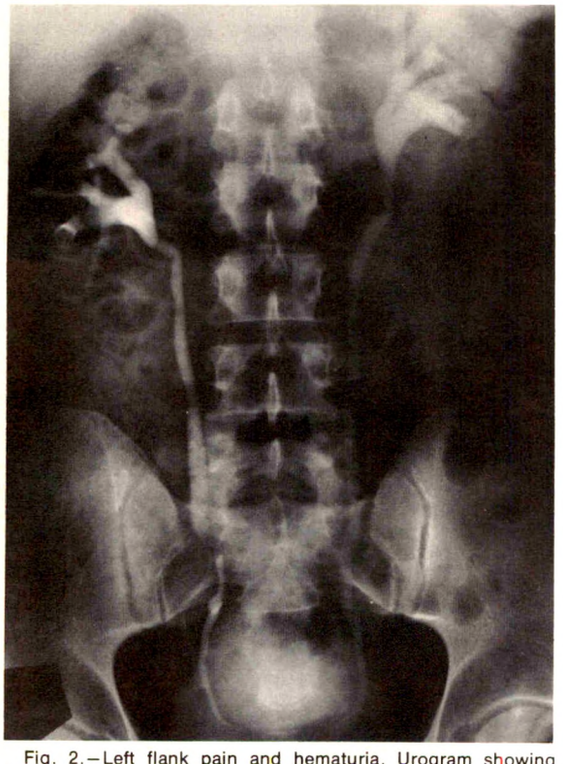

Fig. 2.—Left flank pain and hematuria. Urogram showing definite reduction in radiopacity throughout entire left ureter and renal collecting system, despite equal caliber on both sides.

little or no dilatation of the ureter proximal to the calculus. Thus the functional abnormality, seen on the urogram, of diminished radiopacity of contrast material in the ipsilateral ureter proved important in the radiographic diagnosis. The potential diagnostic utility of this urographic finding in acute unilateral ureteral calculus has rarely been discussed. Bretland [2] suggested it was a sign of continuing obstruction; Hyams [3] postulated that its presence indicated a stone had recently passed through the ureter.

The apparent radiopacity of contrast material is proportional to the concentration of the material times the depth of the element containing that material. If it is assumed that the ureter is a cylinder (i.e., of uniform depth), then diminution in radiopacity implies a reduction in concentration of the contrast agent. Nevertheless, such a reduction in concentration of contrast material may not always be reflected on the radiograph as reduced radiopacity. In vitro experiments have indicated that, given a nearly equal ureteral diameter bilaterally, a difference in ureter iodine concentration of at least 100% is necessary before a difference in radiopacity can be detected on the radiograph [4].

Because in the majority of our patients (nine of 11) the ureters were nearly equal in caliber, we assume that the diminished radiopacity on the obstructed side was due to diminished concentration of contrast material. It is uncertain whether the diminution in concentration takes place within the kidney or is postrenal in location. There is no convincing experimental evidence to support the hypothesis that in acute hydronephrosis an obstructing calculus results in production of relatively dilute urine by the kidney. In fact, Suki et al. [5] showed that acute hydronephrosis in animals results in increase, rather than decrease, in the urinary osmolarity on the hydronephrotic side. Although some investigators suggest that the increased renal blood flow accompanying elevated ureteral pressure may reduce the concentrating capacity of the renal medulla [6], others have disputed this claim [7].

Evaluation of such experimental studies is difficult partly because the degree and duration of ureteral obstruction, the level of hydration, and the presence and type of experimental diuresis used may not accurately reflect the clinical conditions that produced the urographic findings in our patients. Another possible expla-

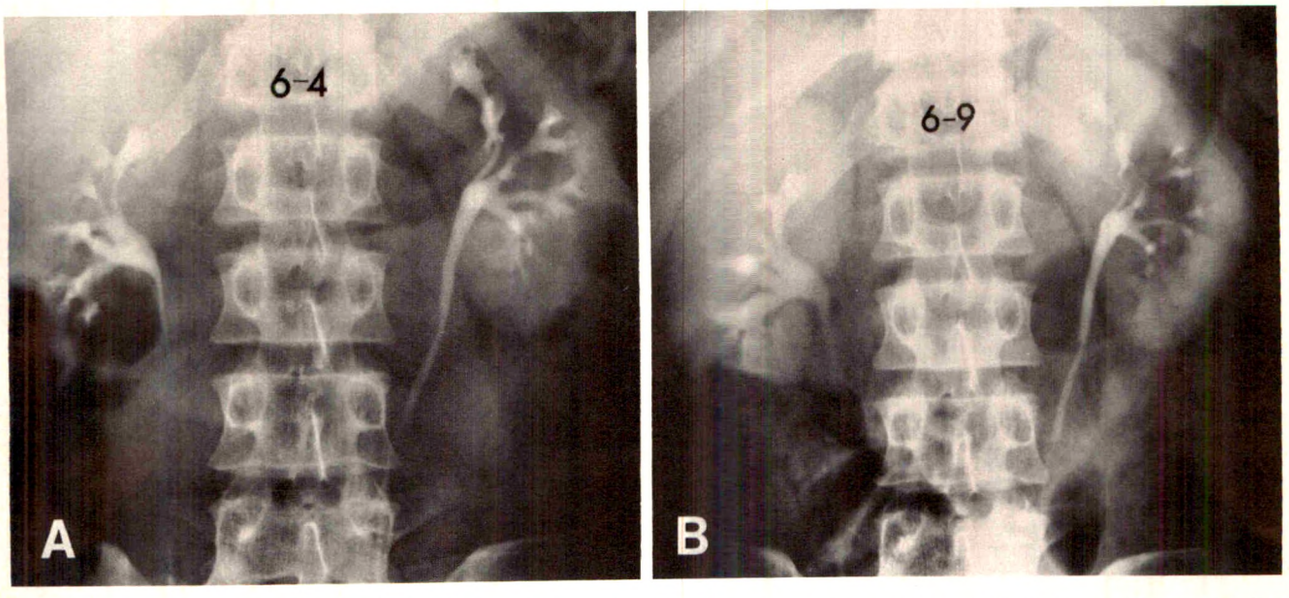

Fig. 3.—*A*, Urogram performed for dysuria showing equal degree of opacification of contrast material in both kidneys and in proximal and distal ureters. *B*, Repeat urogram 5 days later for acute right flank pain and hematuria showing diminished radiopacity on right.

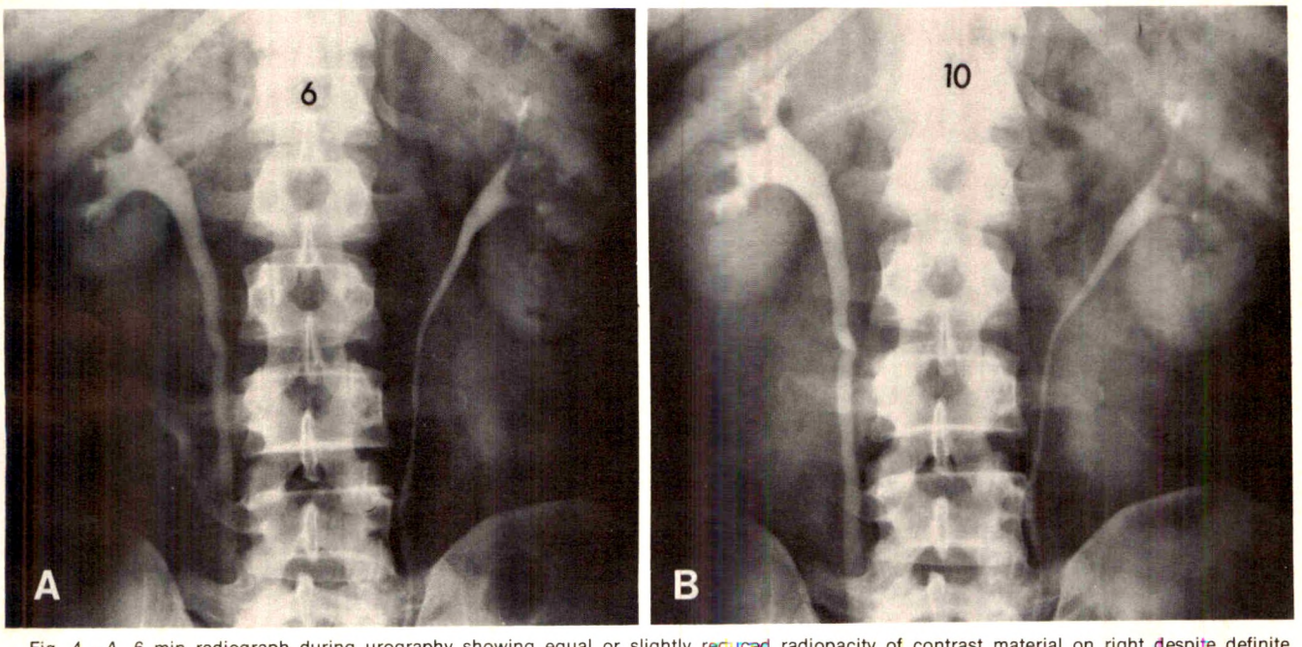

Fig. 4.—*A*, 6 min radiograph during urography showing equal or slightly reduced radiopacity of contrast material on right despite definite pyeloureterectasis. *B*, Film 4 min later showing greater opacity of contrast material on right than on left, indicating that initial dilution of contrast material by more stagnant urine has been superseded by continued excretion into dilated ureter and renal pelvis.

nation of the decreased radiopacity of contrast material is the diuresis associated with relief of renal obstruction [8]. If the ureteral calculus passed into the bladder before or at the beginning of urography, the urographic finding we describe might be a reflection of the decreased concentrating capacity of the kidney following relief of the obstruction.

It is likely that urine is adequately concentrated by the kidney during acute partial ureteral obstruction, but is then diluted by a column of urine in the ureter more stagnant than that in the opposite side (fig. 4). The only way to confirm such a postulated mechanism clinically would be to obtain and evaluate rapid-sequence radiographs during the first 5 min of urography in patients such as ours. Normally the urographic finding we describe is overshadowed by the more conventional findings, especially ureteral dilatation. Our findings indicate that there are degrees and durations of partial ureteral obstruction that can result in reduction of urine flow without producing profound ureteral dilatation. In such

cases, reduction in radiopacity of the contrast material may be useful urographic evidence of acute ureteral calculus obstruction.

Regardless of the mechanism responsible for the reduced radiopacity, it should be apparent that any unilateral renal disease, or any diffuse renal disease that affects the concentrating mechanism of one kidney more than the other, could result in a urographic appearance similar to that described here. Certainly, unilateral diminution in contrast agent radiopacity is occasionally seen during urography in patients with acute pyelonephritis [9], a disease with a clinical appearance close to that of acute calculus.

REFERENCES

1. Elkin M: Obstructive uropathy and uremia. *Radiol Clin North Am* 10:447–465, 1972
2. Bretland PM: *Acute Ureteric Obstruction: A Clinical and Radiological Study*. New York, Appleton-Century-Crofts, 1972
3. Hyams BB: The signs of a passed ureteral stone. *J Can Assoc Radiol* 28:270–273, 1977
4. Duré-Smith P, Rosen R, Stern A, Framow H, Simenhoff M: Physiology of the excretory urogram. III. A densitometric and subjective assessment of changes in contrast medium concentration. *Invest Radiol* 9:104–108, 1974
5. Suki W, Eknoyan G, Rector F, Seldin DW: Patterns of nephron perfusion in acute and chronic hydronephrosis. *J Clin Invest* 45:122–131, 1966
6. Selkurt EE: Effect of ureteral blockade on renal blood flow and urinary concentrating ability. *Am J Physiol* 205:286–292, 1963
7. Suki WN, Guthrie AG, Martinez-Maldonato M, Eknoyan E: Effects of ureteral pressure elevation on renal hemodynamics and urine concentration. *Am J Physiol* 220:38–43, 1971
8. Bercovitch DD, Kasen L, Blann L, Levitt MF: The postobstructive kidney: observations on nephron function after the relief of 24 hr of ureteral ligation in the dog. *J Clin Invest* 50:1154–1165, 1971
9. Silver TM, Kass EJ, Thornbury JR, Konnak JW, Wolfman MW: The radiological spectrum of acute pyelonephritis in adults and adolescents. *Radiology* 118:65–71, 1976

New Observations in Renal Transplants Using Ultrasound

MELVYN R. CONRAD,[1] RICHARD DICKERMAN,[2] IAN L. LOVE,[1] THOMAS CURRY,[1] PAUL PETERS,[2] ALLEN HULL,[3] MARK LERMAN,[3] AND HAROLD HELDERMAN[3]

Using gray scale ultrasound, the parenchymal changes in transplant rejection are reported in five patients. In both acute and chronic rejection, parenchymal sonolucent regions may be imaged due to foci of edema, hemorrhage, or recent infarction. The prognostic significance of these findings is unclear.

Previous investigators have shown that ultrasound is useful in assessing the transplanted kidney. Hydronephrosis may be reliably excluded. Although an increase in the measured volume of the renal transplant has been correlated with transplant rejection [1–3], parenchymal changes due to rejection have not been well documented. These findings are described and correlated with the arteriographic and anatomic changes in five patients, and are representative of findings seen in a larger series of approximately 180 transplant examinations per year.

Materials and Methods

Transverse and oblique scans (i.e., parallel to the surgical scar) of the renal transplant were done at intervals of 0.5–1.0 cm using a 3.5 MHz, medium internal focused transducer. Images were made using the single sweep scanning technique and recorded on a Searle Pho/Sonic analog unit, Searle Pho/Sonic digital unit, or a Picker EDC unit. Time gain compensation and output were set for optimal renal parenchymal detail. In renal transplants without rejection, the renal cortex has a characteristic uniform homogenous grainy acoustic texture. The medullary pyramids are imaged as discrete sonolucentlike structures surrounded by the homogenous parenchymal pattern of the cortex (fig. 1).

Case Reports

Case 1

A 26-year-old white male received a cadaveric renal allograft after 2 years of chronic hemodialysis. Anuria developed postoperatively. On the fifth postoperative day, an arteriogram (fig. 2*A*) showed signs of rejection evidenced by severe pruning of the peripheral vessels, irregularity of the segmental renal arteries, a poor nephrogram, and increased circulation time. A sonogram showed large areas of sonolucency within the renal parenchyma (fig. 2*B* and 2*C*). The patient was treated for rejection with intravenous steroids. Because the clinical response was poor, a transplant biopsy was performed 15 days postoperatively which revealed acute rejection with a small cortical infarct. In the face of continued poor renal function, the patient received three additional courses of antirejection therapy. A sonogram 40 days after transplantation showed the sonolucent regions to be unchanged, and a nephrectomy was performed 2 days later. The gross specimen showed acute rejection evidenced by a boggy, edematous kidney with diffuse areas of recent, punctuate hemorrhage, and areas of recent gross cortical infarction.

Comment. In this patient with both clinical and arteriographic evidence of acute transplant rejection, prominent cortical sonolucent regions were imaged throughout the hospital course. Examination of the gross specimen confirmed the cortical sonolucency to correspond to the morphologic changes of edema, hemorrhage, and recent gross infarcts in the renal parenchyma.

Case 2

A 34-year-old black female received a cadaveric kidney transplant. After 21 days, an arteriogram was performed because of poor renal function. It showed marked irregularity of the large vessels, stretched intrarenal vessels, and an increased circulation time (greater than 11 sec) which was compatible with the vasculitis of acute rejection (fig. 3*A*). Large sonolucent regions were imaged in the renal parenchyma, which persisted until nephrectomy 46 days after transplant (fig. 3*B*). The gross specimen showed multiple recent infarcts in the renal parenchyma due to acute rejection.

Comment. The clinical and arteriographic documentation of the onset of acute rejection was correlated with the appearance of large sonolucent regions within the renal parenchyma due to extensive cortical infarctions, hemorrhage, and edema.

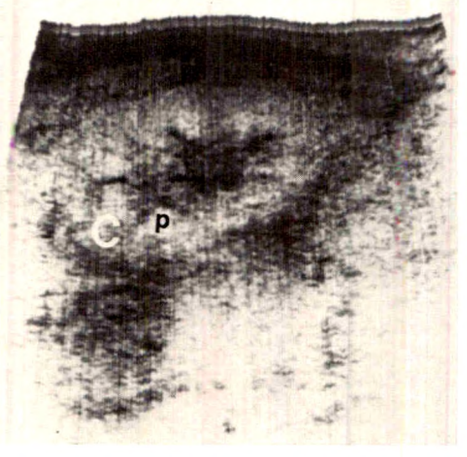

Fig. 1.—Oblique sonogram of renal transplant 3 days after transplantation. Relatively sonolucent-appearing medullary pyramids (P) are surrounded by homogeneous, grainy acoustic texture of renal cortex (C). Dark central echoes arise from renal hilum.

Received January 31, 1978; accepted after revision May 31, 1978.

[1] Department of Radiology, Ultrasound Division, Parkland Memorial Hospital, Southwestern Medical School, 5323 Harry Hines Boulevard, Dallas, Texas 75235. Address reprint requests to M. R. Conrad.

[2] Department of Surgery, Parkland Memorial Hospital, Southwestern Medical School, Dallas, Texas 75235.

[3] Department of Nephrology, Parkland Memorial Hospital, Southwestern Medical School, Dallas, Texas 75235.

© 1978 American Roentgen Ray Society

0361–803X/78/1100–0851 $00.00

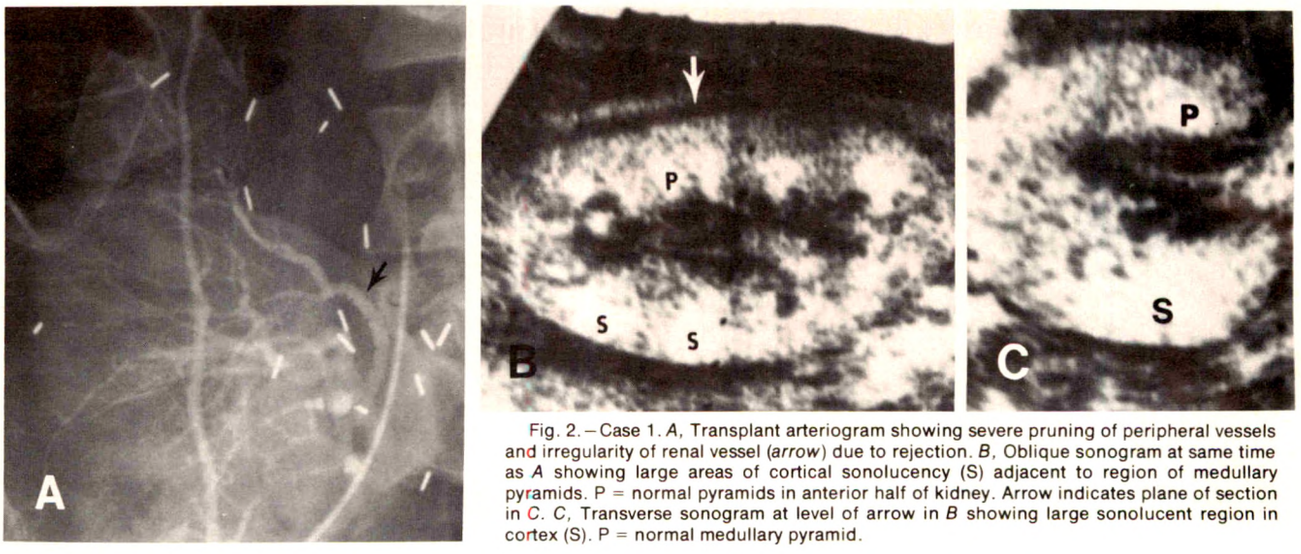

Fig. 2.—Case 1. *A*, Transplant arteriogram showing severe pruning of peripheral vessels and irregularity of renal vessel (*arrow*) due to rejection. *B*, Oblique sonogram at same time as *A* showing large areas of cortical sonolucency (S) adjacent to region of medullary pyramids. P = normal pyramids in anterior half of kidney. Arrow indicates plane of section in *C*. *C*, Transverse sonogram at level of arrow in *B* showing large sonolucent region in cortex (S). P = normal medullary pyramid.

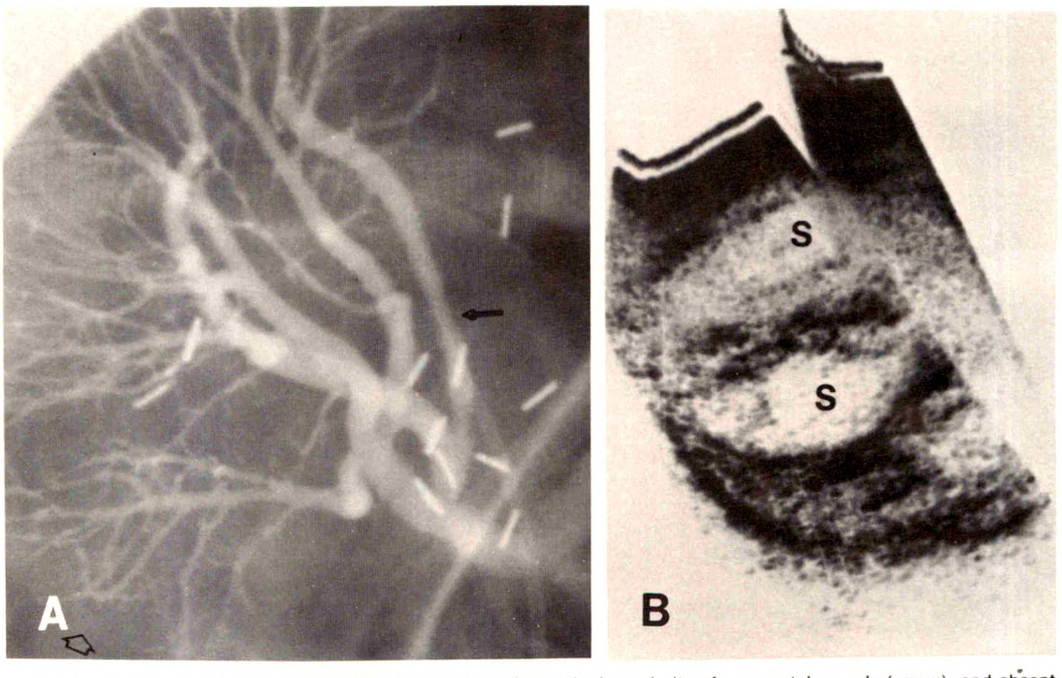

Fig. 3.—Case 2. *A*, Arteriogram showing stretched renal vessels, irregularity of segmental vessels (*arrow*), and absent cortical perfusion (*open arrow*) due to severe transplant rejection. *B*, Sonogram transverse plane at time of *A* showing well defined, large areas of sonolucency (S) in renal cortex due to cortical infarction.

Case 3

A cadaveric renal allograft was performed in an 18-year-old black male suffering from chronic renal failure due to Alport's syndrome. Four days postoperatively, he was treated for acute rejection. A transplant arteriogram 15 days postoperatively showed an infarct in the upper pole of the transplant due to thrombosis of a small upper pole artery which had been anastomosed to the common iliac artery (figs. 4*A* and 4*B*). Sonography showed a large circumscribed region of sonolucency in the posterior portion of the upper pole (figs. 4*C*, 4*D*, and 4*E*).

Comment. The large parenchymal sonolucency imaged in the upper pole region of the renal transplant was due to cortical infarction as documented on the arteriogram.

Case 4

The patient received a renal transplant 2½ years previously, and shortly afterward was successfully treated with steroids and radiation therapy for four or five episodes of acute rejection. During the year preceding the patient's death, a mild gradual deterioration of renal function occurred with a rise in serum creatinine to the 2–3 level which remained there until death after an unsuccessful pancreatic transplant. Several sonograms obtained during the patient's last year demonstrated persistent areas of sonolucency in the renal parenchyma (fig. 5). An arteriogram showed a poor cortical nephrogram, irregular and poorly filled interlobular vessels, and stretched vessels. Because of the patient's relatively stable clinical status and arterio-

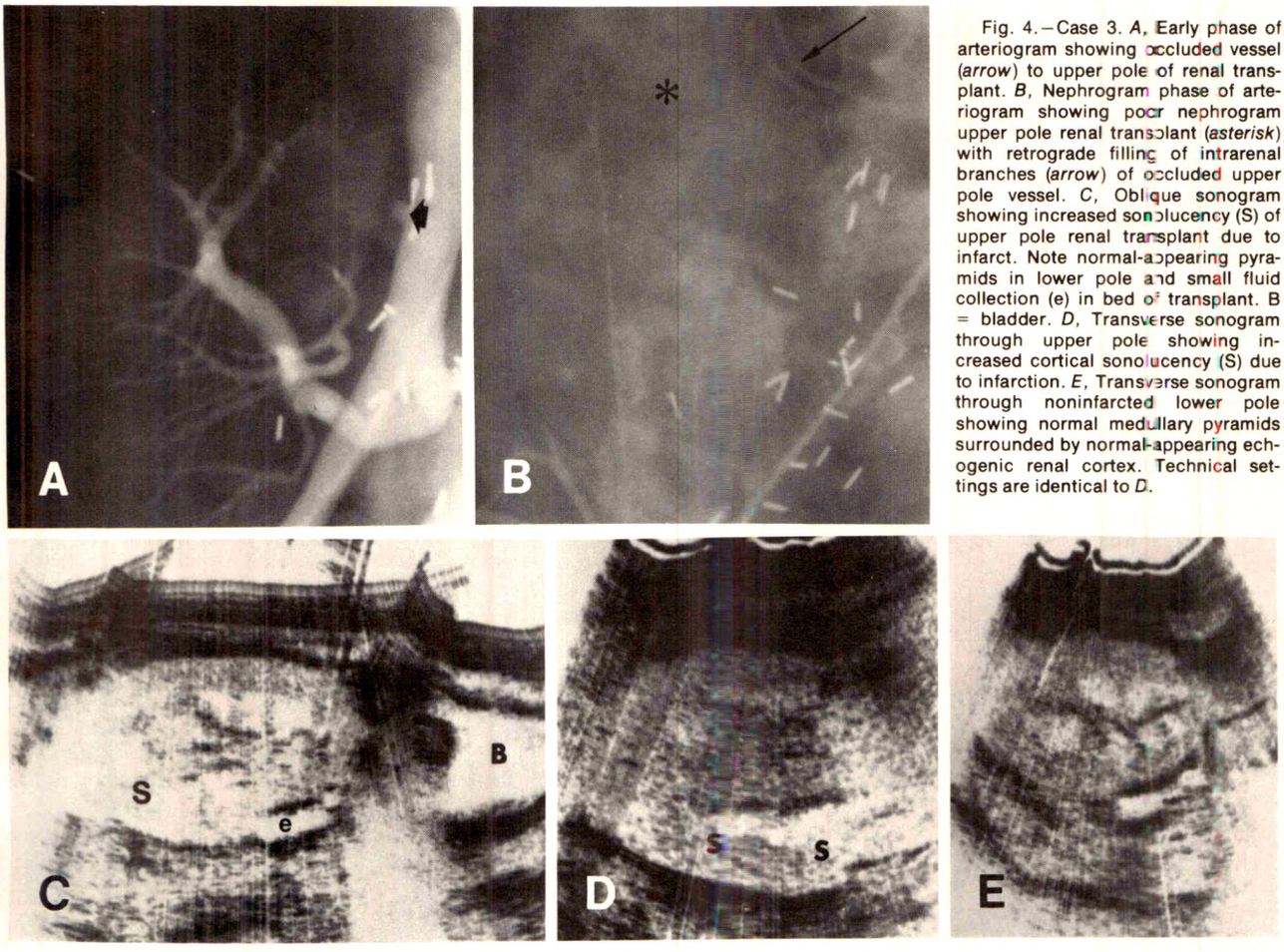

Fig. 4.—Case 3. *A*, Early phase of arteriogram showing occluded vessel (*arrow*) to upper pole of renal transplant. *B*, Nephrogram phase of arteriogram showing poor nephrogram upper pole renal transplant (*asterisk*) with retrograde filling of intrarenal branches (*arrow*) of occluded upper pole vessel. *C*, Oblique sonogram showing increased sonolucency (S) of upper pole renal transplant due to infarct. Note normal-appearing pyramids in lower pole and small fluid collection (e) in bed of transplant. B = bladder. *D*, Transverse sonogram through upper pole showing increased cortical sonolucency (S) due to infarction. *E*, Transverse sonogram through noninfarcted lower pole showing normal medullary pyramids surrounded by normal-appearing echogenic renal cortex. Technical settings are identical to *D*.

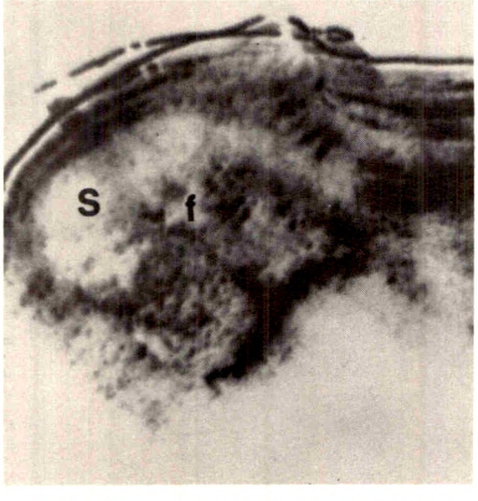

Fig. 5.—Case 4. Transverse section through transplant showing large area of parenchymal sonolucency (S) in patient with chronic rejection. f = normal fluid-filled renal pelvis.

graphic findings, the clinical diagnosis was chronic rejection. Examination of the transplanted kidney at autopsy revealed findings consistent with chronic rejection evidenced by areas of fatty degeneration, edema with interstitial fibrosis, and scattered hemorrhage.

Comment. This patient had documented chronic transplant rejection during the year preceding his demise. The persistent sonolucent parenchymal regions were shown at autopsy to be due to edema, fibrosis, and hemorrhage of chronic rejection.

Case 5

A 40-year-old Latin American male underwent a cadaveric transplant because of renal failure due to chronic renal glomerulonephritis. After 18 days, the patient became febrile and suffered a decrease in urinary output, which failed to respond to a volume challenge. Serum creatinine rose from 2.0 mg/100 ml to 5.2 mg/100 ml; urinalysis showed proteinuria, granular and cellular casts, 5–10 white blood cells per high powered field, and numerous red blood cells per high powered field. Sonography showed marked increased cortical sonolucency within the mid and lower pole of the transplant (fig. 6*A*). Arteriography showed normal major renal vessels with equivocal minimal changes of rejection involving peripheral cortical vessels. A clinical diagnosis of mild acute rejection was made, and four steroid boluses were given. A good clinical response occurred, and the serum creatinine decreased with clearing of the urinary sediment. Repeat sonography 16 days later showed resolution of the cortical sonolucency in the lower pole (fig. 6*B*).

Comment. Resolution of the large area of parenchymal sonolucency in conjunction with the successful treatment of the

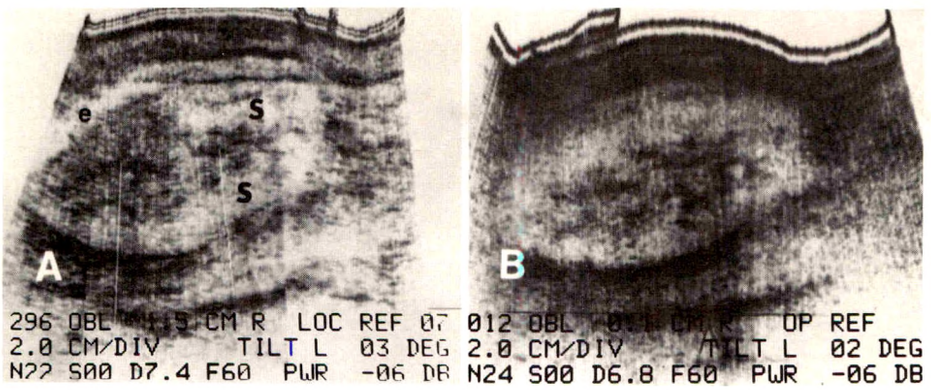

Fig. 6.—Case 5. *A*, Oblique sonographic section through renal transplant showing large area of sonolucency (S) involving lower half of transplant due to acute rejection. e = small perirenal fluid collection. *B*, Oblique sonographic section at level similar to *A* following resolution of acute rejection process. Note relatively normal homogenous cortical echo pattern. Nearly identical technical settings were used in each examination. N = near gain, D = slope in dB/cm, F = far gain. Output = −6 dB in each case.

acute rejection episode suggests that the parenchymal changes were probably due to edema rather than the irreversible changes of renal infarction. Of note is the better documentation by sonography rather than arteriography, in this case, of the changes due to mild acute rejection.

Discussion

The histologic, gross morphologic, and arteriographic changes in acute rejection have been well documented [4]. In acute rejection, cortical ischemia occurs because of renal arterial occlusion due to increased vasomotor constriction and/or fibrinoid thrombi [5]. Cortical ischemia results in variably sized, parenchymal foci of edema, hemorrhage, or infarction [6]. The degree of edema, extent of hemorrhage, and presence or absence of infarction is determined by the severity of the impaired cortical perfusion and vascular occlusion [7].

In this limited study using ultrasound, the appearance of sonolucent regions in the parenchyma of recently transplanted kidneys was shown to correlate by clinical, arteriographic, and gross pathologic examination with the morphologic changes of documented transplant rejection. Examination of the nephrectomy specimen in each of the three cases undergoing severe acute rejection showed the regions of sonolucency to be due to parenchymal foci of edema, hemorrhage, and/or recent cortical infarction. Since the latter processes are homogeneous, containing few interfaces, and result in a decrease in acoustic impedance through the affected parenchyma when compared to the normal renal cortex [8], the appearance of parenchymal sonolucency is not surprising. Similar findings of parenchymal sonolucency were also seen in one case each of chronic rejection (case 4) and renal infaction secondary to arterial thrombosis (case 3).

Other investigators have suggested that transplant rejection may be evidenced by increased echogenicity in the renal parenchyma and/or an increase in the size of the renal pyramids [9]. Increased echogenicity might be expected in chronic rejection due to interstitial fibrosis. However, the low grade edema and inflammation that occurs in chronic rejection [7] may result in a net effect of increased sonolucency, as seen in case 4. The suggestion that the renal pyramids enlarge in rejection [9] most likely is due to parenchymal edema in the adjacent cortex (figs. 2*B* and 4*C*), and not to a real increase in size of the pyramids.

The prognostic significance of these findings is not clear at present. The appearance of well defined parenchymal sonolucencies in a recent transplant probably indicates significant parenchymal ischemia due to acute rejection. Estimation of the degree of ischemia and differentiation between edema and hemorrhage from cortical infarction on the basis of the pattern or degree of sonolucency was not possible. The sonolucency due to each of these processes appears indistinguishable using current ultrasound equipment However, relatively rapid resolution of the findings concomitant with the successful treatment of an acute rejection episode, as in case 5, probably indicates a lesser degree of tissue insult, such as parenchymal edema rather than infarction. In a chronic renal transplant, without baseline studies, it would be difficult to differentiate the parenchymal sonolucency due to an acute rejection episode from that due to the low grade edema and associated interstitial fibrosis of chronic rejection.

The relationship of these findings to acute tubular necrosis and renal cortical necrosis is currently being investigated. Each of these processes affects the entire renal substance in a uniform fashion. Widespread hemorrhagic infarction may be seen with cortical necrosis, and diffuse edema of varying degree occurs in acute tubular necrosis [10, 11]. In contrast, the ischemia of rejection affects the cortex in a random and focal pattern. Consequently, focal parenchymal sonolucency is not anticipated during acute tubular necrosis or cortical necrosis.

ACKNOWLEDGMENTS

We thank Mary Nell Ryals, Mary Starling, and Nancy Schieber for assistance in manuscript preparation.

REFERENCES

1. Bartrum RJ Jr, Smith EH, D'Orsi CJ, Tilney NL, Dantono J: Evaluation of renal transplants with ultrasound. *Radiology* 118:405–410, 1976
2. Fletcher EWL, Leck JW: The radiological size of renal transplants—a retrospective study. *Br J Radiol* 42:892–898, 1969

3. Burgener FA, Schabel SI: The radiographic size of renal transplants. *Radiology* 117:547–550, 1975
4. Foley WD, Bookstein JJ, Tweise M, Gikas PW, Mayor GH, Turcotte JG: Arteriography of renal transplants. *Radiology* 116:271–277, 1975
5. Hollenberg NK, Epstein M, Rosen SM, Basch RI, Oken DE, Merrill JP: Acute oliguric renal failure in man: evidence for preferential renal cortical ischemia. *Medicine* 47:455–474, 1968
6. Heptinstall RH, Kissane JM, McCluskey RT, Porter KA: *Pathology of the Kidney*, vol 2, 2nd ed, Boston, Little, Brown, 1966
7. Deochar SD, Benjamin SP: Pathology of human renal allograft rejection. *Surg Clin North Am* 51:1141–1159, 1971
8. Buddemeyer EU: The physics of diagnostic ultrasound. *Radiol Clin North Am* 13:391–402, 1975
9. Cook JH, Rosenfield AT, Taylor KW: Ultrasonic demonstration of intrarenal anatomy. *Am J Roentgenol* 129:831–835, 1977
10. Duff GL, Murray EG: Bilateral cortical necrosis of the kidney. *Am J Med Sci* 201:428–450, 1941
11. Dunrill MS: A review of the pathology and pathogenesis of acute renal failure due to acute tubular necrosis. *J Clin Pathol* 27:2–13, 1974

Calcified Bodies in Popliteal Cysts: A Characteristic Radiographic Appearance

RONALD P. GOLDBERG[1, 2] AND HARRY K. GENANT[1]

Calcified bodies in popliteal cysts have a characteristic radiographic appearance which can be confirmed by arthrography. Calcified bodies may arise in the true joint due to trauma, arthropathy resulting in joint destruction, or synovial osteochondromatosis. These calcified loose bodies may pass into a popliteal cyst through posterior joint-bursal communications or can arise in a popliteal cyst by chondrometaplasia. Correct radiographic interpretation will exclude soft tissue tumors and vascular lesions as differential considerations. Management of these patients will be determined by the clinical circumstances since neither popliteal cysts nor synovial osteochondromatosis are necessarily symptomatic.

The radiographic finding of multiple calcified bodies posterior to the knee joint can present a confusing diagnostic problem. The differential diagnosis may include soft tissue tumors with calcification, such as fibrosarcoma or synovial sarcoma, or vascular lesions, such as popliteal artery aneurysms or arteriovenous malformations. We recently saw four cases in which this finding was due to calcified bodies in a popliteal (Baker's) cyst. Characteristic plain film findings were confirmed by surgery and/or arthrography in three cases. This paper describes the radiographic findings and considers the pathogenetic mechanisms for calcified bodies localizing in popliteal cysts.

Case Reports

Case 1

A 64-year-old woman was hospitalized with a right popliteal fossa mass. Swelling had been noted for several weeks and intermittent knee pain without obvious cause for 4 months.

Radiography demonstrated multiple dense, round punctate calcifications behind the knee (fig. 1*A*). CT scanning showed a soft tissue mass with dense calcification behind the knee (fig. 1*B*). Femoral arteriography showed normal vessels in the region of the knee with no evidence of aneurysm. Arthroscopy revealed a few pieces of loose cartilage in the joint and some small defects in the articular cartilage thought to be due to osteoarthritis. The synovial lining of the knee joint and suprapatella bursa appeared normal. Intraoperative radiography showed that air introduced into the knee joint extended into a popliteal cyst that contained calcified masses posterior to the knee. A posterior dissection yielded a bursal mass with a necklike extension arising from the joint capsule between the semimembranosus and medial head of the gastrocnemius muscles.

The pathologic specimen was a 6 × 2 cm ovoid mass with multiple small 0.5 cm cartilage bodies. Microscopy revealed cartilaginous tissue growing from the synovium which lined the cyst. Scattered areas of ossification were present in the cartilaginous loose bodies. The diagnosis was synovial osteochondromatosis.

Case 2

A 39-year-old man had chronic right knee pain. History revealed major knee trauma at age 14 years. Radiography showed degenerative changes, including flattening and irregularity of the medial femoral condyle. Calcified bodies were present behind the knee and in the region of the knee joint (figs. 2*A* and 2*B*). Subsequent films of the knee prior to surgery showed a change in position of the calcified bodies (fig. 2*C*). At surgery multiple loose cartilage bodies were seen in the knee joint and in a popliteal cyst. No evidence of cartilaginous metaplasia in the synovium was found, and the loose bodies were felt to be secondary to fragments of cartilage dislodged from the medial femoral condyle.

Case 3

A 67-year-old man had bilateral leg and arm pain. Radiography showed multiple calcified masses posterior to the knee (fig. 3*A*). Arthrography demonstrated that these masses were within a popliteal cyst (fig. 3*B*). The symptoms were felt to be due to cervical spine pathology resulting in cord compression, and surgery was not performed on the knee.

Case 4

A 70-year-old male with malignant melanoma of the scalp complained of severe low back pain radiating down the left leg. Radiography of the knee showed multiple densities posterior to the knee joint. These densities had the radiographic appearance of calcified cartilage (fig. 4). The pain was thought to be unrelated to knee pathology and instead due to an old sciatic nerve injury from an injection. The knee was asymptomatic and no further diagnostic workup was undertaken nor treatment prescribed. The diagnosis, based on the characteristic radiographic appearance, was probable synovial osteochondromatosis in a popliteal cyst.

Discussion

The composition of loose bodies in joints is either entirely cartilage or a combination of cartilage and bone. These bodies may be classified according to their etiologies into three groups [1, 2]: (1) trauma—loose bodies secondary to osteochondral fractures and osteochondritis dissecans [3]; (2) arthropathy—loose bodies associated with joint surface disintegration such as osteoarthritis, infection, and neuropathic joints; and (3) synovial osteochondromatosis—calcified or noncalcified bodies which may be attached to the synovial membrane or

Received May 9, 1978; accepted July 17, 1978.

[1] Department of Radiology, Skeletal Section, University of California Medical Center, San Francisco, California 94143. Address reprint requests to Department of Radiology, Editorial Office, University of California Medical Center, San Francisco, California 94143.

[2] Present address: Department of Radiology, Beth Israel Hospital–Harvard Medical School, 330 Brookline Avenue, Boston, Massachusetts 02215.

© 1978 American Roentgen Ray Society

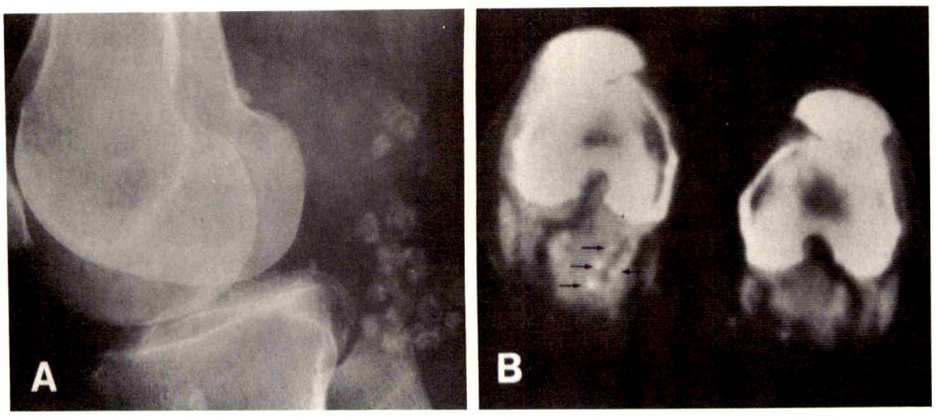

Fig. 1.—*A*, Lateral radiograph showing multiple nodular densities behind knee. Punctate calcifications within nodules are characteristic of cartilage calcification. *B*, CT scan of knees showing small calcifications (*arrows*) within soft tissue mass behind right knee.

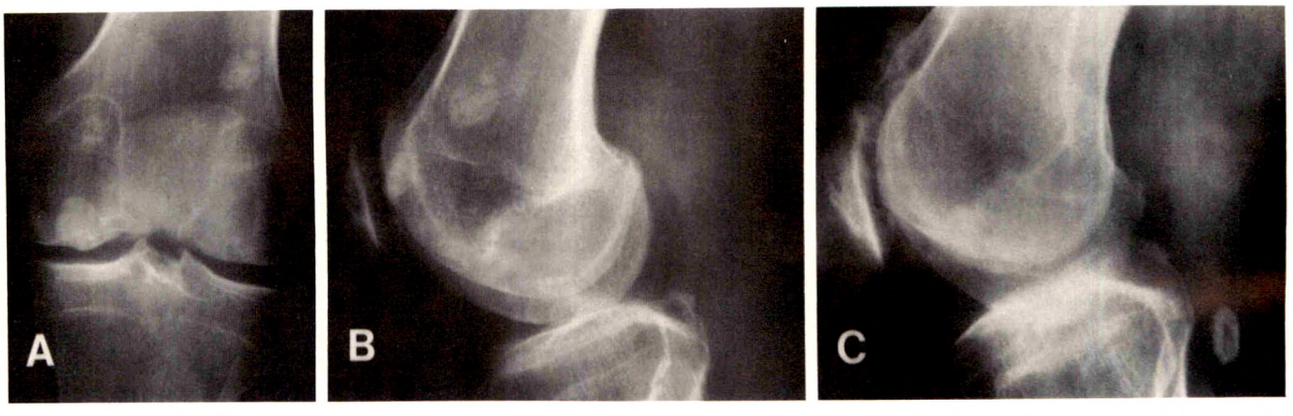

Fig. 2.—*A and B*, Radiographs demonstrating degenerative changes including flattening and irregularity of medial femoral condyle. Calcified bodies are behind knee and in region of joint. *C*, 3 months later calcified bodies have changed position. Change indicates they are loose within knee joint, suprapatella bursa, and popliteal cyst.

loose [4, 5]. Trauma and arthropathy can be grouped together as processes which may affect articular cartilage and secondarily result in calcified or loose joint bodies. However, synovial osteochondromatosis is considered a primary pathologic process of the synovial lining resulting in loose or calcified joint bodies.

The etiology of synovial osteochondromatosis is unknown. It is believed to be a benign form of chondrometaplasia occurring in synovial tissue [5, 6]. The chondroid masses may form in the tips of synovial villi in joints, in bursal synovium [7], or in tendon sheaths. Synovial osteochondromatosis occurs most commonly in the knee joint, but can occur in the hip, shoulder, and elbow [8–11]. Conventional radiography may show soft tissue masses within the joint. These tissue masses may or may not be calcified and may erode the adjacent bone [12]. Arthrography can show multiple small filling defects resulting from either the synovial masses or loose joint bodies [13, 14].

On the basis of a histopathologic study of 30 cases, Milgram [8] believes there are three separate phases of synovial osteochondromatosis. He states that the process starts as active intrasynovial disease, progresses to a transitional phase of osteochondral bodies in the synovium and free in the joint cavity, and, finally, a phase of inactive synovial disease with multiple free joint bodies. The nature of therapeutic intervention should reflect the stage of the process, and synovectomy may be unnecessary in the last phase of synovial osteochondromatosis.

According to Meyerding and Van DeMark [15], popliteal cysts may be produced by either herniation of the synovial membrane through the posterior capsule of the knee joint, or a communication of the knee joint with the semimembranosus or gastrocnemius bursae. These cysts are synovial lined. In a high percentage of cases, popliteal cysts are associated with intraarticular pathology [16]. Lesions such as meniscal tears or rheumatoid synovitis which result in chronic synovial effusion may be causally responsible for some popliteal cysts [17].

We believe there are two explanations for the finding of calcified bodies in popliteal cysts. First, loose joint mice or synovial osteochondromata may induce a joint effusion, which through congenital openings between the semimembranosus or gastrocnemius bursae causes enlarged popliteal cysts. Loose bodies as well as joint fluid can travel from the true joint space to the communicating posterior bursa resulting in the occurrence of calcified bodies in the popliteal cyst. Alternatively, the same radiographic appearance could be produced if the calcified bodies of synovial osteochondromatosis arose de novo as a form of chondrometaplasia in the synovial lined popliteal cysts. Synovial osteochondromatosis arising de novo in a noncommunicating popliteal bursal cyst

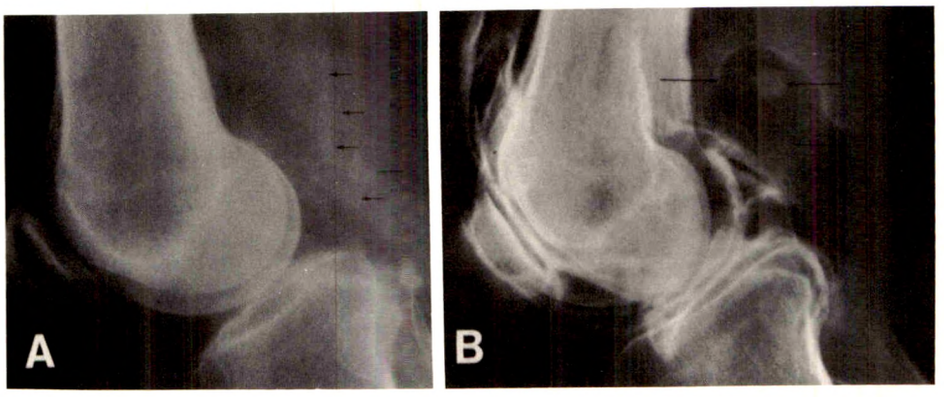

Fig. 3.—*A*, Multiple calcified bodies (*arrows*) posterior to knee joint. *B*, Arthrogram demonstrating calcified bodies (*arrows*) within popliteal cyst. (Courtesy of Dr. Robert Courey, St. Anne's Hospital, Fall River, Mass.)

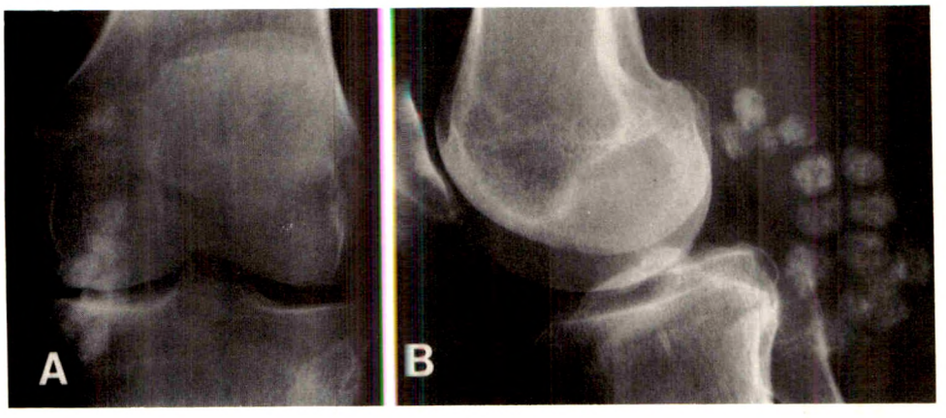

Fig. 4.—Anteroposterior (*A*) and lateral (*B*) films showing multiple calcifications posterior to knee joint with radiographic appearance characteristic of calcified cartilage.

has an identical appearance to synovial osteochondromatosis in a popliteal cyst in which there is communication with the joint [7].

We believe the latter explanation is relevant in case 1 and the former in case 2. The synovial metaplasia seen in the pathologic specimen in case 1 confirmed the diagnosis of synovial osteochondromatosis. In case 2, the history and radiographic findings of previous trauma and the lack of synovial metaplasia implied that the cartilaginous and loose bodies were secondary to the previous trauma and joint destruction. The characteristic radiographic appearances of synovial osteochondromatosis in cases 3 and 4 closely mimic that of case 1 and support a similar pathogenetic mechanism, although surgical proof was not obtained.

ACKNOWLEDGMENT

We thank Dr. Robert Courey for allowing us to use case 3.

REFERENCES

1. Fisher AGT: A study of loose bodies composed of cartilage or of cartilage and bone occurring in joints with special reference to their pathology and etiology. *Br J Surg* 8:493–523, 1921
2. Milgram JW: The classification of loose bodies in human joints. *Clin Orthop* 124:282–291, 1977
3. Milgram JW: Radiological and pathological manifestations of osteochondritis dissecans of the distal femur. *Radiology* 126:305–311, 1978
4. Jones HT: Loose body formation in synovial osteochondromatosis with special reference to etiology and pathology. *J Bone Joint Surg* 6:407–458, 1924
5. Murphy FP, Dahlin DC, Sullivan CR: Articular synovial chondromatosis. *J Bone Joint Surg [Am]* 44:77–86, 1962
6. Aegerter E, Kirkpatrick J: *Orthopedic Diseases*, 4th ed. Philadelphia, Saunders, 1975
7. Symeonides P: Bursal chondromatosis. *J Bone Joint Surg [Br]* 48:371–373, 1966
8. Milgram JW: Synovial osteochondromatosis. *J Bone Joint Surg [Am]* 59:792–801, 1977
9. Leydig SM, Odell RT: Synovial osteochondromatosis. *Surg Gynecol Obstet* 89:457–463, 1949
10. Freund E: Chondromatosis of joints. *Arch Surg* 34:670–685, 1937
11. McIvor RR, King D: Osteochondromatosis of the hip joint. *J Bone Joint Surg [Am]* 44:87–97, 1962
12. Zimmerman C, Sayegh V: Roentgen manifestations of synovial osteochondromatosis. *Am J Roentgenol* 83:680–686, 1960
13. Prager RJ, Mall JC: Arthrographic diagnosis of synovial chondromatosis. *Am J Roentgenol* 127:344–346, 1976
14. Murphy WA, Siegel MJ, Gilula LA: Arthrography in the diagnosis of unexplained chronic hip pain with regional osteopenia. *Am J Roentgenol* 129:283–287, 1977
15. Meyerding MW, Van DeMark RE: Posterior hernia of the knee (Baker's cyst, popliteal cyst, semimembranous bursitis, medial gastrocnenins bursitis and popliteal bursitis). *JAMA* 122:858–861, 1943
16. Burleson RJ, Bickel WH, Dahlin DC: Popliteal cyst. A clinicopathological survey. *J Bone Joint Surg [Am]* 38:1265–1274, 1956
17. Chitwood HM: Posterior medial meniscal lesions and popliteal cysts. *J Bone Joint Surg [Am]* 47:1272–1273, 1965

Complications of Catheter Cerebral Arteriography: Analysis of 5,000 Procedures. I. Criteria and Incidence

RICHARD L. MANI,[1, 2] RONALD L. EISENBERG,[1] EUGENE J. McDONALD, JR.,[1, 3] JAMES A. POLLOCK,[4] AND JOHN R. MANI[5]

Computer analysis of complications of 5,000 catheter cerebral arteriograms performed at four hospitals (two training and two nontraining) revealed a total of 68 complications (1.4%). Eight (0.16%) of these complications were major: five patients required thrombectomy or embolectomy, two had permanent neurologic deficits, and one patient died. The complication rate for the training hospitals (3.9%) was significantly higher than that for the nontraining hospitals (0.9%), but the rates of permanent complications were identical in both groups (0.1%). Reporting criteria and complication types are described.

Catheter cerebral arteriography has achieved increasing acceptance as a technique that provides high degrees of both operator flexibility and patient comfort. Within the last 10 years (1966–1976), it has become the technique of choice in evaluating virtually every suspected intracranial lesion at the University of California San Francisco and its two affiliated training hospitals. Puncture of the femoral artery has replaced puncture of the axillary or brachial artery and direct puncture of the carotid or vertebral artery except in rare instances when (1) occlusion or high grade stenosis of both femoral and iliac arteries prevents passage of the catheter; (2) a vessel is so tortuous it cannot be catheterized; or (3) the referring physician specifically requests that femoral puncture be avoided.

Despite the demonstrated advantages of this technique, outside our institutions there is still widespread reluctance to adopt it because of doubts about its safety [1–4]. These doubts reflect the absence of comprehensive and detailed data on complication rates of catheter cerebral arteriography as currently practiced using the recent advances in catheters, guide wires, contrast media, film and equipment technology, and greater operator proficiency. In every case in which catheter cerebral arteriography is considered, it is the clinician who must ultimately weigh the risks and benefits for the patient. More precise data on the current complication rate of catheter cerebral arteriography will allow this decision to be made with greater confidence.

To investigate the complications of arteriography, we reviewed 5,000 catheter cerebral arteriograms and the medical records of patients evaluated in two training and two nontraining hospitals. This first part of our study presents the criteria used for reporting the complications, classifies the complications into three major types and subtypes, documents the incidence of complication, and compares the complication rates of the nontraining and training hospitals.

Materials and Methods

The four hospitals chosen were well matched. First, the participating neuroangiographers in these hospitals were trained in the same institution (University of California San Francisco) and use virtually identical techniques of catheter cerebral arteriography. Second, the participating hospitals were similar in number of patient beds and number of procedures performed per year (table 1). The level of experience of the angiographers, however, varied considerably between first- and second year radiology residents (supervised) and fully trained neuroangiographers.

In reviewing the medical records and arteriograms from each of the four hospitals, particular attention was paid to angiographers' and nurses' notes and progress notes for the 48 hr period following arteriography. If any evidence of complication was reported, the patient's course was assessed from time of complication until the condition stabilized.

Early in the period of data acquisition, when approximately 1,600 cases had been reviewed (800 from each of the two types of hospital), it became apparent that the incidence of complications in the nontraining hospitals was far less than in the training hospitals. Therefore, in order to investigate possible relationships of the complications to other factors (e.g., clinical and arteriographic diagnoses, age of patient, time of procedure, amount of contrast agent, number and type of vessels catheterized) [5], we extended our data gathering into earlier years, but this time only from the nontraining hospitals so that a comparable number of complications from both types of hospital could be analyzed. The total number of cases collected was 5,000: 813 from the training hospitals from August 1974 to June 1975 and 4,187 from the nontraining hospitals from January 1969 to June 1975.

The procedural and follow-up data pertaining to the 5,000 catheter cerebral arteriograms were recorded on prepared forms, transcribed to punch cards, and analyzed by computer (table 2).

Reporting Criteria

Different authors report results in different ways, making comparison of complications difficult, if not impossible. We combined the criteria of Wishart [6] and Takashi and Kawanani

Received February 7, 1978; accepted after revision August 1, 1978.

[1] Department of Radiology, University of California School of Medicine and Veterans Administration Hospital, San Francisco, California 94121. Address reprint requests to R. L. Eisenberg at Veterans Administration Hospital.

[2] Present address: Department of Radiology, Providence Hospital, 30th and Summit, Oakland, California 94609.

[3] Present address: 10010 Garrett Street, Vienna, Virginia 22180.

[4] Department of Radiology, Sutter General Hospital, Sacramento, California 95816.

[5] Department of Radiology, Franklin Hospital, San Francisco, California 94114.

© 1978 American Roentgen Ray Society

0361–803X/78/1100–0861 $00.00

TABLE 1

Analysis of Participating Radiology Staff

Hospital	No. Beds	Procedures/Yr	Radiology Staff	Comment
Nontraining:				
NT-I	600	600	Two neuroradiologists	Perform 90%–95% of all arteriography
NT-II	275	300	Three board-certified radiologists, no extra arteriographic training	Equally share all arteriography performed
Training:				
T-I	600	750	Two neuroradiologists, two neuroradiology fellows, and two third year residents	90%–95% performed by fellows or residents under direct supervision of neuroradiologists
T-II	275	450	One neuroradiologist, four staff radiologists, and two first or second year residents	90%–95% performed by residents under direct supervision of radiologists

TABLE 2

Analysis of Case Material

Hospital	Years	Procedures		Sex M/F (%)	Age Range (Median) (yr)	Arteries Punctured					
						Femoral		Axillary		Carotid	
		No.	%			No.	%	No.	%	No.	%
Nontraining:											
NT-I	1/1969–6/1975	3,676	72	52/48	1–88(52)	3,631	99	42	1	3	. . .
NT-II	1/1973–6/1975	511	10	59/41	4–94(61)	487	96	17	3	7	1
Training:											
T-I	8/1974–6/1975	513	12	51/49	1–87(52)	464	90	48	9	1	. . .
T-II	8/1974–6/1975	300	6	97/3*	21–89(56)	291	97	9	3	. . .	. . .
Total	. . .	5,000	100	55/44	1–94(53)	4,873	98	116	2	11	0.2

* Veterans Administration Hospital.

[7] and classified complications into three major categories (table 3): local, central nervous system, and systemic or toxic. Subcategories were allocated for each of the major types of complication according to severity and duration. The following definitions were used for interpretation of the data.

Complication. Any unanticipated event deleterious to the health of the patient occurring within 24 hr of the initiation of the arteriographic procedure and which in the judgment of a trained clinical observer resulted from the procedure.

Minor. A complication that does not alter significantly the health or activity of the patient or require extra hospitalization or extraordinary therapy (pertains primarily to complaints of the patient).

Major. A complication that alters significantly the health or activity of the patient and requires extraordinary therapy or hospitalization.

Transient. A complication that persists for 10 days or less.

Permanent. A complication that persists longer than 10 days.

Local. A complication that involves the puncture site or artery or limb.

Central nervous system. A complication that involves any part of the central nervous system.

Systemic or toxic. A complication that involves any body system other than the central nervous system.

Determination of whether a complication is due to the procedure or to the attendant disease is often difficult. For example, a moribund or comatose patient whose clinical course worsens before, during, and immediately after emergency arteriography may demonstrate symptoms of a complication that may or may not be attributable to the procedure. To avoid speculation, we

TABLE 3

Criteria for Reporting Complications Resulting from Catheter Cerebral Arteriography

Criteria	Examples
Local:	
Transient, minor	Subjective complaints of 24 hr or less requiring only supportive therapy
Transient, major	Loss of pulse, cold limbs requiring anticoagulant therapy but not surgery
Permanent, major	Requiring thrombectomy or embolectomy
Death	As result of surgery or limb complication
Central nervous system:	
Transient, minor	Seeing "spots" for 5–10 min after injection
Transient, major	Blindness, paralysis lasting less than 10 days
Permanent, major	Residual field defects, hemiparesis
Death	Following convulsion, stroke
Systemic or toxic:	
Transient, minor	Minor hypotensive episode
Transient, major	Shock, laryngospasm, electrocardiographic changes
Permanent, major	Arrhythmia, electrocardiographic changes, coma
Death	Cardiac arrest

TABLE 4
Total Complications

Complications	Nontraining Hospital			Training Hospital			Total
	NT-I	NT-II	Total	T-I	T-II	Total	
Local:							
Minor transient	. . .	. . .	. . .	2	. . .	2	2
Major transient	. . .	2	2	1	. . .	1	3
Major permanent	2	2	4	. . .	1	1	5
Death	. . .	. . .	. . .	. . .	. . .	. . .	. . .
Subtotal	2(0.06)	4(0.8)	6(0.1)	3(0.6)	1(0.3)	4(0.5)	10(0.2)
Central nervous system:							
Minor transient	. . .	. . .	. . .	5	. . .	5	5
Major transient	17	3	20	14	4	18	38
Major permanent	2	. . .	2	. . .	. . .	. . .	2
Death	1	. . .	1	. . .	. . .	. . .	1
Subtotal	20(0.5)	3(0.6)	23(0.6)	19(3.7)	4(1.3)	23(2.8)	46(0.9)
Systemic:							
Minor transient	3	1	4	2	1	3	7
Major transient	2	1	3	. . .	2	2	5
Major permanent	. . .	. . .	. . .	. . .	. . .	. . .	. . .
Death	. . .	. . .	. . .	. . .	. . .	. . .	. . .
Subtotal	5(0.1)	2(0.4)	7(0.2)	2(0.4)	3(1.0)	5(0.6)	12(0.2)
Total	27(0.7)	9(1.8)	36(0.9)	24(4.7)	8(2.7)	32(3.9)	68(1.4)

Note.—Numbers in parentheses are percentages.

recorded any complication judged by the referring clinician to be a complication of the procedure itself. This may have produced a higher complication rate but one that is probably offset by complications that were "silent" or unobserved.

Results

A total of 68 complications (1.4%) resulted from the 5,000 catheter cerebral arteriographic procedures (table 4). Of these 68 complications, 14 (20.5%) were minor, transient; 46 (68%) were major, transient; and seven (10%) were major, permanent. There was one death (1.5%). The total complication rates for the nontraining hospitals (0.9%) were significantly lower ($P < .001$) than those for the training hospitals (3.9%).

Five patients (0.1%) had local complications that required thrombectomy or embolectomy. There were 41 (0.8%) major central nervous system complications. Of these, 35 were transient neurological deficits requiring 10 min to 48 hr to clear, and three were transient hemiparesis requiring 7–10 days to clear. Two patients had permanent hemiparesis. One patient died after a prolonged abortive attempt to catheterize the left vertebral artery; the postmortem diagnosis was atherosclerosis, dissection and occlusion of the left vertebral artery, and a small right vertebral artery. Systemic complications included five severe hypotensive episodes. In three there was associated laryngospasm that was treated with fluids and steroids. No patient required a tracheostomy nor had a cardiac arrest.

Table 5 shows the six major categories of prearteriographic (clinical) diagnosis in our series. The major discrepancy in the distribution pattern can be seen in the seizure or headache category, in which the number of patients is significantly larger in the nontraining institutions (19%) than in the training institutions (2%). Patients with clinically diagnosed seizure or headache had a high percentage of arteriograms that showed no abnormalities and correspondingly experienced few complications from the procedure. When complications from this category were excluded, the overall complication rates were not greatly altered (table 5).

Discussion

Reported overall complication rates of cerebral arteriography have varied; Feild et al. [8] reported 2.1%, Blain and Resch [9] 23.2%. We found a rate of 1.4% (table 6). Total complication rates reported are often misleading because they do not discriminate the clinically important permanent complications from those that are transient and clinically less significant. Although we found the total complication rate significantly higher for the training hospitals (3.9%) than for the nontraining hospitals (0.9%), the rates of permanent complication were identical (0.1%). Therefore, the difference between the hospital groups lies in the number of transient complications.

Surprisingly, our study revealed an extremely low rate of postarteriographic thrombectomy and embolectomy (five of 5,000, 0.1%), which contrasts greatly to that reported by Jacobsson and Schlossman (14 of 275, 5%), Siegelman et al. (four of 173, 2.3%), and Formanek et al. (2.5%) [22–24]. This discrepancy may be explained by the small size of the selective catheters (no. 5 French) used in over 95% of the cases reported in our study; the investigators just cited used larger catheters (nos. 7 and 8 French). Mani [25] demonstrated that the incidence of postangiographic thrombosis of the punctured artery is related to catheter size.

TABLE 5

Percentage Complications Relative to Clinical Diagnoses

Hospital	Vascular Disease	Tumor	Subarachnoid Hemorrhage	Trauma or Subdural Hematoma	Degenerative Disease	Seizure or Headache	Complication Rate
Nontraining:							
All patients	34	27	11	8	1	19	0.9
Excluding seizure or headache	42	33	14	10	1	. . .	1.0
Training:							
All patients	38	30	20	9	1	2	3.9
Excluding seizure or headache	39	31	20	9	1	. . .	3.7

TABLE 6

Reported Complication Rates of Cerebral Arteriography

Reference	Examination Type	No. Cases	Total Complications (%)	Transient (%)	Permanent (%)	Death (%)	Local or Systemic (%)	Central Nervous System (%)
Codden and Krieger [2]	Direct puncture	546	17.5	15.1	0.8	1.6	8.4	9.1
Lindner et al. [10]	Various approaches	1,000	2.4	1.1	0.5	0.8	NR	NR
Feild et al. [8]	Direct puncture	2,332	2.1	1.5	0.3	0.3	1.1	1.0
Scheinberg and Zunker [11]	Direct puncture	902	3.7	2.8	0.6	0.3	0.8	2.9
Lang [12]	Femorocerebral arteriography	11,402	7.1	7.0	0.1	0.06	3.4	3.7
Halpern [13]	Femorocerebral arteriography	1,000	NR	NR	NR	NR	2.0	NR
Patterson et al. [14]	Direct puncture	604	4.6	3.8	0.6	0.2	NR	4.6
Cullen [4]	Direct puncture	538	3.9	1.9	1.0	1.0	NR	NR
Blain and Resch [9]	Various approaches	99	23.2	22.2	0.0	1.0	9.0	14.2
Silverstein [15]	Various approaches	398	7.6	6.1	1.0	0.5	NR	NR
Perrett and Caldicott [16]	Direct puncture	783	2.3	0.7	0.4	1.2	NR	2.3
Hass et al. [17]	Various approaches	4,748	NR	NR	0.5	0.7	NR	NR
Chynn [18]	Femorocerebral arteriography	436	4.9	4.5	0.0	0.4	NR	4.9
Wishart [6]	Femorocerebral arteriography	447	10.8	9.5	1.3	0.0	5.5	5.3
Feild et al. [19]	Brachial	1,000	4.0	3.2	0.6	0.2	NR	NR
Takahashi and Kawanani [7]	Femorocerebral arteriography	500	2.6	2.5	0.1	0.0	0.9	1.7
Vitek [20]	Femorocerebral arteriography	2,000	2.3	1.5	0.7	0.1	0.8	1.5
Olivecrona [21]	Various approaches	5,531	26.3	26.1	0.2	0.03	21.7	4.6
Present report:	Catheter cerebral arteriography	5,000	1.4	1.2	0.1	0.02	0.4	0.9
Nontraining hospitals	. . .	4,187	0.9	0.8	0.1	0.03	0.3	0.6
Training hospitals	. . .	813	3.9	3.8	0.1	0.0	1.1	2.8

Note.—NR = not reported.

Complications related to the central nervous system were almost invariably transient (43 of 46, 93%). The 38 major, transient complications of the central nervous system were of three definite types: visual, six; motor, 30; and cerebellar, two. They occurred immediately after the manipulation of guide wire or catheter, completion of an injection of contrast material, or termination of the study. We presume these complications were produced by an embolism from the catheter and guide wire combination, atheromatous debris, or, less likely, thrombi from the cardiac wall. The single death occurred in the nontraining hospital with the lowest complication rate and was related to failure to catheterize the vertebral artery.

Systemic complications were hypotension, shock, and laryngospasm, all requiring pressor therapy, fluids, or steroids. Five of the 12 systemic complications were severe and required extraordinary measures for resuscitation; each incident occurred from 30 min to 2 hr after the procedure. The causes of the systemic complications are unknown; however, the remarkably similar times of occurrence of each complication seem to represent a distinct clinical pattern.

Our study indicates a significant relationship between

operator proficiency (length of training) and overall complication rate. The training hospitals, in which neuroradiology fellows or residents perform the neuroangiographic procedures under close supervision, had a complication rate (3.9%) approximately 4.5 times that of nontraining centers (0.9%), which have operators of greater experience. Even within the nontraining hospitals, the complication rate of the radiologists/angiographers was more than twice (1.8%) that of the fully trained neuroradiologists (0.7%).

Is there a complication rate inherently associated with catheter cerebral arteriography? To determine the existence of such a rate, data for two groups of patients from hospital NT-I (greatest operator proficiency, lowest complication rate) were examined. The first group consisted of 856 patients with a clinical diagnosis of headache or seizure (i.e., 84% of the arteriograms showed no abnormalities). The second group consisted of 2,112 patients whose arteriograms showed no abnormalities; 714 of these patients had the diagnosis of headache or seizure. The complication rates were 0.35% and 0.46%, respectively, a difference that was not significant. If it is assumed that these patients had little or no disease that would contribute to the risk of angiography, these figures would then represent a complication rate intrinsic to catheter cerebral arteriography as it is currently practiced at the highest level of operator proficiency.

REFERENCES

1. Baker HL Jr: Cerebral angiography—techniques and results. *Mayo Clin Proc* 35:482–486, 1960
2. Coddon DR, Krieger HP: Circumstances surrounding complications of cerebral angiography: analysis of 546 consecutive cerebral angiograms. *Am J Med* 25:580–589, 1958
3. Cronqvist S, Efsing HO, Palacios E: Embolic complications in cerebral angiography with the catheter technique. *Acta Radiol [Diagn]* (Stockh) 10:97–107, 1970
4. Cullen JF: Visual field defects following cerebral angiography. *Ophthalmol Soc UK Trans* 89:47–55, 1970
5. Mani RL, Eisenberg RL: Complications of catheter cerebral arteriography: analysis of 5,000 procedures. III. Assessment of arteries injected, contrast medium used, duration of procedure, and age of patient. *Am J Roentgenol* 131:871–874, 1978
6. Wishart DL: Complications in vertebral angiography as compared to nonvertebral cerebral angiography in 447 studies. *Am J Roentgenol* 113:527–537, 1971
7. Takahashi M, Kawanani H: Complications of catheter cerebral angiography: an analysis of 500 examinations. *Acta Radiol [Diagn]* (Stockh) 13:248–258, 1972
8. Feild JR, Robertson JT, DeSaussure RL Jr: Complications of cerebral angiography in 2,000 consecutive cases. *J Neurosurg* 19:775–781, 1962
9. Blain JG, Resch JA: Complications of angiography in the stroke patient. *Geriatrics* 21:149–154, 1966
10. Lincner DW, Hardy WG, Thomas LM, Gurdjian ES: Angiographic complications in patients with cerebrovascular disease. *J Neurosurg* 19:179–185, 1962
11. Scheinberg P, Zunker E: Complications in direct percutaneous carotid arteriography. *Arch Neurol* 8:676–684, 1963
12. Lang EK: A survey of complications of percutaneous retrograde arteriography: Seldinger technic. *Radiology* 81:257–263 1963
13. Halpern M: Percutaneous transfemoral arteriography: an analysis of the complications in 1,000 consecutive cases. *Am J Roentgenol* 92:918–934, 1964
14. Patterson RH, Goodell H, Dunning HS: Complications of carotid arteriography. *Arch Neurol* 10:513–520, 1964
15. Silverstein A: Arteriography of stroke. III. Complications. *Arch Neurol* 15:206–210, 1966
16. Perrett LV, Caldicott WJ: Complications of cerebral angiography. *Australas Radiol* 11:107–113, 1967
17. Hass WK, Fields WS, North RR, Kricheff II, Chase NE, Bauer RB: Joint study of extracranial arterial occlusion. II. Arteriography, techniques, sites and complications. *JAMA* 203 961–968, 1968
18. Chynn KY: Transfemoral carotid and vertebral angiography. *Acta Radiol [Diagn]* (Stockh) 9:244–250, 1969
19. Feild JR, Lee L, McBurney RF: Complications of 1,000 brachial arteriograms. *J Neurosurg* 36:324–332, 1972
20. Vitek JJ: Femoro-cerebral angiography: analysis of 2,000 consecutive examinations, special emphasis on carotid arteries catheterization in older patients. *Am J Roentgenol* 118 633–647, 1973
21. Olivecrona H: Complications of cerebral angiography. *Neuroradiology* 14:175–181, 1977
22. Jacobsson B, Schlossman D: Thromboembolism of leg following percutaneous catheterisation of femoral artery for angiography: predisposing factors. *Acta Radiol [Diagn]* (Stockh) 8:109–118, 1969
23. Siegelman SS, Caplan LH, Annes GP: Complications of catheter angiography: study with oscillometry and "pull-out" angiograms. *Radiology* 91:251–253, 1968
24. Formanek G, Frech RS, Amplatz K: Arterial thrombus formation during clinical percutaneous catheterization. *Circulation* 41:833–839, 1970
25. Mani RL: Computer analysis of factors associated with thrombus formation observed on pullout angiograms: preliminary communication. *Invest Radiol* 10:373–384, 1975

Complications of Catheter Cerebral Arteriography: Analysis of 5,000 Procedures. II. Relation of Complication Rates to Clinical and Arteriographic Diagnoses

RICHARD L. MANI[1,2] AND RONALD L. EISENBERG[1]

Clinical (prearteriographic) and arteriographic diagnoses were grouped into six categories each for analysis of central nervous system and systemic complications of 5,000 catheter cerebral arteriograms. Within each category, there was no significant difference in complication rate between clinical and arteriographic diagnoses. The highest complication rates (1.2%–1.9%) were in patients with cerebrovascular occlusive disease, posttraumatic or postoperative conditions, and subarachnoid hemorrhage. Significantly lower complication rates (0.2%–0.5%) were found in patients with tumor, seizure or headache, and patients with normal arteriographic findings.

This communication discusses our investigation of the possible relationship between the central nervous system and systemic complication rates of catheter cerebral arteriography and the clinical (prearteriographic) and arteriographic diagnoses. This information is of importance to the clinician in his appraisal of risk versus benefit to the patient who may undergo catheter cerebral arteriography and to the angiographer in his approach to the procedure.

Materials and Methods

This study is a continuation of a previously described analysis of complications of 5,000 catheter cerebral arteriographic procedures performed in two training and two nontraining hospitals [1]. We chose to evaluate both the clinical and the arteriographic diagnoses because although the arteriographic diagnosis allows for the more accurate reflection of the effect of concurrent disease on the complication rate, when the risk of contemplated arteriography is assessed against benefit by the referring clinician and the radiologist, only the clinical diagnosis is known.

All clinical information was extracted from patient charts. In cases in which more than one clinical (prearteriographic) diagnosis was given, we used the primary (first) clinical diagnosis in the present study. Only 146 of the 5,000 cases (2.9%) had multiple clinical diagnoses.

The arteriographic diagnoses were taken from the radiologist's report. The incidence of cases with more than one arteriographic diagnosis was 1.2% (61 of 5,000). In the cases having multiple arteriographic diagnoses, however, every diagnosis was included in our study because we believe these to be a more factual statement of disease than the clinical diagnosis.

The criteria used for complications of catheter cerebral arteriography were previously described [1]; complications fell into three major categories: local, central nervous system, and systemic or toxic. Only central nervous system and systemic or toxic complications will be discussed in this study because there is no evidence to suggest a relationship between any clinical diagnosis included in this study and local complications.

Results

Clinical Diagnosis

Clinical diagnoses were grouped into six categories for analysis of systemic and central nervous system

TABLE 1

Central Nervous System and Systemic Complications Relative to Clinical Diagnosis

Clinical Diagnosis	Complication Rate (%)	
	Nontraining Hospitals	Training Hospitals
Vascular occlusive disease*	1.2 (17/1,392)	3.5 (11/310)
Tumor†	0.36 (4/1,113)	5.3 (13/246)
Subarachnoid hemorrhage (any cause)	1.3 (6/461)	2.6 (4/153)
Postoperative or posttraumatic conditions	1.2 (4/330)	0 (0/72)
Degenerative cerebral disease‡	0 (0/38)	0 (0/9)
Seizure or headache	0.35 (3/853)	0 (0/23)
Total	0.8 (34/4,187)	3.4 (28/813)

* Stroke, transient ischemic attacks, cerebral insufficiency syndromes, intracerebral hemorrhage.
† Any neoplastic process including abscess.
‡ Encephalopathy, atrophy.

TABLE 2

Central Nervous System and Systemic Complications Relative to Arteriographic Diagnosis

Arteriographic Diagnosis	Complication Rate (%)	
	Nontraining Hospitals	Training Hospitals
Vascular occlusive disease*	1.2 (12/1,013)	4.3 (12/283)
Neoplasm (including abscess)	0.2 (1/530)	5.0 (6/120)
Vascular abnormality†	1.9 (7/367)	3.4 (5/149)
Posttraumatic or postoperative conditions‡	1.3 (2/152)	0 (0/55)
Atrophy, hydrocephalus	2.0 (1/50)	0 (0/25)
Normal§	0.5 (11/2,112)	2.6 (5/195)
Total	0.8 (34/4,224)	3.4 (28/827)

* Including intracerebral hemorrhage in absence of vascular abnormality.
† Including aneurysm, arteriovenous malformation, and associated hemorrhage.
‡ Extracerebral space, cerebral contusion, swelling.
§ No arteriographic evidence of disease.

Received February 7, 1978; accepted after revision August 1, 1978.
[1] Department of Radiology, University of California School of Medicine and Veterans Administration Hospital, San Francisco, California 94121. Address reprint requests to R. L. Eisenberg at Veterans Administration Hospital.
[2] Present address: Department of Radiology, Providence Hospital, 30th and Summit, Oakland, California 94609.

© 1978 American Roentgen Ray Society

0361–803X/78/1100–0867$00.00

TABLE 3

Literature Survey of Central Nervous System and Systemic Complications Relative to Clinical Diagnosis

	Feild et al. [2]	Lindner et al. [3]	Patterson et al. [4]	Blain and Resch [5]	Perret and Nishioka [6]	Silverstein [7]	Hass et al. [8]	Feild et al. [9]	Present Report	
									Nontraining Hospitals	Training Hospitals
Approaches	Direct puncture	Various	Direct puncture	Various	Direct puncture	Various	Various	Retrograde brachial	Catheter cerebral	Catheter cerebral
Vascular occlusive disease:										
Total cases	760	1,199	88	99	...	398	4,748	459	1,392	310
Overall rate	2.6	2.4	11.0	22.0	...	7.6	...	8.7	1.2	3.5
Permanent	0.5	0.5	2.0	0	...	1.0	0.5	...	0.07	0
Death	0.4	1.3	1.0	0	...	0.5	0.7	...	0	0
Tumor:										
Total cases	180	...	231	...	...	...	...	49	1,113	246
Overall rate	1.7	...	0.9	...	...	...	...	4.1	0.4	5.3
Permanent	0	...	...	...	...	...	...	...	0	0
Death	0.6	...	...	...	...	...	...	...	0.09	0
Subarachnoid hemorrhage:										
Total cases	180	...	76	...	5,685	...	...	152	461	153
Overall rate	3.3	...	6.6	...	5.5	...	...	6.6	1.3	2.6
Permanent	0.6	...	0	...	0.5	...	...	...	0.4	0
Death	1.1	...	0	...	0.6	...	...	...	0	0
Headache or seizure:										
Total cases	...	...	187	...	...	...	...	...	853	23
Overall rate	...	...	5.3	...	...	...	...	...	0.4	0
Permanent	...	...	0.5	...	...	...	...	...	0	0
Death	...	...	0	...	...	...	...	...	0	0

Note.—Complication rates (overall, permanent, and death) are percentages.

complications (table 1). In this series, 75% of the total cases and 90% of the complications fell in three categories: vascular occlusive disease, tumor, and subarachnoid hemorrhage. In all three categories, the training hospitals had complication rates significantly higher ($P < .05$) than the nontraining hospitals. In the other three categories (posttraumatic or postoperative conditions, degenerative encephalopathy, and seizure or headache) the differences between the hospital groups were not comparable statistically because of the small sample from the training group.

In the nontraining hospitals, the highest complication rates were in patients with clinically diagnosed vascular occlusive disease, subarachnoid hemorrhage, and posttraumatic or postoperative conditions; these rates were virtually the same (1.2%–1.3%). Significantly lower complication rates within the nontraining group were found in patients with suspected tumor (0.36%) and with seizure or headache (0.35%). The small number of cases in the degenerative encephalopathy and seizure or headache categories preclude a statistical statement.

Arteriographic Diagnosis

The cases of systemic and central nervous system complications generally fell within the same categories of arteriographic diagnosis as clinical diagnosis (table 2). Also, the results in this group were similar in all six categories to those noted in the clinical diagnosis group. Total complication rates were again significantly higher in the training hospitals (3.4%) than in the nontraining hospitals (0.8%). In the nontraining hospitals, the highest complication rates were in patients diagnosed as having vascular occlusive disease (1.2%), arteriovenous malformation or aneurysm (1.9%), and posttraumatic or postoperative conditions (1.3%). Complication rates were significantly lower in patients with tumor (0.2%) and in those demonstrating no abnormalities arteriographically (0.5%).

Discussion

The first part of our investigation [1] demonstrated that the higher complication rates in training hospitals compared to nontraining hospitals reflect the effect of operator proficiency. These findings are also shown in tables 1 and 2. Because the purpose of the present study was to assess the influence of underlying disease processes on the complication rate of catheter cerebral arteriography, the factor of operator proficiency must be either eliminated or minimized. To this end, therefore, our attention is focused on the results of the nontraining hospitals, in which the greater technical skill and experience of the angiographer has minimized the component of operator error.

Our complication rates are lower than previously published complication rates related to specific disease entities [2–11] (tables 3 and 4). In all categories of clinical and arteriographic diagnoses, the overall complication rates of the nontraining hospitals were less than those reported previously; in most instances the differences were statistically significant. Of even greater importance,

TABLE 4

Literature Survey of Central Nervous System and Systemic Complications Relative to Arteriographic Diagnosis

	Codden and Krieger [10]	Present Report	
		Nontraining Hospitals	Training Hospitals
Approaches	Direct puncture	Catheter cerebral	Catheter cerebral
Vascular occlusive disease:			
Total cases	. . .	1,013	283
Overall rate	. . .	1.1	4.3
Permanent	. . .	0	0
Death	. . .	0	0
Neoplasm:			
Total cases	192	530	120
Overall rate	16.7	0.2	5.0
Permanent	0.5	0	0
Death	1.6	0	0
Vascular abnormality/aneurysm:			
Total cases	48	367	149
Overall rate	16.7	1.9	3.4
Permanent	0	0.5	0
Death	2.1	0	0
Normal:			
Total cases	157	2,112	195
Overall rate	17.2	0.5	2.6
Permanent	1.3	0.05	0
Death	1.3	0	0

Note.—Wishart [11] reported an overall complication rate of 12.3% in 179 cases with vascular occlusive disease using a catheter approach. No other information was given. All complication rates (overall, permanent, and death) are percentages.

the incidence of permanent complications and death was lower in all categories for both types of hospital in our study.

Only three reports [2, 4, 9] have documented the complication rates for two or more categories of clinical diagnosis. In all three, as in our study, the complication rates in patients with suspected tumors were lower than in patients with suspected vascular occlusive disease or subarachnoid hemorrhage (table 3).

Several reports [3, 5, 12–14] indicate that patients with vascular occlusive disease have a higher incidence of complication associated with cerebral arteriography than those without vascular disease. Feild et al. [9] stated that "the complications in patients with cerebrovascular disease were found to be 3 to 4 times higher than any other category." In our study, although the complication rate for patients with cerebrovascular occlusive disease was significantly higher than for patients with suspected tumor or with headache or seizure, the rate was not higher than that for patients with subarachnoid hemorrhage associated with aneurysms or arteriovenous malformations or for patients with posttraumatic or postoperative conditions. The contention that there is a greater risk of complication associated with catheter cerebral arteriography in patients with either suspected or proved cerebrovascular occlusive disease is not supported by the results of our study.

REFERENCES

1. Mani RL, Eisenberg RL, McDonald EJ Jr, Pollock JA, Mani JR: Complications of catheter cerebral arteriography: analysis of 5,000 procedures. I. Criteria and incidence. *Am J Roentgenol* 131:861–865, 1978
2. Feild JR, Robertson JT, DeSaussure RL Jr: Complications of cerebral angiography in 2,000 consecutive cases. *J Neurosurg* 19:775–781, 1962
3. Lindner DW, Hardy WG, Thomas LM, Gurdjian ES: Angiographic complications in patients with cerebrovascular disease. *J Neurosurg* 19:179–185, 1962
4. Patterson RH, Goodell H, Dunning HS: Complications of carotid arteriography. *Arch Neurol* 10:513–520, 1964
5. Blair JG, Resch JA: Complications of angiography in the stroke patient. *Geriatrics* 21:149–154, 1966
6. Perret G, Nishioka H: Cerebral angiography: an analysis of diagnostic value and complications of carotid and vertebral angiography in 5,484 patients. *J Neurosurg* 25:98–114, 1966
7. Silverstein A: Arteriography of stroke. III. Complications. *Arch Neurol* 15:206–210, 1966
8. Hass WK, Fields WS, North RR, Kricheff II, Chase NE, Bauer RE: Joint study of extracranial arterial occlusion. II. Arteriography, techniques, sites and complications. *JAMA* 206:961–968, 1968
9. Feild JR, Lee L, McBurney RF: Complications of 1,000 brachial arteriograms. *J Neurosurg* 36:324–332, 1972
10. Codden DR, Krieger HP: Circumstances surrounding complications of cerebral angiography: analysis of 546 consecutive cerebral angiograms. *Am J Med* 25:580–589, 1958
11. Wishart DL: Complications in vertebral angiography as compared to nonvertebral cerebral angiography in 447 studies. *Am J Roentgenol* 113:527–537, 1971
12. Baker HL Jr: Cerebral angiography: techniques and results. *Mayo Clin Proc* 35:482–486, 1960
13. McDowell FH, Schick RW, Frederick W, Dunbar HS: An arteriographic study of cerebrovascular disease. *Arch Neurol* 1:435–441, 1959
14. Pribram HFW: Complications of angiography in cerebrovascular disease. *Radiology* 85:33–37, 1965

Complications of Catheter Cerebral Arteriography: Analysis of 5,000 Procedures. III. Assessment of Arteries Injected, Contrast Medium Used, Duration of Procedure, and Age of Patient

RICHARD L. MANI[1, 2] AND RONALD L. EISENBERG[1]

Complication rates in 5,000 consecutive catheter cerebral arteriograms were assessed with regard to arteries injected, contrast medium used, patient age, and duration of procedure. No statistically significant difference was found between the complication rate when the carotid artery alone was injected and that when the carotid artery was injected in combination with the vertebral artery, the aortic arch, or both. There was also no significant difference between the total complication rates using Conray-60 and Renografin-60. However, although Conray-60 demonstrated no change in complication rate with increased volume, Renografin-60 showed a consistent and significant increase in complication rate with increased volume. Complication rates were also significantly higher when the procedure lasted more than 80 min and in patients more than 40 years old. As might be expected, nontraining hospitals used significantly less contrast material and had significantly shorter procedures than training hospitals.

Various factors have been suggested [1–11] that may influence the complication rate of catheter cerebral arteriography. These include the number and type of arteries catheterized (carotid, vertebral, aortic arch), amount and type of contrast medium injected, duration of the procedure, and age of the patient. We investigated these factors in reviewing the complication rate in 5,000 catheter cerebral arteriographic procedures.

Materials and Methods

This study is a continuation of our analysis of 5,000 consecutive catheter cerebral arteriograms from two training and two nontraining health centers [12, 13]. All material was extracted from patients' charts and technicians' records and was analyzed by computer for statistical significance. All four hospitals used similar angiographic techniques, with no. 5 French polyethylene catheters for selective arteriography. The volume of contrast medium per injection for a given artery was standard in all four hospitals, and all used mechanical injectors.

The overall complication rate for the 5,000 arteriographic procedures was analyzed for number and type of arteries catheterized, amount and type of contrast material injected, duration of the procedure, and age of the patient. The second part of this three-part series [13] demonstrated that the complication rates of catheter cerebral arteriography varied significantly among six categories of clinical diagnosis. Therefore, the case material for the present study was also divided into these diagnostic groups to assess the complication rate according to the above factors.

Results

Type and Number of Arteries Catheterized

In four of the six diagnostic categories (3,360 cases), data were sufficient for statistical analysis (Table 1). In each of the four categories, including the previously demonstrated higher risk category of subarachnoid hemorrhage, no statistically significant differences were found in complication rates according to the vessel or vessels injected. Although the carotid plus vertebral plus aortic arch group showed a complication rate of 7.1% for subarachnoid hemorrhage, the significance of the difference was not determinable statistically because of the small number of patients.

The total complication rates according to the arteries injected varied from 0.3% (carotid plus vertebral) to 2.5% (carotid plus vertebral plus aortic arch), but the differences were not statistically significant. The overall complication rates in patients with more than one artery injected were not significantly different from those with single vessels injected; in fact, the higher complication rate occurred in the patients with single vesse s injected. The complication rate (0.7%) of all vertebral injections (alone and in combination with the carotid artery) was lower than that of carotid injections alone (1.3%), but the difference was not significant; the complication rate of all aortic arch injections (alone or in combination with the carotid) was the same as that of carotid injections alone.

A supplementary analysis to evaluate whether the total number of arteries catheterized or the total number of catheters employed had any effect on complication rates disclosed no statistically significant finding.

Type and Volume of Contrast Agent

The complication rate associated with the use of sodium meglumine diatrizoate (Renografin-60, Squibb) was compared with that using meglumine iothalamate (Conray-60, Mallinckrodt) in 4,187 catheter cerebral arteriographic procedures in the two nontraining hospitals. The first hospital used only Conray-60, while the other changed from Renografin-60 to Conray-60 midway in the study, providing a unique setting for comparative analysis of the two agents. Case material was analyzed by comparing the total complication rates of the two agents and then by comparing the complication rates of

Received February 7, 1978; accepted after revision August 1, 1978.

[1] Department of Radiology, University of California School of Medicine and Veterans Administration Hospital, San Francisco, California 94121. Address reprint requests to R. L. Eisenberg at Veterans Administration Hospital.

[2] Present address: Department of Radiology, Providence Hospital, 30th and Summit, Oakland, California 94609.

© 1978 American Roentgen Ray Society

0361–803X/78/1100–0871 $00.00

TABLE 1

Percentage Complications According to Number and Type of Arteries Injected

Arteries Injected	Clinical Diagnosis				Total
	Cerebrovascular Occlusive Disease	Tumor	Subarachnoid Hemorrhage	Seizure or Headache	
Single:					
Carotid	2.0(7/347)	0.6(2/338)	1.9(3/160)	0.5(1/193)	1.3(13/1,038)
Vertebral	0(0/15)	0(0/38)	0(0/20)	0(0/9)	0(0/82)
Aortic arch	2.3(1/44)	0(0/3)	0(0/8)	0(0/2)	1.8(1/57)
Total	2.0(8/406)	0.5(2/379)	1.6(3/188)	0.5(1/204)	1.2(14/1,177)
Multiple:					
Carotid and vertebral	0.9(2/213)	0.1(1/683)	0.4(1/232)	0.2(1/644)	0.3(5/1,772)
Carotid and aortic arch	0.3(2/612)	0(0/32)	3.8(1/26)	0(0/29)	0.4(3/699)
Carotid, vertebral, and aortic arch	1.9(3/160)	5.0(1/20)	7.1(1/14)	0(0/18)	2.5(5/212)
Total	0.7(7/985)	0.3(2/735)	1.1(3/272)	0.1(1/691)	0.5(13/2,683)

Note.—Data on 3,860 catheter cerebral arteriograms.

TABLE 2

Complication Rates by Volume of Renografin-60 and Conray-60

Contrast Medium	Complication Rate (%)				
	60 ml	70 ml	80 ml	90 ml	100 ml
Renografin-60:*					
Below volume	0.3(2/742)	0.3(4/1200)	0.5(6/1336)	0.5(8/1497)	0.5(9/1642)
At volume and above	1.2(15/1246)	1.6(13/788)	1.7(11/652)	1.9(9/491)	2.3(8/346)
Significance (*P* value)	<.05	<.01	<.01	<.01	<.01
Conray-60:†					
Below volume	0.9(2/229)	1.0(4/416)	1.0(7/682)	0.8(8/995)	0.8(10/1261)
At volume and above	0.7(13/1970)	0.6(11/1783)	0.5(8/1517)	0.6(7/1204)	0.5(5/938)

Note.—Data on 4,187 catheter cerebral arteriograms.
* Total complication rate = 0.86(17/1,988).
† Total complication rate = 0.69(15/2,199). Differences in complication rates by volume were not significant.

the two agents according to volume of contrast material injected. Numbers were too small to compare complication rates of the two agents according to diagnostic category.

No significant difference was found between the total complication rate using Conray-60 (0.69%) and that using Renografin-60 (0.86%). When analyzed by specific volume, however, Conray-60 demonstrated no increase in complication rate with increasing volumes, but Renografin-60 showed a consistent and significant increase in complication rate as the volume of contrast material was increased (table 2).

Table 3 presents the amount of contrast material administered to patients for catheter cerebral arteriography in the two nontraining and two training centers included in our study. In the nontraining centers, less than 100 ml of contrast agent is used for each procedure in over 70% of patients; in the training centers, more than 140 ml of contrast agent is used for each procedure in over 70% of patients.

Duration of Procedure

For this part of the study, 4,795 patients were analyzed. The overall complication rate was significantly greater ($P < .01$) in patients whose procedures lasted longer than 80 min than in patients having shorter procedures (table 4).

As might be expected, the duration of arteriographic procedures in nontraining centers was significantly shorter than in training centers. The nontraining centers showed a significant increase ($P = .04$) in the complication rate among patients whose procedure lasted more than 90 min compared to patients with shorter examinations. The training center population showed no consistent pattern when complication rates were compared with time distribution.

Age of Patient

This analysis included 4,187 patients. Overall, there was a significant and consistent increase in complication rates when patients were above the age of 40 ($P < .01$, table 5). Numbers of patients were too small to statistically assess complication rates by age in the six clinical diagnostic categories previously described [12, 13]. Nevertheless, patients over 60 years old showed a complication rate 2.5 times greater than those under 60 for cerebrovascular occlusive disease, three times greater for tumor, and 16 times greater for seizure or headache.

Discussion

Some authors [1, 4] have suggested that injection of contrast material into the vertebral artery is associated

TABLE 3

Volume of Contrast Material in Training and Nontraining Centers

Volume (ml)	Percentage of Procedures	
	Nontraining Hospitals	Training Hospitals
Less than 100	75	22
100–139	20	7
140 or more	5	71

Note.—Data on 4,187 catheter cerebral arteriograms at nontraining hospitals and 813 at training hospitals.

TABLE 4

Complication Rates According to Duration of Procedure

Procedure Time (min)	Complication Rate (%)		Significance (*P* value)
	Below Time	At Time and Above	
60	1.2(33/2,725)	1.6(34/2,070)	NS
70	1.2(38/3,197)	1.8(29/1,598)	NS
80	1.1(42/3,780)	2.5(25/1,015)	< .01
90	1.2(50/4,136)	2.6(17/659)	< .01

Note.—Data on 4,795 catheter cerebral arteriograms. NS = not significant.

TABLE 5

Complication Rates According to Age of Patient

Age (yr)	Complication Rate (%)		Significance (*P* value)
	Below Age	At Age and Above	
30	0.2(1/660)	0.9(31/3,527)	NS
40	0.1(1/1,082)	1.0(31/3,105)	< .01
50	0.4(7/1,806)	1.0(25/2,381)	< .05
60	0.5(13/2,786)	1.4(19/1,401)	< .02

Note.—Data on 4,187 catheter cerebral arteriograms. NS = not significant.

with a neurologic complication rate higher than that for a carotid injection alone. Wishart [4] found a higher percentage of neurologic complications in patients with combined vertebral and carotid artery injections than in patients with carotid injections alone. However, he could find no difference in the combined neurologic and systemic complication rates (11%) between these two groups. Our study showed no statistically significant difference in neurologic or systemic complication rates in patients who had vertebral injections or aortic arch injections (alone or in combination with carotid) and carotid injections alone.

We found lower rates of complication for single vertebral or aortic arch injections than have been previously reported [2, 3]. Lang [3] described an 11.5% rate of convulsion with injections of the aortic arch; our overall complication rate for aortic arch injections alone or in combination with carotid was only 1.3%. Silverman and co-workers [2] reported a 5% rate of cortical blindness in percutaneous vertebral injections. The overall incidence of cortical blindness as a complication of vertebral arteriography in our study was 0.3% and is totally a reflection of the complications occurring in the training hospitals (eight of 286) rather than the nontraining hospitals (zero of 2,056). This latter finding suggests that the complication of cortical blindness may be related to operator proficiency rather than an inherent risk of vertebral artery injection.

Our results point out the importance of comparing specific volumes of a contrast medium. Although the total complication rates for both Renografin-60 and Conray-60 were not statistically different, analysis according to specific volume demonstrated a clear and consistent increase in complication rate as the volume of Renografin-60 was increased; complication rates of Conray-60 were not affected by volume changes. These data may reflect the greater toxicity of sodium compounds compared to nonsodium compounds. Fischer [5] reported that meglumine salts are better tolerated than the sodium compounds when using the same testing techniques, and he recommends pure meglumine agents for cerebral angiography. Because Renografin-60 was found to be more toxic than Conray-60 at higher volumes, Conray-60 would seem to be the contrast agent of choice for cerebral arteriography—especially in the training hospitals, which generally administer greater volumes of contrast material.

Although a cooperative study on coronary arteriography [6] concluded that the increased duration of a procedure is associated with an increased risk to the patient, Wishart [4] found no significant difference in complication rate with respect to procedure time. The cooperative study included both training and nontraining centers and analyzed a large number of cases (46,904); Wishart [4] reported only on a training institution. Both results agree with our findings (i.e., no consistent pattern in the training centers and a significant increase in complication rate when the training and nontraining centers were combined and the numbers were large). Our study strongly suggests that the complication rate increases when the arteriographic procedure exceeds 80 min.

Some investigators [7–9] have suggested that the complication rates for catheter cerebral arteriography increase significantly in patients over 60 years of age; others [1, 4, 10] have shown no relation between age and complication rates. Although our study disclosed a definitely higher complication rate for patients over the age of 40 years, this higher rate does not increase directly with advancing age; it appears to be relatively constant. Complications are unusual in young patients [9, 11]. In Pribram's series [11], no complications occurred in his seven patients under 30; Patterson et al. [9] reported no permanent complications in 86 patients under the age of 50 years. Our results were similar; only one complication occurred in 1,082 patients under the age of 40 years.

REFERENCES

1. Takahashi M, Kawanani H: Complications of catheter cerebral angiography: an analysis of 500 examinations. *Acta Radiol* 13, part 1:248–258, 1972
2. Silverman SM, Bergman PS, Bender MB: The dynamics of

transient cerebral blindness: report of nine episodes following vertebral angiography. *Arch Neurol* 4:333–348, 1961
3. Lang EK: A survey of complications of percutaneous retrograde arteriography: Seldinger technique. *Am J Roentgenol* 81:257–263, 1963
4. Wishart DL: Complications in vertebral angiography as compared to non-vertebral cerebral angiography in 447 studies. *Am J Roentgenol* 113:527–537, 1971
5. Fischer HW: Contrast media, in *Radiology of the Skull and Brain*, edited by Newton TH, Potts DG, St. Louis, Mosby, 1974, pp 893–907
6. Adams DF, Fraser DB, Abrams HL: The complications of coronary arteriography. *Circulation* 48:609–617, 1973
7. Gibson RD: Complications of cerebral angiography—catheter technique. *Australas Radiol* 15:117–122, 1971
8. McDowell FH, Schick RW, Frederick W, Dunbar HS: An arteriographic study of cerebrovascular disease. *Arch Neurol* 1:435–441, 1959
9. Patterson RH, Goodell H, Dunning HS: Complications of carotid arteriography. *Arch Neurol* 10:513–520, 1964
10. Coddon DR, Krieger HP: Circumstances surrounding complications of cerebral angiography: analysis of 546 consecutive cerebral angiograms. *Am J Med* 25:580–589, 1958
11. Pribram HFW: Complications of angiography in cerebrovascular disease. *Radiology* 85: 33-37, 1965
12. Mani RL, Eisenberg RL, McDonald EJ Jr, Pollock JA, Mani JR: Complications of catheter cerebral arteriography: analysis of 5,000 procedures. I. Criteria and incidence. *Am J Roentgenol* 131:861–865, 1978
13. Mani RL, Eisenberg RL: Complications of catheter cerebral arteriography: analysis of 5,000 procedures. II. Relation of complication rates to clinical and arteriographic diagnoses. *Am J Roentgenol* 131:867–869, 1978

Coronal Computed Tomography: Indications and Accuracy

STUART MASS,[1, 2] DAVID NORMAN,[1] AND THOMAS H. NEWTON[1]

The application of wide aperture scanners to neuroradiology permits improved anatomic definition and localization of intracranial and intraorbital lesions. Coronal scans are most useful in demonstrating lesions of the skull base and apex, distinguishing between infra- and supratentorial lesions, and in determining if a lesion is intra- or extraaxial. Limitations of coronal scans include discomfort in positioning, high spatial frequency artifacts, and additional radiation exposure.

Computed tomography of the brain has been routinely performed in the axial projection with variations in head angulation from −5° to +25° to the canthomeatal line. Large aperture scanners permit placement of the patient in a position suitable for direct coronal scanning, not possible on the earlier small aperture machines [1, 2]. With increased use of this technique, we have observed a number of situations in which the coronal view provides additional and sometimes invaluable information. The relative indications for and limitations of CT scanning of the head in the coronal plane are described.

Technique

All of the available large aperture scanners are suitable for coronal scans. Units which have a gantry that tilts provide more flexibility and are adaptable to a larger patient population. The patient may be placed in the supine position with the neck hyperextended and with a support beneath the shoulders. Some patients find that the prone position with the neck hyperextended is more comfortable. The canthus of the eye or the external auditory meatus are usually used as positioning reference points. Care should be exercised in older patients with a limited range of motion and when hyperextension may impair blood flow to the posterior fossa. Gantry tilt will compensate for a limited range of motion of the neck. In most instances, the plane of section deviates 10°–25° from the plane perpendicular to the canthomeatal line.

Indications

One of the generally accepted principles of geometric tomography is that the plane of section should be perpendicular to the plane of the object [3]. This principle can also be applied to computed tomography. When axial scans are performed tangential to areas of nonhomogenous tissue, such as the skull base, vertex, or adjacent to the ventricles, density averaging may yield inaccurate information. Precise separation of anatomic compartments of similar density, such as infra- and supratentorial structures, may not be possible in the axial plane. In addition, high spatial frequency artifacts, occasionally seen in relation to the petrous bone and frontal sinuses, may be avoided by use of coronal sections. The indications for coronal CT evolve from these basic principles.

Localization of Lesions

Axial CT may detect a lesion, but accurate localization may be difficult. Differentiation between intra-and extraaxial lesions, intra- and extraventricular lesions, and infra- and supratentorial lesions is essential. It is also important to provide the neurosurgeon with all possible information relating a particular lesion to surrounding structures.

Intra- versus extraaxial lesion (case 1). A 61-year-old Mexican American presented with right-sided spasticity and left third nerve palsy of gradual onset. A postcontrast axial CT scan demonstrated a ringlike structure which appeared to involve the suprasellar cistern, hypothalamus, and thalamus (fig. 1*A*). On the basis of the axial studies, it was not possible to determine whether the lesion was intra- or extraaxial. Angiography and pneumoencephalography provided no additional information. The intraaxial location of the lesion which spared the suprasellar cistern was easily demonstrated on coronal CT (fig. 1*B*).

Intra- versus extraventricular lesion (case 2). A 13-year-old girl had symptoms suggestive of a malfunctioning Torkildsen shunt which had been placed for the treatment of aqueductal stenosis. Axial CT demonstrated large ventricles with a shunt tube extending into the right lateral ventricle and the tip apparently within the ventricular cavity (fig. 2*A*). On coronal CT, the tip of the shunt tube was seen to be extraventricular (fig. 2*B*).

Infra- versus supratentorial lesion (case 3). A 31-year-old woman had a history of ataxia, weakness, and syncopal episodes. The axial CT scan demonstrated a lesion along the edge

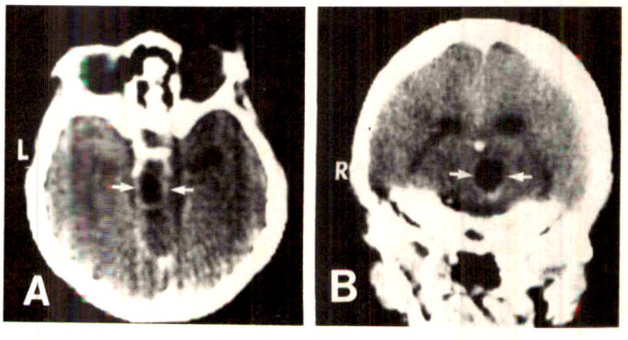

Fig. 1.—Case 1. Axial (*A*) and coronal (*B*) postcontrast scans of cysticercosis cyst. Coronal scan establishes intraaxial location of lesion (*arrows*).

Received May 25, 1978; accepted July 28, 1978.
Presented at the annual meeting of the American Society of Neuroradiology, Hamilton, Bermuda, March 1978.
[1] Department of Radiology, University of California, San Francisco, California 94143. Address reprint requests to D. Norman.
[2] Present address: Department of Radiology, Good Samaritan Hospital, San Jose, California 95124.

© 1978 American Roentgen Ray Society

0361–803X/78/1100–0875 $00.00

of the tentorium at the level of the quadrigeminal cistern (figs. 3*A* and 3*B*). The intense enhancement and smooth margination suggested a supratentorial meningioma. On coronal scans, the lesion was seen to extend both above and below the edges of the tentorium (figs. 3*C* and 3*D*). In this case, the coronal scan appropriately sectioned the tentorium perpendicular to its anatomic plane.

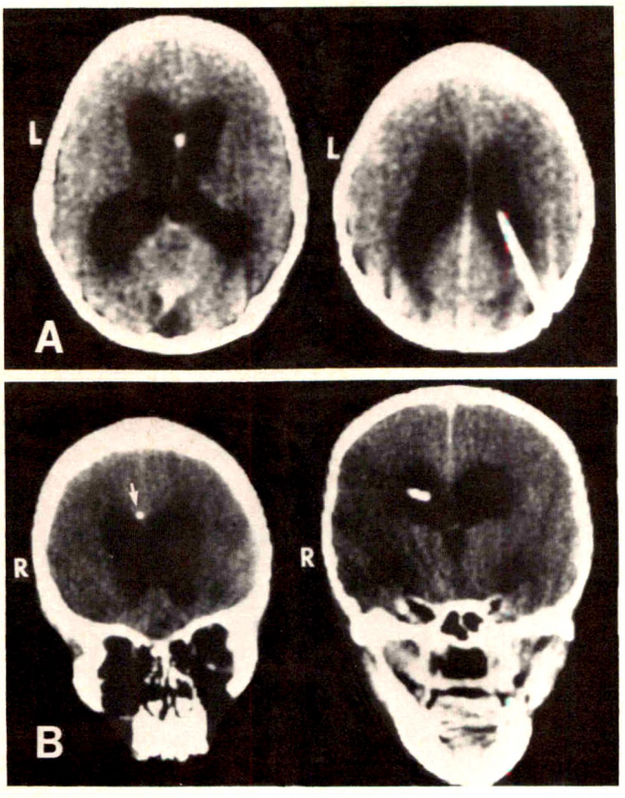

Fig. 2.—Case 2. Axial (*A*) and coronal (*B*) precontrast scans of Torkildsen shunt. Extension of shunt tip beyond confines of ventricle can be seen only on coronal sections (*arrow*).

Lesions Adjacent to Skull Base and Vertex

The supra- and parasellar regions are difficult to evaluate on axial CT scans due to density averaging with the bony calvarium and high spatial frequency artifacts. Scanning in the coronal plane minimizes most density averaging in the suprasellar region. High spatial frequency artifact is not always eliminated in the coronal plane.

Lesion adjacent to skull base (case 4). A 19-year-old man presented with a right fifth sensory and a right sixth cranial nerve palsy. The axial CT scans suggested a subtle area of increased attenuation adjacent to the sphenoid sinus on the right (figs. 4*A* and 4*B*). At the level of the sphenoid sinus on the coronal scans, a definite area of contrast enhancement abutting the right lateral wall of the sphenoid sinus was demonstrated (figs. 4*C* and 4*D*). A fifth nerve neurinoma was removed at surgery.

Lesion adjacent to skull base (case 5). A 39-year-old woman had a history of visual impairment. On the axial postcontrast scan, a round area of decreased attenuation (0–14) in the suprasellar region was demonstrated (fig. 5*A*). The differential diagnosis included a subarachnoid cyst, an epidermoid, or a cysticercosis cyst. The coronal scan (fig. 5*B*) demonstrated that the lesion imposed itself on the anterior recess of the third ventricle and was lobulated, thus favoring a diagnosis of epidermoid tumor, rather than a smoothly marginated subarachnoid cyst or cysticercosis. At surgery an epidermoid tumor was removed.

Lesion arising from calvarium or dura (case 6). A 9-day-old male infant had an intraventricular hemorrhage at 5 days of age. Axial scans demonstrated a hematoma within the lateral, third, and fourth ventricles. High convexity scans were normal (figs. 6*A* and 6*B*). A coronal scan demonstrated an area of increased density in the region of the superior sagittal sinus, indicating superior sagittal sinus thrombosis (fig. 6*C*). This diagnosis was not possible without the use of the coronal scan.

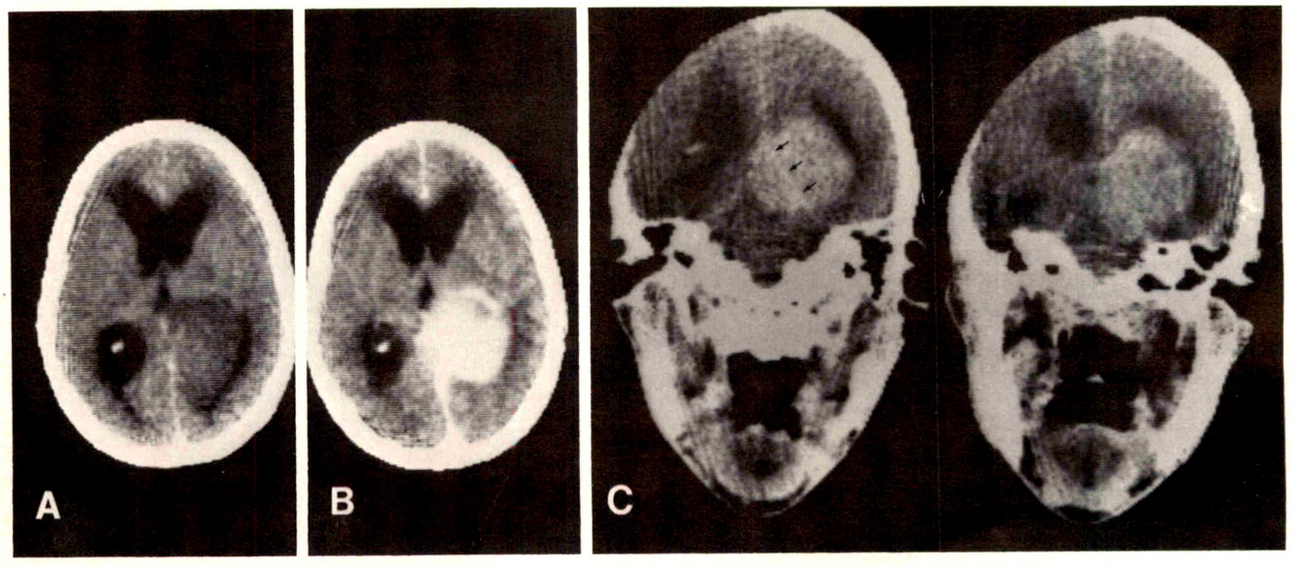

Fig. 3.—Case 3. Axial precontrast (*A*), postcontrast (*B*), and coronal postcontrast (*C*) scans of tentorial meningioma. Involvement of quadrigeminal cistern on axial scans suggests extension of lesion through incisura. Coronal scans demonstrate that lesion extends both above and below tentorium (*arrows*).

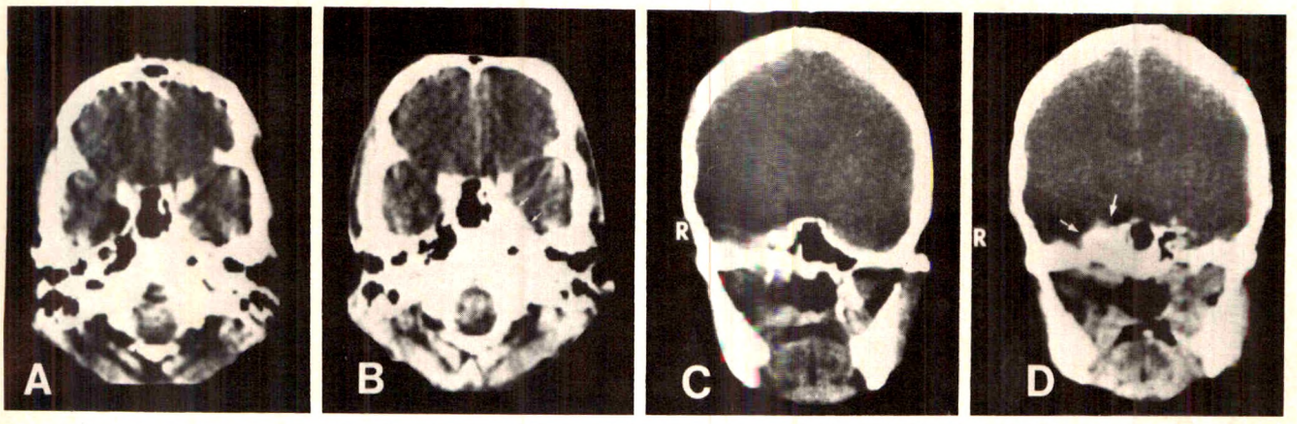

Fig. 4.—Case 4. Axial precontrast (*A*) and postcontrast (*B*) scans showing subtle area of contrast enhancement in medial aspect of right temporal lobe (*arrow*). Coronal precontrast (*C*) and postcontrast (*D*) scans more clearly showing lesion (*arrows*). (Courtesy of Dr. Richard Kramer, Palo Alto Clinic).

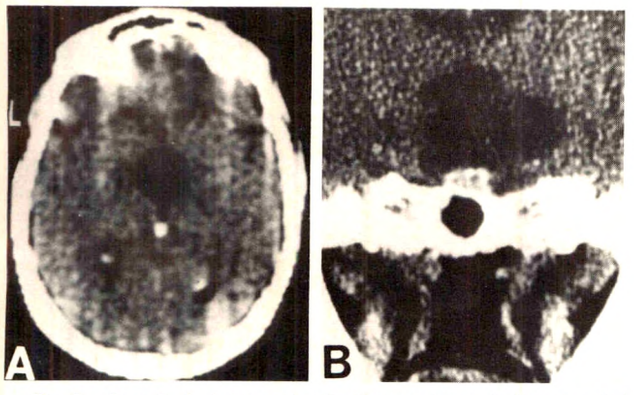

Fig. 5.—Case 5. *A*, Axial postcontrast scan demonstrating rounded low density lesion in region of suprasellar cistern and hypothalamus. *B*, Coronal scan showing definite involvement of suprasellar cistern. Lobulated margins of lesion suggest histologic diagnosis of epidermoid.

Congenital Anomalies

Proper evaluation of congenital anomalies requires a firm understanding of the relation between malformed anatomic structures. Judgments regarding the most effective treatment and/or genetic counseling can then be made. Coronal scans often provide additional anatomic information and are useful in delineating the relationship of cerebrospinal fluid spaces to the ventricular system [4, 5].

Agenesis of corpus callosum (case 7). A 7½-year-old boy presented with mental retardation and ataxia. The axial CT scans revealed an abnormally wide separation of the ventricles (fig. 7*A*). The coronal scan more clearly demonstrated the separation of the lateral ventricles and the high-riding third ventricle (fig. 7*B*).

Subarachnoid cyst (case 8). A 10-year-old girl presented with headaches and ataxia. The axial CT scan (fig. 8*A*) revealed a large posterior fossa cyst. The superior extent of the cyst, the degree of supratentorial extension, and the relation of the cyst to the lateral ventricles was not clear. The coronal scans (fig. 8*B*) demonstrated extension of the cyst through the tentorial incisura and insinuation of the cyst beneath the bodies of the lateral ventricles, with superior displacement of the lateral ventricles.

Orbital Lesions

The optic nerve and muscles of the globe lie in the axial plane. In accordance with the principle of sectioning perpendicular to the plane of the object of interest, these structures can be more easily discriminated and pathologic involvement better delineated in the coronal projection. This also avoids density averaging of these rather small soft tissue structures with adjacent bone [6, 7].

Case 9. A 14-year-old boy had a 1 year history of headaches and scotomata in the left eye. Plain films revealed an osteoma involving the superior medial aspect of the left orbit and the left ethmoid sinuses. Axial CT scans clearly defined the relationship of the lesion to the globe and the optic nerve (fig. 9*A*). Superior extent of the lesion could not be well defined because of averaging with the orbital roof. The coronal scan clearly demonstrated that the lesion did not invade the floor of the anterior fossa (fig. 9*B*).

Limitations of Coronal Scans

Positioning required for coronal scanning may be uncomfortable. High spatial frequency artifacts created by abrupt changes in density may result when the x-ray beam passes through metallic fillings in the patient's teeth or through air in the paranasal sinuses (fig. 10). Although coronal scans may result in additional x-ray dosage to the patient, the additional information provided by a coronal scan often warrants this additional exposure.

Discussion

An alternative approach to direct coronal scans is the computer transformation of axial images. These offer the advantage of simple and comfortable patient positioning. Axial and coronal sections can be obtained in one examination. Data manipulation is flexible, allowing sagittal sections to be obtained. In certain areas, such as the sella, high spatial frequency artifacts associated with teeth or sinus air, as seen in the coronal scans, may be eliminated or reduced. Although attractive in many aspects, the transformed image has some limitations. It requires that thinner sections in the range of 3–5 mm be

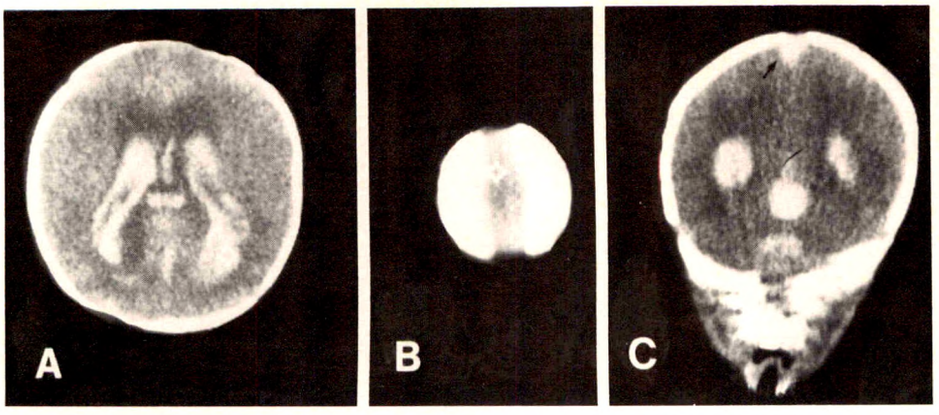

Fig. 6.—Case 6. *A*, Precontrast axial scan showing blood within third and lateral ventricles as well as cisterns. *B*, High convexity scan showing no abnormalities. *C*, Coronal scan confirming presence of blood in lateral, third, and fourth ventricles. High density in region of superior sagittal sinus (*arrow*) indicates superior sagittal sinus thrombosis. (Courtesy of Dr. Robert Scheibel, Sonoma County Community Hospital, Santa Rosa, Calif.)

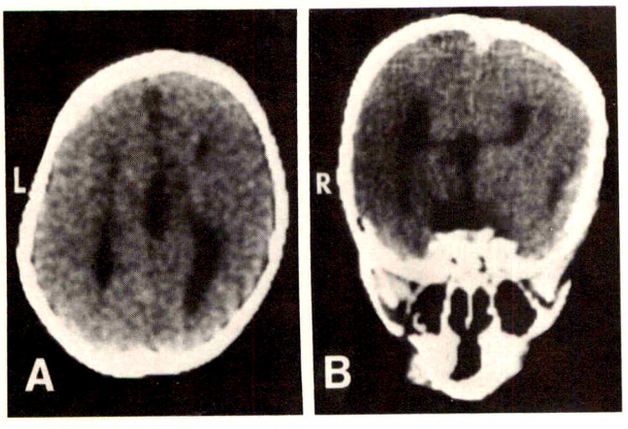

Fig. 7.—Case 7. Precontrast axial (*A*) and coronal (*B*) studies showing separation of lateral ventricles.

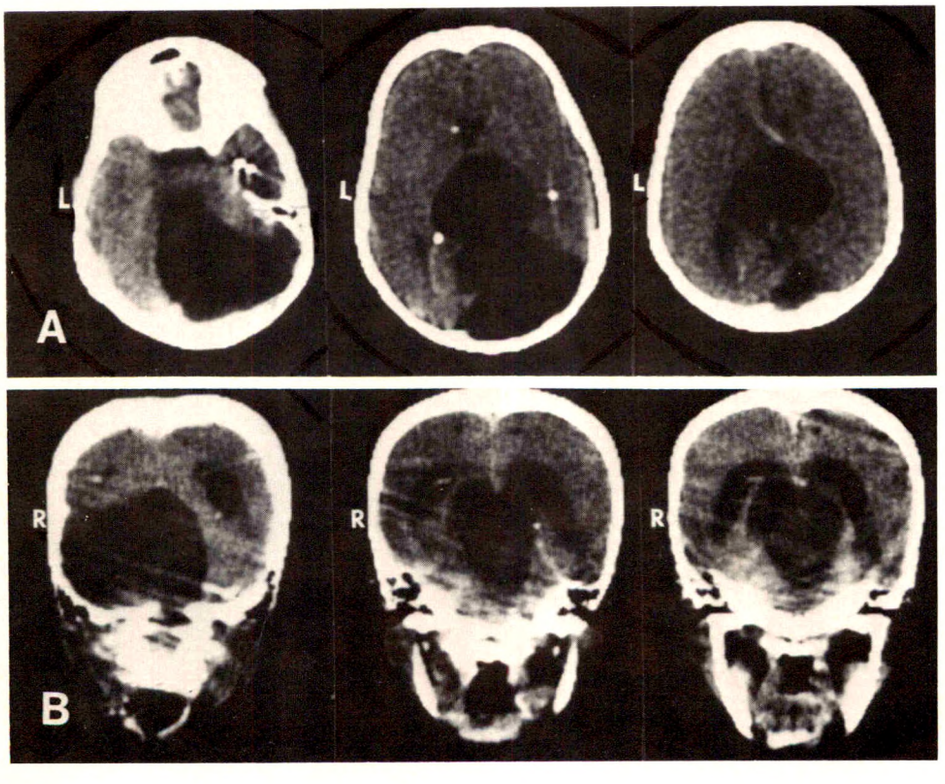

Fig. 8.—Case 8. Axial precontrast (*A*) and coronal (*B*) scans of posterior fossa subarachnoid cyst. Coronal scans better demonstrate relation of cyst to incisura and lateral ventricles.

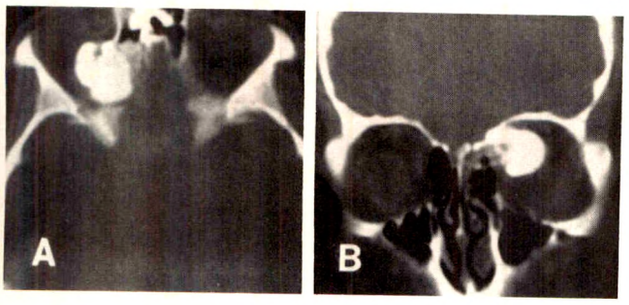

Fig. 9.—Case 9. *A*, Axial scan demonstrating left orbital osteoma involving superior medial aspect of left orbit and displacing globe anteriorly and optic nerve laterally. Relationship of osteoma to floor of anterior fossa is not adequately demonstrated. *B*, Coronal scan clearly demonstrating that lesion is limited to ethmoid sinus and orbit. Anterior fossa and adjacent brain are spared.

Fig. 10.—Case 10. Coronal scan with high spatial frequency artifact secondary to metallic tooth fillings.

performed for maximum clarity and resolution of reconstructed images. This in turn requires increased scanning and processing time. Since most routine studies are not performed with 3–5 mm slices, the need for a transformed image must be anticipated to insure proper sectioning. As this facility becomes more readily available in clinical practice, both methods may become competitive and may also develop their own areas of relative specific indication.

REFERENCES

1. Wolf BS, Nakagawa H, Staulcap PH: Feasibility of coronal views in computed scanning of the head. *Radiology* 120:217–218, 1976
2. Hammerschlag SB, Wolpert SM, Carter BL: Computed coronal tomography. *Radiology* 120:219–220, 1976
3. Littleton JT: *Tomography: Physical Principles and Clinical Applications*. Baltimore, Williams & Wilkins, 1976
4. Byrd SE, Harwood-Nash D, Barry JF, Fitz CR, Boldt DW: Coronal computed tomography of the skull and brain in infants and children. I. Techniques and results. *Radiology* 124:705–709, 1977
5. Byrd SE, Harwood-Nash D, Barry JF, Fitz C, Boldt DW: Coronal computed tomography of the skull and brain in infants and children. II. Clinical value. *Radiology* 124:710–714, 1977
6. Takahashi M, Tamakawa Y: Coronal computed tomography in orbital disease. *J Comput Assist Tomogr* 1:505–509, 1977
7. Tadmor R, New, FJ: Computed tomography of the orbit with special emphasis on coronal sections. *J Comput Tomogr* 2:24–34, 1978

CT Contrast Enhancement in Cerebral Infarction

GEORGE A. NORTON,[1] PULLA R. S. KISHORE,[2] AND JAMES LIN[3]

Computed tomography was used to study 100 patients with ischemic cerebral infarcts. All cases were documented by autopsy, radionuclide imaging, cerebral angiography, or clinical course. Vascular distribution of infarcts was varied and included infarcts of cerebral hemispheres, basal ganglia, and cerebellum. Distinct patterns of enhancement are seen following administration of intravenous contrast material: predominantly peripheral, central, homogeneous, or heterogeneous. Enhancement of the infarcted area usually occurs 1–4 weeks after the onset of clinical symptoms, but was seen as early as the first day or as late as several months after the onset of symptoms. Infarcts showing contrast enhancement may or may not revert to a nonenhanced pattern on follow-up examination for several months. Lesions demonstrating contrast enhancement in cerebrovascular disease may at times be indistinguishable from tumor. Contrast enhancement was the only manifestation of infarction in some instances, and an infarcted area may be completely missed if a postcontrast examination is not performed.

The value of contrast enhancement in assessing brain infarction by computed tomography has become increasingly important. It is now recognized that the appearance of an infarct on CT may be significantly altered by contrast infusion often simulating other pathologic entities. Occasionally, contrast medium may obscure the infarcted site altogether.

Subjects and Methods

One hundred patients with predominantly ischemic brain infarcts were studied using an EMI computed tomographic head unit with 160 × 160 matrix. Except for five patients who were studied with contrast enhancement only, all were examined both with and without intravenous contrast infusion (double scanned). Contrast material was administered at a dose of 2 ml of 30% meglumine diatrizoate per 0.45 kg in the pediatric group. In the adult group 150 ml was infused prior to scanning and an additional 150 ml was infused while performing the second scan. No delayed scans were performed after contrast infusion. Age range was 6 weeks to 87 years (mean, 53 years). Charts were reviewed in all cases. Infarction was documented by autopsy, biopsy, arteriography, radionuclide imaging, or persuasive clinical course.

Results

In this series of 100 randomly chosen cases of ischemic infarction, enhancement of the infarcted area was encountered in 31 patients. Enhancement was seen as early as the first day after onset of clinical symptoms or as late as 9 months after the percipitating event. Mean time of enhancement in this series was 19.7 days; median time was 14 days.

In four cases (13% of the 31 patients), no characteristic decreased density was noted on the precontrast scan; however, after contrast infusion a definite enhancement of the infarcted area was demonstrated (fig. 1). The time intervals between the onset of clinical symptoms and the CT study were 2, 11, 14, and 27 days. The 27 day CT scan of the fourth patient was followed by a 62 day postinfarction scan which demonstrated a characteristic lucency on the precontrast study and persistent enhancement of the infarcted area on the postcontrast CT. All these infarcts were supratentorial, involving the cerebral hemispheres, and demonstrated a homogeneous pattern of contrast enhancement.

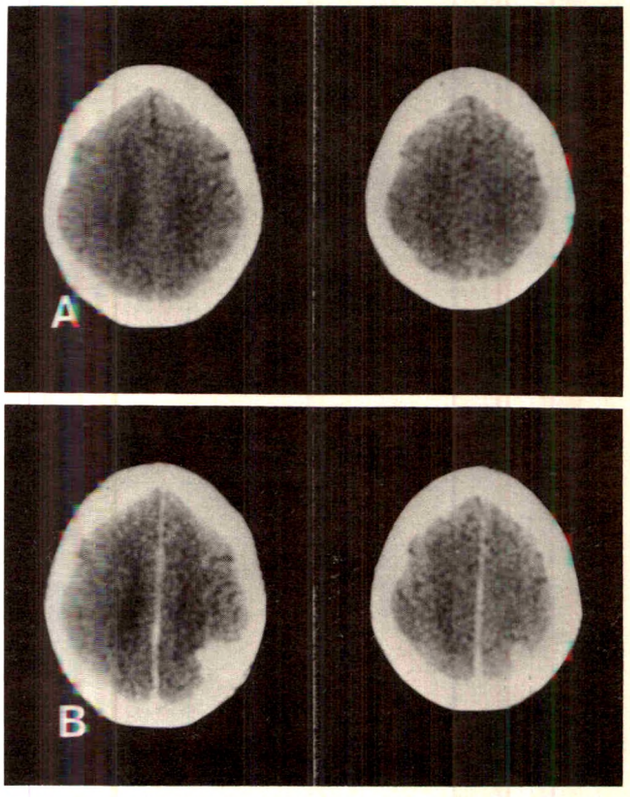

Fig. 1.—77-year-old male 2 weeks after onset of blurred vision. *A*, Precontrast scans showing no lucency in right parietal region. *B*, Postcontrast scans showing right parietal enhancement.

Received August 2, 1977; accepted after revision July 24, 1978.

[1]Department of Diagnostic Radiology, Section of Neuroradiology, University of Kansas Medical Center, Kansas City, Kansas 66103. Present address: Department of Diagnostic Radiology, Duke University Medical Center, Durham, North Carolina 27710.

[2] Department of Diagnostic Radiology, Section of Neuroradiology, University of Kansas Medical Center, Kansas City, Kansas 66103. Present address: Department of Radiology, Medical College of Virginia, Box 728, Richmond, Virginia 23298. Address reprint requests to P. R. S. Kishore.

[3]Department of Neurology, University of Kansas Medical Center, Kansas City, Kansas 66103.

© 1978 American Roentgen Ray Society

0361–803X/78/1100–0881 $00.00

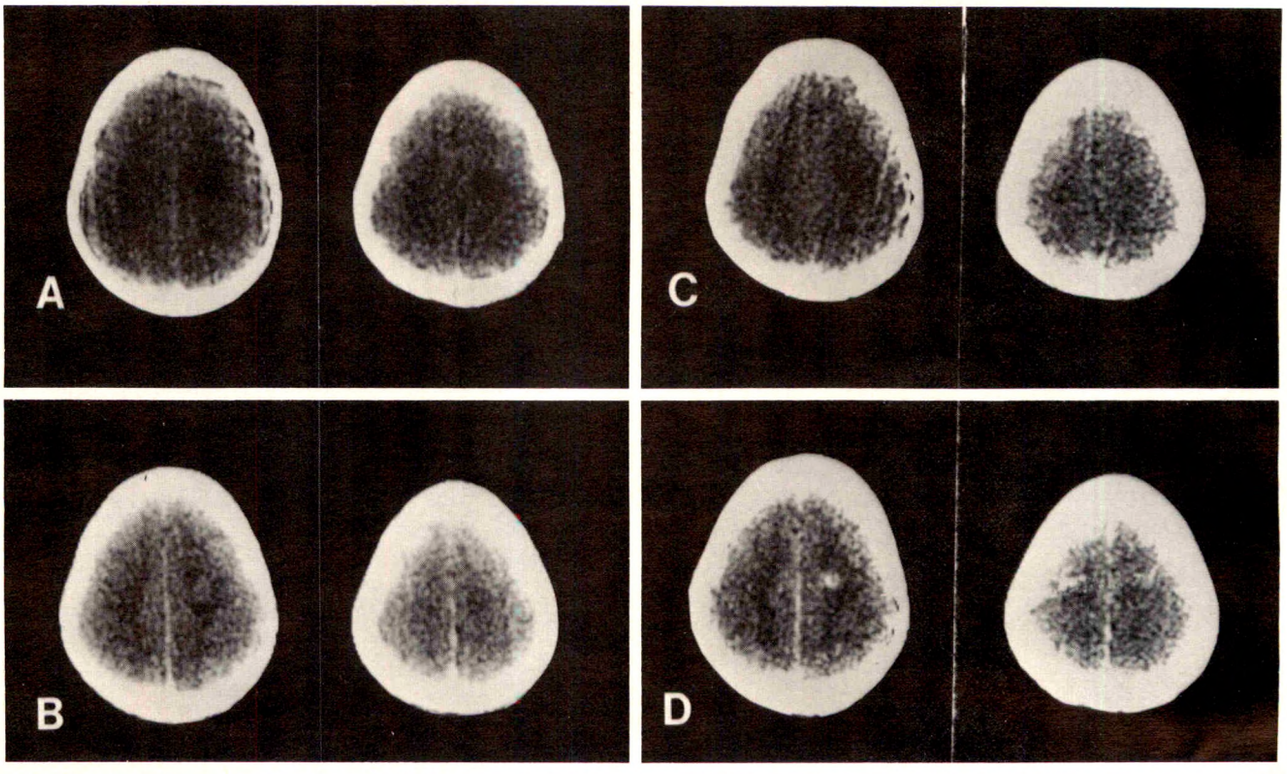

Fig. 2.—16-year-old female *A and B*, 20 days after onset of left side weakness. *A*, Precontrast scans showing right parietal lucency. *B*, Postcontrast scans showing lesion obscured. *C and D*, 12 days earlier. Pre(*C*) and postcontrast (*D*) scans demonstrating significant postcontrast enhancement.

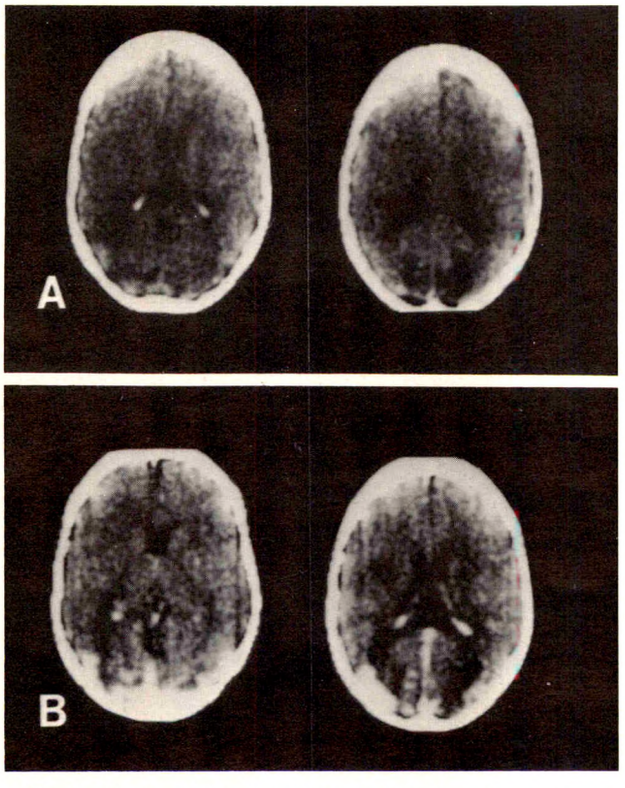

Fig. 3.—49-year-old female with cortical blindness for 17 days. *A*, Precontrast scans showing bilateral occipital lucencies. *B*, Postcontrast scans demonstrating enhancement of lesions.

The remaining 27 patients demonstrated a characteristic lucency involving the infarcted area on the precontrast scan. In one case, characteristic lucency was noted on the precontrast CT; however, the appearance of the infarct was somewhat obscured after the contrast infusion, since the density in this region closely approached that of surrounding normal brain (fig. 2). These cases demonstrate the need for both pre- and postcontrast scanning in suspected ischemic infarction.

Five distinct patterns of contrast enhancement were encountered, designated by their appearance: homogeneous, heterogeneous, central, peripheral, and perihematoma enhancement (figs. 1, 3–6). Contrast enhancement surrounding a cerebral hematoma has been described previously and is presented here only as an additional pattern of contrast enhancement [1, 2].

Including the cases that demonstrated contrast enhancement of the infarcted area on follow-up CT examination, 41 cases showed enhancement. The degree of contrast enhancement was graded as minimal, mild, moderate, or marked. Nine cases demonstrated minimal enhancement of the lesion, 12 showed mild enhancement, 11 were moderately enhanced, and nine were markedly enhanced on the postcontrast CT. From the time of the onset of ictus, 17% of these enhanced scans occurred within 1 week; 29% in 1–2 weeks; 15%, 2–3 weeks; 12%, 3 weeks to 1 month; 12%, 1–2 months; and 15%, later than 2 months. The pattern of enhancement was homogeneous in 22%, heterogeneous in 59%, central in 10%, peripheral in 7%, and surrounding a cerebral

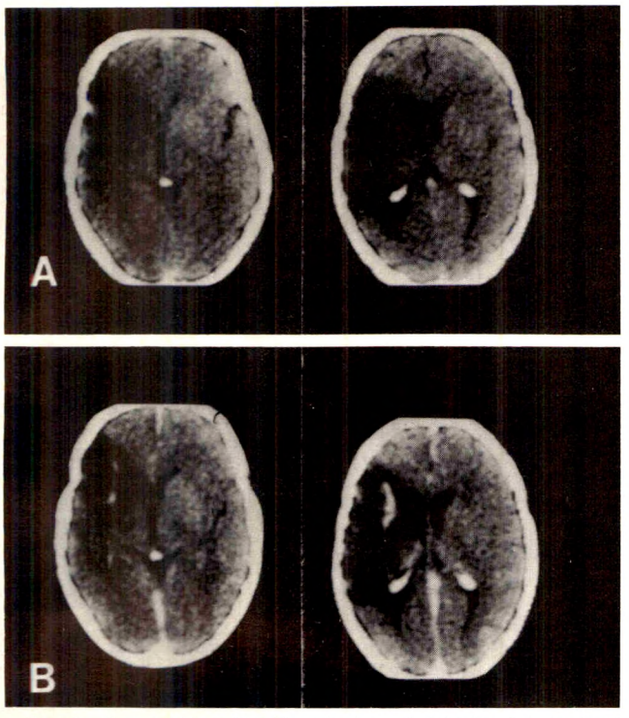

Fig. 4.—46-year-old male with aphasia and right hemiplegia for 9 months. *A*, Precontrast scans demonstrating left frontal, parietal, and temporal lucencies. *B*, Postcontrast scans showing central contrast enhancement in lucent area.

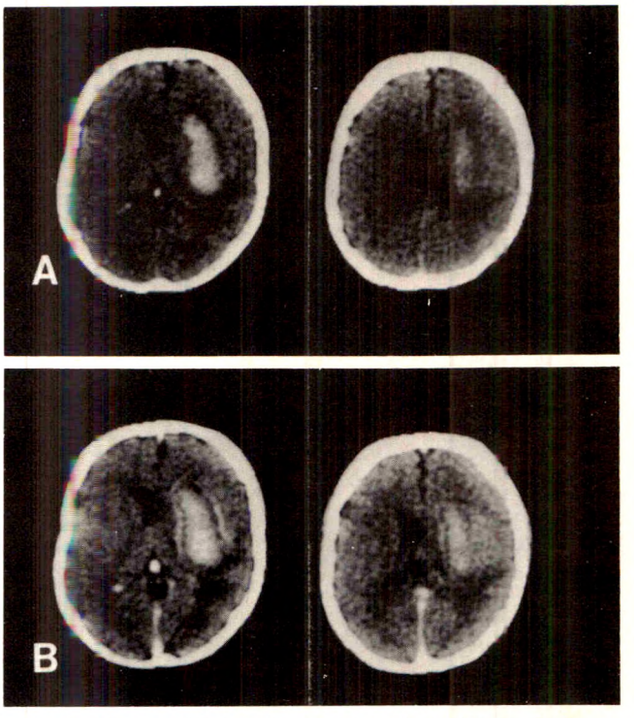

Fig. 6.—58-year-old male with left hemiparesis for 18 days. *A*, Precontrast scans showing right basal ganglia hematoma. *B*, Postcontrast scans showing peripheral enhancement around hematoma.

hematoma in 2%. Correlation of the time of onset of contrast enhancement, degree of enhancement, and pattern of enhancement is shown in table 1.

Of the 22 patients who had more than one CT examination, 12 demonstrated enhancement of the infarcted area following contrast infusion on at least one CT examination. Six patients (55%) reverted from an enhanced to a nonenhanced CT appearance within 3–12 weeks after the initial scan. Eight patients showed a persistent appearance of contrast enhancement from 1 week to 9 months after the initial CT. None of the follow-up examinations demonstrated an increase in the degree of enhancement, while 82% eventually demonstrated no enhancement or less contrast enhancement than on a previous scan. One patient demonstrated a change in pattern from heterogeneous to a central pattern 2 months after the infarct, while another patient changed from homogeneous to heterogeneous 2 months after the infarct. One case showed contrast enhancement 8 days after infarction following a negative study 1 day after the onset of symptoms. This scan demonstrated a homogeneous pattern and subsequently reverted to a nonenhancing study (table 2).

A total of 36 patients had radionuclide brain imaging. In two patients brain scans were done at the referring hospital, and the dates of these scans were not available. The age of infarct at the time of CT and radionuclide scanning in the remaining 34 cases is shown in table 3. Of the 34 cases, 19 showed enhancement of the infarcted area on postcontrast CT scans. In 13 cases a good

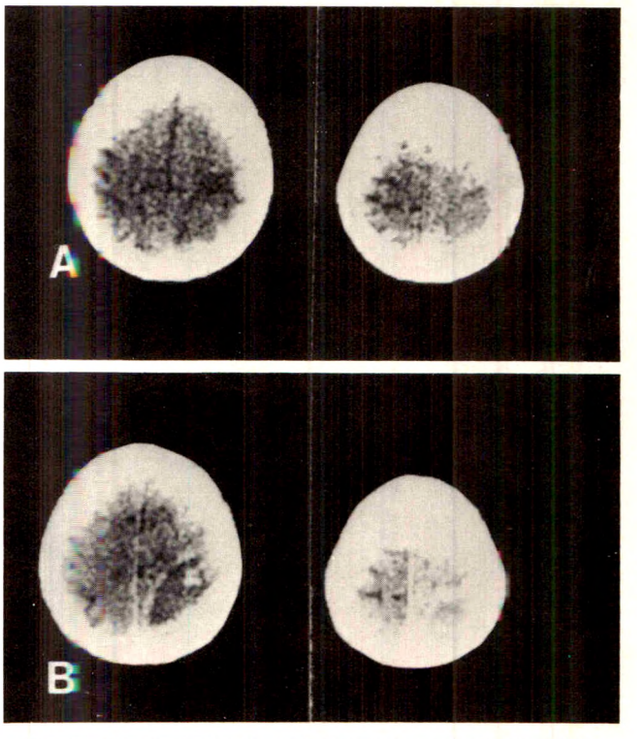

Fig. 5.—76-year-old female with left hemiparesis for 3 months. *A*, Precontrast scans showing lucent lesion in right parietal region. *B*, Postcontrast scans showing peripheral enhancement and small central enhancement in same lesion.

correlation was demonstrated between contrast enhancement on CT examination and a positive radionuclide study. No correlation was noted between the radionuclide uptake and the degree and pattern of contrast enhancement on CT. In the other six cases with contrast enhancement, however, both dynamic and static radionuclide images were negative. In these six cases radionuclide scanning was performed within 6 days of CT; in three of these cases, it was done within 48 hr of CT. In the remaining 15 cases CT revealed no enhancement and the radionuclide study was positive. The time intervals between the two methods are indicated in table 3. In four cases the time intervals were 10, 15, 25, and 45 days between radionuclide scanning and CT. In the remaining 11 cases, the studies were performed within 3 days of each other in 10 and 4 days in one.

TABLE 1

Age of Infarct Correlated with Degree and Pattern of Contrast Enhancement

Age of Infarct (days)	Contrast Enhancement		No. Patients
	Degree	Pattern	
Under 2	Moderate	Homogeneous	1
	Minimal	Heterogeneous	2
	Moderate	Heterogeneous	1
3–4	Minimal	Heterogeneous	1
	Minimal	Peripheral	1
5–7	Minimal	Heterogeneous	1
8–10	Mild	Homogeneous	2
	Mild	Heterogeneous	2
11–14	Moderate	Homogeneous	2
	Marked	Homogeneous	1
	Minimal	Heterogeneous	1
	Mild	Heterogeneous	1
	Marked	Heterogeneous	3
15–21	Minimal	Homogeneous	1
	Mild	Homogeneous	1
	Moderate	Heterogeneous	2
	Marked	Heterogeneous	1
	Moderate	Perihematoma	1
22–30	Marked	Homogeneous	1
	Moderate	Heterogeneous	2
	Marked	Heterogeneous	1
	Marked	Central	1
31–60	Minimal	Heterogeneous	1
	Mild	Heterogeneous	3
	Moderate	Heterogeneous	1
61 or more	Minimal	Heterogeneous	1
	Mild	Central	2
	Marked	Central	1
	Mild	Peripheral	1
	Moderate	Peripheral	1
Total			41

Nine patients showing contrast enhancement by CT had cerebral arteriography. In four patients who had arteriography within 5 days of CT, a significant abnormality was not seen. The remaining five cases showed evidence of infarction as demonstrated by occluded arteries and mass effect. These five angiograms were performed within 24 days of the CT examination. No correlation could be found between angiographic findings and the pattern or degree of contrast enhancement on CT.

Vascular distribution of infarcts in our series was varied. The majority of patients had one or more region of infarction along the anterior, middle, or posterior cerebral arterial distribution. Four patients had basal ganglia infarction and five patients had cerebellar infarction. Basal ganglia and cerebellar infarcts appeared identical to cerebral infarcts on both pre- and postcontrast scans, as expected.

Discussion

The CT appearance of brain infarction varies according to the natural pathophysiologic evolution of the disease. Initially the scan may appear normal. However, usually within a matter of hours a region of relatively decreased density in relation to surrounding brain tissue

TABLE 2

Progression of Enhancement on Follow-up Scanning

Patient No.	Initial Study			Follow-up Study		
	Time Since Ictus (days)	Contrast Enhancement		Time Since Ictus (days)	Contrast Enhancement	
		Degree	Pattern		Degree	Pattern
1	0	Marked	Heterogeneous	17	Marked	Heterogeneous
2	1	None	. . .	8	Mild	Homogeneous
				20	Minimal	Homogeneous
				31	None	. . .
3	2	Moderate	Heterogeneous	23	None	. . .
4	11	Marked	Heterogeneous	38	Moderate	Heterogeneous
5	11	Marked	Heterogeneous	24	Moderate	Heterogeneous
				65	Mild	Central
				200	Mild	Central
6	14	Minimal	Heterogeneous	100	None	. . .
7	17	Moderate	Heterogeneous	24	Moderate	Heterogeneous
				84	None	. . .
8	27	Marked	Homogeneous	62	Minimal	Heterogeneous
9	30	Marked	Central	270	Marked	Central
10	60	Minimal	Heterogeneous	150	None	. . .

TABLE 3

Age of Infarct at CT and Radionuclide Scanning

Patient No.	CT Enhanced, Radionuclide Positive		CT Enhanced, Radionuclide Negative		CT Not Enhanced, Radionuclide Positive	
	CT	Radio nuclide	CT	Radio nuclide	CT	Radio nuclide
1	40	40	2	2	5	4
2	7	3	11	5	90	93
3	17	14	14	8	6	6
4	10	10	5	3	123	120
5	8	14	16	12	3	5
6	14	13	53	55	11	9
7	14	11	. . .	. . .	31	30
8	27	19	. . .	. . .	10	6
9	10	14	. . .	. . .	5	2
10	1	5	. . .	. . .	52	27
11	1	4	. . .	. . .	4	5
12	12	3	. . .	. . .	75	65
13	39	9	. . .	. . .	27	12
14	. . .	. . .	. . .		7	9
15	. . .	. . .	. . .	. . .	62	17

Note.—Age of infarct reported in days.

is identified. Mass effect may or may not be present. As the infarct evolves, the region of relative lower density becomes well defined and often corresponds to a typical arterial distribution. As the infarcted tissue is broken down and removed, the area continues to decrease in density and may become sharply marginated and represent an area of porencephaly. Resulting volume loss caused by old infarction may manifest itself as dilatation of the ipsilateral ventricle [3].

Thus brain infarction presents a spectrum of appearances on CT. It must be stressed that infarction is a dynamic process which may simulate a variety of other conditions. At times it may be indistinguishable from tumor by appearing in a noncharacteristic distribution, showing contrast enhancement and having a significant mass effect (fig. 7). Infarcts demonstrating peripheral enhancement may be confused with abscess or necrotic tumor [3–6]. Contrast enhancement usually begins within the first month after the onset of clinical symptoms [6]. However, the fact that enhancement may persist for several months on follow-up CT makes it difficult to accurately estimate the age of an infarct by CT alone.

Of particular interest were the cases of cerebellar infarction which were readily discernible by CT and appeared identical on both pre- and postcontrast scans to appearances seen with cerebral infarcts.

It has been proposed that the same mechanism allowing uptake of radionuclide in an infarcted area may be responsible for contrast enhancement on CT [3]. However, our series includes many examples in which CT

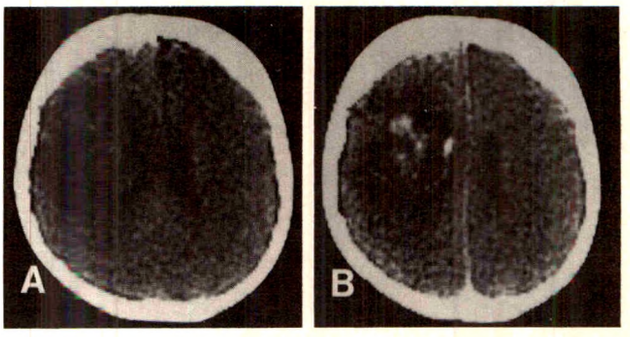

Fig. 7.—24-day-old infarct in left parietal region. *A*, Precontrast scan demonstrating mass effect, not corresponding to typical arterial distribution. *B*, Postcontrast scan showing enhancement in center of lesion, simulating tumor.

enhancement and radionuclide uptake did not occur simultaneously, suggesting that a similar mechanism alone may not be responsible for contrast enhancement. The pathophysiologic mechanism of contrast enhancement has not been clearly defined. Two favored hypotheses are altered permeability of vessels and hypervascularity of the infarcted area [3, 4, 7].

The five patterns of contrast enhancement that we encountered may reflect the size of the occluded vessels, the extent of infarction, or possibly the age of the infarct. In the future, they may be shown to be indicators of the severity of the infarction. Their value at present is to remind the diagnostician that infarction should not be excluded if the classical appearance is not present.

REFERENCES

1. Messina AV: Computed tomography: contrast enhancement in intracerebral hemorrhage (abstr.). *Neuroradiology* 12:50, 1976
2. Zimmerman RD, Leeds NE, Naidich TP: Ring blush with intracerebral hematoma. *Radiology* 122:707–711, 1977
3. Wing SD, Norman D, Pollock JA, Newton TH: Contrast enhancement of cerebral infarcts in computed tomography. *Radiology* 121:89–92, 1976
4. Davis KR, Ackerman RH, Kistler JP, Mohr JP: Computed tomography of cerebral infarction: hemorrhagic, contrast enhancement and time of appearance. *Comput Tomogr* 1:71–86, 1977
5. Yock DH Jr, Marshall WH Jr: Recent ischemic brain infarcts at computed tomography: appearances pre- and postcontrast infusion. *Radiology* 117:599–608, 1975
6. Pollock JA: Stroke, in *Computed Tomography* 1977, edited by Norman D, Korobkin M, Newton TH, St. Louis, Mosby, 1977, pp 255–262
7. Blackwood, Corsellis: *Greenfield's Neuropathology*, 3rd ed. London, Edward Arnold, 1976

Case Reports

Streptococcus bovis Septicemia as a Clue to Colon Neoplasms in Two Cases

THEODORE R. SMITH,[1] STANLEY N. FRIEDMAN,[1] AND HOWARD ADLER[2]

Recently an association between carcinoma and *Streptococcus bovis* endocarditis has been noted [1]. We describe two patients who underwent gastrointestinal evaluation as a result of *Streptococcus bovis* septicemia. Subsequently one was found to have villous adenoma and one colonic adenocarcinoma.

Case Reports

Case 1

A 67-year-old diabetic white female was admitted because of persistent fever for about 2½ months. She had been diagnosed 2 months earlier as having a urinary infection (*E. coli*) and was treated for pyelonephritis with ampicillin, but the fever persisted. After admission, she continued to have a fever of 39°C. The patient had a sister who died of rectal carcinoma. There was no history of specific gastrointestinal or bowel complaints, other than for moderate loss of appetite for several months and several pounds of weight loss. There was no melena or hematochezia, and the stools were guaiac negative. Physical examination failed to reveal significant abnormality, and the abdomen was normal.

Abnormal laboratory values included hematocrit, 29; hemoglobin, 10.7 mg/100 ml; and sedimentation rate, 91. The white blood cell count, urinalysis, blood urea nitrogen, bilirubin, and electrolytes were normal. The patient did have three successive positive blood cultures for *Streptococcus bovis*. These findings and the fever prompted barium enema and air-contrast examination in search of a possible colonic neoplasm. A polypoid, sessile 5–3 cm mass was demonstrated in the distal transverse colon (fig. 1). The lesion was confirmed by colonoscopy and biopsy. The patient subsequently underwent a segmental transverse colectomy. The lesion was described histologically as a villous adenoma with some "intramucosal adenocarcinomatous-like changes" limited to the lamina propria; no frank malignant invasion was noted.

Case 2

A 66-year-old white male diabetic was admitted for the second time because of several hours of shaking chills and sweating. The patient had 2 days of constipation and occasional vomiting, but no melena, bloody stools, or diarrhea. He had a myocardial infarction 1½ years before admission and 1 year before had a mild cerebral infarction. He had undergone a resection of the sigmoid colon 14 years earlier for adenocarcinoma which was without nodal involvement.

Physical examination revealed no acute distress. The abdomen was soft and nondistended. The liver extended 4–6 cm below the right costal margin. There were no masses palpable. Rectal examination revealed a large prostate but no masses.

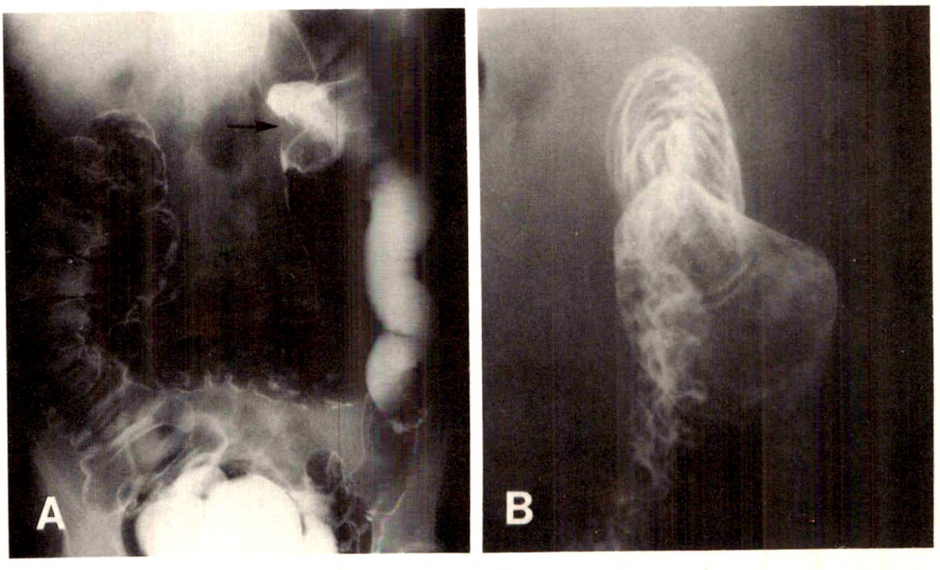

Fig. 1.—*A*, Film showing polypoid villous adenoma (*arrow*) in distal transverse colon. *B*, Postevacuation view of splenic flexure region showing mass.

Received March 28, 1978; accepted after revision July 14, 1978.

[1]Department of Radiology, Albert Einstein College of Medicine, 1300 Morris Park Avenue, Bronx, New York 10461. Address reprint requests to T. R. Smith.

[2]Department of Medicine, Albert Einstein College of Medicine, Bronx, New York 10461.

© 1978 American Roentgen Ray Society

0361–803X/78/1100–0887 $00.00

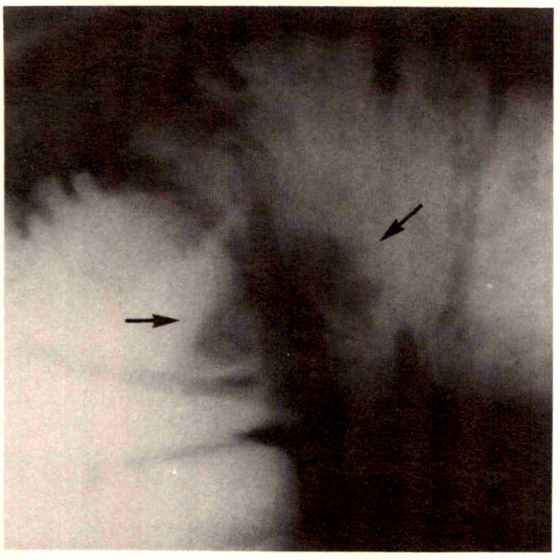

Fig. 2.—Barium enema spot film of hepatic flexure showing lobulated sessile mass (*arrows*).

The temperature was 38.4°C; pulse, 100; respiration, 20; and blood pressure, 140/70. Laboratory data revealed white blood cell count of 7,200 with a shift to the left and a sedimentation rate of 60. Three positive blood cultures grew group D nonenterococci (*Streptococcus bovis*). A liver-spleen scan was normal. The patient was started on 600,000 U of intravenous potassium penicillin every 6 hr. The next day, he was febrile (39.0°C). Repeat blood culture was negative, and the following day the patient became afebrile and remained so.

Barium enema examination revealed a lobulated mass in the region of the hepatic flexure with contour irregularity (fig. 2). Colonoscopy confirmed the mass, and biopsy showed adenocarcinoma. The patient underwent a right hemicolectomy. The lesion was a well differentiated adenocarcinoma which extended through all layers to involve pericolic fat; four lymph nodes showed no tumor.

Discussion

Streptococcus bovis is classified as a nonenterococcal species under the group D streptococci. Laboratory characteristics include ability to grow in bile, hydrolysis of esculin, sensitivity to penicillin, alpha hemolysis on sheep blood agar, positive mannitol fermentation, and inability to grow in 6.5% sodium chloride [1–6].

The work of Klein et al. [1] indicated a fecal carrier rate of about 11% in a nondiseased asymptomatic control group. This was contrasted with 56% incidence in feces of patients with colonic carcinoma, both untreated or with recurrences. The carrier rate did not seem to be affected by gastrointestinal bleeding, recent barium enema examination, age, or colonic stasis. The incidence was about 28% in inflammatory bowel disease (ulcerative colitis and Crohn's disease). Cases of *S. bovis* endocarditis and septicemia have been reported, not only with colonic carcinoma but also with villous adenoma.

Our two cases are added to the few cases previously reported in the nonradiologic literature. We emphasize the importance of evaluating patients for colonic neoplasms who exhibit *S. bovis* septicemia or endocarditis, since this may be the only early manifestation of underlying colonic neoplasm.

REFERENCES

1. Klein RS, Recco RA, Catalano MT, Edberg SC, Casey JI, Steigbigel NH: Association of *Streptococcus bovis* with carcinoma of the colon. *N Engl J Med* 297:800–802, 1977
2. Roses DR, Richman H, Localio SA: Bacterial endocarditis associated with colorectal carcinoma. *Ann Surg* 179:190–191, 1974
3. Ravreby WD, Bottone EJ, Keusch GT: Group D streptococcal bacteremia with emphasis on the incidence and presentation of infections due to *Streptococcus bovis*. *N Engl J Med* 289:1400–1403, 1973
4. Hoppes WL, Lerner PI: Non enterococcal group D endocarditis caused by *Streptococcus bovis*. *Ann Intern Med* 81:588–593, 1974
5. Facklam RR: Recognition of group D streptococcal species of human origin by biochemical and physiological tests. *Appl Microbiol* 23:1131–1139, 1972
6. Deibel RH: The group D streptococci. *Bacteriol Rev* 28:330–366, 1964

Bile Leak into a Hepatic Abscess in a Liver Transplant: Demonstration with ^{99m}Tc-Diethyl-Iminodiacetic Acid

WILLIAM C. KLINGENSMITH, III,[1] LAWRENCE J. KOEP,[2] AND ALAN R. FRITZBERG[1]

There have been only four previous reports of bile leaks detected by radionuclide imaging; two were secondary to trauma [1], one was secondary to spontaneous tear of a bile duct in a patient with biliary atresia [2], and one was associated with an abscess [1]. All four patients were studied with ^{131}I-rose bengal.

We have studied a patient with an orthotopic liver transplant and sepsis with ^{99m}Tc-N,α-(2,6-diethylacetanilide)-iminodiacetic acid (^{99m}Tc-diethyl-IDA) [3]. Serial images over 24 hr clearly demonstrated bile leaking into a circular left hepatic lesion. Surgical exploration revealed an abscess containing bile.

Materials and Methods

The hepatobiliary study was performed by injecting 6 mCi of ^{99m}Tc-diethyl-IDA intravenously and imaging the abdomen in the anterior and right lateral projections at 15, 30, 45, and 60 min (300,000 counts per image) and at 24 hr (20,000 counts per image). ^{99m}Tc-diethyl-IDA was prepared by first making the carrier compound N,α-(2,6-diethylacetanilide)-iminodiacetic acid from 2,6-diethylaniline as previously described [4]. The nuclear magnetic resonance spectrum and elemental analysis of the recrystallized iminodiacetic acid product were consistent with the expected structure. Kits were prepared containing 35 mg of the carrier and 0.35 mg of $SnCl_2 \cdot 2H_2O$ in 0.8 ml at pH 5.8–6.0. The kits were stored frozen under vacuum. Labeling was achieved by adding 40–50 mCi of $^{99m}TcO_4$ in 1.5–2.2 ml. Saline was added as necessary for dilution. Radiochemical purity was ascertained by chromatography on Whatman 3M paper in saline. Labeling was 95% or greater.

Case Report

A 33-year-old male underwent orthotopic liver transplantation 1 year before the present hospital admission because of terminal liver failure secondary to chronic active hepatitis (hepatitis B surface antigen positive) complicated by postnecrotic cirrhosis and hepatic encephalopathy. His posttransplantation course was complicated by episodes of rejection which were controlled with immunosuppressives, and a right hepatic abscess which was drained externally. He was discharged home and for a time did well. Three weeks before the current admission liver function tests deteriorated, and routine blood cultures were positive for mixed organisms. He was rehospitalized with a presumptive diagnosis of cholangitis. Liver function tests deteriorated further, and a liver biopsy revealed mild viral hepatitis without cirrhosis.

A ^{99m}Tc-diethyl-IDA study (total bilirubin, 4.8 mg/dl) demonstrated a moderately sized round marginal lesion in the left lobe of the liver, best seen at 45 min (fig. 1*A*). Delayed passage of activity into the small bowel was seen at 60 min (not shown). Images at 24 hr (total bilirubin now 7.0 mg/dl) showed accumulation of the radiopharmaceutical within the left hepatic lobe lesion (fig. 1*A*). A ^{99m}Tc-sulfur colloid study 6 days later demonstrated progression of the lesion to the point of almost replacing the entire left lobe (fig. 1*B*). A moderate amount of increased bone marrow activity was also noted; no splenic activity was present because of previous splenectomy. Computed tomography performed the same day as the ^{99m}Tc-sulfur colloid study demonstrated a large lesion in the left hepatic lobe which contained an air-fluid level and multiple small areas around the perimeter of the lesion with attenuation coefficient of air (fig. 1*C*).

At surgery a left lobe abscess containing yellow bile was found and drained through the previous epigastric incision. Extensive adhesions precluded exploration of the remainder of the liver or the abdomen. Multiple organisms were cultured from the abscess. A transhepatic cholangiogram at this time demonstrated mild dilatation of the hepatic ducts, intraluminal debris, and free passage of contrast into the small bowel. Since it was felt that the intraluminal debris may have been causing intermittent obstruction, the patient's cholecystojejunostomy was converted to a choledochojejunostomy. The abscess cavity healed without any persisting bile leak.

Discussion

Orthotopic liver transplantation as treatment for terminal liver failure has achieved modest success in terms of survival rate [5]. Common complications, however, include rejection, biliary tract obstruction, and intra- and extrahepatic infection [5]. Because of this combination of functional and anatomic complications, we routinely follow our liver transplant patients with both a hepatobiliary radiopharmaceutical, currently ^{99m}Tc-diethyl-IDA, and ^{99m}Tc-sulfur colloid which gives superior anatomic resolution. Our patient demonstrated the unusual finding of a bile leak into a hepatic abscess in the ^{99m}Tc-diethyl-IDA study.

The four previously reported patients with bile leaks demonstrated by imaging with hepatobiliary radiopharmaceuticals all had fistulous tracts [1, 2]. The biliary tract communicated with the bronchial tree and the skin in one patient [1], the bronchial tree as well as an abscess in a second [1], the lesser sac in a third [1], and the peritoneal cavity in the fourth [2]. The bile leak in our patient was solely into a hepatic abscess without any extrahepatic drainage.

Most hepatic abscesses do not contain bile at surgery. The bile leak in our patient may be related to the pathogenesis of hepatic abscesses in transplanted livers. Obstruction and rejection are frequent contributing factors in the initiation of hepatic abscesses in these pa-

Received May 23, 1978; accepted July 20, 1978.

[1] Division of Nuclear Medicine, University of Colorado Medical Center, 4200 East Ninth Avenue, Denver, Colorado 80262. Address reprint requests to W. C. Klingensmith, III.

[2] Department of Surgery, University of Colorado Medical Center, Denver, Colorado 80262.

© 1978 American Roentgen Ray Society

0361–803X/79/1100–0889 $00.00

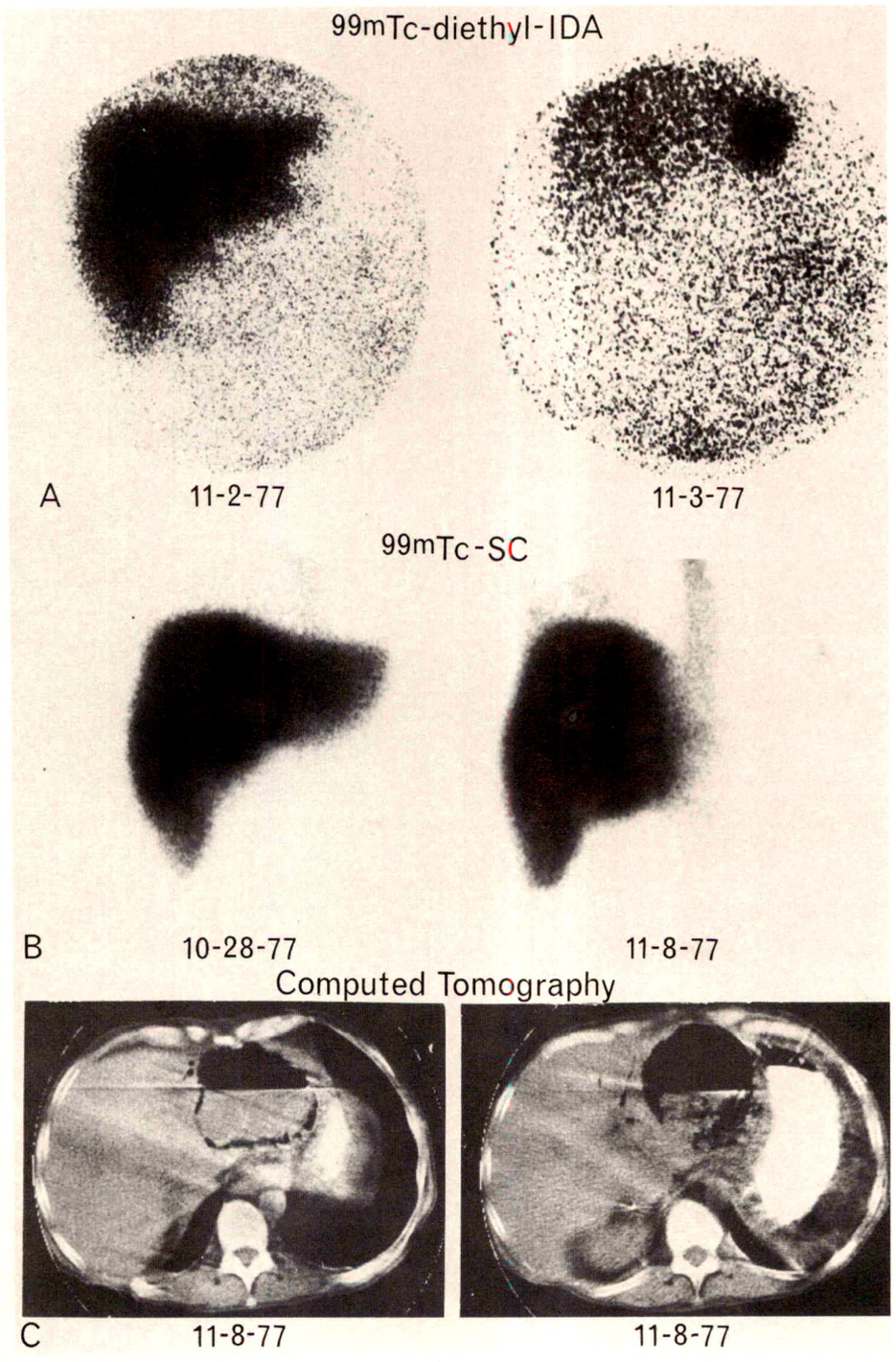

Fig. 1.—*A*, Anterior abdominal images with ^{99m}Tc-diethyl-IDA demonstrating round marginal lesion in left lobe of liver 45 min after injection and bile leak into lesion 24 hr later. *B*, Anterior ^{99m}Tc-sulfur colloid (^{99m}Tc-SC) image showing mildly increased bone marrow activity and normal liver. Eleven days later phagocytic function has been lost in most of left lobe. *C*, CT scan of upper abdomen after oral administration of dilute contrast material demonstrating large lesion in left lobe of liver with air-fluid interface and multiple small areas around margin of lesion which have attenuation coefficient of air.

tients [6]. In our patient intermittent obstruction may have contributed both to abscess formation and the bile leak into the abscess because of elevated biliary duct pressure. Rejection contributes to abscess formation by causing small areas of necrosis which secondarily become infected in these immunosuppressed patients [6]. The process of necrosis prior to infection may contribute to disruption of the biliary ducts, although there was no direct evidence of rejection in our patient.

Newer ^{99m}Tc-labeled hepatobiliary radiopharmaceuticals, such as ^{99}Tc-diethyl-IDA, result in significantly improved images compared to those obtained with ^{131}I-rose bengal or other ^{99m}Tc radiopharmaceuticals such as ^{99m}Tc-pyridoxylideneglutamate [7, 8]. This improvement

in image quality has resulted in better visualization of the intra- and extrahepatic biliary tract and should result in greater sensitivity and specificity in the evaluation of bile leaks and other abnormalities of the hepatobiliary system.

REFERENCES

1. Wiener SN, Vyas M: The scintigraphic demonstration of bile leakage utilizing ^{131}I-rose bengal. *J Nucl Med* 15:1044–1046, 1974
2. Silverberg M, Rosenthall L, Freeman LM: Rose bengal excretion studies as an aid in the differential diagnosis of neonatal jaundice. *Semin Nucl Med* 3:69–80, 1973
3. Wistow BW, Subramanian G, Van Heertum RL, Henderson RW, Gagne GM, Hall RC, McAfee JG: An evaluation of ^{99m}Tc-labeled hepatobiliary agents. *J Nucl Med* 18:455–461, 1977
4. Berovansky A, Lekera A, Urba C: Studies on local anesthetics. XXI. Some derivatives of ω-diethylaminoacetanilide. *J Pharm Assoc Sci Ed* 48:402–404, 1959
5. Starzl TE, Porter KA, Putnam CW, Schroter GPJ, Halgrimson CG, Weil R, Hoelscher M, Reid HAS: Orthotopic liver transplantation in ninety-three patients. *Surg Gynecol Obstet* 142:487–505, 1976
6. Porter KA: Pathology of liver transplantation. *Transplant Rev* 2:129–170, 1969
7. Klingensmith WC, Fritzberg AR, Koep LJ, et al: Clinical comparison of ^{99m}Tc-pyridoxylideneglutamate and ^{131}I-rose bengal in liver transplant patients. Submitted for publication
8. Klingensmith WC, Fritzberg AR, Koep LJ: Clinical comparison of ^{99m}Tc-diethyl-IDA and ^{99m}Tc-pyridoxylideneglutamate for evaluation of the hepatobiliary system. *J Nucl Med* 19:737–738, 1978

Legionnaires Disease

JAMES C. REED,[1] ROBERT McLELLAND, AND PAMELA NELSON

The epidemic of Legionnaires disease, a fulminant, often fatal pneumonia, caused near hysteria and ultimately the demise of a great old hotel, the site of the contagion. The causative organism was identified, but cases continue to surface [1–3].

Successful isolation of the organism at the National Communicable Disease Center followed efforts which involved intraperitoneal inoculation in guinea pigs from lung tissue of one of the original fatal cases and subsequent isolation in the yolk sacs of embryonated chicken eggs. The usual stains were not helpful. While other clinical investigations were continued, a pleomorphic, weakly gram-negative bacillus [4, 5] was demonstrated using a specialized staining technique, which until then had been reserved primarily for the demonstration of spirochetes. We describe the radiographic features of a case of Legionnaires disease.

Case Report

A 30-year-old white woman had sudden onset of fever, chills, malaise, and nonproductive cough. Admission chest radiography (fig. 1*A*) demonstrated extensive left upper lobe consolidation with poorly defined borders and air bronchograms. There was minimal involvement of the right upper lobe. Physical examination revealed an acutely ill woman with a pulse of 140; respirations, 48; and temperature, 39°C. There was increased vocal and tactile fremitus and dullness to percussion over the left lung. Diffuse rales and rhonchi were heard in both lungs, more marked on the left. Cardiovascular, abdominal, and neurologic examinations were normal. Initial leukocytosis was followed by a drop in the white blood cell count to 2,700. The admission blood gases on 70% oxygen by mask showed pH,7.5; pO_2, 37; pCO_2, 24; HCO_3, 16; and oxygen saturation, 72%.

The patient was treated with ampicillin, penicillin, and gentamicin, but fever persisted and hypoxemia worsened. Radiography 3 days later revealed progression, with increasing consolidation of the left upper lobe and diffuse spread through the right lung (fig. 1*B*). Bronchoscopy revealed only mild bronchitis of the left upper lobe with no endobronchial mass lesion. Smears and cultures of bronchial secretions, washings, and brushings were all negative for bacteria, fungi, and acid-fast bacilli. Because there was no evidence of usual bacterial infection by sputum and blood cultures, all antibiotics were discontinued and the patient was started on erythromycin. She was anemic and leukopenic. Quantitative immunoglobulins were universally depressed below 30% of normal. On hospital day 7, because the patient continued to be febrile with no improvement in the radiographic findings and because she required assisted ventilation, an open lung biopsy was performed.

Pathologic examination showed a diffuse infiltrate with lymphocytes, neutrophils, and macrophages with early fibrosis. These findings were interpreted as an organizing pneumonia. All cultures and smears remained negative. On hospital day 8, erythromycin was replaced with tetracycline, and steroids were begun the next day. Over the next several days the patient became afebrile, with radiographic clearing and resolution of her hypoxemia. She developed a leukocytosis with left shift. Serum titres for mycoplasma were positive at 1:8; a repeat study 10 days later was positive at 1:32. Viral serologies and complement fixation titres with fungi and Q-fever were negative. On hospital day 19, radiography showed further clearing and the steroids were discontinued.

Initial and convalescent sera were sent to the Center for Disease Control with confirmation of the diagnosis of Legionnaires disease by the following titres: initial, 1:200; convalescent, 1:1,025. Subsequently, electron microscopy of tissue from the lung biopsy demonstrated intracellular organisms consistent with Legionnaires bacillus.

Follow-up radiography 3 months after the acute pneumonia (fig. 1*C*) revealed persistent large reticular interstitial scars which were most prominent in the left upper lobe. In addition, pulmonary function studies revealed a persistent restrictive defect.

Discussion

This patient's clinical presentation and course were fairly typical when compared to those of other reported cases, both sporadic and from the Philadelphia epidemic [1–4]. In general, early symptomatology has included headache, fever, and myalgias lasting up to 1 week. Many patients develop a nonproductive cough with associated chest pain, often with a pleuritic component. Gastrointestinal symptoms occasionally are seen. Deterioration follows, often to the point of prostration, with markedly elevated temperatures, sometimes associated with confusion. Attempts to culture the offending organism are unsuccessful, and the patient grows worse under conventional therapy for other bacterial infections. Many patients require supplemental oxygen and assisted ventilation but show marked improvement within 24–48 hr on erythromycin or tetracycline. Radiologic improvement tends to lag behind clinical improvement.

While infection apparently stems from an airborne bacterium, the disease is not contagious or communicable. Smokers are more susceptible than nonsmokers [4], and the immunosuppressed patient is at greater risk for infection, as demonstrated by a group of renal transplant patients in Los Angeles [6].

The radiographic features in this case included progressive, bilateral, nonspecific confluent pneumonia which ultimately responded to tetracycline, with an interstitial scarring and restrictive defect on pulmonary function studies remaining 3 months later. The early radiographic findings in our patient are fairly typical [7].

Received March 10, 1978; accepted after revision June 27, 1978.

[1] All authors: Department of Radiology, Duke University Medical Center, Durham, North Carolina 27710. Address reprint requests to J. C. Reed.

© 1978 American Roentgen Ray Society

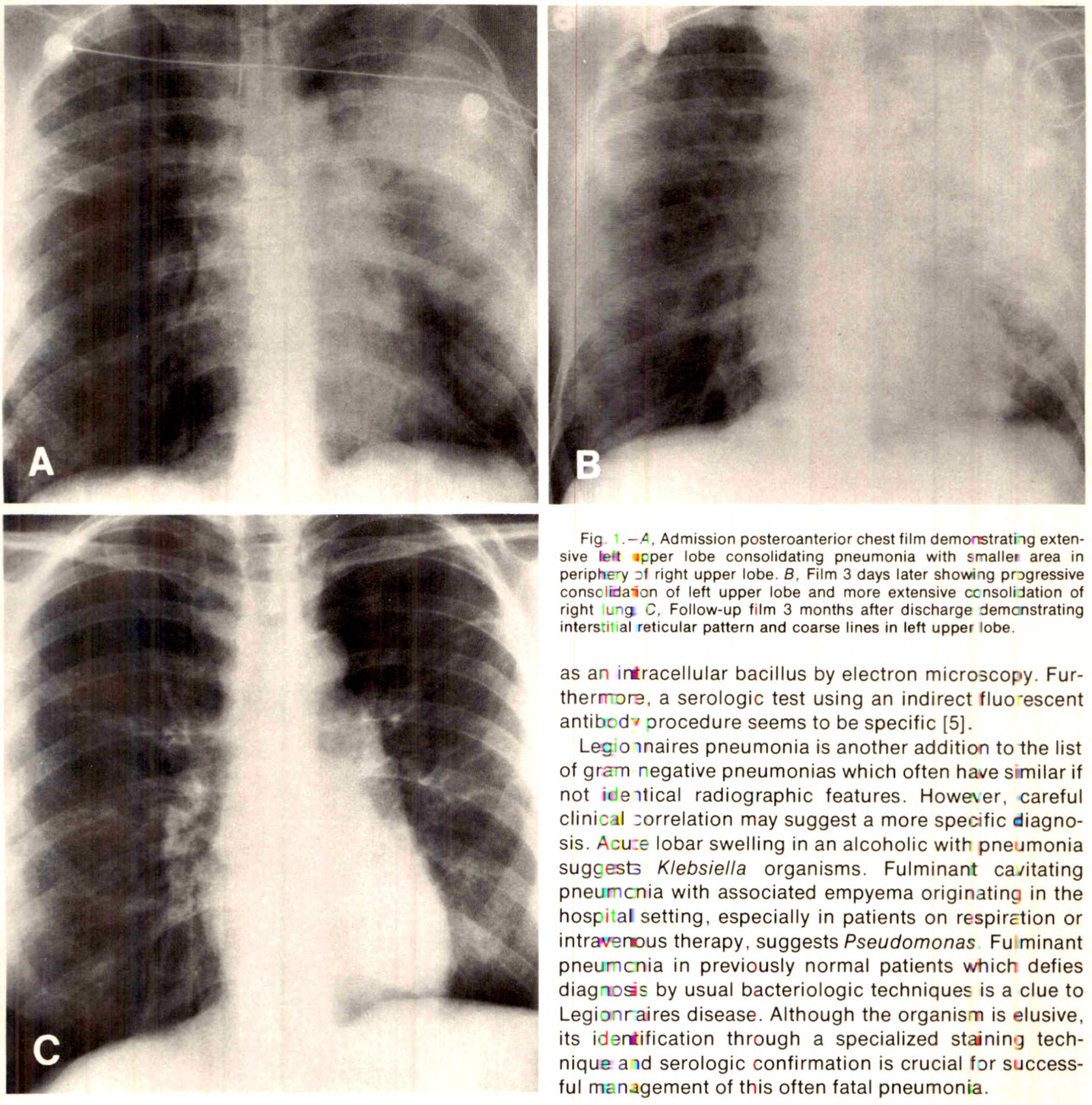

Fig. 1.—*A*, Admission posteroanterior chest film demonstrating extensive left upper lobe consolidating pneumonia with smaller area in periphery of right upper lobe. *B*, Film 3 days later showing progressive consolidation of left upper lobe and more extensive consolidation of right lung. *C*, Follow-up film 3 months after discharge demonstrating interstitial reticular pattern and coarse lines in left upper lobe.

Others have reported initially patchy or fluffy infiltrates which progress to frank consolidation without evidence of significant effusion or of cavitation. In the Philadelphia patients, 50% of the radiographic findings were unilateral. Most went on to resolve completely within 2 weeks to 2 months of clinical improvement [1–4].

Because this unusual bacillus does not stain with hematoxylin and eosin and stains lightly gram negative, if at all, it will usually be missed with conventional examination of sputum, biopsy, or autopsy material. Special staining with the Dieterle silver impregnation method (originally used for the demonstration of spirochetes) will identify the bacillus [8], and it may also be identified as an intracellular bacillus by electron microscopy. Furthermore, a serologic test using an indirect fluorescent antibody procedure seems to be specific [5].

Legionnaires pneumonia is another addition to the list of gram negative pneumonias which often have similar if not identical radiographic features. However, careful clinical correlation may suggest a more specific diagnosis. Acute lobar swelling in an alcoholic with pneumonia suggests *Klebsiella* organisms. Fulminant cavitating pneumonia with associated empyema originating in the hospital setting, especially in patients on respiration or intravenous therapy, suggests *Pseudomonas*. Fulminant pneumonia in previously normal patients which defies diagnosis by usual bacteriologic techniques is a clue to Legionnaires disease. Although the organism is elusive, its identification through a specialized staining technique and serologic confirmation is crucial for successful management of this often fatal pneumonia.

REFERENCES

1. Keys TF: A sporadic case of pneumonia due to Legionnaires' disease. *Mayo Clin Proc* 52:657–660, 1977
2. Jones FL, Beecham HJ III, Dennehy JJ: Sporadic Legionnaires' disease. *JAMA* 239:640–641, 1978
3. Ryerson GG, Lauwasser ME, Block AJ, Barnett BE, Shands JW Jr: Legionnaires' disease: a sporadic case. *Chest* 73:113–114, 1978
4. Fraser DW, Tsai TR, Orenstein W, Parkin WE, Beecham HJ, Sharrar RG, Harris J, Mallison GF, Martin SM, McDade JE, Sheppard CC, Brachman PS, Field Investigation Team: Legionnaires' disease: description of an epidemic of pneumonia. *N Engl J Med* 297:1189–1197, 1977
5. McDade JE, Sheppard CC, Fraser DW, Tsai TR, Redus MA,

Dowdle WR, Laboratory Investigation Team: Legionnaires' disease: isolation of a bacterium and demonstration of its role in other respiratory disease. *N Engl J Med* 297:1197–1203, 1977

6. Bock BV, Kirby B, Eddstein PH, George WL, Snyder L, Owens ML, Hatayama C, Haley CE, Lewis RP, Meyer RD, Finegold SM: Legionnaires' disease in renal transplant recipients. *Lancet* 1:410–413, 1978
7. Dietrich PA, Johnson RD, Fairbank JT, Walke JS: The chest radiograph in Legionnaires' disease. *Radiology* 127:577–582, 1978
8. Chandler FW, Hicklin MD, Blackmon JA: Demonstration of the agent of Legionnaires' disease in tissue. *N Engl J Med* 297:1218–1220, 1977

Ultrasound Diagnosis of Hydatid Disease (Echinococcosis) in Two Cases

DIANE S. BABCOCK,[1, 2] LEONARD KAUFMAN,[1] AND IRIS COSNOW[3]

Echinococcus granulosus is a genus of tapeworm that infects man as an intermediate host. It is not commonly seen in this country, but is fairly common in the large sheep-raising areas of Europe, Asia, the Mediterranean, South America, and Australia. However, there is an increasing incidence among native-born residents in the endemic areas of the Southwest, Alaska, and Canada [1]. Treatment is hampered by the lack of a safe systemic scolicidal agent, making surgical removal the only effective treatment. The high antigenicity of the cyst fluid makes special precautions necessary to prevent spillage of the cyst fluid or daughter cysts into the body tissues. In our two cases, the typical gray scale ultrasound findings of a multicystic mass along with positive serologic tests made the correct diagnosis possible prior to surgery.

Case Reports

Case 1

M. W., a 36-year-old woman native of Yugoslavia who immigrated to the United States at the age of 13, was admitted for routine hysterectomy for chronic cervicitis. History included removal of a hydatid cyst from the right lobe of her liver 10 years previously. Excretory urography showed a large mass in the right kidney (fig. 1*A*). No calcification was seen on the preliminary films. Radionuclide liver scan revealed a small right lobe and, on the posterior view, there was a defect which was suggestive of a recurrent lesion. Gray scale ultrasonography using an Echoview System 80L Ultrasonoscope (Picker Corp.) and a 2.25 MHz transducer revealed a 7 cm multicystic mass in the mid-right kidney (fig. 1*B*). The individual cysts measured 1–3 cm. There was also a multicystic mass above the kidney just beneath the right lobe of the liver (fig. 1*B*). The patient admitted having vague intermittent right flank pressure for some time. The urine sediment contained 1–3 red blood cells and 2–4 white blood cells per high power field. The white blood cell count was 7,000/mm^3 with 2% eosinophils. Serologic tests for *Echinococcus granulosus* were strongly positive. Exploratory surgery via a right subcostal approach revealed a 7 cm cystic mass in the right kidney (fig.1*C*). A second cystic mass was present on the underside of the right lobe of the liver. Both cysts were irrigated with 0.5% silver nitrate solution. A right nephrectomy was performed, and the cyst under the liver was removed intact. Dissection of the kidney revealed a large cyst containing multiple daughter cysts (fig. 1*C*). The postoperative course was uneventful.

Case 2

F. S., a 31-year-old white female native of Yugoslavia living in this country for 10 years, was admitted after 1–2 days of severe upper abdominal pain radiating to the back. The patient experienced two similar episodes 4 months and 4 years prior to admission. Jaundice occurred just prior to this last admission. History included exposure to sheep and dogs for many years in Yugoslavia.

Examination on admission revealed no evidence of acute distress or jaundice. There was no abdominal tenderness. However, a firm globular mass was palpated in the epigastrium. The mass moved with respiration. The white blood cell count was 12,000/mm^3 with 10% eosinophils. The total bilirubin was 3.7 mg/100 ml. Serologic tests for *E. granulosus* were strongly positive. A stool sample revealed many scolices of *E. granulosus*.

Radiographic study of the gallbladder (fig. 2*A*) revealed a curvilinear calcification in the right upper quadrant of the abdomen deforming the gallbladder. The radionuclide liver scan showed a large defect in the hilum of the liver. Gray scale ultrasonography of the abdomen revealed a 7 cm multicystic mass in the hilum of the liver with the smaller cysts ranging from 1–3 cm (fig. 2*B*).

At surgery a large echinococcal cyst was found between the right and left lobes of the liver. The cyst contained multiple daughter cysts which were resected. There was no spillage of the cyst material into the peritoneal cavity. The edges of the cyst were marsupialized. After surgery all the laboratory findings returned to normal, and the patient made an uneventful recovery.

Discussion

There are two species of *Echinococcus* pathogenic to man: *E. granulosus* which forms a single, unilocular cyst and produces symptoms by expansion and compression of adjacent structures, and *E. multilocularis* which is relatively uncommon and produces multilocular or alveolar cysts and spreads through the organ as a highly malignant tumor.

The dog is the definitive host of *E. granulosus* and harbors the adult worm. The adult, not found in man, is 3–6 mm long and lives attached to the villi of the canine small bowel. Eggs from dog feces are swallowed by the intermediate host (sheep, cattle, or man) and hatch in the duodenum. The liberated oncospheres then migrate through the bowel wall to mesenteric venules and enter the portal circulation. The liver acts as the initial filter and is the most common organ involved in man (60%) [2]. Those oncospheres that escape the liver are next filtered by the lungs (25%) [2]. A small percentage enter the systemic circulation and lodge in such places as brain, kidney (2%), and bone. In the sheep-raising areas of the world, including the southwestern United States, *E. granulosus* occurs in the pastoral form with the sheep or cow as the intermediate host and the dog as the

Received March 3, 1978; accepted after revision June 22, 1978.

[1] Department of Radiology, Ravenswood Hospital Medical Center, Chicago, Illinois 60640.

[2] Present address: Department of Radiology, Children's Hospital Medical Center, Elland and Bethesda, Cincinnati, Ohio 45229. Address reprint requests to D. S. Babcock.

[3] Department of Pathology, Ravenswood Hospital Medical Center, Chicago, Illinois 60640.

© 1978 American Roentgen Ray Society

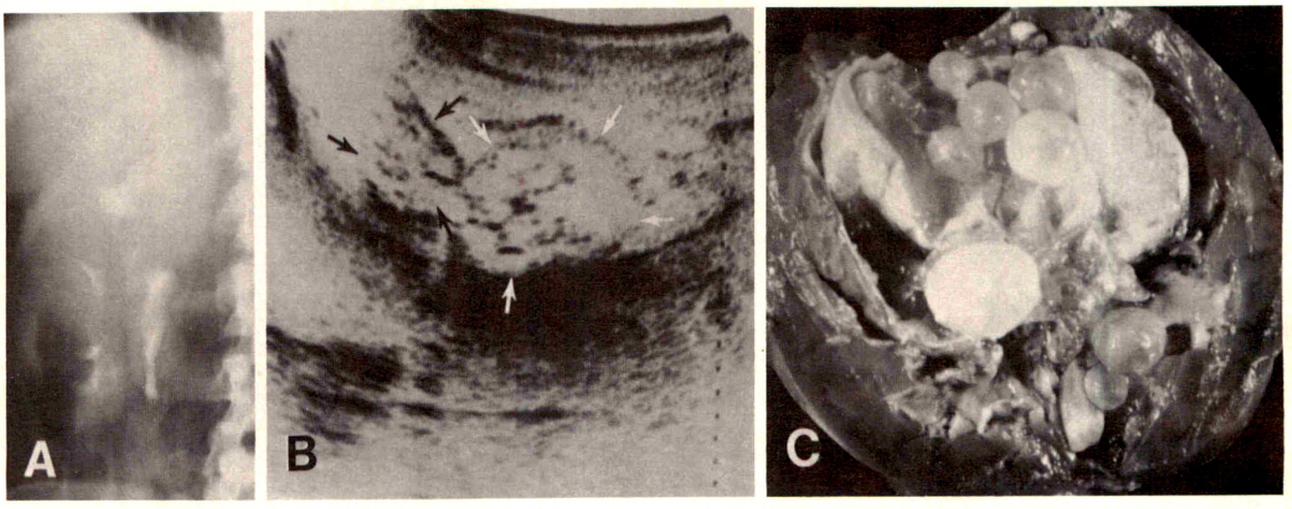

Fig. 1.—Case 1. *A*, Excretory urogram showing mass in right kidney causing splaying of calyces. *B*, Longitudinal ultrasound scan of right kidney with patient prone showing multicystic mass within kidney (*white arrows*) and second multicystic mass above kidney (*black arrows*) and beneath right lobe of liver. *C*, Right nephrectomy specimen. Kidney is bivalved through cysts showing thick cyst wall and multiple daughter cysts within.

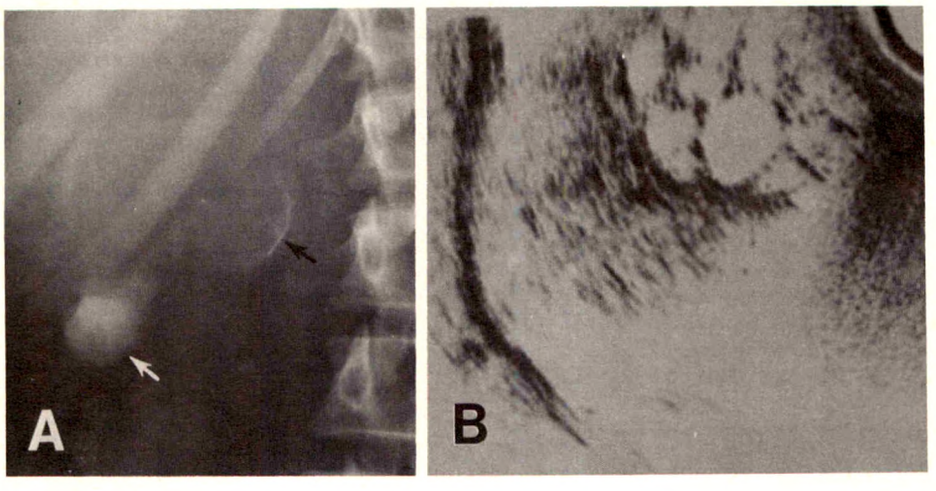

Fig. 2.—Case 2. *A*, Oral cholecystogram showing curvilinear calcifications in cyst wall (*black arrow*) above gallbladder (*white arrow*). *B*, Longitudinal ultrasound scan of liver 6 cm right of midline showing multicystic mass in hilum of liver.

primary host. In Canada and Alaska, *E. granulosus* occurs mainly in the sylvatic form with the moose, caribou, and deer as the intermediate host and the wolf, fox, dog, and rodents as the primary host.

The unilocular hydatid cyst induces a host reaction in the surrounding tissues which form a thick laminated capsule. Daughter cysts and brood capsules bud off from the inner germinal layer producing a multicystic appearance. As the cyst grows, it causes mechanical damage and may interfere with the function of the surrounding organs. The cyst may rupture producing an allergic reaction, even anaphylaxis. Secondary infection may occur, producing signs and symptoms of hepatic abscess. The most common symptom from liver involvement is right upper quadrant abdominal pain. Jaundice may occur if the bile ducts become obstructed [2]. Renal infestation usually results in a painful flank mass and microscopic hematuria [3]. Sometimes daughter cysts are passed in the urine. The patient is usually infected in childhood and the cyst slowly grows for 5–20 years before diagnosis. The cyst may attain a diameter of up to 20 cm. About 20% of patients have multiple cysts; 20%–25% have eosinophilia in the peripheral blood.

Echinococcal disease appears radiographically as a cystic mass lesion in the lungs, liver, or other organs. Some cysts will have calcifications in the wall of the cyst (case 2). If a renal cyst communicates with the collecting system, the cyst may fill with contrast material during excretory urography, and the outline of the daughter cysts can be seen. In noncommunicating cysts, the "goblet" and "crescent" signs have been described in excretory urography [4]. Nephrotomography and angiography may be of value by demonstrating a thick cyst wall.

In both our cases, gray scale ultrasonography demonstrated a mass containing multiple 1–3 cm sonolucent cystic areas. Echinococcal disease should be suspected when such a multicystic mass is seen. Others have reported similar findings [5–7]. King [7] described this

Ultrasound Diagnosis of Hydatid Disease (Echinococcosis) in Two Cases

DIANE S. BABCOCK,[1,2] LEONARD KAUFMAN,[1] AND IRIS COSNOW[3]

Echinococcus granulosus is a genus of tapeworm that infects man as an intermediate host. It is not commonly seen in this country, but is fairly common in the large sheep-raising areas of Europe, Asia, the Mediterranean, South America, and Australia. However, there is an increasing incidence among native-born residents in the endemic areas of the Southwest, Alaska, and Canada [1]. Treatment is hampered by the lack of a safe systemic scolicidal agent, making surgical removal the only effective treatment. The high antigenicity of the cyst fluid makes special precautions necessary to prevent spillage of the cyst fluid or daughter cysts into the body tissues. In our two cases, the typical gray scale ultrasound findings of a multicystic mass along with positive serologic tests made the correct diagnosis possible prior to surgery.

Case Reports

Case 1

M. W., a 36-year-old woman native of Yugoslavia who immigrated to the United States at the age of 13, was admitted for routine hysterectomy for chronic cervicitis. History included removal of a hydatid cyst from the right lobe of her liver 10 years previously. Excretory urography showed a large mass in the right kidney (fig. 1*A*). No calcification was seen on the preliminary films. Radionuclide liver scan revealed a small right lobe and, on the posterior view, there was a defect which was suggestive of a recurrent lesion. Gray scale ultrasonography using an Echoview System 80L Ultrasonoscope (Picker Corp.) and a 2.25 MHz transducer revealed a 7 cm multicystic mass in the mid-right kidney (fig. 1*B*). The individual cysts measured 1–3 cm. There was also a multicystic mass above the kidney just beneath the right lobe of the liver (fig. 1*B*). The patient admitted having vague intermittent right flank pressure for some time. The urine sediment contained 1–3 red blood cells and 2–4 white blood cells per high power field. The white blood cell count was 7,000/mm^3 with 2% eosinophils. Serologic tests for *Echinococcus granulosus* were strongly positive. Exploratory surgery via a right subcostal approach revealed a 7 cm cystic mass in the right kidney (fig.1*C*). A second cystic mass was present on the underside of the right lobe of the liver. Both cysts were irrigated with 0.5% silver nitrate solution. A right nephrectomy was performed, and the cyst under the liver was removed intact. Dissection of the kidney revealed a large cyst containing multiple daughter cysts (fig. 1*C*). The postoperative course was uneventful.

Case 2

F. S., a 31-year-old white female native of Yugoslavia living in this country for 10 years, was admitted after 1–2 days of severe upper abdominal pain radiating to the back. The patient experienced two similar episodes 4 months and 4 years prior to admission. Jaundice occurred just prior to this last admission. History included exposure to sheep and dogs for many years in Yugoslavia.

Examination on admission revealed no evidence of acute distress or jaundice. There was no abdominal tenderness. However, a firm globular mass was palpated in the epigastrium. The mass moved with respiration. The white blood cell count was 12,000/mm^3 with 10% eosinophils. The total bilirubin was 3.7 mg/100 ml. Serologic tests for *E. granulosus* were strongly positive. A stool sample revealed many scolices of *E. granulosus*.

Radiographic study of the gallbladder (fig. 2*A*) revealed a curvilinear calcification in the right upper quadrant of the abdomen deforming the gallbladder. The radionuclide liver scan showed a large defect in the hilum of the liver. Gray scale ultrasonography of the abdomen revealed a 7 cm multicystic mass in the hilum of the liver with the smaller cysts ranging from 1–3 cm (fig. 2*B*).

At surgery a large echinococcal cyst was found between the right and left lobes of the liver. The cyst contained multiple daughter cysts which were resected. There was no spillage of the cyst material into the peritoneal cavity. The edges of the cyst were marsupialized. After surgery all the laboratory findings returned to normal, and the patient made an uneventful recovery.

Discussion

There are two species of *Echinococcus* pathogenic to man: *E. granulosus* which forms a single, unilocular cyst and produces symptoms by expansion and compression of adjacent structures, and *E. multilocularis* which is relatively uncommon and produces multilocular or alveolar cysts and spreads through the organ as a highly malignant tumor.

The dog is the definitive host of *E. granulosus* and harbors the adult worm. The adult, not found in man, is 3–6 mm long and lives attached to the villi of the canine small bowel. Eggs from dog feces are swallowed by the intermediate host (sheep, cattle, or man) and hatch in the duodenum. The liberated oncospheres then migrate through the bowel wall to mesenteric venules and enter the portal circulation. The liver acts as the initial filter and is the most common organ involved in man (60%) [2]. Those oncospheres that escape the liver are next filtered by the lungs (25%) [2]. A small percentage enter the systemic circulation and lodge in such places as brain, kidney (2%), and bone. In the sheep-raising areas of the world, including the southwestern United States, *E. granulosus* occurs in the pastoral form with the sheep or cow as the intermediate host and the dog as the

Received March 3, 1978; accepted after revision June 22, 1978.

[1] Department of Radiology, Ravenswood Hospital Medical Center, Chicago, Illinois 60640.
[2] Present address: Department of Radiology, Children's Hospital Medical Center, Eland and Bethesda, Cincinnati, Ohio 45229. Address reprint requests to D. S. Babcock.
[3] Department of Pathology, Ravenswood Hospital Medical Center, Chicago, Illinois 60640.

© 1978 American Roentgen Ray Society

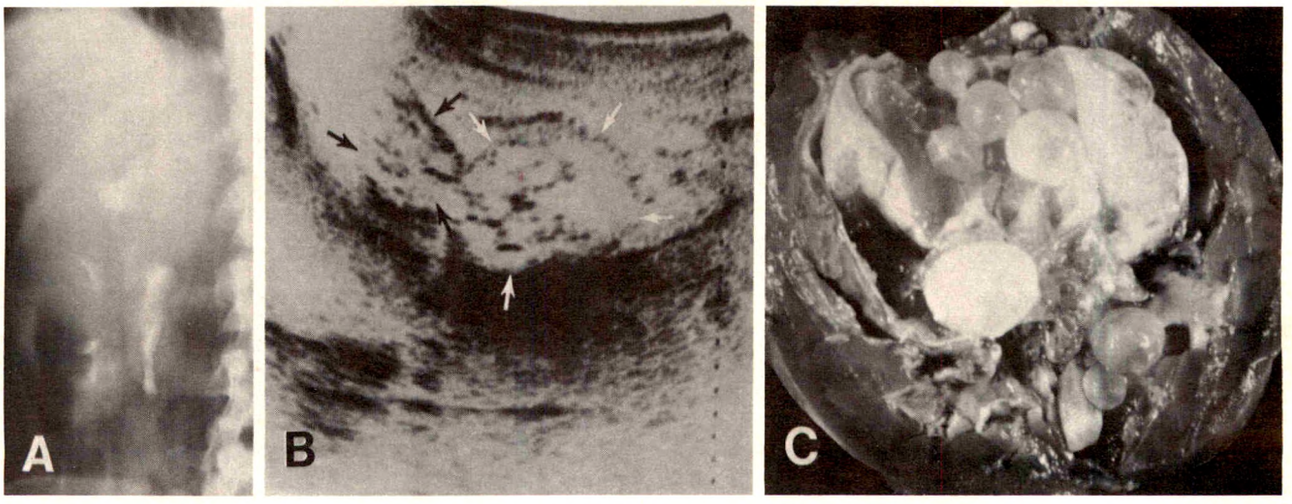

Fig. 1.—Case 1. *A*, Excretory urogram showing mass in right kidney causing splaying of calyces. *B*, Longitudinal ultrasound scan of right kidney with patient prone showing multicystic mass within kidney (*white arrows*) and second multicystic mass above kidney (*black arrows*) and beneath right lobe of liver. *C*, Right nephrectomy specimen. Kidney is bivalved through cysts showing thick cyst wall and multiple daughter cysts within.

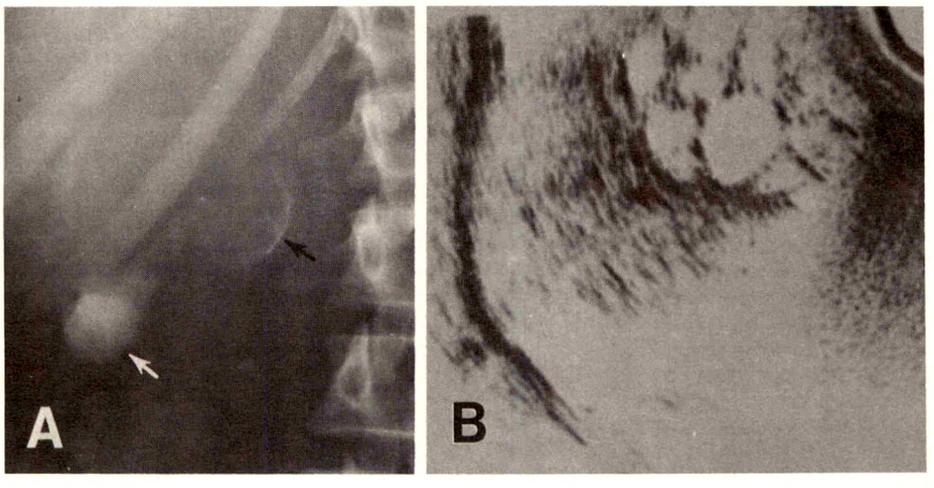

Fig. 2.—Case 2. *A*, Oral cholecystogram showing curvilinear calcifications in cyst wall (*black arrow*) above gallbladder (*white arrow*). *B*, Longitudinal ultrasound scan of liver 6 cm right of midline showing multicystic mass in hilum of liver.

primary host. In Canada and Alaska, *E. granulosus* occurs mainly in the sylvatic form with the moose, caribou, and deer as the intermediate host and the wolf, fox, dog, and rodents as the primary host.

The unilocular hydatid cyst induces a host reaction in the surrounding tissues which form a thick laminated capsule. Daughter cysts and brood capsules bud off from the inner germinal layer producing a multicystic appearance. As the cyst grows, it causes mechanical damage and may interfere with the function of the surrounding organs. The cyst may rupture producing an allergic reaction, even anaphylaxis. Secondary infection may occur, producing signs and symptoms of hepatic abscess. The most common symptom from liver involvement is right upper quadrant abdominal pain. Jaundice may occur if the bile ducts become obstructed [2]. Renal infestation usually results in a painful flank mass and microscopic hematuria [3]. Sometimes daughter cysts are passed in the urine. The patient is usually infected in childhood and the cyst slowly grows for 5–20 years before diagnosis. The cyst may attain a diameter of up to 20 cm. About 20% of patients have multiple cysts; 20%–25% have eosinophilia in the peripheral blood.

Echinococcal disease appears radiographically as a cystic mass lesion in the lungs, liver, or other organs. Some cysts will have calcifications in the wall of the cyst (case 2). If a renal cyst communicates with the collecting system, the cyst may fill with contrast material during excretory urography, and the outline of the daughter cysts can be seen. In noncommunicating cysts, the "goblet" and "crescent" signs have been described in excretory urography [4]. Nephrotomography and angiography may be of value by demonstrating a thick cyst wall.

In both our cases, gray scale ultrasonography demonstrated a mass containing multiple 1–3 cm sonolucent cystic areas. Echinococcal disease should be suspected when such a multicystic mass is seen. Others have reported similar findings [5–7]. King [7] described this

appearance as the "cyst within a cyst" pattern. Careful ultrasound examination can determine the size of the cyst and its relation to surrounding organs. Serologic tests (hemagglutination and flocculation) can then confirm the diagnosis so that proper precautions may be taken at surgery.

REFERENCES

1. Faust EC, Russell PF, Jung RC: *Echinococcus granulosus*, in *Craig & Faust's Clinical Parasitology*, Philadelphia, Lea & Febiger, 1970, pp 541–552
2. Plorde JJ: Echinococciasis, in *Harrison's Principles of Internal Medicine*, edited by Thorn GW, Adams RD, Braunwald E, Isselbacher KJ, Petersdorf RG, New York, McGraw-Hill, 1977, pp 1117–1118
3. Diamond HM, Lyon ES, Hui NT, De Pauw AP: Echinococcal disease of the kidney. *J Urol* 115:742–744, 1975
4. Emmett JB, Witten DM: *Clinical Urography*. Philadelphia, Saunders, 1971
5. Garrett WJ, Kossoff G, Uren RF, Carpenter DA: Gray scale ultrasonic investigation of focal defects on ^{99m}Tc sulphur colloid liver scanning. *Radiology* 119:425–428, 1976
6. Taylor KJW, Carpenter DA, Hill CR, McCready VR: Gray scale ultrasound imagining, the anatomy and pathology of the liver. *Radiology* 119:415–424, 1976
7. King DL: Ultrasonography of echinococcal cysts. *JCU* 1:64–67, 1973

Diffuse Lymphatic Dysplasia with Hepatic Oil Embolism

TAKASHI TATEZAWA[1] AND MASAYOSHI AKISADA[1]

Diffuse abdominal lymphangiectasis with lymphedema of the left leg is reported in a 16-year-old female. Pulmonary, diaphragmatic, renal, and hepatic lymphatics with hepatic oil embolization were demonstrated during bipedal lymphography. This was not associated with chyluria, protein-losing enteropathy, or chylothorax. Presumably this lymphatic abnormality was congenital in origin.

Case Report

F. I., a 16-year-old female, was investigated because of swelling of the left lower extremity for 1 year. On examination, there was moderate edema of the left lower limb, especially of the leg. No other physical abnormalities were found. Renal and liver function tests and blood and urine examinations were normal. The total serum protein was 7.6 g/100 ml; 58% was albumin and 42% globulin. There was no steatorrhea, and the absorption of mono- and disaccharides was normal. Chyluria was not apparent. Except for lymphography, the radiologic examination revealed no significant abnormalities.

Bipedal lymphography was performed injecting 5 ml of Lipiodol Ultra-fluid (Ethiodol) into each side. The lymphatics of the right lower limb were normal. However, in the edematous left lower extremity, an increased number of tortuous lymphatics was opacified with no obvious site of obstruction (fig. 1). In the pelvis there were tortuous and dilated lymphatics in the iliac areas bilaterally with visualization of vessels in the midline, probably in the vulva (fig. 2). Numerous lymphatic channels were seen in the vicinity of the porta hepatis, gallbladder, and liver. The pericalyceal renal lymphatics were densely opacified (figs. 3*A* and 4). Although the thoracic duct was demonstrated only to the level of the diaphragm, the cisterna chyli and the caudal segment of the duct were not dilated. Fine curvilinear vessels along the distribution of the cupola of the diaphragm were considered to represent diaphragmatic lymphatics. A few channels projecting toward the hilum of the lung were thought to be pulmonary lymphatics (fig. 3*B*).

Late phase lymphography revealed numerous small lymph nodes in the paraaortic chain. Persistent opacification of the pericalyceal renal lymphatics was especially obvious on the right. Lipiodol was apparent in and about the liver (fig. 4).

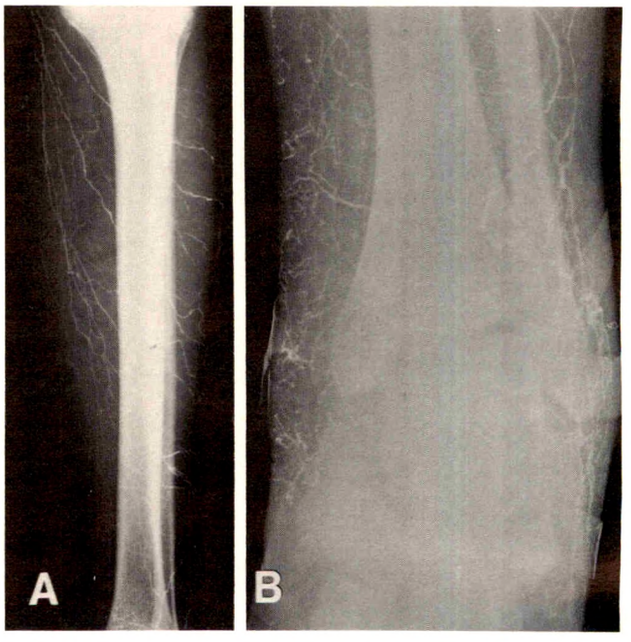

Fig. 1.—Lymphatics of the left leg (*A*) and ankle (*B*) are moderately hyperplastic and ectatic.

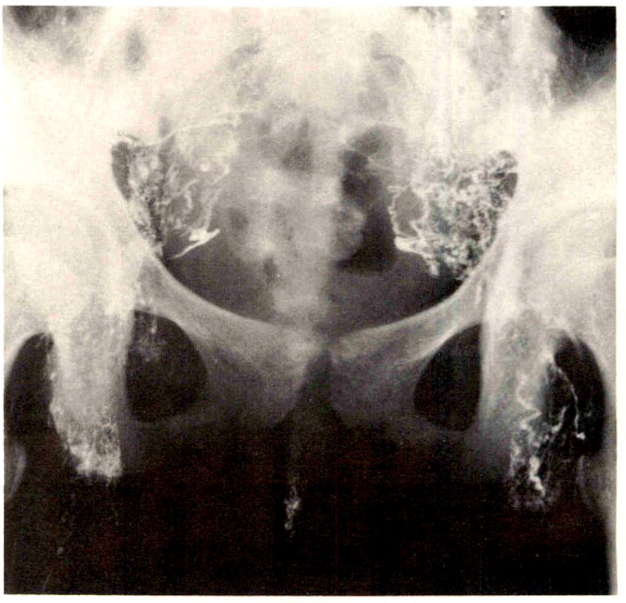

Fig. 2.—Film immediately after lymphogram showing ectatic lymphatic vessels around iliac and vulvar region.

Discussion

Abnormalities of the lymphatics frequently have clinical manifestations such as lymphedema, chyloperitoneum, chyluria, and chylothorax. The etiology of the lymphatic abnormality may be a congenital malformation or acquired obstruction. At times a determination of the etiology is impossible. The term lymphangiectasis refers to a predominance of the ectatic component of the lymphatic abnormality, while lymphangioma denotes a mass effect or tumor [1]. Lymphaticovenous anasto-

Received November 29, 1977; accepted after revision July 6, 1978.
[1] Department of Radiology, Tsukuba University School of Medicine, Niihari-Gun, Ibaraki-Ken 300-31, Japan. Address reprint requests to T. Tatezawa.

© 1978 American Roentgen Ray Society

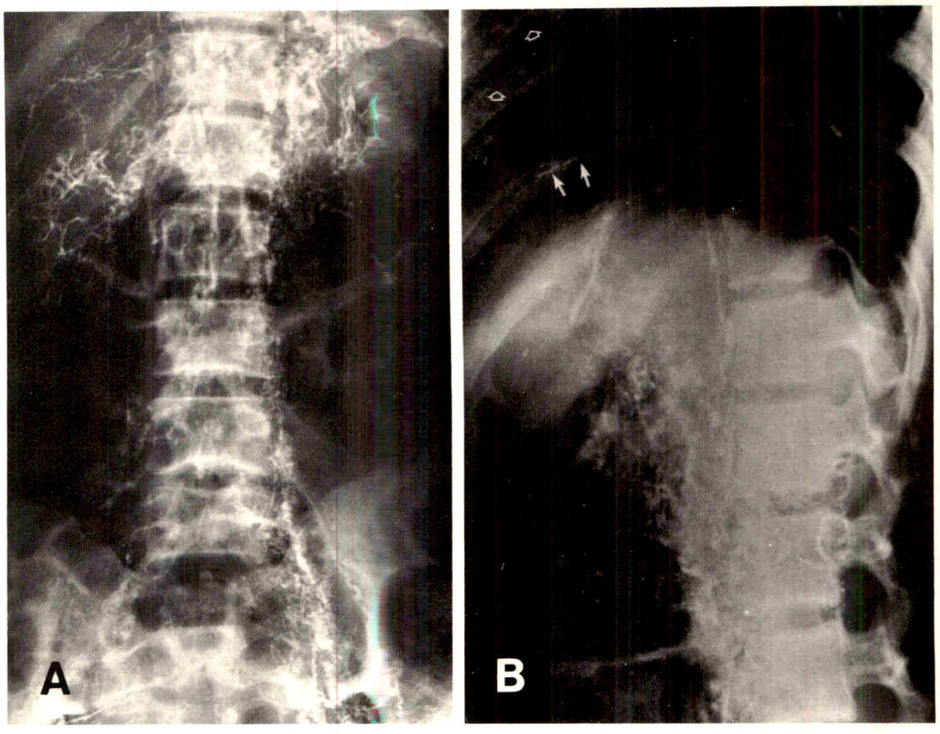

Fig. 3.—Frontal (*A*) and lateral (*B*) views of lymphatic filling phase. Thoracic duct is completely interrupted at level of diaphragm. Caudal segment and cisterna chyli are not dilated. Numerous dilated lymphatics are seen in vicinity of porta hepatis, liver, and gallbladder and within mesentery. Pericalyceal renal lymphatics are well visualized. Note diaphragmatic (*arrows*) and pulmonary (*open arrows*) lymphatics.

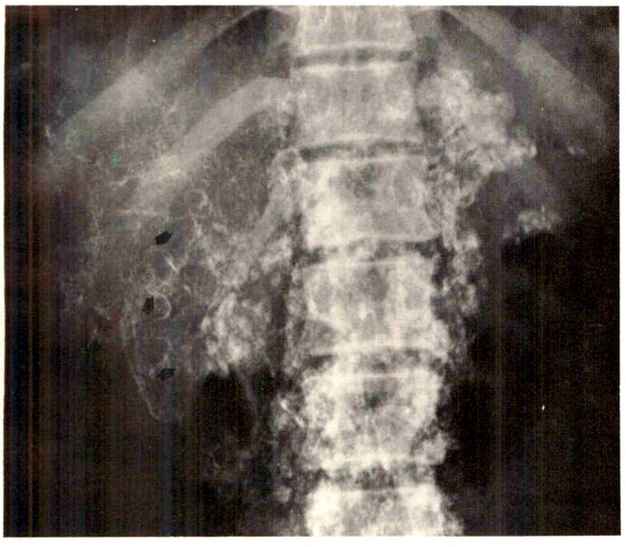

Fig. 4.—Nodal filling phase revealing numerous small lymph nodes of paraaortic lymph chains and Lipiodol within liver. Pericalyceal renal lymphatics are well opacified (*arrows*).

moses, the direct communication between the lymphatics and veins, are explained embryologically in that the primary lymphatic sac buds from the veins.

The term hepatic oil embolism, first described by Leger et al. [2] in 1961, is used to designate a variety of rare conditions in which oil contrast media enters the liver. Though the cause has been debated, hepatic oil embolism theoretically can occur via lymphaticoportal anastomoses or retrograde filling of hepatic lymphatics. Either mechanism may be secondary to lymphatic obstruction, congenital or acquired (infection, trauma including surgical trauma, malignant neoplasms, etc.) [3–5].

In most reported cases, hepatic oil embolism was secondary to obstruction of the thoracic duct or lumbar lymphatics by a malignant tumor in the pelvis or retroperitoneum. It was assumed that hepatic oil embolism was the result of lymphaticoportal anastomoses [3, 4].

In our patient, the thoracic duct was interrupted at the level of the diaphragm with opacification of extensive lymphatic collateral circulation. The deposition of contrast material in the region of the liver (figs. 3*A* and 4) was believed to be primarily within the hepatic capsular lymphatics. The only suggestion of venous filling was in the lateral projection (fig. 3*B*), and this was not sufficiently convincing to implicate lymphaticovenous anastomoses. Therefore, we assume that the hepatic oil embolization in this patient was the result of retrograde filling of hepatic lymphatics.

The visualization of the pericalyceal renal lymphatics was apparently also by retrograde route (fig. 4). The same mechanism was operative in the opacification of the pulmonary lymphatics via the lymphatics of the inferior pulmonary ligament and diaphragm [6] (fig. 3*B*).

Since no obvious obstructing lesion was seen in the posterior mediastinum or retroperitoneum and a local lymphangitis with interruption of the thoracic duct could be excluded, the findings in this patient suggest the occlusion was most likely of congenital origin; that is, a lymphatic dysplasia manifested by diffuse abdominal lymphangiectases and hepatic oil embolism secondary to a congenital lymphatic obstruction or malformation.

REFERENCES

1. Schinas P, Eliades S: Dysplasia of the lymphatic system. *Radiology* 122:357–358, 1977
2. Leger L, Buchet R, Bitry-Boely C, Premont M: Introduction á l'étude de la lymphographie hépatique. *Presse Med* 69:1981–1982, 1961
3. Chavez M, Picard JD, Davis D: Liver opacification following lymphography: pathogenesis and clinical significance. *Surgery* 63:564–570, 1968
4. Akisada M, Tasaki A, Lin S: Hepatic oil embolism: its clinical aspect and pathogenesis. *Nippon Acta Radiol* 28:80–95, 1969
5. Hodes PJ, Dodd GD, Wallace S: Lymphography, in *Gastroenterology*, edited by Bockus HL, Philadelphia, Saunders, 1976, pp 113–132
6. Grant T, Levin B: Lymphangiographic visualization of pleural and pulmonary lymphatics in a patient without chylothorax. *Radiology* 113:49–50, 1974

Free-floating Calculi in the Pericardial Cavity

J. T. LITTLETON[1] AND J. B. CADY[2]

Two relatively large free-floating calculi in the pericardial cavity in a patient with long-standing rheumatic heart disease are the subject of this report. A rather extensive review of the literature failed to disclose any similar calculi within the pericardial sac, nor have we found any report of calcification of epicardial or pericardial rheumatoid granulomata which may have been their origin.

Case Report

A 35-year-old woman was referred to the Robert Packer Hospital because of shortness of breath and edema. History included a prolonged illness at age 13 years with the clinical characteristics of acute rheumatic fever with myocarditis. The heart was enlarged to the left with a grade II/IV rough systolic murmur at the aortic area, radiating to the neck, followed by a low-pitched blowing diastolic murmur along the left sternal border. There was a grade II systolic murmur at the apex with a short thrill. The lungs contained crepitant rales at the bases. Only mild pedal edema was present. The clinical diagnosis was rheumatic heart disease with mitral insufficiency, and aortic stenosis and insufficiency (the latter predominating) with congestive heart failure.

At routine fluoroscopy of the heart, three calcified shadows were seen "dancing" synchronous with cardiac rhythm over the inferior portion of the left apex (fig. 1). The smaller of the three calculi (no. 1) remained stationary relative to other cardiac structures and moved synchronous with systole. The two larger calculi (nos. 2 and 3) had more active motion, and calculus 3 was seen to roll end-on-end (fig. 1). In the supine position, calculus 3 moved widely (fig. 1*B*), while there was lesser displacement of calculus 2. In the lateral projection (fig. 1*C*), two of the calculi were seen to be in a posterior position and the other anterior. It was initially assumed that the two larger calculi were in cardiac chambers, possibly calcified polyps with relatively long stalks, and that calculus 3 was passing from the right ventricle to the right atrium through the tricuspid valve. However, their relative positions in the lateral projection (fig. 1*C*) should have suggested that the calculi were free-floating in the pericardial cavity. Cine studies confirmed the rotational movement of the calculi, further suggesting that they could not be attached to a stalk.

The patient had repeated hospitalizations for congestive failure during the ensuing 12 years and was subsequently found dead in a field near her home. It was estimated that she had been dead 2–3 weeks, and an autopsy authorized by the county coroner was performed by one of us (J. T. Littleton) the next day. Cause of death seemed related to accidental entanglement in a barbed-wire fence under severe winter weather conditions.

The pericardial cavity was smooth and glistening. Lying free within the pericardial cavity were two smooth-surfaced calculi each about 1.8 cm in greatest diameter (fig. 2*A*). At a point about 5 cm superior to the aortic valve, but within the pericardium, there was a reticulated mass of fibrous tissue which included two tiny firm nodules about 0.2 × 0.3 cm in greatest dimension (fig. 1*D*). On the posterior aspect of the heart, there was an area of fibrosis within which was a 0.7 cm calcified mass (fig. 1*D*, calculus 1) of yellow-orange tissue. This calcified nodule is the smaller of the three calculi noted earlier on radiography (figs. 1*A*–1*C*). Sections of the nodule showed it to be confined to the epicardial fat.

Microscopic examination of the myocardium revealed small scattered aggregates of lymphocytes and histiocytes. In occasional foci, there were also scattered polymorphonuclear leukocytes. A very few of the inflammatory cells had the appearance of Anitschkow cells. One or two foci were consistent with Aschoff nodules. There were scattered foci of fibrosis in the myocardium and, in addition, the sections of the papillary muscles showed regions of loss of myocardial fibers. No foci of acute necrosis were identified. A section of the mitral valve showed it to be thickened with hypocellular fibrous tissue. Thick-walled blood vessels extended a moderate distance into the mitral leaflet. In contrast, the aortic valve leaflet had visible vessels almost to its tip.

A section of the right ventricle, including the posterior epicardial nodule (fig. 1, calculus 1), revealed a large region of collagenous epicardial thickening. The nodule was decalcified and appeared to be composed of whorled masses of acellular granular material surrounded by a thick layer of hypocellular collagen (fig. 2*B*). The remaining microscopic findings were noncontributory to the present report. The final pathologic diagnosis was rheumatic heart disease with fibrous thickening of aortic leaflets and apparent insufficiency; calcified partial fusion of mitral valve leaflets with stenosis; residual rheumatic myocarditis; focal nodular calcification of epicardium and calcified loose bodies in the pericardial cavity; hypertrophy of left ventricular myocardium; multiple microscopic healed infarcts; and marked dilatation of left ventricle.

Discussion

Calcification of all cardiac structures has been described in all age groups. Arndt et al. [1] described a case of unusual calcification of the infant heart following infarction. They also reviewed other instances of cardiac calcifications in children, including calcification in endocardial fibroelastosis, myocarditis, intramural fibroma, ischemia, or infarction; and metastatic deposits in hypercalcemic states, such as chronic renal disease, vitamin D intoxication, and infantile hypercalcemia. Calcific deposits have also been reported as pericardial calcification after purulent pericarditis and calcification of the septal muscle mass in idiopathic hypertrophic subaortic stenosis, and with intracardiac tumors such as myxoma and teratoma.

Sutton and Granger [2] described calcification in a

Received August 2, 1977; accepted after revision June 9, 1978.

[1] Robert Packer Hospital, Sayre, Pennsylvania 18840. Present address: Department of Radiology, University of South Alabama College of Medicine, 2451 Fillingim Street, Mobile, Alabama 36617. Address reprint requests to J. T. Littleton.

[2] Robert Packer Hospital, Sayre, Pennsylvania 18840. Present address: 630 South Main Street, Athens, Pennsylvania 18810.

© 1978 American Roentgen Ray Society

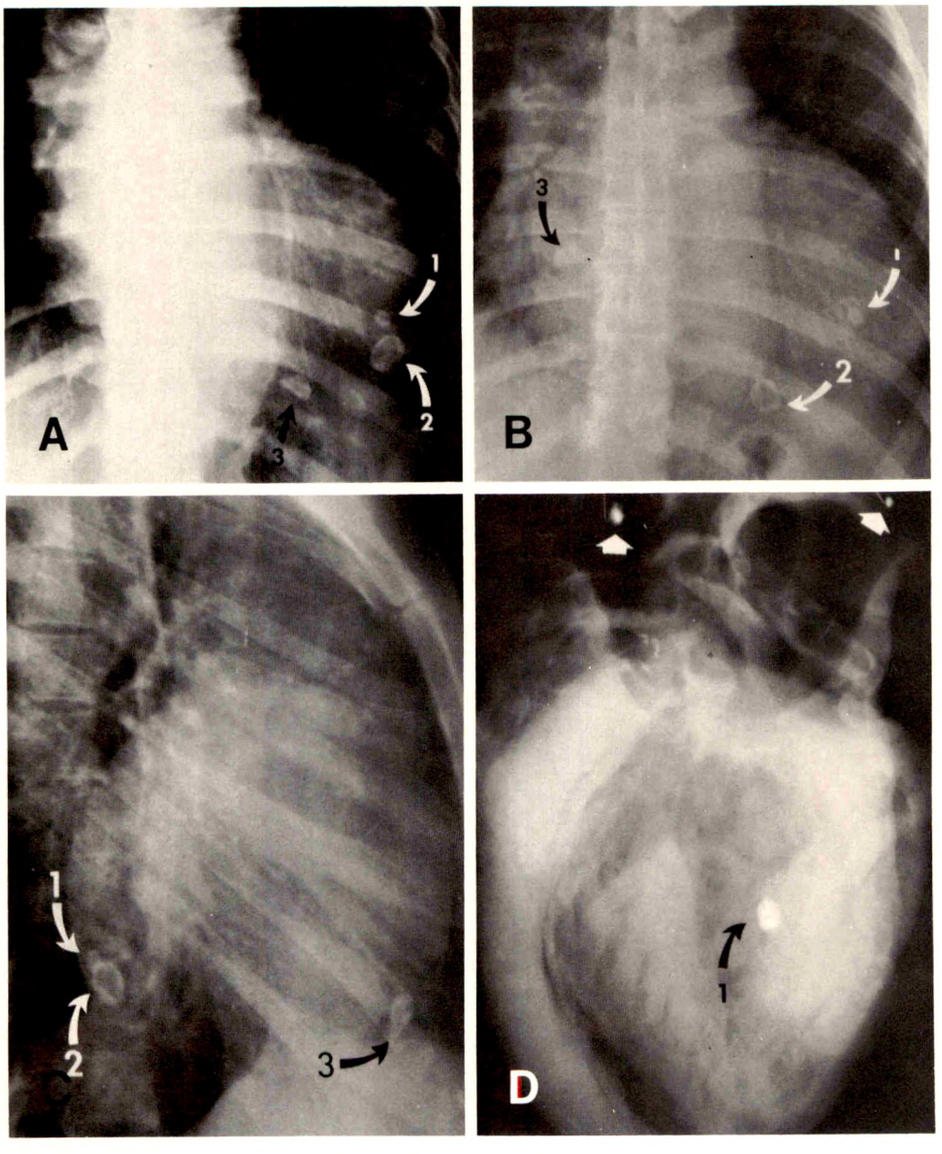

Fig. 1.—*A*, Conventional posteroanterior erect radiograph of chest demonstrating three visible calculi projecting through left margin of heart. Calculus 1 maintained constant position with relation to cardiac activities. Calculus 2 migrated medially and inferiorly with patient in recumbent position. Calculus 3 rotated end-on-end and demonstrated transverse mobility in supine position. *B*, Conventional anteroposterior supine film of chest showing change in position of calculi 2 and 3 with patient recumbent. *C*, Left lateral film of chest with patient in erect position showing relative positions of calculi. *D*, Radiograph of cut specimen of heart showing calcified nidus in each of three otherwise typical rheumatoid nodules. Two smaller calculi (arrowheads) were not appreciated in clinical radiographic studies.

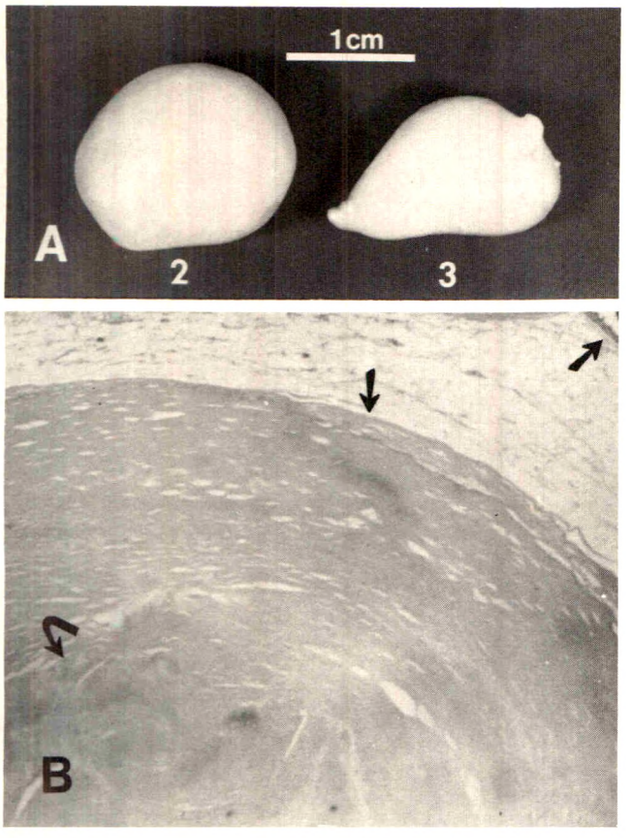

Fig. 2.—*A*, Photograph of calculi 2 and 3, large free-floating calculi recovered from pericardial sac. *B*, Photomicrograph of portion of 0.7 cm nodule, decalcified, in posterior epicardial fat to show cellular relation of calcified central mass. Arrows indicate epicardium and apparent border of calcified tissue. Note scalloped outlines of acellular tissue in center of nodule (*curved arrow*). Original magnification ×25.

mural thrombus. They also described rare causes of intracardiac calcification, such as in tumors (notably an atrial myxoma), metastatic deposits in the myocardium, and calcification of the heart with hydatid disease and Paget's disease. Buenger and Oglesby [3] described calcified polyps within cardiac chambers.

An extensive review of the literature failed to disclose any report of free-floating calculi in the pericardial cavity. The origin of the calculi is a matter of speculation. To our knowledge, calcification of rheumatic nodules has not previously been reported. The fact that there were three smaller calcified foci in granulomatous foci in the epicardium suggests that the two larger calculi may have been extruded from other granulomatous foci in the epicardium or pericardium, perhaps the so-called "milk spots" of chronic or healed rheumatic pericarditis. We would welcome other suggestions.

ACKNOWLEDGMENT

We thank Dr. William C. Luft, Guthrie Clinic and Robert Packer Hospital, for assistance with reviewing and describing the pathologic specimen.

REFERENCES

1. Arnd RD, Smith LE, Po J, Ricchiuti V: Myocardial calcification of the heart following infarction. Detected on the chest roentgenogram: a case report. *Am J Roentgenol* 122:133–136, 1974
2. Sutton D, Granger RG: *A Textbook of Radiology*, 2d ed. Edinburgh, Churchill Livingston, 1975
3. Buenger RE, Oglesby P: Calcified polyp of the heart. *Radiology* 67:531–536, 1956

Focal Perfusion Defect Caused by Sequestration in Two Cases

MICHAEL E. VAN AMAN,[1] THOMAS V. LLOYD, AND JOHN C. JOHNSON

Pulmonary sequestration is a congenital malformation in which a mass of pulmonary tissue, usually in the posterior basilar segment of the lower lobe, has no normal connection with the bronchial tree. The blood supply is systemic, and the venous return is either via the pulmonary veins or azygos system [1, 2]. Pulmonary sequestration is a rare cause of focal perfusion defect on a lung scan.

Case Reports

Case 1

A 34-year-old white female was seen at a community hospital with sudden onset of pleuritic chest pain on the left side. The physical examination and chest radiograph were normal, but the patient had a decreased pO_2 and an abnormal lung scan (fig. 1*A*) showing a perfusion defect in the posterior segment of the left lower lobe. She was treated with anticoagulants and discharged with no further symptoms. She returned 1 month later with a recurrence of the left side chest pain and was transferred to the University Hospital. Pulmonary angiography showed no evidence of pulmonary emboli but did show displacement of the left lower lobe pulmonary arteries around an avascular aerated portion of lung. The levo phase of angiography showed a systemic arterial supply arising from the thoracic aorta at the T11 level supplying a left lower lobe sequestration (fig. 1*B*). The patient has experienced two subsequent episodes of gross hemoptysis, but so far has refused pulmonary surgery.

Case 2

A 19-year-old white female was well until 4 days prior to admission, when she noted a "congested sensation" in her chest and coughed up about 230 ml of bright red sputum. Physical examination and chest radiography from the outpatient department at this time were normal. One day before admission, the patient produced about 115 ml of bright red sputum. She had no chest pain or dyspnea. On admission, physical examination and laboratory studies including blood gases were normal. Posteroanterior chest radiography was interpreted as normal. A lung scan (fig. 2*A*) detected a perfusion defect in the posterior segment of the left lower lobe. An inhalation scan using ^{99m}Tc sulfur colloid (fig. 2*A*) showed a ventilatory defect in the left lower lobe which appeared smaller than the perfusion defect, but in the same anatomic distribution. Pulmonary angiography (fig. 2*B*) showed no evidence of pulmonary embolization. However, the left lower lobe pulmonary arteries were fewer in number than normal and curvilinear, suggesting a mass. Delayed films showed an artery arising from the thoracic aorta at the T9 level supplying a left lower lobe sequestration. Catheterization of the thoracic aorta and selective injection of the two anomalous vessels supplying this sequestered lung were performed 24 hr later (figs. 2*C* and 2*D*). Delayed films of

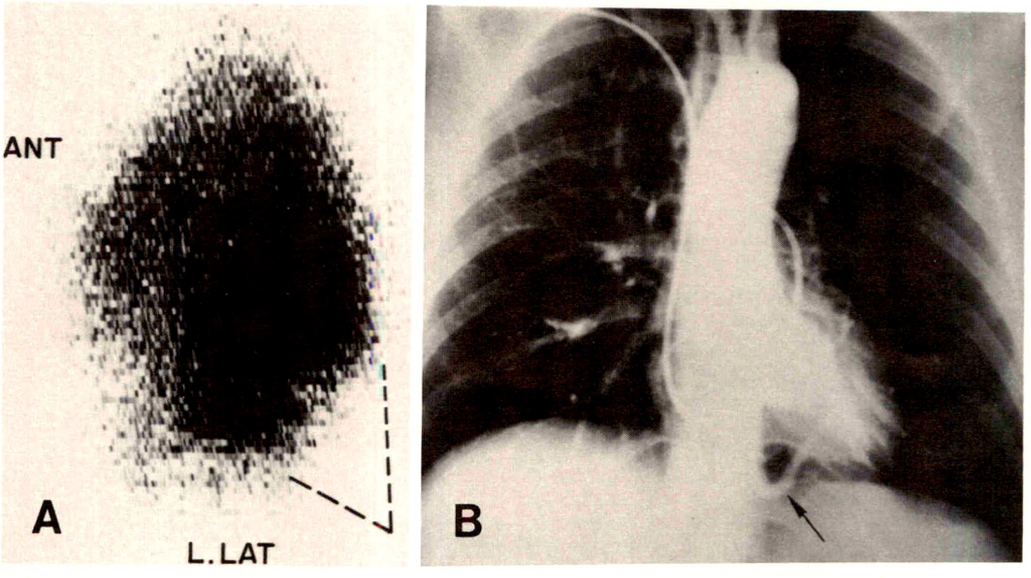

Fig. 1.—Case 1, *A*, Left lateral perfusion lung scan showing segmental perfusion defect in posterior basilar segment. *B*, Levo phase of pulmonary arteriogram demonstrating systemic arterial supply from lower thoracic aorta to left lower lobe sequestration (*arrow*).

Received February 21, 1978; accepted after revision June 23, 1978.
[1]All authors: Department of Radiology, Ohio State University Hospitals, 410 West 10th Avenue, Columbus, Ohio 43210. Address reprint requests to M. E. Van Aman.

© 1978 American Roentgen Ray Society

0361-803X/78/1100-0904 $00.00

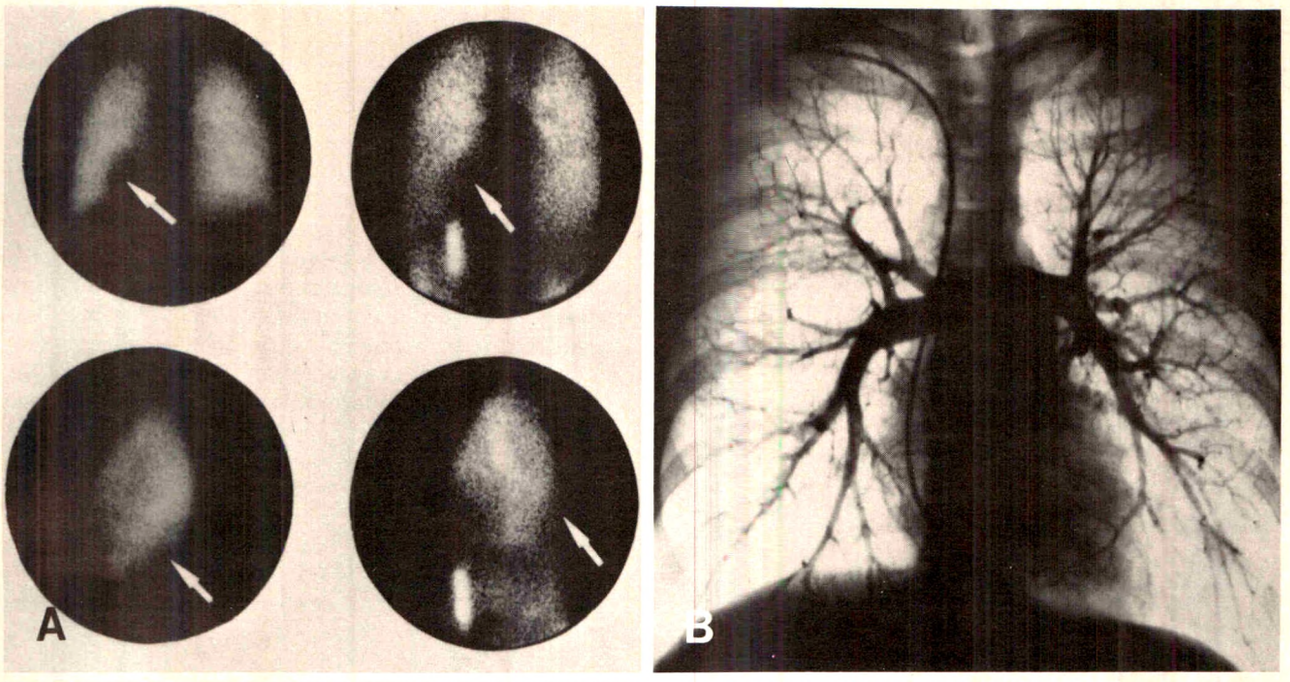

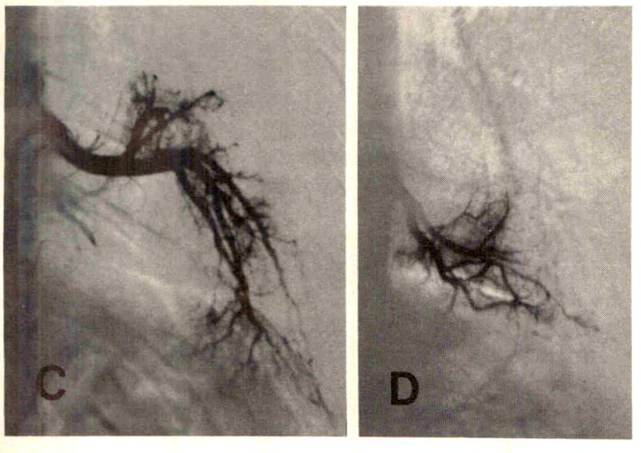

Fig. 2.—Case 2. *A*, Posterior and left lateral views from perfusion lung scan (*left*) showing segmental perfusion defect in posteromedial aspect of left lower lobe (*arrows*). Corresponding view from inhalation lung scan (*right*) showing defect in same area (*arrows*). *B*, Photographic negative of pulmonary arteriogram showing relatively few vessels supplying left base with curvilinear course of some branches suggesting mass effect. *C and D*, Selective injection of two anomalous vessels arising from thoracic aorta supplying sequestered segment of left lower lobe.

the selective injection demonstrated venous return via both the azygos and pulmonary venous system.

Discussion

The high sensitivity and low specificity of the perfusion lung scan is well known and well documented [3–5]. However, sequestration is not usually listed as a cause of false positive lung scans. Our two patients had symptoms very suggestive of embolic episodes; perfusion lung scans were compatible with that diagnosis. Case 2 demonstrated a corresponding ventilation defect, making pulmonary embolus unlikely [6–8].

The presence of unexplained hemoptysis in both patients was very disturbing. We postulate that this was secondary to inflammatory changes in the surrounding normal lung. Such inflammatory changes in association with sequestration are well documented [9] and constitute the rationale for surgical intervention, even when sequestration is found incidentally in an otherwise well patient.

Sequestration should be included in the differential diagnosis of a perfusion defect in the posterior basal segment of either lower lobe. A perfusion-ventilation match and a characteristic location are additional clues to the nonembolic nature of such a defect.

REFERENCES

1. Felson B: The many faces of pulmonary sequestration. *Semin Roentgenol* 7:3–16, 1972
2. Spencer H: *Pathology of the Lung*, 2d ed. Oxford, Pergamon, 1968
3. Bell TK, Ferguson R, McIlbrath EI, Weaver JA: Radioisotope scanning of the lungs. *Thorax* 23:24–32, 1968
4. John PM: The role of lung scanning in pulmonary embolism. *Semin Nucl Med* 1:161–184, 1971
5. Kelly MJ, Elliott LP: The radiologic evaluation of the patient with suspected pulmonary thromboembolic disease. *Med Clin North Am* 59:3–36, 1975
6. Williams O, Lyall J, Vernon M, Croft DN: Ventilation-perfusion lung scanning for pulmonary emboli. *Br Med J* 1:600–602, 1974
7. DeNardo GL, Goodwin DA, Ravaeni R, Detrick PA: Ventilatory lung scan in the diagnosis of pulmonary embolism. *N Engl J Med* 282:1334–1339, 1970
8. Secker-Walker RH, Seigel BA: Use of nuclear medicine in the diagnosis of lung disease. *Radiol Clin North Am* 11:215–241, 1973
9. Khalil KG, Kilman JW: Pulmonary sequestration. *J Thorac Cardiovasc Surg* 70:928–937, 1975

Complications from Intraarterial Lidocaine in Upper Extremity Arteriography

VINCENT P. CHUANG[1] AND WARREN C. WIDRICH[2]

The use of intraarterial lidocaine has been accepted recently as a valuable adjunct in peripheral angiography to decrease or control the pain from contrast medium injection [1–4]. The method was initially evaluated in lower extremity angiography and may be helpful when applied to upper extremity angiography as well. However, during the early experience with this technique for upper extremity angiography, complications have occurred from regurgitation of lidocaine into the cerebral circulation in two patients, one each at two different medical centers. We feel that awareness of this potential complication will help other radiologists avoid similar mistakes.

Case Reports

Case 1

A 29-year-old female was referred to the University of Kentucky Medical Center for evaluation of possible thoracic outlet syndrome. Bilateral subclavian arteriography was performed. The catheter was positioned in the left subclavian artery about 1½ cm distal to the origin of left vertebral artery. One ml of 1% lidocaine (10 mg) was added to every 10 ml of Conray 60. The injection rate was 4 ml/sec for 3 sec; the filming sequence was two films per second for 4 sec, and one film per second for 4 sec. Regurgitation of the contrast medium into the left vertebral artery was observed in the fifth film and subsequently cleared in the sixth film of the sudy. The left subclavian and axillary arteries were normal. The patient experienced severe tinnitus and was unable to respond to questions immediately after arteriography. Her vital signs remained normal. There were no signs of neurologic deficit. She returned to normal conscious status 5 min later. Further angiographic studies, including left and right subclavian arteriograms with left and right arms in hyperextension, were done omitting intraarterial lidocaine without complication.

Case 2

A 47-year-old male was admitted to the Boston Veteran's Administration Hospital complaining of pain and tingling sensation in the right second, third, and fourth fingers for 3 weeks. Physical examination revealed diminished right radial pulse and coldness and ulceration of the tips of the same fingers. Right upper extremity arteriography was performed with the catheter tip in the mid-subclavian artery. Two ml of 2% lidocaine (20 mg) was injected through a three-way stopcock, followed immediately by 15 ml of methyglucamine iothalamate at 10 ml/sec. Several seconds after contrast injection, the patient developed a grand mal seizure but subsequently recovered without residual signs or symptoms.

Discussion

The angiographic evaluation of thoracic outlet syndrome, upper extremity claudication, and digital artery embolism frequently requires multiple arterial injections of contrast medium. The injection of contrast material into the upper extremity arterial system is as painful, and frequently more painful, than injection into the lower extremity. Occasionally, a patient will refuse to have more studies after the initial arteriography, thus making angiographic workup incomplete. Consequently, it was natural to extend the favorable experience of lidocaine in lower extremity arteriography to the upper extremity.

In case 1, the contrast medium regurgitated into the left vertebral artery for 0.5–1 sec, and probably did not total more than 2 ml of contrast medium (or 2 mg of lidocaine). The reaction was thus mild, causing only tinnitus. In case 2, since the lidocaine was given in a bolus injection, it is difficult to estimate the amount that regurgitated into the cerebral circulation. Very possibly, the amount was larger than in case 1. Consequently, the reaction was more severe (i.e., a grand mal seizure).

Both cases occurred early in the development of this technique. Subsequently, we have used intraarterial lidocaine without complication in many upper extremity arteriograms, by assuring that the catheter tip is distal to the third segment of the axillary artery. Currently, we use 2 mg lidocaine per 1 ml contrast medium. This is done by mixing 1 ml of 2% lidocaine with every 10 ml of contrast medium. The arterial flow is estimated by test injection under fluoroscopy and the injection rate is determined accordingly.

A preliminary study comparing subclavian arteriography without lidocaine and brachial arteriography with lidocaine in the same extremity has shown marked reduction of pain in some patients, but others have had minimal or no relief of pain. Individual variation in response to lidocaine is apparently present. A prospective randomized study has not been done.

REFERENCES

1. Guthaner DF, Silverman JF, Hayden WG, Wexler L: Intraarterial analgesia in peripheral angiography. *Am J Roentgenol* 128:737–739, 1977
2. Widrich WC, Singer RJ, Robbins AH: The use of intra-arterial lidocaine to control pain due to aortofemoral arteriography. *Radiology* 124:37–41, 1977
3. Gordon IJ, Westcott JL: Intra-arterial lidocaine: an effective analgesic for peripheral angiography. *Radiology* 124:43–45, 1977
4. Widrich WC, Robbins AH: Adjuvant intra-arterial lidocaine in aorto-femoral arteriography: some further observations. *Radiology*. In press, 1978

Received April 25, 1978; accepted after revision July 20, 1978.

[1] Department of Diagnostic Radiology, University of Kentucky Medical Center, Lexington, Kentucky 40506. Present address: Department of Diagnostic Radiology, M. D. Anderson Hospital and Tumor Institute, 6723 Bertner Avenue, Houston, Texas 77030. Address reprint requests to V. P. Chuang.

[2] Radiology Service, Boston Veterans Administration Hospital, Tufts University School of Medicine, Boston, Massachusetts 02136.

© 1978 American Roentgen Ray Society

Ultrasonic Visualization of a Cervical Cord Cystic Astrocytoma

MICHAEL H. REID

Clinical ultrasound is well known for its ability to provide diagnostic information of abdominal organs and other soft tissue parts. However, its utility in evaluating lesions of the spinal cord has yet to be reported. We used both focused and narrow beam ultrasound to visualize the spinal cord. This report describes the findings in a cervical cystic astrocytoma.

Case Report

A 50-year-old white male automobile mechanic was admitted because of pain, weakness, and numbness in the right arm and fingers for 1½ years, and difficulty walking for 1 year. Neurologic examination confirmed the muscle weakness and hypesthesia. Laboratory results were unremarkable except for a cerebrospinal fluid protein of 103 mg/100 ml. Computed tomography of the cervical and upper thoracic spine was normal. Pantopaque myelography revealed a widened cord from C2 to T1 levels (figs. 1*A* and 1*B*), and air myelography (fig. 1*C*) again showed a widened cord which did not collapse with positional changes of the patient. An ultrasound examination suggested an anterior cystic component accounting for at least part of the cervical cord widening (fig. 2*A*). At decompression laminectomy from C3 through C7, a nonpulsatile enlarged cord with normal vascularity was found. There was no gross evidence of tumor. Needle aspirate from the cord yielded 3 ml of fluid with negative cytology. There was slight transient improvement in symptoms following the laminectomy.

Because of the possibility of a cystic component within the cord, further needle aspiration of the cord was attempted with fluoroscopic guidance, but no fluid could be obtained. Lateral radiography demonstrated the needle tip about midway within the spinal canal. Repeat ultrasound clearly showed the cervical cord with an extensive anterior cystic component which lay just anterior to the needle tip at the previous attempted aspiration (figs. 2*B* and 2*C*). There was no variation in cyst appearance with positional (prone vs. upright) changes. At reoperation, the anterior cyst was identified and tissue fragments were obtained from the area; they were interpreted as a mixed ependymoma and cystic astrocytoma, grade 1. The patient has had some amelioration of symptoms over the subsequent months, but right arm weakness persists.

Discussion

Focused ultrasound [1] was used to evaluate the spinal cord using a 13 mm diameter, 3.5 MHz transducer and a specially fabricated 6 mm diameter, 4.0 MHz transducer. Scans of the cervical cord are obtained posteriorly with the neck flexed, with the best cord definition provided when the scan plane is parallel to the interlaminar spaces. In this fashion, it is possible to obliquely transect the cord between the posterior arches and minimize the effects of overlying bone. The narrow diameter, 4.0 MHz transducer is particularly useful because penetration, beam collimation, and width of interlaminar spaces are closely matched. Flexing the neck to one side to open the interlaminar "window" is occasionally helpful. Longitudinal scans obtained with the neck fully flexed and the transducer off midline and directed toward the cord can be obtained as the transducer passes over the interlaminar spaces. If the ultrasound amplifier gain is reduced to permit rescanning without overwriting the image then arc-sector scans can be formed at each

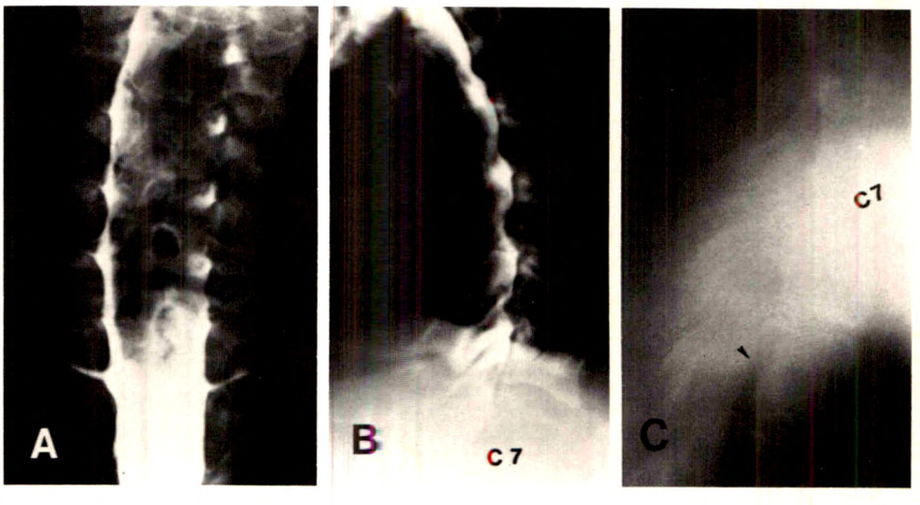

Fig. 1.—*A and B,* Pantopaque myelogram demonstrating extensive cervical cord widening. *C,* Gas myelogram with patient in near-vertical position without change in cervical cord diameter. Gas column is limited by widened cord (*arrow*).

Received January 10, 1978; accepted after revision July 18, 1978.

[1] Department of Diagnostic Radiology, University of California, Davis, School of Medicine, and Sacramento Medical Center, 4301 X Street, Sacramento, California 95817.

© 1978 American Roentgen Ray Society

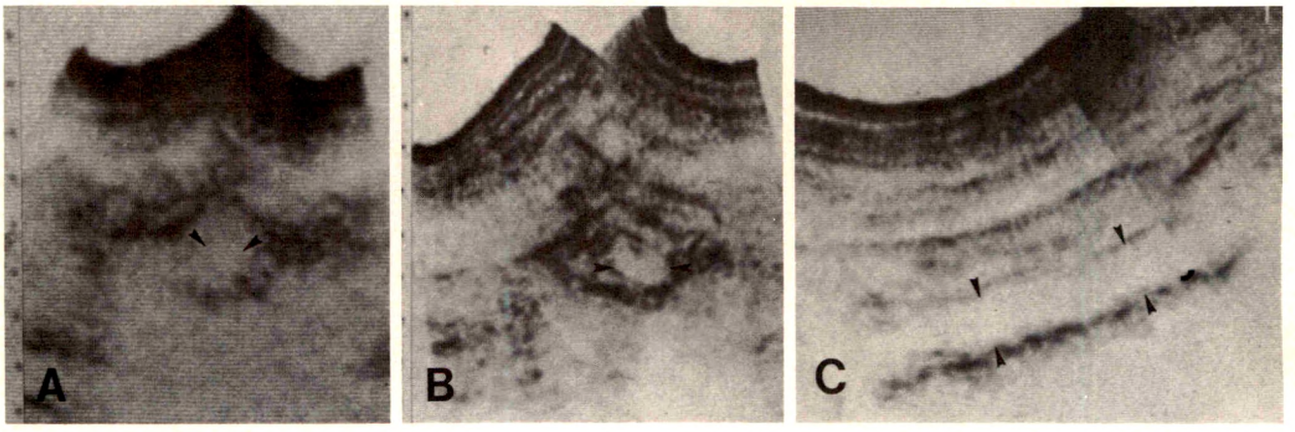

Fig. 2.—*A*, Transverse arc-sector scan of cervical canal at C3-C4 level. Anterior cystic cord lesion (*arrows*) suggested on multiple scans from C2–C3 to C6–C7 levels. *B* and *C*, Post laminectomy transverse (*B*) and longitudinal (*C*) scans of the mid-cervical cord demonstrating large anterior cord cystic lesion (*arrows*) which did not vary with changes in patient position.

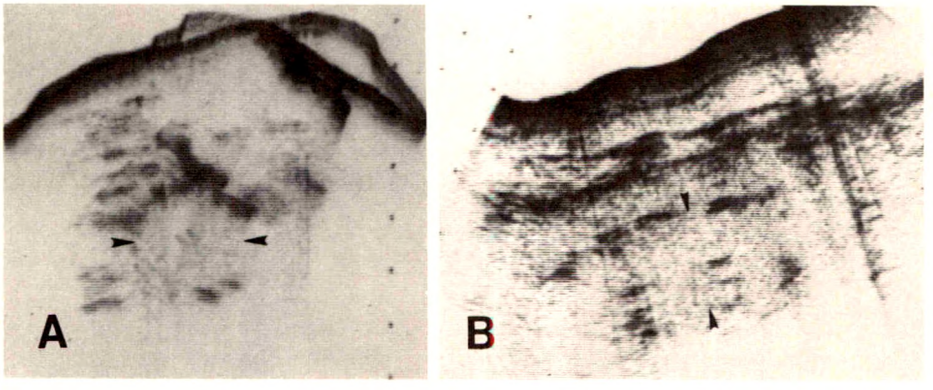

Fig. 3.—*A*, Transverse arc-sector scan of cervical canal of normal young woman at C3–C4 level demonstrating normal spinal cord (*arrows*). Smaller cluster of echoes centrally in cord are nearly always seen and may represent tissue interface at central canal. *B*, Longitudinal arc-sector scan of cervical canal demonstrating normal spinal cord (*arrows*). Intermittent central echoes are reverberation echoes from overlying bony lamina. Scan obtained with transducer off midline (to avoid spinous processes) and angled medially.

interlaminar space on the longitudinal scan. Similarly, transverse arc-sector scans through the open lamina may be obtained (fig. 2*A*). A normal scan of the cervical cord is shown for comparison (fig. 3). The procedure is noninvasive and, if further perfected, may replace air myelography in certain instances.

Widening of the cervical cord over a number of vertebral segments is usually a result of syringomyelia (hydromyelia) or intramedullary tumor such as ependymoma or astrocytoma. Syringomyelia can generally be differentiated from intramedullary cystic tumors by: (1) age (average, 24 vs. 34 years); (2) duration of symptoms (average, 10 vs. 5 years); (3) the fact that paresis and sensory loss are more common in syringomyelia; and (4) cerebrospinal fluid protein levels are nearly always less than 70 mg/100 ml in syringomyelia and above this level in intramedullary neoplasm [2]. Radiologically, measurements of canal width on plain film examination of the cervical spine are occasionally helpful [3]. Pantopaque myelography will confirm the presence of a widened cord; however, the more diagnostic examination is gas myelography, where change in size of the widened cervical cord may be noted with change in patient positioning in nearly all cases of syringomyelia and only minimally in about 25% of cases with cystic neoplasms [2, 4, 5]. A single report using computed tomography in syringomyelia showed three of nine proven cases with positive CT findings [6]. The use of ultrasound throughout the entire spinal canal is currently being evaluated; findings will be reported in a subsequent paper.

REFERENCES

1. Reid MH: Visualization of the bile ducts using focused ultrasound. *Radiology* 118:155–158, 1976
2. Ellertsson AB: Syringomyelia and other cystic spinal cord lesions. *Acta Radiol* (Stockh) 45:403–417, 1969
3. Dolan KN: Expanding lesions of the cervical spinal canal. *Radiol Clin North Am* 15:203–214, 1977
4. Westberg G: Gas myelography and percutaneous puncture in the diagnosis of spinal cord cysts. *Acta Radiol [Suppl]* (Stockh) 252:1–67, 1966
5. Bradac GB: The value of gas myelography in the diagnosis of syringomyelia. *Neuroradiology* 4:41–45, 1972
6. Di Chiro G, Axelbaum SP, Schellinger D, Twigg HL, Ledley RS: Computerized axial tomography in syringomyelia. *N Engl J Med* 292:13–16, 1975

Huge Laparotomy Pad Granuloma Simulating a Gastric Wall Tumor

EDWARD W. CARSKY[1] AND DONALD M. HASWELL[1]

Few reports in the recent literature discuss complications of gauze sponges and laparotomy pads left at surgery [1–3]. Fewer still describe their radiographic appearance [1, 3]. This is understandable in light of the medicolegal liability implied in this technical oversight.

Most patients with a surgical sponge left in the abdomen will develop complications within a matter of weeks or months [4]. Radiography at that time will usually show the opaque marker of the surgical sponge or laparotomy pad, and the condition is surgically corrected. However, when the marker has been present for a long time, the marker may become mottled and granular and may not be correctly identified.

We report a case of a retained laparotomy sponge eroding the stomach wall of a patient 12 years after initial surgery at another institution. The disintegrating opaque marker was obvious, but its significance was not appreciated, and therefore the foreign body granulomatous mass involving the gastric wall was diagnosed as a gastric neoplasm.

Case Report

R. B., a 56-year-old female, was admitted to the emergency room complaining of an enlarging upper abdominal mass, tarry bowel movements, and weakness. Surgical history included cholecystectomy 12 years earlier and a hysterectomy 15 years earlier.

Physical examination revealed a markedly pale female with some respiratory distress and tachycardia of 110. There was a huge, minimally mobile abdominal mass about 25 cm in diameter located primarily in the left upper quadrant. Rectal examination revealed soft tarry stool. The hematocrit was 9 mg/100 ml; calcium, 7.5 mg/100 ml; albumin 2.8 mg/100 ml; bilirubin, 2.6 mg/100 ml with 0.7 mg/100 ml direct and 1.9 mg/100 ml indirect. Other laboratory tests were within normal limits. The plain film of the abdomen (fig. 1*A*) showed a large soft tissue mass in the left upper quadrant with some small oval metallic densities near the periphery of the mass. Abdominal ultrasound demonstrated a large, partially solid, partially cystic mass. The upper gastrointestinal series (fig. 1*B*) revealed that the large mass was intimately associated with the stomach and either arose from or was very intimately applied to it. Angiography showed that the mass arose from the wall of the stomach with hypertrophy of vessels supplying the mass. The gastroepiploic artery was displaced away from the lumen of the stomach, establishing the intramural location of the mass (fig. 1*C*).

Gastroscopy demonstrated an ulcer on the greater curvature of the stomach, with the greater curvature markedly smoothed out and indented by the large extrinsic mass. An attempted brush biopsy of the ulcer base resulted in brisk bleeding.

The patient underwent exploratory surgery with a preoperative diagnosis of gastric leiomyosarcoma. The lesion was found to arise from the wall of the stomach, and a Billroth II procedure was performed. There were numerous adhesions. An abscess which developed on postoperative day 18 was drained and cleared completely on antibiotics.

Examination of the specimen disclosed a mass 27 cm in diameter weighing 4,470 g. On cut section, it was semicystic containing atheromatous material and clotted and unclotted blood. There were two ulcers of the stomach, both of which communicated with this huge "aneurysmlike" cyst. Within the cyst, there was a meshlike foreign body suggestive of gauze. Microscopically under polarized light, the meshlike material had a regular symmetrical pattern. The final pathologic diagnosis was foreign body granuloma secondary to surgical sponge or laparotomy pad.

Discussion

Since Crossin and Crossin [4] reported on 307 cases of retained sponges and laparotomy pads in 1940, there have been few reports of the complication. This is probably the result of improved surgical technique with routine sponge count which has reduced the number of complications, plus limited reporting of this complication because of the potential medicolegal implications.

The pathology as described by Olnick et al. [1] and Crossin and Crossin [4] may be of the exudative or of the aseptic fibrous type. In the exudative type, the body reacts to the foreign substance with abscess formation, often with secondary bacterial invasion. With the development of an abscess, the body will attempt to extrude the foreign material, either externally or into a hollow viscus, usually the small intestine or colon, rarely the bladder. Most abscesses are diagnosed and treated in the early postoperative period because of urgent clinical symptoms.

In the aseptic fibrous type, there is encapsulation in response to the low grade inflammation. In their classic book, Crossin and Crossin [4] showed that this form is the most common type after the sponge has been present for 5 or more years. These may gradually increase in size and are discovered incidentally at surgery for an unrelated condition or because the mass is thought to be a tumor. Our case is an example of the latter and appears to be larger than any of those reported by Crossin and Crossin.

The most important clue is the radiopaque insert which is either monofilament or ribbon. However, it is important to realize that sponge and laparotomy pad inserts can vary markedly in shape and appearance. After about 5 years, these begin to disintegrate so that the opaque portion may change markedly from its original appearance, even resembling mucosal folds in one reported case [3]. Our case is an example of the ribbon type with checkerboard squares that have, with time, separated and rounded off to appear as oval opaque densities. They have separated because the supporting

Received May 12, 1978; accepted July 26, 1978.
[1] Department of Radiology, St. Joseph's Hospital Health Center, Syracuse, New York 13203. Address reprint requests to E. W. Carsky.

© 1978 American Roentgen Ray Society

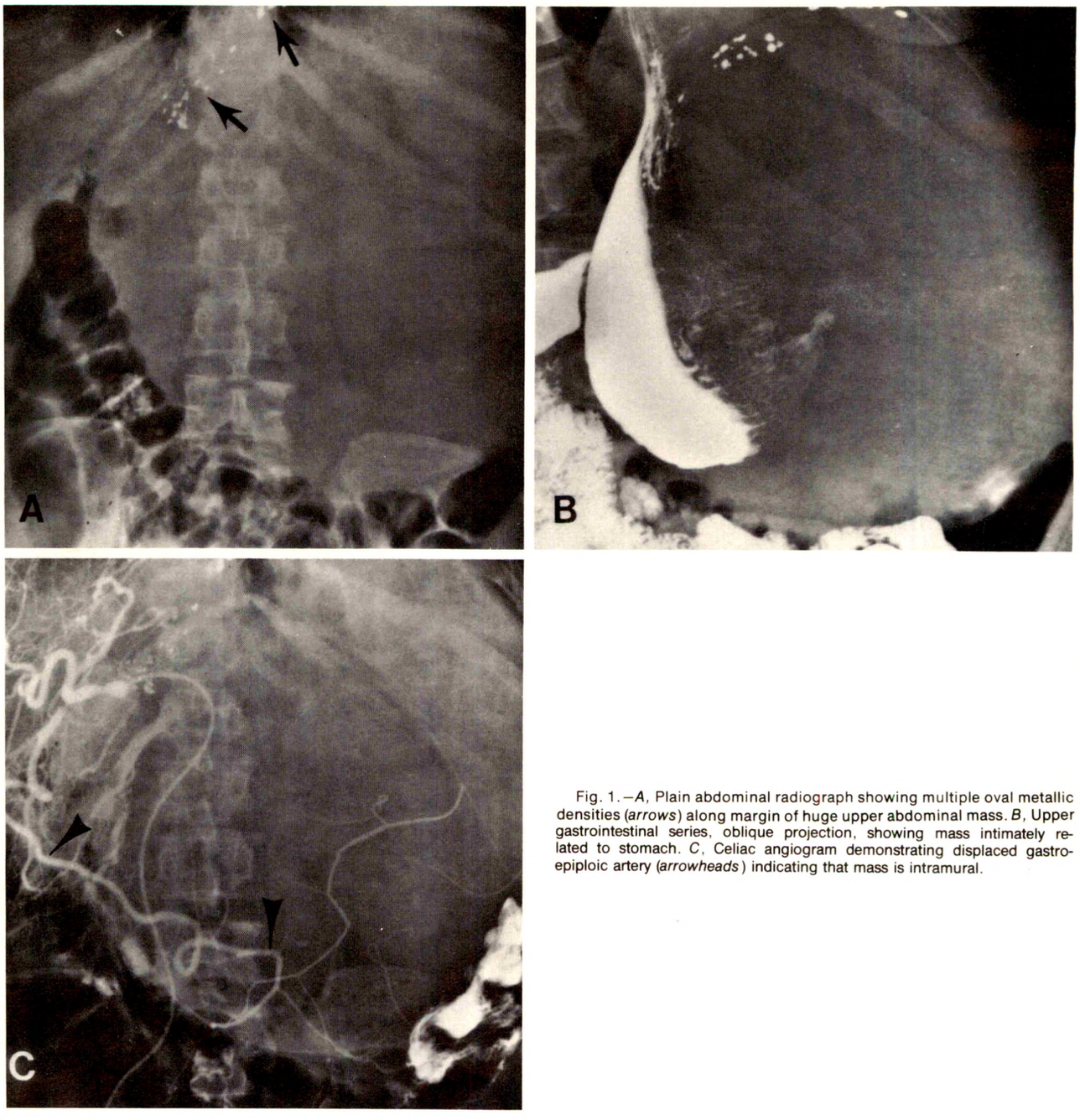

Fig. 1.—*A*, Plain abdominal radiograph showing multiple oval metallic densities (*arrows*) along margin of huge upper abdominal mass. *B*, Upper gastrointestinal series, oblique projection, showing mass intimately related to stomach. *C*, Celiac angiogram demonstrating displaced gastroepiploic artery (*arrowheads*) indicating that mass is intramural.

fabric has deteriorated. Our patient serves as a reminder that this diagnosis should be considered whenever opaque metallic material is seen in association with a mass in a patient who has had prior surgery.

REFERENCES

1. Olnick HM, Weens HS, Rogers JV Jr: Radiological diagnosis of retained surgical sponges. *JAMA* 195:1525–1527, 1955
2. Wells HA Jr, Hyun BH, Mitchell RE: A retained surgical sponge with interesting sequelae. *Am J Med* 35:423–426, 1963
3. Weens HS, Rogers JV Jr: Roentgenologic recognition of radiopaque sponges. *Am J Roentgenol* 61:706–710, 1949
4. Crossin HS, Crossin DF: *Foreign Bodies Left in the Abdomen: the Surgical Problems, Cases, Treatment, Prevention: the Legal Problems, Cases, Decisions, Responsibilities*. St. Louis, Mosby, 1940

Enlargement of the Intervertebral Foramina: An Unusual Cause

DUSHYANT V. PATEL,[1] R. J. LAWRENCE FERGUSON,[2] AND WILLIAM L. SCHEY[1]

Dejerine-Sottas syndrome or hypertrophic interstitial polyneuritis is a rare disease of unknown etiology. It is characterized by thickening of the nerves due to hyperplasia of the sheath of Schwann. The disease may involve one or more peripheral, spinal, or cranial nerves or cauda equina [1–4]. The diagnosis is generally made in later life since the clinical manifestations are not usually apparent in childhood.

We recently examined a 17-year-old male with this disease in whom there was bilateral enlargement of multiple cervical intervertebral foramina. This and other plain film findings have not been mentioned in any reports and are therefore presented in this communication.

Case Report

J. A. B., a 17-year-old black male, was admitted to Michael Reese Medical Center with a 1-month history of pain in the right leg and lower back. The pain in the leg was constant and believed caused by muscle spasm. The back pain was relieved by flexion of the knee and augmented by knee extension associated with hip flexion. The patient developed similar symptoms in the left leg 2 weeks prior to admission. At the time of admission he was unable to walk.

At age 17 years he was hospitalized because of abdominal pain, failure to thrive, headaches, and subcutaneous cordlike nodules down the lateral aspect of the leg. A biopsy of a nodule from the right leg was obtained. The specimen was reported to be a neurofibroma, and the patient was thought to have neurofibromatosis. The family history was noncontributory.

Physical examination at this admission showed a slightly underweight and short individual with normal-sized head. He was well oriented and of normal intelligence. There was marked atrophy of all extremities, especially distally, and the patient had a decreased position sense. The plantar reflexes were normal bilaterally.

The cerebrospinal fluid was clear and colorless. It contained 520 mg/100 ml protein. Electromyographic findings were compatible with peripheral neuropathy. Radiographs revealed marked bilateral enlargement of multiple intervertebral foramina in the cervical spine (fig. 1). In the lumbar region there was scalloping of the dorsum of several lumbar vertebral bodies and a triangular shape of the pedicles at L5.

Myelography was difficult to perform. At the time of lumbar puncture there was slow flow of cerebrospinal fluid. A small amount of Pantopaque was introduced under fluoroscopic control. The column moved slowly and the contrast was thought to be subdural; however, the lateral radiograph confirmed the subarachnoid location of the needle tip and Pantopaque.

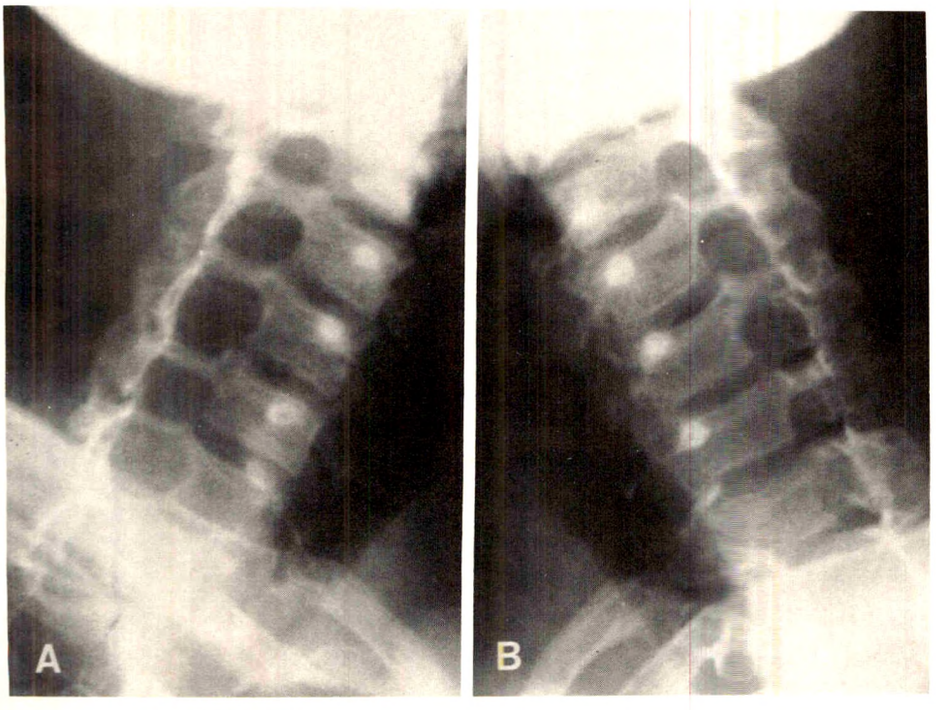

Fig. 1.—Oblique views of cervical spine demonstrating markedly enlarged intervertebral foramina.

Received March 22, 1978; accepted after revision July 26, 1978.

[1] Department of Radiology, Michael Reese Medical Center, 29th Street and Ellis Avenue, Chicago, Illinois 60616. Address reprint requests to D. V. Patel.

[2] Department of Neurosurgery, Michael Reese Medical Center, Chicago, Illinois 60616.

© 1978 American Roentgen Ray Society

0361–803X/78/1100–0911 $00.00

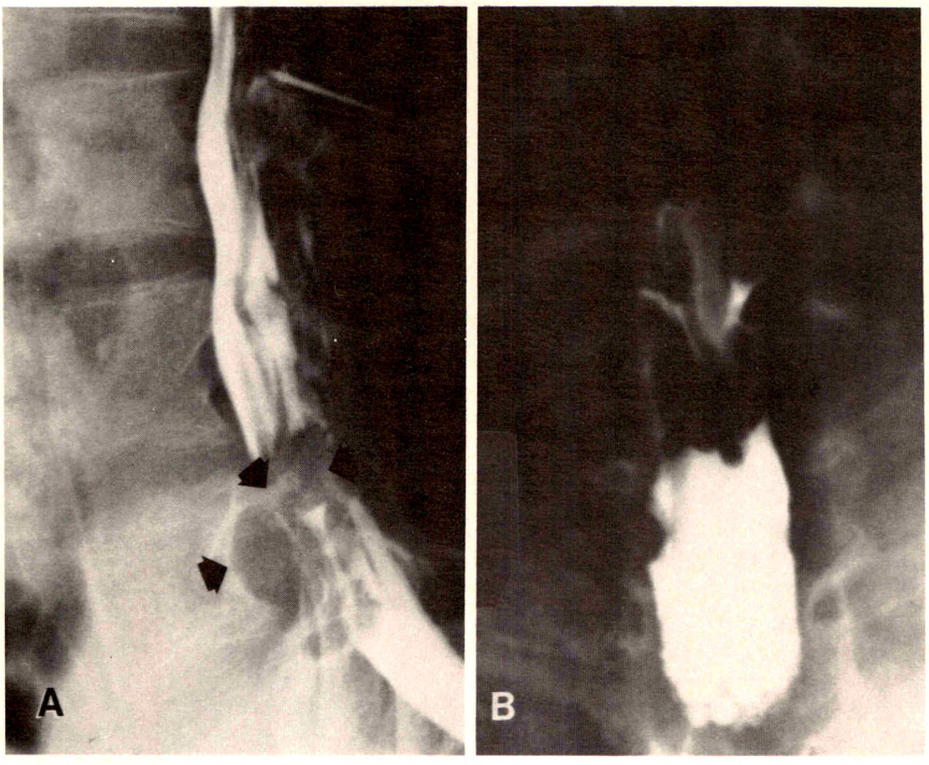

Fig. 2.—*A*, Cross-table lateral radiograph during lumbar myelography. Filling defect in oily contrast (*upper arrows*) demonstrates marked thickening of nerves. Vertical lucencies throughout column of contrast also represent nerve root thickening. Scalloping of dorsal portion of fifth lumbar vertebra is also evident (*lowest arrow*). *B*, Posteroanterior radiograph during myelography demonstrating almost complete obstruction to flow of contrast with narrowing of band of contrast above site of major obstruction.

Additional Pantopaque was then introduced. Linear intradural defects were noted in the lumbar region with areas of nodular defects at the intervertebral disc levels (fig. 2*A*). The dorsal region was not remarkable. There was almost complete obstruction to the flow of contrast medium at C7–T1 with no filling above the C5 level (fig. 2*B*). Nodular defects in the Pantopaque column at C6 and C7 levels were interpreted as partly intradural, but because of incomplete filling, extradural masses could not be excluded. The findings were thought to be due either to multiple intradural tumors with extradural extensions as seen in patients with neurofibromas or hypertrophic interstitial polyneuritis.

Laminectomy was performed in the lower cervical region. Biopsy of a nodular lesion demonstrated changes due to hypertrophic interstitial polyneuritis. Previous biopsy sections from 1969 were reanalyzed by another neuropathologist who felt that those changes were characteristic of Dejerine-Sottas syndrome.

Discussion

The plain film radiographic features of this disease are related to swelling of the sheaths and nerve roots within the vertebral canal and in the intervertebral foramina [1, 5]. They include scalloping of the dorsum of vertebral bodies (perhaps related to pooling of cerebral spinal fluid) [1, 3, 6], an enlarged interpediculate distance, and a triangular configuration of the pedicle. This latter feature is attributed to the chronic increase in intervertebral canal pressures on the medial side and pressure of the thickened nerve root on the inferior aspect [1].

Our patient had striking enlargement of cervical intervertebral foramina bilaterally at several levels. Review of the previous literature and radiographs did not reveal this feature. It is possible that enlarged intervertebral foramina were present but were not recognized due to the failure to obtain oblique projections of the cervical spine.

Enlarged cervical intervertebral foramina have been reported secondary to neurofibromas, dermoids, teratomas, fibromas, absent pedicle, and erosion by a tortuous vertebral artery [7, 8]. Multiple enlarged intervertebral foramina are most often associated with neurofibromatosis [8].

Rao et al. [3] found seven cases of hypertrophic neuropathy with abnormal myelographic findings in the English language literature and added two of their own cases. They did not describe what we believe are important plain film manifestations. Their description of characteristic myelographic findings in addition to those described by other authors include: (1) slow flow of Pantopaque in the subarachnoid space; (2) partial or complete obstruction of the flow of contrast; (3) parallel linear radiolucencies due to enlarged nerve roots; (4) round or oval filling defects located at the level of intervertebral foramina; (5) medial displacement of Pantopaque by enlarged nerve roots; and (6) bizarre appearance to contrast due to large hypertrophied nerves. All of these findings were present in our patient associated with apparently unique enlargement of the cervical intervertebral foramina.

ACKNOWLEDGMENT

We thank Debra James for editing and typing.

REFERENCES

1. Bellon EM, Kaufman B, Tucker ME: Hypertrophic neuropathy: plain film and myelographic changes. *Radiology* 103:319–322, 1972.

2. Brawley BW, Kelly WA: Interstitial hypertrophic neuritis of the eighth cranial nerve: case report. *J Neurosurg* 25:461–463, 1966
3. Rao CVGK, Fitz CR, Harwood-Nash DC: Dejerine-Sottas syndrome in children. *Am J Roentgenol* 122:70–74, 1974
4. Shapiro R: Myelography, 3d ed. Chicago, Year Book Medical Publishers, 1975
5. Harwood-Nash D, Fitz CR: *Neuroradiology in Infants and Children*. St. Louis, Mosby, 1976
6. Hinck VC, Suchden NS: Myelographic findings in hypertrophic interstitial neuritis. *Am J Roentgenol* 95:947–948, 1965
7. Danziger J, Bloch S: The widened cervical intervertebral foramen. *Radiology* 116:671–674, 1974
8. Dolan KD: Expanding lesions of the cervical spine canal. *Radiol Clin North Am* 15:203–214, 1977

Chlamydia trachomatis: A Cause of an Infantile Pneumonia Syndrome

RANDALL H. STICKNEY,[1] JOHN C. BJELLAND,[1] M. PAUL CAPP,[1] R. ROBERT HARRISON,[2] AND RONALD HANSEN[2]

The afebrile infant with a productive cough can pose diagnostic and therapeutic problems. Recent clinical reports have documented *Chlamydia trachomatis* as the etiologic agent in many of these cases [1–3]. These reports also suggest amenability to antimicrobial therapy [2], making early diagnosis essential. Awareness of the radiographic findings of the disease is important in such cases.

Case Report

An afebrile 10-week-old black female with an uneventful neonatal course presented with a 3–4 week history of a productive "stacatto" cough and failure to gain weight. This symptomology and lack of other physical findings led clinicians to diagnose a viral upper respiratory tract infection requiring no further diagnosis or therapy.

One week later the patient's symptoms worsened and diffuse rales and rhonchi were noted on auscultation. This prompted radiographic examination of the chest (fig. 1). Hyperaeration and peribronchial thickening were present, but the principal process was diffuse interstitial infiltrates with some alveolar component.

A complete cell blood count revealed a mild lymphocytosis with several atypical forms, but no eosinophilia was present. Screening techniques for pertussis and mycoplasma were negative, but nasopharyngeal aspirates and urine specimens were positive for *C. trachomatis* and cytomegalic inclusion virus, respectively. The infant was started on a 6 week course of erythromycin and revealed no clinical pulmonary disease after 3 weeks of treatment. Because of the dramatic improvement, final radiographic evaluation was not obtained.

Discussion

C. trachomatis, an inclusion-forming, intracellularly growing organism, is transferred by direct contact and is the causative agent in trachoma, one of the oldest and most prevalent human diseases [4]. The organism has also been identified in both ophthalmia neonatorum and nongonococcal urethritis [5]. A strong correlation between this occular disease of newborns and concurrent maternal genital infection has been described [6]. Studies of nongonococcal urethritis have indicated a high incidence of *C. trachomatis* infection in the adult population [7], but only recently has the organism been postulated as an etiologic agent in an infantile pneumonia syndrome.

Beem and Saxon [1] related *C. trachomatis* nasopharyngitis to a pneumonitis syndrome in infants. They described a disease complex developing gradually over the first 6 weeks of life consisting of rhinorrhea, intermittent nasal obstruction, a "stacatto" cough, variable tachypnea, eosinophilia, and increased levels of IgE and IgM with no fever or major systemic reaction. While early reports were limited to black infants, subsequent studies have not demonstrated a racial predilection [2].

Current reports show the chest radiograph is a valuable diagnostic tool in this disease. In a prospective study of afebrile pneumonias in 50 infants less than 6 months old, 23 patients yielded positive *C. trachomatis* cultures, and 20 of these displayed symmetrical interstitial infiltrates on chest radiographs [3]. As in our patient, 14 of the 20 yielded combined infections with cytomegalic inclusion virus the most common second agent. Of these 14, all but one demonstrated similar interstitial pulmonary infiltrates and hyperaeration. The combined *C. trachomatis* and cytomegalic inclusion virus infection has been isolated by lung biopsy from an infant with this same history and radiographic presentation [8]. Shanley and Josdin [9] question the disease contribution of *C. trachomatis* in this instance, but concede chlamydia could be a frequent cause of infantile interstitial pneumonia. The significance of the mixed infection, as opposed to *C. trachomatis* alone, remains unclear.

The exact pathogenesis in *C. trachomatis* pneumonitis is still under investigation. Beem and Saxon [1] hypothesized that the disease reflects a neonatally acquired colonization of the respiratory tract with expression dependent upon individual sensitivity. Reports in the literature conflict concerning the association between chlamydia ophthalmia neonatorum and this infantile pneumonia syndrome. Hobson and Rees [10] found no correlation in a large population of patients. Yet in another series of 14 infants, 13 of the patients with chlamydia pneumonitis showed evidence of prior conjunctivitis documented by the presence of tear antibody. Three of the 14 had active culture positive conjunctivitis [2].

In the past, chlamydia infections have been treated with a wide variety of antibiotics with a variable response [5]. Preliminary evidence suggests that both erythromycin and sulfa drugs may be effective in this infantile pneumonia syndrome [2]. The place of antimicrobials as opposed to only supportive therapy will probably be decided in the near future.

As with most newly recognized diseases, the literature reflects a certain amount of confusion and disagree-

Received March 7, 1978; accepted after revision July 28, 1978.

[1] Department of Radiology, University of Arizona Health Sciences Center, Tucson, Arizona 85724. Address reprint requests to J. C. Bjelland.

[2] Department of Pediatrics, University of Arizona Health Sciences Center, Tucson, Arizona 85724.

© 1978 American Roentgen Ray Society

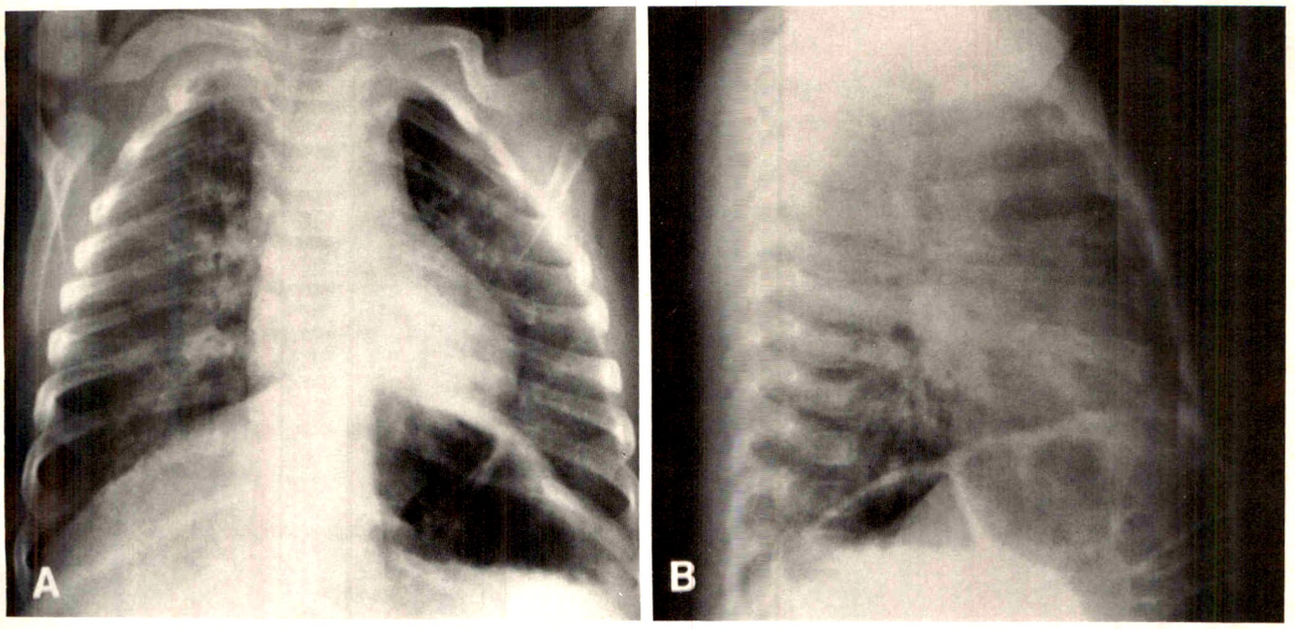

Fig. 1.—Anteroposterior (*A*) and lateral (*B*) views of chest demonstrating interstitial disease, hyperaeration, and peribronchial thickening.

ment. However, we feel that radiologic findings similar to those discussed, when observed in an afebrile infant with chronic cough and the appropriate clinical history, warrant the diagnostic consideration of *C. trachomatis* pneumonitis.

ACKNOWLEDGMENT

We thank Dr. E. Russel Alexander, University of Washington, Seattle, for performing the chlamydial cultures on this infant. Dr. K. J. Kranzler is credited with the initial radiographic presentation of *C. trachomatis* at the September 1976 meeting of the Society for Pediatric Radiology in Atlanta.

REFERENCES

1. Beem MO, Saxon EM: Respiratory tract colonization and a distinctive pneumonia syndrome in infants with chlamydia trachomatis. *N Engl J Med* 296:306–310, 1977
2. Harrison HR, English MG, Lee CK, Alexander ER: *Chlamydia trachomatis* infant pneumonitis: comparison with matched controls and other infant pneumonitis. *N Engl J Med* 298:702–708, 1978
3. Tipple MA, Saxon EM, Radkowski MA, Beem MO: Clinical characteristics of *Chlamydia trachomatis* pneumonia. *Pediatr Res* 11:822, 1977
4. Tang FF, Chang HL, Huang YT, Wang KC: Studies on the etiology of trachoma with special reference to isolation of the virus in chick embryo. *Chin Med J [Engl]* 75:429–447, 1957
5. Grayston JT, Wang J: New knowledge of chlamydiae and the diseases they cause. *J Infect Dis* 132:87–105, 1975
6. Dunlop EMC, Jones BR, Al-Hussaini MK: Infection of the eye and genital tract by TRIC agent II. Clinical and other features of infection of the genital tract associated with trachoma. *Rev Int Trach* 42:14–26, 1965
7. Jacobs NK Jr, Arum ES, Krauf SJ: Nongonococcal urethritis: the role of *Chlamydia trachomatis* pneumonia. *Ann Intern Med* 86:313–314, 1977
8. Frommel CT, Bruhn FW, Schwartzman JD: Isolation of *Chlamydia trachomatis* from infant lung tissue. *N Engl J Med* 296:1150–1152, 1977
9. Shanley JD, Jordin MC: Chlamydia and CMV in pneumonitis. *N Engl J Med* 297:560, 1977
10. Hobson D, Rees E: Chlamydia infection in neonates. *N Engl J Med* 296:398, 1977

Technical Notes

Radiography of LeVeen Type Peritoneovenous Shunts

DAVID B. FREIMAN,[1] ERNEST J. RING,[1] JUAN A. OLEAGA,[1] AND ERNEST F. ROSATO[2]

Peritoneovenous shunts of the LeVeen type have been used for several years for relief of intractable ascites [1]. These shunts consist of silastic tubing extending from the peritoneal cavity subcutaneously into the jugular vein and from there into the superior vena cava. Near the peritoneal end of the shunt, a pressure sensitive valve ensures unidirectional flow and prevents reflux of blood into the tubing and peritoneum.

Although radioisotope scans have been used to indirectly evaluate nonfunctioning shunts [2], recent reports [3, 4] demonstrate the feasibility of direct puncture of the shunt and contrast material injection as a safe method of determining the exact cause of a malfunction. This report describes the causes of a shunt malfunction which can be demonstrated using this method.

Technique

Recently 10 patients were referred to determine the cause of failure of a LeVeen shunt. The shunts were introduced to control intractable ascites due to primary liver disease in eight patients and metastatic tumor in two patients.

The radiographic examinations were performed using techniques previously described [3]. The shunts were directly punctured using a 23 gauge scalp vein needle and opacified with 10 ml of contrast material by forceful hand injection. The shunt tubing is easily palpated and punctured as it courses subcutaneously over the thoracic cage. Serial films were obtained at a rate of 1 film per second for 6 sec beginning in the middle of the injection.

Discussion

A one-way valve is necessary to prevent reflux of blood into the venous end of a LeVeen shunt. The valve must have a low opening pressure (3–5 cm of water) since the pressure gradient between intraabdominal and central venous pressure decreases to very low levels as the ascites is removed. The valve also regulates the speed of ascites removal by closing in response to elevated central venous pressure, thereby preventing a rapid increase in intravascular volume and consequent congestive failure.

Unfortunately, the sensitivity of the valve makes it subject to malfunction. The slightest interference with the outflow of the shunt has a significant effect on ascites removal. If the shunt is partially obstructed by clot formation in the superior vena cava or obturated against a vascular wall, the valve will fail to open. In addition, if the venous end of the shunt is located in a zone of relatively high pressure, such as the right ventri-

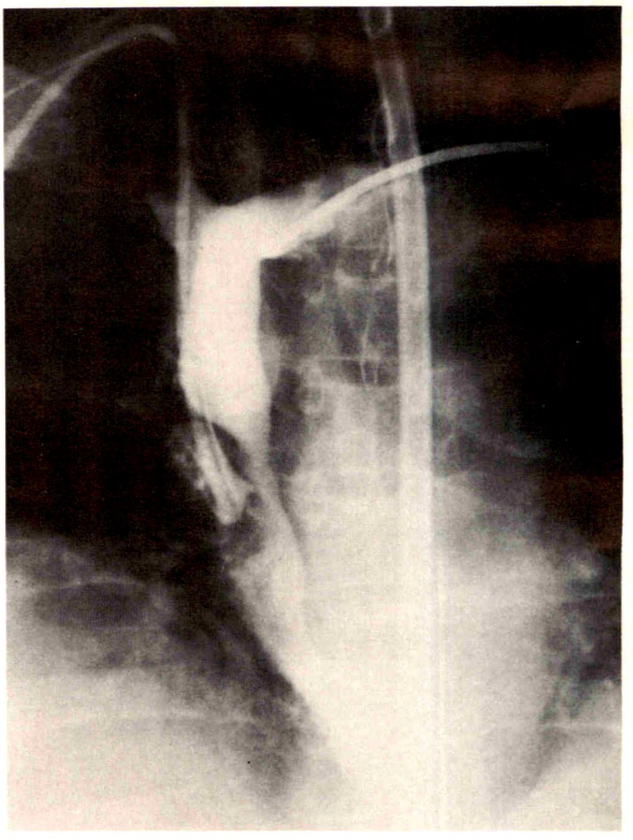

Fig. 1.—Simultaneous injections of contrast into LeVeen shunt and into catheter inserted through vein in left arm into superior vena cava demonstrating clot around distal end of shunt.

Received February 24, 1978; accepted after revision July 18, 1978.

[1] Department of Radiology, Hospital of the University of Pennsylvania, Philadelphia, Pennsylvania 19104. Address reprint requests to D. B. Freiman.
[2] Department of Surgery, Hospital of the University of Pennsylvania, Philadelphia, Pennsylvania 19104.

© 1978 American Roentgen Ray Society

cle, or intraabdominally in the inferior vena cava, there will be no flow through the shunt [4].

Of the 10 patients we studied, five had demonstrable thrombosis at or around the tip of the catheter in the vena cava (fig. 1). The other five had superior vena caval thrombosis, tumor impingement on superior vena cava, catheter obturated against the side wall of the innominate vein, catheter tip in the right atrium, and occluded inflow in the abdomen. The only significant risk to this procedure seems to be reaction to contrast material. Infection should be easily prevented by using standard aseptic technique.

REFERENCES

1. LeVeen HH, Christoudias G, Ip M, Luft R, Falk G, Grosberg S: Peritoneo-venous shunting for ascites. *Ann Surg* 180:580–591, 1974
2. Kirchner N, Hart V: Radionuclide assessment of LeVeen shunt patency. *Ann Surg* 185:145–146, 1977
3. Ring EJ, Rosato EF: Assessment of peritoneo-jugular shunts by direct radiographic examination. *Surg Gynecol Obstet.* In press, 1978
4. Holcroft J, Kresel HY, Prager R, Trunkey D, Jacobs RP: An experience with a LeVeen ascites shunt. *Arch Surg* 111:302–303, 1976

Pathologic Index for Arrangement of Teaching File

RICHARD H. DAFFNER[1]

The majority of teaching cases in departmental or private collections are filed by using the American College of Radiology (ACR) coding system [1]. In using this system, the search for a particular pathologic entity may become cumbersome, since cases are filed almost universally by the anatomic area. As a result of my experience in trying to rapidly retrieve cases, films in our section's teaching file are now filed according to the pathologic entity. The reasoning behind this system derives from the fact that similar lesions in an organ look alike no matter what their location. A lung carcinoma in the right upper lobe is similar to a lung carcinoma in the left lower lobe. Similarly, rheumatoid arthritis of the hand resembles rheumatoid arthritis of the foot, and so on.

Our teaching file is divided into the general anatomic sections as prescribed by the ACR index (head, face, mastoids and neck, spine, skeletal system, heart and great vessels, etc.). However, all entities in these areas are filed according to the *pathologic* index. Figure 1 shows the general arrangement of our teaching jacket. A colored tape representing the first number in the pathologic code is placed on the outside margin of the jacket for easy recognition. If there are two pathologic codes for a case, a second piece of colored tape may be placed immediately above the lowest one. Tapes are placed at the top to rapidly identify cases of special interest.

The gastrointestinal tract and genitourinary tract (ACR codes 70 and 80, respectively) posed a dilemma, which was solved by filing under the individual organ system as a separate entity (table 1). In these two sections, lesions are still filed by pathologic index number. For example, carcinoma of the esophagus is filed numerically under .321 regardless of its location.

This system has been in effect for nearly 3 years and has been simple and easy to use for both residents and staff. Retrieval of information from the file may be done quickly and efficiently.

REFERENCE

1. American College of Radiology: *Index for Roentgen Diagnoses*, 3d ed. Chicago, American College of Radiology, 1975

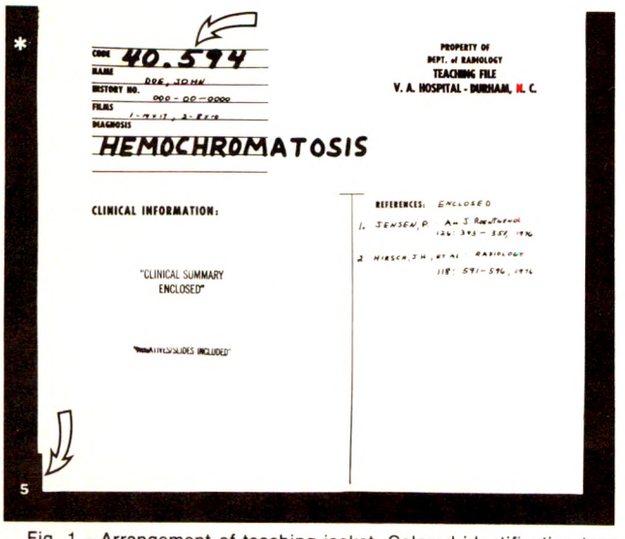

Fig. 1.—Arrangement of teaching jacket. Colored identification tape matches first digit of pathologic index number (*arrows*). Cases of special interest are marked by colored tapes at top of jacket (*asterisk*).

TABLE 1
Filing System

Code and Anatomic Heading	Code and Anatomic Heading
10. Skull and contents	80. Genitourinary system
20. Face, mastoids and neck	81. Kidney
30. Spine and contents	82. Ureter
40. Skeletal system	83. Bladder
50. Heart and great vessels	84. Male urethra, genitalia
60. Lung, mediastinum, and pleura	85. Female urethra, genitalia, fetus, placenta
70. Gastrointestinal system	86. Adrenal
71. Esophagus	87. Extraperitoneal space
72. Stomach	90. Vascular and lymphatic systems
73. Duodenum	00. Breast
74. Small intestine	
75. Colon	
76. Liver, biliary system	
77. Pancreas, spleen	
78. Generalized	
79. Other	

Note.—Modified from American College of Radiology Index [1].

Received May 16, 1978; accepted July 20, 1978.
[1] Department of Radiology, Veterans Administration Hospital and Duke University Medical Center, 508 Fulton Street, Durham, North Carolina 27705.

© 1978 American Roentgen Ray Society

0361-803X/78/1100-0918 $00.00

Progress in Radiology:

Total Body Opacification

N. THORNE GRISCOM[1]

Total body opacification is the phenomenon whereby introduction of iodinated contrast material into the blood stream renders structures differentially radiopaque according to their blood supply. The term implies the physiology: it is the whole body which is opacified, in proportion to the iodine in its plasma and extravascular extracellular fluid at the time of the radiograph. To the density inherent in the tissue before injection is added the opacity of the iodine circulating through and transuding into it. Just as tissues, even those of "water density," have minor intrinsic differences in x-ray absorption [1–3], so they may also have minor differences in blood flow and transudation into the extracellular fluid; the combination of these minor differences often makes the invisible visible.

Until the last few years, this simple concept was useful primarily in pediatric radiology. Now, differential tissue opacification after contrast injection has assumed an unexpected importance, since contrast enhancement is a crucial part of computed tomography. Computed tomography, of course, is much more sensitive to minor differences in x-ray absorption. However, even by ordinary radiography, a few lesions, such as some uterine myomas [4–6], some ovarian tumors [6], some liver tumors [7], and an occasional cerebral glioma, are rendered recognizably opaque during intravenous urography because they temporarily contain more contrast material than the surrounding structures. Other lesions, receiving little or no blood and therefore little or no iodine, stand out as lucencies against opacified adjacent areas. The latter is the classical meaning of total body opacification, and it is this aspect—lucencies recognized by plain film or by noncomputerized tomography after intravenous injection of contrast material—that this review will discuss.

Physiology

Total body opacification occurs not only because of the circulation of iodine in the blood, but also because of transudation of iodine into the extravascular extracellular spaces. Diatrizoate equilibrates into the entire extracellular space [8]. This equilibration starts immediately. It is rapid in some tissues and slower in others [9]. Equilibration into large isolated extravascular spaces, such as fluid collections in serous cavities and cysts, must be fairly slow. In rats, diatrizoate was found 5 min after intravenous injection to have a distribution volume of 26% of body volume; it seemed to be approaching the 28% "sulfate space," considered to be the total (intravascular plus extravascular) extracellular fluid volume. At this time, more than 80% of the contrast material was outside the blood vessels [9]. Organs vary substantially in the volumes of their extracellular spaces; the extracellular space constitutes a large part of the liver, bowel, and skin, for example, which therefore presumably are able to acquire large amounts of contrast material by equilibration [9]. This would be especially true during high dose urography in newborns, when renal extraction is tardy. These varying rates of equilibration and differences in volumes available for equilibration are one reason why neighboring structures may be radiologically distinct from each other at one time after injection and not at another. As the kidneys lower the plasma concentration of diatrizoate, the extravascular contrast material will reequilibrate back into the blood vessels, and these tissue differences will disappear.

Several clear-cut examples of opacification of the extravascular extracellular space are known. Passage of contrast material into the interstitial fluid opacifies the falx cerebri on skull films taken during intravenous urography [10]. The fluid contained in cystic brain tumors has likewise been opacified by intravenously injected contrast material, which has then slowly passed back into the blood for removal by the kidneys [11]. Measurable amounts of iodine have been found in simple renal cysts after intravenous urography and after arteriography [12]. Possibly equilibration into cyst fluid also helps explain the curious late faint opacification of a few neonatal multicystic dysplastic kidneys during intravenous urography [13, 14].

Recent work indicates that diatrizoate enters the intracellular spaces of polymorphonuclear granulocytes, at least in certain circumstances [15]; it also enters the kidney tubule cells to a small extent, and perhaps there are other examples of passage of contrast material into a cell. These phenomena must be quantitatively small, and it is the iodine in the extracellular spaces (intravascular and extravascular) that makes the total body opacification effect possible.

Applications

The pathophysiologic lesions rendered visible by total body opacification include cysts, abscesses, local necrosis, hemorrhage, infarction, fluid accumulation, and locally diminished blood supply [16] (figs. 1–4). The effect has several uses. It identifies abnormalities not recognized by plain films, outlines lesions previously poorly seen, and characterizes a lesion by indicating that it is avascular or hypovascular. However, it does not guaran-

Received March 3, 1978; accepted after revision July 20, 1978.
[1] Department of Radiology, Harvard Medical School, Children's Hospital Medical Center, 300 Longwood Avenue, Boston, Massachusetts 02115.

© 1978 American Roentgen Ray Society

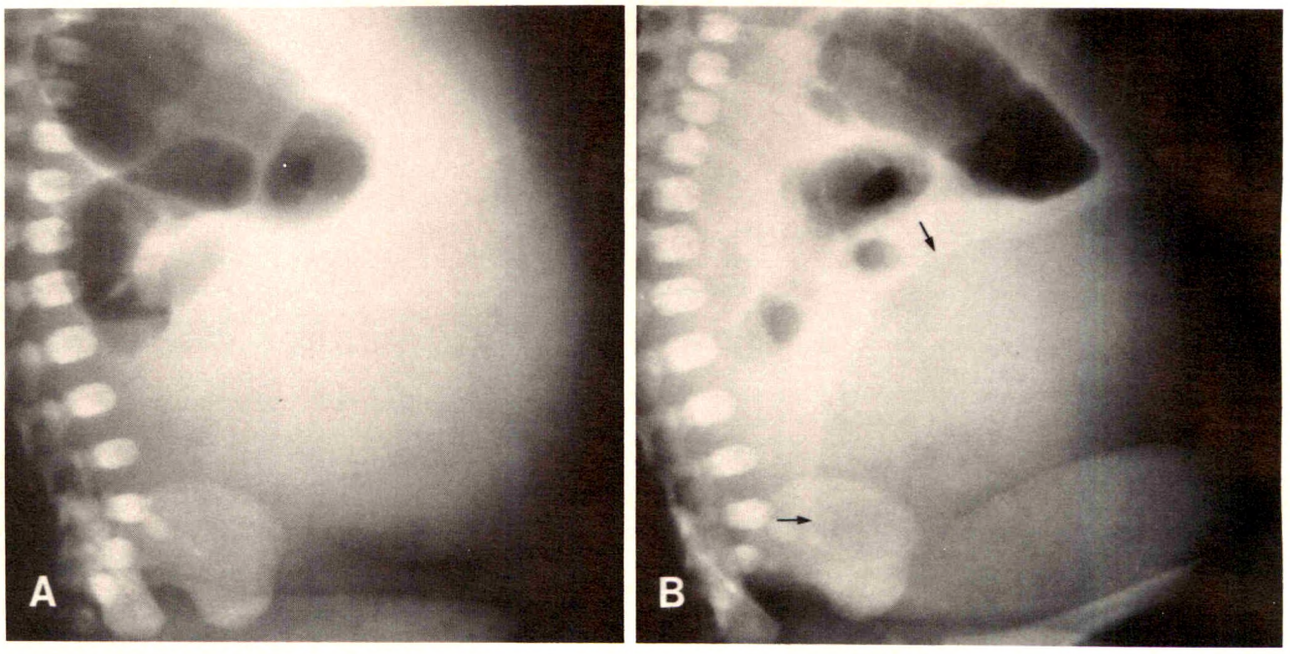

Fig. 1.—Newborn girl with tense abdominal distension. *A*, Preliminary lateral view showing abdominal fullness, small bowel obstruction, and absence of gas or any other definable structure in the lower abdomen. *B*, Film 5 min after intravenous injection of methylglucamine diatrizoate showing distinct lucent mass (*arrows*) occupying much of lower abdomen. Exploratory surgery showed meconium ileus due to cystic fibrosis and perforation; mass was pseudocyst formed by walling off of meconium peritonitis [17]. (Reprinted with permission from [16])

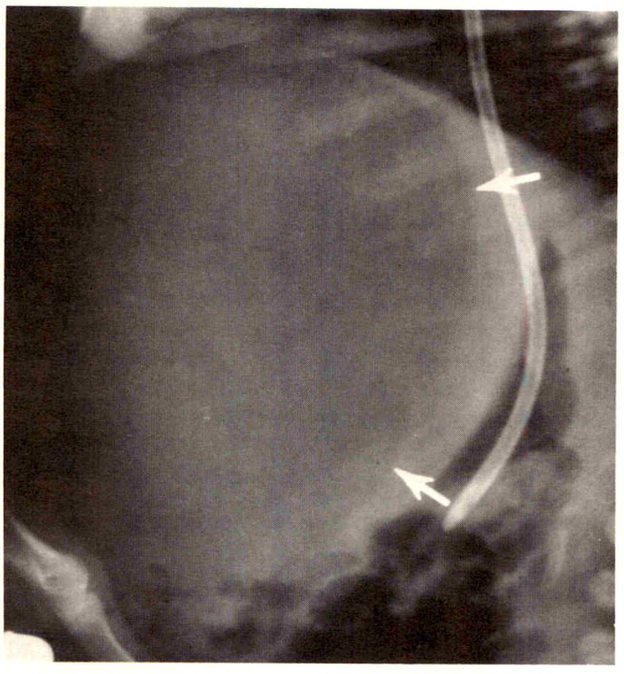

Fig. 2.—Newborn girl with abdominal fullness and questionable upper abdominal cystic mass. Preliminary lateral view depicted liver, anterior abdominal muscles, and diaphragm as one continuous water-density shadow. Film 10 min after injection for urography showing clear-cut lucent intrahepatic lesion (*arrows*). Mass was solitary liver cyst [18].

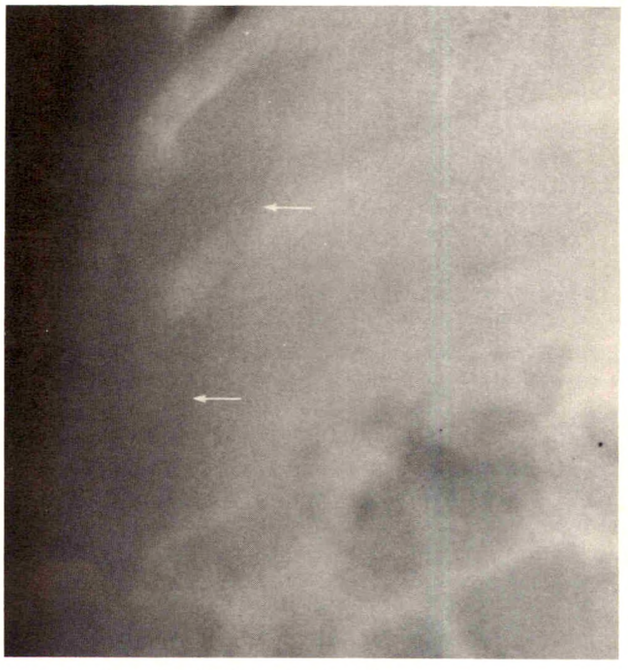

Fig. 3.—2-month-old girl (reported by Martin et al. [16]) with cystic fibrosis, malabsorption, and hypoproteinemia. 5 min urogram with opacification of liver and gut by circulating iodine showing ascites (*arrows*).

tee benignity, since some malignancies are necrotic, hemorrhagic, or otherwise avascular [22]. It makes relatively few diagnoses by itself but is commonly important supportive information.

The effect is especially useful in the evaluation of neonatal abdominal masses [18] for several reasons. Neonatal abdominal masses are usually large at discovery and have often reached a volume sufficient to show the total body opacification effect; the majority of neo-

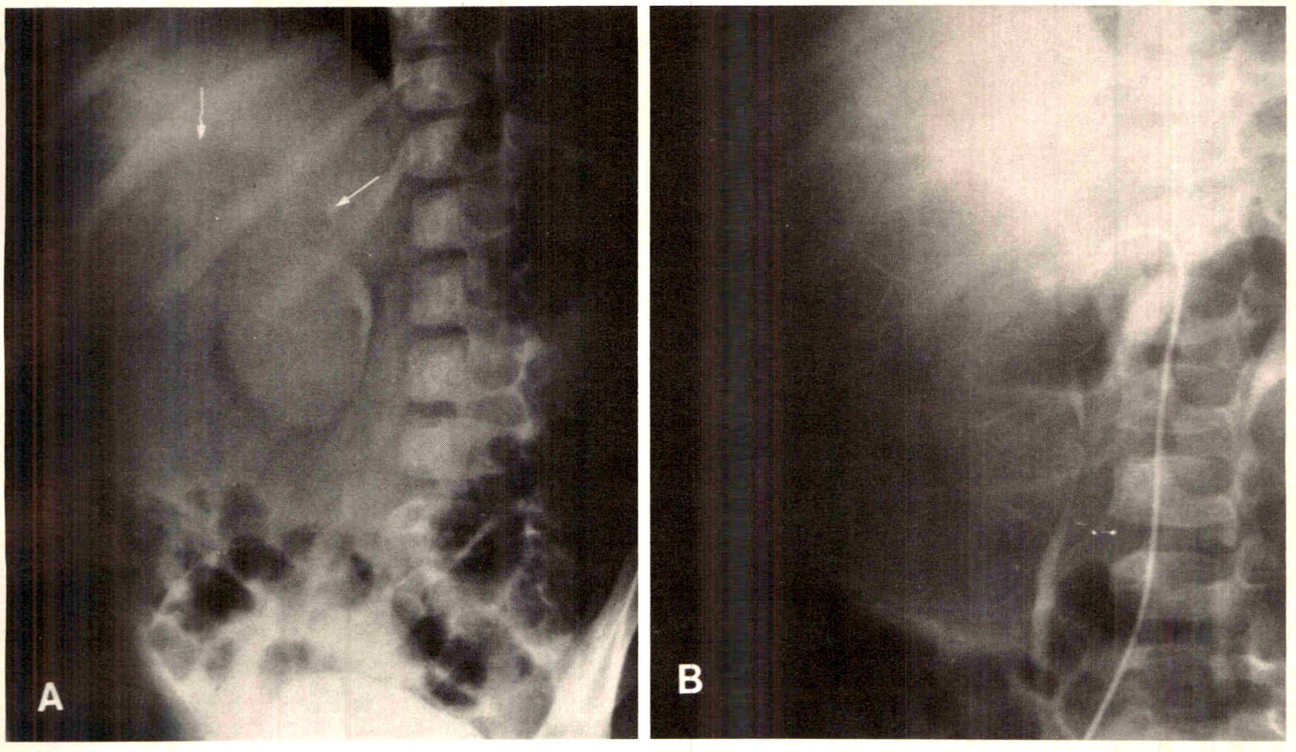

Fig. 4.—4-year-old girl with choledochal cyst. *A*, 20 min oblique urogram showing round lucency (*arrows*) projected over lower two-thirds of kidney, displacing liver upward and bowel downward. *B*, Capillary phase from common hepatic arteriogram showing same lucency, now further demarcated by added density of cyst wall [19]; this rim effect was faintly visible on intravenous urogram. (Earlier films from this angiogram published by Fellows [20] and Rosenfield and Griscom [21].)

natal abdominal masses are avascular; and the relatively low glomerular filtration rate of neonatal kidneys leads to a longer period during which the total body opacification effect can be captured on film. Furthermore, newborns have a smaller scattering volume, and therefore fine differences in image contrast are less likely to be obliterated; there is no need to raise kilovoltage above 70 for the sake of penetration, and thus photoelectric absorption at the k-edge of iodine is maximized; and relatively high doses of diatrizoate are commonly used in neonatal urography, which enhances the total body opacification effect.

Table 1 lists pediatric conditions in which the total body opacification effect has assisted in diagnosis. Table 2 gives some additional adult lesions showing the effect, sometimes made evident by conventional tomography [30, 33, 34, 36–40]. In many of these examples, especially in those masses with inflamed walls and those tumors composed of a relatively vascular wall and a necrotic, hemorrhagic, or cystic center, the increase in density of the wall (fig. 4) accounted for at least part of the appearance of central lucency [5, 6, 15, 19, 30, 41–44]. Tomography during intravenous cholangiography has shown a postoperative subhepatic bile collection by contrast with the opacified liver [45], an example of local opacification rather than whole-body opacification. In principle, lesions of other soft tissue regions (neck, shoulders and arms, thighs and calves) ought to be as demonstrable by the total body opacification effect as abdominal condi-

TABLE 1

Conditions Shown as Lucencies by Total Body Opacification Effect in Children

Type and Condition	Type and Condition
Urinary:	Gastrointestinal:
Multicystic dysplastic kidney (pelvoinfundibular atresia)	Duplication
Severe hydronephrosis	Omental or mesenteric cyst
Renal cyst	Paraduodenal hematoma
Renal vein thrombosis, infarction	Pancreatic pseudocyst
Pyonephrosis, abscess	Volvulus with infarction
Necrotic Wilms' tumor	Mesenteric arterial thrombosis and small bowel infarction [25]
Fetal renal hamartoma [23]	Pseudocyst from prenatal volvulus, perforation, or extreme dilatation
Hydroureter	Gastric dilatation [26]
Dilated bladder	Genital:
Hepatobiliary:	Ovarian cyst
Liver cyst	Cystic ovarian carcinoma
Liver abscess	Hydrometrocolpos
Lymphangiomatous hamartoma of liver	Other:
Hemorrhagic hepatoma	Adrenal hemorrhage
Thrombosed, hemorrhagic, or necrotic hemangioma	Hemorrhagic or necrotic neuroblastoma
Focal liver necrosis	Splenic cyst
Choledochal cyst	Splenic rupture [27]
Hydropic cholecystitis [24]	Ascites
	Extraperitoneal parahepatic hematoma

Note.—Except where noted, all have been seen at Children's Hospital, Boston.

TABLE 2
Conditions Shown by Total Body Opacification Effect in Adults

Type and Condition	Type and Condition
Urinary:	Genital:
Uriniferous perirenal pseudocyst [28]	Necrotic uterine carcinoma [34]
Hepatobiliary	Amniotic cavity [34]
Hydrops of the gallbladder [29]	Other:
Acute cholecystitis [30]	Pancreatic pseudocyst [35]
Dilated hepatic ducts [31]	Anterior meningocele [34]
Hydatid liver cyst [32]	Hypovascular splenic metastasis [36]
Polycystic liver disease [33]	Retroperitoneal mesenchymoma [37]
	Lymphatic cyst [36]
	Adrenal cyst [38]

Note.—These are in addition to the conditions in table 1. List is probably incomplete. Conventional tomography was frequently used.

tions; enhanced computed tomography is beginning to confirm this.

Technique

In children, display of the total body opacification effect to best advantage requires only minor modifications of intravenous urography [46]:

1. Optimal penetration of preliminary films, showing the area of interest in the middle grays.
2. Adjustment of peak kilovoltage to maximize photoelectric absorption at the k-edge of iodine.
3. Proper obliquity of preliminary films, throwing the area of interest free of overlying bowel gas and other structures.
4. Sufficient contrast material.
5. First film about 30 sec after the end of injection, when the contrast material has mixed with the blood but has not yet been appreciably filtrated out by the glomeruli. This film should match the best preliminary film in penetration and obliquity.
6. Tomography when indicated, especially in older children and adults.
7. Later films, to confirm the presence of the lesion or to show that the lucency disappears as the kidneys remove the contrast material from the blood.

The preliminary film should display the soft tissues in the middle gray region, in the steepest part of the characteristic curve of the film-screen combination. Sufficient contrast dosage should be used. Our present schedule for intravenous urography (and for total body opacification) calls for 2 ml of methylglucamine diatrizoate (Renografin 60) per 0.45 kg in early infancy, falling off gradually to 0.5 ml/0.45 kg in adolescence. If a compelling reason existed, we would use even higher doses in later childhood and adolescence. However, large doses of contrast material cause gross alterations in body fluid composition, and the high doses recommended for small infants should be used only if the child is already properly hydrated and should not be raised further without a very strong indication.

The early films should be taken within 1 min of the completion of the injection, although a newborn's slow glomerular filtration allows considerable flexibility in timing. Thereafter opacification will begin to fade, at a rate governed by the rapidity with which the kidneys remove the iodine. Nevertheless, if the first films should be inadequate, later films may be useful; we have seen the effect persist for as long as an hour in a newborn infant. Tomography of the area in question may be helpful. Late films, automatically available with the completion of the urographic part of the study, may show disappearance of the total body opacification effect, confirming the avascular nature of the lucency. In adults, the approach is similar but with emphasis on high doses of contrast material by bolus injection or rapid infusion, prompt filming, tomography, and avoidance of high kilovoltage when possible [30].

Hazards

The hazards of a total body opacification examination are virtually identical to those of intravenous urography [47–50], of which it ordinarily forms a part. The risk of life-threatening idiosyncratic reactions is less in children than in adults [60], but preparations for their occurrence naturally must be made. Large doses of contrast material have very distinct hemodynamic effects, in particular a substantial rise in serum osmolarity, a substantial fall in the hematocrit and in the concentration of normal blood constituents [51], and a rise in the circulating blood volume. The accompanying hypertonic dehydration may lead to cerebral injury, either by vascular damage during the phase of brain shrinkage or by edema during the rehydration phase [52].

These aberrations correct themselves fairly rapidly as the system-insulting diatrizoate exits via the glomerulus. They can be minimized if proper hydration is maintained; in children and especially in newborns dehydration prior to urography is distinctly contraindicated. Because of the sudden increase in circulating blood volume, use of very large volumes of intravenous contrast agents may be dangerous for a patient near circulatory failure [52]. One normal newborn was put into pulmonary edema by the rapid injection of an amount of diatrizoate only slightly above the dosage schedule given above [61]; slower injection may be protective by allowing transudation into the extravascular extracellular spaces to occur and glomerular filtration to begin. Renal decompensation developed in two adults after very high dose arteriography, perhaps because they were not well hydrated during the examination [53], and two other adults had episodes of renal failure after high doses of diatrizoate [62, 63]. Microscopic lesions of "osmotic nephrosis" have been found with some regularity by renal biopsy in adults a few days after intravenous urography or renal arteriography [54], and the same lesions presumably develop in children. The severity of the lesions was dose related and was greater with preexisting renal disease. Later renal biopsies failed to show these lesions. Despite all these warnings, if proper hydration is maintained, if the dosage schedule given above is not exceeded, and if skills and equipment to handle idiosyncratic reactions are readily available, the hazards of intravenous urogra-

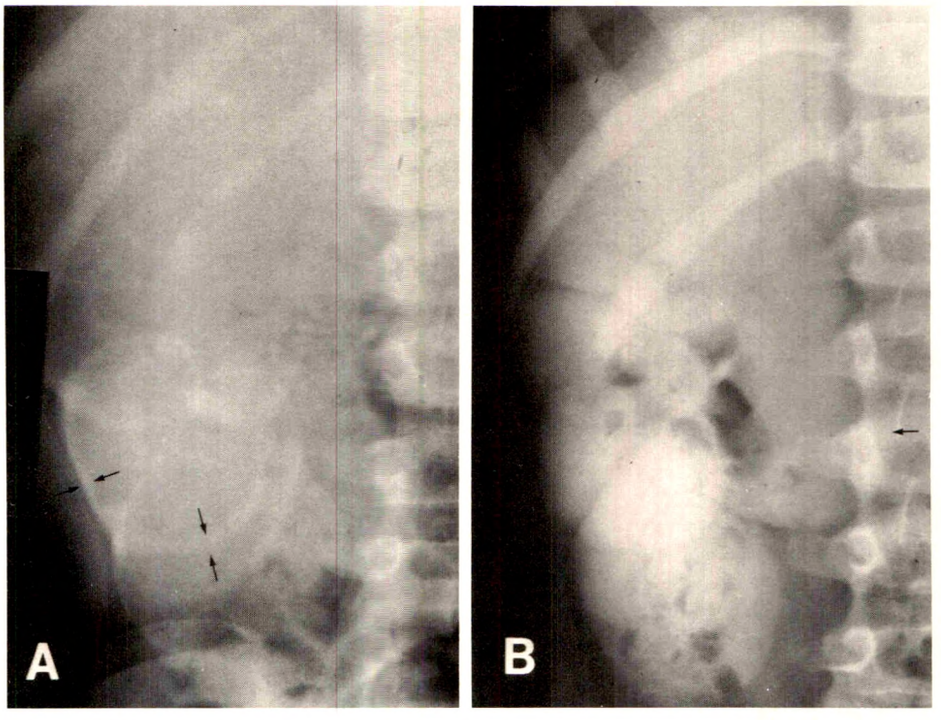

Fig. 5.—7-year-old boy with right flank mass. *A*, 30 sec urogram showing obstructive nephrogram; renal parenchyma (*arrows*) is markedly thinned by grossly ballooned calyces. On radiograph, thin calyceal crescents (see fig. 6) were tentatively identified. *B*, 4 hr film showing opacified calyces, extending from T10 to iliac crest, and ureteropelvic junction obstruction (*arrow*) overlying L3. Pelvicalyceal system was initially of water density, then relatively lucent by total body opacification and by contrast with obstructive nephrogram, and finally relatively dense as it filled with iodinated urine.

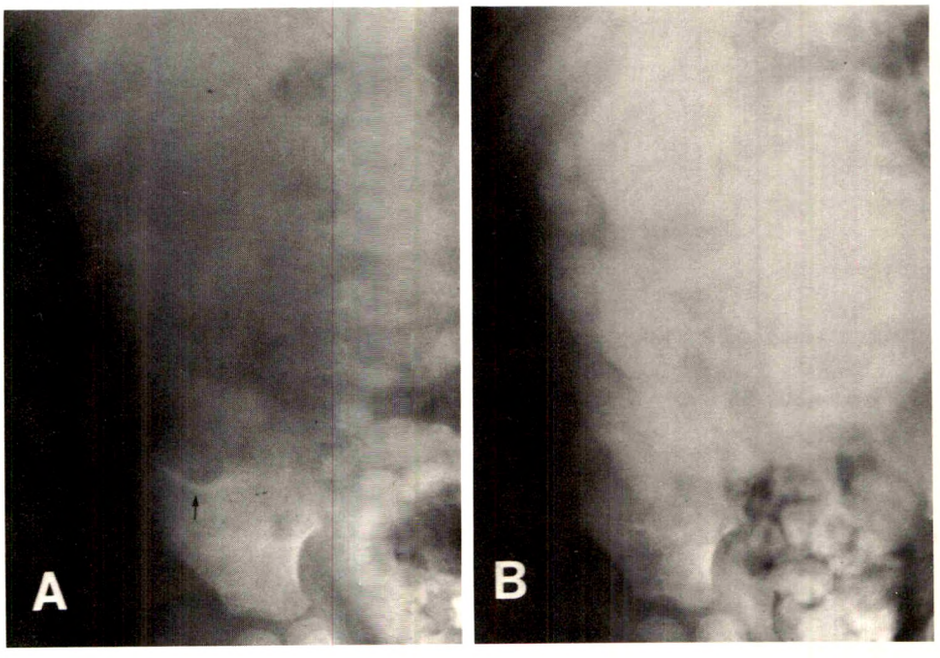

Fig. 6.—15-month-old boy with severe right ureteropelvic obstruction. *A*, 2 min film showing calyceal crescents (*arrow*) [56]. Calyces are relatively lucent, both by comparison with adjacent parenchyma and by total body opacification effect. *B*, 24 hr film showing enormous hydronephrosis, crossing far left of midline.

phy, whether or not it is designed to show total body opacification, are small.

Related Appearances in Obstructive Uropathy

The physiologic characteristics of the kidney (high regional blood flow, glomerular filtration of contrast material, and tubular reabsorption of water) can lead to radiographic appearances superficially similar to the total body opacification effect. One of these is the well known obstructive nephrogram [55], in which the not-yet-opacified urine in the pelvicalyceal system is suddenly visible against the iodine in the renal parenchyma (fig. 5). The calyceal crescent sign of Dunbar and Nogrady [56], a variant of this (fig. 6), is opacification of the flattened renal pyramids adjacent to the distorted calyces by contrast material concentrated within the collecting tubules and papillary ducts of Bellini. Occasionally the

individual dilated ducts of Bellini themselves may be seen as they approach the calyces [57]. But these obstructive phenomena depend on glomerular filtration of contrast material and concentration of iodine by tubular reabsorption of water; they are thus conceptually distinct from the total body opacification effect, which depends merely on disparity in blood flow to and transudation into adjacent structures. Nevertheless, the two effects may coexist, as in severe hydronephrosis, in which the dilated renal pelvis is shown as a lucency, not only because it is an avascular mass adjacent to well vascularized structures, but also because the renal tissue around it has opacified itself by concentrating the contrast material.

Conclusions

Now that angiography, radionuclide scans, and contrast-enhanced computed tomography are so commonplace, it is hard to remember the disbelief which the total body opacification effect aroused. The phenomenon was first reported in 1962 by John O'Connor and Edward Neuhauser at a meeting of the New England Roentgen Ray Society [58]. In that era it was the unformulated assumption that contrast material magically passed nonstop from the injecting needle to the renal pelvis, whence the term "intravenous pyelography." Many of that audience were openly skeptical, concluding that since they had not seen this effect, it was either nonexistent or unimportant. Thus they proved once again the old axiom that we only recognize what is already familiar. Disbelief was so general that an editorial note to "vouch for the accuracy of the authors' claim" was once thought necessary [59]. This is simultaneously humbling and challenging; even now many phenomena must be stalled between our retinas and our higher integrative centers, awaiting some moment of inspired perception.

ACKNOWLEDGMENTS

I thank Drs. William Caldicott, John Kirkpatrick, Robert Lebowitz, David Martin, Edward Neuhauser, and Roy Strand for helpful comments; Andrea Kelton for her assistance; and Donald Sucher for his photographic efforts in conveying the total body opacification effect, which is generally recognized as "difficult to reproduce" [59].

REFERENCES

1. Alfidi R, MacIntyre WJ, Meaney TF, Chernak ES, Janicki P, Tarar R, Levin L: Experimental studies to determine application of CAT scanning to the human body. *Am J Roentgenol* 124:199–207, 1975
2. New PFJ, Scott WR, Schnur JA, Davis KR, Taveras JM: Computerized axial tomography with the EMI scanner. *Radiology* 110:109–123, 1974
3. Mategrano VC, Petasnick J, Clark J, Bin AC, Weinstein R: Attenuation values in computed tomography of the abdomen. *Radiology* 125:135–140, 1977
4. Birnholz JC: Uterine opacification during excretory urography. *Radiology* 105:303–307, 1972
5. Phillips JC, Easterly JF, Langston JW: Contrast enhancement of pelvo-abdominal masses, the rim sign. *Radiology* 112:17–21, 1974
6. Imray TJ: Evaluation of pelvic masses during infusion excretory urography. *Am J Roentgenol* 125:60–65, 1975
7. Wirtanen GW: A new angiographic technique in the diagnosis of liver tumor. *Radiology* 108:51–54, 1973
8. Hegedüs V, Cramer BM, Cockett ATK: Lymphatic distribution of intravenous radiographic contrast media. *Invest Radiol* 9:56–60, 1974
9. Kormano M, Dean PB: Extravascular contrast material, the major component of contrast enhancement. *Radiology* 121:379–382, 1976
10. Gooding CA, Price DC, Newton TH: Experimental studies of falx and tentorial opacification during cerebral angiography. *Radiology* 102:77–82, 1972
11. Messina AV, Potts DG, Rottenberg D, Patterson RH: Computed tomography: demonstration of contrast material within cystic tumors. *Radiology* 120:345–347, 1976
12. Shanser JD, Hedgcock MW, Korobkin MT: Transit of contrast material into renal cysts following urography or arteriography. Paper presented at annual meeting of Radiological Society of North America, Chicago, November 1977
13. Lachman RS, Lindstrom RR, Hirose FM: The "septation sign" in multicystic dysplastic kidney. *Pediatr Radiol* 3:117–119, 1975
14. Young LW, Wood BP, Spohr CH, Panner B: Delayed excretory urographic opacification, a puddling effect, in multicystic renal dysplasia. *Ann Radiol* 17:391–396, 1974
15. Moncada R, Cardoso M, Danley R, Rodriguez J, Kimura K, Pickleman J, Brandly J: Infusion tomography of the gallbladder: mechanism of gallbladder wall opacification in experimental acute cholecystitis. *Am J Roentgenol* 129:587–590, 1977
16. Martin DJ, Griscom NT, Neuhauser EBD: A further look at the total body opacification effect. *Br J Radiol* 45:185–192, 1972
17. Effmann EL, Griscom NT, Colodny AH, Vawter GF: Pseudocysts of bowel and peritoneum in neonatal intestinal obstruction. Paper presented at annual meeting of Radiological Society of North America, Chicago, December 1975
18. Griscom NT: The roentgenology of neonatal abdominal masses. *Am J Roentgenol* 93:447–463, 1965
19. Rabinowitz JG, Kinkhabwala MN, Rose JS: Rim sign in choledochal cyst: additional diagnostic feature. *J Can Assoc Radiol* 24:226–230, 1973
20. Fellows KE: The uses and abuses of abdominal and peripheral arteriography in children. *Radiol Clin North Am* 10:349–366, 1972
21. Rosenfield N, Griscom NT: Choledochal cysts, roentgenographic techniques. *Radiology* 114:113–119, 1975
22. Kurlander GJ, Smith EE: Total body opacification in the diagnosis of Wilms' tumor and neuroblastoma, a note of caution. *Radiology* 89:1075–1076, 1967
23. Berdon WE, Wigger HJ, Baker DH: Fetal renal hamartoma, a benign tumor to be distinguished from Wilms' tumor. *Am J Roentgenol* 118:18–27, 1973
24. Robinson AE, Erwin JH, Wiseman HJ, Kodroff MB: Cholecystitis and hydrops of the gallbladder in the newborn. *Radiology* 122:749–751, 1977
25. Case records of the Massachusetts General Hospital. *N Eng J Med* 295:608–614, 1976
26. Crowe JE, Sumner TE: Combined esophageal and duodenal atresia without tracheosophageal fistula: characteristic radiographic changes. *Am J Roentgenol* 130:167–168, 1978
27. Leape LL, Bordy MD: Neonatal rupture of the spleen. *Pediatrics* 47:101–104, 1971
28. Meyers MA: Uriniferous perirenal pseudocyst: new observations. *Radiology* 117:539–545, 1975
29. Genereux GP, Tchang SPK: Diatrizoate-induced total body opacification in the diagnosis of obstructive cholecystopathy. *J Can Assoc Radiol* 21:242–250, 1970
30. Moncada R, Cardoso M, Danley R, Rodriguez J, Kimura K,

Pickleman J, Brandly J: Acute cholecystitis, 137 patients studied by infusion tomography of the gallbladder. *Am J Roentgenol* 129:583–585, 1977
31. Morin ME, Baker DA, Marsan RE: Demonstration of dilated biliary ducts by total body opacification. *Radiology* 121:307–309, 1976
32. Balikian JP, Mudarris FF: Hydatid disease of the lungs. *Am J Roentgenol* 122:692–707, 1974
33. Hatfield PM, Pfister RC: Splenic and hepatic evaluation during infusion nephrotomography. *Am J Roentgenol* 119:687–691, 1973
34. Love L, Melamed M, Cooper RA, Moncada R, Schwartz H: Infusion tomography of the female pelvis. *Am J Roentgenol* 122:299–307, 1974
35. Lilienfeld RM, Lande A: Pancreatic pseudocysts presenting as thick-walled renal and perinephric cysts. *J Urol* 115:123–125, 1976
36. Mitty HA, Schapira HE: Total body opacification in the adult. *Am J Roentgenol* 115:630–635, 1972
37. Smith AM, Becker JA: Malignant mesenchymoma of the retroperitoneum. *Am J Roentgenol* 104:389–393, 1968
38. Kurti DJ, Patel SK: Diagnosis of adrenal cysts utilizing the principle of total body opacification. *Am J Roentgenol* 119:576–579, 1973
39. Rabushka SE, Love L, Moncada R: Infusion tomography of the gallbladder. *Radiology* 109:549–552, 1973
40. Morgan H, Johnson PM: Splenic masses detected by scintillation imaging and contrast tomography. *Radiology* 97:301–306, 1970
41. Brill PW, Krasna IH, Aaron H: An early rim sign in neonatal adrenal hemorrhage. *Am J Roentgenol* 127:289–291, 1976
42. Stanley P: Total body opacification and the adrenal. *Pediatr Radiol* 5:58, 1976
43. Balsys R, Janousek J, Pulla RSK: Peripheral increased density in CT scanning in the differential diagnosis of intracranial lesions (abstr.). *Invest Radiol* 12:393, 1977
44. Barbaric ZL: Pelvocalyceal wall opacification, a new radiological sign. *Radiology* 123:587–589, 1977
45. Benton C, Hastings E: Intravenous cholangiography—excretion hepatography. *Radiology* 104:61–62, 1972
46. Griscom NT, Neuhauser EBD: Total body opacification. *J Pediatr Surg* 1:76–79, 1966
47. Dunbar JS, Nogrady B: Excretory urography in the first year of life. *Radiol Clin North Am* 10:367–391, 1972
48. Witten DM, Hirsch FD, Hartman GW: Acute reactions to urographic contrast medium. *Am J Roentgenol* 119:832–840, 1973
49. Martin DJ, Gilday DL, Reilly BJ: Evaluation of the urinary tract in the neonatal period. *Radiol Clin North Am* 13:359–368, 1975
50. Talner LB: Functional aspects of uroradiology. *Contrib Nephrol* 5:3–40, 1977
51. Standen JR, Nogrady MB, Dunbar JS, Goldbloom RB: The osmotic effects of diatrizoate (Renografin 60) in intravenous urography in infants. *Am J Roentgenol* 93:473–479, 1965
52. Ansell G: Fatal overdose of contrast medium in infants. *Br J Radiol* 43:395–396, 1970
53. Doust BD, Redman HC: The myth of 1 ml/kg in angiography. *Radiology* 104:557–560, 1972
54. Moreau JF, Droz Y, Sabto J, Jungers P, Keinknecht D, Hinglais N, Michel JR: Osmotic nephrosis induced by water-soluble tri-iodinated contrast media in man. *Radiology* 115:329–336, 1975
55. Elkin M: Radiology of the urinary tract, some considerations. *Radiology* 116:259–270, 1975
56. Dunbar JS, Nogrady MB: The calceal crescent—a roentgenographic sign of obstructive hydronephrosis. *Am J Roentgenol* 110:520–528, 1970
57. Griscom NT, Kroeker MA: Visualization of individual papillary ducts (ducts of Bellini) by excretory urography in childhood hydronephrosis. *Radiology* 106:385–389, 1973
58. O'Connor JF, Neuhauser EBD: Total body opacification in conventional and high dose intravenous urography in infancy. *Am J Roentgenol* 90:63–71, 1963
59. Holt JF, Whitehouse WM: *Year Book of Radiology, 1964–1965*. Chicago, Year Book Medical Publishers, 1965
60. Goodling CA, Berdon WE, Brodeur AE, Rowen M: Adverse reactions to intravenous pyelography in children. *Am J Roentgenol* 123:802–804, 1975
61. McAlister W: Pulmonary edema in a neonate from intravenous urography. Paper presented at the annual meeting of the Society for Pediatric Radiology, Denver, September 1978
62. Borra S, Hawkins D, Duguid W, Kaye M: Acute renal failure and nephrotic syndrome after angiocardiography with meglumine diatrizoate. *N Engl J Med* 284:592–593, 1971
63. Bergman LA, Ellison MR, Dunea G: Acute renal failure after drip-infusion pyelography. *N Engl J Med* 279:1277, 1968

Editorial

Rare Earth Screens and Silver

Compared to conventional calcium tungstate intensifying screens, rare earth screens have the disadvantages of higher cost and unfamiliar exposure characteristics. But they have important advantages as well: their ability to reduce radiation exposure has been emphasized [1], while their potential to conserve silver has been largely ignored.

Wagner [2], during a comparative study of rare earth and calcium tungstate screens, found that XD film, a fine grained film used with a rare earth system (Trimax, 3M Co., St. Paul, Minn.), contained approximately 23% less silver than XM and Kodak RP films. The low silver film was useful because of the increased brightness of the rare earth phosphors. These phosphors operate with increased detection efficiency permitting an exposure reduction of about 50% with no increase in noise (quantum mottle). Combining rare earth screens with the higher silver content films allowed even greater exposure reductions, but at the cost of increased noise.

While reducing radiation exposure is an important goal, reducing silver consumption may also be desirable. Silver is indispensable for manufacture of x-ray film. Industrial consumption of silver in the United States is more than five times greater than mine production [3]. Mine production of silver in the United States has been declining (fig. 1). The success of both mining and salvage is intimately related to the availability of natural gas and other energy supplies [4]. In the future energy shortages may further restrict silver production. Although the successive price increases in silver occurring since 1967 have stimulated salvage (recycling), they have had little effect on primary production. Primary production of silver is relatively insensitive to price, which Cook [5] attributes to depletion and to the special geologic characteristics of silver ores. Depletion of silver, although apparent for many years, for several reasons has not been of great concern. Instead, monetary silver and imports have been substituted for the industrial needs of the United States.

However, some alternatives have been considered. Silver has been more actively recovered from discarded film and photographic solutions. Electrophotography has been touted as a replacement for silver halide radiography. Manufacturers have had some success reducing the silver content in films designed for use with conventional screens, and rumors of a substitute for silver in film have surfaced.

Nevertheless, problems still exist. The supply of monetary silver is finite and diminishing. The two billion troy ounces of silver once held in the United States Treasury have largely disappeared. Mexico and India have restricted exports. Peru, an important supplier, has had declining production.

Over the past 5 years, imports of silver into the United States have averaged 88 million troy ounces per year. If this rate continues, and silver remains near its present price ($5.58 per troy ounce on August 2, 1978), silver imports will contribute about one-half billion dollars per year to our balance of payments deficit. This deficit, by affecting the international value of the dollar, may further increase the cost of imported silver.

Optimal silver recovery is difficult to obtain. Electrolytic recovery units commonly used in hospitals and medical offices are not always installed or monitored carefully. Faraday's law dictates that about 8 A·h of electric current are required to plate 1 troy ounce of silver. Recovery units of proper capacity must be used. Recently an electrolytic recovery unit was installed locally and wired to turn on and off automatically with a processor standby control. This resulted in insufficient power to plate the available silver, which was proved by testing the effluent for its silver content. Approximately 0.375 troy ounces of silver went down the drain with each gallon of fixer. Rewiring the unit to the main processor switch increased silver recovery.

Steel wool metallic cartridges are in common use. Unfortunately, they are frequently changed at improper intervals, and some units have been defective. To insure proper function, their effluent should be tested for its silver residual.

Rigorous studies by radiologists, radiologic organizations, and academic departments to determine the best methods to recover silver in various sized institutions are nonexistent. Issues such as the possible value of using recovery units in tandem and possible ways to recover low tenor solutions have been neglected.

Electrophotography, though useful for special purposes, has failed to replace film radiography. In fact the importance of x-ray film is growing, as it is increasingly used to record CT, ultrasound, nuclear, and thermographic images. It is not certain that there will ever be a chemical substitute for silver in x-ray (and photographic) film. Other light-sensitive chemical processes are far too slow. Research dating to the nineteenth century has failed to find a suitable substitute. The special photosensitivity of silver halides may depend on valence electron energy bands possessed by no element but silver.

In special situations dye coupling does allow substitutions for silver—after the initial exposure. For example, in color photography silver is present in the unexposed

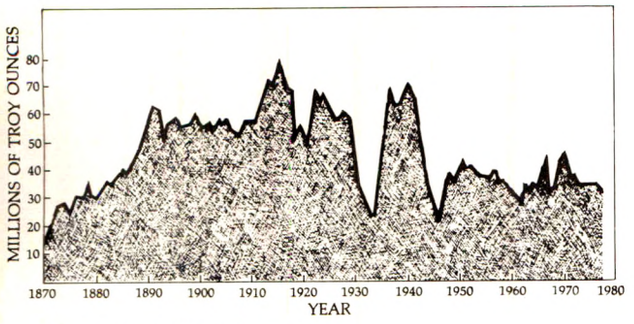

Fig. 1.—Silver production in the United States. Data from [3] and [10].

negative, but is removed from the final product and effectively recycled. A similar process occurs with Medichrome x-ray film (Agfa-Gevaert) [6].

In 1967, 44.8 million m² of x-ray film were shipped in the United States [7]. Five years later 70.6 million m² were shipped. X-ray films have an unusually high silver content. During the early 1960s medical x-ray film commonly contained from .291 to .431 troy ounces/m² of silver [8]. According to two different manufacturers, some films commonly used in recent years have contained approximately .237 troy ounces/m². Further reductions of silver content of films designed for calcium tungstate screens may be limited by considerations of speed and contrast, as well as quality control and a desirable D-max.

In 1975 an estimated 25 million troy ounces of silver were coated on x-ray film in the United States. Mine production in the United States was about 31.5 million troy ounces in 1977 [3]. If consumption of x-ray film continues to grow, the amount of silver used in radiology may soon exceed the amount mined in the United States, even if the silver used in other photographic materials for radiologic purposes is excluded.

Silver is truly a rare element. Its average concentration in the earth's crust is about 0.05 ppm [9]. The rare earths are not so rare. Lanthanum is about 600 times more prevalent than silver. In view of the growing use of x-ray film, declining production of silver, and worsening balance of payments, silver conservation may become increasingly important. The low concentration of silver in the earth's crust, and an even lower concentration in seawater, mandate that effective recycling be performed prior to dilution of wastes [10]. Otherwise silver cannot be economically recovered.

In addition to recycling, other techniques to conserve silver are needed. One approach would be wider use of rare earth screens with fine-grained low silver film. This might be accomplished while simultaneously reducing radiation exposure about 50%, with no adverse effect on image quality. In fact quality could be improved due to the use of shorter exposure times or smaller focal spots.

Rare earth screens have more potential advantages than reducing radiation exposure. When the possibilities of lessening the load on x-ray apparatus, decreasing the negative balance of payments, and conserving a truly precious metal are considered, the indications for wider use of rare earth screens are compelling.

Robert A. Wilson
2705 Loma Vista Road
Ventura, California 93003

REFERENCES

1. Newlin N: Reduction in radiation exposure: the rare earth screen. *Am J Roentgenol* 130:1195–1196, 1978
2. Wagner RF, Weaver KE: Prospects for x-ray exposure reduction using rare earth intensifying screens. *Radiology* 118:183–188, 1976
3. Handy and Harman Company: *The Silver Market 1977, 62d Annual Review*. New York, 1978
4. Wilson RA: Silver and the second law of thermodynamics. *Commodity J* 8:11–13, 1973
5. Cook E: The depletion of geologic resources. *Technol Rev* 77:13–28, 1975
6. Sellir K, Reichmann S: High-density failure of radiographic films. *Acta Radiol* 18:95–112, 1977
7. U.S. Department of Commerce, Bureau of the Census: *1972 Census of Manufacturers*, vol 2, pt. 3, 38B-24. Washington, D.C. Government Printing Office, 1976
8. Determination of silver in a fixing bath: Philip A. Hunt Company. Research Laboratory, July 1963
9. Geochemical distribution of elements, *Encyclopaedia Britannica*, 15th ed, vol 6, 1974, p 702
10. Wilson RA: Conservation of silver. *South Med J* 59:861–863, 1966

Letters

Renal Pseudocalculus

Schabel and Rogers [1] have demonstrated diagnostic problems resulting from the increased enthusiasm for health foods. We encountered a 40-year-old white female from the medical clinic with a 3 week history of moderate left flank pain radiating to the pelvis. A supine film of the abdomen showed a round density superimposed over the inferior pole of the left kidney (fig. 1), and she was referred for excretory urography. The scout film the following day showed no evidence of a left renal calculus. The patient admitted to being a health food enthusiast and to having taken a bone meal vitamin tablet 1 hr before the initial examination.

Radiologists are familiar with the appearance of pills within the gastrointestinal tract, barium in colonic diverticula, and residual Pantopaque in renal cysts [2]. Bone meal vitamin tablets fortified with calcium attain the density of some renal calculi and may give rise to some confusion. While the erroneous assumption of a renal calculus was made by the referring physician, radiologists unaware of the unusual dietary habits of some patients could easily make the same mistake. The fortuitious projection en face of the disk-shaped tablet compounds the confusion. Although the bone meal constituents of this tablet make it slightly more radiopaque, there are no structural features that might have identified it, except to physicians with a high index of suspicion. The usefulness of a scout film prior to excretory urography is reinforced.

Kong Meng Tan
Permanente Medical Group
Richmond, California 94804

REFERENCES

1. Schabel SI, Rogers CI: Opaque artifacts in a health food faddist simulating ovarian neoplasm. *Am J Roentgenol* 130:789–790, 1978
2. Eisenberg RL, Mani RL: Residual Pantopaque in renal cysts: an addition to the differential diagnosis of intra-abdominal heavy metal densities. *Clin Radiol* 29:227–229, 1978

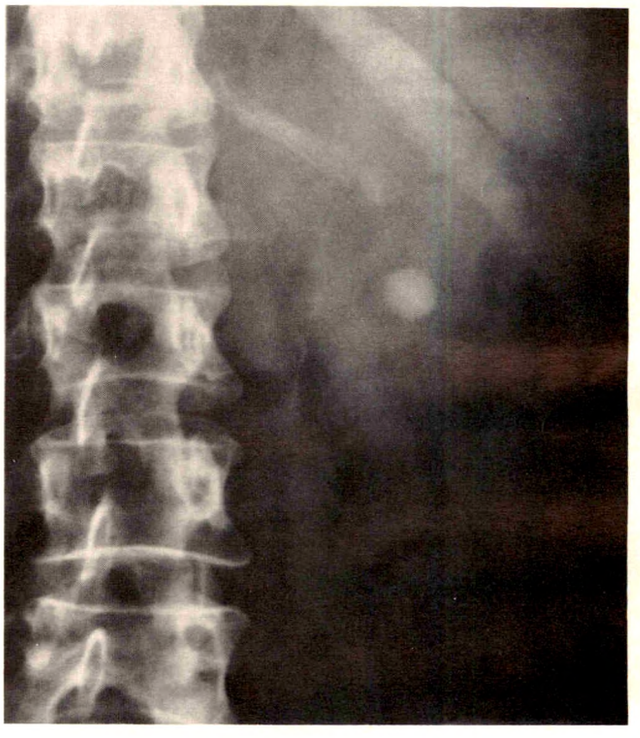

Fig. 1

Summary of American Roentgen Ray Society 1979 Meeting

March 25–30, Sheraton Centre, Toronto, Canada

A description of the meeting including a comprehensive listing of courses and information on the Categorical Course on Neuroradiology, appeared in the October issue of AJR. For reader convenience, **the complete packet of colored registration forms appears in both the October and November AJR issues.** Included are: meeting registration forms backed by the course registration form, hotel reservations, spouses' program, and forms for the tennis tournament and social evening.

In the February issue, AJR will list the papers and exhibits scheduled for presentation during the scientific sessions of the ARRS and SPIE.

Accreditation

All courses meet the criteria for AMA Category I credit.

Meeting Format

Scientific Program. Sessions will be during the latter half of each morning, Monday–Friday, as well as Tuesday and Thursday afternoons. Papers will be grouped by topic and parallel scientific sessions will be held.

Refresher Courses. A full scope of courses will be offered on Monday and Wednesday afternoons and Tuesday, Thursday, and Friday mornings.

Categorical Course on Neuroradiology. This 15 hr course will begin on Sunday, March 25, and continue through Friday, March 30 (except on Wednesday).

Caldwell Lecture. Dr. Joseph Whalen will deliver this prestigious address on Wednesday morning, March 28.

Exhibits

Scientific exhibits will be open on Sunday, March 25, from 7–11 p.m., 7 a.m.–11 p.m. on Monday through Thursday, and 7 a.m. to 1 p.m. on Friday. Technical exhibits will be open from 9 a.m. to 5:30 p.m., Monday through Thursday, and 9 a.m. to 1 p.m. on Friday.

Other Society Meetings

The Society for Pediatric Radiology will meet March 24 and 25. A joint program with ARRS is planned for the morning on March 26. The Society for Photo-Optical Instrumentation Engineers will meet March 25 and 26, and a joint program with this group is anticipated on March 27. The American Thermographic Society will meet March 29–April 1.

Local Activities

Spouses' Program. On March 26, a theater tour and luncheon are scheduled; March 27 features a walk through a maple woods or a bus tour of downtown Toronto. Both groups meet for lunch before visiting "the most Canadian art gallery". On March 28, a day-long tour to Niagara Falls is scheduled with time for shopping. A fashion show and brunch will be March 29. Meals are included in tour prices (Canadian funds) which are listed on the registration form. No receipts or confirmations will be mailed. All tickets and badges should be picked up at the Spouses' Registration Desk, Sheraton Centre Hotel.

Tennis Tournament. March 28 at Mayfair Racquet Club, Downsview, Ontario. Schedule: bus transportation from Sheraton Centre, 11:45 a.m.; luncheon; play; cocktails; trophy presentation; return to hotel, 6:30 p.m. Play is limited to 48. To register, see form.

Golf Tournament. Cancelled this year

Social Evening at Ontario Place. Thursday, March 29, buffet supper at 7:45 p.m. following a happy hour. Film, North of Superior, will follow. Busses will leave Sheraton Centre at 6:30 p.m., return approximately 10 p.m. Tickets are $16.50 (Canadian funds) and will be held at the Spouses' Registration Desk. To register, send form with check (payable to ARRS Dinner).

Meeting Registration

Preregistration by mail will be accepted until March 1 (see form). Late registrants may register on site. Official badges and program booklets will be available at the registration desk, Four Seasons Sheraton Hotel. No registration confirmations will be made.

Course Registration

Register early, enrollment is limited. Registrants should list first, second, and third choices for each period unless they take the categorical course. **Registration in categorical course fills all course time and precludes registration in other courses.** All ticket orders will be filled according to postmark. Fees: $25 for all who take categorical course; other courses, no fee to ARRS members, $3 per course for nonmembers. Payment must accompany instruction order sheet. If enrolling late, send form to Dr. Gedgaudas, Four Seasons Sheraton Hotel, 123 Queen Street West, Toronto, Ontario, Canada. Make checks payable to American Roentgen Ray Society.

Hotel Registration

Reservations will be handled by the ARRS Housing Bureau in Toronto (see form) and must be made by February 25. Participating hotels, prices, and a map are on form.

Fees

Meeting:	
ARRS members	No fee
Nonmembers	$25
Physicians in training (with verification)	15
Courses:	
Categorical course, for all who enroll	25
Other courses, ARRS members	0
Other courses, nonmembers, per course	3

Cancellations and Fee Refund

Course fees will be refunded only if cancellations are received before March 20. Cancellations should be sent to ARRS, 20 North Wacker Drive, Chicago, Illinois 60606.

U.S. POSTAL SERVICE

STATEMENT OF OWNERSHIP, MANAGEMENT AND CIRCULATION

(Required by 39 U.S.C. 3685)

1. TITLE OF PUBLICATION	A. PUBLICATION NO.	2. DATE OF FILING
THE AMERICAN JOURNAL OF ROENTGENOLOGY		9-12-78
3. FREQUENCY OF ISSUE	**A. NO. OF ISSUES PUBLISHED ANNUALLY**	**B. ANNUAL SUBSCRIPTION PRICE**
MONTHLY	12	$ 40.00

4. LOCATION OF KNOWN OFFICE OF PUBLICATION *(Street, City, County, State and ZIP Code) (Not printers)*

301-327 East Lawrence Avenue, Springfield, Illinois 62717

5. LOCATION OF THE HEADQUARTERS OR GENERAL BUSINESS OFFICES OF THE PUBLISHERS *(Not printers)*

CHARLES C THOMAS, PUBLISHER, 301-327 East Lawrence Ave., Springfield, IL 62717

6. NAMES AND COMPLETE ADDRESSES OF PUBLISHER, EDITOR, AND MANAGING EDITOR

PUBLISHER *(Name and Address)*

CHARLES C THOMAS, PUBLISHER, 301-327 East Lawrence Ave., Springfield, IL 62717

EDITOR *(Name and Address)*

Melvin M. Figley, M.D., 403 Pacific National Bank Bldg., 4545 - 15th Ave., N. . Seattle, WA 98105

MANAGING EDITOR *(Name and Address)*

NONE

7. OWNER *(If owned by a corporation, its name and address must be stated and also immediately thereunder the names and addresses of stockholders owning or holding 1 percent or more of total amount of stock. If not owned by a corporation, the names and addresses of the individual owners must be given. If owned by a partnership or other unincorporated firm, its name and address, as well as that of each individual must be given.)*

NAME	ADDRESS
THE AMERICAN ROENTGEN SOCIETY, a non-profit organization incorporated in the District of Columbia	
Dr. James F. Martin, Secretary	300 S. Hawthorne St., Winston-Salem, NC 7103
Dr. Raymond A. Gagliardi, Chairman, Publication Committee	880 Woodward Ave. Pontiac, MI 48055

8. KNOWN BONDHOLDERS, MORTGAGEES, AND OTHER SECURITY HOLDERS OWNING OR HOLDING 1 PERCENT OR MORE OF TOTAL AMOUNT OF BONDS, MORTGAGES OR OTHER SECURITIES *(If there are none, so state)*

NAME	ADDRESS
NONE	

9. FOR COMPLETION BY NONPROFIT ORGANIZATIONS AUTHORIZED TO MAIL AT SPECIAL RATES *(Section 132.122, PSM)*

The purpose, function, and nonprofit status of this organization and the exempt status for Federal income tax purposes *(Check one)*

☐ HAVE NOT CHANGED DURING PRECEDING 12 MONTHS ☐ HAVE CHANGED DURING PRECEDING 12 MONTHS *(If changed, publisher must submit explanation of change with this statement.)*

10. EXTENT AND NATURE OF CIRCULATION	AVERAGE NO. COPIES EACH ISSUE DURING PRECEDING 12 MONTHS	ACTUAL NO. COPIES OF SINGLE ISSUE PUBLISHED NEAREST TO FILING DATE
A. TOTAL NO. COPIES PRINTED *(Net Press Run)*	15,000	14,989
B. PAID CIRCULATION 1. SALES THROUGH DEALERS AND CARRIERS, STREET VENDORS AND COUNTER SALES		
2. MAIL SUBSCRIPTIONS	13,804	14,525
C. TOTAL PAID CIRCULATION *(Sum of 10B1 and 10B2)*	13,804	14,525
D. FREE DISTRIBUTION BY MAIL, CARRIER OR OTHER MEANS SAMPLES, COMPLIMENTARY, AND OTHER FREE COPIES	155	166
E. TOTAL DISTRIBUTION *(Sum of C and D)*	13,959	14,691
F. COPIES NOT DISTRIBUTED 1. OFFICE USE, LEFT OVER, UNACCOUNTED, SPOILED AFTER PRINTING	1,041	298
2. RETURNS FROM NEWS AGENTS	———	———
G. TOTAL *(Sum of E, F1 and 2—should equal net press run shown in A)*	15,000	14,989

11. I certify that the statements made by me above are correct and complete.

SIGNATURE AND TITLE OF EDITOR, PUBLISHER, BUSINESS MANAGER, OR OWNER

Wayne Bolinger Business Manager

12. FOR COMPLETION BY PUBLISHERS MAILING AT THE REGULAR RATES *(Section 132.121, Postal Service Manual)*

39 U. S. C. 3626 provides in pertinent part: "No person who would have been entitled to mail matter under former section 4359 of this title shall mail such matter at the rates provided under this subsection unless he files annually with the Postal Service a written request for permission to mail matter at such rates."

In accordance with the provisions of this statute, I hereby request permission to mail the publication named in Item 1 at the phased postage rates presently authorized by 39 U. S. C. 3626.

SIGNATURE AND TITLE OF EDITOR, PUBLISHER, BUSINESS MANAGER, OR OWNER

Wayne Bolinger Business Manager

(See instructions on reverse)

Abstracts of Current Literature

Chest

The hypertransradiant hemithorax: the importance of lateral decentring, and the explanation for its appearance due to rotation. Joseph AEA, deLacy GJ, Bryant THE, Stoker DJ, Ayr G (Department of Diagnostic Radiology, St. George's Hospital, London, Engand). *Clin Radiol* 29:125–131, March 1978

Experimental evidence is presented indicating that 80% of the increase in unilateral film blackening on the chest radiograph resulting from rotation of the patient is due to asymmetrical absorption of the x-ray beam. Scatter contributes 20% to this increase in blackening. The effect on the radiograph of lateral decentring is also described. In the rotated patient, the hypertransradiant hemithorax always occurs on the side to which the patient is rotated, and is independent of the projection. If this rule is broken, then decentring or a thoracic abnormality is present.

Author Abstract

Vascular pseudo-tumours of the mediastinum in asymptomatic patients. A tomographic study. I. Arteries II. Veins (in English). Westra D (University Hospital, Amsterdam, the Netherlands). *Radiol Clin* 47:100–113 and 47:169–181, 1978

These two articles discuss the radiologic features of asymptomatic mediastinal pseudotumors of vascular origin that were detected accidentally on routine chest radiographs. A distinction is made between vascular pseudotumors of arterial and of venous origin. The first article discusses pseudotumors of arterial origin, the majority of which are based on a tortuous descending aorta, buckling innominate artery, aneurysm of the aorta, or congenital anomalies of the aortic arch and its major branches. The second article deals with the venous category. The majority of venous pseudotumors are caused by dilated mediastinal veins as a result of impaired flow due to congestive heart failure or pericarditis, or increased blood supply due to occlusion or congenital absence of other veins. The author discusses how the vascular nature of these findings can be established; particular attention is on the role of tomography.

Peter F. Winter

Lymphocytic interstitial pneumonitis. Review of 13 cases. Strimlan CV, Rosenow EC III, Weiland LH, Brown LR (E. C. Rosenow III, Mayo Clinic, Rochester, Minnesota 55901). *Ann Intern Med* 88:616–621, 1978

This paper reviews 13 cases of lymphocytic interstitial pnemonitis seen at the Mayo Clinic from 1966 to 1976. This condition is currently regarded as a reactive lymphocytic infiltration of the lung, somewhat analogous to the involvement of the salivary glands in Sjögren's syndrome. Ordinarily patients present with fever, cough, and weight loss that is often accompanied by considerable dyspnea. Chest x-rays usually show bilateral coarse infiltrates; bacteriologic culture studies are negative. Lung biopsies reveal lymphocyte accumulation without formation of germinal centers. As reported in this series, there is a high association with dysproteinemias and it is presumed this may be an immunologic disease. Patients with lymphocytic interstitial pnemonitis are often treated with corticosteroids and immunosuppressive drugs. Although the prognosis is reported by some to be better than that for the malignant lymphonomas, in this series five of 13 patients died in less than 2 years. This report is noteworthy because of the number of cases reported and the excellent review of current literature.

David C. Dale
Department of Medicine
University of Washington

Lung radiography additional techniques without special equipment. Lame EL (VA Hospital, Coatesville, Pennsylvania 19320). *Revista Interam Radiol* 3:93–98, April 1978

Several special techniques have been designed to reveal the lung apices. These are readily learned and may give considerable valuable information, without the use of special equipment. One technique is the use of the fine line grid and/or the moving Bucky. This reduces scatter and gives better detail. The authors also suggest the use of 30 degree or 45 degree oblique exposures of the complete chest, when extensive pulmonary disease exists. It is stated that these views are often of greater value than lateral views since they avoid superimposition of bilateral lesions. When these are used (in the presence of apical disease especially) the clavicle nearest the cassette in the posteroanterior oblique posture should be raised by elevating that arm and resting the hand on the head. This is termed "clavicle high". Usually the apex is seen more clearly.

The McPhedran apical rotation technique consists of use of a small film (20 × 25 cm sharply coned to 13 cm) and small degrees of obliquity for apical tuberculosis, which usually lies posteriorly. Usually 20–25 degrees of obliquity is used with this technique and always with the clavicle high.

The anteroposterior caudad angle ray is taken by having the patient stand or sit erect with scapulae rolled forward. The central ray is angled 25–30 degrees caudad to pass through the apical level. The application of the clavicle high principle to the standard posteroanterior full-size chest film, when the lesion is obscured by the clavicle at its normal level, may be done by raising both arms enough to elevate the clavicle but not so much as to force the patient away from the grid or the Bucky.

Charles M. Nice, Jr.

Pulmonary barotrauma in scuba divers—the role of radiology. Foote GA (Auckland Hospital, Auckland, New Zealand). *Australas Radiol* 21:125–129, June 1977

Direct effects of high pressures on the underwater diver are of no consequence providing the gas in the air containing cavities is at ambient pressure maintained from a high pressure reservoir by way of regulator valves. During ascent, the diver exhales freely to reduce the intrapulmonary pressure and maintain the lung volume constant. Overdistension of part or all of the lung results from resistance to exhalation with subsequent rupture of alveolar walls. This may result in interstitial emphysema, mediastinal emphysema, or pneumothorax. If tears involve pulmonary blood vessels, air may be drawn into the circulation causing air embolism. Pulmonary barotrauma results from either a "free ascent" or due to pulmonary pathology resulting in air trapping.

A case is reported of pulmonary barotrauma and air embolism following a scuba diver's first deep water dive. He lost consciousness on surfacing, regaining normal cerebral function only after several weeks, but was left with some residual spinal damage. Radiographs obtained at the time, and at subsequent examinations, revealed evidence of unilateral emphysema (Swyer-James syndrome) with air trapping during expiration. It is postulated that overexpansion of the abnormal lung occurred during ascent with rupture of alveolar walls, dissection of air into pulmonary veins and systemic air embolism. A second case is presented of a potential scuba diver who was advised against diving because of the discovery of a pulmonary bulla. The importance of chest radiographs during inspiration and expiration of aspiring scuba divers is stressed.

John Branson

Radiologic findings in acute childhood asthma. Gillies JD, Reed MH, Simons FER (Children's Center, Winnipeg, Canada). *J Can Assoc Radiol* 29:28–33, March 1978

The authors retrospectively reviewed the radiographs and clinical and laboratory histories on 178 admissions of 142 children with clinical asthma. Hyperinflation, which was difficult to assess on the radiographs, was demonstrated on only 6% of cases. Other complications such as consolidation (21%), atelectasis (3%), and pneumomediastinum (2%) were demonstrated, usually in the severe or moderately severe asthmatic child. The authors conclude that chest radiographs are justified in the assessment of children presenting with acute asthma due to the significant incidence of pulmonary complications.

Jack M. A. Tishler

Cardiovascular

Portosystemic communications studied by transhepatic portography. Nunez D, Russell E, Yrizarry J, Pereiras R, Viamonte M (School of Medicine, University of Miami, P. O. Box 520875, Biscayne Annex, Miami, Florida 33152). *Radiology* 127:75–79, April 1978

Radiographic findings are reported on the basis of 120 transhepatic portograms. Increasing portal pressure causes reopening of embryonic channels and diversion of venous blood flow to the systemic circulation. Type and number of portosystemic pathways vary from one individual to another.

The three major collateral pathways are: splenorenal, gastrorenal, and anterior parietal. The splenorenal and/or gastrorenal are formed after varices in the stomach appear. Coronary and short gastric vein drain into the left renal vein and through it into the inferior vena cava. Direct drainage from the spleen to the left renal may take place via the pancreatic and retroperitoneal veins. These last two possibilities have been found to present typical angiographic morphology consisting of a large single draining channel running caudad in the left paravertebral gutter to the level of the first lumbar vertebral body. Here the collateral channel drains into the adrenal vein, which dilates and then empties into the left renal vein with an hourglass-like appearance. Connection between portal and systemic veins is in the narrowed region of the hourglass.

The anterior parietal pathway transports portal blood via umbilical and paraumbilical veins draining in the anterior abdominal wall into superficial epigastric veins. The superior epigastric vein drains into the superior vena cava via the internal thoracic vein. The inferior epigastric vein drains into the inferior vena cava via the external iliac vein. Of lesser importance were communications between the inferior mesenteric vein and hemorrhoidal plexus and superior mesenteric vein communications with inferior vena cava. The authors assessed the location, number, and size of collateral channels, as well as the flow pattern. These features were considered when percutaneous embolization was contemplated.

Asher Nov

Relation of cigarette smoking to myocardial infarction in young women. Slone D, Shapiro S, Rosenberg L, Kaufman DW, Hartz SC, Rossi AC, Stolley PD, Miettinen OS (Drug Epidemiology Unit, 10 Moulton Street, Cambridge, Massachusetts 02138). *N Engl J Med* 298:1273–1276, June 8, 1978

This important epidemiological study conducted in 152 hospitals in the Northeast indicates that women who smoke approximately 35 cigarettes per day have a 20-fold increased risk of myocardial infarction. The relative risk is increased modestly even for exsmokers. The risk is approximately two to five times normal for individuals who smoke one to 14 cigarettes per day, three to 12 times normal for those smoking 15–24 cigarettes per day, and the risk is progressive with a linear increase beyond this point with no suggestion of a plateau. Since the individuals with hypertension, previous myocardial infarction, abnormalities of blood lipids, diabetes, severe obesity, and current use of oral contraceptives were excluded, the interrelationships of these factors with smoking was not reported. However, since these factors were excluded, the results of this study very clearly show that the risk of smoking for women is the same as that previously reported for men. As this article points out, there is a steadily increasing rate of cigarette smoking in American women below age 25. Unless this pattern changes this study predicts that premature myocardial infarction in women will be an increasingly frequently encountered medical problem.

David C. Dale
Department of Medicine
University of Washington

The importance of quantitative left ventriculography in coronary heart disease (in French). Solignac A, La Pointe AC, Bourassa MG (Hôtel Dieu. 3840 rue Saint-Urbain, Montreal, P.Q. H2W IT8, Canada). *Ann Radiol* 21:1–7, 1978

It is known that chronic coronary heart disease is accompanied by abnormal contractions of the left ventricle which are of significant importance in the prognosis. This report evaluates the relationship between the ventricular asynergy and the volumetric parameters of the ventricular function.

The patients studied were shown by angiography to have coronary disease with occlusion of more than 70% of its lumen of at least three main coronary arteries. A total of 63 individuals were examined by left cineventriculography. Nineteen cases showed normal left ventricular contractions; in 11 there was minimal ventricular dysfunction, characterized by unisegmental hypokinesia; 15 showed marked ventricular dysfunction: segmental hypokinesia or unisegmental akinesia; in the remaining 18 cases severe ventricular dysfunction was noted, characterized by marked, diffuse hypokinesia, or unisegmental akinesia.

The findings are discussed in detail. The authors conclude that cinceventriculography is the method of choice in the evaluation of the contractility of the left ventricle in patients with coronary disease. It is also possible to determine the telediastolic and telesystolic volumes and the ejection fraction. These and the left ventricular dysfunction should always be analyzed as a routine angiographic evaluation of coronary heart disease.

Antonio F. Govoni

Severe hemorrhage of the lower digestive tract. The value of emergency arteriography (in French). Kunstlinger F, Roche A, Harry G, Busy F, Doyon D (D. Doyon, Faculté Paris-Sud, Service de Radiologie, Hôpital Bicêtre, rue du Général Leclerc, F-94270 Le Kremlin Bicêtre, France). *Ann Radiol* 21:19–24, 1978

Hemorrhages of the lower gastrointestinal tract originating from any segment of bowel between the duodenum and the rectum cannot always be evaluated by endoscopy. However, emergency angiography may localize the hemorrhage.

Six cases with severe rectal bleeding are reported in detail. The lesions demonstrated by angiography were: (1) in the cecum, simple benign ulcer; (2) bleeding diverticulum in the area of anastomosis, status postleft hemicolectomy for diverticulitis; (3) vascular dysplasia of the right colon; (4) ulcer of descending duodenum; (5) rich cecal vascularization with small leakage; (6) hypervascularized tumor of the proximal jejunum which proved to be leiomyoma.

Antonio F. Govoni

Gastrointestinal

The portal triad and hepatic cirrhosis. Witte CL, Witte MH, Dumont AE (University of Arizona School of Medicine, Tucson, Arizona). *Surg Gynecol Obstet* 146:965–974, June 1978

This review article brings together and summarizes the current information regarding the pathophysiology of (1) ascites formation; (2) formation and rupture of esophagogastric var-

ices; and (3) congestive splenomegaly in hepatic cirrhosis. Although this triad is well known, the etiology and progression of these complications involves much more than portal venous hypertension and the resultant passive congestion of the spleen and splanchnic bed. Other important but less well known pathophysiological processes (e.g., increased splanchnic arterial blood flow and its contribution to rupture of gastroesophageal varices and to the development of hypersplenism) are lucidly presented.

Reiley Kidd

Syndrome of Plummer-Vinson (in Spanish). Munyo JC, Leborgne F, Alonso Regules JE (Hospital Pereira Rossell, Montevideo, Uruguay). *Revista Interam Radiol* 3:37–41, Jan 1978

The Plummer-Vinson syndrome or sideropenic dysphagia has been somewhat misunderstood because some patients will have iron deficiency anemia and dysphagia without allowing demonstration of a membrane in the upper esophagus on radiographic examination, whereas other patients may sometimes show what appears to be a thin membrane on the upper portion of the esophagus without having iron deficiency anemia. Hypertrophy of the cricopharyngal sphincter and of the retrocricoid venous plexus may sometimes cause small indentations in the barium column. The indentation produced by the cricopharyngeus is usually posterior whereas those of the venous plexus are seen on the anterior wall of the esophagus. The authors present four female patients who had some degree of glossitis, spoon shaped nails, iron deficiency anemia, and who showed the small thin membranes in the anterior wall of the upper esophagus. Radiographs are reproduced to show the difference between the typical membrane attributed to the Plummer-Vinson syndrome and those which may be due to the cricopharyngal sphincter and the retrocricoidal venous plexus.

Charles M. Nice, Jr.

Profile roentgenographic features of benign greater curvature ulcers. Zboralske FF, Stargardter FL, Harell GS (S068A, Stanford University Medical Center, Stanford, California 94305). *Radiology* 127:63–67, April 1978

Certain roentgenographic features have been considered typical of benign gastric ulcers, based almost entirely on studies of the *lesser* curvature. However, these features frequently are not present on the profile view in benign *greater* curvature ulcers. Moreover, features stated to suggest malignancy in gastric ulcers are commonly simulated by benign greater curvature ulcers. The authors reviewed the profile roentgenographic features of 19 benign greater curvature ulcers and found that they often appeared to be intraluminal and had shouldered edges due to spasm of the surrounding circular muscles. In 6 patients the adjacent gastric contour was scalloped. These features frequently cause radiologists to misinterpret benign greater curvature ulcers as malignant.

Author Abstract

An unusual tumour of the lesser sac. Meredith HC (Medical University of South Carolina, Charleston, South Carolina 29401). *Australas Radiol* 2:140–142, June 1977

A 15-year-old Negro girl is described with a cystadenoma in heterotopic pancreas within the lesser sac. The patient presented with abdominal swelling of 18 months duration. Radiologic investigations, including excretory urogram, barium meal, and barium enema showed displacement of the organs around the mass; ultrasound showed a fluid-filled structure with multiple septations. Angiography revealed the tumor to be vascular in its upper quarter and relatively avascular in its lower three quarters. At laparotomy the mass was found to be free within the lesser sac and clearly free from the pancreas. Histologically the tumor was papillary and cystic, either benign or of very low grade malignancy.

In the literature the incidence of heterotopic pancreas has been variously reported as 1:120 to 1:600 and at necropsy from 0.6%–5.6%. The various anatomic sites include stomach, duodenum, and jejunum which have accounted for the majority (70%). The incidence in the abdomen outside of abdominal organs has been approximately 5%. Heterotopic pancreatic tissue may undergo all the pathologic changes seen in the normally located pancreas. Cystadenomas are a rare tumor and 80% present as an abdominal mass, with a female to male ratio of 9:1. They occur mainly from the fifth decade onwards; most are hypervascular; differentiation between benign and malignant is difficult.

I. Renn

Comparative study between radiology and endoscopy in the diagnosis of duodenal ulcer (in Italian). Liguory CI, Familiari L(Hôpital St. Antoine, Centre d'Endoscopie, 184 rue du Faubourg St. Antoine, F-75571 Paris, France). *Minerva Gastroenterol* 23:285–290, 1977

The authors report on the diagnostic accuracy of diagnosing a duodenal ulcer by radiographic studies and/or endoscopy. From a large series of endoscopies, 240 cases were reviewed in which a duodenal ulcer was either diagnosed by radiographs, endoscopy, or by both. A good diagnostic correlation was found in 134 cases (55.8%). In 68 cases a duodenal ulcer diagnosed radiographically was confirmed in 48 by endoscopy; an ulcer suspected radiographically in 30 was confirmed in eight, while in 13 cases, endoscopy showed scarring; in 126 cases with radiographic diagnosis of deformed bulb, 35 active ulcers were demonstrated.

Antonio F. Govoni

Double contrast examination of the stomach with preliminary thinlayer and pharmacological studies. Correlation between radiology and endoscopy: first results (in French). Clément JP, Burelle H, Corbeau A, Caizergues J (Service Central d'Electroradiologie, Hôpital Sainte-Marguerite, BP 29, F-13274 Marseille, France). *Ann Radiol* 21:33–38, 1978

The procedure presented consists of two main stages, possibly followed by a third. Before the examination, each patient is given isopropamide iodide to obtain gastric hypotony and enable more precise and constant results. In the first stage of the technique, the patient, in the erect position, drinks two mouthfuls of barium (Micropaque) and while he turns himself once or twice, the table is brought to the horizontal position. At this time the anterior wall of the stomach and the antrum are examined and radiographs are taken with the patient in both prone and supine positions. In the second stage, the patient is again in the upright position. At this time he drinks 150–200 cc of barium to which is added 1 cc of an antifoaming agent. Radiographs of the stomach-duodenum are taken in different projections. The patient then rapidly drinks 5–10 cc of water in which 5–10 spoons of ENO salts are dissolved. The table is again brought to the horizontal position and the patient turns around himself once or twice and radiographs are taken in different projections of the various areas of the stomach and duodenal bulb. A third stage consists of additional diluted barium with tension of 130 kV. Generally no more than 12 radiographs are exposed. A comparison between the diagnostic accuracy obtained by this method and by endoscopy was correlated in 190 examinations. A radiographic diagnostic accuracy was noted in 167 cases (87.8%).

Antonio F. Govoni

Double-blind radiographic study of dose response to intravenous glucagon for hypotonic duodenography. Miller RE, Chernish SM, Brunelle RL, Rosenak BD (Indiana University School of Medicine, Indianapolis, Indiana 46202). *Radiology* 127:55–59, April 1978

This study was undertaken to determine a dose response to glucagon during hypotonic duodenography. Fifteen male and

female volunteers received placebo and 0.25 mg, 0.5 mg, 1 mg, and 2 mg of glucagon intravenously, double-blind, and crossover. Onset of drug effect occurred in approximately 45 seconds, regardless of the dose of glucagon given. There was a significant ($p < 0.01$) decrease in gastrointestinal tonicity with all doses. The larger the dose, the greater the duration of drug action. Satisfactory stomach, duodenal, and small bowel hypotonicity for radiography were obtained with 0.25 to 0.5 mg of glucagon given intravenously with few side effects.

Author Abstract

Calcified primary tumors of the gastrointestinal tract. Ghahremani GG, Meyers MA, Port RB (Evanston Hospital–Northwestern University, 2650 Ridge Avenue, Evanston, Illinois 60201). *Gastrointest Radiol* 2:331–339, 1978

Twenty-three examples of calcified primary tumors of the gastrointestinal tract are presented and their radiographic manifestations illustrated. The incidence of calcified primary gastrointestinal tumors are mucinous adenocarcinoma of the colon, (six); mucinous adenocarcinoma of the stomach, (five); hemangioma of the colon, (three); leiomyoma of the esophagus, (two). One example each is presented of gastric neurolemmoma, small intestinal leiomyosarcoma, small intestinal hemangioma, colon colonic leiomyosarcoma, cystadenocarcinoma of the pancreas, and cholangiocarcinoma, and hepatoma. The authors summarize the lesions by character of the calcification and location by stating that a retrocardiac mass containing amorphous calcification is typical of esophageal leiomyoma, calcification similar to that of uterine fibroids may be the feature of gastric leiomyoma or intestinal leiomyosarcoma, sand-like deposits within the stomach or colon suggest mucinous adenocarcinoma, clusters of phleboliths suggest a hemangioma, sunburst type calcification of the pancreas indicates cystoadenoma or cystadenocarcinoma, and aggregates of granular calcification in the liver are diagnostic for metastatic adenocarcinoma of the colon but may rarely be seen in a primary hepatic malignancy. The authors note that the most commonly calcified neoplasm in their series were mucinous adenocarcinomas of the stomach or colon. They note that the presence of mucin possibly acts as an ion exchange resin influencing the deposition of calcium within these carcinomas and their metastases. Calcifications also occur within areas of necrosis and hemorrhage.

Charles A. Rohrmann, Jr.

Giant duodenal ulcers. Eisenberg RL, Margulis AR, Moss AA (Radiology Service, Veterans Administration Hospital, 4150 Clement Street, San Francisco, California 94121). *Gastrointest Radiol* 2:347–353, 1978

The authors present 26 patients in whom giant duodenal ulcers were correctly diagnosed prior to endoscopic confirmation. Clinical and radiographic features are described. The authors emphasize the concept of the ulcer/bulb ratio (ratio of the longest diameter of the ulcer to that of the total bulb length including the ulcer). Only one case in their series was designated as a giant duodenal ulcer by the ulcer/bulb ratio which would not have been designated as such by the classic criteria of size (2.5 cm in diameter). Although the mortality rate of giant duodenal ulcers has been previously reported as up to 40%, only three of the 26 patients in the current series died and only two (8%) could be attributed to the giant duodenal ulcer. Because of these findings, the authors support the concept of intensive medical therapy rather than immediate operative intervention. The authors summarize the significant radiographic features as follows. The giant duodenal ulcer is differentiated from the duodenal bulb by its constancy in size and shape and its lack of normal mucosal pattern. Alterations in the appearance of the pylorus proximally and of the duodenum distal to the ulcer were found with gastric outlet obstruction in four cases. The ulcer often has a nodular floor simulating a polypoid mucosal abnormality but this is felt to represent necrotic pancreas, granulation tissue, or blood clots. An "ulcer within an ulcer" appearance is described where a small area of deeper ulceration is seen in the giant ulcer. This is an important feature to recognize since the smaller ulcer may cause underinterpretation of the large defect. The concept of the ulcer/bulb ratio is advocated by the authors as a diagnostic feature and the ratio should be 0.8 or greater to establish the diagnosis.

Charles A. Rohrmann, Jr.

Genitourinary

The spectrum of angiographic findings in transitional cell carcinoma of the kidney. Cho KJ (University of Michigan Medical Center, Ann Arbor, Michigan 48109). *Australas Radiol* 21:189–194, June 1977

The angiographic findings of 20 patients with transitional cell carcinoma are reviewed. Of the patients, 16 were men and four were women. Average age was 59 years. In 15 patients the diagnosis was made on the angiographic findings which consisted of a combination of the following: tumor vessels, tumor stain, prominent pelvoureteric arteries, arterial encasement, pruned tree appearance, defect in nephrogram, hydronephrosis, and venous invasion or displacement. In five patients, the angiographic findings were normal and in these cases the tumors averaged 1.1 cm in size primarily involved the calyces and were situated within the renal parenchyma. The use of pharmacoangiographic agents improved the angiographic visualization of the tumors in the majority of cases. The differential diagnosis of the angiographic findings is discussed together with differentiation from infectious lesions. The results indicate that the accuracy of angiography is not appreciably greater than excretory urography and retrograde study, but is of value when there is a nonfunctioning kidney (usually due to an obstruction) or when the extent of the tumor and renal vein involvement is to be assessed.

I. Benn

Intraoperative ureteral trauma: a radiologic approach. Barbaric ZL, Wolfe DE, Segal AJ (University of Rochester School of Medicine and Dentistry, Rochester General Hospital, Rochester, New York 14642). *J Can Assoc Radiol* 29:40–43, March 1978

Intraoperative ureteral trauma or ligation is not an uncommon complication of gynecological surgery. The authors report on their experience with 32 cases of ureteral trauma and ligation, approximately one-third as a result of gynecologic surgery, one-third secondary to urologic surgery or instrumentation and one-third due to other general surgical procedures such as sympathectomy, aortoiliac graft, colectomy, and pancreatectomy.

The most common symptoms are abdominal pain and tenderness, usually followed by fever. There is usually a delay, often up to 1 month, because of pain and sedation associated with the operative procedure. This delay may result in increased morbidity and mortality. The authors urge that an excretory urogram be obtained if this complication is suspected. A retrograde pyelogram or percutaneous study may be required for further evaluation and decompression.

Jack M. A. Tishler

Urologic complications in renal homotransplantation. Pastershank SP, Ty M (University Hospital, Saskatoon, Saskatchewan, Canada S7N OW8). *J Can Assoc Radiol* 29:34–39, March 1978

The authors describe their experience with 161 renal transplant patients. Nineteen (11.8%) developed urologic complications. Of these, 18 received cadaver kidneys and one a live donor kidney. In all patients, the ureter was attached to the bladder via a ureteroneocystostomy, and a ureteral stint was used in 13 of these patients. All patients were investigated by excretory urography or fistula tract injection. No nuclear scans were done.

Eighteen patients developed urologic complications 1–56

days after transplantation and one patient 6 years after removal of a rejected transplanted kidney. Nine of these patients developed complications at the ureterovesical area, seven of whom subsequently showed ureterocutaneous fistulae. Two of these patients also went on to stenosis of the lower third of the transplanted ureter. Five patients developed cutaneous fistulae arising from the ureteropelvic area and two of these patients eventually demonstrated ureteropelvic obstruction. One patient had pyelocalyceal and ureterovesical leakage.

The authors emphasize that although rejection is still the most common cause of renal transplant failure, urologic complications may occur in approximately 12% of cases and the mortality rate in these patients may be as high as 47%, usually due to secondary sepsis.

Jack M. Tishler

Musculoskeletal

Arthroscopic examination of the knee. Whipple TL, Bassett FH (Duke University Medical Center, Durham, North Carolina 27710). *Journal Bone Joint Surg* [*Am*]60:444–453, June 1978

Oriented to the orthopedist, this article on knee arthroscopy has information useful to the radiologist who is occasionally involved with knee arthrograms. The authors review some of the previous history of arthroscopy and indicate the standard techniques of this procedure as well as the shortcomings. They also demonstrate with copious pictures and drawings a new technique of polypuncture with percutaneous intraarticular manipulation of the meniscus. This article appears to represent a definite advance in the field of knee arthroscopy and the implications for radiographic review of the knee are multiple. Illustrative case reports and an extensive review of over 50 arthroscopies with intraarticular manipulation are itemized. This type of polypuncture procedure will probably become more common and the ramifications on the approach to difficult knee problems is interesting.

Gerald R. Smith

The influence of thin-section tomography on the treatment of cervical spine injuries. Maravilla KR, Cooper PR, Skiar FH (University of Texas Health Science Center at Dallas, 5323 Harry Hines Boulevard, Dallas, Texas 75235). *Radiology* 127:131–139, April 1978

This study was designed to determine the usefulness of thin section tomography of the cervical spine in trauma patients and its influence on therapy. A total of 79 patients were included in the study. Initial radiographic examination of the cervical spine included plain films in anteroposterior, lateral, and open-mouth odontoid views when possible. Thin section tomography was either performed immediately or following stabilization of systemic injuries. On the basis of clinical examination and initial radiographic examination, patients were divided into three main groups: suspicious radiographic findings, known fracture, and clinical suspicion. Suspicious radiographic findings included subluxation, malalignment, prevertebral soft tissue swelling, vertebral body compression fracture of undetermined age, and "suspicious line". In the known fracture category, tomography was performed to determine extent of an unequivocal fracture seen on plain radiographs. Patients in the clinical suspicion category were those without radiographic abnormalities showing clinical posttraumatic neurological deficit.

Tomographic sections were taken at 5 mm intervals in the anteroposterior and lateral projections when possible. Regions of abnormality requiring further detail were examined in 2 mm intervals.

Cervical spine fractures were considered in five structural categories: (1) vertebral body—19 fractures diagnosed on plain radiographs, 20 on tomography; (2) pedicle—three fractures on plain films, 10 fractures on tomography; (3) lateral mass—nine fractures on plain films, 46 fractures seen on tomography; (4) lamina—six fractures on films, 15 on tomography; (5) spinous processes—two on plain films, three fractures on tomography. Only 35 fractures were identified on plain films as opposed to 94 fracture sites seen on tomographic films.

Fifty-five patients were included in the group showing suspicious plain film findings. Fourteen proved to have fractures, six showed congenital abnormalities and 35 were negative. Of the 24 patients with known fracture on plain radiographs, 13 showed additional fracture sites. Three patients were tomographed because of clinical suspicion of these, two had fractures.

In 14 patients, tomographic findings changed the choice of treatment. Four patients had external immobilization based on plain film findings, one of whom underwent operative fusion as the result of tomography. Six patients received no treatment, while following tomography one patient underwent operative fusion and five patients were treated by external immobilization. In four patients, plain films indicated the need for operative fusion, tomographic findings in two of these patients changed the decision on the type of operative fusion.

Major findings of the study indicated that only 41% of the fractures were identified on closely scrutinized plain film examination. In 14 out of the 79 patients, treatment was altered on the basis of tomographic evaluation. In the suspicious group, 25% proved to have fractures not clearly identified on plain films.

Further indications for tomography are regions which are difficult to evaluate on plain films, such as the cervicothoracic function.

The authors propose the following protocol for radiographic evaluation of the cervical spine in trauma; plain films of the cervical spine with normal findings and normal physical examination necessitate no further workup. If either definite fracture, suspicion of fracture, or neurological deficit are present, tomograms are performed. If a fracture is identified or findings of instability noted, the examination is terminated. If a fracture is identified and instability is questioned, flexion and extension films are obtained. If a fracture is not identified, but a question of instability exists, flexion and extension films are obtained.

Asher Nov

Rupture of the plantar fascia in athletes. Leach R, Jones R, Silva T (Boston University School of Medicine, Boston, Massachusetts). *J Bone Joint Surg* [*Am*] 60:537–539, June 1978

This succinct article deals with the increasingly common problem of foot pain in athletes. The authors describe patients having symptoms similar to a plantar fasciitis who actually had a partial rupture of the plantar fascia. The radiographic findings in this problem are virtually nil but the discussion and description of this problem, as well as the references, are of interest to radiologists.

Gerald R. Smith

Computed tomography of tumors of the musculoskeletal system in children. Berger PE, Kuhn JP (Children's Hospital of Buffalo, 219 Bryant Street, Buffalo, New York 14222). *Radiology* 127:171–175, April 1978

The article is based on findings in 27 patients, 22 patients with malignant tumors—nine cases of Ewing's sarcoma, three osteogenic sarcoma, two rhabdomyosarcoma, one fibrosarcoma, one hemangioendotheliosarcoma, one neuroblastoma, three metastases, two synovial-cell sarcoma. Benign tumors included one osteoid osteoma, two eosinophilic granuloma, one unicameral bone cyst, and one abscess.

Following sedation, both lower or upper extremities were scanned with normal extremities used for comparison. Humeral evaluation was less satisfactory due to motion caused by respiration. Several unique advantages are offered by this modality which include: (1) evaluation of bony abnormalities in difficult regions such as the sacrum and ilium; (2) definition of soft tissue components of bony tumors; (3) recognition of increased density of the medullary space as an expression of pathologic involvement; (4) follow-up of postirradiation or chemotherapy.

With the present experience, the authors do not feel they can distinguish between malignant and benign processes by CT alone.

Asher Nov

Bone infections involving anaerobic bacteria. Lewis RP, Sutter VL, Finegold SM (Infectious Disease Section, Wadsworth Hospital, Los Angeles, California 90073). *Medicine* 57:279–305, July 1978

This report is a detailed survey of the literature of anaerobic bacteria causing osteomyelitis and a review of 58 cases of anaerobic osteomyelitis from the Wadsworth VA Hospital. Typical for papers appearing in the journal *Medicine*, the report is detailed with a complete and up-to-date reference list. Actinomyces infections are the most frequent problem. These infections occur most commonly in the jaw but vertebrae, ribs, and the extremities may be involved. Clinical and radiological features may be difficult to distinguish from tuberculosis when the spine is involved. Correct diagnosis is very important because of the very favorable results which can be achieved generally with penicillin therapy.

The nonactinomycotic anaerobic infections of bone are less common but bacteroides, fusobacterium, anaerobic streptococci, and a variety of other organisms may be at times isolated from bone. Most of the time, these organisms are isolated from nonhematogenous osteomyelitis, specifically cases in which trauma is involved. Quite often these anaerobic bacteria are isolated in association with aerobic bacteria and the causative role of the anaerobes in the infection may not be clear. In this report it is noted that staphylococci are isolated far less frequently with anaerobic bacteria than are the gram negative bacilli.

There are a few important clues for the presence of anaerobes in bone infections. These include gas in the soft tissues, the presence of bacteria having the unique morphology of certain anaerobes, the proximity of the infection to the sinuses, ischemic ulcers, and areas easily contaminated by stool and the presence of a very foul odor in the isolated materials. There are many other noteworthy observations in this report which should be of considerable use to radiologists involved in the diagnosis and management of patients with osteomyelitis.

David C. Dale
Department of Medicine
University of Washington

Nervous System

Computed tomography of the orbit with special emphasis on coronal sections. Part I. Normal Anatomy. Part II. Pathological Anatomy. Tadmor R, New P (Massachusetts General Hospital, Boston, Massachusetts 02114). *J Computer Assisted Tomography* 2:24–34 and 2:35–44, respectively, Jan 1978

In part I, both diagrammatic and CT orbital scans are presented, done in both horizontal and coronal section. Correlation between the actual CT scan and its diagrammatic illustration is carefully made. Particular attention is given to coronal presentations of the orbits.

Part II presents both coronal and standard horizontal CT sections of the orbits. The studies were accomplished on an EMI CT 5000 scanner with a modified 6 mm collimator width. With this particular unit, the radiation dose to the lens for a complete study in the axial plane is 10–12 rads. This dose is reduced to 1½ rads if the scans are obtained with the patient prone, the difference due to the anterior rotation and position of the x-ray tube. A total of 55 patients were examined; selected cases are presented encompassing both benign and malignant tumors, inflammatory processes, and trauma.

Michael Meagher

Evaluation of brain death by contrast-enhanced computerized cranial tomography. Rappaport ZH, Brinker RA, Rovit RL (New York University Medical Center, 550 First Avenue, New York, New York 10010). *Neurosurgery* 2:230–232, May/June 1978

The authors report a typical computed cranial tomographic appearance in four patients with clinical criteria of cerebral death. In each case following the infusion of 100 ml of 60% meglumine diatrizoate, there was no evidence of contrast enhancement of any of the usual intracranial vascular structures including the falx. In one case, a 54-year-old woman with a right parietooccipital abscess, an earlier CT scan with contrast enhancement had visualized both the capsule of the abscess and the falx. Following rupture of the abscess into the ventricular system, the CT scan after contrast administration showed an absence of capsular and falcian enhancement. The three other cases involved head trauma and in addition to showing the absence of contrast enhancement, a diagnosis of acute subdural hematomas could be made in two, one of which had an intracerebral component. The third trauma case had evidence of mass effect without hemorrhage. The authors also suggest a post procedure abdominal radiograph to document renal perfusion and provide initial renal assessment if the patient is a potential kidney donor.

P. M. Chikos

The effect of size, histologic elements and water content on the visualization of cerebral infarcts; a computerized cranial tomographic study. Alcala H, Gado M, Torack RM (Children's Hospital, P.O. Box 20269, Houston, Texas, 77030). *Arch Neurol* 35:1–7, Jan 1978

The authors report radiologic-pathologic correlation in 13 patients who died with a neurological history of stroke. The brain was removed, fixed in formaldehyde, placed in a phantom and scanned in an EMI scanner with a 80 × 80 matrix and a 13 mm slice thickness. Each brain was then cut in the standard reference plane for CT. Visible infarcts were graded small when the largest diameter measured 2 cm; medium when 2.1–5 cm; and large when greater than 5.1 cm. Forty infarcts were graded in this manner and 19 (47.5%) were positive on CT scanning. There is a definite effect of size on CT visualization of cerebral infarcts. Only one of 13 small infarcts were visualized while nine of 16 medium and nine of 11 large infarcts were positive on CT scanning.

Histologic grading, water content, and CT attenuation values were compared in the 26 medium and large infarcts. In the 15 cases which were classified as acute, an abnormal CT image was obtained in seven. The usual tomographic appearance seen in six cases was that of a low density area due to a high content in fluid. However, in the seventh positive case, there was an area of increased attenuation with histologic evidence of an extensive hemorrhagic infarct. Four other acute hemorrhagic infarctions were normal on CT scanning because of the mixture of both edematous and hemorrhagic elements. Two negative acute infarcts were studied within the first 24–36 hr and showed only histologic evidence of diffuse, acute anoxic changes. The last negative infarct was a deep midline brain stem infarction. Five of the seven subacute infarcts (6 days to 3 weeks in age) have typical CT appearances described as zones of well defined low density with attenuation values lower than seen with the acute infarction. In this group abundant phagocytosis and a concomitant increase in neutral fat were noted in addition to edema. Cavitation was not a prominent feature. Two of the subacute lesions were negative on CT scanning and had histologic evidence of extensive calcium and iron content in addition to the low density components. These may represent resolving hemorrhagic infarctions. All six chronic infarctions (defined as being at least 3 weeks old) were positive on CT scanning as areas of diminished density and histologically contained cavitation, residual fats, and gliosis.

Paul M. Chikos

Pediatric Radiology

Dysgerminoma presenting as a calcified abdominal mass with hypercalcemia. Nelken RP, Nieburg PI, Bergstrom WH, Rich-

Advance Registration: 79th Annual ARRS Meeting
Toronto, Ontario, Canada, March 25–30, 1979

If you plan to attend, please fill out the following form.
Official badges and program booklets will be available at the registration desk in the Four Seasons Sheraton Hotel at the time of the meeting. NO CONFIRMATIONS OF REGISTRATIONS WILL BE FORWARDED PRIOR TO THE MEETING.
Preregistration by mail will be accepted only until March 1, 1979. (On site registration will be available.)

MAIL TO: THE AMERICAN ROENTGEN RAY SOCIETY
20 North Wacker Drive, Suite 2920, Chicago, Illinois 60606

Check one box, and include the proper fee in your envelope:
- ☐ Member of the American Roentgen Ray Society (no fee).
- ☐ Nonmember (registration fee $25).
- ☐ Physician in training (registration fee $15). Be sure to include the certification on bottom of this form.

Please print or type:

Name _____

Street _____

City _____

State or Province and zip _____

☐ Check here if you wish a program of events for spouses. Indicate the address to which this is to be sent

Name _____
(Spouse's name you wish printed on badge)

Street _____

City _____

State or Province and zip _____

FOR PHYSICIANS IN TRAINING:

_____ is in training in my department.

_____
Department Chief

_____
Date

_____
Institution

PLEASE COMPLETE BACK FOR COURSE REGISTRATION.

Section on Instruction Order Sheet

It is important to register early for Instruction Courses since the number admitted to each will be limited. It is also important that first, second, and third choices be listed for each period. All ticket orders will be filled according to postmark.

Nonmembers of the American Roentgen Ray Society will pay $3 for each course period. *Nonmembers' fees must accompany this sheet and will not be returned unless cancellation is received before March 20, 1979.*

Members of ARRS, residents in radiology, and nonmembers who are contributing to the program, either by way of an instruction course, a paper, or a scientific exhibit, are not required to pay for these courses but must submit this form.

Tickets for courses will be mailed to those whose order reaches the office of the director on or before March 1. They will be sent to the address below unless directed otherwise. Tickets for late registrants will be available at the Registration Desk of the Section on Instruction at the Four Seasons Sheraton Hotel on and after Sunday morning, March 25.

Please type or print:

_____

Last Name First Name or Initials

_____

Street Address

_____

City State Zip Code

Check one:
☐ Member
☐ Guest
☐ Resident in radiology at:
_____
☐ Scientific exhibitor/paper

I wish to take the Categorical Course on Neuroradiology, five periods, March 25–30. Fee: $25 ☐

Registration in this course precludes registration in any other courses.

Course Registration (for those not taking categorical course). For convenience in selecting your courses consult the condensed schedule of courses. **Be sure to fill out second and third choices for each period.**

Period	First Choice		Second Choice		Third Choice	
	Course No.	Instructor	Course No.	Instructor	Course No.	Instructor
Monday						
Tuesday						
Wednesday						
Thursday						
Friday						

Make checks payable to American Roentgen Ray Society. If mailing late, send to: Dr. Eugene Gedgaudas, Four Seasons Sheraton Hotel, 123 Queen Street West, Toronto, Ontario, Canada.

Application for Hotel Reservations

(DEADLINE: FEBRUARY 25, 1979)

AMERICAN ROENTGEN RAY SOCIETY

MARCH 25–30, 1979

Participating Hotels:	**Singles**	**Doubles**	**Suites**
Four Seasons Sheraton, headquarters hotel	$37, $43 $49	$45, $51, $59	$95–169
Hotel Toronto	$42, $44 $51	$52, $54, $61	$140
Holiday Inn, Downtown Toronto	$34	$42	

(Mail Lower Portion of This Form to Address Listed Below Before FEBRUARY 25, 1979.)

MAIL TO:
ARRS Housing Bureau
Four Seasons Sheraton Hotel
123 Queen Street West
Toronto, Ontario M5H 2M9, Canada

CHOICE OF HOTEL First_____ Second _____ Third _____

ACCOMMODATIONS Single ☐ Double ☐ Twin ☐ 1 Bedroom Suite ☐ Preferred Rate $ _____
Roll-away Bed Requested ☐ 2 Bedroom Suite ☐

Please indicate any special accommodation needs due to a handicap_____

_____

ARRIVAL DATE _____ _____AM _____PM

DEPARTURE DATE _____ _____AM _____PM

Rooms held only until 6:00 PM unless otherwise specified

INDIVIDUAL REQUESTING RESERVATION Name _____
(Please type or print)

Mailing Address _____

_____ ZIP _____

Name(s) of other room occupant(s)_____

_____

(SEE REVERSE SIDE FOR MAP AND SPECIAL INSTRUCTIONS)

Important Information:

1. Reservations must be received by the Housing Bureau no later than FEBRUARY 25, 1979 in order to be assured of written confirmed accommodations.
2. Written confirmation of your reservation will be sent to you by the hotel. Please allow 2–3 weeks for confirmation.
3. All changes such as arrival date, departure date, type room and name changes must be made directly with the hotel after confirmation is received.
4. If you plan to share a room, please send in only one housing form. Be sure to list all names of occupants of rooms. Assignment is delayed until complete information is received.
5. Room assignments will be made in order received. If your choices are not available, the Housing Bureau will assign you to a comparable hotel. If rate requested is not available you will be assigned to the next closest rate available.
6. Hotel reservations will be held only until 6:00 P.M. unless otherwise specified.

HOTELS

FOUR SEASONS SHERATON, HEADQUARTERS HOTEL
Hotel Toronto
Holiday Inn-Downtown Toronto

American Roentgen Ray Society Local Activities
Toronto, Canada, March 26–30, 1979

Spouses' Program

Reservations should be made before March 19. Late requests may not be honored. All tickets and badges are to be picked up at the ARRS Spouses' Registration Desk, Sheraton Centre, Toronto. **No receipts or confirmations will be forwarded prior to that time.**

(Canadian Funds)

Monday, March 26, 10:30 a.m.–2 p.m., St. Lawrence Centre, Backstage at the Theatre, including luncheon _____tickets @ $16 50 $_____

Tuesday, March 27, 9:30 a.m.–4 p.m., Maple Sugar Bush and Canadian Art, including luncheon _____tickets @ $16.00 $_____

Wednesday, March 28, 9:30 a.m.–4:30 p.m., Niagara Falls and Niagara-on-the-Lake, including luncheon _____tickets @ $22.00 $_____

Thursday, March 29, 10:00 a.m.–noon, Fashion, Furs, and Fun, including buffet brunch _____tickets @ $16.00 $_____

Total Enclosed $_____

Please detach and mail with your check (payable in Canadian Funds to ARRS-Convention Consultants of Toronto Ltd.) to: ARRS-Convention Consultants of Toronto Ltd., 961 Eglinton Avenue East, Suite 200, Toronto, Canada M4G 4B5.

NAME_____ADDRESS_____

Annual Tennis Tournament, Wednesday, March 28

The tournament will be at the Mayfair Racquet Club, 3855 Chesswood Drive, Downsview, Ontario. Play will be conventional round-robin style (doubles), alternating on six courts, beginning at 1 p.m. A buffet luncheon at the Mayfair Club precedes the tournament. Cocktails and awards will follow. The entire tournament is sponsored by GAF company. Bus transportation will depart the Sheraton Centre at approximately 11:45 a.m. (following the Caldwell Lecture) with return about 6:30 p.m. Taxis will be available. The tournament is limited to 48 players—first come, first served.

To participate, return completed form to: Dr. D. J. Sieniewicz, Department of Radiology, St. Michael's Hospital, 30 Bond Street, Toronto, Canada M5B 1W8.

NAME_____

ADDRESS_____TELEPHONE _____

_____ZIP CODE _____

Social Evening at Ontario Place, Thursday, March 29

A buffet dinner will be served at the Trillium Restaurant of Ontario Place at approximately 7:45 p.m. following a Happy Hour. A 30–40 min film show will follow, starting with the spectacular film North of Superior. Buses will depart the Sheraton Centre from 6:30 p.m. and return at approximately 10 p.m. Tickets are $16.50 (Canadian funds) and are to be picked up at the ARRS Spouses' Registration Desk, Sheraton Centre. **No receipts or confirmations will be forwarded prior to that time.**

To register, please detach and mail before March 19 with your check (payable to ARRS-Dinner) to: Dr. B. J. Reilly, Department of Radiology, The Hospital for Sick Children, 555 University Avenue, Toronto, Canada M5G 1X8.

NAME_____

ADDRESS_____TELEPHONE _____

_____ZIP CODE _____

man RA (State University Hospital, 750 East Adams Street, Syracuse, New York 13210). *Pediatrics* 61:791–793, May 1978

A 10-year-old white female presenting with anorexia, polyuria, and polydipsia was found to have a large pelvic mass with amorphous calcification, hypercalcemia, and reduced renal function. At operation, a large encapsulated left ovarian tumor was removed. This proved to be a pure dysgerminoma. Following surgery, the hypercalcemia disappeared after 6 months, and renal function improved. Pure dysgerminomas are responsible for one-third of ovarian tumors, but rarely calcify. Calcification is much more frequently seen in dermoid cyst, ovarian teratoma, or gonadoblastoma. The cause of the hypercalcemia is obscure.

B. J. Wood

Large hiatus hernias in infancy and childhood. Daneman A, Kozlowski K (Royal Alexandra Hospital for Children, Sydney, Australia). *Australas Radiol* 21:133–139, June 1977

Four cases of large hiatus hernias in infancy and childhood are presented of a total of 36 cases of all sizes seen between 1965–1976. The literature is also reviewed. Most published cases occur in females, although three of the reported cases are males; the majority occur in the first year of life. Symptoms, when present, are usually related to gastroesophageal reflux and its complications or obstruction which may be also associated with hypertrophic pyloric stenosis or gastric valvulus. Occasionally gastric aspiration with chest infection occurs. All four described cases presented with vomiting.

With large hiatus hernias, abnormalities are invariably present on plain chest films. The stomach is always retrocardiac, often extending to the right of the cardiac silhouette, even to the chest wall, but rarely to the left. The right hemidiaphragm may be depressed but the cardiophrenic angle remains unobscured. With associated intestinal herniations, bowel patterns will be seen. Contrast studies are important to confirm the relative position of the esophagus, stomach, and duodenum and to define such associated abnormalities as gastroesophageal reflux, esophagitis, and subsequent stricture formation. The stomach usually undergoes organoaxial volvulus with potential obstruction at the gastroesophageal junction or pylorus. Hypertrophic pyloric stenosis may also cause obstruction as seen in two of the described cases. Follow-up examination of the bowel is helpful in defining intestinal herniation.

The treatment of choice, advocated by the authors, is surgery with hiatal repair, with or without gastropexy. Prognosis depends more on structural esophageal changes resulting from reflux than the size of the hernia.

John Bramson

Growth, health, and development after neonatal gut surgery: a long-term follow-up. Tejani A, Dobias B, Nangia BS, Mahadevan R (Methodist Hospital, 506 Sixth Street, Brooklyn, New York 11215). *Pediatrics* 61:685–793, May 1978

Growth and development data on 19 children who survived gut surgery in the immediate newborn period are presented. The follow-up period ranges from 7 months to 7.5 years, with a mean of 3 years 8 months. Neonates who undergo gut resection are at a higher risk for delay in height and weight gain compared to those who have gut surgery without resection. Six of the 12 children who had gut resection showed delay in height gain and seven showed delay in weight gain. Of the seven children who had gut surgery but no resection, only one showed delay in height and weight gain after the age of 1 year. An individual approach and careful serial follow-ups are recommended for all children undergoing gut resection in the newborn period. Of the eight children who had psychometric testing in the gut-resected group, only two are normal. Three of the four older children in this group show signs of perceptuomotor defects, suggesting the need for subtesting such children at about 6 years of age so that remedial help, if necessary, may be provided when normal schooling begins.

Author Abstract

Mucocutaneous lymph node syndrome: report of two cases complicated by gallbladder hydrops and diagnosed by ultrasound. Magilavy DB, Speert DP, Silver TM, Sullivan DB (Department of Pediatrics and Communicable Diseases, F6060 Kresge II, University of Michigan Medical Center, Ann Arbor, Michigan 48109). *Pediatrics* 61:699–702, May 1978

Two children are presented who during the course of the mucocutaneous lymph node syndrome developed acute abdominal pain with right upper quadrant mass due to hydrops of the gallbladder. The distended gallbladder was identified in both patients by ultrasound, and in one of the children, the gallbladder was found to return to normal size. Cholecystectomy was performed in the other child. The cystic duct was patent and the microscopic examination showed subacute inflammation. The etiology of the acute hydrops is unknown but is thought to be due to a nonspecific vasculitis or serositis.

B. J. Wood

Wandering spleen in three children. Broker FHL, Fellows K, Treves S (State University Hospital, Oostersingel 59, Groningen, The Netherlands). *Pediatr Radiol* 6:211–214, Feb 1978

Three children are reported with wandering spleen. Two presented with abdominal mass and one with abdominal pain. Technetium scan done in two of the patients was helpful in both instances. The condition is unusual and characterized by abnormal mobility of the spleen, usually associated with abnormal ligamentous attachments. The presentation may be as an acute abdomen due to torsion; or may be as an abdominal mass with or without symptoms.

B. J. Wood

Regional enteritis in children: small bowel disease with normal terminal ileum. Kirks DR, Currarino G (Children's Medical Center, 1935 Amelia Street, Dallas, Texas 75235). *Pediatr Radiol* 7:10–14, April 1978

Of 20 children with regional enteritis seen at Children's Hospital Medical Center, between 1970–1976, four had sparing of the terminal ileum. The diagnosis was made at exploratory laparotomy with biopsy in two of the cases, and on the basis of the radiological appearance in the remaining two. The terminal ileum was normal radiographically and fluoroscopically, and in the two operated cases, on direct inspection as well. All cases were nonstenotic although stenosis has been reported previously in the literature. All patients had systemic symptoms with fever, malaise, fatigue, and loss of weight. Gastrointestinal symptoms, with the exception of abdominal pain were not a feature. The incidence of regional enteritis with normal terminal ileum in the present series was 20%.

B. J. Wood

Posterior urethral valves as a cause of neonatal uriniferous perirenal pseudocyst (urinoma). Morgan CL, Grossman H (Box 3334, Duke University Medical Center, Durham, North Carolina 27710). *Pediatr Radiol* 8:29–32, April 1973

Perirenal urinomas were demonstrated by voiding cystourethrography in two neonates presenting with a left flank mass. Both were secondary to posterior urethral valves, and the infants did well following valve resection. The development of uriniferous perirenal pseudocysts is believed to be due to a tear in the calyceal system secondary to lower urinary tract obstruction. The infant may present with a flank mass or with ascites. Prompt recognition is essential.

B.J. Wood

Cyst formation and cavitation in pulmonary metastases from Wilms' tumor: a report of two cases. Daneman A de Silva M (Royal Alexandra Hospital for Children, Sydney, N.S.W. 2002, Australia) *Pediatr Radiol* 7:4–6, April 1978

The occurrence of cavitation and cyst formation in pulmonary metastasis associated with Wilms' tumor is unusual. The au-

thors present a 5-year-old boy who developed large cysts in the area of previously demonstrated metastasis, and a 13-year-old girl who developed cavitation in two of multiple pulmonary secondaries. Both patients had received chemotherapy and radiotherapy to the lungs. The mechanism of formation of the cysts and cavitation is unknown, but may be due to partial bronchial obstruction in the case of the cysts and to tumor necrosis in the cavities.

B. J. Wood

Miscellaneous

Cytologic evaluation of breast cysts. McSwain GR, Valicenti JF Jr, O'Brien PH (Medical University of South Carolina, Charleston, South Carolina). *Surg Gynecol Obstet* 146:921–925, June 1978

Needle aspiration has become widely accepted as a safe and effective technique for both the diagnosis and the treatment of cystic disease of the female breast. When the characteristic yellow or greenish fluid is obtained, and when the mass disappears after aspiration, open biopsy can thus be avoided. When the aspirated cystic mass contains dark blood or proves to be solid rather than cystic, or when the mass does not resolve completely after aspiration, then open biopsy should be performed.

There has been no general agreement on whether the aspirated fluid should be submitted for cytologic examination routinely. In addressing this question, the authors performed cytologic evaluation of fluid aspirates from all cystic breast masses; aspiration biopsies of solid breast masses and aspirates of fluid from clinically obvious carcinomas were excluded from this series. Of 595 cases, 10 (1.7%) proved to be carcinoma. Four were small solid tumors with a liquid necrotic center, and six were considered intracystic carcinoma. Cystology was falsely negative in one of the 10 cases of carcinoma and was falsely positive in five of the 585 benign cystic masses. Moreover, in most of the carcinomas there was some other indication for open biopsy in addition to a positive cytologic result. Nevertheless, the predictive value of a negative cytologic examination was 99.8%. The authors therefore recommend that fluid aspirated from cystic breast masses always be submitted for cytologic evaluation; a positive result makes open biopsy mandatory for cytologic confirmation prior to mastectomy (36% false positive cytology), and a negative cytologic report should be ignored in the presence of other evidence of carcinoma.

Reiley Kidd

Computer assisted tomography of normal supra renal glands. Brownlie K, Kreel L (Northwick Park Hospital, Watford Road, Middlesex, England). *J Computer Assisted Tomography* 2:1–10, Jan 1978

A total of 90 patients were scanned using a CT 5000 unit. In these patients, both glands were clearly identified in 50, only the right in 10, and only the left in 30. Measurements and positions of both right and left adrenals were demonstrated and certain problems such as lack of ability to separate the right gland from the inferior vena cava are discussed. The authors conclude that CT offers the clearest method of noninvasive imaging of the adrenals.

Michael Meagher

The future of noninvasive medical imaging (in English). Ell PJ, Todd-Pokropek A, Williams ES (Middlesex Hospital Medical School, University College Hospital, London, England). *Fortschr Geb Roentgenstr Nuklearmed* 128:486–490, April 1978

Within the diagnostic armamentarium, the place of many new noninvasive imaging techniques such as radionuclide imaging, ultrasonography, and CT scanning has not been established. The authors present a comparative assessment of the different techniques and present several flow charts illustrating their suggested strategies for an intelligent application of these techniques in the diagnostic workup.

Peter F. Winter

Ultrasonics

Ultrasonic evaluation of "silent regions" in the thyroid scintiscan (in English). Sollikofer ChL, Frank Th, Wewerka J (Department of Nuclear Medicine and Radiation Therapy, Triemli, Zurich, Switzerland). *Nuklearmedizin* 8:16–23, 1978

Thirty-five patients with scintigraphically nonfunctioning thyroid regions not corresponding to palpable nodules were further evaluated by ultrasonography. Suppressed thyroid tissue secondary to an autonomous nodule was suspected on scintigraphic examination in 25 patients with no activity in one entire lobe. Ultrasonography demonstrated thyroid tissue in the nonfunctioning lobe in 23 patients, confirming the diagnosis; in the two remaining patients, ultrasonography did not delineate any thyroid tissue in the scintigraphically silent lobe and the diagnosis of hemiagenesis of the thyroid gland was made. The clinical diagnosis of thyroiditis was made in eight cases; ultrasonography revealed a cystoid pattern in the scintigraphically inactive thyroid regions. In two cases with the clinical diagnosis of myxedema, the sonogram disclosed thyroid tissue with severe scarring and regressive changes, consistent with acquired primary hypothyroidism and excluding a congenital maldevelopment.

Peter F. Winter

Ultrasonic evaluation of extremity soft tissue lesions with arthrographic correlation. Lawson TL, Mittler S (George Washington University Medical Center, 901 23rd Street, NW, Washington, D.C. 20037). *J Can Assoc Radiol* 29:58–61, March 1978

Modern apparatus now permits diagnostic ultrasound to be utilized as a quick, noninvasive method for evaluation of soft tissue lesions of the extremities. The authors used a gray scale echoscope and high frequency transducers of either 3.5 or 5.0 MHz. Contact B scans were obtained using a viscous gel as a sonic bonding agent. Most scans were obtained with the patient supine, but popliteal lesions were scanned with the patient both prone and standing.

Twenty-one patients with suspected knee effusions were examined. Nineteen were shown to have a popliteal cyst, one a patellar bursa rupture, and one a popliteal artery aneurysm. Seven patients with a presumptive diagnosis of cellulitis in the arm and thigh were also examined; three were shown to have an abscess and one a liposarcoma of the thigh. The smallest cyst identified was 1 × 1 × 2 cm. Popliteal cysts were often better demonstrated with the patient standing. The popliteal artery aneurysm mimicked a cyst but was diagnosed by identifying the popliteal artery above and below the mass. A ruptured suprapatellar bursa was identified as a sonolucent fluid collection in the anterior thigh.

The authors emphasize that this method of examination may be the only way to demonstrate a popliteal cyst when the communication between cyst and joint space is obstructed and therefore not demonstrated by arthrography. Also a cyst smaller than 1 cm in diameter or one that is highly separated or that has ruptured may not be visualized by ultrasound.

Jack M. A. Tishler

Radiation Oncology

Radiation induced cycling activity and chemosensitivity of normal tissues. Maruyama Y (University of Kentucky, Lexington, Kentucky 40506). *Revista Interam Radiol* 3:79–87, April 1978

Combined radiation and chemotherapy effects were studied for hemopoietic stem cells using spleen colony method. Cell sensitivity was clearly dependent on when the drug was given

relative to the radiation. This sensitivity change could possibly be the result of an induced recycling or recruitment into proliferative activity of resting or nonproliferating cells. This suggests that toxic effects will be increased when full tumoricidal doses of chemotherapeutic agents and radiation are used concurrently. A review of pertinent clinical literature is also given.

Charles M. Nice, Jr.

Quantitation of differential sensitivity of human-tumor stem cells to anticancer drugs. Salmon SE, Hamburger AW, Soehnlen B, Durie BGM, Alberts DS, Moon TE (Section of Hematology and Oncology, Department of Internal Medicine, University of Arizona Health Sciences Center, Tucson, Arizona 85724). *N Engl J Med* 298:1321–1327, June 15, 1978

The authors performed 32 retrospective or prospective clinical studies in nine patients with myeloma and nine with ovarian cancer treated with standard agents that were tested in vitro. The authors' culture system, as previously described, was utilized for tumor-colony forming cells. Seven patients with myeloma showed drug sensitivity in vitro to agents of the same classes with which they were treated clinically, and in all seven, the in vivo trials including agents of these classes induced at least a partial response (greater than 50% tumor regression). In two patients with myeloma, the assay predicted resistance to one or more of the agents tested and both patients failed to respond. Of the nine ovarian carcinoma patients studied there was apparent resistance to melphalan, carmustine, and adriamycin. In one patient, the development of drug resistance in vivo at the time of relapse from bleomycin therapy was detected and confirmed by rechallange in vivo. In the current study there were 11 cases in which in vitro sensitivity correlated with in vivo sensitivity and one in which it did not. In addition there were 20 cases of in vitro as well as in vivo resistance, and no patient who was resistant in vitro was sensitive in vivo.

Herbert C. Berry

Book Reviews

Breast Carcinoma: The Radiologist's Expanded Role. Edited by Wendy Westinghause Logan. New York: Wiley and Sons, 378 pp., 1977. $32

This concise, highly readable, crisply edited and clearly illustrated "state-of-the-art" review (as of October 1976) will be welcomed by radiologists with a special interest in breast cancer detection. The ambiguous title unfortunately fails to convey either emphasis or depth of scope: (1) a thorough survey of all aspects of mammography with stress on methods of diminishing radiation exposure while maintaining or improving image quality; and (2) descriptions and evaluations of other imaging techniques of potential value for breast cancer detection.

Most of the contributions by 61 recognized experts were derived from a conference held at Roswell Park Memorial Institute in October 1976. The 36 chapters are somewhat arbitrarily divided into five parts, each followed by a panel discussion. The postlude discussions, with their question-and-answer format, tend toward anecdotal and unreferenced proclamations. The chapters, however, are of a far higher standard—invariably illuminating, with current, pertinent references and appropriate, well-reproduced illustrations, tables, and graphs. Candid viewpoints regarding the current breast cancer screening controversy, radiation induction of breast cancer, and the risk-benefit ratio of mammography highlight Part 1.

Part 2 includes discussions of physical factors that affect mammographic images, including scattered radiation, contrast and geometric unsharpness; several chapters devoted to focal spots including magnification radiography with a microfocal spot tube; and the quality assurance roles of the Bureau of Radiological Health and the Regional Centers for Radiological Physics.

Part 3 contains chapters about screening for breast cancer, reduced-dose xeromammography and film-screen mammography, image quality control and radiation exposure (emphasizing surface exposure, since reliable depth-dose data did not appear until August 1977), and, finally, a clinical presentation of magnification mammography complimenting the physical presentation in Part 2.

In Part 4, we glimpse the future: minimal-exposure film-screen techniques, optically enhanced film images, electrostatic imaging, computed tomography, image intensification for xeromammography, and even heavy-particle mammography. The last part of the book, Part 5, honestly describes the conflicting viewpoint regarding the value of thermography in breast cancer screening, with both sides, pro and con, delivering and deflecting polite salvos; also covered in this part are contrast ductography, preoperative needle localization, specimen radiography, needle aspiration-biopsy, and ultrasonography.

The book concludes with an overview by Dr. Logan of the radiologist's role in breast cancer detection. The radiologist is encouraged to obtain a pertinent history, pertinent physical examination, and utilize mammography, thermography, ultrasonography, ductography, and needle aspiration cytology. "Even if . . . the risk is minimal, the radiologist should attempt to perform mammography with as minimal an irradiation exposure as possible *but without sacrificing the information he is seeking*." Finally, the responsibility of the radiologist to promote breast self-examination is stressed. Toward this end there is a facsimile of a pamphlet used by Dr. Logan in her own practice.

Through careful selection and editing of a vast amount of material, Dr. Logan has succeeded in presenting a readable, evenly styled, well-balanced overview of mammography and other imaging techniques for breast cancer detection. Not only are we given a succinct account of things as they are today, we are made aware of the great potential of many imaging techniques to detect breast cancer, and we begin to explore marvelous vistas of things to come.

Richard H. Gold
UCLA School of Medicine
Los Angeles, California 90024

Progress in Pediatric Radiology, vol. 6. Skull, Spine and Contents. Part II: Clinical Aspects. Edited by H. J. Kaufman. Basel: Karger, 304 pp., 1978. $77.50

This small book retains a radiologic emphasis and focus despite the title. Its seven chapters represent articles written by various distinguished authors on limited, defined topics. The first two articles on craniosynostosis and asymmetry of the skull are good conceptual introductions to the radiographic findings and differential diagnoses of these conditions. A chapter on the meninges discusses conditions affecting these structures in children. An excellent review of intracranial calcifications focuses on conditions affecting children and provides valuable, nearly comprehensive discussion of this subject.

A long chapter on neoplasms of the intracranial and intraspinal structures presents in detail the recommended radiologic studies and their findings for each anatomic region of the central nervous system. Emphasis is placed on positive contrast studies of the ventricular system and subarachnoid space particularly for evaluation of posterior fossa lesions. No attempt is made to discuss computed tomography or to cover nonneoplastic conditions. The authors assume the reader possesses a large body of neuroradiologic and neuroanatomic information, and illustrations are used sparingly.

A short article on CT evaluation of diastematomelia attempts to define specific relative indications for the application of this new imaging modality. Fourteen patients are presented in detail.

The final chapter, "Shunts and Complications", is an excellent, thorough review of the radiologic manifestations of the various therapeutic approaches to increased pressure in cerebrospinal fluid spaces. This section is concluded by a dialog

consisting of brief formal comments from several experts as well as a final rebuttal by the authors.

Generally, the book is readable and well illustrated. References are current to 1976. Pediatric radiologists will want to add this book to their libraries. It will also be of value to radiology residents, general radiologists, pediatric neurologists, and neurosurgeons. Unfortunately, the book is overpriced even by 1978 standards.

Joel Blumhagen
Children's Orthopedic Hospital
Seattle, Washington 98105

Current Concepts in Pediatric Radiology, Vol. 1. Edited by Ole Eklöf. New York: Springer International, 147 pp., 1977. $24.90

This thin volume is mainly based on lectures given at the First International Postgraduate Course sponsored by the Swedish Society of Pediatric Radiology in May 1976. It consists of 15 short articles on a wide variety of subjects related to pediatric radiology. These range from discussions of a particular anatomic region—esophagus, terminal ileum, vesicoureteral junction, prostate, hand, and spine—to reviews of particular disease or groups of conditions such as chronic lung disorders, colonic aganglionosis, cystic renal disease, acute renal injury, and hydrocephalus. Highly specialized techniques are described in an article on embolization of pulmonary arteriovenous fistulas via catheter and in another on gastrointestinal fiberendoscopy.

The international flavor of the book is emphasized by the mixture of positive and negative radiographs and widely varied writing styles. The style generally suffers because the articles are transcribed lectures. In written form many appear as meager outlines of their topics, lacking depth and fullness. Several tables (page 6, for example) are very confusing to the reader whereas they may have been clear during the verbal presentation of the lecture.

In contrast to the remainder of the book, several articles stand out as excellent reviews. These include papers on colonic aganglionosis, cystic disease of the kidney, the vesicoureteric junction, and the prostate. Unfortunately some of the concepts presented are not "current" as implied by the book's title, but are actually outdated. For example, arteriography is recommended in the evaluation of simple renal cysts. Other imaging modalities such as radioisotope scintigraphy, ultrasound, and computed tomography are essentially ignored.

For those who attended the course, the book will be a valuable record of the lectures presented. (Others should probably purchase the book on a 30-day free trial basis.) Otherwise the book is not strongly recommended.

Joel Blumhagen
Children's Orthopedic Hospital
Seattle, Washington 98105

Atlas of Gray Scale Ultrasonography. By Kenneth J. W. Taylor. New York: Churchill-Livingstone, 411 pp., 1978. $35

This atlas is intended as an introduction to the many applications of gray scale ultrasound in present day clinical diagnosis. The purpose is well served. Topics include physics, practical aspects of scanning, and normal and abnormal anatomy in abdomen, obstetrics-gynecology, thyroid and thorax. It is well organized and readable. The student is left with an overview of ultrasound imaging and diagnostic capabilities. Therefore, it is an excellent starting point for the beginning ultrasonographer and as a reference to the clinician wondering which patients to send for ultrasound examination.

The radiologist with extensive ultrasonic experience, on the other hand, will not find much new information except in some interesting, rare entities such as hemangioendothelioma of the liver, which he may not have encountered in his own practice. References are limited and ultrasonic guidance of aspiration-biopsy procedures is only briefly mentioned. Except in the chapter on the liver, there is little concerning comparisons of ultrasound, CT, and nuclear medicine as diagnostic modalities.

Ultrasonic images and accompanying line drawings are, for the most part, of high quality. However, some of the radiographs did not reproduce well.

The atlas is an excellent place to start one's exploration of ultrasound and can serve as a review text for the practitioner and the resident studying for the radiology Boards.

Dennis G. Scholl
University of Washington
Seattle, Washington 98195

The Craniovertebral Region in Chronic Inflammatory Rheumatic Diseases. By Yves Dirheimer. Berlin: Springer-Verlag, 173 pp., 1977. $45.10

Dr. Dirheimer has produced a scholarly copiously referenced text concentrating entirely on the "cervicooccipital hinge", that is to say the atlantooccipital and atlantoaxial joints. This is further limited to a discussion of rheumatoid arthritis, ankylosing spondylitis, Still's disease, psoriatic arthritis, and related inflammatory disease as they affect this area. Much of this text centers around atlantoaxial subluxations and a section is included on conservative and surgical management of this complication.

Introductory chapters include sections on the anatomy and physiology of this area as well as the rheumatologic examination and neurologic manifestations. One might therefore question why the interesting embryology of this region was not also discussed particularly as the author refers to congenital malformation which may mimic the manifestations of rheumatic diseases on several occasions. The major portion of the text is devoted to radiographic diagnosis. The radiographs (black on white) are high quality and the illustrations while sometimes abstruse are generally helpful. A brief section on special procedures glosses over arteriography, venography, nuclear medicine, and CT scanning, with only single scans for each. Expansion of the CT section in particular would have been of great

interest. Considering that this is a translation, the text is remarkably free of errors.

This book is of value to the neurosurgeon, orthopedic surgeon, rheumatologist, and general radiologist. It is probably too arcane for the medical student, other than senior residents in radiology. While certainly a valued addition to the library of any larger radiology department, one would doubt that anyone not doing primary work in neuroradiology or bone would purchase a pearl of this price for his own.

David H. Carlson
Tufts-New England Medical Center
Newton-Wellesley Hospital
Newton Lower Falls, Massachusetts 02162

Hip Arthrography. By Paul Grech. Philadelphia: Lippincott, 106 pp., 1977. $19.50

This text provides a good review of hip arthrography in children. It is less complete in the evaluation of the adult hip arthrogram and omits entirely the evaluation of proliferative synovial abnormalities such as synovial chondromatosis and pigmented villonodular synovitis.

The experience with hip arthrography at the Hospital for Special Surgery differs in one or two ways from that presented by the author. First, septic arthritis is not considered a contraindication to a contrast arthrogram. The injection of a small amount of contrast agent is extremely useful in verifying that the needle was intraarticular when the aspiration was obtained, and further, it is useful in evaluating the presence of extracapsular soft tissue abscesses and cartilage destruction. Second, general anesthesia is not necessary to perform a hip arthrogram in young infants. Indeed, no anesthesia at all is necessary. In older infants and children, sedation with or without local anesthesia is sufficient. Third, the chapter on equipment is somewhat dated.

The illustrations vary somewhat in quality but the text is clear and not repetitive.

Amy Beth Goldman
Hospital for Special Surgery
New York, New York 10031

Xeroradiography in Otorhinolaryngology (in Italian and English). By L. Di Guglielmo, R. Campani, P. Garbagna, E. Mira. Amsterdam: Excerpta Medica, 187 pp., 1977.

This atlas of xeroradiography illustrates normal and pathologic conditions related to otorhinolaryngology. This is a well conceived and executed clinicoradiologic work bringing together the expertise of several eminent clinicians.

The purpose of the atlas is to define more precisely the advantages of xeroradiography in imaging pathology of the nasal cavities, pharynx, larynx, and trachea. This was accomplished by comparing xeroradiographs to radiographs from conventional and contrast examinations, and then relating these findings to endoscopic examinations and pathologic specimens.

The atlas is divided into five chapters. The introduction of each briefly reviews x-ray techniques, anatomy, and pathology, concluding with a short discussion that considers the application of xeroradiography to the specific regions. The authors then present well chosen examples to illustrate particular pathology. It is somewhat unfortunate, however, that the xeroradiographic illustrations are not as excellent as one might expect. Although this detracts from the usual crispness of the technique, it does not interfere with the pathologic identification. The English translation of the Italian text is adequate, but not as outstanding as the original.

The atlas represents a valuable addition to the xeroradiographic literature, and will be most useful for visualizing the pathology of the nose, paranasal cavities, and throat.

Nicole F. Bolender
University of Washington
Seattle, Washington 98195

Review of NCRP Radiation Dose Limit for Embryo and Fetus in Occupationally-Exposed Women. NCRP Report No. 53. D.C.: National Council on Radiation Protection and Measurements, 42 pp., 1977. $3.50

Report 53 contains a preface, introduction, conclusions, comments, and two appendices. The report concludes that the 1971 recommendations in Report 38 are current, i.e., limit the embryo-fetus exposure to 0.5 rem. The section of comments shows evidence of a National Council on Radiation Protection number dance to justify rather arbitrary limits. Appendix A is a historical review of the limits. Appendix B, "Status of Knowledge 1976", should have been the main thrust of this report. A short appendix restating the 1971 recommendation could have been attached to that. As it is, Appendix B provides a short summary of our knowledge of teratogenic and carcinogenic effects of prenatal irradiation.

The report has two significant omissions. There is no discussion of the specific risks to the unborn human from radioactive material ingested by the mother. This is a real concern among female technicians in nuclear medicine and radioisotope labs. And, there is no discussion or recommendation for the pregnant woman who has been exposed above the recommended limits. In our pragmatic society it is important to know when preemptive action against a fetus is justified.

As a person who must occasionally counsel radiation workers who are, or would like to be, pregnant, I find this report disappointing. A committee number dance will not convince a woman that her unborn child is safe. A discussion of other normally accepted risks would help give some perspective to an individual's concern.

Although I was disappointed with Report 53, I recommend it for persons responsible for radiation safety of female workers. Fortunately a subsequent report, No. 54, deals with medical exposure of women and is a good supplement to Report 53.

Michael J. O'Brien
Environmental Health and Safety
University of Washington
Seattle, Washington 98195

Understanding Radiography. By Stephen S. Hiss. Springfield, Ill.: Thomas, 365 pp., 1978. $29.50

This text was written by a promising author who has developed an original and refreshing style by utilizing personal experiences to emphasize and explain the material presented. The text contains an agreeable mixture of the old and new concepts of basic radiography, both of which are essential to the modern technologist.

The basic organization includes various sections on radiographic technique, image production, and beam modification. Separate chapters are devoted to tomography, conversion factors, and film critique.

The text is well illustrated with more than 200 figures and the quality of radiographs is excellent. Unfortunately the layout may lead to some confusion since most radiographs that are offered for comparison are found on different pages. Likewise some improperly labeled figures could be confusing for the beginner. Usually, dramatic comparisons are much more effective when smaller portions of the radiograph are grouped on the same page. The coordination of the written material with the illustrative material is not always easy to follow.

The text has been written mainly for the student technologist, but would offer good review to the experienced technologist.

Due to its detail and unusual approach, I would recommend it as a strong reference text if not a supplementary text for any school of radiologic technology.

Shauna R. Carr
11 Antelope Circle
Saint Joseph, Missouri 64507

Synopsis of Radiographic Anatomy with Computed Tomography. By Isadore Meschan. Philadelphia: Saunders, 762 pp., 1978. $31

This text is a synopsis of a previous text, *An Atlas of Anatomy Basic to Radiology* (1975). The original text, which was written specifically for radiologists, has been shortened and sections of computed tomography have been added to entice a wider range of readers. The general style is characteristically Meschan.

The text begins with sections on routine procedures, radiographic technique, radiographic physics, and radiation protection. The ensuing 12 chapters are devoted to the anatomy, positioning, and resulting radiographs of the body systems. Special procedures utilizing contrast media are included. Those chapters concerning the skull and brain are exceptionally well done. The final chapter is devoted entirely to computed tomography.

The format of the text, with exception of the final chapter, is arranged with a positioning sketch, the resulting radiograph, and an outline sketch, which allows easy identification of any structure demonstrated on the radiograph. The format of the final chapter is arranged by an anterior outline sketch on which imaginary scan levels are drawn and numbered. Each level is then demonstrated by a cross-sectional detail sketch and by a CT scan.

The 724 illustrations generally coincide with the written material well enough to allow a flowing, easy to follow text. Most radiographs are of good quality. The detail and outline sketches which accompany them are excellent. A few illustrations of equipment are somewhat outdated, possibly making it difficult for some readers to associate the diagrams with equipment now in use.

A text of this content and quality should be readily accessible in every radiology department for reference. It contains more detail than the average student technologist needs, but it would be well worth the investment for medical students and any radiologically-oriented technologists.

Shauna R. Carr
11 Antelope Circle
Saint Joseph, Missouri 64507

Radiation Protection in Dentistry. Manual on Radiation Protection in Hospitals and General Practice, Vol. 4. By K. Koren and A. H. Wuehrmann. Geneva: World Health Organization, 52 pp., 1977. $4 (ISBN 4 154041 9, available in U.S. from Q Corporation, 49 Sheridan Ave., Albany, NY 12210)

This handbook is a part of a series on radiation protection; this one is intended to provide sufficient information for most radiation concerns in a dental office. It attempts to cover nine major areas in separate chapters: (1) The Need for Radiation Protection; (2) Responsibility; (3) Equipment; (4) Film; (5) Techniques; (6) Film Processing; (7) Patient Dose; (8) General Protection and Monitoring; and (9) Educational Standards.

Although the content would appear to be what a dentist needs, the suggestions and statements in the text are superficial.

I had the impression that the authors did this "off-the-top-of-their-heads" without spending any effort to include substantial material. For example, there are only two paragraphs which deal with voltage. The reader is advised that "Voltage directly controls the quality or penetrability of the X-ray beam and therefore the contrast of the radiograph, the dose, integral patient dose, back scatter, and film exposure." There is no attempt to explain these factors further or to suggest the preferred technique for different diagnostic needs. If the reader understood the paragraph he was far beyond the level of this book; if he was looking for helpful advice, he has the wrong book.

Numerous similar general statements are included without detailed supporting data. In the section on patient dose, it would be useful for a dentist-reader to have a table or graph of typical exposures as a function of technique parameters. And with a little more effort, the authors might suggest the preferred range of techniques for various typical procedures.

There was only a short two paragraph section on shielding; it referred the reader to another publication. Again, a table of typical exposures at normal operator distances would be helpful, together with the effective shielding of standard building material.

With so little technical detail otherwise, it was curious to note that the authors were carefully consistent to express all exposures in both roentgen and SI units, i.e. IR (2.58×10^{-4} C/Kg).

Given the title and the sponsoring organization, together with the prestigious authors and reviewers, one would expect to find a useful and needed handbook. As it is, it does not belong on the bookshelf of dentist or radiation safety professional.

Michael J. O'Brien
Environmental Health and Safety
University of Washington
Seattle, Washington 98195

News

Double Contrast Techniques in GI Radiology

A 3-day seminar, Introduction to Double Contrast Techniques in Gastrointestinal Radiology, will be March 8–10 in Philadelphia. Sponsor is the Department of Radiology, Hospital of the University of Pennsylvania. The International faculty will include: S. Baum, D. Gelfand, V. Gohel, H. Goldstein, H. Herlinger, B. A. Johnson, H. Y. Kressel, I. Laufer, J. O. Op den Orth, R. Miller, and G. Stevenson. The seminar will consist of morning lectures and discussion panels followed by a series of afternoon workshops. Each registrant may choose six of 10 workshops; registration is limited. The seminar will cover the basic principles of performance and interpretation of double contrast techniques throughout the gastrointestinal tract. A total of 18 hr AMA Category I credit is available. Registration fee is $300 ($150 for residents) and includes daily lunch, cocktail reception, and syllabus. For information contact either Dr. Herbert Y. Kressel or Dr. Igor Laufer, Department of Radiology, Hospital of the University of Pennsylvania, 3400 Spruce Street, Philadelphia, Pennsylvania 19104; telephone (215) 662-3264.

Diagnostic Ultrasound Courses

The Division of Diagnostic Ultrasound of Thomas Jefferson University is offering a series of courses for physicians and sonographers. Courses will include: Introduction to Clinical Applications, Cross-Sectional Anatomy with CT and Ultrasound Correlations, Basic and Advanced Physics, Basic and Advanced Abdominal Ultrasound, Basic and Advanced Echocardiography, Obstetrical and Gynecological Ultrasound, Specialized Applications, and Ultrasound Update. Category I credit is available. For complete information, contact: Program Coordinator, Division of Diagnostic Ultrasound, Thomas Jefferson University, 1015 Walnut Street, Philadelphia, Pennsylvania 19107; telephone (215) 928-8533.

Skeletal Symposium

The second annual Skeletal Symposium will be January 20–26 at Sun Valley Lodge, Sun Valley, Idaho. The conference will stress fundamental, practical aspects of bone and joint radiology. Fee is $225; $150 for those in training. The program is approved for 18 hr AMA Category I credit. For further information, contact Michael J. Pitt, M.D., Program Director, Department of Diagnostic Radiology, University of Arizona Health Sciences Center, Tucson, Arizona 85724; phone (602) 626-7368.

Abdominal Real Time Sonography Courses

A series of six, week-long courses on the use of real time ultrasound in abdominal studies will be offered at Bowman Gray School of Medicine on the following dates: December 4–8, 1978; March 12–16, June 11–15, July 16–20, August 6–10, and December 9–13, 1979. While emphasis will be on real time sonography, B-scanning will also be taught. Participants will receive 30 Category I credit hr per week. For further information, please write: James F. Martin, M.D., Director, Center for Medical Ultrasound, Bowman Gray School of Medicine, Winston-Salem, North Carolina 27103.

LSU Diagnostic Radiology Seminar

A problem-oriented diagnostic radiology seminar will be March 15–17 in New Orleans. E. K. Lang is program director. Major topics will include gastrointestinal, genitourinary, bone, chest, neuro, and pediatric radiology. The program carries 18 hr AMA Category I credit. Fee is $200; $110 to a limited number of residents with a letter certifying their status. Guest faculty members include: R. Hattery, Mayo Clinic; J. Madewell, Armed Forces Institute of Pathology; R. Moncada, Loyola University; S. Siegelman, Johns Hopkins Hospital; R. Stanley, Washington University Medical Center; and M. Viamonte, University of Miami. For information, write: Office of Continuing Medical Education, LSU School of Medicine, 1542 Tulane Avenue, New Orleans, Louisiana 70112; telephone (504) 568-6085.

Aspen Uroradiology Seminar

The eighth annual Aspen (Colorado) Uroradiology Seminar presented by the LSU Medical Center is scheduled for February 18–23. The seminar will be divided into two phases with Phase I February 18–21 (fee $220) and Phase II, February 22 and 23 (fee $80). A limited number of residents will be accepted at a special rate. Phase I, a prerequisite for enrolling in the second phase, is the formal didactic part of the seminar and will include presentations and panels by an interdisciplinary faculty of experts. Phase II will provide participants with reviews of visual observations via television and will offer a chance for free exchange of ideas and opinions with the seminar faculty. The course is approved for 36 hr AMA Category I Credit. For additional information contact: Office of Continuing Medical Education, LSU School of Medicine, 1542 Tulane Avenue, New Orleans, Louisiana 70112; telephone (504) 468-6085.

Tennessee Meeting

The fall meeting of the Tennessee Radiological Society will be November 11 and 12 at the University of Tennessee Center for the Health Sciences, Knoxville. Scientific presentations will be made by society members and Morton Bosniak, New York University, and Jim Martin, Bowman Gray School of Medicine. Additional information may be obtained from Dr. T. P. Lynch, Department of Radiology, Memorial Hospital, 1924 Alcoa Highway, Knoxville, Tennessee.

Fleischner Society Ninth Symposium

The Fleischner Society, a multidisciplinary international organization devoted to the study of the chest, announces its 1979 postgraduate course, June 11–13 in Stockholm. Topics will be current problems and important topics in chest disease, anatomy, physiology and clinical medicine with emphasis on radiologic techniques and interpretation. Three days of fully accredited teaching, lectures, a large selection of refresher courses, and some technical exhibits will be presented. Fee is 800 Swedish Krone or $180 U.S. dollars payable to the Fleischner Society. For information write to: Professor B. Nordenström, Department of Radiology, Karolinska Hospital, Stockholm, Sweden.

New Orleans Fall Radiology Conference

A diagnostic radiology seminar will be November 9–11 in New Orleans. Major topics will include a review of current concepts in bone, chest, genitourinary, pediatric, and neuroradiology. The program carries 17 hr AMA Category I credit. Fee is $160; $90 to a limited number of residents. Guest faculty members include: L. Theros, University of California; L. Swischuk and M. Jones, both University of Texas; H. Pollack, University of Pennsylvania; and A. Crummy, University of Wisconsin. In addition, eight members of radiology faculties from the New Orleans area will participate. For information, write: Office of Continuing Medical Education, LSU School of Medicine, 1542 Tulane Avenue, New Orleans, Louisiana 70112; telephone (504) 568-6085.

Practical Advances in Diagnostic Radiology IV

The Department of Radiology, Medical College of Wisconsin, will host its fourth annual postgraduate course, Practical Advances in Diagnostic Radiology, January 13–22 during a Carribean cruise. The trip will originate in New York City. The course is a comprehensive review of recent advances in diagnostic radiology and will emphasize computed tomography, ultrasound, angiography, neuroradiology, gastrointestinal, chest, skeletal, and genitourinary radiology. Fee is $250. The course carries 30 hr AMA Category I credit. For information, write: Dr. E. T. Stewart, Department of Radiology, Milwaukee County Medical Complex, 8700 West Wisconsin Avenue, Milwaukee, Wisconsin 53226.

Musculoskeletal Course and Cruise

Current Concepts in Musculoskeletal Radiology and Orthopedics, a postgraduate course, will be conducted during a Carribean cruise, April 28–May 5. Sponsor is the Musculoskeletal Section, Mallinckrodt Institute of Radiology. Purpose is to review current diagnostic and treatment concepts of various musculoskeletal problems. The course is designed for both radiologists and orthopedists and will illustrate abnormal as well as normal anatomy. AMA Category I credit is available. Fee is $200. For information, write: Dr. L. A. Gilula, Mallinckrodt Institute of Radiology, 510 South Kingshighway Boulevard, St. Louis, Missouri 63110.

CT, Ultrasound, and X-ray

Computed Tomography, Ultrasound, and X-ray: An Integrated Approach is a postgraduate course slated for January 29–February 2 in San Francisco. Sponsor is the University of California, San Francisco. Course objective is to review the major clinical topics for which more than one useful imaging modality is available, to review the basic principles of each technique as it applies to each clinical topic, and to formulate methods to integrate the different modalities into a rational and efficient diagnostic plan. Emphasis will be on CT and diagnostic ultrasound. However, nuclear medicine, angiography, and conventional radiographic approaches to each clinical topic will also be presented.

Guest faculty will include: J. J. Bookstein and G. Leopold, both University of California, San Diego; R. A. Castellino, Stanford University; A. J. Davidson and H. C. Redman, both Mount Zion Hospital, San Francisco; P. B. Hoffer, Yale University; S. R. Reuter, University of California, Davis; S. S. Sagel, Washington University, St. Louis; W. F. Sample, University of California, Los Angeles; B. A. Siegel, Mallinckrodt Institute, St. Louis; and D. H. Stephens, Mayo Clinic. Faculty from the University of California, San Francisco, will also be instructors.

Course fee is $295; $195 for those in training with a letter of verification. Continuing education credit is available. For information contact: Extended Programs in Medical Education, University of California, 1308 Third Avenue, San Francisco, California 94143; telephone (415) 666-2894.

Diagnostic Radiology Course

The twenty-second annual postgraduate course in diagnostic radiology presented by the University of California, San Francisco, will be March 12–16 in San Francisco. The course is designed primarily for the radiologist in clinical practice; it carries 30 hr Category I credit. For information, contact: Extended Programs in Medical Education, University of California, San Francisco, California 94143; telephone (415) 666-4251.

International Symposium and Course on CT

The Fifth International Symposium and Course on Computed Tomography will be April 16–20 in Las Vegas. The symposium is expected to provide an opportunity for those with experience with cranial and body CT to exchange information and ideas on the current state of the art, to explore and identify priorities in research and development, and to promote the best clinical utilization of this modality. The course will serve as a basis for discussions and also consist of a structured series. A physics program is included. AMA Category I credit will be available.

Those wishing to present papers should submit a 100–200 word abstract to: Dr. J. M. Taveras, Program Director, Department of Radiology, Massachusetts General Hospital, Boston, Massachusetts 02114.

Course fee is $160 for physicians; $80 for physicists, hospital administrators, technologists, and others. For further information, write: Mrs. L. T. Haug, Department of Radiology, Massachusetts General Hospital, Boston, Massachusetts 02114.

Gastrointestinal Radiology, Update '79

The San Diego Radiology Research and Education Foundation and the American College of Radiology are offering a seminar, Gastrointestinal Radiology, Update '79, March 9–11 in San Diego. Subjects will include all aspects of gastrointestinal radiology including latest techniques and a general intensive review. Guest faculty will include: J. T. Ferrucci, Jr., Massachusetts General Hospital; H. I. Goldberg, University of California, San Francisco; W. J. Kilman, University of Texas, Dallas; and R. P. Rice, Duke University. Faculty from the University of California, San Diego, will include: J. R. Amberg, R. N. Berk, J. J. Booksteir, F. J. Brahme, D. K. Edwards, III, L. E. Goldberger, B. B. Gosink, E. C. Lasser, G. R. Leopold, L. S. Menuck, and F. W. Scheible.

Fee is $200; 18 hr AMA Category I credit will be given. Registration information is available from M. J. Ryals, Radiology, P. C. Box 2305, La Jolla, California 92038; phone (714) 453-7500, extension 3711.

Selected Topics in Neuroradiology

Selected Topics in Neuroradiology is a seminar slated for February 7–9 in San Diego. Sponsors are the San Diego Radiology Research and Education Foundation and the American College of Radiology. The course will provide an in-depth discussion of selected topics in head and neck radiology with emphasis on ear, nose, and throat; the orbits; and the spine.

Guest faculty will include: S. Cronquist, University of Lund, Sweden; J. T. Diehl, University of Texas, Dallas; K. D. Dolan, University of Iowa; W. N. Hanafee, University of California, Los Angeles; S. Hilal, Neurological Institute, New York City; A. A.

Mancuso, University of California, Los Angeles; T. H. Newton, University of California, San Francisco; and P. T. Siemers, Baylor University. Participating from the University of California, San Diego, will be: W. L. Ashburn, E. F. Bernstein, F. J. Brahme, M. N. Coel, T. G. Georgen, G. D. Greenway, H. E. James, L. E. Kellerhouse, G. R. Leopold, R. B. Livingston, D. Resnick, M. Sovak, J. J. Verba, M. V. Wells, and G. I. Wickbom.

Fee is $225; 22.5 hr AMA Category I Credit will be given. For registration and information, contact M. J. Ryals, Radiology, P. O. Box 2305, La Jolla, California 92038; phone (714) 453-7500, extension 3711.

Cardiovascular Nuclear Medicine

A continuing medical education seminar, Cardiovascular Nuclear Medicine 1978, will be November 11 and 12 at Southwestern Medical School, Dallas. The seminar will be conducted by J. Ritchie, Veteran's Administration Hospital, Seattle; H. Schelbert, University of California, Los Angeles; W. Straus, Harvard; and faculty of Southwestern Medical School. The seminar will carry 15 hr AMA Category I credit. Fee is $225. For information, contact L. L. Wooldridge, Administrative Coordinator, Department of Radiology, Southwestern Medical School, 5323 Harry Hines Boulevard, Dallas, Texas 75235; phone (214) 638-1800, extension 2613.

European Cardiovascular Radiology Congress

The European Society of Cardiovascular Radiology will host its fourth congress, May 3–5 in Nuremberg. Topics are: angiography in pulmonary vascular disease and special treatment methods; angiography in the cervical region including extracerebrovascular disease, angiography of the thyroid and the parathyroid as well as embolization procedures in the cervical region; and image intensifier fluorography. For registration and other information, write: Professor Dr. E. Zeitler, Radiologisches Zentrum, Klinkum Nürnberg, Flurstr. 17, D8500, Nürnberg, West Germany.

LA Bone and Joint Conference

The Los Angeles Bone and Joint Clinical-Pathological-Radiological Correlation Conference meets the third Thursday of each month through May 17. Location is the Center for Health Education, Memorial Hospital Medical Center of Long Beach, 2801 Atlantic Avenue, Long Beach. Sessions run from 7–10 p.m. Participating radiologists include L. Theros, D. Forrester, and D. Resnick. Participating pathologists include C. P: Schwinn, J. Mirra, and R. Terry. Radiographs and histologic slides are studied from 7–7:45 p.m. with discussion following. Three hr CME Category I credit is available for each meeting. There is no fee. For information telephone (213) 595-3811.

Diagnostic Ultrasound Seminar

The Downstate Medical Center of the University of New York, Departments of Radiology and Continuing Education, will host the third annual Spring Weekend Symposium on Diagnostic Ultrasound, April 21 and 22 in New York City. This program will cover basic and advanced theory and technique in obstetrical-gynecologic and abdominal ultrasound. A presymposium on April 20 will be devoted to scanning and interpretation. Participating speakers will be J. A. Becker, R. Filly, J. Haller, J. Hobbins, P. Kahn, E. Kazam, G. Phillips, R. Rosenblatt, R. Sanders, M. Schneider, G. Solish, F. Winsberg, and H-C Yeh. Category I credit is available. For additional information, contact: Department of Radiology, Box 1192, State University of New York, Downstate Medical Center, Brooklyn, New York 11203; phone (212) 270-1601.

Simon Memorial Fellowship

The Fleischner Society announces the establishment of the George Simon Memorial Fellowship Award. Purpose is to honor Dr. Simon by perpetuating his interest in encouraging young physicians and investigators to carry out original work related to diagnostic imaging in the respiratory system. The fellowship will be awarded to that individual who submits the best original work relating to radiologic or other imaging in the respiratory system. The award will consist of a trip to the Fleischner Society meeting and course with all expenses paid, plus a cash prize. The 1979 meeting will be in Stockholm, June 6–13. The fellowship recipient will present his paper at that meeting. Although the paper can be the result of work done by several investigators, the senior author should be the applicant and the majority of the work should be his. Applicants should not be older than 40 years.

Submissions for the 1979 award must be in the form of a complete scientific paper and should be sent to Dr. R. H. Greenspan, Department of Diagnostic Radiology, Yale University School of Medicine, 333 Cedar Street, New Haven, Connecticut 06510, on or before January 1.

San Diego Postgraduate Courses

One and 2 week programs in postgraduate radiology are being offered by the San Diego Radiology Research and Education Foundation and the American College of Radiology. A total of 40 hr CME credit is given per week of study. Fee is $400 for the first week and $200 for each additional week. The program is designed to offer practical, up-to-date information to the practicing radiologist on various aspects of diagnostic radiology. Recent developments will be emphasized such as needle biopsy of pulmonary nodules, skinny needle transhepatic cholangiography, and high resolution magnification techniques in the evaluation of bone disorders. In addition, a review of selected traditional diagnostic approaches in radiology will be offered. Newer modalities such as ultrasound and CT scanning will be included.

Faculty includes: N. P. Alazaraki, J. R. Amberg, W. L. Ashburn, R. N. Berk, J. J. Bookstein, E. J. Brahme, M. N. Coel, D. K. Edwards, D. Feigin, J. V. Forrest, P. J. Friedman, L. Goldberger, B. B. Gosink, S. E. Halpern, C. B. Higgins, M. Kelley, E. C. Lasser, G. R. Leopold, A. Orloff, D. L. Resnick, L. B. Talner, A. T. Taylor, Jr., and G. I. Wickbom.

For registration and information, contact M. J. Ryals, Radiology, P. O. Box 2305, La Jolla, California 92038; (714) 453-7500, extension 3711.

XII Symposium Neuroradiologicum

Giovanni Di Chiro, Chief of the Neuroradiology and Computed Tomography Section of the National Institutes of Health, Bethesda, Maryland, has been elected president of the XII Symposium Neuroradiologicum. The election was in June at the XI Symposium in Wiesbaden, Germany.

The XII Symposium Neuroradiologicum will be in Washington, D.C. October 10–16, 1982. Vice President is Hillier L. Baker, Mayo Clinic; Secretary General is David O. Davis, George Washington University Medical Center.

The Symposium Neuroradiologicum is one of the oldest and most prestigious meetings in the radiologic field. The first symposium was in 1939, in Antwerp, Belgium, and following symposia have taken place every 3–4 years in different countries. Only once before was the symposium held in the United States (New York, 1964).

San Francisco Cancer Symposium

The fourteenth annual San Francisco Cancer Symposium will be March 23 and 24. Title is Body Image, Self-Esteem, and Sexuality in Cancer Patients. Registration fees are as follows. Fees in parentheses are those that will be charged for registration after December 1. Fees: physicians with CMA credit, $100 ($125); nonphysician health professions, with credit, $40 ($50); nonphysician health professionals, without credit, $25 ($35); residents and students, $10 ($10). For information, contact Dr. J. M. Vaeth, West Coast Cancer Foundation, 50 Francisco Street, Suite 200, San Francisco, California 94133; phone (415) 981-4590.

Meeting and Course Review

For reader convenience, a summary of upcoming meetings and courses is provided. Detailed listings of these events appeared in journal issues indicated in parentheses.

CT in Radiotherapy, workshop, March 28–30, Geneva, Switzerland (June).

Courses in Ultrasound, two 8-week postgraduate courses beginning January 8 and April 2, respectively, Winston-Salem, North Carolina (July).

General Diagnostic Radiology, course, February 5–9, Puerto Rico (July).

Diagnosis of Liver Metastases, symposium, November 30–December 2, Brussels (July).

Adjuvant Therapy of Cancer, conference, March 28–31, Tucson (July).

Medical Imaging Meeting, December, Hong Kong and People's Republic of China (August).

CT, Ultrasound, Nuclear Medicine in Pediatrics, symposium, January 18–20, Orlando, Florida (September).

Body CT Course, February 26–March 1, San Diego (Se ber).

Current Concepts in Diagnostic Radiology, course, Fel 12–16, Acapulco, Mexico (September).

Arthrography Course, December 14–16, New York City tember).

Computed Tomography, Ultrasound, and X-ray, course uary 29–February 2, San Francisco (September).

Two Courses: Snowbird and Park City, January 28–Fel 3, Snowbird, Utah, and February 24–March 3, Park Ci Resort, Utah (September).

FDA Invites Comments on Proposed Radiation Prot Recommendation (October).

National Conference on Breast Cancer, March 4–9, A (October).

Thoracic Society: Call for Abstracts, deadline Decem (October).

XII Interamerican Congress of Radiology, July–August Quito, Ecuador (October).

Sixth Congress of Radiation Research, May 13–19, (October).

Noninvasive Imaging in Medicine, symposium, June Lund, Sweden (October).

Conferences on Medical and Biological Engineerin Medical Physics, August 19–24, Jerusalem (October).

L. H. Gray Conference, September 10–14, Cambridg gland (October).

Asian Oceanian Congress of Radiology, October 28–N ber 3, 1979, Singapore (October).

Diagnostic and Therapeutic Angiography, course, I 21–25, Puerto Rico (October).

Research Training Fellowships, deadline January 31, national Agency for Research on Cancer (October).

Diagnostic Ultrasound Preceptor Training Programs Diego, one month programs (October).

Books Received

Receipt of books is acknowledged as a courtesy to the sender. Books that appear of sufficient interest will be reviewed as space permits.

An Atlas of the Human Brain for Computerized Tomography. By T. Matsui, A. Hirano. Tokyo and New York: Igaku-Shoin, 570 pp., 1978. $54.50

Radiology of Trauma. By H. Birzel, R. Bergleiter, E. H. Kuner. Philadelphia: Saunders, 372 pp., 1978. $65

Ultrasonography of Digestive Diseases. By F. S. Weill. St. Louis: Mosby, 505 pp., 1978. $47.50

Contrary to Nature. By M. B. Shimkin. D.C. U.S. Government Printing Office, 498 pp., 1977.

Essentials of Radiology. By P. M. Bretland. Boston: Butterworths USA, 178 pp., 1978. $19.95

Cardiac Catheterization and Angiocardiography, 3d ed. By D. Verel, R. G. Grainger. New York: Churchill Livingstone, 239 pp., 1978. $29.50

Intensive Care Radiology: Imaging of the Critically Ill. Edited by L. R. Goodman, C. E. Putmar . St. Louis: Mosby, 36 1978. $34.50

1978 Year Book of Nuclear Medicine. Edited by J. L. Qui S. M. Spies. Chicago: Year Book Medical, 390 pp., 1978.

Nuclear Medicine: Endocrinology. Edited by B. Rothfeld adelphia: Lippincott, 378 pp., 1978. $37.50

Bone Tumors: General Aspects and Data on 6,221 Cas ed. By D. C. Dahlin. Springfield, Ill.: Thomas, 445 pp., $32.75

Diagnostic Ultrasound in Clinical Obstetrics and Gynec Edited by H. E. Thompson, R. L. Bernstine. New York: W Sons, 192 pp., 1978. $25

The Chemistry of Radiopharmaceuticals. Edited by N. D. del, H. D. Burns, T. Honda, L. W. Brady. New York: Ma 294 pp., 1978. $27.50

L'echocardiographie en pratique clinique (in French). Drobinski, P. Botreau-Roussel, Y. Grosgogeat. Paris: Ma 110 pp., 1978. 45 F

Philips Angiography Systems.

TOTAL BODY COVERAGE WITH THE BROADEST RANGE OF EQUIPMENT

. . . from the only company offering all the choices you need!

Poly Diagnost C

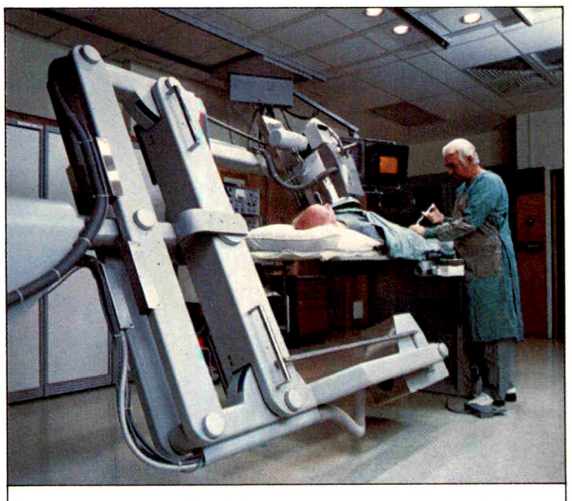

The parallelogram construction of the Poly Diagnost C permits the patient to remain stationary, leaving the physician more relaxed and able to concentrate fully on the procedure. Insuring maximum safety for both patient and operator, the Poly C provides both routine and cranio-caudal views that insure clear, unobstructed views of overlapping vessels. Stenoses which might have been obscured can be detected with a high degree of efficiency and operational ease.

Designed for both the brachial and femoral techniques of cardiac angiography, the Poly C is also successfully used in abdominal and thoracic studies.

Poly Diagnost N

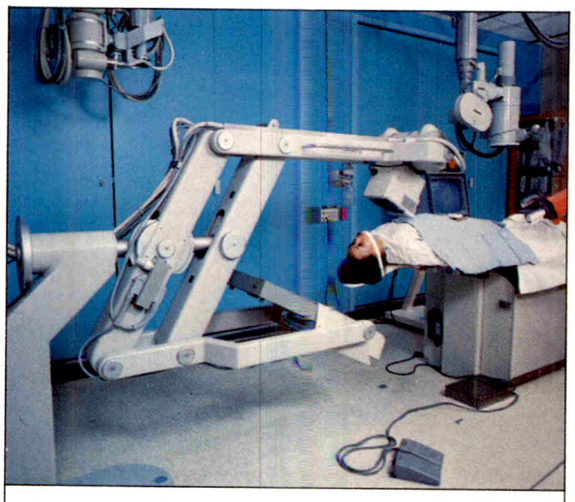

Designed specifically for cerebral angiography at 2:1 magnification, the Poly Diagnost N easily provides views of the patient previously difficult (or impossible) to achieve. The parallelogram construction allows full rotation around the long axis of the body *and* the maximum desirable head-to-foot angulation. The unique construction insures all motions are isocentric and all results are distortion free.

Designed for use in single or bi-plane operation with a Puck rapid film changer, the Poly N lends itself to extensions for more dedicated requirements, such as the latest configuration with a quickly interchangeable image intensifier and a rapid film changer.

PHILIPS MEDICAL SYSTEMS, INC.

710 Bridgeport Avenue, Shelton, Conn. 06484

Philips Angiography Systems.

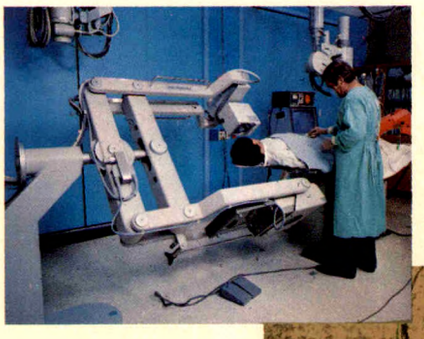

Poly Diagnost N

The first in Philips' family of dedicated cerebral angiography systems with parallelogram construction. For optimum results with isocentric patient positioning for all projections.

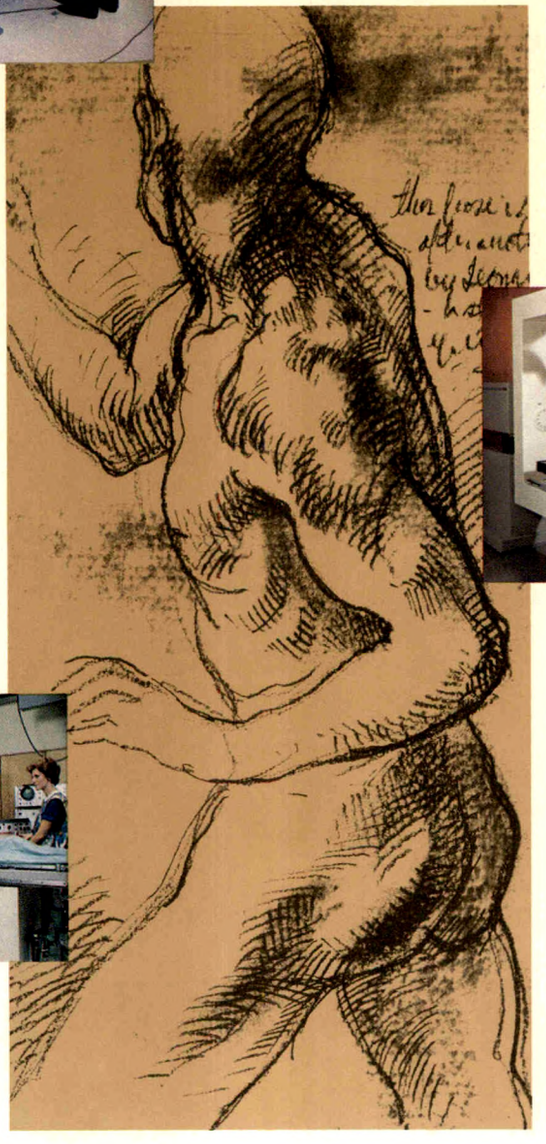

Poly Diagnost UPI

Philips' new universal angiography system for the most flexible filming of cerebral, thoracic, abdominal and peripheral angiography, with full provision for occasional cardiovascular examinations.

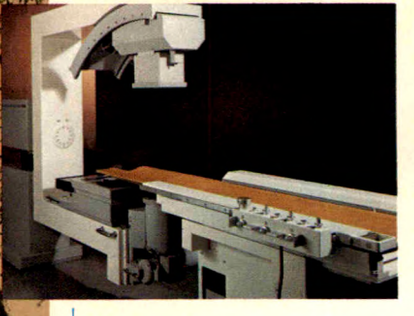

Poly Diagnost C

An extension of the U-arm principle first developed by Philips in the Cardio Diagnost, the Poly C is a dedicated cardiovascular system. Parallelogram construction provides routine and cranio-caudal views without moving the patient, making the Poly C widely used for imaging the thoracic and abdominal areas.

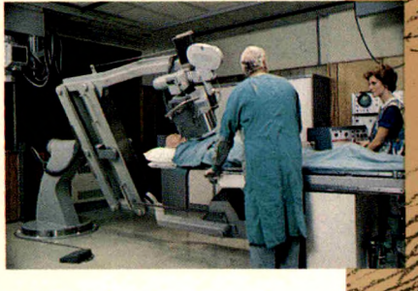

Poly Diagnost UPI

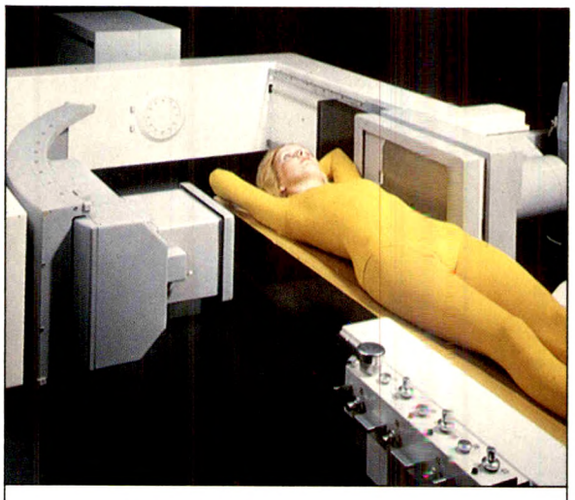

A universal system with revolutionary design, the Poly Diagnost UPI features a rotating U-arm that carries the X-ray tube and an image intensifier and rapid film changer which are quickly interchangeable.

A new experience in examination convenience, the Poly UPI is a masterful combination of system features: free choice of oblique, cranio-caudal and caudo-cranio projections; rapid changeover from fluoroscopy to film changer work; automatic control of object-film distance; motorized height adjustment of both table and U-arm, which provides contact and up to 2:1 geometric enlargement; and a unique boating movement that keeps the object centered in the beam while the object-film distance is automatically controlled in every projection. It's the ideal universal system for angiography!

PHILIPS®

© TM N.V. Philips of Holland

A COMPLETE FAMILY OF IMAGE INTENSIFICATION SYSTEM X-RAY TUBES AND GENERATORS FOR PHILIPS ANGIOGRAPHIC EQUIPMENT.

The 14" Triple-Mode Image Intensifier
Another first from Philips! An amazingly lightweight 14" image intensifier for highly detailed surveys with outstanding results.

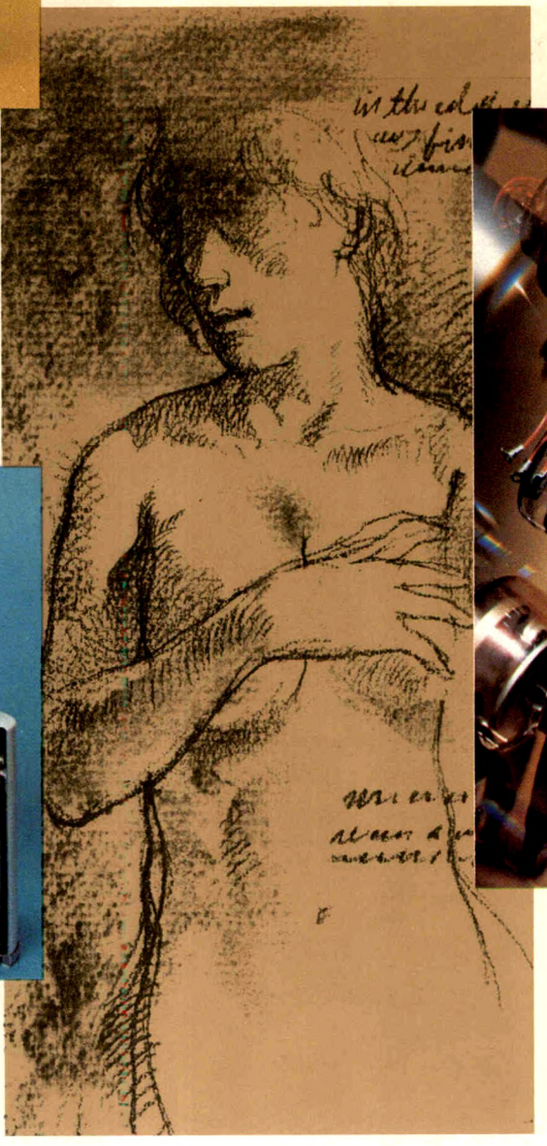

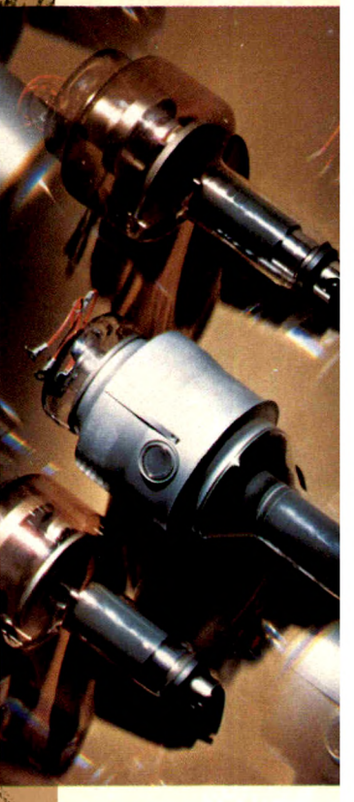

Super Rotalix and Trinodex X-ray Tube
Preferred for exceptic image quality and reli performance in sustai eration, Philips' tubes designed for high loa and superbly efficient dissipation.

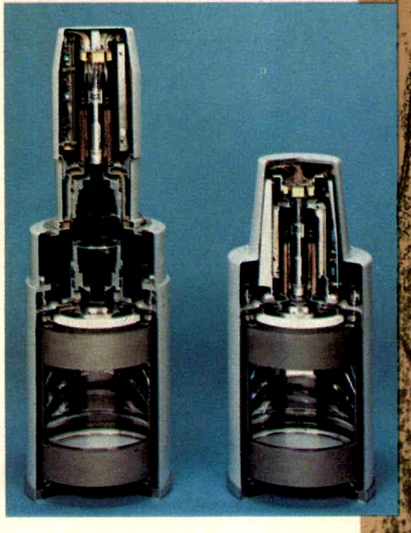

Conventional or Fiber Optic Image Intensifiers
Select from a full range of fields in conventional image intensifiers . . . or Philips' Exclusive Fiber Optic Image Intensification System. Fiber optics provides 30:1 contrast ratio for greater detail, uniform image quality over the entire screen, optimum image transfer and compactness for easy maneuverability.

PHILIPS®
the most reliable family of systems and people in the industry.

A Full Range of Generators
From the very affordab three-phase, high outp Classic line, to a full ra Modular Generators, t computerized Optimus Philips' family of gener combines quality, perf and price for your ever ination need.

Hysterosalpingogram with Salpix Contrast Medium.

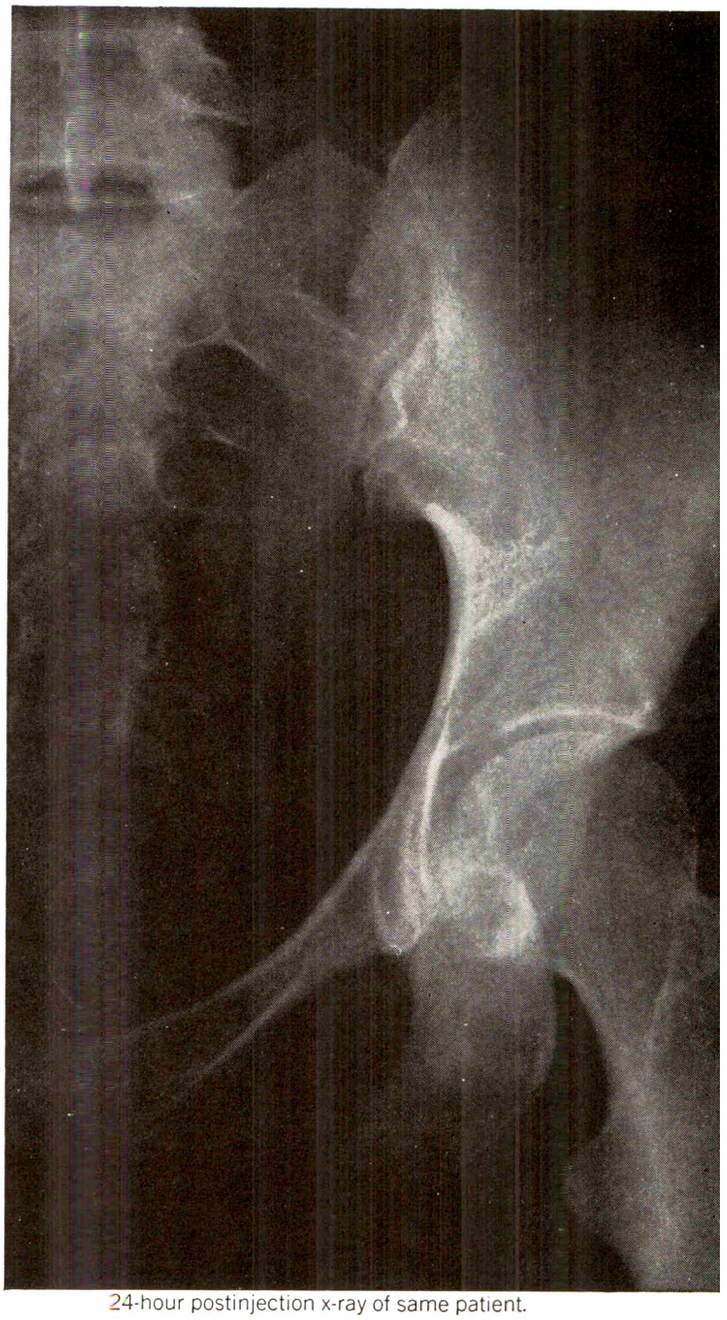

24-hour postinjection x-ray of same patient.

now you see it

now you don't

With Salpix as your contrast medium, your gynecologic patient needn't undergo the 24-hour postinjection x-ray usually required with iodized oils. Water-soluble Salpix leaves virtually no irritating radiopaque residue to produce foreign-body reactions, yet it provides the viscosity needed for adequate visualization.

Contraindications: Contraindications to hysterosalpingography include the presence of severe vaginal or cervical infections, existing or recent pelvic infection, marked cervical erosion or endocervicitis, and pregnancy. The procedure is contraindicated during the immediate pre- or post-menstrual phase.

Sensitivity Test: If indicated in the patient's history, an intracutaneous skin test or sublingual absorption observation may be done with 0.1 cc Salpix.

Warning: Not for intravenous use.

© ORTHO PHARMACEUTICAL CORPORATION 1970

CONTRAST MEDIUM

Salpix

TRADEMARK

EACH CC CONTAINS:
sodium acetrizoate 0.53 g and
polyvinylpyrrolidone 0.23 g

Ortho

ORTHO PHARMACEUTICAL CORPORATION • RARITAN, NEW JERSEY 08869

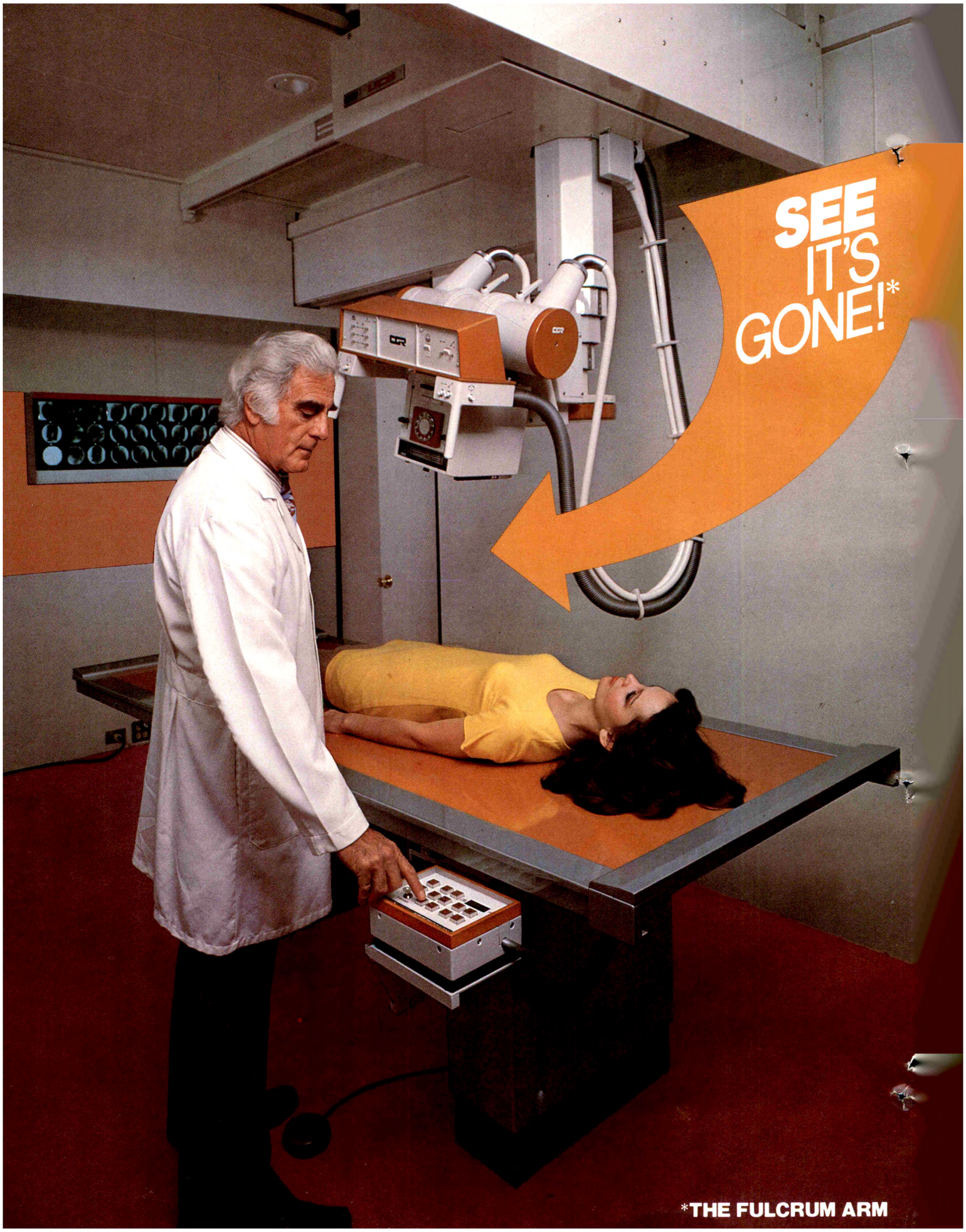
SEE
IT'S
GONE!*
*THE FULCRUM ARM

COMPACT/ SYNCHROTOME.™

CGR'S NEW RADIOGRAPHIC/ TOMOGRAPHIC SYSTEM THAT'S TOTALLY "FULCRUM ARM FREE."

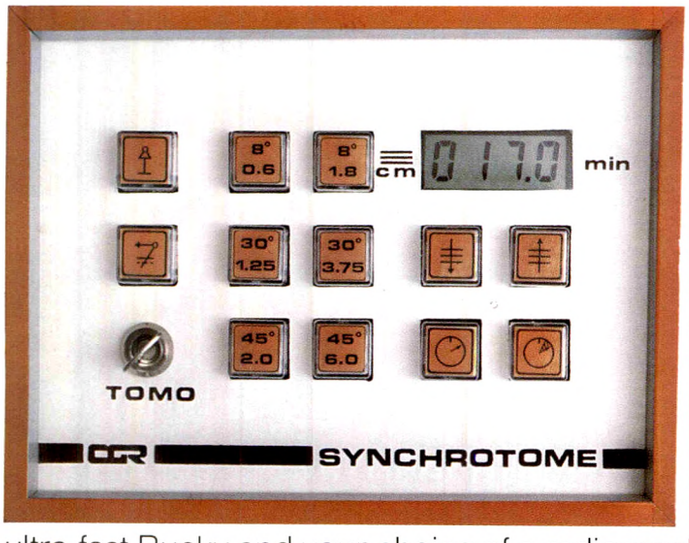

It's a totally new approach to radiography and linear tomography. Starting right out with a superior table: The Compact.

The Compact table gives you an island approach to examination. Complete, obstruction-free access to every side. The large, four-way, floating table top accommodates patients of any size and has extended longitudinal and transverse movement. Table-to-film distance is only 1.6". And the table has an ultra-fast Bucky and your choice of a radiographic grid. Phototiming is optional.

Synchrotome completes the system. The first "fulcrum arm free" linear tomography in the industry. A revolutionary approach using microcomputer electronics. No mechanical linkage whatsoever. Combined with its suspension system it offers complete examination versatility.

Compact/Synchrotome. CGR's cost effective breakthrough in economical radiography/linear tomography.

Your CGR representative has all the details.

CGR MEDICAL CORPORATION 2519 Wilkens Ave
Baltimore, Maryland 21223 (301) 233-2300
CGR CANADA LTÉE-LTD. 500 Boulevard de l'Aéroparc,
Lachute, Québec, Canada, (514) 562-8806
CGR 13 Square Max Hymans,
75741 Paris, France 273-8200

Machlett for high-power chest radiography

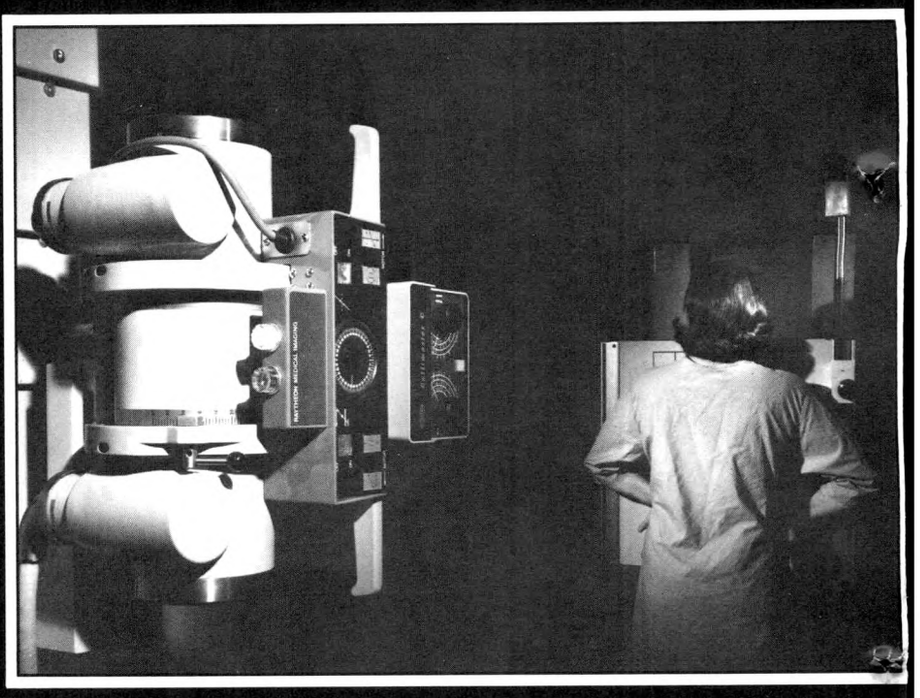

procedure-designed dynamax 68 45/110 x-ray tube

Designed explicitly for high-power chest radiography, including the air gap technique, the Dynamax 68 45/110 provides extended capability for diagnostic information within the chest bone structure. With the large focus rated at 110 kW, the Dynamax 68 45/110 is also extremely well suited to high kV gastro-intestinal studies.

You can obtain a resolution of 7 line pairs/mm with the small focus and 3.3 line pairs/mm with the large focus, with magnification of 1.15 times. Power ratings for the tube are sufficient for extended film distances up to the maximum used for chest radiography.

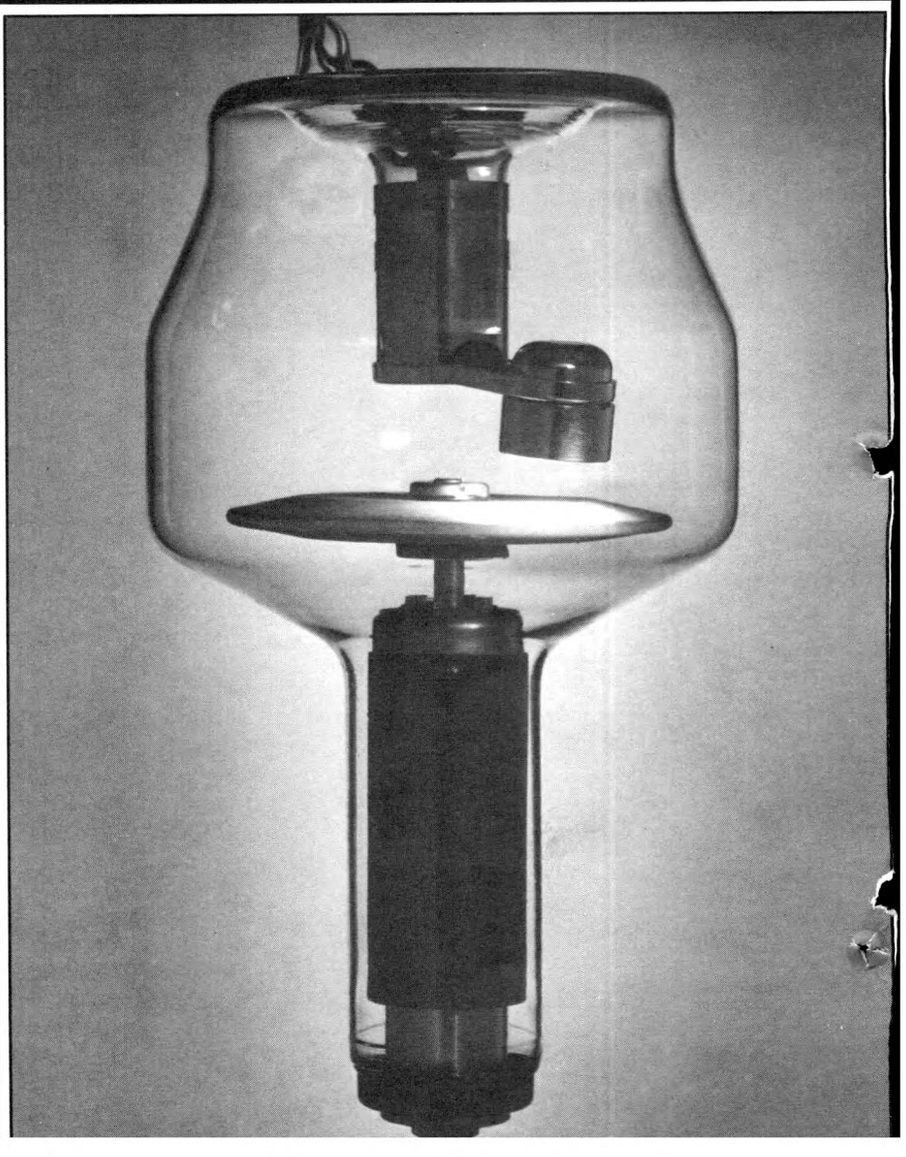

For complete technical information on the Dynamax 68 45/110, or for consultation relative to its application, contact your x-ray dealer or

MACHLETT

The Machlett Laboratories, Incorporated
1063 Hope Street
Stamford, Connecticut 06907

FISCHER X-RAY
introduces...new systems for Radiography/Fluoroscopy

Convenient control aid fluoroscopy and spot filmin

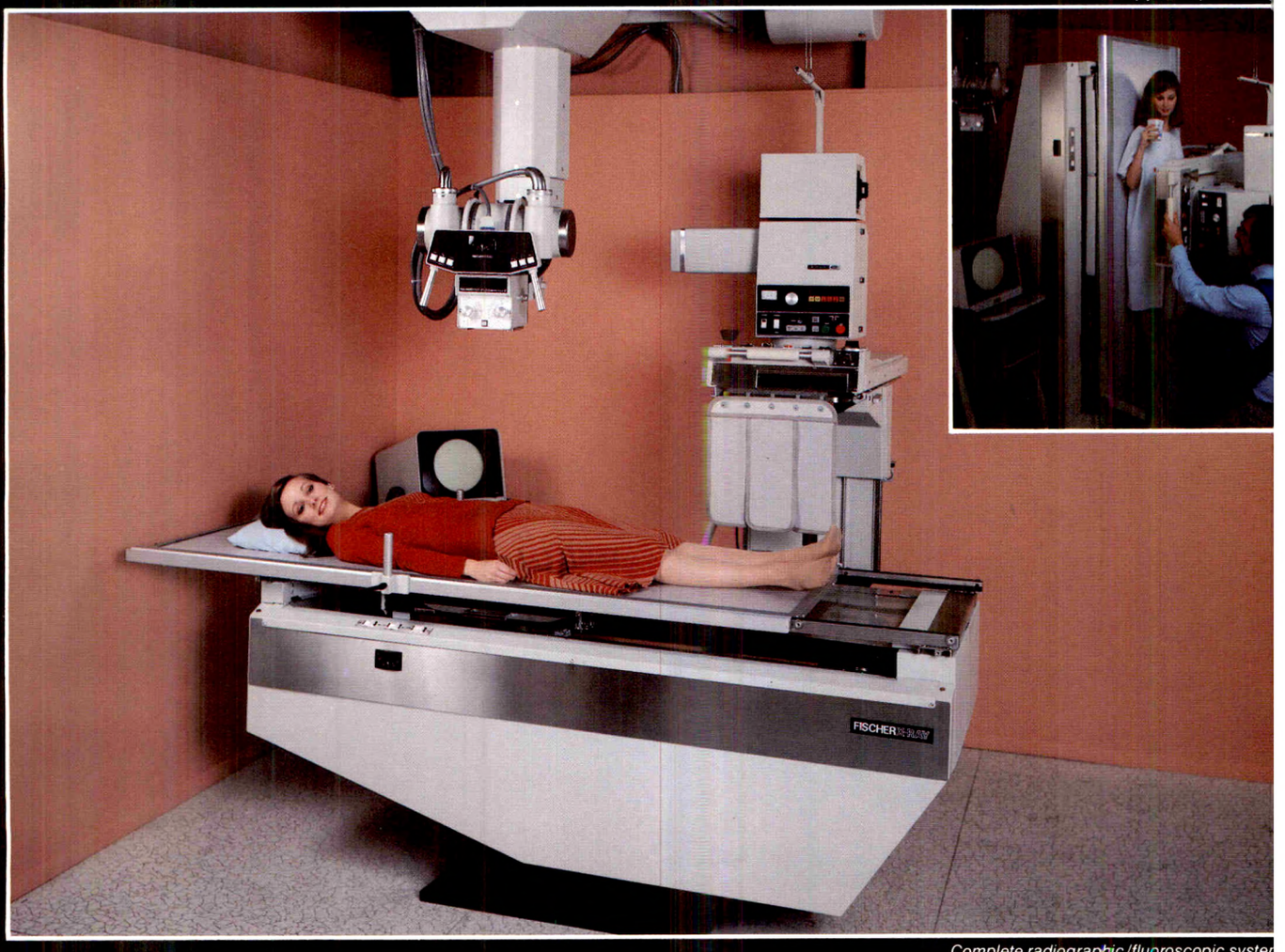

Complete radiographic/fluoroscopic syster

- FX650 or FX525 generator
- 90°/15° Concept 90 table
- 100mm fluoro spot film system

Modular design, economy and exceptional convenience characterize these new R/F systems. The motor driven Concept 90 table has automatic stops at 15° Trendelenburg, horizontal and vertical. Its 4-way top has a unique, 2¼" tabletop-to-film distance for superior image sharpness. Generators include 600mA/150kVp and 500mA/125kVp, both with ionization phototiming for consistent exposures at minimum patient dosage. Fischer's Cascade I Ceiling Tubemount provides 59" of vertical travel; digital display indicates focal distance. The superb optics of the Old Delft "Anodica" camera ensure excellent overall film detail. A unique optical distributor permits shock-free switching from fluoroscopy to film and back within one second.

Write or call for detailed information, or the name of your local Fischer X-Ray Representative.

FISCHER® X-RAY

An established manufacturer of radiographic equipment, serving the medical profession since 1910.

H.G. FISCHER, INC. 3816 N. Carnation Street, Franklin Park, Illinois 60131 • 312/671-5275

FISCHER X-RAY DIVISION • CLAYTON CHEMICAL DIVISION • KATIMA DIVISION

CHARLES C THOMAS • PUBLISHER

PATHOLOGY IN COMPUTED TOMOGRAPHY OF THE BRAIN *by* **Scott D. Henderson,** *Rush-Presbyterian-St. Luke's Medical Center, Chicago.* This reference and guide is designed for use by all persons concerned with computed tomography of the brain. The large number of brain scans included will familiarize the reader with pathology as demonstrated on such scans. The views most respresentative of pathology from over 400 cases are provided. Analyses are presented in general terms to explain as much pathology as the scans are capable of showing. By reading the explanations and studying the scans, the reader will acquire a feeling for the actual physical nature of the pathology involved. *'78, 216 pp. (6 3/8 x 9 5/8), 839 il., $17.50*

AN INTRODUCTION TO THE PHYSICS OF NUCLEAR MEDICINE *by* **Paul N. Goodwin,** *Albert Einstein College of Medicine, Bronx, New York, and* **Dandamudi V. Rao,** *New Jersey Medical School, Newark.* The principles and physics of nuclear medicine are presented in a simple yet comprehensive manner with problems and multiple-choice questions included at the end of each chapter to aid self-study. Topics covered include: the interaction of radiation with matter, scanners, gamma cameras and other imaging devices, statistics of radiation measurements, radiation safety, and radiation dosimetry. Appendices present a list of the elements, conversion factors, physical data for radionuclides and answers to questions and problems. *'77, 164 pp. (6 3/4 x 9 3/4), 44 il., 4 tables, $18.50*

PERCUTANEOUS ANGIOGRAPHY *by* **S. Swamy,** *Michael Reese Medical Center;* **Lewis Irwin Segal,** *Louis A. Weiss Memorial Hospital; and* **S. Mouli,** *Foster-McGaw Medical Center; all of Chicago.* Numerous illustrations explain in detail the basic angiographic techniques while the authors present solutions for many common technical problems in angiography. One section details the programming of standard studies; another is composed of special recipes for the systematic study of common disease processes. The authors also provide in-depth information on angiographic patterns, which are classified according to pathology rather than anatomy, and their relation to gross histological architecture. *'77, 848 pp. (8 1/2 x 11), 1455 il., $80.00*

AN ATLAS OF POLYTOME PNEUMOGRAPHY: With Particular Reference to the Midline Ventricles of the Brain *by* **Taher El Gammal** *and* **Marshall B. Allen, Jr.,** *both of Medical College of Georgia, Augusta, Georgia. Assisted by* **Paul Dyken.** This atlas presents a large number of studies which supplement the study of normal anatomy of the cerebrospinal fluid pathways, and provides comparison for the identification of abnormal structures. Concentration is on the findings of polytome pneumography but, where possible, correlations are made with angiography, positive contrast ventriculography, and CAT examinations. *'77, 480 pp. (8 1/2 x 11), 729 il., $39.50*

A STUDY GUIDE IN NUCLEAR MEDICINE: A Modern Up-to-Date Presentation *compiled and edited by* **Fuad Ashkar, August Miale, Jr.,** *and* **William Smoak,** *all of the Univ. of Miami, Miami, Florida. (22 Contributors)* This book is divided into ten sections covering such topics as basic science, radiopharmaceuticals, principles of radiation therapy, interaction of gamma rays with matter, control of radiation exposure to man, essentials of rectilinear scanning, and cardiovascular imaging. Study questions and references to other material in the field are presented at the end of many chapters. *'75, 488 pp., 312 il., 44 tables, cloth-$22.75, paper-$17.50*

UNDERSTANDING RADIOGRAPHY *by* **Stephen S. Hiss,** *Atlantic City Medical Center, Atlantic City, New Jersey.* A most expansive and detailed text on radiographic technology, this book encompasses the vast and intricate changes that have recently taken place in the field. The descriptive and imaginative manner in which it is written and illustrated makes it unusually informative and enjoyable to read. Great care has been taken to provide a blend of the basic technical factors, their relationship to physics, and their applicability to typical situations with which the technologist will be confronted. Characteristics of the radiographic image, film and processing, intensifying screens, focal distance, the remnant beam, and tomography are among the subjects examined. *'78, 376 pp. (6 3/4 x 9 3/4), 365 il., 4 tables, $29.50*

A STUDY GUIDE TO UNDERSTANDING RADIOGRAPHY *by* **Stephen S. Hiss,** *Atlantic City Medical Center, Atlantic City, New Jersey.* Designed as an adjunct to UNDERSTANDING RADIOGRAPHY, this study guide will help students learn the material and assess their own progress. Its scope and format, which parallel the main text, will be especially helpful to students preparing for the American Registry Examination in X-Ray Technology. There are approximately 1,000 questions arranged by subject matter. These questions will aid the student in reviewing the facts and techniques outlined in each chapter. *'78, 150 pp., 41 il., $6.50, paper*

PALEOPATHOLOGICAL DIAGNOSIS AND INTERPRETATION: Bone Diseases In Ancient Human Populations *by* **R. Ted Steinbock,** *Harvard Medical School, Boston. Foreword by* **T. Dale Stewart.** This book provides a systematic approach to diagnosing bone lesions in excavated skeletal series and interpreting the significance of such diseases in ancient human populations. Chapters discuss the biology and gross anatomy of normal bone to aid in understanding the bone changes produced by pathological conditions, and cover the major traumatic, infectious, nutritional, metabolic, degenerative, and neoplastic diseases of bone. *'76, 440 pp., 274 il., 16 tables, $22.75*

THE ADULT POSTOPERATIVE CHEST *by* **Myron Melamed; Florencio A. Hipona,** *Harvard Medical School, Boston;* **Carlos J. Reynes,** *Loyola Univ., Maywood, Illinois;* **Walter L. Barker,** *Univ. of Illinois, Chicago; and* **Santiago Paredes,** *Boston Univ. School of Medicine, Boston. Foreword by* **Hiram T. Langston.** This study of adult pulmonary and cardiovascular radiography after surgery systematically assesses the extraneous factors imposed upon x-ray film by the surgical act. The book offers an atlas against which problem pictures can be compared for quick identification. *'77, 396 pp., 578 il., 1 table, $31.50*

HEALTH PROTECTION OF RADIATION WORKERS *by* **W. Daggett Norwood,** *Hanford Environmental Health Foundation, Richland, Washington.* This book summarizes present knowledge regarding the hazards to the safety and well-being of persons working with radiation. Basic facts are provided on ionizing radiation, its measurement and dosimetry. Also discussed are established standards for health, safety and environmental protection along with their implementation, diagnosis and therapy for illness or injury. Everyone concerned with protecting the health and safety of radiation workers will greatly benefit from this informative book. *'75, 468 pp., 16 il., 16 tables, $27.50*

Orders with remittance sent, on approval, postpaid

301-327 East Lawrence Avenue • Springfield • Illinois • 62717

For Double Contrast Stomachs, Use

NEW! E-Z-HD™

High Density with High Fluidity Barium Sulfate for Suspension

NOTE THE ANTRAL POLYP (ARROW) AND THE LACELIKE AREAE GASTRICAE IN THE BODY OF THE STOMACH
Film, courtesy of Robert E. Koehler, M.D. Washington University, Dept. of Radiology, St. Louis, Missouri.

Double contrast radiography appears to offer the potential for significant improvements in diagnostic accuracy.

Double contrast studies of the stomach best demonstrate the surface pattern of the stomach (areae gastricae). This leads to improved detection of superfical erosions and ulcers, malignancies, polyps and other benign tumors, and ulcer scars.

E-Z-HD barium sulfate provides the basic ingredient necessary for good double contrast of the stomach.

The higher the density of the barium suspension, the better the coating, E-Z-HD allows for the highest density suspension of any commercial product on the market today: 85% w/w. 250% w/v. E-Z-HD achieves this density while remaining fluid for ease of administration.

- High density
- High fluidity
- Palatable
- Unit dose convenience.

E-Z-HD – The barium for the double contrast examination of the stomach and duodenum.

Optimal Density & Fluidity for the Modern Double Contrast Examination of the Stomach and Duodenum

Refrences:

David W. Gelfand: The Japanese-Style Double Contrast, Examination of the Stomach, Gastrointest Radiol. 1, 7-17 (1976)

Igor Laufer: The Diagnostic Accuracy of Barium Studies of the Stomach and Duodenum – Correlation with Endoscopy, Radiology 115: 569-573, June 1975

Roscoe E. Miller: The Air Contrast Stomach Examination: an overview. Radiology 117: 743-744 Dec. 1975

E-Z-EM

For Further Information Write:

7 Portland Ave.
Westbury, New York 11590
(516) 333-8230

9/77

MPX
120
500
400
125
90
00
GENERAL ELECTRIC
RPX Newsy

A classic breakthrough.

GE's new R&F system saves you time, space, money and dose. And gives you excellent images.

Here's a totally new R&F system that offers you many advantages over existing units—it's a major breakthrough in classical R&F. Let's take a closer look at each component.

Fluoricon® L300 suspensionless intensifier gives you 9″ triple field performance, high frame rate photospot capability and improved imaging in a new lightweight package.

Diagnostic detail is exceptional—with advanced video camera technology and high resolution, high contrast ratio image tubes.

User-selectable dose rate and video gain let you add video gain for imaging obese patients, and provide the lowest dosage for young or thin patients.

When you choose the computerized technic management option at the spotfilmer, unique values of kVp, mA and focus are stored for each spotfilm and photospot procedure. Patient size selection includes pediatrics down to the neonate range.

And the new suspensionless design allows ample clearance for an overhead tube, facilitating radiography and attachment of an optional tomograph. The compact design fits into smaller, problem-sized rooms, giving you large room R&F capability.

RFX™ table and spotfilmer, with user-selectable grids, combines lower dose fluoro and high kVp spotfilms in one easy-to-use system.

The spotfilmer's unique, effort-sensing power assist simulates the feel of an unpowered fluoroscopic screen.

Two-per-second spotfilming with sequence anticipation allows two to four manually sequenced spotfilms without cassette return. Load from the front or rear, with pushbutton changeover.

Diagnostic advantages include automatic masking to format with full field, 2-on-1 vertical or transverse, or 4-on-1 formats. Masking is internal, allowing full field fluoro with the cone in place.

Additional RFX features include: (1) cone lockout for myelography; (2) automatic cassette return; (3) rapid access spotfilming (.75 sec.); (4) arthrographic collimation and ion chamber compensation for 9-on-1 or 6-on-1 formats; and (5) improved radiation protection at all routine angulations.

MPX computerized generator, with Quantamatic™ tx technic management, stores all of your department's standard radiographic settings.

The operator simply presses the appropriate anatomical selection buttons. The microprocessor instantly displays all technic parameters, including kVp, mA, mAs, time, focal spot size and AEC status. And the operator may raise or lower factors to suit special patient situations.

With over 200 programmed AEC and fixed-time technics (on or off the table) available, you can handle virtually every patient size. From infant to obese adult. And any body part, including extremities.

Quantamatic tx technic management gives you consistent, high-quality films. Throughput increases. Costly retakes due to technic error are virtually eliminated. And programmed constant load design extends tube life by optimizing tube loading.

You'd expect it from GE.

Contact your GE representative to get all the facts on this important R&F breakthrough. Fluoricon L300/RFX/MPX....it's a classic.

General Electric Medical Systems, Milwaukee, Toronto, Madrid.

GENERAL ELECTRIC

1950

Conventional image intensifier

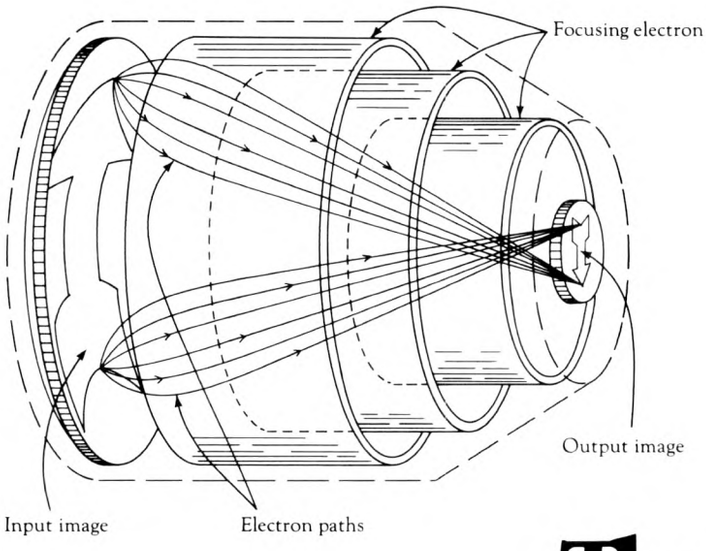

1978

DI's Panel Electron Tube

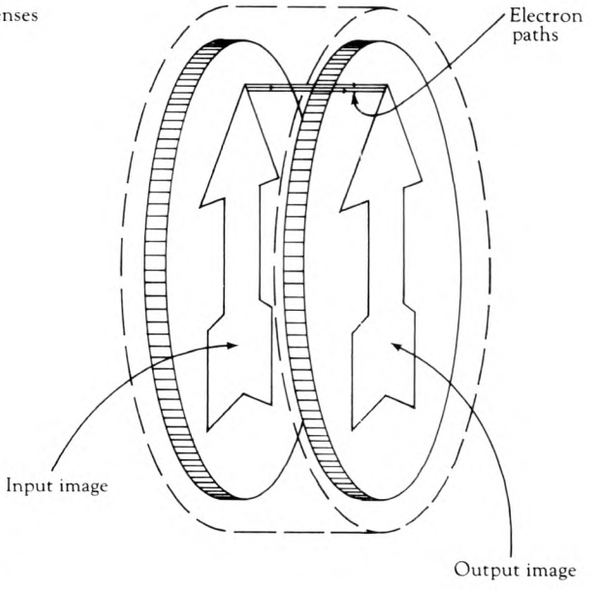

The difference between yesterday and tomorrow.

In 1950, image intensification took fluoroscopy out of the dark ages. But you paid a price—image distortion, peripheral blurring and a bulky "bottle" between you and the patient.

Today Diagnostic Information's Panel Electron Tube provides simple, direct fluoroscopy (PET™ Scope) and low-dose TV fluoroscopy (PET™ TV). PET technology is simple, compact and versatile. It gives you a sharper, more stable image without distortion.

Tomorrow the Panel Electron Tube will do more. It will be the heart of a high-performance nuclear camera and a high-speed CT scanner; provide high-resolution photo spot films; and make possible inexpensive small-film x-rays and large-format imaging. All based on the same innovative technology. All being developed now. By the innovators in image technology, Diagnostic Information, Inc., 246 Sobrante Way, Sunnyvale, CA 94086. (408) 736-3500.

See us at RSNA Booth #1411

Diagnostic Information Incorporated

The Embryogenesis of the Human Skull

An Anatomic and Radiographic Atlas

Robert Shapiro and Franklin Robinson

Drs. Shapiro and Robinson have created an atlas described by Richard L. Sidman as "a solid piece of research, executed with considerable esthetic as well as scholarly finesse, [which] will serve as the definitive study on an important aspect of human fetal development." This will be the basic normative standard reference for studies on developmental skeletal disorders of the head and neck and will be useful in the study of developmental brain diseases. Radiologists will also find this an invaluable tool.
A Commonwealth Fund Book 103 illus., $45.00

Harvard University Press
Cambridge, MA 02138

Harvard

We want you to talk in our library.

Ours is a living library of spoken words. A library of roughly 40,000 textbooks on tape, available free of charge to blind students. Eligible students also include the visually impaired, the learning disabled, and the physically handicapped who cannot handle printed material.

These students continually require new texts. And to fill this need, volunteer readers make tapes in our 29 recording studios across the country.

We urgently need readers with technical or professional backgrounds, and native speakers of foreign languages. If you can spare two hours a week, please volunteer. We are a non-profit organization supported by contributions from the public.

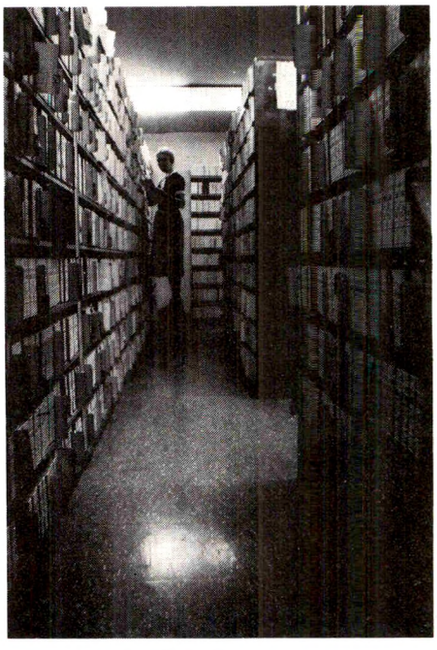

Recording for the Blind . . . . . *an educational lifeline*
215 East 58th St., New York, NY 10022.

Your special procedures

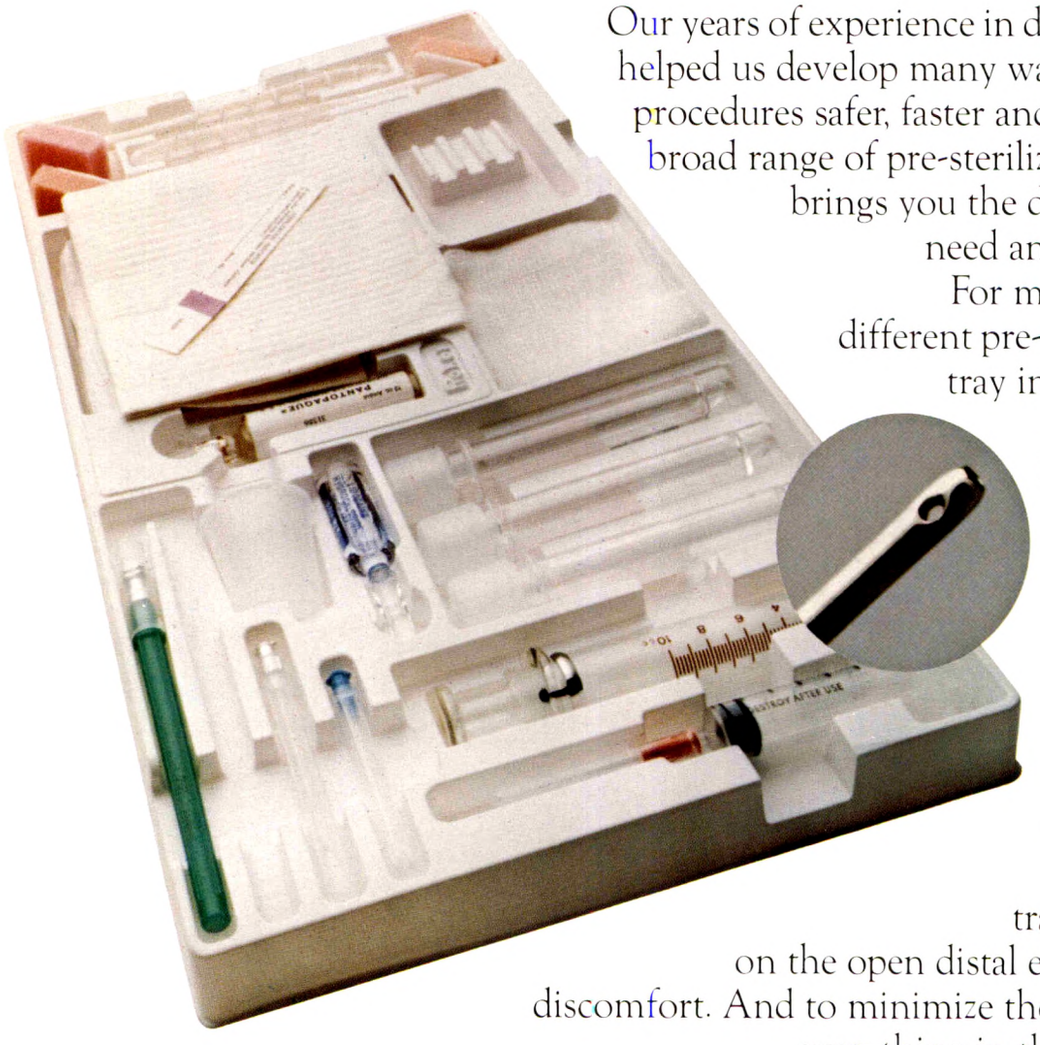

Our years of experience in diagnostic medicine have helped us develop many ways to make your special procedures safer, faster and easier to perform. Our broad range of pre-sterilized trays and accessories brings you the dependable accuracy you need and minimizes your costs.

For myelography, we offer six different pre-sterilized packages. Each tray includes all the essentials, conveniently arranged. So now you can choose the tray that best fits your needs.

Our new aspirating cannula is one example of the special attention we give to myelography. Designed to minimize patient trauma, the rounded edge on the open distal end is less likely to cause discomfort. And to minimize the risk of cross-infection, everything in the package is disposable.

Arthrography also has our special attention. With the exception of prep solution and contrast agent, our new tray has everything you need for single- and double-contrast arthrography...all in one pre-sterilized disposable package. Each item is neatly arranged for ease of use.

Since more often than not arthrography involves the knee, the way to high-quality radiographs is to use the Arthrostress. It maintains the limb or area of interest in the same plane relative to the cassette.

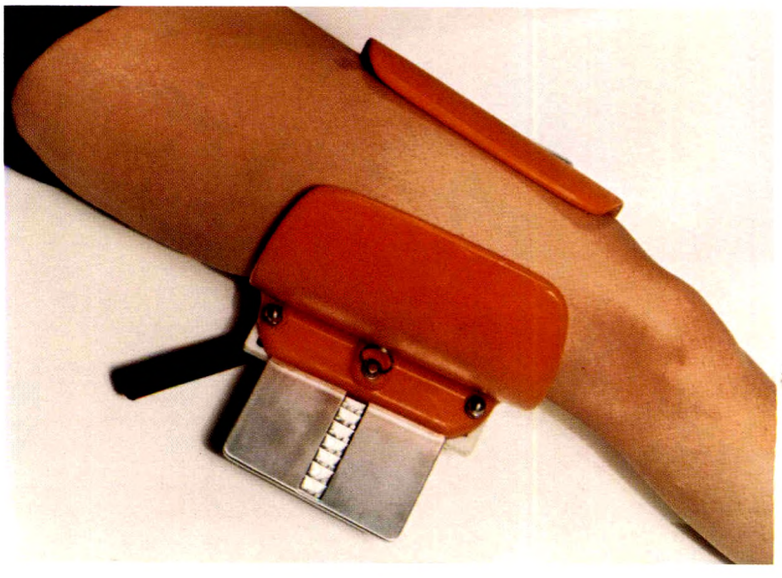

have our special attention.

While waiting, your patients can relax comfortably in our VIP disposable gowns. They're tough, flame-retardant to comply with the Flammable Fabrics Act—and economical, because they eliminate the cost of laundering.

And we suggest you wear our Lite-Gard™ apron for protection and comfort. Available in a variety of colors, these lightweight aprons offer optimum radiographic protection while assuring maximum freedom of movement.

In addition, we can supply you with our complete line of accessories—over 3,000 different supplies ranging from positioning aids, films and chemicals, to processors, cassettes...and so much more.

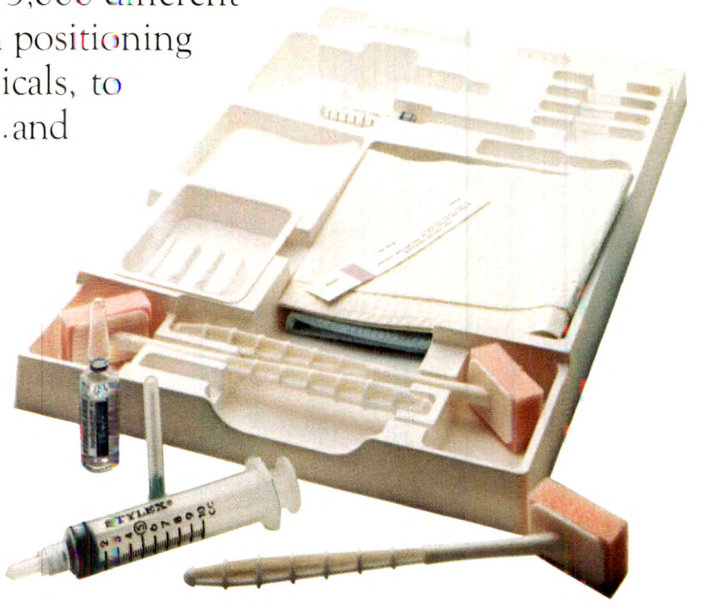

For more information contact your local Picker representative, or write Picker Corporation or Picker International, 595 Miner Road, Cleveland, OH 44143.

PICKER®

ONE OF THE CIT COMPANIES

"Productivity is up 10% to 20%"

"Lower absenteeism"

"You can tell by their attitude—the workers who participate are happier, more cooperative, much sharper"

"We can identify direct savings of $2,000,000 per year"

"The program has had a distinct bearing on staff performance. Our engineering people now have a camaraderie with their counterparts in other departments"

"It started in headquarters. By next year we hope to have it in all our factories and research facilities"

These are actual quotes from executives of large and small companies and organizations in Denver, Omaha, Birmingham, and Greenwich. They're talking about company fitness programs. That's right, many employers now provide facilities or opportunities for exercise for their employees. They are glad they did.

Most began with a concern for employee health and well being. What they have found is a variety of additional benefits. These benefits add up to *increased productivity*—so much so that several companies can demonstrate that the fitness program pays for itself. Add to this improved morale, better internal communications, and employee health. How can you lose? Write us now for more information:

The President's Council on Physical Fitness and Sports
Department B
Washington, D.C. 20201

Employee Fitness: In the long run you will be the winner.

DISCOVER MORE WITH CLEAR DEFINITION

new AMIPAQUE® (metrizamide)

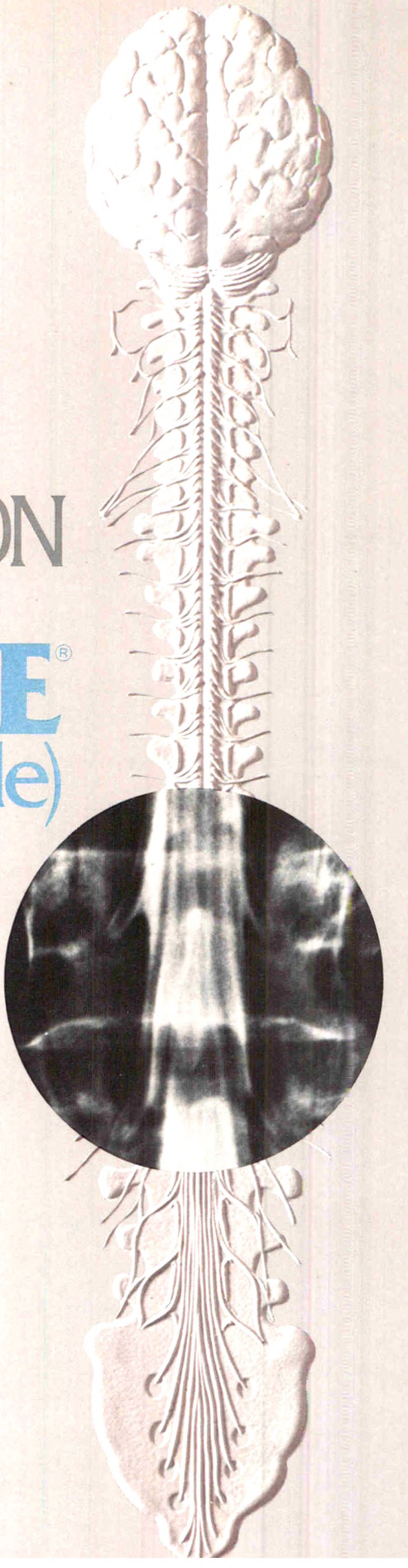

See last page for important product information including warnings, adverse reactions, and prescribing and precautionary recommendations.

COMPARE RADIOGRAPHS

iophendylate

Lumbar myelogram of 27-year-old female (anteroposterior view): Note high-density shadows and failure of contrast medium to adequately fill nerve-root sheaths.

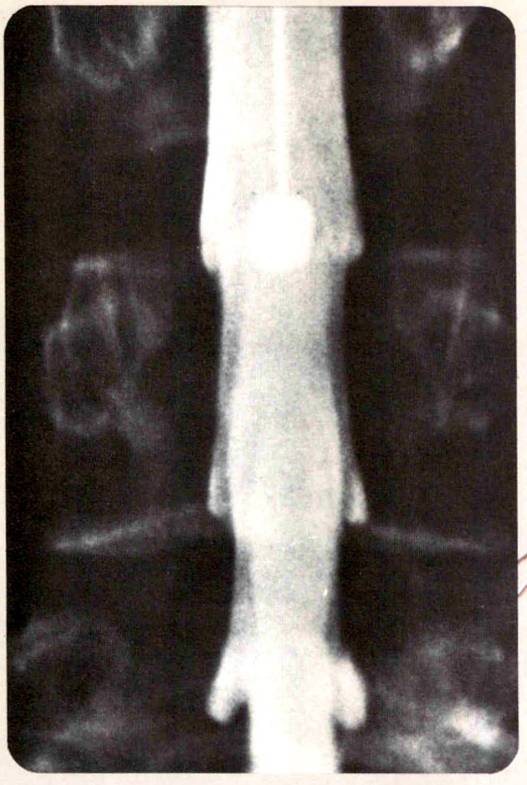

AMIPAQUE (metrizamide)

Lumbar myelogram of 20-year-old male (anteroposterior view): Note graded density of shadows and filling of nerve-root sheaths by the low-viscosity, water-soluble contrast medium.

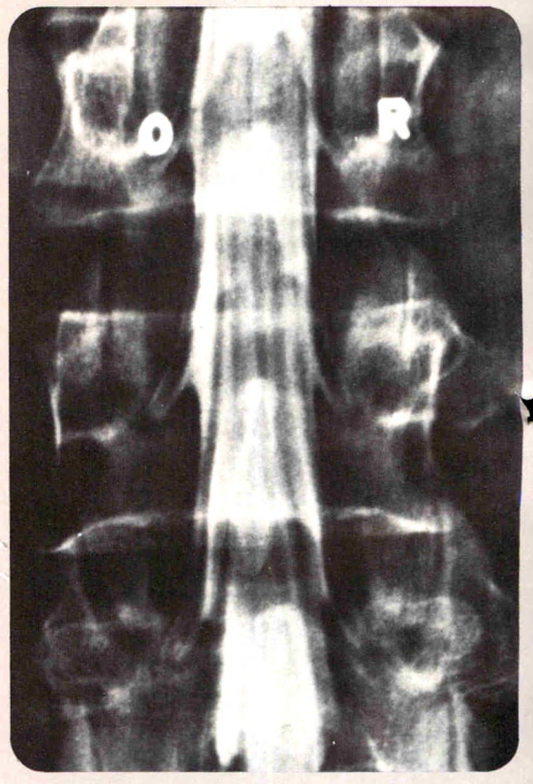

See last page for important product information including warnings, adverse reactions, and prescribing and precautionary recommendations.

CLEARER VISUALIZATION

Water-soluble, low viscosity

- ☐ Miscible with CSF for more uniform distribution around structures in subarachnoid space.[1,2]
- ☐ Flows into and through narrow subarachnoid spaces, fills slender cavities of nerve-root sheaths.[1,3]
- ☐ Usually diffuses around all except total obstructions with a single injection.
- ☐ Radiographic contrast provides nonobscured view of fine details.

Slightly hyperbaric

- ☐ Allows control of contrast distribution during initial phase of radiologic study, if desired.[1,3]

SIMPLIFIED MYELOGRAPHY

Nonionic...does not dissociate in solution

Isotonic with CSF at concentrations most frequently used (170 mgI/ml).

Low viscosity

- ☐ Allows use of narrow-bore needle (22-gauge).
- ☐ Less chance of CSF leakage...less chance of trauma to dura.

Resorbed and excreted mainly via kidneys in 48 hours

- ☐ No need for aspiration or second puncture...lessens potential for neurologic damage.
- ☐ No needle left in place during procedure...facilitates patient manipulation.

PATIENT TOLERANCE

- ☐ In general, the types of adverse reactions following subarachnoid injection of AMIPAQUE are not substantially different from those seen after lumbar puncture alone.
- ☐ The most frequently occurring reactions are headache, nausea, and vomiting.
- ☐ Rarely have reactions been severe or persistent beyond 24 hours.
- ☐ Although metrizamide is relatively safe and, in comparative studies, less toxic than other compounds for these indications, side effects ranging from headache and nausea to epileptic fits, convulsions, slow wave patterns on EEGs, petit mal states, paralysis, and arachnoiditis have occurred with the use of such compounds. Neurologic examinations were performed before and at intervals after the procedures in 1,495 of 1,850 cases. No clinically significant changes were found.

INDICATIONS: lumbar, thoracic, cervical, and total columnar myelography; and for use in computerized tomography of the intracranial subarachnoid spaces following spinal subarachnoid injection.

new **AMIPAQUE**® (metrizamide)

More fully investigated before introduction than any other subarachnoid contrast agent

☐ 158 published reports ☐ 5 years in clinical research ☐ 2 years in U.S. medical centers

Description: Metrizamide, 2-[3-Acetamido-2,4,6-triiodo-5-(N-methylacetamido) benzamido]-2-deoxy-D-glucopyranose, is a compound derived from metrizoic acid and glucosamine. It is a nonionic water-soluble contrast medium with a molecular weight of 789 (iodine content: 48.25%). The chemical structure is as follows:

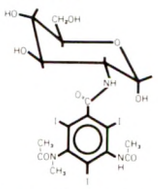

AMIPAQUE (metrizamide) is provided as a sterile, white lyophilized powder. Each 3.75 g/20 ml vial contains 3.75 g metrizamide (1.81 g organically-bound iodine) and 1.2 mg edetate calcium disodium. Each 6.75 g/50 ml vial contains 6.75 g metrizamide (3.26 g organically-bound iodine) and 2.16 mg edetate calcium disodium.

Each 20 ml vial of sterile aqueous diluent contains 0.05 mg/ml sodium bicarbonate in water for injection. pH is adjusted with carbon dioxide, USP, if necessary.

When AMIPAQUE is reconstituted to the lowest recommended concentration (170 mgI/ml) it has a specific gravity of 1.184 at 37°C, is hyperbaric to cerebrospinal fluid, is isotonic with CSF, and has a pH of approximately 7.4.

Clinical Pharmacology: AMIPAQUE is absorbed from cerebrospinal fluid into the bloodstream. Approximately 60 percent of the administered dose is excreted unchanged through the kidneys within 48 hours.

The initial concentration and volume of the medium, in conjunction with appropriate patient manipulation, will determine the extent of the diagnostic contrast that can be achieved. This can be monitored by fluoroscopy.

Following spinal subarachnoid injection, conventional radiography will continue to provide diagnostic contrast for approximately an hour. At 4 to 5 hours contrast is hazy and none is detectable at 24 hours.

Following subarachnoid placement, irrespective of the position the patient has maintained, upward diffusion of AMIPAQUE takes place through the CSF.

After introduction into the lumbar subarachnoid space, computerized tomography (CT) shows CSF contrast enhancement in the thoracic region in about one hour, in the cervical region in about 2 hours, and in the basal cisterns in 3 to 4 hours.

When low doses of AMIPAQUE (see DOSAGE AND ADMINISTRATION) are introduced into the lumbar CSF and moved cephalad under gravity control and examined by CT scanning, they will provide immediate CSF contrast in the basal cisterns. Depending on the specific technique used, the lateral, third, and fourth ventricles may also be visualized. The contrast in this area will markedly diminish at 6 hours and disappear by 24 hours. CSF enhancement will be evident at the cortical sulci and interhemispheric fissures at 6 hours. Between 12 and 24 hours the surfaces of the cerebrum and cerebellum, in contact with the subarachnoid spaces, will develop a "blush" effect on the scan which will normally disappear in 36 to 48 hours. The rate, time, extent of diffusion, and the disappearance or stasis of AMIPAQUE as demonstrated with CT scanning, can be used to detect or infer the presence of CNS abnormalities.

Indications and Usage: AMIPAQUE is indicated for lumbar, thoracic, cervical, and total columnar myelography and for use in computerized tomography of the intracranial subarachnoid spaces following spinal subarachnoid injection.

Contraindications: AMIPAQUE should not be administered to patients with a known hypersensitivity to metrizamide.

Warnings: If grossly bloody CSF is encountered, the possible benefits of a myelographic procedure should be considered in terms of the risk to the patient.

Usage in pregnancy. No teratogenic effects attributable to AMIPAQUE have been observed in reproduction studies in animals. However, before administration of AMIPAQUE to women during pregnancy, the benefit to the patient should be carefully weighed against the possible risk to the fetus.

Until further experience is gained in children younger than 12 years, administration of AMIPAQUE in this age group is not recommended.

Fatal reactions have been associated with the administration of water-soluble contrast media. Although no fatal reactions have been associated with AMIPAQUE, it is of utmost importance that a course of action be carefully planned in advance for the immediate treatment of serious reactions, and that adequate and appropriate facilities and personnel be readily available in case of a severe reaction.

Precautions: Caution is advised in patients with a history of epilepsy, severe cardiovascular disease, chronic alcoholism, multiple sclerosis, or with a history of bronchial asthma or other allergic manifestations.

Before a contrast medium is injected, the patient should be questioned for a history of allergy. Although a history of allergy, including asthma, may imply a greater than usual risk, it does not arbitrarily contraindicate the use of the medium. Premedication with antihistamines to avoid or minimize possible allergic reactions may be considered. No conclusive relationship between severe reactions and antigen-antibody reactions or other manifestations of allergy has been established.

Patients who are receiving anticonvulsants should be maintained on this therapy. Should a seizure occur, intravenous diazepam or sodium phenobarbital is recommended.

Prophylactic anticonvulsant treatment with barbiturates or diazepam orally for 24 to 48 hours should be considered in patients with evidence of inadvertent intracranial entry of a large or concentrated bolus of the contrast medium since there is an increased risk of seizures in such cases.

Any drugs, such as neuroleptics, including phenothiazine derivatives, which lower the seizure threshold should be avoided. These drugs should not be used as premedications. If possible, they should be withdrawn at least 48 hours before the examination and not used for at least 12 hours postprocedure.

In patients with severe renal insufficiency or failure, the drug is excreted by the liver into the bile at a much slower rate. Patients with hepatorenal insufficiency should not be examined unless the possibility of benefit clearly outweighs the additional risk. Reexamination should be delayed for five to seven days.

Adverse Reactions: In general, the adverse reactions following subarachnoid injection of AMIPAQUE are not substantially different from those seen after lumbar puncture alone. The most frequently occurring adverse reactions are headache, nausea, and vomiting. These reactions occur 3 to 8 hours postinjection, almost all occurring within 24 hours. They are usually mild to moderate in degree lasting for a few hours and disappearing within 24 hours. Rarely have the headaches been severe or persisted beyond 24 hours.

Backache, neck stiffness, numbness and paresthesias, leg or sciatic-type pain occurred less frequently, often in the form of a transient exacerbation of preexisting symptomatology. Temperature elevations and dizziness have also been reported.

Rarely, muscle spasm or generalized convulsions have occurred 4 to 8 hours following injection and in some cases were attributed to a history of epilepsy, medication with neuroleptic drugs, or inadvertent overdose. In all cases, treatment with intravenous diazepam or sodium phenobarbital has provided rapid control.

Transient alterations in vital signs may occur, the significance of which is difficult to assess since these parameters may be affected by the procedure or the patient's physical or emotional state.

Other rarely occurring adverse reactions include the following:
Allergy or Idiosyncrasy: chills, pruritus, urticaria, nasal congestion, and dyspnea.
CNS: mild and transitory perceptual aberrations such as hallucinations, depersonalization, anxiety, depression, hyperesthesia, visual and speech disturbances, confusion and disorientation. In addition, malaise, weakness, EEG changes, and meningismus have occurred.
Cardiovascular: chest pain, tachycardia, bradycardia, and arrhythmia.
Other: diarrhea.

Dosage and Administration: The dosage and concentration of AMIPAQUE will depend on the degree and extent of contrast required in the area(s) under examination and on the equipment and technique employed. Concentrations which are approximately isotonic (170 to 190 mgI/ml) are recommended for examination in the lumbar region. For movement of the medium to distant target areas, higher concentrations are recommended to compensate for dilution of AMIPAQUE with CSF.

A total dose of 3000 mg of iodine should not be exceeded.

The recommended usual and maximum doses of AMIPAQUE are summarized in the following table:

DOSAGE TABLE

Procedure	Conc. of Solution (mgI/ml)	Usual Recommended Dose* (ml)	Max. Dose Total (mgI)
Lumbar myelogram	170-190	10-15	2850
Thoracic myelogram	220	12	2640
Cervical myelogram (via lumbar injection)	250-300	10	3000
Cervical myelogram (via lat. cervical inj.)	220	10	2200
Total columnar myelography	250-280	10	2800
CT cisternography (via lumbar inj.)	170-190	4-6	1140

*Refer to RECONSTITUTION TABLE for preparation of Solution

PATIENT MANAGEMENT

PREPROCEDURE: Anesthesia is not necessary. Premedication sedatives or tranquilizers are usually not needed. The use of neuroleptic drugs, including phenothiazine derivatives, should be avoided and such medication should be discontinued, when possible, 48 hours before the procedure (see PRECAUTIONS). Epileptic patients should be maintained on their anticonvulsant medication.

INSTRUCTIONS FOR PREPARATION OF THE SOLUTION: Contents under vacuum. Use only if vacuum is present as evidenced by diluent being drawn into vial when stopper is punctured.

1. Fill a sterile syringe with the exact volume of diluent as indicated in the following RECONSTITUTION TABLE to obtain the desired iodine concentration. *Examples: a.* For vials containing 3.75 g AMIPAQUE: To obtain 170 mgI/ml, use 8.9 ml of diluent; to obtain 190 mgI/ml, use 7.8 ml of diluent. *b.* For vials containing 6.75 g AMIPAQUE: To obtain 170 mgI/ml, use 16.1 ml of diluent; to obtain 190 mgI/ml, use 14.0 ml of diluent.

RECONSTITUTION TABLE

Conc. of Solution (mgI/ml)	Volume of Diluent to be Added 3.75 g Vial (ml)	6.75 g Vial (ml)
170	8.9	16.1
180	8.3	15.0
190	7.8	14.0
220	6.5	11.7
250	5.5	10.0
260	5.2	9.4
270	5.0	9.0
280	4.7	8.5
290	4.5	8.1
300	4.3	7.8
	The volume of the final solution will equal the volume of the diluent + 1.7 ml	The volume of the final solution will equal the volume of the diluent + 3.1 ml

The volume of the final solution will exceed the amount required to achieve the recommended dosage. For precise volume for injection refer to DOSAGE TABLE.

2. Inject the diluent into the vial, and leave the syringe and needle in place.
3. Gently swirl the vial (without shaking) until its contents are dissolved (approximately 3 to 10 minutes). The solution should be clear and colorless to slightly yellow.

Use immediately after reconstitution (see DOSAGE AND ADMINISTRATION). Discard any unused portion.

As with any lumbar puncture, sterile technique must be employed. The lumbar puncture is usually made between L3 and L4, but if pathology is suspected at this level the interspace immediately above or below may be selected. A lateral cervical puncture may also be used.

POSTPROCEDURE: The lumbar puncture needle may be removed immediately following injection since it is not necessary to remove AMIPAQUE after injection into subarachnoid spaces.

Management of the patient is similar to that used following simple lumbar puncture. Maintaining the patient recumbent in bed with the head raised 15° to 30° for 8 hours may reduce the rate of upward dispersion of the medium. The patient may then remain horizontal for a further 16 hours at the discretion of the physician.

How Supplied: *Kits, each containing:* one-3.75 g/20 ml single-dose vial of AMIPAQUE with 1 vial of diluent (NDC 0024-0044-01); or one-6.75 g/50 ml single-dose vial of AMIPAQUE with 1 vial of diluent (NDC 0024-0046-01).
Combination packs, each containing: five-3.75 g/20 ml single-dose vials of AMIPAQUE with 5 vials of diluent (NDC 0024-0044-12); or five-6.75 g/50 ml single-dose vials of AMIPAQUE with 5 vials of diluent (NDC 0024-0046-12).

Protect vials of AMIPAQUE from light.

References: 1. Grainger RG, Kendall BE, Wylie IG: Lumbar myelography with metrizamide—a new non-ionic contrast medium. *Br J Radiol* 49:996-1003, 1976. **2.** Peeters FLM: Myelography with metrizamide. *Radiol Clin* 46:203-213, 1977. **3.** Hindmarsh T: Myelography with the non-ionic water-soluble contrast medium metrizamide. *Acta Radiol [Diagn] (Stockh)* 16:417-435, 1975.

new AMIPAQUE® (metrizamide)

from the originators of the broad line of contrast media

Winthrop

Winthrop Laboratories
New York, N.Y. 10016

What the most demanding radiology departments in America can expect from the second largest film maker in the world.

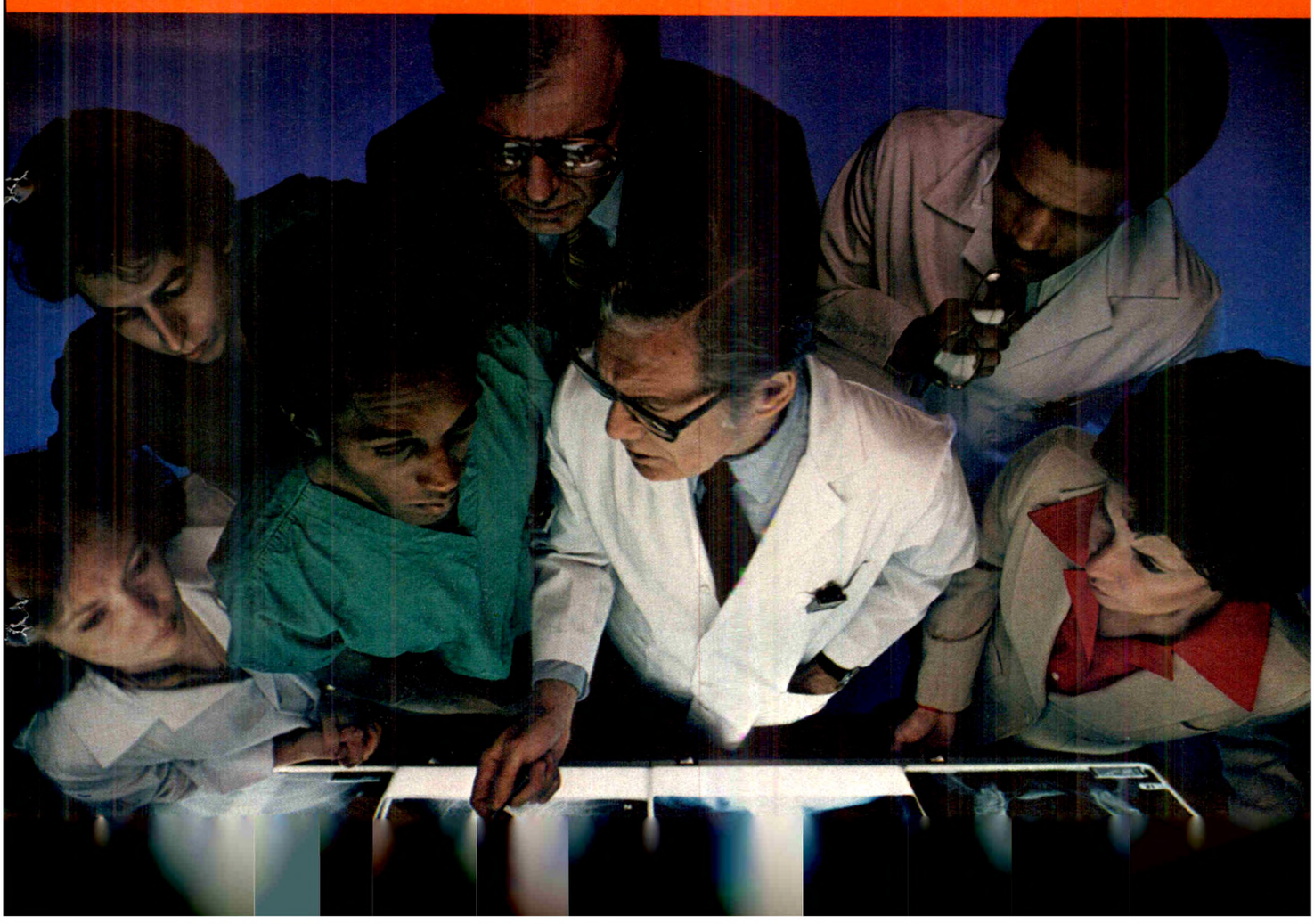

Image quality and service second to none.

A complete line of superior, sensitometrically dependable X-ray films.
All have the finest definition and image quality to help make precise diagnoses. And all offer appropriate speed for the desired technique. Whether it's general purpose radiology, or special procedures, such as cine-fluorography, angiography, or mammography, Agfa-Gevaert Rex has the film to meet your diagnostic needs.

An extensive line of blue-emitting rare earth screens.
Agfa-Gevaert Rex has a full line of rare earth screens that provide for virtually all possible film/screen combinations. Our screens permit reduced patient exposure and increased tube life . . . without sacrificing image quality.

Quality assurance and technical support.
To complement our products and services, Agfa-Gevaert Rex offers innovative support systems designed to save time and labor. Systems like CHEMALERT, our Automatic Processor Monitor and CHEMATIC II Automatic Solution Mixer have demonstrated ability to reduce operating cost and improve overall efficiency.

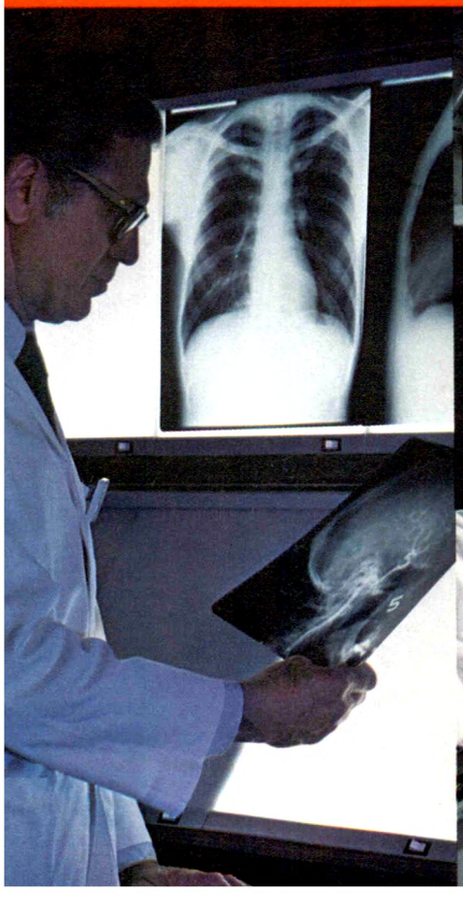

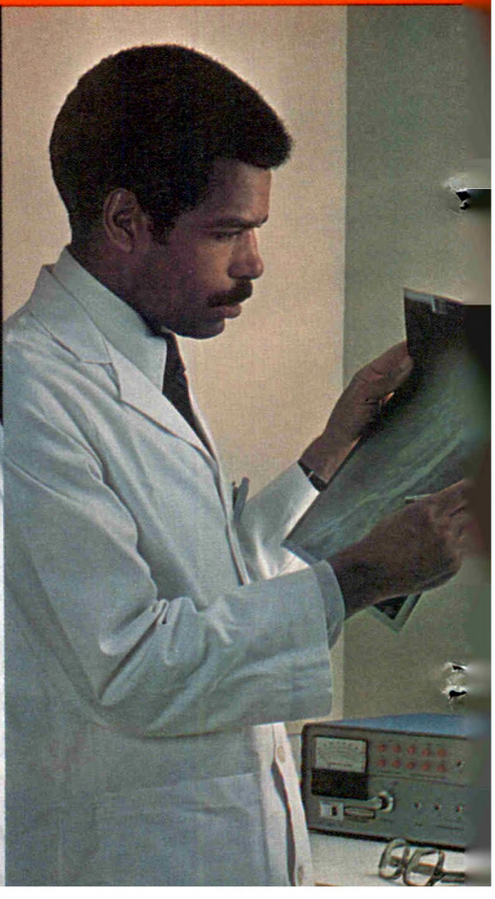

AGFA-GEVAERT REX INC.

A subsidiary of Agfa-Gevaert Group, the second largest film maker in the world. White Plains, N.Y. Tel. 914 682-5650

Quality with economy
Because Agfa-Gevaert is a prime manufacturer and world-wide distributor of base films and emulsions, our film selling price is very competitive. You get the same high quality images to which you are accustomed . . . at a very economical price.

A commitment to education.
In addition to sponsoring hospital training programs, Agfa-Gevaert Rex is opening new Technical Training Centers throughout the country. These Radiological and Technological Education Seminars provide hands-on experience with the latest equipment and imaging technology. You'll have the opportunity to see and hear recognized experts. And many of these seminars will be designed to meet requirements for accredited Continuing Education Programs.

Complementary services
Agfa-Gevaert Rex is committed to the concept that customer service starts with quality film. Experts in X-ray technique, processing, chemistry, and sensitometry, our technical representatives provide the support you need to achieve and maintain maximum efficiency in your department. Once our system is initiated, these specialists will provide the required service on a continuing basis.

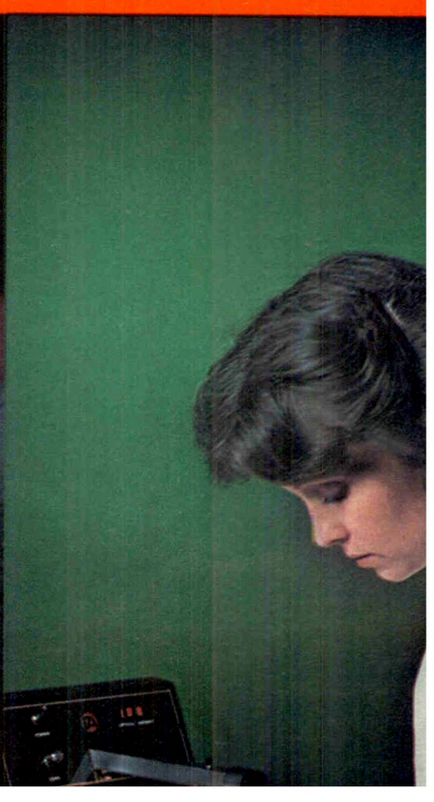

AN INTRODUCTION TO THE PHYSICS OF DIAGNOSTIC RADIOLOGY

SECOND EDITION

EDWARD E. CHRISTENSEN, M.D.
Professor of Radiology,
University of Texas Health Science
Center at Dallas and Parkland Memorial Hospital

THOMAS S. CURRY, III, M.D.
Professor of Radiology,
University of Texas Health Science
Center at Dallas and Parkland Memorial Hospital

JAMES E. DOWDEY, PH.D.
Associate Professor of Radiology
(Physics), University of Texas Health Science
Center at Dallas and Parkland Memorial Hospital

Extremely well written and easy to follow with carefully chosen illustrations, this new and up-dated Second Edition sets forth essential aspects of the physics of diagnostic radiology and incorporates recent advances in radiologic imaging.

The authors introduce the important equipment advances and changes which confront radiologists. New chapters dealing with xeroradiography, computed tomography, ultrasound and radiologic protection have been added to this edition. Chapters on magnification and cinefluorography have been greatly expanded and completely revised. Major updating has been done on chapters dealing with x-ray screens, x-ray film, the radiographic image, image intensifiers and television. Basic principles of diagnostic physics are explained in a non-mathematical manner that avoids technical language and highly theoretical concepts. Numerous illustrations are used to clarify and simplify explanations.

This book will be of value to radiology residents and radiologists both as a text and refresher. It has also proven its usefulness as a textbook for students in programs of radiologic technology. The major portion of the text and illustrations have been used for resident lectures, physics graduate student lectures, and radiologic technologist lectures at the University of Texas Health Science Center at Dallas.

428 pages (7 x 10), illustrated, $18.00

Published August, 1978, ISBN: 0-8121-0636-9, L.C. No. 78-5405

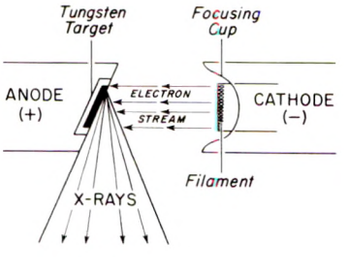

Figure 2-4. *Lateral view of the cathode and anode of a stationary anode x-ray tube*

Plan to visit Booth 3009
Radiological Society of North America
Chicago, Illinois, Nov. 26-30, 1978

LEA & FEBIGER
600 SOUTH WASHINGTON SQUARE, PHILADELPHIA, PA. 19106

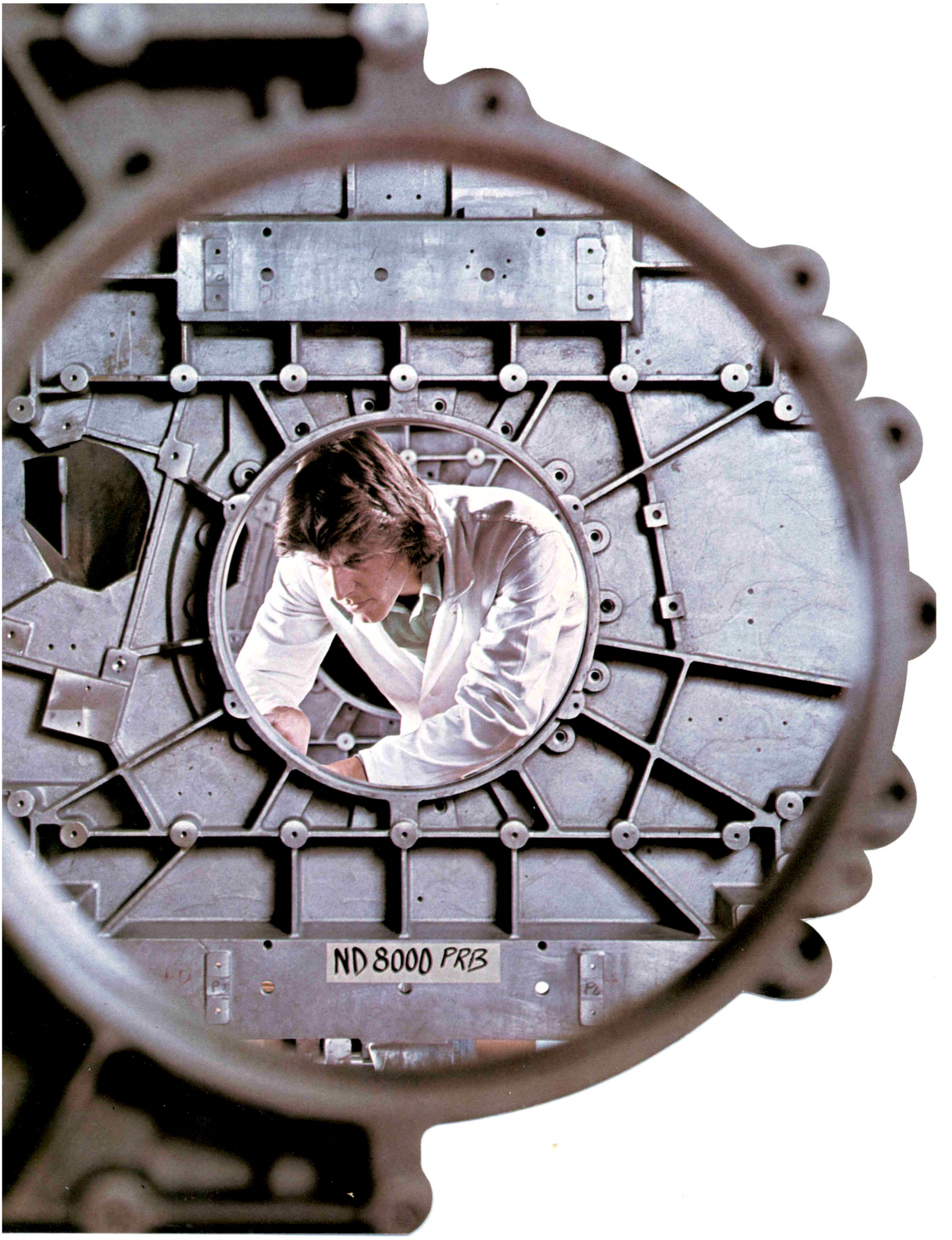
ND 8000 PRB

ND 8000

The gantry provides angulation of ± 30° for exact alignment of the x-ray beam with anatomical reference points. In addition, this motion is most useful for orientation of CT sections with patients who have cervical arthrosis.

The patient couch has a unique swivel motion providing precise adjustment of symmetrical transverse sections. Two structures, such as the optic nerves, can be optimumly visualized in the same scan without difficulty.

Scanners are not universal. And this is a critical factor in neuroradiology. Neuroradiology requires a scanner that's specific to its diagnostic requirements.

CGR ND 8000 is this scanner.

The ND 8000 has unique technology for cranial examinations. A special geometry for the x-ray beam. Specific collimation as well as filtration. And an adapted selective reconstruction program.

The new system is excellent for standard diagnostic procedures and particularly advantageous in trauma cases and pediatric examinations. The ND 8000 facilitates easy definition and excellent scan symmetry.

Examination times are short with immediate data acquisition. To eliminate artifacts. And improve results.

The CGR ND 8000. Significantly advancing the state-of-the-art in computerized tomography of the head.

Call your CGR representative for details

Large fronto-parietal tumor pushing back the right lateral ventricle.

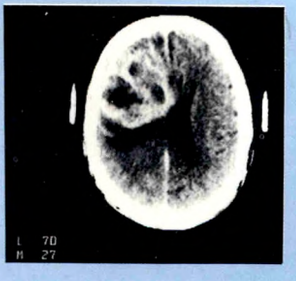

ND 8000

striving for excellence

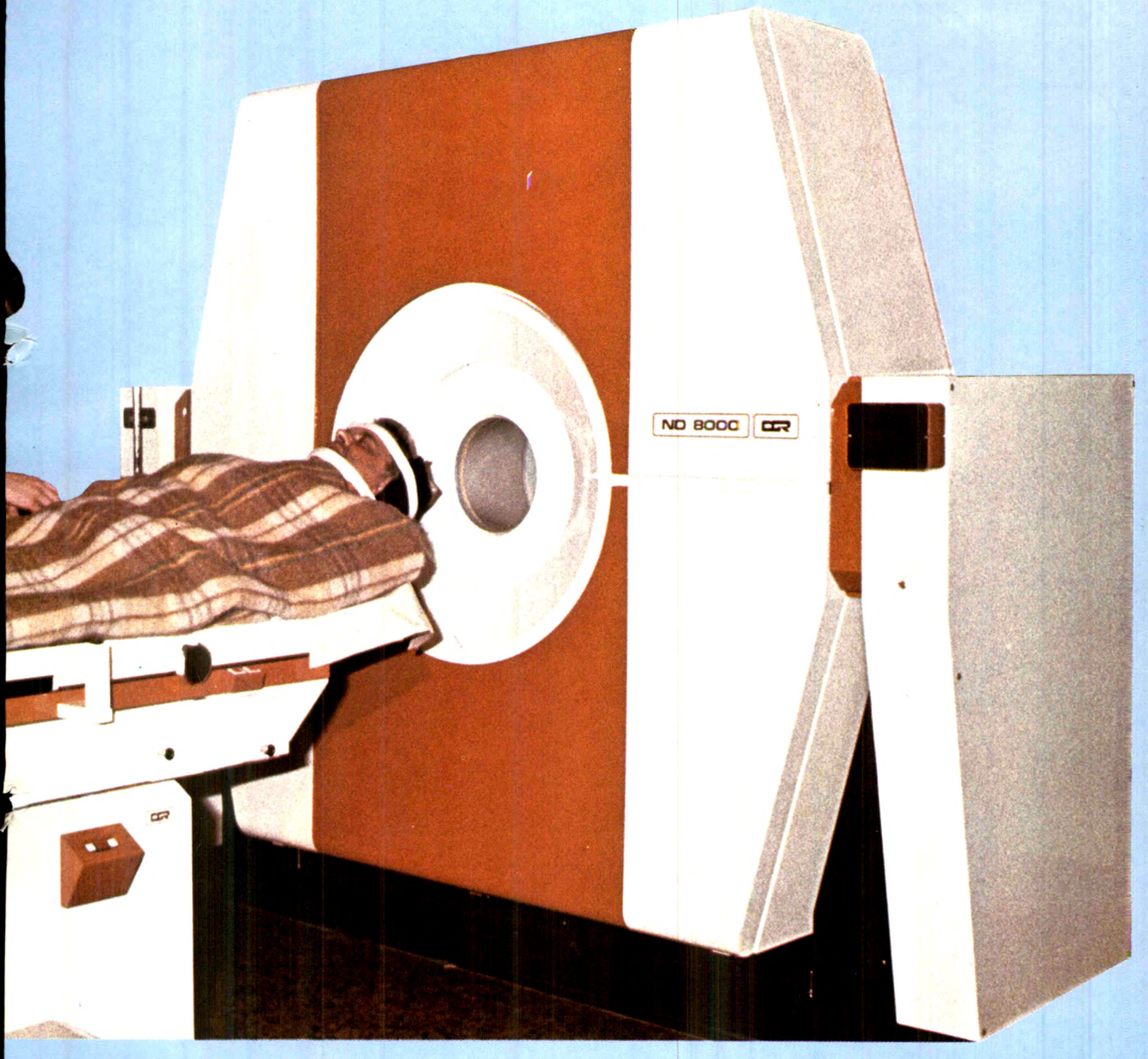

ND 8000

pride of

ND 8000

to see and to interpret

The recording of outstanding data is a necessity but their interpretation and manipulation are still more mandatory.

ND 8000 offers several visualization desks depending upon the kind of data acquisitions and their interpretation.

Without altering the recorded data, a thorough study of the visualized scan is made easier thanks to :

- The integrated microprocessor.
- The independent function of the diagnostic desk.
- An automatic selection of the image processing.
- The easy and immediate measurement.
- The color display of scans to enhance the image visualization.
- The easy reproducibility of all data.

MIDWINTER RADIOLOGICAL CONFERENCE

SPRING ULTRASOUND CONFERENCE

The Continuing Education Committee of the Los Angeles Radiological Society is proud to announce the ***Thirty-First Annual Midwinter Radiological Conference for 1979.*** An outstanding faculty has been invited to speak in Diagnostic and Therapeutic Radiology, Nuclear Medicine, Ultrasound and Computerized Axial Tomography.

The first day will consist of small workshops in all disciplines. The next two days will consist of formal lectures and round-table discussions. A Saturday evening dinner dance is again scheduled. The second largest Radiological Technical Exhibit in the country will be open for viewing on all three days.

The optional 11 days Fifth Annual post conference seminar will be held in New Zealand, Australia and Fiji.

THE THIRTY-FIRST ANNUAL MIDWINTER RADIOLOGICAL CONFERENCE

SPONSOR: The Los Angeles Radiological Society
DATE: January 26, 27, and 28, 1979
LOCATION: Century Plaza Hotel, Los Angeles
California 90067

SPEAKERS:

DIAGNOSTIC RADIOLOGY
- Sidney Wallace, M.D. ..... *M.D. Anderson Hospital, Houston*
- Morton A. Meyers, M.D. ..... *State University, Stonybrook, N.Y.*
- William Martel, M.D. ..... *University of Michigan Medical Center*
- David G. Bragg, M.D. ..... *University of Utah Medical Center*
- R. Thomas Bergeron, M.D. ..... *New York University Medical Center*
- Thomas F. Meaney, M.D. ..... *Cleveland Clinic Foundation*

NUCLEAR MEDICINE
- Paul B. Hoffer, M.D. ..... *Yale University School of Medicine*

ULTRASOUND
- George R. Leopold, M.D. ..... *University of California, San Diego*

RADIATION THERAPY-ONCOLOGY
- Charles G. Moertel, M.D. ..... *Mayo Clinic*
- Oliver H. Beahrs, M.D. ..... *Mayo Clinic*
- Theodore L. Phillips, M.D. ..... *University of California, San Francisco*
- Leonard L. Gunderson, M.D. ..... *Harvard Medical School*
  ..... *Massachusetts General Hospital*
- Robert B. Livingston, M.D. ..... *Veterans Hospital, San Antonio*
- H. J. G. Bloom, M.D. ..... *Royal Marsden Hospital, London, England*

REGISTRATION: Fee of $125.00 includes two luncheons. $75.00 for residents. Workshops: $25.00 each.

ADVANCE REGISTRATION: Earl P. Detrick, M.D.
4415 Lakeview Canyon Road,
Westlake Village, California 91361

HOTEL ACCOMMODATIONS: Convention Manager
Century Plaza Hotel
Los Angeles, California 90067

MESSAGE CENTER: Century Plaza Hotel
(213) 277-2000

NEW ZEALAND, AUSTRALIA, FIJI POST CONVENTION SEMINAR:

January 28 through February 10, 1970. $1375.00 per person includes air fare from Los Angeles, transportation between sites and accommodations. There will be a $195.00 tuition fee for each registrant. This is accredited for 32 hours of Category 1 credit.

FACULTY:
- R. Thomas Bergeron, M.D. ..... *New York University Medical Center*
- William Martel, M.D. ..... *University of Michigan Medical Center*
- Thomas F. Meaney, M.D. ..... *Cleveland Clinic Foundation*
- A. Franklin Turner, M.D. ..... *Arcadia Medical Group, Arcadia, Calif.*
- G. Kossoff ..... *Director-Ultrasound Institute, Sidney, Australia*

No reservations can be accepted after November 15th.

Tech-Mobile: new concepts

Designing a mobile, battery-operated X-ray unit that would be significantly better than any other unit presently available was our goal. We succeeded with Tech-Mobile.

From its simplified controls to its recessed wheels, the sturdy Tech-Mobile was created to give easy maneuverability, reliable operation and consistent high-quality radiographs.

Pushing, pulling and tugging are a thing of the past. Variable-speed, hand-grip controls let you maneuver easily on tile, carpeting or almost anywhere. Simply drive the cordless Tech-Mobile to the patient's bedside. And if Tech-Mobile's safety bumper contacts a door, wall or any other stationary object when traveling forward, it stops immediately and gently reverses to disengage the object. You'll never be stuck in a corner.

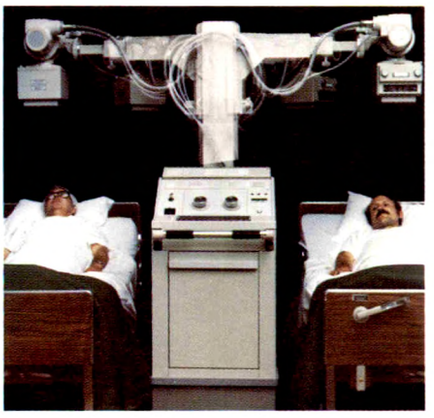

And because Tech-Mobile is only 23 inches (590 mm) wide, it fits easily between beds, doorways and crowded corridors.

Powered completely by a strong nickel-cadmium battery pack, the Tech-Mobile has a 12,000 mAs exposure capacity on hand for a full day's caseload. Then, a standard electrical outlet is all that's needed to recharge the unit to full capacity in a matter of hours.

Minimal effort is required to position the unit. Setting exposure parameters and making the exposure are simplified. And the battery-

in cordless radiography.

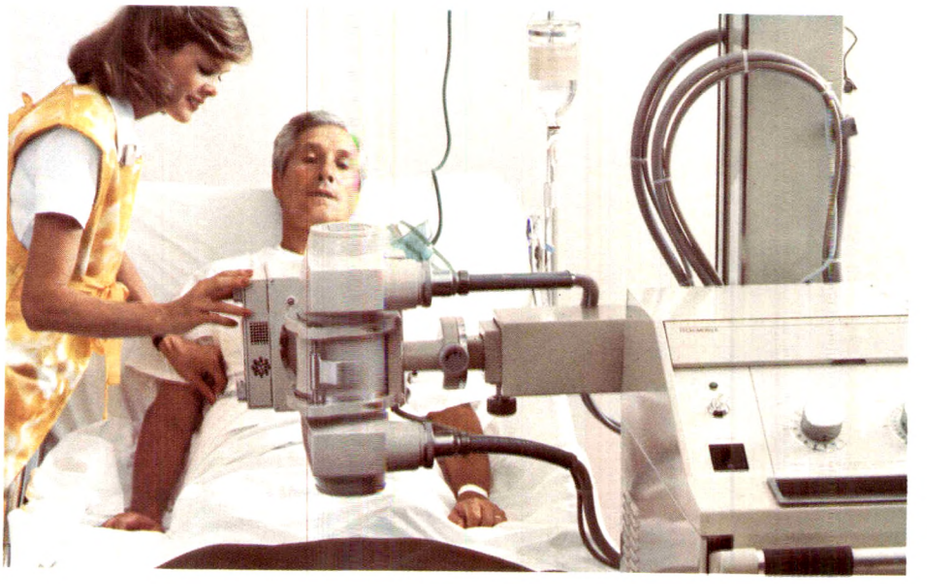

operated Tech-Mobile has no cord or grounding wire, simplifying its use in CCU and ICU. This means spending less time in preparing each procedure.

We even included some convenient extras: an accessory tray to store film markers, a requisition clip, remote collimator field light switch, a large fold-out exposure guide and a convenient apron hook.

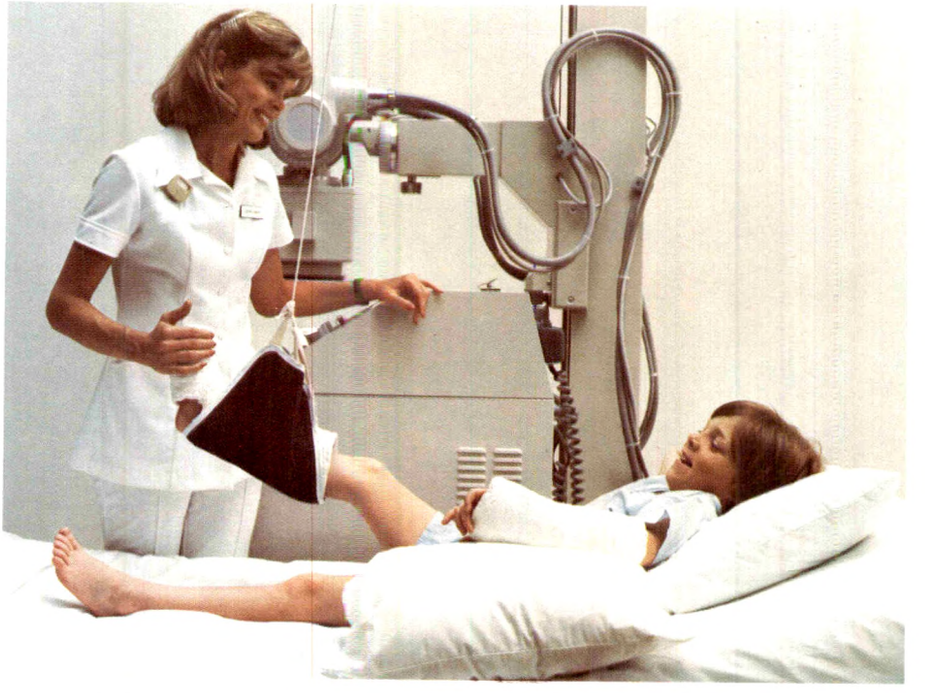

Tech-Mobile is backed by our worldwide service organization. And it can be leased, if you wish, with assistance from our parent, CIT Financial Corporation. For more information about the newest concepts in mobile radiography, contact your local Picker representative, or write Picker Corporation or Picker International, 595 Miner Road, Cleveland, OH 44143.

PICKER®
ONE OF THE CIT COMPANIES

Hanley Space Saver X-Ray and Medical Record Cabinets are installed in most hospitals in America.

Top quality and low price is the reason. It's #1. Regular 5 compartment with doors or open 19½ x 32 x 83. Deluxe Oversize 5 High 23 ¾ x 32 x 88. F.O.B. Factory. **In X-Ray rooms it's the oversize.** Extra depth means easier filing.

AMERICA'S LARGEST DISTRIBUTOR OF X-RAY CABINETS.

HANLEY MEDICAL EQUIPMENT CO.
5614 South Grand X-Ray Division St. Louis, Mo. 63111
Phone 314-351-3359

In reply to advertisers
please mention that you saw
their advertisement in

THE
AMERICAN JOURNAL OF
ROENTGENOLOGY

published monthly for
The American
Roentgen Ray Society
by
CHARLES C THOMAS • PUBLISHER
Springfield, Illinois 62717

CHARLES C THOMAS • PUBLISHER

BONE TUMORS

• **General Aspects and Data on 6,221 Cases** •

Third Edition

By **David C. Dahlin,** *Mayo Clinic, Rochester, Minnesota.* The expanded and updated Third Edition of this respected treatise provides a valuable repository of information. New features for this edition include chapters on benign and malignant histiocytomas; descriptions and illustrations of recognizable types of osteosarcomas and chondrosarcoma; and several novel examples of bone tumor simulators. Throughout the text Doctor Dahlin stresses the importance of accurate roentgenologic interpretation in the assessment of malignant and benign tumors. This emphasis is underscored by the use of numerous illustrations.

A sampling of chapters includes those on osteochondroma, benign osteoblastoma, benign vascular tumors, myeloma, malignant lymphoma of bone, Ewing's tumors, chordoma, and hemangioendothelioma. A special chapter is presented on conditions that commonly simulate primary neoplasms of bone, and include data on fibrous dysplasias, giant cell reparative granulomas, Paget's disease, and many other conditions.

This volume is well on its way to becoming a classic in its field. This new edition continues to provide pathologists and clinicians in radiology, orthopedics and surgery with an unsurpassed review of bone tumor diagnosis and treatment. *'78, 464 pp. (8 1/2 x 11), 740 il., 7 tables, $32.75*

Orders with remittance sent, on approval, postpaid

301-327 East Lawrence Avenue • Springfield • Illinois • 62717

JOIN THE AIR FORCE, PRACTICE AT HOME.

The Air Force has a new Hometown Assignment Program for physicians. If you have the right specialty and if you live in or near a city where an Air Force hospital is located, you could qualify.

You would receive a direct commission, possibly as high as Lt. Colonel, and all the benefits of an Air Force Officer. At the same time you could maintain your present home. Your children could stay in the same schools. You could even take a paid vacation—4 weeks a year!

Here's what you would *lose.*

You wouldn't have to pay malpractice insurance. "Boss" an office staff. Or worry about the thousands of details a small businessman has to deal with.

You could concentrate on practicing medicine.

Get all the details. Talk to your Air Force Recruiter. Or mail in this coupon.

It's a great way of life!
AIR FORCE

Medical Professional Opportunities CJR118
Box 1776, Valley Forge, PA 19481

I would like more information about training and career opportunities in the Air Force Medical Service. I understand there is no obligation.

Name_____ Sex ☐ M ☐ F

Address_____ Apt. #_____

City_____

State_____ Zip_____

Phone_____ Birth Date_____

School_____

Yr. of Degree_____ Specialty_____

THIS BOOK TELLS A LOT ABOUT US ...WITHOUT ONCE MENTIONING OUR NAME

OR OUR PRODUCTS

The name of this volume is *Certificate of Need: An Expanding Regulatory Concept.* Not once in its 944 pages does the name Pfizer appear.

Yet, despite this, we are proud to offer this book to several hundred people in the health care field, with our compliments, as part of an important, new Pfizer program called the Certificate of Need Assistance Program.

A Total C.O.N. Assistance Program

Pfizer's C.O.N. Assistance Program is designed to aid you in the increasingly regulated climate in which medicine now operates. As one of the health care industry's leaders for 129 years, Pfizer feels a responsibility not only to provide quality products but also to join the medical community in its current search for effective ways to comply with these regulations. Typical of these requirements is the Certificate of Need, or C.O.N., which is required in most cases where federal funding is involved in paying for major equipment or plant expansion.

Toll-free C.O.N. Assistance Service

Applying for the C.O.N. can be a complicated process—sometimes confusing, always time-consuming. The Pfizer C.O.N. Assistance Program can help. The two main components of this program are the book, *Certificate of Need: An Expanding Regulatory Concept,* and the toll-free C.O.N. Telephone Service to answer questions about the cost effectiveness of diagnostic equipment, as well as how this information relates to C.O.N. requirements.

To use our C.O.N. Telephone Service just phone 800-221-4688, from 9 a.m.-5 p.m. Monday through Friday. (In New York State, please call 212-573-2030, collect.)

Complimentary Books to Administrators and Radiologists

Many hospital administrators have already received copies of the book. We have also offered it to chief radiologists throughout the country and to certain other medical and administrative personnel who are involved in the purchase of diagnostic equipment.

(Incidentally, if you have not personally received *Certificate of Need: An Expanding Regulatory Concept,* and you take part in major purchasing as a hospital executive or radiologist, you are welcome to a complimentary copy. To receive it, just send us your request on your official letterhead.)

The book, as its title suggests, is a comprehensive, state-by-state compilation of current C.O.N. requirements. We feel that it makes a substantial contribution to understanding this very complex subject. And it is a subject in which we feel a special responsibility, since CT Scanners usually require this document.

Full Range of Pfizer Radiological Services

Now that we have told you how we're making it easier for you to meet the regulatory requirements for buying diagnostic equipment, we'd like to tell you why you should want to.

There's an expert specially qualified to do just that: the Pfizer Medical Systems or Radiologic Sciences Technical Representative.

He'll give you useful, specific information on the one subject that isn't included in the C.O.N. Assistance Program.

Our Products.

Pfizer Inc.
235 East 42nd St.
New York, N.Y. 10017

Advancing the Science of Therapeutics and Diagnostics.

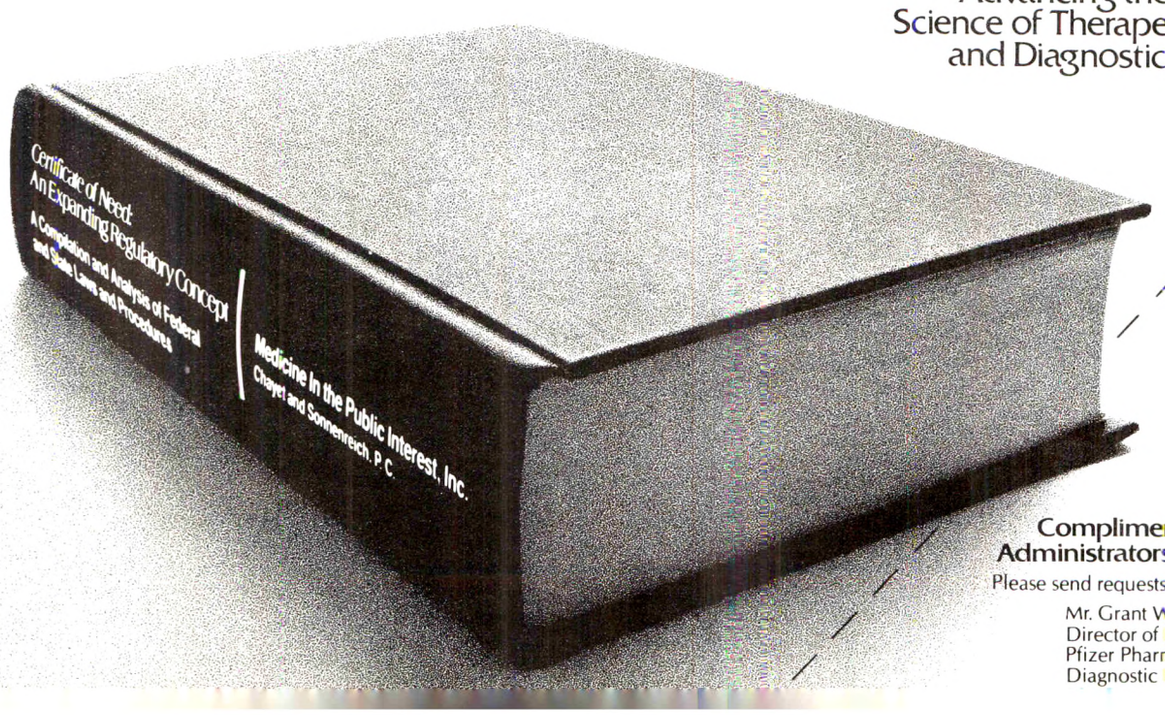

Complimentary books to Administrators and Radiologists.

Please send requests on official letterheads to:

Mr. Grant W. Denison, Jr.
Director of Planning
Pfizer Pharmaceuticals and
Diagnostic Products

SIEMENS

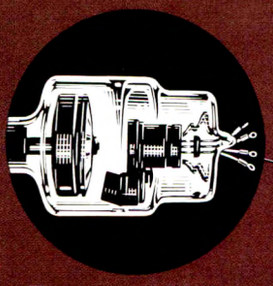

The custom application OPTI-150 CT X-ray tube permits continuous patient scanning at a rate of up to 125 scans/hour.

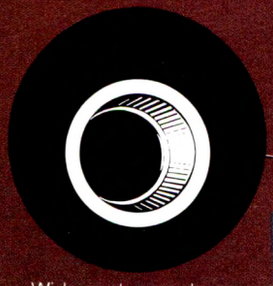

Wide gantry aperture and scan field (both 54 cm. in diameter) facilitate patient handling and positioning.

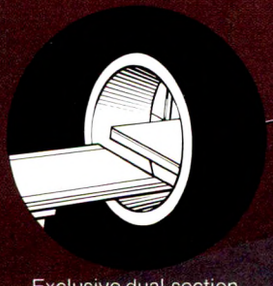

Exclusive dual-section, flat-top table system with motorized patient conveyor.

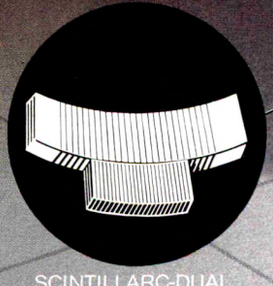

SCINTILLARC-DUAL detector system provides maximized detector utilization with optimized clinical results.

The only CT scanners with instantaneous image reconstruction

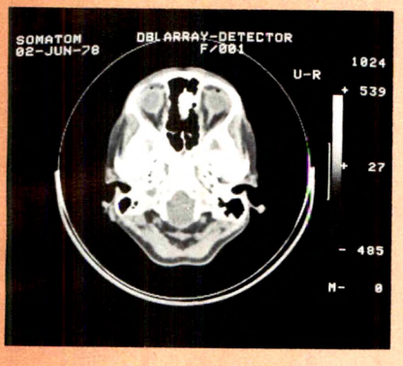

Instantaneous image reconstruction makes the SOMATOM (whole body scanner) and the SIRETOM (head/neck scanner) the most sophisticated computed tomographic systems available today. Upon completion of each scan, the image is immediately available for clinical evaluation. The SOMATOM offers selectable scan times of four and eight seconds while the SIRETOM scan time options are 60, 120, and 180 seconds.

The EVALUSKOP, an independent evaluation console, extends the capability for CT image manipulation and analysis. Programmable and available at the push of a button are window variation, multiple region of interest selection, distance and angle measurement, histogram, magnification, saggital/coronal reconstruction, multiple tomogram displays, tomogram addition and subtraction, and filter manipulation.

Siemens' full line of computed tomographic equipment is designed to fulfill the exacting requirements of CT application. Behind each system definition—X-ray tubes, tables, generators, radiation measurement, and signal processing—is more than 100 years of engineering excellence.

Siemens' world-wide reputation for product support and service is unsurpassed. In the United States alone, Siemens has a technical staff of over 500 trained professionals ready to serve you—should the need arise.

For further information

Please contact your local Siemens Representative or Siemens Corporation, Medical Systems Division, 186 Wood Avenue South, Iselin, New Jersey (201) 494-1000.
In Canada: Siemens Canada Limited, P.O. Box 7300, Pointe Claire 730-P.Q.

Concepts... engineered to radiologic excellence

SIR-408

A New Study Confirms...

THE RSI MAMMOGRAPHIC SYSTEM **INCREASES DIAGNOSTIC ACCURACY**

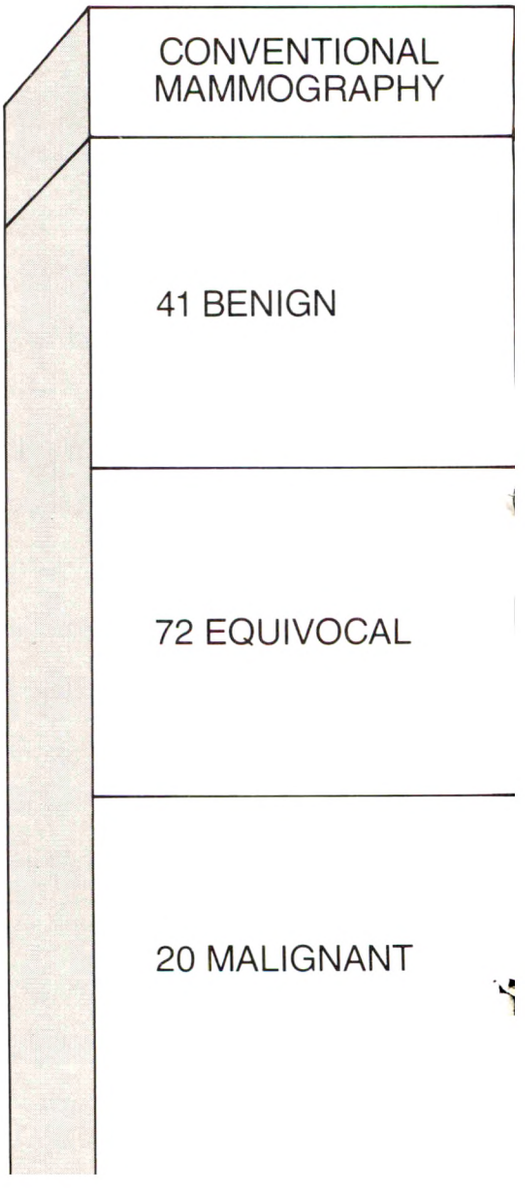

Take a good look at the chart. You'll see the remarkable results of a study published by Dr. Edward A. Sickles, making a clinical comparison of 133 patients who received both conventional mammography and RSI Magnification Mammography. The results were confirmed with pathological diagnosis.*

This new study confirms just how accurate RSI Mammography really is. In fact, Dr. Sickles wrote in 1977, that magnification mammograms are "...clearly superior both quantitatively and qualitatively to conventional contact mammograms."[1]

Diagnostic Accuracy in Mammographic Examinations[2]
Clinical Data of Edward A. Sickles, M.D.
Assistant Professor of Radiology, University of California, San Francisco
Clinical Comparison of 133 Cases

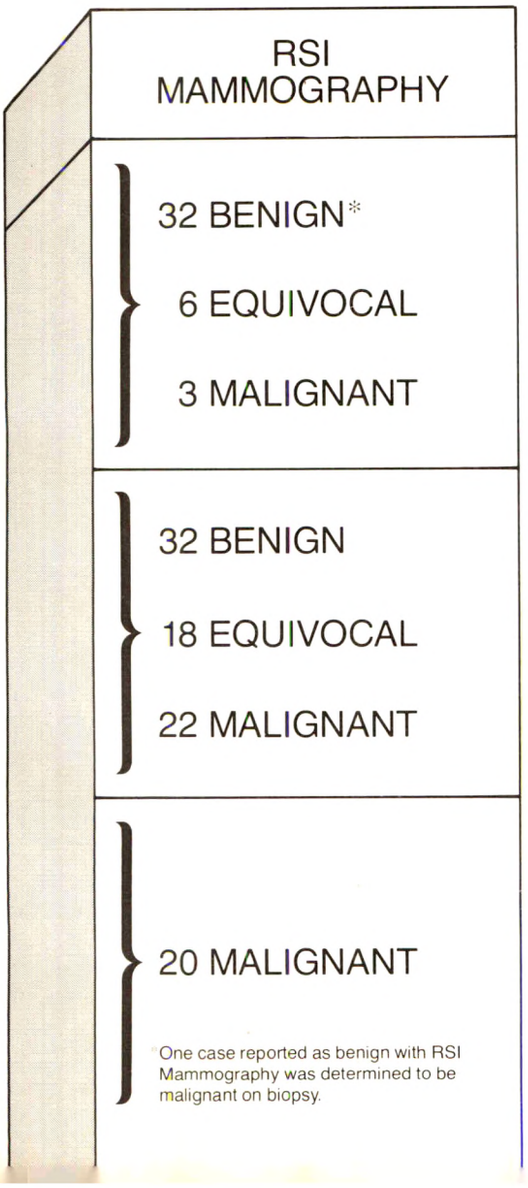

Out of 41 cases diagnosed as benign with conventional mammography, RSI Mammography determined that 3 of these cases were, in fact, malignant. In addition, with conventional mammography alone, 72 cases were diagnosed as equivocal and direct magnification mammography (RSI System) was able to differentiate these as: 22 malignant, 32 benign, and only 18 remained equivocal. This revealing clinical comparison clearly shows that RSI Magnification Mammography increases the certainty in diagnosis, decreases the time between examination and confirmation, and may even reduce the need for biopsy.

In a radiologic symposium presented in New York City, Dr. Sickles remarked, "...in dealing with difficult cases, we considerably improved our diagnostic accuracy [with RSI Magnification Mammography]."[2]

These more accurate diagnoses are the direct result of the capability of the RSI Mammography's System to give you—

- Clearer definition of mass borders
- Improved image sharpness and resolution
- Resolution of malignant microcalcifications often not discernible by conventional mammography
- Delineation of trabecular patterns

The RSI Mammography System offers high-detail resolution in the magnification mode as well as the conventional contact mode. The superior image which results from the exceptionally uniform focal spot provides a new level of confidence in the detection of breast cancer.

For more detailed information on the RSI Mammographic System and a reprint of the study published by Sickles *et al* in 1977, please write or call, Radiologic Sciences Inc., a subsidiary of Pfizer Inc., 235 East 42nd St., New York, N.Y. 10017 (212) 573-7941.

References: 1. Sickles, E.A.; Doi, K.; Genant, H.K.: *Radiology* 125:69-76, October 1977. **2.** Sickles, E.A.: *Microfocal Spot Magnification Mammography.* Presented at a Symposium, New York City, June 1, 1978.

THE RSI MAMMOGRAPHIC SYSTEM

INCREASES DIAGNOSTIC ACCURACY

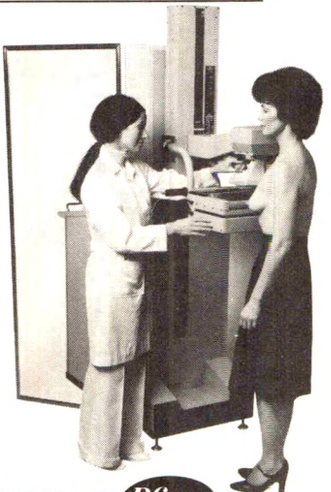

RADIOLOGIC SCIENCES INC. Pfizer
A subsidiary of Pfizer Inc., New York, N.Y. 10017

SIEMENS

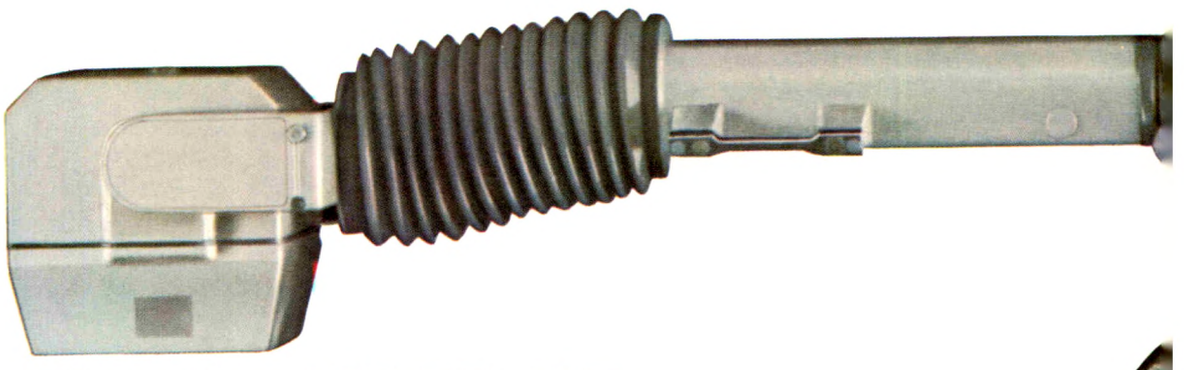

Introducing the MOBIL XR: A revolutionary concept in X-ray systems

Siemens has taken the concept of mobile X-ray systems and redesigned it from top to bottom. The result is total freedom of positioning, exceptional maneuverability, and ease of operation seen only in the MOBIL XR.

Only the MOBIL XR simplifies positioning.
Its innovative flexible extender arm provides a height and distance capability over and above any other mobile X-ray system. Without moving the unit from the foot of the patient's bed, the operator can easily maneuver the X-ray tube housing into any position, including lateral. Typically, at a bed height of 32 inches, the MOBIL XR will allow a 60-inch source-image distance. No other mobile unit can offer this capability.

Only the MOBIL XR has complete computerized organ programming.
By simply activating the push-button controls, the operator can select specific organ programs, reprogram the unit for specialized application techniques, or switch to manual settings. And for functional security, a digital readout displays the Kv, mAs, and battery condition of the unit.

Only the MOBIL XR has a custom-designed cassette tunnel.
It establishes and maintains the proper perpendicular relationship between X-ray tube and film cassette to provide optimum geometric positioning accuracy.

Only the MOBIL XR is easy to clean and keep aseptic.
That's because its design is free of corners, ridges, and hidden surfaces. Bacteria has no place to hide on the smooth fiberglass body of the MOBIL XR.

The Siemens family of mobile X-ray units extends beyond the MOBIL XR to include the KONDIAMOBIL 125 and the SIREMOBIL 2U. All are products of the quality engineering that reflect Siemens' standard of excellence in the field of radiological equipment.

For further information, please contact your local Siemens Representative or Siemens Corporation, Medical Systems Division, 186 Wood Avenue South, Iselin, New Jersey (201) 494-1000. In Canada: Siemens Canada Limited, P.O. Box 7300, Pointe Claire 730-P.Q.

SIR-409

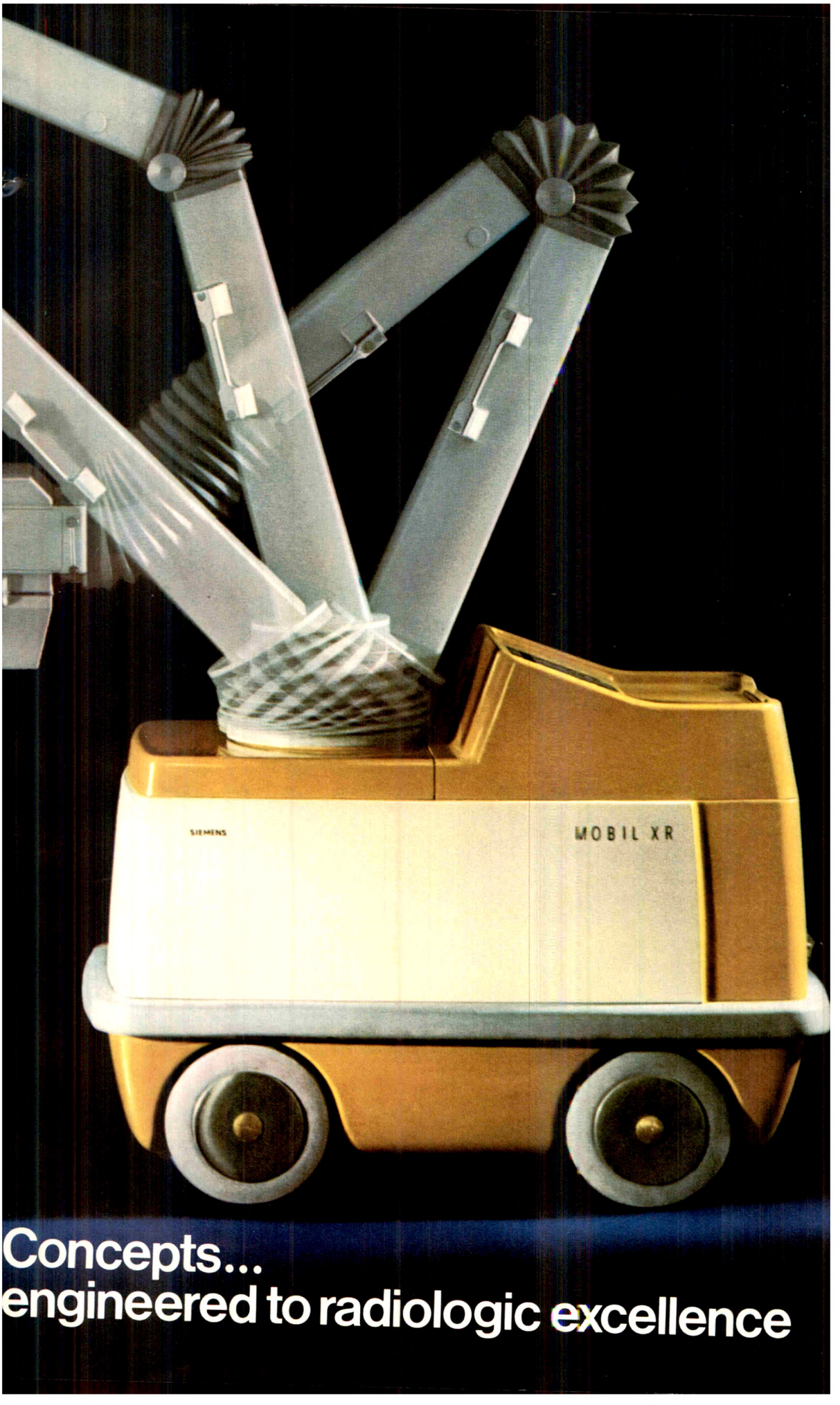

Concepts...
engineered to radiologic excellence

AJR Index to Advertisers

(In Order of Appearance)

Guerbet Laboratory
Sybron/Liebel-Flarsheim
Pyne X-Ray Corporation
The Purdue-Frederick Company
GAF Corporation
E-Z-EM Company
Pfizer Medical Systems
Eastman Kodak Company
Gordon Projectors
G. D. Searle and Company
S and S X-Ray
Atomic Energy of Canada
AMRAD, a Raytheon Company
Dunn Instruments, Inc.
Raytheon Medical Imaging
Eastman Kodak Company
E. R. Squibb and Sons, Inc.
Institute of Continuing Education

• • •

Philips Medical Systems
Ortho Pharmaceutical Corporation
CGR Medical Corporation
Machlett Laboratories
H. G. Fischer, Inc.
Charles C Thomas • Publisher
E-Z-EM Company
General Electric Company
Diagnostic Information
Harvard University Press
Picker Corporation
Winthrop Laboratories
Agfa-Gevaert Rex, Inc.
Lea and Febiger
Philips Medical Systems
Los Angeles Radiological Society
CGR Medical Corporation (Paris)
Picker Corporation
Hanley Medical Equipment Company
Charles C Thomas • Publisher
United States Air Force
Pfizer, Inc.
Seimens Corporation
Radiologic Sciences
Seimens Corporation
E. I. Dupont de Nemours & Company, Inc.
Charles C Thomas • Publisher
General Electric Company
C. V. Mosby Company
Xerox Corporation

CHARLES C THOMAS • PUBLISHER

ANATOMICAL EXERCISES IN COMPUTERIZED TOMOGRAPHY BODY SCANNING

By **Fred C. Shipps,** *Good Samaritan Hospital and Medical Center, Portland, Oregon.* This text is composed of a series of exercises which cover organ systems and areas of interest in current computerized tomography (C.T.) body scanning. As the reader progresses through the various systems, the interrelationship of structures is reinforced.

Included are chapters on:

- *Lungs, Fleura, and Mediastinum*
- *Pancreas*
- *Liver and Biliary Tract*
- *Aorta, Superior Mesenteric Artery, Inferior Vena Cava, and Adrenals*
- *Kidneys and Ureters*
- *Lumber Lymphatics, Thoracic Duct, and Azygos Veins*
- *Pelvis*

In order to offer these scans — all produced by the EMI-tronics 5000 prototype machine presenting a 160 x 160 matrix — in an unadulterated form for study, many images are provided with the labels on transparent overlays. The removal of the overlay will also afford the student an opportunity to review and test his/her ability to recognize the different structures. Color-coded sketches appearing beside many of the scans will aid in the recognition of both the location and the shape of a structure.

The final two sections are comprised of an exercise quiz and an index. The quiz section presents provocative questions to the reader about a series of normal and abnormal scans. Some questions are intentionally misleading and require careful consideration. The author's interpretation appears on the following page. The index, which lists the anatomical and pathological structures covered in the text, offers a quick method of finding those scans that demonstrate a specific structure. *'78, 70 pp. (8 1/2 x 11), 186 il. (63 in color), $22.75, spiral (paper)*

ATLAS OF BRAIN ANATOMY FOR C.T. SCANS
Using EMI Terminology
Second Edition

Prepared by **Fred C. Shipps, J. McAndrew Jones** *and* **Anthony D'Agostino,** *all of Good Samaritan Hospital and Medical Center, Portland, Oregon.* The Second Edition of this atlas surpasses the usefulness even of its predecessor as a reference in computerized tomography and as an instructive tool. The text continues to offer a rapid and convenient review of cross-sectional anatomy of the brain as found on C.T. scans, but it has been greatly expanded with several new chapters and greater precision and clarity in retained material. New chapters are included on the identification of common artifacts; on window width, window level and mu; transferring C.T. findings to the lateral skull film; and on a method of clinicopathological correlations. A section on skull anatomy using the EMItronic Model 5000 Scanner is also presented. The unique self-teaching feature of the original edition, the overlay format, has been retained. No one involved in radiology or neurology will want to overlook this most useful volume. *'77, 60 pp. (8 1/2 x 11), 82 il., $16.75, spiral (paper)*

Orders with remittance sent, on approval, postpaid

301-327 EAST LAWRENCE
SPRINGFIELD • ILLINOIS • 62717

For years we've made it our business to help hospitals control image quality, contain costs and improve patient care. The results speak for themselves.

Imaging Management

DUPONT

REG. U.S. PAT. & TM. OFF.

Imaging Management gets results: Better image quality. Tighter cost containment. Improved patient care.

Supplier involvement with hospital radiology departments probably doesn't sound like a terribly novel idea today, but before 1970 it was. That was when DuPont initiated an in-depth Quality Control Program for hospitals. DuPont led the way then, and today DuPont still sets the pace in quality assurance.

Over the years, DuPont's involvement with its customers has grown beyond the original Quality Control Program. This involvement now includes a range of training and consultation services in all areas of radiology management. For the most part, these newer programs have been aimed at improving cost containment and patient care, which have joined image quality as key department goals.

Today, DuPont can offer the hospital radiology department a selection of imaging services unmatched in depth and variety. The challenge now is to apply these programs and services so that they meet the unique needs of each individual department and produce the specific results that the profession demands.

Imaging Management meets today's needs.

Imaging Management is DuPont's answer to this "challenge to produce results." It is a proven process of selecting, implementing and monitoring those radiology programs that will achieve specific departmental goals rapidly and effectively.

Imaging Management follows an orderly procedure of needs analysis, objective setting and program selection, to produce an action plan that is unique for each radiology site. It provides guidelines and assistance during implementation of the plan and concludes with a quantitative measurement of program results. The entire process is conducted as a "team effort" between the radiology department and DuPont, using the best resources of both.

The whole point: To put you in control.

The Imaging Management Concept recognizes the interrelationship of people, products and services in effective radiology administration. It acknowledges the importance of managing these three variables to achieve specific depart-

mental goals. The whole point is to put you in control of your image quality, costs and patient care, and that's exactly what happens.

Imaging Management not only promises better quality and lower costs; it can also result in a more efficient staff, a more efficient department layout and more efficient administrative procedures.

For the patient, it can mean faster exams, less waiting time and lower X-ray dosage.

The results speak.

Imaging Management principles and techniques have produced results like these at hospitals across the country.

Boston City Hospital saved $7,500 in film costs by reducing repeats 18% and minimizing film spoilage. Radiograph quality and department efficiency improved, too.

St. Luke's Hospital Center in New York City reduced their repeat rate from 10% to 4% and realized a noticeable improvement in department efficiency.

Temple University Hospital in Philadelphia saved over $4,000 a month with improved inventory control and fewer repeats.

Baptist Hospital in Miami cut radiation dosage in half in 90% of their general procedure exams.

Our customers can tell you about dozens of similar successes.

It starts with the use of quality Imaging Products.

The key to effective Imaging Management is quality: Quality of objectives, quality of programs, quality of results. Equally important is quality of products.

DuPont has the widest choice of quality film/screen combinations available for any diagnostic procedure.

Among our more recent innovations: A new line of Medical Recording Films for computed tomography, ultrasound and nuclear medicine; three new film/screen/cassette combinations especially developed for imaging extremities; a new high-capacity processor and chemical mixer.

And, of course, there's the original DuPont Daylight Film Handling System, which makes it possible to do all film

handling, even the processing, in room light. This important development allows you to use satellite units, including computed tomography, ultrasound and nuclear medicine, that are not tied to the darkroom. Technologists can virtually take the X-ray department to the patient, thereby improving patient care.

These and many other quality consumable and equipment products form the foundation for our long-term involvement with hospitals.

People and services wrap it up.

DuPont Technical Representatives are trained to be responsive to radiology departments' needs, to search out ways to help control costs, improve image quality and patient care. To meet these needs, they call on the finest and most complete resource package in the industry... DuPont's series of Imaging Services, including Quality Control, Computerized Cost Analysis, Training in Budget Administration and Management Principles, Layout Assistance, Resident and Student Education, and a full range of technical programs. Working with your radiology team, our Technical Representatives can help develop managerial and technical skills to new levels of proficiency.

DuPont's new Seminar on Imaging Management offers in-depth training.

Radiology department administrators and their assistants, chief technologists, QC coordinators and other hospital personnel are invited to participate in DuPont's new seminar on Imaging Management, to be held at key locations around the country in the months ahead. The seminar will be conducted in half-day segments or as a week-long training program; you can choose the format that best fits your schedule.

For full information, get to know your DuPont Technical Representative.

Your DuPont "TR" is the direct link to Imaging Management. Let him help you develop and implement a management system that will meet the unique needs of your department to control image quality and costs and improve patient care.

Ask him about the Imaging Management Seminar, too. He has more valuable information to offer and a prospectus folder on the training program. Or write DuPont Company, Room 36673, Wilmington, DE 19898.

Imaging Management.
It puts you in control of image quality, costs and patient care.

DUPONT
REG. U.S. PAT. & TM. OFF.

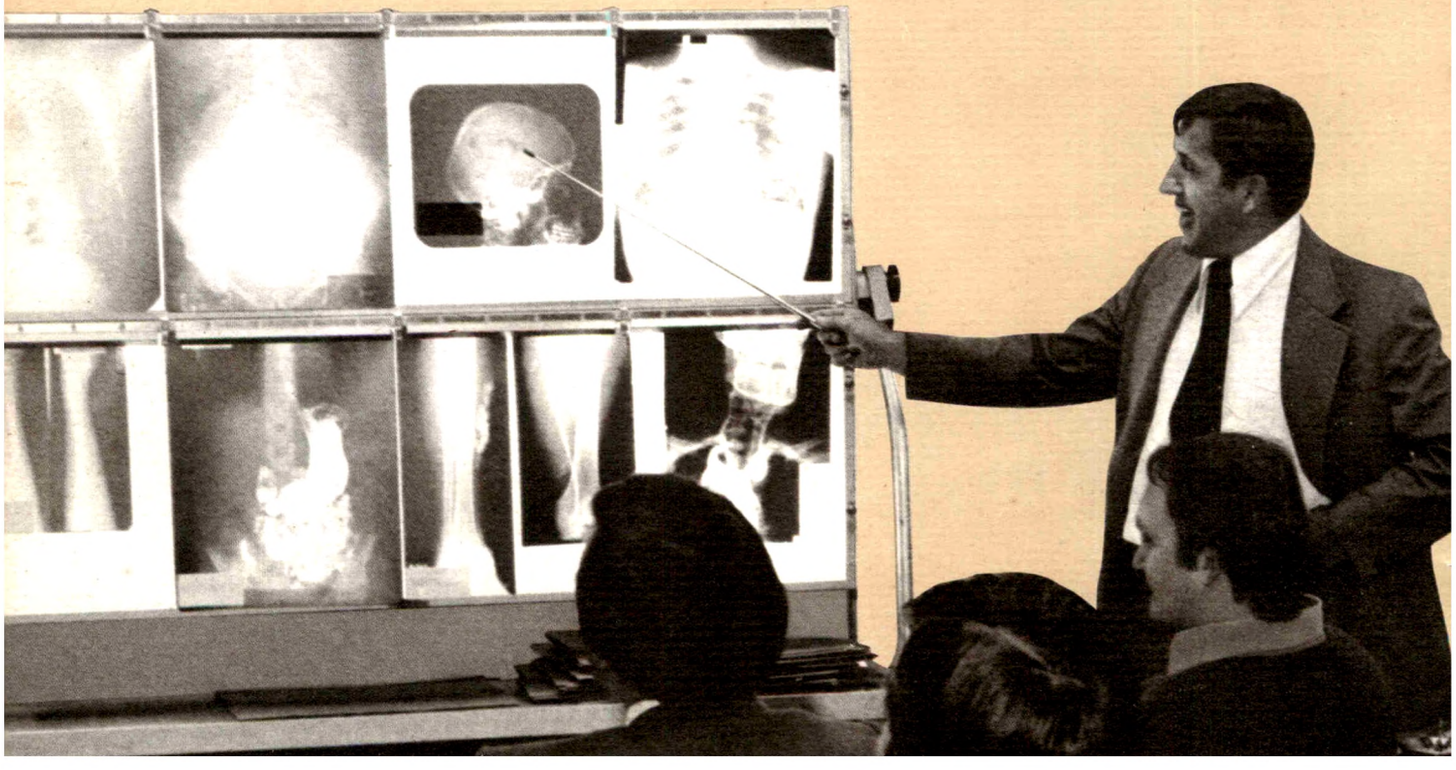

Refine your diagnostic and interpretative skills.

Here's how . . .

A New Book!

COLOR ATLAS OF SECTIONAL ANATOMY: Chest, Abdomen and Pelvis

This impressive atlas promises to become one of the most valuable clinical tools in your field. Designed as a reference for normal radiological appearance, it features a complete set of sections (sagittal, transverse, and coronal) 1 cm. thick — all in full color plates — of the chest, abdomen and pelvis. To aid you in interpretation:

- each plate is accompanied by a labelled line diagram;
- photography is far superior to that in any other atlas on this subject;
- every organ is shown in its natural color since the body was frozen without embalming;
- 60 unmounted slides (ten 35 mm. strips, each with six plates) are included at the back of the book.

This is an excellent opportunity to refine your skills in interpreting scans and recognizing abnormalities, and to increase your understanding of the important spatial relationships of internal structures. But the only way to appreciate how this monumental atlas can help you in practice is to SEE IT YOURSELF! Be among the first to evaluate this landmark volume . . . order your copy today.

By E. A. Lyons, M.D., F.R.C.P. (C). October, 1978. Approx. 304 pages, 283 illustrations, including 138 in full color, plus 60 unmounted 35 mm. transparencies. About $130.00.

New Volume IV!

RADIOLOGY OF THE SKULL AND BRAIN: Ventricles and Cisterns

A major publishing event . . . an encyclopedic treatment of this subject against which all others will be judged . . . a definitive statement on the intricacies of contemporary neuroradiology. You'll recognize — and benefit from — all this and more in the latest addition to this monumental series. Superbly illustrated and completely up-to-date, it displays the ventricles and cisterns by anatomical techniques, ventriculography and pneumoencephalography. Throughout, internationally known neuropathologists, neuroradiologists, neurologists and neurosurgeons share their expertise with such significant topics as:

- techniques and indications for pneumoencephalography and ventriculography;
- pneumoencephalography in congenital anomalies;
- hydrocephalus.

Be among the first to put this outstanding resource to work in your practice. Order your own copy today!

Edited by Thomas H. Newton, M.D. and D. Gordon Potts, M.D.; with 15 contributors. October, 1978. Approx. 704 pages, 1,369 illustrations. About $59.50.

Also of interest . . .

A New Book! **CARDIOVASCULAR ANGIOGRAPHY FOR TECHNOLOGISTS.** By David Garrison, Ph.D. and Anne Donnell, R.T. (ASRT). July, 1979. Approx. 225 pp., 86 illus. **About $13.95.**

A New Book! **INTENSIVE CARE RADIOLOGY: Imaging of the Critically Ill.** Edited by Lawrence R. Goodman, M.D. and Charles E. Putman, M.D.; with 10 contributors. June, 1978. 380 pp., 353 illus. **Price, $34.50.**

A New Book! **ULTRASONOGRAPHY OF DIGESTIVE DISEASES.** By Francis S. Weill, MD. March, 1978. 522 pp., 1,336 illus. **Price, $47.50.**

5th Edition. **Ackerman and del Regato's CANCER: Diagnosis, Treatment, and Prognosis.** By Juan A. del Regato, M.D. and Harlan J. Spjut, M.D. 1977. 1,028 pp., 805 illus. and 4 color plates. **Price, $57.50.**

A New Book! **POSITIONING AND TECHNIQUE HANDBOOK FOR RADIOLOGIC TECHNOLOGISTS.** By Sylvester B. Conte and Douglas H. Kemme. July, 1978. 304 pp., 337 illus. **Price, $8.95.**

A New Book! **COMPUTER METHODS: The Fundamentals of Digital Nuclear Medicine.** By David E. Lieberman, B.S.E.E., M.S.E.E.; with 19 contributors. December, 1977. 244 pp., 215 illus. **Price, $14.95.**

A New Book! **TEXTBOOK OF DIAGNOSTIC ULTRASONOGRAPHY.** By Sandra L. Hagen-Ansert, B.A., R.D., M.S.; illustrations by Eric P. Teichman, R.D., M.S. September, 1978. Approx. 432 pp., 1,200 illus. **About $44.50.**

A New Book! **COMPUTED TOMOGRAPHY OF THE HUMAN BODY: An Atlas of Normal Anatomy.** By Ralph J. Alfidi, M.D.; John Haaga, M.D.; Meredith Weinstein, M.D.; and Jack DeGroot, M.D., Ph.D. December, 1977. 208 pp., 220 illus. **Price, $34.50.**

A New Book! **INTRODUCTION TO DIAGNOSTIC RADIOLOGY: A Correlated Approach to Imaging.** By Richard H. Daffner, M.D. October, 1978. Approx. 400 pp., 626 illus. **About $14.95.**

A New Book! **MATHEMATICS FOR TECHNOLOGISTS IN RADIOLOGY, NUCLEAR MEDICINE AND RADIATION THERAPY.** By Stefano S. Stefani, M.D. and Lincoln B. Hubbard, Ph.D. April, 1979. Approx. 211 pp., 121 illus. **About $9.50.**

To order, call us toll free: (800) 325-4177 ext. 10; in Missouri, call collect (314) 872-8370 ext. 10 during regular business hours. A80848-59-05

MOSBY

TIMES MIRROR

THE C. V. MOSBY COMPANY
11830 WESTLINE INDUSTRIAL DRIVE
ST. LOUIS, MISSOURI 63141

N w imaging v rsatility.

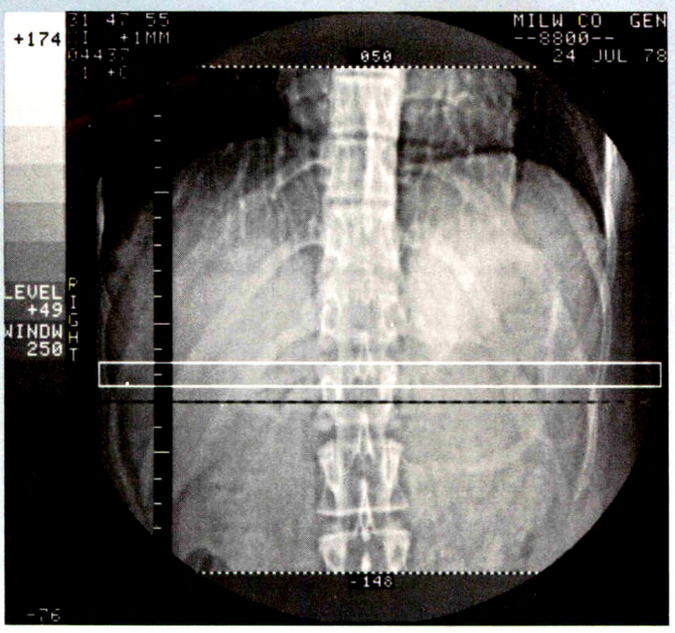

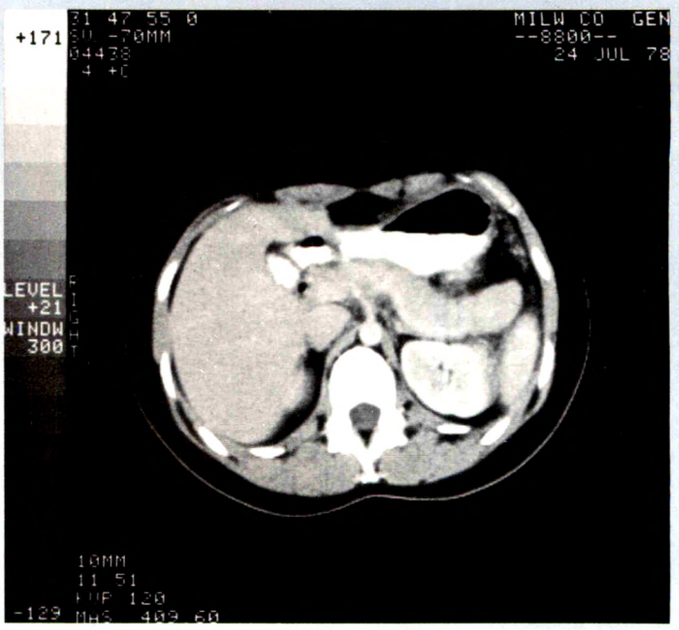

These images demonstrate how ScoutView imaging simplifies pancreatic localization. An axial slice taken at the mid to lower L-1 vertebral level is almost invariably at the takeoff of the superior mesenteric artery from the abdominal aorta, and the body of the pancreas will be included in the same slice.The scan sequence can then be monitored both above and below this level to ensure that the complete pancreas has been studied. Unnecessary slices resulting from attempts to define the level of the pancreas from external landmarks are thus avoided.

The image at the right was taken at the level indicated by the box on the ScoutView image. In this case, the patient has a horizontally oriented pancreas, and the slice taken at this level, following an intravenous bolus injection of 25 cc of Renographin 60, clearly demonstrates the splenic vein and superior mesenteric vein, in addition to the superior mesenteric artery on the posterior surface of the pancreas. Note the obliteration of the spleno-renal angle due to pancreatitis. Gas is present within the distal common bile duct secondary to a previous sphincteroplasty on the ampulla of Vater.

Clinical documentation of ScoutView's usefulness in diagnostic procedures is provided in a new 4-page Medical Systems Report. It's yours for the asking from your GE Medical Systems representative, or write ScoutView, P.O. Box 414 (W-512), Milwaukee, WI 53201.

New operator's console, one part of the ODC package, lets you initiate ScoutView imaging, then position a cursor on the image to select scan locations and plan gantry angulation. The new console also allows set up and control of axial scans, plus viewing of the last slice. When the physician's console is not in use, image analysis can be controlled at the operator's console.

SDC physician's console (far right), standard with CT/T systems, provides complete axial, sagittal and coronal scan image manipulation and analysis capability. With the optional ODC package, this console also displays ScoutView images, which can be analyzed with magnification, angle measure and grid/annotate.

You'd expect it from GE.

GE's new Optional Diagnostic Capability package (ODC) offers these key features:

- **New operator's console with image viewing, manipulation and recording capability**
- **Improved, coordinated anatomical reference system utilizing new table electronics**
- **1.5 mm contiguous axial slice capability**
- **ScoutView™ localization imaging—AP/PA, lateral and oblique**
- **Easily installed on existing CT/T 7800 and 8800 systems**

ScoutView localization provides important new benefits for the CT/T operator. The scanner actually generates a radiograph-like image that is used to accurately plan first and last slice locations, plus the exact gantry angulation needed. Each axial scanning procedure is thus tailored precisely to the anatomy of the individual patient, since the ScoutView image and the axial scans share a coordinated anatomical reference system.

A ScoutView procedure is performed in just 5 to 10 seconds, and the image is reconstructed in less than 40 seconds. Dosage is low, varying from 6 mR to 600 mR depending on technic and patient size.

At the operator's console, ScoutView images and the last slice may be viewed without interrupting diagnostic activity at the physician's console. And when the physician's console is not in use, the operator can perform virtually all image manipulation and recording functions at the operator's console.

ScoutView images can also be displayed, manipulated and analyzed at the physician's console. Because of the coordinated reference system, axial scans can be selected for viewing according to their locations on the ScoutView image.

This new package is further evidence of GE's Continuum concept: to provide important options without major systems changes. This cost-saving concept has brought you GE's fast-reconstruct option, X-2 ultra-high resolution detector, and the Independent Diagnostic Console. And now the ODC with ScoutView imaging.

That's just what you'd expect from GE. The best images and best value...now and in the future.

General Electric Medical Systems,
Milwaukee, Toronto, Madrid.

GENERAL ELECTRIC

ONE-SEVENTH OF YOUR EMPLOYEES MAY BE DYING. HELP SAVE THEIR LIVES.

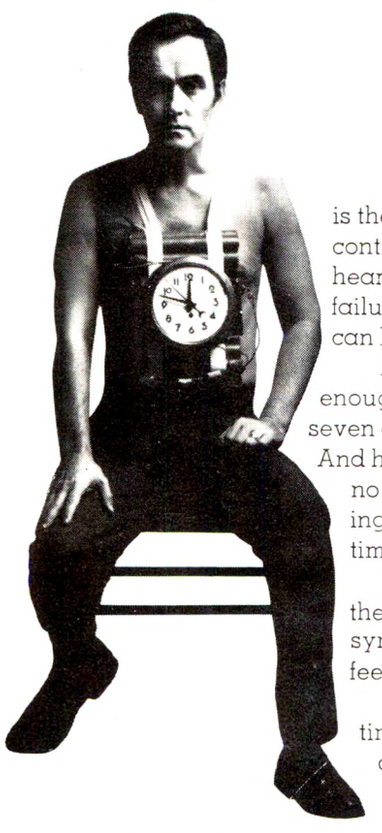

High Blood Pressure is the country's leading contributor to stroke, heart disease and kidney failure. Any of which can kill.

And, frighteningly enough, one out of every seven of your workers has it. And half of them have no idea they're walking around with this time bomb inside them.

That's because there are usually no symptoms. The victim feels fine.

But all the while, the time bomb is ticking away.

Until, suddenly, it explodes.

But you can help. By giving your employees a chance to check their blood pressure. It takes only seconds to measure a person's blood pressure. And it's painless. Best of all, your own medical or nursing personnel can do the job, simply.

When a case of High Blood Pressure is detected, the employee is then referred to a doctor for treatment. And treatment is usually as simple as taking a pill every day.

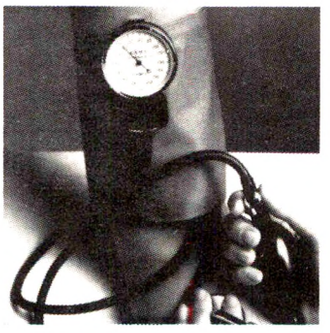

To help you implement this life-saving program, we have a special kit, "Guidelines for High Blood Pressure Control Programs in Business and Industry." The kit includes complete instructions on screening, publicity, referral, follow-up, education. And more.

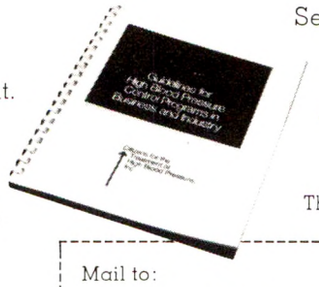

Send for your kit today. It may be the best thing you've ever done for your employees. And your company.

A Public Service of this Magazine & The Advertising Council

Mail to:

National High Blood Pressure Education Program
120/80, National Institutes of Health
Room 1012—Landow Bldg.
Bethesda, Md. 20014

Please send me _____ copy(ies) of "Guidelines for High Blood Pressure Control Programs in Business and Industry."

Name _____

Title _____

Company _____

Address _____

City _____ State _____ Zip _____

HIGH BLOOD PRESSURE
Treat it...and live.

The National High Blood Pressure Education Program, U.S. Department of Health, Education, and Welfare.

HIGH BLOOD PRESSURE EDUCATION CAMPAIGN **BP-2-76**
BUSINESS PRESS AD NO. HBP - 2475 - 76 — 7" x 10" (110 Screen)
Volunteer Agency: DKG, Inc. Volunteer Coordinator: Sanford Buchsbaum, Revlon, Inc.

TWENTY WAYS TO LOOK AT SOUND.

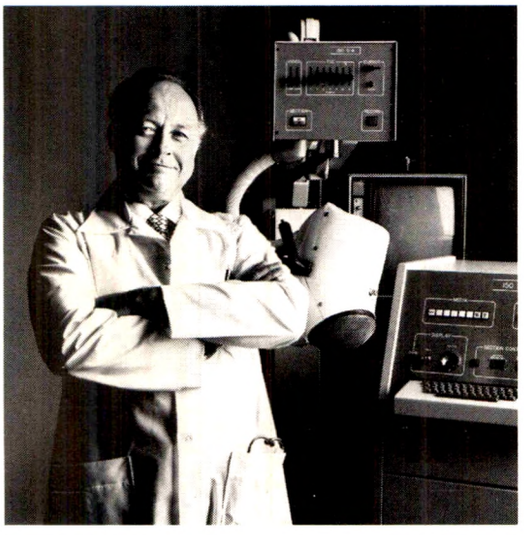

In the Xerox 150 S-4 Real-time Ultrasound System, we've put together many features that are worth looking into.

Here are 20 of them.

1. Excellent lateral resolution: The beam width is 2mm at the skin line, 3mm at 10cm depth and only 4.5mm at the full 20cm depth of scan.

2. Excellent axial resolution: Data is sampled every .8mm along the beam axis.

3. Deep scan penetration: 20cm deep. Enough to accurately diagnose obese patients.

4. Annular array transducer: Provides a dynamically focused pencil-thin beam throughout the entire depth of scan.

5. Dynamic focusing: One transducer does it all. Maximum side-lobe suppression: maximum signal-to-noise ratio in area of interest.

6. Water path system: Minimizes near-field distortion and maximizes field of view.

7. Total digital operation: Digital scan converter-type functions, digital memory, digital microprocessor give you the flexibility for the future and reliability for today.

8. Video invert: Provides viewing and recording of either black on white or white on black images.

9. Image repeatability: Automated operation helps all trained personnel to achieve virtually the same images.

10. Image magnification: A 1.5x enlargement of the displayed image allows easier viewing of small structures.

11. Flicker free images: Displayed on a large 17" TV monitor.

12. Real-time Search mode: Permits rapid orientation thus increasing the number of patients examined.

13. Automated B-scan Study mode: Maximum resolution. Simpler operation. Reduced scanning time.

14. Stop frame mode: Permits detailed study and photography in either real-time or automated B-scan Study mode.

15. Automatic sectioning mode: Provides programmable "tomographic" sections through the anatomy without moving the scanning head.

16. Total system warranty: One year labor; one year parts, including the annular array transducer.

17. Alphanumeric data entry display: Provides input of three full lines, 16 characters each, for a total of 48. Plus an additional line showing scanning head position and image reference data.

18. Multiple hard-copy compatability: Use with your choice of video tape recorder, roll film cameras, instant film cameras, multiformat cameras.

19. Modular construction: Ease of service; accommodates advanced capability design changes.

20. Abdominal versatility: Superior real-time diagnostic evaluation of liver, kidney, spleen, pancreas, gallbladder, aorta and other blood vessels. Complete OB/Gyn studies including the lower uterine segment.

For more information, and a closer look at the Xerox 150 S-4, call Ty Fairchild collect at (213) 351-1579, or write Xerox Ultrasound, 125 N. Vinedo St., Pasadena, CA 91107.

XEROX

XEROX® is a trademark of XEROX CORPORATION.
The Xerox 150 S-4 was developed and is manufactured by Mediscan, Inc., South Windsor, Connecticut.

American Journal of Roentgenology

Vol. 131 November 1978 No. 5

DIAGNOSTIC IMAGING

773 **Radium-induced Malignant Tumors of the Mastoid and Paranasal Sinuses.** *Littman MS, Kirsh IE, Keane AT*
787 **Radiologic and Clinical Assessment of Broad-Spectrum Antibiotic Therapy in Crohn's Disease.** *Moss AA, Carbone JV, Kressel HY*
791 **Association of Squamous Cell Carcinoma of the Head and Neck with Cancer of the Esophagus.** *Goldstein HM, Zornoza J*
795 **Cystic Neoplasms of the Pancreas: New Angiographic and Ultrasonographic Findings.** *Freeny PC, Weinstein CJ, Taft DA, Allen FH*
803 **Lymphangiographic Changes after Radiation Therapy.** *Jonsson K, Libshitz HI, Osborne BM*
807 **High-Dose Renal Pharmacoangiography in the Assessment of Hypovascular Renal Neoplasms.** *Chuang VP, Fried AM*
813 **Optimal Technique of Renal Arteriography in Living Renal Transplant Donors.** *Strauser GD, Stables DP, Weil R III*
817 **Complications in Expanded Polytetrafluoroethylene Arteriovenous Grafts: An Angiographic Study.** *Lemaitre P, O'Regan S, Herba M, Kaye M*
821 **Complication Rate with Supine Phlebography.** *Coel MN, Dodge W*
823 **Flow-directed Balloon Catheterization for Aortofemoral Arteriography Using the Axillary Artery Approach.** *Buonocore E, Lynch TP*
827 **A New Noninvasive Approach to Peripheral Vascular Disease: Thallium-201 Leg Scans.** *Siegel ME, Siemsen JK*
831 **Computed Tomography in the Detection of Retroperitoneal Hemorrhage after Translumber Aortography.** *Bergman AB, Neiman HL*
835 **Detection of Neoplastic Involvement of the Mesentery and Omentum by Computed Tomography.** *Levitt RG, Sagel SS, Stanley RJ*
839 **Computed Tomography of Necrotic Hepatic Metastases.** *Wooten WB, Bernardino ME, Goldstein HM*
843 **CT Diagnosis of Tumor Thrombosis of the Renal Vein and Inferior Vena Cava.** *Marks WM, Korobkin M, Callen PW, Kaiser JA*
847 **Diminished Radiopacity of Contrast Material: A Urographic Sign of Ureteral Calculus.** *Korobkin M, Jacobs RP, Clark RE, Minagi H*
851 **New Observations in Renal Transplants Using Ultrasound.** *Conrad MR, Dickerman R, Love IL, Curry T, Peters P, Hull A, Lerman M, Helderman H*
857 **Calcified Bodies in Popliteal Cysts: A Characteristic Radiographic Appearance.** *Goldberg RP, Genant HK*
861 **Complications of Catheter Cerebral Arteriography: Analysis of 5,000 Procedures. I. Criteria and Incidence.** *Mani RL, Eisenberg RL, McDonald EJ Jr, Pollock JA, Mani JR*
867 **Complications of Catheter Cerebral Arteriography: Analysis of 5,000 Procedures. II. Relation of Complication Rates to Clinical and Arteriographic Diagnoses.** *Mani RL, Eisenberg RL*
871 **Complications of Catheter Cerebral Arteriography: Analysis of 5,000 Procedures. III. Assessment for Arteries Injected, Contrast Medium Used, Duration of Procedure, and Age of Patient.** *Mani RL, Eisenberg RL*
875 **Coronal Computed Tomography: Indications and Accuracy.** *Mass S, Norman D, Newton TH*
881 **CT Contrast Enhancement in Cerebral Infarction.** *Norton GA, Kishore PRS, Lin J*

CASE REPORTS

887 ***Streptococcus bovis* Septicemia as a Clue to Colon Neoplasms in Two Cases.** *Smith TR, Friedman SN, Adler H*
889 **Bile Leak into a Hepatic Abscess in a Liver Transplant: Demonstration with ^{99m}Tc-Diethyl-Iminodiacetic Acid.** *Klingensmith WC III, Koep LJ, Fritzberg AR*
892 **Legionnaires Disease.** *Reed JC, McLelland R, Nelson P*
895 **Ultrasound Diagnosis of Hydatid Disease (Echinococcosis) in Two Cases.** *Babcock DS, Kaufman L, Cosnow I*
898 **Diffuse Lymphatic Dysplasia with Hepatic Oil Embolism.** *Tatezawa T, Akisada M*
901 **Free-floating Calculi in the Pericardial Cavity.** *Littleton JT, Cady JB*
904 **Focal Perfusion Defect Caused by Sequestration in Two Cases.** *Van Aman ME, Lloyd TV, Johnson JC*
906 **Complications from Intraarterial Lidocaine in Upper Extremity Arteriography.** *Chuang VP, Widrich WC*
907 **Ultrasonic Visualization of a Cervical Cord Cystic Astrocytoma.** *Reid MH*
909 **Huge Laparotomy Pad Granuloma Simulating a Gastric Wall Tumor.** *Carsky EW, Haswell DM*
911 **Enlargement of the Intervertebral Foramina: An Unusual Cause.** *Patel DV, Ferguson L, Schey WL*
914 ***Chlamydia trachomatis:* A Cause of an Infantile Pneumonia Syndrome.** *Stickney RH, Bjelland JC, Capp MP, Harrison RR, Hansen R*

TECHNICAL NOTES

916 **Radiography of LeVeen Type Peritoneovenous Shunts.** *Freiman DB, Ring EJ, Oleaga JA, Rosato EF*
918 **Pathologic Index for Arrangement of Teaching File.** *Daffner RH*

919 **Progress in Radiology: Total Body Opacification.** *Griscom NT*

926 **Editorial: Rare Earth Screens and Silver.** *Wilson RA*
928 **Letters**
931 **Abstracts of Current Literature**
946 **Book Reviews**
950 **News**
929 **ARRS 1979 Meeting Summary**

Acc.
13.7.79

AJR

American
Journal of
Roentgenology

December 1978

LIBRARY

Revitalize
Your Tired
R-F
Equipment.
Add a Machlett Cesium Iodide Image Intensifying System
• IRIS 100 TV Viewing & 100mm Spotfilming
• DYNAVISION TV Viewing
• DYNAVIEW Optical Viewing
Superior performance at the right price.
Ask your x-ray dealer for complete information or contact:
MACHLETT
Machlett Laboratories, Incorporated
1063 Hope Street
Stamford, Connecticut 06907
(203) 348-7511
A Raytheon Company

Official Journal
American Roentgen Ray Society
American Radium Society

AJR

Including Diagnostic Radiology • Radiation Oncology • Nuclear Medicine Ultrasonography • Related Sciences

Editor Melvin M. Figley

Associate Editor Rosalind H. Troupin

Assistant Editor John D. Harley

Contributing Editor E. Frederick Lang

Consulting Editorial Board Luther W. Brady • Kent Ellis E. Robert Heitzman • Donald L. King • N. Thorne Griscom Eugene C. Klatte • Kenneth Krabbenhoft • John G. McAfee Russell H. Morgan • Thomas H. Newton • Robert G. Parker Stewart R. Reuter • William B. Seaman • Robert J. Shalek John Storer • Michel M. Ter-Pogossian • Joseph P. Whalen David M. Witten

Editorial Staff K. A. Murray, manager • M. J. Leonard, manuscript editor • J. Anderson, assistant manuscript editor • C. P. Kaiser, secretary

Published monthly by Charles C Thomas, 301-327 East Lawrence Avenue, Springfield, Illinois 62717. All correspondence, except editorial office business, should be addressed to the publisher. Annual subscription rates: $40 ($20 for residents with letter of verification) plus appropriate mailing surcharge (see note next page). Single copies, $5. Undelivered or damaged copies replaced within 60 days of publication; 90 days for foreign subscribers. Allow 90 days for address changes. © 1978 by American Roentgen Ray Society. Second-class postage paid at Springfield, Illinois, and at additional mailing offices. Printed in U.S.A. ISSN 0361-803X

American Roentgen Ray Society

President: Harry Z. Mellins
President Elect: Paul A. Riemenschneider
1st Vice-president: Joseph D. Calhoun
2d Vice-president: Charles E. Bickham, Jr.
Secretary: James F. Martin
Treasurer: Harley C. Carlson

COMMITTEES 1977–1978

Executive Council: H. Z. Mellins, P. A. Riemenschneider, J. D. Calhoun, C. E. Bickham, Jr., J. F. Martin, H. C. Carlson, M. M. Figley, R. G. Evens, B. G. Brogdon, R. A. Gagliardi, E. Gedgaudas, G. A. Kling, T. F. Leigh, S. F. Ochsner, J. F. Wiot, R. E. Buenger, E. C. Klatte, J. P. Tampas, J. L. Gwinn, chairman

Finance and Budget: A. E. James, E. C. Klatte, R. McLelland, J. P. Tampas, R. G. Evens, chairman

Publications: M. P. Capp, K. Ellis, F. F. Ruzicka, Jr., E. R. Heitzman, R. A. Gagliardi, chairman

Editorial Policy: M. M. Figley, E. F. Lang, R. H. Troupin, E. R. Heitzman, K. Ellis, F. F. Ruzicka, Jr., M. P. Capp, R. A. Gagliardi, chairman

Advisory Committee on Education and Research: J. E. Youker, G. Wilson, G. W. Hartman, L. F. Rogers, E. Gedgaudas, chairman

Scientific Exhibits: T. C. Beneventano, G. Dodd, B. G. Brogdon, chairman

Constitution and Bylaws: J. H. Walker, W. M. Whitehouse, J. P. Tampas, chairman

American Board of Radiology Representatives: J. F. Roach, R. W. McConnell, S. W. Nelson

Program Committee: H. Z. Mellins, J. F. Martin, J. L. Gwinn, M. M. Figley, R. A. Gagliardi, B. G. Brogdon, E. Gedgaudas, G. A. Kling, P. Riemenschneider, chairman

Instruction Courses: E. Gedgaudas, director; G. W. Hartman, associate director

American College of Radiology Board of Chancellors Representative: W. B. Seaman

Annual Meeting: March 25–30, 1979, Sheraton Centre, Toronto, Canada

Scientific Program: P. A. Riemenschneider, president elect, Cottage Hospital, Santa Barbara, California 93105

Manager Annual Meeting: George A. Kling, Harper Hospital, Detroit, Michigan 48201

Membership: John L. Gwinn, 4650 Sunset Blvd., Los Angeles, California 90027

Business Office: Keith W. Gundlach, comptroller, American College of Radiology, 20 North Wacker Drive, Chicago, Illinois 60606

American Radium Society

President: Frederick W. George, III
President Elect: Alfred S. Ketcham
1st Vice-president: Julian P. Smith
2d Vice-president: Edwin M. Jacobs
Secretary: Norah duV. Tapley
Treasurer: Simon Kramer

COMMITTEES 1978–1979

Executive: A. S. Ketcham, J. P. Smith, E. M. Jacobs, N. duV. Tapley, S. Kramer, L. W. Brady, R. H. Jesse, F. W. George, F. Rutledge, chairman

Public Relations: V. Marcial, J. Vaeth, C. Honaker, ex-officio, and F. George, chairman

Publication: K. L. Krabbenhoft, D. Hussey, A. Raventos, I. Fix, L. W. Brady, chairman

Scientific Program: R. Parker, J. Durant, A. S. Ketcham, M. S. Mitchell, G. Murphy, F. Rutledge, M. Griem, W. E. Powers, M. Apuzzo, F. George, chairman

Local Arrangements: L. Davis, J. Vaeth, J. Nolan, R. McKenna, J. Slater, J. Stein, J. Scallon, S. Kramer, J. Helsper, chairman

Constitution and Bylaws: A. S. Glicksman, P. J. DiSaia, K. L. Krabbenhoft, chairman

Audiovisual: C. R. Bogardus, J. Helsper, R. Schweitzer, R. H. Jesse, C. Perez, J. Glassburn, A. M. Nisar Syed, R. Young, B. Herrington, F. George, chairman

American Board of Radiology Representatives: J. J. Stein, R. E. King, N. duV. Tapley

American College of Radiology Board of Chancellors Representative: L. W. Brady

American College of Radiology Council Representative: J. del Regato

Editorial Board of AFCOS Newsletter Representative: J. Vaeth

National Council on Radiation Protection and Measurements Liaison Representative: L. W. Davis

Annual Meeting: March 4–8, Los Angeles, California

Scientific Program: F. W. George, III, University of Southern California School of Medicine, Los Angeles, California 90033

Local Arrangements: James Helsper, Pasadena, California

Membership: Norah duV. Tapley, secretary, M. D. Anderson Hospital, 6723 Bertner Avenue, Houston, Texas 77030

Business Office: N. V. Jordan, c/o R. H. Jesse, M. D. Anderson Hospital and Tumor Institute, 6723 Bertner Avenue, Houston, Texas 77030

Mailing note. — Mailing surcharges: U.S. and possessions, none; European countries, $25; Japan, $45; other, $10. European rates apply to Algeria, Austria, Belgium, Czechoslovakia, Denmark, Finland, France, Germany, Great Britain, Greece, Hungary, India, Iran, Ireland, Israel, Italy, Kenya, Luxembourg, Netherlands, Nigeria, Norway, Portugal, Romania, South Africa, Spain, Sweden, Switzerland, Turkey, Uganda, Yugoslavia. All subscriptions to Japan and European countries are delivered by air freight; there is no option for surface mail.

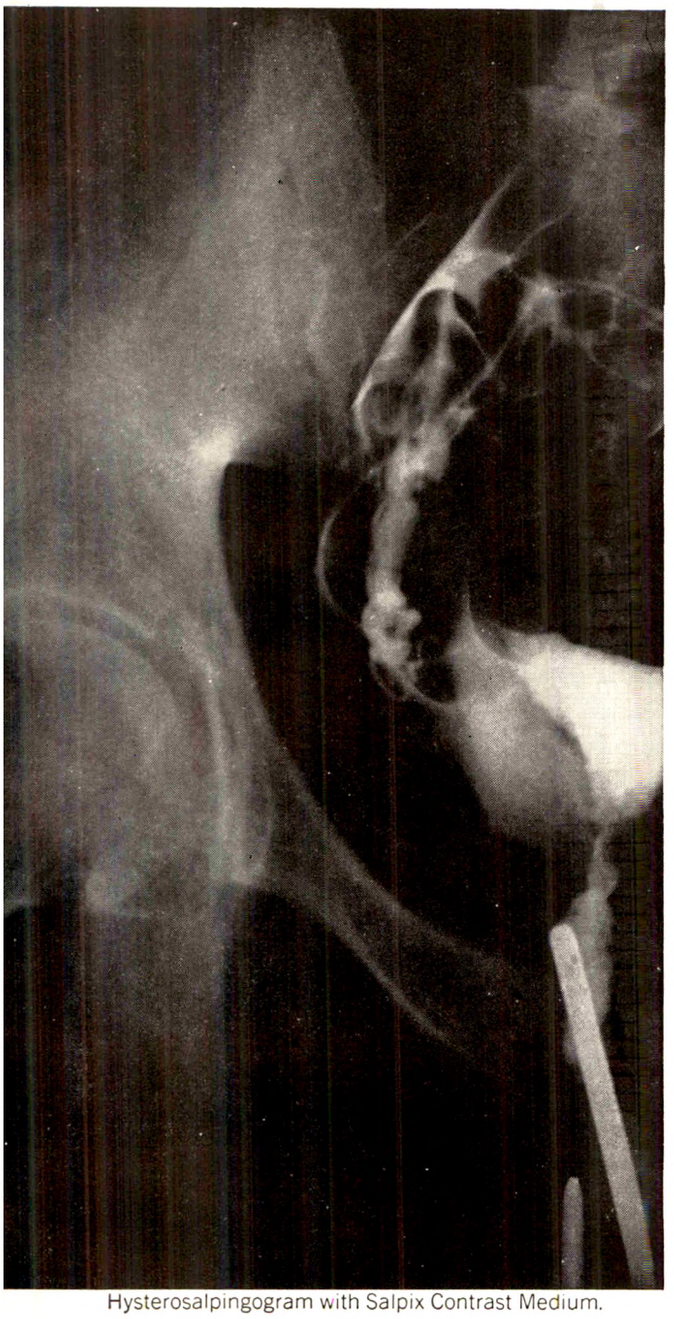

Hysterosalpingogram with Salpix Contrast Medium.

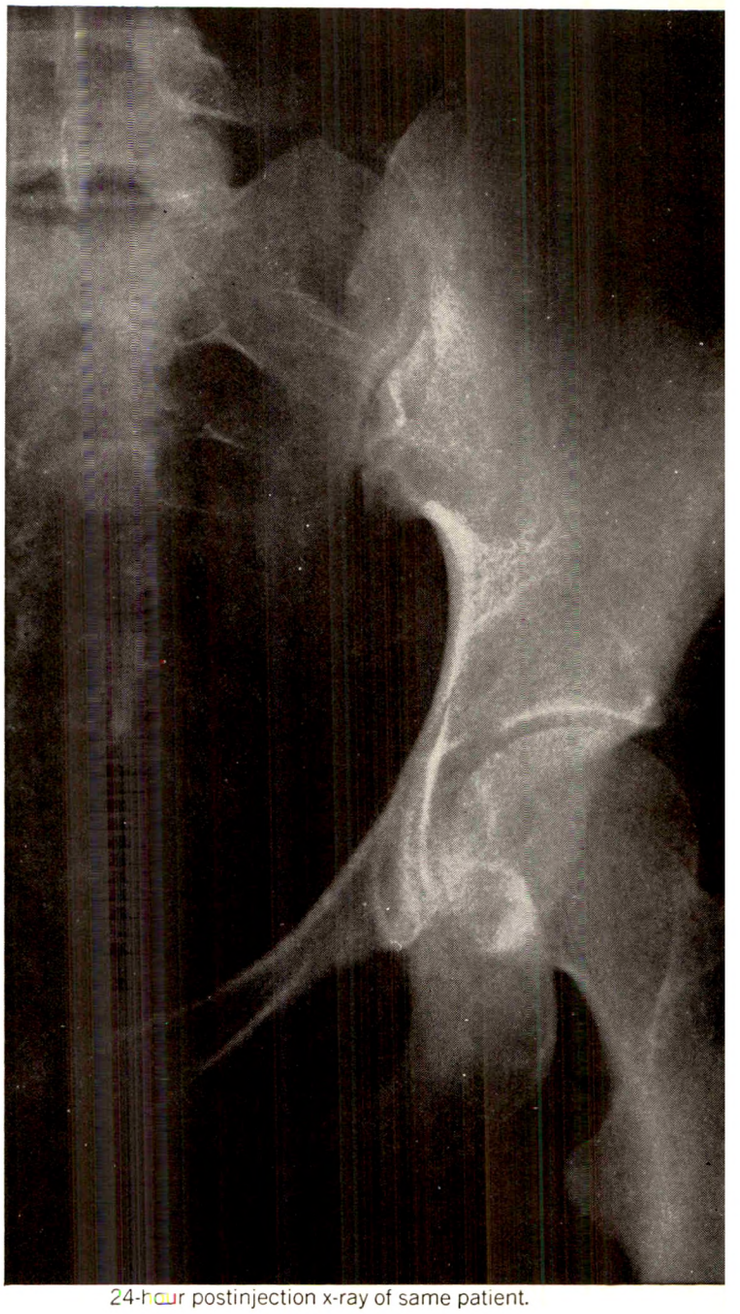

24-hour postinjection x-ray of same patient.

now you see it

now you don't

With Salpix as your contrast medium, your gynecologic patient needn't undergo the 24-hour postinjection x-ray usually required with iodized oils. Water-soluble Salpix leaves virtually no irritating radiopaque residue to produce foreign-body reactions, yet it provides the viscosity needed for adequate visualization.

Contraindications: Contraindications to hysterosalpingography include the presence of severe vaginal or cervical infections, existing or recent pelvic infection, marked cervical erosion or endocervicitis, and pregnancy. The procedure is contraindicated during the immediate pre- or post-menstrual phase.

Sensitivity Test: If indicated in the patient's history, an intracutaneous skin test or sublingual absorption observation may be done with 0.1 cc Salpix.

Warning: Not for intravenous use.

© ORTHO PHARMACEUTICAL CORPORATION 1970

CONTRAST MEDIUM

Salpix

TRADEMARK

EACH CC CONTAINS:
sodium acetrizoate 0.53 g and
polyvinylpyrrolidone 0.23 g

Ortho

ORTHO PHARMACEUTICAL CORPORATION • RARITAN, NEW JERSEY 08869

THIS BOOK TELLS A LOT ABOUT US ...WITHOUT ONCE MENTIONING OUR NAME

OR OUR PRODUCTS

The name of this volume is *Certificate of Need: An Expanding Regulatory Concept.* Not once in its 944 pages does the name Pfizer appear.

Yet, despite this, we are proud to offer this book to several hundred people in the health care field, with our compliments, as part of an important, new Pfizer program called the Certificate of Need Assistance Program.

A Total C.O.N. Assistance Program

Pfizer's C.O.N. Assistance Program is designed to aid you in the increasingly regulated climate in which medicine now operates. As one of the health care industry's leaders for 129 years, Pfizer feels a responsibility not only to provide quality products but also to join the medical community in its current search for effective ways to comply with these regulations. Typical of these requirements is the Certificate of Need, or C.O.N., which is required in most cases where federal funding is involved in paying for major equipment or plant expansion.

Toll-free C.O.N. Assistance Service

Applying for the C.O.N. can be a complicated process—sometimes confusing, always time-consuming. The Pfizer C.O.N. Assistance Program can help. The two main components of this program are the book, *Certificate of Need: An Expanding Regulatory Concept,* and the toll-free C.O.N. Telephone Service to answer questions about the cost effectiveness of diagnostic equipment, as well as how this information relates to C.O.N. requirements.

To use our C.O.N. Telephone Service just phone 800-221-4688, from 9 a.m.-5 p.m. Monday through Friday. (In New York State, please call 212-573-2030, collect.)

Complimentary Books to Administrators and Radiologists

Many hospital administrators have already received copies of the book. We have also offered it to chief radiologists throughout the country and to certain other medical and administrative personnel who are involved in the purchase of diagnostic equipment.

(Incidentally, if you have not personally received *Certificate of Need: An Expanding Regulatory Concept,* and you take part in major purchasing as a hospital executive or radiologist, you are welcome to a complimentary copy. To receive it, just send us your request on your official letterhead.)

The book, as its title suggests, is a comprehensive, state-by-state compilation of current C.O.N. requirements. We feel that it makes a substantial contribution to understanding this very complex subject. And it is a subject in which we feel a special responsibility, since CT Scanners usually require this document.

Full Range of Pfizer Radiological Services

Now that we have told you how we're making it easier for you to meet the regulatory requirements for buying diagnostic equipment, we'd like to tell you why you should want to.

There's an expert specially qualified to do just that: the Pfizer Medical Systems or Radiologic Sciences Technical Representative.

He'll give you useful, specific information on the one subject that isn't included in the C.O.N. Assistance Program.

Our Products.

Pfizer Inc.
235 East 42nd St.
New York, N.Y. 10017

Advancing the Science of Therapeutics and Diagnostics.

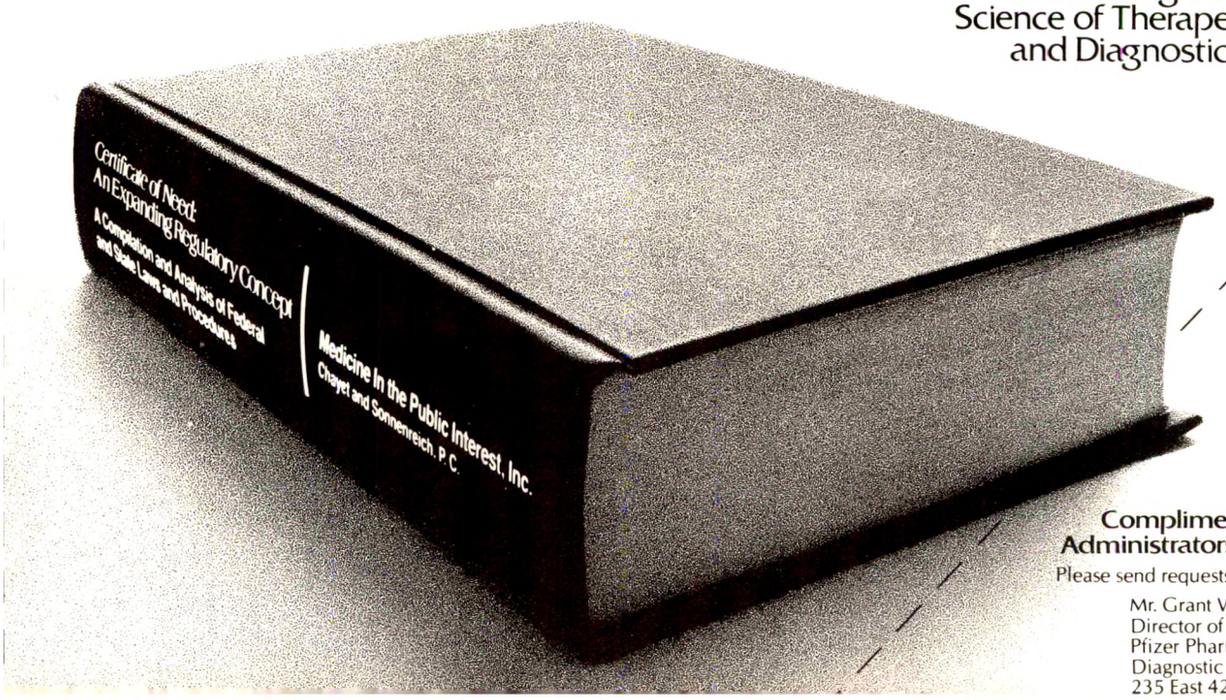

Complimentary books to Administrators and Radiolog

Please send requests on official letterhea

Mr. Grant W. Denison, Jr.
Director of Planning
Pfizer Pharmaceuticals and Diagnostic Products
235 East 42nd St.

clear, clean colon

X-Prep® Liquid

(standardized extract of senna fruit)

versatile bowel evacuant for diagnostic procedures

Versatile in indications

May be used prior to:

G.I. radiography
Urologic radiography
Colonoscopy
Sigmoidoscopy
Other diagnostic bowel procedures

Versatile in administration

May be used:

Alone, in a single dose
Alone, in divided doses, particularly in elderly or debilitated patients
With adjunctive use of citrate of magnesia, laxative suppositories and enemas, as required
As part of other regimens, such as hydration

X-PREP Liquid is formulated specifically for effective bowel evacuation prior to diagnostic procedures. It induces peristalsis through virtually colon-specific action. X-PREP Liquid has been found effective in cleansing the colon for diagnostic evaluation in 95% of 749 patients prepared for barium enemas, intravenous pyelography, or colonoscopy.* Its pleasant taste meets with high patient acceptance, and its ease of administration is appreciated by the patient and nursing staff.

Supplied: X-PREP Liquid (standardized extract of senna fruit) in 2½ fl. oz. bottles (alcohol 7% by volume). X-PREP Powder (standardized senna concentrate) in ¾ oz. containers. **Now Available:** X-PREP™ Bowel Evacuant Kit. Each kit contains: two SENOKOT® S Tablets (standardized senna concentrate and dioctyl sodium sulfosuccinate), one bottle of X-PREP® Liquid 2½ fl. oz., and one RECTOLAX™ Suppository (bisacodyl 10 mg), plus easy-to-follow patient instructions for hydration, clear liquid diet, and the correct time sequence of administering the above laxatives.

*Bibliography available upon request.

Colonoscope, courtesy of Olympus

Gray Pharmaceutical Co., Affiliate
The Purdue Frederick Company

© Copyright 1978, Gray Pharmaceutical Co. Norwalk, CT 06856

A9047 194578

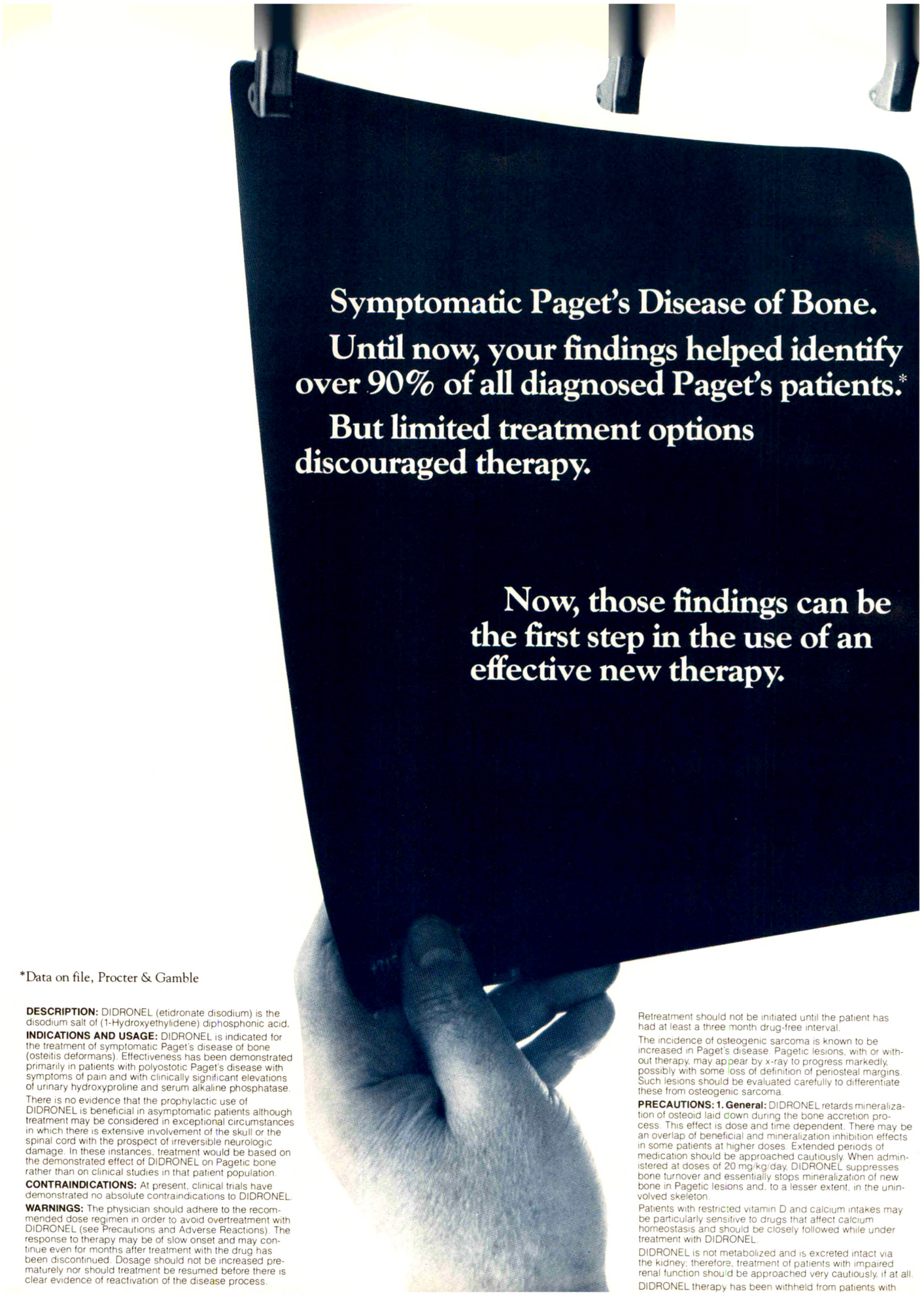

*Data on file, Procter & Gamble

DESCRIPTION: DIDRONEL (etidronate disodium) is the disodium salt of (1-Hydroxyethylidene) diphosphonic acid.

INDICATIONS AND USAGE: DIDRONEL is indicated for the treatment of symptomatic Paget's disease of bone (osteitis deformans). Effectiveness has been demonstrated primarily in patients with polyostotic Paget's disease with symptoms of pain and with clinically significant elevations of urinary hydroxyproline and serum alkaline phosphatase.

There is no evidence that the prophylactic use of DIDRONEL is beneficial in asymptomatic patients although treatment may be considered in exceptional circumstances in which there is extensive involvement of the skull or the spinal cord with the prospect of irreversible neurologic damage. In these instances, treatment would be based on the demonstrated effect of DIDRONEL on Pagetic bone rather than on clinical studies in that patient population.

CONTRAINDICATIONS: At present, clinical trials have demonstrated no absolute contraindications to DIDRONEL.

WARNINGS: The physician should adhere to the recommended dose regimen in order to avoid overtreatment with DIDRONEL (see Precautions and Adverse Reactions). The response to therapy may be of slow onset and may continue even for months after treatment with the drug has been discontinued. Dosage should not be increased prematurely nor should treatment be resumed before there is clear evidence of reactivation of the disease process.

Retreatment should not be initiated until the patient has had at least a three month drug-free interval.

The incidence of osteogenic sarcoma is known to be increased in Paget's disease. Pagetic lesions, with or without therapy, may appear by x-ray to progress markedly, possibly with some loss of definition of periosteal margins. Such lesions should be evaluated carefully to differentiate these from osteogenic sarcoma.

PRECAUTIONS: 1. General: DIDRONEL retards mineralization of osteoid laid down during the bone accretion process. This effect is dose and time dependent. There may be an overlap of beneficial and mineralization inhibition effects in some patients at higher doses. Extended periods of medication should be approached cautiously. When administered at doses of 20 mg/kg/day, DIDRONEL suppresses bone turnover and essentially stops mineralization of new bone in Pagetic lesions and, to a lesser extent, in the uninvolved skeleton.

Patients with restricted vitamin D and calcium intakes may be particularly sensitive to drugs that affect calcium homeostasis and should be closely followed while under treatment with DIDRONEL.

DIDRONEL is not metabolized and is excreted intact via the kidney; therefore, treatment of patients with impaired renal function should be approached very cautiously, if at all.

DIDRONEL therapy has been withheld from patients with

from Procter & Gamble

200 MG TABLETS

DIDRONEL®

ETIDRONATE DISODIUM

The first oral agent that suppresses symptomatic Paget's disease of bone

...Retards the disease

...Relieves signs and symptoms in many patients

...Promotes sustained posttherapy remission

...Bone-specific pharmacologic action

enterocolitis because increased frequency of bowel movements and diarrhea is seen in some patients when DIDRONEL is administered at a dose of 20 mg/kg/day and may be increased occasionally at lower doses.

2. Pregnancy: There is no experience in pregnant women given DIDRONEL. DIDRONEL should be used only when clearly needed in women who are or may become pregnant.

3. Nursing Mothers: It is not known whether this drug is excreted in human milk. As a general rule, nursing should not be undertaken while the patient is on a drug since many drugs are excreted in human milk.

4. Pediatric Use: No data support the use of DIDRONEL in children.

ADVERSE REACTIONS: Increased or recurrent bone pain at existing Pagetic sites and/or the appearance of pain at sites previously asymptomatic has been reported. At the recommended dose (5 mg/kg/day) 1 out of 10 patients reported the phenomena; at higher doses the figure rose to 2 out of 10. In placebo-treated patients, the occurrence was 1 out of 15. In DIDRONEL-treated patients, the pain resolved while therapy was continued in some patients but persisted for several months in others.

Fractures are recognized as a common feature in patients with Paget's disease. The risk of fracture may be increased when DIDRONEL is taken at a dose level of 20 mg/kg/day in excess of 3 months. This risk may be greater in patients with extensive and severe disease, a history of multiple fractures, and/or rapidly advancing osteolytic lesions. It is recommended that the drug be discontinued when fractures occur and that therapy not be reinstated until fracture healing is complete.

Gastrointestinal complaints such as diarrhea, loose bowel movement, and nausea are increased in some patients when DIDRONEL is administered at doses greater than 5 mg/kg/day. The incidence is about 1 out of 15 in both placebo-treated patients and in patients on DIDRONEL, 5 mg/kg/day. The incidence rises to approximately 2 out of 10 in patients treated with DIDRONEL at the dose of 20 mg/kg/day.

DOSAGE AND ADMINISTRATION: Initial Treatment Guidelines: The recommended initial dose of DIDRONEL for most patients is 5 mg/kg/body weight/day, not to exceed a period of six months. Doses above 10 mg/kg should be reserved for use when there is an overriding requirement for suppression of increased bone turnover associated with Paget's disease or when the patient requires more prompt reduction of elevated cardiac output. Treatment with doses above 10 mg/kg/day should be approached cautiously and should not exceed three months duration. Doses in excess of 20 mg/kg/day are not recommended.

DIDRONEL should be administered as a single, oral dose, two hours before eating. It may be given with fruit juice or water. Food, particularly materials high in calcium content such as milk, in the stomach or upper portions of the small intestine may reduce absorption. Therefore, eating should be avoided for two hours before and after drug administration.

Serum phosphate elevations have been observed when DIDRONEL is administered at daily doses of 10 mg/kg body weight/day or above and occasionally at 5 mg/kg/day. This has not been found to be an indication for discontinuing therapy.

Retreatment Guidelines: Retreatment should be undertaken only after a drug-free period of at least three months and after it is evident that reactivation of the disease has occurred. In no case should duration of retreatment exceed the maximum duration of the initial treatment.

How Supplied: DIDRONEL is supplied as a rectangular white tablet containing 200 mg of etidronate disodium. The tablets are packaged in bottles of 250.

For additional information, write Procter & Gamble, Professional Services, P.O. Box 85507, Cincinnati, Ohio 45201, or call (513) 977-5547.

A Product of Procter & Gamble Research

Fleet® Barium Enema Prep Kits: Make us your first choice for fewer retakes.

The greatest defect in colon examinations is in the preparation of the colon.[1]

Fleet® Barium Enema Prep Kits systematize and improve colon prepping because they conform to the recommended method which provides a combination of diet, hydration and proven laxation which stimulates the large and small intestines.[2] The result? Cleaner colons, clearer x-rays and fewer retakes.

All Fleet Prep Kits offer three laxative steps: 1½ oz. of Fleet® Phospho-Soda® followed by four Fleet® Bisacodyl tablets, plus a final cleansing step. Prep Kit 1 offers Fleet® Bisacodyl suppository. Prep Kit 2 offers a large-volume disposable Fleet® Bagenema. And Prep Kit 3 offers our new Fleet® Bisacodyl enema. And all three Prep Kits have easy-to-follow instructions with a choice of flexible time-tables to fit your schedule.

With Fleet Barium Enema Prep Kits, you'll be sure of convenient, dependable, effective colon prepping every time. And that's reason enough to make Fleet Prep Kits your first choice for fewer retakes.

Fleet Barium Enema Prep Kits
for cleaner colons, clearer x-rays and fewer retakes.

Fleet pharmaceuticals
C.B. Fleet Co., Inc.
Lynchburg, Va. 24505

[1]Dr. R.E. Miller, Ad Hoc Committee on Detection of Cancer of the Colon, Detection of Colon Lesions, American College of Radiology, (Chicago, Ill., 1973) p. 76.
[2]Dr. W.R. Eyler, Ibid. pp. 203, 204.

Taking the Pain out of Chest X-rays

Of course, chest x-ray examinations are not normally painful for the patient. However, the heavy patient load this type examination places on radiology departments can create chronic operational PAIN! This PAIN can be in scheduling chest examination patients into various rooms between other studies and the constant trips to and from the darkroom for cassette loading, unloading and film processing. Variable film quality due to different screens, cassettes, x-ray equipment and processor being used, can also contribute to department operation PAIN.

The ULTRARAD Chest System by Liebel-Flarsheim eliminates these operational pains and inefficiencies. When the ULTRARAD Chest System is installed with a dedicated film processor and automatic exposure timing, all your chest radiographs will be of the same high quality because the same screens, grid, x-ray equipment and film processor are used for all chest examinations. In addition, the system will deliver radiographs ready for diagnosis, in less than 2 minutes[1] from time of exposure.

The 100 supply film capacity[2] of the ULTRARAD reduces the greatest operational pain of all; those time consuming trips to and from the darkroom with cassettes, for loading, unloading and film processing.

Let Liebel-Flarsheim take the PAIN out of your chest x-ray examinations—write for our free brochure on PAINLESS CHEST RADIOLOGY.

When used with Kodak model M6 processor
The ULTRARAD is furnished with two supply magazines each capable of holding up to 50 films.

Liebel-Flarsheim Company
Division of Sybron Corporation
111 E. Amity Road,
Cincinnati, Ohio 45215, U.S.A.
(513) 761-2700

SYBRON | Liebel-Flarsheim

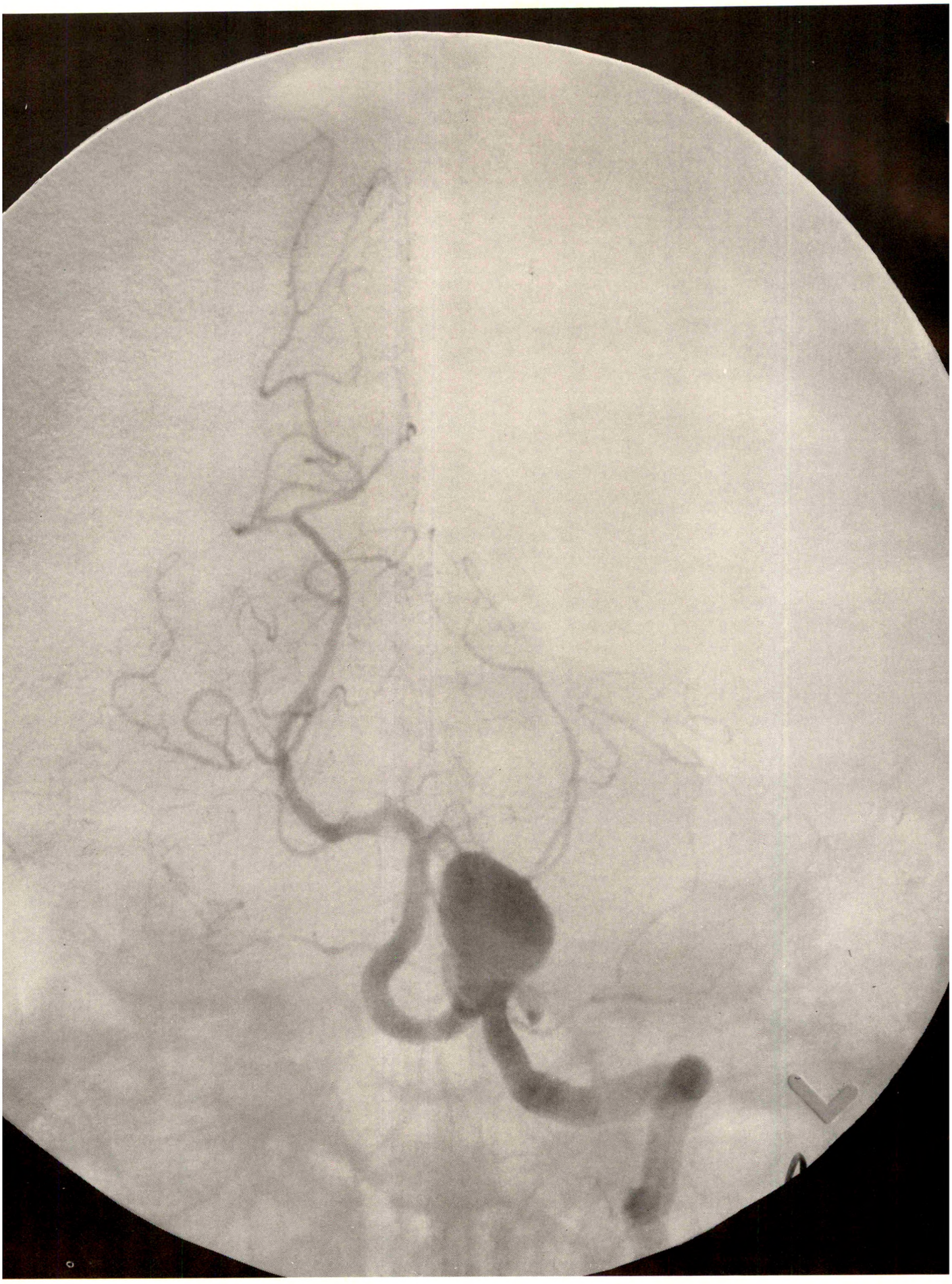

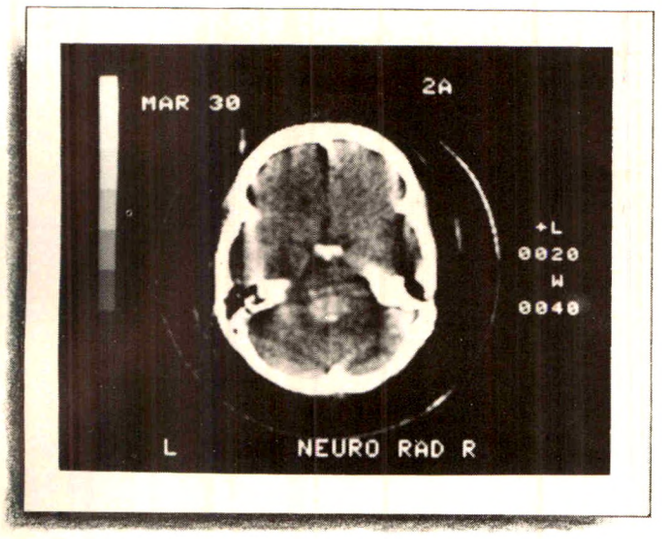

Diagnosis:
Posterior Inferior Cerebellar Artery Aneurysm

Clinical Data:
55 year old woman with diplopia, increasing right-sided weakness and hypoacousis in the left ear of 18 months duration.

CT Scan:
A midline mass is noted in the posterior fossa. The mass is partially calcified and enhanced slightly after contrast infusion. On the basis of this scan it is impossible to determine if this lesion is intra or extra-axial in location.

Left Vertebral Arteriogram:
A large aneurysm arising from the proximal posterior inferior cerebellar artery is shown.

The arteriogram and the CT scan reproductions are both reduced to 79% of their original size.

Angiography and CT scanning.

Each has its own special diagnostic advantages in this era of expanding imaging technology.

Angiography and Elema-Schonander.

For diagnostic specificity.

While CT has proved to be a highly sensitive diagnostic technique, in many cases angiography is necessary to make a specific diagnosis. And, no matter what your angiographic applications are, Elema-Schonander has a sheet-film changer to meet your requirements.

AOT-S Models: Six exp/sec, 30-film capacity AOT-S Models are available to accommodate either 35cm x 35cm (14″ x 14″) or 24cm x 30cm sheet-film sizes.

PUCK Models: Three exp/sec, 20-film capacity PUCK Models, which handle the same sheet-film sizes, are available for applications in which increased mobility, compactness and magnification are important considerations.

Both AOT-S and PUCK sheet-film changers have Elema-Schonander's CFRP (carbon-fiber reinforced plastic) front compression plate for low x-ray attenuation with intimate screen/film contact. Both are punch card controlled for accuracy and convenience. Both can be used for single plane, or biplane simultaneous or alternating sequences.

Call or write for brochures describing the AOT-S and PUCK sheet-film changers. Elema-Schonander, Inc., 699 Lively Blvd., Elk Grove Village, IL 60007. (312) 593-6770.

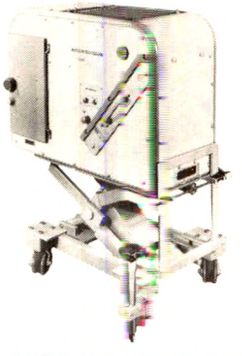

AOT-S Sheet-film Changer

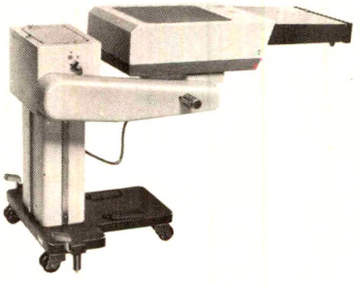

PUCK Sheet-film Changer

elema·schonander

78211

A New Study Confirms...

THE RSI MAMMOGRAPHIC SYSTEM **INCREASES DIAGNOSTIC ACCURACY**

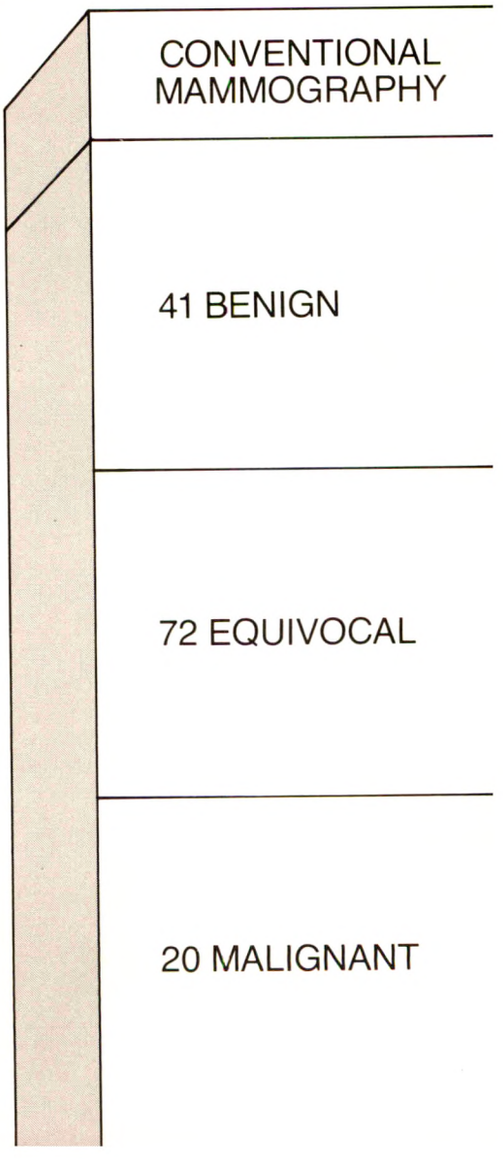

Take a good look at the chart. You'll see the remarkable results of a study published by Dr. Edward A. Sickles, making a clinical comparison of 133 patients who received both conventional mammography and RSI Magnification Mammography. The results were confirmed with pathological diagnosis.*

This new study confirms just how accurate RSI Mammography really is. In fact, Dr. Sickles wrote in 1977, that magnification mammograms are "...clearly superior both quantitatively and qualitatively to conventional contact mammograms."[1]

Diagnostic Accuracy in Mammographic Examinations[2]
Clinical Data of Edward A. Sickles, M.D.
Assistant Professor of Radiology, University of California, San Francisco
Clinical Comparison of 133 Cases

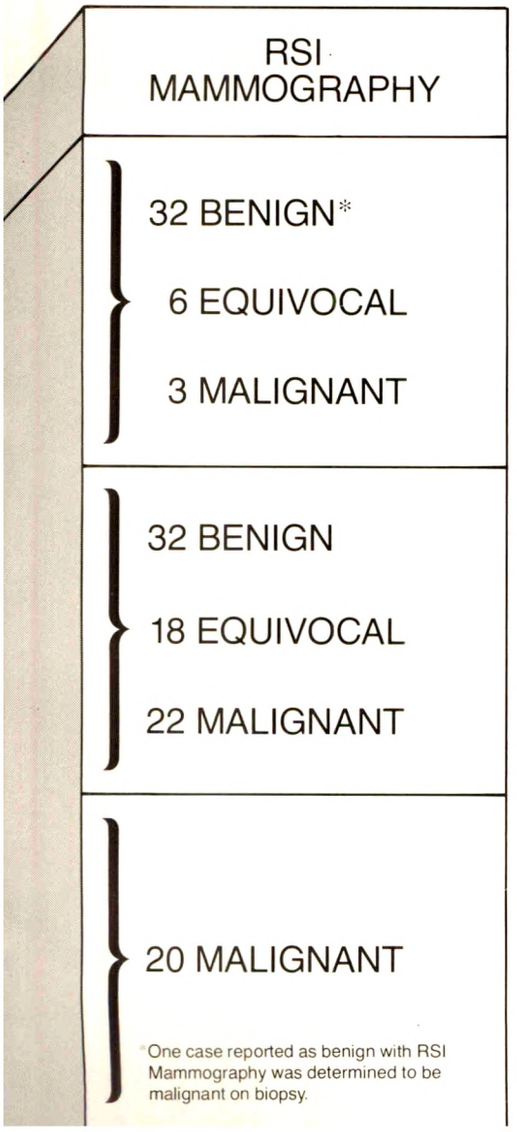

Out of 41 cases diagnosed as benign with conventional mammography, RSI Mammography determined that 3 of these cases were, in fact, malignant. In addition, with conventional mammography alone, 72 cases were diagnosed as equivocal and direct magnification mammography (RSI System) was able to differentiate these as: 22 malignant, 32 benign, and only 18 remained equivocal. This revealing clinical comparison clearly shows that RSI Magnification Mammography increases the certainty in diagnosis, decreases the time between examination and confirmation, and may even reduce the need for biopsy.

In a radiologic symposium presented in New York City, Dr. Sickles remarked, "...in dealing with difficult cases, we considerably improved our diagnostic accuracy [with RSI Magnification Mammography]."[2]

These more accurate diagnoses are the direct result of the capability of the RSI Mammography's System to give you—

- Clearer definition of mass borders
- Improved image sharpness and resolution
- Resolution of malignant microcalcifications often not discernible by conventional mammography
- Delineation of trabecular patterns

The RSI Mammography System offers high-detail resolution in the magnification mode as well as the conventional contact mode. The superior image which results from the exceptionally uniform focal spot provides a new level of confidence in the detection of breast cancer.

For more detailed information on the RSI Mammographic System and a reprint of the study published by Sickles *et al* in 1977, please write or call, Radiologic Sciences Inc., a subsidiary of Pfizer Inc., 235 East 42nd St., New York, N.Y. 10017 (212) 573-7941.

References: 1. Sickles, E.A., Doi, K.; Genant, H.K.: *Radiology* 125:69-76, October 1977. **2.** Sickles, E.A.: *Microfocal Spot Magnification Mammography.* Presented at a Symposium, New York City, June 1, 1978.

THE RSI MAMMOGRAPHIC SYSTEM

INCREASES DIAGNOSTIC ACCURACY

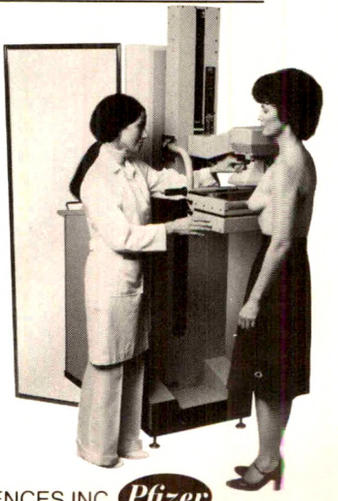

RADIOLOGIC SCIENCES INC. Pfizer
A subsidiary of Pfizer Inc., New York, N.Y. 10017

better

The 600 Beta Series Camera

Nice looking. The camera, we mean.

No need to pout. This camera won't let you make any careless mistakes, like forgetting to pull the dark slide.

Easy access. Takes the pain out of installation and service.

How do you name the heir to a classic?

We needed a way to tell the world that our new generation of 600 Series cameras was part of the original family of multi-format, video display cameras. But different. Totally redesigned for improved performance. But recognizably the same. So we picked the second letter of a classic alphabet – the Greek – and called it the Beta camera. It's second, but not second best. In fact, it's better.

Better than the camera that established the concept of multiple image hard copy on 8"×10" x-ray film? (And has the patent to prove it.) That has sold more units in this country and abroad than any of its numerous imitators? Hard to believe . . . hard to achieve. But true.

Better operating, for one thing. Single-handed front loading. Film cassette and dark slide interlocks that keep you from taking a picture when you shouldn't. Automatic Reset when a new film is loaded so you operate the camera almost without thinking.

We still offer the proven formats. And all the proven features, like flash card data entry, spot meter exposure system and footswitch remote operation. Our components will always be the finest available, including a new, high performance video monitor, Schneider lens and CMOS electronics.

This all pays off where it counts – in image quality. And when you see our images, you'll know for sure that Beta's not only better. It's best.

For more information, call collect or write: Dunn Instruments, Inc., 544 Second Street, San Francisco, CA 94107, (415) 957-1600

Dunn Instruments

The 600 Beta Series Camera

Single-handed front loading. Lets you install the Beta anywhere you like and load it on the run.

Ho hum. Simplified front panel controls make picture-taking a breeze.

Where Beta's best – superb clinical images in any format, positive or negative.

American Journal of Roentgenology Guidelines

Address manuscripts and correspondence to the Editorial Office, 403 Pacific National Bank Building, 4545 15th Avenue N.E., Seattle, Washington 98105; telephone (206)633-2754.

Publication Policy

The Journal publishes original and timely contributions to the advancement of radiologic diagnosis and treatment. Although the content is predominantly clinical, laboratory investigations are accepted when their relevance to clinical practice is demonstrable. Authors should indicate if informed consent was obtained. Decisions on manuscripts are based on the opinions of at least two outside reviewers. Statements within an article are the responsibility of the authors and not the Journal or its publisher. Reviewers receive manuscripts without title pages to protect the identity of authors and to ensure an unbiased review; names of reviewers, in turn, are never revealed to authors.

It is understood that material submitted has not been published and is not currently submitted elsewhere. Portions of the data or illustrations from previously published works may be included if permission release forms accompany the manuscript and such material is clearly credited in the text. Prior publication of abstracts will not prejudice publication of the complete study.

Copyright Information

In accordance with Journal implementation of the new U.S. Copyright Law, authors must release first and subsidiary rights to their manuscript at submission. A dated cover letter, containing signatures of all authors, should state: "We, the authors, assign first and subsidiary rights to the American Roentgen Ray Society in the event that our manuscript (title) is published by AJR." The Journal, in turn, grants authors the right to use portions of their manuscript, without charge, in books or articles of which they are authors or editors.

Manuscript Form

Manuscripts should be typed double-spaced throughout, including references, tables, and figure legends. Tables, footnotes, and figure legends should be on separate sheets, and a separate title page should be provided. In addition to the original typewritten copy, a duplicate copy complete with figures, tables, and references is required. Authors' names should be on title page only and should not be on figures so that author anonymity can be maintained during the review process.

Figures should be submitted as 13 × 18 cm glossy prints, untrimmed and unmounted. Labels and arrows must be of professional quality and should be removable from the prints. Each figure should be numbered to correspond with figure legends, and the top should be indicated. Specific permission for publication of facial photographs of patients is required. Line illustrations and graphs should be drawn in black ink on white background.

References should be cited in the text by number (e.g., [3, 4]). The bibliography should be arranged in the numerical order that references are cited in the text and typed double-spaced throughout. Data for each reference should be arranged according to the uniform style on bibliographic citations adopted by many biomedical journals. Provide all authors' names and inclusive pages. Abbreviations for titles of medical periodicals should conform to those published in *Index Medicus*. Examples:

1. Miller RE, Chernish SM, Skucas J, Rosenak BD, Rodda BE: Hypotonic roentgenography with glucagon. *Am J Roentgenol* 121:264–274, 1974
2. Boijsen E: Superior mesenteric angiography, in *Angiography*, edited by Abrams H, Boston, Little, Brown, 1971, pp 1091–1119

Organization

Title page. Titles should be brief and specific. Include addresses for each author and acknowledgment of grant support when appropriate.

Abstract. A description of the purpose, methods, results and conclusions of the study is required.

Introduction. Clearly state the purpose of the investigation including necessary background facts.

Materials and methods. Decribe the protocol clearly. Use standard abbreviations as presented in the *Council of Biology Editors Style Manual*, 3d ed. Metric measurements should be used throughout.

Results. Present results in logical sequence.

Discussion. Interpret the results to lend meaning and importance to the observations. If hypotheses and speculation are included, they must be labeled as such. When results differ from those of previous investigators, an attempt should be made to explain the discrepancy.

References. Only include references which provide adequate background and present fairly any opposing evidence and concepts. Accuracy of reference data is the responsibility of the author.

Legends. Legends should be brief but should provide sufficient description to interpret the figure.

Special Communications

Case Reports. Concise case reports are accepted if they present unusual experiences that are medically important and educational. Clarity and brevity are essential. After preliminary screening by an editor to determine whether the requirement of medical significance has been met, qualifying papers will undergo the same peer review as major papers.

Technical notes. Brief descriptions of new techniques or significant modifications of older ones which are directly applicable to clinical practice will be accepted.

Letters to the Editor. Letters are subject to editing and condensation. Criticism of published articles should be objective and constructive. Letters may also discuss matters of general interest to radiologists.

Prospective Comparison of Ultrasound and Computed Tomography in the Evaluation of Gynecologic Pelvic Masses

JAMES W. WALSH,[1, 2] ARTHUR T. ROSENFIELD,[1] C. CARL JAFFE,[1] PETER E. SCHWARTZ,[3] JOSEPH SIMEONE,[1] ALAN G. DEMBNER,[1] AND K. J. W. TAYLOR[1]

A prospective evaluation of computed tomography and ultrasound was performed on 24 consecutive patients with suspected pelvic masses. Of the 24 patients, 22 had subsequent surgical identification of abnormalities; two were considered normal on clinical follow-up. Ultrasound provided important clinical information in 17 of 24 patients; CT in 15 of 24 patients. There were three false negative examinations with each method and no false positives. Differentiation between benign and malignant disease could not be made in four of 24 patients by ultrasound and five of 24 patients by CT. Because both imaging techniques depict similar pathology and use similar diagnostic criteria, the two methods tend not to be complementary.

Traditionally the preoperative radiologic evaluation of patients suspected of having a pelvic malignancy is limited to barium enema examination and excretory urography in search of mass effect on the bowel lumen or the urinary tract. Pelvic pneumography which may show the lesion directly is not commonly used. Ultrasound and computed tomography (CT) also permit direct evaluation of the lesion. This paper compares the usefulness and diagnostic accuracy of gray scale ultrasound and CT used prospectively in 17 women with pelvic lesions of undetermined etiology and in seven patients with known pelvic malignancies, prior to "second look" surgery. Several reports indicate the diagnostic accuracy of ultrasound in the evaluation of pelvic masses [1–3]. To our knowledge, only two studies report the use of CT in the definition and delineation of gynecologic pelvic masses [4, 5]. We are not aware of any previous studies in which both methods were prospectively applied to a group of patients with a wide variety of surgically proven lesions.

Subjects and Methods

A group of 24 consecutive female patients thought clinically to have a pelvic mass was prospectively studied by both ultrasound and computed tomography. These imaging procedures were completed within a 3 day period in most patients. Of the 24 patients, 22 had surgical or biopsy confirmation of their disease within 7 days after the imaging studies. Two patients with normal ultrasound and CT scans had normal clinical follow-up for 5 months. Each preoperative study was evaluated independently without the knowledge of other radiographic procedures or of the specific site of disease on pelvic examination. Interpretation from Polaroid film (ultrasound) or film copy (CT) was performed on the day of examination by the radiologist who monitored the study.

All CT examinations were performed on the Pfizer 0200FS ACTA Scanner. The scan duration was 18 sec and the images were displayed on a 320 × 320 matrix and recorded on film. Patients were administered 1 mg of intravenous glucagon to limit bowel peristalsis, 400 ml of 4% Gastrografin to outline the small bowel, and 50–100 ml of intravenous Renografin 60% to outline the urinary tract. Then routine 13-mm-thick sections were taken at 2 cm intervals between centers of sections from the level of the kidneys to below the level of the symphysis pubis. The liver was not routinely studied.

Gray scale ultrasound examinations were performed with the Searle PhoScanic, Picker EDC, or Picker 80L equipment, at a transducer frequency of 2.25 or 3.5 MHz depending upon the patient's size. The pelvis was routinely scanned with the full bladder technique in transverse and sagittal sections at 1 cm intervals. Transverse and sagittal sections of the liver and prone or decubitus sections of each kidney were also performed.

The postoperative pathologic diagnosis was correlated with the official preoperative ultrasound and CT diagnosis in each patient and the results scored. Studies were considered diagnostic when the imaging technique resulted in a specific histologic diagnosis or when a malignant tumor and its organ site were correctly identified. The examination was considered contributory when a combination of the tissue consistency and correct organ, or malignant tumor without organ site, was detected. The procedure was considered nonspecific when the consistency of a pelvic mass was demonstrated, but the specific histologic nature or organ site could not be stated. A false negative was scored when the lesion was not detected. A false positive was scored when predicted pathology was not present at surgery.

Results

The pathologic diagnoses and diagnostic value of the data are classified in table 1. This study includes 22 abnormal and two normal studies. No false positives occurred.

Ovarian Tumors

Six patients had primary ovarian neoplasms. Malignancies included adenocarcinoma, cystadenocarcinoma, and an endodermal sinus tumor. One patient had bilateral ovarian cystadenomas. Ultrasound was diagnostic in five of the six cases of ovarian neoplasm and contributory in one. CT was diagnostic in one case,

Received March 16, 1978; accepted after revision September 12, 1978.
Presented at the annual meeting of the Computerized Tomography Society Seminar, Washington, D.C., February 1978.
[1]Department of Diagnostic Radiology, Yale University School of Medicine, 333 Cedar Street, New Haven, Connecticut 06510. Address reprint requests to A. T. Rosenfield.
[2]Present address: Department of Radiology, Medical College of Virginia, Richmond, Virginia 23298.
[3]Department of Obstetrics and Gynecology, Yale University School of Medicine, New Haven, Connecticut 06510.

© 1978 American Roentgen Ray Society

contributory in three, and nonspecific in two. Careful comparison of ultrasound and CT images showed almost identical gross morphology of the lesions. Solid and cystic areas and septations could be comparatively depicted (fig. 1). The neoplasms were predominantly solid with small cystic components in three cases, predominantly cystic in two cases, and solid with a necrotic central cavity in one case (fig. 2). Hydronephrosis was present by ultrasound in two patients, one of whom was also identified by CT. Gross ascites was demonstrated in one patient by both methods and minimal ascites in another patient by ultrasound. Paraaortic adenopathy was correctly identified by CT in one patient and not detected in one patient by both methods. No hepatic metastases were noted by either method in each of the six patients.

TABLE 1

Types of Pelvic Masses versus Diagnostic Accuracy

	Diagnostic	Contributory	Nonspecific	False Negative	False Positive
Ovarian neoplasm:					
Benign:					
CT	...	1	...	...	...
Ultrasound	1	...	...	...	...
Malignant:					
CT	1	2	2	...	...
Ultrasound	4	1	...	...	...
Recurrent cancer of ovary:					
CT	3	...	...	2	...
Ultrasound	3	...	1	1	...
Ovarian cysts:					
CT	...	...	1	...	...
Ultrasound	...	...	1	...	...
Uterine fibroid:					
CT	1	1	2	...	...
Ultrasound	1	1	2	...	...
Cancer endometrium:					
CT	1	1	...	...	...
Ultrasound	...	2	...	...	...
Cancer cervix:					
CT	...	1	1	...	...
Ultrasound	2	...	...	...	...
Recurrent cancer of cervix:					
CT	1	...	...	1	...
Ultrasound	...	...	...	2	...
Normal:					
CT	2	...	...	...	...
Ultrasound	2	...	...	...	...
Totals:					
CT	9	6	6	3	0
Ultrasound	13	4	4	3	0

Uterine Tumors

Four patients with uterine fibroids presented unexpected difficulties. Both imaging procedures were diagnostic in only one patient. In two patients the abnormality could not be clearly localized to the uterus or ovary. In the fourth patient the complex solid and cystic lesion was so large that an ovarian neoplasm was simulated (fig. 3).

A retrospective comparison of the CT and ultrasound appearance of uterine fibroids revealed a distinct difference in their patterns. On ultrasound three patients showed the typical disrupted internal uterine architecture with focal areas of increased or decreased echogenicity. CT scans in two of these cases demonstrated a uniformly solid uterine consistency (fig. 4). In only one patient did CT show focal zones of decreased attenuation in the uterus. Visualization of fibroid calcification by CT was helpful in only one patient.

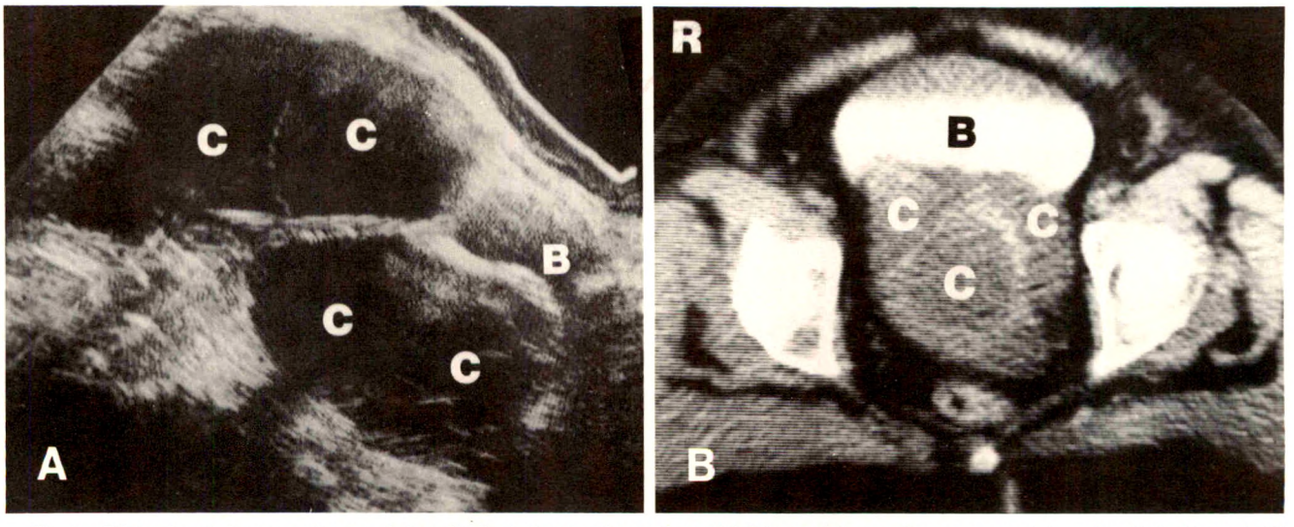

Fig. 1.—Bilateral cystadenomas of ovary. *A*, Longitudinal ultrasound scan through left true pelvis revealing mass consisting of multiple thin cysts (C) with septa. There is no solid component in tumor. (B = bladder.) *B*, CT scan showing multiple cysts (C) separated by septa in retrovesical region.

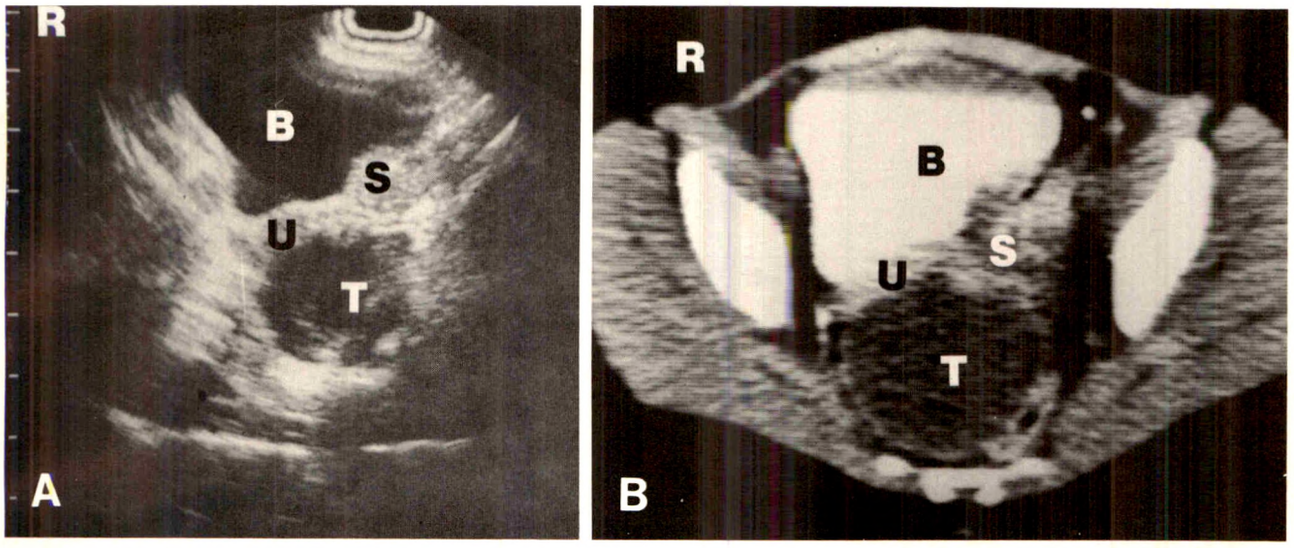

Fig. 2.—Adenocarcinoma of left ovary. *A*, Transverse ultrasound scan through true pelvis showing tumor mass with necrotic center (T) and solid component (S) invading left side of bladder (B). Part of mass is behind uterus (U). *B*, CT scan through true pelvis showing tumor mass with low density center (T) behind uterus (U). Solid component (S) of tumor invades left posterior bladder (B).

Fig. 3.—Uterine fibroid. *A*, Longitudinal ultrasound scan through middle true pelvis showing enlargement of uterus with irregular low level echoes throughout visualized uterine cavity (F) consistent with a fibroid uterus. (B = bladder.) *B*, Transverse ultrasound scan through true pelvis 5 cm above symphysis pubis revealing fibroid uterus (F) with inhomogenous echo pattern indenting left superior portion of bladder (B). *C*, CT scan superior to bladder showing enlargement of uterus (F) with central low density region (*arrowhead*).

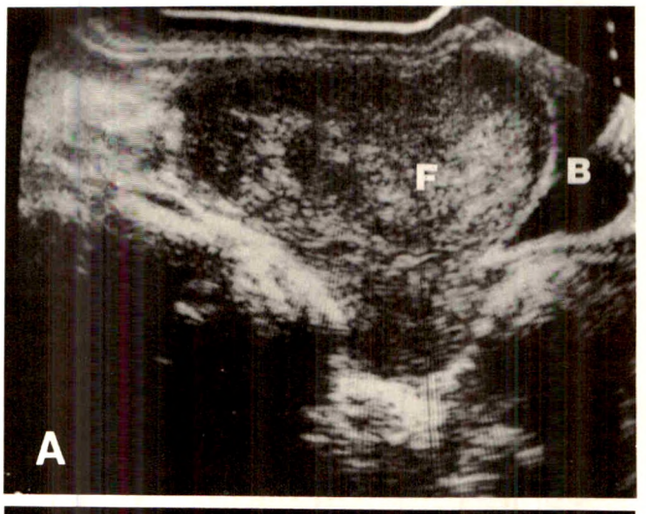

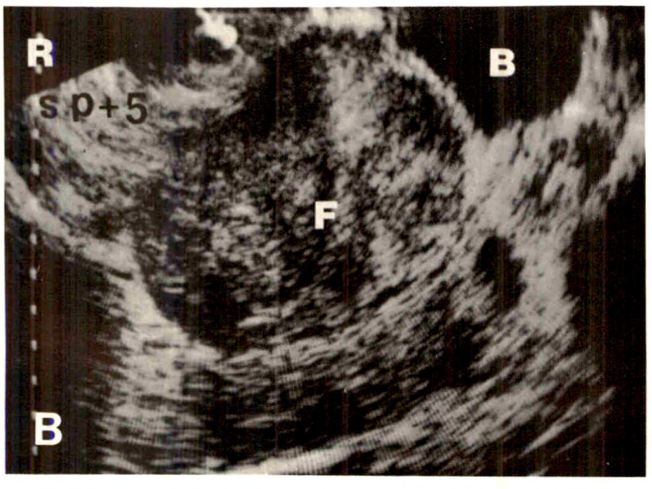

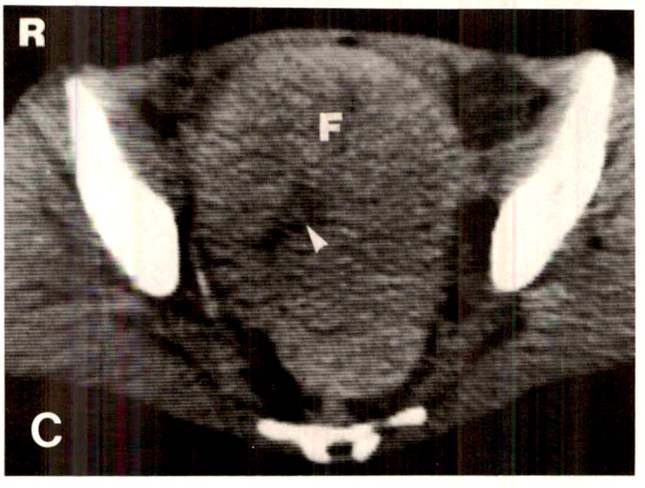

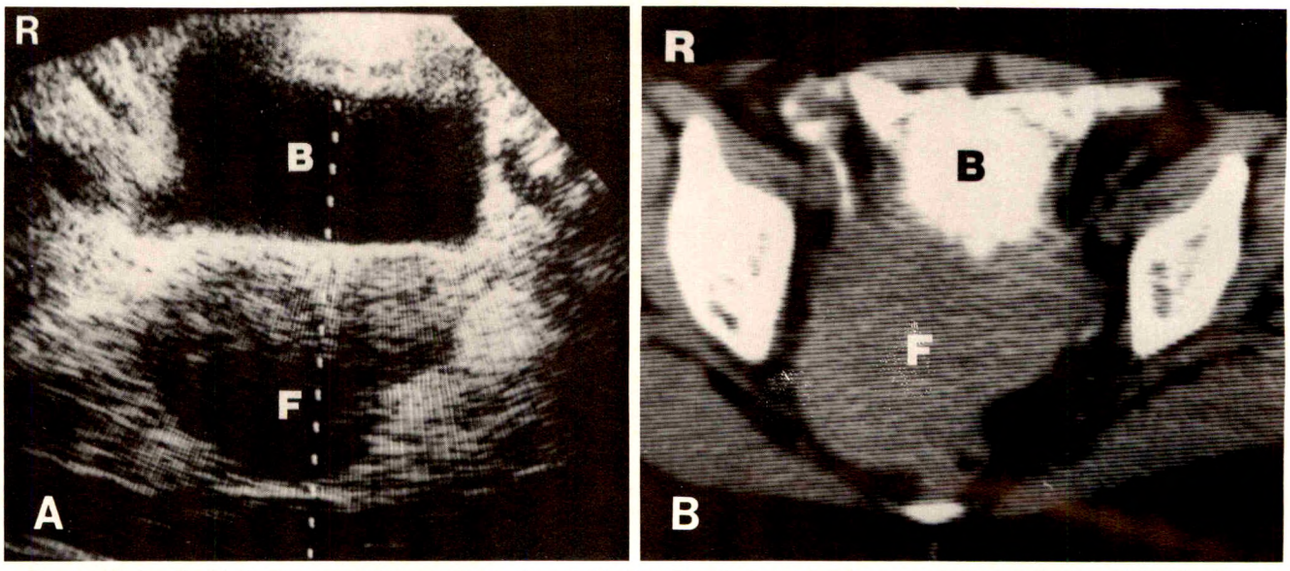

Fig. 4.—Uterine fibroid. *A*, Transverse ultrasound scan through bladder (B) and uterus showing zone of decreased echogenicity (F) with poor transmission of ultrasound beam in uterus consistent with fibroid. Note that uterus is lobulated. *B*, CT scan through true pelvis showing lobulated fibroid uterus (F) with uniform soft-tissue density behind bladder (B).

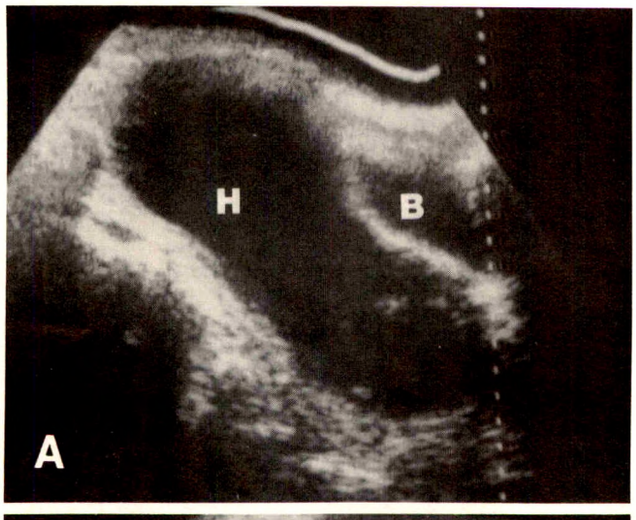

Fig. 5.—Hematometra secondary to carcinoma of endometrium. *A*, Longitudinal ultrasound scan through bladder (B) showing enlarged and fluid-filled uterus (H). Uterine walls are irregular and a few scattered echoes are present in cavity. *B*, Transverse ultrasound scan through true pelvis revealing enlarged uterine cavity filled with liquified blood (H) posterior to bladder (B). *C*, CT scan of true pelvis demonstrating bladder (B) displaced to right by enlarged uterus with low density center (H) representing hematometra.

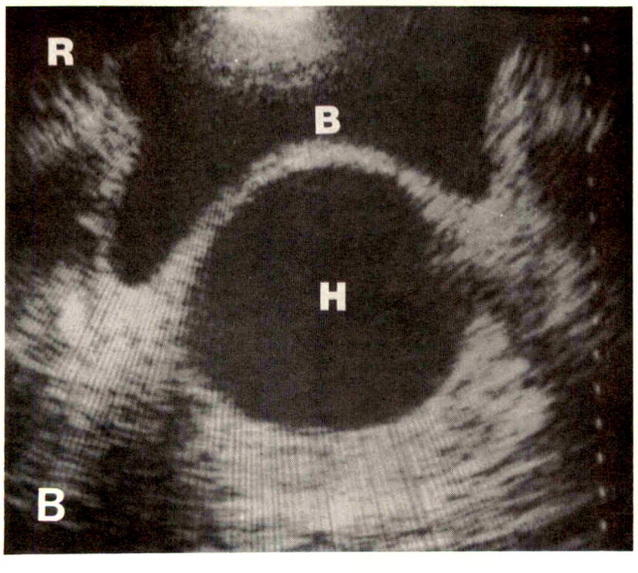

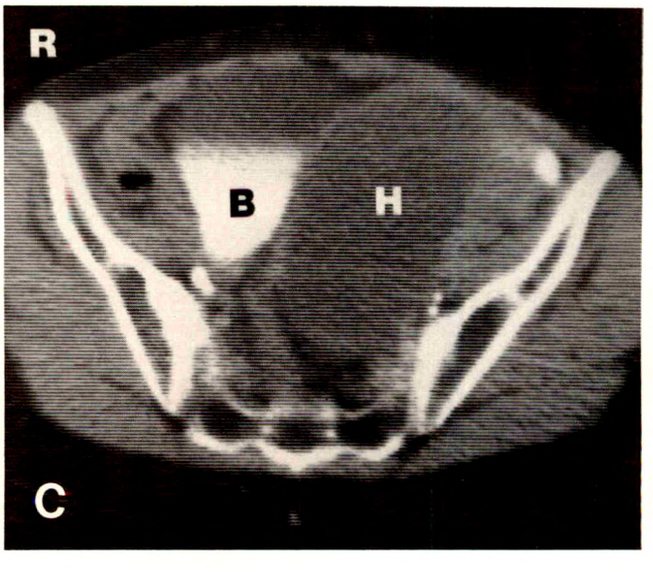

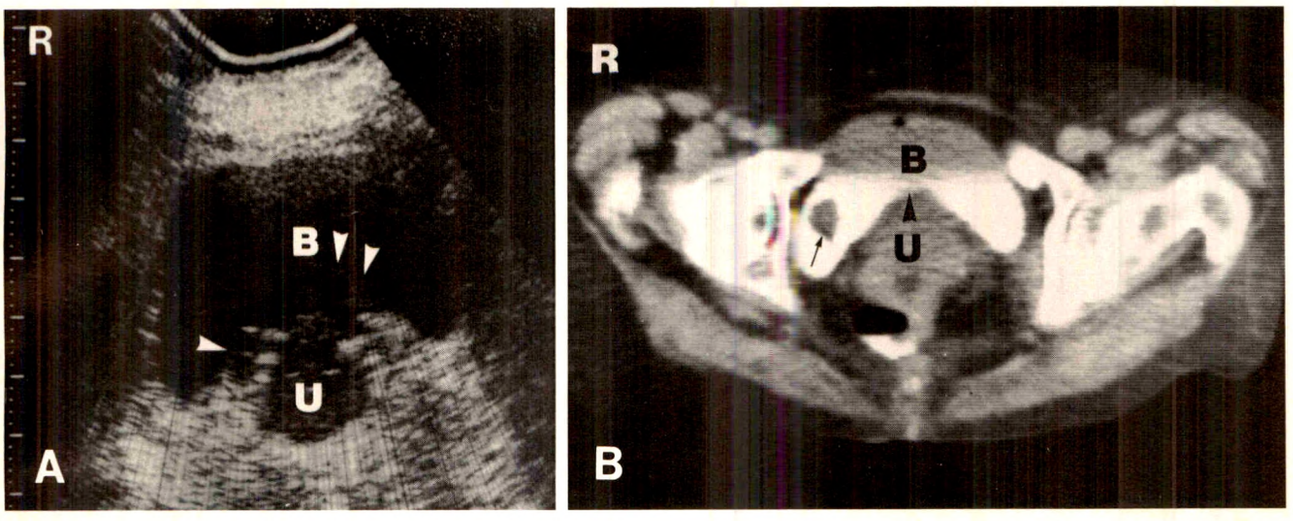

Fig. 6.—Carcinoma of cervix. *A*, Transverse ultrasound scan through true pelvis at level of cervical canal showing enlargement of uterus (U) by solid mass which invades (*arrowheads*) bladder (B). *B*, CT scan through true pelvis demonstrating enlargement of uterus (U) behind bladder (B). Invasion of bladder base (*arrowhead*) is present. Tumor nodule (*arrow*) is seen in right portion of bladder.

Carcinoma of the endometrium was correctly diagnosed by CT in one case. The finding consisted of a large solid mass with irregular necrotic center lying behind the bladder. Contributory ultrasound demonstrated a midline irregular solid pelvic mass with coexistent right hydronephrosis and minimal ascites. In a second patient, ultrasound and CT identified a large midline cystic structure with thick walls as a malignancy (fig. 5). At surgery, hematocolpos and hematometra were removed. Malignant endometrial cells lined the uterine cavity.

Ultrasound was diagnostic in two patients with carcinoma of the cervix, whereas CT was contributory in one and nonspecific in the other. The morphology of the lesions by both methods was that of an irregular solid retrovesical mass in the position of the uterus. In one patient tumor extension into the bladder anteriorly was demonstrated by both studies (fig. 6). Hydronephrosis was identified in both patients by both methods.

Ultrasound was falsely negative in two patients with recurrent cervical carcinoma. In one patient CT demonstrated a mass in the left iliac fossa involving the left iliopsoas muscle. A recurrence involving the sigmoid colon serosa was discovered at surgery. In one patient metastatic tumor involving the perirectal soft tissues, cervix, and posterior vaginal wall was not detected by either method.

Both methods were nonspecific in one patient with two hemorrhagic cysts of the ovary. Two patients with normal imaging procedures had no evidence of pelvic mass on follow up clinical examination.

Discussion

In the preoperative diagnosis and management of patients with gynecologic pelvic masses, gray scale ultrasound or computed tomography can provide significant clinical data. In our series, ultrasound was diagnostic in 13 of 24 examinations. If contributory studies are included, ultrasound yielded important clinical information in 17 of 24 patients. In comparison, CT was diagnostic in nine of 24 patients. Excluding nonspecific and false negative exams, CT provided important clinical data in 15 of 24 patients. Pelvic pathology was undetected by both methods in three patients, each with recurrent tumor.

In patients with an ovarian neoplasm, gray scale ultrasound seems to have an advantage as an imaging technique and is diagnostic in the majority of patients. This primarily results from the ability to view the pelvis rapidly in two planes, demonstrate the ovaries in nearly all cases, and clearly separate the uterus from the adnexae. Ultrasound can also demonstrate small amounts of ascites in the pouch of Douglas and the hepatorenal angle. Hydronephrosis is well demonstrated by both methods. Inability to identify normal ovaries among the other pelvic structures is a limitation of CT.

CT and ultrasound were equally effective in demonstrating recurrent ovarian carcinoma in three of five cases. However, because of several false negative examinations, neither method can eliminate "second look" surgery in the management of ovarian carcinoma. Small deposits of metastatic tumor on the bowel serosa or in the omentum are beyond the current resolution of both ultrasound and CT systems.

In about four of 24 patients examined by ultrasound and five of 24 by CT, a differentiation between benign and malignant disease could not be made. The presence of hydronephrosis was a particularly valuable sign of malignancy with relatively small lesions, and routine renal imaging proved useful in this regard. Nonetheless, it remains extremely difficult to distinguish a solid ovarian tumor from a pedunculated fibroid by either method.

In patients with cervical carcinoma, ultrasound seems to have advantages over CT because the easily obtained sagittal projection more adequately demonstrates the

U. OF MEDICINE

anatomic relationship of the cervix to the vaginal canal and the body of the uterus. In this projection, changes in consistency, size, and organ outline are more easily seen. Carcinoma of the endometrium is well depicted on both methods.

Recurrent cervical carcinoma was not successfully evaluated in this study. None of the patients in this series had pelvic lymphadenopathy and only two patients had paraaortic lymph node metastases. Thus, the imaging techniques were not specifically tested for this form of pathology.

We conclude that at present, ultrasound is an effective screening technique for the presence of gynecologic pelvic masses and the evaluation of their consistency. CT provides comparable diagnostic information. Although the accuracy rate of ultrasound was slightly higher than CT, our numbers were too small for statistical analysis. Because both imaging techniques depict similar pathology and use similar diagnostic criteria, the two methods tend not to be complementary for pathology in the true pelvis. Except for questions of tumor recurrence, the routine use of both techniques for a diagnosis of pelvic masses may not be justified.

REFERENCES

1. Kobayashi M: Use of diagnostic ultrasound in trophoblastic neoplasms and ovarian tumors. *Cancer* 38:441–452, 1976
2. Levi S, Delval R: Value of ultrasonic diagnosis of gynecological tumors in 370 surgical cases. *Acta Obstet Gynecol Scand* 55:261–266, 1976
3. Bowie JD: Ultrasound of gynecologic pelvic masses: the indefinite uterus and other patterns associated with diagnostic error. *JCU* 5:323–328, 1977
4. Schapiro RL, Chiu LC: An introduction to abnormal computed anatomy. III. The pelvis. *Comput Axial Tomogr* 1:219–225, 1977
5. Redman HC: Computed tomography of the pelvis. *Radiol Clin North Am* 15:441–448, 1977

Sonolucent Areas in the Placenta: Sonographic and Pathologic Correlation

BEVERLY A. SPIRT,[1] EUGENE H. KAGAN,[2] AND RICHARD M. ROZANSKI[1]

With the advent of gray scale ultrasonography, the internal structure of the placenta can be defined in great detail. Subchorionic sonolucent areas visualized on antepartum sonograms correlate with areas of subchorionic fibrin deposition, hematoma, and cystic degeneration in the term placenta. These lesions are apparently of no clinical significance. However, diffuse intraplacental sonolucent cystic lesions are abnormal and are seen in both hydatidiform mole and hydropic swelling of the placenta.

The recent advances in ultrasound imaging have made it possible to visualize in greater detail the internal structure of the placenta. Differences in the echo pattern of the placenta at various stages of gestation have been described [1, 2]. In addition to these normal variations, we noted focal sonolucent areas within the placenta in a number of patients. This paper presents sonographic, pathologic, and clinical correlation of this finding.

Subjects and Methods

Ten cases of subchorionic sonolucent areas and one case of diffuse intraplacental sonolucent areas were studied with pathologic correlation. An example of hydatidiform mole is also included for comparison. Ultrasonography was performed with a Unirad Sonograph II (GZD). The more recent studies were performed with a 3.5 MHz transducer, 13 mm or 19 mm in diameter, and earlier studies with a 2.25 MHz transducer, 19 mm in diameter. After delivery, the placentas were examined grossly by both the pathologist and the sonographer. The placentas were serially sectioned in the vertical plane at 1 cm intervals in the fresh state. They were then fixed in 10% formalin and appropriate histologic sections were taken.

Results

We noted subchorionic sonolucent areas in about 10%–15% of obstetric sonograms. Placentas were obtained in 10 cases in which such lesions were documented. The pathologic findings in each case were similar.

Diffuse intraplacental sonolucent lesions are uncommon. They occur in cases of hydatidiform mole and in hydatidiform swelling of an otherwise normal placenta. The placenta obtained in one case of diffuse intraplacental sonolucent lesions, in an apparently viable pregnancy, had the pathologic changes of hydatidiform swelling.

Representative Case Reports

Case 1: Subchorionic Sonolucent Areas

A 25-year-old woman had two previous stillbirths. Base line sonography requested at 23 weeks in view of this history, demonstrated multiple subchorionic sonolucent areas (fig. 1*A*). A follow-up study at 29 weeks demonstrated a large (12 × 2 cm) confluent subchorionic sonolucent space (fig. 1*B*). The sonolucent areas appeared smaller on repeat sonography at 34 weeks gestational age (fig. 1*C*). The pregnancy was uneventful. The patient went into spontaneous labor at term and delivered a healthy child. Upon gross examination of the placenta, multiple subchorionic cysts were identified. The chorionic membrane appeared thickened and opaque (fig. 1*D*). Beneath the chorion were large deposits of fibrin which had undergone cystic degeneration. Proteinaceous material was found within the cystic space (fig. 1*E*).

Case 2: Subchorionic Sonolucent Areas

A 22-year-old gravida three patient underwent sonography for confirmation of dates. The examination demonstrated multiple subchorionic sonolucent areas (fig. 2*A*) in a 35 week pregnancy. A follow-up examination at 38.5 weeks confirmed the previous findings. One week after the second sonogram, the patient went into spontaneous labor and delivered a healthy child. The placenta, delivered spontaneously intact, contained multiple raised white subchorionic areas corresponding to the subchorionic lesions noted on sonography (fig. 2*B*). Microscopic examination of these areas demonstrated fibrin deposition with evidence of fresh hemorrhage (fig. 2*C*). Hemosiderin was present, indicating older hemorrhage.

Case 3: Diffuse Intraplacental Sonolucent Lesions

A 17-year-old primigravida had severe preeclampsia. The urinary human chorionic gonadotropin level was within normal limits. Blood pressure was 180/100 and she had 3 plus proteinuria. Sonography at 17 weeks demonstrated a large placenta with multiple cystic spaces (fig. 3*A*). Fetal movement was present. Shortly after sonography, the patient experienced a grand mal seizure and was hyperreflexic. A hysterotomy was performed. A 14 cm fetus with spina bifida and a 450 g placenta was removed (fig. 3*B*). The placenta contained multiple cystic areas. Within 12 hr after surgery, blood pressure and reflexes had returned to normal. Only trace proteinuria was present. Microscopic examination of the placenta demonstrated avascular villi with hydropic change, but without trophoblastic

Received February 7, 1978; accepted after revision August 9, 1978.
Presented at the annual meeting of the American Roentgen Ray Society, Boston, September 1977.
[1]Department of Radiology, State University of New York, Upstate Medical Center, Syracuse, New York 13210. Address reprint requests to B. A. Spirt.
[2]Department of Pathology, Crouse-Irving Memorial Hospital, Syracuse, New York 13210.

© 1978 American Roentgen Ray Society

0361–803X/78/1200–0961 $00.00

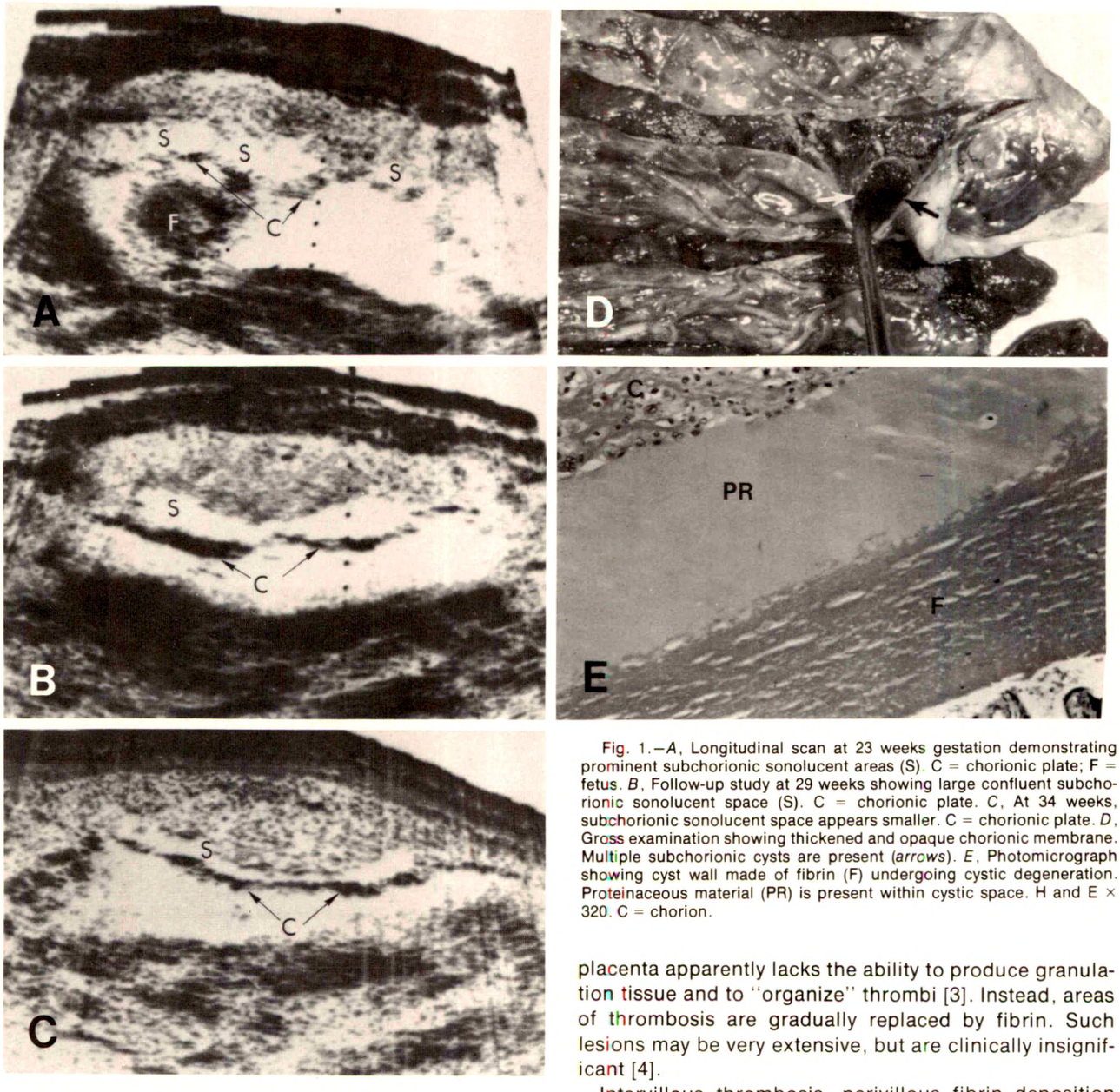

Fig. 1.—*A*, Longitudinal scan at 23 weeks gestation demonstrating prominent subchorionic sonolucent areas (S). C = chorionic plate; F = fetus. *B*, Follow-up study at 29 weeks showing large confluent subchorionic sonolucent space (S). C = chorionic plate. *C*, At 34 weeks, subchorionic sonolucent space appears smaller. C = chorionic plate. *D*, Gross examination showing thickened and opaque chorionic membrane. Multiple subchorionic cysts are present (*arrows*). *E*, Photomicrograph showing cyst wall made of fibrin (F) undergoing cystic degeneration. Proteinaceous material (PR) is present within cystic space. H and E × 320. C = chorion.

proliferation (fig. 3*C*). Areas of normal placental tissue were present as well.

Discussion

Subchorionic Fibrin Deposition

Significant subchorionic fibrin deposition is seen grossly in varying degrees in at least 15% of "normal" placentas [3]. It usually appears as triangular laminated yellow-white plaques which may range in size from a few millimeters to several centimeters. Fresh clot or secondary cyst formation is sometimes found within the plaques.

Subchorionic fibrin deposition is thought to be the result of stasis of maternal blood in the intervillous space beneath the chorion, which leads to thrombosis. The placenta apparently lacks the ability to produce granulation tissue and to "organize" thrombi [3]. Instead, areas of thrombosis are gradually replaced by fibrin. Such lesions may be very extensive, but are clinically insignificant [4].

Intervillous thrombosis, perivillous fibrin deposition and true infarction also result in macroscopic fibrin plaques within the placenta [3, 5]. We have not diagnosed any of these lesions sonographically.

Diffuse Intraplacental Sonolucent Lesions

Hydatidiform mole. A hydatidiform mole is an abnormal placenta in which most or all of the villi form grapelike vesicles. The sonographic pattern in hydatidiform mole is suggestive of multiple cysts (fig. 4*A*). Multiple grapelike cysts are noted on gross examination (fig. 4*B*). Avascular villi, hydropic change, and trophoblastic proliferation are demonstrated microscopically (fig. 4*C*). Invasive mole and metastatic choriocarcinoma are complications of true hydatidiform molar disease.

Hydatidiform swelling. The term "hydatidiform swell-

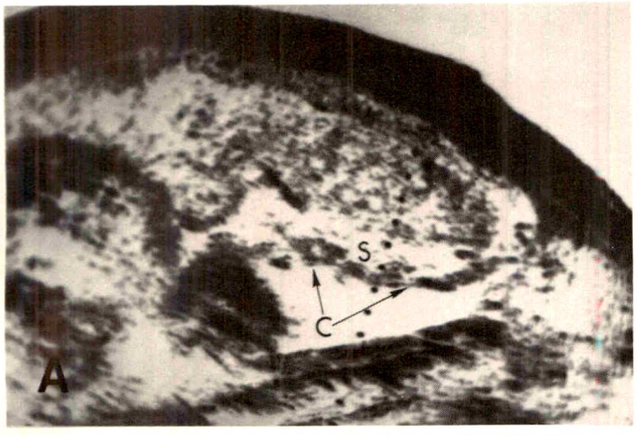

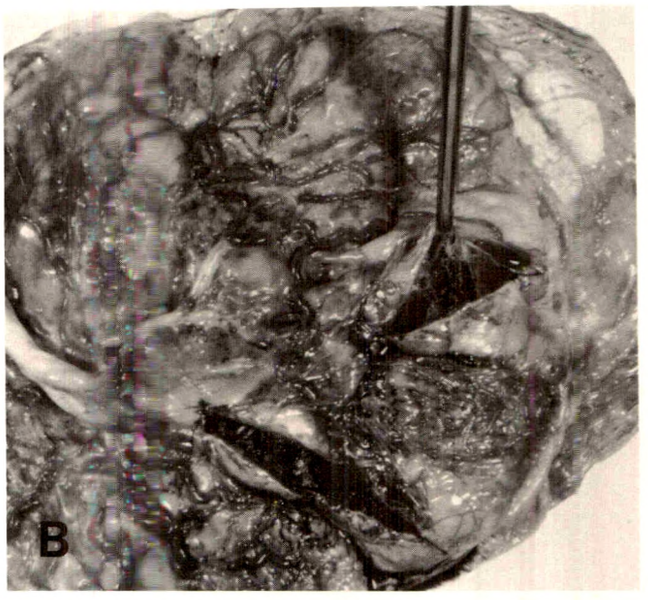

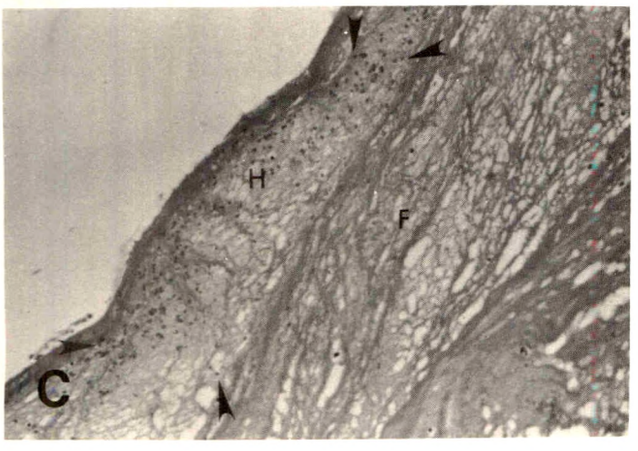

Fig. 2.–*A*, Longitudinal sonogram at 35 weeks showing large subchorionic sonolucent area (S). C = chorion. *B*, Gross examination of placenta showing multiple raised grey-white subchorionic areas. *C*, Photomicrograph of subchorionic lesion showing fibrin deposition (F) with evidence of fresh hemorrhage (H, *arrows*). H and E × 320.

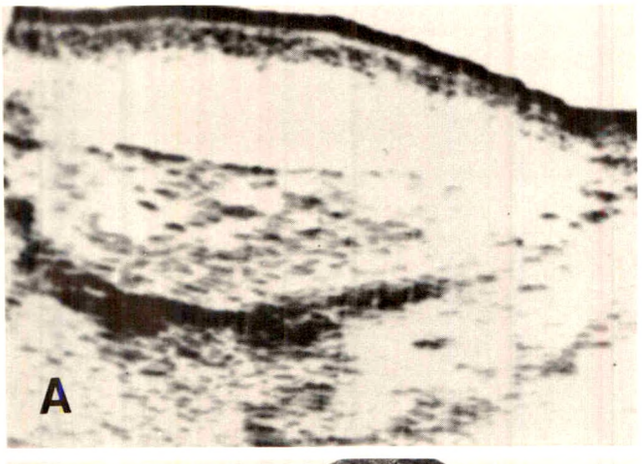

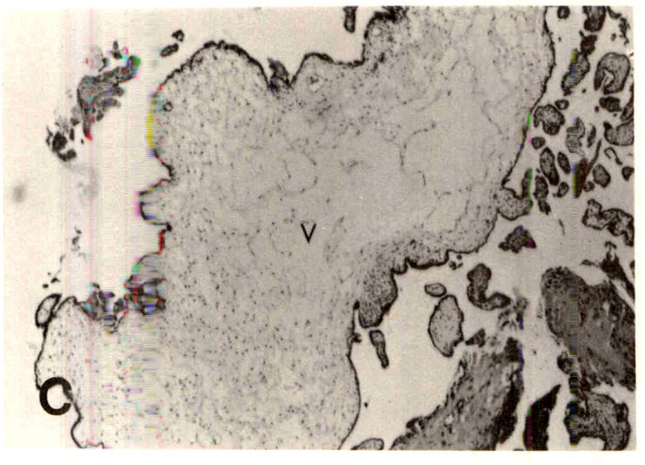

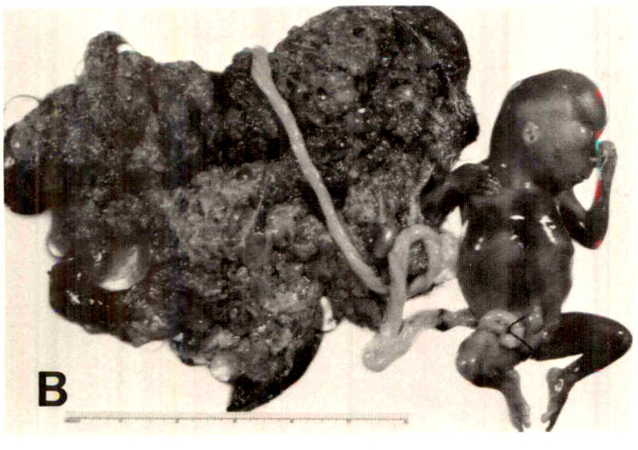

Fig. 3.–*A*, Longitudinal sonogram at 17 weeks showing multiple intraplacental sonolucent areas. *B*, Hysterotomy specimen demonstrating 14 cm fetus and 450 g placenta with multiple cystic areas. *C*, Photomicrograph showing avascular villus (V) with hydropic change, but without trophoblastic proliferation.

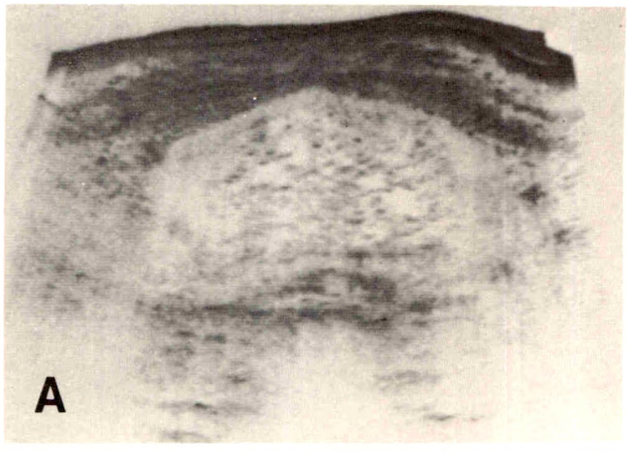

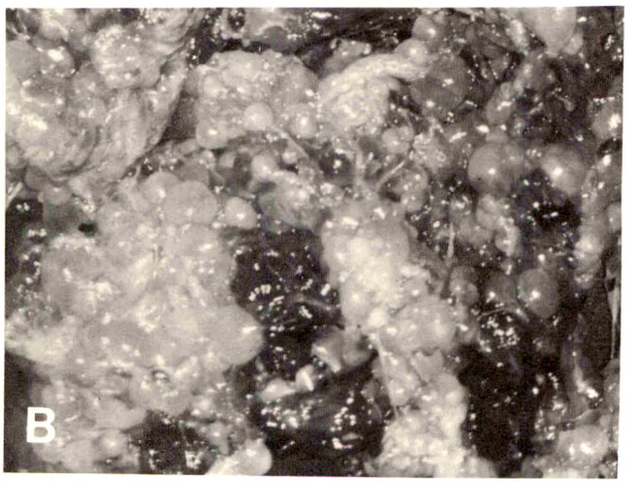

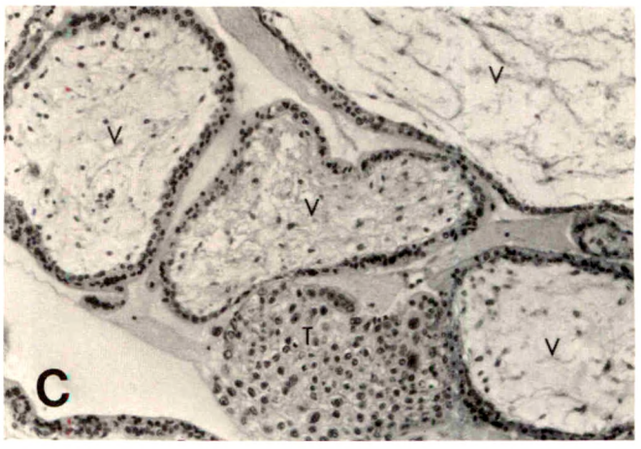

Fig. 4.—*A*, Sonogram of hydatidiform mole showing vesicular echo pattern. *B*, Gross examination showing multiple grapelike cysts. *C*, Photomicrograph showing avascular villi (V), hydropic change, and trophoblastic proliferation (T). H and E × 80. *B and C* courtesy of Dr. David B. Jones, Department of Pathology, Upstate Medical Center, Syracuse, New York.

ing" refers to varying degrees of hydropic change and avascularity without significant trophoblastic proliferation in an otherwise normal placenta. Hydropic swelling may be associated with an abortion, or with a stillborn or living fetus. Significant trophoblastic proliferation is not present and malignant change does not occur. Hydatidiform swelling should be distinguished from hydatidiform mole because of its different prognosis [6].

The sonographic pattern of the placenta in hydatidiform swelling is indistinguishable from that of hydatidiform mole. However, the presence of a fetus favors the diagnosis of hydatidiform swelling. The rare association of a true mole with a fetus is presumed to represent a binovular conception with the fetus and normal placenta from one ovum and the molar tissue from the abnormal ovum.

We reviewed multiple case reports of coexistent fetus and "hydatidiform mole" [7–12], including rare cases with a living fetus. Most of these cases are poorly documented in terms of their pathologic findings, and the distinction between true hydatidiform mole and hydatidiform swelling is not clearly made. Benirschke and Driscoll [4] observed that none of the cases of reported "moles" associated with large fetuses, viable fetuses, and twins developed malignant trophoblastic disease. While this may reflect incomplete reporting, they suggest that these lesions are different from the classic hydatidiform moles in pathogenesis and prognosis.

Conclusions

Subchorionic sonolucent areas are fairly common. These correlate with areas of increased subchorionic fibrin deposition, hematoma, and cystic degeneration, and are apparently not clinically significant. The placenta is an organ with considerable reserve capacity. Most macroscopic lesions are clinically insignificant unless they involve a large portion of the placental substance.

Diffuse intraplacental sonolucent lesions are an abnormal finding seen in both hydatidiform mole and in hydropic swelling of the placenta. Grossly, these latter two entities may appear similar. However, they appear to differ in microscopic findings and in their prognostic implications.

ACKNOWLEDGMENTS

We thank our obstetrical colleagues in the Greater Syracuse Area for their cooperation: Lori Champlin for technical assistance, John Hodgson and Charles Reiner for photography, and Virginia Renehan for clerical assistance.

REFERENCES

1. Fisher CC, Garrett W, Kossoff G: Placental aging monitered by grey scale echography. *Am J Obstet Gynecol* 124:483–488, 1976
2. Winsberg F: Echographic changes with placental aging. *JCU* 1:52–55, 1973
3. Fox H: White infarcts of the placenta. *J Obstet Gynaecol Br Commonwealth* 70:980–991, 1963
4. Benirschke K, Driscoll SG: *The Pathology of the Human Placenta*. New York, Springer, 1967
5. Fox H: Morphological pathology of the placenta, in *The Placenta and Its Maternal Supply Line*, edited by Gruenwold P, Baltimore, University Park Press, 1975, pp 197–220
6. Ziel HA Jr: Coexistence of fetus and hydropic swelling of placental villi. *Obstet Gynecol* 21:502–505, 1963

7. Ballas S, Peyser MR, Toaff R: Diagnosis of hydatidiform mole with and without coexistent fetus by non-stored image echography. *Obstet Gynecol* 50:182–185, 1977
8. Barone CM: Ultrasonic diagnosis of hydatidiform mole with a coexistent fetus. *Radiology* 124:798, 1977
9. Bruse JE: Hydatidiform mole with coexistent fetus. *Proc R Soc Med* 65:864–865, 1972
10. Jones WB, Lauersen NH: Hydatidiform mole with coexistent fetus. *Am J Obstet Gynecol* 122:267–272, 1975
11. Beischer NA: Hydatidiform mole with co-existent fetus. *J Obstet Gynaecol Br Commonwealth* 68:231–237, 1961
12. Brown DB: A case of co-existing hydatidiform mole and living child. *J Obstet Gynaecol Br Commonwealth* 64:446–447, 1957

Analysis of Ultrasonographic Criteria in the Evaluation for Ectopic Pregnancy

THOMAS W. BROWN,[1] ROY A. FILLY,[2] FAYE C. LAING,[1] AND JUDY BARTON[3]

To assess the usefulness of ultrasound in diagnosing ectopic pregnancy, the ultrasonographic findings, pregnancy test results, and proven diagnoses in 148 patients referred for evaluation for ectopic pregnancy were reviewed. Of these patients, 33 were subsequently proven to have ectopic gestations. The ultrasonograms were coded for uterine size, intrauterine gestation sac, adnexal mass, adnexal ring, cul-de-sac fluid, or normal findings. With a positive pregnancy test, the presence of an intrauterine gestation sac excludes the diagnosis of ectopic pregnancy. Of those patients with positive pregnancy tests and no intrauterine gestation sac, 73% had ectopic pregnancy. All patients with normal ultrasonograms had other diagnoses. With a negative pregnancy test, the intrauterine findings are not helpful, and evaluation of the adnexa is more important. An adnexal ring is a significant, though not absolute, indicator of ectopic pregnancy. A normal scan excludes this diagnosis. Other criteria were not significant. A clinical approach to the evaluation for ectopic pregnancy, based on the data accumulated in this study, is suggested.

The clinical diagnosis of ectopic pregnancy is frequently difficult [1]. Since ultrasonography is capable of providing detailed images of pelvic organs, the ultrasonographer is often asked to assist in the evaluation of patients suspected of harboring an ectopic gestation. Although the typical sonographic appearance of ectopic pregnancy was described nearly 10 years ago [2] and is often considered "classic," in our experience the ultrasonograms of many patients with ectopic pregnancies did not conform to this original description. Moreover, other conditions that clinically mimicked ectopic pregnancy frequently yielded ultrasonograms which were remarkably similar to those seen in patients with ectopic pregnancies. The increase in clinical demand for ultrasonographic evaluations in such patients and the lack of statistically tested results on this subject led to the following study.

Subjects and Methods

The medical records and ultrasonograms of 166 patients referred for ultrasonography to one of three medical centers (a university hospital, a university-affiliated county hospital, and a private practice) during an 18 month period were reviewed. Nearly all of these patients were referred for evaluation of clinically suspected ectopic pregnancy. In the remaining patients, ectopic pregnancy was not suspected prior to ultrasonographic examination. Eighteen patients were excluded due to inadequate follow-up. Data on the remaining 148 patients were accumulated and evaluated. In 11 patients, a histologic diagnosis was never made. However, these patients were followed sufficiently long to clinically exclude the diagnosis of ectopic pregnancy.

All patients were scanned with commercially available gray scale equipment and real-time units when available. Routine longitudinal and transverse scans were performed in the supine position in all cases. When deemed necessary, scans in other planes of section or different patient positions were added.

The ultrasonographic data collected in each case included the following: the uterine dimensions, presence or absence of an intrauterine gestation sac, fluid in the cul-de-sac, adnexal mass, or a gestational sac in an ectopic location. A well defined mass in the cul-de-sac or extending from the cul-de-sac into the adnexa was considered as an adnexal mass. Adnexal masses which appeared ringlike (i.e., were sonolucent and bounded by a thick, well defined echogenic wall) were grouped separately (fig. 1). Fetal echoes within such a ring were considered confirmatory of an extrauterine gestation sac.

In all patients, the data collected included the results of a pregnancy test if available. The type of pregnancy test used in each case was not evaluated. However, the vast majority were standard urinary immunologic tests for human chorionic gonadotropin. Surgical, laparoscopic, or clinical proof of diagnosis was available and noted in each case.

In tabulating the data, the patients were divided into two major groups: those with positive pregnancy tests, and those with negative pregnancy tests. The nine patients in whom pregnancy test results were unknown or not obtained were excluded, leaving 139 patients for comparison. Each entry in these two groups was then coded for the presence or absence of proven ectopic pregnancy. The patients were statistically evaluated for the sonographic criteria described above (excluding uterine dimension). In addition, cross-tabulation for the coexistence of two of the ultrasonographic criteria was obtained for each group, comparing those patients with and those without ectopic pregnancy. Statistical analysis was obtained in most cases by the corrected chi-square test; in the few analyses where appropriate, the Fisher's exact test was used.

After measurement of the length, width, and anteroposterior dimension of the uterus, an assessment of uterine volume was made by using a simplified formula for a prolate elipse ($V = L \times W \times AP \times 0.5233$) [3]. When one or more of the three uterine dimensions could not be measured or when an intrauterine pregnancy was demonstrated, the case was excluded from the volume computations and comparison. Because of the variance distribution and size of the groups involved, the standard *t*-test was applied to the log of the uterine volume as well as the uterine volume per se. Two-tail probabilities were obtained.

In order to assess whether or not the mass seen on the ultrasonogram actually represented the ectopic pregnancy, the

Received May 26, 1978; accepted after revision September 12, 1978.
R. A. Filly is a James Picker Scholar of the Picker Foundation.
[1]Department of Radiology, San Francisco General Hospital Medical Center, San Francisco, California 94110. Address reprint requests to T. W. Brown.
[2]Department of Radiology, University of California Medical School, San Francisco, California 94143.
[3] Suite 1003, 3300 Webster Street, Oakland, California 94609.

© 1978 American Roentgen Ray Society

0361-803X/78/1200-0967 $00.00

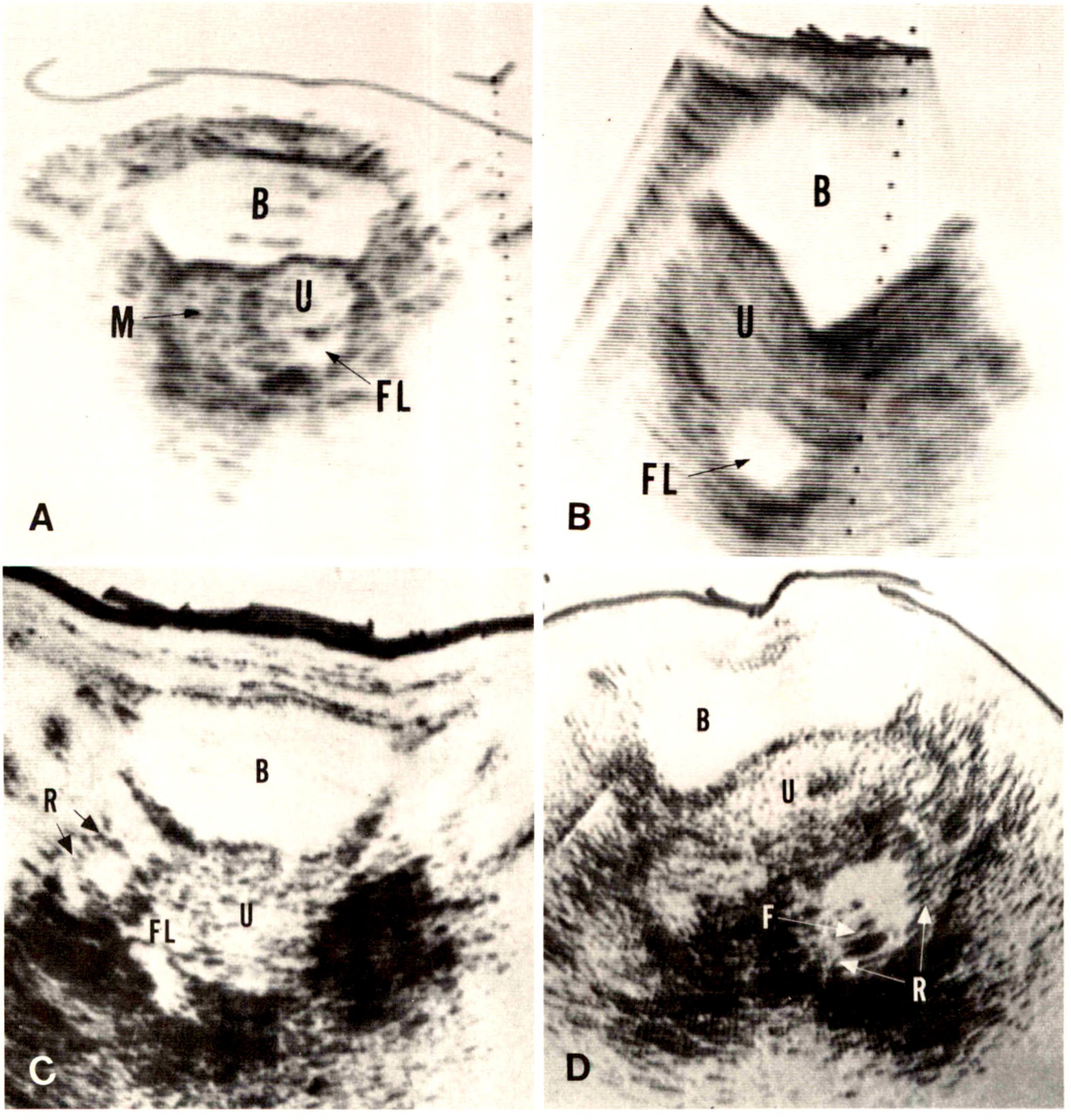

Fig. 1.—4 patients with adnexal findings in ectopic pregnancy. *A*, Transverse scan showing solid right adnexal mass which proved to be ectopic gestation. *B*, Longitudinal scan showing sonolucent mass in cul-de-sac representing hemorrhage or ovarian cyst; absence of thick wall indicates that this is not ectopic gestation sac. *C*, Transverse scan showing sonolucent mass bounded by thick echogenic wall. Mass proved to be ectopic gestation. This is characteristic "adnexal ring." *D*, Transverse scan showing adnexal ring containing fetal echoes in cul-de-sac. B = bladder; F = fetus; Fl = fluid (hematoma or ovarian cyst); M = solid mass, R = thick-walled adnexal ring; U = uterus.

side on which the pregnancy was found at surgery was compared with the side on which the mass was seen at the time of ultrasonographic evaluation.

Results

The distribution of patients in this study on the basis of pregnancy test results is shown in table 1. Of 69 patients who had positive pregnancy tests, 22 had ectopic pregnancies and 47 had other diagnoses. Of 70 patients who had negative pregnancy tests, eight had ectopic pregnancies and 62 had other diagnoses. In nine patients, the pregnancy test was not performed; three of these had ectopic pregnancies. All final diagnoses, tabulated on the basis of pregnancy test results, are recorded in table 1.

The results obtained from analysis of the scans of

TABLE 1

Patient Population

Final Diagnosis	Pregnancy Test			Total
	Positive	Negative	?	
Nonectopic:				
Intrauterine pregnancy	39	0	0	39
Pelvic inflammatory disease	0	20	3	23
Ovarian cyst	0	11	0	11
Unexplained pain, resolved	2	8	1	11
Ruptured ovarian cyst	0	6	0	6
? missed abortion	2	2	0	4
Dysfunctional bleeding	0	4	0	4
Retained products, postabortion	4	0	0	4
Pelvic adhesions	0	4	0	4
Endometriosis	0	2	0	2
Fibroids	0	1	1	2
Other	0	4	1	5
Subtotal	47	62	6	115
Ectopic	22	8	3	33
Total	69	70	9	148

those patients with positive pregnancy tests showed several significant findings. All of the criteria tested (i.e., cul-de-sac fluid, adnexal mass, adnexal ring, or absence of intrauterine gestation sac) had significant value as indicators of ectopic pregnancy. No patient with an intrauterine gestational sac had an ectopic pregnancy ($P = 0.00$). All patients with adnexal rings (three cases) had ectopic pregnancy ($P = 0.035$). The presence of fluid in the cul-de-sac or any adnexal mass was very suggestive of ectopic pregnancy ($P = 0.002$ and 0.0005, respectively). Performing complex cross-tabulations on this data confirmed the above findings and yielded no additional pertinent information. None of the patients with ectopic pregnancy and positive pregnancy tests had a normal scan. Although two patients in this group had no demonstrable adnexal mass, fluid in the cul-de-sac was present in both instances.

Eight (27%) of the 30 patients who had a positive pregnancy test and no intrauterine gestation sac had a final diagnosis other than ectopic pregnancy. Of these, four had retained products of conception after therapeutic abortion, two proved subsequently to have intrauterine pregnancies not demonstrated at the time of ultrasonographic evaluation, and two had negative pregnancy tests on follow-up examination. These two were presumed either to have had false positive pregnancy tests initially or recent spontaneous abortions.

Analysis of the results in those patients with negative pregnancy tests were remarkably dissimilar. Of all the criteria tested, the only one found to be significant in the differentiation of ectopic pregnancy from other diagnoses was the presence of an adnexal ring ($P = 0.02$). However, this probability was based only on the presence of adnexal rings in two patients with ectopic pregnancy, as opposed to one patient with an adnexal ring that proved to be a tubovarian abscess. Complex cross-tabulations demonstrated a single significant criterion. The absence of fluid in the cul-de-sac when an adnexal ring was seen was more significant as an indicator of ectopic pregnancy ($P = 0.006$) than either criterion alone. This probability resulted from comparison of the three patients with adnexal rings, in which only the tubovarian abscess had associated cul-de-sac fluid.

Again, all of the patients with ectopic pregnancy had abnormal scans. In each of these patients an adnexal mass was demonstrated, but this characteristic was not diagnostic ($P = 0.17$) because many patients with other diagnoses also had adnexal masses. Finally, none of the patients in the group with negative pregnancy tests had an intrauterine gestational sac. Consequently, in dramatic contrast to the group with positive pregnancy tests, the intrauterine findings were not a statistically significant criterion ($P = 0.24$).

The following results were obtained from measurement of uterine dimensions, volumes, and log volumes. The mean uterine length showed a statistically significant difference between the ectopic and nonectopic groups (9.2 vs. 7.5 cm, respectively, $P = 0.003$) as did the uterine width (5.5 vs. 4.6 cm, respectively, $P < 0.02$). While the uterine volume measurements were quite disparate (111.66 vs. 79.36 cm^3), the distribution and variance of the computed volumes resulted in no statistical significance. The relationship of the log of the uterine volumes (1.99 vs. 1.77) however, did prove to be significant ($P = 0.004$). However, the standard deviation from the mean was in each case larger than the difference between the means of the ectopic and nonectopic groups.

When the surgically proven location of the ectopic pregnancies was compared to the side on which a mass was seen at the time of ultrasonographic evaluation, a discrepancy was found in seven of the 30 applicable cases.

Discussion

Ultrasound has been used as a diagnostic tool in the evaluation of ectopic pregnancy for almost a decade. Early publications [2, 4, 5] demonstrated remarkable accuracy in the diagnosis of ectopic pregnancy with bistable ultrasound equipment. The slightly enlarged uterus containing no gestational sac, associated with an irregular adnexal mass, "ectopic fetal head," or fluid in the cul-de-sac, became the "classic" appearance of an ectopic pregnancy on ultrasound. A recent report by Maklad and Wright [6] claimed greater than 90% accuracy in the diagnosis of ectopic pregnancy with gray-scale equipment. However, our experience suggested that relying on these "classic" criteria yielded many false negative and false positive diagnoses. Other pathologic conditions at times have ultrasonographic appearances similar to those seen in patients with ectopic pregnancies. Furthermore, ultrasonograms of patients with ectopic pregnancies may be unusual and confusing. This impression provided the impetus for reevaluation of the role of ultrasound in the diagnosis of ectopic pregnancy.

The clinical diagnosis of ectopic pregnancy is often difficult. The problem is compounded when the immunologic urinary pregnancy test is negative, as it fre-

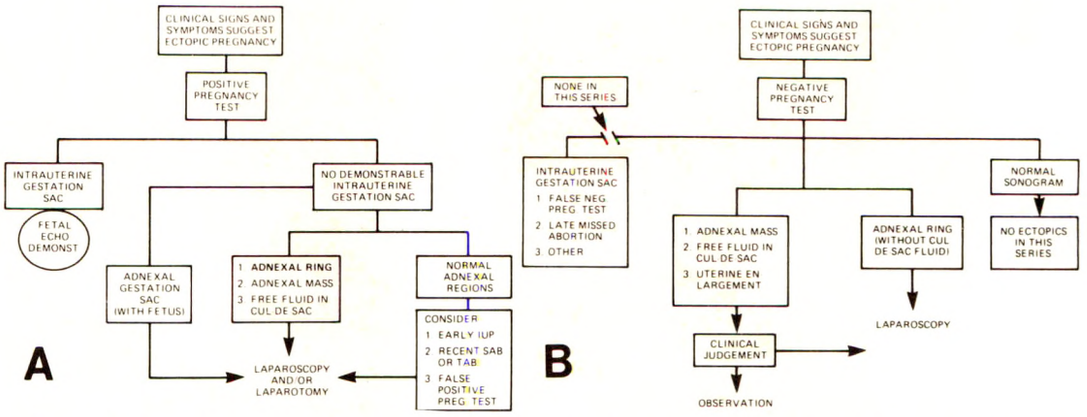

Fig. 2.—Schematic approaches recommended for evaluation for ectopic pregnancy in patients with positive (*A*) and negative (*B*) pregnancy tests.

quently is in patients with ectopic pregnancies[7] (27% of the ectopics in this series). Prior to ultrasonography, the value of the urinary immunologic pregnancy test in evaluation of ectopic pregnancy was negligible [8]. If negative, the results might well be false negative. If positive, the clinician had no easy means of determining whether the pregnancy was inside or outside of the uterus. However, given the ability of ultrasound to demonstrate early intrauterine pregnancies [9], correlation of the results of the pregnancy test with those of the ultrasonogram can aid significantly in the assessment of the patient. For this reason, patients were compared separately on the basis of their pregnancy test results.

The results of this study, and the clinical approach they suggest, are summarized in figure 2. The presence or absence of a gestational sac within the uterus, coupled with a positive pregnancy test, provide the basis for the most reliable interpretation of the ultrasonogram. If the pregnancy test is positive and the ultrasonogram demonstrates an intrauterine gestational sac, then the diagnosis of ectopic pregnancy is effectively excluded (it is estimated that only one in 30,000 pregnancies will have coexisting intrauterine and ectopic gestation [10]). An ectopic pregnancy was present in 73% of the patients in this series who had a positive pregnancy test and no demonstrated intrauterine pregnancy. In this situation, it may be helpful to carefully evaluate the adnexal regions. If no abnormalities (i.e., masses or fluid in the cul-de-sac) are found, ectopic pregnancy is unlikely, since all patients in this study with ectopic pregnancy demonstrated abnormal findings. Those patients without an intrauterine gestational sac who do have adnexal masses, particularly ringlike structures or fluid in the cul-de-sac, should undergo laparoscopy or laparotomy, because of the high incidence of ectopic pregnancy in this group.

With a negative pregnancy test, the intrauterine findings become less helpful, and the adnexal findings more important in evaluation for ectopic pregnancy. None of the 70 patients in this series with negative pregnancy tests demonstrated an intrauterine gestational sac, whether ectopic pregnancy was present or not. This situation nullifies the most effective ultrasonographic criterion for the exclusion of ectopic pregnancy.

If examination of the adnexal and cul-de-sac regions reveals no abnormal findings the diagnosis of ectopic pregnancy is again highly unlikely (no cases in this series). If, on the other hand, an adnexal mass or fluid in the cul-de-sac is demonstrated, an ectopic pregnancy may or may not be present, since many other clinical entities also yield similar sonographic findings. By contrast, the presence of a ringlike structure in the adnexa, particularly in the absence of cul-de-sac fluid, was significant for the presence of ectopic pregnancy. However, the sample in the negative pregnancy test group consisted of only two patients. Since tubovarian abscess, appendiceal abscess, and possibly other masses can mimic an adnexal ring, this criteria may be less reliable than indicated statistically. Consequently, in those patients with negative pregnancy tests and abnormal adnexal or cul-de-sac findings, ultrasound will not be definitive in the evaluation for ectopic pregnancy. The decision of whether or not to perform laparoscopy or laparotomy will depend largely on the level of clinical suspicion.

A disappointing feature of the study was that the adnexal findings are frequently confusing and lack specificity. Even a ringlike structure in the adnexa is not diagnostic. If the ectopic gestation is leaking, aborted, ruptured, or chronic, with fresh blood or clot in the adnexal regions, differentiation from other clinical entities is difficult. In addition, in seven of 30 instances the adnexal mass identified on the ultrasonogram was on the side opposite the ectopic pregnancy. It is quite probable that ovarian cysts and/or hematomas were imaged while the ectopic gestation was missed. If this is the case, it may also be true that masses demonstrated on the same side as the ectopic pregnancy represented some structure other than the ectopic, as well. Obviously, this could not be tested.

Furthermore, given the fact that corpus luteum cysts are common in normal early pregnancies, the statistical suggestion that the presence of an adnexal mass with positive pregnancy test indicates the presence of ectopic

pregnancy is a curious one. This observation possibly reflects the fact that when an intrauterine pregnancy was identified, the diagnosis of ectopic pregnancy was excluded, and a less detailed scan of the adnexal regions was performed. Although these facts do not appear to have altered the statistical results of this study, they stress the nonspecificity of a demonstrated adnexal mass when evaluating a patient suspected of harboring an ectopic gestation.

Excluding those patients with intrauterine gestation sacs, the mean length, width, and log volume of the uterus were significantly larger in those patients with ectopic pregnancy than in those without. Unfortunately, a single standard deviation overlapped the mean value in the corresponding opposite group. Consequently, although it is interesting that of those patients referred to rule out ectopic pregnancy, the uterus is statistically larger in those patients with ectopic pregnancy than in those without, this criterion is not reliable for differentiation of these two groups.

ACKNOWLEDGMENTS

We thank Barbara Brunnenmeyer, Linda London, Valerie Nelson, and Cheryl Wilson for technical assistance in performing the many ultrasonograms used in this study. Our appreciation is also extended to Dr. David Martinez for permission to review records and ultrasonograms from his practice, and to Nickolin Casciani for her efforts in the preparation of this manuscript.

REFERENCES

1. Chez RA, Moore JG: Diagnostic errors in the management of ectopic pregnancy. *Surg Gynecol Obstet* 117:589–596, 1963
2. Kobayashi M, Hellman L, Fillisti L: Ultrasound: an aid in the diagnosis of ectopic pregnancy. *Am J Obstet Gynecol* 103:1131–1140, 1969
3. Gohari F, Berkowitz PC, Hobbins JC: In utero prediction of IUGR by determination of total intrauterine volume. *Am J Obstet Gynecol* 127:255–260, 1977
4. Donald J: Diagnostic uses of sonar (ultrasonic echo sounding) in obstetrics and gynecology, in *Advances in Obstetrics and Gynecology*, edited by Marcus SL, Marcus G, Baltimore, Williams & Wilkins, 1967, pp 314–329
5. Zacutti A, Brugnoli CA: Usefulness of ultrasonic scanning in the diagnosis of ectopic pregnancy. *Acta Eur Fertil* 2:445–468, 1970
6. Maklad NF, Wright CH: Grey scale ultrasonography in the diagnosis of ectopic pregnancy. *Radiology* 126:221–226, 1978
7. Hall RE, Todd WD: The suspected ectopic pregnancy. A review of 500 cases. *Am J Obstet Gynecol* 81:1220–1229, 1961
8. Breen JL: A 21-year survey of ectopic pregnancies. *Am J Obstet Gynecol* 106:1004–1009, 1970
9. Blackwell RJ, Shirley I, Farnan D, Michael CA: Ultrasonic B-scanning after less than 6 weeks amenorrhea. *Br J Obstet Gynecol* 82:108–114, 1975
10. Hellman LM, Pritchard JA: *Williams Obstetrics*, 14th ed. New York, Meredith Corp, 1971

Uterine Anomalies Associated with Renal Agenesis: Role of Gray Scale Ultrasonography

ANDREW M. FRIED,[1] MICHAEL OLIFF,[1,2] EMERY A. WILSON,[3] AND JOSEPH WHISNANT[4]

Anomalies of the female genital tract were successfully characterized by gray scale ultrasonography in three cases; all three were found in association with unilateral renal agenesis. Findings at intravenous urography prompted ultrasound studies. The high incidence of genital tract anomalies associated with unilateral renal agenesis, particularly in females, indicates ultrasonography be used to examine the pelvis (as well as the renal bed). Further diagnostic procedures can then be assessed on a more informed basis.

Pathologic descriptions of unilateral renal agenesis date at least to 1609 (Consiliorum) and possibly to Aristotle. A variety of associated anomalies of the genital tract are well documented in modern literature. Since the incidence of such anomalies in females has been reported as high as 69.9% [1], discovery of a congenital solitary kidney by intravenous urography should prompt evaluation of the female genital tract. We recently encountered three such cases. To our knowledge, gray scale ultrasound studies of this situation have not previously been reported.

Case Reports

Case 1

D. K., a 15-year-old white female gravida O para O, had abnormal uterine bleeding and a pelvic mass. Physical findings on admission included a soft anterior adenexal mass on the right about 8 cm in diameter, normal external genitalia, and a foul vaginal discharge that subsequently grew *E. coli* on culture. Excretory urography revealed absence of the right kidney with compensatory hypertrophy of the left; cystoscopy confirmed a left hemitrigone. Ultrasonography demonstrated a complex right 6 cm adenexal mass in close contiguity with the uterus (fig. 1). Oblique scans suggested a septum, and the preoperative diagnosis of bicornuate uterus with occlusion of the right horn was made. After 5 days of parenteral antibiotic therapy, the right adenexal mass was smaller by clinical examination. At laparoscopy, a bicornuate uterus was observed, united at the upper part of the cervix; the right horn was still some 2 cm larger than the left. The tubes and ovaries were normal.

Case 2

S. S., a 21-year-old white female, was found to have a solitary hypertrophied left kidney at excretory urography performed for recurrent urinary tract infections. Cystoscopy demonstrated a left hemitrigone with no identifiable right ureteral orifice. Ultrasonography imaged a small slender uterus canted to the left (figs. 2*A* and 2*B*).The small dimensions of the uterus (1.5 cm anteroposterior diameter by 2.5 cm wide), coupled with its displacement led to the suspicion of a unicornuate uterus [2]. Hysterosalpingography confirmed the presence of a solitary left cornu with a normal fallopian tube (fig. 2C).

Comment. This case illustrates the usual situation in which most of the genital anomalies have been found on the same side as the agenetic kidney [1].

Case 3

B. S., a 42-year-old mentally retarded white female had a history of recurrent urinary tract infections. At excretory urography she had a solitary left kidney; at cystoscopy, no right ureteral orifice or hemitrigone could be identified. Gray scale ultrasound demonstrated a symmetrically bilobed uterus with a clearly defined midline septum; the configuration was felt to represent a bicornuate uterus (fig. 3). Because of the patient's age, mental status, and the extreme unlikelihood of fertility being significant, no further workup of her genital tract was considered warranted.

Discussion

Previous reports have focused on varying aspects of unilateral renal agenesis and associated genital anomalies; the reported incidence of this association varies [3–8]. In a comprehensive review study Collins [9] found 367 cases of unilateral renal agenesis in 337,488 autopsies, an incidence of 0.1%. The overall incidence of associated anomalies was 58%, with 48% having specific genital anomalies. Fortune [10] found genital anomalies in 69.9% of females with congenital solitary kidneys and in 21.2% of males; Longo [1] found a 54.1% incidence in females and 45.9% in males. The Müllerian duct system develops at a later stage in embryogenesis than the Wolffian duct and is therefore more likely to undergo malformation, which has been postulated to account for the higher incidence of associated genital anomalies in females than males. It is accepted that anomalies of the genital tract occur in a significant percentage of patients with unilateral renal agenesis, and at least a modest female predominance is generally held.

The most common malformations of the female genital tract associated with an absent kidney are bicornuate and unicornuate uterus; a complete spectrum of septation anomalies involving both uterus and vagina are also described [9, 11, 12]. Anomalies of the fallopian tubes and ovaries are reported with considerably less frequency.

Received June 13, 1978; accepted August 10, 1978.
[1] Department of Diagnostic Radiology, University of Kentucky Medical Center, Lexington, Kentucky 40506. Address reprint requests to A. M. Fried.
[2] Present address: Hardin Memorial Hospital, Elizabethtown, Kentucky 42701.
[3] Department of Obstetrics and Gynecology, University of Kentucky Medical Center, Lexington, Kentucky 40506.
[4] Department of Surgery/Urology, University of Kentucky Medical Center, Lexington, Kentucky 40506.

© 1978 American Roentgen Ray Society

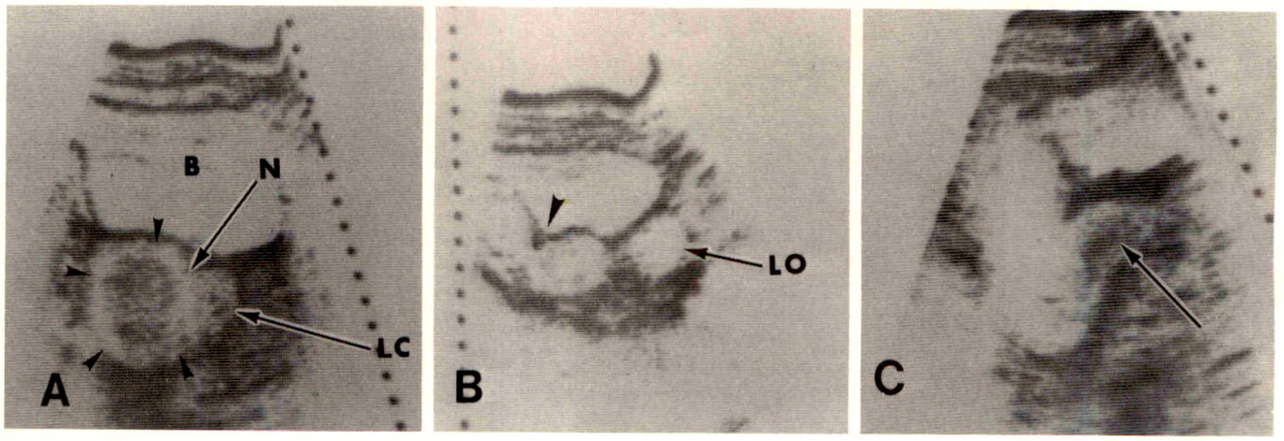

Fig. 1.—Case 1. *A*, Transverse scan about 6 cm above symphysis. Note rounded complex mass (*arrowheads*) representing right cornu of uterus and notch between cornua (N). (LC = left uterine cornu, B = bladder.) *B*, Lower oblique scan better demonstrating division between cornua of uterus (*arrowhead*). (LO = left ovary.) *C*, Longitudinal scan 3 cm right of midline demonstrating enlarged right cornu; echogenicity in region of endocervical canal felt to represent purulent material (*arrow*).

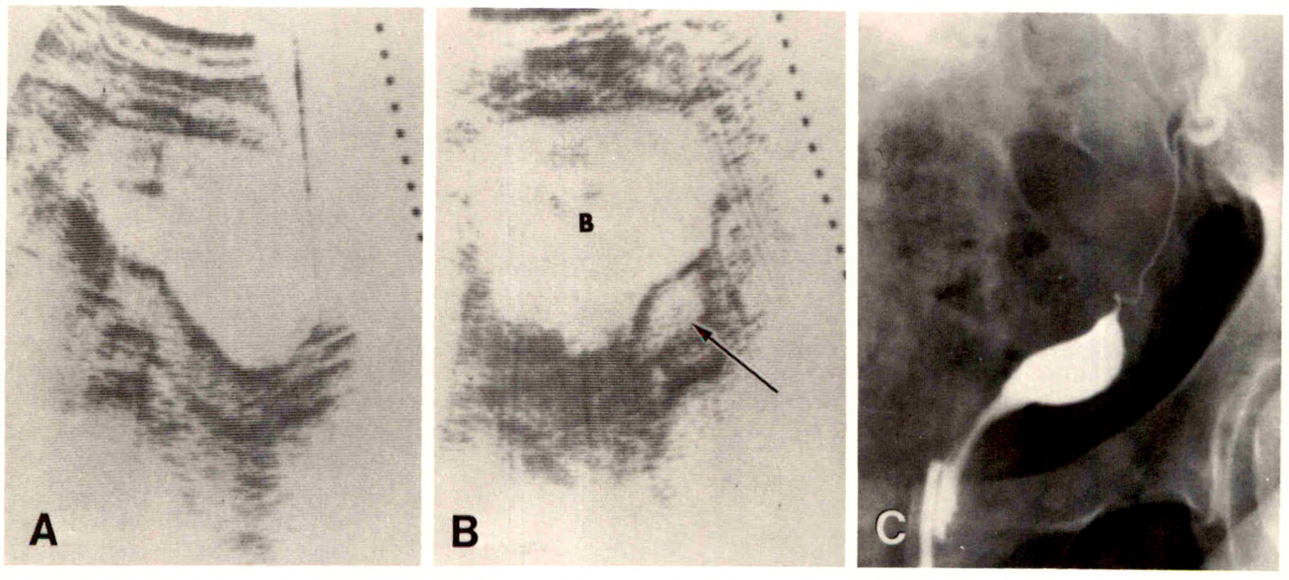

Fig. 2.—Case 2. *A*, Longitudinal scan 4 cm left of midline; left cornu of the uterus is 1.5 cm in anteroposterior diameter. *B*, Transverse scan 4 cm above symphysis. Note only 2.5 cm wide left cornu visible (*arrow*) (B = bladder.) *C*, Hysterosalpingogram confirming solitary left cornu and tube.

Reports of ultrasonographic studies of uterine anomalies have been scant and largely confined to the pregnant and puerperal uterus using bistable equipment [13–19]. With bistable equipment, Haller et al. [20] concluded that "abnormalities of septation of the immature uterus cannot be identified" although Bennett [21] successfully demonstrated one case of uterus bicornis unicollis in the nonpregnant state. Our experience with gray scale ultrasonography in delineating such abnormalities in three nulliparous women suggests that currently available units can provide significant diagnostic information in such cases.

Several considerations make this application of gray scale ultrasonography significant. Hysterosalpingography, the only other currently available imaging technique for identifying uterine anomalies, is not a satisfactory screening method. It can be difficult, if not impossible, in the pediatric and adolescent female and is at least moderately invasive in any age group. Nonetheless, the frequency with which genital anomalies are found in association with unilateral renal agenesis dictates further evaluation of the female genital tract.

The role of ultrasonography in evaluating the unilateral nonvisualized kidney is well established [22–27]. Successful delineation of uterine anomalies by gray scale ultrasonography suggests an extension of the logical sequence of diagnostic procedures. We propose that the kidney not visualized at intravenous urography first be examined ultrasonographically. Failure to delineate a kidney on ultrasound should suggest possible unilateral renal agenesis, and the female pelvis should then be examined to evaluate the uterus and adenexal structures

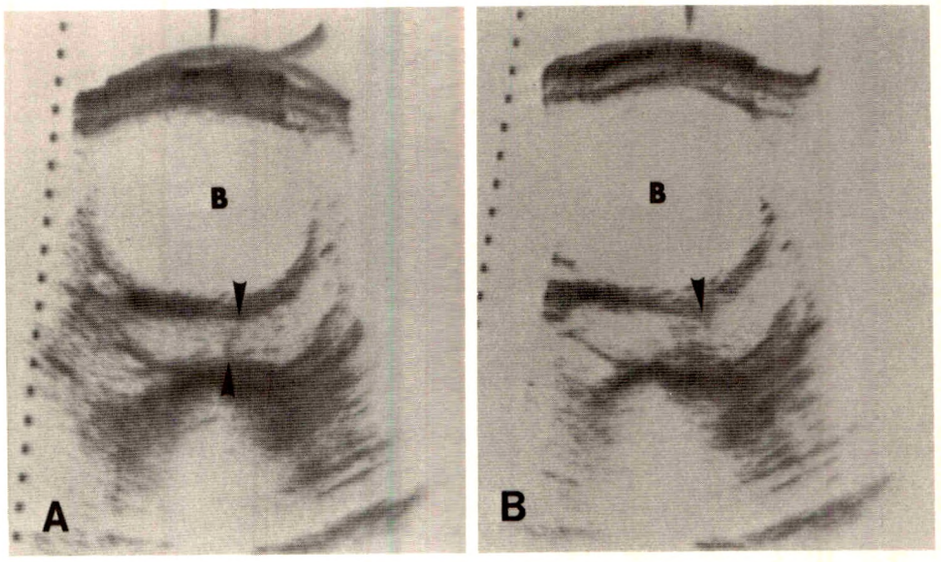

Fig. 3.—Case 3. *A*, Transverse scan 4 cm above symphysis. Note septum (*arrowheads*) dividing two uterine cornua. (B = bladder.) *B*, Slightly oblique transverse scan at same level more clearly demonstrating notch between cornua (*arrowhead*).

for congenital malformations. On the basis of ultrasonographic findings, the patient's age, symptomatology, and clinical setting, a more informed decision can then be reached concerning further diagnostic procedures (e.g., hysterosalpingography and laparoscopy).

ACKNOWLEDGMENT

We thank Nancy Lail for preparing the manuscript.

REFERENCES

1. Longo VJ, Thompson GJ: Congenital solitary kidney. *J Urol* 68:63–68, 1952
2. Miller EI, Thomas RH, Lines P: The atrophic postmenopausal uterus. *JCU* 5:261–263, 1977
3. Ashley DJB, Mostofi FK: Renal agenesis and dysgenesis. *J Urol* 83:211–230, 1960
4. Meiraz D, Fischelovitch J, Lazebnik J: Agenesis of the kidney associated with congenital malformation of the seminal vesicle. *Br J Urol* 45:541–544, 1973
5. Furtado AJL: Three cases of cystic seminal vesicle associated with unilateral renal agenesis. *Br J Urol* 45:536–540, 1973
6. Friedrich M: Eine utero-vaginale Doppelmissbildung mit anschliessender Schwangerschaft. *Geburtshilfe Frauenheilkd* 32:602,1972
7. Braasch WF, Merricks JW: Clinical and radiological data associated with congenital and acquired single kidney. *Surg Gynecol Obstet* 67:281–286, 1938
8. Schumacker HB: Congenital anomalies of the genitalia associated with unilateral renal agenesis. *Arch Surg* 37:586–602, 1938
9. Collins DC: Congenital unilateral renal agenesia. *Ann Surg* 95:715–726, 1932
10. Fortune CH: The pathological and clinical significance of congenital one-sided kidney defect, with the presentation of three new cases of agenesia and one of aplasia. *Ann Intern Med* 1:377–399, 1927
11. Vinstein AL, Franken EA: Unilateral hematocolpos associated with agenesis of the kidney. *Radiology* 102:625–627,1972
12. Radasch HE: Congenital unilateral absence of the urogenital system and its relation to the development of the Wolffian and Muellerian ducts. *Am J Med Sci* 136:111–118, 1908
13. Kobayashi M, Hellman LM, Cromb E: *Atlas of Ultrasonography in Obstetrics and Gynecology*, 7th ed. New York, Appleton-Century-Crofts, 1972
14. Arger PH, Zarembok I: Ultrasound efficacy in evaluation of lower genitourinary tract anomalies. *JCU* 3:61–63, 1975
15. Szoke E, Kiss D: The use of ultrasonic echo technique in the diagnosis of developmental anomalies of the uterus. *Ann Chir Gynaecol* 66:59–61, 1977
16. Shkolnik A: B-mode ultrasound and the non-visualizing kidney in pediatrics. *Am J Roentgenol* 128:121–125,1977
17. Von Miscky LI: Gynecologic ultrasonography, in *Diagnostic Ultrasound*, edited by King DL, St. Louis, Mosby, 1974, pp 207–241
18. Fisch AE, Jacobson JB: Ultrasound findings in segmental uterine distension. *JCU* 4:209–212, 1976
19. Bennett MJ: Puerperal ultrasonic hysterography in the diagnosis of congenital uterine malformations. *Br J Obstet Gynecol* 83:389–392, 1976
20. Haller JC, Schneider M, Kassner EG: Ultrasonography in pediatric gynecology and obstetrics. *Am J Roentgenol* 128:423–429, 1977
21. Bennett MJ II: The ultrasonic diagnosis of uterine fundal abnormalities. *Excerpts Medical International Congress* 363:262–268, 1975
22. Sanders RC: The place of diagnostic ultrasound in the examination of kidneys not seen in excretory urography. *J Urol* 114:813–821,1975
23. Goldberg BB, ed: *Abdominal Gray Scale Ultrasonography*. New York, Wiley, 1977
24. Marangola JF, Bryan PJ, Azimi F: Ultrasonic evaluation of the unilateral nonvisualized kidney. *Am J Roentgenol* 126:353–362,1976
25. Hasch E: Ultrasound in the investigation of the kidney and urinary tract in children. *Acta Paediatr Scand* 63:42–48, 1974
26. Sweet EM: The place of nephrosonography in renal investigation in childhood. *Ann Radiol* 20:25, 1977
27. Teele RL: Ultrasonography of the genitourinary tract in children. *Radiol Clin North Am* 15:109–128, 1977

Gray Scale Features of Hematomas: An Ultrasonic Spectrum

JEFFREY D. WICKS,[1] TERRY M. SILVER,[1] AND ROBERT L. BREE[2]

Forty-eight B-scan ultrasound examinations were performed on 25 patients with hematomas. Hematomas are usually spherical or ovoid within the abdomen, and lentiform within the pleural space or abdominal wall. They generally decrease in size with time, and usually have irregular walls. Hematomas contain a variable amount of internal echoes during the first month, and then gradually become anechoic. The sonographic appearance is not specific; an abscess may have a similar appearance. An old, anechoic hematoma may contain a gelatinous material which cannot be aspirated.

The value of ultrasonic scanning to diagnose intraabdominal hematomas has been reported [1, 2]. Ultrasonography has also been used to diagnose hematomas of the rectus sheath [3–5], spleen [6], and retroperitoneum and extremity in hemophiliacs [7–9]. A variety of sonographic appearances has been noted. We examined the gray scale ultrasonic spectrum of hematomas and correlated sonographic appearance with age of the hematoma.

Materials and Methods

Standard contact B-scanning techniques were performed using commercially available gray scale ultrasound equipment. Images were obtained at 1–2 cm intervals in sagittal and transverse planes, with 2.25, 3.5, or 5.0 MHz transducers, and recorded on Polaroid or x-ray film.

The charts of 99 patients with abnormal fluid collections diagnosed by ultrasound were reviewed retrospectively. In 25 patients, these abnormal fluid collections were determined to be hematomas by surgical exploration (12), by percutaneous needle aspiration (five), or by significant drop in hematocrit with no other source of blood loss (eight). Patients excluded from the study included those with febrile postoperative courses and reduced hematocrit or those with bloody aspirates that had positive cultures.

A total of 48 ultrasound examinations was performed on the 25 patients. The age of the hematoma was estimated for each examination based on the date of onset of symptoms and/or drop in hematocrit. Size, shape, amount of internal echoes, presence of septation, and regularity of the wall were evaluated on each examination. Internal echoes were graded as follows on a scale of 0–4: 0 = completely echo free; 1 = a few scattered nonreverberatory echoes within an echo-free lesion; 2 = more internal echoes than grade 1, but less than one-half of the area of the lesion contained echoes; 3 = area with echoes equals echo-free area; and 4 = area of lesion containing echoes exceeds echo-free area. Regularity of the wall was graded as smooth, slighly irregular, or irregular.

Results

The ages of the hematomas at examination ranged from 1 day to about 1 year. Of 25 cases, 17 were single examinations. In eight patients, multiple examinations were performed. The periods of follow-up were 4–217 days.

Shape and Location

The shapes of hematomas seemed to be determined by their location. The hematomas (intraperitoneal, five; pelvic, seven; retroperitoneal, one; hepatic, two; and extremity, one) were all ovoid or spherical. Even the intraperitoneal hematomas that occurred in partially limited spaces, such as the anterior and posterior subhepatic spaces, were ovoid. Hematomas found in the following locations were lentiform: abdominal wall (six), pleural space (two), and perirenal space (one). This configuration reflects the ease of dissection of the fluid collection along well defined tissue planes.

Size

On initial examination, hematomas ranged 4–23 cm in greatest dimension. Of the eight cases with follow-up examinations, two initially increased in size, while six decreased in size. The two that increased were clinically

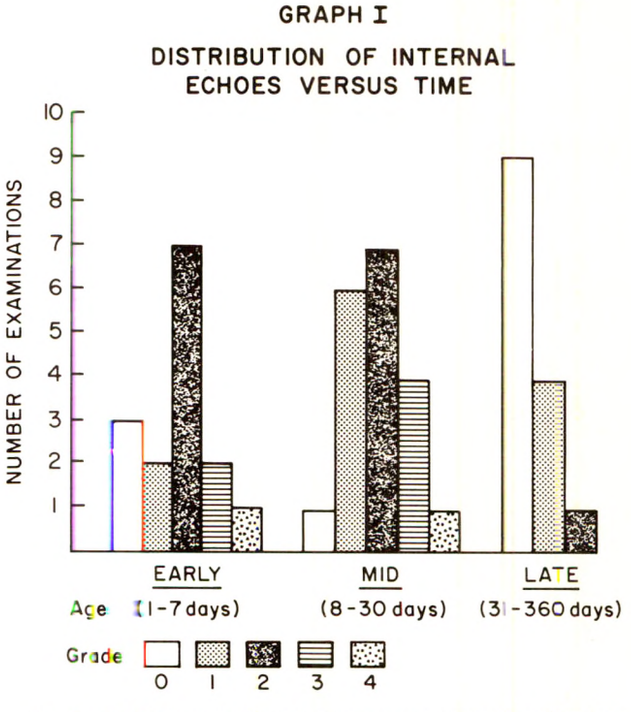

Fig. 1.—Distribution of internal echoes versus time. Note that late hematomas contain significantly fewer echoes than those of early or middle ages.

Received June 13, 1978; accepted after revision September 12, 1978.
[1] Department of Radiology, University of Michigan Hospital, Ann Arbor, Michigan 48109. Address reprint requests to J. D. Wicks.
[2] Department of Radiology, Toledo Hospital, Toledo, Ohio 43606.

© 1978 American Roentgen Ray Society

0361–803X/78/1200–0977 $00.00

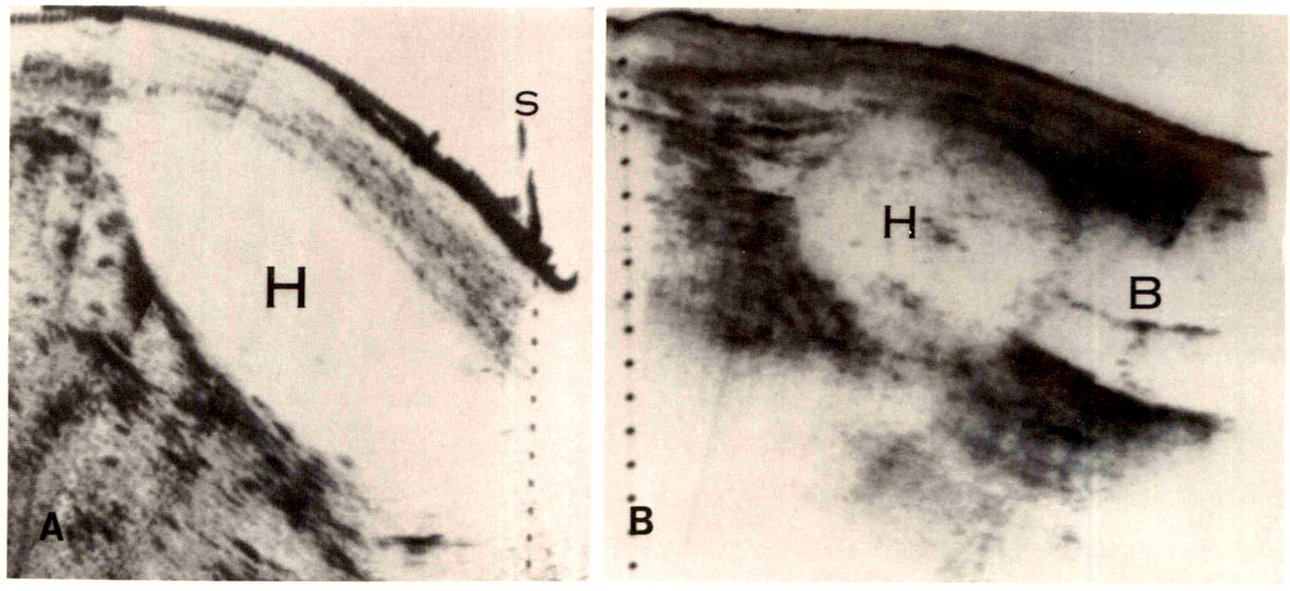

Fig. 2.—1-day-old hematomas. *A*, Longitudinal midline postvoiding scan of pelvis of 45-year-old female being treated with heparin for pulmonary emboli. Note oval anechoic hematoma (H) with slightly irregular walls. S = symphysis. *B*, Longitudinal midline scan of pelvis of 45-year-old female 1 day after vaginal hysterectomy. Spherical hematoma (H) has irregular walls and grade 2 internal echoes. Bladder (B) has internal echoes from drainage device.

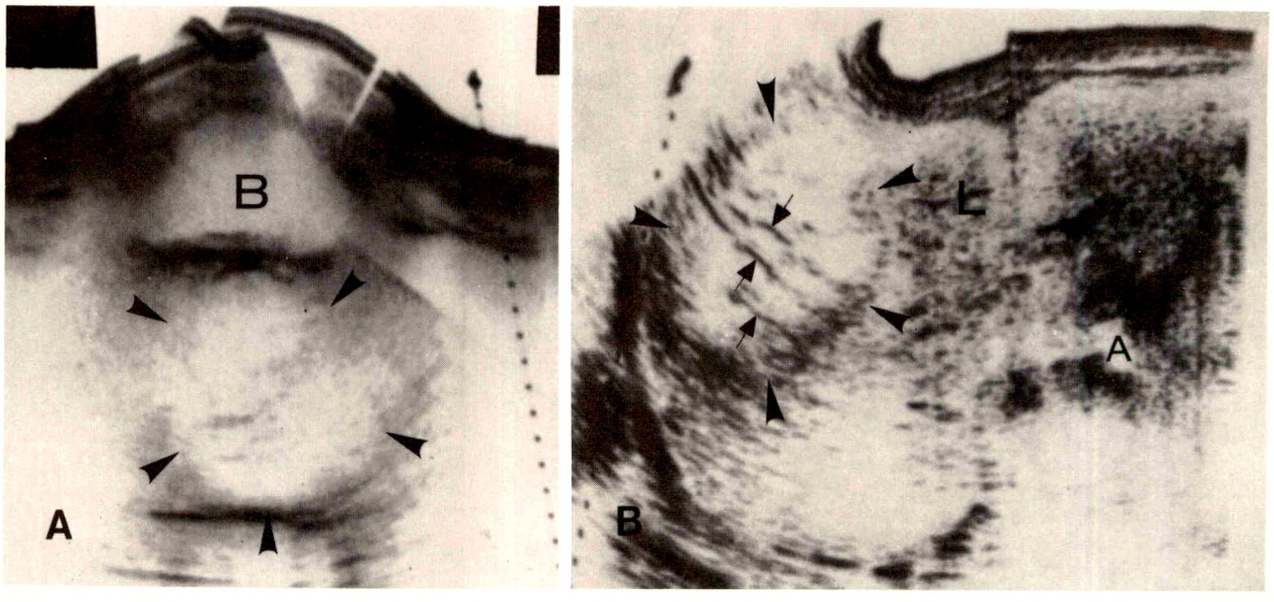

Fig. 3.—1- to 4-week-old hematomas. *A*, 12-day-old hematoma. Transverse scan of pelvis of 77-year-old male after abdominoperineal resection for carcinoma of rectum. Hematoma (*arrowheads*) has slightly irregular walls and grade 2 internal echoes. Bladder (B) contains reverberatory echoes. *B*, 23-day-old hematoma. Transverse scan angled cephalad at level of xyphoid of 27-year-old male injured in auto accident. Intrahepatic hematoma (*arrowheads*) has irregular wall, grade 2 internal echoes, and septae (*arrows*). L = liver, A = aorta.

and surgically considered to be due to continued bleeding. Two that initially decreased eventually stabilized and did not change over the subsequent 30 day follow-up period preceding percutaneous aspiration. The other four hematomas gradually decreased.

Wall Characteristics

Of 25 cases, 22 (88%) hematomas had irregularity of the wall at some time. Once irregular, the wall continued to be irregular on subsequent examinations. Of these, one had smooth walls at 3 days and developed irregular walls by day 9. Three cases of smooth-walled hematomas were of 5, 7, and 360 day durations.

Internal Echoes

Figure 1 shows the distribution of internal echoes compared with the age of the hematoma. Old hematomas seem to contain fewer echoes. There is no difference statistically between the early (1–7 days) and middle (8–30 days) ages. However, late hematomas (31–360 days)

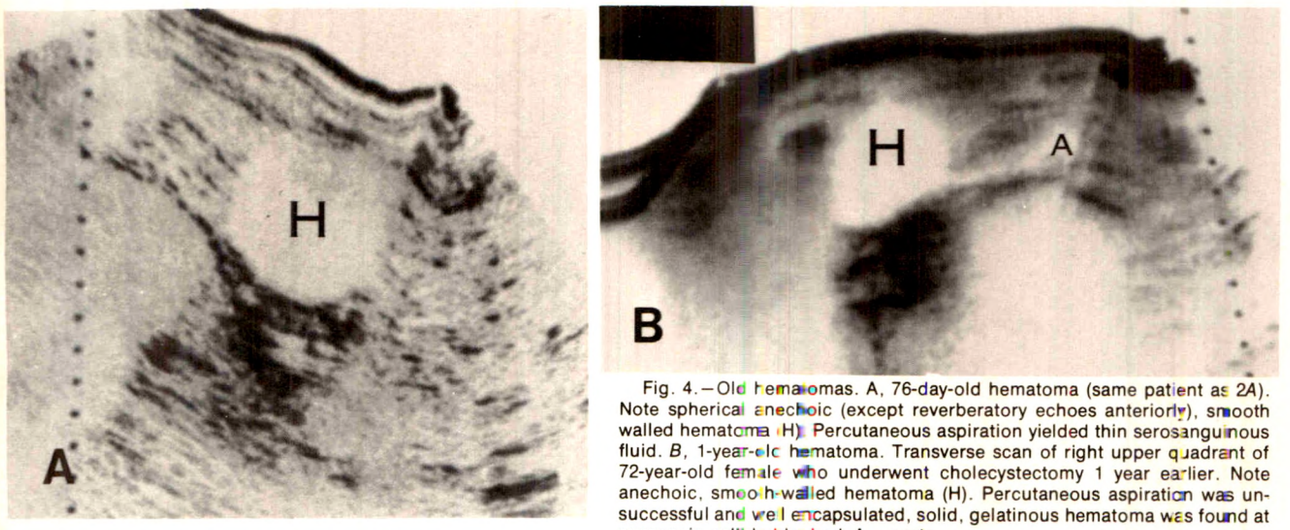

Fig. 4.—Old hematomas. A, 76-day-old hematoma (same patient as 2A). Note spherical anechoic (except reverberatory echoes anteriorly), smooth walled hematoma (H). Percutaneous aspiration yielded thin serosanguinous fluid. *B*, 1-year-old hematoma. Transverse scan of right upper quadrant of 72-year-old female who underwent cholecystectomy 1 year earlier. Note anechoic, smooth-walled hematoma (H). Percutaneous aspiration was unsuccessful and well encapsulated, solid, gelatinous hematoma was found at surgery in gallbladder bed. A = aorta.

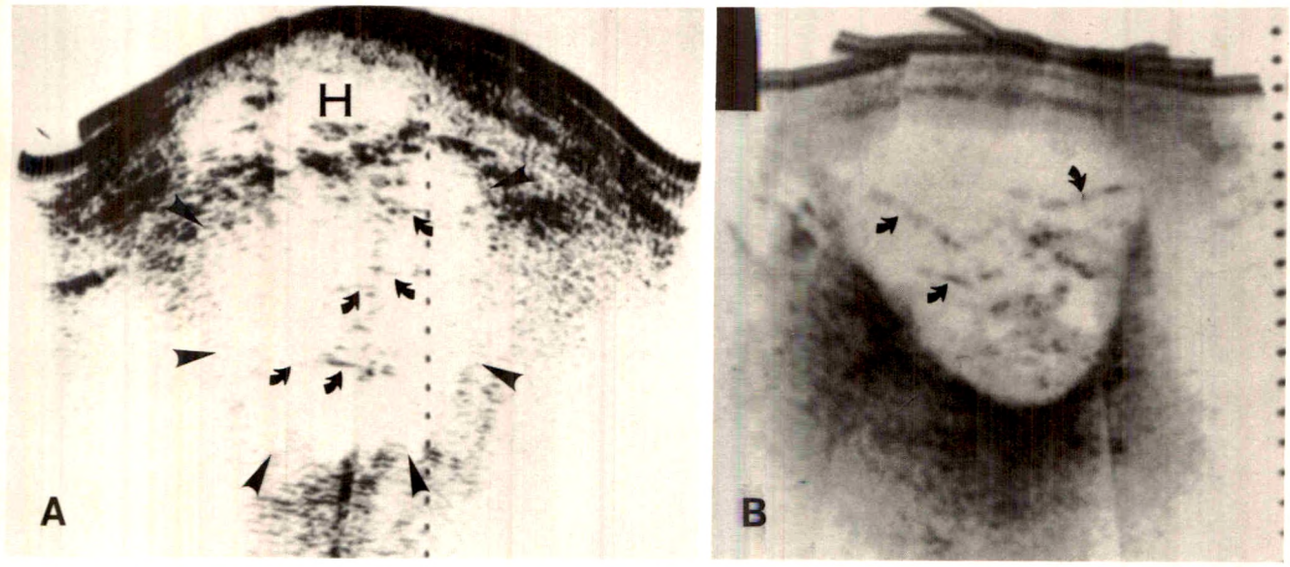

Fig. 5.—Septation. *A*, 8-day-old hematoma. Transverse scan of lower abdomen of 55-year-old male treated with heparin. Lentiform hematoma (H) in anterior abdominal wall has irregular walls and grade 1 internal echoes. Note another hematoma deeper within abdomen (*arrowheads*) with irregular walls, grade 2 internal echoes, and septae (*arrows*). *B*, Abscess. Transverse scan of lower abdomen of 60-year-old male with *Bacteroides* abscess. Note septation (*arrows*) similar to that in 5*A*.

contain significantly fewer echoes ($P < 0.01$) than the early or middle groups. The pattern of decreasing internal echoes as the hematoma aged was noted in seven of eight cases with multiple follow-up examinations.

Septation

Septation within the hematoma was present in 11 of 25 cases (44%). This finding was noted at 5–30 days. In one case, the septae were not present at 1 day, appeared by day 6 and were not present at reexamination at 27 days.

Discussion

Kaplan and Saunders [2] demonstrated in vitro that fresh unclotted or homogeneously clotted blood had no internal echoes. With fragmentation of the clot, internal echoes were found. Our cases generally support these experimental findings.

Four cases were initially scanned within the first 24 hr of symptoms or the documented period of hematocrit drop (fig. 2). Two of four had no internal echoes while the others were graded as 1 and 2. No pathologic correlation was available in these cases. Six cases underwent aspiration or surgical drainage during the period of 1–4 weeks postbleeding. Surgical descriptions were "old partially clotted blood" or "partially organized hematoma." These cases had internal echoes ranging from grades 1–3. Figure 3 shows two cases that are representative of 1- to 4-week-old hematomas.

Two hematomas of estimated age older than 10 weeks have pathologic correlation (fig. 4). Although both cases were anechoic sonographically, one contained a thin serosanguinous fluid and the other a solid gelatinous material pathologically. Two cases of intrahepatic hematomas also became anechoic by 10 weeks. Although no pathologic correlation is available in these cases, a case of hepatic hematoma, discovered 1 year after injury, reported by Shapiro et al. [10] documents the solid gelatinous nature of the hematoma. Even if a hematoma is suspected and appears anechoic sonographically, percutaneous aspiration may be unsuccessful in an old hematoma.

It is difficult to definitively diagnose a fluid collection as a hematoma on the basis of the sonographic appearance alone [1]. Both hematomas and abscesses may appear similar sonographically [11]. Both transmit sound well and have internal echoes and irregular walls. When located intraabdominally, both abscesses and hematomas tend to be spherical or ovoid and will displace adjacent organs. Although septation was present in 44% of the hematomas studied (fig. 5*A*), and has been described in blood-containing endometriomas [12], it does not seem to be a specific sign. Figure 5*B* shows a lower abdominal fluid collection which has a septated appearance similar to the hematoma cases. Percutaneous aspiration yielded a purulent, light brown fluid which contained gram-negative rods and cultured two strains of *Bacteroides*. Septae have also been reported within a loculated pleural effusion [13]. We have also noted septae within lymphoceles.

Although the clinical setting is helpful in suggesting the nature of an abnormal fluid collection, ultrasound-guided percutaneous aspiration can provide a specimen for analysis [14]. The sonographic appearance of the hematoma does not allow one to absolutely predict a fluid specimen will be obtained (an old anechoic hematoma may contain a nonaspiratable, gelatinous material). However, all attempted aspirations of our hematomas containing echoes yielded a bloody aspirate. Laing and Filly [13] reported a similar experience with attempted aspiration of pleural opacities.

ACKNOWLEDGMENT

We thank Dr. Dennis Fryback for statistical analysis.

REFERENCES

1. Jensen F, Pedersen JF: The value of ultrasonic scanning in the diagnosis of intraabdominal abscesses and hematomas. *Surg Gynecol Obstet* 139:326–328, 1974
2. Kaplan GN, Sanders RC: B-scan ultrasound in the management of patients with occult abdominal hematomas. *J Clin Ultrasound* 1:5–13, 1973
3. Lee PWR, Bark M, Macfie J, Pratt D: The ultrasound diagnosis of rectus sheath hematoma. *Br J Surg* 64:633–634, 1977
4. Kaftori JK, Rosenberger A, Pollack S, Fish JH: Rectus sheath hematoma: ultrasonic diagnosis. *Am J Roentgenol* 128:283–285, 1977
5. Hamilton JV, Flinn G, Haynie CC, Cefalo RC: Diagnosis of rectus sheath hematoma by B-mode ultrasound: a case report. *Am J Obstet Gynecol* 125:562–565, 1976
6. Kristensen JK, Buemann B, Kuhl E: Ultrasonic scanning in the diagnosis of splenic hematomas. *Acta Chir Scand* 137:653–657, 1971
7. McVerry BA, Vicary FR, Vohe J, Dormandy KM: Ultrasonography in the management of haemophilia. *Lancet* 1:872–874, 1977
   Bilateral pseudotumors of the pelvis in a patient with Christmas disease: with notes on localization by radioactive scanning and ultrasonography. *Am J Roentgenol* 121:173–186, 1974
9. Nowotny C, Niessner H, Lechner K: Sonography: a method of localization of hematomas in hemophiliacs. *Hemostasis* 5:129–135, 1976
10. Shapiro HN, McBride CM, Luna MA: Hematoma of the liver discovered one year after injury. *Am J Surg* 113:833–836, 1967
11. Doust BD: Abscesses, hematomas, and other fluid collections, in *Abdominal Gray Scale Ultrasonography*, edited by Goldberg BB, New York, Wiley, 1977, pp 231–259
12. Sandler MA, Karo JJ: The spectrum of ultrasonic findings in endometriosis. *Radiology* 127:229–231, 1978
13. Laing FC, Filly RA: Problems in the application of ultrasonography for the evaluation of pleural opacities. *Radiology* 126:211–214, 1978
14. Holm HH, Pedersen JF, Kirstensen JK, Rasmussen SN, Hancke S, Jensen F: Ultrasonically guided percutaneous puncture. *Radiol Clin North Am* 13:493–503, 1975

Comparison of Whole Lung Tomography and Computed Tomography for Detecting Pulmonary Nodules

JOHN R. MUHM,[1] LARRY R. BROWN, JOHN K. CROWE, PATRICK F. SHEEDY II, ROBERT R. HATTERY AND DAVID H. STEPHENS

Detecting pulmonary metastasis is important when planning surgical therapy, radiotherapy, or chemotherapy in patients with known malignancy. A series of 91 patients was studied by both whole lung tomography and computed tomography (CT) of the lungs. More pulmonary nodules were detected with CT than with whole lung tomography in 32 (35%) of the patients. Of the 91 patients in the study, 31 had resection of some or all of the pulmonary nodules. In 27 patients, the nodules were primary or metastatic malignant lesions. Bilateral pulmonary nodules were detected with CT in 13 patients when whole lung tomography had demonstrated nodules in only one lung. CT has replaced whole lung tomography as the method preferred by the authors for detecting pulmonary nodules in selected patients at risk to develop pulmonary metastasis.

It is well established that more lesions in the pulmonary parenchyma and the mediastinum can be detected with whole lung tomography than with conventional plain radiography of the chest [1]. Recent publications have also shown that more pulmonary nodules can be detected by CT than by whole lung tomography [2–6]. This report describes our experience with 91 patients who had both whole lung tomography and CT of the lung for the detection of pulmonary nodules.

Subjects and Methods

Between October 1975 and August 1977, 91 patients had both whole lung tomography and lung CT to detect pulmonary nodules. Malignancy had been proven in 88 patients and they were being studied for possible pulmonary metastasis. Of the 88 patients, 37 had osteogenic sarcoma; seven had primary lung carcinoma; six had Ewing's sarcoma; four had fibrosarcoma of the soft tissues; three each had carcinoma of the colon, synovial sarcoma, liposarcoma, and breast carcinoma; two each had rhabdomyosarcoma, fibrous histiocytoma, melanoma, and malignant teratoma; and 14 each had one other type of carcinoma or sarcoma. Some of these patients had already had the primary malignant lesion resected, while others had a known primary neoplasm that had not yet been resected. One patient had malignant cells in the sputum and was being studied to find the primary neoplasm. Two patients with no known malignancy had a solitary pulmonary nodule detected by conventional radiography and had whole lung tomography and CT as part of their preoperative evaluation.

Whole lung tomography was performed at 125 kVp using a 15° linear arc. Tomographic cuts were performed at 1 cm intervals. The entire chest from apex to base was included on each 35.6 x 43.2 cm film. Tomographic cuts were begun at posterior ribs and continued until the anterior ribs were visualized.

CT was performed with a prototype EMI CT-5000 body scanner and an EMI CT-5005 body scanner. Each machine has a scan time of 18 sec. Sequential CT scans without contrast material were performed at intervals of 1.5 cm, and the chest was scanned from the apex of the lung to the posterior costophrenic angle.

The initial interpretations of the whole lung tomographic examinations and the CT examinations are used in this study, so the results discussed here are not a retrospective evaluation of either the whole lung tomographic examination or the CT examination. Both examinations were usually performed the same day. The radiologist who interpreted the whole lung tomographic examination was usually not the radiologist who interpreted the CT examination. In the first six cases, the results of the whole lung tomographic examinations were available to the radiologist interpreting the CT examination, but in the remainder the two examinations were conducted by different radiologists and interpreted independently.

Results

More pulmonary nodules were detected by CT than by whole lung tomography in 32 (35%) of the 91 patients. In five of the 32 patients, whole lung tomography showed no pulmonary nodules, but CT showed one or more. In 13 patients, one nodule had been seen on whole lung tomography, but two or more were detected by CT. In 14 patients, two or more nodules were detected by whole lung tomography, while CT showed even more nodules. In 13 of the 32 patients, bilateral pulmonary nodules were detected by CT after whole lung tomography demonstrated nodules in only one lung.

In four patients fewer nodules were detected by CT than by whole lung tomography. In one patient, whole lung tomography demonstrated two pulmonary nodules, while only one was seen on CT. Subsequent surgery removed the two metastatic nodules seen on whole lung tomography, and confirmed a false negative CT examination. In two patients, CT did not demonstrate a nodule that had been demonstrated with conventional chest radiographs and whole lung tomography. However, since both these patients were too large to fit completely into the aperture of the gantry, the CT examination did not include the lung portion containing the nodule. In the fourth patient whole lung tomography showed a 2 cm mass in the lingula and a questionable 1 cm nodular density in the right lung. CT demonstrated the left lung nodule, but showed that the right lung was normal. Follow-up examinations of this patient during the next

Received April 21, 1978; accepted after revision August 21, 1978.
This work was supported in part by Research Grant CB-53886C from the National Institutes of Health, Public Health Service.
[1]All authors: Department of Diagnostic Radiology, Mayo Clinic and Mayo Foundation, Rochester, Minnesota 55901. Address reprint requests to J. R. Muhm.

© 1978 American Roentgen Ray Society

0361–803X/78/1200–0981 $00.00

year show no evidence of a nodule in the right lung. Review of the whole lung tomograms suggests that the initial CT interpretation was correct and that the positive interpretation of the initial whole lung tomograms was incorrect.

In three patients, there was a false positive CT interpretation because no lesions were found at surgery which corresponded to the density seen on the CT examination. In one of these patients with a Ewing's sarcoma, CT showed a 1.5 cm nodule in the right middle lobe and a 5 mm subpleural nodular density in the right lower lobe (fig. 1). At thoracotomy, a 1.5 cm metastatic lesion was removed from the right middle lobe, but the surgeon could not palpate a parenchymal nodule that would correspond with the subpleural density seen in the right lower lobe. In another patient with a previous large-cell carcinoma of the right lung, CT demonstrated a 2.5 cm mass in the left lung apex and a 1 cm nodular density in the lingula (fig. 2). At surgery, a 2.5 cm metastatic lesion was resected from the apex of the left upper lobe, but the surgeon could not palpate a parenchymal nodule in the lingula corresponding to the density seen on CT. In both these cases, follow-up radiographs of the chest over 18 months show no evidence of pulmonary nodules. The third patient had a left upper lobectomy for an in situ squamous cell carcinoma of the left upper lobe bronchus. CT examination had demonstrated a 1 cm nodular density in the left upper lobe, but the pathologist did not find a parenchymal nodule in the resected left upper lobe (fig. 3).

All of the false positive and false negative CT interpretations were in the first 29 cases of the study, indicating that accuracy increased as more experience was gained in interpreting CT examinations.

Of the 91 patients, 31 had thoracotomy or median sternotomy within 10 days after CT examination and resection of some or all of the nodules demonstrated with CT. In 25 of the 31 patients, the resected nodules were primary or metastatic malignant lesions. In two patients previously described as having false positive results, additional nodules detected only with CT were resected and shown to be metastatic lesions, while one of the additional nodules in each patient was not found by the surgeon. In the other patient with false positive CT results, no pulmonary nodule was found after left upper lobectomy. In two patients, the nodule was a benign granuloma due to *Histoplasma capsulatum*. One patient had several nodules that proved to be suture granulomas from previous resections of metastatic nodules of synovial sarcoma. None of the resected nodules were subpleural lymph nodes.

Thoracotomy or median sternotomy was performed in 18 of the 32 patients in whom more nodules were detected by CT than by whole lung tomography. Three of these patients had the false positive CT examinations previously described; in the other 15 the nodules proved to be metastatic lesions. In eight of the 15 patients with proved metastases, all the additional nodules detected by CT were resected. In four patients, the surgeon described the lung as "studded with metastases," and no attempt was made to remove all the nodules that had been detected by CT. A unilateral thoracotomy was performed in three patients. All the nodules that had been detected by CT in that lung were removed, but CT

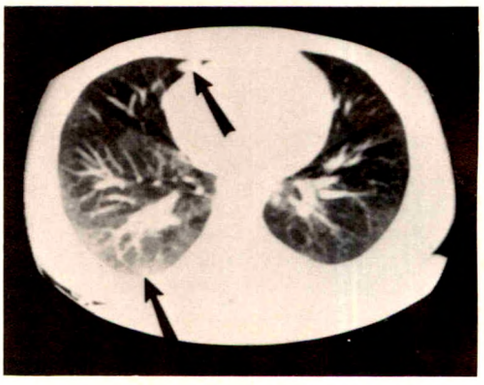

Fig. 1.—CT of 18-year-old girl with Ewing's sarcoma showing 15 mm metastatic lesion (*upper arrow*) in right middle lobe and 5 mm nodular density not found at thoracotomy (*lower arrow*).

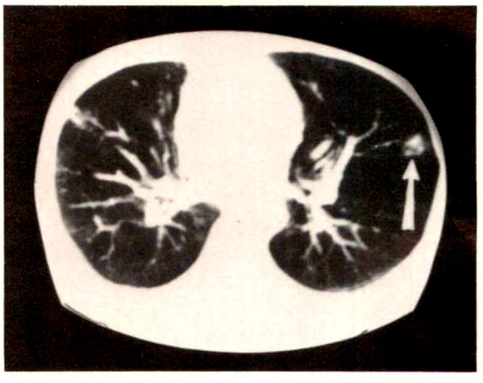

Fig. 2.—CT of 62-year-old man with metastatic large-cell carcinoma of right lung showing 15 mm nodular density (*arrow*) in lingula not found at thoracotomy. Note postoperative fibrosis anteriorly in right midlung.

Fig. 3.—CT of 66-year-old man with carcinoma in situ of left upper lobe (*arrow*) showing 1 cm nodular density not found by pathologist after left upper lobectomy.

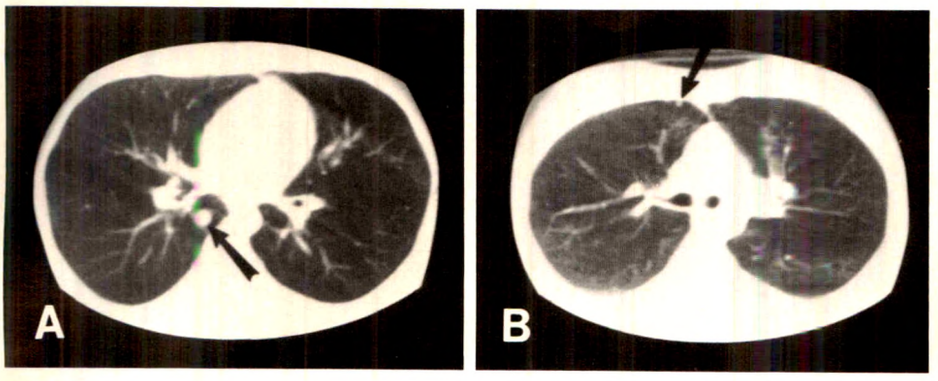

Fig. 4.—CT of 18-year-old boy with osteogenic sarcoma. *A*, Previously undetected 15 mm metastatic lesion (*arrow*) behind right hilum. *B*, Previously undetected 5 mm subpleural metastatic lesion (*arrow*).

had shown bilateral nodules, and the nodules in the other lung were not removed.

The finding of more pulmonary nodules by CT than by whole lung tomography altered the clinical course in 20 of the 32 patients. In five patients, this information obviated the need for further surgery, either thoracotomy or laparotomy, and made chemotherapy the treatment of choice. In the other 15 patients, the additional information was helpful in their surgical management. In two of these 15 patients, the presence of the nodules seen with CT led to thoracotomy for resection of the nodule or nodules. In four patients, a median sternotomy was performed rather than a thoracotomy, because bilateral nodules had been detected. In one patient in whom bilateral nodules were detected by CT this information was responsible for both the decision to operate and the performance of a median sternotomy rather than a thoracotomy. In one patient, a right thoracotomy was planned, but the CT examination indicated a left thoracotomy instead. In seven patients, resection of pulmonary nodules was planned, and detection of additional nodules with CT directed the surgeon to these additional nodules at thoracotomy.

Discussion

Because resection of pulmonary metastatic lesions improves the survival rate in certain types of malignancies [7, 8], for several years we have used whole lung tomography to detect pulmonary metastases, especially in patients who have malignant bone tumors and soft tissue sarcomas. Our early clinical experience with CT of the lungs showed that more pulmonary nodules could be detected by CT than by either conventional chest radiography or plain-film whole lung tomography [3,4] and our current findings confirm this.

More nodules can be detected by CT than by whole lung tomography for two reasons. First, the transverse orientation of the CT images eliminates the confusing shadows caused by superimposed cardiovascular and bony structures (fig. 4). Second, the format of the CT image (looking for a white spot against a dark gray background) makes identifying pulmonary nodules easier with CT than with whole lung tomography, in which nodules are seen as a lighter gray spot against a darker gray background.

Identifying pulmonary nodules on CT is straightforward when the nodule is larger than the pulmonary vessels in the same portion of the lung (fig. 4*A*). When pulmonary nodules are the same size as pulmonary vessels or smaller than the vessels in the same area, CT interpretation is more difficult. If a density on the CT image is continuous with a vascular structure on the same scan or on an adjacent scan, it probably represents a vascular structure rather than a pulmonary nodule. If the density on the CT image is near the periphery of the lung and is larger than blood vessels located a similar distance away from the chest wall or is definitely not connected to the vessels in the area, the density more likely represents a pulmonary nodule (fig. 4*B*). Nodules very close to the diaphragm and nodules in the subpleural region can be difficult to detect on static film or Polaroid CT images taken at fixed window settings. Frequently only a portion of a nodule is included in the 13 mm thickness of the scan, or a nodule will be overshadowed by a portion of the diaphragm that is partially included in the scans near the lung base. Electronic manipulation of the image display is essential in detecting such nodules. However, caution must be used when assigning significance to nodular densities less than 5 mm in diameter that are located in the subpleural portions of the lungs. Although this is an area frequently involved by metastatic disease, small areas of pleural thickening or subpleural fibrosis may give the appearance of a peripheral nodule. Therefore, unless numerous other larger nodules are seen in the lung or a previous comparable CT scan is available for comparison, we are hesitant to interpret these densities as representing metastasis. We believe CT scanning is the most reliable method for clinically following these densities, because juxtadiaphragmatic and subpleural densities seen on CT examinations are usually difficult, if not impossible, to detect by conventional radiographic techniques, including conventional plain-film tomography.

Contrary to other findings [2, 6, 9, 10], almost all the pulmonary nodules detected only with CT in our study were metastatic lesions. In 15 (83%) of 18 patients in whom CT demonstrated more pulmonary nodules than

had whole lung tomography, resection confirmed that the nodules demonstrated only by CT were metastatic lesions. Of the 91 patients, 31 had pulmonary nodules demonstrated by CT resected, and the nodules in 27 of these patients were metastatic lesions. The high proportion of proved metastatic nodules in this series is partly due to careful selection of patients for CT examination. We are primarily studying patients with known malignancies that have a tendency to metastasize to the lungs. Pulmonary nodules found in this clinical setting are generally metastatic.

When a solitary pulmonary density is detected by CT in a patient with no known malignancy, our approach is the same as it is in the patient with a solitary pulmonary nodule detected on a chest radiograph. Any previous films of the patient are evaluated to determine if the nodule was present previously and, if so, to see if it has enlarged. Localized plain-film tomography is performed to determine if the density represents a nodule or is merely an area of fibrosis or pleural thickening. If the density is a nodule, plain-film tomography is used to determine if the nodule is calcified. In certain patients, CT can determine if the nodule is calcified or not, especially if the nodule is large, but in most, localized plain-film tomography is more accurate than CT. Because of the "partial volume" effect, the CT numbers for calcified nodules may be higher than, equal to, or lower than those for an uncalcified nodule, depending on how much aerated lung is included in the 13 mm scan thickness.

Because more pulmonary metastastic lesions can be detected with CT than with whole lung tomography, and particularly because bilateral nodules have been detected with CT when whole lung tomography has demonstrated only unilateral nodules, we now use a combination of stereo chest radiography and CT for detecting pulmonary metastasis in selected patients. This policy has the enthusiastic support of our oncologists and thoracic surgeons. Before beginning CT of the lung, 50 to 60 whole lung tomographic examinations were performed each month, but now 10 to 15 whole lung tomographic studies are done each month and 70 to 80 CT scans are done each month in an effort to detect pulmonary metastasis.

REFERENCES

1. Neifeld JP, Michaelis LL, Doppman JL: Suspected pulmonary metastases: correlation of chest x-ray, whole lung tomograms, and operative findings. *Cancer* 39:383–387, 1977
2. Jost RG, Sagel SS, Stanley RJ, Levitt RG: Computed tomography of the thorax. *Radiology* 126:125–136, 1978
3. Muhm JR, Brown LR, Crowe JK: Detection of pulmonary nodules by computed tomography. *Am J Roentgenol* 128:267–270, 1977
4. Muhm JR, Brown LR, Crowe JK: Use of computed tomography in the detection of pulmonary nodules. *Mayo Clin Proc* 52:345–348, 1977
5. Kollins SA: Computed tomography of the pulmonary parenchyma and chest wall. *Radiol Clin North Am* 15:297–308, 1977
6. Schaner EG, Chang AE, Doppman JL, Conkle DM, Flye MW, Rosenberg SA: Comparison of computed and conventional whole lung tomography in detecting pulmonary nodules: a prospective radiologic-pathologic study. *Am J Roentgenol* 131:51–54, 1978
7. Thomford NR, Woolner LB, Clagett OT: The surgical treatment of metastatic tumors in the lungs. *J Thorac Cardiovasc Surg* 49:357–363, 1965
8. Martini N, Huvos AG, Miké V, Marcove RC, Beattie EJ Jr: Multiple pulmonary resections in the treatment of osteogenic sarcoma. *Ann Thorac Surg* 12:271–278, 1971
9. Schaner EG, Chang AE, Doppman JL, Conkle DM, Rosenberg SA: Comparison of computed and conventional whole lung tomography in the detection of pulmonary metastases (abstr). *J Comput Assist Tomogr* 1:363, 1977
10. Neifeld JP, Doppman JL: Author's comment. *Invest Radiol* 12:477–478, 1977

Radiographic Manifestations of Pulmonary *Mycobacterium kansasii* Infections

EDWARD E. CHRISTENSEN,[1] GERAL W. DIETZ,[1] CHAI HO AHN,[2] JOHN S. CHAPMAN,[3] ROBERT C. MURRY,[1] AND GEORGE A. HURST[2]

The radiographic characteristics of 187 pristine cases of pulmonary *Mycobacterium kansasii* infection are reviewed. The cases were selected from a total of 309 patients with two positive sputum cultures. All but three of the 187 patients had pulmonary disease. The progenitive focus of disease almost always involved the upper lobes, the right side (72%) more often than the left (50%). Upper lobe disease began posterior to the trachea in every case. Only one patient had disease that originated in an atypical location, that is, in the superior segment of the right lower lobe. The most frequent radiographic abnormality was cavitation (96% of diseased patients). The classical description of a thin walled cavity (or cavities) occurred in 33% of patients. A cicatricial reaction was common (two-thirds of cases). About 63% of patients had endobronchial spread. The likelihood of endobronchial disease decreased as the distance from the progenitive focus increased. Pleural effusions and adenopathy were rare. In an individual case, it is not possible to differentiate between pulmonary *M. tuberculosis* and *M. kansasii* infections.

Mycobacterium kansasii is one member of a group of organisms which are called the atypical mycobacteria. The group was called "atypical" because it differed bacteriologically from *M. tuberculosis,* the "typical" causative organism for human tuberculosis. In the Runyon [1] classification of the atypical mycobacteria, *M. kansasii* is classified as group I organism. It is closer to the tubercle bacillus, both bacteriologically and clinically, than any of the other atypical organisms [2–4]. It produces a creamy white colony that matures in from 14–21 days. The colonies turn from white to yellow-orange upon exposure to light, thus the name photo (light) chromogen (color).

The epidemiology of *M. kansasii* infection is not understood and the source of human infections is unknown. The disease is not considered contagious from one human to another, so infected patients need not be isolated. The incidence of disease varies a great deal from one section of the country to another. It is exceedingly uncommon in New England [5], but quite common in the central portions of the United States. Most large reports have come from Texas, Kansas, Illinois, and Louisiana [6–10].

Subjects and Methods

Patient Selection

We retrospectively studied the radiographic characteristics of pulmonary mycobacteriosis kansasii. All patients were from the University of Texas Health Center at Tyler (formerly the East Texas Chest Hospital). The study covered a 17-year period from September 1959 to September 1976. Patients with at least two positive sputum cultures growing at least 100 colonies of *M. kansasii* were considered potential candidates for the study. Those with only one positive culture, with fewer than 100 colonies, or with only one positive gastric aspirate were excluded. A total of 309 patients met this initial test. Their charts and radiograms were reviewed, and 187 pristine cases were selected for this study. These patients had no previous history of a mycobacterial infection, no other sputum pathogen within 6 months of the admission chest radiography, at least one posteroanterior and lateral chest examination, and not more than 30 days of antituberculous therapy. Only 17% of the patients in the pristine group had any treatment prior to the first radiograph.

A total of 122 (40%) of the 309 patients with two positive cultures failed at least one of the tests for inclusion in the pristine category: 40 had been treated more than 30 days, 24 had a second organism within 6 months of the first radiograph (usually *M. tuberculosis* but occasionally group II, III, or IV mycobacteria or a fungus), 39 gave a history of previous tuberculosis, and 19 were discarded for miscellaneous reasons (no radiographs, previous pulmonary resections, complicating bronchogenic carcinoma, radiation therapy, etc.).

Definitions

Words like patchy, fibronodular, fibrocavitary, interstitial, reticular, nodular, fluffy, and so on had different meanings to each of the authors. Newell et al. [11] had similar problems when they attempted to set down a definitive nomenclature for tuberculosis. Instead of forcing our nomenclature on the films, we tried to let the radiographic images serve as their own definitions. To accomplish this, we photographically reduced the posteroanterior films of the pristine cases to a 12.7 × 17.8 cm format. All of these smaller films could be displayed at one time, so it was easy to search for cases that had a similar radiographic appearance. While we could not agree on descriptive terms, we could identify recurring patterns of disease. The few descriptive terms that we did use are illustrated in figure 1 and defined as follows:

Focus of disease—an area of homogeneous confluent and/or cavitary pulmonary disease greater than 1 cm. Two or more foci could be present in a lobe, provided the foci were clearly separated by apparently normal lung. We differentiated foci into two types: progenitive foci and secondary foci.

Progenitive focus of disease—the focus that was judged to be the initial site of infection. When two sites were equally involved, both were considered progenitive foci. Even with moderate asymmetry, both were called progenitive foci when

Received April 28, 1978; accepted after revision September 7, 1978.

[1] Department of Radiology, University of Texas Health Science Center at Dallas, 5323 Harry Hines Boulevard, Dallas, Texas 75235. Address reprint requests to E. E. Christensen.

[2] Department of Medicine, University of Texas Health Science Center at Tyler, Tyler, Texas 75701.

[3] Department of Internal Medicine, University of Texas Health Science Center at Dallas, Dallas, Texas 75235.

© 1978 American Roentgen Ray Society

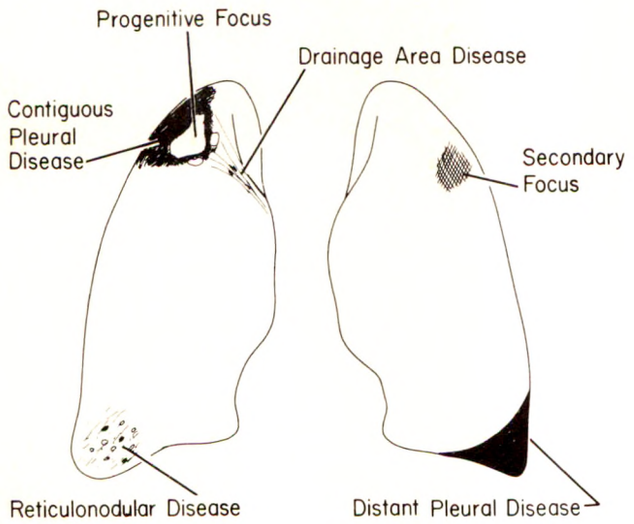

Fig. 1.—Diagram of descriptive terms.

they were cavitary and located in the posterior portions of the upper lobes.

Secondary focus of disease—a focus that appeared smaller and lower in position than the progenitive focus from which it originated. Secondary foci were considered areas of endobronchial spread.

Drainage areas of disease—linear- and nodular-appearing disease between a focus of infection and the adjacent hilum.

Reticulonodular disease—all parenchymal lung disease not included in the previous definitions. Reticulonodular disease was considered endobronchial spread. At times it was primarily reticular, at other times it was entirely nodular, but it usually was a combination of the two.

Endobronchial spread—all pulmonary parenchymal disease other than a progenitive focus with its drainage area disease. Secondary foci and all reticulonodular disease were categorized as endobronchial spread. We defined a secondary focus as one that was anatomically lower (or equal in height) and smaller in size than a progenitive focus.

Contiguous pleural disease—pleural disease, or apparent pleural disease, between a progenitive focus of infection and the adjacent chest wall. When the pleural disease was adjacent to a cavity, it was impossible to determine how much of the thickening actually represented the wall of the cavity.

Distant pleural disease—pleural thickening and/or fluid remote from a focus, usually in the lateral or posterior costophrenic angles.

Results

Age, Race, and Sex Distribution

The median age of patients in the pristine group was 50 years. A distinct age difference occurred between males and females. Median age of males was 52 years; females, 41 years. The youngest patient was an 18-year-old white male and the oldest a 93-year-old Latin male. Patients were white (80%), black (18%), and Latin (2%). The disease was about four times as common in males (81%) as in females (19%).

Associated Nontuberculosis Disease

Chronic obstructive pulmonary disease was the only nontuberculosis disease that occurred with significant frequency. This diagnosis was made on the basis of overexpanded lungs, that is, flattened diaphragms and an increase in the anteroposterior diameter of the chest. The degree of overexpansion was graded as minimal (34%), moderate (21%), and advanced (6%). The diagnosis of bullous emphysema was only made when we could actually see the walls of blebs or bullae. Bullous disease (39%) was graded by severity as minimal (20%), moderate (11%), and advanced (8%).

TABLE 1

Radiographic Classification of *M. kansasii* Infections by Extent of Pulmonary Lesions

Classification	No. Patients	(%)
Normal (no visible disease)	3	(1.6)
Minimal	4	(2.1)
Moderately advanced	80*	(42.8)
Far advanced	100†	(53.5)
Total	187	(100)

* Of these, 29 were only because of cavitation.
† Of these, 43 were only because of cavitation.

Extent of Disease

The extent of disease was assessed according to the 1961 classification of pulmonary tuberculosis [12]. Table 1 summarizes the extent of disease in the 187 patients in our study group. Three patients had normal radiographs, even though they had two positive cultures. The infection was either moderately or far advanced in 98% of the diseased patients. One of the reasons for this relatively advanced stage of disease is the cavitary nature of *M. kansasii* infections. This old classification of tuberculosis is heavily weighted towards cavitary disease, and almost all *M. kansasii* infections are cavitary.

Distribution of Pulmonary Infection

The disease was unilateral in 59% of patients and bilateral in the remainder. When the disease was unilateral, the right side was infected more than twice as often as the left. In 17% of the patients with unilateral infections, the disease was extensive (fig. 2). The right upper lobe was the most diseased lobe in 115 patients (63%), the left upper lobe in 74 patients (41%), and each of the lower lobes in two patients (1%). The total is more than 100% because occasionally two lobes were equally involved. The disease was confined to one lobe in 80 patients (43%): 28% in the right upper lobe and 15% in the left upper lobe. The upper lobes were diseased in all but one of the 80 patients with single lobe disease. The exception was in the superior segment of the right lower lobe of a 34-year-old white male (fig. 3). He did not have diabetes, nor was he a compromised host. The other patients with their most extensive disease in the lower lobes also had upper lobe involvement and the lower lobe disease probably represented extensive endobronchial spread.

Table 2 shows the segmental distribution of disease within the involved lobes. On the lateral view, the anterior wall of the trachea was used to separate the anterior segments from the other segments of the upper lobes.

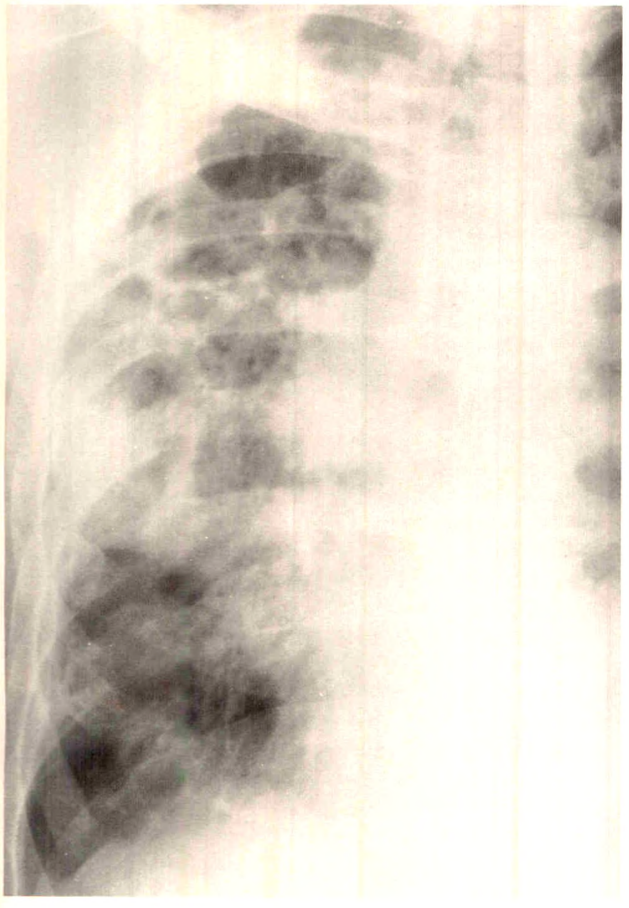

Fig. 2.—Extensive unilateral *M. kansasii* infection.

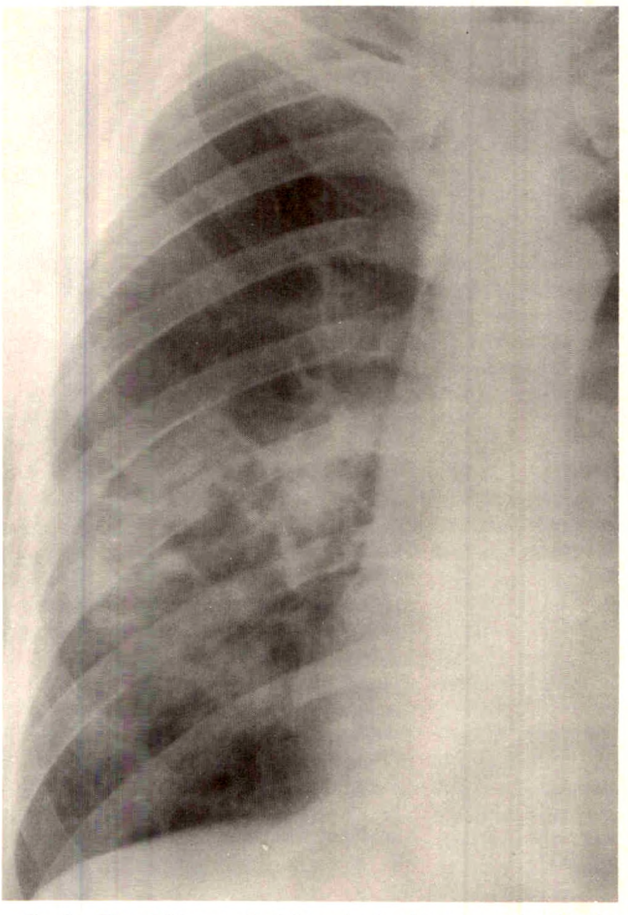

Fig. 3.—Film of 34-year-old white male showing unusual location for focus of *M. kansasii* infection in superior segment of right lower lobe.

Occasionally a large progenitive focus extended into the anterior or lingular segments. However, in each of these instances, the disease was extensive and originated in a more posterior site. No patient had disease that was limited to the anterior portion of an upper lobe.

The disease involved the apical portions of the lungs in 157 patients (85%) and the subapex in 155 patients (84%). In 97% of patients, the disease involved either the apex, subapex, or both. Only six patients had infections that spared the apical and/or subapical regions. One of these was the patient with disease limited to the superior segment of the right lower lobe. The other five patients had disease too low in the lungs to be considered subapical, but even in these patients, the disease originated posterior to the trachea.

The lungs were divided radially into three zones: (1) perihilar, (2) midlung, and (3) peripheral. Only 15% of progenitive foci were limited to a single zone. In one of these patients, the disease was perihilar. The others were equally divided between the midlung and peripheral zones. The patient with perihilar disease had large bullae replacing most of the lung in the midlung and peripheral zones. When the disease involved more than one zone, the midlung and peripheral zones were involved with almost equal frequency. The perihilar zone was diseased about one-third as often as the other two zones. The zone judged to be maximally involved was equally divided between the mid and peripheral zones.

TABLE 2

Lobar and Segmental Distribution of Progenitive Foci in 184 Patients

Lobe	No. Patients	Segment	Diseased Segments	Only Diseased Segment
Right upper	134	Apical	121	12
		Posterior	122	12
		Anterior	51	0
Left upper	92	Apical-posterior	92	68
		Anterior	23	0
		Superior lingular	4	0
		Inferior	2	0
Right lower	1	Superior	1	1

Note.—Total is more than 184 because some patients had bilateral progenitive foci.

Cavitation

Many patients had bullous emphysema; in these patients, it was occasionally impossible to differentiate between cavitation and bullae. Nevertheless, in each

TABLE 3

Characteristics of 252 Cavitary Foci

Characteristics of Cavities	Percentage of Foci
Number:	
1 cavity	12
2–5 cavities	28
5 or more cavities	60
Greatest dimension of largest cavity (cm):	
Under 2	31
2–3.9	41
4–6	19
More than 6	9
Infiltrate cavitated (%):	
(20)	18
(40)	44
(60)	24
(80)	14
Air-fluid level	8

Note.—Total includes 26 cavitary secondary foci.

case we attempted to make the differentiation. Of 299 foci of infection, 252 were judged to be cavitary. The foci that were not cavitary were usually smaller and, in most cases, probably represented secondary foci. We measured the largest cavity and estimated both the number of cavities and the percentage of the infiltrate that had cavitated (table 3). In 88% of patients, cavities were multiple. In 28% of the cavitary foci, the largest cavity was 4 cm or more in greatest dimension, and in most cases cavitation involved a large percentage of the total disease process.

Air-fluid levels occurred in 8% of cavitary foci. Usually only one cavity contained an air-fluid level, even though multiple cavities may have been present. The percentage of the cavity that was fluid-filled was always minimal, never exceeding 20% of the estimated volume of the cavity.

Drainage Area Disease

Linear and nodular disease between a progenitive foci and adjacent hilum was called drainage area disease (fig. 1). It usually took the form of linear stranding along the bronchovascular tree supplying the progenitive focus as shown in figure 4. It was exceedingly common, occurring to some extent in 80% of right upper lobe and 57% of left upper lobe progenitive foci.

Scarring and Volume Loss

A cicatricial reaction was common, especially when the disease was extensive. Volume loss was present in 68% of upper lobe progenitive foci: in 41% the volume loss was minimal, in 18% moderate, and in 9% severe. To be judged severe, a lobe had to be markedly contracted, (i.e., almost completely destroyed).

Patterns of Disease for Upper Lobe Foci

Cavitation was the most consistent feature of *M. kansasii* infections. In reviewing all of the full size chest films, including tomograms when available, cavitation was present in 96% of patients with radiographic disease. In reviewing the smaller photographic reproductions, cavitary disease was the predominate radiographic feature in 85% of the upper lobe foci. In the other 15%, infiltrative disease predominated. The cavitary disease was divided into two major subdivisions depending on whether there was one predominate cavity (47%) or multiple cavities without a predominate one (38%). These broad categories were further subdivided into seven patterns. Bilateral disease was frequently asymmetrical so that the two lungs had to be categorized separately. Approximately the same percentages of each category occurred on the two sides, but the right was more often diseased. The seven patterns are:

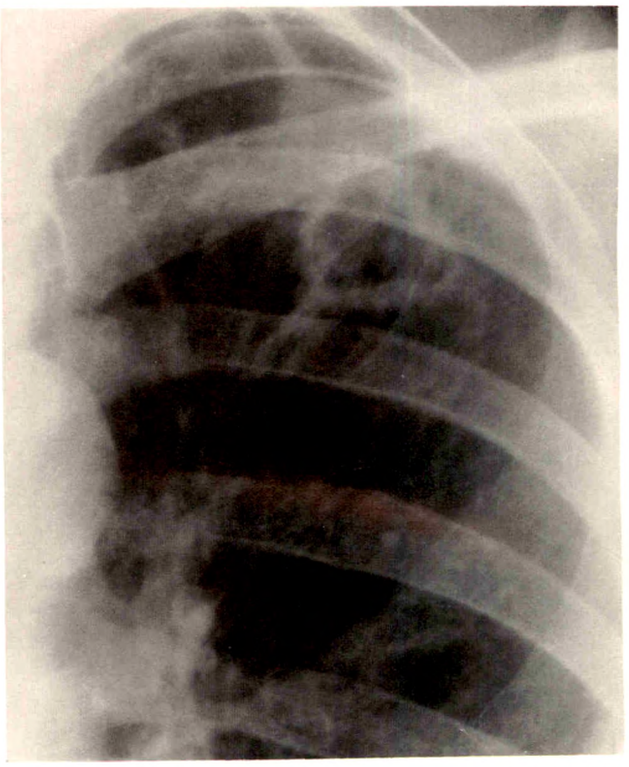

Fig. 4.—Pattern 1 consisting of one predominate cavity with little or no surrounding parenchymal disease.

Pattern 1: One predominate cavity with little or no surrounding parenchymal disease. This category was reserved for solitary thin-walled cavities with little or no surrounding parenchymal disease like the cavity shown in figure 4. This is the classic pattern usually described as a prototype for atypical mycobacteriosis [13–15]. Only 8% of patients had this pattern.

Pattern 2: One predominate cavity with a moderate amount of surrounding parenchymal disease (fig. 5). This was the most common pattern occurring in 28% of lungs.

Pattern 3: One predominate cavity with extensive surrounding parenchymal disease was found in 11% of diseased lungs (fig. 6).

Pattern 4: Multiple cavities (no predominate one) with minimal to moderate amounts of surrounding parenchy-

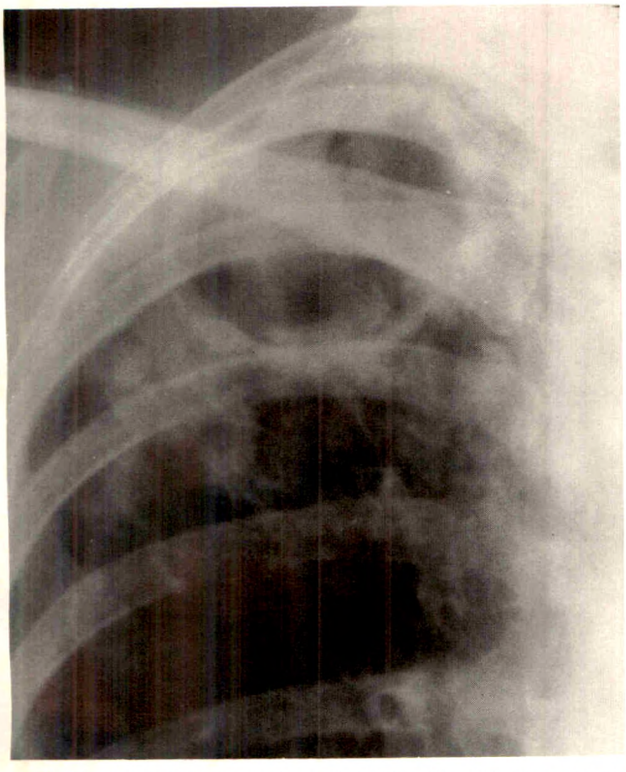

Fig. 5.—Pattern 2 is one predominate cavity with moderate amount of surrounding parenchymal disease.

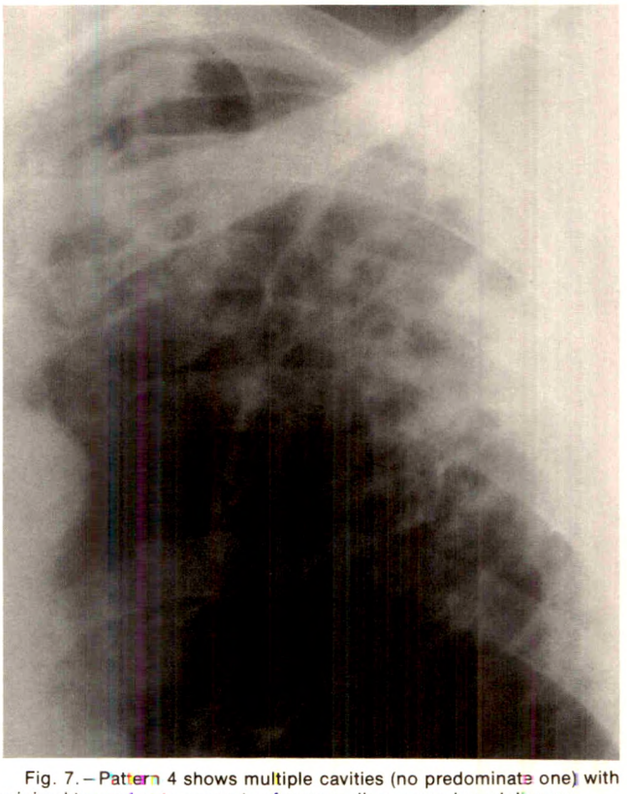

Fig. 7.—Pattern 4 shows multiple cavities (no predominate one) with minimal to moderate amounts of surrounding parenchymal disease.

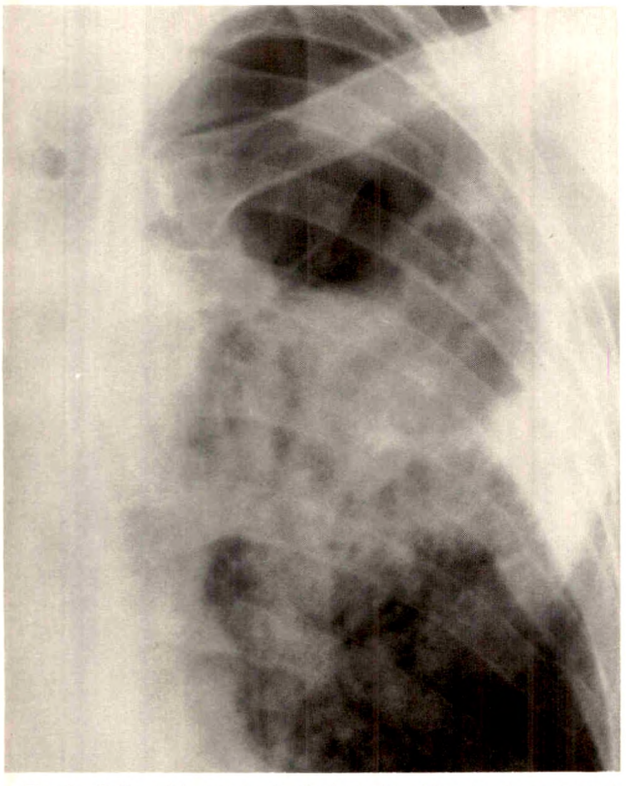

Fig. 6.—Pattern 3 is one predominate cavity with extensive surrounding parenchymal disease.

mal disease (fig. 7). This was the second most frequent pattern, occurring in 25% of diseased lungs. A few of these lesions, especially those with thin-walled cavities, may actually represent bullae and not areas of pulmonary necrosis. Some cases would probably meet other radiologists' definition of "thin-walled" cavitary disease. If they are included, the percentage of patients with thin-walled cavities is 33% (8% pattern 1 and 25% pattern 4).

Pattern 5: Multiple cavities (no predominate one) with extensive surrounding parenchymal disease (fig. 8). Some 13% of all lesions had a similar appearance.

Pattern 6: Small parenchymal infiltrates with little or no cavitation.

The last two patterns are characterized by predominately infiltrative disease. However, even in these patients there were frequently small cavities. Nevertheless, for these last two patterns infiltration was the predominate radiographic feature.

Small parenchymal infiltrates were more common in the left lung where they accounted for 17% of the disease, as opposed to only 9% on the right (fig. 9). The probable explanation for the difference between the two sides is that the disease usually started on the right and the smaller left-sided infiltrates represented secondary foci of endobronchial spread. The overall incidence of pattern 6 disease was 12%.

Pattern 7: Large parenchymal infiltrates with little or no cavitation (fig. 10). Only 3% of upper lobe foci were

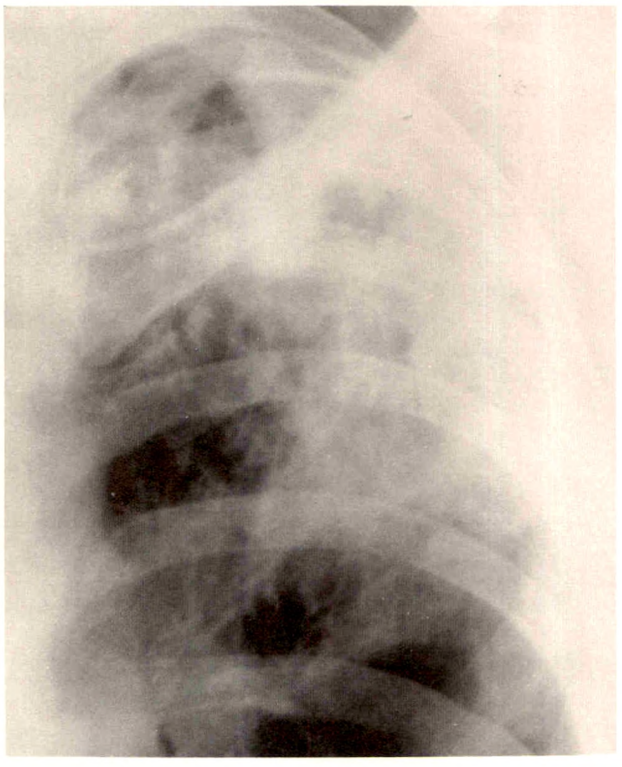

Fig. 8.—Pattern 5 consisting of multiple cavities (no predominate one) with extensive surrounding parenchymal disease.

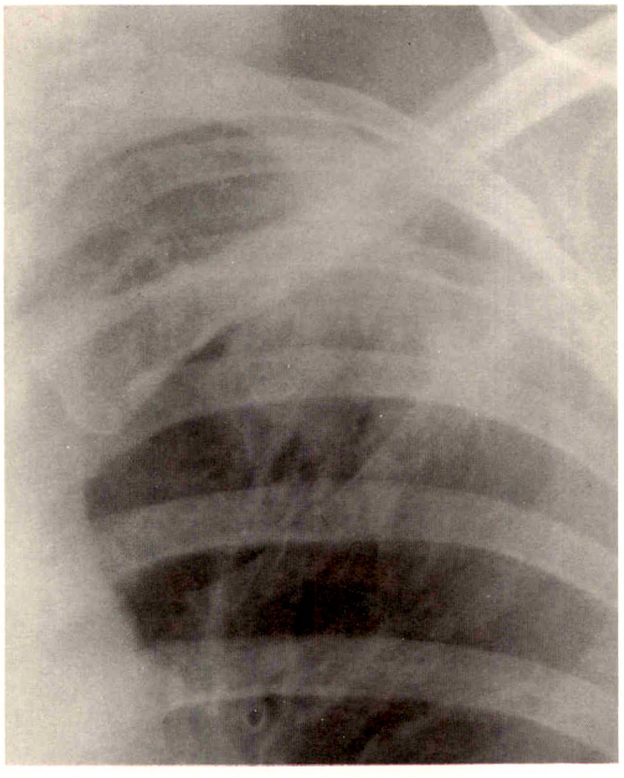

Fig. 9.—Pattern 6 is small parenchymal infiltrates with little or no cavitation.

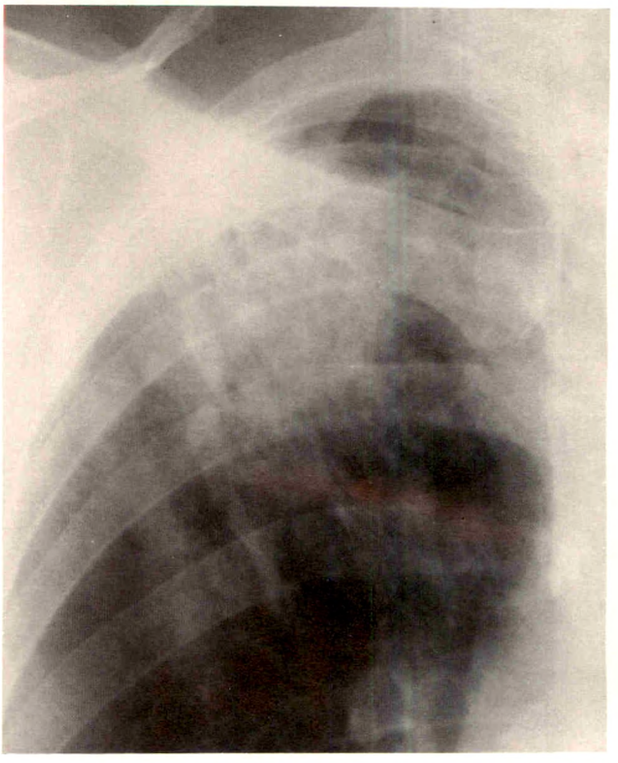

Fig. 10.—Pattern 7 shows large parenchymal infiltrates with little or no cavitation.

of this variety. *M. kansasii* produces a necrotizing granulomatous infection. When the disease has been present long enough to become extensive, a prerequisite for inclusion in the category, necrosis usually dominates the radiographic picture.

Adenopathy

Only one patient had unequivocal adenopathy, a 34-year-old white male with far advanced cavitary disease in the right upper lobe and extensive spread into the right lower and middle lobes. The adjacent right hilar and paratracheal lymph nodes were enlarged. No follow-up films were available. Three other patients had equivocal evidence of adenopathy. In these, an enlarged azygos vein, adjacent pleural thickening, or superimposed nodular pulmonary disease may have been responsible for the radiographic appearance.

Pleural Disease

Pleural disease was divided into two types: (1) distal pleural disease remote from a focus of infection; and (2) contiguous pleural disease adjacent to a focus of infection. Decubitus films were available on only a few patients so we were usually uncertain about the character and chronicity of the distant pleural disease. Seven patients (4%) had a clearly defined edge of pleural thickening and/or fluid blunting either a lateral or posterior costophrenic sulcus, four on the right and three on the left. The quantity of fluid, if indeed the pleural

disease was an effusion, was always minimal, never more than a few hundred milliliters.

Contiguous pleural thickening was present along the adjacent chest wall in 37% of upper lobe progenitive foci. In 18% the maximum thickening measured less than 1 cm, in 16% between 1 and 2 cm, and in 3% over 2 cm (fig. 11). It was frequently impossible to know how much of the thickening was truly pleural and how much represented parenchymal disease in the wall of an adjacent cavity.

Endobronchial Spread

We defined endobronchial spread as disease remote from the progenitive site(s), at a lower or equal height in the lungs, and less mature appearing. Size, cavitation, and the degree of cicatricial reaction were used to assess maturity. Endobronchial spread occurred in 63% of diseased patients. Two principal types of endobronchial disease were recognized: (1) reticulonodular disease with the individual lesions less than 1 cm; and (2) larger, more confluent lesions greater than 1 cm. The larger lesions, called secondary foci, were occasionally cavitary. All lower and middle lobe disease, even when cavitary, was considered endobronchial in origin. The only exception was the one patient with disease confined to the superior segment of the right lower lobe. Reticulonodular disease was extremely variable in its radiographic appearance. It ranged from a fine and sparse reticular infiltrate to extensive near-confluent nodular disease. At times, reticulonodular disease appeared acinar with poorly defined 5–6 mm nodules, while at other times the nodules had crisply defined margins. The nodules ranged in numbers from one to many dozens.

In general, the lung closest to the progenitive focus was at greatest risk. Of the 134 patients with a progenitive focus in the right upper lobe, 34% had intralobar endobronchial spread. Most were reticulonodular and could have been called satellite lesions. The incidence of endobronchial spread diminished as the distance from the parent lobe increased. The right lower lobe (23%) was more frequently involved than the right middle lobe (18%), but the difference was minimal; and superior segment disease (20%) was more common than disease in the basilar segments (16%), but again the difference was minimal. To determine cross-over spread from the right upper lobe to the left lung, 43 patients with concommitant left upper lobe progenitive foci were subtracted from the original 134 patients, leaving a total of 91 patients at risk. Cross-over to the left upper lobe (15%) was more common than to the left lower lobe (5%).

A total of 91 patients had left upper lobe progenitive foci. This number was reduced to 48 patients for cross-over spread because 43 of the 91 patients also had right upper lobe progenitive foci. Endobronchial spread from the left upper lobe was similar to that from the right upper lobe with one exception. Lingular disease was a great deal more common from the left upper lobe (46%) than right middle lobe disease was with a right upper lobe progenitive focus (18%). The explanation for the difference is probably the proximity of the lingular bronchus. While the right middle lobe bronchus originates 2–3 cm from the right upper lobe bronchus, the lingular bronchus shares a common origin with the rest of the left upper lobe. The radiographic picture of lingular endobronchial spread was quite characteristic. From the progenitive focus in the apex, which was frequently cavitary, reticulonodules spread throughout the left midlung and more confluent foci in the inferior lingula developed (fig. 12). The incidence of endobronchial spread to other portions of the lungs from a left upper lobe progenitive focus was: left lower lobe 34%, right upper lobe 19%, right lower lobe 13%, right middle lobe 4%.

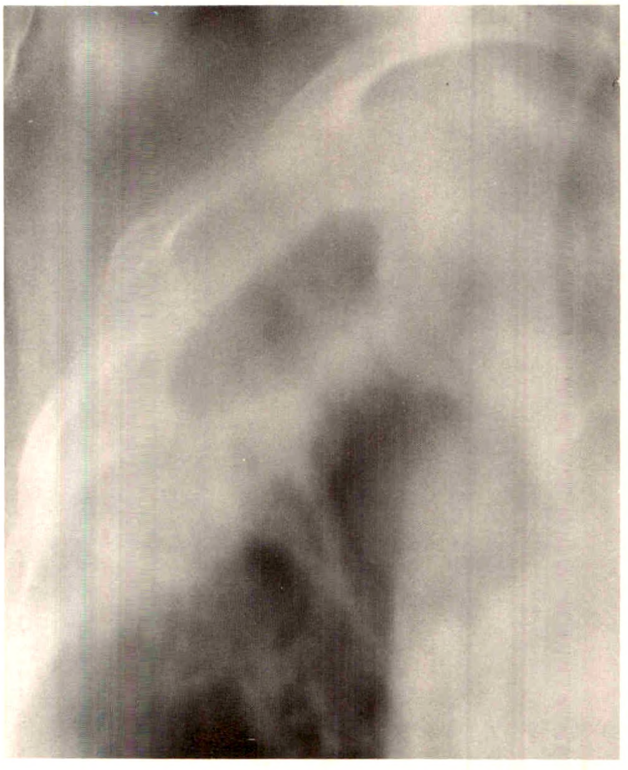

Fig. 11.—Film showing extensive contiguous pleural disease around cavitary right upper lobe focus.

Endobronchial spread was reticulonodular in character about twice as often as it was confluent, that is, formed a secondary focus. The two lungs were similar in this respect. With only a few exceptions, intralobar endobronchial spread was reticulonodular in character.

Discussion

Patients with two positive sputum cultures (over 100 colonies) of *M. kansasii* usually have radiographic evidence of disease. Only three of our pristine cases (1.6%) had normal chest radiographs. The age, race, and sex distribution of our cases is consistent with other reports in the literature [10, 16]. The disease occurs predomi-

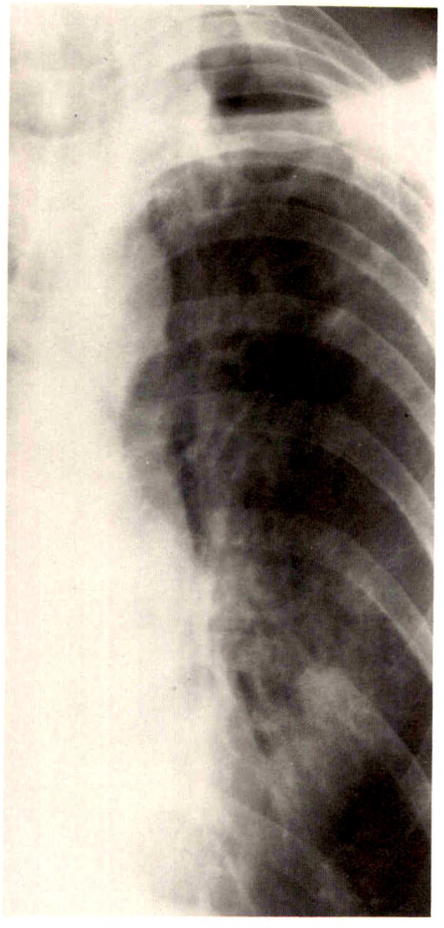

Fig. 12.—Endobronchial spread from cavitary focus in left upper lobe with reticulonodular disease in midlung region and secondary focus in inferior lingular segment.

nately in white males with a mean age of about 50 years. The most important associated disease is chronic obstructive pulmonary disease, which was radiographically evident in 61% of our patients. This is similar to the spirometrically determined 69% incidence of chronic obstructive pulmonary disease reported by Ahn et al. [6] on the same group of patients. Bullous emphysema of some degree was present in 39% of patients.

The most predictable characteristic of pulmonary *M. kansasii* infections is its distribution. Of 80 patients with disease confined to a single lobe, all but one involved the upper lobes, 51 on the right and 28 on the left. The lone exception was in the superior segment of the right lower lobe. When the upper lobe disease was confined to a single segment, the segment was always either the apical, posterior, or apical-posterior, depending on the side. Another common radiographic characteristic of pulmonary *M. kansasii* infections is cavitation, which occurred in 96% of our cases. The cavities were frequently multiple (88%) and often more than 4 cm in diameter (27%). The size, shape, and smoothness of cavity walls were extremely variable and not felt to be characteristic enough to distinguish *M. kansasii* from other cavitary lung diseases. The so-called classical radiographic picture of a thin-walled cavity [13–15] was found in 33% of cases, 8% with one predominate cavity and 25% with multiple cavities.

A cicatricial reaction was common, especially when the disease was far advanced. About two-thirds of the patients had some volume loss, usually minimal, but in 9% of patients, one lobe was markedly contracted.

Adenopathy and pleural effusions were both rare. Only one patient had unequivocal adenopathy. A few (4%) had a pleural meniscus that could have represented an effusion, but because we did not have decubitus films we were never certain. Even in these cases, the quantity of fluid was not more than a few hundred milliliters. No patients had an empyema.

It has been stated that endobronchial spread is less common with *M. kansasii* than with *M. tuberculosis* [15, 17]. The exact incidence of endobronchial spread for a comparable study group of *M. tuberculosis* patients is unknown, but the incidence of endobronchial spread for our *M. kansasii* patients was 63%. The likelihood of endobronchial spread decreases as the distance from the progenitive focus increases. Thus, the parent lobe, the one containing the progenitive focus, was the most frequent site of spread.

We intend to look at a comparable study group of patients infected with *M. tuberculosis* so that we can compare the two diseases. However, at this time we do not feel that we have radiographic criteria which can differentiate an individual case of *M. kansasii* infection from one of *M. tuberculosis*.

ACKNOWLEDGMENTS

We thank Glenda Parkison for manuscript preparation, Jan Dolph for assistance with graphics, Nancy Schreiber for photography, John Moore and Curtis Chaney for technical assistance in Dallas, and Mary Bailey and Reba Hackney for technical assistance in Tyler.

REFERENCES

1. Runyon EH: Anonymous mycobacteria in pulmonary disease. *Med Clin North Am* 43:273–290, 1959
2. Klug KA, Pratt PC: Experimental immunization of guinea pigs with photochromogenic acid-fast bacilli. *Am Rev Respir Dis* 85:78–93, 1962
3. Marmorsteine BL, Scheinhorn DJ: The role of nontuberculous mycobacterial skin test antigens in the diagnosis of mycobacterial infections. *Chest* 67:320–324, 1975
4. Youmans GP, Youmans AS: The measurement of the response of immunized mice to infection with mycobacterium tuberculosis var hominis. *J Immunol* 78:318–329, 1957
5. Warring FC Jr: Mycobacteria in a New England Hospital: a study of mycobacterial species in the sputum of patients with chronic pulmonary disease. *Am Rev Respir Dis* 98:965–977, 1968
6. Ahn CH, Nash DR, Hurst GA: Ventilatory defects in atypical mycobacterioses. *Am Rev Respir Dis* 113:273–280, 1976
7. Christianson LC, Dewlett HJ: Pulmonary disease in adults associated with unclassified mycobacteria. *Am J Med* 29:980–991, 1960
8. Jenkins DE, Bahar D, Chofnas I: Pulmonary disease due to atypical mycobacteria: current concepts, in *Transactions of*

the 19th Conference on Chemotherapy of Tuberculosis, edited by V. A. Department of Medicine and Surgery, Central Office, D.C.: U.S. Government Printing Office 1960, pp 224–229
9. Lester W: Unclassified mycobacterial disease. *Am Rev Med* 17:351–360, 1966
10. Rauscher CR, Kerby G, Ruth WE: A ten year clinical experience with mycobacterium kansasii. *Chest* 66:17–19, 1974
11. Newell RR, Chamberlain WE, Rigler L: Descriptive classification of pulmonary shadows. *Am Rev Tuberculosis* 12:556–584, 1954
12. *Diagnostic Standards in the Classification of Tuberculosis*, New York, National Tuberculosis Association, 1961
13. Chapman JS: *The Anonymous Mycobacteria in Human Disease*, Springfield, Ill. Thomas, 1960
14. Fraser RG, Paré JAP: *Diagnosis of Diseases of the Chest*, Philadelphia, Saunders, 1970
15. Wiot JF, Spitz HB: Atypical pulmonary tuberculosis. *Radiol Clin North Am* 111:191–196, 1973
16. Chapman JS: *The Atypical Mycobacteria and Human Mycobacterioses*, New York, Plenum, 1977
17. Anderson DH, Grech P, Townshend RH, Jephcott AE: Pulmonary lesions due to opportunistic mycobacteria. *Clin Radiol* 26:461–469, 1975

Identification of Thoracic Isomerism from the Plain Chest Radiograph

BENIGNO SOTO,[1] ALBERT D. PACIFICO,[2] ARTHUR S. SOUZA, JR.,[1] LIONEL M. BARGERON, JR.,[3] RUFINO ERMOCILLA,[4] AND INA L. TONKIN[1]

Plain chest radiographs of 14 patients with congenital cardiac malformations associated with situs ambiguus were retrospectively reviewed to establish diagnostic radiographic signs from both frontal and lateral projections. Cardiac diagnosis was previously established by angiocardiography in each of the 14 patients and by supplemental anatomic inspection in 10. Right thoracic isomerism was present in six patients and left thoracic isomerism in eight.

Analysis of frontal projections showed similar length of right and left bronchus (mean ratio, 1.13 ± 0.09) in each patient, and similar anatomic relations between each bronchus and its respective pulmonary artery (i.e., eparterial or hyparterial), previously shown to be useful radiographic signs of situs ambiguus.

The diagnosis of situs ambiguus could also be suspected from the lateral projection of the plain chest film, a finding not previously reported. This projection usually shows the right and left bronchus posterior to the respective pulmonary artery in patients with right isomerism (usually associated with asplenia) and each bronchus inferior and anterior to the corresponding pulmonary artery in those with left isomerism (usually associated with polysplenia).

Radiographic criteria were listed for diagnosis of situs ambiguus and for separation into left and right isomerism from each projection to compare their usefulness. Frontal and lateral films from 14 patients in the study group (situs ambiguus) were compared with the 29 patients in a control group (three with situs inversus and 26 with situs solitus). These 86 films were randomized and reviewed "blindly" by three radiologists in 258 observations. Eleven errors in diagnosis (4.3%) were made by the observers: one film of a patient with situs inversus was diagnosed as situs solitus and 10 films of patients with situs ambiguus were incorrectly reported as situs solitus. A total of 84 observations was made of 14 patients with situs ambiguus with two false negatives and no false positives. A total of 48 observations of eight patients with left isomerism was made with seven errors. A total of 36 observations of patients with right isomerism was made with four errors . There was no significant difference between the false positive and false negative error rate using frontal or lateral views ($P < 0.50$).

These data permit the conclusion that the frontal and lateral views of the plain chest film are independently equally useful in allowing the suspicion of the diagnosis of situs ambiguus and in separating left from right isomerism.

Introduction

The lungs, liver, spleen, stomach, and atria are usually asymmetric organs and the term situs is used to define their position relative to the midline or sagittal plane [1]. Situs solitus indicates the normal position of the viscera and situs inversus, their mirror image location. Situs ambiguus describes the condition in which usually asymmetric structures tend to be symmetrical [2]. Van Mierop et al. [3] suggested the term isomerism to describe symmetrical morphology; this can be further subdivided into right and left subsets to describe patients with bilateral "right sidedness" or "left sidedness."

There is a strong tendency toward situs ambiguus in patients with asplenia or polysplenia syndromes, the former tending to have right and the latter left isomerism [3]. Patients with these syndromes often have multiple severe congenital cardiac malformations, usually more severe in those with asplenia, although splenic absence and the presence of multiple spleens have been found in patients without cardiac malformations [4]. Shinebourne et al. [5] indicated that the splenic "state" is difficult to establish clinically and conveys less information than direct demonstration of the type of isomerism from bronchial anatomy. Clinically it is useful to diagnose situs ambiguus and the type of isomerism in patients with congenital cardiac malformations, since this permits improved planning of cardiac catheterization studies.

Pulmonary situs seems to be best indicated by bronchial anatomy which does not always correspond to pathologic evaluation of lung lobulation [6, 7]. The length of each main-stem bronchus and the relation to its respective pulmonary artery provide the most reliable clinical prediction of thoracic situs [8–10]. Normally the right main-stem bronchus is posterior and superior to the right pulmonary artery and the left main-stem bronchus anterior and inferior to the left pulmonary artery [1, 9]. The opposite relation exists in patients with situs inversus. Most authors agree that pulmonary situs defined by bronchial anatomy and atrial situs are concordant and, therefore, that identification of bronchopulmonary artery anatomy permits reasonably reliable designation of atrial situs [3, 10].

Proper identification of the situs of cardiac atria provides the foundation for systematic classification of congenital cardiac malformations using the segmental approach described and modified by various authors [5, 8, 11–13]. Thus identification of thoracic situs may allow presumption of atrial situs and permit reasonable conjectures as to the anatomy of underlying congenital heart disease.

Received December 7, 1977; accepted after revision August 21, 1978.

[1] Division of Cardiac Radiology, University of Alabama School of Medicine, 619 South 19th Street, Birmingham, Alabama 35233. Address reprint requests to B. Soto.

[2] Department of Surgery, University of Alabama School of Medicine, Birmingham, Alabama 35233.

[3] Department of Pediatric Cardiology, University of Alabama School of Medicine, Birmingham, Alabama 35233.

[4] Department of Pathology, University of Alabama School of Medicine, Birmingham, Alabama 35233.

0361–803X/78/1200–0995 $00.00

© 1978 American Roentgen Ray Society

TABLE 1: Cardiac Malformations

Case	Sex and Age	Atria	Ventricular Relation*	Aortoventricular Valves	Ventricular Great Artery Connection	Systemic Veins	Pulmonary Veins	Associated Anomalies	Cardiac Axis†
Right isomerism (group 1)‡:									
1	M, 7½ y	Two	Normal	Common	Discordant	Normal	Normal	PS, CAV	R
2	F, 3 d	Common	Common	Single	DOV	R & LSVC	TAPVC to RSVC	PS	L
3	M, 1 d	Common	Common	Single	DOV	IAC, LSVC	Hypoplastic and anomalous	PDA	L
4	F, 1 m	Common	Inverted	Two	Concordant	IAC, LSVC	TAPVC to LSVC	PAV, CoA, PDA	R
5	F, 16 m	Common	Normal	Common	DORV	Normal	TAPVC to RSVC	PS, CAV	L
6	F, 17 y	Common	Common	Single	DOV	R & LSVC	TAPVC to LSVC	PS	R
Left isomerism (group 2)‡:									
7	M, 31 y	Two	Inverted	Two	Discordant	IAC; R & LSVC	Normal	ASD, VSD	L
8	M, 1 y	Common	Normal	Two	Concordant	IAC; R & LSVC	Normal	VSD	L
9	M, 1 w	Common	Common	Single	DOV	IAC; R & LSVC	Normal	Interrruption of Ao. arch. PDA	L
10	M, 7 y	Common	Normal	Two	Concordant	IAC	TAPVC to RA	Hypoplastic LA	R
11	M, 2 d	Two	Inverted	Common	Concordant	R & LSVC	PAPVC to RA	PAV, CoA, PDA	R
12	F, 1 y	Common	Normal	Two	DORV	IAC; R & LSVC	Normal	PS, CAV	R
13	F, 10 w	Common	Normal	Common	Concordant	IAC; R & LSVC	Not identified	CoA	L
14	M, 29 y	Two	Normal	Two	Concordant	Normal	Normal	VSD	L

Note.—SVC = superior vena cava, L = left, R = right; TAPVC and PAPVC = total and partial anomalous pulmonary venous connection; PS = pulmonic stenosis; CAV and PAV = complete and partial atrioventricular canal; IAC = interruption of inferior vena cava with azygous or hemiazygous continuation; PDA = patent ductus arteriosus; CoA = coarctation; ASD and VSD = atrial and ventricular septal defect; LA = left atrium; DOV = double outlet ventricle; DORV = double outlet right ventricle; y = year; d = day; m = month; w = week.

* Normal = Left ventricle leftward of right ventricle; Inverted = left ventricle rightward of right ventricle; Common = univentricular heart.

† Base to apex orientation. ‡ Each patient had two atrial appendages similar to the normal right (group 1) and left (group 2) atrial appendages.

This study was undertaken to determine the limitations in predicting thoracic situs from the plain chest radiograph and to compare the usefulness of the lateral view which previously has not been recognized as helpful, with the validity of the more widely recognized analysis from frontal projections.

Subjects and Methods

Fourteen patients with situs ambiguus underwent cardiac evaluation at the University of Alabama in Birmingham between February 1974 and October 1977. There were nine males and five females ranging in age from 1 day to 31 years. Cardiac catheterization and angiocardiography were performed on each patient. Anatomic observations were recorded in 10 patients, seven who underwent intracardiac operation and three additional nonoperated patients at postmortem examination.

The cardiac malformations determined by angiocardiography and anatomic inspection are described for each study group in table 1. Patients were separated into two subsets according to the anatomy of the atrial appendages and the relation of each main-stem bronchus to its corresponding pulmonary artery. Six patients in group 1 had right thoracic isomerism with each atrial appendage resembling the morphology of a right atrial appendage. The left and right pulmonary arteries were located anterior and inferior to their corresponding main-stem bronchus (fig. 1). Group 2 consisted of eight patients with left isomerism, each having their left and right side atrial appendages similar in morphology to the usual left atrial appendage (fig. 2). Group 2 patients had left and right pulmonary arteries located superior and posterior to the corresponding main-stem bronchus. The anatomy of the atrial appendages was directly verified in 10 patients as detailed above. Angiographic examples of patients with right (group 1) and left (group 2) thoracic isomerism are shown in figures 3 and 4.

Plain chest radiographs of 26 patients with situs solitus and three with situs inversus served for control. Ten patients had isolated aortic stenosis; eight, isolated ventricular septal defect; eight, isolated atrial septal defect; two, tetralogy of Fallot; and one, the complete form of common atrioventricular canal. The situs of the atria was anatomically verified at surgery in each patient.

One frontal and one lateral radiograph from each of the 43 patients (86 total films) were randomized (eight patients with situs ambiguus and left isomerism, six with situs ambiguus and right isomerism, three with situs inversus, and 26 with situs solitus). Each randomized film was reviewed "blindly" and separately by two radiologists with special training in cardiovascular disease (observers 1 and 2) and by one general radiologist (observer 3). A total of 258 observations was made (86 × 3) using a list of diagnostic criteria.

Situs ambiguus was diagnosed when, on the *frontal* view, each bronchus had similar length (see below) and each bronchus and its respective pulmonary artery were similarly positionally related. On the *lateral* projection, situs ambiguus was diagnosed when the right and left pulmonary arteries were located either both anterior or posterior to the tracheobronchial tree and when the appearance of the main-stem bronchi were similar (i.e., both morphologic right or left). The right main-stem bronchus typically has a posterior stripe due to interface with the adjacent lung parenchyma (figs. 5*B* and 6*B*). In contrast, the left main-stem bronchus does not have this mark because it is adjacent to the left pulmonary artery which has a density similar to that of the bronchial wall.

Left isomerism was diagnosed from the frontal view when each pulmonary artery was identified superior to each bronchus and right isomerism when each was inferior. Left isomerism was designated from the lateral view when each pulmonary

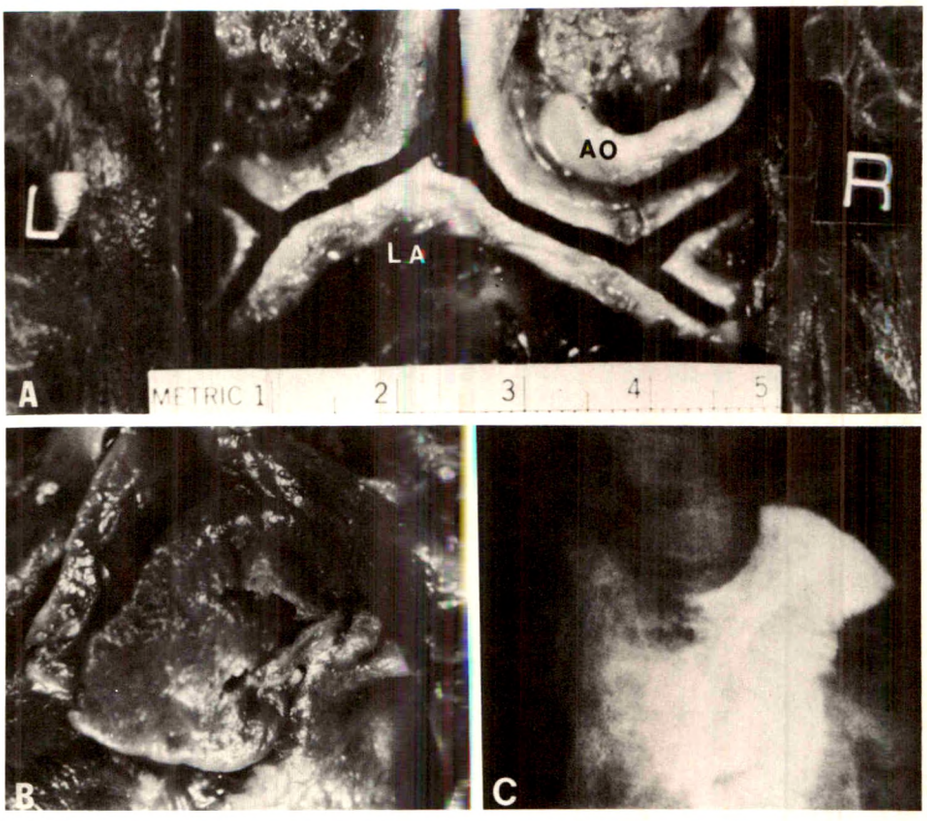

Fig. 1.—*A*, Posterior view of specimen with right isomerism showing similar length of right and left bronchi. Pulmonary arteries not visible because of their anteroinferior location. Descending thoracic aorta (Ao) has been reflected superiorly to visualize bronchus. LA = left atrium. *B*, Anatomic view of morphologic right atrial appendage which was located on left side. *C*, Angiogram with injection of contrast material into typical morphologic right atrial appendage located to left.

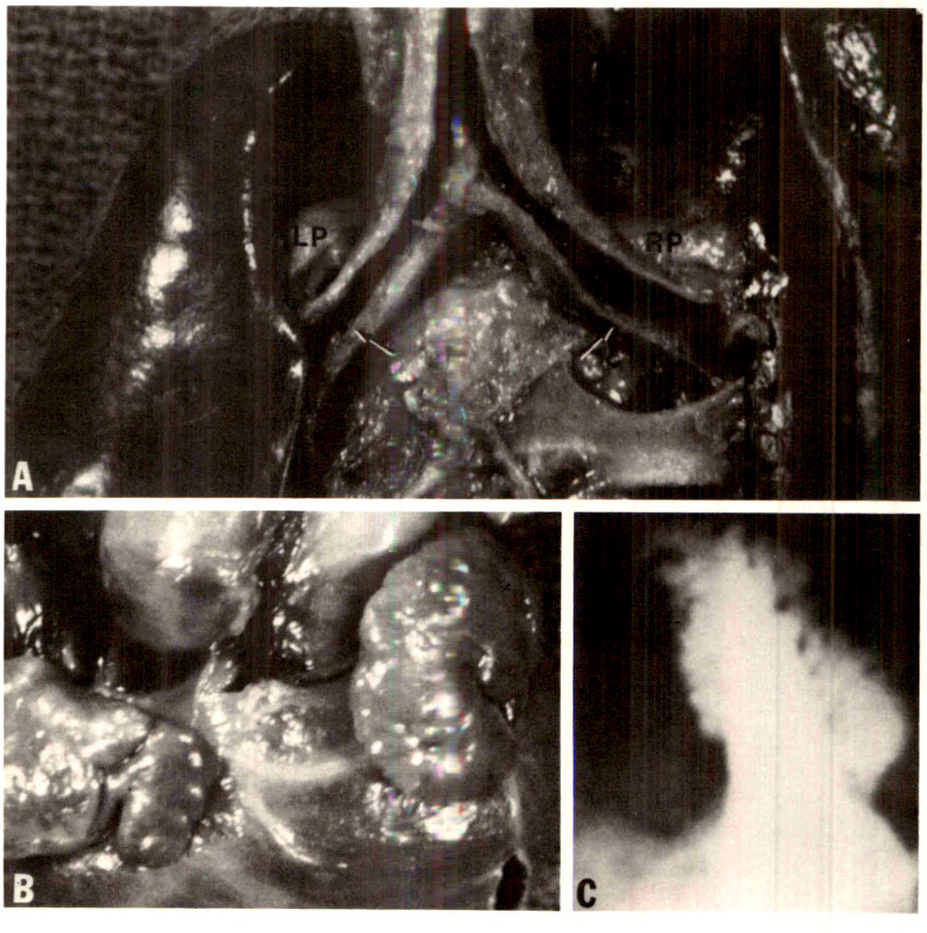

Fig. 2.—*A*, Posterior view of specimen with left isomerism showing origins of right and left upper bronchi (arrows). Similar length of each main-stem bronchus is apparent. Right (RP) and left (LP) pulmonary arteries, above corresponding bronchi, curve posteriorly at lung hilum. *B*, Bilateral morphologic left atrial appendages. *C*, Selective injection of contrast material into morphologic left atrial appendage which was located on right.

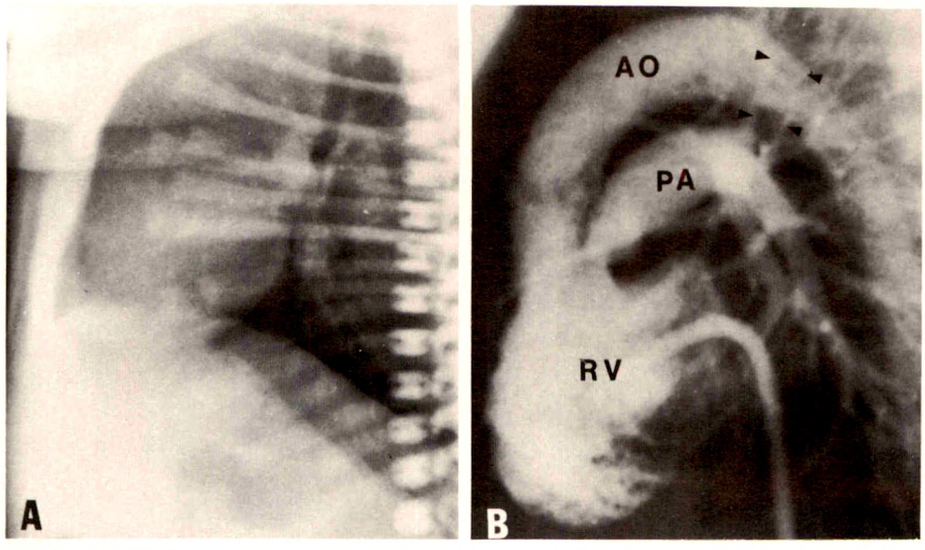

Fig. 3.—Patient with right isomerism. *A*, Lateral view of chest film. Neither pulmonary artery can be visualized posterior to tracheobronchial tree. *B*, Right ventricular (RV) angiocardiogram showing right and left pulmonary arteries (PA) anterior to tracheobronchial tree (*arrows*). AO = aorta.

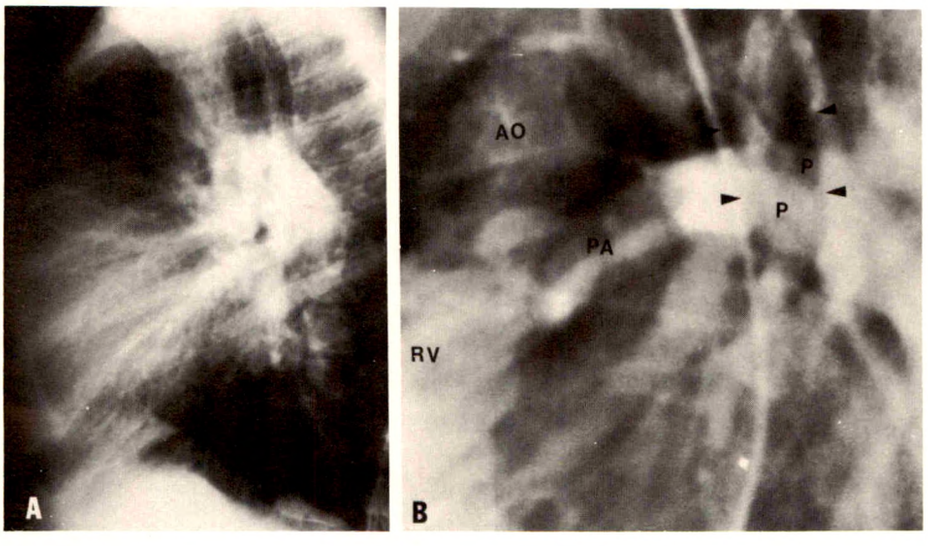

Fig. 4.—Patient with left isomerism. *A*, Lateral view of chest film showing pulmonary arteries posterior to tracheobronchial tree. *B*, Right ventricular (RV) angiocardiogram showing negative shadow of tracheobronchial tree (*arrows*); each pulmonary artery (P) crosses posteriorly. AO = aorta, PA = main pulmonary artery.

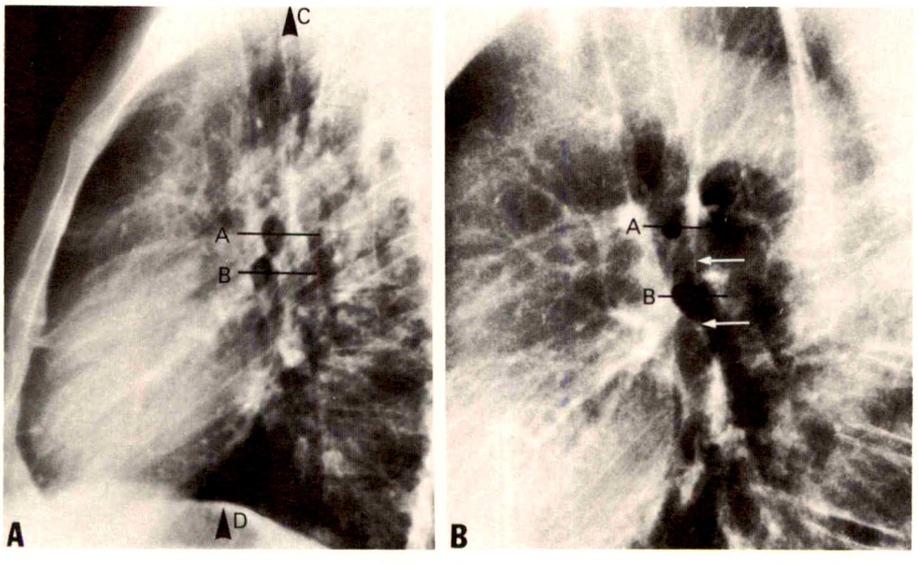

Fig. 5.—Lateral view of situs ambiguus with left isomerism (*A*) compared with situs solitus (*B*). Lines A and B define center of each upper lobe bronchus and the arrowheads C and D, height of thorax. Distance between each bronchus is smaller in patients with isomerism than those with lateralization. Posterior stripe in B (situs solitus) (*arrows*) identifies right bronchus.

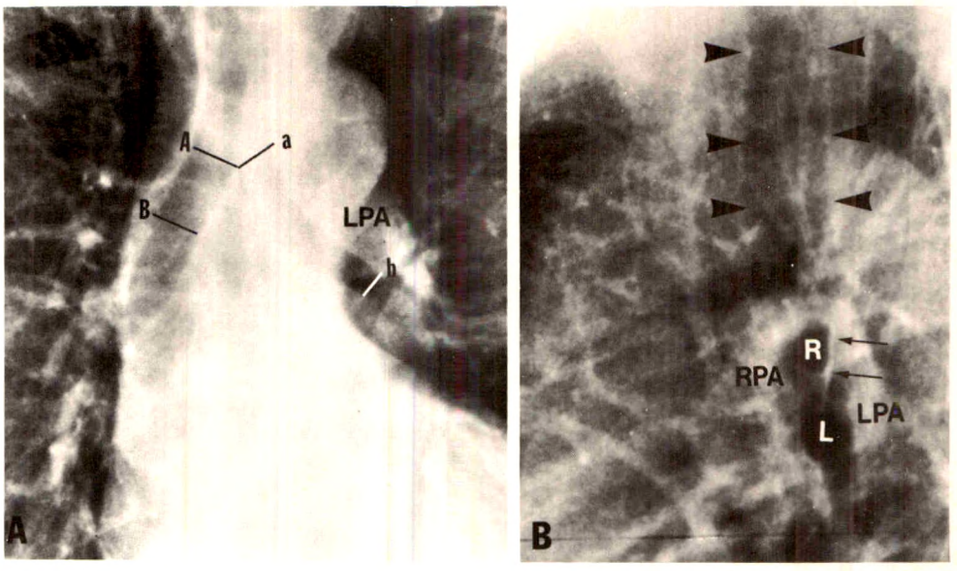

Fig. 6.—Frontal (*A*) and lateral (*B*) views of chest radiograph of normal subjects (situs solitus). *A*, Lines A and a are drawn from carina to lateral aspect of each bronchus perpendicular to long axis. Lines B and b are similarly drawn at origin of right and left upper bronchi. Distance A–B and a–b are length of each main-stem bronchus. Left pulmonary artery (LPA) is located superior and posterior to left upper bronchus. Right pulmonary artery is not seen. *B*, Trachea (*arrowheads*) and origin of right (R) and left (L) upper bronchi. Right pulmonary artery (RPA) is anterior to right (R) bronchus and left pulmonary artery (LPA) is posterior to left (L) bronchus. Posterior stripe (*arrows*) identifies right main-stem bronchus.

artery was superior and posterior to each bronchus and right isomerism when each was anterior.

Separate contingency tables were constructed for frontal and lateral views for each observer. From these we calculated the false negative (number of false negatives/actual positives) and false positive (number of false positives/actual negatives) rates for: (1) the diagnosis of ambiguus versus nonambiguus situs, (2) left isomerism, and (3) right isomerism. Contingency tables were also constructed to examine interobserver correlation.

Length of each main-stem bronchus was measured on the frontal view of the plain chest film and their ratio calculated. This was the distance between the lines drawn perpendicular to the long axis of each main-stem bronchus at the level of the carina and at the origin of each upper lobe bronchus (fig. 6*A*). The lateral projection was analyzed by measuring the height of the thorax and the distance between the center of the origin of the left and right upper bronchi and a ratio calculated to normalize for differences in patient size (fig. 5*A*).

The frontal chest radiographs were taken in the upright posteroanterior view centering the x-ray beam in the middle of the posterior aspect of the thorax parallel to the sagittal plane. Children were supported in the upright position in front of the x-ray film. Lateral projections were made with the left side of the patient in contact with the film and the x-ray beam directed perpendicular to the saggital plane. The focus-film distance was 183 cm.

Results

The "blind" analysis of the 86 randomized frontal and lateral chest films by three observers resulted in 258 observations. There were 11 errors in diagnosis (4%): one film of a patient with situs inversus was diagnosed as situs solitus and 10 films of patients with situs ambiguus were incorrectly reported as situs solitus in one, incorrect isomerism in seven, and unidentifiable isomerism in two. Considering the diagnosis of situs ambiguus, there were 84 observations of 14 patients with two false negatives (2%). The errors were made by observer 2 who diagnosed situs solitus from the frontal view and situs nonambiguus from the lateral view of the same patient with right isomerism. The false negative error rate of this observer was 7% (1 of 14). There were no false positive errors in the discrimination of nonambiguus versus ambiguus situs.

The false negative and false positive error rates for the classification of left versus right isomerism by each observer individually and collectively from each projection is shown in table 2. There was no difference in error rate between frontal and lateral view, $P = 0.50$ for left isomerism and $P = 1.0$ for right isomerism.

Bronchial length measured from the frontal view of the plain chest film showed a left/right ratio of 1.00–1.36 (1.13 ± 0.09, mean ± SD) for the 14 patients with situs ambiguus. In the control group this range was 1.85–2.75 (2.33 ± 0.08, mean ± SD) ($P < 0.01$).

The height of the thorax and the distance between the midpoint of each bronchus was measured from the lateral projection from the group with right and left isomerism and compared with the control group with asymmetric situs. A ratio of these measurements, calculated in an effort to normalize the data, was 7.03–15.75 (11.92 ± 2.64, mean ± SD) for patients with asymmetric situs and 19.28–57.00 (29.54 ± 9.75, mean ± SD) for patients with situs ambiguus ($P < 0.001$).

The typical lateral view of patients with left isomerism showed each bronchus anterior to the respective pulmonary artery, similar to the relation of the left bronchus and left pulmonary artery in normal subjects (fig. 7). Conversely, each bronchus was posterior to the respective pulmonary artery in patients with right isomerism (fig. 8), similar to the right bronchopulmonary artery relation in normal subjects.

Discussion

Patients with right isomerism and usually associated

TABLE 2
Error Rates

Observer No.	View	Left Isomerism		Right Isomerism	
		False Negative (n = 8)	False Positive (n = 35)	False Negative (n = 6)	False Positive (n = 37)
1	AP	1 (12)	1 (3)	1 (17)	1 (3)
	Lat	1 (12)	0	0	1 (3)
2	AP	0	0	1 (17)	0
	Lat	0	0	1 (17)	0
3	AP	3 (38)	0	0	2 (5)
	Lat	2 (25)	0	1 (17)	2 (5)
Total	AP	4 (17)	1 (1.0)	2 (11)	3 (3)
	Lat	3 (12)*	0 *	2 (11)†	3 (3)†

Note.—Numbers in parentheses are percentages. AP = anteroposterior, Lat = lateral.
* P = 0.50.
† P = 1.0.

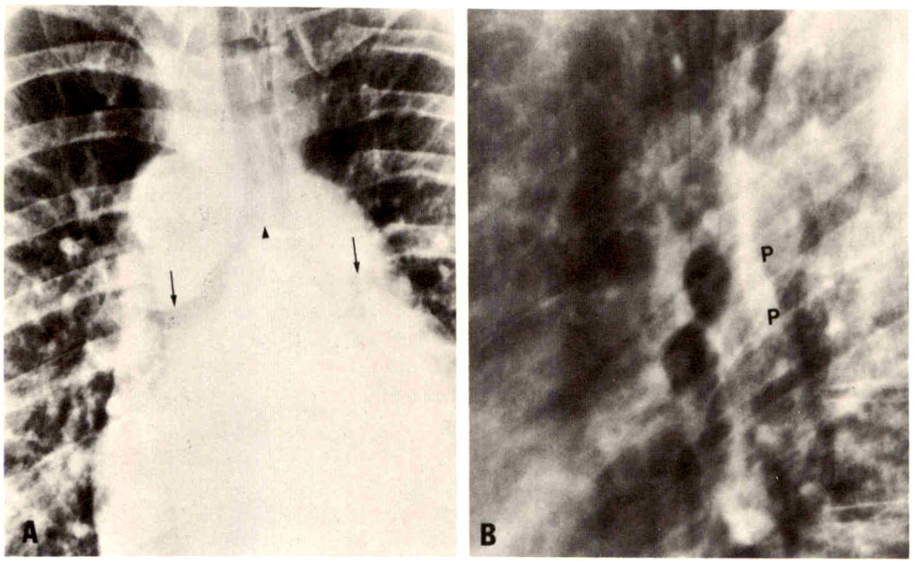

Fig. 7.—Patient with left isomerism and levocardia. *A*, Frontal chest film retouched to show bronchi. Origin of each upper lobe bronchus (*arrows*) is of similar distance from carina (*arrowhead*). *B*, Lateral view showing pulmonary arteries (P) posterior to tracheobronchial tree, indicating bilateral left bronchi. Right and left upper bronchi are closer together than in normal chest film. Note lack of posterior stripe indicating absence of right bronchi.

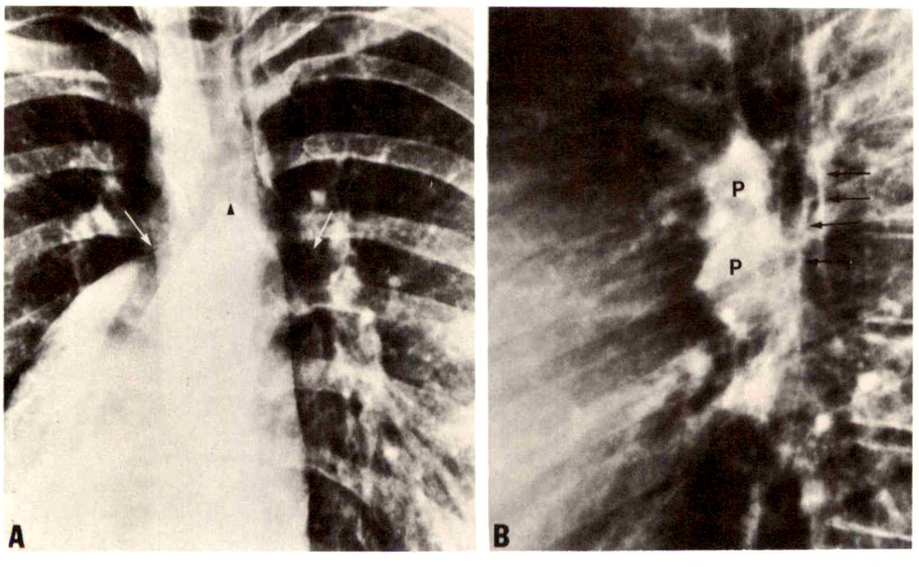

Fig. 8.—Patient with right isomerism and dextrocardia. *A*, Frontal chest film retouched to show bronchi. Carina (*arrowhead*) and origin of right and left upper bronchi (*arrows*) shows similarity in bronchial length. Pulmonary arteries on both sides are inferior to respective bronchi. *B*, Lateral film showing tracheobronchial tree posterior to each pulmonary artery (P), indicating bilateral right bronchi. Double posterior bronchial stripes (*arrows*) further identify bilateral right bronchi.

asplenia have cardiac malformations commonly including anomalous pulmonary venous connection, atrioventricular canal, single ventricle, pulmonary stenosis or atresia, and transposition [8]. In contrast, patients with left isomerism, usually associated with polysplenia, often have double-outlet right ventricle, left-side obstructive lesions, ventricular septal defect, and anomalies of systemic more often than pulmonary venous return [8]. They often have interruption of the inferior vena cava with hemiazygous vein continuation. The high probability that these cardiac malformations exist can be predicted from knowledge of right or left thoracic isomerism, and this information is clinically useful in preparing for cardiac catheterization studies.

It is important to note disagreement in the literature with regard to the proper designation of the atria in the presence of situs ambiguus or when a common atrium is present. Van Praagh [12] believes the atria cannot be properly named in these circumstances, while Lev et al. [6] require the presence of an atrial septum for precise morphologic atrial identification but accepts the morphology of the atrial appendages for presumptive designation. Contrarily, Stanger et al. [8] and Van Mierop et al. [3] believe the atrium may be defined solely on the basis of atrial appendage morphology. However, most authors agree that patients with pulmonary symmetry usually have hearts with bilateral atrial appendages similar to either the normal right or left atrial appendage. The normal right atrium has a fossa ovalis and limbus on its septal surface, the crista terminalis on its lateral wall, and a trabeculated appendage with a broad base and dome-shaped apex. The left atrium is free of these structures and has a narrow-based fingerlike appendage. When the septum is absent (common atrium), a frequent finding in patients with situs ambiguus, distinction of left and right atria cannot be made using septal elements. Instead appendage morphology and the presence or absence of a crista terminalis must be relied on for presumptive designation, if such differentiation is to be made by gross examination or by angiography. Clinically therefore, we believe it is useful to try to identify thoracic situs from bronchial anatomy visible on the plain chest radiograph in order to determine the situs of the atria.

This study confirms the previously recognized usefulness of the frontal view of the chest film to diagnose thoracic situs by measurement of bronchial length. In situs *nonambiguus* (solitus or inversus), the ratio of left/right main-stem bronchial length is greater than 1.71 [10]. In this study, this ratio in 29 control subjects was 2.33 ± 0.28 SD and ranged from 1.85 to 2.75. In patients with situs ambiguus, the ratio of left/right main-stem bronchial length, measured from the frontal view is less than 1.4 [10]. This was confirmed in our 14 patients with situs ambiguus whose mean ratio was 1.13 ± 0.09 SD, ranging between 1.00 and 1.36.

This study indicates that the lateral view is as useful for prediction of thoracic situs as is the frontal view. The interbronchial distance on the lateral projection of patients with situs ambiguus was normalized for variations in patient size by calculating a ratio of the height of the thorax/interbronchial distance. This ratio was less than 15.75 in 29 patients with situs nonambiguus and greater than 19.28 for those with situs ambiguus. The shorter interbronchial distance on lateral chest films of patients with situs ambiguus is the result of similar length of each main-stem bronchus.

The positional relation of the bronchi and their respective pulmonary arteries is also useful in differentiating thoracic ateralization from thoracic isomerism. This relation also permits differentiation of right from left thoracic isomerism in those patients with situs ambiguus. Right isomerism is present when each pulmonary artery is identified anterior to its respective bronchus and when a double stripe is found posterior to each bronchus. In contrast, left isomerism is present when each pulmonary artery is superior to its respective bronchus and the posterior stripe is not identifiable. The diagnosis of situs ambiguus from the lateral view, using these criteria, was associated with no false positive errors and a 2% false negative error rate. The separation into left and right isomerism was less precise, having a false negative rate of 12% and a false positive rate of 1.4%. These error rates were not different from those present from analysis of frontal projections.

In practice, a radiologist would have both frontal and lateral films available simultaneously and it is therefore possible that he would be more likely to make a correct diagnosis. In contrast we recognize that during this evaluation, the observers were aware that some films were of patients with situs ambiguus, while in practice this occurrence might be completely unexpected and would tend to reduce diagnostic accuracy.

ACKNOWLEDGMENTS

We thank Dr. Eugene Blackstone for helping to design and analyze the randomization study. We also acknowledge the assistance of Gail Stewart, James Craig, and Vicki Overton in the preparation of this manuscript.

REFERENCES

1. Brandt PW, Liebow AA: Right pulmonary isomerism associated with venous, splenic, and other anomalies. *Lab Invest* 7:469–504, 1958
2. Van Mierop LHS, Wiglesworth FW: Isomerism of the cardiac atria in the asplenia syndrome. *Lab Invest* 11:1303–1315, 1962
3. Van Mierop LHS, Eisen S, Schiebler GL: The radiographic appearance of the tracheobronchial tree as an indicator of visceral situs. *Am J Cardiol* 26:432–435, 1970
4. Ivemark B: Implications of agenesis of the spleen on the pathogenesis of conotruncus anomalies in childhood. *Acta Paediatr Scand* 44(suppl 104):1–110, 1955
5. Shinebourne EA, Macartney FJ, Anderson RH: Sequential chamber localization—logical approach to diagnosis in congenital heart disease. *Br Heart J* 38:327–340, 1976
6. Lev M, Liberthson RR, Eckner FAO, Arcille RA: Pathologic anatomy of dextrocardia and its clinical implications. *Circulation* 37:979–999, 1968
7. Liberthson RR, Hastreiter AR, Sinha SN, Bharati S, Novak

GM, Lev M: Levocardia with visceral hetrotaxy-isolated levocardia: pathologic anatomy and its clinical implications. *Am Heart J* 85:40–54, 1973

8. Stanger P, Rudolph AM, Edwards JE: Cardiac malpositions. *Circulation* 56:159–172, 1977
9. Landing BH, Lawrence TK, Payne VC, Wells TR: Bronchial anatomy in syndromes with abnormal visceral situs, abnormal spleen and congenital heart disease. *Am J Cardiol* 128:456–462, 1971
10. Partridge MC, Scott O, Deverall PB, Macartney FJ: Visualization and measurement of the main bronchi by tomography as an objective indicator of thoracic situs in congenital heart disease. *Circulation* 51:188–196, 1975
11. Van Praagh R: The segmental approach to diagnosis in congenital heart disease. *Birth Defects* 8:4–23, 1972
12. Van Praagh R: Terminology of congenital heart disease. *Circulation* 56:139–143, 1977
13. Kirklin JW, Pacifico AD, Bargeron LM, Soto B: Cardiac repair in anatomically corrected malposition of the great arteries. *Circulation* 48:153–159, 1973

Congenital Pulmonary Atresia: Photographic Subtraction as an Aid in Recognizing Hypoplastic Pulmonary Arteries

RICHARD E. FULTON[1] AND GEORGE D. DAVIS[1]

Photographic subtraction is a valuable adjunct for studying patients with pulmonary atresia, ventricular septal defect, and systemic pulmonary collateral vessels. In about 9% of 282 patients, it helped identify the true central pulmonary arteries and whether or not they were confluent. This technique, used retrospectively in evaluating patients previously considered inoperable, has permitted recall of several patients for repeat study and probable corrective or palliative surgery.

Direct surgical correction or first-stage palliation of congenital pulmonary atresia with ventricular septal defect is possible in most patients, but it is largely dependent on angiographic demonstration of the presence of true central pulmonary arteries [1, 2]. Recognizing the presence, size, and confluence (or nonconfluence) of pulmonary arteries, especially when the arteries are very hypoplastic, is often difficult because they are obscured by the many systemic collateral arteries to the lungs that indirectly connect with the true pulmonary arteries. In the past, failure to recognize the presence of true pulmonary arteries resulted partly from a lack of familiarity with this appearance, but more often from these arteries being obscured by the maze of overlapping vessel opacities. The end effect was that many patients erroneously classified as having Collett-Edwards type IV truncus were excluded from surgical consideration [3].

Photographic subtraction of appropriately chosen large film angiograms on these patients has been proven a very useful technique both in retrospective analysis of previously studied patients and as an on-line decision-making measure during cardiac catheterization. In this application it guides selective catheterization and filming

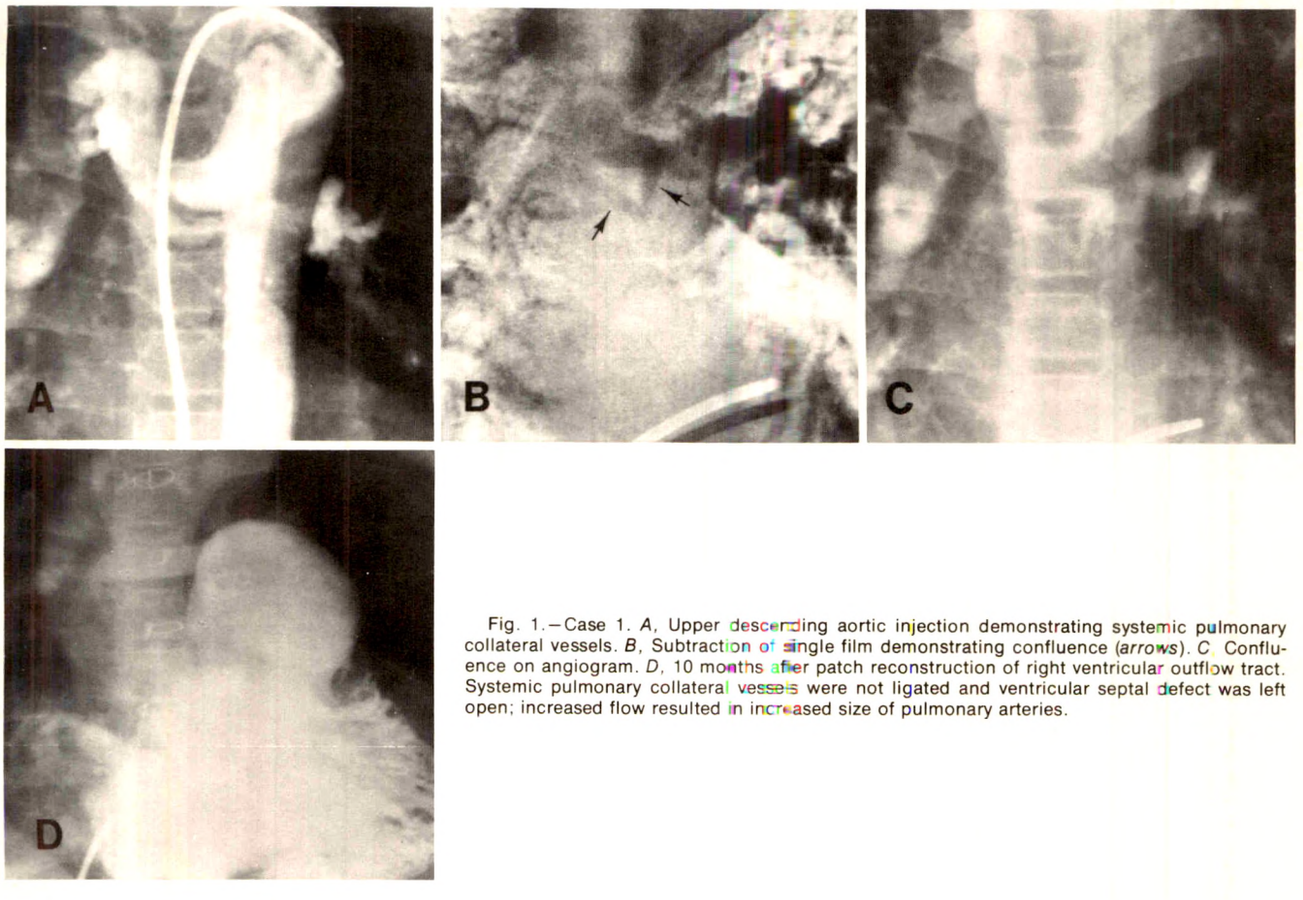

Fig. 1.—Case 1. *A*, Upper descending aortic injection demonstrating systemic pulmonary collateral vessels. *B*, Subtraction of single film demonstrating confluence (*arrows*). *C*, Confluence on angiogram. *D*, 10 months after patch reconstruction of right ventricular outflow tract. Systemic pulmonary collateral vessels were not ligated and ventricular septal defect was left open; increased flow resulted in increased size of pulmonary arteries.

Received October 5, 1977; accepted after revision September 5, 1978.
This paper was presented at the annual meeting of the American Roentgen Ray Society, Boston, September 1977.
[1] Department of Diagnostic Radiology (G. D. Davis, emeritus), Mayo Clinic and Mayo Foundation, Rochester, Minnesota 55901. Address reprint requests to R. E. Fulton.

© 1978 American Roentgen Ray Society

0361–803X/78/1200–1003 $00.00

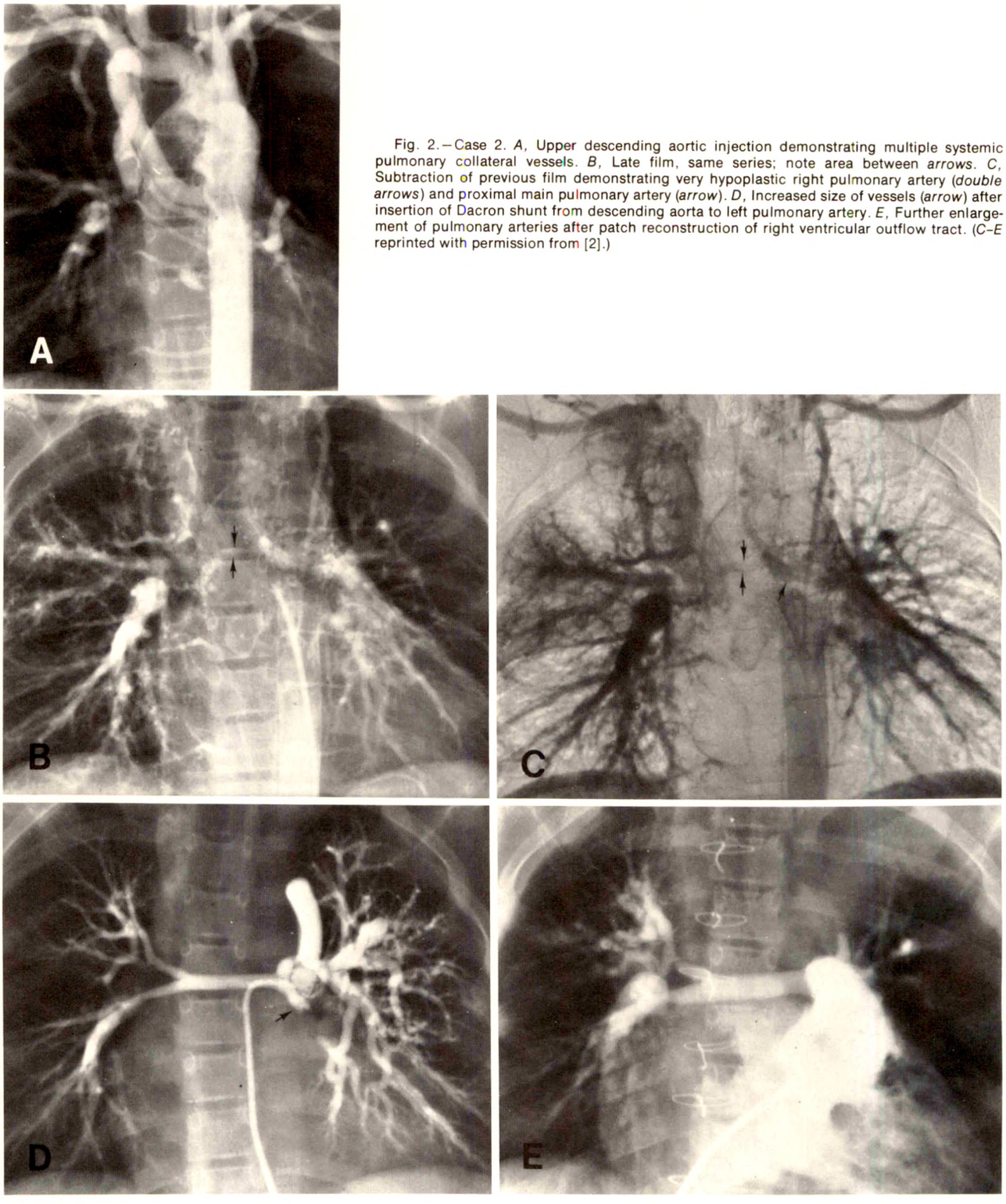

Fig. 2.—Case 2. *A*, Upper descending aortic injection demonstrating multiple systemic pulmonary collateral vessels. *B*, Late film, same series; note area between *arrows*. *C*, Subtraction of previous film demonstrating very hypoplastic right pulmonary artery (*double arrows*) and proximal main pulmonary artery (*arrow*). *D*, Increased size of vessels (*arrow*) after insertion of Dacron shunt from descending aorta to left pulmonary artery. *E*, Further enlargement of pulmonary arteries after patch reconstruction of right ventricular outflow tract. (*C–E* reprinted with permission from [2].)

of systemic collaterals to the lungs and has been used routinely in this manner since 1974.

Case Material and Results

From January 1962 through July 1977, 282 patients with congenital pulmonary atresia and ventricular septal defect were studied by cardiac catheterization and large film biplane angiocardiography. Photographic subtraction was used to restudy the angiocardiograms of 76 of the patients seen before 1974 in whom no central pulmonary arteries were recognized on the original study. By using early films (usually those of right ventricular

and ascending aortic injections) in the angiograms as masks, and printing selected later films against the mask, we distinguished the presence of late-filling true central pulmonary arteries from the early-filling, but paralleling or overlapping, "bronchial" or similar systemic collateral arteries. In 19 (25%) of the 76, previously undetected pulmonary arteries were recognized.

Since 1974, photographic subtraction, together with selective catheterization of all accessible systemic collateral arteries, has been a routine procedure in studying patients with pulmonary atresia. In six of 37 (16%) patients since 1974 whose central pulmonary arteries were not initially recognized in the study, photographic subtraction was essential in establishing the true anatomic diagnosis and in determining subsequent surgical decisions.

Thus, in the entire group of 282 patients, including both some in whom central pulmonary arteries could be seen and some in whom they could not be recognized, photographic subtraction was essential in establishing the presence and size of true central pulmonary arteries in 25 patients (8.9%).

Representative Case Reports

The following four examples illustrate the value of photographic subtraction in defining the presence of true central pulmonary arteries.

Case 1

A boy, first catheterized at age 3 months, was diagnosed as having pulmonary atresia with ventricular septal defect and bronchial vessels only. At age 3 he was catheterized again at another institution with the same diagnosis. When referred to us at 9 years of age, he had a hemoglobin level of 19.9 g/dl and was becoming increasingly fatigued. Thorough radiographic evaluation, including selective injection of the systemic collateral vessels, was done. Initial review of the films revealed no evidence of central pulmonary arteries, but photographic subtraction identified a very hypoplastic central pulmonary artery confluence (figs. 1*A*–1*C*). This patient had a palliative reconstruction of the right ventricular outflow tract, with the ventricular septal defect left open. He has done well postoperatively. The size of the vessels more than doubled after the introduction of the increased flow (fig. 1*D*), and at a follow-up study 10 months later the hemoglobin level was 15.0 g/dl. Total correction is planned.

Case 2

A 4-year-old girl had central pulmonary arteries that would not have been identified without photographic subtraction. She had extremely hypoplastic yet confluent right and left pulmonary arteries and a remnant of a proximal main pulmonary artery (figs. 2*A*–2*C*). These vessels could not be seen by only selective collateral vessel injections. A Dacron shunt was inserted from the upper descending aorta to the left pulmonary artery in 1975. Postoperative study showed enlarged pulmonary arteries (fig. 2*D*). By 1976, the patient's clinical condition was deteriorating due to stenosis of the graft. After restudy, patch reconstruction of the right ventricular outflow tract was done for further palliation, with the ventricular septal defect left open (fig. 2*E*). Considerable clinical improvement resulted. (Some elements of this case courtesy of [2].)

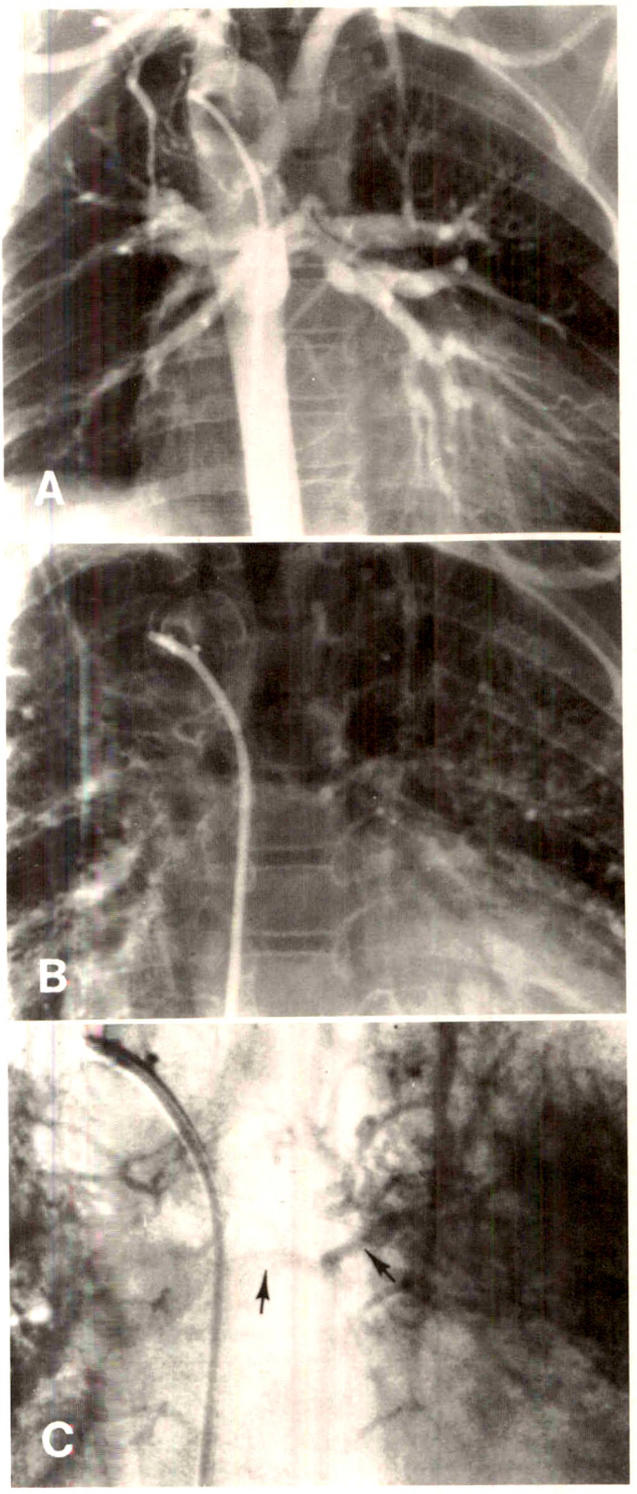

Fig. 3.—Case 3. *A*, Upper descending aortogram demonstrating multiple systemic pulmonary collateral vessels possibly coming from single origin with no evidence of true central pulmonary arteries. *B*, Late film aortogram raising question of true central confluent pulmonary arteries. *C*, Subtraction of previous film confirming right and left pulmonary arteries (*arrows*) confluent with atretic proximal main pulmonary artery remnant.

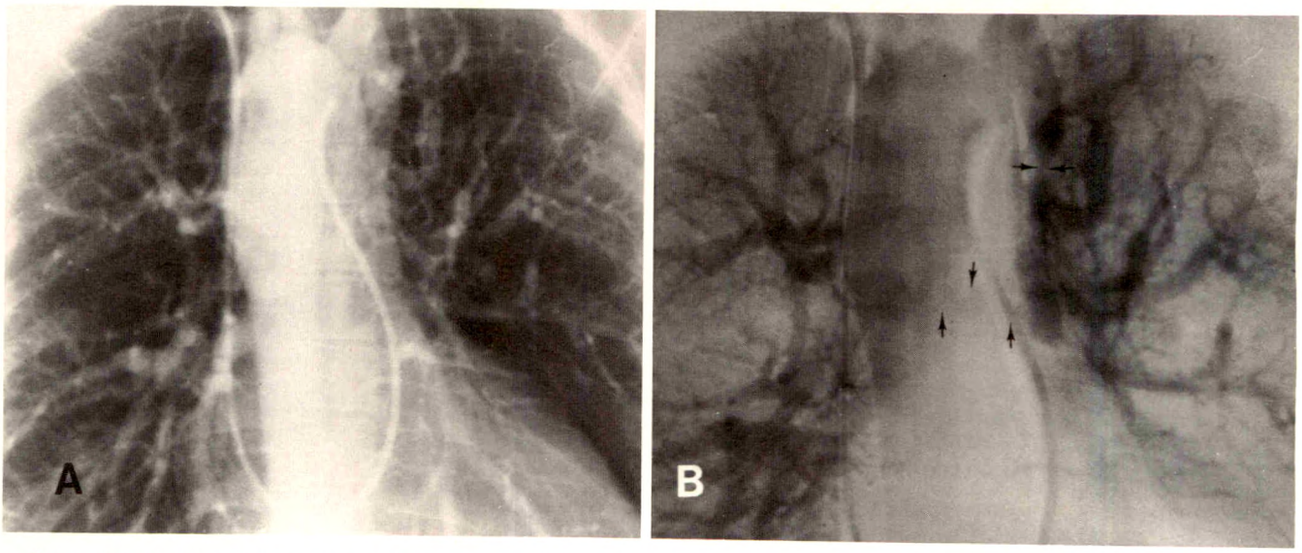

Fig. 4.—Case 4. *A*, Upper descending thoracic aortogram of 1972 study. No apparent true central pulmonary arteries. *B*, Subtraction of same 1972 film demonstrating relatively large right pulmonary artery (*three arrows*), confluent point, and stenotic left Blalock-Taussig anastomosis to left pulmonary artery (*double arrows*), sole supply to pulmonary arteries.

Case 3

A 10-year-old girl was originally diagnosed as having pulmonary atresia, ventricular septal defect, and bronchial arteries only. True confluent central pulmonary arteries were not recognized. Retrospective reevaluation with the subtraction technique identified confluent, hypoplastic central pulmonary arteries (fig. 3). The patient has been offered restudy.

Case 4

A 26-year-old woman had a previous diagnosis of "type IV truncus." At age 3 she had a left "Blalock-Taussig anastomosis" to the "left pulmonary artery." Reexamination by us in 1972 revealed pulmonary atresia, ventricular septal defect, and bronchial vessels only. There was a functioning shunt to what was considered a left bronchial artery. No pulmonary arteries were recognized. During retrospective review, the subtraction technique demonstrated a relatively large right pulmonary artery, confluence, and a stenotic left Blalock-Taussig anastomosis to the left pulmonary artery (fig. 4). The patient has been contacted and is returning for restudy.

Discussion

Photographic subtraction has been extremely helpful in many areas of diagnostic radiology [4–6]. To our knowledge, it has not been applied to cardiac radiology for several reasons, chiefly the following:

1. The subtraction technique has primarily been used by radiologists, and cardiologists involved in angiographic evaluation of patients with congenital heart disease are not familiar with it.

2. Cardiac and respiratory motion hinders good subtraction technique because there must be no movement of the area of interest between the radiographic views to be subtracted.

3. Cineradiography is currently preferred to large film format by most cardiac angiographers. In our experience, very hypoplastic pulmonary arteries coursing in the midst of multiple systemic collaterals are more readily recognized on large serial films, because these permit more detailed display and film-by-film analysis, and also because photographic subtraction is done more readily on-line during the study.

Since 1974, we have routinely made selective injections into all accessible systemic pulmonary collateral vessels [7–9] and have used the subtraction technique to define the anatomy of pulmonary blood supply, and especially to determine the presence or absence of confluent pulmonary arteries and, if present, their size and the extent of their parenchymal distribution [10].

Flow through very hypoplastic pulmonary vessels can be increased with a shunt or, if the vessels are confluent, by outflow tract reconstruction. Experience from our institution indicates that in the growing child these hypoplastic vessels may enlarge to a size that will later allow complete repair as a second-stage procedure [2, 11]. Even if the arteries do not enlarge to this extent, the palliation achieved by establishing increased flow through these vessels is often greatly beneficial. Most patients (88% in our experience) diagnosed with pulmonary atresia and ventricular septal defect will have at least one pulmonary artery and thus may be candidates for surgery.

Our experience and the data here confirm that photographic subtraction can be a valuable aid in the diagnostic evaluation of patients with suspected pulmonary atresia, ventricular septal defect, and confluent hypoplastic central pulmonary arteries. We suggest reviewing previous studies recorded on the static film format and using the subtraction technique to help identify those patients who may have been misinterpreted as having no central pulmonary arteries. This is important since nearly 90% of these patients encountered by us [10] had at least one demonstrable true pulmonary artery. Many patients

with hypoplastic true pulmonary arteries are candidates for palliative surgery and some can be considered for definitive repair as a second-stage procedure.

REFERENCES

1. Edwards JE, McGoon DC: Absence of anatomic origin from heart of pulmonary arterial supply. *Circulation* 47:393–398, 1973
2. Gill CC, Moodie DS, McGoon DC: Staged surgical management of pulmonary atresia with diminutive pulmonary arteries. *J Thorac Cardiovasc Surg* 73:436–442, 1977
3. Sotomora RF, Edwards JE: Anatomic identification of so-called absent pulmonary artery. *Circulation* 57:624–633, 1978
4. Fulton RE, Sheedy PF II, McIlrath DC, Ferris DO: Preoperative angiographic localization of insulin-producing tumors of the pancreas. *Am J Roentgenol* 123:367–377, 1975
5. Winkler NT: Roentgenographic subtraction technique. *Radiol Technol* 39:339–346, 1968
6. Powell DF, Baker HL Jr, Laws ER Jr: The angiographic findings in pituitary adenomas. *Radiology* 110:589–595, 1974
7. Pacifico AD, Kirklin JW, Bargeron LM Jr, Soto B: Surgical treatment of common arterial trunk with pseudotruncus arteriosus. *Circulation* 50 (suppl. 2):20–25, 1974
8. McGoon MD, Fulton RE, Davis GD, Ritter DG, Neill CA, White RI Jr: Systemic collateral and pulmonary artery stenosis in patients with congenital pulmonary valve atresia and ventricular septal defect. *Circulation* 56:473–479, 1977
9. Levin DC, Baltaxe HA, Goldberg HP, Engle MA, Ebert PA, Sos TA, Levin AR: The importance of selective angiography of systemic arterial supply to the lungs in planning surgical corrections of pseudotruncus arteriosus. *Am J Roentgenol* 121:605–613, 1974
10. Davis GD, Fulton RE, Ritter DG, Mair DD, McGoon DC: Congenital pulmonary atresia with ventricular septal defect: angiographic and surgical correlates. *Radiology* 128:133–144, 1973
11. McGoon DC, Baird DK, Davis GD: Surgical management of large bronchial collateral arteries with pulmonary stenosis or atresia. *Circulation* 52:109–118, 1975

Radiographic and Echocardiographic Evaluation of Newborns Treated with Indomethacin for Patent Ductus Arteriosus

DAVID K. EDWARDS,[1] CHARLES B. HIGGINS,[1] T. ALLEN MERRITT,[2] THOMAS G. DiSESSA,[2] AND WILLIAM F. FRIEDMAN[2]

A series of 33 consecutive preterm newborns who were treated with indomethacin, a drug which acts to close the patent ductus arteriosus, were studied retrospectively to examine the efficacy of chest radiography and echocardiography in diagnosing the presence of a significant patent ductus arteriosus. Radiographic changes in pulmonary vascular engorgement, pulmonary edema, and cardiac size on the anteroposterior film tended to precede the clinical changes of shunt appearance and resolution. The echocardiographic left atrial to aortic ratio (LA/Ao) supplemented the radiographic findings. The time of disappearance of the ductus arteriosus shunt, as judged by clinical findings, was identified accurately by radiographic and echocardiographic findings in the majority of cases; errors of under- and overestimation occurred in a minority of patients. In assessing both the presence and the resolution of the shunt, greater reliability was possible by using both radiographic and echocardiographic findings than by using either method alone.

Pulmonary overcirculation from prolonged patency of the ductus arteriosus is a frequent and often life-threatening problem in premature newborn infants [1–3]. Preoperative diagnosis of a patent ductus arteriosus is usually nonangiographic, involving clinical markers, chest radiographic changes [4], and echocardiography [4, 5].

The radiographic and echocardiographic changes that follow ductus arteriosus ligation have been described [4], but little information is available regarding the changes that occur when there is nonsurgical resolution. Surgical closure of the ductus arteriosus has the advantage that the surgery itself provides a therapeutic endpoint. No such distinct endpoint exists when the ductus arteriosus closes spontaneously or when nonsurgical maneuvers are used to close it.

Accurate diagnosis of ductus arteriosus patency has become imperative because of the recent development of pharmacologic agents that affect the ductus arteriosus. Prostaglandin E_1 has been shown to dilate the ductus arteriosus [6–8], while inhibitors of prostaglandin synthesis act to close the ductus [6, 9, 10]. Indomethacin is a potent inhibitor of prostaglandin synthetase that has been used with considerable [9–11] but not invariable [12] success in effecting nonsurgical closure of the ductus arteriosus in clinical trials. When such an agent is used, it is desirable to identify markers by which success of therapy may be judged.

The purpose of our study was to compare retrospectively the radiographic, echocardiographic, and clinical findings in a series of 33 preterm newborns who were treated with indomethacin after clinical signs of a significant patent ductus arteriosus. In addition to documenting the chronology of the diagnostic findings, a specific effort was made to determine the accuracy of chest radiography used independently to determine the time and therapeutic success of ductus closure.

Subjects and Methods

Sequential radiographs were evaluated in 33 preterm infants who exhibited clinical signs of patent ductus arteriosus and in whom pharmacologic closure of the ductus was attempted with indomethacin. The use of this drug was as described elsewhere [9, 11, 13]. The radiographs were examined by two of us (D. E. and C. H.) working together without knowledge of the dates of indomethacin administration or of the patient's clinical course; subsequently these data were noted from the patients' records.

Initial chest radiographs were examined to identify each patient's initial radiographic diagnosis. Cardiothoracic ratios (C/T) were measured on all films as described elsewhere [4]. Times were noted at which the C/T began to increase, when it reached its maximum, and when it began to decrease. Similar times were noted for the onset, maximum, and reduction in pulmonary vascular enlargement and pulmonary edema. Weighing these factors and the overall radiographic course, a subjective estimate was made of the time when the final dose of indomethacin was administered. An estimate was also made of the success of shunt closure.

Echocardiographic data were available for 23 patients; echocardiograms were measured as previously described [4]. The left atrial to aortic root ratio (LA/Ao) was noted at its maximum, immediately preceding, and following the course of indomethacin therapy. The left ventricular end diastolic dimension was measured on 17 patients as described elsewhere [14].

The patients in this series were treated at two hospitals: 24 at University Hospital in San Diego and nine at Sunrise Hospital in Las Vegas. Average gestational age at birth determined by examination was 30.3 weeks (range, 26–35) and average birthweight was 1,336 grams (range, 640–2,700). Three patients were described as small for gestational age; the remainder were of normal size. Of the 33 patients, 18 were male. The clinical records were examined when these were available (23 patients) to determine the ages at which significant clinical findings

Received May 12, 1978; accepted after revision September 7, 1978.
C. B. Higgins is the recipient of U.S. Public Health Service Research Career Development Award, grant no. K04 HL00201 from the National Heart and Lung Institute.

[1] Department of Radiology, University of California Hospital, 225 West Dickinson Street, San Diego, California 92103. Address reprint requests to D. K. Edwards.
[2] Department of Pediatrics, University of California Hospital, San Diego, California 92103.

© 1978 American Roentgen Ray Society

0361–803X/78/1200–1009 $00.00

TABLE 1

Correlation of Clinical and Radiographic Observations

Mean Age (Days)	Clinical	Radiographic and Echocardiographic
5.1 (1–17)	...	Enlargement of pulmonary vessels
5.3 (2–12)	Significant murmur noted	...
5.9 (1–15)	...	Enlargement of cardiac size
6.6 (2–17)	...	Onset of pulmonary edema
7.5 (3–14)	Bounding pulses noted	...
9.4 (4–33)	Peak of clinical symptoms	...
9.4 (3–34)	First indomethacin dose	...
9.7 (1–35)	...	Maximum cardiac size
10.2 (5–35)	...	Maximum vessel enlargement
10.2 (5–33)	...	Maximum LA/Ao ratio
10.3 (4–31)	...	Maximum pulmonary edema
11.7 (3–36)* (4–39)†	Final indomethacin dose	Radiographic estimate of final dose
13.0 (3–43)	...	Cardiac size decrease
13.3 (6–43)	...	Pulmonary vessel decrease
13.8 (6–43)	...	Pulmonary edema decrease
14.3 (6–47)	Clinical symptom resolution	...

Note.—Numbers in parentheses are ranges.
* Clinical.
† Radiographic and echocardiographic.

suggesting a patent ductus arteriosus were initially noted, reached a maximum, and resolved.

Results

Radiographic Observations

The primary radiographic diagnosis for 26 patients was respiratory distress syndrome. Four patients demonstrated what has been termed "immature lung" [15], with minimal granularity and no significant airbronchograms. Two patients exhibited no discernable pulmonary parenchymal disease, but had congestive heart failure that was initially mild. One patient had an initially normal chest radiograph, but within a few days developed findings characteristic of Wilson-Mikity syndrome [16].

The time course of the findings of pulmonary vascular enlargement, pulmonary edema, and enlarged cardiac silhouette is summarized in table 1. All patients during their clinical courses exhibited enlargement of pulmonary vessels, manifested by appearance of numerous hilar and perihilar en face vessels ("shunt vessels"). Initial pulmonary plethora appeared at 1–17 days of age (average, 5.1 days); these enlarged vessels tended to be the first manifestation of patent ductus arteriosus. Vessel enlargement was maximal at 10.2 days of age, and discernable decrease was observed at an average of 13.3 days. Pulmonary edema was observed in all but one patient. The average age at onset was 6.6 days. Edema was maximal at 10.3 days, and began to decrease at 13.8 days.

Cardiothoracic ratio (C/T) averaged 52.5% on the initial chest film. Onset of discernable enlargement over the initial value was noted at an average of 5.9 days, and maximal C/T occurred at 9.7 days. Decrease in cardiac size occurred at 13.0 days. Maximum C/T never exceeded 60% in 21 patients. Of these 21 patients, five demonstrated an increase in C/T of 5% or more, while the remainder showed lesser increases. A total of 17 patients had maximum C/T increases of less than 5%. Of these patients, 16 demonstrated over the sequence of films an increase and subsequent decrease in C/T that paralleled clinical symptomatology, even though the change was less than 5%. One patient demonstrated no discernable increase in cardiac size during his hospital course, and two patients never exhibited a decrease after enlargement of their cardiac silhouettes. The latter two patients did not have subsequent chest radiographs.

All patients but one required assisted ventilation during their hospital courses. A wide variety of pulmonary abnormalities, many probably related to assisted ventilation, were observed. These included varying degrees of atelectasis (14 patients), pleural effusion (two), aspiration (three), pneumothorax (six), pneumomediastinum (one), pneumopericardium (one), and interstitial emphysema (eight patients). Hyperaeration was not a frequent finding.

Echocardiographic Observations

The echocardiograms obtained in 23 infants showed a peak left atrial to aortic root (LA/Ao) ratio of 0.8–0.9 in four infants, suggesting a moderate left to right shunt, and a peak ratio of 1.0 or greater in 12 infants, suggesting a large-volume shunt [17]. The average peak LA/Ao ratio was 1.0 (range, 0.5–1.4). The average age at the peak LA/Ao ratio was 10.2 days. The average LA/Ao ratio prior to initiation of indomethacin was 0.9 (range, 0.4–1.4), and after the course of the drug was 0.6 (range, 0.4–1.0). The LA/Ao ratio decreased after indomethacin therapy in all but one patient. All patients who exhibited elevated LA/Ao ratios also demonstrated enlarged left ventricular end diastolic dimension, in the 17 patients for whom this was measured.

Of the seven patients with LA/Ao of less than 0.8, absolute cardiomegaly (C/T more than 60%) was seen in two patients, and four patients exhibited significant increase in C/T (more than 5%). Only one patient with normal LA/Ao ratio demonstrated neither cardiomegaly nor significant increase in C/T. However, this patient did

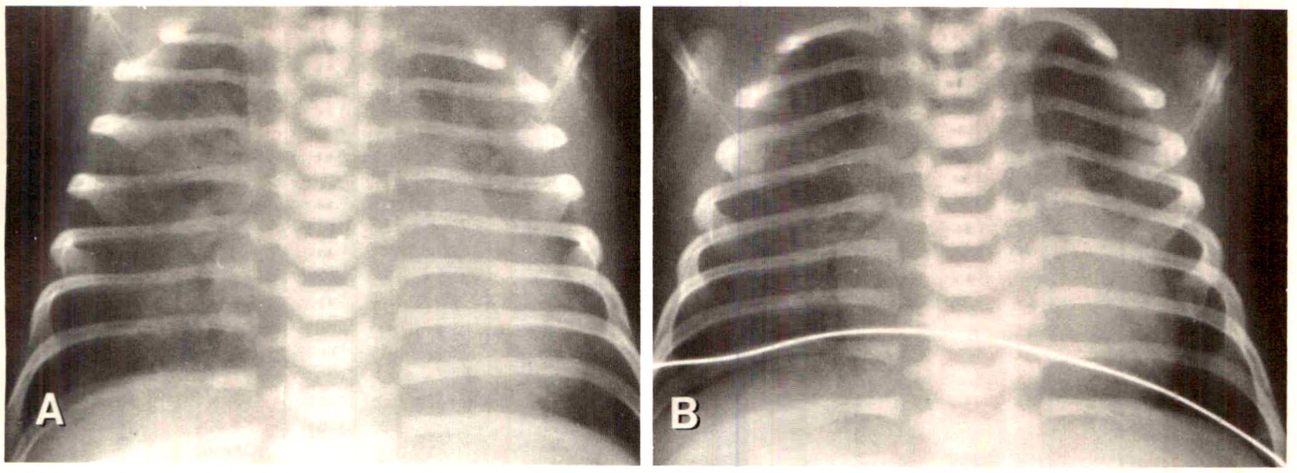

Fig. 1.—Patient who exhibited gradual clearing after drug therapy. *A*, Anteroposterior view of chest prior to indomethacin administration. *B*, Film after indomethacin therapy showing partial resolution of pulmonary plethora and edema.

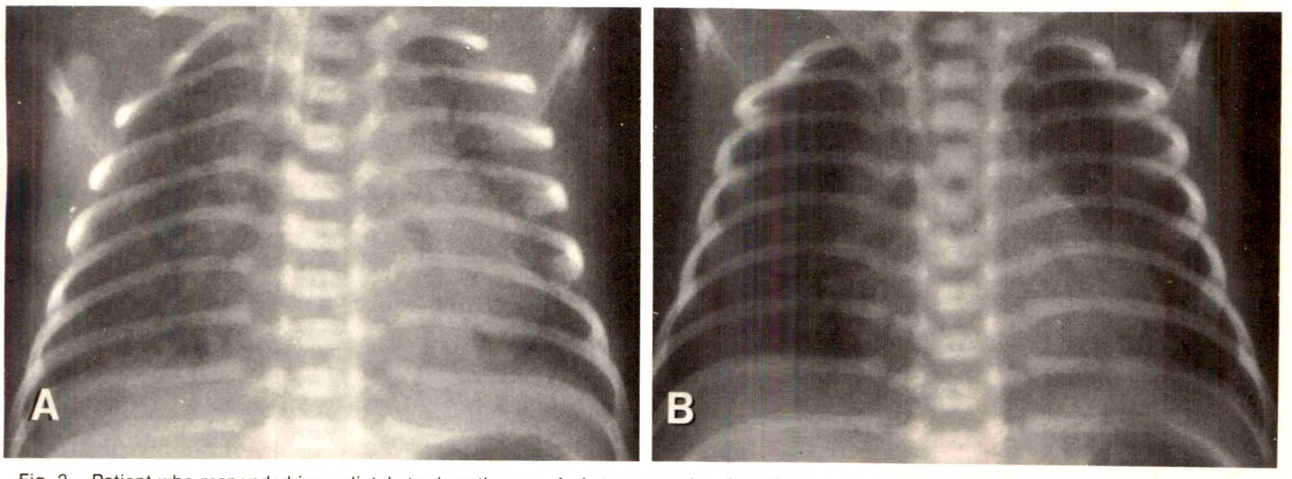

Fig. 2.—Patient who responded immediately to drug therapy. *A*, Anteroposterior view of chest prior to indomethacin administration. *B*, Film 1 day after indomethacin therapy showing marked clearing of cardiomegaly, and pulmonary plethora and edema.

exhibit pulmonary plethora and edema. Thus in all patients either radiographic or echocardiographic signs of a large volume shunt were identified prior to indomethacin therapy.

Clinical Evaluation

A chronologic summary of the major clinical events is presented in table 1. The first time a significant murmur was noted was at an average age of 5.3 days; the average peak of clinical symptoms was 9.4 days, the same average time as the first dose of indomethacin. The average time of clinical resolution was 14.3 days.

Four patients were felt to have recurrent patent ductus arteriosus after indomethacin therapy and underwent ductal ligation. Radiographically three of these four appeared to have improved in terms of shunt-related abnormalities but had not entirely resolved; in the fourth infant the radiographic abnormalities appeared to have resolved completely. At surgery the patent ductus arteriosus was very small (2 mm) in the latter patient, and persisting moderate-sized in the other three.

Radiographic Estimation of Indomethacin Therapy

When the radiographic estimate of the date of successful indomethacin therapy was compared with the actual time of the final dose (that is, the dose that was felt clinically to have closed the ductus), the radiographic estimate lay within 24 hr of the actual time in 17 cases (52%). In seven cases, the radiographic estimate of successful therapy was earlier than the final dose by up to 5 days; in nine cases the radiographic estimate was past the time of the final dose by up to 6 days. The average estimated time of the final dose of indomethacin was 11.7 days, which was the same as the average actual time.

Subsequent examination of the nine cases in which the radiographic estimate of successful therapy was later than the actual final indomethacin dose revealed that these cases exhibited resolution that occurred slowly over several days. An example of a patient who exhibited slow clearing is shown in figure 1, which may be contrasted with a patient who exhibited marked immediate clearing after indomethacin therapy (fig. 2).

Examination of the seven cases in which the radiographic signs of significant improvement preceded the actual completion of indomethacin therapy revealed that, in four cases, the volume of the left-to-right shunt was probably small prior to indomethacin treatment because the C/T was below 60% and the peak LA/Ao ratio (in the two cases measured) was only 0.6. In three of these cases, two doses of indomethacin were administered after radiographic clearing of what appeared to be small shunts. In one of these patients, persisting respiratory dependency led eventually to ductal ligation; as predicted radiographically, this patient had a very small patent ductus arteriosus. In the other four cases, radiographic findings suggested significant improvement after the first dose of indomethacin, but clinical findings prompted additional doses.

Of the 16 patients in whom radiographic assessment of successful therapy was erroneous, 11 were among the 23 patients on whom echocardiography was done. Of these 11, five patients demonstrated decreases in LA/Ao ratio from 1.0 or above to below 0.8 with indomethacin therapy. Had this LA/Ao ratio drop been used in conjunction with the radiographic findings, the number correct would thus have been 17 of 23, or 74%. In the remaining five patients, neither the LA/Ao ratio nor the radiographs reflected the exact time of shunt closure as defined by clinical evidence of closure.

Discussion

In evaluating the onset of a significant shunt across a patent ductus arteriosus in a newborn infant, the current study supports a previous report [4] that indicative changes on the chest radiograph are contemporary with and often in advance of clinical detection of a significant heart murmur. The sequence of clinical and radiographic changes is more striking than the average times of these observations would suggest (table 1), because in many cases radiographic evaluation was not requested until after there was clinical suspicion of a shunt.

In examining the radiographic indices of significant shunt, the most sensitive were engorged pulmonary vessels, which were observed with all patients except one. The size of the cardiac silhouette was a relatively insensitive index of shunt severity. Absolute cardiomegaly (C/T more than 60%) was seen in only 36% of patients, and significant increase in C/T (more than 5%) was seen in only 48%. A large number of patients (48%) demonstrated neither absolute cardiomegaly nor significant increase in C/T.

The other numerical variable examined in this study was the echocardiographic LA/Ao ratio. Like the C/T findings, this ratio was not always indicative of clinical status. In 48% of 23 cases, the peak LA/Ao ratio was below 1.0, and in 30% the peak was below 0.8, the value which probably represents the lower limit for a moderate left-to-right shunt [17].

In diagnosing ductus arteriosus shunt closure, the use of the radiographs was only modestly successful. The average estimation of the date of indomethacin administration coincided with the average date of the final indomethacin dose, but there were errors of up to 5 and 6 days in either direction. Accuracy within 24 hr was attained with only 52% of patients. Of the factors that may contribute to this inaccuracy, possibly the most important is that the standard for radiographic evaluation in this study was clinical assessment of the shunt. The accuracy of clinical evaluation is always open to question in the absence of direct evidence. This factor, together with partial or incomplete ductus closure, may have contributed to the error made in seven cases in which the radiographs would have suggested cessation of therapy before it was actually discontinued.

In nine cases the radiographs alone would have suggested a need for additional doses of indomethacin. In the majority of these patients clearance of pulmonary plethora and/or edema was relatively slow. It is speculated that this type of error may relate to slow clearance of fluid; transient oliguria is a known side-effect of indomethacin therapy in infancy [9]. In considering the accuracy of radiographic evaluation of patent ductus arteriosus shunt, it is worth noting that with the four cases who underwent surgical ligation, the final radiographs predicted the operative findings correctly.

It may be concluded from this study that radiographic changes are a fairly reliable indicator of the appearance of a significant ductus arteriosus shunt, if the changes of pulmonary vascular enlargement and pulmonary edema are weighed more heavily than measurable changes in the cardiothoracic (C/T) ratio. If the C/T is considered together with the echocardiographic LA/Ao ratio, greater accuracy is possible than with using either measurement alone. The exact time of ductus closure is not reliably estimated by any of the variables examined in this study , although again greater accuracy is attained by using echocardiographic data together with the radiographs than by using either alone. More reliable indices of shunt closure than those examined here need to be developed in order to monitor the effects of pharmacologic agents such as indomethacin.

REFERENCES

1. Kitterman JA, Edmunds LH Jr, Gregory GA, Heymann MA, Tooley WH, Rudolph AM: Patent ductus arteriosus in premature infants. Incidence, relation to pulmonary disease and management. *N Engl J Med* 287:473–477, 1972
2. Neal WA, Bessinger FB Jr, Hunt CE, Lucas RV Jr: Patent ductus arteriosus complicating respiratory distress syndrome. *J Pediatr* 86:127–131, 1975
3. Rudolph AM, Heymann MA: Medical treatment of the ductus arteriosus. *Hosp Prac* 12:57–65, 1977
4. Higgins CB, Rausch J, Friedman WF, Hirschklau MJ, Kirkpatrick SE, Goergen TG, Reinke RT: Patent ductus arteriosus in preterm infants with idiopathic respiratory distress syndrome. Radiographic and echocardiographic evaluation. *Radiology* 124:189–195, 1977
5. Laird WP, Fixler DE: Echocardiography of premature infants with pulmonary disease: a noninvasive method for detecting large ductal left-to-right shunts. *Radiology* 122:455–457, 1977
6. Elliott RB, Starling MB, Neutz JM: Medical manipulation of the ductus arteriosus. *Lancet* 1:140–142, 1975
7. Heymann MA, Rudolph AM: Ductus arteriosus dilatation by

prostaglandin E_1 in infants with pulmonary atresia. *Pediatrics* 59:325–329, 1977

8. Lang P, Freed MD, Rosenthal A, Castaneda AR, Nadas AS: The use of prostaglandin E_1 in an infant with interruption of the aortic arch. *J Pediatr* 91:805–807, 1977
9. Friedman WF, Hirschklau MJ, Printz MP, Pitlick PT, Kirkpatrick SE: Pharmacologic closure of patent ductus arteriosus in the premature infant. *N Engl J Med* 295:526–529, 1976
10. Heymann MA, Rudolph AM, Silverman NH: Closure of the ductus arteriosus in premature infants by inhibition of prostaglandin synthesis. *N Engl J Med* 295:530–533, 1976
11. Friedman WF, Heymann MA, Rudolph AM: Commentary: new thoughts on an old problem—patent ductus arteriosus in the premature infant. *J Pediatr* 90:338–340,1977
12. Neal WA, Kyle JM, Mullett MD: Failure of indomethacin therapy to induce closure of patent ductus arteriosus in premature infants with respiratory distress syndrome. *J Pediatr* 91:621–623, 1977
13. Friedman WF, Printz MP, Kirkpatrick SE: Blockers of prostaglandin synthesis—a novel therapy in the management of the premature infant with patent ductus arteriosus, in *Advances in Prostaglandin and Thromboxane Research,* edited by Coceani F, Olley PM, New York, Raven, 1978, pp 373–381
14. Hirschklau MJ, DiSessa TG, Higgins CB, Friedman WF: Echocardiographic diagnosis: pitfalls in the premature infant with a large patent ductus arteriosus. *J Pediatr* 92:474–477, 1978
15. Parker BR, Pinckney LE, Johnson JD, Northway WH Jr: Immature lung syndrome (abstr). *Clin Res* 24:194A, 1976
16. Hodgman JE, Mikity VG, Tatter D, Cleland RS: Chronic respiratory distress in the premature infant: Wilson-Mikity syndrome. *Pediatrics* 44:179–195, 1969
17. Sahn DJ, Vaucher Y, Williams DE, Allen HD, Goldberg SJ, Friedman WF: Echocardiographic detection of large left to right shunts and cardiomyopathies in infants and children. *Am J Cardiol* 38:73–79, 1976

Intermittent Bleeding from Minute to Minute in Acute Massive Gastrointestinal Hemorrhage: Arteriographic Demonstration

THOMAS A. SOS,[1] JACK G. LEE,[2] DAVID WIXSON,[1, 3] AND KENNETH W. SNIDERMAN[1]

Acute massive gastrointestinal hemorrhage can be intermittent from minute to minute. This phenomenon is documented by arteriography in three patients. Failure to demonstrate active bleeding by angiography therefore may not prove cessation of bleeding or indicate an inadequate examination.

Arteriography occupies an important role in the localization [1] and treatment [2, 3] of gastrointestinal hemorrhage. The pioneering work of Baum and others demonstrated that temporary and occasionally permanent control of gastrointestinal hemorrhage may be achieved by transcatheter infusion [2] or embolization [3] techniques. High risk emergency surgical procedures can thus be deferred until the patient's medical condition improves. It is thus especially frustrating when, in patients clinically documented to have massive active gastrointestinal hemorrhage, a site of extravasation cannot be demonstrated by visceral panangiography. An explanation not previously demonstrated angiographically is the intermittency of even massive active gastrointestinal bleeding. We recently studied three patients in whom clinically documented acute gastrointestinal hemorrhage was demonstrated by only one of two or three identical selective arteriograms performed within a few minutes.

Case Reports

Case 1

A 61-year-old white male was admitted after 24 hr of episodic bright red and melanotic stools. He denied a previous history of gastrointestinal bleeding and had no abdominal pain. The only significant finding on physical examination was orthostatic hypotension (180/100 mm Hg supine and 140/100 mm Hg sitting). Hematocrit was 25% and the hemoglobin 8.0 gm/dl. Nasogastric aspirate was free of blood. Sigmoidoscopy to 20 cm demonstrated melanotic stools from above. On the day of admission the patient continued to have melena mixed with bright red blood and received two units of packed cells and one unit of whole blood.

Emergency arteriography was performed. Superior mesenteric arteriography demonstrated no bleeding. Selective inferior mesenteric arteriography was then performed (fig. 1). The first angiographic series was centered to include the sigmoid colon (fig. 1*A*); no bleeding was seen. For complete coverage of the entire inferior mesenteric artery distribution, a second angiographic series covered the splenic flexure at an identical injection rate and volume (fig. 1*B*). Active bleeding into a proximal sigmoid diverticulum was demonstrated at the lower margin of the field, which overlapped the midzone of the first arteriographic series. A few minutes later, a third angiographic series was performed at the same injection rate and volume in the right posterior oblique projection for better localization of the bleeding site (fig. 1*C*); no bleeding was demonstrated.

The patient was treated by conservative medical therapy; after receiving nine more units of blood, he stabilized. Barium enema examination showed diffuse diverticulosis of the entire colon. Surgery was not performed and the patient was discharged without further episodes of bleeding.

Case 2

A 66-year-old white man was admitted for evaluation of an upper gastrointestinal hemorrhage. A week before admission he developed acute gastrointestinal bleeding which was successfully treated medically, but before diagnostic studies could be completed he left the hospital against medical advice. On the day of the present admission, the patient vomited coffee ground materials, passed five black tarry stools, and had a syncopal episode. He had a long history of heavy alcohol consumption and, 5 years earlier, a bleeding ulcer was controlled with medical management and multiple transfusions. Because of a cerebral vascular accident 1 year earlier, he received coumadin anticoagulation until the onset of the present illness. On admission, hemoglobin was 9.6 gm/dl and there was clinical evidence of moderate bleeding.

After a transfusion of several units of whole blood, visceral angiography was performed (figs. 2*A* and 2*B*). Celiac arteriography demonstrated extravasation of contrast material in the second portion of the duodenum (fig. 2*A*). Right posterior oblique celiac angiography performed immediately afterward at identical injection rate and volume revealed no bleeding (fig. 2*B*). Injection of the superior mesenteric artery to rule out bleeding through the inferior pancreaticoduodenal artery was also negative (fig. 2*C*). Vasopressin infusion was ineffective in controlling the hemorrhage and the patient was taken to surgery. An acute actively bleeding ulcer was found on the posterior wall of the second portion of the duodenum.

Case 3

A 76-year-old man was admitted with a severe gastrointestinal hemorrhage evidenced by multiple tarry stools. On admission, hemoglobin was 8 gm/dl. History included diverticulitis and Anacin ingestion. Physical examination demonstrated orthostatic hypotension. A nasogastric tube did not return bloody aspirate. After transfusion of eight units of whole blood, the patient continued to bleed briskly.

Superior mesenteric arteriography was performed; this included two separate identical injections covering first the upper and then the lower abdomen (fig. 3). On the first injection there

Received April 20, 1978; accepted after revision August 10, 1978.
This work was supported in part by National Institutes of Health grant no. 1 to 1 HL05966-03CAR.

[1] Department of Radiology, Division of Cardiovascular Radiology, New York Hospital-Cornell Medical Center, 525 East 68th Street, New York, New York 10021. Address reprint requests to T. A. Sos.
[2] Department of Radiology, St. Luke's Hospital, San Francisco, California 94110.
[3] Present address: Department of Radiology, Bethesda Naval Medical Center, Bethesda, Maryland 20014.

© 1978 American Roentgen Ray Society

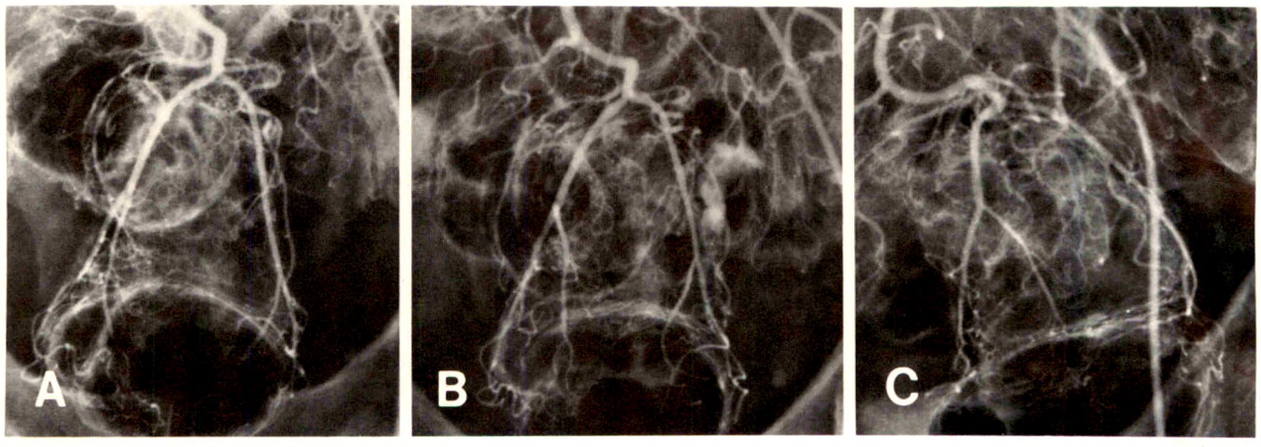

Fig. 1.—Case 1: inferior mesenteric arteriograms of 61-year-old man with active lower gastrointestinal bleeding. *A*, Anteroposterior view showing normal rectosigmoid colon. *B*, Anteroposterior view a few minutes later showing bleeding in proximal sigmoid colon. *C*, Right posterior oblique view a few minutes after *B*. No bleeding is seen.

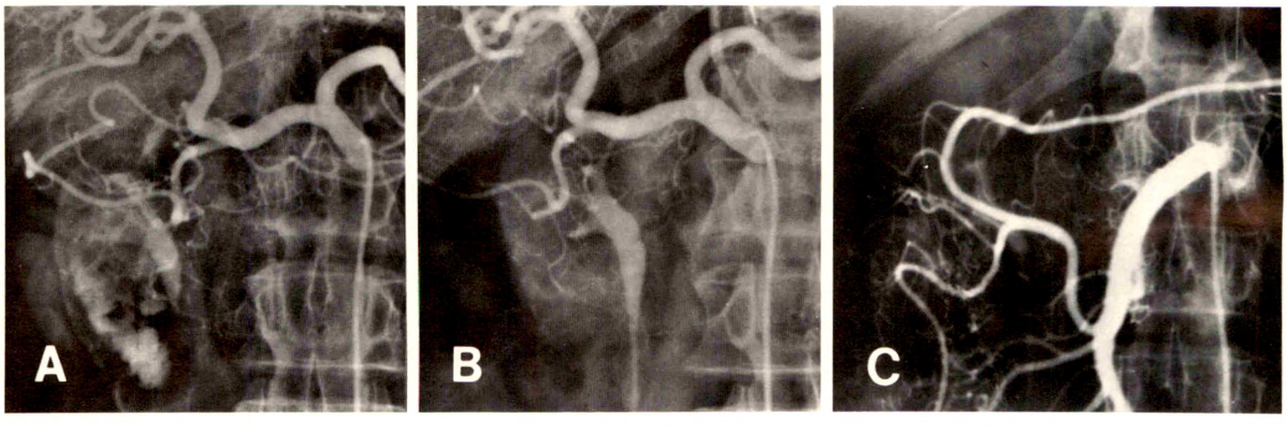

Fig. 2.—Case 2: 66-year-old man with acute upper gastrointestinal hemorrhage. *A*, Celiac arteriogram, anteroposterior view, showing massive extravasation from superior pancreaticoduodenal artery into duodenum. *B*, Celiac arteriogram, right posterior oblique view soon after *A*. No evidence of bleeding. *C*, Superior mesenteric arteriogram, anteroposterior view soon after *B*, showing filled inferior pancreaticoduodenal artery. No bleeding is seen.

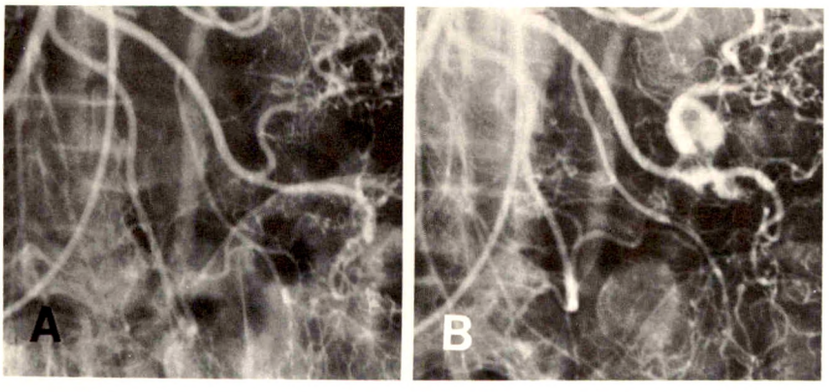

Fig. 3.—Case 3: superior mesenteric arteriograms of 76-year-old man with acute upper gastrointestinal hemorrhage. *A*, Anteroposterior view. No evidence of bleeding is seen. *B*, Anteroposterior view a few minutes later showing extravasation from jejunal artery.

was no demonstrable bleeding (fig. 3*A*). On the second examination, the upper part of the field overlapped the lower part of the first angiographic field; in this series extravasation of contrast material was seen from a jejunal artery which was not bleeding in the first series (fig. 3*B*). The patient was immediately taken to surgery and a diverticulum was found about 46 cm from the ligament of Treitz. Pathologic examination of the specimen demonstrated a 1.6 cm acquired diverticulum of the jejunum and a 0.1 cm ulcer in the tip of the diverticulum immediately overlying and eroding into a small muscular artery.

Discussion

Visceral angiography is a well established technique in detecting and controlling gastrointestinal hemorrhage. Prior to angiography, patients often undergo

endoscopy in an attempt to localize the site of bleeding. Both endoscopists and angiographers have encountered patients with acute massive gastrointestinal hemorrhage in whom they failed to demonstrate the bleeding site. Demonstration of variceal bleeding by angiography is notoriously difficult, but arterial bleeding at rates over 0.5 ml/min is usually well seen [1]. Presently recognized and documented causes for failure to demonstrate gastrointestinal bleeding by arteriography include: (1) hemorrhage at a rate too slow to demonstrate by angiography (<0.5 ml/min); (2) venous (variceal) bleeding; (3) technical problems, including injection into the wrong artery, nonselective injection, inadequate injection rate and/or volume, and failure to include the bleeding site on the angiographic field; (4) permanent cessation of bleeding; and (5) temporary cessation of bleeding due to hypotension (vasovagal reaction or blood loss) or intermittent bleeding (arteriographically documented in this paper).

We believe our three cases document a transient phenomenon—the intermittent minute-to-minute nature of even acute massive gastrointestinal hemorrhage. As documented, such bleeding can occur from branches of all the major arteries to the gastrointestinal tract: the inferior mesenteric artery (case 1), the celiac artery (case 2), and the superior mesenteric artery (case 3).

The mechanism for the intermittency is not clear; localized spasm in arteriolar branches may be responsible. It is probably too transient to be related to blood loss and/or vasovagal reaction. None of our three patients had clinical evidence of changes in their hemodynamic status during the course of angiographic examinations, and the injected major vessels or their branches showed no change in caliber from study to study.

Baum [4] and Casarella et al. [5] suggested that gastrointestinal hemorrhage can be intermittent in nature; Casarella et al. reported two patients with colonic diverticular hemorrhage in whom negative angiographic studies were followed by positive ones within 30 min. They postulated that the bleeding may have been provoked by the vasodilatory action of the contrast medium [6]. In our patients, however, hemorrhage was demonstrated on the first but not the second or third arteriogram in case 2, and in case 3 on the second, but not the first or third arteriogram.

This phenomenon may be more frequent than recognized, because in many patients a repeat injection is not needed to cover the entire distribution of an artery, or because in cases of repeated injections the bleeding site may not be located in overlapping areas of the two angiographic fields. Lack of demonstration of a bleeding point therefore does not necessarily represent either an inadequate examination or cessation of the hemorrhage, but rather a very transient phenomenon. This makes it increasingly important that patients with acute gastrointestinal hemorrhage undergo thorough endoscopy to find the bleeding site(s), and that the status of patients with upper gastrointestinal hemorrhage be monitored during the angiographic study. In patients with upper gastrointestinal hemorrhage, the nasogastric aspirate should be checked frequently; in those with lower gastrointestinal bleeding, accurate monitoring unfortunately is not possible.

We hesitate to recommend repeated contrast injections in patients with acute gastrointestinal hemorrhage and negative arteriography. However, a trial infusion of vasopressin into the appropriate artery may be indicated in clinically continuing gastrointestinal bleeding localized by endoscopy, even if such hemorrhage is not demonstrated by arteriography.

REFERENCES

1. Nusbaum M, Baum S: Radiographic demonstration of unknown sites of gastrointestinal bleeding. *Surg Forum* 14:374–375, 1963
2. Baum S, Nusbaum M: The control of gastrointestinal hemorrhage by selective mesenteric arterial infusion of vasopressin. *Radiology* 98:497–504, 1971
3. Rösch J, Dotter CT, Brown MJ: Selective arterial embolization: a new method for control of acute gastrointestinal bleeding. *Radiology* 102:303–306, 1972
4. Baum S: Angiography, in *Gastroenterology*, 3d ed., vol 1, edited by Bockus HL, Philadelphia, Saunders, 1974, p 828
5. Casarella WJ, Kanter IE, Seaman WB: Right sided colonic diverticula as cause of acute rectal hemorrhage. *N Engl J Med* 286:450–453, 1972
6. Steckel RJ, Rösch J, Ross G, Grollman JH Jr: New developments in pharmacoangiography (and arterial pharmacotherapy) of the gastrointestinal tract. *Invest Radiol* 6:199–211, 1971

Protean Manifestations of Mycotic Aneurysms

STEPHEN L. KAUFMAN,[1] ROBERT I. WHITE, JR., DONALD P. HARRINGTON, KLEMENS H. BARTH, AND STANLEY S. SIEGELMAN

Nine patients examined by arteriography were shown to have mycotic aneurysms involving the thoracic aorta, subclavian artery, renal artery, middle cerebral artery, hepatic artery, and splenic artery. Patients presented with sepsis, chest pain, mediastinal mass, headache, hypertension, and intraperitoneal bleeding. Etiologic factors included endocarditis, septicemia, drug abuse, and poorly controlled soft-tissue infection. Most mycotic aneurysms were virulent processes with rapid progression and only three of the nine patients (33%) survived. Since mycotic aneurysms may be associated with rapid progression and poor prognosis, early recognition is mandatory.

Since William Osler's 1885 description [1] of an aortic aneurysm arising secondary to bacterial endocarditis, the term "mycotic" aneurysm has been used to describe any aneurysm due to an infectious process involving the arterial wall. Although the incidence of mycotic aneurysms has decreased in the postantibiotic era [2], they are not rare. Mycotic aneurysms occur in patients of all ages; they may involve any systemic vessel and thus may be responsible for a wide spectrum of clinical disturbances [3–8].

This report describes nine patients with mycotic aneurysms encountered within a 7-year period. Since mycotic aneurysms may be associated with a rapid progression and poor prognosis, early recognition and treatment is mandatory.

Case Material

A computerized search of the Johns Hopkins Hospital Disease and Operative Index and review of the records of the Division of Cardiovascular Radiology for the period 1971–1977 revealed nine patients with mycotic aneurysms. Clinical records, surgical notes, and autopsy results were reviewed. Angiographic studies were performed in all nine patients.

Findings

Clinical and radiographic findings are summarized in table 1.

Location of Aneurysm

Mycotic aneurysms were intrathoracic in six of the nine patients, the thoracic aorta being involved in five of these. In two patients the aneurysm originated from the ascending thoracic aortic, in one patient from the aortic arch, and in two patients from the descending thoracic aorta. The intrathoracic portion of an anomalous right subclavian artery was involved with intrathoracic aneurysm in the sixth patient. Two patients had intraabdominal mycotic aneurysms; a renal artery mycotic aneurysm occurred in one of these. The second patient with intraabdominal mycotic aneurysms had multiple aneurysms within the hepatic and splenic circulation. The final patient had mycotic aneurysms involving intracerebral vessels.

Clinical Findings

The five males and four females were 6–64 years old (mean, 37). Five of the six patients with intrathoracic aneurysm had chest or back pain. Cervical and upper extremity venous engorgement occurred in two patients (cases 1 and 4). The patient with hepatic and splenic artery mycotic aneurysms (case 7) had acute blood loss and hemoperitoneum. The patient with the renal artery aneurysm (case 8) had hypertension several months after an episode of subacute bacterial endocarditis. The patient with intracerebral aneurysms (case 9) had headache without focal neurologic signs or evidence of subarachnoid hemorrhage.

Sepsis, as evidenced by fever and leukocytosis, occurred with mycotic aneurysms regardless of location. Seven of the nine patients were septic at presentation. In the other two patients the aneurysms were discovered 2–3 months after successful therapy for subacute bacterial endocarditis. Of these two patients, one had renal artery aneurysm with hypertension (case 8) and one had aneurysm of the ascending thoracic aorta (case 5). The latter was asymptomatic at presentation; the aneurysm was detected on a follow-up chest radiograph.

Predisposing Conditions

Four patients had bacterial endocarditis. In three the endocarditis occurred on abnormal valves involved with congenital or rheumatic heart disease; the fourth had acute endocarditis on a previously normal mitral valve (case 7). In one patient, a mycotic aneurysm was associated with a coarctation of the aorta (case 3); he was asymptomatic before presenting with mycotic aneurysm. One patient was a known intravenous drug abuser (case 4). In cases 1 and 2 the mycotic aneurysm occurred on areas of severe atherosclerosis. In case 6 the aneurysm resulted from a spreading paravertebral abscess. Three patients had diabetes mellitus.

Bacteriology

Staphlococcus aureus was the causative organism in four patients; *E. Coli* was isolated in two patients; and

Received March 22, 1978; accepted after revision August 1, 1978.

[1] All authors: Russel H. Morgan Department of Radiology and Radiological Science, Johns Hopkins Medical Institutions, Baltimore, Maryland 21205. Address reprint requests to S. L. Kaufman.

© 1978 American Roentgen Ray Society

0361–803X/78/1200–1019 $00.00

TABLE 1
Summary of Findings

Case No.	Age and Sex	Location of Aneurysm	Associated Conditions	Symptoms/Signs	Radiographic Findings	Organism	Outcome
Intrathoracic:							
1	64, F	Ascending thoracic aorta	Atherosclerosis, diabetes	Chest pain, fever, cervical venous distension	Mediastinal enlargement containing gas density radiolucencies	*E. coli*	Died
2	61, F	Aortic arch	Atherosclerosis, diabetes	Back pain, fever	Mediastinal enlargement containing gas density radiolucencies	*E. coli**	Died
3	11, M	Descending thoracic aorta	Coarctation of the aorta	Back pain, absent pulses lower extremities	Posterior mediastinal mass	*S. aureus*	Died
4	33, M	Descending thoracic aorta	Heroin addiction	Fever, chest pain, cervical venous distension	Mediastinal enlargement	*S. aureus*	Died
5	6, M	Ascending thoracic aorta	Congenital aortic stenosis, previous bacterial endocarditis	Asymptomatic	Anterior mediastinal mass	Negative cultures	Aneurysm resected
6	59, M	Subclavian artery	Long term steroid medication, uncontrolled soft tissue infection	Fever, back and shoulder pain	Mediastinal enlargement	*S. aureus*	Died
Intraabdominal:							
7	62, F	Splenic and hepatic arteries	Acute bacterial endocarditis, diabetes	Fever, abdominal pain, hemoperitoneum	. . .	*S. aureus*	Died
8	13, F	Renal artery	Rheumatic mitral stenosis, previous bacterial endocarditis	Hypertension	. . .	*S. viridans*	Spontaneous thrombosis of aneurysm
Intracerebral:							
9	23, M	Middle cerebral artery	Congenital mitral stenosis, bacterial endocarditis	Fever, headache	. . .	*S. epidermidis*†	Recovered on antibiotics

* Cultured at postmortem examination.
† Cultured at exploratory surgery.

Staphlococcus epidermidis and *Streptococcus viridans* were each isolated in one patient. All cultures proved negative in one patient. In two other patients multiple blood cultures were negative and the organism was isolated on cultures taken either at surgery or at postmortem examination. Both of these patients had undergone prior antibiotic therapy.

Plain Radiographic Findings

Plain chest radiographs were positive in the six patients with intrathoracic mycotic aneurysms. Generalized mediastinal enlargement or a localized mediastinal mass was present in all cases (figs. 1*A*, 3, and 5*A*). Tracheal deviation was frequently seen. Mottled radiolucencies of gas density were present within the mediastinum in the two diabetic patients with intrathoracic aneurysms (cases 1 and 2) (fig. 1*B*). Esophagrams in these two patients were negative except for extrinsic deviation.

Angiography

Angiographically the aortic mycotic aneurysms were saccular and arose eccentrically from one wall of the aorta (fig. 1*C*, 2, and 3*C*). The mycotic aneurysm in the patient with coarctation (case 3) occurred in the immediate poststenotic segment of the descending thoracic aorta (fig. 2). Thoracic aortography showed a mycotic aneurysm emanating from an aberrant subclavian artery in the final patient with intrathoracic aneurysm (case 6) (fig. 5*B*). Multiple mycotic aneurysms within the substance of the liver and spleen were seen in the patient with hemoperitoneum and blood loss (case 7) (figs. 4*A* and 4*B*).

Right renal arteriography in the hypertensive patient (case 8) revealed an aneurysm of the dorsal branch of the right renal artery (fig. 6*A*). Flow to the renal parenchyma was delayed within the distribution of the aneurysmal vessel and the arterial branch to the left upper pole was occluded with distal infarction. Renal vein renin sampling in this patient revealed lateralization to the right kidney (right renal vein, 15.9 ng/ml/hr; left renal vein, 5.6 ng/ml/hr). Right carotid arteriography revealed two small aneurysms in peripheral branches of the right middle cerebral artery in the patient with intracerebral mycotic aneurysm (case 9) (fig. 7).

Treatment and Prognosis

All patients were treated with appropriate antibiotics. Surgery was attempted in five of the six patients with intrathoracic aneurysms. In four of these cases the aneurysms ruptured during surgery due to extensive surrounding soft tissue infection and friability of the vessel walls. The aneurysm was successfully resected in the fifth patient (case 5). This aneurysm was sterile at the time of surgery. The patient with hepatic and splenic artery aneurysms refused surgery. Gelfoam embolization of the hepatic and splenic arteries (fig. 4*C*) temporarily stopped the bleeding; however, the patient subsequently rebled and died. Followup angiography 18 months after initial examination in the patient with the renal artery aneurysm (case 8) revealed that the aneurysm had spontaneously thrombosed (fig. 6*B*). The patient was normotensive at the time of the follow-up study and renal vein renin levels were normal.

Overall mortality in the series was 67% (six of nine patients). Mortality associated with aneurysms involving the aorta was 80% (four of five), while mortality associated with aneurysms of peripheral vessels was 50% (two of four). Mortality in aneurysms caused by *S. aureus* and *E. coli* was 100% (six of six), while there was no mortality associated with aneurysms caused by other organisms.

Discussion

Although the incidence of mycotic aneurysm has decreased since the advent of antibiotics [2], the occurrence of nine mycotic aneurysms in a 7-year period in one institution indicates that while uncommon, they are not rare. Mycotic aneurysm constituted 2.6% of 338 aneurysms over a 50-year period spanning both the pre- and postantibiotic eras [7]. Mycotic aneurysms have been described in virtually every artery; however, the aorta has been the most common site [3, 6, 7], as was found in five of the nine cases reported here.

The clinical presentation of mycotic aneurysms is related to the vessel involved. Chest or back pain occurred in five of the six cases with intrathoracic aneurysms. Venous engorgement secondary to superior vena cava compression was seen in cases 1 and 4. The patient with mycotic aneurysms of the hepatic and splenic arteries (case 7) had hemoperitoneum. Hepatic artery mycotic aneurysms may alternatively be associated with hematemasis, hematobilia, and jaundice [9–11]. Splenic artery mycotic aneurysms may present as splenic abscesses [12]. Our patient with renal artery mycotic aneurysm (case 8) had hypertension. Previously, renal mycotic aneurysms have been associated with hematuria [13, 14]. Although isolated renal artery aneurysms have been related to hypertension [15, 16], we believe this is the first recorded case of a mycotic renal artery aneurysm presenting in this manner. Renin levels from the kidney involved with the aneurysm were significantly elevated, indicating that this kidney was the source of hypertension. Renin determination was especially important in this case, as abnormalities were also present in the opposite kidney. The patient with intracerebral mycotic aneurysm (case 9) had headache without focal neurologic signs or hemorrhage, although these latter findings have been encountered with intracerebral mycotic aneurysms [17].

Sepsis, evidenced by fever and leukocytosis, was present with mycotic aneurysms regardless of location. Seven patients were septic at presentation with the aneurysm. In the two exceptions (cases 5 and 8), mycotic aneurysms appeared several months after successful antibiotic therapy for bacterial endocarditis.

Clinical clues to the presence of mycotic aneurysm exist in the concomitant occurrence of several conditions associated specifically with the development of

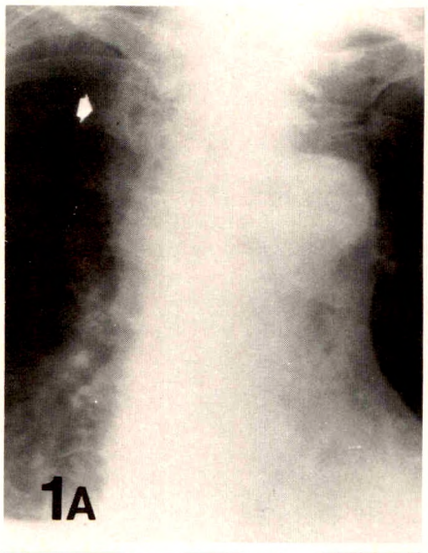

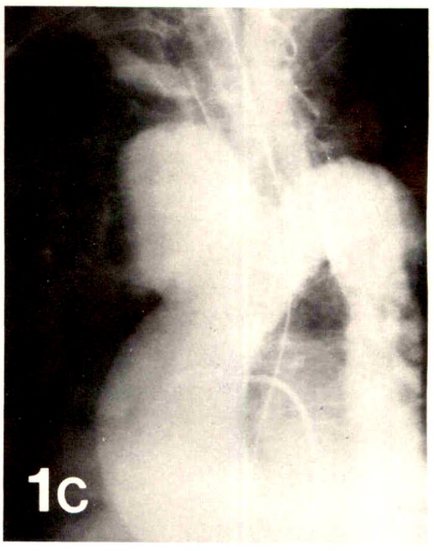

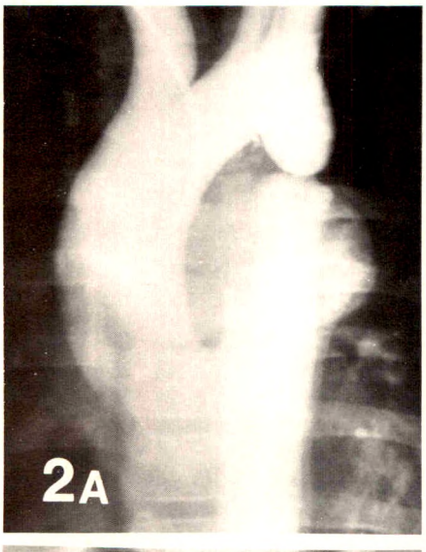

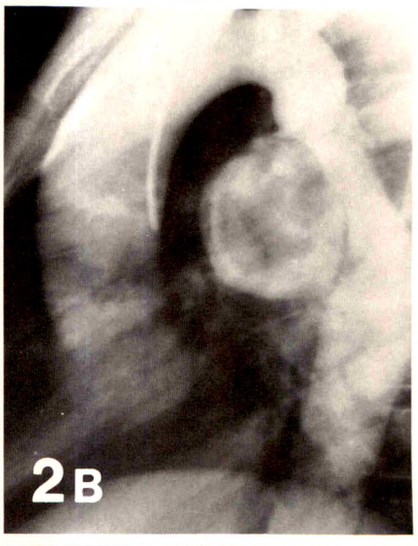

Fig. 1.—Case 1. *A*, Posteroanterior chest radiograph demonstrating widened mediastinum with scattered radiolucencies of gas density (*arrow*) and calcification of aortic arch. *B*, Tomogram confirming mediastinal gas. *C*, Levo phase of pulmonary arteriogram showing saccular mycotic aneurysm originating from ascending aorta.

Fig. 2.—Case 3. Anteroposterior (*A*) and lateral (*B*) projections of thoracic aortogram showing saccular mycotic aneurysm originating distal to aortic coarctation.

Fig. 3.—Case 5. Posteroanterior (*A*) and lateral (*B*) chest radiographs showing 3 cm mass in anterior mediastinum adjacent to ascending aorta. *C*, Thoracic aortogram demonstrating saccular aneurysm arising from ascending aorta with aortic regurgitation.

Fig. 4.—Case 7. *A*, Arteriogram of right branch hepatic artery demonstrating several aneurysms (*arrows*) within right lobe of liver. *B*, Splenic arteriogram showing intrasplenic

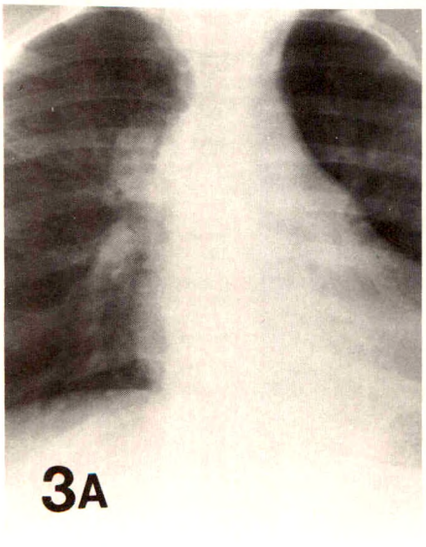

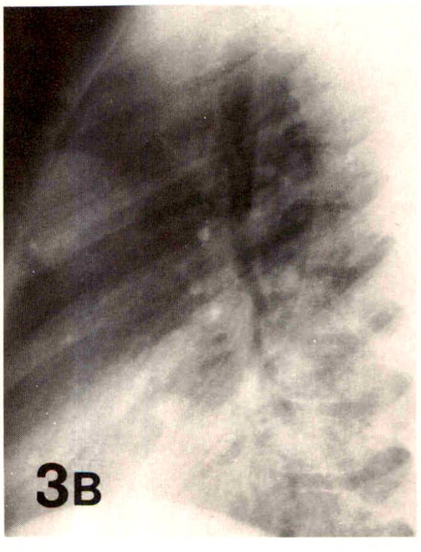

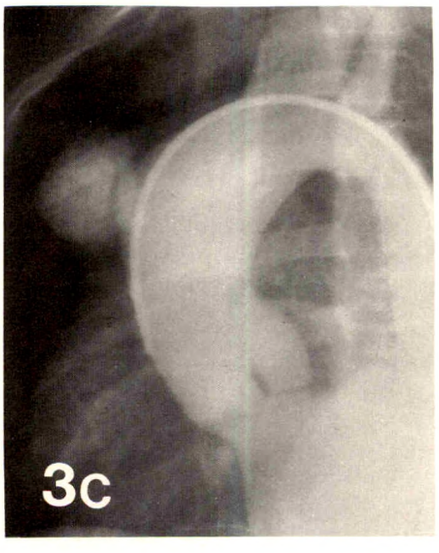

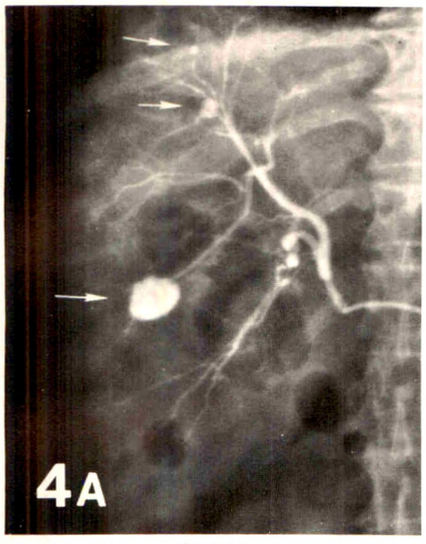

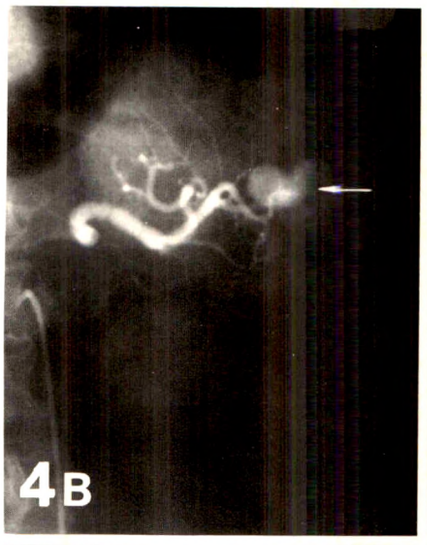

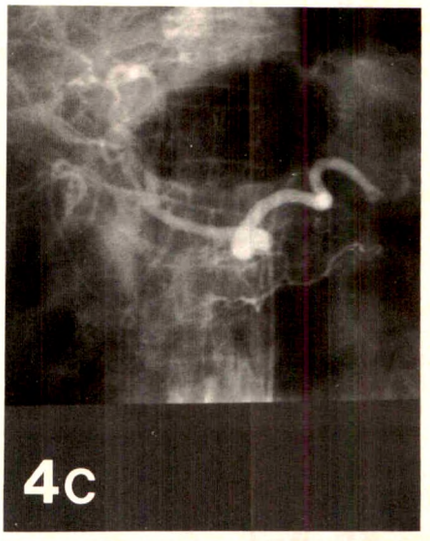

aneurysm (*arrow*). *C*, Celiac arteriogram after Gelfoam embolization demonstrating occlusion of splenic and right hepatic arteries.

Fig. 5.—Case 6. *A*, Posteroanterior chest radiograph showing superior mediastinal widening with shift of trachea to right; left pleural effusion is present. *B*, Subtracted right posterior oblique projection of thoracic aortogram showing aneurysm (*small arrows*) originating from anomalous right subclavian artery (*large arrow*).

Fig. 6.—Case 8. *A*, Right renal arteriogram showing aneurysm originating from dorsal branch of right renal artery and delayed flow to renal parenchyma within distribution of aneurysmal vessel (*arrows*). *B*, Followup arteriogram 18 months later showing that aneurysm has thrombosed; some loss of renal parenchyma in previously ischemic region.

Fig. 7.—Case 9. Anteroposterior view of right carotid arteriogram showing bilobed aneurysm (*large arrow*) originating from anterior sylvian branch of middle cerebral artery; a smaller aneurysm (*small arrow*) originates from posterior parietal branch. Note mass effect with shift of anterior cerebral artery across midline.

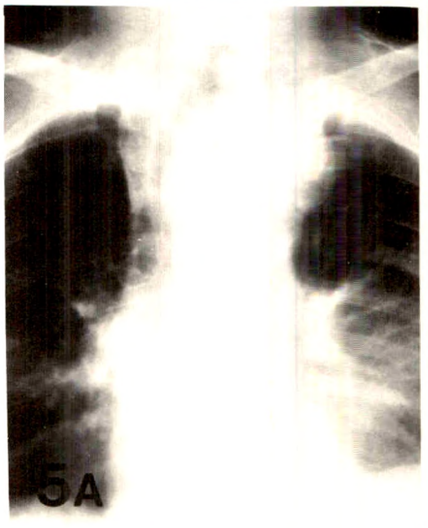

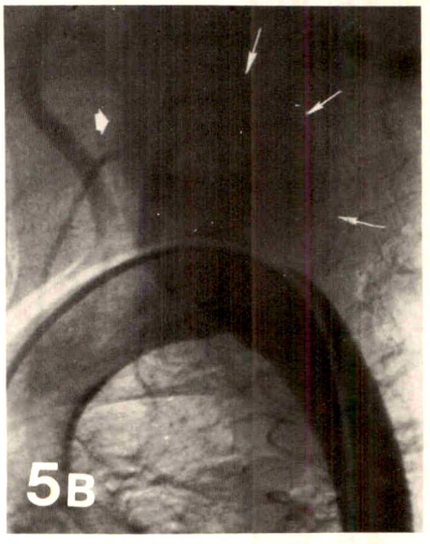

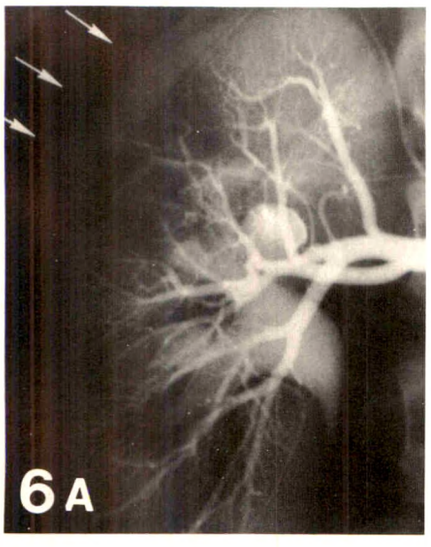

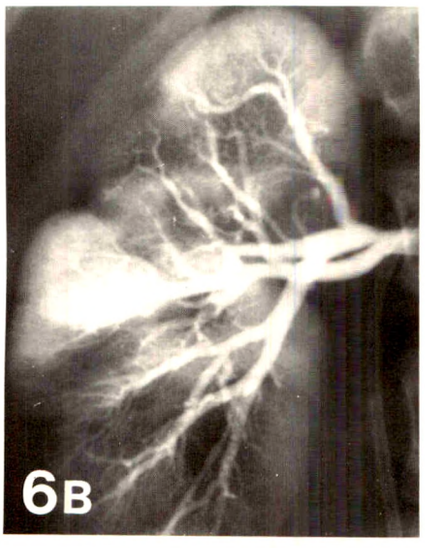

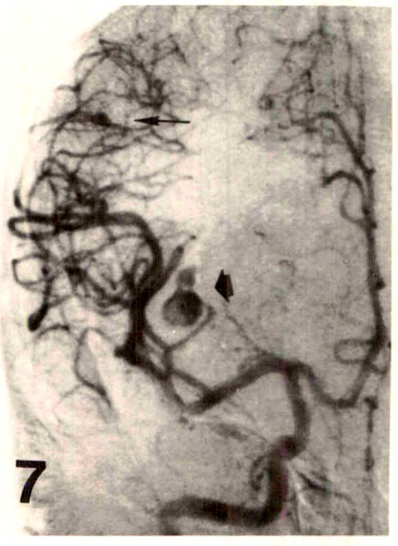

mycotic aneurysm or generally with increased susceptibility to infection. Four of the patients in our series had bacterial endocarditis. In three of these the endocarditis occurred on abnormal valves involved with congenital or rheumatic heart disease. The presence of congenital or acquired cardiac valvular disease and clinical symptoms and signs of bacterial endocarditis or a recent history of endocarditis should immediately suggest the possibility of secondary mycotic aneurysm formation when appropriate localizing findings are also present.

In cases 1 and 2 the mycotic aneurysms occurred on areas of severe atherosclerosis. These cases represent the so-called primary mycotic aneurysms, in which bacteremia from an often occult, distant source of infection results in infection of diseased vessel wall with aneurysm formation [6, 18, 19]. Coarctation of the aorta has also been associated with mycotic aneurysm [20–22]. In contrast to most other types of aneurysms complicating coarctation, mycotic aneurysms most often occur just distal to the area of coarctation [21, 22]. Localized fibrous intimal thickening occurs in the immediate poststenotic area resulting from trauma caused by the jet of blood passing through the coarctation and striking the aortic wall; this intimal damage predisposes the poststenotic segment to infection [21, 22].

Three of our nine cases had diabetes mellitus. Diabetes generally predisposes patients to infection, and it is not surprising that mycotic aneurysm may complicate this condition. The patient with a subclavian artery aneurysm (case 6) secondary to poorly controlled soft tissue infection had been on steroids for many years, thereby increasing his general susceptibility of infection. One patient was an intravenous drug abuser (case 4). Infectious complications in heroin addicts resulting from nonsterile intravenous injection techniques are well known. Both systemic and pulmonary artery mycotic aneurysms have been described in these individuals [12, 20, 23].

S. aureus was the most commonly occurring pathogen in our series (four cases); *E. coli* was the pathogen in two cases. *S. epidermidis* and *S. viridans* were each isolated in one case, and all cultures were negative in one case. In two other cases multiple blood cultures were negative and the organism was isolated only upon cultures taken at surgery or postmortem examination. This may have been related to prior antibiotic administration in these patients. Failure to identify a specific pathogen is not uncommon and in one series cultures were negative in almost half of all cases [6].

Plain chest radiography was abnormal in all six intrathoracic mycotic aneurysms. The mycotic aneurysms involving intrathoracic vessels exhibited either a generally enlarged mediastinum or a localized mediastinal mass. Deviation of the trachea or the esophagus frequently occurred. Mottled radiolucencies of gas density were present within the enlarged mediastinum in the two diabetic patients with intrathoracic aneurysms. *E. coli* was the causative organism in both cases. Gas formation associated with mycotic aneurysms in diabetics has not been previously noted, although the entities of emphysematous cholecystitis and emphysematous pylonephritis are well known in diabetics. Esophagrams in these two patients were negative except for extrinsic deviation. An esophagram should be performed in the presence of gas in the mediastinum to exclude an esophageal perforation.

Angiography is necessary for the definitive diagnosis of mycotic aneurysms regardless of location and is recommended when the diagnosis is initially suspected. Angiographically the mycotic aneurysms originating from the aorta were saccular and, when viewed in the proper projection, emanated eccentrically from one wall of the vessel. However, this appearance is not entirely specific and may also be seen with aneurysms of other etiologies [8]. Therefore, the correct angiographic diagnosis of mycotic aneurysm is a function of the association of the rapid appearance or development of the aneurysm, signs of infection, and the presence of predisposing conditions. Aneurysms associated with coarctation of the aorta occurring in the immediate poststenotic segment should be suspected as being mycotic.

Intracranial mycotic aneurysms are somewhat more specific in that they tend to occur more peripherally than the more commonly occurring congenital aneurysms at the circle of Willis [17, 24]. The middle cerebral artery is the most frequent site for intracerebral mycotic aneurysms [17]. The differential diagnosis of peripheral intracerebral aneurysms includes metastatic choriocarcinoma and left atrial myxoma [24].

The patient with hepatic and splenic artery mycotic aneurysms and hemoperitoneum underwent transcatheter embolization with Gelfoam. This was temporarily successful in arresting bleeding; however, the patient rebled and expired. Transcatheter embolization may have a place in the therapy of quiescent mycotic aneurysms in suitable circulations; however, surgery with vigorous antibiotic coverage is the most appropriate therapy for acutely infected lesions [14, 25, 26].

The high mortality rate of mycotic aneurysms reported here (67%) indicates the lethality of this entity even with antibiotics and sophisticated methods of vascular surgery. The prognosis of mycotic aneurysms is related to their location and the virulence of the organism involved. Peripheral aneurysms have a better prognosis than those involving the aorta [8, 14] (80% mortality involving the aorta in our study, compared with 50% mortality involving peripheral vessels). The mortality for mycotic aneurysms caused by *S. aureus* and *E. coli* was 100%. The aneurysms caused by less virulent organisms in our remaining three patients responded to antibiotic therapy and these patients constituted the three survivors in the series. With a more virulent organism, the aneurysm and associated infection may progress rapidly with early rupture; with a less virulent organism, a febrile course of weeks to months may ensue before rupture [6, 25]. However, rupture can be expected to occur in up to 75% of cases [6, 14]. The prognosis, while generally poor, is much worse if the aneurysm has already ruptured [14],

emphasizing the need for early diagnosis. In addition to the possibility of rupture, the longer the delay in making the diagnosis the more widespread the surrounding soft tissue infection becomes, making successful therapy more difficult [8]. Even sterile, apparently quiescent aneurysms have been known to rupture [6] and therapy is recommended. Case 8 is unique in that spontaneous complete thrombosis of the renal artery aneurysm was demonstrated on follow-up angiography. We consider rupture in this situation extremely unlikely, and since this patient's blood pressure also has reverted to normal no further therapy is contemplated.

REFERENCES

1. Osler W: The Gulstonian lectures on malignant endocarditis. *Br Med J* 1:467–470, 1885
2. Bennett DE, Cherry JK: Bacterial infection of aortic aneurysms: a clinicopathologic study. *Am J Surg* 113:321–326, 1967
3. Stengel A, Wolferth CC: Mycotic (bacterial) aneurysms of intravascular origin. *Arch Intern Med* 31:527–554, 1923
4. Wood BP, Young LW, Elbadawi NA: Primary mycotic aneurysm in infancy and childhood. *Am J Roentgenol* 118:109–115, 1973
5. Cliff MM, Soulen RL, Finestone AJ: Mycotic aneurysm—A challenge and a clue. *Arch Intern Med* 126:977–982, 1970
6. Bennett DE: Primary mycotic aneurysms of the aorta. *Arch Surg* 94:758–765, 1967
7. Parkhurst GF, Decker JP: Bacterial aortitis and mycotic aneurysm of the aorta. A report of twelve cases. *Am J Pathol* 31:831–835, 1955
8. Weintraub RA, Abrams HL: Mycotic aneurysms. *Am J Roentgenol* 102:354–362, 1968
9. Gupta S, Cope V: Hepatic artery aneurysm as a cause of gastrointestinal bleeding. *Br J Radiol* 45:726–728, 1972
10. Stack BHR, Runkin JT, Bentley RJ: Hepatic artery aneurysm after staphlococcal endocarditis. *Br Med J* 2:659–660, 1968
11. Sukerhar AN, Dulay CC, Anandappa E, Asokan S: Mycotic aneurysm of the hepatic artery. *Radiology* 124:444, 1977
12. Jacobs RP, Shanser JD, Lawson DL, Palubinskas AJ: Angiography of splenic abscesses. *Am J Roentgenol* 122:419–42[illegible], 1974
13. Clark RE, Jacobson AC, Petty WE: Intrarenal mycotic (false) aneurysm secondary to staphlococcal septicemia. *Radiology* 115:421–422, 1975
14. Mundth ED, Darling RC, Alvarado RH, Buckley MJ, Linton RR, Austen WG: Surgical management of mycotic aneurysm and the complications of infection in vascular reconstructive surgery. *Am J Surg* 117:460–470, 1969
15. Barry WF Jr, Seuk KK: Renal artery aneurysms. *Am J Roentgenol* 98:132–136, 1966
16. Vaughan TJ, Barry WF Jr, Jeffords DL, Johnsrude IS: Renal artery aneurysms and hypertension. *Radiology* 99:287–293, 1971
17. Zimmet I, Johnson BL Jr: Angiography in the management of intracerebral mycotic aneurysms. *Arch Intern Med* 122:349–352, 1968
18. Crane AR: Primary multilocular mycotic aneurysm of the aorta. *Arch Pathol Lab Med* 24:634–641, 1937
19. Rewell STR: Primary mycotic aneurysms. *Ann Intern Med* 22:431–440, 1945
20. Jaffe RB, Condon VR: Mycotic aneurysms of the pulmonary artery and aorta. *Radiology* 116:291–298, 1975
21. Khazei AH, Cowley RA: Mycotic aneurysm associated with coarctation of the aorta. *Am Surg* 33:325–329, 1967
22. Edwards JE: Aneurysms of the thoracic aorta complicating coarctation. *Circulation* 48:195–201, 1973
23. Jaffe RB, Koschmann EB: Intravenous drug abuse: pulmonary cardiac and vascular complications. *Am J Roentgenol* 109:107–119, 1970
24. Olmstead WW, McGee TP: The pathogenesis of peripheral aneurysms of the central nervous system. A subject review from the AFIP. *Radiology* 123:661–666, 1977
25. O'Connor TW, Lord RSA, Tracy CG: Treatment of mycotic aneurysms. *Med J Aust* 2:1161–1164, 1972
26. Nasseth DC, Deterling RA Jr: Surgical management of mycotic aneurysms. *Surgery* 50:347–353, 1961

Transcatheter Occlusion of the Arterial Supply to Arteriovenous Fistulas with Gianturco Coils

THOMAS A. LAYNE,[1, 2] ETHEL J. FINCK,[1] AND WILLIAM D. BOSWELL[1]

Transcatheter occlusive therapy is finding widespread clinical application. Numerous types of occlusive devices have been described. This report details the first three cases of occlusion of the arterial supply to arteriovenous fistulas with Gianturco stainless steel coils. Patients benefiting from this approach include those who refuse or cannot tolerate surgery, those in whom previous surgery failed, and those with chronic fistulas in whom surgery is likely to fail. The angiographer should make sure the coil is completely within the desired vessel, the feeding vessel is smaller than the coil to prevent passage through the fistula, and there is adequate collateral flow to distal organs to prevent infarction after occlusion of a major artery. This technique is useful as a nonsurgical treatment for a variety of arteriovenous fistulas and is within the capability of any experienced angiographer.

Preoperative transcatheter occlusion of the arterial supply of various abdominal tumors using Gianturco stainless steel coils with wool strands is becoming more common [1]. Use of these coils in experimentally created arteriovenous fistulas in dogs and in two cases of human renal arteriovenous fistulas was recently described [2, 3]. In the humans, the coils were placed in the fistulas from the venous side. This report describes our experience using these coils to occlude the feeding artery to arteriovenous fistulas.

Case Reports

Case 1

R. C., a 16-year-old male, was shot in the right groin with a single shotgun blast. He presented in hemorrhagic shock and underwent immediate repair of severe arterial and venous injury. The right superficial femoral artery was resected and replaced with a graft from the left saphenous vein. Numerous smaller injuries to the profunda femoris were repaired. Venous bleeders were tied off. The patient recovered and was discharged without symptoms.

However, at a clinic visit 3 weeks after surgery, a loud machinerylike bruit was heard over the right thigh. Percutaneous angiography revealed multiple arteriovenous fistulas involving the profunda femoris artery and vein. Retrograde flow was noted in many veins, as well as a large pseudoaneurysm of the profunda femoris artery (fig. 1*A*).

Since no single fistulous communication was found at surgery, the angiographers embolized the profunda femoris artery. Two Gianturco coils were placed in the artery at the level of the pseudoaneurysm. Angiography performed immediately after embolization showed occlusion of the artery and nonfilling of the pseudoaneurysm and arteriovenous fistulas. The patient had mild fever to 38.4°C for 24 hr after embolization. He did not complain of pain nor exhibit other symptoms. Repeat angiography 2 months later again showed no arteriovenous communication (fig. 1*B*). After 10 months the patient is asymptomatic, with a negative physical examination.

Case 2

J. S., a 63-year-old man, was beaten and had a broomstick inserted into his rectum during a robbery. He presented in shock with massive rectal bleeding. At surgery, a 16 cm laceration of the rectum was found. No definite injury of a major vessel was identified. The patient bled several times after removal of the rectal packing. Angiography revealed an arteriovenous fistula from the left hypogastric artery to the corresponding vein, with a large pseudoaneurysm of the hypogastric artery (fig. 2*A*). The right femoral artery was catheterized, and the catheter was manipulated around the aortic bifurcation into the left hypogastric artery. Two coils were placed in the hypogastric artery. Angiography immediately after embolization demonstrated complete occlusion of the fistula and pseudoaneurysm (fig. 2*B*). The patient developed a slight fever (37.9°C), which returned to normal 48 hr after embolization. He was discharged 3 weeks after embolization, and had no further complaints during the 9-month follow-up.

Case 3

P. S., a 55-year-old female, had hematuria and dysuria for 4 days. Medical history revealed a mastectomy for unknown cause in 1971 in Mexico. In addition, the patient had been taking digoxin and Lasix for valvular heart disease for 4 years. Physical examination revealed a widened pulse pressure, bounding distal pulses, systolic and diastolic murmurs compatible with mitral stenosis and mitral regurgitation, bilateral basilar rales, and a palpable left lower quadrant abdominal mass with a bruit and thrill.

Chest radiography showed marked cardiomegaly and increased pulmonary vascularity with cephalic redistribution. Excretory urography revealed delayed and markedly decreased left renal function. Provisional diagnosis was valvular heart disease, with high output failure secondary to probable renal arteriovenous fistula. At angiography, a large renal arteriovenous fistula with a huge draining vein was found (fig. 3*A*). The patient refused surgery. While recognizing potential complications of renal embolization, in this instance nonsurgical occlusion of the main feeding artery was considered the best treatment of the fistula. It was hoped that leaving the smaller feeding artery patent would supply blood to the small amount of residual functioning renal tissue.

Prior to embolization, the cardiac output measured 10.2 l/min by the cardiogreen method. Two Gianturco coils were inserted into the left main renal artery and the patient showed immediate clinical improvement. Cardiac output dropped to 5.2 l/min, pulse from 104 to 65 beats/min, and blood pressure from 160/90 to 110/58. Aortography at placement of the coils showed

Received January 4, 1978; accepted after revision August 22, 1978.

[1] Department of Radiology, Los Angeles County-University of Southern California Medical Center, 1200 North State Street, Los Angeles, California 90033. Address reprint requests to E. J. Finck.

[2] Present address: 7 Greenbrier Drive, Missoula, Montana 59801.

© 1978 American Roentgen Ray Society

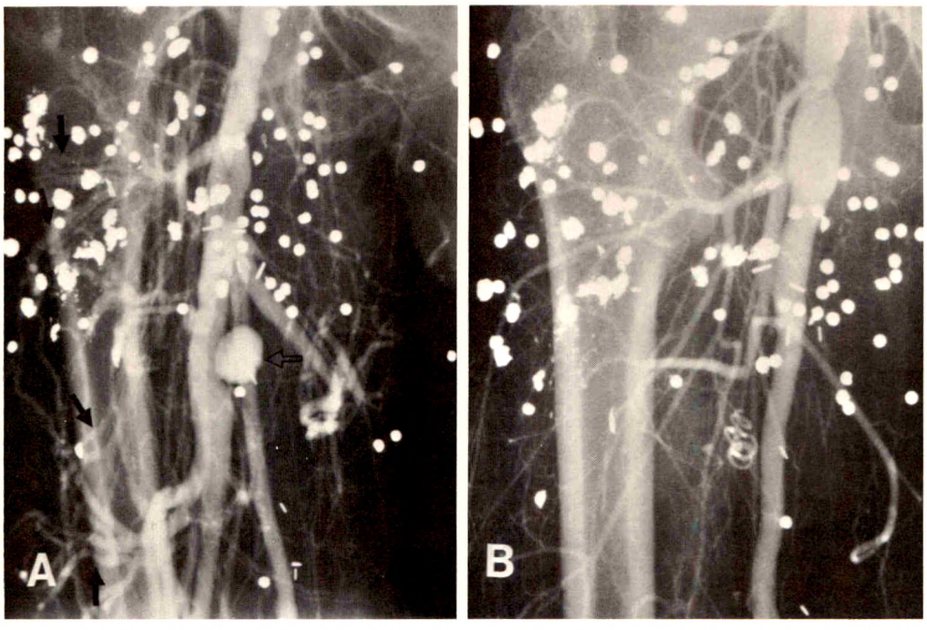

Fig. 1.—Case 1, femoral arteriograms. *A*, Early arterial phase demonstrating large pseudoaneurysm (*open arrow*) of profunda femoris artery. Note opacification of numerous veins indicating arteriovenous shunting (*closed arrows*). *B*, Occlusion of profunda femoris 2 months after embolization. Pseudoaneurysm is occluded and there is no evidence of arteriovenous shunting.

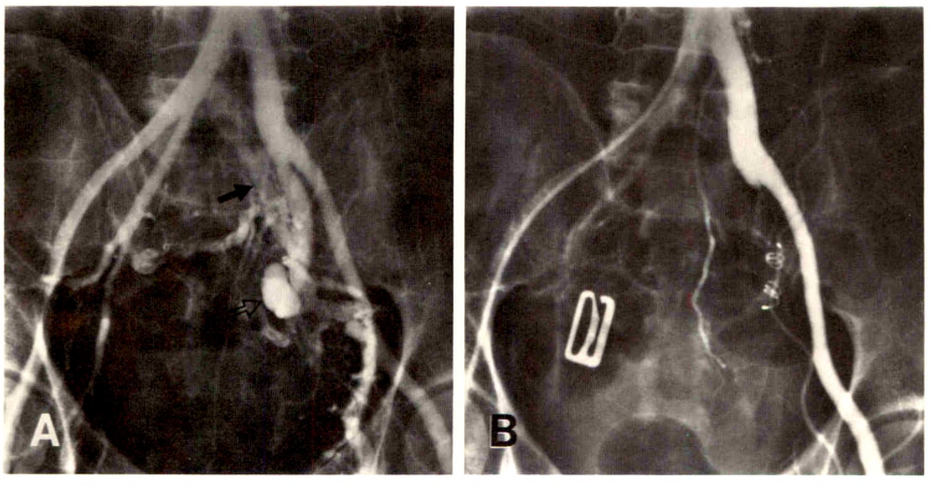

Fig. 2.—Case 2, midarterial phase arteriograms. *A*, Internal iliac vein drains early (*closed arrow*) and there is a large pseudoaneurysm (*open arrow*) of hypogastric artery. *B*, Two coils in hypogastric artery; arteriovenous fistula is closed. Clot has propagated proximally to artery origin.

complete occlusion of the main feeding artery without filling of the large draining vein (fig. 3*B*).

Immediately after embolization, the patient developed mild nausea and vomiting. She had chills and fever to 38.1°C. All symptoms had disappeared at 48 hr., and she was discharged after 5 days. Cardiac status showed continuing improvement. Murmurs were no longer present and echocardiography demonstrated a normal mitral valve. Murmurs heard on admission were believed to be caused by the high flow rate across the valve, rather than to organic disease. The hematuria and dysuria were resolved at discharge. Unfortunately, the patient returned to Mexico and has been lost to follow-up. Exact cause of the arteriovenous fistula has not been determined.

Discussion

Transcatheter vascular occlusive therapy for various clinical indications [4–8] using a wide variety of materials [5, 7–10] has been described. In 1976 Grace et al. [11] reviewed the various materials and techniques. More recently, Anderson et al. [2] described the placing of wire coils in surgically created arteriovenous fistulas in dogs. Wallace et al. [3] reported treating two arteriovenous fistulas by placing the coils in the fistulous segment via a venous approach. Stanley and Cubillo [7] reported closure of two cases of arteriovenous fistulae using Gelfoam. The present case reports are, to our knowledge, the first to describe use of the coils to occlude the arterial supply to arteriovenous fistulas.

The embolizations were carried out using the Gianturco–Wallace–Anderson arterial embolization set. Cases 2 and 3 were catheterized via a transfemoral approach. In case 1 the catheter was placed directly in the vessel exposed at surgery. The catheters were preformed in our lab, using steam to conform to the vascular anatomy, as demonstrated on preembolization angiograms. In case 2 some slight difficulty was experienced in catheter placement because the catheter was inserted in the left hypo-

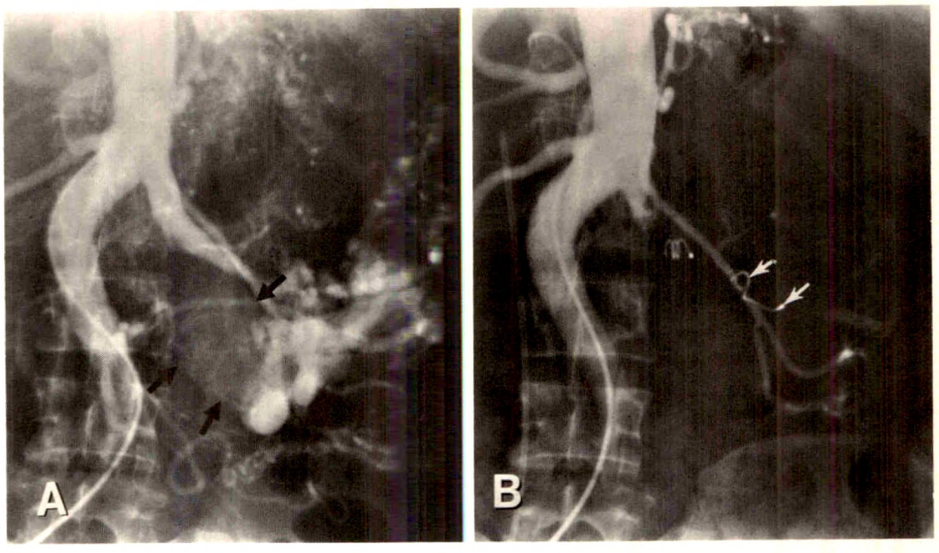

Fig. 3.—Case 3. *A*, Aortogram showing tangled mass of fistulous vessels in lower pole of left kidney. Note huge draining vein (*arrows*). *B*, Postembolization arteriogram demonstrating occlusion of artery and absence of large draining vein. Distal coil (*arrows*) was considerably larger than artery, preventing complete coiling.

gastric artery from the right side. Initially, a visceral catheter with a hooked curve was placed over the aortic bifurcation and a guide wire inserted around the bifurcation and down into the left hypogastric. Subsequently the visceral catheter was exchanged and the embolization catheter inserted. No difficulty was encountered in inserting any of the coils.

It should be emphasized that occlusion of the supplying artery must not compromise the blood supply to vital tissues. In cases 1 and 2 adequate collateral flow around the profunda femoris and hypogastric arteries, respectively, permitted sacrifice of these large arteries. In case 3 a smaller feeding branch was left patent to provide blood to the remaining renal tissue. If collateral flow is inadequate or marginal, the risk of infarcting a vital organ or even an entire extremity must be strongly considered.

Ideally, the size of the coil should be slightly larger than the artery to be occluded. If the coil is smaller than the artery supplying the fistula or than the fistula itself, embolization of the coil into the venous circulation and even to the heart and lungs could occur. The artery to be embolized should be carefully measured using arteriography before inserting the coil. If any doubt exists about the size of the artery, simultaneous catheterization of the draining vein with a wire snare could prevent loss of the coil into the main venous circulation.

In each of our three cases, clot propagated rapidly in a retrograde fashion along the occluded vessel to the closest major branch of the artery (or to the origin, if there were no major branches). Anderson et al. [2] reported that coils placed so that a portion protruded either into the arterial or the venous side from the fistula caused thrombosis of the artery or vein, in addition to the fistula. Care must be taken to make sure the coil has been placed beyond any major branches that should be saved, and the coil must be entirely within the desired artery to avoid forming a nidus of clot within the parent vessel. Clot could also form in the arteriovenous fistula itself and embolize into the pulmonary circulation. Stanley and Cubillo [7] reported this complication in one of two patients embolized with Gelfoam. This did not occur in our series.

Finally, it must be emphasized that since the coil is not actually within the fistula, the possibility exists that collateral flow will reopen the fistula at some future time. While this has not occurred in two of our patients at 9 and 10 months, patients should be followed for recurrence of symptoms. However, for patients who refuse surgery, for those who cannot tolerate surgery, and for those in whom surgery has failed, embolization of the feeding artery may be the only alternative, and on the basis of our experience may offer long-term relief.

We feel that occluding arteriovenous fistulas by obstructing the feeding artery is applicable in a variety of locations and types of fistulas. If an arteriovenous fistula has one single communication, placement of a coil within the fistula itself may be possible. However, in many instances the communications are multiple or the actual fistula may be inaccessible, preventing direct insertion of the coil into the fistula. By occluding the feeding artery, obliteration of the fistula can be accomplished and surgery may be avoided.

ACKNOWLEDGMENTS

We thank Ellen Duncan and Marie Adrianos for their assistance with this manuscript.

REFERENCES

1. Goldstein HM, Wallace S, Anderson JH, Bree RL, Gianturco C: Transcatheter occlusion of abdominal tumors. *Radiology* 120:539–545, 1976
2. Anderson JH, Wallace S, Gianturco C: Transcatheter intravascular coil occlusion of experimental arteriovenous fistulas. *Am J Roentgenol* 129:795–798, 1977
3. Wallace S, Gianturco C, Anderson JH, Goldstein HM, Davis JL, Bree RL: Therapeutic vascular occlusion utilizing steel coil technique: clinical applications. *Am J Roentgenol* 127:331–337, 1976

4. Doppman JL, DiChiro G, Ommaya AY: Percutaneous embolization of spinal cord arteriovenous malformations. *J Neurosurg* 34:48–55, 1971
5. Kerber C: Experimental arteriovenous fistula creation and percutaneous catheter obstruction with cyanoacrylate. *Invest Radiol* 10:10–17, 1975
6. Luessenhop AJ, Spence WT: Artificial embolization of cerebral arteries: report of a case of arteriovenous malformation. *JAMA* 172:1153–1155, 1960
7. Stanley RJ, Cubillo E: Nonsurgical treatment of arteriovenous malformations of the trunk and limb by transcatheter arterial embolization. *Radiology* 115:609–612, 1975
8. Robles C, Carrasco-Zanini J: Treatment of cerebral arteriovenous malformations by muscle embolization. *J Neurosurg* 29:603–608, 1968
9. Kricheff II, Madayag M, Braunstein P: Transfemoral catheter embolization of cerebral and posterior fossa arteriovenous malformations. *Radiology* 103:107–111, 1972
10. Gianturco C, Anderson JH, Wallace S: Mechanical devices for arterial occlusion. *Am J Roentgenol* 124:428–435, 1975
11. Grace DM, Pitt DF, Gold RE: Vascular embolization and occlusion by angiographic techniques as an aid or alternative to operation. *Surg Gynecol Obstet* 143:469–482, 1976

Mammographic Parenchymal Patterns as Risk Indicators for Incident Cancer in a Screening Program: An Extended Analysis

PETER M. KROOK[1]

In a screening program of self-referred women, different mammographic parenchymal patterns were related to significantly different rates for developing breast cancer. The risk of cancer detection subsequent to a negative mammographic examination was 7.6 times greater for women in the highest parenchymal risk class compared with the lowest, an increase in risk comparable to that of a personal history of breast cancer and greater than that reported for any other combination of historical risk factors. These differences are qualitatively similar to, but of a lesser magnitude than, those in previous reports which were based on symptomatic women with previous negative mammograms. Data suggest this difference in risk is inherent between parenchymal patterns, rather than indicating difficulty in identifying small cancers in dense breasts. Findings of differential parenchymal risk, coupled with other risk factors, may lead to concentrating mammographic screening on a smaller segment of the population, thus improving the benefit-to-cost ratio.

Mammography is widely accepted as beneficial for evaluating breast abnormalities and for screening women over 50 years old. Screening mammography is controversial in women younger than 50 because of theoretical concerns of carcinogenesis from even very low doses of ionizing radiation. Current efforts to reduce radiation dose and its presumed risk to each patient include use of improved film-screen combinations, negative mode xeromammography, single view mammography, and more penetrating x-ray beams.

Identifying women at significantly greater risk to harbor or subsequently develop breast cancer would improve the benefit-to-cost (financial plus possible carcinogenesis) ratio for the entire patient population by concentrating mammographic screening on those at high risk and reducing the use of mammography (with its possible radiation dangers) in those at low risk. Wolfe [1, 2] reported that the risk of developing breast cancer after a negative mammogram varies according to the breast parenchymal pattern, and a preliminary analysis of 36 such cancers by Krook et al. [3] found a qualitatively similar, but quantitatively lower, variation in risk. Wilkinson et al. [4] tended to support the thesis, demonstrating a correlation between breast parenchymal patterns and cancer risk by comparing 42 patients whose breast cancer was discovered on initial and subsequent screening with 84 matched controls. This view was challenged by Egan and Mosteller [5], whose analysis of mammograms from 1963 to 1972 suggests increased short-term risk is solely due to difficulty in identifying small cancers in dense breasts.

In an analysis of data from the Virginia Mason Medical Center Breast Cancer Detection Demonstration Project of 79 lesions detected subsequent to a negative mammogram in self-referred women, the rates of prevalent and incident cancer were determined for each age group and parenchymal pattern class. The rates of incident cancer in each parenchymal pattern class in the second and third screenings were compared with the rates in the fourth and fifth screenings. (Prevalent cancer is present in the population for an unknown length of time and detected at the initial screening or within 6 months. Incident cancer is detected more than 6 months after negative initial screening.) In addition, the relations between parenchymal pattern and personal or family history of breast cancer were examined.

Subjects and Methods

In September 1973, 10,053 self-referred women over 35 enrolled in a program of yearly clinical breast examination, thermography, and xeromammography, and were instructed in monthly breast self-examination. Suspicious findings on physical examination and/or mammography prompted immediate biopsy or reevaluation within 6 months. As of February 1978, 93% of the 504 recommended biopsies were performed, revealing 155 lesions. Of the 33 patients in whom biopsy has not yet been accomplished, 14 are indeterminate and 19 are believed to be benign after continued observation. As of December 1977, 86% of the original enrollees still actively participated in the program. Of the remainder, 3.5% moved, 0.5% died, 3.0% withdrew due to radiation concern, 0.2% had double mastectomies, and the remaining 6.8% withdrew for a variety of other reasons.

Of the 79 incident lesions found, the 14 lesions (18%) detected only by physical examination were not interpreted as malignant by xeromammography. Twelve lesions (15%) were detected in the interval between examinations. Xeromammography alone detected 23 (29%) and helped clarify only minor physical abnormalities in at least ten others. In five of these cases, minor abnormalities found on initial screening that were not considered suspicious enough to warrant biopsy later developed into detectable carcinoma.

Since April 1976 xeromammograms have been classified according to the Wolfe system [1, 2]: N1 = parenchyma composed primarily of fat with at most small amounts of "dysplasia"; P1 = parenchyma chiefly composed of fat with prominent ducts involving up to one-fourth of breast volume; P2 = prominent ducts involving more than one-fourth of breast volume; and Dy = severe involvement with "dysplasia" often obscuring an underlying prominent duct pattern.

Two groups of 1,000 patients each were randomly selected from the entire patient population. The first group was chosen

Received May 12, 1978; accepted after revision August 16, 1978.
This work was supported by the National Cancer Institute, Grant No. 1-CN-55304, and the American Cancer Society.
[1] Department of Radiology, The Mason Clinic, P. O. Box 900, Seattle, Washington 98111. Address reprint requests to P. M. Krook.

© 1978 American Roentgen Ray Society

when the Wolfe system had been used 12 months; age and parenchymal pattern were recorded for each patient. A second group was chosen 14 months later; age, parenchymal pattern, and personal or family history of breast cancer were recorded. About 94% of the mammograms had been prospectively classified at screening without knowledge of the patient's age, physical findings, or historical data. The remaining 6% were classified when the groups were selected and before other patient information was revealed. To approximate the average percentage of the population in each age group and parenchymal pattern class in a population ever increasing in age, the average of the first and second samples was used to analyze the incident cancer data.

The second group was used to examine the relation between history and parenchymal pattern. The relative with breast cancer was available in 73% of the patient history forms, and this information was recorded as close relative (mother or sister) or close plus distant relative (including grandmother or aunt). Only the number of relatives with a previous history of breast cancer was available for the remaining 27% of the sample, and these were recorded only in the close plus distant column.

To eliminate bias caused by recognizing a lesion, radiologists classified all breasts harboring lesions from among a blind selection of mammograms that included films from the nondiseased breast and single breast mammograms with benign diagnoses.

Findings

Table 1 shows the distribution of the sample populations in each age and parenchymal pattern combination. As Wolfe noted, the Dy frequency is considerably reduced in the oldest age groups.

Table 2 presents the number of incident cancers and the rate per 1,000 screenees in each age and parenchymal pattern combination calculated for an average of 9,400 screenees during the study. The incident cancer rate in the Dy class increases markedly from 4/1,000 in the 35–39 age group to 40/1,000 in the 60+ age group, and for the entire population the rate increases steadily as the parenchymal pattern class progresses from N1 to Dy. This parenchymal pattern difference in cancer risk is significant ($P < 0.01$, χ^2 test with Yates correction) for the entire population and for the 50–59 and 60+ age groups.

Table 3 compares the number and rate of incident cancer for each parenchymal pattern group in the second and third screens with the fourth and fifth screens. All of the third screens, 80% of the fourth screens, and 27% of the fifth screens have been accomplished. Although the incident cancer rates are slightly higher on the fourth and fifth screens for P1 and P2 and are considerably higher for Dy, these differences are not significant in a series of this size ($P > 0.25$).

Table 4 provides (1) the fraction of the sample population with a close relative with breast cancer history in each age and parenchymal pattern combination (factored for the 73% rate of detailed history forms); (2) the fraction with a close or distant family history of breast cancer; and (3) the fraction with a personal history of breast cancer. Parenchymal patterns are not significantly different in either close or close plus distant family history of breast cancer, although there is a slight tendency for the higher risk classes to have a higher rate of close plus distant relatives with a history of breast cancer. Of the incident cancer patients, two N1, five P1, five P2, and three Dy patients had a close family history of breast cancer, and two N1, seven P1, nine P2, and nine Dy patients had a close plus distant family history of cancer (not a statistically significant difference). Personal history of breast cancer in the combined P2 and Dy class is significantly different ($P < 0.01$) from the combined N1 and P1 class; however, only one each of N1, P1, P2, and Dy patients with incident cancer had a prior history of breast cancer, indicating that the correlation in the entire population between parenchymal pattern and personal history of cancer is not directly responsible for the difference in incident cancer rates between the various parenchymal pattern classes.

TABLE 1

Parenchymal Classes by Age

	35–39	40–44	45–49	50–59	60+	All Ages
N1	1.1	2.9	3.5	8.2	4.9	20.6
P1	1.8	4.3	3.6	10.4	6.1	26.2
P2	2.3	5.2	5.4	11.6	8.1	32.6
Dy	5.0	5.2	4.7	4.1	1.6	20.6
Total	10.2	17.6	17.2	34.3	20.7	100.0

Note.—Data given in percentages.

TABLE 2

Incident Cancers by Age

	35–39	40–44	45–49	50–59	60+	All Ages
No. in entire population:						
N1	0	0	1	3	0	4
P1	0	3	0	7	7	17
P2	1	0	5	16	5	27
Dy	2	7	5	11	6	31
Total	3	10	11	37	18	79
Rate per 1,000 screenees:						
N1	0	0	3.0	3.9	0	2.1
P1	0	7.4	0	6.9	12.3	6.9
P2	4.4	0	9.9	14.7	6.6	8.9
Dy	4.3	14.4	11.3	28.8	40.0	16.0
Total	3.1	6.0	6.8	11.5	9.2	8.4

TABLE 3

Incident Cancer Rate Per 1,000 Screenees

	2nd and 3rd Screens*	4th and 5th Screens†
N1	0.7	0.5
P1	2.0	2.8
P2	2.7	3.2
Dy	4.0	7.8

* 19,330 total examinations.
† 9,480 total examinations.

TABLE 4

Population with History of Breast Cancer (fraction)

	35–39	40–44	45–49	50–59	60+	All Ages
Close family history:						
N1	0	0.19	0.10	0.14	0.18	0.15
P1	.26	.11	.21	.15	.15	.16
P2	.07	.08	.05	.15	.15	.12
Dy	.15	.21	.19	.19	.25	.19
Close or distant family history:						
N1	.33	.21	.25	.18	.21	.21
P1	.31	.22	.25	.31	.22	.26
P2	.20	.25	.13	.22	.33	.25
Dy	.42	.36	.30	.14	.24	.30
Personal history:						
N1	0	0	0	0	.043	.010
P1	0	0	0	0	.015	.004
P2	0	0	.018	.025	.094	.036
Dy	0	0	.047	.048	.059	.026

Discussion

Reports by Krook et al. [3], Mendel et al. [6], and Wolfe [7] identify a small but consistently higher rate of prevalent cancer in the P2 plus Dy class, indicating a real difference in the propensity of the different parenchymal classes to harbor a prevalent cancer. Wolfe [1, 2] first determined the rate of cancer detection subsequent to negative mammograms in the different parenchymal patterns. His patients were referred for examination, and follow-up by tumor registry, hospital records, or patient questionnaires was obtained. In his two combined series, Wolfe found a relative risk of 31 for incident cancers in the Dy class compared with the N1 class, and a relative risk of 6 for the P2 plus Dy class compared with the N1 plus P1 class.

Egan and Mosteller [5] challenged the long term significance of this finding. Their series of 327 prevalent and 54 incident breast lesions showed a decreased risk of prevalent cancer in their class 3 and 4 breasts (similar to Wolfe's P2 and Dy classes). This was followed by a markedly elevated risk (26) of class 4 (Dy) compared with class 1 (N1) for a 3-year period. However, incidence rates for the 14 lesions detected 38–88 months after the initial negative mammogram were nearly the same in all classes. They concluded that breast parenchymal pattern correlated only with the possibility of failing to detect a lesion. Three items are noteworthy: (1) the patient population analyzed produced 381 lesions in only 6,540 patients, indicating a patient population vastly different from ours; (2) over half the incident lesions (28 of 54) were detected before 1965, when mammography may have been less sensitive on initial examination than today; and (3) Egan and Mosteller's is the only major series in which markedly fewer cancers were detected in the P2 and Dy patterns on initial examination (which may be related to the first two items). Their finding that there is no difference in relative risk for the different parenchymal patterns in the 14 lesions occurring more than 36 months after negative mammogram is at distinct variance with our series of 17 lesions occurring more than 36 months after a negative examination, of which 10 were Dy, 5 were P2, and 2 were P1.

Wilkinson et al. [4], in a series of combined prevalent and incident cancer, demonstrated a relative risk of 5.8 for the Dy class compared with N1. This somewhat lower relative risk is probably explained by having combined prevalent lesions, which have a small relative risk difference, with incident lesions, which have a greater difference in relative risk. However, the report did not provide enough information to separate these factors.

In our study, a relative risk of 7.6 exists for incident cancer in the Dy class over the N1 class. The four parenchymal pattern classes are significantly different ($P < 0.01$ for entire population), indicating the necessity for intensive rescreening of the Dy class. The P2 class has a slightly greater risk than the P1 class, but these two classes occupy an intermediate position between N1 and Dy. This difference between classes remains qualitatively constant after age 40 with a relative Dy-to-N1 risk of 7.8 in the 40–49 age group and 13.0 for the 50+ age group.

The rate of incident cancer in the Dy class is markedly increased compared with the N1 class, which agrees with Wolfe's results, although quantitatively of lesser degree. The certainty of the relative risk calculation in this study is limited by its size (only four lesions in the N1 class) and the 4 year maximum follow-up. If Wolfe's hypothesis that there is a considerable difference in the relative propensities of the various parenchymal classes to develop incident cancers is correct, then one would expect an increasingly greater concentration of the incident cancers in the P2 and Dy classes as the period of follow-up lengthens, and the calculated relative risk of Dy versus N1 would increase with time. If the hypothesis is incorrect, and the increased early risk of incident cancer in the P2 and Dy classes represents only the difficulty in identifying prevalent cancer in dense breasts, the calculated relative risk would decrease with time.

The increased risk of prevalent or prevalent plus incident cancer in the P2 and Dy classes in four of five reports, the increased risk of incident cancer for the first 3 years of screening in all reports, the finding that P2 plus Dy women have had significantly more breast lesions prior to enrollment, and the known difficulty in identifying small lesions in dense breasts suggest that both factors contribute to the increased risk. The numbers and length of follow-up in this series are insufficient to fully elucidate the relative effects of these factors, but the constant or increasing risk through the fifth screening indicates that the risk associated with denser parenchymal patterns is comparable to or slightly greater than that of small lesion identification. Longer periods of follow-up and combined series are needed to calculate the inherent relative risk of developing incident cancer in each parenchymal pattern class versus the risk of not detecting prevalent cancer in a dense breast.

The abilities of the classifier and the patient population characteristics also affect the relative risk. Wolfe placed 7% of 5,284 patients and 17.1% of 1,930 patients in the Dy class. Our series places 20.6% of the combined sample populations in the Dy class. Assuming that a "true" Dy has the greatest risk of incident cancer, classifiers who place more and presumably lower risk patients into the Dy class reduce the calculated relative risk. Also, our patient population was self-referred, rather than referred by physicians. This difference may affect subsequent detection of incident cancers: the symptomatic patients referred for mammography in Wolfe's first series are different from the patients in our study because his patients developed 56 incident lesions in 5,284 patients (10.6 lesions per 1,000 screenees) to only 79 incident lesions in 9,400 patients (8.4 lesions per 1,000 screenees) in this series, which has been followed for a slightly greater average length of time. In addition, women in different series may well have significant differences in other risk factors such as personal or strong family histories of breast cancer. The number of women having previous cancer is not sufficient to explain the difference in incident cancer rates in our series, but marked differences between patient populations might well have a greater effect. Nevertheless, for the first 4 years of screening, it is possible to demonstrate a large and significant increase in risk for women in the Dy class compared with those in the N1 class, and an appreciable increase in risk for the P2 plus Dy class compared with the N1 plus P1 class.

Screening mammography in women less than 50 years old is controversial because (1) the risk of carcinogenesis of the low radiation doses currently used for mammography is estimated but uncertain; (2) the risk of carcinogenesis for patients with different physical or historical risk factors is unknown; and (3) a controlled study of mammographic screening in this age group has not been performed since the advent of improved technology such as xeromammography, leaving only estimates of the benefits that may accrue to women in a screening program. These factors contribute to conflicting estimates of the benefits and costs in lives. Bailar [8] and Bross and Blumenson [9] estimated that the risk of carcinogenesis is comparable or somewhat greater than the potential number of lives saved in the under 50 age group. In contrast, reports by Gregg [10] and Letton et al. [11] suggest a net benefit to women under age 50, and Seidman [12] estimated that the benefits of an initial screening are 10–100 times the costs in the 40–49 age group with second screen benefits of about 5–46 times the cost.

Until a carefully controlled trial of screening mammography with a 20–30 year follow-up quantifies the long-term benefits and costs for the various age and risk factor groups, screening programs for women under 50 might best be reserved for women at greatest risk for developing breast cancer. This position has been adopted by the Breast Cancer Detection Demonstration Projects, and screening mammograms in the under 50 age group are routinely performed only on women with personal history of breast cancer (risk about 6 times the no risk group) and women with a close family history of breast cancer (risk about 2). Factors excluded in determining screening groups are breast surgery, lumps, thickenings, discharge (risk about 2–3), menarche prior to age 12, or failure to bear a live child by age 30 (risk about 1.25). A strategy of screening all women at age 40, rescreening all women with a Dy pattern, and rescreening those with a P2 pattern in the 45–49 age group would concentrate the screening program on those women with a relative risk greater than 5 times that of the remaining women in the 40–49 age group.

Further study is needed to define optimum screening intervals in the various age-pattern combinations. The N1 class generates so few incident cancers that, unless there are strong historic indications, rescreening may be worthwhile only at lengthy intervals. After age 50, the P1 class develops an appreciable number of cancers, and by age 60 is comparable to the P2 class, so that fairly frequent screening would seem prudent. The Dy class after age 40 and the P2 class after age 45 have a markedly increased rate of incident cancer calling for frequent (perhaps annual) routine screening. Our study shows fairly constant values for the risks of incident cancer in each parenchymal pattern class over the 4 years of study. Longer follow-up is needed to identify any change in relative risk or other indications for a corresponding alteration in screening intervals.

Conclusions

Our study demonstrated that breast parenchymal pattern classes in self-referred women have significantly different risk values for developing incident cancers; the relative risk for the greatest risk group compared with the least is comparable to the risk observed in women with a personal history of breast cancer and is greater than that noted for other historic risk factors. Further evidence that this is an inherent property of the parenchymal pattern and not just failure to identify prevalent

cancer includes (1) the finding in three of four studies of slightly increased rates of prevalent cancer in the higher parenchymal risk groups; (2) the markedly increased rate of combined prevalent plus incident cancer in the Dy class in one study; (3) the finding that women in the higher risk pattern classes are significantly more likely to have had a previous breast cancer (although this finding fails to explain the marked increase in incident cancer risk); and (4) the absence of a decrease in relative risk of Dy versus N1 over the length of our study.

The various parenchymal patterns reach a high risk at different ages: the incidence of cancer is extreme in the Dy class after age 40; the P2 class is associated with a high rate of incident cancer after age 45; and the P1 class developed a significant number of cancers after age 50. In contrast to the N1 class, which produces very few incident cancers, the P1 and P2 patterns are associated with an intermediate rate of cancer development, and the Dy pattern develops 7.6 times as many incident cancers as the N1 pattern in the entire population. Until a controlled study is performed quantifying the benefits and costs of mammographic screening and defining appropriate screening intervals, our findings support a strategy of screening all women over age 40, intensively and regularly rescreening all women in the Dy class, and frequently rescreening women in the P2 class after age 45 and in the P1 class after age 50. The remainder of the population would best be served by infrequent mammographic examinations unless there are strong historic indications or physical abnormalities.

ACKNOWLEDGMENT

We thank Evelyn Hadaway for help in assembling the data.

REFERENCES

1. Wolfe JN: Breast patterns as an index of risk for developing breast cancer. *Am J Roentgenol* 126:1130–1139, 1976
2. Wolfe JN: Risk for breast cancer development determined by mammographic parenchymal pattern. *Cancer* 37:2486–2492, 1976
3. Krook F, Carlile T, Bush W, Hall M: Mammographic parenchymal patterns as a risk indicator for prevalent and incident cancer. *Cancer* 41:1093–1097, 1978
4. Wilkinson E, Clopton C, Gordonson J, Green R, Hill A, Pike M: Mammographic parenchymal pattern and the risk of breast cancer. *J Natl Cancer Inst* 59:1397–1400, 1977
5. Egan R, Mosteller R: Breast cancer mammography patterns. *Cancer* 40:2087–2090, 1977
6. Mendel L, Rosenbloom M, Naimark A: Are breast patterns a risk index for breast cancer? A reappraisal. *Am J Roentgenol* 128:547, 1977
7. Wolfe JN: Breast patterns. *Am J Roentgenol* 128:703, 1977
8. Bailar JC: Mammography—a contrary view. *Ann Intern Med* 84:77–84, 1976
9. Bross I, Blumenson L: Screening random asymptomatic women under 50 by annual mammographies: does it make sense? *J Surg Oncol* 8:437–445, 1976
10. Gregg E: Radiation risks with diagnostic X-ray. *Radiology* 123:447–454, 1977
11. Letton H, Wilson J, Mason E: The value of breast screening in women less than fifty years of age. *Cancer* 40:1–3, 1977
12. Seidman H: Screening for breast cancer in younger women: life expectancy gains and losses. *CA* 27:66–87, 1977

Radiology of the Jugular Tubercles

ANNE G. OSBORN,[1] W. ROBERT BRINTON, AND WAYNE H. SMITH

The jugular tubercles are two small protuberances that arise from the inferolateral margins of the clivus and project posterosuperiorly over the hypoglossal canals. The jugular tubercles are clearly seen on routine anteroposterior temporal bone tomograms and may be identified on axial or coronal CT scans. Varying widely in size and configuration, these structures are usually somewhat ovoid but can be elongated, gently squared, or asymmetric. Despite this variation in size and appearance, no normal instances were found in which the superior surface of the jugular tubercles appeared either flattened or concave. The radiology of the normal and pathologic jugular tubercle is described. The material outlined was derived from radiographic studies of both dried skulls and a variety of normal and abnormal clinical cases.

The jugular tubercles are two small bony protuberances arising from the inferolateral margins of the clivus. While the radiographic anatomy of their better-known neighbors, the jugular foramina, has been thoroughly studied [1–3], the jugular tubercles themselves have received scant attention in radiologic literature. Although earlier authors described the jugular tubercles as inconstant and often difficult to recognize [4], these structures are readily identifiable on high quality anteroposterior hypocycloidal temporal bone tomograms and axial or coronal CT scans of the skull base.

This paper describes the normal gross and radiographic anatomy of the jugular tubercles, their normal variations, and alterations in a variety of pathologic conditions. In several instances, subtle alterations in the contour of the tubercles were the sole abnormalities present on initial studies.

Subjects and Methods

Anteroposterior hypocycloidal 1 mm tomograms through the jugular tubercles were obtained in 30 dried adult skulls and 25 normal patients initially referred for evaluation of the internal auditory canals or cochlea. In all instances the contours of the tubercles and adjacent structures were mapped on tracing paper. In three dried skulls, a thick barium paste was inserted into the hypoglossal canals and the tomograms repeated.

Normal Gross and Radiographic Anatomy

The jugular foramen is a large golf club–shaped aperture in the skull base lying at the posterior end of the petrooccipital fissure. Just medial to the lower border of the jugular foramen is a rounded elevation, the jugular tubercle. Arising from the concave inferolateral margins of the clivus, the jugular tubercles project posterosuperiorly over the hypoglossal canals (fig. 1). On their posteriolateral aspects, the tubercles may present an oblique furrow or shallow groove created by the glossopharyngeal, vagus, and accessory nerves as they course toward the jugular foramina [5].

The jugular tubercles are often not clearly seen on standard plain films of the skull. Careful, high quality tomography is essential for accurate delineation of their size, shape, and position.

Thin-section anteroposterior hypocycloidal tomograms through the posterior part of the jugular tubercles show the medial meatus of the hypoglossal canal (filled with barium in fig. 2*A*). More anteriorly, the typical jugular tubercles resemble an eagle head or beak as they arc over the obliquely oriented hypoglossal canals (fig. 2*B*). The petrooccipital fissures and adjacent jugular foramina can easily be identified in these sections.

The jugular tubercles vary widely in size and shape. While some authors find the interjugular distance useful in identifying expansile posterior fossa mass lesions [4, 6], we doubt measurements of the intertubercular distance are dependable. The extreme variability in shape of jugular tubercles made exact measurements and statements regarding configuration of doubtful value. The tubercles most often appear somewhat ovoid but are also elongated, gently squared, or asymmetric with one tubercle either considerably smaller than the other or shaped quite differently (fig. 3*A*). Even when the tubercles are somewhat square, the normal superior surface is always slightly rounded.

The configuration of the jugular tubercles also varies depending on the portion of the tubercle contained in the plane of section. Posterior cuts may show ovoid tubercles that appear quite different when sectioned more anteriorly (fig. 3*B*). This variation in shape from one plane to another precludes precise statements regarding the frequency of any particular configuration. Nevertheless, we found no normal instances in which the superior surface of the jugular tubercles appeared either flattened or concave.

On axial CT scans, prominent jugular tubercles appear as obliquely oriented ovoid areas of bone-equivalent attenuation paralleling the petrous axis (fig. 4*A*). They are usually contained in sections obtained just below the internal auditory meati. If the tubercles are asymmetric or if the patient is incorrectly positioned, only one tubercle may be apparent (fig. 4*B*). The tubercles are also often identifiable on high quality coronal CT scans [7]. Since the jugular tubercles are surrounded by components of the basilar craniovertebral venous plexus [8,

Received May 2, 1978; accepted after revision August 21, 1978.
Presented at the annual meeting of the American Society of Neuroradiology, New Orleans, Louisiana, February 1978.
[1] All authors: Department of Radiology, University of Utah College of Medicine, 50 North Medical Drive, Salt Lake City, Utah 84132. Address reprint requests to A. G. Osborn.

© 1978 American Roentgen Ray Society

0361–803X/78/1200–1037 $00.00

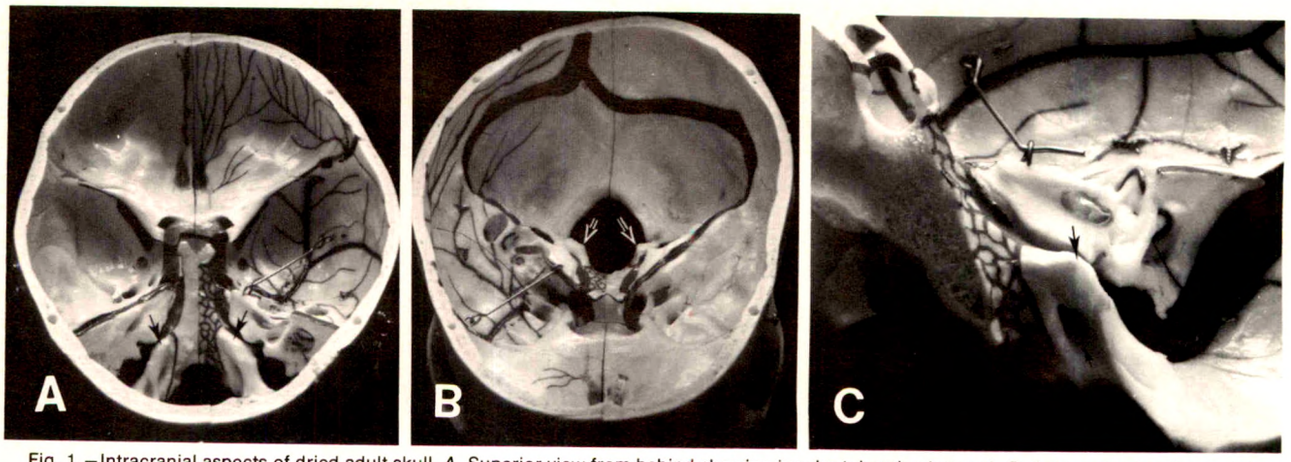

Fig. 1.—Intracranial aspects of dried adult skull. *A*, Superior view from behind showing jugular tubercles (*arrows*). *B*, Anterosuperior (Towne) view; jugular tubercles (*arrows*) are projected over foramen magnum. *C*, Medial view of jugular tubercle (*large arrow*) arching over hypoglossal canal (*small arrow*). Shallow groove on posterolateral aspect of tubercle is created by glossopharyngeal, vagus, and accessory nerves.

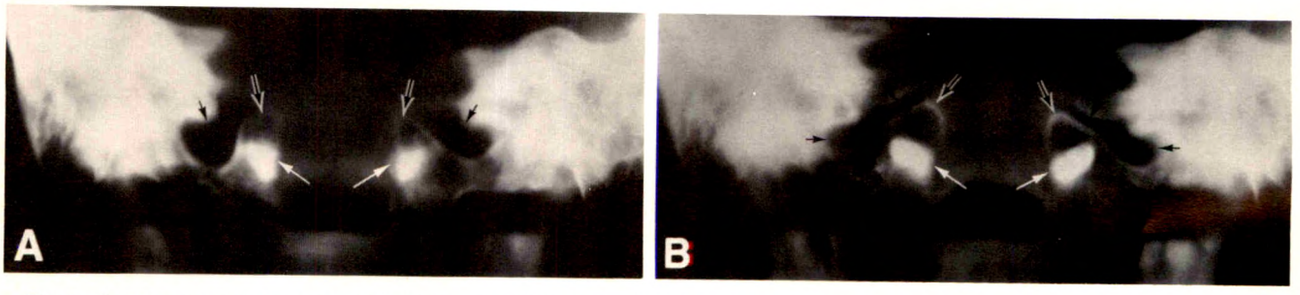

Fig. 2.—Anteroposterior 1 mm hypocycloidal tomograms through jugular tubercles in dried skull. *A*, Jugular tubercles (*outlined arrows*) arc over obliquely oriented, barium-filled hypoglossal canals (*white arrows*). Note jugular foramina (*black arrows*). *B*, 4 mm anterior to *A*. Jugular tubercles (*outlined arrows*) resemble eagle head with beak curving over hypoglossal canals (*white arrows*). Note jugular foramina (*black arrows*) and petrooccipital fissure (*black arrowheads*).

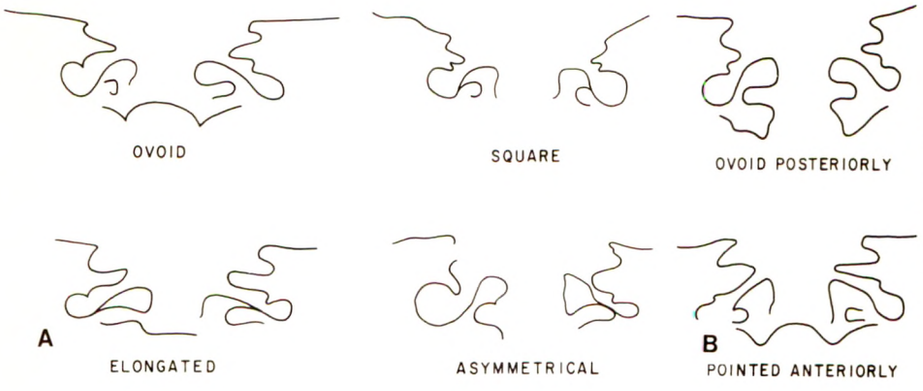

Fig. 3.—Tracings from anteroposterior temporal bone tomograms of different anatomical specimens. *A*, Jugular tubercles appear highly variable, even from side to side, though superior surface is always gently rounded. *B*, More posterior sections showing ovoid jugular tubercles. On cuts 4 mm more anterior tubercles appear elongated and pointed.

9], they may show some increase in apparent size with intravenous contrast enhancement (fig. 5). This appearance should not be mistaken for a cerebellopontine angle mass lesion, such as an acoustic neurinoma.

Other than considerable variation in size and configuration, anomalies of the jugular tubercles are unusual. In the presence of a persistent hypoglossal artery, an enlarged hypoglossal canal is present in the base of the tubercle [10, 11].

Pathological Anatomy

The jugular tubercles may be destroyed by a variety of malignant or locally invasive processes. We have seen eight such cases (three cerebellopontine angle subarachnoid cysts, two glomus tumors, two metastatic lesions, and one chordoma). Three cases are presented here to demonstrate typical pathologic alterations of the jugular tubercles. Tumors such as metastatic carcinoma

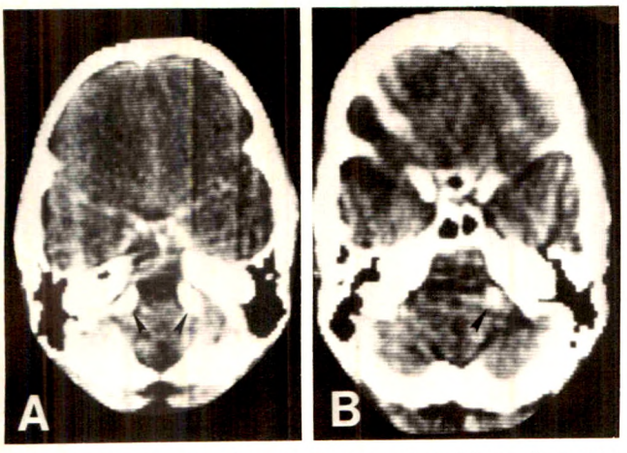

Fig. 4.—Noncontrast-enhanced CT scans of skull base. *A*, Jugular tubercles (*arrows*) in normal patient. *B*, Asymmetrical jugular tubercles. Right tubercle (*arrow*) seen as ovoid area of bone-equivalent attenuation paralleling petrous ridge.

Fig. 6.—Anteroposterior hypocycloidal tomogram in patient with clivus chordoma. Right jugular tubercle is intact (*arrowhead*); left jugular tubercle (*outlined arrow*) has been completely eroded.

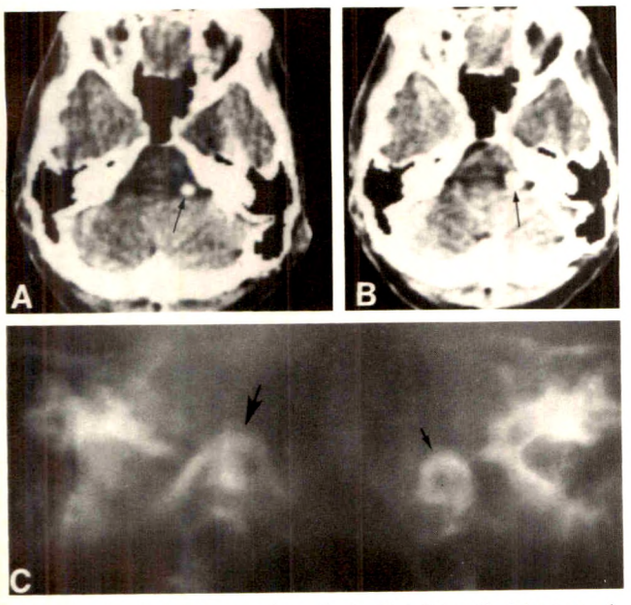

Fig. 5.—*A and B*, CT scans in patient with left hemifacial spasm. *A*, Without contrast enhancement. Prominent right jugular tubercle appears as unilateral ovoid density (*arrow*) protruding into right cerebellopontine angle cistern. *B*, With contrast enhancement. Tubercle appears larger (*arrow*) due to increased attenuation of surrounding veins. *C*, Anteroposterior temporal bone tomogram demonstrating asymmetric jugular tubercles with right tubercle (*large arrow*) significantly more prominent than left (*small arrow*). Angiography subsequently disclosed tortuous vertebrobasilar artery looping into left cerebellopontine angle. (Case courtesy of James S. Moore, Jr., St. Joseph's Hospital, St. Paul, Minn.)

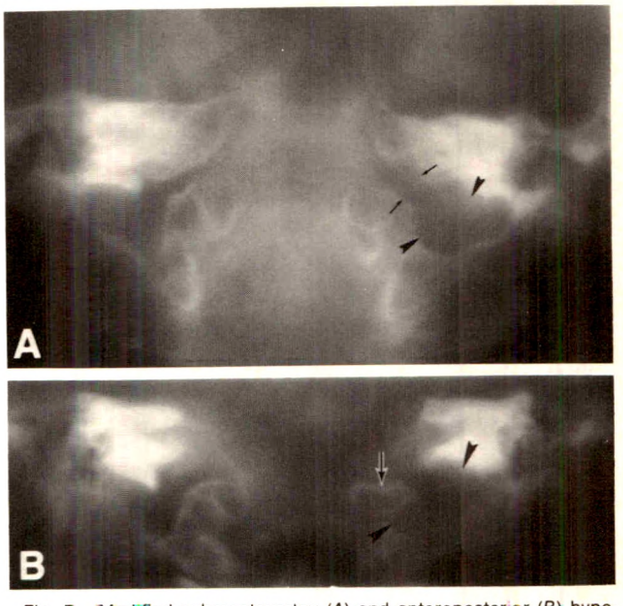

Fig. 7.—Modified submentovertex (*A*) and anteroposterior (*B*) hypocycloidal tomograms in patient with chemodectoma of left jugular fossa. Fossa (*arrowheads*) is enlarged and its cortical margins disrupted; extension of mass into cerebellopontine angle cistern is indicated by erosion and widening of the petrooccipital fissure (*small arrows*) and concavity of the left jugular tubercle (*outlined arrow*). Angiography disclosed typical glomus jugulare tumor.

or clivus chordoma (fig. 6) may affect the jugular tubercles either by extension from adjacent structures in the skull base or by hematogenous spread [12].

Benign tumors involving the cerebellopontine angle, jugular foramen [1, 2], petrous temporal bone [13, 14], or hypoglossal canal [10, 11] may also affect the tubercles by direct extension. Neurinomas, meningiomas [13–16], primary cholesteatomas [17, 18], glomus jugulare tumors, and remote posterior fossa tumors [6] can all produce detectable alterations in configuration of the adjacent jugular tubercle. In one such case (fig. 7), an enlarged left jugular fossa was present with obliterated effaced cortical margins. A widened petrooccipital fissure and the superiorly concave left jugular tubercle indicated extension of the lesion into the cerebellopontine angle cistern. Angiography disclosed a typical chemodectoma. Tumor extension into the left cerebellopontine angle cistern over the jugular tubercle was documented at surgery.

Other benign lesions may affect the jugular tubercles. Paget's disease or fibrous dysplasia of the skull base

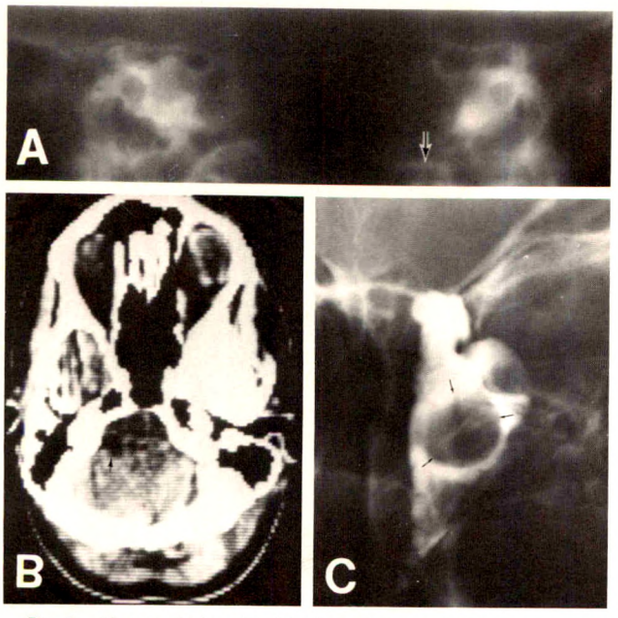

Fig. 8.—20-year-old female with bilateral congenital deafness, absent labyrinthine function, and 6 year history of progressive tinnitus and vertigo. Initial anteroposterior tomograms showed typical Mondini malformation. *A*, More posterior section disclosing normal right jugular tubercle, but flattening of left tubercle (*arrow*). *B*, CT scan suggesting possible cyst in left cerebellopontine angle cistern (*arrow*). *C*, Pantopaque cisternogram disclosing 2 cm well demarcated left cerebellopontine angle mass (*arrows*). Surgery confirmed radiographic diagnosis of subarachnoid cyst.

may involve the tubercles as part of the generalized disease process. In some instances of benign mass lesions in the adjacent cerebellopontine angle, subtle alteration in the contour of the jugular tubercles may be the only initial radiographic abnormality. We have seen three cases of cerebellopontine angle subarachnoid cyst in which flattening or compression of the tubercles provided the first diagnostic clues suggesting the presence of a localized mass (fig. 8). In our experience, flattening or compression of the jugular tubercles has always been abnormal and should prompt further clinical and radiologic investigation.

REFERENCES

1. Kim SK, Capp MP: Jugular foramen and early roentgen diagnosis of glomus jugulare tumor. *Am J Roentgenol* 97:597–606, 1966
2. Shapiro R: Compartmentation of the jugular foramen. *J Neurosurg* 36:340–343, 1972
3. Sutton JS: The normal jugular spur, jugular foramen, and jugular bulb as visualized on skull and temporal bone radiographs. *Radiology* 128:109–117, 1978
4. DiChiro G, Anderson WB: The clivus. *Clin Radiol* 16:211–223, 1965
5. Gray H: *Anatomy of the Human Body*, 29th American ed., edited by Goss CM, Philadelphia, Lea and Febiger, 1973
6. Kruyff E, Munn JD: Further experiences with a new sign in posterior fossa tumors. *J Can Assoc Radiol* 14:116–118, 1963
7. Byrd SE, Harwood-Nash DC, Barry JF, Fitz CR, Boldt DW: Coronal computed tomography of the skull and brain in infants and children. I. technique and results. *Radiology* 124:705–709, 1977
8. Braun JP, Tournade A, Ammerich H: Transverse anastomoses of the veins at the base of the brain. *Neuroradiology* 12:167–169, 1976
9. Braun JP, Tournade A: Venous drainage in the craniocervical region. *Neuroradiology* 13:155–158, 1977
10. Valvassori G, Kirdani M: The abnormal hypoglossal canal. *Am J Roentgenol* 99:705–711, 1967
11. Wardell GA, Goree JA, Jimenez JP: The hypoglossal artery and hypoglossal canal. *Am J Roentgenol* 118:528–533, 1973
12. Kendall BE, Lee BCP: Cranial chordomas. *Br J Radiol* 50:687–698, 1977
13. Phelps PD, Toland JA, Sheldon PWE: Erosions of the petrous temporal bone. *J Laryngol Otol* 84:1205–1230, 1970
14. Goldman AM, Martin JE: Tumors involving the temporal bone. *Radiol Clin North Am* 8:387–402, 1970
15. Montgomery WW: Cystic lesions of the petrous apex: transsphenoid approach. *Ann Otol Rhinol Laryngol* 86:429–435, 1977
16. Gacek RR: Diagnosis and management of primary tumors of the petrous apex. *Ann Otol Rhinol Laryngol* 84 (suppl 18):1–20, 1975
17. Derlacki EL: Congenital cholesteatoma of the middle ear and mastoid. *Arch Otolaryngol* 97:177–182, 1973
18. Brookler KH, Pulec JL, Hallberg OE: Congenital cholesteatomas of the temporal bone. *Arch Otolaryngol* 90:449–452, 1969

Technetium-99m Pertechnetate as an Indicator of Gastric Mucosal Proliferation

DAVID V. PECORA,[1] VIDYA SAGAR,[2] AND JOSEPHINE PICCONE[2]

Gastric mucosa was removed from five dogs and allowed to regenerate. Serial scintiscans after administration of ^{99m}Tc pertechnetate revealed gradual increase in gastric radioactivity, so that by 4 weeks it appeared as intense as preoperatively. By this means it was possible to follow the progress of gastric mucosal regeneration. The authors suggest that serial ^{99m}Tc scintiscanning might prove useful in evaluating the hypothesis that Barrett esophagus is due to replacement of esophageal squamous epithelium by gastric columnar epithelium.

In Barrett syndrome, ectopic gastric mucosa is found in the esophagus extending for varying distances orad from the cardia. Many investigators believe that the condition represents persistence of columnar epithelium found in the embryo. But Goldman and Beckman [1], after observing a patient with peptic esophagitis in whom a stricture and columnar epithelium migrated cephalad, suggested that Barrett epithelium may be an acquired condition and may represent a healing response of the esophagus to injury. Adler [2] subsequently presented convincing evidence that the peptic digestive process tends to destroy squamous mucosa normally found in the esophagus and that during the reparative phase, columnar mucosa extends into the esophagus to cover ulcerated areas.

It has been demonstrated that radioactive ^{99m}Tc pertechnetate is secreted by the normal gastric mucosa predominantly in the mucus-secreting cells [3]. Berquist et al. and others [4–6] have also shown that radioisotope scintigraphy may be useful in identifying patients who have ectopic gastric-type mucosa within the esophagus. The possibility arises that serial studies of individual patients might confirm the theory that Barrett epithelium originates at the gastric junction and advances up the esophagus. Our study attempted to establish how early proliferative gastric mucosa could be identified by determining the time after mucosal stripping that regenerating epithelium could be identified by the radioactive label.

Materials and Methods

Five beagles were anesthetized with intravenous pentobarbital. Under sterile conditions, the stomach was exposed and incised in the long axis. By blunt and sharp dissection, the mucosa was removed except for small areas near the pylorus and cardia in four dogs. In one dog, mucosa was stripped from the prepyloric region to and including the lower esophagus. Bleeding was easily controlled by pressure. The stomach was then closed using two layers of continuous 2-0 chromic catgut.

The secretion of free acid after the administration of intravenous histalog was tested prior to stripping the mucosa by the application of Congo red dye and pH paper to the mucosal surface. The test was repeated when dogs underwent subsequent exploratory surgery after the gastric mucosa had regenerated. Microscopic sections were made of the full thickness of the gastric wall before stripping, after stripping, and at subsequent exploration after mucosal regeneration.

Images of the stomach were obtained preoperatively in the anterior and left lateral projections after the intravenous administration of 5 mCi of ^{99m}Tc pertechnetate using a Searle Pho/Gamma IV camera and a converging collimator. For each image, 500,000 counts were collected on a 20 × 25 cm film through a "Microdot" imager. Postoperative images were obtained at weekly intervals using the same technique.

Results

Of the five dogs, one died 41 days after surgery. This animal developed a lower esophageal obstruction where esophageal mucosa had been stripped. The other four dogs survived until the end of the study 75, 115, 153, and 183 days after stripping at which times the mucosa had regenerated completely.

Histologic sections showed that the stripping procedure had removed all but traces of glandular elements. After regeneration, full thickness sections of the gastric wall showed the mucosa to be thinner and flatter than normal (fig. 1). The gastric glands were shallow. Almost all cellular elements were of the mucus-secreting type. Chief and parietal cells were rare. The pathologist reported that the mucosa appeared "atrophic." Secretory studies revealed markedly decreased or absent secretion of free acid.

The preoperative scans showed uptake of ^{99m}Tc pertechnetate uniformly throughout the stomach (figs. 2 and 3). One day after surgery no uptake was seen, except where gastric mucosa had been spared. Serial scans demonstrated a gradual increase in the area of uptake of radioactivity. By 4 weeks after surgery, the entire stomach was visualized in all animals. Although quantitative studies were not performed, the intensity of uptake appeared the same as preoperatively.

Discussion

Our observations indicate that regenerating gastric mucosa takes up ^{99m}Tc pertechnetate at an early stage in the repair process. This suggests that the method could be used clinically in following patients with esophagitis who are suspected of developing Barrett syndrome.

Received October 25, 1977; accepted after revision August 8, 1978.

[1] Department of Surgery, Thomas Jefferson University, Philadelphia, Pennsylvania, and Veterans Administration Center, 1601 Kirkwood Highway, Wilmington, Delaware 19805. Address reprint requests to D. V. Pecora in Delaware.

[2] Department of Nuclear Medicine, Thomas Jefferson University, Philadelphia, Pennsylvania, and Veterans Administration Center, Wilmington, Delaware 19805.

© 1978 American Roentgen Ray Society

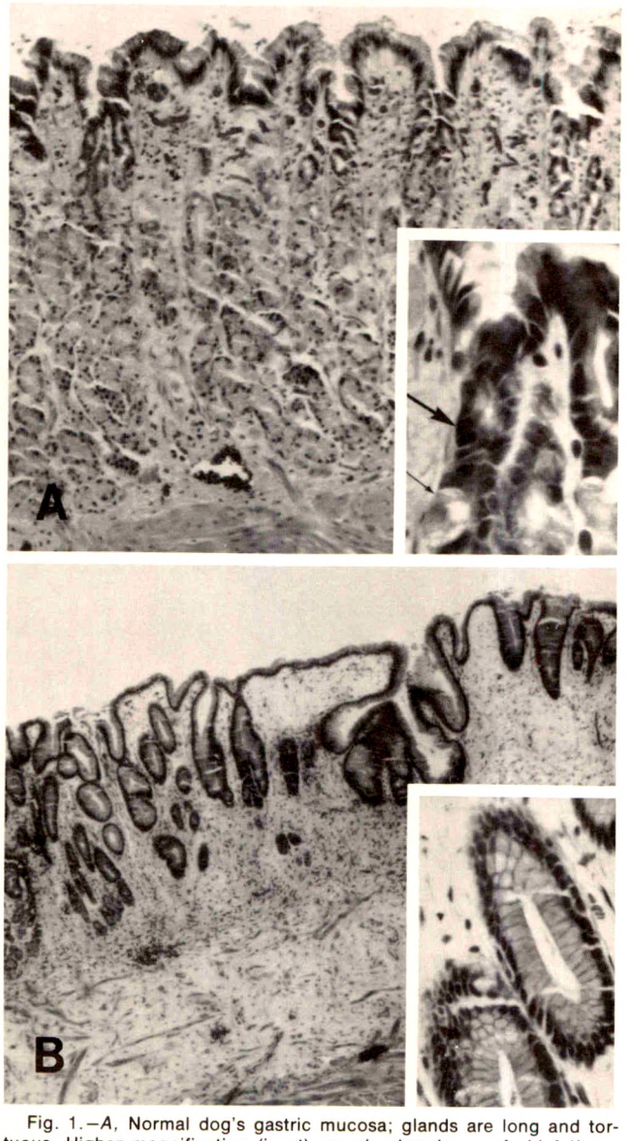

Fig. 1.—*A*, Normal dog's gastric mucosa; glands are long and tortuous. Higher magnification (inset) reveals abundance of chief (*large arrow*) and parietal cells (*small arrow*). Mucous cells appear cuboidal with clear cytoplasm. Chief cells contain darkly stained pigment. Parietal cells appear spherical or triangular and occupy peripheral position near basement membrane. *B*, Regenerated gastric mucosa 75 days after stripping. Gastric glands are shallow. In inset, only rare chief and parietal cells can be identified. Almost all cells are mucous type containing clear cytoplasm.

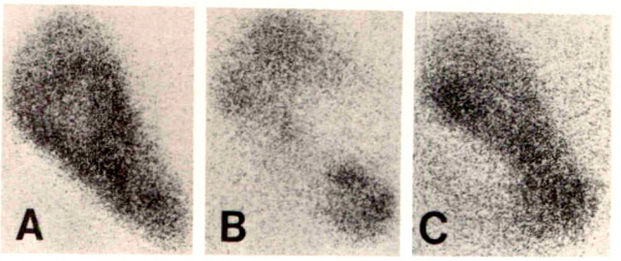

Fig. 2.—*A*, Preoperative scintiscan of stomach. *B*, 8 days after mucosal stripping, denuded area does not concentrate pertechnetate. *C*, 90 days after stripping, mucosa has regenerated and concentrates pertechnetate throughout stomach.

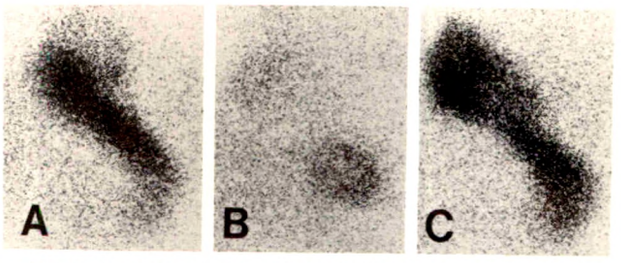

Fig. 3.—*A*, Preoperative image showing pertechnetate concentration in mucosa of whole stomach. *B*, 7 days after surgery, pertechnetate is absent from stripped area. *C*, 34 days after surgery, gastric mucosa has regenerated. Pertechnetate is concentrated as preoperatively throughout whole stomach.

The hypothesis advanced by Adler [2] is appealing, but requires further study. Paull et al. [7] described three types of columnar epithelium above the lower esophageal sphincter in Barrett esophagus: atrophic gastric fundic type epithelium with parietal and chief cells closest to the stomach, junctional-type epithelium with cardiac mucous glands next, and distinctive specialized columnar epithelium with a villiform surface, mucous glands, and intestinal-type goblet cells most cephalad.

Lippman et al. [8] reported that after stripping, regenerating gastric mucosa first consisted entirely of mucous cells and subsequently developed increasing numbers of parietal and chief cells. With time, the appearance of the mucosa changed from a mucous gland intestinal type to a more normal appearing gastric mucosa. The regenerative phases seem to resemble progressively the specialized columnar, junctional, and atrophic gastric fundic types, respectively, of Paull et al. This histologic evolution further supports Adler's hypothesis that esophageal mucosal replacement begins from below.

Having demonstrated that regenerating gastric mucosa can be identified by pertechnetate we are studying patients with esophagitis hoping to demonstrate whether or not gastric mucosa can be shown to progress up the esophagus from the stomach.

REFERENCES

1. Goldman MC, Beckman RC: Barrett syndrome. *Gastroenterology* 39:104–110, 1960
2. Adler RH: The lower esophagus lined by columnar epithelium. *J Thorac Surg* 45:13–32, 1963
3. Chaudhuri T, Polak J: Autoradiographic studies of distribution in the stomach of Tc-99m pertechnetate. *J Nucl Med* 17:559, 1976
4. Berquist TH, Nolan NG, Stephens DH, Carlson HC: Radioisotope scintigraphy in diagnosis of Barrett's esophagus. *Am J Roentgenol* 123:401–411, 1975
5. Mangla JC, Brown M: Diagnosis of Barrett's esophagus by pertechnetate radionuclide. *Am J Dig Dis* 21:324–328, 1976
6. Priebe CJ Jr, Marsden DS, Lazarevic B: The use of 99m technetium pertechnetate to detect transplanted gastric mucosa in the dog. *J Pediatr Surg* 9:605–613, 1974
7. Paull A, Trier JS, Dalton MD, Camp RC, Loeb P, Goyal RK: The histologic spectrum of Barrett's esophagus. *N Engl J Med* 295:476–480, 1976
8. Lippman HN, Sheldon DB, Longmire WP: Further observations on the return of secretory function following gastric mucosal stripping in the dog. *Surgery* 40:212–222, 1956

Drip Infusion Urography with Meglumine Iodamide

ALAN H. ROBBINS,[1] ARTHUR T. ROSENFIELD,[2] NICHOLAS F. PIZZOLATO,[3] GERALD A. IRWIN,[4] CHARLES E. PUTMAN,[2] STEPHEN G. GERZOF,[1] AND SIDNEY ULREICH[2]

In a double-blind study of 283 patients (140 given iodamide and 143 diatrizoate), meglumine iodamide 24% produced a significantly greater degree of opacification than meglumine diatrizoate 30% ($P < 0.01$ to $P < 0.001$) in the renal calyces during the early phase of drip infusion pyelography. The agents were infused at a dose of 4.5 ml/kg, up to a maximum volume of 300 ml, over a period of about 10 min. The incidence and nature of laboratory abnormalities and clinical adverse reactions produced by the drugs were similar. No severe reactions occurred. The apparent superiority of the iodamide solution in the early stage of excretion, despite its lower iodine content, may be due to the partial secretion of iodamide by the renal tubules, as observed in other studies.

The safety and effectiveness of meglumine iodamide as a contrast agent for excretory urography have been extensively demonstrated in clinical trials in Europe and Asia, and, more recently, in the United States and Canada [1–9]. Iodamide is similar to diatrizoate in molecular structure, differing only in an additional carbon linkage on one of the side chains (fig. 1).

The results of some animal [10, 11] and clinical studies [12, 13] suggest that, unlike other contrast agents, iodamide may be secreted by the renal tubules, thus possibly producing greater concentrations of iodine in the collection system, and hence better and more rapid opacification during the early phase of excretion. However, other studies found no evidence of tubular secretion [14, 15].

This report presents further data on the safety and effectiveness of meglumine iodamide (Renovue-DIP, Squibb) in comparison with meglumine diatrizoate (Reno-M-DIP, Squibb) for drip infusion urography. The data were acquired following the same predesigned protocol at four participating institutions. The protocol was approved by the committees overseeing human investigation in each hospital.

Subjects and Methods

In a double-blind study, 283 patients requiring excretory urography received an intravenous infusion of 4.5 ml/kg (up to a maximum of 300 ml) of either meglumine iodamide or meglumine diatrizoate, according to a predetermined randomization schedule. The duration of the infusion was about 10 min.

Meglumine iodamide was given to 140 patients (100 male and 40 female) as a 24% sterile aqueous solution containing 111 mg of organically bound iodine per milliliter. Meglumine diatrizoate was administered to 143 patients (102 male and 41 female) as a 30% sterile aqueous solution with 141 mg of organically bound iodine per milliliter. The patients given iodamide ranged in age from 18 to 87 years (average, 49.8) and those given diatrizoate ranged from 18 to 83 years (average, 51.8).

Pretreatment renal function was considered (1) normal, with creatinine clearance of 80–180 ml/min, and normal blood urea nitrogen and serum creatinine; (2) mild impairment with creatinine clearance of 50–80 ml/min, and blood urea nitrogen and serum creatinine increased by 25% or less above the upper limit for normal; (3) moderate impairment, with creatinine clearance of 10–50 ml/min, and blood urea nitrogen and serum creatinine increased by 25%–50% above the upper limit for normal; or (4) severe impairment, with creatinine clearance less than 10 ml/min, and blood urea nitrogen and serum creatinine increased more than 50% above the upper limit for normal. Pretreatment renal function was normal in 126 patients in the iodamide group and in 124 of the diatrizoate group. Of those with abnormal renal function in the iodamide group, the impairment was mild in eight, moderate in four, and severe in two. In the diatrizoate group, impairment was mild in 10, moderate in seven, and severe in two.

For most patients, the reason for the urographic procedure was a preliminary diagnosis of urinary tract disease. Other, less frequent reasons were abdominal complaints, hypertension, extraurinary tract tumor, and routine radiologic workup. Patients with severe renal or hepatic dysfunction were generally excluded from the study.

Vital signs were monitored before, during, and 4 hr after the infusion and a laboratory profile was obtained before and after infusion. The minimum laboratory follow-up involved a urinalysis, hemogram, and serum urea nitrogen, creatinine, and total bilirubin concentrations at 24 hr after infusion. However, about one-half of the patients were followed-up more extensively (urinalysis, hemogram and SMA-12 plus serum creatinine and SGPT) at 2- and 48–96 hr after infusion. In addition, complete 12-lead electrocardiograms were performed on 70 patients (34 in the iodamide group and 36 diatrizoate) before, during, and after the infusion.

Serial exposures of the abdomen were obtained before and at 5, 10, 20, 30, and 45 min after the start of infusion. Additional films were taken after 45 min if satisfactory opacification had not occurred. Radiologists other than the principal investigators evaluated the films. They were blinded to the drug, the patient, and the time at which the films were taken. Except for a small number of films that were lost or judged technically inadequate (as with over- or under-exposure), the films from all 283 patients were evaluated. For each film, scores were assigned to nine areas of the urinary tract (the right and left parenchyma, calyces, pelves, ureters, and the urinary bladder) as follows: 0

Received December 15, 1977; accepted after revision September 19, 1978.
This work was supported by grants from the Squibb Institute for Medical Research, Princeton, New Jersey 08540.
[1] Department of Radiology, Veterans Administration Hospital, Tufts University School of Medicine, Boston, Massachusetts 02130. Address reprint requests to A. H. Robbins.
[2] Department of Radiology, Yale University School of Medicine, New Haven, Connecticut 06504.
[3] Northport Veterans Administration Hospital, Northport, New York 11768.
[4] Department of Radiology, Nassau County Medical Center, East Meadow, New York 11554.

© 1978 American Roentgen Ray Society

0361–803X/78/1200–1043 $00.00

= no opacification; 1 = faint opacification, structure minimally visualized; 2 = dense or optimal opacification. Although the scoring was basically qualitative, the blinded method of evaluation and the population size were considered sufficient to balance the variations among radiologists. In addition, the principal investigators evaluated the clinical performance of the contrast agents as satisfactory or unsatisfactory, considering both the safety and effectiveness of the drugs.

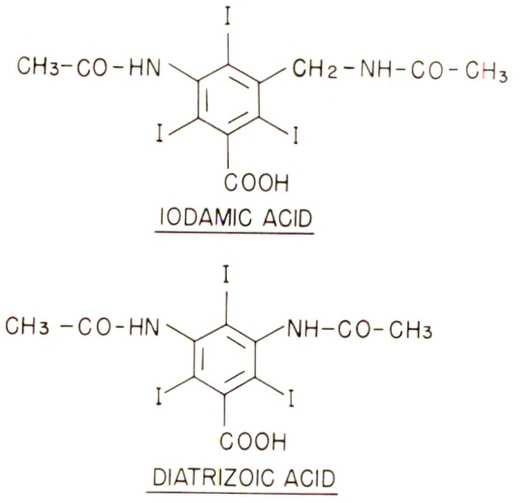

Fig. 1.—Acid forms of iodamide and diatrizoate.

Results

Degree and Speed of Opacification

The opacification scores, including means, are presented in table 1. For bilateral sites, the better opacified side in each film has been recorded. The table does not include data from 23 patients treated with iodamide and 28 with diatrizoate, all of whom had abnormal pretreatment renal function and/or radiologic evidence of obstruction of the urinary tract.

Iodamide produced dense opacification in the renal calyces more frequently at the earlier times (i.e., 5 and 10 min after the start of the infusion) than did diatrizoate. Thus, the mean opacification scores were significantly higher for iodamide in the calyces at 5 min ($P < 0.001$) and 10 min ($P < 0.01$). There were no significant differences between the contrast agents in opacifying the renal parenchyma, the pelves, ureters, or urinary bladder.

TABLE 1

Comparison of Urinary Tract Opacification by Iodamide and Diatrizoate in Patients With Normal Renal Function

Time (min) and Opacity	Parenchyma		Calyces		Pelves		Ureters		Bladder	
	Iodamide	Diatrizoate	Iodamide	Diatrizoate	Iodamide	Diatrizoate	Iodamide	Diatrizoate	Iodamide	Diatrizoate
5:										
Dense	55	60	67	39	70	55	40	27	19	20
Faint	55	48	47	71	37	52	55	57	50	45
None	6	5	2	3	9	6	21	29	47	52
Mean	1.42	1.49	1.56**	1.32	1.53	1.43	1.16	0.98	0.76	0.73
10:										
Dense	58	65	91	69	94	85	70	60	63	61
Faint	51	36	22	37	18	20	40	39	45	35
None	4	5	0	0	1	1	3	7	5	9
Mean	1.48	1.57	1.81*	1.65	1.82	1.79	1.59	1.50	1.51	1.50
20:										
Dense	46	63	92	92	92	96	82	79	99	105
Faint	56	44	19	23	18	19	27	32	9	6
None	9	8	0	0	1	0	1	4	1	3
Mean	1.33	1.48	1.83	1.80	1.82	1.83	1.74	1.65	1.90	1.89
30:										
Dense	33	44	84	80	89	90	77	72	97	99
Faint	56	50	19	24	14	14	25	30	6	1
None	15	1	1	0	1	0	2	4	1	3
Mean	1.17	1.33	1.80	1.77	1.85	1.87	1.72	1.64	1.92	1.93
45:										
Dense	20	24	60	59	65	63	50	48	79	86
Faint	54	64	29	40	24	36	35	42	10	9
None	17	12	2	1	2	1	6	10	2	4
Mean	1.03	1.12	1.64	1.58	1.69	1.62	1.48	1.38	1.85	1.83

Note.—Omitted from this table are data from 23 patients treated with meglumine iodamide and 28 with meglumine diatrizoate, all of whom had abnormal pretreatment renal function and/or radiologic evidence of obstruction of the urinary tract. The number of radiograms obtained decreased slightly with time because individual patients did not require the full schedule of films. Also, a few films were considered technically inadequate for evaluation. Mean opacification scores were weighted by counting each dense, faint, and none as 2, 1, and 0, respectively.

** Mean opacification score is significantly higher for iodamide than diatrizoate ($P < 0.001$).

* Mean opacification score is significantly higher for iodamide than diatrizoate ($P < 0.01$).

The mean time required to produce dense opacification of the various sites was also compared for patients in whom dense scores had been recorded. The number of patients in whom the first dense opacification was observed in a given site at each time was multiplied by the time (5, 10, 20, 30, or 45 min). The mean times were calculated from this and compared by the *t* test. The only significant difference occurred in the calyces where mean time required to produce dense opacification was significantly less for iodamide than for diatrizoate ($P < 0.01$).

Radiologic and Clinical Findings

The radiologic findings were normal in 65 (46%) of the patients given meglumine iodamide and in 73 (51%) of the patients given meglumine diatrizoate. Obstructive uropathy was diagnosed in nine patients given iodamide and in 12 given diatrizoate. In the latter group there were three whose pretreatment renal function was abnormal. Radiologic diagnoses for the other patients included pyelonephritis, ureteral obstruction or calculi, renal tumors or calculi, and prostatic enlargement.

The clinical performance of the contrast agents was judged satisfactory in all 140 patients given iodamide and in 141 of the 143 patients given diatrizoate.

Abnormal Laboratory Test Results

The results of laboratory follow-ups were similar for the contrast agents: 88 abnormalities were observed in 50 (36%) of the patients given iodamide and 90 were observed in 43 (30%) of the patients given diatrizoate. Abnormal values were counted separately each time they occurred in a given test (at 24 or at 48–96 hr after infusion), and their relationship to the drug was judged by a physician who was unaware of the drug given.

The abnormalities noted were typically transient and not associated with any clinically apparent complaint. The most frequently observed hematologic change was a mild eosinophilia—seven abnormal tests in the iodamide group and 16 in the diatrizoate group. The number of seemingly drug-related abnormalities is shown for five test categories in table 2.

Some of the data concerning renal function tests are worth examining further. It should be noted that no patient demonstrated clinical signs of renal failure and any observed alteration in renal function testing was a purely chemical event. Thirteen patients (9%) in the diatrizoate and 18 patients (12.8%) in the iodamide group showed alteration in tests of renal function. While four of these diatrizoate patients had associated hypertension and two had impaired renal function, none had associated diabetes. Of the 18 iodamide patients, three had associated hypertension and two had diabetes, but none had preexisting renal insufficiency.

Indeed there seemed to be generally poor correlation of renal function deterioration after contrast with preexisting abnormal renal function per se. In the iodamide group 14 patients had preexisting renal function impairment (eight mild, four moderate, and two severe). Only one of these patients, a diabetic, showed change in renal function after contrast. In the diatrizoate group 19 patients had preexisting renal function impairment (10 mild, seven moderate, two severe). Two patients (one with hypertension, the other with diarrhea) demonstrated transient deterioration of renal function tests after receiving the drug.

TABLE 2

Laboratory Abnormalities

Test Category	Iodamide ($N = 50$)	Diatrizoate ($N = 43$)
Hemogram	12	27
Urinalysis	15	19
Renal function	27	23
Liver function	21	15
Other blood chemistry	13	6
Total	88	90

There were 11 patients with hypertension in each study group. Three in the iodamide group and four in the diatrizoate group showed some deterioration of renal function tests. Two of the 10 patients with diabetes in the iodamide group showed decreased renal function after examination, whereas none of the eight in the diatrizoate group showed similar change. There was no strong correlation between any other associated conditions and abnormal renal function tests after infusion pyelography.

Clinical Adverse Reactions

Of the patients given iodamide, 19 (14%) experienced 23 clinical adverse reactions (18 mild reactions and five moderately severe, that is, requiring and responding immediately to treatment). The reactions included eight instances of urticaria and seven of nausea and/or vomiting. Of the patients given diatrizoate, 14 (10%) had 18 reactions (14 mild and four moderate) including six instances of urticaria and five of nausea and/or vomiting.

Electrocardiographic Evaluation

Electrocardiographic changes possibly due to the contrast agents occurred during or shortly after the infusion in four patients given iodamide and in eight given diatrizoate. Ischemic changes associated with a clinical anginal episode occurred in one patient given iodamide and premature ventricular beats occurred in the other three. Electrocardiograms from two patients given diatrizoate showed ischemic changes, one transient and without clinical symptoms, the other associated with angina (this patient showed subsequent enzyme changes indicating minor myocardial injury). Three patients given diatrizoate developed occasional premature ventricular beats and three others had transient increases in cardiac rate.

Discussion

Both drugs are highly effective urographic agents. These results support a recent study that found meglumine iodamide to be at least as effective as diatrizoate (the meglumine and sodium salts combined) when the agents were administered as intravenous bolus injections [9]. In this study, however, iodamide showed statistically significant advantages in opacifying the upper portions of the renal collecting system during the period of infusion. This advantage is even more notable with regard to the 20% lower content of iodine in the iodamide than in the diatrizoate solution for infusion. Since the advantage was largely one of the speed of opacification rather than the ultimate density obtainable, this particular factor admittedly, may be of limited clinical significance despite being statistically so.

Preliminary studies have suggested that, unlike other contrast agents, iodamide may be secreted by the renal tubules [10–13]. This could produce a higher concentration of the agent in the urine, and thus greater opacification, in the early phase of excretion from the kidney.

Iodamide and diatrizoate seem to be comparable in terms of safety. There were fewer patients with electrocardiographic changes after receiving iodamide than after receiving diatrizoate and, although more patients had laboratory abnormalities after iodamide, the total number of abnormalities was greater after diatrizoate. The number of patients with clinical adverse reactions was slightly higher in the iodamide group, but most of the reactions in both drug groups were mild and transient.

In view of the rash of recent reports relating iodinated contrast agents to renal failure [16–21] it is important to note that the new agent, iodamide, is also associated with an apparent deterioration of renal function in a greater percentage of patients with preexisting diabetes or hypertension than in those without. It is of interest that of the 33 patients with preexisting abnormal renal function studied with either drug, only three showed evidence of deterioration. One was a diabetic, another hypertensive, and the other was suffering from diarrhea. This raises some question as to whether preexisting abnormal renal function in the absence of another compromising problem such as diabetes or hypertension does in fact render a patient more susceptable to renal toxicity when confronted by contrast agent as has been suggested* [16–21].

In conclusion, these data, combined with those from earlier studies, indicate that meglumine iodamide is an effective contrast agent for excretory urography that may offer advantages over other agents currently used, such as meglumine diatrizoate, in the degree and speed of opacification of the upper portions of the renal collecting system.

*Editors note. – See Editorial, this issue.

REFERENCES

1. Bellizzi C: A study of the renal elimination of a new contrast medium: iodamide. *Radiobiol Radiother Fis Med* 21:217–224, 1966
2. Chiesa A, Biodoli F: Remarks on the use of iodamide, a new water-soluble contrast medium for urography and angiography. *Quad Radiol* 31:557–570, 1966
3. Corsi M, Tassini T: Remarks on the use of a new water-soluble contrast medium, iodamide 300, in urography and cerebral angiography. *Quad Radiol* 34:187–206, 1969
4. de Langen JE, Hermans J: Comparative multiclinical studies of iodamide and diatrizoate in excretory urography. *Radiology* 106:73–76, 1973
5. Goy W, Pohlenz O: A new contrast medium for excretion urography. *Arzt Praxis* 18:1461–1462, 1966
6. Kamdar KN, Lapsia KC: Comparative radiological studies of urologic contrast media with Uromiro. *Indian J Radiol* 21:211–217, 1967
7. Mean A, Pasquier J: Intravenous urography with a new contrast product: Uromiro. *Praxis* 56:945–950, 1967
8. Sneider P, Reichman P: New radiological contrast materials available in South Africa—a preliminary communication. *S Afr J Radiol* 41:5–9, 1967
9. Gerzof SG, Robbins AH, Unger G, Zaki A, Wickis EA: Double-blind comparison of meglumine iodamide and Renografin-60 for excretory urography. *Am J Roentgenol* 128:211–215, 1977
10. DiFazio LT: Summary of preclinical studies, clinical trials and experience. *Clinical Pharmacology Investigator's Brochure for SQ 21,981,* Princeton, NJ, Squibb Institute for Medical Research, 1973
11. Bonati F, Rosati GF, Zanichelli V: Renal clearances of urographic contrast agent in the rabbit. *Radiol Med* (Torino) 6:577–587, 1976
12. Bollerup AC, Hesse B, Steiness E: Renal handling of iodamide and diatrizoate: evidence of active tubular secretion of iodamide. *Eur J Clin Pharmacol* 9:63–67, 1976
13. Magno L: A study of the renal clearance of iodine-containing contrast media for urography and angiography. *Radiol Med* (Torino) 52:253–266, 1966
14. Weissenstein H, Suterlin F, Feller E: Renal examinations with iodamide-iod^{131}. *Radiologe* 9:60–64, 1969
15. Wurdinger H: I^{131}-et kettiertes iodamide in der isotopennephrographie. *Arzneim Forsch* 16:662–664, 1966
16. Alexander RD, Berkes SL, Abuelo JG: Contrast media-induced oliguric renal failure. *Arch Intern Med* 138:381–384, 1978
17. Weinrauch LA, Robertson WS, D'Elia JA: Contrast media-induced acute renal failure. *JAMA* 239:2018–2019, 1978
18. Swartz RD, Rubin JE, Leeming BW, Silva P: Renal failure following major angiography. *Am J Med* 65:31–37, 1978
19. Carvallo A, Rakowski TA, Argy WP Jr, Schreiner GE: Acute renal failure following drip infusion pyelography. *Am J Med* 65:38–45, 1978
20. VanZee BE, Hoy WE, Talley TE, Jaenike JR: Renal injury associated with intravenous pyelography in nondiabetic and diabetic patients. *Ann Intern Med* 89:51–54, 1978
21. Shafi T, Chou SY, Porush JG, Shapiro WB: Infusion intravenous pyelography and renal function. *Arch Intern Med* 138:1218–1221, 1978

Shoulder Arthrography as a Treatment Modality

LOUIS A. GILULA,[1] PERRY L. SCHOENECKER,[2] AND WILLIAM A. MURPHY[1]

Some patients undergoing shoulder arthrography with a stiff and painful joint have a small volume capsule or a frozen shoulder. In certain cases when the rotator cuff is intact, the arthrographic procedure has been therapeutic and joint distention has effected a return to normal function. Four such cases are presented.

Differential diagnoses of patients undergoing shoulder arthrography with pain and limited range of motion should include rotator cuff tear, adhesive capsulitis (frozen shoulder), and a syndrome characterized by pain and stiffness [1]. We report four patients with stiff and painful shoulder who have benefited therapeutically from arthrography. We believe that intraarticular local anesthetic, capsular distention, and assisted exercise may combine as a therapeutic method.

Technique

Anterior needle placement with the patient supine (rather than posterior oblique) is used to maximize patient comfort and minimize soft-tissue thickness between skin and joint. Meglumine iothalamate 60% (15 ml) is diluted with 12 ml sterile saline and 3 ml sterile 1% xylocaine. After intracapsular verification, contrast solution is injected until the joint space is fluoroscopically distended, or until the patient experiences a full or slightly uncomfortable sensation. After needle removal, the patient sits up and is gently assisted through as full and painless a range of motion as possible. No forceful manipulation is attempted, such as is performed under general anesthesia for adhesive capsulitis (frozen shoulder) [1, 2]. Routine radiographs in anteroposterior position with internal and external rotation and axillary views are obtained. If the initial exercise results in increased range of motion, further range of motion exercise of the shoulder is performed after the radiographs are obtained.

Case Reports

Case 1

A 50-year-old male was seen 1 year after he had suffered a stretch injury to his shoulder by falling from a ladder. The shoulder was constantly painful and stiff and he was unable to abduct beyond 40°. Arthrography demonstrated a small capsule without an axillary recess (fig. 1); the rotator cuff was intact. With passive range of motion exercise, contrast extravasated from the subscapularis bursa. By the end of the procedure, the patient actively abducted his shoulder to 110°. At follow-up 2 years later, the patient had minimal pain, improved motion dating from the time of arthrography, and no functional limitation.

Case 2

A 50-year-old male had a painful stiff right shoulder 2 months after fracture of the inferior glenoid rim. Active abduction was limited to 65°. At arthrography, a borderline small joint capsule was evidenced by a small axillary recess and a very small subcoracoid bursa. The capsule margin was slightly lobulated and no rotator cuff tear was present. Assisted range of motion exercise was performed at arthrography, and 140° of active abduction was obtained without contrast extravasation. On follow-up examination, the patient demonstrated further improvement in range of motion and was able to return to work as a truck driver with only occasional mild shoulder pain.

Case 3

A 47-year-old male fell over a fence and injured his right shoulder. Three weeks after injury he had only 60° abduction and 90° flexion of his shoulder. Internal and external rotation was markedly limited. During arthrography, contrast material entered the joint with more than usual resistance. At first the joint was very small, but during injection it gradually, although incompletely, distended and contrast material escaped through the bicipital tendon sheath. The rotator cuff was intact and range of motion quickly improved with passive exercise. He then satisfactorily resumed his pastime of fishing, and follow-up 1 year later demonstrated normal pain-free motion.

Case 4

A 60-year-old male with bronchogenic carcinoma developed a stiff and painful right shoulder which persisted for 2 months without documented injury. He could abduct his arm only to 20°. Arthrography demonstrated an intact rotator cuff, a small capsule without an axillary recess, and extravasation from the subcapsularis bursa. No bone or soft-tissue metastases were demonstrated. Improved range of motion accompanied gentle passive exercise. On follow-up examination, the patient had no further complaints of shoulder pain or stiffness. He died 2 months later of metastatic cancer.

Discussion

The arthrographic appearance of rotator cuff tear and adhesive capsulitis have been well described [1–8]. Neviaser [1] classified capsulitis and its treatment into three groups. The group with the most severe adhesive disease, or frozen shoulder, included long-term management problems with advanced clinical and arthrographic findings. These patients required surgical intervention. The group with moderate involvement was characterized by arm abduction limited to less than 90° and joint volume reduced to 5–10 ml at arthrography (normal joint volume: 16–35 ml [2]). These patients were treated with manual manipulation under general anesthesia.

The group with the mildest clinical disease, the "stiff and painful shoulder" syndrome, was characterized by

Received March 28, 1978; accepted after revision August 9, 1978.
[1] Mallinckrodt Institute of Radiology, 510 South Kingshighway Boulevard, St. Louis, Missouri 63110. Address reprint requests to L. A. Gilula.
[2] Division of Orthopaedic Surgery, Department of Surgery, Washington University School of Medicine, St. Louis, Missouri 63110.

© 1978 American Roentgen Ray Society

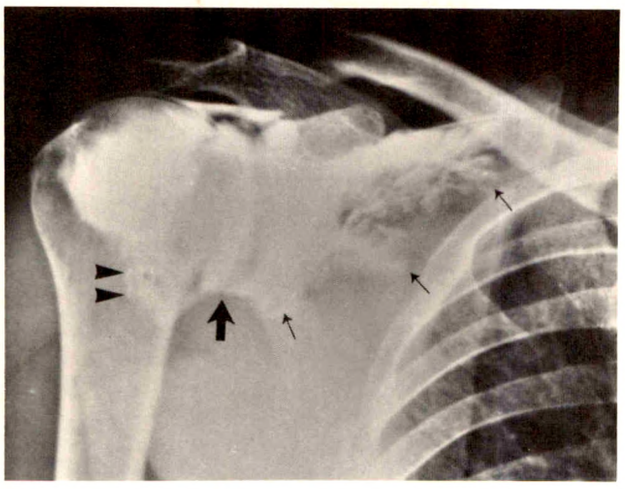

Fig. 1.—Case 1: Absent axillary recess is manifested as concavity (*large arrow*) in capsular contour. Contrast extravasated from subscapularis bursa into subscapularis muscle (*small arrows*) and filled bicipital tendon sheath (*arrowheads*). Rotator cuff is intact.

limited scapulohumeral motion. Although less than normal, abduction was usually greater than 90° and intraarticular volume about 10–12 ml. Neviaser [1] treated these patients with physical therapy, exercise, and gentle manipulation, and found that most patients returned to normal in 3–6 months. In the past, treatment of similar shoulder problems has included watchful waiting, physical therapy, range of motion exercises, systemic antiinflammatory medication, and intraarticular injection of local anesthetic and steroids [1, 9–13]. Since each of our patients improved immediately after a single arthrogram and no further treatment was necessary, we feel arthrography should be viewed as a possible treatment method.

No scar formation was demonstrated at arthrography, even though the joint capsules were of small volume, containing only 5–15 ml of contrast material before extravasation. It is unclear what causes the pain and stiffness in this group, but perhaps the small volume capsule follows a nonspecific capsular inflammatory reaction [9, 14], or an autoimmune response resulting from breakdown of collagen or mucopolysaccharide from portions of the articular soft tissues [15]. Although it is uncertain why our patients responded to the combination of joint distention, intraarticular local anesthetic, and assisted range of motion, we believe this combination may counteract irritation or stretch subradiographic adhesions.

Others have attempted to increase range of shoulder motion with combined arthrography and joint distention [3, 5, 13, 16], but have often found repeated intervention necessary [5, 9]. Andren and Lundberg [3] treated 128 shoulders ranging from "moderate stiffness" (26 patients) to "rigid" (64 patients), and all but two responded with increased mobility. Full and permanent recovery occurred immediately in two-thirds of the "moderate stiffness" group and one-fifth of the "rigid" group. No complications have been documented in the literature among such patients.

Of 160 patients undergoing shoulder arthrography during the past 4 years, four have been convincingly treated by the arthrographic procedure. However, these numbers potentially underestimate the usefulness of this treatment method. In part, this is because we have traditionally performed shoulder arthrography as a diagnostic tool rather than as therapeutic intervention [3]. Furthermore, it has been performed by various staff members and residents without uniform sensitivity to the possible treatment of a small capsule or frozen shoulder by further distention. To identify this subpopulation of patients undergoing shoulder arthrography, it is only necessary to consider those who have pain and limited scapulohumeral motion with a small volume joint capsule.

Improved range of motion will occur immediately, but this improvement must be maintained by active range of motion for several days after arthrography [3]. Steroid instillation at the time of arthrography has been suggested to prolong the therapeutic result [13]; however, we have not used steroids. Success in our patients is measured by return to normal activity without further medication or treatment other than continued range of motion exercises.

REFERENCES

1. Neviaser JS: *Arthrography of the Shoulder*. Springfield, Ill., Thomas, 1975
2. Lundberg BJ: The frozen shoulder. Clinical and radiographical observations. The effect of manipulation under general anesthesia. Structure and glycosaminoglycan content of the joint capsule. Local bone metabolism. *Acta Orthop Scand [Suppl]* 119:1–59, 1969
3. Andren L, Lundberg BJ: Treatment of rigid shoulders by joint distention during arthrography. *Acta Orthop Scand* 36:45–53, 1965
4. Killoran PJ, Marcove RC, Freiberger RH: Shoulder arthrography. *Am J Roentgenol* 103:658–668, 1968
5. Reeves B: Arthrographic changes in frozen and post-traumatic stiff shoulders. *Proc R Soc Med* 59:827–830, 1966
6. Holstein A, Lewis GB: Adhesive capsulitis of the shoulder—a clinical review of management. *J Bone Joint Surg [Am]* 49:202, 1967
7. Ennevaara K: Painful shoulder joint in rheumatoid arthritis. *Acta Rheum Scand [Suppl]* 11:1–116, 1967
8. Nelson CL, Burton RI: Upper extremity arthrography. *Clin Orthop* 107:62–72, 1975
9. Roy S, Oldham R: Management of the painful shoulder. *Lancet* 1:1322–1324, 1976
10. Bateman JE: *The Shoulder and the Neck*. Philadelphia, Saunders, 1972
11. DePalma AF: *Surgery of the Shoulder*. Philadelphia, Lippincott, 1973
12. Richardson AT: The painful shoulder. *Proc R Soc Med* 68:731–736, 1975
13. MacNab I, Hastings D: Rotator cuff tendinitis. *Can Med Assoc J* 99:91–98, 1968
14. Neviaser JS: Adhesive capsulitis of the shoulder: a study of pathological findings in periarthritis of the shoulder. *J Bone Joint Surg [Am]* 27:211–222, 1945
15. MacNab I: Rotator cuff tendinitis. *Ann R Coll Surg Engl* 53:271–287, 1973
16. Older MWJ, McIntyre JL, Lloyd GJ: Distension arthrography of the shoulder joint. *Can J Surg* 19:203–207, 1976

Association of Diffuse Idiopathic Skeletal Hyperostosis (DISH) and Calcification and Ossification of the Posterior Longitudinal Ligament

DONALD RESNICK,[1] JOSE GUERRA, JR.,[1] CHARLES A. ROBINSON,[2] AND VINTON C. VINT[3]

Diffuse idiopathic skeletal hyperostosis (DISH) is a common ossifying diathesis in middle-aged and elderly patients characterized by bone proliferation along the anterior aspect of the spine and at extraspinal sites of ligament and tendon attachment to bone. Four patients with DISH revealed extensive calcification and ossification of the posterior longitudinal ligament in the cervical spine. Review of cervical spine radiographs in 74 additional patients with DISH demonstrated bony hyperostosis of the posterior aspect of the vertebrae in 41%, posterior spinal osteophytosis in 34%, and posterior longitudinal ligament calcification and ossification in 50%. These ligamentous findings, which have previously been described almost exclusively in Japanese people, appear to be an additional skeletal manifestation of DISH.

Diffuse idiopathic skeletal hyperostosis (DISH) is a common disorder characterized by bone proliferation in axial and extraaxial sites [1–3]. The most characteristic abnormalities in this condition are ligamentous calcification and ossification along the anterolateral aspect of the vertebral bodies with localized osteophytosis. Changes in extraspinal locations are also frequent, including ligament and tendon calcification and ossification, paraarticular osteophytes, and bony excrescences at sites of ligament and tendon attachment to bone. Alterations along the posterior aspect of the vertebrae are rarely mentioned in this condition.

Ossification of the posterior longitudinal ligament of the cervical spine has been reported in a large number of Japanese patients and in a few non-Japanese individuals [4–13]. This ossification, which has a characteristic appearance on radiographs, may be associated with cervical myelopathy [4, 5, 7, 8, 10, 12] or produce no symptoms and signs [5, 10, 11, 13–15].

Recently we investigated four patients who demonstrated extensive posterior longitudinal ligament calcification in the cervical spine on initial evaluation. Subsequently, additional radiographs revealed findings of DISH. We present these four patients in detail and describe the incidence of radiographic abnormalities along the posterior aspect of cervical vertebral bodies and intervertebral discs in a large number of patients with DISH.

Case Reports

Case 1

A 71-year-old white man was evaluated at the Hospital of Scripps Clinic because of left lower extremity pain and weakness for 15 years. The pain began as a tingling sensation on the dorsum of the left foot and progressed to involve the ankle, knee, hip, and left buttock. An extensive neurologic and orthopedic evaluation 4 years prior to the current evaluation included myelography and electromyography with inconclusive results. The present physical examination outlined herpes zoster on the left buttock, pronounced restriction of motion of the cervical spine, and muscle atrophy and decreased pain and sensation in the left lower extremity. Laboratory evaluation was unremarkable, although nonspecific electromyographic alterations were apparent in the left leg.

Radiographic examination revealed the findings of DISH, including calcification and ossification along the anterior aspect of the entire vertebral column (fig. 1*A*), bony excrescences about the pelvis, and paraacetabular osteophytes. Prominent calcification and ossification of the posterior longitudinal ligament was noted in the cervical spine (fig. 1*B*). Lumbar myelography demonstrated no significant abnormalities; the cervical canal was not examined. The final impression after extensive neurologic evaluation was that the symptoms were probably related to nerve root involvement in the lumbosacral spine, and that they were accentuated by the presence of herpes zoster.

Case 2

A 57-year-old white man had a complicated medical history which included pulmonary resection for a granuloma related to coccidioidomycosis, adult-onset diabetes mellitus, type IV hyperlipoproteinemia, hypertension, and a hydrocele of the left testicle. His current evaluation at the Hospital of Scripps Clinic for increasing pain and stiffness in the neck and lower back for several years revealed marked restriction of motion of the cervical spine with paraspinous muscle spasm. Some restriction of motion in the lumbar spine with flattening of the lumbar lordosis was also evident. Laboratory examination was unremarkable.

Radiographic evaluation outlined findings of DISH, including new bone formation along the anterolateral aspect of the entire vertebral column, paraacetabular bony excrescences, sacroiliac joint osteophytosis, and patellar hyperostosis. Radiography including tomography of the cervical spine outlined exuberant calcification and ossification of the posterior longitudinal ligament (figs. 2*A* and 2*B*) which was further documented on computed tomography (fig. 2*C*). The patient was referred for appropriate physical therapy.

Case 3

A 64-year-old white man was seen at the Hospital of Scripps Clinic because of low back and lower extremity pain for about 13 years which had required lower lumbar laminectomy for "three slipped discs." Additional musculoskeletal complaints were numbness and tingling of both thighs, pain and stiffness

Received June 30, 1978; accepted after revision August 28, 1978.
This work was supported in part by Veterans Administration grant no. 7406.
D. Resnick is a Picker Scholar of the Picker Foundation.
[1] Department of Radiology, University of California School of Medicine, Veterans Administration Hospital, 3350 La Jolla Village Drive, San Diego, California 92161. Address reprint requests to D. Resnick.
[2] Department of Internal Medicine, Hospital of Scripps Clinic, San Diego, California 92037.
[3] Department of Radiology, Hospital of Scripps Clinic, San Diego, California 92037.

© 1978 American Roentgen Ray Society

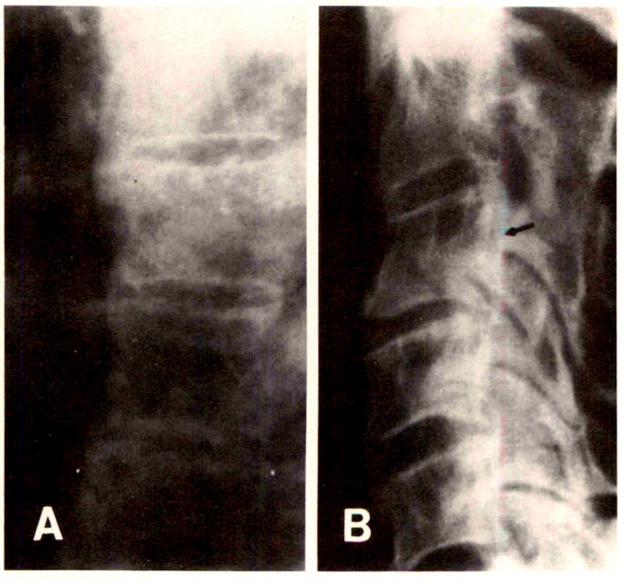

Fig. 1.—Case 1. *A*, Flowing calcification and ossification along anterior aspect of mid and lower thoracic spine. *B*, Note calcification and ossification of posterior longitudinal ligament in cervical spine (*arrow*).

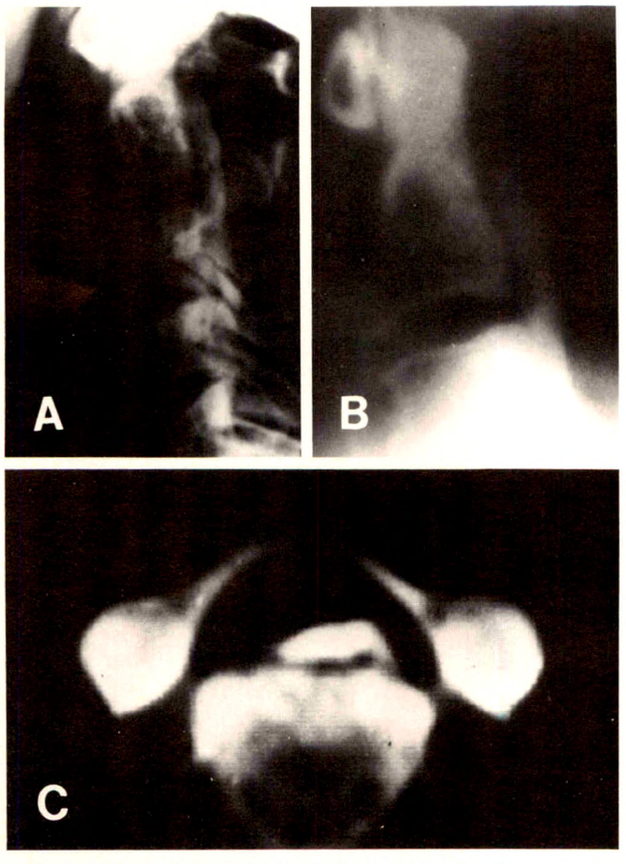

Fig. 2.—Case 2. *A*, Lateral radiograph of cervical spine demonstrating extensive calcification and ossification of posterior longitudinal ligament. Observe radiolucency between radiodense ligament and posterior surface of second cervical vertebral body. *B*, Tomogram demonstrating calcified and ossified posterior longitudinal ligament. *C*, CT scan at level of one cervical vertebral body outlining radiodense ligament separated from posterior aspect of vertebral body.

in the cervical spine, and mild discomfort in the region of the achilles tendon associated with "heel spurs." Physical findings included significant restriction of cervical spine motion, paraspinous muscle spasm of the cervical region, and restriction of forward flexion in the lumbar spine. Neurologic examination and laboratory analysis were within normal limits.

Radiography outlined the changes of DISH, including prominent anterior spinal new bone formation (fig. 3*A*), paraacetabular osteophytes, calcification of iliolumbar ligaments, and pelvic bony excrescences. Cervical spine radiography demonstrated calcification and ossification of the posterior longitudinal ligament (fig. 3*B*). The patient was referred for physical therapy.

Case 4

A 57-year-old white man was evaluated at the Veterans Administration Hospital for pain and decreased range of motion in the neck for several years. The patient also noted pain and numbness along the lateral aspect of the right arm. Previous medical history included Ménière's disease. Laboratory analysis was unrewarding, but electromyography outlined absent sensation of the right arm along the distribution of the ulnar nerve. There was no evidence of motor radiculopathy.

Radiography demonstrated the alterations of DISH with deposition of bone along the anterolateral aspect of the vertebral column, and extensive calcification and ossification of the posterior longitudinal ligament in the cervical spine (fig. 4). Although myelography was recommended, the patient was lost to follow-up.

Cervical Spine Changes in DISH

Review of cervical spine radiographs in 74 patients who met our previously published criteria for DISH [2] documented definite abnormalities along the posterior aspect of the vertebral bodies in 55 patients (74%). These abnormalities could be divided into three types which frequently were found together:

1. Bony hyperostosis (fig. 5). Bony eburnation or sclerosis along the posterior aspect of the vertebral bodies was apparent in 30 patients (41%). This abnormality was most apparent in the upper cervical vertebrae and produced "highlighting" or "whitening" of the posterior cortex.

2. Osteophytosis. Osteophytes protruding from the posterior aspect of the vertebral bodies were noted in 25 patients (34%). They were most frequent in the mid and lower cervical region where they produced bony excrescences, typically small, which protruded into the spinal canal.

3. Posterior longitudinal ligament calcification and ossification. Ligamentous calcification and ossification were apparent in 37 patients (50%). These deposits, particularly frequent in the upper cervical spine, were of variable size, linear in distribution, bumpy in contour, and typically were separated from the subjacent vertebral body by a radiolucency of variable thickness.

These three types of radiographic abnormalities were commonly, but not invariably, associated with alterations along the anterior aspect of the cervical spine which included osteophytes and flowing ossification anterior to the vertebral bodies and intervertebral discs. Although thoracolumbar changes were invariably present allowing

the diagnosis of DISH, there was no definite correlation between the extent of abnormality along the posterior aspect of the cervical vertebrae and that in the thoracolumbar region.

Discussion

Although DISH and posterior longitudinal ligament calcification and ossification have received considerable attention in the medical literature, their possible association has rarely been mentioned. Arlet et al. [16] analyzed 40 patients with cervical myelopathy and noted the frequency of vertebral hyperostosis in these patients. Of the 40 patients, 17 (43%) had both DISH and acquired stenosis of the cervical canal related to bony proliferation along the posterior aspect of the vertebral bodies. The pattern of proliferation included findings similar to those noted in our investigation, such as hyperostosis, osteophytosis, and ligament calcification and ossification.

Ono et al. [17] investigated 166 patients with ossification of the posterior longitudinal ligament. Symptoms in these patients, including motor and sensory disturbances in the lower extremity, were particularly prominent when the ossified posterior longitudinal ligament occupied 60% of the sagittal diameter of the cervical spine. Of 160 patients in that report, 71 (44%) demonstrated concomitant hyperostosis on the anterior aspect of the vertebral column. Postmortem examination of two patients with both posterior longitudinal ligament calcification and DISH revealed that the ossification of the posterior longitudinal ligament was particularly prominent in its superficial layer, whereas the unossified deep layer was thickened, creating a radiolucency between the ossified ligament and underlying vertebral body. At the craniocervical junction, histologic evaluation outlined proliferation of cartilagelike cells and hyperplasia of the matrix within the posterior longitudinal ligament. These findings did not document the sequence of events which occurs in this condition, but suggested that although anterior and posterior longitudinal ligament calcification and ossification frequently coexist, definite and remarkable differences in their pathology can be noted.

Although patients with posterior longitudinal ligament ossification may be asymptomatic [13], a variety of symptoms and signs have been associated with this disorder [4–12]. Parasthesias may vary from intermittent sensations, including numbness or tingling of several digits of one or both upper extremities, to extensive and severe anesthesia of the trunk and lower extremities [6]. Motor disturbances, such as weakness, incoordination, and instability, may be encountered in upper and lower extremities. Additional symptoms may include head and neck pain and stiffness, urinary and rectal incontinence and

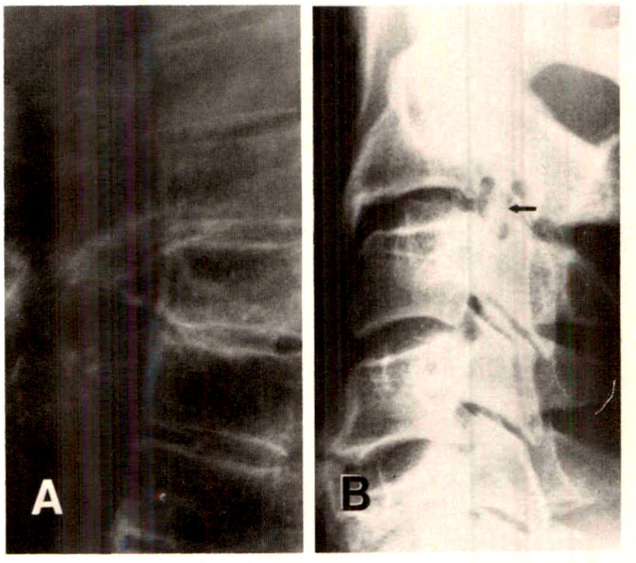

Fig. 3.—Case 3. *A*, Typical flowing ossification in thoracic spine. *B*, Calcification and ossification of posterior longitudinal ligament at level of second and third cervical vertebral bodies (*arrow*).

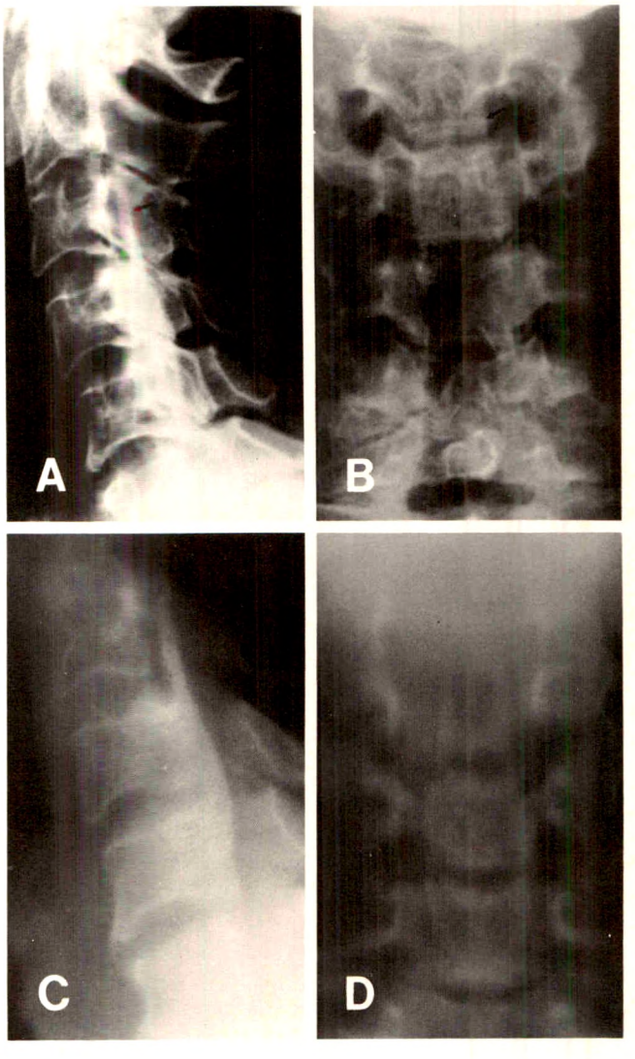

→

Fig. 4.—Case 4. *A and B*, Lateral and frontal radiographs of cervical spine demonstrating widespread calcification and ossification of posterior longitudinal ligament (*arrows*). *C and D*, Lateral and frontal tomograms better delineating these findings.

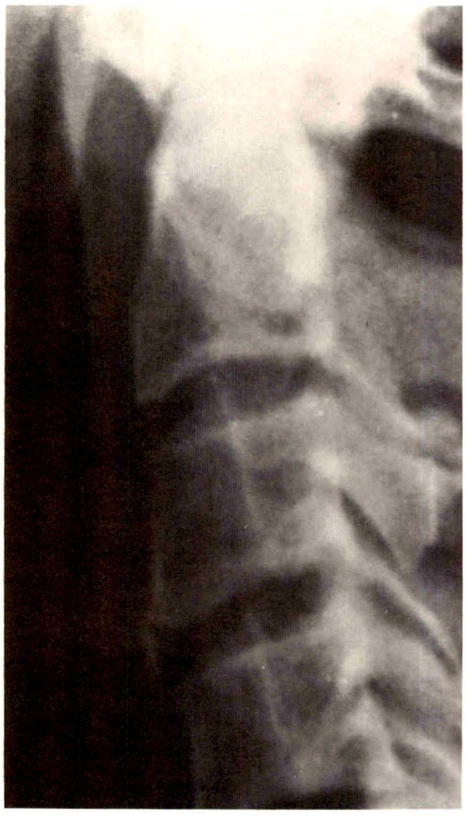

Fig. 5.—Hyperostosis of posterior surface of second, third, and fourth cervical vertebral bodies.

dysfunction, and loss of libido. On physical examination, patients may reveal muscle atrophy, fasciculations, hyperreflexia, and sensory loss. The reported incidence of these findings has varied considerably, and the symptoms and signs are, in general, nonspecific, being present in other disorders of the spinal canal and cord.

Our previous investigations of patients with DISH did not emphasize abnormalities of the posterior aspect of the cervical vertebrae, although we did note some patients with DISH who revealed posterior longitudinal ligament ossification, and others who demonstrated small posterior cervical spine osteophytes and hyperostosis [18]. It is apparent from our closer evaluation of these and additional patients with DISH that such alterations are frequent in the disease. Furthermore, our recent experience with the four patients reported here suggests that posterior longitudinal ligament calcification and ossification in the cervical spine may become extensive in this disorder.

This observation is important, as deposition of calcium and bone along the posterior aspect of the vertebral bodies and intervertebral discs may compromise the integrity of the spinal cord, leading to significant neurologic findings. Some of the neurologic abnormalities in three of these four patients (cases 1, 3, and 4) may indeed have resulted from such ossification; it is therefore imperative that the radiologist search diligently for these changes. Thus, lower extremity muscle atrophy and senosry loss in case 1, numbness and tingling of the thigh in case 3, and upper extremity numbness and sensory loss in case 4 may have been related to posterior longitudinal ligament ossification. Tomography of the spine may be necessary for adequate evaluation; in one of our patients, computed tomography revealed not only the presence of posterior longitudinal ligament calcification and ossification but the extent of spinal canal impingement. Human et al. [19] previously described a patient with cervical myelopathy in whom computed tomography documented the presence and extent of ossification within the posterior longitudinal ligament.

It is apparent from this review that a great number of patients with DISH will reveal significant posterior vertebral abnormalities. Although we have not analyzed cervical spine radiographs in an age- and sex-matched "normal" control population, our brief review of about 20 cervical spine examinations in elderly patients yielded some with bony hyperostosis and minor degrees of osteophytosis. Posterior longitudinal ligament calcification and ossification were not apparent, suggesting that these latter changes are indeed associated with DISH. If DISH is considered a frequent disease in this country with an incidence that may reach 12% of middle-aged and elderly patients [18], calcification and ossification of the posterior longitudinal ligament should no longer be regarded as findings almost confined to Japanese individuals.

REFERENCES

1. Resnick D, Shaul SR, Robins JM: Diffuse idiopathic skeletal hyperostosis (DISH): Forestier's disease with extraspinal manifestations. *Radiology* 115:513–524, 1975
2. Resnick D, Niwayama G: Radiographic and pathologic features of spinal involvement in diffuse idiopathic skeletal hyperostosis (DISH). *Radiology* 119:559–568, 1976
3. Forestier J, Rotes-Querol J: Senile ankylosing hyperostosis of the spine. *Ann Rheum Dis* 9:321–330, 1950
4. Nakanishi T, Mannen T, Toyokura Y, Sakaguchi R, Tsuyama N: Symptomatic ossification of the posterior longitudinal ligament of the cervical spine. *Neurology* 24:1139–1143, 1974
5. Bakay L, Cares HL, Smith RJ: Ossification in the region of the posterior longitudinal ligament as a cause of cervical myelopathy. *J Neurol Neurosurg Psychiatr* 33:263–268, 1970
6. Takahashi M, Kawanami H, Tomonaga M, Kitamura K: Ossification of the posterior longitudinal ligament. A roentgenologic and clinical investigation. *Acta Radiol [Diagn]* (Stockh) 13:25–36, 1972
7. Soo YS, Sachdev AS: Calcification in the posterior longitudinal ligament as a cause of cervical myelopathy. *Med J Aust* 1:743–744, 1971
8. Op den Orth JO: Die Verkalkung bzw. Verknocherung des Ligamentum Longitudinale Posterius der Halswirbelsaule. *Fortschr Geb Roentgenstr Nuklearmed* 122:442–445, 1975
9. Lagemann VK: Hintere Langsbandverkalkungen kombiniert mit virbelkorperexkavationen. *Fortschr Geb Roentgenstr Nuklearmed* 116:834–835, 1972
10. Minagi H, Gronner AT: Calcification of the posterior longitudinal ligament: a cause of cervical myelopathy. *Am J Roentgenol* 105:365–369, 1969

11. Hiramatsu Y, Nobechi T: Calcification of the posterior longitudinal ligament of the spine among Japanese. *Radiology* 100:307–312, 1971
12. Nagashima C: Cervical myelopathy due to ossification of the posterior longitudinal ligament. *J Neurosurg* 37:653–660, 1972
13. Nakanishi T, Mannen T, Toyokura Y: Asymptomatic ossification of the posterior longitudinal ligament of the cervical spine. *J Neurol Sci* 19:375–381, 1973
14. Yanagi T: Ossification of the posterior longitudinal ligament. A clinical and radiological analysis of forty-six cases. *Brain Nerve* 22:909–921, 1970
15. Palacios E, Brackett CE, Leary DJ: Ossification of the posterior longitudinal ligament associated with a herniated intervertebral disc. *Radiology* 100:313–314, 1971
16. Arlet PJ, Pujol M, Buc A, Geraud G, Gayrard M, Latorzeff S: Rôle de l'hyperostose vertebrale dans les myelopathies cervicales. *Rev Rhum Mal Osteoartic* 43:167–175, 1976
17. Ono K, Ota H, Tada K, Hamada H, Takaoka K: Ossified posterior longitudinal ligament. A clinicopathologic study. *Spine* 2:126–138, 1977
18. Resnick D, Shapiro RF, Wiesner KB, Niwayama G, Utsinger PD, Shaul SR: Diffuse idiopathic skeletal hyperostosis (DISH). Ankylosing hyperostosis of Forestier and Rotes-Querol. *Semin Arthritis Rheum* 7:153–187, 1978
19. Hyman RA, Merten CW, Liebeskind AL, Naidich JB, Stein HL: Computed tomography in ossification of the posterior longitudinal spinal ligament. *Neuroradiology* 13:227–228, 1977

Intraarticular Methyl Methacrylate: A Complication of Hip Surgery

CHANDRAKANT C. TAILOR,[1] WILLIAM A. MURPHY, AND EMILY L. SMITH

Methyl methacrylate, used as a grout during hip arthroplasty, can inadvertently become lodged between acetabular and femoral components during surgery. After resumption of ambulation, crescentic fragments may extrude into the pseudocapsule. If mobile methyl methacrylate fragments lodge within the joint, late surgical failure may result because of methyl methacrylate's abrasive character. Two cases of total hip replacement and one case of femoral arthroplasty are reported in which intraarticular methyl methacrylate was identified retrospectively; all three patients remain asymptomatic at the time of the report.

Numerous complications of total hip arthroplasty are known [1]. Methyl methacrylate, used as a grout in hip arthroplasty, may lodge between the acetabular and femoral components during surgery. Three cases of this complication are reported.

Case Reports

Case 1

A 66-year-old woman with right hip arthritis since age 16 underwent cup arthroplasty in 1967. Between 1970 and 1977, four total hip replacements were necessary due to various complications. In September 1977, she became unable to flex her right knee more than 30° and developed right hip, buttock, and thigh pain.

Intraoperative radiography in April 1977 (fig. 1*A*) showed a density interposed between the prosthetic femoral head and the acetabular cup, although this finding was not recognized at that time. Follow-up radiography in June 1977 (fig. 1*B*) showed a crescentic density at the superolateral aspect of the joint. The crescentic mold of methyl methacrylate had displaced from its position between the femoral and acetabular components, but remained in an intraarticular location within the postoperative pseudocapsule.

Case 2

A 75-year-old woman underwent right femoral head and neck replacement following subcapital femoral fracture. Intraoperative radiography in June 1977 (fig. 2A) showed methyl methacrylate interposed between the natural acetabulum and the prosthetic femoral head; again, this finding was not appreciated at the time. Follow-up radiography in August 1977 (fig. 2*B*) showed extrusion of multiple methyl methacrylate crescents into the pseudocapsule.

Case 3

A 91-year-old woman sustained an intertrochanteric fracture of the left femur, which was treated by compression screw internal fixation. When the internal fixation device loosened 20 months later, the patient underwent total hip arthroplasty. Intraoperative radiography (fig. 3*A*) in December 1976 showed methyl methacrylate interposed between the acetabular and femoral components. Follow-up radiography (fig. 3*B*) in June 1977 showed a crescent of methyl methacrylate within the pseudocapsule.

Comment. In all three cases, intraarticular presence of methyl methacrylate was detected retrospectively on review of intraoperative radiographs. So far all three patients have remained asymptomatic.

Discussion

During the past two decades, hip arthroplasty and total hip replacement have helped rehabilitate many patients previously incapacitated by severe degenerative or rheumatoid arthritis, avascular necrosis, intertrochanteric or femoral neck fractures, and other causes of chronic pain or loss of motion [2]. Replacement surgery requires removal of the diseased part and insertion of a femoral component alone or in combination with an acetabular component. These prosthetic parts are fixed in position with barium impregnated methyl methacrylate, which acts as a grout.

At surgery, methyl methacrylate is mixed from powdered monomer and liquid resin. While still semisolid, the polymer is used to fix the prosthetic components, which must be held firmly in place until the grout has hardened. The acetabular component is fixed first, followed by the femoral component. After the components are firmly seated in bone, the prosthetic hip joint is reduced. Because of methyl methacrylate's initial semisolid form, it is not uncommon to find small amounts extruded into pockets not visible to the surgeon, although care is taken to control its flow. The three cases reported here demonstrate this situation. As the prosthetic hip joint was being reduced, a small amount of methyl methacrylate became interposed between the joint surfaces. When hardened, the methyl methacrylate retained the crescentic shape of the articular surface. All three cases had their hip surgery at the same hospital using similar surgical techniques.

In each instance, when ambulation was resumed, the methyl methacrylate cast displaced and migrated within the joint, coming to rest within the pseudocapsule, away from the articular surfaces. The displaced fragments of methyl methacrylate should be differentiated from the heterotopic bone formation frequently seen about prosthetic hips. Methyl methacrylate can be recognized by its uniform density and globular nature, while heterotopic bone formation has the variable appearance of myositis ossificans. Crescentic fragments, as in our cases, should be recognized as methyl methacrylate. As demonstrated by case 2, multiple fragments may be present. None of

Received May 26, 1978; accepted after revision September 11, 1978.

[1] All authors: Mallinckrodt Institute of Radiology, 510 South Kingshighway, St. Louis, Missouri 63110. Address reprint requests to C. C. Tailor.

© 1978 American Roentgen Ray Society

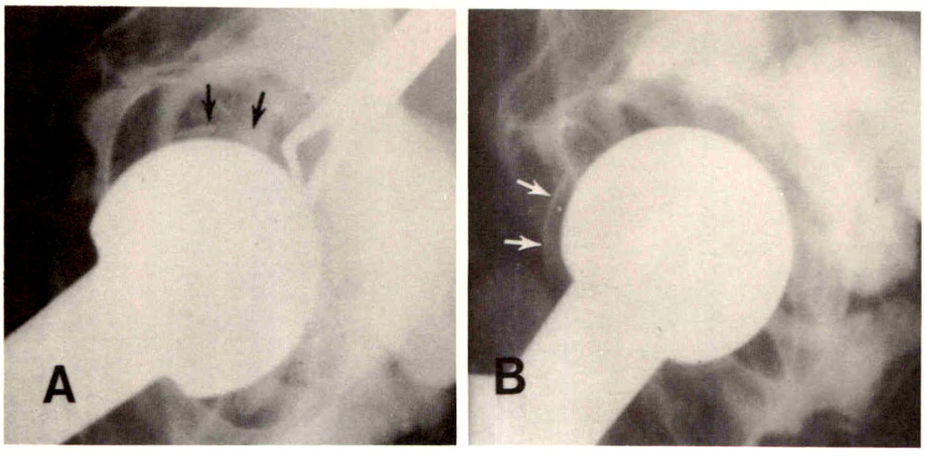

Fig. 1.—Case 1. *A*, Crescentic shadow (*arrows*) between femoral head and acetabular cup during surgery. *B*, 2 months later, methyl methacrylate (*arrows*) extruded into pseudocapsule.

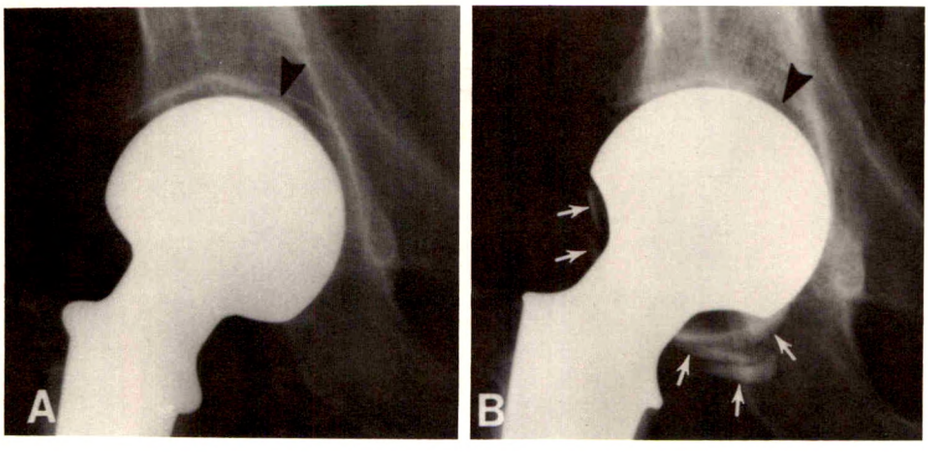

Fig. 2.—Case 2. *A*, density (*arrow*) between femoral head and acetabulum during surgery. *B*, 2 months later, multiple crescentic fragments of methyl methacrylate (*arrows*) extruded into pseudocapsule, displaced from original position (*arrowhead*).

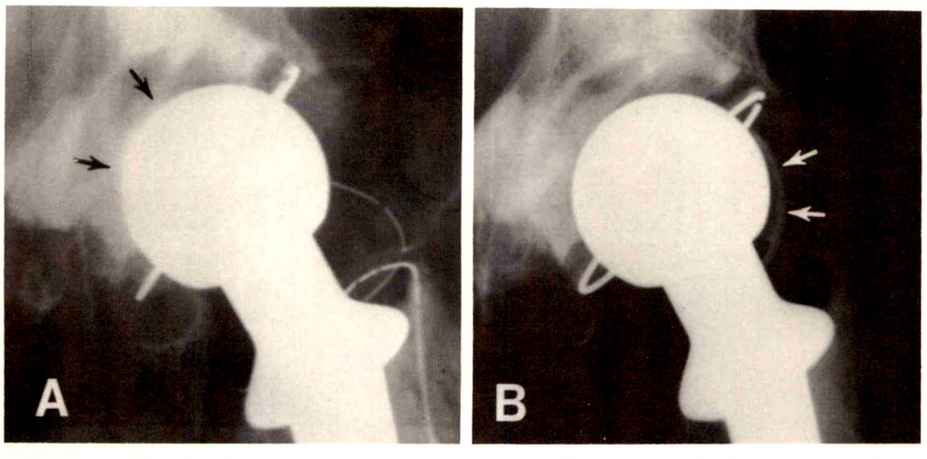

Fig. 3.—Case 3. *A*, Methyl methacrylate (*arrows*) interposed between femoral head and acetabular cup during surgery. *B*, 6 months later, methyl methacrylate (*arrows*) extruded into pseudocapsule.

our patients has experienced a problem directly related to the intracapsular fragments, although such a problem could occur. If one or more of the fragments were to become interposed between the articular surfaces once again, mechanical compromise of joint function could result. In addition to pain and decreased motion, dysfunction might manifest as subluxation, dislocation, locking, or rapid deterioration of the components.

Foreign body interposition between hip arthroplasty components has been reported. Fragments of wire su-

tures used to reattach an osteotomized greater trochanter have caused persistent dislocation and late prosthetic failure [3, 4]. Eftekhar et al. [1] tabulated two cases of prosthetic subluxation from methyl methacrylate fragments lodged between the femoral head and acetabular cup. As demonstrated by our three cases, the intracapsular position of mobile methyl methacrylate fragments can be recorded prior to any complication. The surgeon is then alerted to the causative agent for acute complication. At this time, it seems unnecessary to remove these fragments unless a complication occurs.

REFERENCES

1. Eftekhar NS, Kiernan HA, Stinchfield FE: Systemic and local complications following low-friction arthroplasty of the hip joint. *Arch Surg* 111:150–155, 1976
2. Harris WH: Current concepts: total joint replacement. *N Engl J Med* 297:650–651, 1977
3. Campbell RE, Marvel JR Jr: Concomitant dislocation and intraarticular foreign body: a rare complication of the Charnley total hip arthroplasty. *Am J Roentgenol* 126:1059–1062, 1976
4. Bronson JE: Articular interposition of trochanteric wires in a failed total hip replacement. *Clin Orthop* 121:50–52, 1976

Postoperative Bony Stenosis of the Lumbar Spinal Canal: Evaluation of 164 Symptomatic Patients with Axial Radiography

ROBERT M. QUENCER,[1] F. REED MURTAGH,[1] M. JUDITH D. POST,[1] HUBERT L. ROSOMOFF,[2] AND NORMAN A. STOKES[1]

Computed tomography (CT) and transverse axial tomography (TAT) were used to study the lumbar spines of 164 patients with persistent or recurrent low back pain and/or radiculopathy. Of those patients with previous spinal fusion and of those with previous disectomy, 43% and 28%, respectively, demonstrated bony stenosis of the lumbar spinal canal. Of the patients who underwent surgery for this narrowed canal, 91% showed clinical improvement.

A stenotic spinal canal is a structural abnormality which may be focal, segmental, or generalized and is caused by bony or soft tissue encroachment upon the canal and/or neural foramina. If infection, uncomplicated disc herniation, tumor, and tumorlike conditions are excluded, there are two basic categories of canal stenosis, congenital or acquired [1]. Congenital causes include developmental stenosis and achondroplasia. Acquired causes include spondylosis, spondylolithesis, trauma, iatrogenic causes, or any combination of these etiologies [1–6].

Although iatrogenic causes of canal stenosis have been mentioned [2, 3, 6–13] only one study has been devoted exclusively to the study of canal stenosis after both lumbar laminectomy and lumbar fusion [7]. In that study myelography was the primary radiographic method used to diagnose a narrowed canal. However, the density of Pantopaque will obscure early changes of canal stenosis and will give only limited information concerning the lateral recesses and the intervertebral foramina [3, 12, 14]. Kirkaldy-Willis et al. [12] found that myelography occasionally will fail to reveal the presence of stenosis, particularly when protrusion of enlarged articular processes produces, in cross section, a cloverleaf configuration of the canal. In those myelograms, the anteroposterior and lateral dimensions of the canal will appear to be within normal limits.

In conventional plain film radiography of the lumbar spine, measurements of the interpedicular distance [15], the intervertebral foramen [16], or the anteroposterior limits of the spinal canal [17] are even less effective than myelography in detecting a narrowed spinal canal. Previous reports [4, 18] indicate that the maximum area of canal narrowing occurs posterior to the pedicles at the level of the articular processes. In fact, Verbiest [18] reported seven cases of developmentally narrowed canals, all of whom had normal interpedicular measurements. The exact dorsal and ventral borders of the intervertebral foramen are frequently hard to define and this measurement has only a fair correlation [16] with the true sagittal width of the canal as determined on Pantopaque myelography. The anteroposterior dimension of the canal which theoretically could more correctly assess canal size, compared with interpedicular distance or intervertebral foramen measurement [18, 19], is difficult to determine [17, 20]. Attempts have even been made to eliminate variables such as patient size and radiographic magnification factors by establishing canal to vertebral body ratios [20] in hopes of more accurately defining canal stenosis. These ratios however are rarely, if ever, used.

Because of the limitations of plain film radiography and myelography in determining spinal canal size, a mode of imaging the spine in an axial plane, such as transverse axial tomography (TAT) or computed tomography (CT), is desirable. The ability of both of these methods to determine the presence of a stenotic canal has been reported [3, 6, 14, 21] and isolated examples of lumbar fusion overgrowths on CT and TAT have been shown [3, 6, 14]. However there are no previous reports of the use of axial radiography in a large series of postoperative lumbar spine patients to determine the presence of bony canal stenosis.

In this study we used axial radiography in 164 symptomatic postoperative lumbar spine patients to determine the incidence of postdisectomy and postfusion bony canal stenosis. Of those patients with canal stenosis, clinical follow-up was obtained in 80%, which allowed us to measure the significance of these radiographic findings.

Subjects and Methods

Over a 3 year period, 164 patients who had undergone one or more previous lumbar spine operations were seen at the University of Miami/Jackson Memorial Medical Center for evaluation of continued, recurrent, or worsening of low back pain and/or radicular symptoms. The patients were divided into two groups: (1) those with prior surgery for disc herniation (110 cases) and (2) those who had prior posterior lumbar fusion (54 cases). Within the first group a wide spectrum of bone excision was seen including minimal laminectomy defects, wide laminectomies, partial facetectomies, and foraminotomies,

Received October 4, 1977; accepted after revision August 16, 1978.
Presented in part at the annual meeting of the American Roentgen Ray Society, Boston, September 1977 and the American Society of Neuroradiology, New Orleans, February 1978.

[1] Department of Radiology, University of Miami Medical Center, Jackson Memorial Hospital, Biscayne Annex, Miami, Florida 33152. Address reprint requests to R. M. Quencer.
[2] Department of Neurological Surgery, University of Miami Medical Center, Jackson Memorial Hospital, Miami, Florida 33152.

© 1978 American Roentgen Ray Society

reflecting variability in surgical approach for disc herniation. Because of that complex situation, this group will simply be called postdiscectomy. Within the second group, the posterior lumbar fusion was either the only procedure performed or it was preceded by one or more spinal operations. This group will be called postfusion. The percentage of patients with canal stenosis was determined for each group. Clinical follow-up was obtained from patient records. Of the patients operated on for canal stenosis, the number who improved clinically after surgery were those who felt that the procedure was a success. No attempt was made to grade the degree of improvement.

Transverse axial tomography (TAT) and computed tomography (CT) were used to evaluate the size and contour of the bony lumbar canal. TAT was performed with the Toshiba Radiotherapeutic Unit (Toshiba Medical Co., Carson, Calif.) in which the image of a 3-mm-thick section of the spine is recorded on standard radiographic film. CT was performed on the General Electric CT/T scanner in which mathematically reconstructed 10-mm-thick sections will image not only the osseous structures of the spine but the associated soft tissues. Although we routinely use an opaque marking system [13, 14] for determining the level of axial sectioning with CT and TAT, the use of surrounding landmarks [22] is also used with CT to confirm the level which has been sectioned. Multiple axial sections from at least the L3 through the S1 level were obtained and when clinically indicated, higher or lower levels were included.

Both methods show that from L1 through L5 the canal changes from an oval to a triangular configuration and that there is a variation in shape between the articular osseous segments which alternate in sequence along the length of the lumbar spine [3, 13, 14, 22, 23]. At the articular segments Gargano [13] determined with TAT the range of normal for the interfacet distance at the lower portion of L5-S1 (30–38 mm), the upper portion of L5-S1 (27–36 mm), and at the L4-L5 level (22–31 mm). Normal interfacet distances at the various lumbar levels have also been determined with CT of the spine [22] and they are comparable to those found with TAT.

Although we measured the interfacet distances in our cases, we also used the presence of abnormal bony contours such as thickened lamina, a flattened triangular shape of the canal, and hypertrophied articular facets [6, 14, 22, 24, 25] to determine canal narrowing since these factors are more sensitive indicators of the presence of bony canal stenosis or focal bony changes involving the lateral recesses or neural foramina. With posterior lumbar fusions, osseous overgrowth may obliterate normal bony landmarks such as the facet joints, lamina, and articular processes so in these cases also the overall size and shape of the canal rather than any specific measurement is of primary importance.

Results

Of the 110 postdiscectomy patients, 94 were examined with TAT and 16 with CT: canal stenosis was found in 28 by TAT and in three by CT, an incidence of 28% (table 1). Of 54 postfusion patients, 46 were examined with TAT and eight by CT: canal stenosis was found in 19 by TAT and in four by CT, an incidence of 43% (table 1). Combining the postfusion and postdisectomy groups yields an overall incidence of 33% bony canal stenosis in the symptomatic postoperative lumbar spine patient.

Clinical follow-up was obtained on 43 of the 54 patients with canal stenosis (table 2). Nine of the 31 postdiscectomy patients and 14 of the 23 postfusion patients underwent surgery; eight (of nine) postdiscectomy patients and 13 (of 14) postfusion patients experienced symptomatic improvement following removal of the offending bone, a combined overall improvement of 91%. Of those patients who were not operated on, five refused surgery, nine were treated with medical and/or psychiatric support, and in five a decision concerning their future clinical management is pending. In one, an incidental postoperative pseudomeningocele discovered at myelography was successfully repaired.

Because image reproducibility for publication is better with CT than with TAT our findings are illustrated below with CT of the spine even though the majority of patients were examined with transverse axial tomography.

Representative Case Reports

Case 1: Postdiscectomy Stenosis

A 55-year-old male had an L5 laminectomy and discectomy for a left sided L5-S1 herniated nucleus pulposus 2 years prior to admission. That operation failed to relieve his symptoms and over the past 6 months there was an actual increase in his low

TABLE 1

Symptomatic Postoperative Spinal Patients

	Total Patients	No. with Canal Stenosis
Postdiscectomy:		
Examined by TAT	94	28
Examined by CT	16	3
Total	110	31(28)
Postfusion:		
Examined by TAT	46	19
Examined by CT	8	4
Total	54	23(43)

Note. – Numbers in parentheses are percentages.

TABLE 2

Clinical Follow-Up

	Post-discectomy	Postfusion	Totals
Underwent surgery:			
Improved	8	13	21
No change	1	1	2
Refused surgery	3	2	5
Medical/psychiatric management	7	2	9
Incidental pseudomeningocoele	1	. . .	1
Decision pending	3	2	5
Lost to follow-up	8	3	11
Total	31	23	54

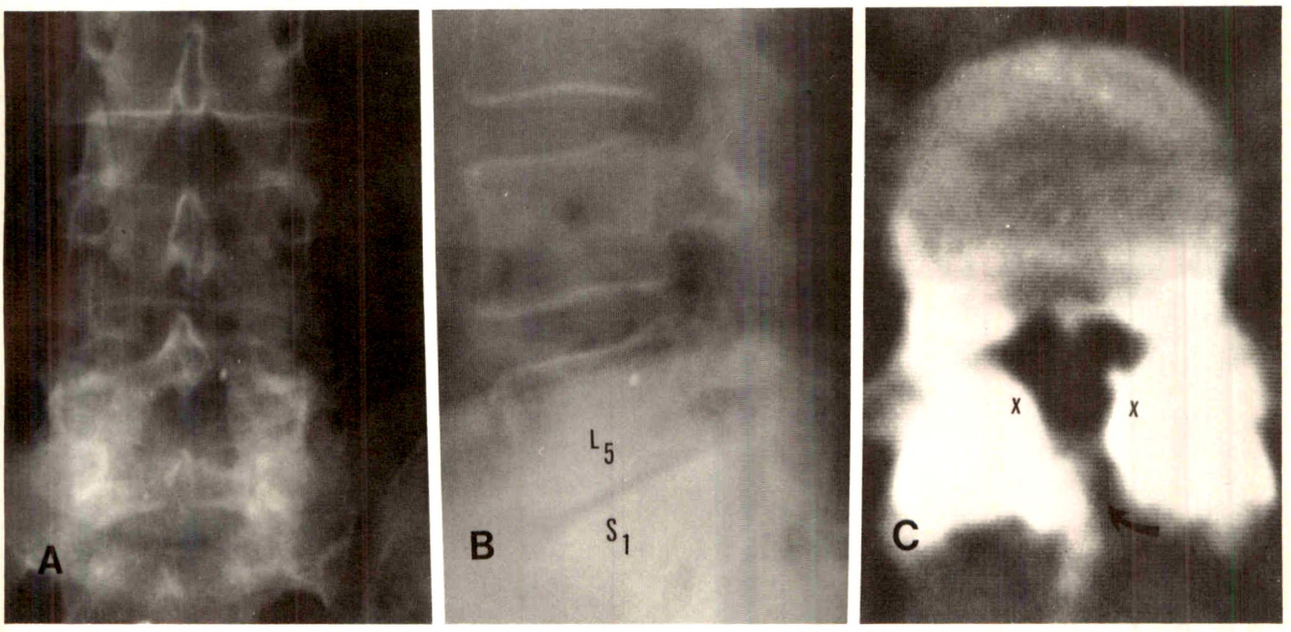

Fig. 1.—Case 1: postdiscectomy stenosis. *A*, Anteroposterior lumbar spine showing L5 laminectomy done for left sided L5-S1 herniated nucleus pulposus. *B*, Lateral film showing degenerative sclerosis of both L5–S1 facet joints associated with marked disc space narrowing and sclerosis of adjacent portions of L5 and S1 vertebral bodies. *C*, CT scan at L5-S1 showing facet sclerosis and hypertrophy (x) encroaching upon spinal canal. Upper portion of left laminectomy defect is seen (*arrow*).

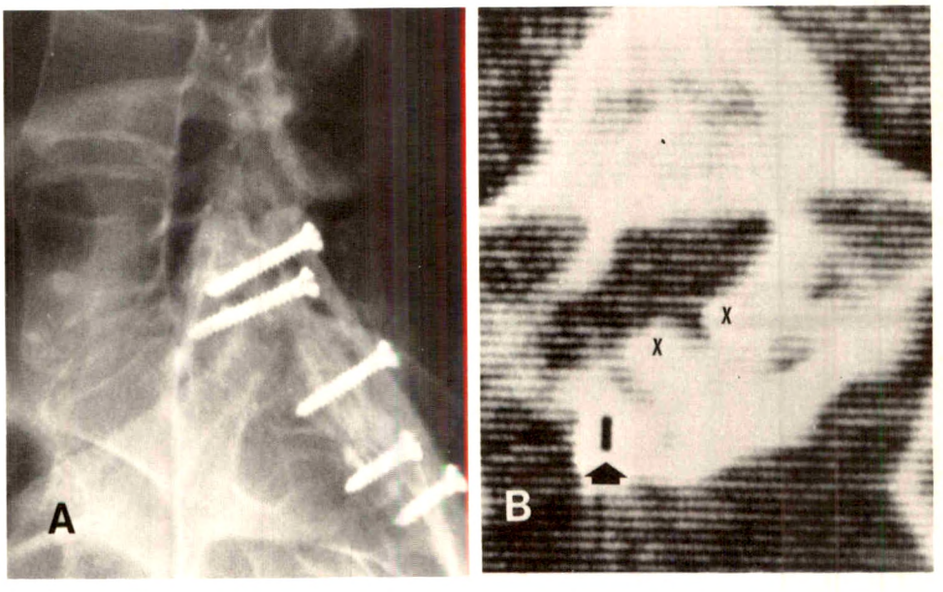

Fig. 2.—Case 2: postfusion stenosis (fusion overgrowth). *A*, Lateral lumbosacral spine film showing metallic screws and posterior bone graft extending from L5 through midsacral region. *B*, CT scan at L5–S1 level showing asymmetric bony stenosis of spinal canal, with dorsal and left lateral bony encroachment (x). Cursor (*arrow*) is seen on one metallic screw

back pain. Plain films of the lumbar spine (figs. 1*A* and 1*B*) showed the postsurgical changes at L5, disc space narrowing at L5–S1, sclerosis of the adjacent vertebral end plates, and degenerative changes of the L5–S1 facet joints bilaterally. The extent of spinal canal stenosis secondary to the hypertrophied articulating facets at L5–S1 is seen on the CT scan at that level (fig. 1*C*).

Case 2: Postfusion Stenosis

Fusion overgrowth.—A 32-year-old female with prior L4–L5 and L5–S1 discectomies had dowel graft fusion of her lower lumbar spine from L5 through S3. She experienced gradually increasing low back pain over the next 4 years. The lateral spine film (fig. 2*A*) showed the posterior fusion mass and the metallic screws, but even with anteroposterior and oblique films the canal width could not be accurately determined. CT of the spine at L5–S1 (fig. 2*B*) showed bony overgowth at the fusion site with consequent encroachment of the spinal canal.

Case 3: Postfusion Stenosis

Degenerative changes above a lumbar fusion.—A 45-year-old male with prior L4–L5 and L5–S1 discectomies and an L4 through S1 posterior spinal fusion (fig. 3*A*) had gradual recurrence of low back pain. A CT scan through the lower lumbar

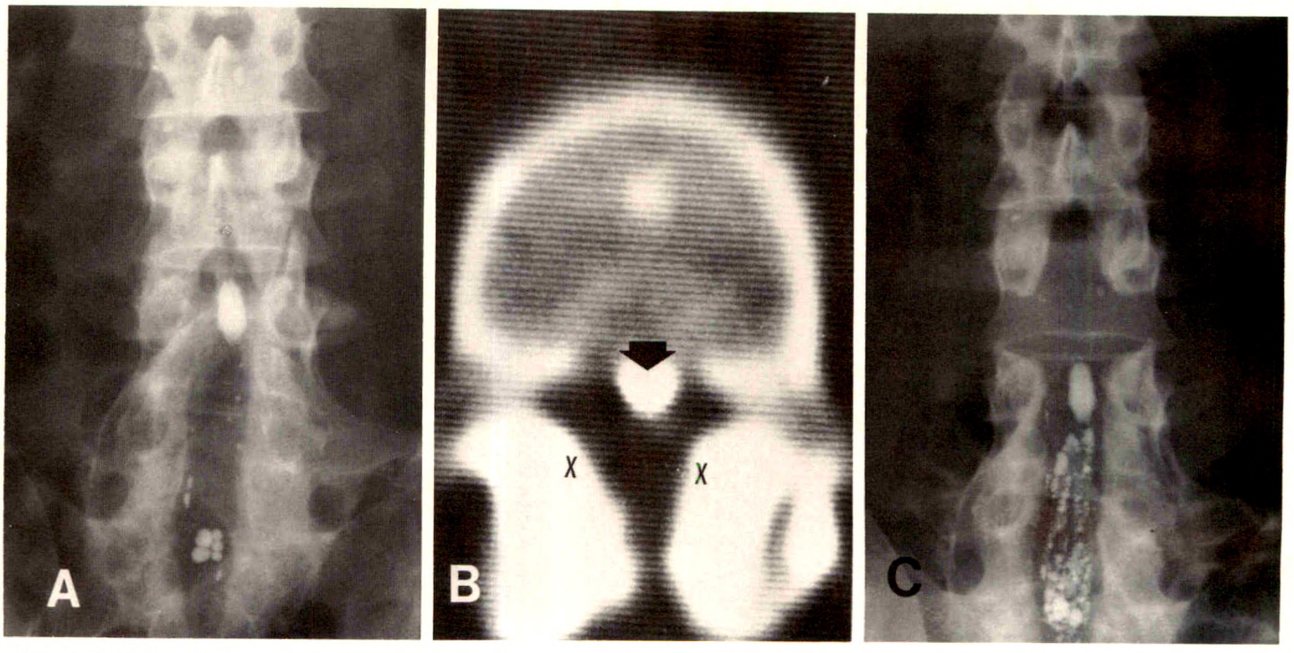

Fig. 3.—Case 3: postfusion stenosis (spondylosis above fusion). *A*, Anteroposterior lumbar film showing L4, L5, and S1 laminectomy and L4 through S1 posterior lumbar fusion. *B*, CT scan at L3–L4 (first mobile section above fusion) showing degenerative and hypertrophied articulating facets (x) resulting in stenotic canal. Axial sections through areas of prior fusion showed no evidence of stenotic canal or bony overgrowth. Droplet of Pantopaque is present along ventral surface of canal at L3–L4 (*arrow*). *C*, Postoperative anteroposterior film showing removal of superior and inferior articulating facets at L3–L4 along with L3 lamina. There was marked symptomatic improvement.

spine showed no evidence of fusion overgrowth, but at L3–L4 there was evidence of substantial facet enlargement causing a narrowed canal (fig. 3*B*). There was symptomatic improvement after an L3 laminectomy and complete bilateral facetectomies at L3–L4 (fig. 3*C*).

Discussion

In the previously operated lumbar spine the recurrence or persistence of low back symptoms may be due to disc reherniation, disc herniation at another level, arachnoiditis,.epidural scarring, infection, mechanical instability, retained foreign body, a surgically produced arachnoidal cyst, spinal stenosis, functional causes, or a combination of any of the above. Radiographic evaluation of these patients has traditionally included plain films of the lumbar spine and, when necessary, myelography. Although both are adequate in diagnosing many of the structural abnormalities occurring in the postoperative spine, they are frequently inaccurate in diagnosing a stenotic canal, particularly when there is only moderate bony prominence. For these reasons we feel that axial radiography is an equally important method in the evaluation of these symptomatic patients.

Bony canal stenosis usually does not receive much consideration as a diagnostic possibility in the symptomatic postoperative patient, particularly in the absence of a prior posterior lumbar fusion. It has been the primary subject of only a few articles [7, 11], although various investigators have acknowledged its existence by mentioning postoperative canal stenosis as either part of a review of the entire subject of the stenotic canal or in discussing the results of lumbar fusion [2, 3, 6, 9, 10, 26, 27]. Brodsky [7] reviewed 552 cases of lumbar stenosis and found, with myelography, 231 cases (41%) in previously operated spines (125 postlaminectomy, 106 postfusion). The canal narrowing was due not only to thickened lamina, medially protruding articulating facets, and spondolytic spurs, but also due to soft tissue prominence such as thickened ligamentum flava, thickened dura, and scar tissue. Wedge et al. [10] indicated that of 130 cases of canal stenosis, 20 were iatrogenic (13 postdiscectomy, seven postfusion). Measurements of the lumbar spinal canal in the anteroposterior and lateral dimensions of plain films were used in that study.

Our study differed from these investigations in two major respects: (1) we set out to determine the incidence of bony canal stenosis in the symptomatic postoperative patient and (2) we utilized axial radiography rather than myelography or routine radiography in diagnosing canal stenosis. Our results indicate that bony canal stenosis is a surprisingly common finding in the symptomatic postoperative patient. It was found in 28% of patients with prior discectomies and 43% of patients with previous posterior lumbar fusions, an overall incidence of 33% (tables 1 and 2). Our data do not define whether the narrowed canal was present preoperatively, developed as a direct result of surgery or developed postoperatively as part of a progressive degenerative spondylosis.

Iatrogenic causes of bony canal stenosis are usually considered to be related to hypertrophy of a posterior

bone graft [2, 3, 6, 7, 9, 10, 14, 27] with overgrowth into the canal especially when an interlaminar fusion mass has been used [7]. There is apparently no difference in the incidence of canal stenosis whether the fusion is solid or pseudoarthrosis exists [7]. Because of the occurrence of postoperative spinal stenosis [7, 28] when posterior grafts between the lamina and spinous processes have been used, posterolateral intertransverse process fusions are advocated whenever possible.

Less well recognized than fusion overgrowths, but nonetheless of great importance, is the bony canal stenosis seen in postdiscectomy patients. Although in these cases the narrowed canal may result from thickened lamina following periosteal stripping [7] during laminectomy or from degenerative changes of the facet joints after a partial facetectomy, it is possible that a stenotic canal was undiagnosed prior to the initial surgery [2, 7, 9, 28–36]. Tile et al. [29] reviewed 15 cases of canal stenosis in patients who had prior surgery and felt, in re-reading the surgical notes, that all those patients had a stenotic canal not originally recognized by the surgeon. Ehni [35] sums up this problem by suggesting that the removal of a disc in a patient with lumbar spondylosis as though the disc were the sole abnormality "invites therapeutic failure."

The development of a narrowed canal postoperatively as part of an ongoing degenerative spondylosis may occur after either a discectomy or fusion procedure. Surgical removal of disc material from the intervertebral disc space may incite changes within zygoapophyseal joints similar to those caused by primary disc degeneration. As Harris and MacNab [37] pointed out, the nucleus pulposus is normally the area over which vertebral bodies move with positional change, but that with disc degeneration this motion now occurs posteriorly through the facet joints. With repeated flexion-extension movements, damage to these joints can occur with resultant degenerative hypertrophy of the articulating facets and facet subluxation. After a fusion, degenerative changes causing stenosis may occur at the upper end of the graft [10] or there may be increased and accelerated spondylosis at the next higher mobile segment [33].

The most important factor we investigated in this study was the significance of bony canal stenosis in the symptomatic postoperative lumbar spine patient. The clinical follow-up of these patients (table 2) clearly indicates the help which can be offered to those patients who have a narrowed canal. Of those patients who underwent surgery, clinical improvement was achieved in 89% in the postdiscectomy group and 93% in the postfusion group, a combined success rate of 91%. In previously operated spines, clinical improvement in the vast majority of patients has been reported following the removal of overgrowth fusion masses [2, 11, 26]. Brodsky [7] reported his postsurgical results as a whole and did not show the difference between the postlaminectomy and postfusion categories. Even with that limitation, if his excellent, good, and fair results are considered together there was an 85% clinical improvement in the 231 cases. In another study [29], which reported the surgical treatment of canal stenosis, there was excellent, good, or fair results in five of six cases (83%) of iatrogenic stenosis. These surgical results are similar to ours.

The amount of bone which is removed varies with the length and configuration of the stenotic canal. A laminectomy alone in these cases is usually insufficient for adequate canal decompression, frequently necessitating sufficient resection of the articulating facets [2, 7, 36] to widen the canal and unroof the lateral recesses.

Since many patients with an underlying stenotic canal are probably operated upon for what is considered by the clinician to be simply a herniated disc, we recommend preoperative axial radiography in all patients who are being considered for disc surgery whenever the clinical history is not typical for an acutely herniated disc or the myelogram and/or plain films suggests an abnormal bone canal configuration.

REFERENCES

1. Arnoldi CC, Brodsky AE, Cauchoix HV, Crock HV, Dommisse GF, Edgar MA, Gargano FP, Jacobson RE, Kirkaldy-Willis WH, Kurihara A, Langenskiold A, Macnab I, McIvor GWD, Newman PH, Paine KWE, Russin LA, Sheldon J, Tile M, Uris MR, Wilson WE, Wiltse LL: Lumbar spinal stenosis and nerve root entrapment syndromes. *Clin Orthop* 115:4–5, 1976
2. Schatzker J, Pennal GF: Spinal stenosis, a cause of cauda equina compression. *J Bone Joint Surg [Br]* 50:606–618, 1968
3. Sheldon JJ, Russin LA, Gargano FP: Lumbar spinal stenosis. Radiographic diagnosis with special reference to transverse axial tomography. *Clin Orthop* 115:53–67, 1976
4. McIvor GWD, Kirkaldy-Willis WH: Pathological and myelographic changes in the major types of lumbar spinal stenosis. *Clin Orthop* 115:72–76, 1976
5. Gill GG, Manning JG, White HL: Surgical treatment of spondylolisthesis without spinal fusion. Excision of the loose lamina with decompression of the nerve roots. *J Bone Joint Surg [Am]* 37:493–520, 1955
6. Jacobson RE, Gargano FP, Rosomoff HL: Transverse axial tomography of the spine. II. The stenotic spinal canal. *J Neurosurg* 42:412–419, 1975
7. Brodsky AG: Post laminectomy and post fusion stenosis of the lumbar spine. *Clin Orthop* 115:130–139, 1976
8. Paine KWE: Results of decompression for lumbar spinal stenosis. *Clin Orthop* 115:96–100, 1976
9. Pennal GF, Schatzker J: Stenosis of the lumbar spinal canal. *Clin Neurosurg* 18:86–105, 1971
10. Wedge JH, Kirkaldy-Willis WH, Kinnard P: Lumbar spinal stenosis, in *Disorders of the Lumbar Spine*, edited by Helfet AJ, Lee DMG, Philadelphia, Lippincott, 1978, pp 51–58
11. Kestler OC: Overgrowth (hypertrophy) of lumbosacral grafts, causing a complete block. *Bull Hosp Joint Dis* 27:51–57, 1966
12. Kirkaldy-Willis WH, Paine KWE, Cauchoix J, McIvor G: Lumbar spinal stenosis. *Clin Orthop* 99:30–50, 1974
13. Gargano FP: Transverse axial tomography of the spine. *CRC Crit Rev Clin Radiol Nucl Med* 7:279–328, 1976
14. Sheldon JJ, Sersland T, LeBorgne J: Computed tomography of the lower lumbar vertebral column. *Radiology* 124:113–118, 1977

15. Schlesinger EB, Taveras JM: Factors in the production of cauda equina syndromes in lumbar discs. *Trans Am Neurol Assoc* 78:263–265, 1953
16. Epstein BS, Epstein JA, Lavine L: The effect of anatomic variations in the lumbar vertebrae and spinal canal on cauda equina and nerve root syndromes. *Am J Roentgenol* 91:1055–1063, 1964
17. Eisenstein S: Measurements of the lumbar spinal canal in two racial groups. *Clin Orthop* 115:42–48, 1976
18. Verbiest H: A radicular syndrome from developmental narrowing of the lumbar vertebral canal. *J Bone Joint Surg [Br]* 36:230–237, 1954
19. Verbiest H: Further experiences on the pathological influence of a developmental narrowness of the bony lumbar vertebral canal. *J Bone Joint Surg [Br]* 37:576–583, 1955
20. Jones RAL, Thompson JLG: The narrow lumbar canal. A clinical and radiological review. *J Bone Joint Surg [Br]* 50:595–605, 1968
21. Gargano FP, Jacobson R, Rosomoff H: Transverse axial tomography of the spine. *Neuroradiology* 6:254–258, 1974
22. Lee BCP, Kazam E, Newman AD: Computed tomography of the spine and spinal cord. *Radiology* 128:95–102, 1978
23. Jacobson RE, Gargano FP, Rosomoff HL: Transverse axial tomography of the spine. I. Axial anatomy of the normal lumbar spine. *J Neurosurg* 42:406–411, 1975
24. Hammerschlag SB, Wolpert SM, Carter BL: Computed tomography of the spinal canal. *Radiology* 121:361–367, 1976
25. Burton CV: Lumbar arachnoiditis. *Spine* 3:24–30, 1978
26. Paine KWE, Haung PWH: Lumbar disc syndrome. *J. Neurosurg* 37:75–82, 1972
27. Williams P, Yglesias L: Lumbosacral facetectomy for post fusion persistent sciatica. *J Bone Joint Surg* 15:579–590, 1933
28. Helfet AJ, Lee DMG: Segmental intervertebral instability and its treatment, in *Disorders of the Lumbar Spine,* edited by Helfet AJ, Lee DMG, Philadelphia, Lippincott, 1978, pp 69–111
29. Tile M, McNeil SR, Zarins RK, Pennal GF, Garside SH: Spinal stenosis. Results of treatment. *Clin Orthop* 115:104–108, 1976
30. Epstein JA, Epstein BS, Lavine L: Nerve root compression associated with narrowing of the lumbar spinal canal. *J Neurol Neurosurg Psychiatry* 25:165–176,1962
31. Reily J, Yong-Hing K, MacKay RW, Kirkaldy-Willis WH: Pathological anatomy of the lumbar spine, in *Disorders of the Lumbar Spine,* edited by Helfet AJ, Lee DMG, Philadelphia, Lippincott, 1978, pp 26–50
32. King AB: Back pain due to loose facets of the lumbar vertebrae. *Johns Hopkins Med J* 97:271–283,1955
33. Clark K: Significance of the small lumbar spinal canal. Cauda equina syndromes due to spondylosis. II. Clinical and surgical significance. *J Neurosurg* 31:495–498, 1969
34. Wilson LES: Spinal stenosis: the narrow lumbar canal syndrome. *Clin Orthop* 122:244–248, 1977
35. Ehni G: Significance of the small lumbar canal. Cauda equina syndromes due to spondylosis. I. Introduction. *J Neurosurg* 31:490–494, 1969
36. Rosomoff HL: Bony encroachment of the lumbar spine. A cause of low back surgery failure. *J Fla Med Assoc* 63:884–888, 1976
37. Harris RI, Macnab I: Structural changes in the lumbar intervertebral disc: their relationship to low back pain and sciatica. *J Bone Joint Surg [Br]* 36:304–322, 1954

Diagnostic Oncology Case Studies

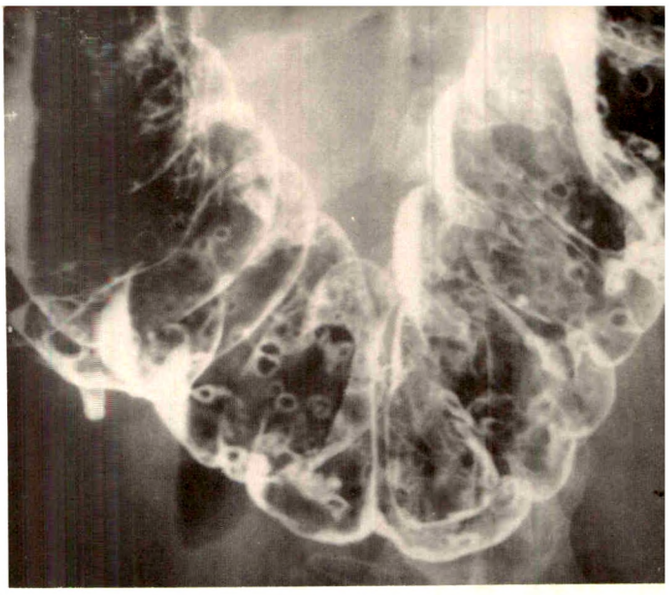

Colonic Polyposis and Cancer

In October 1972, a 57-year-old caucasian male had a sigmoidoscopy for rectal bleeding and was found to have two nonsessile 2 cm diameter adenomatous polyps at about 20 cm; these were removed with the use of snare and electrocautery. In addition, five smaller polyps were destroyed by electrofulguration. Barium enema examination after the procedure revealed no additional polyps, and a repeat barium enema in March 1974 was normal (Figs. 1*A* and 1*B*). Vague abdominal complaints associated with anemia prompted upper gastrointestinal and small bowel studies which showed an abnormality in the duodenum. In April 1974, the patient underwent a Whipple procedure for adenocarcinoma of the duodenum. Cholecystojejunostomy was performed for biliary drainage. Postoperatively the patient developed obstructive jaundice with an apparent stricture of the cystic duct. At reexploration the gallbladder was removed and a choledochojejunostomy performed. Histopathologic examination of the specimen revealed an unsuspected superficial adenocarcinoma of the gallbladder mucosa, without evidence of muscle invasion.

Because of recurrent rectal bleeding, a repeat sigmoidoscopy was done in July 1977, revealing two additional polyps in the rectum. Barium enema examination with air contrast showed multiple polyps throughout the colon (lead picture). In addition, the study strongly suggested the presence of a circumferential carcinoma involving the proximal transverse colon (fig. 1*C*). Skeletal survey revealed no osteomas or jaw cysts. In October 1977, the patient underwent subtotal colectomy with ileoproctostomy, and pathologic examination revealed innumerable adenomatous polyps throughout the colon, a desmoic tumor of the mesentery, and an adenocarcinoma extending through to the colonic serosa (Duke's B2) in the hepatic flexure. No metastatic lymph nodes or liver deposits were noted at surgery. Six months later, the patient remains free of symptoms and proctoscopic examination is negative.

Discussion

The radiographic findings in multiple polyposis of the colon can be subtle, especially if the polyps are small [1]. Small polyps occasionally may be hidden in the barium-filled colon (especially when the barium is too dense and/or there is improper radiographic technique or bowel preparation [2]), but they may be revealed with a double-contrast enema after adequate bowel preparation. With the standard barium enema examination, an overall "miss" rate of 42% for polyps of variable size was reported by Wolff et al. [3]. Comparing complete colonoscopy findings with barium air-contrast studies, Williams et al. [4] found that 85% of all polyps had been detected on the preceding double-contrast enema. In another series using double-contrast technique [5] only 5% of polyps were missed, and all of these were under 1 cm in diameter.

This is another in a bimonthly series of case reports prepared by A. Robert Kagan and Richard J. Steckel (Southern California Permanente Medical Group, 1510 North Edgemont, Los Angeles, California 90027, and UCLA Jonsson Comprehensive Cancer Center, 924 Westwood Boulevard, Suite 650, Los Angeles, California 90024, respectively) to present and discuss contemporary problems and procedures in the identification and staging of neoplasms. Case contributed by Aroor Rao (Department of Radiation Therapy, Southern California Permanente Medical Group, Los Angeles, California 90027), A. Khazin (Department of Surgery, Southern California Permanente Medical Group, San Diego, California 92120), and A. Fremland (Department of Radiology, Southern California Permanente Medical Group, San Diego, California 92120). Address reprint requests to R. J. Steckel.

© 1978 American Roentgen Ray Society

In the patient reported here, it took nearly 5 years from the initial examination to make the diagnosis of colonic polyposis; by that time, adenocarcinoma of the hepatic flexure had developed as well as two malignancies at other levels of the gastrointestinal tract. When multiple polyps were first found on proctoscopy, a more strenuous effort should have been made to rule out multiple colonic polyposis [6]. Although controversy still exists and good technique *is* paramount, we believe that a negative barium enema examination should have been followed in this patient by a careful double-contrast study and possibly by colonoscopy, as well as upper gastrointestinal and small bowel series. In other words, a patient with multiple rectosigmoid polyps and bleeding should be studied more aggressively at the onset to rule out polyposis.

Isolated colonic polyps 1–2 cm or less in diameter have a 1%–2% incidence of concurrent cancer, whereas polyps greater than 2 cm in diameter have a 20% incidence of malignancy [7]. By histologic type, only 5% of all adenomatous polyps develop cancer as opposed to 40% of villous adenomas [8]. The eventual incidence of large bowel cancer in patients with otherwise uncomplicated polyposis coli is high. Of 617 patients reviewed by Bussy [9] 66.8% are known to have developed intestinal cancer. If those first seen *after* initial diagnosis (most of whom had already been treated by colectomy) are excluded, the large bowel cancer incidence increased to 78.8% of 500 study subjects. Multiple polyposis of the colon is usually, but not always, a familial disease and is inherited as a simple autosomal dominant with a high (95%) degree of penetrance. Therefore, all first-degree family members of patients with polyposis should be studied. Multiple polyposis usually becomes symptomatic in early adulthood with diarrhea and hematochezia. Our patient is unusual, since he first became symptomatic in the sixth decade.

Other inherited gastrointestinal polyposis syndromes include Peutz-Jeghers syndrome, Gardner syndrome, generalized juvenile polyposis, and the Turcot syndrome. All of these are inherited as Mendelian autosomal dominants except for Turcot syndrome, which may be an autosomal recessive disorder. Peutz-Jeghers syndrome is characterized by generalized polyposis (polyps of the small intestine are frequent) and melanin spots on the lips, buccal mucosa, and/or digits. There is a 2%–3% risk of gastrointestinal cancer in this condition, often in the duodenal region [10]. Gardner syndrome is characterized by the triad of colonic polyps (rarely the small intestine), osteomas and jaw cysts, and soft tissue tumors (desmoids, fibromas, lipomas, and epidermoid cysts). The predisposition to colonic cancer is as marked as with familial colonic polyposis, but with an additional risk of carcinoma in the pancreatoduodenal region [11].

Fig. 1.—*A and B*, Conventional (single-contrast) barium enema, March 1974, giving no evidence of additional polyps in colon. *C*, Barium-filled phase of air-contrast study (see lead picture), July 1977, showing annular carcinoma in proximal transverse colon. Note that most polyps seen in lead picture are *not* demonstrated in this phase of study.

Generalized juvenile polyps are usually diagnosed in the first decade of life, with polyps usually involving the colon and rectum (occasionally the small intestine and stomach). Recently, the risk of cancer in this syndrome has been reassessed and found to be somewhat increased over the general population [12]. Turcot syndrome is characterized by colonic polyps and malignant tumors of the brain [13]. Some "crossover" between the various syndromes has been observed, and the present case may be an example.

Colonic polyposis is often managed by subtotal colectomy and attempted preservation of the rectum, with frequent proctologic surveillance and fulguration of rectal polyps when they are detected. The premise for subtotal rather that total colectomy is that the cancers may originate in "benign" polyps; therefore, if newly-developed polyps in the rectum are treated promptly, the rectum may be safely preserved. However, Moertel et al. [14] reported that among 143 *sub*total colectomy patients whose polyposis involved the rectum, 31 subsequently developed rectal cancer despite frequent proctosigmoidoscopic surveillance. The risk of cancer developing subsequently in the rectum after subtotal colectomy is higher if polyps were noted in this segment prior to surgery. The risk of subsequent development of rectal carcinoma after subtotal colectomy is also greater in female patients, as well as in patients with a carcinoma in the resected colon.

In summary, any patient with or without a family history of polyps who has two or more polyps at proctosigmoidoscopic examination, should have a double-contrast enema study after careful bowel preparation and an upper gastrointestinal series. Colonoscopy should be considered depending on the result of these studies. Patients with several of the polyposis syndromes are at a high risk of developing a gastrointestinal carcinoma; therefore, a careful initial diagnostic workup and persistent surveillance are requisites for proper management.

REFERENCES

1. Marshall RH, Linder AE, Maklansky D: Familial polyposis. *Am J Gastroenterol* 67:177–184, 1977
2. Laufer I: The double-contrast enema: myths and misconceptions. *Gastrointest Radiol* 1:19–31, 1976
3. Wolff WI, Shinya H, Geffen A, Ozoktay S, DeBeer R: Comparison of colonoscopy and the contrast enema in five hundred patients with colorectal disease. *Am J Surg* 129:181–186, 1975
4. Williams CB, Hung RD, Loose H: Colonoscopy in the management of colon polyps. *Br J Surg* 61:673–682, 1974
5. Laufer I, Smith NC, Mullens JE: The radiological demonstration of colorectal polyps undetected by endoscopy. *Gastroenterology* 70:167–170, 1976
6. Thoeni RF, Margolis AR: The state of radiographic technique in the examination of the colon: a survey. *Radiology* 127:317–323, 1978
7. Welin S, Yonker J, Spratt JS Jr: The rate and patterns of growth of 375 tumors of large intestine and rectum observed serially by double-contrast enema studies (Malmo technique). *Am J Roentgenol* 90:673–682, 1974
8. Morsen BC: Evolution of cancer of the colon and rectum. *Cancer* 34:845–849, 1974
9. Bussey HJR: *Familial Polyposis Coli*. Baltimore, The Johns Hopkins University Press, 1973
10. Dozois RR, Judd ES, Dohlin DC, Bartholomew LG: The Peutz-Jegher's syndrome; is there a predisposition to the development of intestinal malignancy. *Arch Surg* 98:509–577, 1969
11. Schnur PL, David E, Brown PL Jr, Beahrs OH, Remine WH, Harrison EG Jr: Adenocarcinoma of duodenum and Gardner syndrome. *JAMA* 223:1229–1232, 1973
12. Stempel JJ, Kent TH, Summers RW: Juvenile polyposis and gastrointestinal carcinoma: a study of a kindred. *Ann Intern Med* 83:639–646, 1975
13. Turcot J, Despois JP, St. Purre F: Malignant tumors of central nervous system associated with familar polyposis of colon: report of two cases. Drs. Colon and Rectum 2:465–468, 1959
14. Moertel CG, Hill HR, Adsen MA: Management of multiple polyposis of the large bowel. *Cancer* 28:160–164, 1971

Case Reports

Pheochromocytoma with Reversible Renal Artery Stenosis

WILLIAM F. VELICK,[1] JOSEPH J. BOOKSTEIN AND LEE B. TALNER

Pheochromocytoma is a well-recognized cause of renal artery stenosis with at least 25 cases reported in the English literature. In approximately 75% of these cases the pheochromocytoma arose from the lumbar sympathetic chain on the side of the stenosis and in the region of the renal hilum. In the others the tumor involved the ipsilateral adrenal gland and often extended into the renal hilum. The stenoses were frequently attributed to compression or stretching of the renal artery by the tumor.

We describe a patient in whom renal artery stenosis regressed following treatment with propranolol and phenoxybenzamine, suggesting an adrenergic mechanism as the cause.

Case Report

A 23-year-old male was found to have mild hypertension during an employment physical examination. Two years later an excretory urogram showed parenchymal atrophy of the lower pole of the right kidney and renovascular hypertension was suspected. VMA was normal.

An aortogram performed prior to selective renal angiography showed severe stenoses of the major divisions of the right renal artery (fig. 1*A*). Selective arteriography more clearly revealed the stenoses (fig. 1*B*). The lower pole of the kidney was atrophic. Several small tortuous vessels in the renal hilum were thought to represent collaterals. Late films showed a faint tumor blush below the renal hilum that had been misinterpreted as duodenal stain.

Renal vein renin activities lateralized to the right kidney: upper pole vein 11.4, lower pole vein 6.0, and left renal vein 3.8 ng/ml/hr. Because of the location and multiplicity of stenoses and because the hypertension responded satisfactorily to propranolol, surgery was not recommended.

Four months later the patient returned with palpitations, headache, syncope, and blood pressure 250/160 mm/Hg. VMA was 23 mg/24 hr (0.5–12 nl) and catecholamines were greater than 700 mg/24 hr (0–103 nl). Blood pressure was controlled with phenoxybenzamine and propranolol.

Angiography demonstrated a hypervascular 6 × 10 cm tumor of the right renal hilum with tumor vessels and blush, no change in the renal contour, and almost complete disappearance of renal artery branch stenoses (fig. 2). At surgery the tumor surrounded the renal artery but no stenosis was noted. Histologic examination confirmed the diagnosis of pheochromocytoma with no evidence of tumor necrosis or malignancy. No renal artery tissue was available for examination.

Postoperatively blood pressure measured 130/95 without medication. Catecholamines were normal and the patient was asymptomatic. Follow-up examination 2 mo later revealed persistent mild hypertension. Repeat angiography revealed occlusions of several posterior segmental renal arteries with reconstitution by prominent sinus collaterals (fig. 3). These occlusions probably occurred during the operation when difficulties

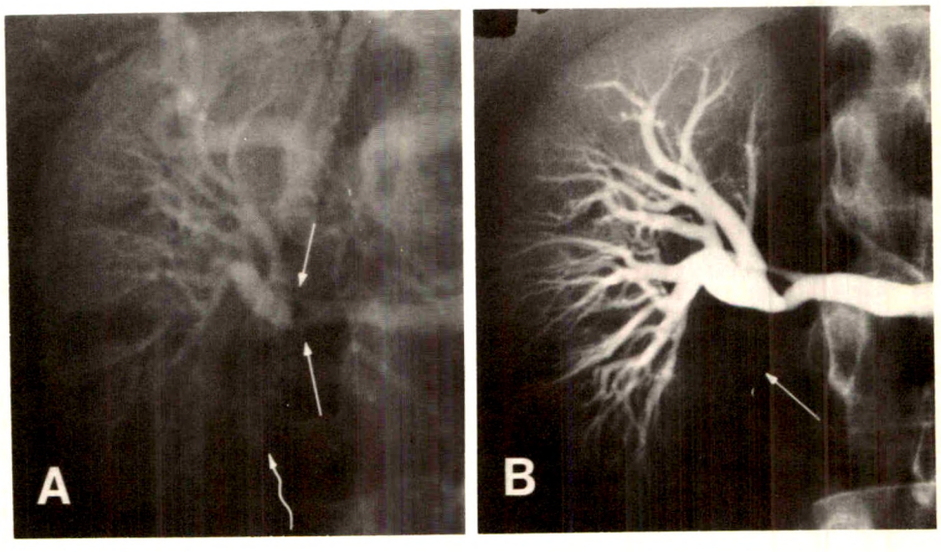

Fig. 1.—Films showing stenoses of right renal artery. *A*, Aortogram showing faint stenoses (*arrows*). Note peculiar ringlike stain medial to atrophic lower pole of right kidney (*curved arrow*). *B*, Selective magnification arteriogram demonstrating stenoses, atrophic lower pole of kidney, and a few tortuous vessels (*arrow*) thought to participate in collateral flow to a segmental branch.

Received February 10, 1978; accepted after revision August 9, 1978.

[1] All authors: Department of Radiology, University of California Medical Center, 225 Dickinson Street, San Diego, California 92103. Address reprint requests to J. J. Bookstein.

© 1978 American Roentgen Ray Society

0361–803X/78/1200–1069 $00.00

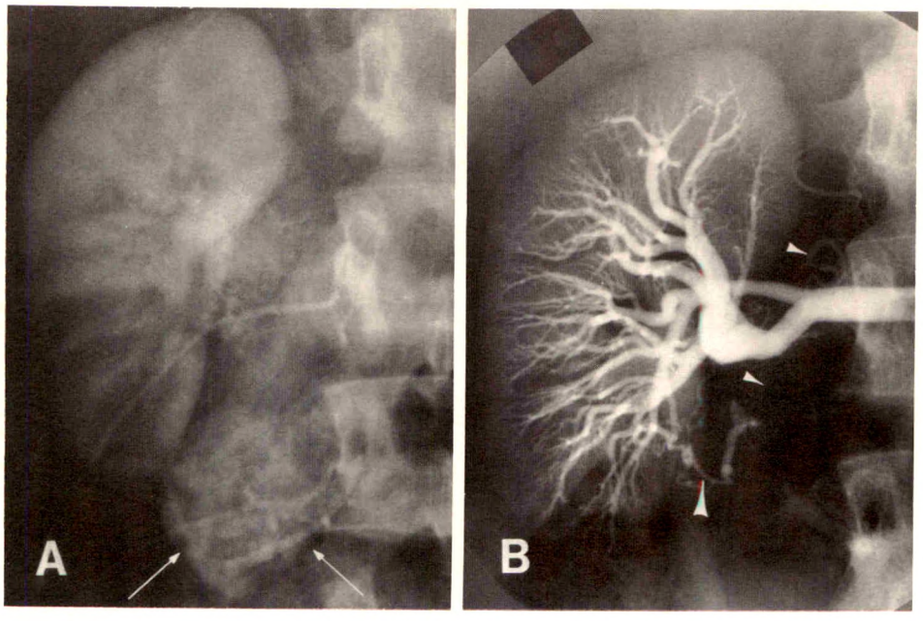

Fig. 2.—*A*, Repeat aortogram 3 months later. Catheter is at much higher position and shows more impressive tumor stain (*arrows*). *B*, On selective arteriography renal stenoses have almost disappeared though some irregularity remains. Inferior adrenal arteries (*arrowheads*) and perforating capsular branches (*arrow*) lead to tumor.

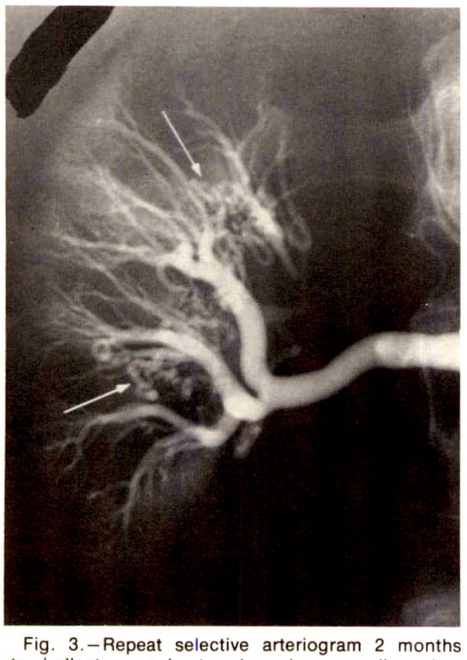

Fig. 3.—Repeat selective arteriogram 2 months later indicates renal artery branches were ligated at surgery; note collaterals in renal sinus (*arrows*). Later films showed delayed nephrogram of upper pole secondary to collateral flow.

in excising the tumor necessitated ligation of several vessels. The continued mild hypertension is thought to be renovascular in origin.

Discussion

Previous reports have enumerated presumed causes of renal artery narrowing associated with pheochromocytoma [1, 2]. Stenoses have usually been attributed to direct compression or encasement. This case clearly demonstrates that the stenosis can be functional and reversible and suggests local pharmacologic effects of catecholamines as an etiologic mechanism. The ipsilateral elevation of renal vein renin activity is assumed to be secondary to the renal artery stenosis. In this case, a direct cause and effect relationship between adrenergic blockade and regression of stenosis seems likely, but cannot be proven. A coincidental change in tumor morphology could have occurred, or a transient constriction might have relaxed independently of the blocking drugs.

Four other cases in the literature document a transient or reversible renal artery stenosis with pheochromocytoma. Boijsen et al. [3] reported a patient in whom the renal artery and branches were narrowed on the aortogram but were normal in caliber on the selective renal artery injection. The pheochromocytoma was in the renal hilum. Sutton [4] illustrated a case in which a renal artery stenosis was observed during a hypertensive reaction. Following phentolamine the stenosis disappeared. A patient reported by Ishihashi et al. [5] had a left adrenal pheochromocytoma surrounding a narrowed renal artery. This tumor was removed and a follow-up angiogram 4 months later showed no remaining stenosis. Ecoiffier et al. [6] reported a patient with renal artery stenoses in addition to splenic and inferior mesenteric stenoses; at postmortem examination these had disappeared.

With catecholamine excess, spasm is not unique to the renal arteries. Claudication in the extremities and gangrene due to large and small vessel involvement have been reported [7]. Catecholamine induced myocarditis and intestinal ischemia have been reported in several patients with pheochromocytoma. Again the pathogenesis is thought to be severe vasospasm [8–10]. These incidences differ from the present case, however, insofar as the pheochromocytomas were remote from the involved vessels.

Reports in the literature describe a variety of histologic arterial abnormalities in pheochromocytoma [11]. Renal artery stenoses have been secondary to intimal fibrosis or proliferation [2, 12]. The intima may be atherosclerotic [3, 13] and the media normal or thickened. Small arterioles in the kidney have been shown to resemble those in nephrosclerosis [14]. Nonspecific interstitial mononuclear cell infiltrate, hyalinized glomeruli, and subcapsular renal scars near the site of the tumor have been described [2, 14].

Although severe renal artery stenosis is rare in patients with pheochromocytoma, we have seen mild stenoses of renal arteries in four of eight cases at this institution. Similar mild stenoses were seen in eight of 27 renal artery studies by Christenson et al. [15]. In one of their cases, as in ours, the stenosis was hemodynamically significant [12].

REFERENCES

1. Naidich TP, Sprayregen S, Goldman AG, Siegelman SS: Renal artery alterations associated with pheochromocytoma. *Angiology* 23:488–499, 1972
2. Rosenheim ML, Ross EJ, Wrong OM, Hodson CJ, Davies DR, Smith JF: Unilateral renal ischemia due to compression of a renal artery by pheochromocytoma. *Am J Med* 34:735–740, 1963
3. Boijsen E, Williams CM, Judkins MP: Angiography of pheochromocytoma. *Am J Roentgenol* 98:225–232, 1966
4. Sutton D: The radiological diagnosis of adrenal tumors. *Br J Radiol* 48:237–258, 1975
5. Ishihashi M, Takenchi A, Yokoyama S: Pheochromocytoma with renal artery stenosis and high plasma renin activity. *Jpn Heart J* 16:741–748, 1975
6. Ecoiffier J, Fournier A, Leduc G, Plainfosse MC: Quelle signification peut-on accorder a la decouverte arteriographique de "stenoses" au cours des pheochromocytomes. *La Press Medicale* 78:2325–2328, 1970
7. Scharf Y, Nahir M, Plavinic Y, Ben-Arieh J: Intermittent claudication with pheochromocytoma. *JAMA* 215:1323–1324, 1971
8. Radtke WE, Kazmier FJ, Rutherford BD, Sheps SG: Cardiovascular complication of pheochromocytoma crisis. *Am J Cardiol* 35:701–705, 1975
9. Van Vliet PD, Burchell HB, Titus JL: Focal myocarditis associated with pheochromocytoma. *N Engl J Med* 274:1102–1108, 1966
10. Rosati LA, Augur NA: Ischemic enterocolitis in pheochromocytoma. *Gastroenterology* 60:581–585, 1975
11. James TN: DeSubitaneis mortibus. XIV. On the cause of sudden death in pheochromocytoma. *Circulation* 54:348–356, 1976
12. Van Way CW, Michelakis AM, Alper BJ, Hutcheson JK: Renal vein renin in a patient with renal hilar pheochromocytoma and renal artery stenosis. *Ann Surg* 172:212–217, 1970
13. McBride JW, Fitz A: Renal artery stenosis, pheochromocytoma and erythrocytosis. *Am J Med* 51:403–411, 1971
14. Castleman B, Scully RE, McNeely BU: Case records of the Massachusetts General Hospital. *N Engl J Med* 288:1010–1018, 1973
15. Christenson R, Smith CW, Burko H: Arteriographic manifestations of pheochromocytoma. *Am J Roentgenol* 126:567–575, 1976

Embolization for Postbiopsy Renal Arteriovenous Fistula: Effective Occlusion Using Homologous Clot

ROBERT J. ROSEN,[1] LAURA FELDMAN, AND AUDREY R. WILSON

The development and now widespread use of percutaneous needle biopsy as a major diagnostic method in renal disease has been accompanied by an increasing frequency of reported complications. An important and potentially very serious complication is development of intrarenal arteriovenous fistulae. In the present case, life-threatening hematuria secondary to fistula formation followed renal biopsy and was successfully treated using selective arterial embolization. Angiographic and pathologic confirmation of persistent arterial occlusion with autologous clot 6 and 12 days after embolization was obtained.

Case Report

A 41-year-old white male was admitted in chronic renal failure with a diagnosis of adult hemolytic-uremic syndrome. Blood pressure on admission was 180/110; blood urea nitrogen, 181; and creatinine, 12.0. The patient was placed on hemodialysis. Renal arteriography showed changes consistent with nephrosclerosis. Percutaneous needle biopsy of the left kidney demonstrated intravascular fibrin deposition compatible with hemolytic-uremic syndrome. The patient developed massive hematuria requiring transfusion of 12 units of blood to stabilize blood pressure while on hemodialysis 3 days after biopsy. There was continued massive hematuria; emergency arteriography demonstrated an arteriovenous fistula supplied by an accessory renal artery to the lower pole of the left kidney but no bleeding site (fig. 1*A*). Embolization of the accessory renal artery was performed using 5 ml of autologous clot. Arteriography immediately after embolization confirmed complete occlusion of the vessel and consequent closure of the fistula (fig. 1*B*). A small amount of hematuria for the next 3 days was believed to be caused by infarction of the lower pole of the left kidney.

Persistence of the hematuria resulted in repeat arteriography 6 days after embolization to exclude reopening of the fistula. Continued occlusion of the accessory lower pole vessel was demonstrated with no evidence of recanalization. The hematuria decreased gradually over the next several days. The patient suffered cardiac arrest 6 days after the third arteriography (12 days after embolization); resuscitation attempts were unsuccessful. Autopsy revealed infarction of the lower pole of the left kidney and a perinephric hematoma of moderate size (fig. 2*A*). The accessory artery to the lower pole contained adherent thrombus (fig. 2*B*). Death was thought to result from an unrelated, overwhelming aspiration pneumonia.

Discussion

Arteriovenous fistula formation is relatively common following percutaneous needle biopsy of the kidney.

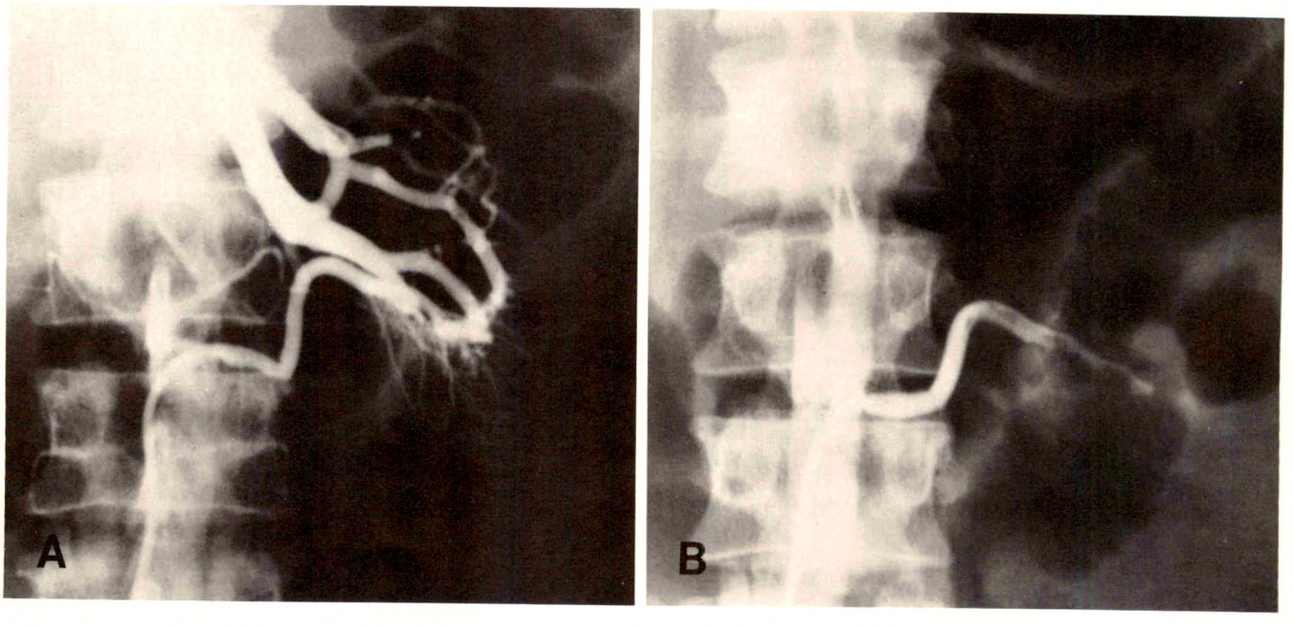

Fig. 1.—Arteriograms. *A*, Arteriovenous fistula supplied by accessory lower pole renal artery. No bleeding is demonstrated. *B*, Complete occlusion of lower pole vessel with consequent closure of fistula after embolization. Note localized ileus over embolized kidney.

Received April 20, 1978; accepted after revision August 25, 1978.

[1] All authors: Diagnostic Radiology, Hahnemann Medical College and Hospital, 230 North Broad Street, Philadelphia, Pennsylvania 19102. Address reprint requests to A. R. Wilson.

© 1978 American Roentgen Ray Society

0361–803X/78/1200–1072 $00.00

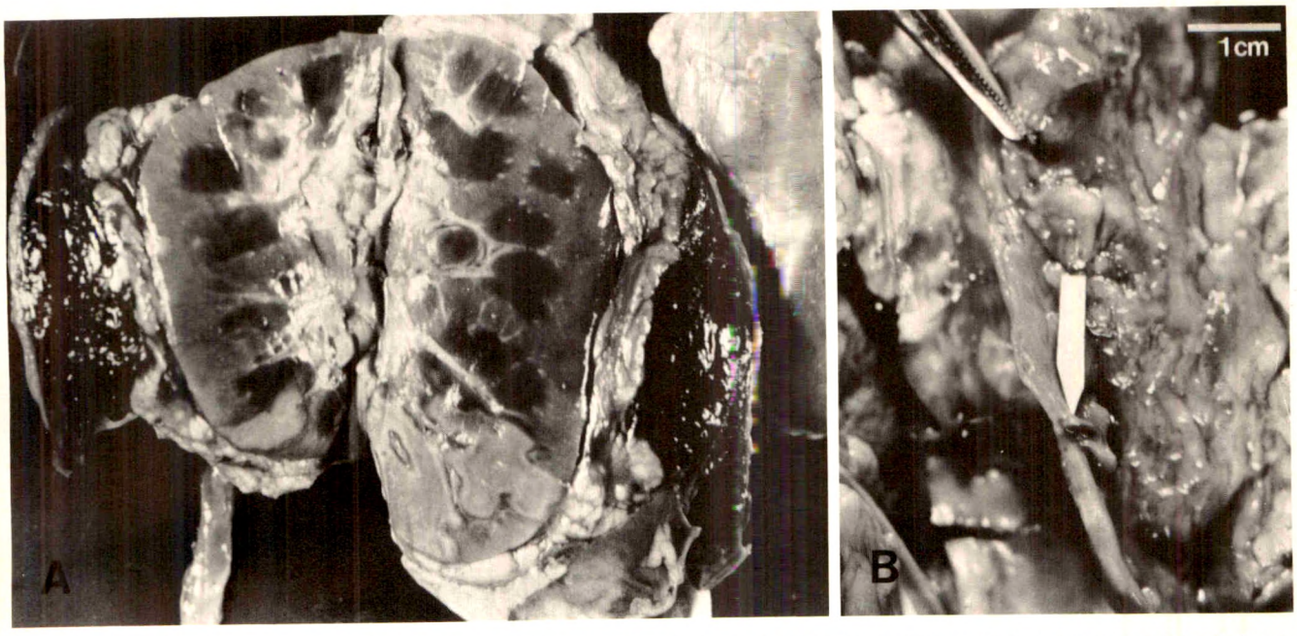

Fig. 2.—Embolized kidney at autopsy. *A*, Infarction of lower pole and moderate-sized perinephric hematoma. *B*, Anterior view of abdominal aorta and accessory lower pole renal artery opened longitudinally demonstrating adherent thrombus at renal vessel origin (*arrow*). Tissue at right is perinephric fat.

Reported incidence is as high as 36% in patients with hypertension [1], the major risk factor in fistula development [1–3]. Nephrosclerosis is also considered a predisposing cause [2]. Most fistulae (70%) close spontaneously between 2 weeks and 18 months, so conservative therapy is advocated in the absence of any serious clinical complications [3]. Potential complications include life-threatening hematuria, hypertension, decreased renal function, congestive heart failure, retroperitoneal hematoma, and abdominal pain [1–6].

Successful embolization of a postbiopsy arteriovenous fistula was first reported by Bookstein and Goldstein [7] in 1973. Various materials, including Gelfoam, autologous clot, muscle tissue, fat, and metal shot fragments have been used to occlude these fistulae. Lysis of autologous clot has been reported to occur within hours except in the region of the fistula itself [4, 6, 8–10]. However, not all autologous clots undergo lysis. The present case demonstrates persistent occlusion of the embolized renal artery 6 and 12 days after embolization, with resulting infarction of the lower pole.

Reported sequelae of the embolization procedure include flank pain, slight temperature elevation, and transient hematuria (present in this case) [1]. No cases of renovascular hypertension have been reported after this procedure, possibly due to the complete infarction, rather than any ischemia, of the involved segment of kidney. In the present case, an accessory renal artery supplied the lower pole of the kidney where the fistula was located, permitting selective embolization of the lower pole and sparing the major portion of the kidney.

ACKNOWLEDGMENT

We thank James P. Fullin for assistance in preparing pathologic material.

REFERENCES

1. Silverberg DS, Dossetor JB, Eid TC, Mant MJ, Miller JDR: Arteriovenous fistula and prolonged hematuria after renal biopsy treatment with epsilon aminocaproic acid. *Can Med Assoc J* 110:671–672, 1974
2. Ekelund L, Gothlin J, Lindholm T, Lindstedt E, Mattsson K: Arteriovenous fistulas following renal biopsy with hypertension and hemodynamic changes. *J Urol* 108:373–376, 1972
3. O'Brien DP, Parott TS, Walton KN, Lewis EL: Renal arteriovenous fistulas. *Surg Gynecol Obstet* 118:1305–1311, 1964
4. Messing E, Kessler R, Kavaney PB: Renal arteriovenous fistulas. *Urology* 8:101–107, 1976
5. Cangiano JL, Kest L: Use of a G-suit for uncontrollable bleeding after percutaneous renal biopsy. *J Urol* 107:360–361, 1972
6. Barbaric ZL, Cutcliff WB: Control of renal arterial bleeding after percutaneous biopsy. *Urology* 8:108–111, 1976
7. Bookstein JJ, Goldstein HM: Successful management of postbiopsy arteriovenous fistula with selective arterial embolization. *Radiology* 109:535–536, 1973
8. Warren BA: Fibrinolytic activity of vascular endothelium. *Br Med Bull* 20:213–216, 1964
9. Silber SJ, Clark RE: Treatment of massive hemorrhage after renal biopsy with angiographic injection of clot. *N Engl J Med* 292:1387–1388, 1975
10. Silber S: Renal trauma: treatment by angiographic injection of autologous clot. *Arch Surg* 110:206–207, 1975

Demonstration of Pancreatic Cysts in Adult Polycystic Disease by Computed Tomography and Ultrasound

ALI SHIRKHODA[1] AND CAROL A. MITTELSTAEDT[1]

Although the term polycystic disease is usually attributed to the kidneys, the involvement of other organs such as the liver, pancreas, lungs, spleen, ovaries, testes, epididymis, thyroid, uterus, and bladder may occur [1]. It is apparent that polycystic disease is not often suspected antimortem as it has been estimated that 75% of cases remain undiagnosed [2]. With the advent of ultrasound and computed tomography (CT), unsuspected visceral cysts may be identified, localized, and, if necessary, punctured. To our knowledge, demonstration of pancreatic cysts in adult polycystic disease by CT and ultrasound has not been reported. We present such a case, probably Potter type III adult polycystic disease [3].

Case Report

A 65-year-old female with chondrosarcoma of the left iliac bone had a limp and left lower quadrant pain. Several months before admission she had undergone a partial left hemipelvectomy. She was suspected to have recurrence on the basis of a plain pelvic radiographic examination. The history was otherwise negative. Although the patient was not known to be hypertensive, her sister and mother died secondary to hypertension and heart disease. On physical examination, the only positive finding, other than the pelvic surgical scar, was an enlarged liver and a blood pressure of 140/90 mm Hg. Biochemistry of the blood and urine were normal except for anemia.

CT of the pelvis, performed using an Ohio Nuclear Delta Scan 50, confirmed the diagnosis of recurrent tumor. Since the liver was enlarged, the right lobe was incidently seen in one of the more superior cuts through the pelvis. Because of an unsuspected well circumscribed area of low absorption value (water density on Delta Unit) within the liver, additional tomographic cuts were obtained through the upper abdomen. Since the patient had a history of allergy to iodine, no contrast injection was performed. Multiple well circumscribed areas of low density were found throughout both lobes of the liver (fig. 1*A*). The kidneys were slightly enlarged with suspected cystic lesions. In addition, there were well circumscribed cystic areas in the body and tail of the pancreas (fig. 1*B*). At this point, the diagnosis of adult polycystic disease was tentatively made. For confirmation, ultrasound examination of the abdomen and kidneys was performed using a 2.25 mHz transducer and a conventional gray scale machine. As with CT, multiple round, well defined cystic (sonolucent) areas were demonstrated within the liver, kidneys and pancreas (fig. 2). A liver cyst puncture performed with ultrasound guidance yielded clear fluid.

Discussion

Osathanondh and Potter [3] recently established a classification for polycystic kidney disease which includes three types.

1. Potter type I cystic disease results from hyperplasia of the interstitial portions of the collecting systems and corresponds to infantile polycystic disease.

2. Potter type II cystic disease demonstrates interstitial inhibition of ampullary activity on microdissection and incorporates several entities—the hypergenetic or disgenetic cystic kidney, the multicystic dysplastic kidney, and the unilateral circumscribed multilocular cyst.

3. Potter type III cystic disease involves one or more of several abnormalities of development, wherein the calyces are often abnormal, the papilla absent, and varying numbers of normal and abnormal nephrons and tubules are intermixed. Any portion of the nephron or tubule may be cystic, with Bowman's space and the angle of the loop of Henle most commonly involved. Potter type III cystic disease corresponds to adult type polycystic disease of the kidneys.

Potter type III, or adult polycystic renal disease, is generally believed to be a progressive, frequently familial, bilateral cystic degeneration which is often associated with involvement of the other viscera and hypertension as well as intracranial aneurysm. Hatfield and Pfister [2] studied 399 patients with pathologically proven multiple cysts in both kidneys and found 58 of them also had associated cysts of the liver and pancreas, assumed to represent adult polycystic disease. The incidence of pancreatic cysts in an autopsy series has been estimated to be 9% [1] with cysts of the lung and other viscera being less common.

Hepatic, pancreatic, and renal cysts are easily demonstrated with computed tomography [4, 5] and ultrasound [6]. Pancreatic cysts should be differentiated from pseudocyst, abscess, and necrotic tumor. However, in a patient with multiple cysts in the kidneys and liver, these differential considerations would be very unlikely. Before the advent of CT and ultrasound, hepatic cysts were recognized in only about one-third of living patients with adult polycystic disease. However, in an autopsy series [1], 43% of patients with polycystic kidneys had concomitant liver cysts, and about 53% of those with hepatic cysts had polycystic kidneys. Davis [7] in his study of 241 cases of polycystic liver, demonstrated that in 136 cases (56%) the kidneys were also cystic. In another study [8], 16 patients with adult polycystic disease were studied by gray scale ultrasound and in 50% of the cases, liver cysts were detected.

In our patient, the detection of multiple hepatic lesions

Received April 21, 1978; accepted after revision August 9, 1978.

[1] Department of Radiology, Division of Imaging, University of North Carolina School of Medicine, Chapel Hill, North Carolina 27514. Address reprint requests to A. Shirkhoda.

© 1978 American Roentgen Ray Society

0361–803X/78/1200–1074 $00.00

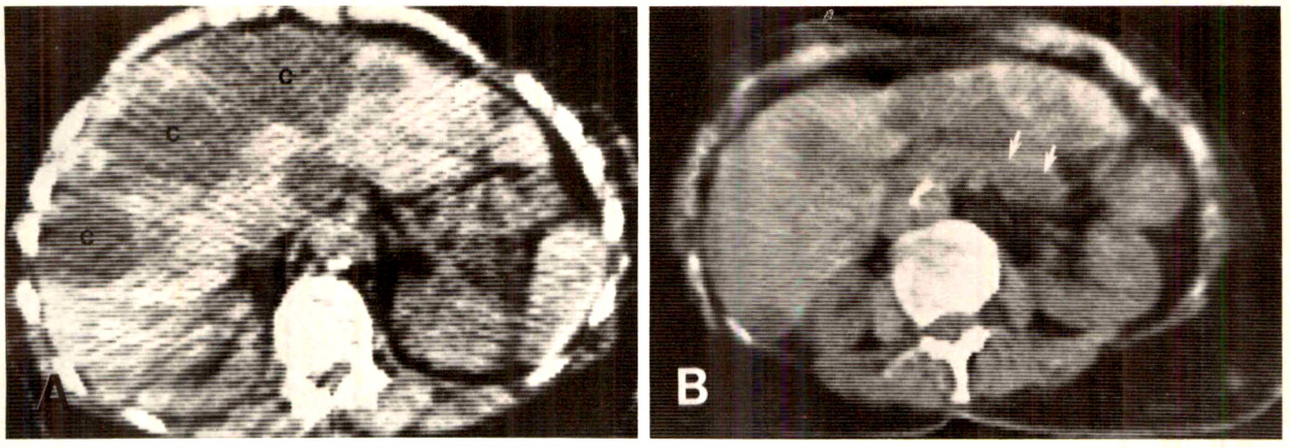

Fig. 1.—CT scans of liver and pancreas. *A*, Transverse cut through liver and kidney showing multiple relatively well circumscribed areas of low attenuation value demonstrating multiple cysts (c). *B*, One or probably two areas of low attenuation in pancreas (*arrows*) representing cysts. Again multiple cysts in liver are noted.

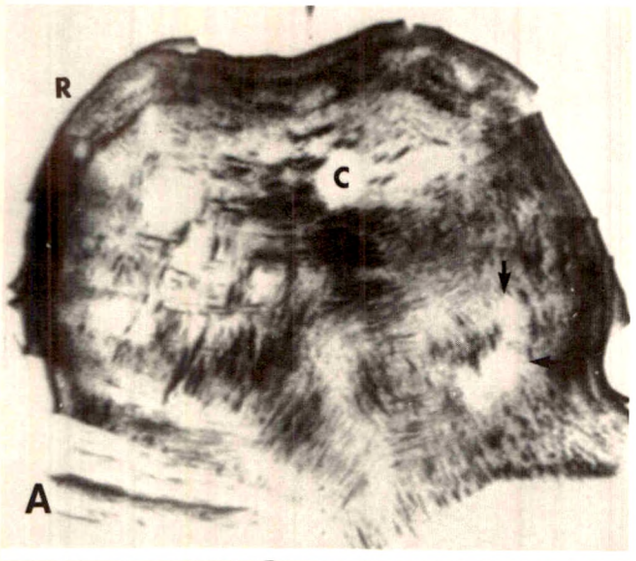

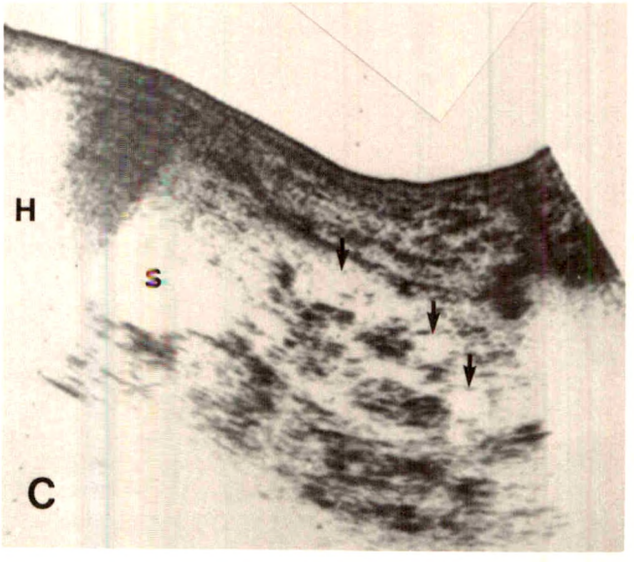

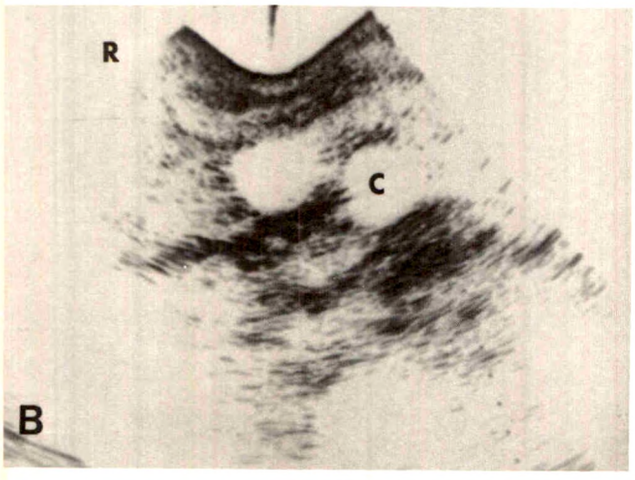

Fig. 2.—Sonographic evaluation of liver, pancreas, and kidney. *A*, Transverse scan 8 cm above umbilicus demonstrating multiple sonolucent areas within both lobes of liver. Single sonolucent structure with strong through-transmission is seen below left lobe of liver representing cyst (C) within pancreas. Multiple cysts (*arrows*) in left kidney. *B*, Scan 2.5 cm below xyphoid, with caudal angulation of transducer to evaluate pancreas, showing two adjacent cysts, one in posterior aspect of left lobe of liver and one (C) in pancreas. *C*, Longitudinal scan of left kidney in prone position demonstrating multiple small cysts throughout entire kidney (*arrows*), particularly in region of cortex. Similar findings were observed on right side. S = spleen, H = head.

was made incidentally. The documentation of their cystic nature by the combination of CT, ultrasound, and cyst puncture and the identification of similar renal and pancreatic lesions allowed a confident diagnosis of adult polycystic disease (Potter type III), and an incorrect diagnosis of hepatic metastases in a patient with a known neoplasm was avoided.

REFERENCES

1. Bosniak MA, Ambos MA: Polycystic kidney disease. *Semin Roentgenol* 10:133–143, 1975
2. Hatfield PM, Pfister RC: Adult polycystic disease of the kidneys (Potter type 3). *JAMA* 222:1527–1531, 1972
3. Osathanondh V, Potter EL: Pathogenesis of polycystic kidneys. *Arch Pathol* 77:459–512, 1964

Pseudomass of the Liver Due to Pleural Effusion and Inversion of the Diaphragm

BARRY T. KATZEN,[1] WALTER S. CHOI, MICHAEL H. FRIEDMAN, IRA J. GREEN, WILLIAM V. HINDLE, AND ALLAN ZELLIS

Numerous recent reports have shown the remarkable ability of CT scanning to demonstrate abnormalities of the liver and biliary tree, so that it is now accepted as a definitive diagnostic modality. However, CT scanning has inherent limitations because it presents images in a cross-sectional plane, and gross anatomic alterations are occasionally somewhat difficult to analyze without other reference planes. Our case demonstrates this feature and the need for complementary imaging modalities, such as arteriography and sagittal plane ultrasound.

Case Report

A 35-year-old physicist presented with shortness of breath and right chest pain. Chest films demonstrated a moderate-sized right pleural effusion (fig. 1). Aspiration revealed adenocarcinoma. A search for primary neoplasm and metastases was performed with upper gastrointestinal and small bowel series, barium enema, excretory urography, and radionuclide bone and liver scans. The liver scan revealed an abnormality in the dome of the right lobe of the liver suggesting replacement by neoplastic disease (fig. 2*A*). Computed tomography of the liver (fig. 2*B*) demonstrated a large area of decreased attenuation in the right upper quadrant, having the appearance of an intrinsic lesion of the right lobe of the liver. Attenuation coefficients measured in the range close to water density.

Visceral arteriography was undertaken to evaluate the apparent liver mass and search for primary lesion. Selective injection of contrast in the common hepatic artery (fig. 2*C*) demonstrated marked downward displacement of the liver so that the right lobe lay inferiorly to the left of midline. In addition, the right kidney was displaced inferiorly by a downward directed curvilinear density representing the inverted right hemidiaphragm. Because of this confusing constellation of findings, the patient underwent ultrasound examination (fig. 2*D*), which demonstrated a large fluid collection on transverse and sagittal sections. The diaphragm was clearly shown to be inverted and in direct apposition to the superior pole of the right kidney. Aspiration of this fluid by thoracentesis resulted in reversal of these findings. No other source of tumor was demonstrated.

Discussion

Inversion of the left hemidiaphragm by large pleural effusion has been documented [1–3]. However, presumably due to the presence of the liver in the right upper quadrant, inversion of the right hemidiaphragm has not been previously noted. In a recent report of the value of CT of the liver [4], a false positive diagnosis of cyst in the dome of the right lobe of the liver was demonstrated from a small right pleural effusion. In our patient the marked downward displacement of the liver, associated with inversion of the diaphragm, suggested intrahepatic pathology. It is not clear why the fluid did not redistribute posteriorly in the pleural space in the horizontal positions. Perhaps it was trapped by adhesions. Moreover, additional fluid may have accumulated in the 1-week interval between initial chest radiograph and abdominal evaluation.

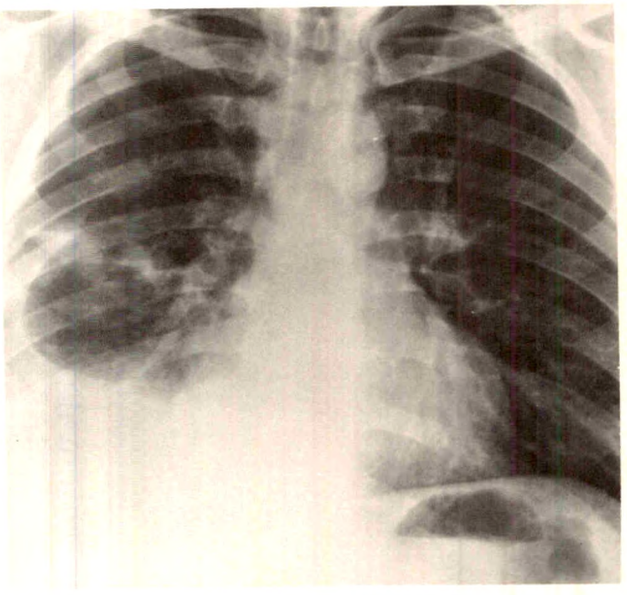

Fig. 1.—Chest film demonstrating moderate-sized right pleural effusion.

The confusion in diagnosis was partly due to cross-sectional imaging, which in the future may be eliminated if computer assisted sagittal reconstruction becomes more commonplace. Until then the interpretation of liver CT scans in the presence of right pleural effusions should be made with caution. When an inverted diaphragm is suspected, ultrasound may be helpful.

REFERENCES

1. Swingle JA, Logan R, Juhl JH: Inversion of the left hemidiaphragm. *JAMA* 208:863–864, 1969
2. Mulvey RB: The effect of pleural fluid on the diaphragm. *Am J Roentgenol* 84:1080–1085, 1965
3. Rogers CI, Meredith HC: Osler revisited: an unusual cause of inversion of the diaphragm. *Radiology* 125:596, 1977
4. Levitt RG, Sagel SS, Stanley RJ, Jost RG: Accuracy of computed tomography of the liver and biliary tree. *Radiology* 124:123–128, 1977

Received March 28, 1978; accepted after revision July 26, 1978.

[1] All authors: Department of Radiology, Alexandria Hospital, 4320 Seminary Road, Alexandria, Virginia 22314. Address reprint requests to B. T. Katzen.

© 1978 American Roentgen Ray Society

0361–803X/78/1200–1077 $00.00

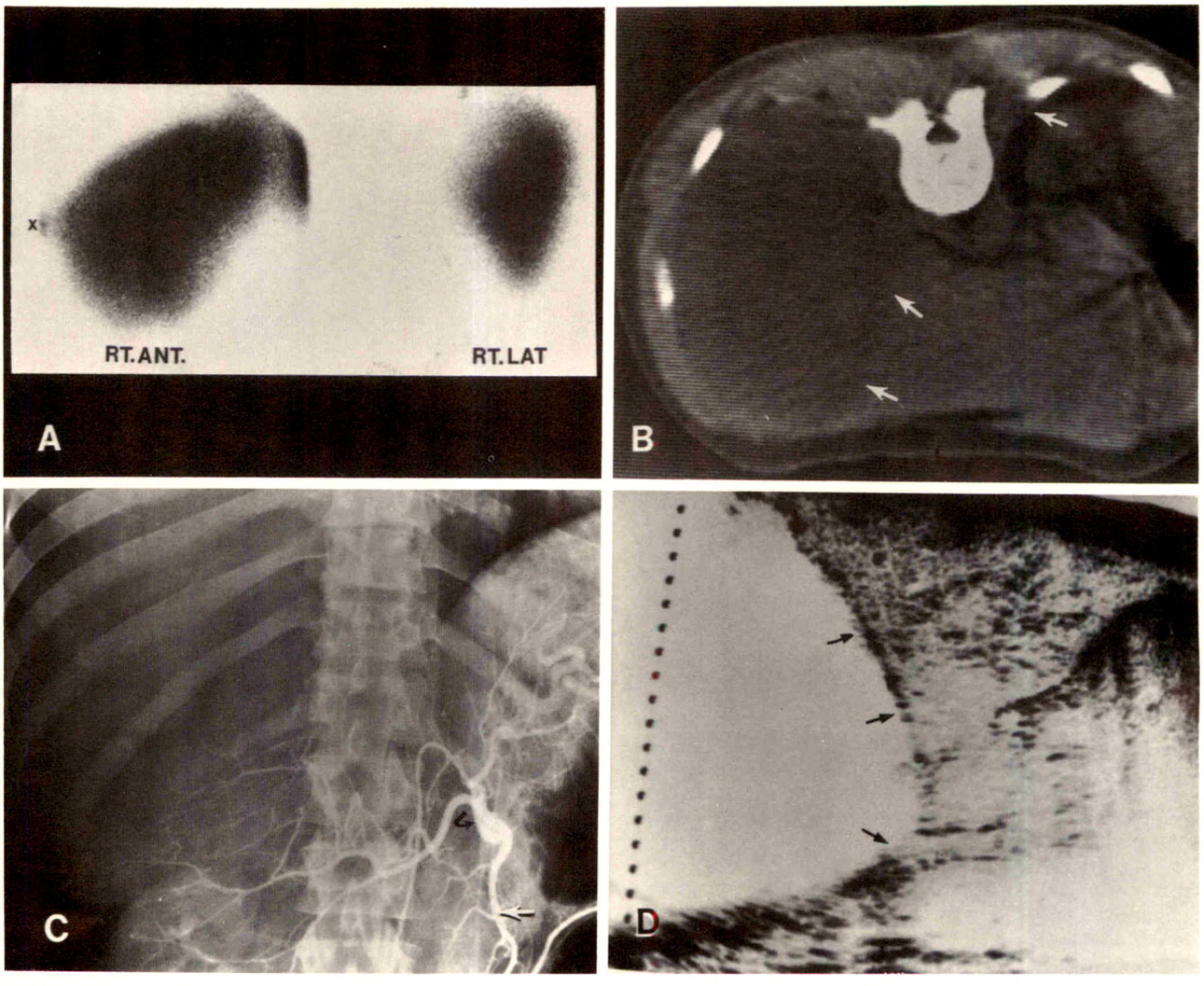

Fig. 2.—*A*, Radionuclide scan of liver demonstrating somewhat horizontal appearance of dome of right lobe of liver. *B*, Prone CT scan showing area of decreased attenuation in region of right lobe of liver (*arrows*). *C*, Arterial phase of selective hepatic arteriogram demonstrating shift of liver and duodenum across midline. Note common hepatic artery (*black arrow*) and gastroduodenal artery (*white arrow*). *D*, Sagittal sonograph of abdomen 3 cm right of midline demonstrating that diaphragm is inverted in direct apposition to superior pole of kidney (*arrows*). Large sonolucency is compatible with pleural effusion above it.

Cathartic Colitis

SEUK KY KIM,[1] RICHARD D. GERLE, AND RICHARD ROZANSKI

The radiographic findings of cathartic colon [1] have been well known since Heilbrun [2] first reported this entity in 1943. Despite the characteristic radiographic changes seen in this entity, the pathogenesis and pathology have not been well understood. We have studied the pathology of cathartic colon and have correlated the pathological changes with the radiographic findings.

Case Report

A 67-year-old white female began using laxatives for chronic constipation during childhood and progressed to daily use of cascara in her teens.

Following surgery for an anal fissure at age 50, the patient developed anal stenosis. She required increasingly larger amounts of laxatives, which eventually resulted in liquid stools. Prior to admission she complained of mild abdominal gaseous distension and distress. Physical examination and laboratory findings were normal except for anal stenosis. A barium enema (fig. 1) demonstrated shortening of the proximal colon with a smooth mucosa and a lack of haustral markings. The terminal ileum was also smooth and dilated. The rectosigmoid was not remarkable. In addition to inconsistent constrictions in the proximal colon, a fixed and persistent stricture was seen at the hepatic flexure causing proximal dilation and poor evacuation. Since the patient was a known laxative abuser, a radiographic diagnosis of cathartic colon was made. However, because of the presence of a fixed stricture that had not been described in cathartic colon and some similarity of radiologic findings to ulcerative colitis, the possibility of cancerous degeneration of chronic ulcerative colitis was considered and a right hemicolectomy was performed. At surgery the ascending colon was considerably dilated but the colon was otherwise unremarkable. Palpation of the stenotic area revealed some thickening of the intestinal wall.

Gross examination of the surgical specimen of the ascending colon (fig. 2*A*) showed a normal serosal surface. The mucosa was atrophic and smooth with punctate, superficial ulcerations. Gross appearance of the stenotic area of the colon was similar to that of the rest of the colon.

Microscopy (fig. 2*B*) showed markedly atrophic mucosa with chronic inflammation and paneth cell metaplasia. Healing superficial ulcerations were noted. The cellular infiltrates were predominantly mononuclear cells, but a large number of eosinophils were also seen, raising the possibility of an allergic reaction to cathartics. Examination of the myenteric plexus was normal. Microscopic examination of the stenotic area, however, revealed markedly thickened muscularis mucosa distorted by fibrosis. The fibrosis extended to the submucosa, which was infiltrated by fat. Muscularis layers were normal. The stricture was therefore due to thickening of the muscularis mucosa and submucosal fibrosis.

Discussion

Radiology

Because history of laxative abuse is often not volunteered by a patient, the radiologist may be puzzled by the findings of a barium enema. The radiographic changes of cathartic colon are similar to those of burned-out ulcerative colitis: smooth mucosa, loss of haustration, and a general shortening of the colon. However, certain features may enable the entities to be distinguished in certain cases. We reviewed the findings of nine cases of cathartic colon and found these to be similar to those described by Plum et al. [1]. Cathartic colon predominantly involves the right colon, often sparing the rectosigmoid region. However, it may involve the entire colon and the terminal ileum, the latter having an appearance of the so-called "backwash ileitis" seen in ulcerative colitis. Shortening of ascending colon can be marked, but unlike ulcerative colitis, the shortened segments remain remarkedly distensible. Inconstant luminal constriction or "pseudo strictures" are seen at fluoroscopy and most commonly occur at the hepatic flexure. True stricture of the colon has not been previously reported. When these characteristic findings are seen in a patient with long standing cathartic abuse, the diagnosis of cathartic colon is certain.

Pathology

In our experience the pathologic changes associated with cathartic colon are nonspecific. Jones [3] first reported the pathologic findings in 1967. He described dark brown colonic mucosa with a white reticular streaking resembling alligator skin; there was excessive submucosal fat and atrophy of the muscle layer. Bockus et al. [4] showed that certain laxatives cause pigmentation of colonic mucosa. In 1968, Smith [5] used the same colon specimen for microscopic examination of the myenteric plexus and described degeneration of neurons and axons. He postulated that laxatives are neurotoxic agents that cause myenteric damage.

The second case of cathartic colon pathology was reported by Urso et al. [6] in 1975. In this case, the colon was dilated and the mucosa was atrophic and smooth with multiple punctate superficial ulcerations measuring 2–3 mm. Thickening of muscularis mucosa and submucosal fibrosis were noted.

We reviewed the pathologic slides of the case described by Urso et al. [6]. The microscopic findings were

Received February 17, 1978; accepted after revision August 2, 1978.
Presented at the annual meeting of the American Roentgen Ray Society, Washington, D.C., September 1976.
[1] All authors: Department of Radiology, Upstate Medical Center, 750 East Adams Street, Syracuse, New York 13210. Address reprint requests to S. K. Kim.

© 1978 American Roentgen Ray Society

similar to those in our case. Findings in both cases included smooth atrophic colonic mucosa with multiple punctate superficial ulcers, chronic inflammation with resultant thickening of muscularis mucosa, and submucosal fatty infiltration and fibrosis. The main muscular layer and myenteric plexus were normal. The degeneration of neurons described by Smith [5] was not appreciated in either case.

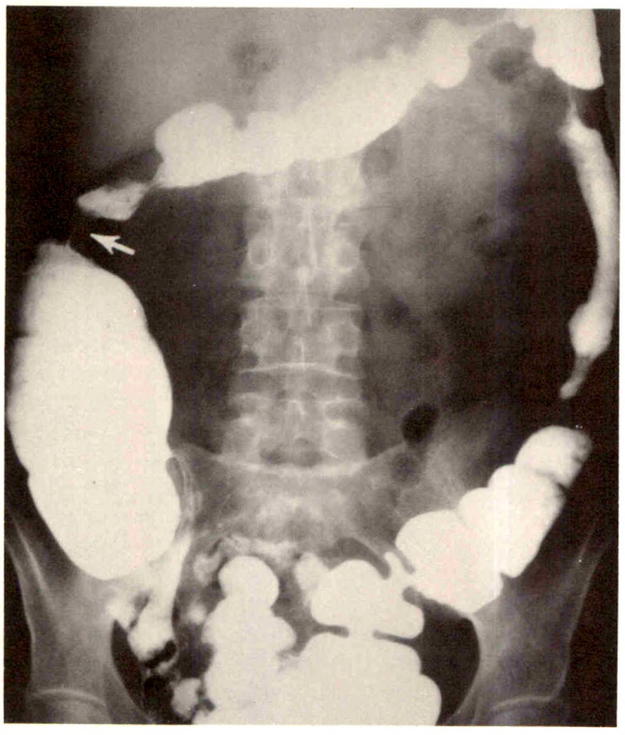

Fig. 1.—Barium enema showing smooth mucosa, lack of haustration shortening, inconstant constrictions, and smooth terminal ileum. Note true stricture with proximal dilation at hepatic flexure (*arrow*).

Goulston et al. [7] reported that benign strictures seen in ulcerative colitis are due to hypertrophy of the muscularis mucosa. This same pathology was found to be the cause of the stricture in our case. All of the pathologic findings of cathartic colon resemble those of chronic ulcerative colitis in remission; our pathologists were unable to distinguish between these entities in the cases reviewed.

Pathophysiology

A chronic colitis appears to develop with prolonged cathartic use, but the only symptom of colitis is a laxative-induced diarrhea. The pathophysiology of cathartic colon can only be postulated. It is possible that direct mucosal irritation by a cathartic for prolonged periods may produce a chronic colitis. Burned-out ulcerative colitis results from years of intermittent exacerbation of acute colitis, which is clinically apparent. However, cathartic colitis, similar both radiologically and pathologically to burned-out ulcerative colitis, develops without a clinically obvious acute phase.

ACKNOWLEDGMENT

We thank Dr. F. P. Urso for use of his pathologic slides.

REFERENCES

1. Plum GE, Weber HM, Sauer WG: Prolonged cathartic abuse resulting in roentgen evidence suggestive of enterocolitis. *Am J Roentgenol* 83:919–925, 1960
2. Heilbrun N: Roentgen evidence suggesting enterocolitis

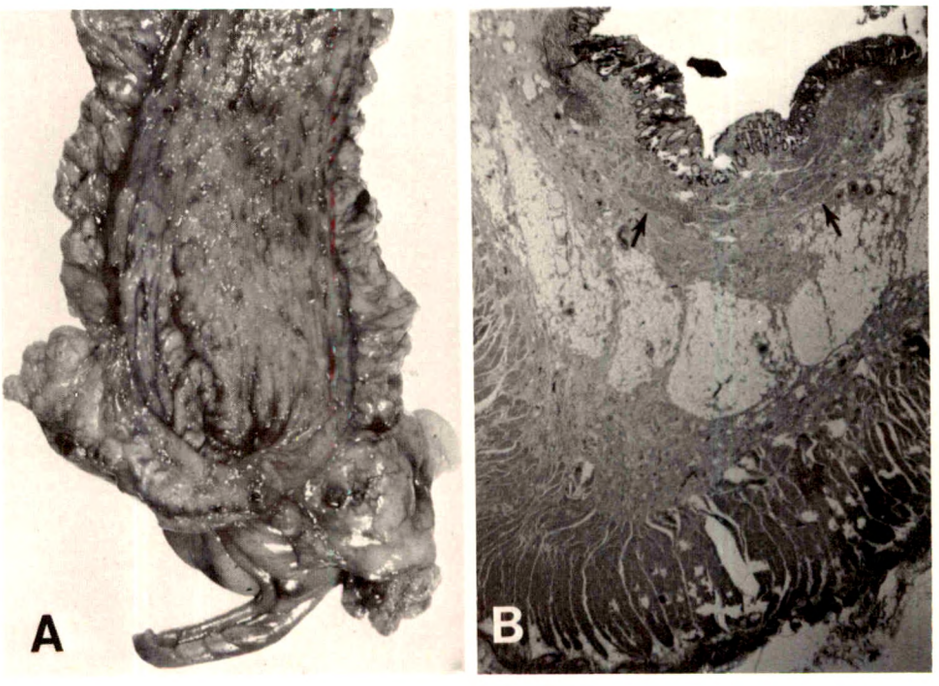

Fig. 2.—*A*, Surgical specimen of ascending colon showing smooth, atrophic mucosa with punctate superficial ulcers (dark spots). Stenotic hepatic flexure is in distal-most portion of specimen at top. *B*, Microphotograph of colon at stenotic area. Mucosa is atrophic with chronic inflammation (top). Note thickened muscularis mucosa (*arrows*). Submucosal fat infiltration, fibrosis, and circular muscles are normal.

associated prolonged cathartic abuse. *Radiology* 41:486–491, 1943
3. Jones FA: Cathartic colon. *Proc R Soc Med* 60:503–504, 1967
4. Bockus HL, Willard JH, Bank J: Melanosis coli: the etiologic significance of the anthracene laxatives. *JAMA* 101:1–6, 1933
5. Smith B: Effect of irritant purgatives on the myenteric plexus in man and the mouse. *Gut* 9:139–143, 1968
6. Urso FP, Urso MJ, Lee CH: The cathartic colon: pathologic findings and radiological/pathological correlation. *Radiology* 116:557–559, 1975
7. Goulston SJM, McGovern VJ: The nature of benign strictures in ulcerative colitis. *N Engl J Med* 281:290–295, 1969

Multinodular Primary Amyloidosis of the Lung: Diagnosis by Needle Biopsy

JEAN-PAUL BIERNY[1]

To date fewer than thirty cases of multinodular primary amyloidosis of the lung have been reported in the medical literature [1–14]. Only one was diagnosed by needle biopsy [9]. An additional case diagnosed promptly by lung needle biopsy is reported here.

Case Report

R. K., a 65-year-old white male, was hospitalized for surgical correction of an inguinal hernia. He was otherwise healthy and without any symptoms referable to the lungs. A routine preoperative chest radiograph showed multiple bilateral lung masses of soft tissue density ranging in size from 1.5–5.5 cm (fig. 1). These masses did not contain any calcification and were sharply circumscribed. There were no hilar nodes and the mediastinum was normal. A percutaneous lung needle biopsy of one of the lung nodules was performed uneventfully as an outpatient procedure. The biopsy material had a waxy consistency, and microscopic evaluation showed typical features of amyloidosis (fig. 2*A*) including some bony trabeculae (fig. 2*B*). Additional laboratory investigation was undertaken to rule out multiple myeloma or another underlying cause. These investigations, including marrow biopsy and serum protein electrophoresis were normal.

Discussion

Nodular pulmonary amyloidosis is rare. It can present as a single mass or as multiple nodules varying in size from a few mm to several cm, sometimes containing calcifications, bony trabeculae [8], or cavitation. The nodules usually have no distinguishing feature other than occurring in asymptomatic patients. The differential diagnosis most prominently includes metastases, granulomas, and less common entities such as alveolar cell carcinoma, hamartomas, lymphoma, periarteritis nodosa, and multiple septic emboli.

The nodules in this otherwise asymptomatic patient were initially suspected to represent metastases from an unknown primary carcinoma. Investigation of such an occult entity might have been expensive, lengthy, and somewhat uncomfortable for the patient. Usual tests include sputum cytology, liver scan, thyroid scan, excretory urography, an upper gastrointestinal series, and barium enema. Instead, it was elected to confirm the diagnosis of metastatic cancer by lung needle biopsy and, based on the microscopic appearance, direct and shorten the search for the primary carcinoma.

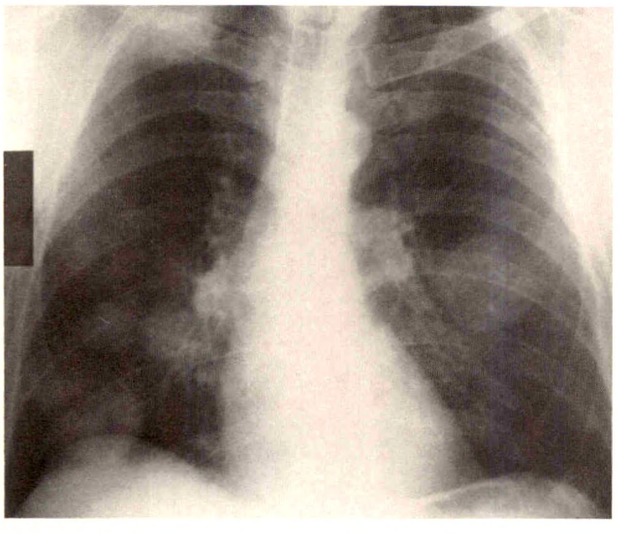

Fig. 1.—Chest radiography showing multiple soft tissue masses of various sizes in both lung fields.

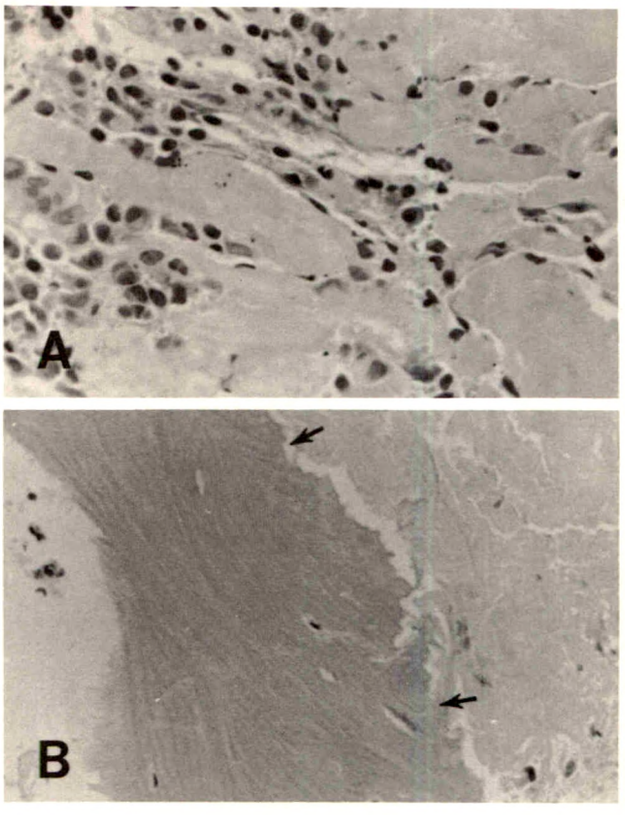

Fig. 2.—Histologic section. *A*, Amyloid material, lymphocytes, and plasma cells are shown. All are characteristic of amyloidosis. *B*, Amyloid material with bony trabeculae (*arrows*).

Received December 16, 1977; accepted after revision August 8, 1978.
[1] Radiology Ltd., 5410 East Pima Street, Tucson, Arizona 85712.

© 1978 American Roentgen Ray Society

0361–803X/78/1200–1082 $00.00

Lung needle biopsy was performed with a modified 18 gauge Franseen needle [15], which obtains a good core of tissue for histologic examination, rather than a smear of aspirated cells for cytologic study. The technique has been described by McCartney et al. [16], and includes a guiding Jelco sleeve, constant suction, and injection of a coagulated blood "patch" through the sleeve as it is withdrawn at the end of the procedure. This technique is comfortable and safe enough to be performed routinely on an outpatient basis (W. Boyd, personal communication) as are other lung needle biopsy techniques [17].

The pathologist identified amyloidosis on the specimen without difficulty, and the diagnosis was unequivocal enough to assume the other lung nodules represented the same process. The diagnosis singularly expedited the patient's workup, eliminating further search for a primary carcinoma and limiting testing to exclude major diseases associated with amyloidosis, mainly multiple myeloma. The patient's condition is unchanged 1 year after the procedure.

REFERENCES

1. Wang CC, Robbins LL: Amyloid disease. Its roentgen manifestations. *Radiology* 66:489–500, 1956
2. Barrington Prowse C: Amyloidosis of the lower respiratory tract. *Thorax* 13:308–320, 1958
3. Weiss L: Isolated multiple nodular pulmonary amyloidosis. *Am J Clin Pathol* 33:318–329, 1960
4. Schuller H, Bollin H, Linder E, Stenran U: Tumor-forming amyloidosis of the lower respiratory system. *Chest* 42:58–67, 1962
5. Cotton RE, Jackson JW: Localized amyloid tumors of the lung simulating malignant neoplasm. *Thorax* 19:97–103, 1964
6. Brown I: Primary amyloidosis. *Clin Radiol* 15:358–367, 1964
7. Hayes V, Berhardt H: Solitary amyloid mass of the lung. *Cancer* 24:20–25, 1969
8. Teixidor HS, Bachman AL: Multiple amyloid tumors of the lung. *Am J Roentgenol* 111:525–529, 1971
9. Gordonson JS, Sargent EN, Jacobson G, Turner AF: Roentgenographic manifestations of pulmonary amyloidosis. *J Can Assoc Radiol* 23:269–272, 1972
10. Dyle PC, Denary JF, Delavan JW, Rasmussen RA: Pulmonary amyloidoma. *Am J Clin Pathol* 61:301–305, 1974
11. Keller A, Staffen A, Syre G: Zur Problematik der isolierten tumorformige Amyloidose der Lunge. *Thoraxchirurgie* 22:86–93, 1974
12. Siong C, Johnson HA: Multiple nodular pulmonary amyloidosis. *Thorax* 30:178–185, 1975
13. Rabin IJ, Hilser CL, Scheinnan HZ, McKenna PJ: Amyloid pseudotumor of the lung. *Mt Sinai J Med* NY 33:168–173, 1976
14. Gariepy J, Phaneus D, Charbonneau R: Amyloidose nodulaire multiple du poumon. *Union Med Can* 105:1227–1230, 1976
15. Arnston T, Boyd W: Percutaneous biopsy using a safe, effective needle. *Radiology* 127:265, 1978
16. McCartney T, Tait D, Stilson N, Seidel GS: A technique for the prevention of pneumothorax in pulmonary aspiration biopsy. *Am J Roentgenol* 120:872–875, 1974
17. Lalli A, McCormack L, Zelch M, Reich N, Belovich D: Aspiration biopsies of chest lesions. *Radiology* 127:35–40, 1978

Editor's note:

The feature of this case report that attracted my attention is the directness with which a very uncommon situation was precisely identified and with minimal inconvenience to the patient. Such directness is the purpose for constructing algorithms for diagnostic workup of various common clinical problems. It provides a solid basis for effective cost containment, an objective that commands attention from all of us in medicine. Where radiologic methods are involved, such directness can only be achieved when the radiologist actively participates in the selection of procedures. This is not the case in many practices today. However, the radiologist must have more than just technical ability. He must be a clinician, knowledgeable of the yield and costs of alternative procedures as well as the therapeutic potential of the entities with which he may be dealing. As the reader, would you take exception to the expeditious workup described here? If so, please respond through the Letters section.

MMF

Abdominal Twiddler's Syndrome

BRUCE A. RODAN,[1] JAMES E. LOWE,[2] AND JAMES T. T. CHEN[1]

Since inception of permanent cardiac pacing, the literature has flourished with reports of complications. One such entity is the pacemaker twiddler's syndrome, named when Bayliss et al. [1] described a patient who dislocated a transvenous electrode by unconscious or habitual "twiddling" of the impulse generator. Other reported cases [2–5] pertain to transvenous electrodes with a subpectoral impulse generator. We describe a lead fracture of a transmediastinal epicardial pacemaker secondary to twiddling.

Case Report

In March 1974 a 73-year-old woman presenting with an episode of syncope was found to be in complete heart block, and a transmediastinal epicardial pacemaker was implanted (figs. 1*A* and 2*A*). The patient did well until she was admitted to Duke University Medical Center with congestive heart failure in July 1977, after she sensed a "pinching feeling over the box" with radiation to the chest.

At surgery the old pulse generator was found rotated 180°, although the twisted pacing wires were intact (fig. 2*B*). A new impulse generator was implanted and the patient recovered uneventfully.

For the next 6 months the patient was relatively asymptomatic until she experienced an episode of lightheadedness followed by temporary loss of consciousness. In the emergency room she had episodes of complete heart block alternating with periods when her pacemaker appeared to function normally. She complained of intermittent nagging pains in the left upper quadrant since insertion of the new impulse generator. Physical examination revealed an obese female with an intermittently slow heart rate. The electrocardiogram recorded periodic failure of the pacemaker to capture the ventricle. Chest and abdominal radiographs revealed marked stretching and coiling of both pacer wires as they exited the battery pack (figs. 1*B* and 2*C*).

While lying on her left side in the Radiology Department, the patient suffered a syncopal episode associated with pacemaker failure. Pressure to the impulse generator reproduced the failure and resulted in intermittent third degree heart block and presyncope. After the patient was rolled supine the pacemaker functioned appropriately.

The patient received a temporary transvenous pacemaker in the Coronary Care Unit and the following day she was taken to the operating room for generator and electrode testing. The electrode leads were found to be twisted 19 times; the insulation of one lead was fractured and the wire partially broken. This wire was capped and the intact wire was connected to a Medtronic 5973 unipolar impulse generator. Good thresholds were attained. The generator was securely fastened to the pacemaker pocket to prevent further twiddling. The patient's recovery was unremarkable.

Discussion

Plain film radiography is a valuable tool in the evaluation of cardiac pacemakers. The gamut of detectable complications has recently been described by Sorkin et al. [2]. In our case the radiographic findings were confirmed at surgical exploration. Tension resulting from the twisted leads eventually caused a disruption of the insulation over the electrode. Radiographs taken in July 1977 (fig. 2*B*) demonstrated the twisting, but the significance was not appreciated.

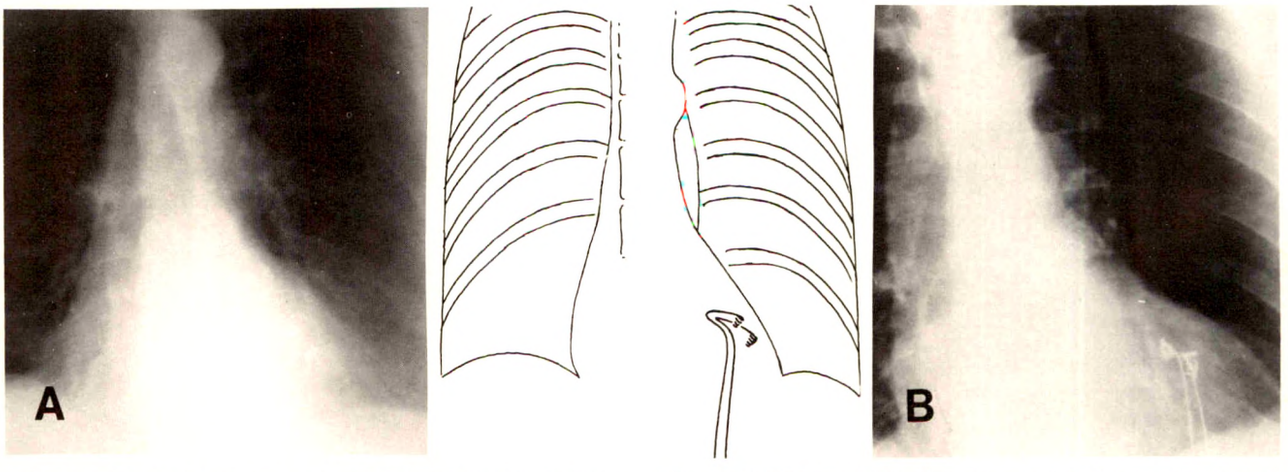

Fig. 1.—Posteroanterior chest radiographs. *A*, Shortly after implantation of transmediastinal pacemaker. Note normal curve of pacemaker wires and electrodes (accompanied by line drawing). *B*, 4 years later after patient developed symptoms of pacemaker malfunction. Note stretched wires, absence of previous curve, and electrodes closer together.

Received May 2, 1978; accepted after revision August 2, 1978.

[1] Department of Radiology, P. O. Box 3808, Duke University Medical Center, Durham, North Carolina 27710. Address reprint requests to B. A. Rodan.
[2] Department of Surgery, Duke University Medical Center, Durham, North Carolina 27710.

© 1978 American Roentgen Ray Society

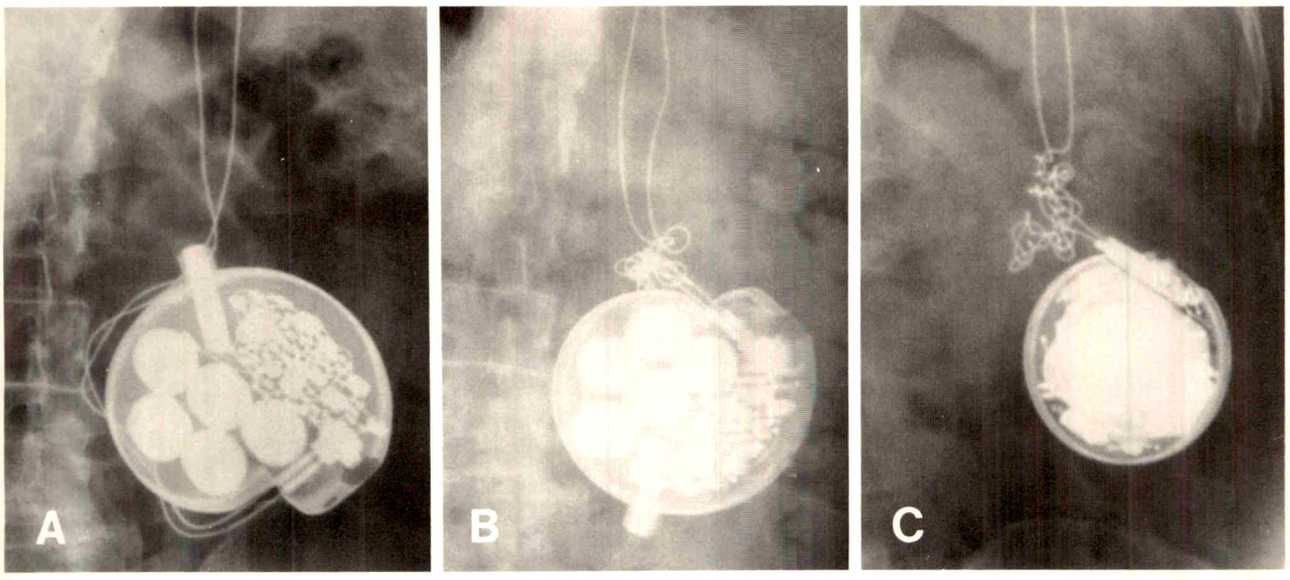

Fig. 2.—Abdominal films. *A*, Film 1 year after initial implant shows normal relationship between wires and impulse generator. *B*, Film 2 years later shows rotation of impulse generator 180° and that wires close to generator are twisted. *C*, 6 months after implantation of new impulse generator, additional twisting is evident.

The mechanism of pacemaker twiddler's syndrome has been well described. Impulse generator rotation can occur spontaneously or as a result of patient manipulation [1–4]. Abdominal discomfort reported by our patient may have induced her to manipulate the impulse generator. We hypothesize that the broken insulation caused intermittent short circuiting of the pacemaker impulses by grounding them to the abdominal soft tissues. The history suggests that this occurred for 6 months prior to detection.

Previously described cases of pacemaker twiddler's syndrome pertain almost exclusively to transvenous electrode dislodgment. To our knowledge, this is the first report in the radiologic literature of "abdominal twiddler's syndrome" associated with a transmediastinal epicardial pacemaker.

ACKNOWLEDGMENT

We thank Vera Mills for help in manuscript preparation.

REFERENCES

1. Bayliss CE, Beanlands DS, Baird RJ: The pacemaker twiddler's syndrome: a new complication of implantable transvenous pacemakers. *Can Med Assoc J* 99:371–373, 1968
2. Sorkin RP, Schuurmann BJ, Simon AB: Radiographic aspects of permanent cardiac pacemakers. *Radiology* 119:281–286, 1976
3. Tegtmeyer CJ, Deignan JM: The cardiac pacemaker: a different twist. *Am J Roentgenol* 126:1017–1018, 1976
4. Meyer JF, Fruehan CT, Delmonico JE: The pacemakers twiddler's syndrome: a further note. *J Thorac Cardiovasc Surg* 67:902–907, 1974
5. Tegtmeyer CJ: Complications of cardiac pacemakers. *Am Fam Physician* 14:66–75, 1976

Computed Tomography of Circumcaval Ureter

WARREN B. GEFTER,[1] PETER H. ARGER,[1] CHARLES B. MULHERN,[1] HOWARD M. POLLACK,[1] AND ALLAN J. WEIN[2]

Circumcaval ureter is an uncommon anomaly in which the proximal right ureter courses medially behind and then anteriorly around the inferior vena cava so as to partially encircle it. Varying degrees of ureteral obstruction result, at times requiring surgical correction [1, 2]. Diagnosis is usually aided by intravenous urography and further supported by retrograde ureteropyelography. Confirmation of the circumcaval position of the ureter requires techniques that simultaneously delineate both the ureter and the vena cava. Inferior venacavography combined with ureteral catheterization is usually employed [3].

Computed tomography (CT) has enabled us to demonstrate a circumcaval ureter. In many cases this simple noninvasive technique may eliminate the need for the more invasive methods formerly used.

Case Report

A 19-year-old black male admitted to the Hospital of the University of Pennsylvania with abdominal pain had no history of urinary tract infections, flank pain, or hematuria. Intravenous urography suggested a circumcaval ureter (fig. 1). Ultrasound of the right kidney confirmed hydronephrosis and proximal hydroureter, but the point of obstruction was not identified. The distal ureter was obscured by bowel gas. CT was done to confirm the presence of a circumcaval ureter using an EMI CT 5005 body scanner with 18 sec scan time. An intravenous infusion of 300 ml meglumine iothalamate (Conray 30) was used for contrast enhancement. Serial scans of selected sections demonstrated the progressive opacification of the proximal dilated ureter and then the retrocaval portion of the ureter. When the contrast material reached the retrocaval portion, lower abdominal compression was applied to distend and demonstrate the distal ureter (fig. 2). Surgical correction was subsequently accomplished.

Discussion

Circumcaval ureter, one of several forms of retrocaval ureter, results from anomalous development of the inferior vena cava. The infrarenal portion of the vena cava normally develops from the dorsally located supracardinal vein. Infrequently the subcardinal vein, lying ventral to the ureter, persists as the major portion of the vena cava. When this occurs, the ureter passes behind and around the medial aspect of the inferior vena cava as it courses to the bladder [1, 2].

This anomaly occurs in about one in 1,000 persons with a 2.8:1 male/female ratio [1, 3]. While it may be discovered as an incidental radiographic or autopsy finding, the abnormality usually leads to symptoms related to ureteral obstruction, including flank pain, recurrent infection, renal calculi, and hematuria [1–5]. Because hydronephrosis develops gradually, circumcaval ureter usually is not manifested before the third or fourth decade, although it has been found at all ages [3–6].

Possible causes of the ureteral obstruction include compression by the inferior vena cava, kinking of the ureter just proximal to the retrocaval segment, crossing gonadal or lumbar veins, and stricture or encasement by a localized fibrosis of the retrocaval segment [4, 5]. Significant ureteral obstruction requires surgical correction. Treatment includes division, transposition, and reanastomosis, with resection of the retrocaval segment if stenotic or redundant. Asymptomatic patients or those with minimal caliectasis may not need surgery but should be followed closely [1, 3, 5, 6].

Intravenous urography in circumcaval ureter reveals a characteristic medial deviation of the upper third of the ureter, which hooks sharply toward the pedicle of the third or fourth lumbar vertebra, producing a "reverse J" configuration (fig. 1). Although several cases without obstruction have been reported, varying degrees of hydronephrosis are usually present [7]. The retrocaval segment and the distal ureter frequently are not opacified. The latter may be demonstrated by retrograde

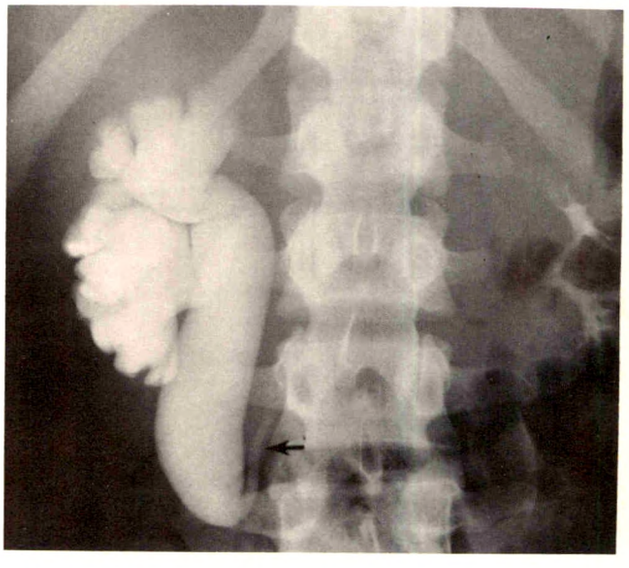

Fig. 1.—30-min follow-up film from intravenous urogram showing dilated proximal ureter and ureteral segment of near normal diameter with "reverse J" configuration (*arrow*).

Received April 4, 1978; accepted after revision August 17, 1978.

[1] Department of Radiology, Hospital of the University of Pennsylvania, 3400 Spruce Street, Philadelphia, Pennsylvania 19104. Address reprint requests to W. B. Gefter.

[2] Department of Urology, Hospital of the University of Pennsylvania, Philadelphia, Pennsylvania 19104.

© 1978 American Roentgen Ray Society

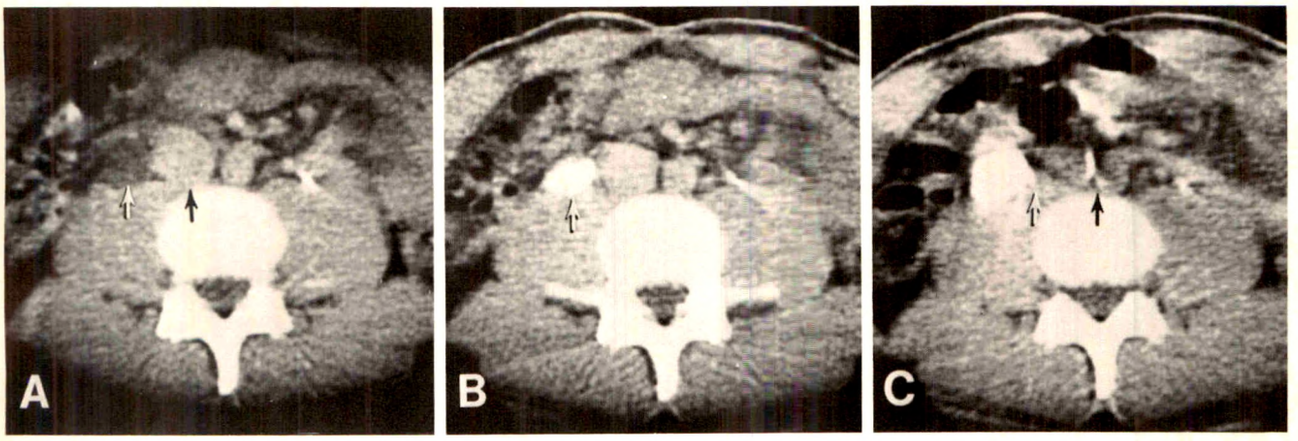

Fig. 2.—CT scans in region of "reverse J" ureteral deformity. *A*, Dilated, nonopacified proximal ureteral segment (*white arrow*); note relationship to inferior vena cava (*black arrow*). *B*, Delayed scan at same level demonstrating opacification of dilated ureteral segment (*white arrow*). *C*, Further delayed scan at same level using lower abdominal compression. Note opacification of undilated "reverse J" segment right of inferior vena cava (*white arrow*) and portion of opacified distal ureter medial to vena cava (*black arrow*) confirming circumcaval course of ureter.

ureteropyelography, which reveals an "italic S" or sickle-shaped ureter [2–6].

In order to confirm the diagnosis preoperatively, a number of techniques have been used to simultaneously display the courses of the ureter and inferior vena cava. These have included inferior venacavography in conjunction with either ureteral catheterization, retrograde ureteropyelography, or infusion pyelography. Stereoscopic views obtained with catheters in both the ureter and vena cava have also been used [1–5].

Because CT performed with intravenous contrast material normally visualizes both the vena cava and the ureters, this simple technique could document a suspected circumcaval ureter, as well as exclude other causes of ureteral displacement. In our case, closely spaced transverse sections through the retrocaval portion in a craniocaudad direction showed successive portions of the ureter and demonstrated unequivocal evidence of its circumcaval position (fig. 2).

An abdominal compression band was used to better distend the retrocaval portion of the ureter. In cases with higher degrees of obstruction, it may be difficult to visualize the distal ureter using intravenously administered contrast, and CT with a ureteral catheter would be required. CT is expected to nearly eliminate the need for venacavography and catheterization procedures to demonstrate this anomaly, and it may become the method of choice in all cases where information about anteroposterior relationships of the ureter is desired.

REFERENCES

1. Johansson NT, Nilsson SV, Schersten T, Schvarcz J, Weiland PO: Retrocaval ureter: report of a case and short review of the literature. *Scand J Urol Nephrol* 3:53–58, 1969
2. Witten DM, Myers GH, Utz DC: *Emmett's Clinical Urography. An Atlas and Textbook of Roentgenologic Diagnosis*, 4th ed. Philadelphia, Saunders, 1977
3. Shown TE, Moore CA: Retrocaval ureter: 4 cases. *J Urol* 105:497–501, 1971
4. Brito RR, Zulian R, Albuquerque J, Borges HJ: Retrocaval ureter. *Br J Urol* 45:144–152, 1973
5. Pitt DC: Retrocaval ureter: report of a case diagnosed preoperatively by intravenous and retrograde pyelography. *Radiology* 84:699–702, 1965
6. Kenawi MM, Williams DI: Circumcaval ureter: a report of four cases in children with a review of the literature and a new classification. *Br J Urol* 48:183–192, 1976
7. Crosse JE, Soderdahl DW, Teplick SK, Clark RE: Nonobstructive circumcaval (retrocaval) ureter. *Radiology* 116:69–71, 1975

Periosteal Chondromas of the Anterior Tibial Tubercle: Two Cases

SANDRA G. KIRCHNER,[1] HELENE PAVLOV,[2] RICHARD M. HELLER,[1] AND JEREMY J. KAYE[1]

Periosteal, or juxtacortical, chondromas are relatively uncommon benign cartilaginous neoplasms usually seen in young adults. We present two cases of this unusual tumor, both of which had a similar appearance in an atypical location.

Case Reports

Case 1

E. G., an 8-year-old boy, noted a painless lump below the left knee 2 months before admission to the Hospital for Special Surgery. The mass did not interfere with his normal activities, and he seemed otherwise in excellent health. Physical examination revealed a 5 cm firm, nonmovable mass in the area of the left anterior tibial tubercle. The mass was only slightly tender to persistent palpation; the overlying skin was slightly erythematous without local heat. The affected knee had full range of motion and there was no vascular or neurologic deficit.

Laboratory examinations, chest radiography, and excretory urography were normal. Radiography of the left knee (figs. 1*A* and 1*B*) revealed a partially calcified and ossified soft-tissue mass in the region of the anterior tibial tubercle. Minimal erosive defects of the underlying cortex were present. Excisional biopsy was performed. The pathologic specimen (fig. 1*C*) revealed a partially calcified and ossified soft-tissue mass. Microscopic examination of the specimen resulted in the diagnosis of periosteal or juxtacortical chondroma. Follow-up examinations of this patient have revealed no clinical or radiographic evidence of recurrence.

Case 2

T. D., a 6-year-old boy, had a mass on the left leg just below the knee noted 4 months before admission to Vanderbilt University Hospital. The mass was reported to have increased in size over this 4 month period, and the child had complained of pain for the preceding 2 weeks. Physical examination revealed a 2 cm firm, nonmobile mass in the region of the left tibial tubercle. There was no evidence of inflammation in the area, and the neurologic and vascular examinations were normal.

Laboratory examinations were within normal limits. Radiography of the left knee (fig. 2) revealed a partially calcified mass in the soft tissues anterior to the proximal tibia. The underlying tibia appeared relatively normal. Biopsy of the lesion was performed, and the pathologic diagnosis was periosteal chondroma. The patient is now asymptomatic, but the lesion continues to grow and excision is planned.

Discussion

Periosteal chondromas were initially clearly recognized as entities separate from osteochondromas and enchondromas by Lichtenstein and Hall [1] in 1952. In 1956, Jaffe [2] described nine additional patients with this lesion, and proposed the name juxtacortical chondroma. From these and subsequent reports [3–8], a characteristic pattern for this lesion has emerged.

The periosteal or juxtacortical chondroma is most commonly seen in children and young adults, occurring in the tubular bones of the hands and feet. It is also found fairly frequently in the long bones of the extremities. The initial complaint is most often that of a localized swelling, which may gradually increase in size even after puberty. When pain is present, it is usually described as dull and aching, and the tumor may be tender to palpation.

Periosteal chondromas have characteristic radiographic features: (1) a localized soft-tissue mass, which may contain cartilaginous calcifications or ossification; and (2) erosion of the underlying cortex with subjacent sclerosis. On occasion, a delicate shell of periosteal new bone formation may be seen to outline the soft-tissue tumor.

Pathologically, the tumor has a microscopic appearance similar to that of an enchondroma; there may be more cellularity in the lobules of hyaline cartilage. Subjacent cortical sclerosis may be evident on excisional biopsies. Successful treatment is usually obtained by en bloc excision or by excision with curettement of the underlying bone.

The differential diagnosis of periosteal chondroma includes other tumors of periosteal origin, osteochondroma, fibrous cortical defect, cortical desmoid, chondrosarcomas, osteosarcomas, and synovial sarcomas. It must be kept in mind that periosteal chondroma may have atypical radiographic features, including the absence of calcification within the cartilaginous mass and minimal or absent erosion of the adjacent cortex. There may be localized areas of destruction within the underlying bone.

The two cases presented here are unusual in several respects. They occurred in an unusual location, the anterior tibial tubercle. Indeed, this location was of some concern to the surgeons caring for these patients because of the possible effects of total excision on subsequent growth in this area. The radiographic features of cortical saucerization and sclerosis were minimal in these patients. Additionally, the radiographs of the second patient actually demonstrated a well demarcated destructive area in the underlying cortex.

Atypical radiographic features of periosteal chondromas have been previously described by Meyer [9], Merlino and Nixon [10], and Cooke and Pearce [11]. Cases described by these authors were all similar in that no changes were observed in the underlying bone.

Received June 2, 1978; accepted August 3, 1978.

[1] Department of Radiology and Radiological Sciences, Vanderbilt University Medical Center, Nashville, Tennessee 37232. Address reprint requests to S. G. Kirchner.

[2] Department of Radiology, Hospital for Special Surgery, 535 East 70th Street, New York, New York 10021.

© 1978 American Roentgen Ray Society

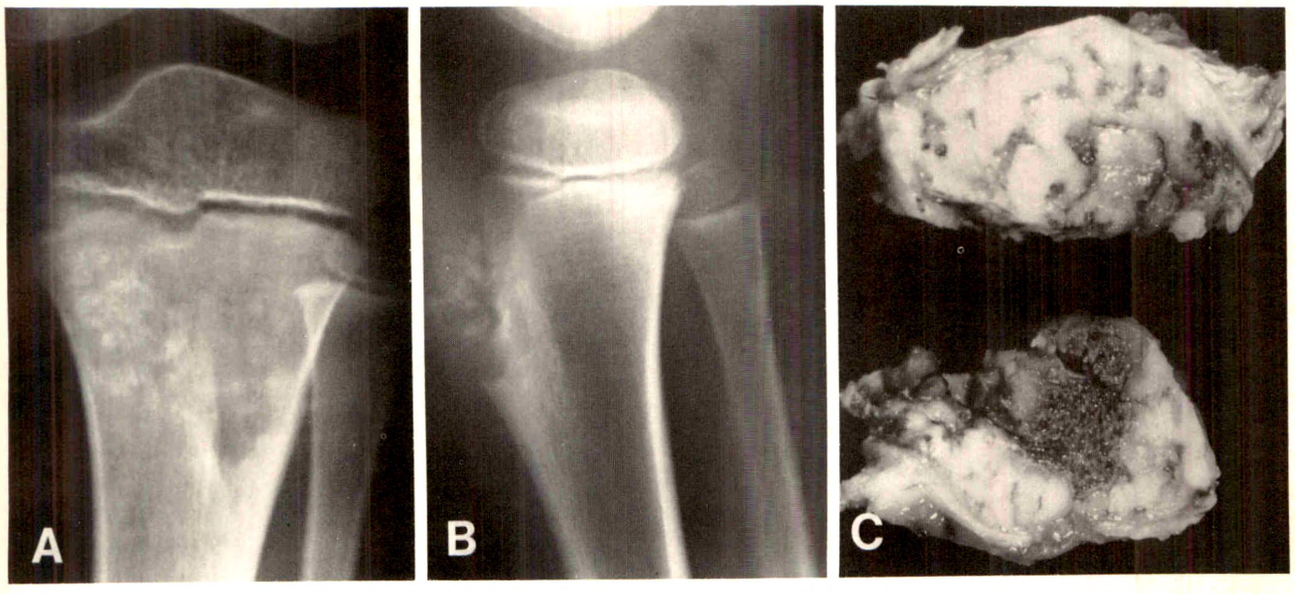

Fig. 1.—Frontal (*A*) and lateral (*B*) projections of proximal left tibia reveal large, poorly marginated mass projecting anteriorly from area of tibial tubercle with multiple dense calcifications within mass and bulging of soft tissues anterior to it. Adjacent anterior aspect of tibia is slightly irregular. *C*, Biopsy specimen showing cartilaginous mass surrounded by fibrous tissue on one side and by bone on other. Note irregular trabecular pattern of underlying bone.

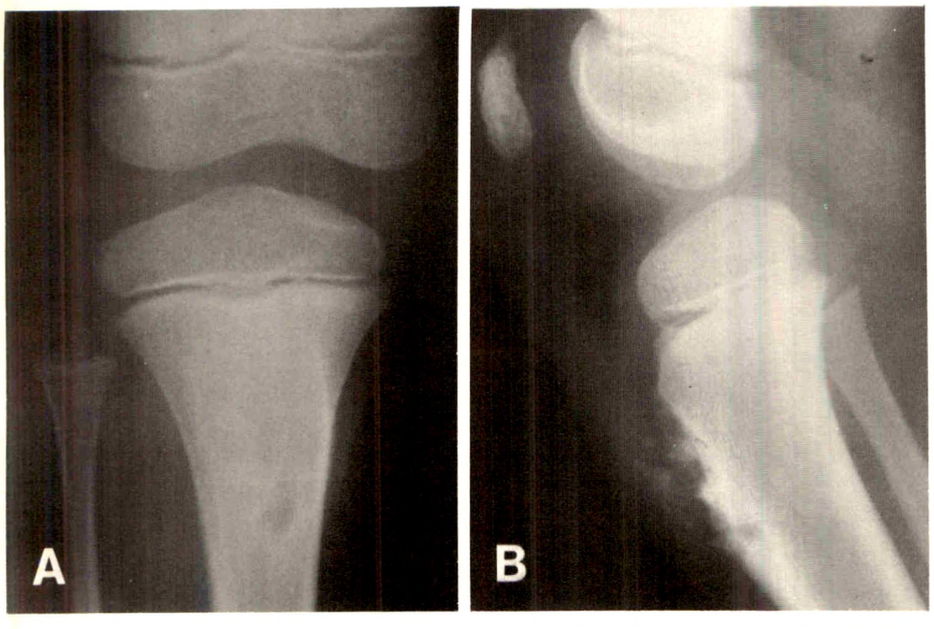

Fig. 2.—Frontal (*A*) and lateral (*B*) projections of proximal left tibia revealing soft-tissue mass in area of anterior tibial tubercle. Mass contains multiple cartilaginous calcifications. Small radiolucency is present in anterior cortex of tibia at lower margin of the lesion. Little underlying cortical erosion or new bone formation is present.

REFERENCES

1. Lichtenstein L, Hall JE: Periosteal chondroma. A distinctive benign cartilage tumor. *J Bone Joint Surg* [Am] 34:691–697, 1952
2. Jaffe HL: Juxtacortical chondroma. *Bull Hosp Joint Dis* 17:20–29, 1956
3. Feinberg SB, Wilber MC: Periosteal chondroma. A report of two cases. *Radiology* 66:383–386, 1956
4. Alcott DL, Dubansky M: Periosteal chondroma. A report of a case. *Am J Clin Pathol* 26:294–295, 1956
5. Cary GR: Juxtacortical chondroma. *J Bone Joint Surg* [Am] 47:1405–1407, 1965
6. Jacobson SA: Epichondroma. A supraosseous benign tumor of cartilage. *Bull Hosp Joint Dis* 26:93–101, 1965
7. Nosanchuk JS, Kaufer H: Recurrent periosteal chondroma. Report of two cases and a review of the literature. *J Bone Joint Surg* [Am] 51:375–380, 1969
8. Rockwell MA, Saiter ET, Enneking WF: Periosteal chondroma *J Bone Joint Surg* [Am] 54:102–108, 1972
9. Meyer R: Juxtacortical chondroma. *Br J Radiol* 31:106–107, 1958
10. Merlino AF, Nixon JE: Periosteal chondroma. Report of an atypical case and review of the literature. *Am J Surg* 107:773–776, 1964
11. Cooke GM, Pearce JG: Periosteal chondroma. Report of two cases with atypical radiologic features. *J Can Assoc Radiol* 27:301–303, 1976

Intraarterial Nitroprusside Treatment for Ergotism

JAMES W. HUSTED,[1] ERNEST J. RING,[2] AND LEONARD F. HIRSH[3]

Peripheral ischemia and gangrene are well known complications of ergotamine tartrate. This may be due to either overdosage or individual hypersensitivity to normally tolerated doses [1]. Because of characteristic angiographic features, angiography may be the first clue to the proper diagnosis in these patients. Withdrawal of the ergotamine will eventually reverse the spasm [2]. However, if a limb is in a pregangrenous state, more aggressive measures are necessary. Therapy has been quite varied and unpredictable.

Recently, O'Dell et al. [3] reported a case of ergotamine spasm successfully treated by infusion of nitroprusside. We have had similar success with intraarterial nitroprusside in a patient with a pregangrenous foot.

Case Report

A 37-year-old female had sudden onset of a severe left frontal headache 2 months before admission. Angiography revealed two left intracavernous aneurysms. In the month preceding admission, the patient used 18 tablets and three suppositories of Cafergot for headache, a total of 24 mg of ergotamine tartrate. On admission, the remainder of her medical history was not relevant to the clinical problem. The general physical and neurologic examinations were negative, with good femoral and distal pulses bilaterally.

The day after admission, a left carotid Selverstone clamp was placed to treat the intracavernous carotid aneurysms. Partial closure of the clamp was performed 3 days later. That day, the patient complained of pain in both legs. The femoral pulses were markedly diminished bilaterally with absent peripheral pulses and a cool, cyanotic right foot.

During the first 4 days after admission, the patient received 11 Cafergot suppositories, a total of 22 mg of ergotamine tartrate, for left frontal headache. No more than three suppositories were used in any one day. During this time, she also received intermittent diazepam, propoxyphene hydrochloride, aspirin, and oxycodone hydrochloride. Because of apparent lower limb ischemia, arteriography was performed. Procedure via the axillary route demonstrated severe spasm of both external iliac, femoral, and peripheral arteries (fig. 1*A*).

Despite a continuous epidural block with local anesthetic, intravenous low molecular weight dextran, and intravenous hydrocortisone, the right foot continued to be cold and painful. A line of ischemic demarcation appeared in the right mid-calf. A catheter was placed in the distal abdominal aorta; repeat pelvic angiography revealed no significant change. Twenty-four hours after the first signs of ischemia, a continuous infusion of sodium nitroprusside was begun through this catheter. Treatment was begun at 18 μg/min and increased to 84 μg/min. At this level of infusion, there was little change in the patient's normal systolic blood pressure of 80 mm Hg, as monitored by a radial arterial catheter.

One hour after the beginning of intraarterial nitroprusside, the right foot felt slightly warmer but was still painful. The infusion was continued for about 14 hr before it was tapered and changed to intravenous nitroprusside which was maintained at 36 μg/min for 24 hr longer. Repeat angiography prior to intravenous therapy (fig. 1*B*) revealed disappearance of the arterial spasm on the right. At this time, the right posterior tibial pulse was palpable and the right foot was warm and pink. Although the left leg was asymptomatic, there was little angiographic improvement of the peripheral vessels. Pulses returned to the left foot before completion of the intravenous infusion.

The patient then developed deep venous thrombophlebitis of the right calf, confirmed by phlebography and treated by heparinization. Completion of closure of the Selverstone clamp was carried out. The patient was discharged on sodium warfarin after healing of her surgical wound and resolution of the acute thrombophlebitis. At follow-up 3 months later she had developed right foot drop due to an ischemic peroneal nerve palsy, as well as causalgialike pain in the right foot. Fortunately, her headache had disappeared.

Discussion

Ergotamine produces both direct peripheral vasoconstriction and alpha-adrenergic blockade [4]. The recommended safe maximal dosage is six tablets (6 mg) or two suppositories (4 mg) per attack. Total weekly dosage should not exceed 10 mg [5]. The excellent absorption of the drug through the rectal mucosa and the ease of administration increase the danger of intoxication from the use of rectal suppositories. Increased sensitivity to ergot alkaloids may be present in septic states and impaired liver function [6, 7]. Ergotism may occur as a result of chronic ingestion of therapeutic dosages of ergotamine, as a result of acute ingestion of small amounts of ergot drugs in individuals hypersensitive to them, or, as in our patient, due to overdosage [1].

The treatment of ergotamine-induced vasospasm has been controversial. Sympathetic and epidural blockades have been advocated. However, it is not surprising that these therapies have failed, since ergotamine acts directly on smooth muscle and not through neural pathways. Direct vasodilators provide a more logical treatment approach. However, systemic niacin, tolazoline, papaverine hydrochloride, and hydralazine have all had limited success.

Several recent articles [3, 4, 8] indicate the benefits of systemic nitroprusside infusion in conjunction with other therapies in the treatment of ergotamine poisoning. Sodium nitroprusside, a potent, direct-acting vasodilator, seems well suited for treatment of this condition. It can be precisely titrated to avoid hypotension because

Received March 20, 1978; accepted after revision August 22, 1978.

[1] Department of Radiology, Crozer-Chester Medical Center, Chester, Pennsylvania 19013. Address reprint requests to J. W. Husted.
[2] Department of Radiology, Hospital of the University of Pennsylvania, Philadelphia, Pennsylvania 19104.
[3] Department of Neurosurgery, Hahnemann Medical College, Philadelphia, and Crozer-Chester Medical Center, Chester, Pennsylvania 19013.

© 1978 American Roentgen Ray Society

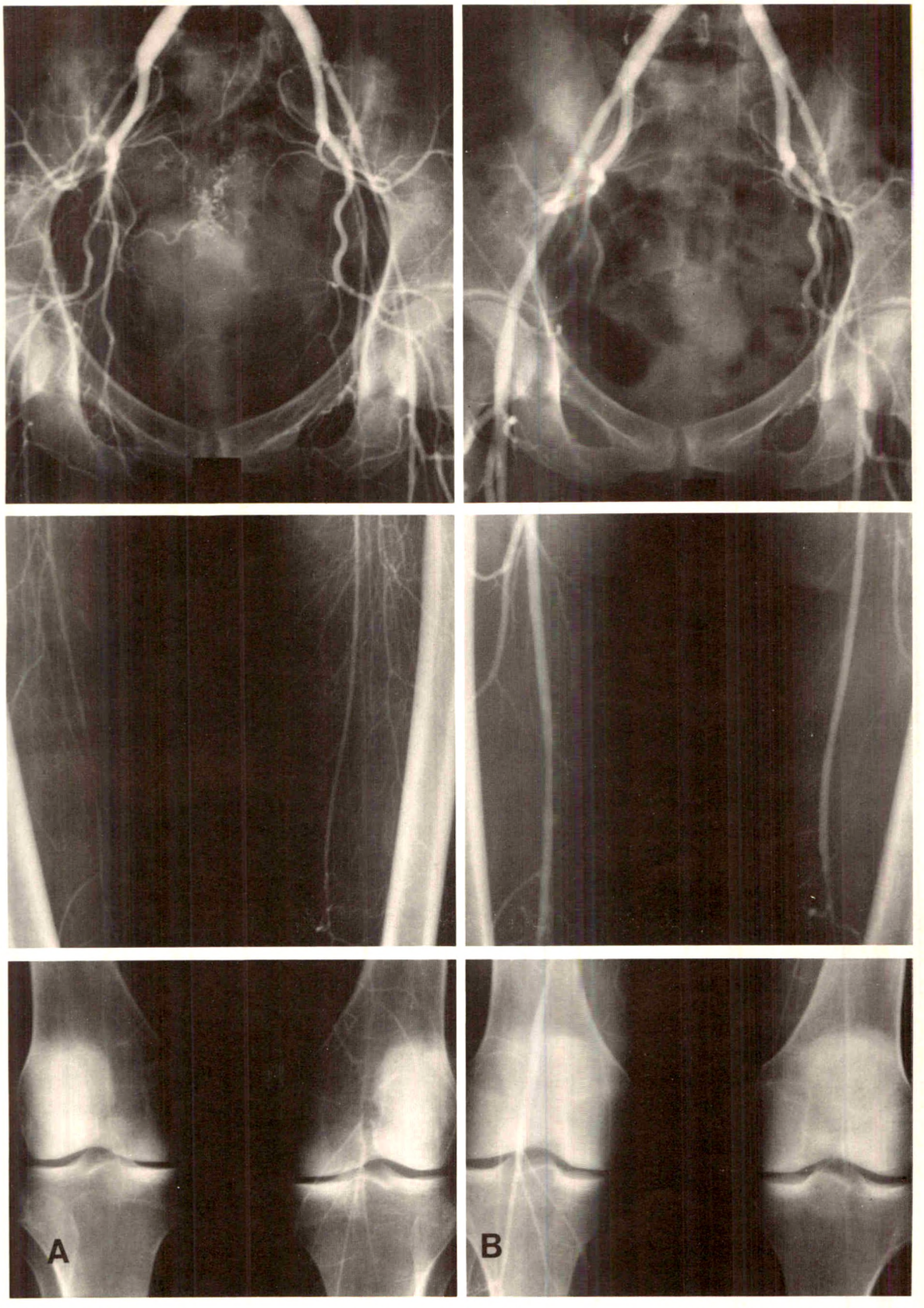

Fig. 1.—*A*, Original angiogram demonstrating bilateral spasm of external iliac, common and superficial femoral, and popliteal arteries. Collateral circulation also visible. *B*, Film after 14 hr of nitroprusside infusion above aortic bifurcation showing marked improvement of vessels on right. Spasm in left external iliac, superficial femoral, and peripheral arteries with collateral circulation persists. Right posterior tibial pulse was normal at this time.

of its rapid onset and cessation of action. In addition, tachyphylaxis has not been reported [4, 8, 9].

During treatment with nitroprusside, precise blood pressure monitoring and control, preferably with an arterial catheter, are strongly recommended. These techniques were essential in this case, because undesired hypotension could have easily produced cerebral ischemia distal to the partially closed carotid artery. In addition, in this patient intraarterial delivery was chosen for more selective action on the affected leg. The subsequent intravenous infusion was to prevent reactive vasospasm after withdrawal of the vasodilator, which although rare has been reported [8]. Despite infusion above the aortic bifurcation and into angiographically similar iliac vessels, the initial effects were much more dramatic in the ischemic leg, an unexplained but quite beneficial effect.

The injection factors for both pre- and posttherapy angiography were identical, using a total of less than 200 ml of contrast material for multiple injections during each study. There were no obvious effects of the contrast agent on the circulation in the limbs during or after the procedures.

The angiographic findings of arterial spasm and collateral circulation are usually bilaterally symmetric with areas of severe narrowing. These may be quite extensive, becoming more severe distally, or may be quite localized. In the lower extremities, which are most commonly affected, the spasm is usually in the superficial femoral arteries, although it may be in the iliac arteries. Thrombosis is a rare complication. Carotid [10], axillary [6], renal [11], and coronary [12] arteries may rarely be involved.

In 1936, Yater and Cahill [13] reported the first angiogram of bilateral gangrene of the feet due to administration of ergotamine tartrate. They described peripheral arterial occlusion with collaterals. No arterial spasm was demonstrated; however, angiography was done almost 6 weeks after the ergot was discontinued.

Although experience is very limited, our observations support those of O'Dell et al. [3] and Carliner et al. [4] that closely monitored intraarterial or intravenous infusion of nitroprusside may be an effective treatment of ergotamine-induced peripheral ischemia.

REFERENCES

1. Bagby RJ, Cooper RD: Angiography in ergotism. *Am J Roentgenol* 116:179–186, 1972
2. Sutton D, Preston BJ: Angiography in peripheral ischemia due to ergotism: report of two cases. *Br J Radiol* 43:776–780, 1970
3. O'Dell CW, Davis GB, Johnson AD, Safdi MA, Brant-Zawadzki M, Bookstein JJ: Sodium nitroprusside in the treatment of ergotism. *Radiology* 124:73–74, 1977
4. Carliner NH, Denune DP, Finch CS, Goldberg LI: Sodium nitroprusside treatment of ergotamine-induced peripheral ischemia. *JAMA* 227:308–309, 1974
5. Sandoz Pharmaceuticals: *Physician's Desk Reference* 31:1372, 1977
6. Kramer RA, Hecker SP, Lewis BI: Ergotism: report of a case studied arteriographically. *Radiology* 84:308–311, 1965
7. Johnsson KA: Angiography in two cases of ergotism. *Acta Radiol* (Stockh) 57:280–284, 1962
8. Andersen PK, Christensen KN, Hole P, Juhl B, Rosendahl T, Stokke D: Sodium nitroprusside and epidural blockade in the treatment of ergotism. *N Engl J Med* 296:1271–1273, 1977
9. Schlant RC, Tsagaris TS, Robertson RJ: Studies on the acute cardiovascular effects of intravenous sodium nitroprusside. *Am J Cardiol* 9:51–59, 1962
10. Richter AM, Banker VP: Carotid ergotism. *Radiology* 106:339–340, 1973
11. Fedotin MS, Hartman C: Ergotamine poisoning producing renal arterial spasm. *N Engl J Med* 283:518–520, 1970
12. Schwalb H: Coronary spasm following ergotamine medication. *Munch Med Wochenschr* 117:1437, 1975
13. Yater WM, Cahill JA: Bilateral gangrene of the feet due to ergotamine tartrate used for pruritis of jaundice: report of a case studied arteriographically and pathologically. *JAMA* 106:1625–1631, 1936

Ulnar Artery Aneurysms: Angiographic Considerations in Two Cases

ROBERT F. LATSHAW[1] AND WILLIAM A. WEIDNER[1]

Most ulnar artery aneurysms in the hand and wrist result from trauma [1, 2]. They are often associated with occupational trauma [3–5], particularly workers who repeatedly hammer or push fixed objects with their palms. The aneurysms are usually located in the distal ulnar artery at the level of the carpal hamate bone [1, 3, 4, 6]. Diagnostic arteriography of the hand and wrist is sometimes technically difficult and requires the use of pharmacologic agents or nerve blockade.

Case Reports

Case 1

A 29-year-old white male was admitted to Hershey Medical Center complaining of a cool sensation and numbness in the middle, ring, and little fingers of his right hand. A right-handed auto mechanic, he daily used air impact wrenches at work. He had no history of cardiac problems, diabetes, or arteriosclerosis. Examination revealed slight cyanosis and decreased temperature to palpation in the right middle, ring, and little fingers. All upper extremity pulses were normal and bilaterally symmetric and laboratory findings were within normal limits.

Arteriography on the fifth hospital day demonstrated normal subclavian, axillary, and brachial arteries in neutral and abducted arm positions. After intraarterial Priscoline, hand and wrist arteriography demonstrated an ulnar artery aneurysm at the level of the carpal hamate bone (fig. 1).

Case 2

An 18-year-old white male was admitted to Hershey Medical Center with pain in the hypothenar region of his left hand and subsequent pain and cyanosis of the left little finger. He had locked himself inside a walk-in freezer at work and had repeatedly struck the exit door with the hypothenar eminence of his left hand to arouse attention of fellow workers.

Angiography on admission demonstrated severe vasospasm. Repeat arteriography after local blocks of the radial and ulnar

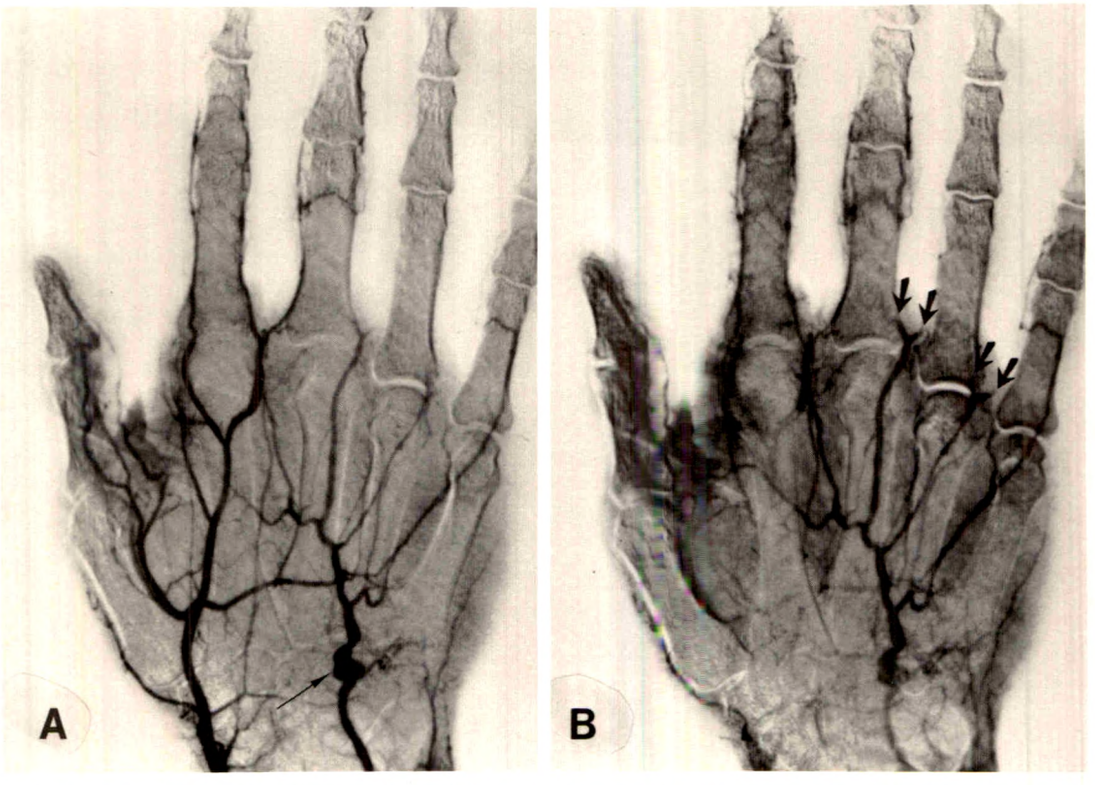

Fig. 1.—Case 1, Subtraction angiograms. *A*, Arterial phase showing ulnar artery aneurysm (*arrow*) at level of hamate bone. Superficial palmar arch is incomplete; radial artery contributes to arterial blood supply to ulnar aspect of index finger and radial aspect of middle finger. *B*, Later film showing multiple occlusions (*arrows*) of proper digital arteries to middle, ring, and little fingers.

Received April 4, 1978; accepted after revision August 29, 1978.

[1] Department of Radiology, Milton S. Hershey Medical Center, Pennsylvania State University College of Medicine, Hershey, Pennsylvania 17033. Address reprint requests to R. F. Latshaw.

© 1978 American Roentgen Ray Society

0361–803X/78/1200–1093 $00.00

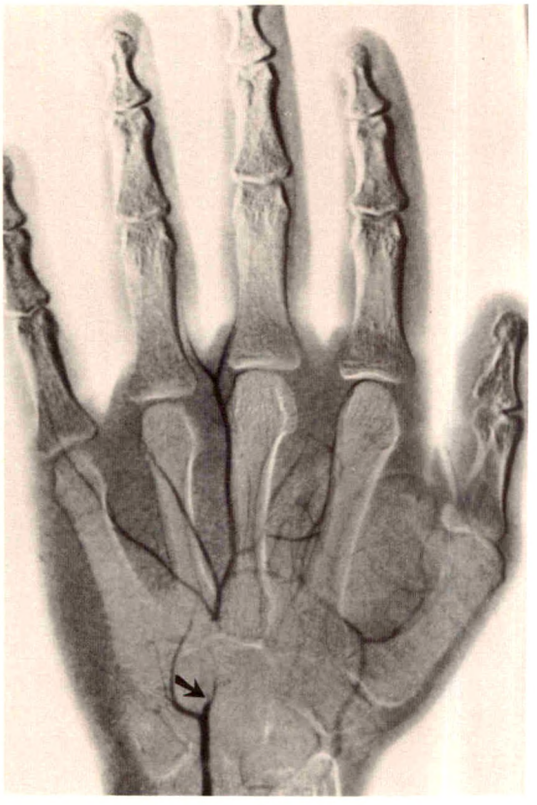

Fig. 2.—Case 2. Subtraction film of arterial phase showing complete occlusion of ulnar artery at level of hamate bone from thrombosed ulnar artery aneurysm (*arrow*). Note diffuse vasospasm involving superficial palmar arch and its branches.

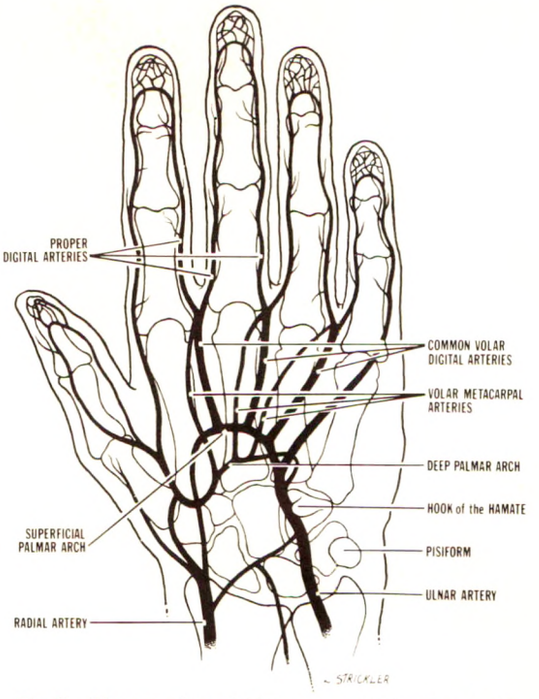

Fig. 3.—Diagram of arterial blood supply to hand and wrist demonstrating classic normal arterial distribution. Note especially relation of ulnar artery to hook of the hamate; most ulnar artery aneurysms occur here.

nerves at the elbow demonstrated improved distal perfusion and complete ulnar artery occlusion at the level of the carpal hamate bone (fig. 2). A thrombosed ulnar artery aneurysm was resected at surgery.

Discussion

True ulnar aneurysms usually follow blunt nonpenetrating trauma; false ulnar artery aneurysms more commonly result from direct penetrating arterial injuries. Ulnar artery aneurysms resulting from occupational trauma most often occur in the dominant hand of manual laborers whose work involves repetitive use of the hand to strike, push, or turn fixed objects. Conn et al. [3] reported that ulnar artery aneurysms may also occur as part of the hypothenar hammer syndrome, a posttraumatic digital ischemia following repetitive nonpenetrating trauma. Trauma can result in aneurysm formation, arterial spasm, occlusion, or any combination of these [3]. Most aneurysms of the hand and wrist involve the ulnar artery at the carpal hamate bone level in the hypothenar eminence. It is postulated that with trauma the ulnar artery is hammered against the hook of the hamate bone, which acts as an anvil.

Arteriography is presently the most accurate method for diagnosing and locating ulnar artery aneurysms, and it is valuable in evaluating associated arterial spasm and occlusion. Arteriography may help exclude other etiologies of ischemia of the hand, such as thoracic outlet syndrome, arteriosclerosis, or thromboangiitis obliterans. An understanding of the arterial supply to the hand and wrist is necessary in performing and interpreting upper extremity arteriography. Figure 3 illustrates the classic normal arterial pattern with respect to underlying carpal bones; however, variations are common.

Coleman and Anson [7] studied 650 gross anatomic hand dissections and classified the findings into subgroups of complete and incomplete superficial palmar arches. To summarize their findings, the arterial blood supply to the hand is primarily from the ulnar and radial arteries, with about 10% of individuals having a persistent median artery. The ulnar artery is usually the major artery to the hand. It divides into a deep and superficial branch in Guyon's canal, and is bounded ventrally by the volar carpal ligament and laterally by the hook of the hamate and pisiform bones. The superficial branch continues "unprotected" 1–2 cm further before turning below the palmar aponeurosis. In this short segment, the artery is covered only by several fibers of the palmaris brevis muscle, subcutaneous tissue, and skin. This large superficial branch terminates in the superficial palmar arch, completed in 79% of individuals by a smaller superficial branch of the radial artery [7]. The common volar digital arteries arise from the superficial arch and transmit the principal blood supply to the fingers [4]. They anastomose with the volar metacarpal arteries, which are branches of the deep palmar arch. At the

interdigital webs, the common volar digital arteries divide into the proper digital arteries, which supply the little, ring, and middle fingers and the ulnar side of the index finger. The radial artery terminates in the deep palmar arch and anastomoses with a smaller branch of the ulnar artery. This arch is complete in about 97% [7] and gives rise to the digital artery to the radial side of the index finger and to the major artery of the thumb.

Diagnostic angiography of the hand and wrist is difficult and is not always achieved without pharmacoangiography or nerve block. Brachial arteriography has been the recommended approach [8]. However, brachial arteriography limits positioning, and arterial spasm may be a significant problem. Currently, arteriography is usually performed from a transfemoral approach using Seldinger technique. This method permits examination of the proximal arteries of the upper extremity. At Hershey Medical Center, a 100 cm no. 5 French polyethylene end-hole catheter is advanced into the midportion of the brachial artery for angiography of the hand. Diatrizoate meglumine 60% (Squibb) is injected at 5–7 ml/sec for a total volume of 20–25 ml. A fluoroscopically monitored test injection of contrast determines when filming starts. Ten to twelve films are exposed at a rate of one film per second. Occasionally, small vessel filling in the hand is not optimal, and pharmacoangiography may be useful. Reported drugs used include Priscoline [9, 10] and phentolamine [9] (Ciba Pharmaceutical Co.) and bradykinin [11]. When pharmacoangiography fails, local nerve block or stellate ganglion block can be used, although they are time consuming (nerve block may delay arteriography as long as 30 min). Subtraction technique and magnification views are also important in improving small vessel detail in angiography of the hand.

REFERENCES

1. Smith JW: True aneurysms of traumatic origin in the palm. *Am J Surg* 104:7–12, 1962
2. Spittel JA Jr: Aneurysms of the hand and wrist. *Med Clin North Am* 42:1007–1010, 1958
3. Conn J Jr, Bergan JJ, Bell JL: Hypothenar hammer syndrome: post-traumatic digital ischemia. *Surgery* 68:1122–1128, 1970
4. Benedict KT Jr, Chang W, McCready FJ: The hypothenar hammer syndrome. *Radiology* 111:57–60, 1974
5. Gallis H, Kushlick AR: Ulnar artery aneurysms of the hand. *Surgery* 73:478–480, 1973
6. Klement HE, Burget GC, Morgan JA, Kutz JE, Atasoy E: Aneurysms of the hand. *Arch Surg* 106:554–557, 1973
7. Coleman SS, Anson BJ: Arterial patterns in the hand based upon a study of 650 specimens. *Surg Gynecol Obstet* 113:409–424, 1961
8. Callaghan L: Angiography of the hand: guidelines for interpretation. *Radiology* 102:331–335, 1972
9. Higgins CB, Hayden WG: Palmar arteriography in acrocyanosis. *Radiology* 119:85–90, 1976
10. Wilmer H, Kay R, Eisenbrey BA: Pharmacologic aids in angiography of the upper extremity. *Radiology* 121:150–154, 1974
11. Eriksson E, Helmus G, Hemmingsson A: On the use of bradykinin in arteriography of the arm. *Australas Radiol* 18:345–349, 1974

Technical Notes

A Transparent Head Support for Magnification Cerebral Angiography

L. D. CROMWELL[1] AND W. E. MOORE[1]

The increased use and popularity of magnification neuroangiography has provided an opportunity for minor equipment revision. The traditional headboard on most angiotables is usually not much wider than the width of the patient's head. Historically, this was for ease in placing the patient's head next to the lateral changer. Because magnification radiography uses an air gap between the patient's head and the film changer, some restrictions on headboard size and design are eliminated.

These restrictions on design of the traditional headboard gave rise to several minor problems. Occasionally its narrow width made positioning difficult, especially for demented or combative patients. This was further complicated because the headboard was not transparent. In addition, its wood core produced significant x-ray absorption.

We have taken advantage of the conditions offered by magnification to design a headboard which overcomes these problems. The design requirements were that the new headboard be wide and optically transparent to facilitate patient positioning and eliminate headboard artifacts caused by off-center head placement. A further requirement was that the new headboard be less radiopaque than the traditional wood-core headboard.

A number of different materials were considered including Styrofoam and Lexan (General Electric). We elected to test Lexan because of its tensile strength, low x-ray attenuation, and transparency.

Design

An easily constructed modification can be made with plywood and a Lexan window. Although the window can be any size, we arbitrarily chose 30.5 × 35.6 cm (fig. 1). The long dimension parallels the long axis of the patient and aids in obtaining oblique views of the common carotid bifurcation during transient ischemic attack workups. The plywood is an exterior grade, 2 cm thick, and serves as a support for the window. The window of .32 cm Lexan is recessed into the plywood support so that it is flush with the upper surface. The device is fastened to the table with the same hardware used for the traditional headboard.

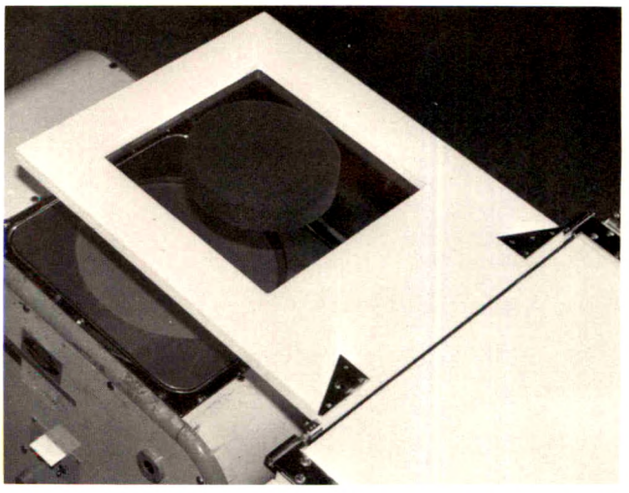

Fig. 1.—Photograph of window headboard illustrating compatibility with Spectrum table (Spectrum X-Ray Corp., Westville, N.J.). Headboard in positioned over Schonander changer. Sponge in middle of window simulates patient's head.

Two types of exposure measurements were made for purposes of cross-checking results. Measurements were made on the head portion of an average man phantom so that reproducible positioning and total exposure presented no problems. Thermoluminescent dosimeters were fastened to various sites. In addition, an ion chamber was placed beneath the headboard. Exposures were made with both the old and new headboards fastened in place.

Results

Our experience indicates use of the Lexan window headboard and routine magnification neuroangiography makes the procedure easier and at the same time enhances the results.Positioning is easier and the films are free of annoying headboard artifacts.

Using 64 kVp, 18 mAs with the conventional headboard, 3.1 mR reached the changer. With the same settings, 4.3 mR reached the changer when the Lexan headboard was installed. This resulted in dark films unless the setting were lowered. We found that 64 kVp,

Received April 28, 1978; accepted after revision September 5, 1978.
W. E. Moore is a James Picker Scholar of the Picker Foundation.
[1] Department of Radiology, University of Washington School of Medicine, Seattle, Washington 98195. Address reprint requests to L. D. Cromwell.

© 1978 American Roentgen Ray Society

12 mAs resulted in comparable optical densities. Using these two techniques, the patient exposure dropped from above 400 mR/film to about 300 mR/film. Alternately, because of the lower attenuation, lower kilovoltage could be used, thereby increasing radiographic contrast.

The unusual strength of Lexan (flexure yield, 5,000 kg/cm²; impact yield, 3,000 cm/kg/cm²) [1] combined with the low cost and low x-ray absorption make it a satisfactory headboard material. A sheet 0.32 cm thick is sufficiently strong for all types of cranial angiography when supported as described.

REFERENCE

1. *The Encyclopedia of Chemical Technology*, 2d ed, vol 16. New York, Wiley-Interscience, 1972

Transurethral Conversion of a Percutaneous Ureteral Stent to an Indwelling Stent

LAWRENCE R. BIGONGIARI,[1] KYO RAK LEE,[1] WINSTON K. MEBUST,[2] JOHN FORET,[2] AND JOHN W. WEIGEL[2]

When retrograde ureteral stent placement by cystoscopy has failed, various techniques of percutaneous nephrostomy offer palliation to the patient with supravesical ureteric obstruction [1]. If an angiographic guide wire can be introduced into the bladder via percutaneous nephrostomy, percutaneous ureteral stent placement can be accomplished [2, 3]. Abdominal surgery is avoided and the patient voids naturally. We recently converted a percutaneous ureteral stent to an indwelling stent transurethrally.

Materials and Methods

A 79-year-old white male, known to have prostatic carcinoma with painless bone metastases, was admitted for evaluation of abdominal pain and swelling of the left leg 2 months after palliative pelvic irradiation. Intravenous urography demonstrated right hydronephrosis and hydroureter with mass effect on the right side of the bladder and nonvisualization of the left kidney. Cystoscopic examination revealed local recurrence of adenocarcinoma of the prostate with bilateral ureteral obstruction. A right percutaneous nephrostomy was performed with placement of an Ingram catheter (Sherwood Medical Industries Inc., St. Louis, Mo.) in the renal pelvis. External irradiation was again applied to the tumor. The patient's symptoms abated and he was discharged.

Two months later an attempt at retrograde placement of a Gibbons catheter (Heyer-Schulte Corp., Goleta, Calif.) led to ureteral perforation. Four days after that, a 0.89 cm guide wire was maneuvered through the nephrostomy, down the ureter, and into the urinary bladder. Some gentle probing was needed to pass the point of obstruction. A Cook No. 8 French Teflon aortogram catheter (Cook, Inc., Bloomington, Ind.) with 10 sideholes at the tip and six extra sideholes punched in its midportion was placed over the guidewire without difficulty as an antegrade ureteral stent (fig. 1*A*). The catheter was sewn to the skin and occluded proximally so that urine entered the sideholes in the midportion of the catheter and exited in the bladder.

One month later, the patient had one episode of leakage of urine around the stent at the skin site. Local skin irritation was present around the tube. The patient expressed a strong desire to have the tube removed from his side. At cystoscopy under

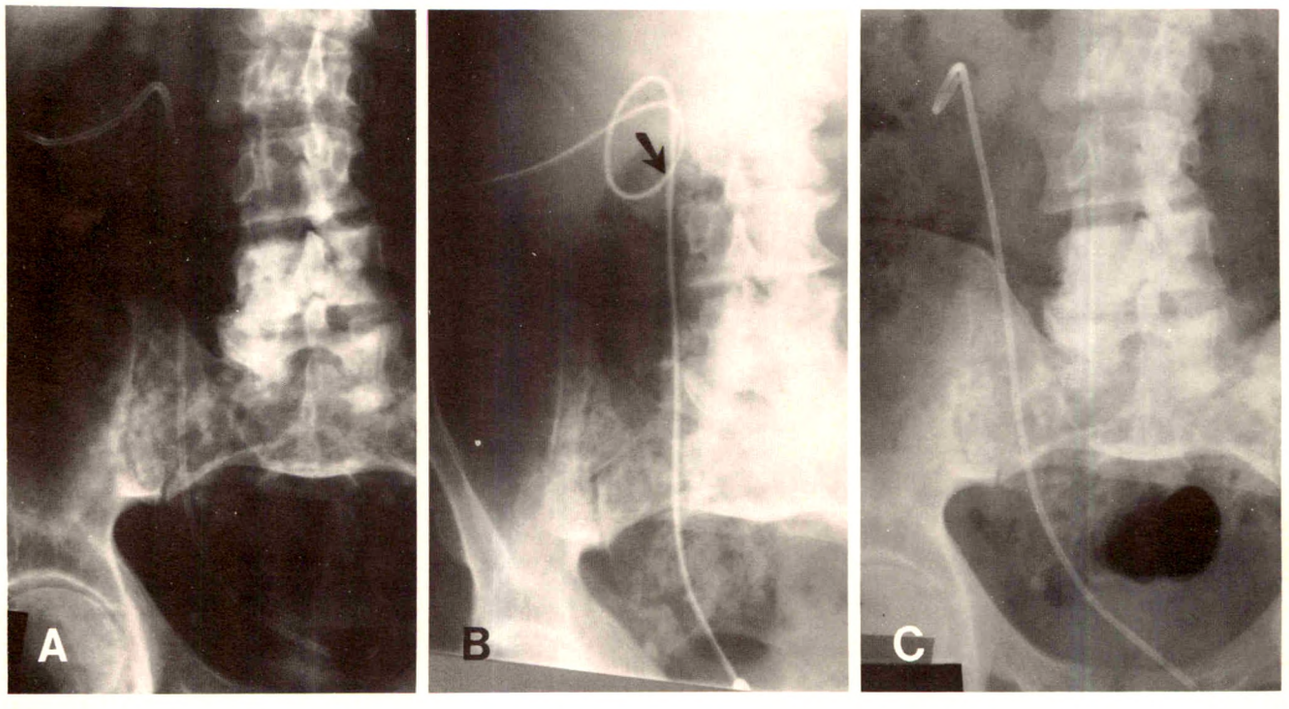

Fig. 1.—*A*, No. 8 French Teflon catheter with proximal sideholes advanced over guide wire previously placed in bladder via percutaneous nephrostomy. Note sclerotic metastases in spine. *B*, No. 8 French pigtail polyethylene catheter advanced over guide wire retrieved from bladder. Tip of pigtail (*arrow*) pushed out percutaneous catheter and coiled in renal pelvis. *C*, Final position of indwelling pigtail stent.

Received June 23, 1978; accepted after revision September 5, 1978.

[1] Section of Uroradiology, Department of Diagnostic Radiology, Kansas University Medical Center, Rainbow Boulevard at 39th Street, Kansas City, Kansas 66103. Address reprint requests to L. R. Bigongiari.

[2] Section of Urology, Department of Surgery, Kansas University Medical Center, Rainbow Boulevard at 39th Street, Kansas City, Kansas 66103.

© 1978 American Roentgen Ray Society

light general anesthesia, a 0.89 cm J-tipped guide wire was passed down the stent from the flank. This guide wire was grasped by the endoscopist and brought out the patient's penis. A Cook ureteral indwelling pigtail stent (no. 8 French polyethylene) was then introduced over this guide wire from below using an additional length of catheter as a pusher. The pigtail stent pushed the antegrade catheter out the patient's side. When the position of the pigtail in the renal pelvis was confirmed (fig. 1*B*), the percutaneous catheter and guide wire were withdrawn from the flank. A follow-up film showed the pigtail tightly coiled in the renal pelvis with the opposite end of the catheter in the urinary bladder (fig. 1*C*). The patient was discharged with no limitations on his physical activity and has remained symptom free on 6 week follow-up.

Discussion

Goldin [2] described the use of percutaneous nephrostomy to place ureteral splints in five patients. Barbaric et al. [3] reported transluminal dilation and ureteral stent placement in surgically ligated ureters in dogs via percutaneous nephrostomy. He suggested burying the occluded proximal end of the tube subcutaneously. More recently, Miller et al. [4] described a technique of affixing a Gibbons tube to the distal end of an antegrade percutaneous stent catheter so that the Gibbons tube can be pulled into place as an indwelling ureteral stent. Their strategy is similar to ours, but their tactics are quite different

The percutaneous techniques avoid surgery in debilitated and terminally ill patients while providing urinary diversion. Blood loss is minimal, if any, and hospitalization can be brief. Renal function can be maintained while primary therapy is considered and applied. The percutaneous approach to stent placement may succeed when the cystoscopic approach has failed. Because of the lack of external appliance, indwelling ureteral stents provide higher quality of life than nephrostomy tubes. Our simple technique allows conversion of a percutaneous to an indwelling stent.

REFERENCES

1. Stables DP, Ginsberg NJ, Johnson ML: Percutaneous nephrostomy: a series and review of the literature. *Am J Roentgenol* 130:75–85, 1978
2. Goldin AR: Percutaneous ureteral splinting. *Urology* 10:165–168, 1977
3. Barbaric ZL, Gothlin JH, Davies RS: Transluminal dilatation and stent placement in obstructed ureters in dogs through the use of percutaneous nephrostomy. *Invest Radiol* 12:534–536, 1977
4. Miller RP, Reinke DB, Smith A, Lange P: The introduction of Gibbons' ureteral stents facilitated by antecedant percutaneous nephrostomy. *J Urol*. In press, 1979

Special Article:

National Guidelines and Standards for Health Planning: Their Relation to Radiology

RONALD G. EVENS[1]

Introduction

Planning has long been recognized as an important concept in radiology. Providing improved radiologic services has always required a systematic approach to departmental design, equipment selection, and personnel utilization. However, such planning usually focused on the individual office or hospital operations and seldom considered community, state, or national issues. Much the same could be said for planning in other medical disciplines.

A system of health planning was first required by congressional legislation in 1966 (Public Law 89-749) which mandated the development of local comprehensive health planning councils and established a certificate of need (CON) reveiw process for new health care proposals. Local planning councils were organized with several objectives, including data gathering, long-range planning for each local area, and the approval or disapproval of capital expenditure projects. In general, the local planning councils did little planning and their primary role was to review and comment on specific projects.

The federal initiative for health planning was strengthened in 1972 when Section 1122 was added to the Social Security Act under Public Law 92-603. Section 1122 required prior approval by both local and state planning agencies for any capital expenditure exceeding $100,000, or for any significant change in clinical services when reimbursed with federal funds through Title V (Maternal and Child Health), Title XVIII (Medicare), or Title XIX (Medicaid). Section 1122 gave "teeth" to the planning process, for denial of reimbursement would be a major problem to most health care institutions. The planning process remained essentially the same with CON reviews at the local and state level, and a continuing responsibility for long-range planning and data collection.

No one was particularly happy with the directives of Section 1122. Medical providers found them restrictive, highly bureaucratic, and inconsistent. Planning agencies were hampered by a lack of data, had difficulty in developing long-range plans, and often stimulated considerable controversy with individual project reviews. The congressional and legislative branches of the federal government were dissatisfied with progress in cost containment or improvements in medical care accessibility.

Further revision of planning activities was legislated by Congress in the National Health Planning and Resource Development Act of 1974 (Public Law 93-641), hereafter called the Act. This Act mandated extensive restructuring of the system for health planning, redefining the geography of local planning areas, adding consumer representation to planning agencies, and broadening the scope of responsibility delegated to health planning and development agencies. Each local planning agency (Health Systems Agency, or HSA) and state agency (each state will have two agencies: a State Health Planning and Development Agency [SHPDA] and a Statewide Health Coordinating Council [SHCC]) was required to develop a health system plan for its local area and criteria and standards for specific health service needs to guide the HSA and state agencies in making informed decisions on individual projects. A criterion is defined as a "measurable characteristic of a health service" and a standard as "the quantitative and/or qualitative value assigned to a particular criterion." The health systems plans of individual HSAs are to be coordinated by the state agency into an overall state plan.

The Act specifically directed the secretary of Health, Education, and Welfare to guide the 205 HSAs and state agencies in designing their health planning systems, including "standards respecting the appropriate supply, distribution, and organization of health resources." The secretary was directed to develop a set of national goals expressed (where practicable) in quantitative terms. The House and Senate reports were somewhat different, but both generally agreed that the concept of the secretary's guidance included a set of national guidelines to serve as a framework within which HSAs and state agencies could develop health plans specific to their area and population.

Developing National Guidelines and Standards

Soon after the enactment of Public Law 93-641 (January 4, 1975), the Department of Health, Education, and Welfare (DHEW) established an interagency committee to coordinate the development of guidelines, commissioned a series of studies on various topics, and sought public input on suggested areas for national guidelines and specific standards. More than a year later, in August 1976, a draft of suggested guidelines covering approximately 24 content areas, both broad and specific, was circulated. In October 1976, a second draft of four broad goals and several specific standards was circulated.

Received August 21, 1978; accepted after revision September 14, 1978.

[1]Department of Radiology, Washington University School of Medicine, and Mallinckrodt Institute of Radiology, 510 South Kingshighway, St. Louis, Missouri 63110. Address reprint requests to R. G. Evens.

© 1978 American Roentgen Ray Society

The development of national guidelines continued to move slowly until mid-1977 when the secretary directed DHEW to "get moving"; perhaps related to his concern about the rising costs of medical care, he directed speedy development and release of *specific* standards. On September 23, 1977, the Health Resources Administration of DHEW published a set of guidelines and standards related to eleven specific areas. Guidelines were developed internally and with little public input.

The September 23 guidelines stimulated a wave of protest as more than 50,000 comments were received in response. Many concerns were expressed on specific standards, the impact of the guidelines on rural hospitals and teaching facilities, and the loss of local control and responsibility for health planning. While the secretary's initial intent was to modify the guidelines of September 23 and issue a final rule in a short period of time, he decided to issue a second set of guidelines after convening a series of public meetings that included several radiologists. A revised set of guidelines was published in the *Federal Register* on January 20, 1978 with multiple changes in specific standards and inclusion of some degree of flexibility in using the standards by local HSAs and state agencies. Apparently the January 20 guidelines elicited a much smaller response and the National Guidelines for Health Planning were published in the *Federal Register* on March 28, 1978, with little change from those of January 20. The secretary has announced that general goals and further guidelines will be issued in the future.

The Guidelines and Radiology

The guidelines define specific standards for general hospital beds, obstetric services, neonatal units, pediatric services, open heart surgery, cardiac catheterization, radiation therapy, and CT scanners. While all the guidelines impact radiology, standards directly relating to radiologic services will be discussed in some detail.

Cardiac Catheterization

> (1) There should be a minimum of 300 cardiac catheterizations, of which at least 200 should be intracardiac or coronary artery catheterizations, performed annually in any adult cardiac catheterization unit within three years after initiation.
>
> (2) There should be a minimum of 150 pediatric cardiac catheterizations performed annually in any unit performing pediatric cardiac catheterizations within three years after initiation.
>
> (3) There should be no new cardiac catheterization unit opened in any facility not performing open heart surgery.
>
> (4) There should be no additional adult cardiac catheterization unit opened unless the number of studies per year in each existing unit in the health service area(s) is greater than 500 and no additional pediatric unit opened unless the number of studies per year in each existing unit is greater than 250.

The discussion accompanying the cardiac catheterization standards justifies their development because these services are expensive and require a highly skilled staff. They recognize that pediatric facilities have special considerations. They are designed to encourage the development of diagnostic and treatment facilities in the same institution.

Megavoltage Radiation Therapy

> (1) A megavoltage radiation therapy unit should serve a population of at least 150,000 persons and treat at least 300 cancer cases annually, within three years after initiation.
>
> (2) There should be no additional megavoltage units opened unless each existing megavoltage unit in the health service area(s) is performing at least 6,000 treatments per year.
>
> (3) Adjustments downward may be justified when travel time to an alternate unit is a serious hardship due to geographic remoteness, based on analyses by the HSA.

The guidelines justify these standards because radiation therapy is expensive. They define megavoltage radiation therapy as cobalt-60 or higher energy radiation, and also define a treatment as a single patient visit without consideration for the number of treatment ports. A local HSA or state agency may be able to adjust the standard due to geographic remoteness (travel time of patients) or for "special purpose" or "very high energy" units.

Computed Tomography (CT) Scanners

> (1) A computed tomographic scanner (head and body) should operate at a minimum of 2,500 medically necessary patient procedures per year, for the second year of its operation and thereafter.
>
> (2) There should be no additional scanners approved unless each existing scanner in the health service area is performing at a rate greater than 2,500 medically necessary patient procedures per year.
>
> (3) There should be no additional scanners approved unless the operations of the proposed equipment will set in place data collection and utilization review systems.

Again, the standards are justified because of expense. A single procedure includes all diagnostic studies performed on the same visit, in the same area of anatomy, and with the same diagnostic interest. The definition was specifically developed to count a patient examination with and without intravenous contrast material as a single procedure. The standards state that this level of activity should be possible in a 50–55 hr week and with a head to body ratio of 60/40. No basis for possible adjustments are given, but the guidelines state that special consideration can be given to institutions with more than one scanner, CT scanners used for clinical research, and in installations with high proportions of seriously ill or pediatric patients. "Medically necessary" is not further defined but is only applied to the standards for CT scanners. The standard requiring data collection is also unique to CT.

Comment

The guidelines are the first serious attempt to regulate the productivity of individual medical facilities. Whether

the guidelines will be used for guidance or serve as a rigid set of rules that force local medical services and radiologic facilities to fit a national standard is a critical issue. The statutory language in Public Law 93-641 states that local HSAs should give "appropriate consideration" and local health systems plans should "take into account" and be "consistent with" the guidelines. While no such language refers to the state agencies, by inference the state health systems plan should also "be consistent" since a state plan is made up of local health systems plans. Although the concept of the guidelines was to serve as a framework within which HSAs and states could develop plans unique to their population and medical needs, rigid federal control is certainly a possibility.

The secretary indicates a *close* relationship between the guidelines and the criteria and standards developed by HSAs and state agencies. The secretary states that local criteria and standards utilized for CON review and health systems plans must be "consistent." In order for local standards and plans to be consistent with the guidelines, they must be the same or *more* stringent. For example, a local HSA standard for CT activity that is consistent with the guidelines would be 2,600 patient procedures annually but a local standard of 2,400 patient procedures per year would not.

While adjustment of the guidelines by an HSA or state agency is possible, any adjustment must be supported by *detailed analysis* and *justification* and is subject to review and comment by the state agency. It is unclear whether the secretary can require consistency when an HSA and state agency standard or plan conflict with the guidelines, since the secretary does not have statutory authority to accept or reject adjustments. In any case, adjustments at the local or state level will require persistence, hard work, and dedication. (Pending congressional legislation would delete the requirement that local and state plans be "consistent" with the Guidelines [HR 11488 and S2410].) The rigidity of the guidelines will undoubtedly be a key issue in the question of local versus national responsibility for health planning.

In addition to the question of federal versus local control over health planning, several additional issues addressed in the guidelines are important to radiology:

1. Planning is focused on large geographic regions, not on the individual hospital or medical facility. HSAs and state agencies must develop plans for their geographic region and the plans of individual institutions must conform to regional goals. This approach will undoubtedly emphasize varying diagnostic and therapeutic capabilities in medical facilities and the distinction between primary, secondary, and tertiary health care. Note that standards for cardiac catheterization facilities require the coordination of diagnostic and therapeutic resources in the same institution, and the standards for CT encourage sharing of services. While certain diagnostic and therapeutic resources, such as cardiac catheterization and radiation therapy, may be coordinated over large geographic regions, other more frequently used diagnostic resources such as CT will be difficult to assign to a limited number of medical centers. Limiting medical resources is especially difficult in sparsely populated areas and may result in long distances or travel time.

2. Medical terminology has been defined at a federal level. The guidelines specifically define a CT "procedure," a radiation therapy "treatment," and a cardiac catheterization "procedure." These terms were defined with the purpose of restricting the number of expensive radiographic units and do not have the same meaning as currently defined in many radiologic practices. Such definitions may very well influence medical practice without sound medical justification. A CT study with and without contrast material on the same day is accounted as one procedure, while the same examination performed on two separate days will be counted as two procedures. A radiation therapy treatment plan requiring several treatment portals will be counted as a single treatment. Undue emphasis on activity statistics could encourage 2 day CT scans and single portal per day radiation therapy.

The standards for CT also require that patient procedures be "medically necessary." To some planners, medically necessary indicates a procedure that detects pathologic abnormality. Negative examinations are often as important to patient care as a positive examination and a medical definition of "medically necessary" is very important.

3. Future planning will be related to previous planning decisions. All standards directly relating to radiology consider the activity of existing installations. This approach gives a veto power to current facilities. No future cardiac catheterization, radiation therapy, or CT installations can be developed until all existing facilities meet the standard of activity. Outmoded radiographic equipment, units that escaped CON legislation, or poorly planned facilities can restrict the installation of new and improved facilities for patient care.

4. No distinction is made for replacement of existing equipment. The guidelines do not distinguish between a completely new radiographic service versus replacing or remodeling older equipment if the cost is more than $100,000 (likely to be increased to $150,000). Changes in radiologic equipment may not be possible unless all facilities in the HSA and state are meeting the standards. It is quite conceivable that an important new technology, for example a sizable reduction in radiation dose per examination, could not be approved for installation.

5. Limitations on equipment location will create special problems with diagnostic services. The guidelines are designed to limit placement of expensive services to a relatively few institutions and encourage shared use of equipment by several medical care providers. This concept is relatively easy to implement when considering certain specialized therapeutic modalities; more difficult but possible with specialized diagnostic procedures for which the patient may be electively admitted, but exceedingly difficult when the diagnostic procedure is used in many clinical conditions. CT has diagnostic use in many diseases of the central nervous system, diagnosis or staging of common cancers (lung, lymphoma, pancreas), and evaluation of postoperative complica-

tions. These clinical problems occur in most medical care facilities and are not electively encountered. Denial of important diagnostic capability will be perceived as a major problem to physicians, administrators, *and* patients. Sequestering facilities such as CT can have a major impact on a medical facility, but there are other examples—if a major hospital loses cardiac catheterization capabilities, can it maintain an adequate cardiology service?

The guidelines represent a new era in medical care and radiology. They emphasize cost effectiveness, but do so inconsistently. If one compares the required utilization intensity of radiologic equipment, there are great differences among the three types of facilities. In order to meet the standards, a cardiac catheterization unit would have to be active about 12–15 hr/week, a radiation therapy installation about 30–40 hr/week, and a CT installation about 50–80 hr/week, even though these installations are of comparable initial cost and require about the same number of support personnel. While cost reduction and high quality can be compatible, often they cannot. Standards for cardiac catheterization are at a level to encourage better quality services, but the standards for radiation therapy and CT are primarily related to cost containment and define what a facility *can do* rather than what it *should do*. Efficiency is important but an "assembly line" approach to diagnostic radiologic examinations can result in "assembly line" medical care.

The guidelines are established by federal policy and will not disappear; they can be adjusted at the local and state level. As currently written, the guidelines clearly reduce accessibility to radiologic services and may reduce their quality. Informed radiologists can influence their impact by emphasizing the need to consider quality, accessibility, and concern for the patient, as well as cost, in the planning process.

International Cancer Research Workshop on Low Dose Rate Teletherapy

EDITED BY J. FRANK WILSON

The International Cancer Research Workshop on Low Dose Rate Teletherapy was held in Lake Geneva, Wisconsin, May 4 and 5, 1978. Proceedings will be published later. Inquiries regarding the Proceedings as well as for reprints of this section should be directed to J. F. Wilson, Department of Radiation Therapy, Medical College of Wisconsin, 8700 West Wisconsin Avenue, Milwaukee, Wisconsin 53226. This project was supported by funds provided in part by the International Cancer Research Data Bank Programme of the National Cancer Institute, National Institutes of Health (U.S.), under contract no. NOl-CO-65341 with the International Union Against Cancer.

CONTENTS

Theoretical Considerations

Dose-Rate Effects in Radiation Therapy and Radiation Biology. Hall EJ
The Importance of D_q. Phillips TL
Implications of the D_q Initial Portion of the Survival Curve for Low Dose Rate Teletherapy. Elkind MM
Tissue Responses to Multiple Small Doses of Irradiation. Withers HR
Comparison of Low Dose Rate and Fractionated Irradiation for the Early Reactions of Skin and Intestinal Mucosa. Dutreix J, Loirette M, Boisserie G, Wambersie A, Stienon-Moes MR
Alteration of Cellular Proliferation in Various Cell Lines Exposed to Low Dose Rate Irradiation. Bedford JS

Current Laboratory Findings

Response of Bone Marrow and Tumor Cells to Acute and Protracted Irradiation. Tubiana M, Boisserie G
Variations in Radiosensitivity and in Dose Rate Effects Among Various Types of Cultured Cells, Tumours and Normal Tissues. Barendson GW
Effects of Single and Fractionated Doses Applied at Low-Dose Rates on Rat Skin and R-1 Rhabdomyosarcoma. Kal HB
The Dose Rate Factor of In Vivo Continuous Low Dose Rate Irradiation of Tumor and Normal Tissues. Fu KK
Modification of Gastrointestinal Death in Mice Exposed to Whole and Partial Body Exposures of Low Dose Rate Irradiation. Swartz HM, Reichling G, Stark R, Been A, Wilson JF

Clinical Considerations

Historical Perspectives of Clinical Radiotherapy at a Low Dose Rate. Pierquin B
The Potential for Clinical Exploitation of Low Dose Rate Teletherapy. Suit HD, Brown BW, Soriano A
Current Results of an E.O.R.T.C. Trial Comparing Low Dose Rate and Classical Fractionated Treatments of Base of Tongue Epitheliomas. Baillet F
Clinical Applications of Hyperfractionated (HFI) (8 and 16 fractions per day) Concentrated Irradiation. Castera D, Loirette M, Dutreix J
Clinical Experience with Low Dose Rate Therapy at the Rotterdam Radiotherapy Institute. Kuipers Tj
Low Dose Rate Teletherapy of Unresectable Carcinoma of the Pancreas. Results of a Pilot Study. Wilson JF

THEORETICAL CONSIDERATIONS

Dose-Rate Effects in Radiation Therapy and Radiation Biology:

Hall EJ (Radiological Res. Lab., College of Physicians and Surgeons of Columbia Univ., New York, NY 10032)

A very wide spectrum of dose-rates has been used in experimental radiobiology and clinical radiotherapy. The range of interest for low dose-rate teletherapy spans from about 50 to 200 rad/hour. Repair of sublethal damage can take place during the long exposures necessary for the accumulation of doses in the therapeutic range. For cells irradiated in culture, the survival curves for acute x-ray exposures at high dose-rate have an appreciable initial shoulder. As the dose-rate is reduced, the slope of the survival curves becomes shallower and the shoulder becomes smaller. At the dose-rates of interest in low dose-rate teletherapy, survival approximates to an exponential function of dose. The magnitude of the dose-rate effect varies with the cell system; it is large for cells which accumulate and repair sublethal radiation damage effectively, and small for cell systems that do not. Survival curves for low dose-rate irradiations can be made much steeper by the concurrent application of a modest level of hyperthermia. A six hour exposure at 41°C, given during or immediately after irradiation, steepens the survival curve by a factor of two, although it does not of itself kill any cells. Hyperthermia and low dose-rate irradiation may prove to be an effective combination. For cells with a mitotic cycle shorter than, or comparable to, the exposure time, there is a further dose-rate effect due to cellular proliferation which can take place during a protracted irradiation. The efficacy of a given dose-rate of gamma-rays on a cycling cell population depends on a number of factors. These include the intrinsic radiosensitivity of the cells and their ability to repair sublethal damage, their mitotic cycle time, and the extent to which cells accumulate at a sensitive phase of the mitotic cycle as a result of prolonged exposure. There is evidence from a number of studies with cells cultured in vitro that cells accumulate in G_2 or M during a continuous low dose-rate irradiation. This accumulation is reflected in an increased radiosensitivity of a cell population as judged by their response to an acute x-ray exposure following a long irradiation at low dose-rate. Many radiotherapists regard low dose-rate radium implants as the treatment of choice "par excellence" for some types of human tumors. This alleged superiority of implants over conventional fractionated beam therapy may be due to a) the localized dose distribution characteristic of an implant, b) the low dose-rate per se, as a result of which energy is deposited continuously at low dose-rate rather than intermittently at high dose-rate, c) the fact that the total dose is delivered in 7 days in contrast to 7 weeks. If the alleged superiority of implants is a result of the localized dose distribution, then their advantages will not be shared by low dose-rate teletherapy. On the other hand, if the reported efficacy of implants stems from radiobiological factors, resulting from the protracted continuous exposure, then beam teletherapy at low dose-rate could prove to be superior to conventional multifraction regimens. At the present time some of the principles associated with low dose-rate irradiation have been elucidated in radiobiological studies. However, controlled clinical trials will be needed to prove whether the cost and inconvenience of low dose-rate beam teletherapy are justified by a greatly improved result at the clinical level.

The Importance of D_q:

Phillips TL (Div. of Radiation Oncology, Univ. of California, San Francisco, CA 94143)

The D_q is a relatively old concept in radiobiology, and derives from the formula for cell survival based on multitarget theory. It is expressed by the following equation: $D_q = D_0 \ln(n)$. Thus it is a measure of the width of the potential for the accumulation of sublethal damage in mammalian cells. D_q is important because it predicts the ability to accumulate and/or repair sublethal damage. It is a major input into any time-dose relationship and will predict dose rate and fractionation effects. Because the size of the D_q depends on radiation quality, it will also predict changes in the RBE.

The D_q is influenced by tissue type, cell age, hypoxia, radiation quality, dose rate, chemical agents, and hyperthermia. The D_q may be measured indirectly in vivo by determining the rads recovered per fraction when a 2-fraction exposure is compared to a single fraction exposure. The value of $D_2 - D_1$ in this situation is equal to the D_q. Using this technique, the indirectly derived D_q is seen to increase from 135 rads for bone marrow to 375 for lung, 400 for small intestinal mucosa, 700 for brain, 715 for kidney, and 845 for esophagus.

Cells are known to have little or no shoulder and essentially zero D_q during the mitotic phase; are known to show very little repair under severe hypoxia; and are known to demonstrate a very small shoulder or absent shoulder under conditions of hyperthermia, at least above 42-43° C.

Radiation quality influences the D_q, with decreasing D_q's occurring with increasing LET. For example, the estimated D_q

© 1978 American Roentgen Ray Society

based on either $D_2 - D_1$ data or extrapolated survival curves for intestinal crypt cells decreases from around 350 rads for cesium, cobalt, or 4 MeV radiation to 200 rads for helium peak irradiation, 0 rads for carbon peak, neon plateau or peak, and argon plateau or peak radiations. Conversely, 15 MeV neutrons show a D_q estimated at 150 rads.

Dose rate influences the D_q in that as dose rates approach 1 rad/minute, the D_q drops for intestinal crypt cells from 400 to 0 rads using ^{137}Cs and from 370 to 0 rads for EMT6 tumor cells.

Certain chemical agents may also influence the D_q as they reduce or inhibit the repair of sublethal damage. Most agents cause only a small effect on the D_q however, with D_q's for ^{137}Cs reduced from 350 rads to around 300 rad with actinomycin, adriamycin, BCNU, 5-fluorouracil, methotrexate, cis-platinum, and vincristine given two hours before irradiation. Cyclophosphamide has no influence on the D_q, and bleomycin, at a dose of 100 mg/kg, reduces the D_q to zero. Two-dose survival ratios confirm the findings of a reduced D_q with the drugs mentioned above, with the greatest reduction in survival ratio occurring with bleomycin and cis-platinum.

Thus it can be seen that the D_q is an important term in radiobiology as applied to radiotherapy, even though it may not apply to certain newer formulae for cell survival. It does predict the ability of cells to repair sublethal damage under a range of situations which can arise clinically and, therefore, can be useful in predicting the effects which would occur at low dose rates.

Implications of the Initial Portion of the Survival Curve for Low Dose Rate Teletherapy: Elkind MM (Div. Biological & Med. Res., Argonne National Lab., Argonne, IL 60439)

Low dose rate teletherapy may be viewed as an extension of fractionation teletherapy to larger and larger numbers of smaller and smaller doses. Accordingly, it is logical to think of the radiobiology involved as a projection of the radiobiology of acute, single exposures to hyperfractionation. This approach leads to the inference that the initial shape of the single-cell survival curve critically influences the shape of the isosurvival curve (i.e., the dependence of total dose, TD, to reach a given level of survival on the number of fractions, N). In particular, if the single-cell survival curve has a zero initial slope, the isosurvival curve TD increases with N without limit. But if the initial slope is negative--such that the beginning of the curve is described by a negative exponential--TD rises to a plateau. The level of this plateau decreases with increasing steepness of the initial slope (or the smaller the D_o of the initial slope).

It is well known that the shape of a single-cell survival curve depends upon the dose rate of the radiation exposure. Even if cell division during exposure is discounted, at a low dose rate repair of sublethal damage will occur during exposure, and hence fewer cells are killed. The resulting change in shape of the survival curve is generally attributed to a flattening of the mid- to large-dose portion of the curve because the initial negative slope is customarily assumed to represent a contribution to cell killing from so-called "single-hit" action. Single-hit effects do not require the accumulation of damage for expression; hence, they are assumed not to be modifiable by reducing the dose rate.

A theorem of T. A. Hall--overlooked for many years--indicates that exponential, so-called "single-hit" survival can result when absorption events are accumulated in the target in a particular way. The relevance of this theorem in the context of potentially lethal damage and its repair was recently discussed. In particular, it was pointed out that repair competence may play a major role in influencing the sensitivity of cells exposed to radiations of different qualities.

The applicability of these considerations to therapy depends upon if, and in which direction, the initial slope of a survival curve will change with reduced dose rate. If the beginning of the curve becomes less steep, because some events are repaired during exposure, the total dose required to sterilize a tumor--or to produce a given level of damage in normal tissue--will be larger than predicted on the basis of the shape of the acute-exposure survival curves of the respective cells in question. As in other unconventional modes of radiation therapy, therefore, a differential in the influence of repair on the initial slopes of the survival of normal tissue cells versus tumor tissue cells may be the factor determining the relative efficacy of low dose rate teletherapy compared to conventional fractionated teletherapy. (Work supported by the U. S. Department of Energy.)

Tissue Responses to Multiple Small Doses of Irradiation: Withers HR (Sect. Experimental Radiotherapy, Univ. of Texas System Cancer Ctr., M. D. Anderson Hosp. and Tumor Inst., Houston, TX 77070)

Responses of tissues to doses of about 200 rads are of interest to radiotherapists but are difficult to quantitate. Most tissues will not manifest detectable injury from single doses of 200 rads, and alternative methods must be used, none of which is entirely satisfactory. The slope of the survival curve over the range of dose/fraction may be estimated from the slope of a survival curve measured over a range of higher doses if the higher doses are given as multiple equal dose fractions. If dose fractions are sufficiently small, requiring a large number of fractions, and if sublethal injury from each dose fraction is completely repaired, the multifraction survival curve slope will approximate the initial slope of the survival curve. Also, if dose fractions are small enough that all killing is through non-repairable injury, then further dose fractionation results in no additional dose requirement for a certain effect. Using these methods it has been estimated that the D_o value for the dose survival curve for jejunal crypt cells, over the dose range of 140-210 rads, lies between 350 and 450 rads. Although most cell killing by 200 rads is from non-repairable (single-hit) mechanisms, the curve has begun to diverge from exponential. Other methods give results that show general agreement with these values.

This investigation was supported in part by NIH grant CA-11138.

Comparison of Low Dose Rate and Fractionated Irradiation for the Early Reactions of Skin and Intestinal Mucosa: Dutreix J, Loirette M, Boisserie G (Institut Gustave-Roussy, Villejuif, France) and Wambersie A, Stienon-Moes MR (Centre des Tumeurs, UCL Brussells, Belgium)

For fractionated irradiation the isoeffect total dose increases with fraction number. When the overall time is kept constant the dose increase can be ascribed to the additional cellular repair between fractions, more precisely to less cell killing due to accumulation of sublethal injuries when the fraction size diminishes.

The total dose increases to a maximum which is reached when the fraction size becomes sufficiently small that the cell killing at each fraction is entirely due to direct lethal events. For the biological systems considered this situation is achieved when the fraction size is less than 2.00 Gy.

Disregarding the additional dose needed to compensate for repopulation, and which is related to the overall time of the treatment, the isoeffect dose increases for human skin desquamation from 13 Gy (single dose) to 22 Gy (maximum) and for LD 50/5 days after abdominal irradiation on mice, from 12.50 Gy to 22.00 Gy.

For continuous irradiation one expects the isoeffect total dose to increase monotonously with irradiation time on account of the cellular repair taking place during the irradiation.

Calculations have been made on a 2 component cell model assuming a random repair of sublethal injuries; they allow computing the isoeffect dose as a function of the irradiation time.

Experiments have been carried out on mice with abdominal irradiation: the LD 50 at 5 days increases with the irradiation time from 12.40 Gy (acute dose) to 20.20 Gy (6 h.) and 22.00 Gy (14 h.). These values are in excellent agreement with the computed values. Thus, the dose increase with the irradiation time can be explained by the repair of sublethal injuries and there is no evidence for any significant role of other mechanisms.

Low dose rate and acute irradiation have been compared by simultaneously treating bilateral supraclavicular fields to human skin desquamation (250 kVp). For irradiation times up to 12 hours the total dose equivalent to 13.00 Gy acute dose is much less than expected from the calculation (at 12 hour the observed value is 15.00 Gy instead of 20.50. Reactions to 13.00 Gy acute dose were comparable to those produced by 15.00 Gy delivered in 12 hours whereas the predicted necessary dose was 20.50 Gy. The skin therefore appears to be somewhat more sensitive to low dose rate irradiation than predicted; this is, as suggested by other experiments reported at this meeting, hypothetically ascribed to a modification of the cell age distribution with an accumulation of cells in a sensitive phase. For irradiation time of 24 hours (actually 3 x 8 hours in 3 days) the total dose is 22.00 Gy, the value predicted by the computation.

Thus for this 24 hour irradiation time the isoeffect dose is explained by the repair of sublethal injuries while for irradiation times up to 12 hours it is necessary to consider that some other radiobiological mechanisms play an important role.

A therapeutic advantage of the curietherapy schedule with respect to conventional fractionation cannot be ascribed to the repair of sublethal injuries: in both cases the cells are killed by directly lethal events. It is not likely that repopulation and reoxygenation can bring an advantage for the short duration of curietherapy. The role of other radiobiological mechanisms, suggested for skin desquamation (and other experiments), requires some attention.

Alteration of Cellular Proliferation in Various Cell Lines Exposed to Low Dose Rate Irradiation: Bedford JS (Colorado State Univ., Dept. of Radiology and Radiation Therapy, Fort Collins, CO 80521)

In six different mammalian cell lines, a detailed life cycle analysis has been performed during low dose rate exposure to determine the redistribution during the cell cycle in an attempt to explain variations in low dose rate survival among the lines.

The cell cycle progression of mitotically-synchronized HeLa cells was examined for various dose rates from 10 to 270 rad/hr. and for hyperfractionated doses during one cell cycle. At 37 rad/hr., the HeLa cells progressed through the G1 and S phases without delay. Then a delay in the G2 phase preceded an accumulation of cells in mitosis in the absence of cell division. This pattern could be repeated by administering fractionated doses such that the dose per hour was equivalent to 37 rad/hr., e.g., a 148 rad dose every 4 hours.

At dose rates higher than 37 rad/hr., division is prevented also. However, as the dose rate is lowered, more cell division occurs. The cell survival curves of log phase HeLa cells cluster together at low dose rates but separate at higher rates. The dose rate of 37 rad/hr. is more effective in cell killing than are the higher rates as a result of the redistribution of cells in more sensitive phases during the lower dose rate exposure.

However, in the Chinese hamster V79 cell line which has a much shorter doubling time of 10 hours than does HeLa, a dose rate of 37 rad/hr. does not inhibit the increase in cell number; even at 154 rad/hr., one cell doubling occurs. The survival curves for dose rates of 74 to 270 rad/hr. are similar. In the pig kidney cell line, which has a doubling time similar to that of HeLa cells (28 hours), more cell division occurs at 37 rad/hr. than occurs in HeLa cells. The survival curves are similar for dose rates of 37 to 270 rad/hr.

In summary, it appears that when continuous irradiation to some cell lines slows or stops cells in their progression through the cell cycle, the redistribution that occurs in the cell cycle can counteract the effect produced from repair of sublethal damage to the extent that in some cases the low dose rate is more effective in cell killing than is the higher dose rate. This phenomenon may be important in the response of tumors and normal tissue to low dose rate teletherapy.

CURRENT LABORATORY FINDINGS

Response of Bone Marrow and Tumor Cells to Acute and Protracted Irradiation: Tubiana M, Boisserie G (Institut Gustave-Roussy, Villejuif, France)

The dose survival of hemopoietic stem cells (CFU_S) is not significantly influenced by the dose rate for dose rates ranging from 600 rads/min to 30 rads/hour.

However the interpretation of CFU_S survival is complex because radiation does not only kill the CFU_S but also triggers the differentiation and the proliferation of the surviving cells. For instance for very low dose rates (40 to 80 rads/day) the initial slope is equal to that observed for higher dose rates, but subsequently a plateau is observed, probably due to an increase in the proliferative rate of the surviving stem cells.

We have assessed the LD_{50} at 30 days after total body irradiation on BALB/c mice with a fractionated irradiation up to 8 fractions (in 48 hours) and with a continuous irradiation up to 21 hours (unpublished data). For the fractionated irradiation, the total dose levels off at 920 rads when the fraction number increases (the dose increased by a factor 1.2 with respect to the single fraction acute irradiation LD_{50}: 720 rads). There is no dose increase between 4 fractions and 8 fractions. This observation is consistent with a full repair of sublethal injuries between fractions and the absence for fractions of 115-230 rads of cell killing due to an accumulation of sublethal injuries.

For continuous irradiation the LD_{50} is slowly increased when the irradiation duration increases up to 4 hours (dose rate 3 rads/min.); the LD_{50} is increased with respect to the LD_{50} for an acute single dose. The ratio (1.15) is close to the ratio 1.2 observed for 4 and 8 fractions. This suggests that at the dose rate of 3 rads/min. there is already little cell killing by accumulation of sublethal injuries. If there were not any other mechanism involved, this ratio should not increase for longer periods of irradiation. Actually when the period of irradiation is further extended up to 21 hours, the ratio increases up to 1.46 and is much higher than expected from the repair of sublethal injuries. This increase cannot be explained by hemopoietic cell repopulation because this hypothesis would require a doubling time of 2 hours. Two other explanations deserve discussion: reassortment of cells in a radioresistant phase of the cell cycle or, more likely, a slow repair process that might be related to repair of potentially lethal damage.

Anyhow the discrepancy between the effects of low dose rate irradiation on LD_{50} and hemopoietic stem cell survival shows that CFU_S survival is not a good criterion for medullary damage. If one counts nucleated bone marrow cells instead of CFU, the relative efficiency of high dose rate versus low dose rate is 1.47, a value similar to that observed for LD_{50}.

The response of an experimental tumor (NCTC 2472) to a dose rate of 50 rads/hour was also studied; the kinetic data and the cell survival as measured by an in vitro cloning technique were collected. Labeling indices decreased with increasing time of irradiation; the mitotic indices dropped initially but tended to recover. Under continuous irradiation the ascites cells accumulated in G_2 at a rapid rate. After 40 hr 61% of the cells were in G_2 phase (versus 5% in the controls), whereas after an acute irradiation, cells temporarily accumulated in G_1 phase. The time interval during which this accumulation is observed is dose dependent. Survival curves of cells from solid tumors show no evidence of hypoxic cells down to a survival level of 10^{-3}; cells from acutely irradiated tumors yielded biphasic survival curves with 10 to 20% of the cells being hypoxic. For this experimental tumor, the difference in the effectiveness of continuous and acute irradiation is small.

Variations in Radiosensitivity and in Dose Rate Effects Among Various Types of Cultured Cells, Tumours and Normal Tissues: Barendson GW (Radiobiological Inst. of Organization for Health Research TNO, Rijswijk, The Netherlands)

Among different types of tumours as well as among different types of normal tissues considerable variation has been observed with respect to responses to single and fractionated doses of ionizing radiation and to low dose rate treatments. These differences are determined by the responsiveness of constituent cells that have the capacity for unlimited proliferation or that are required to maintain the structure and function of normal tissues, but other factors, e.g. cell proliferation kinetics, supply of oxygen and nutrients, and host responses can also play a part.

Studies of the radiosensitivity of cells cultured from different types of experimental carcinomas and sarcomas in rats have demonstrated that large differences are observed between the survival curves for X-rays. For large single doses differences in radiosensitivity amount to at least a factor of three. For fractionated doses of 100 to 200 rad, responses are determined mainly by the initial slopes of survival curves which may differ by at least a factor of 5. Since the effectiveness of small doses of 100 rad per fraction, administered at short intervals adequate to allow all sublethal damage to be repaired, is expected to be equal to that of treatments at dose rates of 50-100 rad per hour, it can be inferred that different types of tumours may also show considerable differences in responses to treatments at low dose rates. These differences are expected to be at least as large as differences among the initial slopes of survival curves of the cells in culture derived from the experimental tumours studied.

The cells in culture derived from experimental rat tumours, can be transplanted in syngeneic animals and give rise to solid tumours which have been studied with respect to their responses to irradiation, e.g. by analysis of growth delay, cure rate or clonogenic capacity of constituent cells after culturing in vitro. The results of these studies have shown that tumours grown by inoculation of cells that were very resistant in vitro, do not always show a large resistance in vivo with respect to growth delay or with respect to doses required to obtain eradication, although in some cases, e.g. a ureter squamous cell carcinoma, a good correlation is obtained. For other tumours, e.g. a rat rhabdomyosarcoma, the cells cultured in vitro are not extremely resistant, but with fractionated treatments extending over 4-6 weeks, accelerated cell proliferation caused the tumours to be relatively resistant with respect to growth delay or eradication.

With respect to tolerance of normal tissues to irradiation at high and low dose rates, considerable variation is also observed among different types of tissues. For the tolerance of spinal cord in rats, assessed through evaluation of paralysis, a large decrease in effectiveness per unit dose with increasing numbers of fractions administered over periods of several weeks and a large effect of reduction in dose rate were observed. For other tissues e.g. skin, the effect of increasing numbers of fractions and of changes in dose rate is smaller than for the central nervous system.

It is concluded that an advantage of low dose rate treatments, relative to fractionated daily treatments with 200-300 rad per fraction, administered over periods of 4-6 weeks, will depend on the type of tumour treated and on the type of normal tissue that is considered critical for the site to be irradiated.

Effects of Single and Fractionated Doses Applied at Low-Dose Rates on Rat Skin and R-1 Rhabdomyosarcoma: Kal HB (Radiobiological Institute TNO, Rijswijk, The Netherlands)

Experiments have been carried out to investigate the effectiveness of single and fractionated doses applied at different

dose rates on tumour cell survival in vitro and for induction of tumour and skin responses. Single doses of X or gamma rays were applied at dose rates of 40 to 150 rad/h. Four daily doses of X-rays were administered at a dose rate of 340 rad/h and acute irradiations were performed at a dose rate of 340 rad/min. The results of the in vitro experiments on R-1 tumour cells show that 1) the effectiveness per unit dose of the gamma radiation decreased with decreasing dose rate, 2) during continuous irradiation applied at dose rates of 4-75 rad/h sublethal damage is repaired and 3) R-1 cells continue to progress through G_1 and S phases at a normal rate but are delayed in their progression through G_2+M.

The rat R-1 rhabdomyosarcoma was irradiated in vivo and tumour cell survival was assayed in vitro. The results show that 1) no dose rate effects on cell survival were present in the range of 75 to 150 rad/h, 2) low dose rate irradiation was less effective per unit dose by a factor of 1.45 as compared to acute irradiation indicating that sublethal damage is repaired during continuous irradiation, 3) reoxygenation occurred so rapidly that the fraction of hypoxic cells remains essential constant and 4) cells are accumulated into a more radiosensitive phase of the cell cycle during continuous irradiation. A skin transplantation technique has been employed for assessment of radiation induced damage to rat skin. Continuous irradiation at a dose rate of 85 rad/h provides a large sparing effect per unit dose as compared to acute irradiation with a factor of 1.8.

Tumour growth delay and severity of skin injury of the rat foot were used as endpoints to evaluate the effectiveness of four daily doses of X-rays applied at a dose rate of 340 rad/h as compared with four daily doses at high dose rate. Treatments of doses administered at the high dose rate were more effective in inducing tumour growth delay as compared with treatments of doses applied at the low dose rate. No significant differences in skin reactions per unit dose were observed when doses were applied at a dose rate of 340 rad/h as compared with acute irradiation providing that animals were anaesthetized with Nembutal. When the mixture Ethrane and oxygen was used as an anaesthetic the treatments applied at the lower dose rate were more efficient per unit dose implying that protracted use of Ethrane interferes with repair processes.

The therapeutic gain observed for single doses at dose rates of about 100 rad/h as compared to acute irradiation could not be observed for fractionated irradiation at a dose rate of 340 rad/h. This might indicate that the dose rates of about 100 rad/h presently used in clinical telecobalt therapy cannot be increased to 340 rad/h without loss of therapeutic gain.

The Dose Rate Factor of In Vivo Continous Low Dose Rate Irradiation of Tumor and Normal Tissues: Fu KK (Univ. of California, San Francisco, Div. of Radiation Oncology, San Francisco, CA 94143)

Low dose rate irradiation is assuming increasing importance clinically because of the increased use of interstitial radiotherapy and external beam total body and partial body irradiation in the treatment of malignant lymphomas, leukemias, disseminated and localized carcinomas, and in bone marrow transplants. In general, the biological effectiveness decreases with decrease of dose rate for a given dose of radiation. When low dose rate irradiation is used as a form of teletherapy, for it to be more advantageous than teletherapy with conventional dose rates, it is necessary that there is greater sparing of normal tissues than of tumors.

In order to quantify the variation of effectiveness with the variation of dose rate, I would like to introduce the term dose rate factor (DRF) which is the ratio of the doses for acute and protracted exposures that result in the same biological effect:

$$\text{DRF} = \frac{\text{Isoeffect dose for acute exposure}}{\text{Isoeffect dose for protracted exposure.}}$$

The DRF decreases with decrease of biological effect as the dose rate decreases. For a given dose rate, the therapeutic ratio is equal to the ratio of DRF's for tumor and for normal tissue at the same dose level:

$$\text{Therapeutic Ratio} = \frac{\text{DRF}_{\text{Tumor}}}{\text{DRF}_{\text{Normal Tissue}}}.$$

If there is greater sparing of normal tissue than of tumor, then the DRF will be smaller for the normal tissue than for the tumor and the therapeutic ratio will be greater than 1.

In order to evaluate the potential advantages of low dose rate teletherapy, the DRF's for the EMT_6 tumor and mouse jejunal crypt cells and bone marrow CFU's were determined from their dose response curves for in vivo continuous irradiation with Cesium 137 at .54, .92, 4.5, 36, and 274 rad/min. For the EMT_6 tumor, DRF's were also determined from dose response curves to in vivo continuous irradiation with Californium 252 neutrons at 78 and 17.6 rad/hr. The DRF's varied with: 1) dose rate, 2) tissue type, 3) biological endpoint or dose, and 4) quality of the radiation. For the EMT_6 tumor, the DRF varied from 0.54 to 0.9 with Cesium 137 irradiation at dose rates ranging from .54 to 36 rad/min. at the 10% survival level. There was no change in DRF with Californium 252 irradiation between 17.6 and 78 rad/hr. For the jejunal crypt cells, the DRF ranged from .53 to .78 at the level of 10 surviving cells/circumference with Cesium 137 irradiation at .92 to 36 rad/min. For the bone marrow CFU's, the DRF's were .69, 1.0, 1.88 and 1.88 with Cesium 137 irradiation at 36, 4.5, .92, and .54 rad/min. at the 10% survival level.

With Cesium 137 irradiation at 4.5 rad/min. at comparable dose levels, the DRF for the EMT_6 tumor was not significantly different from that for the bone marrow CFU's but was greater than that for the jejunal crypt cells. Thus, if the small intestine is the dose limiting normal tissue in the treatment volume, low dose rate irradiation would be more advantageous therapeutically than conventional dose rate irradiation. The increased sparing of the small bowel but less sparing of the hemcpoietic cells with low dose rate irradiation would also support the use of low dose rate teletherapy in the management of malignant lymphomas, leukemias, and in bone marrow transplants. Whether low dose rate teletherapy would also be more advantageous in the treatment of other types of malignant neoplasms needs to be verified by the ongoing clinical studies. However, the potential therapeutic gain with low dose rate teletherapy must be balanced against the impracticality of protracted time of exposure and immobilization of patients for this form of treatment.

Modification of Gastrointestinal Death in Mice Exposed to Whole and Partial Body Exposures of Low Dose Rate Irradiation: Swartz HM, Reichling G, Stark R, Been A, Wilson, JF (Medical College of Wis., Milwaukee, WI 53226)

X-irradiation was administered to the gastrointestinal tract of mice at an acute dose rate (90 rad/min) or low dose rates (2.2 rad/min or 6.3 rad/min). The effects on gastrointestinal deaths were assessed by determining the $LD_{50/6}$ following either whole and partial body exposures.

The approximate $LD_{50/6}$ for whole body irradiation were: 1300 rad at 89 rad/min versus 2200 rad for 2.2 rad/min or 6.3 rad/min. Shielding the head and thorax yielded higher $LD_{50/6}$ values. Results for irradiation of only the lower half of the body were approximately: 1600 rad at 89 rad/min compared to 2600 rad for 2.2 rad/min or 6.3 rad/min.

These results provide experimental data that are pertinent to the use of low dose rate teletherapy of human subjects. They confirm that the tolerance of the gastrointestinal tract to acute effects of radiation is greatly increased when the dose rate is lowered. Within the limitation of our experimental method, no difference was observed between dose rates of 2.2 rad/min and 6.3 rad/min. Both of these rates were quite sparing compared to 89 rad/min. This sparing effect was not diminished by using partial rather than whole body irradiation. These results suggest that it may be possible to overcome of the clinical limitations on irradiation of the gastrointestinal tract by avoiding the radiation reactions that currently limit the tolerable radiation dose. It is now essential that the long term effects of low-dose rate irradiation of the gastrointestinal tract be investigated.

CLINICAL CONSIDERATIONS

Historical Perspectives of Clinical Radiotherapy at a Low Dose Rate: Pierquin B (Service de Radiotherapie, Hospitalo Univ. Henri Mondor, Creteil, France)

The utilization of low dose rate irradiation (LDR) in clinical radiotherapy has not been fully exploited except in curietherapy with radium. Concerning teleradiotherapy, only COUTARD, in the 1930's, studied the slow delivery of a radiation dose, but the overall treatment time remained prolonged over several weeks as with classical fractionated technique. Renewed development in curietherapy with Iridium 192 permitted me to become aware of the interesting possibilities of LDR to allow delivery of a very high dose in a very short total time. Euphemistically, "6000 rad in 6 days rather than in 6 weeks". Based on experience with more than 3000 patients treated with Iridium 192 between 1960 and 1970 and especially my experience with over 250 patients treated to large target volumes for cervical lymph node recurrences, I acquired the clinical conviction that LDR to a dose of 1000 rad and up to 2000 rad daily was well tolerated by the normal tissues but that the tumor, even when entirely poorly oxygenated, remained radiosensitive and locally radiocurable. On this basis, the risk was taken in January, 1970 of irradiating by telecobalt LDR, several patients who presented with very advanced tumors in head and neck sites. Since there is an isoeffect plateau between the dose rates of 30 and 100+ rad/hour, I was able to treat these first patients

with daily doses approximating 900 rad delivered over 8 to 9 hours at the rate of 1.5 to 2 rad/minute. Eight years of experience (1970-1978) with 120 patients thus treated, more than half of whom had oral cavity or oropharyngeal lesions has led to the following conclusions:

1. The most practical recommendable method of administering LDR is as a split-course consisting of two series of 3250 rad separated by a 3 week rest interval, delivering 800 rad daily at a dose rate of 1.5 rad/minute. Total dose therefore equals 6500 rad calculated at our reference isodose, habitually 90% of the dose at the center of the target volume.
2. The effect on the skin is very reduced; 0.25 vs. 2.3 in the OERTC study comparing LDR with classical fractionated irradiation.
3. The effect on the tumor at short and medium term observation appears much more efficacious: (factor of 2 in favor of LDR in the same study).
4. Necroses did not occur more frequently than with classical fractionated technique.
5. Soft tissue sarcomas appear very radiosensitive to LDR (11 of 12 locally controlled).
6. The small intestine appears very tolerant of LDR. Four patients treated for pancreatic cancer tolerated irradiation without nausea or diarrhea, however, treatment was via relatively small portals measuring approximately 10 x 12 x 6.
7. We must study further the optimization of this technique and explore the possibility of finding the optimal dose rate. It is hoped that it will be the highest possible low dose rate to allow treating more patients daily per therapy machine. As of May, 1978 we have confirmed that our last several patients have tolerated well doses of 800 rad given at 2.5 to 3 rad/minute.
8. Studies conducted in close conjunction with our radiobiological colleagues will permit us to better determine the optimization of dose rate as a function of the radiosensitivity of each normal or tumor tissue. This optimization equally applies to the notion of "split" course radiotherapy: when should a split occur and of what duration?
9. Comparative trials should be organized and conducted to compare LDR vs. hyperfractionated irradiation vs. neutron therapy. I propose a meeting for this purpose in 1980 or 1981 in Creteil. Such a meet will assemble a small group of representatives of the teams of clinicians and radiobiologists interested in these irradiation modalities.

The Potential for Clinical Exploitation of Low Dose Rate Teletherapy*: Suit HD (Dept. of Radiation Medicine, Massachusetts General Hosp., Harvard Medical School, Boston, MA 02114), Brown BW (Dept. of Biomathematics, M. D. Anderson Hospital and Tumor Inst., Univ. of Texas, Houston, TX 77030) and Soriano A (Director of Cancer Management, Massachusetts General Hosp., Boston, MA 02114)

The question being considered in this symposium is: would clinical results of external beam radiation therapy be improved by employing low dose rates, viz. ≈1-3 rads min^{-1} given in series of quite protracted exposures? The stimulus for this question is a widely held clinical opinion that the best results achieved in radiation therapy are those obtained using interstitial therapy. The physical characteristics of the latter feature dose rates of approximately 40 rads hr^{-1}, single dose and continuous irradiation, short overall treatment time (3-8 days), and treatment volume confined to the palpable tumor and its immediately surrounding normal tissues. Clinical experience has demonstrated unequivocally that external beam therapy combined with low dose rate intracavitary therapy for carcinoma of the uterine cervix has yielded superior results to that which can be obtained using very aggressive external beam techniques alone. However, recent results from centers employing remote control afterloading systems for their intracavitary therapy but utilizing quite high dose rates have obtained results which apparently are approximately comparable to those using the more traditional low dose rate intracavitary therapy. This clinical finding indicates that the advantage of the intracavitary was not the consequence of a low dose rate but rather the superior dose distribution which made feasible the administration of high total doses. All of the experience of radiation therapy has shown that where dose distribution has been improved such that higher total doses could be employed, the tumor control probability is increased. Our own interpretation of the results of interstitial therapy is that the predominant factor which has contributed to the superior results is the better dose distribution and not the low dose rate.

There would be two radiobiologic advantages which may be a feature of low dose rate continuous irradiation. These are: 1) a reduced oxygen enhancement ratio, 2) greater opportunity for radiation inactivation of cells as they pass through the more sensitive phases of the cell replication cycle. It is almost certainly true that both of these advantages would, however, obtain for irradiation given in multiple fractions of small doses. For example, several fractions per day of doses in the range of 50-100 rads per fraction.

There appear to be several significant technical problems inherent in the use of the prolonged exposure periods which are necessary in low dose rate external beam therapy. Specifically there would almost of necessity be some decrement in the quality of the dose distribution pattern over that which could be achieved with high dose rate conventional external beam therapy technique. Treatment volume would have to be relaxed in order to be certain that the target volume was covered during all of each protracted radiation sessions. This would be the consequence of a prolonged time of immobilization, i.e. for radiation administered at 50-100 rad hr^{-1} for a total of 6-9 hrs per treatment. This would mean that highly sophisticated radiation therapy techniques would not be readily feasible and there would surely be a tendency to employ simple techniques, i.e. single field or parallel opposed portals. Further, the low dose rate protracted technique would be difficult for those treatment problems where contiguous areas were to be treated; for example, head and neck carcinoma (primary plus lower neck), ca of the breast (chest wall and supraclavicular regions).

The effectiveness of radiation given continuously at various dose rates or as fractionated high dose rate irradiation was considered by reference to a model which features a combination of the single hit, single target and the multi-target, single hit inactivation. Equation for survival fraction is:

$$S = e^{-\omega D/D_0}\left[1 - (1 - e^{-(1-\omega)D/D_0})^n\right]$$

where ω = the proportion of energy absorbed in production of non-reparable damage. In an analysis of the performance of this model there was no detected advantage of the continuous low dose rate irradiation over highly fractionated irradiation (small dose per fraction). For example, at dose rates of the order of 50-100 rads per hour or dose per fraction of 100 rads or less the total dose required to achieve a survival fraction of 10^{-5} would be the same for the two approaches (n values of 4-10, repair half time for repair of damaged site of ≤60 min). The highly fractionated or the continuous low dose rate irradiation may be more effective than conventional fractionation schedule because of the OER or more favorable age density distribution or the use of shorter overall time but radiobiologically they appear to be approximately equivalent. These new approaches are potentially very interesting and certainly warrant a serious clinical investigation.

*This work was supported in part by DHEW Grant #CA13311.

Current Results of an E.O.R.T.C. Trial Comparing Low Dose Rate and Classical Fractionated Treatments of Base of Tongue Epitheliomas: Baillet F (Service de Radiotherapie, Centre Hospitalo Univ. Henri Mondor, Creteil France)

This trial was preceded by preliminary studies of low dose rate irradiation of 70 patients on the service of Pierquin at Creteil. Initially forty-five patients with advanced ENT tumors (T > 4 cm. in all cases except 3) were treated with one of two techniques both employing the low hourly dose rate of 0.8 to 1.8 Gy per hour to a daily dose of 6 to 8 Gy. Technique A consisted of 70 Gy as a single course; Technique B of 65 to 70 Gy as a split-course with a rest interval of 3 weeks at mid-course. Fifteen patients were treated with Technique A; 30 with Technique B. Cutaneous reactions with Technique A were extremely mild but no visible reaction occurred with Technique B. Marked mucosal reactions occurred in 14 of 15 with Technique A vs. 4 of 30 with Technique B. Complete disappearance of tumor at 3 months was observed in 33 of 45 patients. Tumor disappearance was essentially the same with either technique (60% Technique A vs. 54% Technique B). Necrosis has occurred in 15 of 25 patients who have not relapsed (6/11 T3, 9/14 T4). Severe of nine occurred with Technique A compared to 8 of 16 with Technique B. Based on this data, low dose rate irradiation was concluded to be safe if given as a split-course and to produce tumor disappearance more frequently than expected with classical fractionated irradiation. On this basis the current trial was organized in January, 1976 comparing Technique B vs. classical fractionated irradiation of 70 Gy total dose administered as 5 fractions of 2 Gy per week. Reduction of irradiated volume is made at 45 Gy with fractionated therapy and at 35 Gy with low dose rate technique to shield the cervical spinal cord. To date 16 patients, 8 in either arm of the study have completed treatment with the following observations: cutaneous reactions graded from 0 to 3 were greater by a factor of 10 with the fractionated technique. Mucosal reactions were identical for both schedules. Tumor disappearance occurred more frequently with low dose rate technique, 75% vs. 50% at 3 months. In April, 1978 5 of 8 patients treated with the low dose rate technique are alive, 4 of 8 treated with the fractionated technique. Necrosis occurred

in one fourth of the patients in either group. In the low dose rate group 3 of the 8 patients are alive without relapse or necrosis and 0/8 in the fractionated technique group. The poor prognostic influence of preexisting ulceration appears to be overcome with the low dose rate technique, there being only 3 relapses in 5 cases who had initial ulceration, 3 of 3 treated with the fractionated technique. Our preliminary conclusion is that a better result is being obtained with low dose rate irradiation in such cases.

Clinical Applications of Hyperfractionated (HFI) (8 and 16 fractions per day) Concentrated Irradiation: Castera D and Loirette M (Centre J. Godinot, Reims, France) Dutreix J (Institut G. Roussy, Villejuif, France)

In a comparative study measuring human skin desquamation 16 fractions of 0.45 Gy per day given at 30 minute intervals over 3 consecutive days was found to be biologically equivalent to reactions produced by 2 x 8.5 Gy in 3 days, to 27 Gy given as fractionated irradiation over 3 weeks and to the low dose rate schedule of 22 Gy given at 0.92 Gy per hour (2 x 4 hours daily). In a second preliminary therapeutic study 11 patients with advanced head and neck lesions were treated for palliation with 250 kV X-Rays giving 16 fractions per day to total skin doses of 26 to 30 Gy. Moderate to brisk dry desquamation peaked at 25 days and was repaired at 40 days; mucositis peaked at 10 days and was repaired by 20 days. Tumor regression was appreciable at 10 to 20 days. This sequence of reactions was similar to that observed with concentrated irradiation given in 2 fractions of 9 Gy in 3 days. In 5 patients a second series was given after a rest interval of 3 to 6 weeks; in 2 there was no evidence of local disease at the time of death at 20 months. In a third clinical study 56 patients with head and neck tumors (9 T2, 43 T3, 4 T4-NON1, 34 N2N3, 22) were treated with cobalt 60 teletherapy with curative intent given as 8 fractions per day of 0.90 Gy at 2 hour intervals over 5 consecutive days repeated after a 2-week rest interval. This resulted in administration of 7.2 Gy per day, 36 Gy per series and 72 Gy total dose. Practically all primary lesions remain clinically controlled except for 4 clinical suspicions of recurrence. In 9, node residua required surgical excision which healed without complication or subsequent recurrence. Brisk mucositis was repaired at 2 months in 75% of cases; it has persisted more than 4 months in 3 patients. Four patients had laryngeal edema; 1 requiring tracheotomy. This series of patients has been compared to a series of 54 patients previously treated with conventional fractionation (70 Gy/7 weeks) treated through similar portals. With the HFI schedule early mucosal reaction was greater but of shorter duration. Xerostomia was more marked and late cervical fibrosis was more frequent but was asymptomatic. Local control of the primary tumor was superior with HFI (4 failures vs. 14) but control of lymph node metastasis was less (9 failures vs. 3). The survival rate at 6, 12, 18 and 23 months is higher for HFI (63% vs. 30% at 23 months) suggesting a benefit with HFI but a clinical trial is necessary for confirmation. Fatal complications of hemorrhage or extended necrosis were similar with the two schedules (7 HFI vs. 10 conventional).

Clinical experience with Low Dose Rate Therapy at the Rotterdam Radiotherapy Institute: Kuipers, Tj (Rotterdamsch Radiotherapeutisch Inst., Rotterdam, The Netherlands)

In a pilot study, 66 sites in 63 patients have been treated with low dose rate telecobalt therapy in order to advance knowledge of therapeutic indications and contra-indications for this type of treatment. Mainly palliative results have been strived after. The poor prognosis of recurrent gynecological malignancies seemed to justify the admission into this pilot study of patients suffering from this type of disease.

Case reports from a few other centers mentioning some favorable results in non-gynecological sarcomas, were the reason for also including various malignant soft tissue tumors. Most of the leiomyosarcomas, however, originated from the myometrium.

Patients remained in the treatment room for 5-6 hours per day and were repositioned every 20-30 minutes. Short rest intervals were allowed for nourishment and elimination. The dose rate at the centre of the tumor was 1.0 - 1.2 Gy/hour. Treatment was given through anterior and posterior pelvic portals measuring as large as 14 x 14 cm. to a dose of 5 Gy, whereas sarcomas of a limb received 6-8 Gy a day. Five fractions per week were given. The total dose for pelvic tumors was usually 50-60 Gy, applied in two equal courses separated by an interval of 2-3 weeks.

Sarcomas of a limb received a total dose of 60-70 Gy. During the first portion of the study, lower total doses were applied. The long daily treatment time was not always well supported; therefore, in a number of patients treatment was partially given with conventional megavoltage methods precluding evaluation. Poor selection of patients early in the study resulted in a total of 18 non-evaluable cases.

Remarkable reduction of tumor volume (up to 90% and more) was observed in the leiomyosarcomas. The best results were seen in the two patients with a recurrent mixed-mesodermal tumor: one of them appears to be free of tumor more than three years after low dose teletherapy.

The results show that for a carcinoma of the cervix, recurrent following full course of initial radiotherapeutic treatment, the addition of low dose rate teletherapy results in a high rate of severe complications. In other cases, recurrent following surgery and post-operative irradiation as initial treatment, a reasonable palliation was achieved without complications if the post-operative vaginal application had given only about 50% of tolerance dose at the surface.

Recurrent ovarian carcinoma usually requires a high dose in a large volume. Therefore, external low dose rate irradiation is not the treatment of first choice, yet some palliation was achieved in a few such patients.

Overall, twenty-two recurrent carcinomas of the cervix, twelve other gynecological or urologic tumors and fourteen soft tissue sarcomas were treated yielding a total of forty-eight evaluable sites. In these, excellent or good palliation was noted in sixteen, twelve obtained moderate palliation and twenty responded poorly. Eleven severe complications were encountered.

Low Dose Rate Teletherapy of Unresectable Carcinoma of the Pancreas. Results of a Pilot Study: Wilson JF (Medical College of Wis., Milwaukee, WI 53226)

In the United States today pancreatic cancer is the 4th most common fatal malignancy following carcinoma of the lung, breast and large bowel, there being only 1% overall survivorship at five years. Two significant barriers to progress in radiation therapy of pancreatic cancer have been the notorious difficulty in accurately localizing such lesions and the proximity of critical organs which tolerate irradiation poorly, principally small bowel, kidney, liver and spinal cord. Experience during the past 20 years has shown clearcut dose dependency of local control confirming that tumor doses of less than 3500 to 4000 rad conventionally administered are probably ineffectual. Clinical and experimental studies strongly suggest the sparing effect of low dose rate irradiation is different for different organs but particularly for the gastrointestinal tract which seems to show remarkable adaptability and can tolerate higher doses of radiation than were previously thought possible if delivered at lower dose rates. Six patients have been evaluated for inclusion in a pilot study; four have actually completed treatment (2 excluded due to mental incompetence). Patients received cobalt 60 teletherapy through portals measuring an average of 12 to 14 cm^2 with an SSD varying between 68 and 75 cm. to give a dose rate of 95 rad per hour at the center of the tumor. Minimum total tumor doses of 5300 to 6150 rad were administered. Such irradiation was extremely well tolerated by patients producing minimal or no acute side effects during treatment. Karnofsky performance status improved in one patient and did not change in the other three. Cutaneous reactions were extremely mild consisting of only an extremely faint erythema at the end of treatment. One patient died of disseminated cancer after 28 weeks. Postmortem examination confirmed a profound radiation effect in the tumor; minimal or no radiation effect was evident in the irradiated adjacent intestine, skin or kidney. Profound histological changes were also noted within the liver substance characterized by marked hepatocellular damage in conjunction with an unusual bile duct proliferation suggesting an individual adaptability to low dose rate irradiation of various cell lines within a single organ. This phenomenon is currently being studied further in a laboratory model. Of the remaining three patients, one is alive with disease at 26 weeks; local recurrence is suspected in another at 12 weeks and the fourth is doing well 10 weeks postirradiation.

From Earlier Pages . . .

A wise old Roentgenologist
  Was sailing o'er the sea;
He looked a sorry Pessimist,
  As ill as he could be.
He muttered with a bitter laugh
  As to the rail he hied,
"I need no silly radiograph
  To show me my inside!" [1]

This ephemeral stanza appeared in our Journal in April 1916, and it was not an isolated item. Obviously, the character and content of the Journal have changed since early issues, when poetry appeared from time to time. The first volume of the *American Journal of Roentgenology* was printed in 1913. It was developed to serve the needs of a society of about 180 members, to publish the papers which had been presented at their meetings, and to permit exchange of ideas among this small membership. The predecessor of the Journal, the *American Quarterly of Roentgenology,* had more limited functions. The new Journal was a monthly publication, and the expansion required a considerable increase in material.

Some of the growing pains were evident. The entire first issue was a memorial to a prominent member of the Society, Charles Lester Leonard. This issue began with a full-page, somber poetic elegy in his praise. The remainder of the issue was devoted to a report by Dr. Leonard describing examination of the gastrointestinal tract with x-rays, and it concluded with a long bibliography of his writings.

The second issue was in the format with which we have become familiar: original articles, editorials, news and notes, and abstracts of the current literature. Nevertheless, the editor included much material which he knew would interest the small, closely knit membership. Poetry was frequently published. In 1914 there was a full-page anonymous parody of Andrew Lang's poem "Pen and Ink" [2]. A closely spaced 2 page series of three poems by Caroline Bartlett Crane, wife of A. W. Crane, president of the Society in 1916, memorialized a dinner given by her at their home in Kalamazoo [3]. The poem named many of the prominent radiologist-guests, and apologized to those omitted because of the strictures of rhyme and meter. In August 1918, there was a full-page untranslated poem in ungrammatical French describing the training of x-ray technicians in France during the war [4]. Some of the language is not in cultured use, and the absence of a translation may have been in the interests of delicacy. The informality of the entire publication is indicated by the inclusion of a poem by 12-year-old Helen Ashbury in 1920 [5]. (A young Baltimore radiologist, H. E. Ashbury, is included in the formal photograph of the 12th annual meeting of the ARRS in Richmond, Virginia, in 1911 [6].)

Despite this informality, it is interesting to note that the contributors to the Journal in 1914 did not consider themselves pioneers. Dr. Lewis Gregory Cole in a discussion of the value of the negative examination [7] was able to write "In the early days of Roentgenology, I well remember. . . . " and to contrast that with his present time, November 1914!

Gradually, with increase in size of the membership, there occurred some loss of the informal intimacy of the members, and, no doubt, some sense of self-awareness developed. The poetry, and the doggerel, gradually disappeared. Although the Journal adopted, and maintained, a more serious mein, befitting its purpose, even then the fine arts were not entirely neglected, but took a somewhat more appropriate form. For several years a spokesman for the city which was to host the annual meeting was permitted the excess of hyperbole, orotundity, and euphuism in his invitation to the membership. This invitation appeared as an editorial several months before the meeting. These sometimes florid presentations included photographs of the countryside surrounding the host city, and these illustrations were frequently strikingly picturesque. There were photographs of craggy mountain vistas around Chattanooga [8], waterfalls near Minneapolis [9], architecture in Minneapolis and Washington [10]. A remarkable, cigar-smoking angler appeared, unaccountably, in two poses, one with a boat background [11] and another in a lake forest scene [9], and in both he proudly displayed the same string of nine immense lake trout.

The Journal has continued to adapt with the times. The enticement to attend the meetings is now in the form of quality of information rather than geography. With the impressive growth in the circulation of the Journal, the membership has become a relatively much smaller part of the readership, and thus the responsibility is of a different nature, and to readers with a more catholic outlook. Rather than including poetry, the Journal must be a repository for organized, collected information as well as a means of recording announcements of work presenting the leading edge of radiology, such as the papers given at the annual meetings. In his presidential address of 1970 [12], John F. Roach pointed out that the Society rests on two pillars: the Journal and the educational experiences afforded by the annual meetings. These continue to complement each other.

E. Frederick Lang

© 1978 American Roentgen Ray Society

REFERENCES

1. PPG: Obvious! *Am J Roentgenol* 3:207, 1916
2. Anonymous: Tube and Screen. *Am J Roentgenol* 2:528, 1915
3. Crane CB: Poems written by Caroline Bartlett Crane for a dinner given at her home to a number of visiting roentgenologists. *Am Quart Roentgenol* 4:237–238, 1913
4. Anonymous: Premieres impressions d'un élève manipulateur. *Am J Roentgenol* 5:388, 1918
5. Ashbury H: X-ray. *Am J Roentgenol* 7:484, 1920
6. Grigg ERN: *The Trail of the Invisible Light*. Springfield, Ill, Thomas, 1963, pp 201–202
7. Cole LG: Negative diagnosis of surgical lesions of the stomach and cap. *Am J Roentgenol* 2:497–506, 1914
8. Manges WF: The nineteenth annual meeting. *Am J Roentgenol* 5:392–395, 1918
9. Anonymous: Minneapolis. *Am J Roentgenol* 7:310–315, 1920
10. Pfender CH: Washington. *Am J Roentgenol* 8:409–413, 1921
11. Anonymous: Twenty-first annual meeting. Further suggestions about the trip. *Am J Roentgenol* 7:358–359, 1920
12. Roach JF: The president's address. *Am J Roentgenol* 110:673–674, 1970

Editorial

Contrast-Induced Acute Renal Failure

Acute oliguric renal failure is an uncommon, but recognized complication of the use of iodinated radiographic contrast media, and renewed attention has been given to this problem with a succession of papers in major medical journals [1–6]. These reports should remind radiologists that, although modern contrast agents are well tolerated by large numbers of patients, they are not completely innocuous substances. Indeed, they may induce occult renal injury with greater frequency than is commonly appreciated and this injury may be permanent. How does this happen?

Although the exact pathogenetic mechanisms involved in contrast-induced renal failure remain obscure, theories invoking a wide variety of factors have been proposed. Killen and Lance [7] attributed the nephrotoxicity of commonly used angiographic contrast media to a direct effect on tubular epithelium. All gradations of injury, from cloudy swelling to cellular dissolution, were noted in tubular cells. However, the glomeruli were spared.

Postlethwaite and Kelley [8] noted the considerable uricosuric effect of iodinated contrast materials, especially cholecystographic agents, and postulated that acute uric acid nephropathy could account for occasional cases of renal failure after their administration. The uricosuric effect of these agents seemed to be caused by enhancement of uric acid secretion by proximal and distal convoluted tubular cells. The theory is supported by the observation that this effect is completely inhibited by prior administration of pyrizinamide, a drug believed to specifically and completely block the tubular secretion of urate. The uricosuria produced by contrast agents may be accompanied by precipitation of urate in the tubular lumen, causing obstruction to the flow of urine and possibly cellular injury.

Berdon et al. [9] suggested that contrast exposure could induce precipitation of Tamm-Horsfall protein, a natural constituent of urine, in normal patients. They proposed that this mucoprotein is capable of forming a viscid gel that can partially or totally block urine flow through the tubules in the proper setting of dehydration, relative oliguria, and specific urine protein and electrolyte concentration. Further investigation of this, and other contrast-protein interactions, is needed to assess its importance in the pathogenesis of transient renal failure.

The hemodynamic changes following intravascular administration of iodinated contrast media are of particular interest. In peripheral vascular beds, a drop in peripheral resistance and an effective increase in blood flow are observed. These phenomena are in large part related to the osmolarity of the injected material [10, 11]. Sodium content and pH of the contrast do not seem to be significant in this regard. In the kidney, however, iodinated contrast agents have consistently been shown to decrease total renal blood flow in experimental animals [12–14]. Some investigators [15, 16] have observed crenation, spherocyte formation, and decreased pliability of red blood cells in the presence of various contrast materials and have related these phenomena to the hypertonicity of these agents. They proposed that the nonpliable erythrocytes, unable to pass through capillary beds, cause sludging and therefore decreased flow in the renal microcirculation. Studying the microcirculation of the bat's wing, Wiedeman [16] noted abnormal platelet clumping and adherence of white blood cells to vessel walls, and implied that direct endothelial damage was also a significant factor.

One must of course consider the unique features of renal circulation in any discussion of hemodynamic changes induced by hyperosmolar substances such as iodinated contrast media. Talner and Davidson [13] found a decrease in renal extraction of *p*-aminohippuric acid accompanied by a transient fall in renal blood flow, after the administration of various contrast agents, hypertonic saline, and mannitol directly into the renal artery of dogs. Aortic and renal artery pressure did not change significantly, and they suggested intrarenal vasoconstriction as a possible explanation for these effects. It would be attractive to implicate the macula densa and juxtaglomerular apparatus here, since the juxtaglomerular apparatus is thought to play a major role in the autoregulation of renal blood flow. It has been shown that sodium content and osmolarity of tubular fluid can influence glomerular filtration, presumably mediated by macula densa cells. Whether a similar type of feedback mechanism regulates renal blood flow after arteriography remains to be determined.

The decrease in renal blood flow might alternatively reflect a change in the complex system of regional blood flow in the kidney. Four regions, each with different flow characteristics, have been identified in acute experiments by autoradiography. These are (1) cortex, (2) outer medulla–inner cortex, (3) inner medulla, and (4) perirenal and hilar fat. The rate of flow is most rapid in the cortical compartment, which receives about 88% of the total nutrient blood flow in the normal kidney [17]. Rerouting of blood from the cortex to the medulla (Trueta shunting) may occur in the end stages of such renal disorders as collagen vascular diseases, malignant nephrosclerosis,

© 1978 American Roentgen Ray Society

0361–803X/78/1200–1113 $00.00

chronic glomerulonephritis, and also in transplant rejection. This is thought to indicate high resistance in the renal cortex, leading to decreased perfusion in this region with respect to the remainder of the kidney. Recently, Tadavarthy et al. [18] reported temporary Trueta shunting in normal kidneys during renal angiography. The mechanism of this phenomenon and its relevance to contrast-induced renal failure are unknown and may warrant further investigation in connection with the other hemodynamic effects of contrast agents.

One might question how this theoretical information applies to the clinical situation. Specifically, can the high risk patient be identified, and what prophylactic measures might be instituted to decrease the incidence of acute oliguric renal failure after contrast studies? The clinical profiles of patients who develop acute renal failure following the administration of iodinated contrast material would suggest that vascular factors are more significant than any tubular cytotoxic effects. Diabetics are at increased risk to develop acute oliguric renal failure after receiving radiocontrast agents, especially in the presence of dehydration and azotemia [6, 19, 20]. In this regard, it should be mentioned that while dehydration could accentuate any of the previously described effects of contrast, adequate hydration does not seem to necessarily protect against renal failure [2, 21, 22].

All of the patients described by Diaz-Buxo et al. [23] had been diabetic for a minimum of 6 years, and all had clinical evidence of diabetic retinopathy, neuropathy, and nephropathy. Harkonen and Kjellstrand [24] studied 29 diabetic patients in whom excretory urography was performed as a routine investigation of renal status and not because of sudden changes in renal function. Exacerbation of preexisting renal insufficiency after pyelography was noted in 76% of these patients, and in nine patients there was irreversible deterioration of renal function. The main risk factors seemed to be early-onset diabetes and more severe degrees of renal insufficiency before the study.

More recently, Van Zee et al. [4] noted an incidence of acute oliguric renal failure of about 5% after excretory urography, in a group of high risk patients which included diabetics and nondiabetics. This is to be compared with an overall incidence of less than 1% in unselected populations. Of the nondiabetic group, 14 of 15 had recognized renal disease due to hypertension (five patients), glomerulonephritis (three), hydronephrosis (three), and gouty nephropathy, polycystic disease, and mild transplant rejection (one patient each). It is noteworthy that all but two patients were well hydrated at the time of urography. These findings support an impression that small vessel disease may significantly predispose to contrast-induced renal failure. Tubular epithelial cell toxicity in such compromised kidneys may be a secondary and additive phenomenon rather than an initiating event in renal failure in this setting. Although intratubular contrast concentrations may actually be less than normal, the period of exposure is prolonged and each nephron handles a larger fraction of the administered dose. Direct tubular damage may therefore occur. Urate nephropathy may also play some role, since many patients are hyperuricemic due to underlying renal insufficiency. This nevertheless does not seem to be the major determinant of contrast-induced renal failure, since not all patients who develop this complication have elevated serum uric acid prior to study.

The high incidence of acute renal failure in susceptible groups of patients may be partially explained by the relatively large doses of contrast used for drip infusion urography and some angiographic examinations. Gruskin et al. [12] observed that hematuria did not occur in infants undergoing cardiac catheterization when the dose of contrast did not exceed 3 ml/kg. Other investigators [4, 21] have also postulated a dose-related effect, but consistent dose-response relationships have not been demonstrated to date either clinically or experimentally [3]. Further study of this question is needed, but from the available data it is not unreasonable to conclude that the maximum safe dose of contrast is probably less than 5 ml/kg, and undoubtedly much less in patients with underlying renovascular disease and/or hyperuricemia.

In summary, clinical and experimental data seem to identify the patient at high risk to develop contrast-induced acute renal failure as having either or both of the following: (1) small vessel renal disease, diabetic or otherwise, and (2) hyperuricemia, either primary or secondary to underlying renal insufficiency. If possible, alternatives to contrast examinations should be found for such patients. However, if necessary diagnostic information cannot be obtained other than by contrast examination, then doses of iodinated contrast media should be kept to a minimum, and an adequate state of hydration should be maintained. The benefits of preserving renal blood flow and controlling serum and urine uric acid have yet to be ascertained by controlled clinical trials.

Margery Heneghan
New York Hospital–Cornell Medical Center
New York, New York 10021

REFERENCES

1. Carvallo A, Rakowski TA, Argy WP, Schreiner GE: Acute renal failure following drip infusion pyelography. *Am J Med* 65:38–45, 1978
2. Shafi T, Chou S, Porush J, Shapiro WB: Infusion intravenous pyelography and renal function effects in patients with chronic renal insufficiency. *Arch Intern Med* 138:1218–1221, 1978
3. Swartz RD, Rubin JE, Leeming BW, Silva P: Renal failure following major angiography. *Am J Med* 65:31–37, 1978
4. Van Zee BE, Hoy WE, Talley TE, Jaenike JR: Renal injury associated with intravenous pyelography in nondiabetic and diabetic patients. *Ann Intern Med* 89:51–54, 1978
5. Wagoner RD: Acute renal failure associated with contrast agents. *Arch Intern Med* 138:353, 1978
6. Weinrauch LA, Robertson WS, D'Elia JA: Contrast media-induced acute renal failure. *JAMA* 239:2018–2019, 1978
7. Killen D, Lance EM: Experimental appraisal of the agents employed as angiocardiographic and aortographic contrast media. II. Nephrotoxicity. *Surgery* 47:260–265, 1960

8. Postlethwaite AE, Kelley WN: Uricosuric effect of radiocontrast agents. *Ann Intern Med* 74:854–862, 1971
9. Berdon WE, Schwartz RH, Becker J, Baker DH: Tamm-Horsfall proteinuria: its relationship to prolonged nephrogram in infants and children and to renal failure following intravenous urography in adults with multiple myeloma. *Radiology* 92:714–722, 1969
10. Krovetz LJ, Mitchell BM, Neumaster T: Hemodynamic effects of rapidly injected hypertonic solutions into the heart and great vessels. *Am Heart J* 74:453–462, 1967
11. Sako Y: Hemodynamic changes during arteriography. *JAMA* 183:253–261, 1963
12. Gruskin AB, Oetliker OH, Wolfish NM, Gootman NL, Bernstein J, Edelmann CM: Effects of angiography on renal function and histology in infants and piglets. *J Pediatr* 76:44–48, 1970
13. Talner L, Davidson AJ: Effect of contrast media on renal extraction of PAH. *Invest Radiol* 3:301–309, 1968
14. Talner L, Davidson AJ: Renal hemodynamic effects of contrast media. *Invest Radiol* 3:310–317, 1968
15. Derrick JR, Brown RW, Livanec G, Bond TP, Guest NM: Experimental effects of selective arteriography on the microcirculation. *Am J Surg* 116:712–714, 1968
16. Wiedeman MP: Vascular and intravascular responses to various contrast media. *Angiology* 14:107–109, 1963
17. Thorburn GD, Kopald HH, Herd JA, Hollenberg M, O'Morchoe CCC, Barger AC: Intrarenal distribution of nutrient blood flow determined with krypton^{85} in the unanesthetized dog. *Circ Res* 13:290–307, 1963
18. Tadavarthy SM, Castaneda W, Amplatz K: Redistribution of renal blood flow caused by contrast media. *Radiology* 122:343–348, 1977
19. Krumlovsky FA, Simon N, Santhanam S, DelGreco F, Roxe D, Pomeranc MM: Acute renal failure association with administration of radiographic contrast material. *JAMA* 239:125–127, 1978
20. Port FK, Wagoner RD, Fulton RE: Acute renal failure after angiography. *Mayo Clin Proc* 121:544–550, 1974
21. Ansari Z, Baldwin DS: Acute renal failure due to radiocontrast agents. *Nephron* 17:28–40, 1976
22. Pillay VKG, Robbins PC, Schwartz FD, Kark RM: Acute renal failure following intravenous urography in patients with long-standing diabetes mellitus and azotemia. *Radiology* 95:633–636, 1970
23. Diaz-Buxo JA, Wagoner RD, Hattery RR, Palumbo PJ: Acute renal failure after excretory urography in diabetic patients. *Ann Intern Med* 83:155–158, 1975
24. Harkonen S, Kjellstrand CM: Exacerbation of diabetic renal failure following intravenous pyelography. *Am J Med* 63:939–946, 1977

Letters

Single-Contrast/Double-Contrast GI

In reference to the article "Double-blind Study of Single and Double Contrast Upper Gastrointestinal Examinations Using Endoscopy as a Control" [1], the many variables which enter into such a study prevent a valid conclusion. In fact, it is indeed not logical for one who has not personally conducted the fluoroscopic examination to be responsible for an informative and accurate interpretation of spot films and overhead films. Attempts to interpret radiographs without the most important aspect of the examination is a corner into which we sometimes paint ourselves.

Certainly any properly conducted so-called "single-contrast examination" should find sufficient gas in the stomach to produce a double-contrast study of the antrum and of the duodenum. It is agreed that distension of the stomach with gas in some instances adds materially to the examination, but that should be "dealer's choice." I would safely state that an experienced examiner doing a meticulous upper gastrointestinal study can outperform the advocates solely relying on the double-contrast method, as Montagne et al. report. But the idea of blind interpretation of only those films presented to an interpreter without his own insight and know-how is fraught with error.

The study should probably have included another control via examining either the same or an additional 100 patients *twice by the same method.* In other words, 100 patients by the contrast method at two intervals closely related and another 100 by the conventional method on two successive similar intervals. I realize that all of this is difficult, but otherwise the study lacks validity. It is well known that the endoscopist is not the ultimate arbiter no matter what his expertise or experience.

John H. Walker
Mason Clinic
Seattle, Washington 98111

The article by Montagne et al. [1] substantiates the findings which I have published on many occasions in letters and articles. There is no reason when performing a gastrointestinal series, that both air studies and the ordinary barium meal examination with high kilovoltage and compression cannot be used. My results over the years have been excellent. Air studies alone will frequently miss obvious lesions. There is no question, however, that this method is best for superficial ulcers and gastritis. Historically, it may be of interest that for many years Dr. Crohn inserted a Levin tube for gastric analysis as an office procedure and then sent the patient to me for films. Utilizing the nasogastric tube, I performed air studies with high-density barium followed by conventional upper gastrointestinal series.

Richard H. Marshak
1075 Park Avenue
New York, New York 10028

REFERENCE

1. Montagne JP, Moss AA, Margulis AR: Double-blind study of single and double contrast upper gastrointestinal examinations using endoscopy as a control. *Am J Roentgenol* 130:1041–1045, 1978

Reply

The purpose of our paper was to evaluate the accuracy of the double-contrast examination of the stomach and duodenum if performed as the only examination of the upper gastrointestinal tract and to compare this with the single-contrast upper gastrointestinal series. To equalize the two examinations, our approach was to compare the two as much in a double-blind fashion as possible. Therefore the protocol called for separating the films of the single- and double-contrast examinations, and having examiners who were not familiar with the patients do the readings separately. This obviously put the single-contrast examination at a disadvantage, but since the value of the single-contrast examination has been documented over many years, we did not elect to again substantiate its value using fluoroscopy with compression and all the other technical advantages that may be possible.

We did not review the films on the 100 patients twice, since the purpose of the study was not to examine the reliability of the examiners against themselves, but to duplicate as much as possible the clinical situation in which the films are read and reported. Our results do not detract from the value of either the single- or double-contrast examination, but demonstrate that by using the advantages of each, overall results will be improved.

The endoscopist may not be the ultimate arbiter no matter what his expertise or experience, but the only ultimate arbiter is autopsy and we were not skillful enough to be able to design a study based on autopsy proof.

We are very grateful that Dr. Marshak agrees with our findings and conclusions and feel that his experience and expertise further contribute to the validity of the paper.

Albert A. Moss
Alexander R. Margulis
Jean-Philippe Montagne
University of California
San Francisco, California 94143

Lymphography vs. CT of Lymphomas

As stated in the paper "Accuracy of Computed Tomography in Detecting Intraabdominal and Pelvic Adenopathy in Lymphoma" [1], CT undeniably has a significant role in the workup of patients with lymphoma. However, it is questionable if at this point all the answers are in and if it is yet time to draw conclusions based on such a limited sample of patients.

To be specific, when results were presented, lymphomas should not have been lumped into one group but subdivided into Hodgkin's and non-Hodgkin's lymphomas. There is a difference in the presenting stage between these two subgroups. Non-Hodgkin's lymphomas usually present in more advanced clinical stages, therefore frequently appearing as a bulky tumor, where CT or ultrasound are probably of much value. In 5%–10% of patients with Hodgkin's lymphoma, one finds only minimal or no enlargement of nodes which are diseased. However, the structural changes in these nodes can easily be recognized lymphography but, because their size is essentially normal, not by CT. Since therapy depends on extent of the disease, it is important to identify these patients.

The paper does not specify how many of the patients with positive CT scans belonged to the Hodgkin's and how many to

the non-Hodgkin's group. Nor is there any mention as to how extensive the disease was. Did most have significantly enlarged nodes? Was the entire retroperitoneum involved? Were only single nodes or nodal groups involved?

As far as the accuracy of the so-called "normal" group is concerned, clinical staging is not accurate enough. The claims that clinical follow-up can be used as a proof that interpretation is correct reminds me of papers published in the 1960s regarding accuracy of lymphography. True accuracy of lymphography was only established after the results of the methodical studies, including staging laparotomies done by the Stanford group, were published. Only then were we able to learn the true criteria for interpretation of the lymphograms. Similar rigid criteria should be applied to CT before conclusions are drawn.

I must take issue with the statement that lymphography has no real advantage over CT when following patients. In most instances sufficient contrast medium remains in the node to allow recognition of nodal changes for at least a year, if not longer. During that time a single plain film of the abdomen is all that is needed to compare with previous studies. This is far simpler, cheaper, and less time-consuming than repeating a CT scan at intervals of 2–3 months as is usually done after lymphangiography.

While time may prove that CT and ultrasound are as sensitive or more sensitive than lymphography, the limited experience available now does not justify suggesting that CT or ultrasound be used for staging of lymphomas. Accuracy of 84% is not acceptable. It is the patient with minimal involvement that we want to find early; it is easy to identify the one with obvious disease. It is questionable if one needs lymphography if the CT or ultrasound are positive, but is it justified to conclude, with the limited information available, that the negative CT reliably reflects the stage of the disease? Are we willing to accept a small error in correct staging of potentially curable patients? These questions must also be answered before one discards the tedious, but fairly reliable lymphography.

P. Ruben Koehler
University of Utah Medical Center
Salt Lake City, Utah 84132

REFERENCE

1. Lee JKT, Stanley RJ, Sagel SS, Levitt RG: Accuracy of computed tomography in detecting intraabdominal and pelvic adenopathy in lymphoma. *Am J Roentgenol* 131:311–315, 1978

Reply

It is true that 5%–10% of patients with Hodgkin's lymphoma may have minimal or no enlargement of nodes which, in fact, are diseased. We did not encounter such a case during the time of the study which was reported. Recently, we saw a patient who had a "normal" CT scan despite an inguinal node biopsy positive for Hodgkin's disease. Lymphangiography was recommended in that instance and showed replaced but normal-sized lymph nodes. It is clearly stated in the discussion of our paper that "lymph nodes which are normal in size but replaced with tumor will not be distinguished as abnormal by CT."

We agree with Dr. Koehler that clinical staging is not accurate enough and cannot be relied upon as the final proof for the so-called "normal" group. In our paper, the accuracy of CT is computed only on the cases with surgical or autopsy proof. The overall accuracy in our series is 90% and not 84% as alluded to. The 84% is simply a percentage of agreement between the CT scan and the lymphangiogram in the 37 patients who had both CT and lymphangiography but no surgical staging procedure.

Nowhere in our paper does the statement "that lymphography has no real advantage over CT when following patients, . . ." appear. We did state that "lymphangiography has only a transient advantage over CT in following patients and the latter is a more valuable tool for long-term follow-up." The amount of residual contrast medium remaining in the lymph nodes after lymphangiography is quite variable. Although it is probably true that most patients will have sufficient contrast medium retained in the nodes for a diagnostic abdominal film up to 6 months later (1 year sounds a bit long to us), only less than one-half of the relapses in Hodgkin's disease occur in the first 15 months, whereas the rest of the recurrences occur within the first 5 years [1]. It is doubtful that any significant percentage of patients will have enough residual contrast medium by that time. Having worked with CT for 3 years in patients who have had both CT and lymphangiography, we have been impressed with the large number of cases in which the follow-up abdominal film either had insufficient contrast remaining in the nodes to allow for a firm diagnostic opinion or, even worse, appeared deceptively normal or unchanged when, in fact, subsequent CT demonstrated a significant increase in node size in other locations such as the mesentery or other nodes which had no residual contrast material within them. We are in the process of accumulating a series of these cases in order to press this point further.

The overall accuracy of CT in lymphoma in our series of 31 surgically proven cases is 90%. The overall accuracy of lymphangiography in lymphoma in the series of Castellino et al. is 92% [2]. The difference between CT and lymphangiography is that the former may have a 14%–15% false negative rate, whereas the latter may have up to a 25% false positive rate. The chance that CT will miss an involved node is no greater than lymphangiography over-calling a hyperplastic lymph node.

Joseph K. T. Lee
Robert J. Stanley
Stuart S. Sagel
Robert G. Levitt
Mallinckrodt Institute of Radiology
St. Louis, Missouri 63110

REFERENCES

1. Weller SA, Glatstein E, Kaplan HS, Rosenberg SA: Initial relapses in previously treated Hodgkin's disease. *Cancer* 37:2840–2846, 1976
2. Castellino FA, Billingham M, Dorfman RF: Lymphographic accuracy in Hodgkin's disease and malignant lymphoma with a note on the "reactive lymph node as a cause of most false-positive lymphograms." *Invest Radiol* 9:155–165, 1974

Ultrasound of Tumor Extension to IVC

I read with interest the article entitled "Ultrasonic Detection of Renal Tumor Extension into the Inferior Vena Cava" [1]. The authors felt that "only one previous case of intracaval tumor extension demonstrated by ultrasonography has been reported in the English language literature." I wish to point out an article written by me entitled "The Inferior Vena Cava: Mass Effects," in the March 1978 issue of the *AJR* [2]. In that article, six patients were presented with mass effects on the vena cava from a variety of tumors. In one of these patients, with renal cell

Howard G. Bayley, 1914–1978

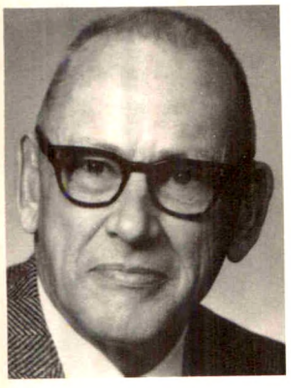

Howard G. Bayley, 63, a community leader in Beaver Dam, Wisconsin, died May 25, 1978 in Georgetown University Hospital while undergoing emergency surgery for a ruptured abdominal aortic aneurysm.

Dr. Bayley was born December 21, 1914 in Battle Creek, Michigan; he received his B.S. degree from Battle Creek College in 1938. His medical degree was awarded by Northwestern University Medical School in 1942 and he interned at Milwaukee County Hospital, 1942–1943, before serving 3 years in the U.S. Army. He was acting radiologist at the Veterans Administration Hospital, Marion, Indiana in 1946 and 1947. In 1947 he became one of my first residents in radiology at the Veterans Administration Hospital, Wood (Milwaukee), Wisconsin, in a training program associated with Marquette University Medical School.

In 1950, Dr. Bayley became the first permanent staff radiologist for St. Joseph's Hospital (now known as Beaver Dam Community Hospital); Waupun Memorial Hospital, Columbus Community Hospital, and Lutheran Hospital, Beaver Dam. He also formed the Radiology Associates of Beaver Dam, Inc. and was the guiding force when he took over as director of the four small departments of radiology for the hospitals he served; in a relatively short time he had busy, well organized departments in each institution.

Howard Bayley was highly intelligent, an excellent radiologist, religious, and a man highly regarded by his medical colleagues and by many highly placed nonmedical friends in an extensive community. His nonmedical appointments to boards and commissions in his local community were numerous. For 28 years he was actively involved in activities of the Boys Scouts of America at county, state, and national levels. He received many awards from this organization, among his most cherished was the Silver Beaver Award, the highest honor a volunteer may receive.

Dr. Bayley was equally active in the medical profession in his local community and at state and national levels as well. Among the various positions in which he served were: diplomat, American Board of Radiology; member, American College of Radiology, and later a fellow; councilor to the American College of Radiology from Wisconsin. In addition he was an active member of numerous societies including the Radiological Society of North America and the American Roentgen Ray Society.

Above all Howard Bayley was an excellent radiologist who was deeply involved in his specialty. He remained friendly, low key, and always available for friendly consultation with his medical colleagues. His contribution in elevating the standards of medical practice in his community was superior. He is survived by his widow, Ardeth, a son, James B. Bayley, a sister, Roberta Bennett, and a brother, Dr. Ned Bayley.

Theodore J. Pfeffer
Milwaukee, Wisconsin 53226

Bernard S. Epstein, 1908–1978

Bernard S. Epstein, a leading radiologic author and educator, died May 5. Born February 12, 1908 in New York City, he remained in New York state as both a student and resident in radiology and received his M.D. from the University of Rochester School of Medicine and Industry in 1932. He trained in radiology at the Jewish Hospital of Brooklyn and Montefiore Hospital, New York City, before serving as a radiologist to Montefiore Hospital and Jewish Sanitarium and Hospital for Chronic Diseases from 1936–1939. Later Dr. Epstein was an associate radiologist with the Jewish Hospital of Brooklyn before assuming responsibility for the Department of Radiology at Long Island Jewish Hillside Medical Center in 1954.

In 1975, Dr. Epstein left New York to participate in the development of the Department of Radiology at the University of Texas Medical School in San Antonio. He was actively engaged in that career at the time of his death.

Throughout his professional life, he remained intimately involved with the educational aspects of radiology, serving as both associate clinical and clinical professor of radiology at Albert Einstein College of Medicine and later as a visiting professor at the same institution. He was professor of radiology at the State University of New York, Stoney Brook, from 1971–1975.

Diseases of the spinal column were of special interest to Dr. Epstein and provided the stimulus for the majority of his more than 170 scientific publications. His best known work was *The Spine: A Radiologic Text and Atlas* which was published in four editions.

Dr. Epstein is survived by his wife, Kay Epstein, now of New York City; a son, Richard Epstein; daughters, Alice Pomper and JoAnn Rubin; a brother, Dr. Joe Epstein; and grandchildren.

Malcolm D. Jones
San Antonio, Texas

In Memorium

The Journal notes with sorrow the deaths of members of the American Roentgen Ray Society between September 1977 and August 1978.

Life
Traian Leucutia
Clyde A. Stevenson

Emeritus
Percy D. Hay, Jr.
Clarence P. Truog

Active
Bernard Wolf
Charles F. Ingersoll
Charles P. Oderr
Alexander S. MacMillan, Jr.
Wendell Dietz
Bernard S. Epstein

Abstracts of Current Literature

Chest

Transbronchial mucus transfer of bronchogenic carcinoma. Cattaneo SM, Zipf RE, Johnson OE, Everhart LS (3545 Olentangy River Road, Columbus, Ohio 43214). *J Thorac Cardiovasc Surg* 75:585–594, April 1978

The metastatic transfer of cells from a primary bronchogenic carcinoma to other portions of the lung as a result of mucus embolization and inoculation has been postulated. However, prior to this report, an actual case had not been documented. A 45-year-old man with hemoptysis demonstrated a discrete 5 cm mass in the left lower lobe and a 1 cm nodule in the left upper lobe. At surgery, the left lower lobe mass was found to be a poorly differentiated squamous cell without evidence of lymphatic invasion. The left upper lobe nodule was an identical carcinoma located endobronchially, without adjacent epithelial dysplasia. The authors consider these findings diagnostic of endobronchial spread.

W. Richard Webb

Reversible respiratory disease in beryllium workers. Sprince NL, Kanarek DJ, Weber AL, Chamberlin RI, Kazemi H (Pulmonary Unit, Massachusetts General Hospital, Boston, Massachusetts 02114). *Am Rev Respir Dis* 117:1011–1017, June 1978

Survey of a beryllium extracting and processing plant was performed in 1971, and peak air concentrations of beryllium 50 times the accepted level were found. Among 214 employes, radiographic changes of interstitial disease (berylliosis) were present in 31, hypoxemia was found in 20, and 11 had both hypoxemia and abnormal radiographs. A follow-up survey in 1974 showed a significant decrease in air concentrations of beryllium, primarily due to better plant ventilation. Nine of 18 men with interstitial disease detected radiographically in 1971 and available for follow-up in 1974 had normal chest radiographs; improvement in hypoxemia also occurred. These findings indicate that, to some extent, the radiographic and clinical findings of berylliosis are reversible, perhaps reflecting acute inflammation.

W. Richard Webb

Distribution of HLA antigens in idiopathic pulmonary fibrosis. Fulmer JD, Sposovska MS, von Gal ER, Crystal RG, Mittal KK (Building 10, Room 6-N-260, National Institutes of Health, Bethesda, Maryland 20014). *Am Rev Respir Dis* 118:141–147, July 1978

In recent years groups of histocompatibility (HLA) antigens have been related to various hereditary diseases. To determine whether there is an association between the major histocompatibility system and idiopathic pulmonary fibrosis, the distribution of 35 antigens of HLA loci A and B was determined among 33 patients with idiopathic pulmonary fibrosis and 329 matched controls. Although certain antigens tended to be more prevalent among patients with idiopathic pulmonary fibrosis, there were no significant differences in the frequencies of the HLA-A and HLA-B antigens between the two groups of patients. Subtle associations may exist, but the authors conclude that HLA-A and HLA-B loci are not strongly related to development of this disease.

W. Richard Webb

Measurement of lung density by computed tomography. Wegener O, Koeppe P, Oeser H. (Klinikum Steglitz, Free University of Berlin, Hindenbergdamm 30, D1000 Berlin 45). *J Computer Assisted Tomography* 2:263–273, July 1978

Tomograms of the lungs were obtained with an EMI CT 5005 whole body scanner. With a nominal slice thickness of 13 mms, the standard deviation for water was 18.1 EMI units. Measurement of the density of each lung was provided over a selected field and a histogram of this level obtained. Clinical application of this technique is demonstrated by comparing histograms of normal patients versus patients with obstructive and restrictive lung disease. The technique appears to offer an objective and sensitive measurement of hydration in the lung, particularly useful in patients undergoing hemodialysis.

Michael J. Meagher

Computed tomography of solitary pulmonary nodules: Experience with scanning times longer than breath holding. Raptopoulos V, Schellinger D, Katz S (University of Massachusetts Medical Center, 55 Lake Avenue, Worchester, Massachusetts 01650). *J Computer Assisted Tomography* 2:55–60, Jan 1978

A total of 31 patients with solitary pulmonary nodules (18 benign and 13 malignant proven by either tissue biopsy or prolonged follow-up) were evaluated by a CT scanner with a scan time of approximately 6 min. Comparison was made between CT findings and findings on the standard posteroanterior chest radiograph. All nodules which showed calcium content by conventional radiographic techniques also showed evidence of calcium on CT. In five additional patients, calcium content within a solitary pulmonary nodule was suspected but not proven on conventional tomograms while proven by CT. Of 18 nodules in which there was no evidence of calcium on conventional tomograms, CT revealed evidence of calcium in five cases. The lack of calcium content was confirmed by CT in the remaining 13 patients.

After analysis of the findings of the CT "tomograms", CT evidence of calcium appeared to be the most important feature of benignancy.

Michael J. Meagher

Pulmonary nocardiosis. Balikian JP, Herman PG, Kopit S (Harvard Medical School, 25 Shattuck Street, Boston, Massachusetts 02115). *Radiology* 126:569–573, March 1978

Pulmonary nocardiosis is an airborne infection due to *Nocardia asteroides*. Nocardiosis is seen in the immunocompromised patient, either due to underlying systemic disease or immunosuppresive therapy. Symptomatology may include malaise, anemia, dry cough, fever, pleuritic chest pain, or respiratory failure but patients with chest film abnormality may be asymptomatic.

Specific diagnosis may be made by percutaneous needle aspiration, core biopsy, transbronchial biopsy, or open lung biopsy. Recovery of the organism from sputum is generally unsuccessful. Samples of tissue are stained with gram, acid-fast, and Gomori silver stains. The organisms are filamentous branching, gram-positive, and acid-fast, and should be grown for at least 2 weeks in aerobic media. The pathologic lesions are combinations of granuloma and suppuration. Three expressions are known: (1) solitary lung abscess; (2) slow progressive fibrosis; (3) acute necrotizing pneumonia.

Radiographic findings include: (1) small solitary nodule; (2) multiple nodules; (3) cavitary pneumonias; (4) bilateral patchy bronchopneumonia; (5) subpleural plaque-like infiltrate; (6) empyema and bronchopleural fistula. When cavitary lesions are present, they are thick walled.

Specific therapy is sulfonamides which should be continued for months to a year in order to cure and prevent relapse. Early specific treatment may achieve as high as 75% survival.

Asher Nov

Cardiovascular

Echocardiographic differentiation of partial and complete atrioventricular canal. Bass JL, Bessinger FB Jr, Lawrence C (Box 94, University of Minnesota Hospitals, 420 Southeast Delaware Street, Minneapolis, Minnesota 55455). *Circulation* 57:1144–1150, June 1978 (by permission American Heart Association)

Retrospective examination of echocardiograms was performed in 34 patients with persistent atrioventricular canal who had undergone cardiac catheterization. Characteristic findings in 16 patients with partial atrioventricular canal were lack of continuity of mitral and tricuspid valves, paradoxical interventricular septal motion, definite E and A waves of the mitral valve anterior leaflet echoes and late systolic anterior motion of the mitral valve. Eighteen patients with persistent atrioventricular canal had an interventricular communication and were classified as having the complete form. They characteristically had continuous mitral and tricuspid valves, normal interventricular septal motion, disorganized mitral valve anterior leaflet echoes, and normal systolic mitral valve motion.

Combining these findings allowed differentiation of 31 of the 34 patients (91%) as having partial or complete atrioventricular canal. Determining the presence of a ventricular septal defect from loss of interventricular septal echoes was unsatisfactory. The severity of mitral insufficiency could not be estimated from echocardiograms of our patients with partial atrioventricular canal.

Author Abstract

Echocardiographic estimation of pulmonary artery pressure in transposition of the great arteries. Gutgesell HP (Pediatric Cardiology, Texas Children's Hospital, 6621 Fannin, Houston, Texas 77030). *Circulation* 57:1151–1153, June 1978 (by permission American Heart Association).

To determine their usefulness in estimating pulmonary artery pressure, left ventricular systolic time intervals were determined by echocardiography in 65 patients with dextro-transposition of the great arteries. The systolic time intervals were measured from recordings of pulmonary valve motion at 100 mm/sec paper speed.

The preejection period (PEP) and the ratio of this period to left ventricular ejection time (PEP/LVET) were directly related to pulmonary artery pressure. The strongest correlations were that between PEP/LVET and pulmonary artery diastolic pressure ($r = 0.70$) and that between PEP/LVET and the ratio of mean pulmonary pressure to mean systemic pressure ($r = 0.71$).

A value of PEP/LVET of less than 0.26 was consistently associated with pulmonary artery diastolic pressures of less than 20 mm/Hg and, in 28 of 31 patients, pulmonary artery pressure less than one-third of mean systemic arterial pressure. Pulmonary hypertension was present in 18 of 22 patients with PEP/LVET of 0.30 or greater; elevated PEP/LVET was also present in four patients with abnormalities of cardiac rhythm or conduction, two of whom also had angiographic evidence of myocardial dysfunction.

Author Abstract

Gastrointestinal

Computerized tomography and nuclear imaging of the liver. A comparative study in 83 cases (in English). Scherer U, Buell U, Rothe R, Eisenburg J, Schildberg FW, Meister P, Lissner J (Radiologische Klinik der Universitaet Muenchen, Klinikum Grosshadern, D-8000 Muenchen 70, Federal Republic of Germany). *Eur J Nucl Med* 3:71–80, 1978

Computed tomography and nuclear liver scanning were compared in 83 patients in which the presence or absence of liver diseases could be assessed further by means of invasive diagnostic procedures such as biopsy, laparoscopy, laparotomy, and/or autopsy. The percentage of true negative cases was 94% for CT and 91% for nuclear liver scanning, and the percentage of true positive diagnosis was 94% for CT and 81% for nuclear liver scanning. CT did not only yield higher true negative and true positive rates, but was also superior in determining the number and size of space-occupying hepatic lesions. Furthermore, CT was pathognomonic for circumscript hepatic disease processes such as cysts, metastases, obstructive jaundice, and perhaps echinococcal disease. Nuclear imaging was superior in detecting cirrhosis.

Peter F. Winter

^{133}Xe uptake by fatty livers. Sutherland JB, McCarthy DS, Mark RJ, Thorlakson TK (University of Manitoba, 700 William Avenue, Winnipeg, Canada). *J Can Assoc Radiol* 29:82–84, June 1978

The authors believe that the 5 min rebreathing of ^{133}Xe and oxygen may be a useful and simple method to accurately study patients for excessive fat accumulation in the liver. Eighteen morbidly obese patients had their respiratory functions studied by xenon ventilation and perfusion scans, as well as liver biopsies and liver function tests. All were performed prior to jejunoileal bypass surgery and at 12 and 24 months following surgery. It became apparent that there was an unusual accumulation in the right upper quadrant in the majority of patients who were also shown to have fatty liver.

Jack M.A. Tishler

Computed tomography in surgical pancreatic emergencies. Pistolesi G (Policlinico Di Borgo Roma, Verona, Italy). *J. Computer Assisted Tomography* 2:165–169, April 1978

Of 186 patients with pancreatic disease studies, seven pancreatic surgical emergencies were retrospectively examined. CT scanning of the pancreatic regions in those patients was found to be highly beneficial in planning the need for and type of surgical intervention.

Michael Meagher

The radiology of ileosigmoid knot. Young WS, White A, Grave GF (University of Natal, Durban, South Africa). *Clin Radiol* 29:211–216, March 1978

The findings on the radiographs of 14 cases of ileosigmoid knot are presented and analyzed. The clinical features and pathology of the condition are briefly described. The key radiologic features consist of a dilated loop of pelvic colon, evidence of small intestinal obstruction, and retention of feces in an undistended proximal colon. The dilated loop usually lies in the right side of the abdomen and the limbs taper inferiorly into the right lower quadrant. Medial deviation of the distal descending colon is an inconsistent but highly specific finding. The radiographs readily permit distinction from primary volvulus of the small intestine and from nonobstructive surgical emergencies such as perforated viscus and ruptured ectopic pregnancy. The combination of radiographic findings may however be simulated by volvulus of the right colon, closed loop small intestinal obstruction and by volvulus of the pelvic colon complicated by peritonitis. The differential diagnosis is discussed and the value of sigmoidoscopy, rather than barium enema, emphasized.

Author Abstract

The retrorectal space. Teplick SK, Stark P, Clark RE, Metz JR, Shapiro JH (Boston City Hospital, Boston, Massachusetts). *Clin Radiol* 29:177–184, March 1978

Ninety-nine adults with an enlarged retrorectal space on barium enema examination have been evaluated. Measurements were based on previously described methods using the lateral view of the barium filled rectum. In 38.4% of cases there was no lesion (normal variations). The rest were classified as inflammatory conditions, tumors, and miscellaneous lesions. It is concluded that an increased width of the presacral space per se does not necessarily connote a lesion. Pathologic widening of the space is usually associated with changes of the contour of the rectum, abnormalities of the sacrum, or other alterations of the presacral soft tissues.

Author Abstract

Hemorrhagic pseudocysts of the spleen in pancreatitis (in French). Paris JC, L'Herminé C, Roger J, Houcke P, Foucart H. *Ann Radiol* 21:25–32, 1978 (Service de Radiologie Est, C. H. U., F-59307, Lille Cedex, France).

Pancreatic pseudocysts containing blood are a relatively rare complication of pancreatitis. This study reports 14 cases. Patient ages ranged from 28–60 years; most were between 30–50 years. In two cases the pseudocysts were the initial manifestation which led to the diagnosis of pancreatitis. In six patients the symptoms were only minimal and the development of the pseudocyst led to the diagnosis of pancreatitis. The remaining six patients were known cases of pancreatitis.

The standard radiologic examinations with and without contrast medium showed pancreatic calcifications, the usual pressure effect with displacement in adjacent structures by the enlarged spleen, in one case stenosis of splenic flexure by extrinsic pressure was demonstrated. In two cases, findings included pseudocyst of the tail of the pancreas and pleural effusion. The diagnosis was easily made by angiography which demonstrated the subcapsular collection of fluid. Numerous, clear illustrations accompany the article.

Antonio F. Govoni

Musculoskeletal

Idiopathic multicentric osteolysis. Whyte MP, Murphy WA, Kleerekoper M, Teitelbaum SL, Avioli LV (Division of Bone and Mineral Metabolism, Washington Universty School of Medicine, St. Louis, Missouri 63110). *Arthritis Rheum* 21:367–376, April 1978

Idiopathic multicentric osteolysis is a rare disorder characterized by multifocal articular bone destruction begining in childhood. Typically, pain and swelling follows an episode of trauma, persists during childhood, and remits during adolescence leaving variable deformity of the hands and feet. The carpal and tarsal bones are invariably affected. This paper reports two affected members of a family and suggests a hereditary pathogenesis. Histologically, synovium, articular cartilage, and bone appear normal and the abnormality is a proliferation of joint fibrous tissue.

D. M. Forrester

The hip joint in Paget's disease (Paget's "coxopathy"). Guyer PB, Dewbury KC (Royal South Hants Hospital, Southampton, England). *Br J Radiol* 51:574–578, Aug 1978

Three hundred patients with Paget's disease around the hip joint are compared with 300 control patients who did not have Paget's disease. The incidence of joint degeneration in the two groups is similar at all ages, and there appears to be no predisposition to joint degeneration in patients who have Paget's disease. A feature of the hip joints is that in approximately half there is joint narrowing to less than 3 mm affecting a portion or the whole of the joint surface, which, together with the incidence of protrusio acetabuli, is probably a specific manifestation of the joint changes associated with Paget's disease.

Author Abstract

Radiographic evaluation of tibial plateau fractures. Newberg AH, Greenstein R (Massachusetts General Hospital, Boston, Massachusetts 02114). *Radiology* 126:319–323, Feb 1978

The radiographs and records of 42 patients with 43 tibial plateau fractures are presented. Tibial plateau fractures are classified into six types. Type 1 injuries are displaced or nondisplaced split fractures of tte lateral plateau resulting from pure abduction injury. Types 2 and 3 are a central depressed and split depressed fractures resulting from abduction and axial compression. Type 4 is a total depression fracture without comminution. These are likely to occur in the medial tibial plateau. Type 5 is anterior or posterior split fractures without central depression, while type 6 is described as comminuted "T" or "Y" fractures. These result from vertical compression.

The greater frequency of lateral tibial plateau fractures relates to several factors: (1) an anterior flattened portion of the lateral femoral condyle; (2) less uniformity in the distribution of stress; (3) smaller numbers of trabeculae in the lateral tibial plateau as opposed to medial; and (4) greater frequency of trauma on the lateral aspect.

These fractures are radiographically evaluated by anteroposterior and lateral radiographs. Due to a normal 10° downward slope of the posterior aspect of the tibial plateau, a 15° caudad angulation on the anteroposterior view may be advantageous. Stress views are useful in evaluating ligamentous injury. A supplemental cross table lateral projection may be employed to detect a fat fluid level indicating intraarticular fracture.

The most accurate anatomic detail is afforded by tomographic evaluation in both anteroposterior and lateral views. The exact definition of the fracture anatomy will determine the therapeutic approach. Types 1 and 2 are treated conservatively while type 3 is treated surgically. It is further agreed that depressions of greater than 5 mm are an indication of an open reduction. There is uniform agreement that depressions of 10 mm and more should be treated surgically. Therapeutic goals are to obtain stability, normal range of motion, and a painless joint.

Asher Nov

The assessment of prognosis in Perthes' disease. Dickens D (Royal Childrens' Hospital, Flemington Road, Parkville, Victoria 3052, Australia). *J Bone Joint Surg* [Br] 60:189–194 May 1978

In a series of 70 children suffering from Perthes' disease, the author notec a close correlation between the clinical and radiologic end results. He felt the most reliable radiologic factors indicating prognosis were the extent of the uncovering of the femoral head, the Catterall grouping, presence of calcification in the outer limit of the acetabulum, and the degree of lateral displacement of the femoral head from the acetabulum. Thus, the radiologic features that were described were thought to be quite helpful in predicting residual sequelae.

Gerald R. Smith

Is chondromalacia patellae a separate clinical entity? Abernethy P, Townsend P, Rose R, Radin E (Department of Orthopaedics, Princess Margaret Rose Orthopaedic Hospital, Edinburgh EH10 7ED, Scotland). *J Bone Joint Surg* [Br] 60:205–210, May 1978

In a review of 100 patellas from patients who died from nonmalignant disease, the authors found a remarkably high necropsy incidence (85% of cartilage deterioration of the central medial facet of the patella) associated with the rather low incidence of symptoms in the general population. The authors suggest that the surgical finding of softening of the articular cartilage of the medial facet should be considered an incidental finding. The persistent pain and tenderness of the patellofemoral joint should not be regarded as "chondromalacia" but as some other disorder such as a facet lesion, osteochondral injury, patella malalignment syndrome, synovial impingement or some type of arthritic disorder. The confusion surrounding the entity of chondromalacia would be reduced by considering the medial facet changes as asymptomatic, age-related physiologic change which does not require surgical intervention. The authors believe that patients who have persistently tender patello-femoral joints should be investigated for alternative causes of pain and that these causes should be specifically treated.

Previous articles have indicated that the diagnosis of chondromalacia patellae is not necessarily a radiographic prerogative and this particular article lends credence that such a radiographic diagnosis should be avoided and that alternative disease processes should be entertained.

Gerald R. Smith

The biology of fracture healing in long bones. McKibbin B (Traumatic and Orthopaedic Surgery, Cardiff Royal Infirmary, Cardiff CF2 1SZ, Wales). *J Bone Joint Sur* [Br] 60:150–161, May 1978

In this scholarly and well written treatise, the author endeavors to review and clarify the current theories of bone healing.

Three basic mechanisms of bone healing are indicated in the article. Any mechanism can occur depending on the stabilization of the fracture. The "external callus" which is the most rapid of all the processes, normally predominates in fractures treated by external fixation. The "late medullary callus" predominates when the external callus response has failed. This process is usually slow and is assisted by immobilization of the bone. A "primary bone union" may occur and is characterized by extreme slowness of the healing. This method is not really a primary method of union but rather a remodeling process which occurs late in the normal healing process.

The author notes that the advantages of a rigidly fixed injured limb are great even though the actual healing process may be slow with this method. He suggests that ideal healing occurs following a procedure which preserves security without imposing total rigidity of the bone. The optimal method of stimulating bone healing has not yet been firmly established.

Gerald R. Smith

Nervous System

Computed tomography in spontaneous intracerebral haematomas. Kendall BE, Radue EW (National Hospital for Nervous Diseases, Queen Square, London, W.C.1, England). *Br J Radiol* 51:563–573, Aug 1978

The typical computed tomographic features of a recent intracerebral hematoma are a homogenous region of increased attenuation surrounded by a well demarcated relatively narrow low attenuation ring. The pathology of the ring is controversial, but it corresponds well with a zone of ischemic necrosis which is observed around most intracerebral hematomas examined at autopsy.

Observations are made on spontaneous intracerebral hematomas and on blood samples which confirm that extravasated blood clot undergoes a variable degree of retraction which is completed within 6 hr. This suggests that the low attenuation ring in recent hematoma is due to damage caused by the greater volume of the precontracted hemorrhage on the surrounding brain.

CT abnormalities in intracerebral hematomas were studied; features which were useful in distinguishing spontaneous hematomas and those which affected prognosis are discussed.

Author Abstract

Transfemoral selective angiography in the investigation of cerebral ischaemic disease—review of 400 consecutive studies. I. Technique and evaluation of method. *Australas Radiol* 21:31–38, March 1977. II. **Pathological findings.** Palmer FJ, Briscoe PJ, Sorby WA, Barry BP, Williams RM (Prince Henry Hospital, Sydney, Australia). *Australas Radiol* 21:116–121, June 1977

In this two-part series, the authors reviewed 400 consecutive studies. The technique employed was selective four-vessel angiography, in which extracranial arteries were demonstrated in turn by injections of contrast into the innominate, the right and left common carotid, and the left subclavian arteries, by transfemoral selective catheterization. The authors achieved a 95.5% success rate, and found the left carotid artery more difficult to catheterize selectively than the others. Supplementary arch aortography was not required and intracranial carotid studies were not routinely done nor advocated, except to exclude a more distal lesion which would contraindicate operative attack on a proximal lesion. Average time for the study was 40 min. Neurologic complications developed in four patients (1%) with one death (0.25%).

The pathologic findings included arterial occlusions in 37 patients (9.25%), stenosis in 220 patients (55%), and atheromatous plaques (<50% stenosis) in 316 patients (79%). Subclavian steal was found in two patients, both on the left side. No extracranial disease was detected in 84 patients (21%). Sites of disease were analyzed for the different types of lesion.

The authors concluded that selective four-vessel angiography combines ease and safety with excellent demonstration of both extracranial and intracranial arteries, and that it is the method of choice in the investigation of cerebral ischemic disease.

G. Lim

CT scanning in middle fossa arachnoid malformations. Smith RJ, Zacks DJ (University of Alberta Hospital, Edmonton, Alberta, Canada T6G 2B7). *Clin Radiol* 29:161–169, March 1978

The typical appearances of middle fossa arachnoid malformations as seen by computed tomography, are presented in six cases of 3,700 unselected CT scans performed in the preceding 2 years. These lesions have well-defined borders, the anterior border often conforming to the configuration of the greater sphenoid wing, and the posterior border merging into the Sylvian fissure medially. They exhibit the same attenuation coefficients as cerebrospinal fluid, ranging from 0 to +8 EMI units. Their size varies. They produce less mass effect than might be expected, even when their size is considerable. Their appearance does not change after infusion of contrast material. Although arachnoid malformations occur in many intracranial sites, the site of predilection appears to be the middle cranial fossa. The clinical presentation and subsequent management of the six cases is briefly described. The pathogenesis and common clinical presentation associated with these lesions is discussed.

Author Abstract

Spinal cord angiography using 4× magnification. Shiozawa Z, Tanaka Y, Makino N, Sugita K (Division of Radiological Sciences, Institute of Clinical Medicine, University of Tsukuba, Sakura Village, Niihari-Gun, Ibaraki Prefecture 300–31, Japan). *Radiology* 127:181–184, April 1978

Seventeen patients underwent myelography and selective arteriography. Three had cervical lesions, 11 thoracic, and three lumbar. Conventional angiography demonstrated a lesion in 10 of the patients. Lesions included four arteriovenous malformations, two metastatic tumors, a single case of anterior spinal artery syndrome, one vertebral hemangioma, one intramedullary spinal cord tumor, and one vertebral sarcoma.

Selective arteriography of the spinal cord developed by Dichiro and Djindjian is applied in the diagnosis of arteriovenous malformations and hemangioblastoma of the spinal cord. In planning therapy for arteriovenous malformations, whether radical resection, intradural ligation of feeding vessels, or nonsurgical embolization, magnification arteriography will provide otherwise unavailable information. This information consisted of: (1) feeding arteries and draining veins; (2) the course of the radiculomedullary arteries, including the artery of Adamkiewicz; (3) communicating branches; (4) position and course of the anterior spinal artery; (5) pathologic changes of the vessel wall.

Equipment used was autobiased microfocal x-ray tube (0.05 mm). Factors were 120 kVp, 3mA, and 0.1 sec. Film was Fuji Rx-S film and Kyokko MS (medium speed) intensifying screens. Tube was 25 cm from the object and 100 cm from the film yielding 4× magnification ratio. This equipment allowed for fluoroscopy during angiography, and abnormal areas could be selectively magnified with a restricted field of 4 × 4 cm. A Toshiba DRX-89H was used for magnification arteriography and a Toshiba KXO-1000 serial angiography unit with focal spot of 2 mm was used for conventional angiography.

Angiography was performed using the Seldinger technique from the femoral or right axillary artery. A red Kifa catheter

(o.d., 2 mm) with flexible J-shaped tip 2.5–3.0 cm long was utilized. Contrast material was Conray-60. In vessels other than the vertebral artery, 3–4 ml of contrast were injected with spot angiography at 1 sec intervals for 3 sec. If an abnormality was suspected, 7–8 ml were injected with serial angiography performed at two frames/sec for 3 sec and 1 frame/sec up to 15 sec. If an abnormality was revealed, magnification arteriography in the anteroposterior view only was performed. For suspected cervical lesions, bilateral selective vertebral angiography, costocervical arteriography, ascending cervical, first intercostal artery angiography were performed. In suspected thoracic or lumbar lesions, intercostal and lumbar arteries were selectively injected and filmed.

Asher Nov

Computer assisted tomography in primary malignant lymphomas of the brain. Kazner E et al. (Oberarzt Der Neurochirurgischen Klinikim, Klinikim Grosshadern der Ludwig Maximilians-Universitat Muchen, Marchioninistrasse, 15, 8000 Munchen 70, Federal Republic of Germany). *J Computer Assisted Tomography* 2:125–134, April 1978

Analysis by computed tomography of 10 patients with histiologically verified primary malignant lymphomas of the brain is reported. Primary lymphoma nodules in the brain present as slightly increased density nodular masses in scans done without contrast and increase considerably in attenuation after intravenous contrast enhancement. The appearance of nodular lymphomas of the brain in a given case is indistinguishable from that of a meningioma, primary or metastatic malignancy or a pituitary adenoma. However, the blurred margins of many tumor nodules seem to be a useful diagnostic clue for malignant lymphomas, and this may be explained by diffuse infiltration of surrounding tissue with tumor cells. Diffusely growing malignant lymphomas produced completely different CT scan patterns. In these patients, the precontrast scan showed the tumor to represent an area of decreased brain density.

Michael J. Meagher

Foreign body embolization of retinal arteries as a complication of carotid angiography. Nehen AM, Damgarrd-Jensen L, Hansen PE. (Aarhus, Kommune-hospital, University of Aarhus, DK-8000 Aarhus C, Denmark). *Neuroradiology* 15:85–88, April 27, 1978

The authors describe two cases of foreign body embolization of the retinal arteries which occurred during percutaneous carotid angiography. Both patients were female and not artherosclerotic. The patients complained of a partial loss of vision immediately after carotid angiography and in each case a single radiopaque foreign body estimated to be slightly less than 100 microns in diameter was seen within a retinal arteriole. After 9 and 11 months of follow-up only minimal improvement in the visual field defects has been observed. The angiographic technique described is not unusual. The contrast material was transferred from the vial to an open basin via a plastic syringe and disposable needle. A glass syringe with a metal plunger and tip was then used to hand inject contrast through plastic tubing. All components of this system had been vigorously flushed with saline prior to use. Foreign bodies observed were thought to consist of a hard material and the authors thought they might consist of grinding dust from syringe tips. Particles of this order of magnitude are at the limit of unaided vision and are therefore difficult to detect. The reported incidence of embolus to the retinal artery is one tenth of 1% and in most cases consisted of emboli from artheromatous plaques which were usually white or yellow in color. The visual field defects were occasionally reversible but often permanent. The authors recommend immediate ophthalmologic evaluation of any patient complaining of visual distress following angiography and suggest a trial of vasodilators such as amyl nitrite.

Paul M. Chikos

Malignant melanoma metastatic to the central nervous system. Enzmann DR, Kramer R, Norman D, Pollock J (Stanford University Medical Center, Stanford, California 94305). *Radiology* 127:177–180, April 1978

CT appearance of metastatic malignant melanoma is discussed on the basis of the findings in 33 patients: 25 males and eight females. Additional studies performed were radionuclide brain scans in 15 patients and cerebral angiograms in 11. Metastatic sites included: 17 frontal lobe; 15 parietal, eight temporal, seven occipital, and three posterior fossa.

Twenty patients (61%) showed a single metastatis; 12 patients (36%) showed multiple metastases; and one patient showed diffuse subarachnoid spread without parenchymal abnormality. In eight patients (40%), a single lesion showed typical CT appearance of metastasis consisting of round well defined abnormal density focus with surrounding edematous zone. The majority of lesions appeared indistinguishable from primary brain tumors.

When a single lesion was noted on preenhanced scans, generally only that one lesion was seen following enhancement. When multiple lesions were noted, contrast enhancement revealed additional metastatic foci. Lesions appeared as dense abnormal foci which showed homogeneous enhancement following injection of contrast material.

Malignant melanoma is the third most common metastatic tumor to the brain, following lung and breast carcinoma. Differential considerations of a CT appearance suggesting hemorrhagic metastases include lung and renal malignancies, choriocarcinoma, and arteriovenous malformations. Dense peripheral lesions with homogeneous contrast enhancement need to be differentiated from an angioma. Diffuse contrast enhancement of the subarachnoid area may be caused by granulomatous arachnoiditis, subarachnoid hemorrhage, and meningeal carcinomatosis.

Metastatic malignant melanoma to the brain carries a poor prognosis. However, recognition of a surgically removable lesion may prolong survivial very significantly.

Asher Nov

Pediatric Radiology

Hyperalimentation catheter passing into the spinal canal causing temporary paraplegia. McAlister WH, Keating JP, Shackleford GD (Mallinckrodt Institute of Radiology, Washington University School of Medicine, 510 South Kingshighway Boulevard, St. Louis, Missouri 63110). *Pediatr Radiol* 7:119–120, 1978

Hyperalimentation instituted in a 4-month-old female for prolonged diarrhea was associated with fever and decreased use of the lower extremities 5 days after insertion of a polyethylene catheter which was believed to have been in the inferior vena cava near the right atrium. X-rays at the time of paraplegia showed the catheter to lie in the spinal canal. Extradural, retroperitoneal, and pelvic masses of extravasated fluid were present. Following withdrawal of the catheter, there was a gradual return to normal and no neurological defects were seen in the child at 8 years of age. This must be added to the increasing list of complications with intravenous hyperalimentation. Catheter position should be checked in frontal and lateral projections.

B. J. Wood

Computer reconstructed sagittal and coronal CT scans: applications in neurological disorders of infants and children. Maravilla KR, Kirks DR, Maravilla AM (University of Texas Health Science Center, 5323 Harry Hines Boulevard, Dallas, Texas 75235). *Pediatr Radiol* 7:65–69, 1978

Thin-section, nonoverlapping transverse head scans can be reconstructed in sagittal and coronal planes using computer manipulation. More precise information is possible regarding

the nature and extent of the lesions, aiding the surgeon in his approach, and the radiotherapist in treatment planning. The radiation dose for the entire head study by thin-section was 3.4 rads to the skin using Artronix neuro CT scanner.

B. J. Wood

Extragonadal endodermal sinus (yolk sac) tumor. Brasch RC, de Lorimier AA, Herzog RJ, Van Natta FC (University of California, Medical Center, San Francisco, California 94143). *Pediatr Radiol* 7:115–118, 1978

Endodermal sinus tumor is an unusual neoplasm of germ cell origin. Some 80% occur in the ovaries or testes of young adults or children; 20% are extragonadal. It is one of the few malignancies associated with increased levels of alphafetoprotein. The clinical, angiographic, and pathologic features of a retroperitoneal endodermal sinus tumor occurring in a 19-month male are reported.

B. J. Wood

The radiology of neonatal necrotizing enterocolitis. A review of 47 cases and the literature. Daneman A, Woodward S, deSilva M (Hospital for Sick Children, 555 University Avenue, Toronto, Canada). *Pediatr Radiol* 7:70–77, 1978

Forty-seven neonates with necrotizing enterocolitis were reviewed and the radiologic findings assessed. Dilatation of the bowel was found to be the most important early and prognostic sign, being present in more than 90%. The degree of dilatation related with the clinical severity. Intramural gas was seen in 60% and portal venous gas in only five cases. These latter two signs were evanescent and were not felt to be of prognostic significance. Thirty-two cases were treated medically in the acute phase and of these, six died, five developed strictures, and 21 had uneventful courses. Fifteen cases were treated surgically in the acute stage. Of these, seven died. Two of the eight survivors developed strictures. The authors indications for surgery included free air, intraperitoneal fluid, diminished bowel gas with asymmetrical loops, and persistently dilated bowel loops.

B. J. Wood

Diverticula of the bladder in children. Boechat MI, Lebowitz RL (Children's Hospital Medical Center, 300 Longwood Avenue, Boston, Massachusetts 02115). *Pediatr Radiol* 7:22–28, April 1978

Diverticula of the bladder in infants and children are most frequently due to mucosal protrusions through a congenital muscular defect and are primary. Most occur near the ureterovesical junction and may or may not be associated with reflux. Other sites of muscle defects occur less commonly. On voiding cystourethrography, an ectopic ureterocele may be visualized as a diverticulum. The newborn is most apt to have significant morbidity associated with diverticula of the bladder. Secondary types of diverticula are usually due to obstruction associated with valves or with a myelomeningocele. Other causes are: postureteral reimplantation, suprapubic tube site, and fistula remnant after repair of a high imperforate anus. Diverticula also occur with increased frequency in association with other conditions such as absence of the abdominal musculature, kinky hair syndrome, William's syndrome, Ehlers-Danlos syndrome, and cutis laxa. The detection of bladder diverticula depends upon examination by voiding cystourethrography since they are frequently missed on bladder films during excretory urography.

B. J. Wood

Neonatal death dwarfism (report of 17 cases). Kozlowski K (Royal Alexandra Hospital for Children, Sydney, Australia). *Australas Radiol* 21:164–183, June 1977

Seventeen cases of the rarer types of neonatal dwarfism are reported. Newborn chondrodystrophic dwarfism is a field in which radiographic examination is superior to any other single method of investigation and often a definitive diagnosis can be established on the basis of a single radiograph.

Cases for this study came from various parts of Australia and elsewhere. The cases include:

Majewski Syndrome. This is characterised by short limb dwarfism, polydactyly, branchydactyly, narrow thorax, protuberant abdomen, facial, and complex internal abnormalities.

Meckel-Gruber Syndrome. This comprises a triad of occipital encephalocele, polydactyly and cystic kidneys, together with associated features of jaw, feet, and intestinal abnormalities, and shortening of the limbs. This condition would seem to have an autosomal recessive inheritance and resembles trisomy 13.

Homozygous Achondroplasia. This short limb dwarf died shortly after birth in respiratory insufficiency. Both parents suffered from achondroplasia. Radiographic changes were more severe than in achondroplasia and similar to thanatophoric dwarfism, which are more quantitative than qualitative.

Cloverleaf Skull Syndrome. This is an etiologically nonspecific development defect regarded as extreme congenital craniostenosis of the acrocephalic type, with features similar to Crouzon's or Apert's disease or related conditions. It is usually associated with peripheral dysostosis-like changes. In the case reported the axial skeleton and long tubular bones were normal.

Chondrodysplasia punctata. The recessive (rhizomelic type) is much rarer than the dominant type. The prognosis is poor and most children die in the first year of life.

Osteogenesis imperfecta (congenital recessive severe form). The congenital recessive form of osteogenesis imperfecta is a rare, although well recognized type of neonatal dwarfism. It is characterized by a large head, deformed extremities, hypotonia, and blue sclerae. The radiographic findings are diagnostic. The disease is to be differentiated from the lethal form of hypophosphatasia.

Campomelic Dwarfism is characterised by a peculiar facies, narrow thorax, bowing of the long bones with cutaneous dimpling at the site of bowing, deformities of the feet, generalized hypotonia, failure to thrive, and respiratory distress. The rare occasional survivors are mentally retarded.

Achondrogenesis. Several cases of achondrogenesis are described. Achondrogenesis is characterised by short trunk, micromelia, hydropic appearances and death in utero or soon after birth. All of the cases were recessively inherited. The authors believe that there are four well differentiated types of achondrogenesis which can be recognized on radiographic examination alone. These are achondrogensis I, as reported by Parenti and Fraccaro. Achondrogenesis II as delineated by Goard and Kozlowski as "thanatophoric dwarfism II", and achondrogenesis III as reported by Harris et al. as "pseudoachondrogenesis with fractures".

Three cases of neonatal death dwarfism (two of them familial) with some distinct features are reported and a tentative designation of achondrogenesis IV is proposed. The authors regard as unlikely the possibility that achondrogenesis IV may represent different stages or a variant of achondrogenesis I, II, or III.

In every case of lethal neonatal dwarfism, photographs, radiographs, biochemical, histologic, and histochemical studies should be performed. This may help to classify this group of diseases and finally establish the causative biochemical defect.

T. J. Hanks

The value of intravenous pyelogram and micturating cystourethrogram in the newborn. Acton CM (Mercy Maternity Hospital, Melbourne, Australia). *Australas Radiol* 21:156–160, June 1977

The aim of the study was to assess the diagnostic yield from radiologic examination of the urinary tract by micturating cystourethrogram and excretory urography in the newborn population. From 19,377 live births over a 4-year period, 160 newborn infants were studied.

The method of examination was described in detail and the following points are worth noting. In those infants with urinary

tract infection micturating cystourethrogram was not done until 7 days after diagnosis of the infection by suprapubic bladder puncture and appropriate treatment. Solution neomycins 0.3% was used as a base for the contrast medium.

The most common indication for investigation was urinary tract infection accounting for 80% of cases. Other indications included abdominal mass, raised blood urea, and family history of renal disease. Males accounted for 82% of cases. Ages varied, but most were between 2 and 4 weeks of age. No serious complications occurred, only minimal hematuria on a few occasions.

Radiologic abnormalities were present in almost half the cases, justifying the procedures in the newborn period. The commonest abnormality was vesicoureteric reflux and the majority of these were of grade III severity. Follow-up examination of a number of these infants at 6 and 18 months showed that a large proportion had ceased to reflux. Other abnormalities were found in association with reflux, including hydronephrosis in seven cases, although hydronephrosis due to obstruction was also found in five additional cases. The kidney was not visualised in five instances and a pathologic cause was found in each case.

John Branson

Miscellaneous

Detection of subcutaneous metastases by computed tomography. Dunnick N, Schaner E, Doppman J (Clinical Center, National Institutes of Health, Bethesda, Maryland 20014). *J Computed Assisted Tomography* 2:275–279, July 1978

Five patients are described in whom subcutaneous spread of neoplastic disease was demonstrated. One patient had carcinoma of the lung, two patients ovarian carcinoma, and two patients malignant melanoma. All patients demonstrated diffusely disseminated disease. In these patients, body CT scanning allowed initial detection and subsequent repeat measurement of the size of subcutaneous nodules. The CT scan also offered an excellent tool for localization of these lesions for percutaneous or excisional biopsy. Good quality photographs are presented demonstrating the lesions well outlined in subcutaneous fatty tissues.

Michael J. Meagher

Adrenal cortical tumors with low attenuation coefficients equals a pitfall in computed tomography diagnosis. Schaner E, Dunnick N, Doppman J, Strott C, Gill JR, Javadpour N (Clinical Center, National Institutes of Health Building 10, Room 6-S211, Bethesda, Maryland 20014). *J Computer Assisted Tomography* 2:11–15, Jan 1978

The authors state that CT will visualize the left adrenal in 80% of cases, the right in 50% of cases. Lesions as small as 1 cm can be identified with attenuation coefficients similar to liver and kidney (64–80 Houndsfield units). Ten surgically proven adrenal lesions were scanned with a CT 5,000 EMI unit (320 × 320 matrix), six tumors were of density similar to liver or kidney but four tumors had a coefficient markedly lower than surrounding tissues (16–35 HU) and it is suggested that these lesions are high in fat and/or sterol content.

Michael J. Meagher

Nuclear Medicine

A gamma camera method for quantitation of split renal function in children followed for vesicoureteric reflux. Tamminen TE, Riihimaki EJ, Tahti EE (Children's Hospital, University of Helsinki, SF-00290 Helsinki 29, Finalnd). *Pediatr Radiol* 7:78–84, 1978

A method for quantitative estimation of split renal function using a computerized gamma camera system is described. Forty-two children and adolescents with existing or preexisting vesicoureteric reflux and recurrent urinary tract infection were investigated. Total renal clearance of DTPA was calculated with a disappearance curve derived from the largest extrarenal area in the field of view of a gamma camera with diverging collimator. Split renal function was estimated with the slopes of second phase renograms. The plasma disappearance clearance of DTPA, calculated using one compartment model with two late blood samples, gave similar results with the clearance estimated from the body disappearance curves. The proportional planimetric renal parenchymal areas had good correlation with the split clearance estimated from renogram slopes. The method offers data on renal function and urinary tract dynamics which is very valuable in the follow-up of children with recurrent urinary tract infection and vesicoureteric reflux.

Author Abstract

The use of multiple radionuclide scanning in the differentiation of upper abdominal lesions. Andrews JT (Royal Melbourne Hospital, Melbourne, Australia). *Australas Radiol* 2:150–155 June 1977

This study is to evaluate the usefulness of the extension of the reticuloendothelial system liver scan, by a triple or quadruple radionuclide study, in the diagnosis of upper abdominal masses. The value of the study is well established but will not differentiate benign from malignant lesions, therefore, the addition of the blood pool scan will help with diagnostic accuracy and is less traumatic than the hepatic angiogram. The value of the technique is more limited in studying tumors outside the liver substance, and here, the addition of other radionuclides, such as selenomethionine and gallium which may be concentrated in tumors, can be helpful.

All 20 patients in this series presented with upper abdominal problems and were studied on a 7.6 or 12.7 cm crystal Picker Magna-scanner. The scans were thought to be helpful in 17 of the 20 patients, seven having benign and 13 having malignant lesions. Several cases were described and illustrated in detail.

The blood pool scan was found to be at least partially vascular in most of the neoplastic lesions, and avascular in all nonneoplastic conditions, excelt as expected in one case of Osler's disease. The selenomethionine and gallium studies were negative in benign lesions and showed increased uptake in most tumors. The author points out that in most cases a combination of two radionuclides is all that is needed for maximum scan diagnosis.

I. Benn

Book Reviews

Diagnosis of Diseases of the Chest, vols. 1 and 2, 2d ed. By Robert G. Fraser and J. A. Peter Paré. Philadelphia: Saunders, 656 pp. (vol. 1) and 639 pp. (vol. 2), 1977 and 1978,respectively. $26/vol.

A best seller in the early and mid-1970's, the first edition of this work proved invaluable for two reasons: it not only became the standard reference work in chest radiology but also served as an authoritative and readable textbook. The second edition, much revised, will continue this tradition. It has expanded from two to four volumes, the first two of which are currently available; the remaining two are expected shortly. The two available volumes amply fulfill the promise of updating and improvement.

And updated it is. The number of references in these first two volumes totals 6,047, an increase of some 40% over the first edition. Most of this increase is from the literature of the past decade. The second edition, like the first, is a model of a medical reference work.

The new volume 1 covers the normal chest, the spectrum of methods of chest examination, radiologic signs, and congenital diseases. The new volume 2 covers infections, immune diseases, neoplasia, thromboembolism, pulmonary hypertension, and edema. Volume 3 will cover a miscellany of remaining disease categories while volume 4 will feature "decision trees" of differential diagnosis as well as tabular and other ready reference material.

The opening chapter on the normal chest contains much contemporary material on anatomy and physiology; this chapter alone serves as an exemplary monograph. New material, moreover, surfaces in practically all parts of the book, but particularly noteworthy additions and revisions appear on lung biopsy, infections in the immunocompromised host, pulmonary edema, occupational diseases, pulmonary manifestations of drug abuse, airway obstruction, and pulmonary development abnormalities.

Readers should be mindful that, although based on the radiograph principally, this work is an authoritative general diagnostic review in chest disease. Solid clinical material on biochemical, skin, and pulmonary function tests, for instance, will be of use to all physicians involved in chest disease, not just to radiologists. Although long, the text is readily readable. The quality of illustrations ranges from adequate to excellent.

The only problem with the second edition is that it contains such a huge mass of information that the general reader may feel reluctant to turn to page one and just start reading. However, if readers do just that, they will find a marvelously detailed table of contents for the first chapter that will enable them to pick out whatever may be their pleasure. With attention to the tables of contents and appropriate selectivity, any reader can study topics of interest. In the preface, the authors express the worry that the sheer size of this edition will deter the student. It shouldn't.

For such a classic *magnum opus,* the price is quite reasonable. Like the first edition, the second should be on the desk or nearby shelf of every radiologist and physician involved with chest disease.

John H. M. Austin
Columbia-Presbyterian Medical Center
New York, New York 10032

A Guide for Automatic Radiographic Processing and Film Quality Control. By Cynthia C. Kirby, William E.J. McKinney, and Thomas T. Thompson. Chicago: American Society of Radiologic Technologists, 105 pp., 1975. $4

"Radiography begins and ends in the darkroom" is as true today as it was many years ago. The advent of automatic processing held promise of accurate, reproducible developing of x-ray film. The discovery of phenidone and related chemicals heralded the era of 90 sec processing. Yet today we are faced with a recognized problem in radiographic quality, attributable in part to inaccurate and irreproducible film processing.

The cause of inaccurate and irreproducible processing is almost always a lack of knowledge of processor operation, and its limitations. This book, along with its companion 16 video tapes, is the first extensive work which attempts to explain what happens inside the magical box known as an automatic processor. It succeeds admirably.

The book is designed to be used in a classroom situation, but is organized as a self teaching aid. Each chapter is called a "Lesson", and sequentially takes the student through an overview, statement of learning objectives, outline of material, laboratory exercises, and review questions.

The first three lessons provide the background information required for the rest of the book. The next 10 lessons describe the eight subsystems in an automatic processor, indicating how failure of any subsystem affects the resulting radiographs. The final three lessons are perhaps the most useful, giving excellent pointers on trouble-shooting, artifact interpretation, and consistent film quality.

This book, and its companion video tapes, should be included in the training of every radiologic technologist. However, it may be too detailed for the average technologist interested in self-education.

William E. Moore
University of Washington
Seattle, Washington 98195

Atlas of Cardiovascular Nuclear Medicine. Edited by H. W. Strauss, B. Pitt, J. Rouleau, I. K. Bailey, and H. N. Wagner. St. Louis: Mosby, 194 pp., 1977. $42.50

This book is primarily an atlas written by authors who have had a major impact in this field. We are fortunate to share their considerable wealth of experience in thallium myocardial imaging and gated blood pool ventricular function studies.

The book is divided into six sections including the appendix. Chapter one describes the physiological and technical factors related to maximizing image quality, such as selected aspects of thallium kinetics, collimator selection, and patient

positioning. There is an outline of points to consider when reviewing the images obtained. The discussion on equilibrium blood pool imaging includes a description of both first pass and equilibrium techniques including advice on view selection and methods for calculating several indices of ventricular function (including ejection fraction, end-diastolic volume, and end-systolic volume). The discussion on infarct-avid imaging is brief. This 48 page chapter (including references) includes most, if not all of the essential features required to perform thallium and equilibrium blood pool ventricular function studies.

Numerous examples of thallium and gated blood pool studies are included in the second chapter on myocardial infarction. The quality of the figures, as elsewhere in the book, is generally excellent. The format for discussion is a series of patient studies; these are generally well done. Numerous examples are given of the appearance of a thallium defect in each useful view. The ventricular function studies demonstrate the appearance of enlarged chambers, contractile abnormalities, and aneurysms.

The chapter on ischemia begins with a brief summary of the sensitivity and specificity of thallium imaging for detection of coronary disease and ischemia when patients are exercised to maximum on the bicycle. The utility of the test is demonstrated through a number of case studies.

The last two chapters focus on cardiomyopathy and congenital heart disease. In the appendix, the reader is asked patient oriented questions based on an accompanying microfiche slide.

It is difficult to say anything very bad about the book. The title of this atlas may be somewhat misleading in that the focus is primarily on thallium myocardial imaging and the blood pool ventricular function analysis. Infarct avid scanning is mentioned, albeit briefly, and intracardiac shunt detection and quantitation is mentioned only in passing. I have not found thallium imaging helpful in identifying idiopathic hypertrophic subaortic stenosis. The chapter on ischemia would benefit from a list of references. There are a modest number of proofreading errors, primarily in the first chapter. These points are minor, however, and do not appreciably detract from the overall excellent quality of this work. A potential drawback is the price.

This book would be an important addition to the library in every facility practicing cardiovascular nuclear medicine.

Gene B. Trobaugh
Harborview Medical Center
Seattle, Washington 98104

Gallium-67 Imaging. Edited by Paul B. Hoffer, Carlos Beckerman, and Robert E. Henkin. New York: Wiley and Sons, 174pp., 1978. $22

This monograph is an excellent review of the current status of gallium-67 imaging. The book is divided into three main sections which discuss the fundamentals of gallium imaging, the use of gallium in inflammatory disease, and the use of gallium in neoplastic disease.

The first part is on fundamentals and contains sections discussing localization of gallium, imaging technique, and normal patterns of localization. The section on imaging technique by Hoffer is a clear discussion of the many technical factors that go into producing quality gallium images. In addition to discussing factors involved, the section contains practical advice on implementation of suggestions and a description of the types of imaging devices available.

The second part of the book is devoted to the methods of diagnosing inflammatory disease. The excellent introductory section on anatomy and pathology of intraabdominal abcesses is followed by a section on radiographic and ultrasonic methods of diagnosing intraabdominal abcesses, and a section on gallium-67 and the diagnosis of inflammatory disease. The organization of these sections forms a unified presentation of the anatomic-pathologic basis for analysis of the intraabdominal abcesses as well as available techniques to determine their presence. The section on gallium imaging reviews the major causes and common locations of inflammatory disease in the abdomen. There is also an excellent discussion of nonabdominal disease which includes inflammatory disease in the chest, central nervous system, and bones and joints.

The third part of the book, use of gallium in neoplastic disease, is a discussion of the individual diseases starting with malignan lymphoma. This is followed by lung carcinoma, testicular malignancies, childhood malignancies, a miscellaneous section covering hepatoma, melanoma, and leukemia, and finally a section which discusses organ systems in which gallium-67 is of limited use.

This excellent book stresses fundamental principles and practical applications of gallium imaging. Although written by several authors, it is well edited and suffers little from multiple authorship. The printing, illustrations, and image reproduction are all excellent. The only notable absence is a section on general principles. The application of gallium-67 to neoplastic diseases would have served as an excellent introduction to the sections on the individual diseases.

This book should be read by anyone interested in this imaging modality. It would be of use not only to the specialist in nuclear medicine but to other physicians, technologists, and physicists.

G. Donald Frey
Medical University of South Carolina
Charleston, South Carolina 29401

Medical Cyclotrons in Nuclear Medicine. Progress in Nuclear Medicine, vol. 4. 4th Medical Cyclotron Users Conference, Miami Beach, Florida, 1976. Edited by Aldo N. Serafini and Joe E. Beaver. Basel: Karger, 201 pp., 1978. $44

This publication is an outgrowth of the Medical Cyclotron Users Conference held in March 1976. As such, the title of the book is somewhat of a misnomer, in that the conference dealt with the methods of production and chemical separation of radionuclides for use in nuclear medicine, not only by compact "medical" cyclotrons but also at larger research cyclotrons and other particle accelerator facilities.

The production and accessibility of compact medical cyclotrons has made possible the rapidly expanding utilization of diagnostic procedures based on the use of a variety of radiopharmaceuticals. Among these are those which utilize the short-lived positron emitter radioisotopes. Their use is made possible by the recent development of improved positron imaging devices, and their potentials still remain to be realized. Most welcome in this regard is an article by M. Phelps and E. Hoffman on the future role of cyclotrons and positron imaging in nuclear medicine. This article attempts to define some necessary general characteristics of medical cyclotrons and their use in the hospital environment. On the other hand, many new and better radioisotopes are demanded by nuclear medicine techniques

which are not producible with compact cyclotrons, and these must still be produced by the larger research accelerator facilities.

The more than two dozen articles in the book are separated into three categories: (1) Production Aspects; (2) Chemistry Overview; and, (3) Clinical Application of Cyclotron Produced Products. However, this grouping is somewhat arbitrary as the subject matter of many of the articles consists of program overviews at approximately 12 accelerator facilities in North America, and one in England at the Hammersmith Hospital where the radionuclides programs in clinical medicine and medical research run concurrently with a very active neutron radiotherapy program.

Although many of the articles are somewhat repetitive in their scientific content, one does gain some perspective in the current applications of accelerators in nuclear medical research.

Jüri Eenmaa
University of Washington
Seattle, Washington 98195

Soft Tissues of the Extremities. A Radiologic Study of Rheumatic Disease. Comprehensive Manuals in Radiology, vol. 1. By W. J. Weston and D. G. Palmer. New York: Springer-Verlag, 128 pp., 1978. $30

This monograph attempts to pinpoint the early soft tissue changes in rheumatoid disease and represents the combined effort of a radiologist and rheumatologist. Separate chapters discuss the shoulder, elbow, wrist and hand, hip, knee, ankle and tarsus, and foot. Each chapter includes a brief review of the normal radiologic anatomy followed by a description of selected tissue changes related to various pathology including rheumatoid disease. Considerable attention is given to the fat lines and arthrographic demonstration of the bursae surrounding these joints.

Given the title *A Radiologic Study of Rheumatic Disease*, it was somewhat surprising that only about 30% of the text was directly related to rheumatic disease. The chapters are adequately illustrated, but more detailed radiographs and drawings would have been welcomed.

It should be mentioned that the specific changes described by the authors as being secondary to rheumatoid disease are also macroscopically characteristic of other pathologic conditions. Examples are fungal infections, hemophilia, and villonodular synovitis, entities which all produce pathologic proliferations of the synovium. The monograph leads one to conclude that rheumatoid disease is but one capable of producing similar radiographic changes.

This review will be of interest to physicians dealing with soft tissues of the extremities.

Nicole Bolender
University of Washington
Seattle, Washington 98195

Radiology of the Liver, vol. 13 in Saunders Monographs in Clinic Radiology. By James G. McNulty. Philadelphia: Saunders, 437pp., 1977.$27.50

This text briefly deals with normal anatomy and its variation, all aspects of imaging techniques, and appropriate techniques in the diagnosis of liver disorders. The chapters are well organized with a bibliography at the end of each section.

Chapter One briefly reviews normal liver anatomy and its variations.

Chapter Two discusses the various imaging techniques in liver disorders. The tables in this chapter summarize the present day knowledge of indications and usefulness of investigative imaging techniques in various liver and gallbladder disorders.

The remaining chapters deal with pathophysiology, radiologic diagnosis, and the value of other various diagnostic imaging techniques in liver disorders: congenital and hereditary, traumatic, inflammatory, neoplastic, and those related to systemic disease.

This book would make an invaluable addition to medical libraries and radiology departments. I highly recommend this work as a reference to gastroenterologists, radiologists, and radiology residents dealing with liver disorders.

Halappa G. Hakkal
Georgetown University Hospital
Washington, D.C. 20007

Radiologic Examination of the Orohypopharynx and Esophagus. The Barium Swallow. By Constantino Zaino and Thomas C. Beneventano. New York: Springer-Verlag, 317 pp., 1977. $54.80

This is the only current American monograph on diseases of the esophagus and its associated structures, and will replace the only other available book that was written by Brombarts. The authors are well known. Zaino has published *The Pharyngoesophageal Sphincter* in 1970 and also *The Lower Esophageal Vestibular Complex*. These basic works are summarized in this book and help clarify two difficult areas in the radiologic study of the esophagus. Beneventano is well known as a lecturer and his lectures in the American College of Radiology refresher course series are outstanding.

The book provides a good summary of available techniques. There is an excellent chapter on embryology accounting for developmental abnormalities which are frequently seen in clinical practice. The important subject of hiatal insufficiency and hernia is very well covered in 11 pages. The authors stress dynamic studies of the esophagus. One section I found extremely valuable was the check list of observations during and following a barium swallow. It helps make one aware of the careful procedure to follow in examining the esophagus. The term "barium swallow" was used in reference to this check list: a term I dislike because of its rather vague usage to describe either the examination of the esophagus or examination of the esophagus, stomach, and duodenum.

The book is extremely well written and a joy to read and should be in every practicing radiologist's collection.

Leonard Goldberg
272 Roncesvalles Avenue
Toronto, Canada M6R 2M2

Books Received

Receipt of books is acknowledged as a courtesy to the sender. Books that appear of sufficient interest will be reviewed as space permits.

Beyond Malpractice: Compensation for Medical Injuries. A Policy Analysis. Institute of Medicine. DC: National Academy of Sciences, 88 pp., 1978. $6.50

Cancer: A Problem of Developmental Biology. By G. B. Pierce, R. Shikes, L. M. Fink. Englewood Cliffs, N. J.: Prentice-Hall, 242 pp., 1978. $15.95

Cancer Therapy by Hyperthermia and Radiation. Edited by C. Streffer, D. van Beuningen, F. Dietzel, E. Röttinger, J. E. Robinson, E. Scherer, S. Seeber, K.-R. Trott. Baltimore: Urban & Schwarzenberg, 344pp., 1978. $39.50

Cerebral Computed Tomography: A Text-Atlas. By L. A. Weisberg, C. Nice, M. Katz. Philadelphia: Saunders, 337 pp., 1978. $22.50

The Cervical Spine in Trauma. Advanced Exercises in Diagnostic Radiology, vol. 11. 1st ed. By A. J. Gerlock, Jr., S. G. Kirchner, R. M. Heller, J. J. Kaye. Philadelphia: Saunders, 167pp., 1978. $8.95

Clinical Application of Carcinoembryonic Antigen Assay. Proceedings of a Symposium, Nice, Oct. 7–9, 1977. Edited by B. P. Krebs, C. M. Lalanne, M. Schneider. Amsterdam: Excerpta Medica, 501 pp., 1978.$78.25

Competency-Based Curriculum Development in Medical Education: An Introduction. By W. C. McGaghie, A. W. Sajid, G. E. Miller, T. V. Telder. Geneva: World Health Organization, 91 pp., 1978. $4.50

The Diagnostic Limitations of Computerised Axial Tomography. Edited by J. Bories. Berlin: Springer-Verlag, 220 pp., 1978. $27

Environmental Health Criteria 5: Nitrates, Nitrities, and N-Nitroso Compounds. United National Environment Programme and World Health Organization. Geneva: World Health Organization, 107 pp., 1978. $5

Gynecologic Oncology. Edited by L. McGowan. New York: Appleton-Century-Crofts, 435 pp., 1978. $35

An International Neutron Dosimetry Intercomparison. ICRU Report 27. International Commission on Radiation Units and Measurements. DC: ICRU Publications, 54 pp., 1978.

Modern Concepts in Brain Tumor Therapy: Laboratory and Clinical Investigations. NCI Monograph 46. Edited by A. E. Evans. DC: U.S. Government Printing Office, 250 pp., 1977. $8

Myelography, Textbook and Atlas. By I. O. Skalpe, O. Sortland. Oslo: Tanum-Norli, 104 pp., 1978. N. kr. 98

Pain and Profit. The Politics of Malpractice. By S. Law, S. Polan. New York: Harper & Row, 305 pp., 1978. $12.95

Pediatric Radiology. Edited by J. G. Rabinowitz. Philadelphia: Lippincott, 513 pp., 1978. $50

Positioning and Technique Handbook for Radiologic Technologists. By S. B. Conte, D. H. Kemme. St. Louis: Mosby, 265 pp., 1978. $8.95

Prevention and Detection of Cancer. Part I—Prevention. Volume 2—Etiology, Prevention Methods. Edited by H. E. Nieburgs. New York: Marcel Dekker, 1,232 pp., 1978. $62.50

Radiographic Positioning and Related Anatomy, 2d ed. By I. Meschan. Philadelphia: Saunders, 590 pp., 1978. $21.75

Radiologic Exploration of Impotence. By J.-F. Ginestie, A. Romieu. The Hague: Martinus Nijhodf, 134 pp., 1978. 50 guilders

Roentgenologic Anatomy of the Lung. By H. Yamashita. Tokyo: Igaku-Shoin, 389 pp., 1978. $79.50

Steroid Contraception and the Risk of Neoplasia. Report of a WHO Scientific Study Group. Technical Report Series 619. Geneva: World Health Organization, 54 pp., 1978. $3

AJR Reviewers and Abstractors, 1978

The journal acknowledges with special pleasure the work of the following individuals in reviewing manuscripts, selecting and writing abstracts of the literature, and preparing book reviews. The quality of the journal is directly dependent on these valuable contributions. The editors and editorial staff are most sincerely appreciative.

D. Adams
A. Alavi
R. J. Alfidi
T. N. K. Allan
D. Allen
H. Arii
J. K. Aston
C. A. Athanasoulis
H. L. Atkins
J. H. M. Austin
S. P. Axelbaum
R. Baker
H. Baltaxe
M. Baron
R. J. Bartram, Jr.
J. A. Becker
M. H. Becker
J. Bentson
R. M. Berk
H. Berry
N. Blank
D. M. Blaufox
J. D. Blumhagen
N. F. Bolender
J. J. Bookstein
M. L. M. Boone
S. Borden, IV
M. A. Bosniak
W. D. Boswell, Jr
L. Brady
R. T. Bramson
J. Branson
R. L. Bree
B. A. Brill
R. C. Brown
R. F. Brown
J. B. Buchanan
R. E. Buenger
H. Burko
M. Burrell
W. L. Caldwell
M. A. Capitanio
D. H. Carlson
H. Carlson
E. Carlsson
S. R. Carr
S. Carter
W. J. Casarella
G. W. Casarett
A. Chait
A. A. Chambers
C. H. J. Chang
R. L. Chard, Jr.
N. E. Chase
C. Chesnut
P. Chikos
K. Cho
E. E. Christensen
G. M. Christensen
V. P. Chuang
J. L. Clements, Jr.
W. P. Cockshott
G. C. Coggs
C. Cole-Beuglet
W. G. Connor
S. H. Conrad
C. M. Coulam
G. W. Cox
L. Cromwell
A. Crummy
J. J. Cunningham
R. H. Daffner
D. C. Dale
D. B. Darling
A. J. Davidson
K. Davis
J. Denney
R. Dinsmore
G. D. Dodd
M. Donner
J. Doppman
B. Doust
J. S. Dunbar
P. Dure-Smith
W. Eckelman
J. Edeiken
S. Edell
J. Eenmaa
R. L. Egan
K. Ellis
J. Eltringham
R. G. Evens
J. Farman
S. A. Feig
K. Fellows
A. H. Felman
J. Fennessy
F. B. Ferguson, Jr.
J. T. Ferrucci
D. C. Figge
R. A. Filly
H. R. Fishback, Jr.
R. A. Flom
E. Fordham
D. M. Forrester
E. A. Franken
G. Frankl
R. Fraser
R. Frech
P. C. Freeny
R. Freiberger
A. K. Freimanis
G. D. Frey
R. M. Friedenberg
G. W. Friedland
M. Friedman
P. J. Friedman
D. E. Fuller
T. O. Gabrielson
G. Gamsu
G. Gates
B. B. Gay, Jr.
M. I. Gelman
H. K. Genant
A. Gerdes
A. J. Gerlock, Jr.
M. Glickman
R. H. Gold
B. B. Goldberg
H. Goldberg
L. Goldberg
M. E. Goldberg
A. B. Goldman
H. S. Goldman
H. M. Goldstein
L. R. Goodman
B. B. Gosink
A. F. Govoni
C. B. Graham
R. Gramiak
R. Greene
L. D. Greenfield
R. J. Griep
T. W. Griffin
N. T. Griscom
J. H. Grollman
H. G. Hakkal
J. M. Halls
G. Hamilton
G. E. Hanks
D. Harrington
G. B. C. Harris
R. D. Harris
D. Harwood-Nash
R. R. Hattery
V. M. Haughton
T. R. Havrilla
S. M. Hecht
D. Heimbach
E. R. Heitzman
S. Hellman
F. Hendrickson
S. J. Hessel
F. Hipona
P. J. Hodes
L. B. Holman
R. A. Holmes
J. Holt
M. Huckman
R. A. Hyman
K. L. Jackson
H. Jacobson
R. Jaffe
M. Janower
P. S. Jensen
M. L. Johnson
P. M. Johnson
D. Jones
R. F. Jones
H. U. Jüttner
A. R. Kagan
C. R. V. Kamath
J. J. Karo
C. J. Kay
J. Kaye
T. Keats
W. A. Kelly
J. G. Kereiakes
R. Kidd
S. A. Kieffer
F. C. Killien
D. L. King
J. A. Kirkpatrick
D. R. Kirks
M. D. Kiviat
E. C. Klatte
P. R. Koehler
M. Korobkin
J. F. Kotalik
K. L. Krabbenhoft
J. Kurzban
A. F. Lalli
B. Lane
E. F. Lang
M. S. Lapayowker
E. C. Lasser
J. S. Laughlin
R. L. Lebowitz
T. G. Lee
J. C. Leonidas
G. R. Leopold
J. R. LePage
D. C. Levin
S. H. Levitt
J. Li
W. W. Logan
J. W. Loop
E. A. Lyons
N. F. Maklad
M. T. Margolis
R. H. Marshak
W. Martel
J. E. Martin
L. O. Martinez
R. Mazess
J. G. McAfee
B. L. McClennan
R. McLelland
J. J. McCort
M. J. Meagher
F. J. Miller
R. R. Million
D. Moody
W. E. Moore
R. H. Morgan
R. D. Moseley, Jr.
P. Moskowitz
A. Moss
J. Muhm
T. P. Naidich
H. L. Neiman
W. B. Nelp
J. A. Nelson
H. Newmark, III
T. H. Newton
C. Nice
A. Norman
D. Norman
C. H. Northrop
A. Nov
R. A. Novelline
S. B. Novy
M. J. O'Brien
A. E. Oestreich
R. E. O'Mara
S. Order
B. Parker
R. G. Parker
A. G. Peck
R. C. Pfister
L. A. Phillips
N. D. Poe
H. M. Pollack
G. D. Potter
D. G. Potts
A. K. Poznanski
J. A. Purdy
J. Rabinowitz
J. N. Rasey
D. F. Reese
B. J. Reilly
D. Resnick
H. Ricketts
R. Robinson
L. F. Rogers
C. A. Rohrmann, Jr.
F. D. Rollo
N. S. Rosenthal
T. Rudd
C. Rumbaugh
F. Ruzicka
J. Sackett
S. Sagel
W. F. Sample
R. C. Sanders
E. N. Sargent
M. Sarwar
G. R. Scanlon
D. G. Scholl
H. M. Schreiber
R. M. Scott
R. Schulz
W. B. Seaman
R. J. Shalek
J. Shapiro
P. F. Sheedy, II
W. H. Shehadi
S. S. Siegelman
T. M. Silver
P. Simkin
E. B. Singleton
M. L. Skolnick
E. H. Smith
G. Smith
J. Smith
W. M. Smoak
R. Soulen
R. P. Spencer
L. Squire
D. P. Stables
R. J. Stanley
W. B. Steel
E. A. Stevens
G. M. Stevens
J. Storer
R. Strand
M. Takahashi
L. B. Talner
H. Taybi
K. J. W. Taylor
R. N. Taxin
A. W. Templeton
F. Templeton
M. M. Ter-Pogossian
F. D. Thomas
J. R. Thornbury
J. M. Tishler
S. Treves
G. B. Trobaugh
M. Viamonte, Jr.
V. Vix
S. Wallace
W. J. Walls
J. Walter
A. C. Waltman
W. R. Webb
J. F. Weigen
J. P. Whalen
R. I. White
T. T. White
M. H. Wholey
T. R. Whyte
W. Widrich
L. Wiegenstein
W. A. Wilcox
R. H. Wilkinson
F. Winsberg
P. F. Winter
J. Wiot
D. Witten
M. J. Wizenberg
J. N. Wolfe
A. H. Wolson
B. J. Wood
P. Wootton
R. Worsnop
J. S. T. Yao
J. Youker
L. W. Young
H. Yune
C. J. Zylak

News

American Board of Radiology Examinations

Dates have been set for the 1979 and 1980 written and oral examinations given by the American Board of Radiology. The written portion of the examination will be offered at 14 selected sites. All candidates must attend two half-day sessions on Thursday afternoon, June 21 and Friday morning June 22, 1979 or on Thursday afternoon, October 9 and Friday morning October 10, 1980. Deadline for filing for examination in any given year is September 30 of the preceding year.

Beginning in 1979, only one oral examination will be held each year and that examination will be in June. The 1979 examination will be the week of June 11 at the Mariott Hotel in Chicago. The 1980 oral examination will be the week of June 2 at Executive West, Louisville, Kentucky.

Complete details are available from the American Board of Radiology, Kahler East, Rochester, Minnesota 55901; telephone (507) 282-7838.

1979 Midwinter Radiological Conference

The thirty-first annual Midwinter Radiological Conference sponsored by the Los Angeles Radiological Society will be January 26–28. The first day will consist of small workshops in all disciplines while the following two days will be formal lectures and round-table discussions. The second largest radiological technical exhibition the country will be open all days. In addition, an optional 10-day postconference seminar will be in New Zealand, Australia, and Fiji.

Speakers will include: S. Wallace, M. D. Anderson Hospital, Houston; M. A. Meyers, State University, Stonybrook, New York; W. Martel, University of Michigan; D. G. Bragg, University of Utah; R. T. Bergeron, New York University Medical Center; T. F. Meaney, Cleveland Clinic; P. B. Hoffer, Yale University; G. R. Leopold, University of California, San Diego; C. G. Moertel and O. H. Beahrs, both Mayo Clinic; T. L. Phillips, University of California, San Francisco; L. L. Gunderson, Harvard; R. B. Livingston, Veterans Hospital, San Antonio; and H. J. G. Bloom, Royal Marsden Hospital, London, England.

Conference fee is $125; $75 for residents; workshops are $25 each. For advance registration, contact Dr. E. P. Detrick, 4415 Lakeview Canyon Road, Westlake Village, California 91361.

Faculty for the postconvention seminar will be: R. T. Bergeron, W. Martel, T. F. Meaney, plus A. F. Turner, Arcadia (California) Medical Group, and G. Kossoff, Ultrasound Institute, Sydney, Australia.

Dates for the postconvention seminar are January 28–February 9. Cost is $999 per person, including air fare from Los Angeles, transportation between sites, and accommodations. There will be an additional $195 tuition fee per registrant. This seminar will carry 36 hr AMA Category I credit.

AFIP Diagnostic Radiology Seminars

The Armed Forces Institute of Pathology, Washington, D.C., has scheduled four seminar courses in diagnostic radiology. All are designed to offer radiologists a summary of the most important morphologic principles that underlie the evaluation of radiologic signs. Dates and course contents are:

January 8–12, bone and gastrointestinal only; May 7–11, August 27–31, and November 12–16, general courses including bone, chest, gastrointestinal, and genitourinary.

Course fee is $250; $175 for residents with a letter of verification. Military and other federal salaried physicians are exempt from the fee. The seminars carry 35 hr AMA Category I credit.

Faculty will include: J. E. Madewell, J. E. Lichtenstein, W. D. Wehunt, D. S. Hartman, and M. S. Lesar.

Sponsors are the Armed Forces Institute of Pathology, the American College of Radiology, and the American Registry of Pathology.

Nonfederal registration applications may be obtained from: American Registry of Pathology, Attn: Radiologic Pathology Seminars, Armed Forces Institute of Pathology, Washington, D.C. 20306.

Military and other federally salaried physicians should contact: Associate Director for Education, Armed Forces Institute of Pathology (EDZ), Washington, D.C. 20306.

Course Slated for Mexico City

Loyola University of Chicago and the Mexican Society of Radiology have announced a two-part course to be in Mexico City, February 5–8. Part I is Radiology of the Genitourinary System while Part II is Radiology of the Head and Neck. Fee is $200; $100 for residents and fellows with verification. For additional information, contact Dr. R. Moncada, Department of Radiology, Loyola University Medical Center, 2160 South First Avenue, Maywood, Illinois 60153.

Pacific Endocurietherapy Society Meet

The winter meeting of the Pacific Endocurietherapy Society will be December 15–17 in Maui, Hawaii. A total of 12 hr CME Category I credit is available. For information contact: Dr. H. S. Frey, 5522 Sepulveda Boulevard, Van Nuys, California 91411; phone (213) 997-1522.

Radiation Biology in Cancer Research

Radiation Biology in Cancer Research will be the topic of the thirty-second annual Symposium on Fundamental Cancer Research to be in Houston February 27–March 2. Subjects will include responses at low doses; targets and effects; delayed effects in tissues; tissue effects no definitely attributable to cell killing; tumor biology; and potential applications of radiobiology to radiotherapy. Cochairmen are Dr. H. R. Withers and Dr. R. E. Meyn.

For additional information contact S. C. Stuyck, M. D. Anderson Hospital and Tumor Institute, Houston, Texas 77030; telephone (713) 792-3030.

Nuclear Medicine Computer Council Symposium

The annual Society of Nuclear Medicine Computer Council topical symposium will be in Phoenix, Arizona, January 21–22. This year's program will include "state of the art" seminars hosted by the commercial research and development community. The seminars will review operating systems as they support clinical data processing and recent developments in computerized nuclear cardiology.

For further information contact: Dr. D. Gilday, Division of Nuclear Medicine, The Hospital for Sick Children, 555 University Avenue, Toronto M5G 1X8, Ontario, Canada.

AFIP Alumni Course

The radiologic alumni of the Armed Forces Institute of Pathology will host a post-graduate course, Radiologic-Pathologic Concepts in Diagnostic Radiology, March 1–4, 1979 in Deerfield Beach, Florida. The course is designed to be a reunion of AFIP faculty and graduates. Lectures from all organ systems emphasizing radiologic-pathologic correlation will be presented. Faculty includes Doctors Theros, Reeder, Allman, Cavanagh, Korsower, Reed, Olmsted, Madewell, Feigin, and Lichtenstein. The course will be approved for 21 hr AMA Category I Credit. Fee is $275. For registration and information, contact Dr. W. W. Olmsted, Radiologic Alumni of AFIP, Box 34847, West Bethesda, Maryland 20034.

Clinical Advances in CT

The Computerized Tomography Society will hold its third annual seminar, Clinical Advances in CT, March 10 and 11, near Washington, D.C. Application is being made for AMA credit and American Association of Family Physicians credit. Registration is limited to 250. For further information, write Mrs. B. Mossman, National Biomedical Research Foundation, Georgetown University Medical Center, 3900 Reservoir Road, N.W., Washington, D.C. 20007; phone (202) 625-2121.

Big Sky Radiology Conference

The third annual Big Sky Radiology Conference will be February 6–9 in Big Sky, Montana. The course is approved for 18 hr AMA Category I credit. Fees are $150; $75 for residents with verification.

Conference format will be a combination of didactic lectures and a self-study series. General subject areas will be head and body computed tomography, pediatrics, bone and joint, neuroradiology, and ultrasound. Sessions will be scheduled to allow adequate time for recreational activities.

Faculty will be: J. Edeiken, Thomas Jefferson University; C. Fagan and L. E. Swischuk, both University of Texas, Galveston; D. C. Harwood-Nash, Hospital for Sick Children, Toronto, Canada; D. H. Stephens, Mayo Clinic; and V. B. Graves, conference chairman, Great Falls, Montana.

For information, contact: Dr. V. Graves, Department of Radiology, Columbus Hospital, P. O. Box 5013, Great Falls, Montana 59403.

Canadian Radiologists Annual Meeting

The forty-second annual meeting of the Canadian Association of Radiologists will be in Vancouver, Canada, June 24–28. This will be a combined meeting with the medical and biological sections of the Canadian Association of Physicists. The diagnostic program will include a categorical refresher course in ultrasound, refresher courses in general diagnostic radiology, and proferred papers in all aspects of diagnostic radiology. Application has been made for Category I AMA approval.

The radiation oncology program will feature a symposium on Charged Particle Therapy with international speakers and a trans Canada review of 3,000 patients with carcinoma of the larynx. The Gordon Richards Memorial Lecture will be given by Dr. Harold E. Johns.

Postconvention tours are available to Alaska, Hawaii, and the Canadian Rockies.

For further information contact Alva Pentecost, executive secretary, Canadian Association of Radiologists, Suite 806, 1440 Ste. Catherine Street West, Montreal, Quebec, Canada, H3G 1R8. Telephone (514) 866-2035.

Multidisciplinary Aspects of Brain Tumor Therapy

A 3-day conference on all aspects of experimental and clinical brain tumor therapy will be June 8–10 in Lake Garda, Italy. Cochairmen are Professor P. Paoletti and Dr. M. D. Walker. This conference will include major sections on Experimental Brain Tumors, The Biology and Diagnosis of Brain Tumor, Principles of Therapy, and Current Therapeutic Studies. In addition there will be a day devoted to free communications. Purpose is to provide the most recent information available from both experimental laboratories and clinical investigations and includes the specialities of neurooncology, neurology, neuropathology, neurosurgery, radiotherapy, and neurodiagnostics. Deadline for submission of a 200 word abstract of new data (not previously presented) is January 15.

Abstracts or requests for additional information should be sent to: Dr. M. D. Walker, National Cancer Institute, 31/4B32, Bethesda, Maryland 20014.

Radiology of Bone and Chest Diseases

Radiology of Bone and Chest Disease with Emphasis on Radiologic-Pathologic Correlation is a seminar scheduled for April 23–27 in San Diego. The course is divided into a half week each of bone and chest diseases and is designed to broaden the skills of radiologists, pathologists, and clinicians. Sponsors are the San Diego Radiology Research and Education Foundation and the American College of Radiology.

Program director is D. S. Feigin and guest faculty include: J. E. Madewell, Armed Forces Institute of Pathology, and E. G. Theros, University of California, Los Angeles. Faculty from the University of California, San Diego, will include: D. S. Feigin, P. J. Friedman, C. B. Higgins, G. D. Greenway, and D. L. Resnick.

Fee is $300; $125 for residents and interns. The program carries 34 hr AMA Category I credit. For those participating in a half-week session, fee is $200; $75 for residents and interns with 17 hr AMA Category I credit.

For registration and information, contact: M. J. Ryals, Radiology, P. O. Box 2305, La Jolla, California 92038; telephone (714) 453-7500, extension 3711.

Radiology of the Chest

The Department of Radiology, Duke University Medical Center, will present its seventh annual tutorial postgraduate course, Radiology of the Chest, April 2–6 in Durham, North Carolina. C. E. Putman is program chairman.

All facets of chest disease will be covered including diagnostic techniques. A detailed abstract book with references will be provided.

Guest faculty will be: R. E. Coleman, Salt Lake City, R. G. Fraser, Birmingham, Alabama; E. R. Heitzman, Syracuse, New York; T. C. McLoud, Boston; and F. S. Stitik, Baltimore. Faculty from Duke University will be: J. T. T. Chen, E. L. Effman, R. McLelland, D. F. Merten, P. C. Pratt, C E. Putman, C. E. Ravin, J. C. Reed, H. A. Saltzman, H. O. Sieker, and W. G. Young.

A total of 30 hr AMA Category I credit will be available.

For additional information, contact: Dr. R. McLelland, Radiology-Box 3808, Duke University Medical Center, Durham, North Carolina 27710; telephone (919) 684-4397.

Skeletal Radiology Course

A Skeletal Radiology Postgraduate Course, sponsored by Albert Einstein College of Medicine, will be May 14–18 in New York City. Additional information is available from Miss R.

Ditizio, coordinating secretary, Radiology Department, Jacobi Hospital, Room 4N21, Pelham Parkway and Eastchester Road, Bronx, New York 10461.

Controversies in Radiology and Medicine

Controversies and Advances in Radiology and Medicine is a postgraduate course started for March 4–9 at Smugglers' Notch Ski Area, Jeffersonville, Vermont. Tufts University School of Medicine is sponsor. The course is designed for internists, surgeons, and radiologists. Major topics will be: Lung Cancer Today; Atherosclerosis: Abdominal Aortic and Peripheral Arterial Disease Update; Venous Thrombosis and Embolism; and Imaging and Intervention in the Septic Patient. A total of 26 hr AMA Category I credit is available. Fees are $200; $125 for residents.

Additional information may be obtained from Office of Continuing Education, Tufts University School of Medicine, 136 Harrison Avenue, Boston, Massachusetts 02111; telephone (617) 956-6579.

General Diagnostic Radiology

The Department of Radiology of Southwestern Medical School, University of Texas Health Science Center at Dallas, is offering a diagnostic radiology seminar, February 15–17 in Dallas. Program director is K. R. Maravilla.

Guest faculty will include: G. Dodd, University of Texas Health Science Center, Houston; R. Freiberger, Cornell University; J. G. Rabinowitz, Mount Sinai School of Medicine.

Faculty from Southwestern Medical School will be: J. Reynolds, E. E. Christensen, T. S. Curry, III, G. C. Curry, A. M. K. Maravilla, K. R. Maravilla, M. Conrad, J. T. Diehl, G. W. Dietz, R. W. Parkey, R. H. Epstein, W. Kilman, M. J. Landay, B. Ellman, M. Gordon, H. Chapa, S. E. Lewis, and G. Currarino.

A total of 20 hr AMA Category I credit is available. Fee is $250.

For information contact: L. L. Wooldrige, Administrative Coordinator, Department of Radiology, Southwestern Medical School, 5323 Harry Hines Boulevard, Dallas, Texas 75235; phone (214) 638-1800, extension 2613.

Spring Physics Seminar

The Southern California Chapter, American Association of Physicists in Medicine, will host its annual Spring Seminar, April 23–25 in Las Vegas. The program will include tutorial sessions plus contributed papers. Tutorial sessions will cover diagnostic imaging (three sessions); cardiac imaging and physiologic data extraction (four sessions); and quality assurance in radiation therapy (four sessions). Continuing Medical Education credit will be available. Information is available from Dr. N. A. Baily, Department of Radiology, 5046 Basic Sciences Building, M010, University of California at San Diego, La Jolla, California 92093.

Nuclear Radiology Workshop

A Nuclear Radiology Workshop will be May 4 and 5 at the University of Michigan, Ann Arbor. Approximately 11 hr AMA Category I credit will be available. For additional information, write: Department of Postgraduate Medicine and Health Professions Education, University of Michigan Medical School, Towsley Center for Continuing Medical Education, Ann Arbor, Michigan 48109.

Diagnostic Ultrasound Course

The Johns Hopkins Medical Institutions Department of Radiology and Nuclear Medicine is presenting a 5-day course, Advanced Practicum in Diagnostic Ultrasound, December 11–15. This course is designed for the practicing ultrasonographer. There will be morning didactic lectures, demonstrations, question and answer periods, and afternoon practical experience in gray scale, B-scan and real time scanning. Fee is $400. AMA Category I credit is available. Enrollment is limited to 20 students. Also available are basic courses for the novice ultrasonographer, held at 2 month intervals. For information contact Dr. R. C. Sanders, Department of Radiology Ultrasound Laboratory, Johns Hopkins Hospital, Baltimore, Maryland 21205; telephone (301) 955-8450.

Ultrasound Seminar

The Division of Ultrasound, Hoag Memorial Hospital, Newport Beach, California, announces its Second Annual Advanced Techniques Seminar will be January 6. Registrants should have prior scanning experience and basic anatomic knowledge. No scanning will be done at the seminar. Speakers will include: E. I. Miller and R. H. Thomas, both Hoag Memorial Hospital; L. Scharzman, University Hospital, San Diego; J. Forsythe, La Jolla Veterans Hospital; R. Clark, UCLA Center for the Health Sciences; and P. Lines and H. Bussey, both Picker Corporation.

The program carries 6 hr continuing education credit. Information is available from: Advanced Techniques Seminar, P. O. Box 7205, Newport Beach, California 92663.

Meeting and Course Review

For reader convenience, a summary of upcoming meetings and courses is provided. Detailed listings of these events appeared in journal issues indicated in parentheses.

CT in Radiotherapy, workshop, March 28–30, Geneva, Switzerland (June).

Courses in Ultrasound, two 8-week postgraduate courses beginning January 8 and April 2, respectively, Winston-Salem, North Carolina (July).

General Diagnostic Radiology, course, February 5–9, Puerto Rico (July).

Adjuvant Therapy of Cancer, conference, March 28–31, Tucson (July).

CT, Ultrasound, Nuclear Medicine in Pediatrics, symposium, January 18–20, Orlando, Florida (September).

Body CT Course, February 26–March 1, San Diego (September).

Current Concepts in Diagnostic Radiology, course, February 12–16, Acapulco, Mexico (September).

Computed Tomography, Ultrasound, and X-ray, course, January 29–February 2, San Francisco (September).

Two Courses: Snowbird and Park City, January 28–February 3, Snowbird, Utah, and February 24–March 3, Park City Ski Resort, Utah (September).

National Conference on Breast Cancer, March 4–9, Atlanta (October).

XII Interamerican Congress of Radiology, July–August 1979, Quito, Ecuador (October).

Sixth Congress of Radiation Research, May 13–19, Tokyo (October).

Noninvasive Imaging in Medicine, symposium, June 6–9, Lund, Sweden (October).

Conferences on Medical and Biological Engineering and Medical Physics, August 19–24, Jerusalem (October).

L. H. Gray Conference, September 10–14, Cambridge, England (October).

Asian Oceanian Congress of Radiology, October 28–November 3, 1979, Singapore (October).

Diagnostic and Therapeutic Angiography, course, March 21–25, Puerto Rico (October).

Research Training Fellowships, deadline January 31, International Agency for Research on Cancer (October).

Diagnostic Ultrasound Preceptor Training Programs, San Diego, one month programs (October).

Double Contrast Techniques in GI Radiology, seminar, March 8–10, Philadelphia (November).

Diagnostic Ultrasound Courses, series, Philadelphia (November).

Skeletal Symposium, January 20–26, Sun Valley, Idaho (November).

Abdominal Real Time Sonography Courses, March 12–16, June 11–15, July 16–20, August 6–10, December 9–13, 1979, Winston-Salem, North Carolina (November).

LSU Diagnostic Radiology Seminar, March 15–17, New Orleans (November).

Aspen Uroradiology Seminar, February 18–23, Aspen, Colorado (November).

Fleischner Society Ninth Symposium (and course), June 11–13, Stockholm, (November).

Practical Advances in Diagnostic Radiology IV, course, January 13–22, Carribean cruise (November).

Musculoskeletal Course and Cruise, April 28–May 5, Carribean (November).

CT, Ultrasound, and X-ray, course, January 29–February 2, San Francisco (November).

Diagnostic Radiology Course, March 12–16, San Francisco (November).

International Symposium and Course on CT, April 16–20, Las Vegas (November).

Gastrointestinal Radiology, Update '79, seminar, March 9–11, San Diego (November).

Selected Topics in Neuroradiology, seminar, February 7–9, San Diego (November).

European Cardiovascular Radiology Congress, May 3–5, Nuremberg, West Germany (November).

LA Bone and Joint Conference, continuing once monthly course, Los Angeles, (November).

Diagnostic Ultrasound Seminar, April 21 and 22, New York City (November).

San Diego Postgraduate Courses, 1 and 2-week programs (November).

San Francisco Cancer Symposium, March 23 and 24 (November).

October Figure Quality

I have just received the October issue of AJR and I am upset with the quality of illustration reproduction in the paper by Greenfield et al., 131:651–655. The quality of the original prints was good, but the end product detracts from the message we wished to transmit.

Christos A. Athanasoulis
Section of Vascular Radiology
Massachusetts General Hospital
Boston, Massachusetts 02114

Reply

The Editorial Office shares Dr. Athanasoulis's disappointment with the quality of illustrations in the October issue. Many were far from the quality it seeks and, in fact, quite dissimilar to intermediate prints that indicated satisfactory end results. AJR's printer, Waverly Press, is investigating the problem. We will not cease in our efforts to carry illustrations that do justice to the author's material and his expectations.

MMF

Summary of American Roentgen Ray Society 1979 Meeting

March 25–30, Sheraton Centre, Toronto, Canada

A description of the meeting including a comprehensive listing of courses and information on the Categorical Course on Neuroradiology, appeared in the October issue of AJR. For reader convenience, **the complete packet of colored registration forms appears in both the October and November AJR issues.** Included are: meeting registration forms backed by the course registration form, hotel reservations, spouses' program and forms for the tennis tournament and social evening.

In the February issue, AJR will list the papers and exhibits scheduled for presentation during the scientific sessions of the ARRS and SPIE.

Accreditation

All courses meet the criteria for AMA Category I credit.

Meeting Format

Scientific Program. Sessions will be during the latter half of each morning, Monday–Friday, as well as Tuesday and Thursday afternoons. Papers will be grouped by topic and parallel scientific sessions will be held.

Refresher Courses. A full scope of courses will be offered on Monday and Wednesday afternoons and Tuesday, Thursday, and Friday mornings.

Categorical Course on Neuroradiology. This 15 hr course will begin on Sunday, March 25, and continue through Friday, March 30 (except on Wednesday).

Caldwell Lecture. Dr. Joseph Whalen will deliver this prestigious address on Wednesday morning, March 28.

Exhibits

Scientific exhibits will be open on Sunday, March 25, from 7–11 p.m., 7 a.m.–11 p.m. on Monday through Thursday, and 7 a.m. to 1 p.m. on Friday. Technical exhibits will be open from 9 a.m. to 5:30 p.m., Monday through Thursday, and 9 a.m. to 1 p.m. on Friday.

Other Society Meetings

The Society for Pediatric Radiology will meet March 24 and 25. A joint program with ARRS is planned for the morning on March 26. The Society for Photo-Optical Instrumentation Engineers will meet March 25 and 26, and a joint program with this group is anticipated on March 27. The American Thermographic Society will meet March 29–April 1.

Local Activities

Spouses' Program. On March 26, a theater tour and luncheon are scheduled; March 27 features a walk through a maple woods or a bus tour of downtown Toronto. Both groups meet for lunch before visiting "the most Canadian art gallery". On March 28, a day-long tour to Niagara Falls is scheduled with time for shopping. A fashion show and brunch will be March 29. Meals are included in tour prices (Canadian funds) which are listed on the registration form. No receipts or confirmations will be mailed. All tickets and badges should be picked up at the Spouses' Registration Desk, Sheraton Centre Hotel.

Tennis Tournament. March 28 at Mayfair Racquet Club, Downsview, Ontario. Schedule: bus transportation from Sheraton Centre, 11:45 a.m.; luncheon; play; cocktails; trophy presentation; return to hotel, 6:30 p.m. Play is limited to 48. To register, see form.

Golf Tournament. Cancelled this year

Social Evening at Ontario Place. Thursday, March 29, buffet supper at 7:45 p.m. following a happy hour. Film, North of Superior, will follow. Busses will leave Sheraton Centre at 6:30 p.m., return approximately 10 p.m. Tickets are $16.50 (Canadian funds) and will be held at the Spouses' Registration Desk. To register, send form with check (payable to ARRS Dinner).

Meeting Registration

Preregistration by mail will be accepted until March 1 (see form). Late registrants may register on site. Official badges and program booklets will be available at the registration desk, Four Seasons Sheraton Hotel. No registration confirmations will be made.

Course Registration

Register early, enrollment is limited. Registrants should list first, second, and third choices for each period unless they take the categorical course. **Registration in categorical course fills all course time and precludes registration in other courses.** All ticket orders will be filled according to postmark. Fees: $25 for all who take categorical course; other courses, no fee to ARRS members, $3 per course for nonmembers. Payment must accompany instruction order sheet. If enrolling late, send form to Dr. Gedgaudas, Four Seasons Sheraton Hotel, 123 Queen Street West, Toronto, Ontario, Canada. Make checks payable to American Roentgen Ray Society.

Hotel Registration

Reservations will be handled by the ARRS Housing Bureau in Toronto (see form) and must be made by February 25. Participating hotels, prices, and a map are on form.

Fees

Meeting:	
ARRS members	No fee
Nonmembers	$25
Physicians in training (with verification)	15
Courses:	
Categorical course, for all who enroll	25
Other courses, ARRS members	0
Other courses, nonmembers, per course	3

Cancellations and Fee Refund

Course fees will be refunded only if cancellations are received before March 20. Cancellations should be sent to ARRS, 20 North Wacker Drive, Chicago, Illinois 60606.

Radiologic Societies

International Societies

Fleischner Society. Secretary K. Ellis, Columbia-Presbyterian Medical Center, 622 West 168th St, New York, NY 10032
Inter-American College of Radiology. Secretary, G. Morillo, Dept Radiology, Jackson Memorial Hospital, 1611 NW 12th Ave, Miami, FL 33136
International Commission on Radiological Protection. Secretariat, F. D. Sowby, Clifton Ave, Sutton, Surrey SM2 5PU, England
International Skeletal Society. Secretary-Treasurer, J. Edeiken, Radiology Dept, Thomas Jefferson University Hospital, 11th and Walnut Sts, Philadelphia, PA 19107
International Society of Radiology. Hon. Secretary-Treasurer, W. A. Fuchs, Dept of Diagnostic Radiology, University Hospital, Inselspital, CH-3010 Bern, Switzerland

U.S. National Societies

American Association of Physicists in Medicine. Secretary, J. Wright, Radiology Dept, Geisinger Medical Center, Danville, PA 17821
American Board of Radiology. Secretary, C. A. Good, Kahler East, Rochester, MN 55901
American College of Radiology. Executive Director, W. C. Stronach, 20 N Wacker Drive, Chicago, IL 60606. Annual meetings: 1979, Sept 16–20, Chicago, IL; 1980, Sept 21–25, New Orleans, LA
American Institute of Ultrasound in Medicine. Executive Secretary, D. LaMaster, PO Box 25065, Oklahoma City, OK 73125. Annual meetings: 1979, Aug 23–31, Montreal. Spring educational meetings: 1978, April 4–9, Puerto Rico; 1979, Feb 23–March 3, Lake Tahoe; 1980, March 1–6, Hilton Head
American Nuclear Society. Program Chairman, T. D. Tarr, U.S. Energy Research and Development Administration Mail Station A-436 Office of Assistant Administrator for Nuclear Energy, Washington, DC 20545
American Radium Society. Business office: N. V. Jordan, Office of the Secretariat, c/o M. D. Anderson Hospital, 6723 Bertner Drive, Houston, TX 77030. Annual meetings: 1979, March 4–8, Los Angeles; 1980, April 27–May 1, Philadelphia
American Roentgen Ray Society. Secretary, J. F. Martin, 300 S Hawthorne Rd. Winston-Salem, NC 27103. Annual meetings: 1979, March 25–30, Toronto; 1980, April 22–25, Las Vegas; 1981, March 24–27, San Francisco
American Society of Neuroradiology. Secretary, T. El Gammel, Medical College of Georgia, Augusta, GA 30902. Annual meeting: May 20–24, 1979, Toronto
American Society of Therapeutic Radiologists. Secretary, W. J. Taylor 1100 9th Ave, Seattle, WA 98101. Annual meeting: 1979, Oct 23–27, New Orleans
American Thermographic Society. Executive Director, N. M. Oldfield, PO Box 2055, Gaithersburg, MD 20760
Association of University Radiologists. Secretary-Treasurer, J. R. Thornbury, University of Michigan, Ann Arbor, MI 48109. Annual meeting: 1979, May 6–10, Rochester, NY
Health Physics Society. Executive Secretary, R. J. Burk Jr, 4720 Montgomery Lane, Bethesda, MD 20014
National Medical Association. Secretary, E. Mapp, Episcopal Hospital, Philadelphia, PA 19148
North American Society of Cardiac Radiology. Secretary-Treasurer, E. Carlsson, University of California, San Francisco, CA 94143
Radiation Research Society. Executive Director, R. J. Burk Jr. 4720 Montgomery Lane, Bethesda, MD 20014
Radiological Society of North America, Inc. Secretary, T. A. Tristan, Fifteenth Floor, One MONY Plaza, Syracuse, NY 13202. Annual meeting: 1978, Nov 26–Dec 1, Chicago; 1979, Nov 25–30, Atlanta, GA; 1980, Nov 16–21, Dallas, TX
Section on Radiology, American Medical Association. Secretary, A. Raventos, Dept Radiology, School of Medicine, University of California, Davis
Society of Cardiovascular Radiology. Secretary-Treasurer, W. J. Casarella. Columbia-Presbyterian Medical Center, New York, NY 10032
Society of Chairmen of Academic Radiology Departments. Secretary-Treasurer, D. Bragg, University of Utah, Salt Lake City, UT 84132
Society of Gastrointestinal Radiologists. Secretary-Treasurer, R. Berk, University Hospital, San Diego, CA 92103
Society of Nuclear Medicine. President, 475 Park Avenue S, New York, NY 10016
Society for Pediatric Radiology. Secretary, B. P. Wood, University of Rochester Medical Center, 601 Elmwood Ave, Rochester, NY 14642
Society of Photooptical Instrumentation Engineers. Secretary, A. H. Gott, Aerospace Corp. PO Box 92957, Los Angeles, CA 90009.
Society of Uroradiology. Secretary-Treasurer, R. C. Pfister, Massachusetts General Hospital, Boston, MA 02114

U.S. State and Local Societies

ALABAMA
Alabama Academy of Radiology. Secretary-Treasurer, J. L. Wayland, 401 West College St, Florence, AL 35630
Section of Radiology, National Medical Association. Secretary, I. Brooks, Dept. Radiology, Veterans Administration Hospital, PO Box 51[illegible], Tuskegee, AL 36083
Southern Radiological Conference. Secretary-Treasurer, J. W. Maxwell, PO Box 2144, Mobile, AL 36601

ALASKA
Alaska Radiological Society. Chapter ACR. Secretary-Treasurer, J. J. Kottra, 3200 Providence Ave, Anchorage, AK 99504

ARKANSAS
Arkansas Chapter of ACR. Secretary-Treasurer, J. A. Gill, PO Box 1827, Fort Smith, AR 72902

ARIZONA
Arizona Radiological Society. Chapter of ACR. Secretary, A. Newman, PO Box 5099, Phoenix, AZ 85010

CALIFORNIA
California Radiological Society, California Chapter of ACR. Executive Secretary, J. M. Allen, 1225 8th St, Suite 590, Sacramento, CA 95814
East Bay Radiological Society. Secretary-Treasurer, J. J. Branscom, PO Box 175, Alamo, CA 94507
Los Angeles Radiological Society. Secretary J. E. Scallon. South Bay Hospital, 514 N Prospect, Redondo Beach, CA 90277
Northern California Radiological Society. Secretary-Treasurer, V. C. Poirier, Mercy San Juan Hospital, 6501 Coyle Ave, Carmichael, CA 95608
Northern California Radiotherapy Association. Secretary-Treasurer, J. D. Earle, Stanford Medical Center, Stanford, CA 94305
Orange County Radiological Society. R. L. Argue, 100 E Valencia Mesa Dr, Fullerton, CA 93632
Radiological Society of Southern California. Secretary-Treasurer, D. E. Blickenstaff. La Jolla Radiology Medical Group, 7849 Fay Ave, La Jolla, CA 92037
Redwood Empire Radiological Society. Secretary, H. B. Peterson, 357 Perkins St, Sonoma, CA 95476
San Diego Radiological Society. President, D. J. Fleischli, 7849 Fay Ave, La Jolla, CA 92037
San Francisco Radiological Society. Secretary-Treasurer, P. A. Brodey, Dept Radiology, Mount Zion Hospital, San Francisco, CA 94115
South Bay Radiological Society. Secretary, R. Wirtz, Redwood Medical Clinic, 2900 Whipple Ave, Redwood City, CA 94062
South Coast Radiological Society Chapter of ACR. Secretary-Treasurer, B. R. Schnier, Dept of Radiology, Cottage Hospital, Pueblo at Bath, Santa Barbara, CA 93105
Southern California Radiation Therapy Society. Secretary-Treasurer, J. Stuhlborg, 514 N Prospect, Redondo Beach, CA 90277
Western Neuroradiological Society. Secretary-Treasurer, A. N. Hasso, Loma Linda University Medical Center, Loma Linda, CA 92354

COLORADO
Colorado Radiological Society. Secretary, P. Danner, St. Anthony Hospital, Denver, CO 80204
Rocky Mountain Radiological Society. Secretary-Treasurer. J. M. Grogan, 4200 E 9th Ave, Denver, CO 80206. Annual meeting: Aug 16–18, 1979, Denver

CONNECTICUT
Connecticut Valley Radiologic Society. Secretary-Treasurer G. N. LaPierre, 759 Chestnut St, Springfield, MA 01107
Radiological Society of Connecticut, Inc. Secretary, E. F. Fox, 300 Main St, Briston, CT 06010

DELAWARE
Delaware Chapter of ACR. Secretary, E. S. Schubert, Wilmington Medical Center, PO Box 1951, Wilmington, DE 19899

DISTRICT OF COLUMBIA
Section on Radiology, Medical Society of the District of Columbia. Secretary-Treasurer, A. M. Zelna, 21 Masters St, Potomac, MD 20854

FLORIDA
The Florida Radiological Society, Chapter of ACR. Secretary, S. H. Sarasohn, PO Box, 610544, North Miami, FL 33161
The Florida West Coast Radiological Society, Inc. Secretary-Treasurer, M. Silbiger, 1 Davis Blvd, Suite 103, Tampa, FL 33606
Greater Miami Radiological Society. Secretary, J. A. Schneider, 1131 N 35 Ave, Hollywood, FL 33021
North Florida Radiological Society. Secretary, C. E. Bender, 1430 16th Ave S, Jacksonville Beach, FL 32250
Northeast Florida Radiological Society. Secretary, O. L. Jeter Jr, Orange Park Community Hospital, Orange Park, FL 32073

GEORGIA
Atlanta Radiological Society. Secretary-Treasurer, J. H. Larose, Dept Nuclear Medicine, South Fulton Hospital, East Point, GA 30344
Georgia Radiological Society. Chapter of ACR. Secretary, T. Vanderzalm, Medical College of Georgia, Augusta, GA 30902

HAWAII
Hawaii Radiological Society, Chapter of ACR. Secretary-Treasurer, M. Meagher, 1301 Punchbowl St, Honolulu, HI 96808

ILLINOIS
Chicago Radiological Society, Division of the Illinois Radiological Society, Chapter of ACR. Secretary-Treasurer, H. J. Lasky, 55 E Washington St. Suite 1735, Chicago, IL 60602
Illinois Radiological Society, Inc, Chapter of ACR. Secretary, R. D. Dooley, Hinsdale Medical Center, Hinsdale, IL 60521

INDIANA
Indiana Roentgen Society of ACR. Secretary, W. S. Tirman, 919 Jefferson Blvd, South Bend, IN 46617
Tri-State Radiological Society. Secretary, T. Harmon, St. Mary's Hospital, Evansville, IN 47750

IOWA
Iowa Radiological Society, Chapter of ACR. Secretary-Treasurer, D. L. Roberson, 1948 First Ave NE, Cedar Rapids, IA 52402

KANSAS
Kansas Radiological Society, Chapter of ACR. Secretary-Treasurer, R. H. Baehr, 310 Medical Arts Bldg, Topeka, KA 66604

KENTUCKY
Bluegrass Radiological Society. Secretary-Treasurer, J. King, 3313 Overbrook Dr, Lexington, KY 40504
Kentucky Chapter of ACR. Secretary-Treasurer, A. Lieber, University of Kentucky Medical Center, Lexington, KY 40506

LOUISIANA
Ark-La-Tex Radiological Society. Secretary, E. K. Lang, LSU School of Medicine, Shreveport, LA 71101
Louisiana Radiological Society, Chapter ACR. Secretary-Treasurer, S. L. Smith, 250 Vincent Ave, Metairie, LA 70005
Louisiana-Texas Gulf Coast Radiological Society. Secretary-Treasurer, J. Romero III, PO Box 3146, Lake Charles, LA 70602
Section on Radiology, Southern Medical Association. Secretary, M. Sullivan, 1514 Jefferson Highway, New Orleans, LA 70121

MAINE
Maine Radiological Society, Chapter of ACR. Secretary-Treasurer, P. E. Giustra. Penobsot Bay Medical Center, Rockland, ME 04841.

MARYLAND
Maryland Radiological Society, Chapter of ACR. Secretary, S. M. Goldman, Sinai Hospital of Baltimore, Belvedere at Greenspring Avenues, Baltimore, MD 21215

MASSACHUSETTS
Massachusetts Radiological Society, Chapter of ACR. Secretary, A. H. Robbins, 150 S Huntington Ave, Boston, MA 02130
New England Roentgen Ray Society. Secretary, H. F. Gramm, 185 Pilgrim Road, Boston, MA 02215.
New England Society for Radiation Oncology. Secretary, S. P. Kadish St. Vincent Hospital, 25 Winthrop St, Worcester, MA 01604
Northeastern Society for Radiation Oncology. Secretary, C. C. Wang, Massachusetts General Hospital, Boston MA 02114

MICHIGAN
Michigan Radiological Society, Chapter of ACR. Secretary-Treasurer, F. P. Shea, Bon Secours Hospital, 468 Cadieux, Grosse Pointe, MI 48230
Michigan Society of Therapeutic Radiologists. Secretary, K. E. Murdock, 302 Kensington Ave, Flint, MI 48502

MINNESOTA
Minnesota Radiological Society, Chapter of ACR. Secretary-Treasurer, J. B. Marta, 125 W College Ave, St. Paul, MN 55102

MISSOURI
Greater Kansas City Radiological Society. President-Secretary, G. D. Dixon, St Luke's Hospital, 44th & Wornall Road, Kansas City, MO 64111
Greater St. Louis Society of Radiologists. Secretary-Treasurer, D. G. Spalding, 621 S New Ballas Rd, St. Louis, MO 63141
Missouri Radiological Society, Chapter of ACR. Secretary-Treasurer, E. M. Herman, 701E 63rd St, Kansas City, MO 64110

MISSISSIPPI
Mississippi Radiological Society, Chapter of ACR. Secretary-Treasurer, J. B. Barlow, 514B E Woodrow Wilson, Jackson, MS 39216

MONTANA
Montana Radiological Society. Secretary-Treasurer, E. Drouillard, St. Patrick Hospital, Missoula, MT 59801

NEBRASKA
Nebraska Chapter of ACR. Secretary-Treasurer, W. H. Northwall, Good Samaritan Hospital, Kearney, NB 68847

NEW HAMPSHIRE
New Hampshire Chapter of ACR. Secretary-Treasurer, E. P. Kane, Claremont General Hospital, Claremont, NH 03743

NEW JERSEY
Radiological Society of New Jersey, Chapter of ACR. Secretary, A. J. Scher, 8 Lord William Penn Dr, Morristown, NJ 07083

NEW MEXICO
New Mexico Society of Radiologists, Chapter of ACR. Secretary, W. M. Jordan, 1100 Central Ave SE, Albuquerque, NM 87106

NEW YORK
Bronx Radiological Society, New York State, Chapter of ACR. Secretary-Treasurer, L. J. Corbin, 1369 Rosendale Ave, Bronx, NY 10472
The Brooklyn Radiological Society. Secretary-Treasurer, E. Arida, 450 4th Ave, Brooklyn, NY 11215
Buffalo Radiological Society. Secretary, A. Favorito, 166 Soldiers Pl, Buffalo, NY 14222
Central New York Radiological Society. Secretary-Treasurer, P. A. Randall, Upstate Medical Center, 750 E Adams St, Syracuse, NY 13210
Kings County Radiological Society. Secretary, M. Moore, 7815 Bay Parkway, Brooklyn, NY 11214
Long Island Radiological Society. Secretary, R. Meisell, 84 Beverly Road, Great Neck, NY 11021
Mid-Hudson Radiological Society. Secretary-Treasurer, W. D. Stiehm, 37 Flower Hill Rd, Poughkeepsie, NY 12603
New York Roentgen Society. Secretary-Treasurer, N. E. Leeds, Montefiore Hospital, 111 E 210th St, New York, NY 10467
New York State Chapter of ACR. Secretary-Treasurer, A. F. Keegan, 6 Secor Dr. Port Washington, NY 11050
Northeastern New York Radiological Society. Secretary, D. R. Morton, Dept Radiology, St. Claire's Hospital, Schenectady, NY 12304
Rochester Roentgen Ray Society. Secretary-Treasurer, R. E. Tobin, 135 Drumlin View Dr, Mendon, NY 14506
Westchester County Radiological Society. Secretary, H. Kessler, Radiological Group, 45 Ludlow St, Yonkers, NY 10705

NEVADA
Nevada Radiological Society, Chapter of ACR. Secretary, C. F. Veverka, Carson Tahoe Hospital, Carson City, NV 89701

NORTH CAROLINA
Catawba Valley Radiological Society. Secretary, J. N. Owsley, 18 13th Ave NE, Hickory, NC 28601
North Carolina Chapter of ACR. Secretary-Treasurer, M. A. Jones, Durham County Hospital, Durham, NC 27705
Southeastern Chapter Society of Nuclear Medicine. Secretary, V. J. Sodd, University of Cincinnati Medical Center, Cincinnati, OH 45267

NORTH DAKOTA
North Dakota Radiological Society, Chapter of ACR. Secretary, H. C. Walker Jr, PO Box 624, Devils Lake, ND 58301

OHIO
Cleveland Radiological Society. Secretary-Treasurer, J. B. McCoy, Elyria Medical Arts Bldg, Suite 12, Elyria, OH 44035
Greater Cincinnati Radiological Society. Secretary-Treasurer, C. D. Eversole, 722 Scott St, Covington, KY 41011
Northwestern Ohio Radiological Society. Secretary, P. C. Chandnani, Medical College of Ohio, C. S. 10008, Toledo, OH 43699
Miami Valley Radiological Society. President, G. W. Bretz, 520 IBM Bldg. 33 W 1st St. Dayton OH 45402

Ohio State Radiological Society, Chapter of ACR. Secretary, W. Howland, Aultman Hospital, 2600 Sixth St SW, Canton, OH 44710

OKLAHOMA
Northwestern Oklahoma Radiological Society. Secretary, W. L. Lavendusky, 100 Center Plaza Suite C, Tulsa, OK 74119
Oklahoma State Radiological Society, Chapter of ACR. Secretary, B. G. Eaton, 2508 Stillmeadow Rd, Edmond, OK 73034

OREGON
Oregon Radiological Society Chapter of ACR. Secretary-Treasurer, A. I. Kostiner, 8535 SW Bohmann Parkway, Portland, OR 97233

PENNSYLVANIA
Greater Delaware Valley Ultrasound Society. Secretary, W. G. M. Ritchie, Temple University School of Medicine, Philadelphia, PA 19140
Northeastern Pennsylvania Area Radiologists. Secretary-Treasurer, A. S. Haber, 181 Wilson Dr, Hazelton, PA 18201
Pennsylvania Radiological Society. Secretary R. Farrell, 201-6 Medical Arts Bldg, Scranton, PA
Philadelphia Roentgen Ray Society. Secretary, M. E. Haskin, 230 N Broad St, Philadelphia, PA 19102
Pittsburgh Roentgen Society. Secretary, R. J. Clearfield, Citizens General Hospital, 651 Fourth Ave, New Kensington, PA 15068

RHODE ISLAND
Radiological Society of Rhode Island, Chapter of ACR. Secretary, F. H. Scola, Rhode Island Hospital, Providence, RI 02902

SOUTH CAROLINA
South Carolina Radiological Society, Chapter of ACR. Secretary, G. W. Brunson, 4315 Woodleigh Rd, Columbia, SC 29206

TENNESSEE
Memphis Roentgen Society. Secretary-Treasurer, D. R. Ramey, Baptist Memorial Hospital, 899 Madison Ave, Memphis, TN 38140
Middle Tennessee Radiological Society. Secretary-Treasurer, H. P. Pendergrass. Vanderbilt University Hospital, Nashville, TN 37232
Tennessee Radiological Society, Chapter of ACR. Secretary-Treasurer, J. W. Grise, Methodist Hospital, 1265 Union Ave, Memphis TN 38104

TEXAS
Central Texas Radiology Society. Secretary-Treasurer, E. J. Schoolar, Scott and White Clinic, Temple, TX 76501
Dallas-Fort Worth Radiology Society. Secretary-Treasurer, J. T. Telle, 900 W Randol Mill Road, #120 Arlington, TX 76012
Houston Radiological Society. Secretary, T. S. Harle, 103 Jones Library Bldg, Texas Medical Center, Houston, TX 77030
San Antonio Civilian Military Radiological Society. Secretary, J. M. Chao, Diagnostic Clinic, San Antonio, TX
Texas Radiological Society, Chapter of ACR. Secretary-Treasurer, D. N. Dysart, Scott and White Clinic, Temple, TX 76501

VERMONT
Vermont Radiological Society, Chapter of ACR. Secretary, P. Dietrich, Medical Center Hospital of Vermont, Burlington, VT 05401

VIRGINIA
Mid-Shenandoah Valley Radiological Society. Secretary, K. L. Dwyer, King's Daughters Hospital, Staunton, VA 24401
Richmond Radiological Society. Secretary, M. Vinik, 9504 Carterwood Rd, Richmond, VA 23229
Virginia Chapter of ACR. Secretary-Treasurer, C. P. Winkler, 3500 Kensington Ave, Suite 2-A, Richmond, VA 23221

WASHINGTON
Pacific Northwest Radiological Society. Secretary-Treasurer, K. D. Moores, 1118 9th Ave, Seattle, WA 98101.
Washingon State Radiological Society, Chapter of ACR. J. F. Sailer, 200 15th Ave E, Seattle, WA 98102. Annual meeting: May 11-13, Portland, OR

WEST VIRGINA
West Virginia Radiological Society, Chapter of ACR. Secretary-Treasurer, A. W. Goodwin II, 200 Medical Arts Bldg, Charleston, WV 25301

WISCONSIN
Milwaukee Roentgen Ray Society. Vice President, T. C. Lipscomb, 1004 N 10th St, Milwaukee, WI 53233
Society of Nuclear Medicine, Central Chapter. G. J. Weir Jr., Marshfield Clinic, Marshfield, WI 54449
Wisconsin Radiological Society. Chapter of ACR. Secretary-Treasurer, J. Unger, Wood VA Hospital, Wood, WI 53193
Wisconsin Society of Therapeutic Radiologists. Secretary, M. Greenberg, Milwaukee County General Hospital, 8700 W Wisconsin Ave, Milwaukee, WI 53222

WYOMING
Wyoming Radiological Society, Chapter of ACR. Secretary, T. E. Hettinger, 1609 E 19th ST, Cheyenne, WY

Canada

Canadian Association of Radiologists. Honorary Secretary, M. J. Palayew, Suite 806, 1440 St, Catherine St W, Montreal, Quebec, Canada H3G 1R8. Annual meetings: 1979, Sept 15-20, Vancouver; 1980, Oct 4-9, Montreal
Edmonton and District Radiological Society. Secretary, B. Caplan, 12320 103rd Ave, Edmonton, Alberta T5N ORZ, Canada
Toronto Radiological Society. Secretary, H. Shulman, Sunnybrook Hospital, 2075 Bayview Avenue, Toronto, Ontario, Canada

Central and South America

Asociacion Costarricense de Radiologia. Secretary, F. A. Arguedas Haug, Apartado 8-5340, San Jose, Costa Rica
Colegio Brasileiro de Radiologia. Secretary-General L. C. C. Teixeira, 01311 Avenida Paulista, 491, 13th Floor, cj. 132, São Paulo, Brazil
Sociedad Chilena de Radiologia. Secretary, M. Neira, Casilla 13426, Santiago, Chile
Sociedad Colombiana de Radiologia. Secretary-General, G. Sanchez Sanchez, Bogota, Colombia
Sociedad Peruana De Radiologia. Secretary-General, E. de Olazaval Tejada, Colegio Médico del Perú, Casilla de Correo 2306, Lima Perú.
Sociedad de Radiologia del Atlantico. Secretary, R. Fernandez, Calle 40 #41-110, Baranquilla, Colombia
Sociedad de Radiologia. Radiotherapéutica y Medicine Nuclear de Rosario. Secretary-General, M. Muñoz, Santa Fe 1798, Rosario, Argentina

Europe

Bavarian-American Radiologic Society. Secretary, S. A. O'Byrne, Radiology Service, Stuttgart, West Germany, 5th General Hospital, APO NY 09154
British Institute of Radiology. Honorary Secretary, D. H. Trapnell, P. N. T. Wells, 32 Welbeck St, London, W1M/7PG, England
Čekoslovenska Radiologická Společnost. Secretary, J. Kolář, Clinic for Diagnostic Radiology ILF, 180 81 Praha 8, Budinova 2, Czechoslovakia
Danish Radiological Society. Secretary General, J. Praestholm, Radiological Dept I, Bispebjerg Hospital, DK-2400, Copenhagen NV, Denmark
Deutsch Rontgengesellschaft. President, W. Frik, Dept Radiology, Techn Univ Aachen, D-5100 Aachen, Goethestrasse 27/29, West Germany
European Society of Paediatric Radiology. Permanent Secretary, C. Fauré, Service de Radiologie, Hôpital Trousseau, 8-28, av du Dr. Arnold Netter, 75 571, Paris CEDEX 12, France. Annual meeting and postgraduate course: April 30-May 1, Köln.
Faculty of Radiologists (of Ireland). Honorary Secretary, M. Ryan, Faculty of Radiologists, Royal College of Surgeons in Ireland, Stephen's Green Dublin 2, Ireland
The Hospital Physicists' Association. Honorary Secretary, R. F. Mould, Westminister Hospital, Physics Dept. Page St Wing, London SW1P2AR, England
Norsk Forening for Medicinsk Radiologi. General Secretary, A. Skjennald, Ullevål sykehus, Oslo, Norway
Netherlandse Vereniging voor Radiologie. Secretary, H. E. Schütte, Dept Radiology, Elizabeth Gasthuis, Haarlem, Netherlands
Royal College of Radiologists. Secretary, P. D. Thomson, 28 Portland Pl, London, W1N4DE, England
Scandinavian Radiological Society. Secretary-General, C-E. Unnérus, Havsvindsv 5C, C2120 Esbo 12 (Hagalund-Tapiola), Finland
Schweizerische Gesellschaft für Radiologie und Nuklearmedizin. Soclete Suisse de Radiologie et de Medecine Nucleaire. Secretary, G. A. Schoch, 7 Gellerstrasse, CH—4052 Basal, Switzerland
Sociedad Española de Radiologia y Electrologia Médicas y de Medicina Nuclear. Secretary-General, P. G. Barberá, Villanueva, Madrid 1, Spain
Societá Italiana di Radiologia Medica e Medicina Nucleare. Administrative Secretary, R. Dall'Acqua, Ospedale Mauriziano, 10128, Torinc, Italy
Société Française de Radiologie Médicale, Nucléaire et Electrologie. Secretary-General, J. Sauvegrain, Hôpital des Enfants-Malades, 149 Rue de Sèvres, 75730 Paris Cedex 15, France.
Société Francaise de Neuroradiologie. Secretary-General, R. Djindjian, 16, rue de l'Universite 75, Paris 7°, France
Svensk Forening för Medicinsk Radiologi. Secretary, H. Ringertz, Dept Pediatric Radiology, Karolinska Sjukhuset, S—104 01 Stockholm, Sweden

Africa

Association of Radiologists of West Africa. Honorary Secretary, A. A. Obisen, Dept Radiology, University College Hospital, Ibadan, Nigeria
Radiological Society of South Africa. Secretary, A Visser, PO Box 8850, Johannesburg, South Africa
South African International Radiological Congress. Director, P. Sneider, PO Box 4878, Johannesburg, South Africa

Near East and Asia

Bengal Radiological Association. Honorary Secretary, B. Chatterji, 262 Rash Behari Ave, Calcutta 700019, India

Indian Radiological Association. Honorary General Secretary, S. P. Aggarwal, 10-B Kasturba Ghandi Marg, New Delhi 110001, India

Indonesian Radiological Society. Secretary, G. Sasmitaatmadja, Radiology Dept, University of Indonesia, Salemba 6, Jakarta, Indonesia

Philippine College of Radiology. Secretary-Treasurer, A. Chavez, Box 1284, Commercial Center, Makati, Rizal, D-708, Philippines

Radiological Society of Thailand. Secretary, D. Prabbasawat, Dept Radiology, Siriraj Hospital Faculty of Medicine, Mahidol University, Bangkok 7, Thailand

Royal Australasian College of Radiologists. Honorary Secretary, B. Roberts, 37 Lower Fort St, Millers Point, NSW 2000, Australia

American Journal of Roentgenology

Please enter my subscription as follows:

Beginning with _____ (*month*), _____ (*year*).

Name _____

Address _____

City and State _____ Zip Code _____

Specialty _____

Amount enclosed $ _____

Annual subscription rates: $40 ($20 for residents with letter of verification) plus appropriate mailing surcharge. Mailing surcharges: U.S. and possessions, none; European countries,* $25; Japan, $45; other, $10. Subscriptions to Japan and European countries are delivered by air freight. There is no option for surface mail.

Send this form and remittance to Charles C Thomas, Publisher, 301-327 East Lawrence Avenue, Springfield, Illinois 62717.

* The European mailing surcharge applies to the following countries. All receive Journal delivery via air freight to Europe. Algeria, Austria, Belgium, Czechoslovakia, Denmark, Finland, France, Germany, Great Britain, Greece, Hungary, India, Iran, Ireland, Israel, Italy, Kenya, Luxembourg, Netherlands, Nigeria, Norway, Portugal, Romania, South Africa, Spain, Sweden, Switzerland, Turkey, Uganda, Yugoslavia.

Author Index Volume 131

Index key: b = book review, c = case report, e = editorial, l = letter, o = obituary, t = technical note

Abrams HL, McNeil BJ: Computed tomography: cost and efficacy implications, 81
Adler H, see Smith TR
Adler O, see Rosenberger A
Ahn CH, see Christensen EE
Akisada M, see Tatezawa T
Alazraki N, see Weissberg DL
Alford BA, see Lees RF
Ali MV, see Shenoy SS
Aliabadi P, Shafiepoor H: Bronchography in the recognition of congenital cystic bronchiectasis, 255
Allen FH, see Freeny PC
Amplatz K, see Probst P
Anderson WA, see Lees RF
Antonioli DA, see Joffe N
Archer MC: Herman C. Sehested, 1901-1978 (o), 755
Arger PH, see Gefter WB
Armstrong JD Jr, see Prescott SM
Arroyo F, see Pueyo I
Athanasoulis CA, see Greenfield AJ
Austin JHM: Diagnosis of disease of the chest (b), 1128

Babcock DS, Kaufman L, Cosnow I: Ultrasound diagnosis of hydatid disease (echinococcosis) in two cases (c), 895
Bahr AL, Hodges FJ III: Efficacy of computed tomography of the head in changing patient care and health costs: a retrospective study, 45
Baker DH, see Slovis TL
Baldwin GN, see Haaga JR
Balthazar EJ, Schechter LS: Air in gallbladder: a frequent finding in gallstone ileus, 219
Bargeron LM Jr, see Soto B
Barkin JS, see Pereiras RV
Barnes JC, see Lester PD
Barth KH, Strandberg JD, Kaufman SL, White RI Jr: Chronic vascular reactions to steel coil occlusion devices, 455
Barth KH, see Kaufman SL
Barton J, see Brown TW
Becker M, see Weissberg DL
Bein ME, Putnam CE, McLoud TC, Mink JH: A reevaluation of intrathoracic lymphadenopathy in sarcoidosis, 409
Bellon EM, see Rashad FA
Bender CE, see Brown ML
Berdon WE, see Slovis TL
Berenberg AL, see Hall FM
Bergman AB, Neiman HL: Computed tomography in the detection of retroperitoneal hemorrhage after translumbar aortography, 831
Berlin L: The clean colon: whose responsibility? (l), 183
Bernardino ME, Danziger J, Young SE, Wallace S: Computed tomography in ocular neoplastic disease, 111
-----, see Wooten WB
Beven E, see Haaga JR
Bierny J-P: Multinodular primary amyloidosis of the lung: needle biopsy (c), 1082
Bigongiari LR, Lee KR, Mebust WK, Foret J, Weigel JW: Transurethral conversion of a percutaneous ureteral stent to an indwelling stent (t), 1099
Bilaniuk LT, see Zimmerman RA
Birnbaum W, see Sargent EN
Bjelland JC, see Stickney RH
Black EB, see Wittenberg J
Black GA, Carsky EW: Duodenal tuberculosis (c), 329
Bledin AG, see Rabin MS
Blum J, Reed JC, Pizzo SV, Thompson WM: Miliary aspergillosis associated with alcoholism (c), 707
Blumhagen J: Current concepts in pediatric radiology (b), 947
-----: Progress in pediatric radiology, vol. 6. Skull, spine and contents (b), 946
Boechat MI, Gilsanz V, Fellows KE: Subclavian artery as the first branch of the aortic arch: A normal variant in two patients (c), 721
Boex RM, see Wepfer JF
Bolender N, Cromwell LD, Wendling L: Fracture of the occipital condyle (c), 729
-----: Soft tissues of the extremities. A radiologic study of rheumatic disease (b), 1130
-----: Xeroradiography in ortorhinolaryngology (b), 948
Bookstein JJ, see Velick WF
Borlaza GS, see Kuhns LR
Boswell WD, see Layne TA
Boyd DP, see Brasch RC
Bradenham BP, see Kelvin FM
Bramson RT: Pediatric radiology (b), 193
Brasch RC, Boyd DP, Gooding CA: Computed tomographic scanning in children: comparison of radiation dose and resolving power of commercial CT scanners, 95
-----, Korobkin M, Gooding CA: Computed body tomography in children: evaluation of 45 patients, 21
Braver JH, see Pugatch RD
Bree RL, see Wicks JD
Brenbridge ANAG, see Lees RF
Brill PW, see Kleinman PK
Brinley G, see Christensen EE
Brinton WR, see Osborn AG
Brooks RA, see Chew E
Brown LR, see Muhm JR
Brown ML, Swee RG, Olson RJ, Bender CE: Pulmonary uptake of ^{99m}Tc diphosphonate in alveolar microlithiasis (c), 703
Brown TW, Filly RM, Laing FC, Barton J: Ultrasonographic criteria of ectopic pregnancy, 967
Bruce D, see Zimmerman RA
Brugarolas A, see Pueyo I
Budge AF, see Lester PD
Buonocore E, Lynch TP: Flow-directed balloon catheterization for aortofemoral arteriography using the axillary artery approach, 823
Burrell M, see Gold J
Buschi AJ, see Lees RF
Bynum LJ, see Landay MJ

Cady JB, see Littleton JT
Callen PW, see Marks WM
Capp MP, see Stickney RH
Carbone JV, see Moss AA
Carlson D, see Carlson DH
Carlson DH, Carlson D, Simon H: Benign multilocal cystic nephroma, 621
-----: The craniovertebral region in chronic inflammatory rheumatic diseases (b), 947
Carr SR: Synopsis of radiographic anatomy with computed tomography (b), 949
-----: Understanding radiography (b), 949
Carroll BA: Gallstones: in vitro comparison of physical, radiographic, and ultrasonic characteristics, 223
-----, Sample WF: Pancreatic cystadenocarcinoma: CT body scan and gray scale ultrasound appearance (c), 339
Carsky EW, Haswell DM: Huge laparotomy pad granuloma simulating a gastric wall tumor (c), 909
-----, see Black GA
Carter BL, see Emami B
-----, see Pilepich MV
Casal GL, see Martinez LO
Casarella WJ, Knowles DM, Wolff M, Johnson P: Focal nodular hyperplasia and liver cell adenoma: radiologic and pathologic differentiation, 393
Casarett GW: Clinical radiobiology (b), 365
Chambers E, see Friedman AC
Chang AE, see Schaner EG
Chang CHJ, Sibala JL, Fritz SL, Gallagher JH, Dwyer SJ III, Templeton AW: Computed tomographic evaluation of the breast, 459
Chang J, Katzen B, Sullivan KP: Transcatheter Gelfoam embolization of posttraumatic bleeding pseudonaneurysms, 645
Chapman JS, see Christensen EE
Chard RL: Clinical pediatric oncology (b), 565
Charlton OP, see Miller MD
Chen JTT, see Rodan BA
Chew E, Weiss GH, Brooks RA, DiChiro G: Effect of CT noise on detectability of test objects, 681
Chiu LC, see Cornell SH
Cho KJ, Martel W: Recognition of splenic vein occlusion, 439
-----, Thornbury JR: Severe reactions to contrast material by three consecutive routes: intravenous, subcutaneous, and intraarterial (c), 509
Choi WS, see Katzen BT
Christensen EE, Dietz GW, Ahn CH, Chapman JS, Murry RC, Hurst GA: Radiography of pulmonary Mycobacterium kansasii infections, 985
-----, Landay MJ, Dietz GW, Brinley G: Buckling of the innominate artery simulating a right apical lung mass, 119
-----, see Landay MJ
Christensen FK, see Levy JM
Christie JH, see Cornell SH
Chuang VP, Clements DL: A modified punch card for extending filming program of a puck changer (t), 534
-----, Fried AM: High-dose renal pharmacoangiography in the assessment of hypovascular renal neoplasms, 807
-----, Widrich WC: Complications from intraarterial lidocaine in upper extremity arteriography (c), 906
Chung KJ, see Hesselink JR
Cimmino CV: Anonymity of reviewers (l), 358
Cimochowski GE, see MacMahon H
Clark RE, see Korobkin M
Clark RL, see Cuttino JT Jr
Clements DL, see Chuang VP
Coel MN, Dodge W: Complication rate with supine phlebography, 821
Coleman RE, see Prescott SM
Conkle DM, see Schaner EG
Conrad MR, Dickerman R, Love IL, Curry T, Peters P, Hull A, Lerman M, Helderman H: New observations in renal transplants using ultrasound, 851
Cooperberg PL: Biliary duct ultrasound (l), 556
Cornell SH, Chiu LC, Christie JH: Diagnosis of extracerebral fluid collections by computed tomography, 107
Correa-Paz F, see Haughton VM
Cosnow I, see Babcock DS
Coulam CM: Computed tomography of the human body: An atlas of normal anatomy (b), 564
Crade M, Taylor KJW, Rosenfield AT, de Graaf CS, Minihan P: Surgical and pathologic correlation of cholecystosonography and cholecystography, 227
-----, Taylor KJW, Rosenfield AT: Water distention of the gut in the evaluation of the pancreas by ultrasound (t), 348
Cromwell LD, Moore WE: A transparent head support for magnification cerebral angiography (t), 1097
-----, see Bolender N
-----, see Keating JW
Crowe JK, see Muhm JR
Crummy AB, see Hesselink JR
Cunningham ME, see Roberts FF
Curry T, see Conrad MR
Cushing B, see Slovis TL

Cuttino JT Jr, Clark RL, Fried FA, Stevens PS: Microradiographic demonstration of pyelolymphatic backflow in the porcine kidney, 501

Daffner RH: Pathologic index for arrangement of teaching file (t), 918
Daggett WM, see Miller SW
Dalinka MK, see Giesecke SB
Danzig LA, see Resnick D
Danziger J, see Bernardino ME
Davis GD, see Fulton RE
Deane RSD, see Gallant TE
Deeb ZL, Martin TA, Kerber CW: Traction device for use with polytome table (t), 732
de Graaf CS, see Crade M
Dembner AG, see Walsh JW
DeNardo GL, see Glass EC
Deren MM, see Glanz S
deSantos LA, Rosengren J-E, Wooten WB, Murray JA: Osteogenic sarcoma after the age of 50: a radiographic evaluation, 481
DeWard LA, see Wochos JF
DiChiro G, see Chew E
Dickerman R, see Conrad MR
Dietrich PA, see Gallant TE
Dietz GW, see Christensen EE
Dinsmore RE, see Miller SW
DiSessa TG, see Edwards DK
Dodge W, see Coel MN
Dolinskas C, see Zimmerman RA
Doppman JL, see Schaner EG
Dublin AB, Richey DC: Pseudoocclusion of a superficial temporal-middle cerebral artery bypass (c), 162
Dwyer SJ III, see Chang CHJ

Ecker MD, Jay B, Keohane MF: Procarbazine lung (c), 527
Edell S: Ultrasonics in clinical diagnosis (b), 193
Edwards DK, Higgins CB, Merritt TA, DiSessa TG, Friedman WF: Radiographic and echocardiographic evaluation of newborns treated with indomethacin for patent ductus arteriosus, 1009
Eenmaa J: Medical cyclotrons in nuclear medicine (b), 1130
Eisenberg RL, see Mani RL
Emami B, Melo A, Carter BL, Munzenrider JE, Piro AJ: Value of computed tomography in radiotherapy of lung cancer, 63
Enzman DR, see Norman D
Ermocilla R, see Soto B
Evens RG: National guidelines and standards for health planning: their relation to radiology, 1101

Faer MJ, Messerschmidt GL: Nonfatal pulmonary air embolism: radiographic demonstration (c), 705
Faling LJ, see Pugatch RD
-----, see Robbins AH
Farooki ZA, see Slovis TL
Feldman PS, see Lees RF
-----, see Rosen RJ
Fellows KE, see Boechat MI
-----, see Levin DC
Felman AH, see McCook TA
Ferguson FB Jr: Orbit roentgenology (b), 192
Ferguson L, see Patel DV
Ferrucci JT Jr, see Harley WD
-----, see Wittenberg J
Figley MM: The mediastinum: radiologic correlations with anatomy and pathology (b), 191
Filly RM, see Brown TW
Finck EJ, see Layne TA
Fineberg HV: Evaluation of computed tomography: achievement and challenge (e), 1
-----, see Wittenberg J
Fischer EP, see Lindell MM Jr
Fishback HR Jr: Fundamental physics of radiology (b), 566
-----:A practical approach to modern x-ray equipment (b), 565
Flehinger BJ, Melamed MR, Heelan RT, McGinnis CM, Zaman MB, Martini N: Accuracy of chest film screening by technologists in the New York early lung cancer detection program, 593
Fleischer AC, James AE Jr, Millis JB, Julian C: Differential diagnosis of pelvic masses by gray scale sonography, 469
Fletcher BD: Pleural herniation in respiratory distres syndrome (1), 358
Flye MW, see Schaner EG
Foret J, see Bigongiari LR
Franklin J Jr, see Sniderman KW
Freeny PC, Weinstein CJ, Taft DA, Allen FH: Cystic neoplasms of the pancreas: new angiographic and ultrasonographic findings, 795
-----, Rosoff L Jr: Pancreatic duct obstruction: a new observation during fine needle percutaneous transhepatic cholangiography (c), 521
Freiman DB, Ring EJ, Oleaga JA, Rosato EF: Radiography of LeVeen type peritoneovenous shunts (t), 916
Fremland A, see Kagan AR
Frey GD: Gallium-67 imaging (b), 1129
Fried AM, Oliff M, Wilson EA, Wisnant J: Uterine anomalies associated with renal agenesis, 973
-----, see Chuang VP
Fried FA, see Cuttino JT Jr
Friedland GW: Progress in radiology: historical review of the changing concepts of lower esophageal anatomy: 430 B.C.-1977, 373
Friedman AC, Chambers E, Sprayregen S: The normal and abnormal left superior intercostal vein, 599
Friedman MH, see Katzen BT
Friedman SN, see Smith TR
Friedman WF, see Edwards DK
Fritz SL, see Chang CHJ
Fritzberg AR, see Klingensmith WC III
Fullenlove TM: Percy Douglas Hay, 1899-1977 (o), 755
Fullerton GD, see Wochos JF
Fulton RE, Davis GD: Congenital pulmonary atresia: photographic subtraction for recognizing hypoplastic pulmonary arteries, 1003
Furman RS, see Giustra PE

Gallagher JR, see Chang CHJ
Gallagher TJ: Easy coronal scans (t), 535
Gallant TE, Dietrich PA, Shinozaki T, Deane RSD: Simple device to measure patient position on portable chest radiographs (c), 169
Ganchan RP, see Prescott SM
Garbutt JT, see Kelvin FM
Garcia-Muniz JL, see Pueyo I
Gefter WB, Arger PH, Mulhern CB, Pollack HM, Wein AJ: Computed tomography of circumcaval ureter (c), 1086
Gelfand DW, see Ott DJ
Genant HK, see Goldberg RP
Gennarelli T, see Zimmerman RA
Gerle RD, see Kim SK
Gerzof SG, see Robbins AH
Giesecke SB, Dalinka MK, Kyle GD: Lisfranc's fracture-dislocation: a manifestation of peripheral neuropathy, 139
Gilbert HA, see Kagan AR
Gilsanz V, see Boechat MI
Gilula LA, Schoenecker PL, Murphy WA: Shoulder arthrography as a treatment modality, 1047
Girdany BR, see Ledesma-Medina J
Giustra PE, Wickenden JW, Furman RS, Wickenden RW, Killoran PJ: Multiple contrast injections in epidural venography, 485
Glanz S, Ravin CE, Deren MM: Benign pneumoperitoneum following median sternotomy incision, 267
Glass EC, DeNardo GL: Abnormal peripheral distribution of thallium-201 due to arteriosclerosis (c), 718
Goergen TG, see Resnick D
Gold J, Rosenfield AT, Sostman D, Burrell M, Taylor KJW: Nonfunctioning islet cell tumors of the pancreas: Radiographic and ultrasonographic appearance in two cases (c), 715
Gold RH: Breast carcinoma: the radiologist's expanded role (b), 946
Goldberg HI, see Shanser JD
Goldberg L: Radiologic examination of the orohypopharynx and esophagus (b), 1130
Goldberg RP, Genant HK: Calcified bodies in popliteal cysts: a characteristic radiographic appearance, 857
Goldman AB: Hip arhtrography (b), 948
Goldman RL, see Kushnet MW
Goldstein HM, Katragadda CS: Prone view ultrasonography for pancreatic tail neoplasms, 231
-----: Ultrasound of tumor extension to IVC (1), 1118
-----, Zornoza J: Association of squamous cell carcinoma of the head and neck with cancer of the esophagus, 791
-----, see Wooten WB
Goldstein SA, see Widrich WC
Goller DS, see Merten DF
Gooding CA, see Brasch RC
Gordon IJ: Evaluation of suspected deep venous thrombosis in the arteriosclerotic patient (c), 531
Gordonson J, Quinn M, Kaufman R, Van Den Tweel JG: Mediastinal lymphadenopathy and undifferentiated connected tissue disease: case report and review (c), 325
-----, see Sargent EN
Gosink BB: Ultrasound of tumor extension to IVC (1), 1117
Gray JE, Taylor KW, Hobbs BB: Detection accuracy in chest radiography, 247
Green IJ, see Katzen BT
Green WM, see Spiegel RM
Greene R: Pleural herniation in respiratory distress syndrome (1), 357
-----, see McLoud TC
Greene RE, see Miller SW
Greenfield AJ, Athanasoulis CA, Waltman AC, LeMoure ER: Transcatheter embolization: prevention of embolic reflux using balloon catheters, 651
Greenfield LD: New methods in tumor localization (b), 763
-----: Pineal tumors (b), 192
Greenway G, see Resnick D
Griscom NT: Progress in radiology: total body opacification, 919
Guerra J Jr, see Resnick D
Guillamondegui OM, see Lindell MM Jr
Gulver GJ, see Shenoy SS
Guthaner DF, see Walter JF
Guzzetta LR, see Stephenson TF

Haaga JR, Baldwin GN, Reich NE, Beven E, Kramer A, Weinstein A, Havrilla TR, Seidelmann FE, Namba AH, Parrish CM: CT detection of infected synthetic grafts: preliminary report of a new sign, 317
Hakkal HG: Radiology of the liver (b), 1130
Hall FM, Berenberg AL: Selective use of the oblique projection in mammography, 465
-----: Radiographs in cervical spine trauma (1), 555
Hanafee WN, see Matsubara R
Hansen R, see Stickney RH
Harley WD, Kirkpatrick RH, Ferrucci JT Jr: Gas in the bile ducts (pneumobilia) in emphysematous cholecystitis, 661
Harrington DP, see Kaufman SL
Harris RD: The lymphoid system. Methods of clinical investigations (b), 566
Harrison RR, see Stickney RH
Haswell DM, see Carsky EW
Hattery RR, see Muhm JR
Haughton VM, Ho KC, Larson SJ, Unger GF, Correa-Paz F: Comparison of arachnoiditis produced by meglumine iocarmate and

metrizamide myelography in animal model, 129
Haverling M, Johanson H: Computed sagittal tomography of the orbit (t), 346
Havrilla TR, see Haaga JR
Hecht SM: Cross-sectional anatomy - an atlas for computerized tomography (b), 764
Heelan RT, see Flehinger BJ
Heilbrun N: Intraluminal duodenal diverticulum (1), 556
Helderman H, see Conrad MR
Heller RM, see Kirchner SG
Helms CA: Pseudocysts of the humerus, 287
Heneghan M: Contrast-induced acute renal failure (e), 1113
Herba M, see Lemaitre P
Hernandez RJ, Poznanski AK, Hopwood NJ, Kelch RP: Incidence of growth lines in psychosocial dwarfs and idiopathic hypopituitarism, 477
-----, see Pueyo I
Hershgold EL, see Prescott SM
Hessel SJ: Coronary artery surgery: a critical review (b), 565
Hesselink JR, Chung KJ, Peters ME, Crummy AB: Congenital partial eventration of the left diaphragm, 417
Higgins CB, see Edwards DK
Hindle WV, see Katzen BT
Hirsh LF, see Husted JW
Ho KC, see Haughton VM
Hobbs BB, see Gray JE
Hodges FJ III, see Bahr AL
Hopwood NJ, see Hernandez RJ
Hounsfield GN: Potential uses of more accurate CT absorption values by filtering, 103
Hull A, see Conrad MR
Hurst GA, see Christensen EE
Husted JW, Ring EJ, Hirsh LF: Intraarterial nitroprusside treatment for ergotism (c), 1090
Hutson D, see Pereiras RV
Hyman RA: Gastrointestinal angiography, 2d ed. (b), 364

Ikeda MK, see Wittenberg J
Irwin GA, see Robbins AH
Isaacs I: Hysterographic double-outlined uterine cavity: a sign of unsuspected pregnancy, 305

Jackson DC, see Limberakis AJ
Jackson KL: Advances in radiation biology (b), 765
Jacobs RP, see Korobkin M
-----, see Schrumpf JD
Jacobson G, see Sargent EN
Jacobson JJ, see Ulreich S
Jaffe CC, see Walsh JW
James AE Jr, see Fleischer AC
Jay B, see Ecker MD
Jimenez JR, see Pueyo I
Jing BS, see Lindell MM Jr
Joffe N, Antonioli DA: Atypical appearances of benign hyperplastic gastric polyps, 147
Johanson H, see Haverling M
Johnson JC, see Van Aman ME
Johnson P, see Casarella WJ
Johnson WC, see Robbins AH
-----, see Widrich WC
Jona JZ, see Selke AC Jr
Jones MD: Bernard S. Epstein, 1908-1978 (o), 1119
Jonsson K, Libshitz HI, Osborne BM: Lymphangiographic changes after radiation therapy, 803
Julian C, see Fleischer AC
Jüttner HU: Radiology of the gallbladder and bile ducts (b), 364

Kagan AR, steckel RJ: Diagnostic oncology case studies: radiologic investigation of bloody ascites, 697
-----, Steckel RJ, Rao A, Gilbert HA: Diagnostic oncology case studies: "Maxillary sinusitis" and cancer: the role of polytomography, 321
-----, Steckel RJ, Rao A, Khazin A, Fremland A: Diagnostic oncology case studies: colonic polyposis and cancer, 1065
Kagan EH, see Spirt BA
Kahn PC, see Leonidas JC
Kaiser JA, see Marks WM
Kalisher L, see McLoud TC
Kamath CRV: Handbook of clinical nuclear medicine (b), 364
Katragadda CS, see Goldstein HM
Katzen BT, Choi WS, Friedman MH, Green IJ, Hindle WV, Zellis A: Pseudomass of the liver due to pleural effusion and inversion of the diaphragm (c), 1077
-----, see Chang J
Kaufman L, see Babcock DS
Kaufman R, see Gordonson J
Kaufman SL, White RI Jr, Harrington DP, Barth KH, Siegelman SS: Protean manifestations of mycotic aneurysms, 1019
-----, see Barth KH
Kay CJ: Obstetrical diagnosis by radiographic, ultrasonic, and nuclear methods (b), 765
Kaye JJ, see Kirchner SG
Kaye M, see Lemaitre P
Keane AT, see Littman MS
Keating JW, Cromwell LD: Remote effects of neuroblastoma, 299
Kelch RP, see Hernandez RJ
Kelvin RM, Oddson TA, Rice RP, Garbutt JT, Bradenham BP: Double contrast barium enema in Crohn's disease and ulcerative colitis, 207
Keohane MF, see Ecker MD
Kerber CW, see Deeb ZL
Khazin A, see Kagan AR
Killoran PJ, see Giustra PE
Kim SK, Gerle RD, Rozanski R: Cathartic colitis (c), 1079
King DL, see Spiegel RM
Kirchner SG, Pavlov H, Heller RM, Kaye JJ: Periosteal chondromas of the anterior tibial tubercle: two cases (c), 1088
Kirkpatrick RH, see Harley WD
-----, see Wittenberg J
Kirks DR, see Lester PD
Kirsh IE, see Littman MS
Kishore PRS, see Norton GA
-----, see Roberts FF
Kleinman PK, Brill PW, Whalen JP: Anterior pathway for transdiaphragmatic extension of pneumomediastinum, 271
Klingensmith WC III, Koep LJ, Fritzberg AR: Bile leak into a hepatic abscess in a liver transplant: demonstration with ^{99m}Tc-diethyl-iminodiacetic acid (c), 889
Knowles DM, see Casarella WJ
Koehler PR: Lymphangiography vs. CT of lymphomas (1), 1116
Koep LJ, see Klingensmith WC III
Kogutt MS: Systemic air embolism secondary to respiratory therapy in the neonate: six cases including one survivor, 425
Konrad H, see Matsubara R
Kopits SE, see Schatz SL
Korobkin M, Jacobs RP, Clark RE, Minagi H: Diminished radiopacity of contrast material: a urologic sign of ureteral calculus, 847
-----, see Brasch RC
-----, see Marks WM
-----, see Shanser JD
Kramer A, see Haaga JR
Kressel HY, see Moss AA
Krook PM: Mammographic parenchymal patterns as risk indicators for cancer, 1031
Kuhns LR, Borlaza GS, Seigel R, Thornbury JR: External anatomic landmarks of the abdomen related to bertebral segments: applications in cross-sectional imaging, 115
Kunhardt B, see Pereiras RV
Kushnet MW, Goldman RL: Lipoma of the corpus callosum associated with a frontal bone defect (c), 517
Kyle GC, see Giesecke SB

Laing FC, see Brown TW
Landay MJ, Christensen EE, Bynum LJ: Pulmonary manifestation of acute aspiration of gastric contents, 587
-----, see Christensen EE
Lang EF: From earlier pages, 181, 734, 1111
Larson EB, Omenn GS, Loop JW: Computed tomography in patients with cerebrovascular disease: impact of a new technology on patient care, 35
-----, Omenn GS, Magno J: Impact of computed tomography on the care of patients with suspected hydrocephalus, 41
Larson SJ, see Haughton VM
Lash JR: M. Wendell Dietz, 1922-1977 (o), 755
Latshaw RF, Rohrer GV: Semierect and erect position in percutaneous transhepatic cholangiography (c), 171
-----, Weidner WA: Ulnar artery aneurysms: angiographic considerations in two cases (c), 1093
Lawson TL: Ectopic pregnancy: criteria and accuracy of ultrasonic diagnosis, 153
Layne TA, Finck EJ, Boswell WD: Transcatheter occlusion of the arterial supply to arteriovenous fistulas with gianturco coils, 1027
Ledesma-Medina J, Reid BS, Girdany BR: Colitis cystica profunda (c), 529
Lee JG, see Sos TA
Lee JKT, Stanley RJ, Sagel SS, Levitt RG: Accuracy of computed tomography in detecting intraabdominal and pelvic adenopathy in lymphoma, 311
-----, Stanley RJ, Sagel SS, Levitt RG: Lymphangiography vs CT of lymphomas (1), 1117
-----, Stanley RJ, Sagel SS, McClennan BL: Accuracy of CT in detecting intraabdominal and pelvic lymph node metastases from pelvic cancers, 675
Lee KR, see Bigongiari LR
Lees RF, Feldman PS, Brenbridge ANAG, Anderson WA, Buschi AJ: Inflammatory cysts of the pelvic peritoneum, 633
-----, Alford BA, Brenbridge ANAG, Buschi AJ, Williamson BRJ: Sonographic appearance of duodenal atresia in utero (c), 701
Lemaitre P, O'Regan S, Herba M, Kaye M: Complications in expanded polytetrafluoroethylene arteriovenous grafts: an angiographic study, 817
LeMoure ER, see Greenfield AJ
Leonidas JC, Moylan FMB, Kahn PC, Ramenofsky ML: Ventilation-perfusion scans in neonatal regional pulmonary emphysema complicating ventilatory assistance, 243
Lerman M, see Conrad MR
Lester PD, Budget AF, Barnes JC, Kirks DR: Gastric emphysema in infants with hypertrophic pyloric stenosis, 421
-----, McAlister WH: Pneumopelvigraphy in childhood, 607
Leung K, see Merten DF
Levin DC, Fellows KE, Sos TA: Angiographic demonstration of complications resulting from the Waterston procedure, 431
Levine A, see Pais MJ
Levitt RG, Sagel SS, Stanley RJ: Detection of neoplastic involvement of the mesentery and omentum by computed tomography, 835
-----, see Lee JKT
Levy JM, Christensen FK, Nykamp FW: Detection of a cerebrospinal fluid fistula by computed tomography (c), 344
Lewis D, see Rabin MS
Libshitz HI, see Jonsson K
Limberakis AJ, Mossler JA, Roberts L Jr, Jackdon DC, Thompson WM: Leukemic infiltration of the colon (c), 725
Lin J, see Norton GA
Lindell MM Jr, Jing BS, Fischer EP, Guillamondegui OM, Wallace S: Laryngocele, 259

Littleton JT, Cady JB: Free-floating calculi in the pericardial cavity (c), 901
Littman MS, Kirsh IE, Keane AT: Radium-induced malignant tumors of the mastoid and paranasal sinuses, 773
Lloyd TV, see Van Aman ME
Lowe JE, see Rodan BA
Logan WW: Technologist guide to mammography (b), 191
Loop JW, Lusted LB: Special report: American College of Radiology diagnostic efficacy studies, 173
-----, see Larson EB
Love IL, see Conrad MR
Lubin J, see Martinez LO
Lund DA, see Ulreich S
Lusted LB, see Loop JW
Lynch TP, see Buonocore E

MacMahon H, O'Connell DJ, Cimochowski GE: Pedunculated endotracheal metastasis (c), 713
Magno J, see Larson EB
Mandell GA: Association of antral diaphragms and hypertrophic pyloric stenosis, 203
Manheimer LH, see Martinez LO
Mani JR, see Mani RL
Mani RL, Eisenberg RL, McDonald EJ Jr, Pollock JA, Mani JR: Complications of catheter cerebral arteriography: analysis of 5000 procedures. I. Criteria and incidence, 861
-----, Eisenberg RL: Complications of catheter cerebral arteriography: analysis of 5000 procedures. II. Relation of complication rates to clinical and arteriographic diagnoses, 867
-----, Eisenberg RL: Complications of catheter cerebral arteriography: analysis of 5000 procedures. III. Assessment of arteries injected, contrast medium used, duration of procedure, and age of patient, 871
Marcia-Moran M, see Pueyo I
Margulis AR, see Moss AA
Marks WM, Korobkin M, Callen PW, Kaiser JA: CT diagnosis of tumor thrombosis of the renal vein and inferior vena cava, 843
Marshak RH: Single-contrast/double-contrast GI (1), 1116
Martel W, see Cho KJ
Martin TA, see Deeb ZL
Martinez LO, Manheimer LH, Casal GL, Lubin J: Malignant fistulae of the gastrointestinal tract, 215
Martini N, see Flehinger BJ
Marx WJ: Reduction of jejunogastric intussusception during upper gastrointestinal examination (c), 334
Mass S, Norman D, Newton TH: Coronal computed tomography: indications and accuracy, 875
Matsubara R, Konrad H, Hanafee WN: Incudostapedial joint in health and disease, 307
McAlister WH, see Lester PD
-----, see Shackelford GD
-----, see Siegel MJ
McClennan BL, see Lee JKT
McCook TA, Felman AH: Esophageal atresia, duodenal atresia, and gastric distention: report of two cases (c), 167
McDaniel DC, see Prescott SM
McDonald EJ Jr, see Mani RL
McDonald MM, see Rumack CM
McGinnis CM, see Flehinger BJ
McLelland R, see Reed JC
McLoud TC, Kalisher L, Stark P, Greene R: Intrathoracic lymph node metastases from extrathoracic neoplasms, 403
-----, see Bein ME
McNeil BJ, see Abrams HL
Mebust WK, see Bigongiari LR
Mehigan JT, see Walter JF
Meiers W, see Pereiras RV
Melamed MR, see Flehinger BJ
Melo A, see Emami B
Merritt TA, see Edwards DK
Merten DF, Leung K, Goller DS: Infant botulism: an unusual cause of intestinal hypomotility (c), 523
Messerschmidt GL, se Faer MJ
Miller FJ Jr, see Schroeder FM
Miller MD, Charlton OP: Reply to "radiographs in cervical spine trauma" (1), 555
Miller RE: The clean colon: whose responsibility? (1), 182
Miller SW, Dinsmore RE, Greene RE, Daggett WM: Coronary, ventricular, and pulmonary abnormalities associated with rupture of the interventricular septum complicating myocardial infarction, 571
Millis JB, see Fleischer AC
Minagi H, see Korobkin M
Mind JH, see Bein ME
Minihan P, see Crade M
Mittelstaedt CA, see Shirkhoda A
Montagne JP, see Moss AA
Moore WE: A guide for automatic radiographic processing and film quality control (b), 1128
-----, see Cromwell LD
Moss AA, Carbone JV, Kressel HY: Radiologic and clinical assessment of broad-spectrum antibiotic therapy in Crohn's disease, 787
-----, Margulis AR, Montagne JP: Single-contrast/double-contrast GI (1), 1116
Mossler JA, see Limberakis AJ
Moylan FMB, see Leonidas JC
Muhm JR, Brown LR, Crowe JK, Sheedy PF II, Hattery RR, Stephens DH: Tomography for detecting pulmonary nodules, 981
Mulhern CB, see Gefter WB
Munzenrider JE, see Emami B
-----, see Pilepich MV
Murphy WA, see Gilula LA
-----, see Tailor CC
Murray JA, see DeSantos LA
Murry RC, see Christensen EE
Murtagh FR, see Quencer RM

Nabseth DC, see Widrich WC
Namba AH, see Haaga JR
Neiman HL, see Bergman AB
Nelson JA, see Schroeder FM
Nelson P, see Reed JC
Newell JD, see Resnick D
Newton TH, see Norman D
-----, see Mass S
-----, see Robertson WD
Niwayama G, see Resnick D
Norman D, Enzman ER, Newton TH: Optimal contrast dosage in cranial computed tomography, 687
-----, see Mass S
Norton GA, Kishore PRS, Lin J: CT contrast enhancement in cerebral infarction, 881
Nykamp PW, see Levy JM

O'Brien MJ: Radiation protection in dentistry (b), 949
-----: Review of NCRP radiation dose limit for embryo and fetus in occupationally-exposed women (b), 948
Oleaga JA, see Freiman DB
O'Connell DJ, see MacMahon H
Oddson TA, see Kelvin FM
Oliff M, see Fried AM
Olson RJ, see Brown ML
O'Meara OP, see Rumack CM
Omenn GS, see Larson EB
O'Regan S, see Lemaitre P
Osborn AG, Brinton WR, Smith WH: Radiology of the jugular tubercles, 1037
Osborne BM, see Jonsson K
Ott DJ, Gelfand DW: Colorectal tumors: Pathology and detection, 691

Pacifico AD, see Soto B
Pais MJ, Levine A, Pais SO: Coccygeal ribs: development and appearance in two cases (c), 164
Pais SO, see Pais MJ
Parrish CM, see Haaga JR
Passano WM Sr: Authors of scientific articles and the copyright act of 1976 (e), 355
Passariello R, see Rossi P
Patel DV, Ferguson L, Schey WL: Enlargement of the intervertebral foramina: an unusual cause (c), 911
Pavlov H, see Kirchner SG
Pecora DV, Sagar V, Piccone J: Technetium-^{99m}pertechnetate as an indicator of gastric mucosal proliferation, 1091
Pereiras RV, Meiers W, Kunhardt B, Troner M, Hutson D, Barkin JS, Viamonte M: Fluoroscopically guided thin needle aspiration biopsy of the abdomen and retroperitoneum, 197
Perez CA, see Ragan DP
Peters ME, see Hesselink JR
Peters P, see Conrad MR
Peterson DH: J. Richard Aurelius, 1897-1977 (o), 756
Pfeffer TJ: Howard G. Bayley, 1914-1978 (o), 1119
Philippart AI, see Slovis TL
Phillips LA: Emmett's clinical urography (b), 763
Piccone J, see Pecora DV
Pilepich MV, Rene JB, Munzenrider JE, Carter BL: Contribution of computed tomography to the treatment of lymphomas, 69
Piper S, see Resnick D
Piro AJ, see Emami B
Pizzo SV, see Blum J
Pizzolato NF, see Robbins AH
Pollack HM, Wills JS: Radiographic features of ureteral endometriosis, 627
-----, see Gefter WB
Pollock JA, see Mani RL
Post MJD, see Quencer RM
Potter GD: Atlas of brain anatomy for CT scans using EMI terminology (b), 191
Poznanski AK, see Hernandez RJ
Prescott SM, Tikoff G, Coleman RE, Richards KL, Armstrong JD Jr, Hershgold EL, McDaniel DC, Ganchan RP: ^{131}I-labeled fibrinogen in the diagnosis of deep vein thrombosis of the lower extremities, 451
Probst P, Rysavy AJA, Amplatz K: Improved safety of splenoportography by plugging of the needle tract, 445
Pueyo I, Jimenez JR, Hernandez J, Brugarolas A, Garcia-Moran M, Garcia-Muniz JL, Arroyo F: Carcinoid syndrome treated by hepatic embolization (c), 511
Pugatch RD, Braver JH, Robbins AH, Faling LJ: CT diagnosis of pericardial cysts (c), 515
-----, see Robbins AH
Putnam CE, see Bein ME
-----, see Robbins AH

Quencer RM, Murtagh FR, Post MJD, Rosomoff HL, Stokes NA: Postoperative bony stenosis of the lumbar spinal canal: 164 symptomatic patients, 1059
Quinn M, see Gordonson J

Rabin MS, Bledin AG, Lewis D: Polypoid leukemic infiltration of the large bowel (c), 723
Ragan DP, Perez CA: Efficacy of CT-assisted two-dimensional treatment planning: analysis of 45 patients, 75
Ramenofsky ML, see Leonidas JC
Rankin RS, see Schroeder FM
Rao A, see Kagan AR
Rashad FA, Bellon EM: Arteriovenous malformation of the right leaf of the diaphragm communicating with vascular malformation of the right lung (c), 507
Ravin CE, see Glanz S
Reed JC, McLelland R, Nelson P: Legionnaires disease (c), 892
-----, see Blum J
Reed JO, see Slovis TL
Reich NE, see Haaga JR
Reid BS, see Ledesma-Medina J

Reid MC: Ultrasonic visualization of a cervical cord cystic astrocytoma (c), 907
Reilly BJ, see Slovis TL
Rene JB, see Pilepich MV
Reningers SA, Spigos DG: Pseudoaneurysm of the arterial anastomosis in a renal transplant (c), 525
Resnick D, Greenway G, Vint VC, Robinson CA, Piper S: Selective involvement of the first carpometacarpal joint in scleroderma, 283
-----, Guerra J Jr, Robinson CA, Vint VC: Diffuse idiopathic skeletal hyperostosis (DISH) and calcification of the posterior longitudinal ligament, 1049
-----, Newell JD, Guerra J Jr, Danzig LA, Niwayama G, Goergen TG: Proximal tibiofibular joint: anatomic-pathologic-radiographic correlation, 133
-----, see Weissberg DL
Reuter SR: On behalf of translumbar aortography (e), 733
-----, see Walter JF
Rice RP, see Kelvin FM
Richards KL, see Prescott SM
Richey DC, see Dublin AB
Ring EJ, see Freiman DB
-----, see Husted JW
Robbins AH, Pugatch RD, Gerzof SG, Faling LJ, Johnson WC, Sewell DH: Observations on the medical efficacy of computed tomography of the chest and abdomen, 15
-----, Rosenfield AT, Pizzolato NF, Irwin GA, Putnam CE, Gerzof SG, Ulreich S: Drip infusion urography with meglumine iodamide, 1043
-----, see Pugatch RD
-----, see Widrich WC
Roberts FF, Kishore PRS, Cunningham ME: Routine oblique radiography of the pediatric lumbar spine: is it necessary?, 297
Roberts L Jr, see Limberakis AJ
Robertson WD, Newton TH: Radiologic assessment of pituitary microadenomas, 489
Robinson CA, see Resnick D
Rodan BA, Lowe JE, Chen JTT: Abdominal twiddler's syndrome, 1084
Rohlfing BM, see Shanser JD
Rohrer GV, see Latshaw RF
Roland JM, see Udoff EJ
Rosato EF, see Freiman DB
Rosen RJ, Feldman L, Wilson AR: Embolization for postbiopsy renal arteriovenous fistula (c), 1072
Rosenberg SA, see Schaner EG
Rosenberger A, Adler O: Fine needle aspiration biopsy in the diagnosis of mediastinal lesions, 239
Rosenfield AT, see Crade M
-----, see Gold J
-----, see Robbins AH
-----, see Walsh JW
Rosengren JE, see deSantos LA
Rosoff L, see Freeny PC
Rosomoff HL, see Quencer RM
Rossi P, Passariello R, Simonetti G: Control of a traumatic vertebral arteriovenous fistula by a modified gianturco coil embolus system (c), 331
Rozanski R, see Kim SK
Rozanski RM, see Spirt BA
Rubin BE: Extravasation of thiodol into deep tissues of the foot: a complication of lymphangiography (c), 342
Rubin SA: Radiographic spectrum of pleuropulmonary tularemia, 277
Rudikoff JC, see Rumack CM
Rumack CM, McDonald MM, O'Mears OP, Sanders BB, Rudikoff JC: CT detection and course of intracranial hemorrhage in premature infants, 493
Rysavy JA, see Probst P

Sagar V, see Pecora DV
Sagel SS, see Lee JKT
-----, see Levitt RG
Sample WF, see Carroll B
Sanders BB, see Rumack CM
Sargent EN, Gordonson J, Jacobson G, Birnbaum W, Shaub M: Bilateral pleural thickening: a manifestation of asbestos dust exposure, 579
Sarwar M: Atlas of polytome pneumography: with particular reference to the midline ventricles of the brain (b), 754
Schaffer DL, see Wittenberg J
Schaner EG, Chang AE, Doppman JL, Conkle DM, Flye MW, Rosenberg SA: Comparison of computed and conventional whole lung tomography in detecting pulmonary nodules: a prospective radiologic-pathologic study, 51
Schatz SL, Kopits SE: Proximal femoral focal deficiency, 289
Schechter LS, see Balthazar EJ
Schey WL, see Patel DV
Schoenecker PL, see Gilula LA
Scholl DG: Atlas of gray scale ultrasonography (b), 947
Schroeder FM, Miller FJ Jr, Nelson JA, Rankin RS: Gastrointestinal angiographic findings in systemic amyloidosis, 143
Schrumpf JD, Sommer G, Jacobs FP: Bleeding simulated by the distal internal pudendal artery stain, 657
Schwartz PE, see Walsh JW
Seaman WB: The areae gastricae (e), 564
Seidelmann FE, see Haaga JR
Seigel R, see Kuhns LR
Selke AC Jr, Jona JZ: The hook sign in type 3 congenital colonic atresia (t), 350
Sewell DH, see Robbins AH
Seymour EQ: Aortoesophageal fistula as a complication of aortic prosthetic graft (c), 160
Shackelford GD, Siegel MJ, McAlister WH: Subglottic edema in acute epiglottitis in children, 603
-----, see Siegel MJ
Shafiepoor H, see Aliabadi P
Shanser JD, Korobkin M, Goldberg HI, Rohlfing BM: Computed tomographic diagnosis of obstructive jaundice in the absence of intrahepatic ductal dilatation, 389
Shaub M, see Sargent EN
Sheedy PF II, see Muhm JR
Shenoy SS, Culver GJ, Ali MV: Reply to "intraluminal duodenal diverticulum" (1), 556
Shinozaki T, see Gallant TE
Shirkhoda A, Mittelstaedt CA: Pancreatic cysts in adult polycystic disease by computed tomography and ultrasound (c), 1074
Sibala JL, see Chang CHJ
Siegel ME, Siemsen JK: A new noninvasive approach to peripheral vascular disease: thallium-201 leg scans, 827
Siegel MJ, McAlister WL, Shackelford GD: Radiographic findings in ovarian teratomas in children, 613
-----, see Shackelford GD
Siegelman SS, see Kaufman SL
Siemsen JK, see Siegel ME
Silver TM, see Wicks JD
Simeone J, see Walsh JW
Simon H, see Carlson DH
Simonetti G, see Rossi P
Slovis TL, Cushing B, Reilly BJ, Farnocki ZQ, Philippart AI, Berdon WE, Baker DH, Reed JO: Wilms' tumor to the heart: clinical and radiographic evaluation, 263
Smith EL, see Tailor CC
Smith TR, Friedman SN, Adler H: Streptococcus bovis septicemia as a clue to colon neoplasms in two cases (c), 887
Smith WH, see Osborn AG
Sniderman KW, Franklin J Jr, Sos TA: Successful transcatheter Gelfoam embolization of a bleeding cecal vascular ectasia (c), 157
-----, see Sos TA
Sommer G, see Schrumpf JD
Sos TA, Lee JG, Wixson D, Sniderman KW: Intermittent bleeding in acute massive gastrointestinal hemorrhage: arteriographic demonstration, 1015
-----, see Levin DC
-----, see Sniderman KW
Sostman D, see Gold J
Soto B, Pacifico AD, Souza AS Jr, Bargeron LM Jr, Ermocilla R, Tonkin IL: Identification of thoracic isomerism from the plain chest radiograph, 995
Souza AS Jr, see Soto B
Spiegel RM, King DL, Green WM: Ultrasonography of primary cysts of the liver, 235
Spigos DG, see Renigers SA
Spirt BA, Kagan EH, Rozanski RM: Sonolucent areas in the placenta: sonographic and pathologic correlation, 961
Sprayregen S, see Friedman AC
Stables DP, see Strauser GD
Stanley JC, see Walter JF
Stanley RJ, see Lee JKT
-----, see Levitt RG
Stark P, see McLoud TC
Steckel RJ, see Kagan AR
Stephens DH, see Muhm JR
Stephenson TF, Guzzetta LR, Tagulinao OA: CT-guided seldinger catheter drainage of a hepatic abscess (c), 323
Stevens PS, see Cuttino JT Jr
Stickney RH, Bjelland JC, Capp MP, Harrison RR, Hansen R: Chlamydia trachomatis: A cause of an infantile pneumonia syndrome (c), 914
Stokes NA, see Quencer RM
Strandberg JD, see Barth KH
Strauser GD, Stables DP, Weil R III: Optimal technique of renal arteriography in living renal transplant donors, 813
Sullivan KP, see Chang J
Swee RG, see Brown ML
Sybert VP: Pheochromocytomas in von Hippel-Lindau disease (1), 736

Taft DA, see Freeny PC
Tagulinao OA, see Stephenson TF
Tailor CC, Murphy WA, Smith EL: Intraarticular methyl methacrylate: a complication of hip surgery, 1055
Tan KM: Renal pseudocalculus (1), 928
Tatezawa T, Akisada M: Diffuse lymphatic dysplasia with hepatic oil embolism (c), 898
Taylor A, see Weissberg DL
Taylor KJW, see Crade M
-----, see Gold J
-----, see Walsh JW
Taylor KW, see Gray JE
Templeton AW, se Chang CHJ
Thompson WM, see Blum J
-----, see Limberakis AJ
Thornbury JR, see Cho KJ
-----, see Kuhns LR
Tikoff G, see Prescott SM
Tonkin IL, see Soto B
Trobaugh GB: Atlas of cardiovascular nuclear medicine (b), 1129
Troner M, see Pereiras RV

Udoff EJ, Roland JM, White RI Jr: Coronary artery anomaly in double-outlet right ventricle (c), 710
Ulreich S, Lund DA, Jacobson JJ: Spontaneous rupture of a calyceal diverticulum during urography (c), 337
-----, see Robbins AH
Unger GF, see Haughton VM
Uzzell B, see Zimmerman RA

Van Aman ME, Lloyd TV, Johnson JC: Focal perfusion defect caused by sequestration in two cases (c), 904
Van den Tweel JG, see Gordonson J
Van Zwalenburg BR: Clarence Peter Truog, 1901-1978 (o), 756
Velick WF, Bookstein JJ; Pheochromocytoma with reversible renal artery stenosis

(c), 1069
Viamonte M, see Pereiras RV
Vint VC, see Resnick D

Walker JH: Giant papilloma of the thoracic esophagus (c), 519
-----: Single-contrast/double-contrast GI (1), 1116
Wallace S, see Bernardino ME
-----, see Lindell MM Jr
Walsh JW, Rosenfield AT, Jaffe CC, Schwartz PE, Simeone J, Dembner AG, Taylor KJW: Comparison of ultrasound and computed tomography gynecologic pelvic masses, 955
Walter JF, Stanley JC, Mehigan JT, Reuter SR, Guthaner DF: External iliac artery fibrodysplasia, 125
Waltman AC, see Greenfield AJ
Weidner WA, see Latshaw RF
Weigel JW, see Bigongiari LR
Weil R III, see Strauser GD
Wein AJ, see Gefter WB
Weinstein A, see Haaga JR
Weinstein CJ, see Freeny PC
Weiss GH, see Chew E
Weissberg DL, Resnick D, Taylor A, Becker M, Alazraki N: Rheumatoid arthritis and its variants: analysis of scintiphotographic, radiographic, and clinical examinations, 665
Wendling L, see Bolender N
Wepfer JF, Boex RM: Mesonephric duct remnants (Gartner's duct), 499
Whalen JP, see Kleinman PK
White RI Jr, see Barth KH
-----, see Kaufman SL
-----, see Udoff EJ
White TT: Postcholecystectomy syndromes: a clinical approach to etiology, diagnosis, and management (b), 566
Wickenden RW, see Giustra PE
Wicks JD, Silver TM, Bree RL: Gray scale features of hematomas: an ultrasonic spectrum, 977
Widrich WC, Robbins AH, Nabseth DC, Johnson WC, Goldstein SA: Pitfalls of transhepatic portal venography and therapeutic coronary vein occlusion, 637
-----, see Chuang VP
Wilcox WA: Ultrasonography of the eye and orbit (b), 565
Williamson BRJ, see Lees RF
Wills JS, see Pollack HM
Wilson AR, see Rosen RJ
Wilson EA, see Fried AM
Wilson RA: Rare earth screens and silver (e), 926
Winter J: Efficiency of utilization of a computed tomography scanner, 89
Wisnant J, see Fried AM
Wittenberg J, Fineberg HV, Black EB, Kirkpatrick RH, Schaffer DL, Ikeda MK, Ferrucci JT Jr: Clinical efficacy of computed body tomography, 5
Wixson D, see Sos TA
Wochos JF, Fullerton GD, DeWerd LA: Mailed thermoluminescent dosimeter determination of entrance skin exposure and half-value layer in mammography, 617
Wolff M, see Casarella WJ
Wooten WB, Bernardino ME, Goldstein HM: Computed tomography of necrotic hepatic metastases, 839
-----, see deSantos LA
Wootton P: S.I. units in medicine (b), 763
Wyckoff HO: Spcial report: international system of units (SI), 536

Young SE, see Bernardino ME

Zaman MB, see Flehinger BJ
Zellis A, see Katzen BT
Zimmerman RA, Bilaniuk LT, Gennarelli T, Bruce D, Dolinskas C, Uzzell B: Cranial computed tomography in diagnosis and management of acute head trauma, 27
Zoronoza J, see Goldstein HM

Subject Index Volume 131

Index key: a = abstract, b = book review, c = case report, e = editorial ex = exhibit, l = letter, t = technial note

The majority of the subjects in the Journal can be classified readily as a disease entity, a diagnostic procedure or a treatment method. These can be brought together rationally in their application to some body part or region. Accordingly, the basic organization of this index is anatomic and, to the extent possible and convenient, entries are listed under a body part or region. Entities that affect more than one body part or disease, procedures, or methods for which there are numerous titles are given independent listing as well. Other subjects not readily referenced anatomically are listed alphabetically. Original articles, abstracts of literature, book reviews, and editorials are indexed. News items and books received are not listed. A given entry will be listed at least once, often twice, and occasionally three times. For brevity, titles of articles and abstracts are often permuted.

A

Abdomen, see also pelvis; specific organ
  Anterior pathway for transdiaphragmatic extension of pneumomediastinum, 271
  Benign pneumoperitoneum following median sternotomy incision, 267
  Clinical efficacy of computed body tomography, 5
  Computed body tomography in children, 21
  Congenital pneumoperitoneum anomalies in umbilical region (a), 190
  Diagnostic oncology case studies: investigation of bloody ascites, 697
  Dysgerminoma presenting as calcified mass with hypercalcemia (a), 936
  External landmarks related to vertebral segments, 115
  Fluoroscopically guided thin needle aspiration biopsy of retroperitoneum and, 197
  Imperforate anus and colon calcification with prune belly syndrome (a), 759
  Medical efficacy of CT of chest and, 15
  Multiple radionuclide scanning in differentiation of lesions (a), 1127
  Total body opacification (e), 919
  Twiddler's syndrome (c), 1084
Abscess see also specific organ, region
  Bile leak into hepatic, demonstration with Tc-diethyl-iminodiacetic acid (c), 889
  Brain, angiographic diagnosis (a), 561
  CT medical efficacy of chest and abdomen, 15
  Hepatic, CT-guided Seldinger catheter drainage (c), 323
  Nonamebic liver, endoscopic retrograde cholangiography (a), 559
Accelerators, see therapeutic radiology, technique
Achalasia, see stomach
Acinus, see lung
Acrocephalosyndactyly, see bone, dysostoses; skull
ACTA scanner, see computed tomography
Addison's disease, see adrenals
Adenoma, see specific organ, region
Adrenals
  Cortical tumors of, with low attenuation coefficients, CT (a), 1127
  CT of normal suprarenal glands (a), 944
  Pheochromocytoma with reversible renal artery stenosis (c), 1069
  Pheochromocytomas in von Hippel-Lindau disease (l), 736
  Remote effects of neuroblastoma, 299
  Ultrasonography (a), 760
Aganglionosis, see colon
Alzheimer's disease, see brain
American College of Radiology
  Special report: diagnostic efficacy studies, 173
American Roentgen Ray Society
  Comprehensive meeting information: president's invitation (e), 737
  Section on instruction: courses scheduled for 1979 annual meeting, 739
  From earlier pages, 1111
  1979 meeting, Toronto, 180; 929
Amyloidosis
  Gastrointestinal angiography in systemic, 143
Anastamoses, see arteries
Aneurysm, see also specific artery; aorta; heart
  Mycotic, protean manifestations, 1019
  Pseudoaneurysm of arterial anastomosis in renal transplant (c), 525
  Ulnar artery, angiographic considerations, 1093
Anger camera, see radionuclide imaging
Angiocardiography, see heart
Angiography, see also specific organ, artery
  Bleeding simulated by internal pudendal stain, 657
  Gastrointestinal (b), 364
  Intermittent bleeding in acute massive gastrointestinal hemorrhage, 101E
Angiography, complications
  Catheter cerebral arteriography: I. criteria, incidence, 861
  Catheter cerebral arteriography: II. rates and diagnoses, 867
  Catheter cerebral arteriography: III. arteries, contrast medium, duration, age, 871
  CT of retroperitoneal hemorrhage after translumbar, 831
  Foreign body embolization of retinal arteries complication of carotid (a), 1125
  Intraarterial lidocaine in arteriography (c), 906
  Renovascular hypertension after umbilical arterial catheterization (a), 558
  Supine phlebography, 821
Angiography, embolism therapy
  Gelfoam, bleeding cecal vascular ectasia (c), 157
  Occlusion of arterial supply to arteriovenous fistulas with Gianturco coils, 1027
  Postbiopsy renal arteriovenous fistula (c), 1072
  Prevention of reflux using baloon catheters, 651
  Transcatheter, posttraumatic bleeding, 645
  Vertebral arteriovenous fistula control by Gianturco coil (c), 331
Angiography, technique
  Aortofemoral flow-directed balloon catheterization, 823
  Axial cineangiography in congenital heart disease: I. technical and anatomic considerations (a), 185
  Axial cineangiography in congenital heart disease: II. specific lesions (a), 359
  Complications of cerebral: III. assessment of arteries, contrast medium, procedure, age, 871
  Contralateral compression in carotid (a), 188
  Extended indications for carboxyangiography (a), 185
  High-dose pharmacoangiography in hypovascular renal neoplasms, 807
  Improved splenoportography by plugging needle tract, 445
  Intraarterial nitroprusside treatment for ergotism (c), 1090
  Modified punch card to extend program of puck changer (t), 534
  Renal transplant donors, 813
  Right posterior oblique projection in hypertension (a), 557
  Translumbar aortography (e), 733
  Transparent head support for magnification cerebral (t), 1096
  Vascular reactions to steel coil occlusion devices, 455
Ankle
  Ligamentous anatomy of (a), 187
Antrum, see stomach
Anus
  Imperforate, and colon calcification with prune belly syndrome (a), 759
Aorta
  Abdominal, in spina bifida cystica (a), 557
  Acute traumatic rupture of, displacement of nasogastric tube (a), 185
  Aortoesophageal fistula complication of prosthetic graft (c), 160
  CT detection of infected synthetic grafts, 317
  CT of retroperitoneal hemorrhage after translumbar aortography, 831
  Flow-directed balloon catheterization for aortofemoral arteriography, 823
  Subclavian artery as first branch of (c), 721
  Translumbar aortography (e), 733
Aortic arch, see aorta
Aqueduct of Sylvius, see brain
Aqueduct, vestibular, see ear
Arachnoid, see also meninges; brain
  Arachnoiditis produced by meglumine iocarmate and metrizamide myelography, 129
  Spinal cysts in children (a), 362
Arnold-Chiari malformation, see brain
Arteries, see also angiography; arteriovenous malformation; thrombosis; specific artery, organ, region
  Complications in expanded polytetrafluoroethylene grafts: angiography, 817
  Gastrointestinal angiography in systemic amyloidosis, 143
  Intraarterial nitroprusside treatment for ergotism (c), 1090
  Noninvasive approach to peripheral vascular disease, thallium-201 leg scans, 827
  Origin of left gastric (a), 757
  Systemic air embolism secondary to respiratory therapy in neonate, 425
  Ulnar aneurysms: angiographic considerations, 1093
Arteries, cerebral, see also brain, blood vessels; cerebral

angiography
Pseudoocclusion of superficial temporal-middle bypass (c), 162
Arteries, coronary, see coronary arteries
Arteries, femoral
Abnormal distribution of thallium-201 due to arteriosclerosis (c), 718
Flow-directed balloon catheterization for, arteriography, 823
Intraarterial nitroprusside treatment for ergotism (c), 1090
Arteries, iliac
External fibrodysplasia, 125
Arteries, pulmonary, see pulmonary arteries
Arteries, subclavian
First branch of aorta (c), 721
Arteries, vertebral
Control of fistula by Gianturco coil embolus (c), 331
Arteriosclerosis, see also specific blood vessel
Abnormal peripheral distribution of thallium-201 (c), 718
Evaluation of suspected deep venous thrombosis (c), 531
Noninvasive approach: thallium-201 leg scans, 827
Arteriovenous malformation
Control of vertebral fistula by Gianturco coil embolus (c), 331
Diaphragm and lung (c), 507
Embolization for postbiopsy renal fistula (c), 1072
Transcatheter occlusion of arterial supply to fistulas with Gianturco coils, 1027
Arthritis, see also spine; specific joint
Juvenile ankylosing spondylitis (a), 187
Lead intoxication and, of hip from bullet fragments (a), 361
Sterno-manubrial articulation in ankylosing spondylitis and Reiter's syndrome (a), 361
Arthritis, rheumatoid
Scintiphotographic, radiographic, and clinical examinations, 665
Arthrography, see also specific joint
Hip (b), 948
Treatment by shoulder, 1047
Asbestos
Bilateral pleural thickening, 579
Ascites
Diagnostic oncology case studies: investigation of bloody, 697
LeVeen type peritoneovenous shunts (t), 916
Aseptic necrosis, see bone or part
Aspergillosis, see also organ
Miliary, alcoholism (c), 707
Astrocytoma, see brain, neoplasm
Atomic bomb and atomic energy, see radiation
Atrial septal defect, see heart, congenital abnormalities
Atrium, see heart
Auditory canal, see ear
Aurelius, J. Richards, 1897-1977 (o), 756
Azygography, see venography

B

Basal cell nevus syndrome, see bone, dysostoses
Bayley, Howard G., 1914-1978 (o), 1119
Beryllium
Reversible respiratory disease in workers (a), 1121
Bile ducts, see also cholangiography; gallbladder
CT diagnosis of obstructive jaundice in absence of intrahepatic dilatation, 389
Gas (pneumobilia) in emphysematous cholecystitis, 661
Percutaneous transhepatic cholangiography (t), 171
Postcholecystectomy syndromes: clinical approach to etiology, diagnosis, and management (b), 566
Radiology of gallbladder and bile ducts (b), 364
Bile ducts, obstructions
Percutaneous transhepatic drainage (a), 558
Bile ducts, ultrasound
Biliary duct ultrasound (1), 556
Normal and dilated biliary tree (a), 760
Biliary tract, see bile ducts; gallbladder; liver
Biopsy, see also specific organ
Fine needle aspiration, mediastinal lesions, 239
Fluoroscopically guided thin needle aspiration, of abdomen and retroperitoneum, 197
Multinodular primary amyloidosis of lung: needle (c), 1082
Bird fancier's disease, see lung, diseases
Bladder
Diverticula of, in children (a), 1126
Quantitation of split renal function in children followed for vesicoureteric reflux by gamma camera (a), 1127
Bone, see also specific bone or disease
Clinical efficacy of computed body tomography, 5
CT of musculoskeletal disorders, 55
Fracture healing biology in long (a), 1124
Bone, developmental abnormalities
International nomenclature of constitutional diseases of bone, 352
Proximal femoral focal deficiency, 289
Bone, diseases
Findings in commercial divers (a), 361
Idiopathic multicentric osteolysis (a), 1123
Scintigraphy in osteonecrosis (a), 362
Bone, dysostoses
International nomenclature of constitutional diseases of bone, 352
Neonatal death dwarfism (a), 1126
Bone, growth and development
Changes in mineral density during growth (a), 543
Growth lines in psychosocial dwarfs and idiopathic hypopituitarism, 477
Bone, infection
Anerobic bacteria and (a), 936
Bone, marrow
Histopathologic studies of the liver following intravenous colloidal ^{198}Au therapy (a), 363
Bone, metabolic abnormalities
Bone calcium by local neutron activation of hand; correlation with absorptiometry and histomorphometry (a), 550
Bone mineral content after surgical treatment of primary hyperparathyroidism (a), 544
Childhood renal disease (a), 544
Etiological factors in osteoporosis using femoral trabecular pattern index (a), 551
International nomenclature of constitutional diseases of bone, 352
Microradioscopic morphometry of intracortical resorption in hand bones: normals and chronic renal failure patients (a), 551
Oophorectomized monkeys (a), 546
Photon absorptiometry in metabolic bone diseases (a), 543
Postmenopausal women (a), 543
Primary hyperparathyroidism (a), 552
Radiographic photodensitometry and maintenance hemodialysis (a), 552
Radiogrammetric and absorptiometric measurements in bone-losing patients (a), 551
Secondary hyperparathyroidism associated with chronic renal disease (a), 187
Bone, mineral measurement
Analysis of two 99m-Tc-Sn-diphosphonates with different binding characteristics (a), 553
Automatic image analysis of bone biopsies: digital processing (a), 549
Ballet dancing and weight lifting--effects (a), 541
Bibliography of methods of tissue and, using radiation absorption and scattering (a), 540
Bone mass and soft tissue, in acromegaly (a), 543
Calcium content analysis in vivo with CT (a), 548
Childhood renal disease (a), 544
Clinical applicability of, by photon absorptiometry (a), 541
Clinical experience with Bonn x-ray bone scanner (a), 544
Compton scattering (a), 546
Compton scattering, progress in (a), 546
Correlation between calcium concentration of bones and CT numbers (a), 547
CT of bone changes in lower extremities of human amputees (a), 547
Data using isowidth and percentile curves (a), 541
Densitometry of cortical bone by CT (a), 547
Direct photon absorptiometry in small infants (a), 542
Dual photon absorptiometry system: HpGe detector and microprocessor controller (a), 540
Elderly vegetarian females (a), 542
Etiological factors in osteoporosis using femoral trabecular patterns index (a), 551
Exponential bone loss in postmenopausal women (a), 543
Gamma-ray CT analysis of trabecular and compact bone: estrogen, testosterone, growth hormone in children (a), 547
Gamma photon-absorptiometry and radiogrammetry (a), 551
Hindlimb densitometry in normal beagle dogs (a), 545
Histomorphometry and noninvasive methods of (a), 549
Increase in, after surgical treatment of primary hyperparathyroidism (a), 544
$1,25(OH)_2D_3$ in patients with renal osteodystrophy (a), 545
Lithium-treated manic depressive patients (a), 543
Mass in blacks (a), 541
Microradioscopic morphometry of intracortical resorption in hand bones in normals and chronic renal failure patients (a), 551
Multiple energy CT (a), 548
Neutron activation analysis of partial body calcium using californium-252 (a), 550
Numerical filtering for error elimination by finite photon beam size (a), 540
Oophorectomized monkeys (a), 546
Paget's disease (a), 543
Partial body calcium measurements by IVNAA in long-term studies (a), 550

Patients on hemodialysis and following renal transplantation (a), 543
Photodensitometry cortical index comparison with (a), 552
Photodensitometric evaluation of bone fracture repair (a), 552
Photon-absorptiometric and histomorphometric measurements (a), 541
Photon absorptiometry in hemodialysed and transplant patients in Newcastle upon Tyne (a), 545
Photon absorptiometry in metabolic bone diseases (a), 543
Photon absorptiometry in New Zealand white rabbit (a), 546
Photon absorption profiles and influence of fat on (a), 540
Postnatal, in infants (a), 542
Primary hyperparathyroidism (a), 552
Quantification in growing rats by gamma-ray CT (a), 547
Quantitation of experimental fracture mineralization (a), 545
Quantitative CT (a), 548
Quantitative microradiographic studies of mineralization of bone tissue (a), 549
Radiogrammetric and absorptiometric measurements in bone-losing patients (a), 551
Radiographic photodensitometry and maintenance hemodialysis (a), 552
Report on 1976 and 1978 symposia on (a), 541
Serial measurements of density during growth (a), 543
Single source Compton scattering methods (a), 547
Size of body and mass (a), 541
Skeletal calcium using californium-252 source (a), 550
Spinal, by CT in patients, controls, phantoms (a), 548
99m-Tc HEDP at 24 hr index of metabolic bone disease (a), 553
Thyrocalcitonin effect on ^{18}F uptake in spinal cord injuries (a), 553
Total-body calcium with radiographic photodensitometry and photon absorptiometry measurements (a), 551
Vertebral mineral by CT scanning (a), 549
X-ray bone densitometer (a), 546
Bone, mineralization
Bone calcium by local neutron activation of hand; correlation with absorptiometry and histomorphometry (a), 550
Bone, mutable abnormalities
Bone mineral content of patients on hemodialysis and following renal transplantation (a), 543
Effect of $1,25(OH)_2D_3$ in patients with renal osteodystrophy (a), 545
Photon absorptiometry in hemodialysed and transplant patients (a), 545
Bone, neoplasm
Aneurysmal bone cyst (a), 187
CT of tumors of musculoskeletal system in children (a), 935
Osteogenic sarcoma after age 50, 481
Periosteal chondromas of anterior tibial tubercle (c), 1088
Bone, radionuclide scanning
Scintigraphy in diagnosis of osteonecrosis (a), 362
Book reviews
Advances in radiation biology, 765
Atlas of brain anatomy for CT scans using EMI terminology, 191
Atlas of cardiovascular nuclear medicine, 1128
Atlas of gray scale ultrasonography, 947
Atlas of polytome pneumography: with particular reference to the midline ventricles of the brain, 764
Breast carcinoma: the radiologist's expanded role, 946
Clinical pediatric oncology, 565
Clinical radiobiology, 365
Coronary artery surgery, a critical review, 565
Craniovertebral region in chronic inflammatory rheumatic diseases, 947
Cross-sectional anatomy--an atlas for CT, 764
CT of the human body: an atlas of normal anatomy, 564
Current concepts in pediatric radiology, 947
Diagnosis of diseases of the chest, 1128
Emmett's clinical urography, 763
Fundamental physics of radiology, 566
Gallium-67 imaging, 1129
Gastrointestinal angiography, 364
Guide for automatic radiographic processing and film quality control, 1128
Handbook of clinical nuclear medicine, 364
Lymphoid system. Methods of clinical investigations, 566
Mediastinum: radiologic correlations with anatomy and pathology, 191
Medical cyclotrons in nuclear medicine, 1129
Neuroradiology case studies: 110 case histories related to neuroradiology, 764
New methods in tumor localization, 763
Obstetrical diagnosis by radiographic, ultrasonic, and nuclear methods, 765
Orbit roentgenology, 192
Pediatric radiology, 193
Pineal tumors, 192
Postcholecystectomy syndromes: a clinical approach to etiology, diagnosis, and management, 566
Practical approach to modern x-ray equipment, 565
Progress in pediatric radiology, vol 6. Skull, spine and contents, 946
Radiation protection in dentistry, 949
Radiologic examination of the orohypopharynx and esophagus, 1130
Radiology of the gallbladder and bile ducts, 364
Radiology of the liver, 1130
Review of NCRP radiation dose limit for embryo and fetus in occupationally-exposed women
S.I. units in medicine, 763
Soft tissues of the extremities. A radiologic study of rheumatic disease, 1130
Synopsis of radiographic anatomy with computed tomography, 949
Technologist's guide to mammography, 191
Ultrasonics in clinical diagnosis, 193
Ultrasonography of the eye and orbit, 565
Understanding radiography, 949
Xeroradiography in otorhinolaryngology, 948
Bowel, see colon; intestine; gastrointestinal tract
Brachydactyly, see bone, dysostoses
Brachytherapy, see therapeutic radiology
Brain, see also arachnoid; computed tomography, cranial; cerebral angiography; meninges
Angiographic diagnosis of abscesses (a), 561
Atlas of polytome pneumography: with particular reference to the midline ventricles of the brain (b), 764
Neuroradiology case studies: 110 case histories related to neuroradiology (b), 764
Progess in pediatric radiology, vol. 6. Skull, spine and contents (b), 946
Protean manifestations of mycotic aneurysms, 1019
Brain, angiography, see also cerebral angiography
Abscesses (a), 561
Brain, blood vessels
CT in patients with cerebrovascular disease, 35
Pseudoocclusion of superficial temporal-middle cerebral artery bypass (c), 162
Transfemoral selective angiography in cerebral ischaemic disease (a), 1124
Brain, computed tomography
Atlas of brain anatomy for CT scans using EMI terminology (b), 191
Cerebrovascular disease, 35
Computer reconstructed sagittal and coronal scans: applications in pediatric neurological disorders (a), 1125
Contrast enhancement in cerebral infarction, 881
Detection of cerebrospinal fluid fistula (c), 344
Diagnosis and management of acute head trauma, 27
Effect of size, histologic elements and water content on visualization of cerebral infarcts (a), 936
Efficacy of, and health costs, 45
Evaluation of brain death by contrast enhanced (a), 936
Extracerebral fluid collections, 107
Frontal and lateral views reconstructed from EMI axial slices (a), 188
Impact on diagnosis of hydrocephalus, 41
Indications and accuracy, 875
Intracranial hemorrhage in premature infants, 493
Middle fossa arachnoid malformations (a), 1124
Noncontrast, in suspected brain tumor (a), 362
Pediatric head trauma (a), 362
Primary malignant lymphomas (a), 1125
Protocol for contrast enhancement in (a), 561
Radionuclide imaging and, in evaluation of ischemic stroke (a), 362
Sign of subarachnoid bleeding in pediatric head trauma patients (a), 362
Spontaneous intracerebral hematomas (a), 1124
Brain, cysts, see brain, neoplasm; computed tomography, cranial
Brain, hemorrhage
CT in premature infants, 493
Brain, infarction
CT contrast enhancement, 881
CT evaluation of size, histologic elements, and water content on visualization of (a), 936
CT in patients with cerebrovascular disease, 35
CT and radionuclide imaging in evaluation of ischemic stroke (a), 362
Transfemoral selective angiography in investigation of cerebral ischemic disease (a), 1124
Brain, neoplasm
Abnormal CT scans in asymptomatic children with acute lymphocytic leukemia (a), 761
CT in primary malignant lymphomas (a), 1125
Lipoma of corpus callosum with frontal bone defect (c), 517
Malignant melanoma metastatic to central nervous system (a), 1125
Medulloblastomas demonstrated by CT (a), 188

Noncontrast CT scanning in suspected brain tumor (a), 362
Pheochromocytomas in von Hippel-Lindau disease (1), 736
Pineal tumors (b), 192
Radiation therapy of brain-stem tumors compared with pinealoma (a), 363
Radiologic modalities in acoustic neurilemomas (a), 189
Remote effects of neuroblastoma, 299
Brain, radionuclide imaging
CT and, in evaluation of ischemic stroke (a), 362
Breast, see also mammography
Age at first pregnancy and breast parenchymal pattern (a), 562
Angiography of (a), 363
Cytologic evaluation of cysts (a), 944
Breast, neoplasm
Accuracy of mammography (a), 190
Breast carcinoma: radiologist's expanded role (b), 946
CT evaluation of, 459
Estrogen receptors and response to chemotherapy in (a), 760
Gastrointestinal manifestations of (a), 758
Parenchymal patterns as risk indicators for cancer, 1031
Radiology of tumors in male (a), 190
Breast, radiography, see mammography
Bronchi, see also lung
Atresia (a), 757
Bronchography in congenital cystic bronchiectasis, 255
Bursa, see specific joint

C

Caffey's disease, see bone, diseases
Calcification, see specific disease, organ, or region
Cancer, see neoplasm; therapeutic radiology; radiation biology; specific organ, region, and neoplasm
Carotid artery, see arteries; cerebral angiography
Cataract, see eye
Cathartics, see colon
Cauda equina, see spinal cord
Cavography, see venae
Cecum, see colon
Cephalhematoma, see skull
Cephalometry, see skull
Cerebellopontine angle, see brain
Cerebral angiography, see also brain; brain, angiography; brain, neoplasm; specific blood vessel
Complications. I. Criteria and incidence, 861
Complications. II. Relation to clinical and arteriographic diagnoses, 867
Complications. III. Assessment of arteries injected, contrast medium used, duration of procedure and patient age, 871
Foreign body embolization of retinal arteries, complication of carotid (a), 1125
Transfemoral selective in cerebral ischaemic disease (a), 1124
Transparent head support for magnification (t), 1096
Cerebral arteries, see brain; arteries, cerebral
Cerebral palsy, see body parts
Cervix, see uterus
Chemotherapy, see also specific drug
Estrogen receptors and response to chemotherapy in metastatic breast cancer (a), 760
Pulmonary complications of renal transplantation: low-dose immunosuppression (a), 184
Pulmonary, pleural and thoracic changes complicating (a), 184
Procarbazine lung (c), 527
Quantification of differential sensitivity of human-tumor stem cells to anticancer drugs (a), 945
Radiation induced cycling activity and chemosensitivity of normal tissues (a), 944
Chest, see thorax; specific organ
Chloroquine, see chemotherapy
Cholangiography, see also bile ducts; gallbladder
Erect position in percutaneous transhepatic (t), 171
Pancreatic duct obstruction observed during transhepatic (c), 521
Cholangitis, see bile ducts
Cholecystitis, see gallbladder
Choledochal cyst, see bile ducts
Cholografin, see cholangiography
Chondroblastoma, see bone, neoplasm
Chondrosarcoma, see bone, neoplasm
Choroid plexus, see brain
Coccyx
Coccygeal ribs (c), 164
Colitis
Cathartic (c), 1079
Double contrast barium enema in Crohn's disease and ulcerative, 207
Collimators, see radiography, apparatus
Colon, see also gastrointestinal tract; colitis
Calcifications in small bowel of infants with total aganglionosis (a), 759
Cathartic colitis (c), 1079
Clean colon: whose responsibility? (1), 182
Colitis cystica profunda (c), 529
Gelfoam embolization of bleeding cecal vascular ectasia (c), 157
Hook sign in type 3 congenital atresia (t), 350
Imperforate anus and, calcification with prune belly syndrome (a), 759
Ischemic colitis and stricture after hemolytic-uremic syndrome (a), 562
Lower digestive tract severe hemorrhage: emergency arteriography (a), 932
Prophylactic doxycycline for traveler's diarrhea (a), 758
Radiology of ileosigmoid knot (a), 1122
Radiology of neonatal necrotizing enterocolitis (a), 1126
Retractile mesenteritis as colonic obstruction (a), 186
Strongyloides stercoralis (a), 758
Colon, neoplasm
Colorectal tumors: pathology and detection, 691
Leukemic infiltration (c), 725
Leukemic infiltration of large bowel (c), 723
Polyposis and cancer, 1065
Resection and anastomosis following preoperative irradiation of rectosigmoid (a), 761
Streptococcus bovis septicemia as clue to (c), 887
Colon, radiography
Double contrast barium enema in Crohn's disease and ulcerative colitis, 207
ECG changes during barium enema: protective role of B-receptor blocking agents (a), 360
Colonoscopy, see endoscopy
Computed tomography
Absorption values by filtering accuracy, 103
Body, in children, 21
Breast, 459
Clinical efficacy of body, 5
Comparison of radiation dose and resolving power of commercial scanners, 95; erratum, 735
Cost and efficacy implications, 81
Cross-sectional anatomy--an atlas for CT (b), 764
CT of the human body: an atlas of normal anatomy (b), 564
Efficacy of CT-assisted 2-dimensional treatment planning, 75
Efficiency of scanner use, 89
Evaluation: achievement and challenge (e), 1
Medical efficacy of, in chest and abdomen, 15
Musculoskeletal disorders, 55
Noise on detectability of test objects, 681
Patient and personnel exposures (a), 362
Radiation dose and resolving power of commercial scanners, 95
Sagittal of orbit (t), 346
Subcutaneous metastases (a), 1127
Computed tomography, abdominal
Accuracy in detecting intraabdominal and pelvic adenopathy in lymphoma, 311
Adrenal cortical tumors with low attenuation coefficients: pitfall (a), 1127
Children: evaluation of 45 patients, 21
Circumcaval ureter (c), 1086
Clinical efficacy, 5
Comparison of ultrasound and, in gynecologic pelvic masses, 955
Conventional whole lung tomography, and, in detecting pulmonary nodules, 51
CT-guided Seldinger catheter drainage of hepatic abscess (c), 323
Diagnosis of obstructive jaundice in absence of intrahepatic ductal dilatation, 389
Diagnostic oncology case studies: bloody ascites, 697
Hepatic tumor demonstration with iodinated fat emulsion (a), 186
Infected synthetic grafts, detection, 317
Lymphography vs. CT of lymphomas (1), 1116
Lymph node metastases from pelvic cancers, 675
Lymphomas, treatment, 69
Medical efficacy of chest and, 15
Necrotic hepatic metastases, 839
Neoplastic involvement of mesentery and omentum, 835
Nuclear imaging and, of liver (a), 1122
Pancreatic cystadenocarcinoma: gray scale ultrasound and, appearance (c), 339
Pancreatic cysts in adult polycystic disease by ultrasound and (c), 1074
Renal transplant problems (a), 560
Retroperitoneal hemorrhage after translumbar aortography, 831
Surgical pancreatic emergencies (a), 1122
Tumor thrombosis of renal vein and inferior vena cava, 843
Whole-body scanning in pediatric radiology (a), 759
Computed tomography, cranial
Abnormal scans in asymptomatic children with acute lymphocytic leukemia (a), 761
Brain death evaluation (a), 936
Cerebrospinal fluid fistula detection (c), 344

Cerebrovascular disease: impact on patient care, 35
Computer reconstructed sagittal and coronal scans: applications in pediatric neurological disorders (a), 1125
Contrast enhancement in cerebral infarction, 881
Coronal: indications and accuracy, 875
Diagnosis and management of acute head trauma, 27
Efficacy and health costs, 45
Extracerebral fluid collections, 107
Frontal and lateral views reconstructed from EMI axial slices (a), 188
Impact on diagnosis of hydrocephalus, 41
Intracranial hemorrhage in premature infants, 493
Medulloblastomas (a), 188
Middle fossa arachnoid malformations (a), 1124
Noncontrast scanning: limited value in suspected brain tumor (a), 362
Optimal contrast dosage, 687
Pediatric head trauma: acute general cerebral swelling (a), 362
Primary malignant lymphomas (a), 1125
Protocol for contrast enhancement (a), 561
Radionuclide and, in ischemic stroke (a), 362
Sign of subarachnoid bleeding in pediatric head trauma patients (a), 362
Size, histologic elements, and water content on visualization of cerebral infarcts (a), 936
Spontaneous intracerebral hematomas (a), 1124
Computed tomography, skeletal
Bone changes in lower extremities of human amputees (a), 547
Calcium concentration of bone correlation and CT numbers (a), 547
Calcium content analysis in vivo (a), 548
Densitometry of cortical bone (a), 547
Gamma-ray CT analysis of trabecular and compact bone: treatment with estrogen, testosterone and growth hormone in children (a) 547
Multiple-energy CT for measurement of bone mineral content (a), 548
Postoperative bony stenosis of lumbar spinal canal: 164 symptomatic patients, 1059
Quantification of bone mineralization in growing rats by gamma-ray CT (a), 547
Quantitative (a), 548
Spinal bone mineral determination in patients, controls, and phantoms (a), 549
Tumors of musculoskeletal system in children (a), 935
Vertebral mineral (a), 549
Computed tomography, technique
Contrast enhancement in cranial (a), 561
Coronal, 875
Easy coronal (t), 535
Noise on detectability of test objects, 681
Optimal contrast dosage, 687
Computed tomography, thoracic
Clinical efficacy, 5
Conventional whole lung tomography and, in detecting pulmonary nodules, 51
Lung density measurement (a), 1121
Medical efficacy of chest and abdomen, 15
Pericardial cysts (c), 515
Pulmonary nodule detection, 981
Radiotherapy of lung cancer and, 63
Solitary pulmonary nodules: scanning times longer than breath holding (a), 1121
Contrast media
Contrast-induced acute renal failure (e), 1113
Drip infusion urography with meglumine iodamide, 1043
New water-soluble iodinated myelographic medium with reduced convulsive effects (a), 561
Severe reactions by three consecutive routes (c), 509
Coronary arteries, see also heart
Anomaly in double outlet right ventricle (c), 710
Cineangiography, left ventriculography, and ^{201}Tl-scintigraphy relationships (a), 363
First decade of aortocoronary bypass grafting, 1967-1977. A review (a), 359
Neovascularity and fistula formation, sign of mural thrombus (a), 185
Surgery: a critical review (b), 565
Underfilled: pre- and postoperative observations on recipient arterial quality and left ventricular function after surgery of (a), 359
Ventricular, pulmonary, and abnormalities with rupture of interventricular septum, 571
Corpus callosum, see brain
Cowper's duct, see urethra
Craniofacial dysostosis, see bone, dysostoses
Craniopharyngioma, see brain, neoplasm
Craniosynostosis, see bone, dysostoses
Crohn's disease
Double contrast barium enema in ulcerative colitis and, 207
Radiologic and clinical assessment of broad-spectrum antibiotic therapy in, 787
Regional enteritis in children: small bowel disease with normal terminal ileum (a), 943
Crouzon's disease, see bone, dysostoses
Cushing's syndrome, see also pituitary
Selective transsphenoidal resection of pituitary microadenomas (a), 761
Cyclotrons, see therapeutic radiology; specific radionuclide
Cystic fibrosis, see specific organ
Cystography, see bladder; radiography
Cystourethrography, see bladder; radiography; urethra
Cysts, see specific organ or region

D

Deafness, see ear
Delta scanner, see computed tomography
Design of radiological facilities, see radiology, practice
Desmoid tumor, see neoplasm
Diaphragm
Arteriovenous malformation of lung and (c), 507
Congenital partial eventration of left, 417
Large hiatus hernias in infancy and childhood (a), 943
Dietz, M. Wendall, 1922-1977 (1), 755
Diphosphonate, see specific organ or region
Dislocation, see also specific joint
Lisfranc's fracture-dislocation: manifestation of peripheral neuropathy, 139
Diverticulitis, see colon
Diverticulum, see organ
Doppler ultrasound, see ultrasound
Dosimetry
CT: comparison of radiation dose and resolving power of commercial CT scanners, 95; erratum, 735
Exposures to patient and personnel in CT (a), 362
International system of units (e), 536
S.I. units in medicine (b), 763
Thermoluminescent dosimeter determination of exposure in mammography, 617
Ductus arteriosus, see heart
Duodenum, see also gastrointestinal tract; intestine
Acute upper gastrointestinal hemorrhage (a), 559
Dose response to glucagon during hypotonic radiography (a), 759
Esophageal and, atresia and gastric distention (c), 167
Giant ulcers (a), 934
Glucagon double-blind radiographic study for hypotonic duodenography (a), 933
Intraluminal diverticulum (1), 556
Radiology and endoscopy comparison in diagnosis of ulcers (a), 933
Sonography of atresia in utero (c), 701
Tuberculosis (c), 329
Dura mater, see meninges

E

Ear
Ceruminous tumor of jugular foramen (a), 189
Incudostapedial joint, 307
Echinococcosis, see specific organ or region
Echocardiography, see heart, ultrasound
Editorials
Areae gastricae, 554
Authors of scientific articles and the copyright act of 1976, 355
Contrast-induced acute renal failure, 1113
Evaluation of CT: achievement and challenge, 1
From earlier pages, 181, 734, 1111
Rare earth screens and silver, 926
Translumbar aortography, 733
Education
ARRS section on instruction: 1979 annual meeting, 739
Pathologic index for arrangement of teaching file (t), 918
Effusion, see specific region
Electron beam therapy, see therapeutic radiology
Electronic imaging, see radiography
Embolism, see also thrombosis
Nonfatal pulmonary air (c), 703
Suspected pulmonary, and negative pulmonary arteriogram, patient course (a), 757
Systemic air, secondary to respiratory therapy in neonate, 425
Embolism, therapeutic
Carcinoid syndrome treated by hepatic embolization (c), 511
Gelfoam embolization of bleeding cecal vascular ectasia (c), 157
Transcatheter embolization of posttraumatic bleeding, 645
Transcatheter embolization: prevention of reflux using balloon catheters, 651

Vascular reactions to steel coil occlusion devices, 455
Vertebral arteriovenous fistula control by Gianturco coil embolus (c), 331
EMI scanner, see computed tomography
Encephalography, see brain
Endoscopic retrograde cholangiography, see also organ
Nonamebic liver abscesses (a), 559
Endoscopy
Acute upper gastrointestinal hemorrhage (a), 559
Comparative study: radiology, and, in duodenal ulcer diagnosis (a), 933
Enteritis, see intestine
Enterocolitis, see colon; intestine
Ependymoma, see brain, neoplasm
Epidermoids, see skull; brain
Epiglottis
Subglottic edema, 603
Erratum
Comparison of radiation dose and resolving power of commercial CT scanners (95), 735
Epstein, Bernard S. 1908-1978 (o), 1119
Esophagus, see also stomach
Aortoesophageal fistula complication of prosthetic graft (c), 160
Carcinoma of head and neck with cancer of, 791
Changing concepts of anatomy of lower: 430 B.C.-1977, 373
Duodenal and, atresia and gastric distention (c), 167
Foreign body: cause of stridor (a), 562
Giant papilloma of thoracic (c), 519
Large hiatus hernias in infancy and childhood (a), 943
Radiologic examination of orohypopharynx and (b), 1130
Technetium-99m pertechnetate as indicator of gastric mucosal proliferation, 1041
Tracheal collapse following atresia repair (a), 189
Transhepatic portal venography and therapeutic coronary vein occlusion, 637
Trauma (a), 757
X-ray diagnosis of cancer (a), 559
Exophthalmos, see eye; orbit
Eye
CT in ocular neoplastic disease, 111
Ultrasonography or orbit and (b), 565

F

Fabry's disease, see intestine
Falx cerebri, see meninges
Feil-Klippel syndrome, see bone, dysostoses
Femur
Osteochondritis dissecans of distal (a), 560
Proximal focal deficiency, 289
Fibrinogen
^{131}I-labeled, in deep vein thrombosis, 451
Fibrosis, see specific organ or region
Filters, see radiography, apparatus; therapeutic radiology
Fistula, see also organ
Aortoesophageal complication of aortic prosthetic graft (c), 160
Cerebrospinal fluid, by CT (c), 344
Gastrointestinal tract, 215
Fontanelle, see skull
Foot
Extravasation of Ethiodol into tissues of: complication of lymphangiography (c), 342
Lisfranc's fracture-dislocation: peripheral neuropathy, 139
Rupture of plantar fascia in athletes (a), 935
Foreign bodies, see specific organ or part
Forestier's disease, see bone, dysostoses
Fractionation, see dosimetry; radiation biology; therapeutic radiology
Fracture, see also specific bone
Healing in long bones (a), 1124
Lisfranc's fracture-dislocation: peripheral neuropathy, 139
Occipital condyle (c), 729
Photodensitometric evaluation of bone repair (a), 552
Quantitation of experimental, mineralization: new technique (a), 545
Radiographic evaluation of tibial plateau (a), 1123
Thin-section tomography in treatment of cervical spine injuries (a), 935

G

Gallbladder, see also bile ducts
Air: frequent finding in gallstone ileus, 219
Gallstones; in vitro comparison of physical, radiographic, and ultrasonic characteristics, 223
Gas in bile ducts (pneumobilia) in emphysematous cholecystitis, 661
Mucocutaneous lymph node syndrome (a), 943
"Phrygian cap" deformity with bistable and gray scale ultrasound (a), 562
Radiology of, and bile ducts (b), 364
Surgical and pathologic correlation of cholecystosonography and cholecystography, 227
Gallium-67
Imaging (b), 1129
Gastrointestinal tract
Acute upper, hemorrhage, new observations (a), 559
Angiography (b), 364
Angiography in systemic amyloidosis, 143
Antacid titration in prevention of acute, bleeding. Trial in 100 patients (a), 758
Calcified primary tumors (a), 934
Growth, health, and development after neonatal gut surgery (a), 943
Huge laparotomy pad granuloma simulating gastric wall tumor (c), 909
Infant botulism: intestinal hypomotility (c), 523
Intermittent bleeding in acute massive hemorrhage: arteriographic demonstration, 1015
Malignant fistula, 215
Metastatic breast carcinoma and (a), 758
Primary intestinal "Mediterranean" type lymphoma (a), 758
Prophylactic doxycycline for travelers' diarrhea. Double blind study (a), 758
Radiologic and clinical assessment of broad-spectrum antibiotic therapy in Crohn's disease, 787
Reduction of jejunogastic intussusception during examination of upper (c), 334
Severe hemorrhage of emergency arteriography of lower (a), 932
Single contrast/double-contrast (1), 1116
Small bowel malabsorption and malignancy of (a), 758
Strongyloides stercoralis colitis (a), 758
Gelfoam, see embolism, therapeutic
Genitals, see specific organ
Genitourinary tract, see urinary tract; urography; specific organ
Glioblastoma, see brain, neoplasm
Goiter, see thyroid
Gold
Histopathologic studies of liver following intravenous colloidal ^{198}Au therapy (a), 363
Grafts, vascular
Complications in expanded polytetrafluoroethylene, angiography, 817
Graves's disease, see thyroid
Gynecology, see ovary; pregnancy; uterus

H

Hand
Involvement of first carpometacarpal joint in scleroderma, 283
Patients with systemic lupus erythematosus (a), 560
Hay, Percy Douglas 1899-1977 (o), 755
Heart, see also arteries; coronary arteries; pericardium
Abdominal twiddler's syndrome (c), 1084
Atlas of cardiovascular nuclear medicine (b), 1128
Axial cineangiography in congenital disease (a), 359
Axial cineangiography in congenital disease. I. technical and anatomic considerations (a), 185
Complications from Waterston procedure, 431
Coronary artery surgery: critical review (b), 565
Coronary cineangiography, left ventriculography, and ^{201}Tl-scintigraphy (a), 363
Coronary neovascularity and fistula formation, sign of mural thrombosis (a), 185
ECG changes during barium enemas, protective role of B-receptor blocking agents (a), 360
First decade of aortocoronary bypass grafting (c), 359
Free-floating calculi in pericardial cavity (c), 901
Persistent positive technetium-99m stannous pyrophosphate myocardial scintigrams after myocardial infarction (a), 185
Quantitative left ventriculography (a), 932
Radiographic identification of prosthetic valves (a), 359
Systolic anterior motion of mitral valve in absence of asymmetric septal hypertrophy (a), 359
Tricuspid regurgitation with echocardiography and peripheral vein injection (a), 186
Underfilled coronary artery: pre- and postoperative observations on recipeint arterial quality and left ventricular function after surgery (a), 359
Wilms' tumor to, 263
Heart, congenital abnormalities
Anatomically corrected malposition: association with juxtaposition of atrial appendages and right aortic arch (a), 558
Apex echocardiography, two-dimensional technique (a), 558
Axial cineangiography (a), 359
Axial cineangiography. I. Technical and anatomic considerations

(a), 185
Complications from Waterston procedure, 431
Contrast echocardiographic techniques in critically ill infants with cardiac pulmonary disease (a), 186
Double-outlet right ventricle (c), 710
Echocardiographic differentiation of partial and complete atrioventricular canal (a), 1122
Echocardiographic estimation of pulmonary artery pressure (a), 1122
Identification of thoracic isomerism from plain chest radiograph, 995
Prolonged prostaglandin E_1 infusion in cyanotic (a), 760
Pulmonary atresia: photographic subtraction for recognizing hypoplastic pulmonary arteries, 1003
Radiographic and echocardiographic evaluation of newborns treated with indomethacin for patent ductus arteriosus, 1009
Routine urography following angiocardiography (a), 361
Heart, infarction
Coronary cineangiography, left ventriculography, and ^{201}Tl-scintigraphy (a), 363
Coronary, ventricular, and pulmonary abnormalities with rupture of interventricular septum, 571
Detection of mycardial scar tissue by m-mode echocardiography (a), 360
Persistent positive technetium-99m stannous pyrophosphate myocardial scintigrams (a), 185
Relation of cigarette smoking to, in young women (a), 932
Heart, ultrasound
Contrast technique in critically ill infants with cardiac and pulmonary disease (a), 186
Detection of myocardial scar tissue by m-mode (a), 360
Detection of tricuspid regurgitation with, and peripheral vein injections (a), 186
Differentiation of partial and complete atrioventricular canal (a), 1122
Estimation of pulmonary artery pressure in transposition of the great arteries (a), 1122
Radiographic and, evaluation of newborns treated with indomethacin for patent ductus arteriosus, 1009
Recognition of ruptured chordae tendineae (a), 360
Systolic anterior motion of mitral valve in absence of asymmetric septal hypertrophy (a), 359
Hemangioendothelioma, see organ or region
Hemangiopericytoma, see organ or region
Hemihypertrophy, see organ or region
Hemolytic-uremic syndrome
Ischemic colitis and stricture (a), 562
Hemorrhage, see specific disease, organ, or system
Hepatoma, see liver, neoplasm
Hernia, see also specific organ
Large hiatus, in infancy and childhood (a), 943
Hip
Arthrography (b), 948
Intraarticular methyl methacrylate: complication of surgery, 1055
Lead intoxication and traumatic arthritis, secondary to retained bullet fragments (a), 361
Paget's disease (a), 1123
Prognosis in Perthes' disease (a), 1123
Proximal femoral focal deficiency, 289
Histiocytosis, see neoplasm
Hodgkin's disease, see also lymphoma
Pregnancy outcome of patients with (a), 563
Holt-Oram syndrome, see bone, dysostoses; heart
Humerus
Pseudocysts, 287
Hyaline membrane disease, see respiratory distress syndrome
Hydatidiform mole, see uterus
Hydromyelia, see spinal cord
Hyperinsulinism, see pancreas, neoplasm
Hyperparathyroidism, see parathyroid, hyperparathyroidism
Hypothalmus, see brain
Hypotonic duodenography, see duodenum; radiography
Hysterography, see uterus; radiography
Hysterosalpingography, see uterus

I

Innominate artery
Buckling, simulating right apical lung mass, 119
Instruction, see education
Insulinoma, see pancreas, neoplasm
Intervertebral disc, see spine, intervertebral disc
Intestine, see also duodenum; gastrointestinal tract
Air in gallbladder: frequent in gallstone ileus, 219
Assessment of antibiotic therapy in Crohn's disease, 787
Calcifications in small bowel of infants with total colonic aganglionosis (a), 759
Infant botulism: cause of, hypomotility (c), 523
Neonatal necrotizing enterocolitis: indication for surgery (a), 190
Primary lymphoma of "Mediterranean" type (a), 758
Radiology of ileosigmoid knot (a), 1122
Radiology of neonatal necrotizing enterocolitis (a), 1126
Reduction of jejunogastric intussusception during upper gastrointestinal examination (c), 334
Regional enteritis in children: small bowel disease with normal terminal ileum (a), 943
Small-bowel malabsorption and gastrointestinal malignancy (a), 758
Intussusception, see specific organ
Iocarmate
Arachnoiditis produced by meglumine iocarmate and metrizamide myelography, 129
Iodamide
Drip infusion urography with meglumine, 1043
Ischium, see pelvis
Islands of Langerhans, see pancreas

J

Jarcho-Levin syndrome, see spine
Jejunum, see intestine
Joint, see also specific joint; arthritis
Anatomic-pathologic-radiographic correlation in proximal tibiofibular, 133
Calcified bodies in popliteal cysts: radiography, 857
First carpometacarpal, in scleroderma, 283
Prognosis in Perthes' disease (a), 1223
Rheumatoid arthritis: scintiphotographic, radiographic, and clinical examinations, 665

K

Kidney, see also urinary tract; urography; renal arteries
Efficacy of CT, 5
Fluoroscopically guided thin needle aspiration biopsy of abdomen and retroperitoneum, 197
Microradiography of pyelolymphatic backflow in porcine, 501
Posterior urethral valves causing neonatal urinifercus perirenal pseudocyst (urinoma) (a), 943
Renal pseudocalculus (1), 928
Spontaneous rupture of calyceal diverticulum during urography (c), 337
Ultrasonic detection of nonopaque calculi (a), 760
Ultrasonography in management of unexplained failure (a), 760
Kidney, abnormalities
Uterine anomalies and agenesis, 973
Kidney, angiography
Embolization for postbiopsy renal arteriovenous fistula (c), 1072
High-dose renal pharmacoangiography in hypovascular renal neoplasms, 807
Optimal technique for transplant donors, 813
Kidney, cyst
Benign multilocal, 621
Kidney, failure
Bone mineral content of patients on hemodialysis and following renal transplant (a), 545
Bone mineral status in childhood (a), 544
Contrast-induced (e), 1113
Effect of $1,25(OH)_2D_3$ in renal osteodystrophy (a), 545
Ischemic colitis and stricture after hemolytic-uremic syndrome (a), 562
Microradiscopic morphometry of intracortical resorption in hand bones in normal and (a), 551
Photon absorptiometry in haemodialysed and transplant patients (a), 545
Radiographic photodensitometry and maintenance hemodialysis (a), 552
Radiogrammetric and absorptiometric measurements in bone-losing patients and subperiosteal resorption (a), 551
Kidney, neoplasm
Angiographic findings in transitional cell (a), 934
Benign multilocal cystic nephroma, 621
Cyst formation and cavitation in pulmonary metastases from Wilms' tumor (a), 943
High-dose renal pharmacoangiography in hypovascular, 807
Pheochromocytomas in von Hippel-Lindau disease (1), 736
Ultrasound of extension to IVC (1), 1117
Kidney, transplant
Bone mineral content on hemodialysis after (a), 545
Children 1-5 year old (a), 579
CT in (a), 560
$1,25(OH)_2D_3$ in renal osteodystrophy (a), 545
Photon absorptiometry in haemodialysed and transplant patients (a), 545
Ultrasound, 851
Urologic complications (a), 934

Kidney, ultrasound
Nonopaque renal calculi (a), 760
Pancreatic cysts in adult polycystic disease by CT and (c), 1074
Renal transplants, 851
Tumor extension to IVC (1), 1117
Unexplained renal failure (a), 760
Klippel-Feil syndrome, see bone, dysostoses
Knee
Arthroscopic examination (a), 935
Calcified bodies in popliteal cysts, 857
Chondromalacia patellae (a), 1123
Osteochondritis dissecans of distal femur (a), 560
Tibial plateau fractures (a), 1123

L

Larsen's syndrome, see bone; specific joint
Larynx
Carbon dioxide laser in pediatric airway lesions (a), 759
Head, neck, and esophageal cancer, 791
Laryngocele, 259
Subglottic edema in acute epiglottitis, 603
Xeroradiography in otorhinolaryngology (b), 948
Laurence-Moon-Bardet-Biedl syndrome, see bone, dysostoses
Lead poisoning
Traumatic arthritis and, of hip secondary to retained bullet fragments (a), 361
Legionnaires disease
(c), 892
Lens, see eye
Letters
Anonymity of reviewers, 358
Biliary duct ultrasound, 556
Clean colon: whose responsibility?, 182
Intraluminal duodenal diverticulum, 556
Lymphography vs. CT of lymphomas, 1116
Pheochromocytomas in von Hippel-Lindau disease, 736
Pleural herniation in respiratory disress syndrome, 357
Radiography in cervical spine trauma, 555
Renal pseudocalculus, 928
Single-contrast/double-contrast GI, 1116
Ultrasound of tumor extension to IVC, 1117
Leukemia
Abnormal CT in asymptomatic children with acute lymphocyte, after prophylactic treatment of central nervous system (a), 761
Infiltration of colon (c), 725
Infiltration of large bowel (c), 723
Lidocaine
Arteriography (c), 906
Liposarcoma, see specific organ
Liver, see also bile ducts
Bile leak into abscess demonstrated by Tc-diethyl-iminodiacetic acid (c), 889
Blood flow in contusions: traumatic "arterioportal fistulae" (a), 185
CT-guided Seldinger catheter drainage of abscess (c), 323
Endoscopic retrograde cholangiography in nonamebic abscesses (a), 559
Fluoroscopically guided thin needle aspiration biopsy of abdomen and retroperitoneum, 197
Histopathologic studies after intravenous colloidal ^{198}Au therapy (a), 363
^{133}Xe uptake in fatty (a), 1122
Portal triad and hepatic cirrhosis (a), 932
Portosystemic communications studied by transhepatic portography (a), 932
Pseudomass due to pleural effusion and diaphragm inversion (c), 1077
Radiology (b), 1130
Ultrasound diagnosis of hydatid disease (echinococcosis) (c), 895
Liver, computed tomography
Efficacy, 5
Necrotic metastases, 839
Nuclear imaging and (a), 1122
Obstructive jaundice in absence of intrahepatic ductal dilatation, 389
Seldinger catheter drainage of abscess (c), 323
Tumor with iodinated fat emulsion (a), 186
Liver, neoplasm
Carcinoid syndrome treated by embolization (c), 511
CT of necrotic metastases, 839
Focal nodular hyperplasia and liver cell adenoma, 393
Infancy and childhood (a), 558
Palliation of metastasis (a), 563
Liver radionuclide imaging
Bile leak into abscess: demonstration with Tc-diethyl-iminodiacetic acid (c), 889
CT and (a), 1122
Pseudomass due to pleural effusion and inversion of diaphragm (c), 1077
Liver, ultrasound
Hydatid disease (echinococcosis) (c), 895
Primary cysts, 235
Vessels and biliary tract (a), 190
Lung, see also bronchi; pleura
Arteriovenous malformation of diaphragm and (c), 507
Barotrauma in scuba divers (a), 931
Bronchial atresia (a), 757
Buckling of innominate artery simulating right apical mass, 119
Chest dimensions in spontaneous pneumothorax (a), 757
CT and conventional whole lung tomography in detecting nodules, 51
Cyst formation and cavitation in metastases from Wilms' tumor (a), 943
Diagnosis of chest diseases (b), 1128
Efficacy of CT, 5
Essential fatty acids, prostaglandins, and respiratory distress syndrome of newborn (a), 561
Focal perfusion defect caused by sequestration (c), 904
Hypertransradiant hemithorax: appearance due to rotation (a), 931
Identification of thoracic isomerism from plain chest radiograph, 995
Left superior intercostal vein, 599
Massive hemorrhage: surgical treatment (a), 184
Medical efficacy of CT of chest and abdomen, 15
Multinodular primary amyloidosis: needle biopsy (c), 1082
Nonfatal air embolism (c), 705
Procarbazine (c), 527
Pulmonary, pleural, and thoracic changes complicating chemotherapy (a), 184
Radiation pneumonitis complicated by Pneumocystis carinii (a), 557
Radiography techniques without special equipment (a), 931
Radiologic findings in acute childhood asthma (a), 931
Renal transplant; low-dose immunosuppression (a), 184
Suspected embolism and negative arteriogram (a), 757
Lung, computed tomography
Density measurement (a), 1121
Solitary nodules: experience with scanning times longer than breath holding (a), 1121
Whole lung tomography and, for detecting nodules, 981
Lung, diseases
Bronchography in congenital cystic bronchiectasis, 255
Course of usual and desquamative interstitial pneumonia (a), 557
Distribution of HLA antigens in idiopathic fibrosis (a), 1121
Manifestations of acute aspiration of gastric contents, 587
Miliary aspergillosis associated with alcoholism (c), 707
Pleural herniation in respiratory distress syndrome (1), 357
Reversible respiratory disease in beryllium workers (a), 1121
Uptake of ^{99m}Tc diphosphonate in alveolar microlithiasis (c), 703
Ventilation-perfusion scans in neonatal emphysema complicating ventilatory assistance, 243
Lung, edema
Coronary, ventricular, and pulmonary abnormalities with rupture of interventricular septum, 571
Lung, infection
Chlamydia trachomatis: cause of infantile pneumonia syndrome (c), 914
Legionnaires disease (c), 892
Lymphocytic interstitial pneumonitis (a), 931
Nocardiosis (a), 1121
Radiographic spectrum of pleuropulmonary tularemia, 277
Radiography of, in Mycobacterium kansasii, 985
Lung, neoplasm
Accuracy of chest film screening by technologists, 593
CT in radiotherapy, 63
Pedunculated endotracheal metastasis (c), 713
Transbronchial mucus transfer of bronchogenic (a), 1121
Whole lung tomography and CT in detection of, 981
Lung, radionuclide imaging
Focal perfusion defect caused by sequestration (c), 904
Uptake of ^{99m}Tc diphosphonate in alveolar microlithiasis (c), 703
Ventilation-perfusion scans in neonatal emphysema complicating ventilatory assistance, 243
Lupus erythematosis
Hands in patients with systemic (a), 560
Mediastinal lymphadenopathy and undifferentiated connective tissue disease (c), 325
Lymph node, see also Hodgkin's disease; lymphography; lymphoma
CT in metastases from pelvic cancers, 675
Fluoroscopically guided thin needle aspiration biopsy of abdomen and retroperitoneum, 197
Intrathoracic metastases from extrathoracic neoplasms, 403
Lymphangiographic changes after radiation therapy, 803
Mediastinal lymphadenopathy and undifferentiated connective tissue disease (c), 325
Reevaluation of intrathoracic lymphadenopathy in sarcoidosis, 409

System, methods of clinical investigations (b), 566
Lymphangiography, see lymphography
Lymphatics
Diffuse dysplasia with hepatic oil embolism (c), 898
Lymphogranuloma, see Hodgkin's disease
Lymphography, see also lymph node; lymphoma
Changes after radiation therapy, 803
CT and, of lymphoma (1), 1116
Diffuse lymphatic dysplasia with hepatic oil embolism (c), 898
Extravasation of Ethiodol into tissues of foot; complication of (c), 342
Lymphoma, see also Hodgkin's disease
CT in detecting intraabdominal and pelvic adenopathy in, 311
CT in primary malignant, of brain (a), 1125
CT in treatment of, 69
Lymphangiography vs. CT of (1), 1116

M

Macroradiography, see radiography
Mammography, see also breast
Accuracy in 655 histologically verified cases (a), 190
Breast tumors in male (a), 190
Influence of age at first pregnancy on breast parenchymal pattern (a), 562
Intensity of scattered radiation (a), 190
Oblique projection, 465
Parenchymal patterns as risk indicators for cancer, 1031
Technologist guide to (b), 191
Thermoluminescent dosimeter determination of exposure, 617
Mastoid
Radium-induced malignant tumors of paranasal sinuses and, 773
McArcle's disease, see kidney, failure
Mediastinum
Anterior pathway for transdiaphragmatic extension of pneumomediastinum, 271
Buckling of innominate artery simulating right apical lung mass, 119
Clinical efficacy of body CT, 5
CT diagnosis of pericardial cysts (c), 515
Fine needle aspiration biopsy in diagnosis of lesions, 239
Intrathoracic lymph node metastases from extrathoracic neoplasms, 403
Left superior intercostal vein, 599
Lymphadenopathy and undifferentiated connective tissue disease (c), 325
Medical efficacy of CT of chest and abdomen, 15
Neural tumors of the thorax: review from AFIP (a), 184
Radiologic correlations with anatomy and pathology (b), 191
Reevaluation of intrathoracic lymphadenopathy in sarcoidosis, 409
Right paratracheal stripe in children (a), 759
Vascular pseudo-tumours; tomographic. I. arteries (a), 931
Medulla oblongata, see brain
Medullary sponge kidney, see kidney, cyst
Megacolon, see colon
Megalencephaly, see brain
Melanoma
Malignant, metastatic to central nervous system (a), 1125
Meninges, see also arachnoid
CT detection of cerebrospinal fluid fistula (c), 344
Thoracic and lumbar dural ectasia in 2 year old (a), 759
Meningioma, see brain, neoplasm
Mesentery
Isolated desmoids (fibromatosis) (a), 360
Neoplastic involvement by CT of omentum and, 835
Retractile mesenteritis: presentation as colonic obstruction (a), 186
Metaphyses, see bone
Metrizamide
Arachnoiditis produced by meglumine iocarmate and, myelography, 129
Microangiography, see angiography
Mitral valve, see also heart
Echocardiographic recognition of ruptured chordae tendineae (a), 360
Systolic anterior motion in absence of asymmetric septal hypertrophy (a), 359
Mucolipidosis, see bone, metabolic abnormalities
Myelography
Comparison of arachnoiditis produced by meglumine iocarmate and metrizamide, 129
New water-soluble iodinated contrast medium with reduced convulsive effects (a), 561
Spinal arachnoid cysts in children (a), 362
Myelomeningocele, see spinal cord
Myelopathy, see spinal cord
Myocardium, see heart
Myoglobinuria, see kidney, failure

N

Necrotizing enterocolitis, see colitis
Neoplasm, see also radiation biology; therapeutic radiology, specific organ, region, neoplasm
Carcinoma of head and neck with cancer of esophagus, 791
Clinical pediatric oncology (b), 565
New methods in localization of (b), 763
Radium-induced malignant tumors of mastoid and paranasal sinuses, 773
Nerves
Enlargement of intervertebral foramina: unusual cause (c), 911
Neuroblastoma, see specific organ
Neuroradiology, see brain; cerebral angiography; nerves
Noonan's syndrome, see heart
Nose
Treatment of lesions of pediatric airway: carbon dioxide laser (a), 759
Nuclear medicine, see also specific disease, organ, region
Handbook of clinical (b), 364
Nuclide, see specific radionuclide

O

Obituaries
Aurelius, J. Richards, 1897-1977, 756
Bayley, Howard B., 1914-1978, 1119
Dietz, M. Wendell, 1922-1977, 755
Epstein, Bernard S., 1908-1978, 1119
Hay, Percy Douglas, 1899-1977, 755
Sehested, Herman C., 1901-1978, 755
Truog, Clarence Peter, 1901-1978, 756
Observer performance, see radiographs, interpretation; radiography
Obstetrics, see pregnancy; uterus
Occlusion, see embolism; thrombosis
Oculoauriculovertebral syndrome, see ear; eye; spine
Omentum
Neoplastic involvement by CT of mesentery and, 835
Ophthalmology, see eye; orbit
Oral cavity
Head, neck, and esophageal cancer, 791
Oram-Holt syndrome, see bone, dysostoses; heart
Orbit
Computed sagittal tomography (t), 346
CT in ocular neoplastic disease, 111
CT of coronal sections (a), 936
Roentgenology (b), 192
Ultrasonography of eye and (b), 565
Ossicles, auditory, see ear
Osteoarthritis, see arthritis; specific bone or joint
Osteodystrophy, see bone, metabolic abnormalities
Osteomyelitis, see bone, infection
Osteoporosis, see bone, metabolic abnormalities
Osteosarcoma, see bone, neoplasm
Osteotomy, see bone
Ostium primum defect, see heart
Otolaryngology, see ear
Ovary
Diagnosis of pelvic masses by gray scale sonography, 469
Dysgerminoma as calcified abdominal mass with hypercalcemia (a), 936
Extragonadal endodermal sinus (yolk sac) tumor (a), 1126
Pneumopelvigraphy in childhood, 607
Teratomas in children, 613
Ultrasound and CT in gynecologic pelvic masses, 955

P

Pacemakers, see heart
Paget's disease
Bone mineral content measurements (a), 543
Hip joint (Paget's "coxopathy") (a), 1123
Pancreas
Clinical and radiographic studies of carcinoma: diagnosic efficacy of angiography (a), 360
Clinical efficacy of CT, 5
CT in surgical emergencies (a), 1122
Cystic neoplasms; angiography and ultrasonography, 795
Duct obstruction during transhepatic cholangiography (a), 521
Fluoroscopically guided thin needle aspiration biopsy of abdomen and retroperitoneum, 197
Hemorrhagic pseudocysts of spleen in pancreatitis (a), 1123
Medical efficacy of CT of chest and abdomen, 15
Unusual tumor of lesser sac (a), 933
Pancreas, neoplasm
Angiography and ultrasonography of cystic, 795
Clinical and radiologic studies; diagnostic efficacy of angiography (a), 360

Cystadenocarcinoma: CT body scan and gray scale ultrasound (c), 339
High-dose, small volume irradiation treatment (a), 563
Nonfunctioning islet cell tumors (a), 715
Pancreas, ultrasound
Cystadenocarcinoma: CT body scan and gray scale (c), 339
Cystic neoplasms: angiography and, 795
Cysts in adult polycystic disease by CT and (c), 1074
Low dose rate teletherapy of unresectable carcinoma of, pilot study (a), 1110
Nonfunctioning islet cell tumors (c), 715
Prone view for tail neoplasms, 231
Water distention of gut in evaluation (t), 348
Papillary necrosis, see kidney
Parathyroid
Ultrasonography (a), 760
Parathyroid, hyperparathyroidism
Bone disease in primary (a), 552
Increase in bone mineral content after surgery of primary (a), 544
Primary, bone mineral measurement (a), 552
Secondary, associated with chronic renal disease (a), 187
Parietal bone, see skull
Patella
Chondromalacia: separate clinical entity? (a), 1123
Patent ductus arteriosus, see heart, congenital abnormalities
Pediatric radiology, see specific procedure or disease
Pelvis, see also specific pelvic bone; organ
Inflammatory cysts of peritoneum, 633
Retrorectal space (a), 1122
Pericardium
CT diagnosis of cysts (c), 515
Free-floating calculi in cavity (c), 901
Periostitis, see bone
Peritoneum
Diagnostic oncology case studies: investigation of bloody ascites, 697
Extragonadal endodermal sinus (yolk sac) tumor (a), 1126
Inflammatory cysts of pelvic, 633
Radiography of LeVeen type peritoneovenous shunts (t), 916
Unusual tumor of lesser sac (a), 933
Perthes' disease, see hip
Pharynx
Head, neck, and, with esophageal cancer, 791
Plummer-Vinson syndrome (a), 933
Radiologic examination of orohypopharynx and esophagus (b), 1130
Pheochromocytoma, see adrenals
Phlebography, see venography; specific organ, procedure
Phocomelia, see specific extremity
Pigeon breeder's disease, see lung, diseases
Pituitary
Bone mass and soft tissue measurements in acromegaly (a), 543
Cushing's disease, selective transsphenoidal resection of microadenomas (a), 761
Placenta
False, previa: clinical observation (a), 563
Sonolucent areas: sonographic, pathologic correlation, 961
Ultrasonic diagnosis of previa: value of postvoid scan (a), 563
Platyspondyly, see spine
Pleura
Bilateral thickening: asbestos dust exposure, 579
Localized mesothelioma: benign and malignant (a), 557
Pseudomass of liver due to pleural effusion and inversion of diaphragm (c), 1077
Pneumatosis intestinalis, see intestine
Pneumocystis carinii
Radiation pneumonitis complicated by (a), 557
Pneumoencephalography, see brain
Pneumoperitoneum, see also peritoneum
Anterior pathway for transdiaphragmatic extension of pneumomediastinum, 271
Benign, after median sternotomy incision, 267
Congenital anomalies in umbilical region in (a), 190
Pneumopelvigraphy in childhood, 607
Pneumothorax, see also pleura
Chest dimensions in spontaneous (a), 757
Polydactyly, see bone, dysostoses
Polyphosphate, see specific organ, region scanned
Polyps, see specific organ
Popliteal artery, see arteries
Porencephaly, see brain
Portal vein
Improved splenoportography by plugging needle tract, 445
Intrahepatic blood flow in liver contusions: traumatic "arterioportal fistulae" concept (a), 185
Portosystemic communications studied by transhepatic portography (a), 932
Splenic vein occlusion, 439
Therapeutic coronary vein occlusion and transhepatic angiography, 637
Pregnancy, see also uterus; placenta; radiation, injurious effects; radiation biology
Hysterographic double-outlined uterine cavity: sign of unsuspected, 305
Obstetrical diagnosis by radiographic, ultrasonic, and nuclear methods (b), 765
Ultrasound in ectopic, 153; 967
Prune belly syndrome, see abdomen; urinary tract
Procarbazine
Lung (c), 527
Prostaglandin
Essential fatty acids, respiratory distress syndrome of newborn and (a), 561
Prolonged E_1 infusion in cyanotic congenital heart disease (a), 760
Pseudo-Hurler polydystrophy, see bone, metabolic abnormalities
Pseudotruncus arteriosus, see pulmonary arteries; heart
Pulmonary arteries, see also heart; embolism; arteriovenous malformation; thrombosis
Congenital atresia: photographic subtraction for recognizing hypoplastic, 1003
Patient course with suspected embolism and negative arteriogram (a), 757
Pulseless disease, see arteries
Pyelography, see urography
Pylorus, see stomach
Pyrophosphate, see specific organ

R

Radiation biology, see also dosimetry; neoplasm; radiation; radiation, injurious effects; specific disease, organ, region, radionuclide
Advances in (b), 765
Clinical (b), 365
Cycling activity and chemosensitivity of normal tissues (a), 944
Effect of ultrasound alone and with x-rays on chromosomes in vivo (a), 762
Radiation biology, sensitization studies
Importance of D_q (a), 1105
Variations in radiosensitivity and dose rate effects among various types of cultured cells (a), 1107
Radiation biology, time dose studies
Alteration of cellular proliferation in cell lines exposed to low dose rate irradiation (a), 1107
Applications of hyperfractionated (HFI) (8 and 16 fractions per day) concentrated irradiation (a), 1110
Clinical exploitation of low dose rate teletherapy (a), 1109
Comparison of low dose rate and fractionated irradiation for early reactions of skin and intestinal mucosa (a), 1106
Dose-rate effects in radiation therapy and radiation biology (a), 1105
Dose rate factor of in vivo continuous low dose irradiation of tumor and normal tissues (a), 1108
Historical perspectives of clinical radiotherapy at low dose rate (a), 1108
Implications of initial portion of survival curve for low dose rate teletherapy (a), 1106
Importance of D_q (a), 1105
Modification of gastrointestinal death in mice exposed to whole and partial body exposures of low dose rate irradiation (a), 1108
Response of bone marrow and tumor cells to acute and protracted irradiation (a), 1107
Single and fractionated doses applied at low-dose rates on rat skin and R-1 rhabdomyosarcoma (a), 1107
Tissue responses to multiple small doses of irradiation (a), 1106
Variations in radiosensitivity and dose rate effects among various types of cultured cells (a), 1107
Radiation, injurious effects, see also therapeutic radiology
From earlier pages, 734
Malignant tumors of mastoid and paranasal sinuses, 773
Review of NCRP radiation dose limit for embryo and fetus in occupationally-exposed women (b), 948
Radiation measurement, see also dosimetry
International system of units (e), 536
S.I. units in medicine (b), 763
Radiation physics
Fundamental physics of radiology (b), 566
Radiation protection
Dentistry (b), 949
Review of NCRP radiation dose limit for embryo and fetus in occupationally-exposed women (b), 948
Radiation therapy, see therapeutic radiology
Radiculography, see myelography
Radiographs, interpretation
Accuracy of chest film screening, 593
Current concepts in pediatric radiology (b), 947
Detection accuracy in chest, 247

Pediatric radiology (b), 193
Radiography, see also specific organ, procedure
From earlier pages, 181
Oblique, of pediatric lumbar spine: is it necessary?, 297
Synopsis of radiographic anatomy with CT (b), 949
Understanding (b), 949
Radiography, apparatus
Device to record patient position on portable chest radiographs (t), 169
Easy coronal scans (t), 535
Guide for automatic radiographic processing and film quality control (b), 1128
Modified punch card for extending filming program of puck changer (t), 534
Practical approach to modern (b), 565
Rare earth screens and silver (e), 926
Traction device for Polytome table (t), 732
Transparent head support for magnification cerebral angiography (t), 1096
Radiography, exposures, see also dosimetry
Patient and personnel in computed axial tomography (a), 362
Thermoluminescent dosimeter determination in mammography, 617
Radiography, image quality
CT absorption values by filtering, 103
CT: comparison of radiation dose and resolving power of commercial CT scanners, 95
Guide for automatic radiographic processing and film quality control (b), 1128
Radiography, technique
Lung, without special equipment (a), 931
Oblique projection in mammography, 465
Pneumoperitoneum in congenital anomalies in umbilical region (a), 190
Rare earth screens and silver (e), 926
Single-contrast/double-contrast GI (1), 1116
Total body opacification, 919
Radiology, practice
American College of Radiology diagnostic efficacy studies, 173
CT: achievement and challenge (e), 1
CT: cost and efficacy implications, 81
Efficiency of CT scanner, 89
National guidelines and standards for health planning, 1101
Noninvasive medical imaging (a), 944
Pathologic index for teaching file (t), 918
Radionuclide, see specific radionuclide, organ scanned
Medical cyclotrons in nuclear medicine (b), 1129
Radionuclide imaging
Atlas of cardiovascular nuclear medicine (b), 1128
Gallium-67 imaging (b), 1129
Rucionuclide scanning
Multiple, in differentiation of upper abdominal lesions (a), 1127
Radium
Mastoid and paranasal sinus malignant tumors, induced, 773
Rectum
Colitis cystica profunda (c), 529
Colorectal tumors, 691
Rectrorectal space (a), 1122
Reflux, see stomach; ureter
Renal arteries, see also kidney; arteriovenous malformation
Pseudoaneurysm of arterial anastomosis in transplant (c), 525
Transplant donors, arteriography, 813
Renal arteries, stenosis
Pheochromocytoma with reversible (c), 1069
Right posterior oblique projection in aortography of hypertensive patients (a), 557
Renal hypertension
Complication of umbilical arterial catheterization (a), 558
Respiratory distress syndrome
Essential fatty acids, prostaglandins, and, in newborns (a), 561
Pleural herniation in (1), 357
Radiography and echocardiography in newborns treated with indomethacin for patent ductus arteriosus, 1009
Systemic air embolism secondary to, in neonate, 425
Respiratory tract, see specific organ
Retroperitoneum
Clinical efficacy of computed body tomography, 5
Fluoroscopically guided thin needle aspiration biopsy of abdomen and, 197
Medical efficacy of CT of chest and abdomen, 15
Retractile mesenteritis as colonic obstruction (a), 186
Retrorectal space (a), 1122
Rheumatoid arthritis
Craniovertebral region in chronic inflammatory rheumatic diseases (b), 947
Mediastinal lymphadenopathy and undifferentiated connective tissue disease (c), 325
Soft tissues of the extremities. Radiologic study of rheumatic disease (b), 1130
Ribs
Coccygeal (c), 164
Roentgenograms, see radiographs; radiography

S

Sacroiliac joint
HLA-B27-negative sacroilitis: manifestation of familial Mediterranean fever in childhood (a), 561
Sacrum, see also pelvis
Sacral agenesis (a), 560
Sarcoidosis
Reevaluation of intrathoracic lymphadenopathy in, 409
Sarcoma, see specific organ
Scintigraphy, see radionuclide imaging
Scleroderma
Mediastinal lymphadenopathy and undifferentiated connective tissue disease (c), 325
Screens, see radiography, appartus
Scrotum
Gray scale ultrasound of (a), 562
Sehested, Herman C. 1901-1978 (o), 755
Semilunar cartilages, see knee
Shields, see therapeutic radiology
Shoulder
Arthrography as treatment, 1047
Sigmoid, see colon
Sinus
Xeroradiography in otorhinolaryngology (b), 948
Sinus, nasal
Diagnostic oncology case studies; maxillary sinusitis and cancer: role of polytomography (c), 321
Radium-induced malignant tumors of mastoid and paranasal sinuses, 773
Skeleton, see bone
Skull
Ceruminous tumor of jugular foramen (a), 189
Fracture of occipital condyle (c), 729
Jugular notch (a), 189
Lipoma of corpus callosum with frontal bone defect (c), 517
Progress in pediatric radiology, vol 6. Skull, spine, and contents (b), 946
Radiology of jugular tubercles, 1037
Small bowel, see intestine; gastrointestinal tract
Soft tissue
CT of tumors of musculoskeletal system in children (a), 935
Detection of subcutaneous metastases by CT (a), 1127
Extremities. Radiologic study of rheumatic disease (b), 1130
Gray scale features of hematomas: ultrasonic spectrum, 977
Ultrasonic evaluation of extremity, lesions with arthrographic correlation (a), 944
Sphenoid sinus, see sinus, nasal
Spinal canal, see spine; spinal cord
Spinal cord, see also arachnoid; meninges; myelography
Angiography using 4x magnification (a), 1124
Hyperalimentation catheter passing into spinal canal causing temporary paraplegia (a), 1125
Malignant melanoma metastatic to central nervous system (a), 1125
Neuroradiology case studies (b), 764
New water-soluble iodinated myelographic contrast medium with reduced convulsive effects (a), 561
Radiographs in cervical spine trauma (1), 555
Thyrocalcitonin on ^{18}F uptake in injuries of (a), 553
Spinal cord, neoplasm
Ultrasonic visualization of cervical cord cystic astrocytoma (c), 907
Spine, see also sacroiliac joint
Abdominal aorta in spina bifida cystica (a), 557
Craniovertebral region in chronic inflammatory rheumatic diseases (b), 947
CT of musculoskeletal disorders, 55
Diffuse idiopathic skeletal hyperostosis (DISH) and calcification of posterior longitudinal ligament, 1049
Enlargement of intervertebral foramina: unusual cause (c), 911
External landmarks of abdomen related to vertebral segments, 115
Hyperalimentation catheter passing into spinal canal causing temporary paraplegia (a), 1125
Infections (a), 561
Juvenile ankylosing spondylitis (a), 187
Multiple contrast injections in epidural venography, 485
Postoperative bony stenosis of lumbar spinal canal, 1059
Progress in pediatric radiology, vol 6. Skull, spine and contents (b), 946
Radiographs in cervical trauma (1), 555
Radiology of sterno-manubrial articulation in ankylosing spondylitis and Reiter's syndrome (a), 361
Routine oblique radiography of pediatric lumbar, 297
Sacral agenesis (a), 560
Scoliosis (a), 361

Thin-section tomography in treatment of cervical injuries (a), 935
Thoracic and lumbar dural ectasia in 2-year-old (a), 759
Spine, intervertebral disc
Epidural venography in diagnosis of lumbar disc herniation (a), 188
Herniations: cartilaginous (Schmor's) nodes (a), 188
Spleen
Conservative surgery for injuries of (a), 562
Hemorrhagic pseudocysts in pancreatitis (a), 1123
Improved splenoportography by plugging needle tract, 445
Vein occlusion, 439
Wandering, in three children (a), 943
Spondylitis, see spine
Staphylococcus, see specific organ
Sternum
Radiologic examination of sterno-manubrial articulation in ankylosing spondylitis and Reiter's syndrome (a), 361
Stomach, see also gastrointestinal tract
Acute upper gastrointestinal hemorrhage (a), 559
Antral diaphragms and hypertrophic pyloric stenosis, 203
Areae gastricae (e), 554
Atypical benign hyperplastic gastric polyps, 147
Benign greater curvature ulcers (a), 933
Disseminated histoplasmosis producing hypertrophic gastric folds (a), 558
Gastric emphysema in infants with hypertrophic pyloric stenosis, 421
Gastric polyposis due to multiple hyperplastic adenomatous polyps (a), 559
Huge laparotomy pad granuloma simulating gastric wall tumor (c), 909
Lower esophageal anatomy: 430 B.C.-1977, 373
Mass screening of cancer in Japan. I. life saving vs. loss (a), 559
Reduction of jejunogastric intussusception during upper gastrointestinal examination (c), 334
Single-contrast/double-contrast GI (1), 1116
Technetium-99m pertechnetate as indicator of gastric mucosal proliferation, 1041
Transpyloric extension of gastric carcinoma (a), 560
Streptococcus, see specific organ
Subdural, see meninges
Subtraction, see radiography
Sutures, see skull
Syndrome, see by name
Synostosis, see skull
Synovitis, see arthritis
Synovium, see specific joint

T

Talus, see ankle
Tarsus, see foot
Teeth
Remineralization of enamel by saliva substitute in irradiated patients (a), 760
Tendon, see specific part, joint
Terotoma, see specific organ, region
Tetralogy of Fallot, see heart, congenital abnormalities
Thallium-201
Abnormal peripheral distribution of, due to arteriosclerosis (c), 718
Noninvasive approach to peripheral vascular disease, leg scans, 827
Relationships between coronary cineangiography, left ventriculography, and ^{201}Tl-scintigraphy (a), 363
Scintigraphy, new method for imaging of uterus (a), 363
Therapeutic radiology
CT in radiotherapy of lung cancer, 63
CT in treatment of lymphomas, 69
Efficacy of CT-assisted 2-dimensional treatment planning, 75
Fletcher gamma-ray colpostat system (a), 563
Lymphangiographic changes after, 803
Remineralization of enamel by saliva substitute in irradiated patients (a), 760
Therapeutic radiology, technique
Clinical exploitation of low dose rate teletherapy (a), 1109
Current results of an E.O.R.T.C. trial comparing low dose rate and classical fractionated treatments of base of tongue epitheliomas (a), 1109
Experience with low dose rate therapy at Rotterdam radiotherapy institute (a), 1110
Historical perspectives of clinical radiotherapy at low dose rate (a), 1108
Low dose rate teletherapy of unresectable carcinoma of pancreas: pilot study (a), 1110
Thorax, see also specific organ, region
Anterior pathway for transdiaphragmatic extension of pneumomediastinum, 271
Benign pneumoperitoneum following median sternotomy incision, 267
Clinical efficacy of computed body tomography, 5
Congenital partial eventration of left diaphragm, 417
Device to record patient position on portable chest radiographs (t), 169
Diagnosis of disease of (b), 1128
Medical efficacy of CT of abdomen and, 15
Neural tumors (a), 184
Protean manifestations of mycotic aneurysms, 1019
Radiographic aspects of total parenteral nutrition during infancy (a), 562
Thromboembolism, see embolism; thrombosis
Thrombosis, see also embolism
Evaluation of suspected deep venous, in arteriosclerotic patient (c), 531
^{131}I-labeled fibrinogen in deep vein, 451
Thyroid, ultrasound
"Silent regions" in thyroid scintiscan (a), 944
Tibia
Proximal tibiofibular joint: anatomic-pathologic-radiographic correlation, 133
Radiographic evaluation of plateau fractures (a), 1123
Tomography, see also specific organ, region
Atlas of Polytome pneumography: with particular reference to midline ventricles of brain (b), 764
Computed and conventional whole lung tomography in detecting pulmonary nodules, 51
Postoperative bony stenosis of lumbar spinal canal, 1059
Traction device for Polytome table (t), 732
Whole lung and CT for detecting pulmonary nodules, 981
Tongue
Current results of E.O.R.T.C. trial comparing low dose rate and classical fractionated treatments of base of tongue epitheliomas (a), 1109
Trachea
Collapse following esophageal atresia repair (a), 189
Pedunculated endotracheal metastasis (c), 713
Right paratracheal stripe in children (a), 759
Transposition of great vessels, see heart, congenital abnormalities
Treatment planning, see therapeutic radiology
Tricuspid valve, see also heart
Detection of regurgitation with echocardiography and peripheral vein injections (a), 186
Truog, Clarence Peter 1901-1978 (o), 756
Trophoblastic disease, see specific organ, part
Truncus arteriosus, see heart, congenital abnormalities
Tuberculosis, see also specific organ
Duodenal (c), 329

U

Ulcers, see specific organ
Ultrasound, see also specific organ, region
Adrenal (a), 760
Atlas of gray scale (b), 947
Clinical diagnosis (b), 193
Duodenal atresia in utero (c), 701
Ectopic pregnancy: accuracy of diagnosis, 153
Effect, alone and in combination with x-rays on chromosomes in vivo (a), 762
Extremity soft tissue lesions with arthrographic correlation (a), 944
Eye and orbit (b), 565
Gallstones: in vitro comparison of physical, radiographic, and characteristics, 223
Gray scale features of hematomas, 977
Gray scale of scrotum (a), 562
Inflammatory cysts of pelvic peritoneum, 633
Liver, primary cysts, 235
Obstetrical diagnosis by radiographic, nuclear, and (b), 765
Parathyroid (a), 760
"Phrygian cap" deformity with bistable and gray scale (a), 562
Prone view for pancreatic tail neoplasms, 231
Surgical and pathologic correlation of cholecystosonography and cholecystography, 227
Visualization of cervical cord cystic astrocytoma (c), 907
Water distention of gut in evaluation of pancreas (t), 348
Umbilicus
Pneumoperitoneum in congenital anomalies in umbilical region (a), 190
Ureter
CT of circumcaval (c), 1086
Diminished radiopacity of contrast material: sign of calculus, 847

Endometriosis, 627
Gamma camera method for quantification of split renal function in children followed for vesicoureteric reflux (a), 1127
Intraoperative trauma (a), 934
Transurethral conversion of percutaneous stent to indwelling stent (t), 1098
Urethra
Posterior valves as cause of neonatal uriniferous perirenal pseudocyst (urinoma) (a), 943
Urinary tract, see also specific urinary organ
Emmett's clinical urography (b), 763
Gamma camera method for quantification of split renal function in children followed for vesicoureteric reflux (a), 1127
Spontaneous rupture of calyceal diverticulum during urography (c), 337
Transurethral conversion of percutaneous ureteral stent to indwelling stent (t), 1098
Urography following angiocardiography in congenital heart abnormalities (a), 361
Urography
Diminished radiopacity of contrast material: sign of ureteral calculus, 847
Drip infusion with meglumine iodamide, 1043
Emmett's clinical (b), 763
Uterus, see also pregnancy
Endometriosis, 627
Fletcher gamma ray colpostat system (a), 563
Hysterographic double-outlined cavity: sign of unsuspected pregnancy, 305
Pneumopelvigraphy in childhood, 607
Stage 1 endometrial carcinoma management (a), 761
Thallium-201 scintigraphy, radionuclide imaging of uterus (a), 363
Uterus, ultrasound
Anomalies with renal agenesis, 973
Criteria of ectopic pregnancy, 967
CT and, in gynecologic pelvic masses, 955
Diagnosis of pelvic masses by gray scale, 469
Diagnosis of placenta previa: value of postvoid scan (a), 563
Dynamic uterus by time-lapse echography (a), 562
False placenta previa (a), 563
Sonolucent areas in placenta: sonographic and pathologic correlation, 961

V

Vagotomy, see gastrointestinal tract
Valsalva sinus, see aorta
Varices, see also vein
Transhepatic portal venogaphy and therapeutic coronary vein occlusion, 537
Vascular sling, see pulmonary arteries
Vein, see also angiography: embolism; arteriovenous malformation; portal vein; thrombosis; specific organ
Complications in expanded polytetrafluoroethylene arteriovenous grafts: angiography, 817
CT of tumor thrombosis of renal and inferior vena cava, 843
Evaluation of suspected deep thrombosis in arteriosclerotic patient (c), 531
Extended indications for carboxyangiography (a), 185
^{131}I-labeled fibrinogen in thrombosis, 451
Left superior intercostal, 599
Multiple contrast injections in epidural venography, 485
Splenic occlusion, 439
Venae cavae
CT of tumor thrombosis of renal vein and inferior, 843
Ultrasound of tumor extension (1), 1117
Venography, see also angiography; specific vein, organ, region
Complication rate with supine phlebography, 821
Epidural in diagnosis of lumbar disc herniation (a), 188
Ventricles, see brain; heart
Ventricular septal defect, see heart, congenital abnormalities
Ventriculography, see brain; radiography; heart
Vertebrae, see spine
Vesicoureteral reflux, see ureter
Volvulus, see specific organ

X

Xenon
^{133}Xe uptake by fatty livers (a), 1122

Official Journal
American Roentgen Ray Society
American Radium Society

Volume 131

AJR

Including Diagnostic Radiology • Radiation Oncology • Nuclear Medicine Ultrasonography • Related Sciences

Editor Melvin M. Figley

Associate Editor Rosalind H. Troupin

Assistant Editor John D. Harley

Contributing Editor E. Frederick Lang

Consulting Editorial Board Luther W. Brady • Kent Ellis • E. Robert Heitzman • Donald L. King • N. Thorne Griscom • Eugene C. Klatte • Kenneth Krabbenhoft • John G. McAfee • Russell H. Morgan • Thomas H. Newton • Robert G. Parker • Stewart R. Reuter • William B. Seaman • Robert J. Shalek • John Storer • Michel M. Ter-Pogossian • Joseph P. Whalen • David M. Witten

Editorial Staff K. A. Murray, manager • M. J. Leonard, manuscript editor • J. Anderson, assistant manuscript editor • C. P. Kaiser, secretary

Published monthly by Charles C Thomas, 301–327 East Lawrence Avenue, Springfield, Illinois 62717. All correspondence, except editorial office business, should be addressed to the publisher. Annual subscription rates: $40 ($20 for residents with letter of verification) plus appropriate mailing surcharge (see note next page). Single copies, $5. Undelivered or damaged copies replaced within 60 days of publication; 90 days for foreign subscribers. Allow 90 days for address changes. © 1978 by American Roentgen Ray Society. Second-class postage paid at Springfield, Illinois, and at additional mailing offices. Printed in U.S.A. ISSN 0361-803X

American Roentgen Ray Society

President: Harry Z. Mellins
President Elect: Paul A. Riemenschneider
1st Vice-president: Joseph D. Calhoun
2d Vice-president: Charles E. Bickham, Jr.
Secretary: James F. Martin
Treasurer: Harley C. Carlson

COMMITTEES 1977–1978

Executive Council: H. Z. Mellins, P. A. Riemenschneider, J. D. Calhoun, C. E. Bickham, Jr., J. F. Martin, H. C. Carlson, M. M. Figley, R. G. Evens, B. G. Brogdon, R. A. Gagliardi, E. Gedgaudas, G. A. Kling, T. F. Leigh, S. F. Ochsner, J. F. Wiot, R. E. Buenger, E. C. Klatte, J. P. Tampas, J. L. Gwinn, chairman

Finance and Budget: A. E. James, E. C. Klatte, R. McLelland, J. P. Tampas, R. G. Evens, chairman

Publications: M. P. Capp, K. Ellis, F. F. Ruzicka, Jr., E. R. Heitzman, R. A. Gagliardi, chairman

Editorial Policy: M. M. Figley, E. F. Lang, R. H. Troupin, E. R. Heitzman, K. Ellis, F. F. Ruzicka, Jr., M. P. Capp, R. A. Gagliardi, chairman

Advisory Committee on Education and Research: J. E. Youker, G. Wilson, G. W. Hartman, L. F. Rogers, E. Gedgaudas, chairman

Scientific Exhibits: T. C. Beneventano, G. Dodd, B. G. Brogdon, chairman

Constitution and Bylaws: J. H. Walker, W. M. Whitehouse, J. P. Tampas, chairman

American Board of Radiology Representatives: J. F. Roach, R. W. McConnell, S. W. Nelson

Program Committee: H. Z. Mellins, J. F. Martin, J. L. Gwinn, M. M. Figley, R. A. Gagliardi, B. G. Brogdon, E. Gedgaudas, G. A. Kling, P. Riemenschneider, chairman

Instruction Courses: E. Gedgaudas, director; G. W. Hartman, associate director

American College of Radiology Board of Chancellors Representative: W. B. Seaman

Annual Meeting: March 25–30, 1979, Sheraton Centre, Toronto, Canada

Scientific Program: P. A. Riemenschneider, president elect, Cottage Hospital, Santa Barbara, California 93105

Manager Annual Meeting: George A. Kling, Harper Hospital, Detroit, Michigan 48201

Membership: John L. Gwinn, 4650 Sunset Blvd., Los Angeles, California 90027

Business Office: Keith W. Gundlach, comptroller, American College of Radiology, 20 North Wacker Drive, Chicago, Illinois 60606

American Radium Society

President: Frederick W. George, III
President Elect: Alfred S. Ketcham
1st Vice-president: Julian P. Smith
2d Vice-president: Edwin M. Jacobs
Secretary: Norah duV. Tapley
Treasurer: Simon Kramer

COMMITTEES 1978–1979

Executive: A. S. Ketcham, J. P. Smith, E. M. Jacobs, N. duV. Tapley, S. Kramer, L. W. Brady, R. H. Jesse, F. W. George, F. Rutledge, chairman

Public Relations: V. Marcial, J. Vaeth, C. Honaker, ex-officio, and F. George, chairman

Publication: K. L. Krabbenhoft, D. Hussey, A. Raventos, I. Fix, L. W. Brady, chairman

Scientific Program: R. Parker, J. Durant, A. S. Ketcham, M. S. Mitchell, G. Murphy, F. Rutledge, M. Griem, W. E. Powers, M. Apuzzo, F. George, chairman

Local Arrangements: L. Davis, J. Vaeth, J. Nolan, R. McKenna, J. Slater, J. Stein, J. Scallon, S. Kramer, J. Helsper, chairman

Constitution and Bylaws: A. S. Glicksman, P. J. DiSaia, K. L. Krabbenhoft, chairman

Audiovisual: C. R. Bogardus, J. Helsper, R. Schweitzer, R. H. Jesse, C. Perez, J. Glassburn, A. M. Nisar Syed, R. Young, B. Herrington, F. George, chairman

American Board of Radiology Representatives: J. J. Stein, R. E. King, N. duV. Tapley

American College of Radiology Board of Chancellors Representative: L. W. Brady

American College of Radiology Council Representative: J. del Regato

Editorial Board of AFCOS Newsletter Representative: J. Vaeth

National Council on Radiation Protection and Measurements Liaison Representative: L. W. Davis

Annual Meeting: March 4–8, Los Angeles, California

Scientific Program: F. W. George, III, University of Southern California School of Medicine, Los Angeles, California 90033

Local Arrangements: James Helsper, Pasadena, California

Membership: Norah duV. Tapley, secretary, M. D. Anderson Hospital, 6723 Bertner Avenue, Houston, Texas 77030

Business Office: N. V. Jordan, c/o R. H. Jesse, M. D. Anderson Hospital and Tumor Institute, 6723 Bertner Avenue, Houston, Texas 77030

Mailing note.—Mailing surcharges: U.S. and possessions, none; European countries, $25; Japan, $45; other, $10. European rates apply to Algeria, Austria, Belgium, Czechoslovakia, Denmark, Finland, France, Germany, Great Britain, Greece, Hungary, India, Iran, Ireland, Israel, Italy, Kenya, Luxembourg, Netherlands, Nigeria, Norway, Portugal, Romania, South Africa, Spain, Sweden, Switzerland, Turkey, Uganda, Yugoslavia. All subscriptions to Japan and European countries are delivered by air freight; there is no option for surface mail.

American Journal of Roentgenology

Vol. 131 **July 1978** **No. 1**

MEDICAL EFFICACY OF CT

1 **Editorial: Evaluation of Computed Tomography: Achievement and Challenge.** *Fineberg HV*

5 **Clinical Efficacy of Computed Body Tomography.** *Wittenberg J, Fineberg HV, Black EB, Kirkpatrick RH, Schaffer DL, Ikeda MK, Ferrucci JT Jr*

15 **Observations on the Medical Efficacy of Computed Tomography of the Chest and Abdomen.** *Robbins AH, Pugatch RD, Gerzof SG, Faling LJ, Johnson WC, Sewell DH*

21 **Computed Body Tomography in Children: Evaluation of 45 Patients.** *Brasch RC, Korobkin M, Gooding CA*

27 **Cranial Computed Tomography in Diagnosis and Management of Acute Head Trauma.** *Zimmerman RA, Bilaniuk LT, Gennarelli T, Bruce D, Dolinskas C, Uzzell B*

35 **Computed Tomography in Patients with Cerebrovascular Disease: Impact of a New Technology on Patient Care.** *Larson EB, Omenn GS, Loop JW*

41 **Impact of Computed Tomography on the Care of Patients with Suspected Hydrocephalus.** *Larson EB, Omenn GS, Magno J*

45 **Efficacy of Computed Tomography of the Head in Changing Patient Care and Health Costs: A Retrospective Study.** *Bahr AL, Hodges FJ III*

51 **Comparison of Computed and Conventional Whole Lung Tomography in Detecting Pulmonary Nodules: A Prospective Radiologic-Pathologic Study.** *Schaner EG, Chang AE, Doppman JL, Conkle DM, Flye MW, Rosenberg SA*

55 **Computed Tomography of Musculoskeletal Disorders.** *Wilson JS, Korobkin M, Genant HK, Bovill EG Jr*

63 **Value of Computed Tomography in Radiotherapy of Lung Cancer.** *Emami B, Melo A, Carter BL, Munzenrider JE, Piro AJ*

69 **Contribution of Computed Tomography to the Treatment of Lymphomas.** *Pilepich MV, Rene JB, Munzenrider JE, Carter BL*

75 **Efficacy of CT-assisted Two-dimensional Treatment Planning: Analysis of 45 Patients.** *Ragan DP, Perez CA*

81 **Computed Tomography: Cost and Efficacy Implications.** *Abrams HL, McNeil BJ*

89 **Efficiency of Utilization of a Computed Tomography Scanner.** *Winter J*

95 **Computed Tomographic Scanning in Children: Comparison of Radiation Dose and Resolving Power of Commercial CT Scanners.** *Brasch RC, Boyd DP, Gooding CA*

DIAGNOSTIC IMAGING

103 **Potential Uses of More Accurate CT Absorption Values by Filtering.** *Hounsfield GN*

107 **Diagnosis of Extracerebral Fluid Collections by Computed Tomography.** *Cornell SH, Chiu LC, Christie JH*

111 **Computed Tomography in Ocular Neoplastic Disease.** *Bernardino ME, Danziger J, Young SE, Wallace S*

115 **External Anatomic Landmarks of the Abdomen Related to Vertebral Segments: Applications in Cross-sectional Imaging.** *Kuhns LR, Borlaza GS, Seigel R, Thornbury JR*

119 **Buckling of the Innominate Artery Simulating a Right Apical Lung Mass.** *Christensen EE, Landay MJ, Dietz GW, Brinley G*

125 **External Iliac Artery Fibrodysplasia.** *Walter JF, Stanley JC, Mehigan JT, Reuter SR, Guthaner DF*

129 **Comparison of Arachnoiditis Produced by Meglumine Iocarmate and Metrizamide Myelography in an Animal Model.** *Haughton VM, Ho KC, Larson SJ, Unger GF, Correa-Paz F*

133 **Proximal Tibiofibular Joint: Anatomic-Pathologic-Radiographic Correlation.** *Resnick D, Newell JD, Guerra J Jr, Danzig LA, Niwayama G, Goergen TG*

139 **Lisfranc's Fracture-Dislocation: A Manifestation of Peripheral Neuropathy.** *Giesecke SB, Dalinka MK, Kyle GC*

143 **Gastrointestinal Angiographic Findings in Systemic Amyloidosis.** *Schroeder FM, Miller FJ Jr, Nelson JA, Rankin RS*

147 **Atypical Appearances of Benign Hyperplastic Gastric Polyps.** *Joffe N, Antonioli DA*

153 **Ectopic Pregnancy: Criteria and Accuracy of Ultrasonic Diagnosis.** *Lawson TL*

CASE REPORTS

157 **Successful Transcatheter Gelfoam Embolization of a Bleeding Cecal Vascular Ectasia.** *Sniderman KW, Franklin J Jr, Sos TA*

160 **Aortoesophageal Fistula as a Complication of Aortic Prosthetic Graft.** *Seymour EQ*

162 **Pseudoocclusion of a Superficial Temporal–Middle Cerebral Artery Bypass.** *Dublin AB, Richey DC*

164 **Coccygeal Ribs: Development and Appearance in Two Cases.** *Pais MJ, Levine A, Pais SO*

167 **Esophageal Atresia, Duodenal Atresia, and Gastric Distention: Report of Two Cases.** *McCook TA, Felman AH*

TECHNICAL NOTES

169 **Simple Device to Measure Patient Position on Portable Chest Radiographs.** *Gallant TE, Dietrich PA, Shinozaki T, Deane RSD*

171 **Semierect and Erect Position in Percutaneous Transhepatic Cholangiography.** *Latshaw RF, Rohrer GV*

173 **SPECIAL REPORT: American College of Radiology Diagnostic Efficacy Studies.** *Loop JW, Lusted LB*

180 **79th ARRS Meeting Information**

181 **From Earlier Pages**

182 **Letters**

184 **Abstracts of Current Literature**

191 **Book Reviews**

194 **News**

American Journal of Roentgenology

Vol. 131 **August 1978** **No. 2**

DIAGNOSTIC IMAGING

197 **Fluoroscopically Guided Thin Needle Aspiration Biopsy of the Abdomen and Retroperitoneum.** *Pereiras RV, Meiers W, Kunhardt B, Troner M, Hutson D, Barkin JS, Viamonte M*

203 **Association of Antral Diaphragms and Hypertrophic Pyloric Stenosis.** *Mandell GA*

207 **Double Contrast Barium Enema in Crohn's Disease and Ulcerative Colitis.** *Kelvin FM, Oddson TA, Rice RP, Garbutt JT, Bradenham BP*

215 **Malignant Fistulae of the Gastrointestinal Tract.** *Martinez LO, Manheimer LH, Casal GL, Lubin J*

219 **Air in Gallbladder: A Frequent Finding in Gallstone Ileus.** *Balthazar EJ, Schechter LS*

223 **Gallstones: In Vitro Comparison of Physical, Radiographic, and Ultrasonic Characteristics.** *Carroll BA*

227 **Surgical and Pathologic Correlation of Cholecystosonography and Cholecystography.** *Crade M, Taylor KJW, Rosenfield AT, de Graaff CS, Minihan P*

231 **Prone View Ultrasonography for Pancreatic Tail Neoplasms.** *Goldstein HM, Katragadda CS*

235 **Ultrasonography of Primary Cysts of the Liver.** *Spiegel RM, King DL, Green WM*

239 **Fine Needle Aspiration Biopsy in the Diagnosis of Mediastinal Lesions.** *Rosenberger A, Adler O*

243 **Ventilation-Perfusion Scans in Neonatal Regional Pulmonary Emphysema Complicating Ventilatory Assistance.** *Leonidas JC, Moylan FMB, Kahn PC, Ramenofsky ML*

247 **Detection Accuracy in Chest Radiography.** *Gray JE, Taylor KW, Hobbs BB*

255 **Bronchography in the Recognition of Congenital Cystic Bronchiectasis.** *Aliabadi P, Shafiepoor H*

259 **Laryngocele.** *Lindell MM Jr, Jing BS, Fischer EP, Guillamondegui OM, Wallace S*

263 **Wilms' Tumor to the Heart: Clinical and Radiographic Evaluation.** *Slovis TL, Cushing B, Reilly BJ, Farooki ZQ, Philippart AI, Berdon WE, Baker DH, Reed JO*

267 **Benign Pneumoperitoneum Following Median Sternotomy Incision.** *Glanz S, Ravin CE, Deren MM*

271 **Anterior Pathway for Transdiaphragmatic Extension of Pneumomediastinum.** *Kleinman PK, Brill PW, Whalen JP*

277 **Radiographic Spectrum of Pleuropulmonary Tularemia.** *Rubin SA*

283 **Selective Involvement of the First Carpometacarpal Joint in Scleroderma.** *Resnick D, Greenway G, Vint VC, Robinson CA, Piper S*

287 **Pseudocysts of the Humerus.** *Helms CA*

289 **Proximal Femoral Focal Deficiency.** *Schatz SL, Kopits SE*

297 **Routine Oblique Radiography of the Pediatric Lumbar Spine: Is It Necessary?** *Roberts FF, Kishore PRS, Cunningham ME*

299 **Remote Effects of Neuroblastoma.** *Keating JW, Cromwell LD*

305 **Hysterographic Double-outlined Uterine Cavity: A Sign of Unsuspected Pregnancy.** *Isaacs I*

307 **Incudostapedial Joint in Health and Disease.** *Matsubara R, Konrad H, Hanafee WN*

311 **Accuracy of Computed Tomography in Detecting Intraabdominal and Pelvic Adenopathy in Lymphoma.** *Lee JKT, Stanley RJ, Sagel SS, Levitt RG*

317 **CT Detection of Infected Synthetic Grafts: Preliminary Report of a New Sign.** *Haaga JR, Baldwin GN, Reich NE, Beven E, Kramer A, Weinstein A, Havrilla TR, Seidelmann FE, Namba AH, Parrish CM*

321 **Diagnostic Oncology Case Studies: "Maxillary Sinusitis" and Cancer: The Role of Polytomography.** *Contributed by Rao A, Gilbert HA*

CASE REPORTS

323 **CT-guided Seldinger Catheter Drainage of a Hepatic Abscess.** *Stephenson TF, Guzzetta LR, Tagulinao OA*

325 **Mediastinal Lymphadenopathy and Undifferentiated Connective Tissue Disease: Case Report and Review.** *Gordonson J, Quinn M, Kaufman R, Van den Tweel JG*

329 **Duodenal Tuberculosis.** *Black GA, Carsky EW*

331 **Control of a Traumatic Vertebral Arteriovenous Fistula by a Modified Gianturco Coil Embolus System.** *Rossi P, Passariello R, Simonetti G*

334 **Reduction of Jejunogastric Intussusception during Upper Gastrointestinal Examination.** *Marx WJ*

337 **Spontaneous Rupture of a Calyceal Diverticulum during Urography.** *Ulreich S, Lund DA, Jacobson JJ*

339 **Pancreatic Cystadenocarcinoma: CT Body Scan and Gray Scale Ultrasound Appearance.** *Carroll B, Sample WF*

342 **Extravasation of Ethiodol into Deep Tissues of the Foot: A Complication of Lymphangiography.** *Rubin BE*

344 **Detection of a Cerebrospinal Fluid Fistula by Computed Tomography.** *Levy JM, Christensen FK, Nykamp PW*

TECHNICAL NOTES

346 **Computed Sagittal Tomography of the Orbit.** *Haverling M, Johanson H*

348 **Water Distension of the Gut in the Evaluation of the Pancreas by Ultrasound.** *Crade M, Taylor KJW, Rosenfield AT*

350 **The Hook Sign in Type 3 Congenital Colonic Atresia.** *Selke AC Jr, Jona JZ*

352 **SPECIAL REPORT: International Nomenclature of Constitutional Diseases of Bone**

355 **Editorial: Authors of Scientific Articles and the Copyright Act of 1976.** *Passano WM Sr*

357 **Letters**

359 **Abstracts of Current Literature**

364 **Book Reviews**

366 **News**

369 **Radiologic Societies**

American Journal of Roentgenology

Vol. 131 September 1978 No. 3

373 **Progress in Radiology: Historical Review of the Changing Concepts of Lower Esophageal Anatomy: 430 B.C.–1977.** *Friedland GW*

389 **Computed Tomographic Diagnosis of Obstructive Jaundice in the Absence of Intrahepatic Ductal Dilatation.** *Shanser JD, Korobkin M, Goldberg HI, Rohlfing BM*

393 **Focal Nodular Hyperplasia and Liver Cell Adenoma: Radiologic and Pathologic Differentiation.** *Casarella WJ, Knowles DM, Wolff M, Johnson PM*

403 **Intrathoracic Lymph Node Metastases from Extrathoracic Neoplasms.** *McLoud TC, Kalisher L, Stark P, Greene R*

409 **A Reevaluation of Intrathoracic Lymphadenopathy in Sarcoidosis.** *Bein ME, Putman CE, McLoud TC, Mink JH*

417 **Congenital Partial Eventration of the Left Diaphragm.** *Hesselink JR, Chung KJ, Peters ME, Crummy AB*

421 **Gastric Emphysema in Infants with Hypertrophic Pyloric Stenosis.** *Lester PD, Budge AF, Barnes JC, Kirks DR*

425 **Systemic Air Embolism Secondary to Respiratory Therapy in the Neonate: Six Cases Including One Survivor.** *Kogutt MS*

431 **Angiographic Demonstration of Complications Resulting from the Waterston Procedure.** *Levin DC, Fellows KE, Sos TA*

439 **Recognition of Splenic Vein Occlusion.** *Cho KJ, Martel W*

445 **Improved Safety of Splenoportography by Plugging of the Needle Tract.** *Probst P, Rysavy JA, Amplatz K*

451 **^{131}I-labeled Fibrinogen in the Diagnosis of Deep Vein Thrombosis of the Lower Extremities.** *Prescott SM, Tikoff G, Coleman RE, Richards KL, Armstrong JD Jr, Hershgold EL, McDaniel DC, Ganchan RP*

455 **Chronic Vascular Reactions to Steel Coil Occlusion Devices.** *Barth KH, Strandberg JD, Kaufman SL, White RI Jr*

459 **Computed Tomographic Evaluation of the Breast.** *Chang CHJ, Sibala JL, Fritz SL, Gallagher JH, Dwyer SJ III, Templeton AW*

465 **Selective Use of the Oblique Projection in Mammography.** *Hall FM, Berenberg AL*

469 **Differential Diagnosis of Pelvic Masses by Gray Scale Sonography.** *Fleischer AC, James AE Jr, Millis JB, Julian C*

477 **Incidence of Growth Lines in Psychosocial Dwarfs and Idiopathic Hypopituitarism.** *Hernandez RJ, Poznanski AK, Hopwood NJ, Kelch RP*

481 **Osteogenic Sarcoma after the Age of 50: A Radiographic Evaluation.** *deSantos LA, Rosengren JE, Wooten WB, Murray JA*

485 **Multiple Contrast Injections in Epidural Venography.** *Giustra PE, Wickenden JW, Furman RS, Wickenden RW, Killoran PJ*

489 **Radiologic Assessment of Pituitary Microadenomas.** *Robertson WD, Newton TH*

493 **CT Detection and Course of Intracranial Hemorrhage in Premature Infants.** *Rumack CM, McDonald MM, O'Meara OP, Sanders BB, Rudikoff JC*

499 **Mesonephric Duct Remnants (Gartner's Duct).** *Wepfer JF, Boex RM*

501 **Microradiographic Demonstration of Pyelolymphatic Backflow in the Porcine Kidney.** *Cuttino JT Jr, Clark RL, Fried FA, Stevens PS*

CASE REPORTS

507 **Arteriovenous Malformation of the Right Leaf of the Diaphragm Communicating with Vascular Malformation of the Right Lung.** *Rashad FA, Bellon EM*

509 **Severe Reactions to Contrast Material by Three Consecutive Routes: Intravenous, Subcutaneous, and Intraarterial.** *Cho KJ, Thornbury JR*

511 **Carcinoid Syndrome Treated by Hepatic Embolization.** *Pueyo I, Jiménez JR, Hernández J, Brugarolas A, García-Morán M, García-Muñiz JL, Arroyo F*

515 **CT Diagnosis of Pericardial Cysts.** *Pugatch RD, Braver JH, Robbins AH, Faling LJ*

517 **Lipoma of the Corpus Callosum Associated with a Frontal Bone Defect.** *Kushnet MW, Goldman RL*

519 **Giant Papilloma of the Thoracic Esophagus.** *Walker JH*

521 **Pancreatic Duct Obstruction: A New Observation during Fine Needle Percutaneous Transhepatic Cholangiography.** *Freeny PC, Rosoff L Jr*

523 **Infant Botulism: An Unusual Cause of Intestinal Hypomotility.** *Merten DF, Leung K, Goller DS*

525 **Pseudoaneurysm of the Arterial Anastomosis in a Renal Transplant.** *Renigers SA, Spigos DG*

527 **Procarbazine Lung.** *Ecker MD, Jay B, Keohane MF*

529 **Colitis Cystica Profunda.** *Ledesma-Medina J, Reid BS, Girdany BR*

531 **Evaluation of Suspected Deep Venous Thrombosis in the Arteriosclerotic Patient.** *Gordon IJ*

TECHNICAL NOTES

534 **A Modified Punch Card for Extending Filming Program of a Puck Changer.** *Chuang VP, Clements DL*

535 **Easy Coronal Scans.** *Gallagher TJ*

536 **International System of Units (SI).** *Wyckoff HO*

539 **Bone Measurement Conference.** *Mazess RB*

554 **Editorial:** The Areae Gastricae. *Seaman WB*

555 **Letters**

557 **Abstracts of Current Literature**

564 **Book Reviews**

568 **News**

American Journal of Roentgenology

Vol. 131 **October 1978** **No. 4**

DIAGNOSTIC IMAGING

571 **Coronary, Ventricular, and Pulmonary Abnormalities Associated with Rupture of the Interventricular Septum Complicating Myocardial Infarction.** *Miller SW, Dinsmore RE, Greene RE, Daggett WM*

579 **Bilateral Pleural Thickening: A Manifestation of Asbestos Dust Exposure.** *Sargent EN, Gordonson J, Jacobson G, Birnbaum W, Shaub M*

587 **Pulmonary Manifestations of Acute Aspiration of Gastric Contents.** *Landay MJ, Christensen EE, Bynum LJ*

593 **Accuracy of Chest Film Screening by Technologists in the New York Early Lung Cancer Detection Program.** *Flehinger BJ, Melamed MR, Heelan RT, McGinnis CM, Zaman MB, Martini N*

599 **The Normal and Abnormal Left Superior Intercostal Vein.** *Friedman AC, Chambers E, Sprayregen S*

603 **Subglottic Edema in Acute Epiglottitis in Children.** *Shackelford GD, Siegel MJ, McAlister WH*

607 **Pneumopelvigraphy in Childhood.** *Lester PD, McAlister WH*

613 **Radiographic Findings in Ovarian Teratomas in Children.** *Siegel MJ, McAlister WH, Shackelford GD*

617 **Mailed Thermoluminescent Dosimeter Determination of Entrance Skin Exposure and Half-Value Layer in Mammography.** *Wochos JF, Fullerton GD, DeWerd LA*

621 **Benign Multilocal Cystic Nephroma.** *Carlson DH, Carlson D, Simon H*

627 **Radiographic Features of Ureteral Endometriosis.** *Pollack HM, Wills JS*

633 **Inflammatory Cysts of the Pelvic Peritoneum.** *Lees RF, Feldman PS, Brenbridge ANAG, Anderson WA, Buschi AJ*

637 **Pitfalls of Transhepatic Portal Venography and Therapeutic Coronary Vein Occlusion.** *Widrich WC, Robbins AH, Nabseth DC, Johnson WC, Goldstein SA*

645 **Transcatheter Gelfoam Embolization of Posttraumatic Bleeding Pseudoaneurysms.** *Chang J, Katzen BT, Sullivan KP*

651 **Transcatheter Embolization: Prevention of Embolic Reflux Using Balloon Catheters.** *Greenfield AJ, Athanasoulis CA, Waltman AC, LeMoure ER*

657 **Bleeding Simulated by the Distal Internal Pudendal Artery Stain.** *Schrumpf JD, Sommer G, Jacobs RP*

661 **Gas in the Bile Ducts (Pneumobilia) in Emphysematous Cholecystitis.** *Harley WD, Kirkpatrick RH, Ferrucci JT Jr*

665 **Rheumatoid Arthritis and Its Variants: Analysis of Scintiphotographic, Radiographic, and Clinical Examinations.** *Weissberg DL, Resnick D, Taylor A, Becker M, Alazraki N*

675 **Accuracy of CT in Detecting Intraabdominal and Pelvic Lymph Node Metastases from Pelvic Cancers.** *Lee JKT, Stanley RJ, Sagel SS, McClennan BL*

681 **Effect of CT Noise on Detectability of Test Objects.** *Chew E, Weiss GH, Brooks RA, Di Chiro G*

687 **Optimal Contrast Dosage in Cranial Computed Tomography.** *Norman D, Enzmann DR, Newton TH*

691 **Progress in Radiology: Colorectal Tumors: Pathology and Detection.** *Ott DJ, Gelfand DW*

697 **Diagnostic Oncology Case Studies: Radiologic Investigation of Bloody Ascites.** *Contributed by Steckel RJ*

CASE REPORTS

701 **Sonographic Appearance of Duodenal Atresia in Utero.** *Lees RF, Alford BA, Brenbridge ANAG, Buschi AJ, Williamson BRJ*

703 **Pulmonary Uptake of ^{99m}Tc Diphosphonate in Alveolar Microlithiasis.** *Brown ML, Swee RG, Olson RJ, Bender CE*

705 **Nonfatal Pulmonary Air Embolism: Radiographic Demonstration.** *Faer MJ, Messerschmidt GL*

707 **Miliary Aspergillosis Associated with Alcoholism.** *Blum J, Reed JC, Pizzo SV, Thompson WM*

710 **Coronary Artery Anomaly in Double-Outlet Right Ventricle.** *Udoff EJ, Roland JM, White RI Jr*

713 **Pedunculated Endotracheal Metastasis.** *MacMahon H, O'Connell DJ, Cimochowski GE*

715 **Nonfunctioning Islet Cell Tumors of the Pancreas: Radiographic and Ultrasonographic Appearances in Two Cases.** *Gold J, Rosenfield AT, Sostman D, Burrell M, Taylor KJW*

718 **Abnormal Peripheral Distribution of Thallium-201 due to Arteriosclerosis.** *Glass EC, DeNardo GL*

721 **Subclavian Artery as the First Branch of the Aortic Arch: A Normal Variant in Two Patients.** *Boechat MI, Gilsanz V, Fellows KE*

723 **Polypoid Leukemic Infiltration of the Large Bowel.** *Rabin MS, Bledin AG, Lewis D*

725 **Leukemic Infiltration of the Colon.** *Limberakis AJ, Mossler JA, Roberts L Jr, Jackson DC, Thompson WM*

729 **Fracture of the Occipital Condyle.** *Bolender N, Cromwell LD, Wendling L*

TECHNICAL NOTE

732 **Traction Device for Use with Polytome Table.** *Deeb ZL, Martin TA, Kerber CW*

733 **Editorial: On Behalf of Translumbar Aortography.** *Reuter SR*

734 **From Earlier Pages**

736 **Letters**

737 **1979 ARRS Comprehensive Meeting Information**

755 **Memorials**

757 **Abstracts of Current Literature**

763 **Book Reviews**

767 **News**

769 **Radiologic Societies**

735 **Erratum**

American Journal of Roentgenology

Vol. 131 **November 1978** **No. 5**

DIAGNOSTIC IMAGING

773 **Radium-induced Malignant Tumors of the Mastoid and Paranasal Sinuses.** *Littman MS, Kirsh IE, Keane AT*

787 **Radiologic and Clinical Assessment of Broad-Spectrum Antibiotic Therapy in Crohn's Disease.** *Moss AA, Carbone JV, Kressel HY*

791 **Association of Squamous Cell Carcinoma of the Head and Neck with Cancer of the Esophagus.** *Goldstein HM, Zornoza J*

795 **Cystic Neoplasms of the Pancreas: New Angiographic and Ultrasonographic Findings.** *Freeny PC, Weinstein CJ, Taft DA, Allen FH*

803 **Lymphangiographic Changes after Radiation Therapy.** *Jonsson K, Lidshitz HI, Osborne BM*

807 **High-Dose Renal Pharmacoangiography in the Assessment of Hypovascular Renal Neoplasms.** *Chuang VP, Fried AM*

813 **Optimal Technique of Renal Arteriography in Living Renal Transplant Donors.** *Strauser GD, Stables DP, Weil R III*

817 **Complications in Expanded Polytetrafluoroethylene Arteriovenous Grafts: An Angiographic Study.** *Lemaitre P, O'Regan S, Herba M, Kaye M*

821 **Complication Rate with Supine Phlebography.** *Coel MN, Dodge W*

823 **Flow-directed Balloon Catheterization for Aortofemoral Arteriography Using the Axillary Artery Approach.** *Buonocore E, Lynch TP*

827 **A New Noninvasive Approach to Peripheral Vascular Disease: Thallium-201 Leg Scans.** *Siegel ME, Siemsen JK*

831 **Computed Tomography in the Detection of Retroperitoneal Hemorrhage after Translumber Aortography.** *Bergman AB, Neiman HL*

835 **Detection of Neoplastic Involvement of the Mesentery and Omentum by Computed Tomography.** *Levitt RG, Sagel SS, Stanley RJ*

839 **Computed Tomography of Necrotic Hepatic Metastases.** *Wooten WB, Bernardino ME, Goldstein HM*

843 **CT Diagnosis of Tumor Thrombosis of the Renal Vein and Inferior Vena Cava.** *Marks WM, Korobkin M, Callen PW, Kaiser JA*

847 **Diminished Radiopacity of Contrast Material: A Urographic Sign of Ureteral Calculus.** *Korobkin M, Jacobs RP, Clark RE, Minagi H*

851 **New Observations in Renal Transplants Using Ultrasound.** *Conrad MR, Dickerman R, Love IL, Curry T, Peters P, Hull A, Lerman M, Helderman H*

857 **Calcified Bodies in Popliteal Cysts: A Characteristic Radiographic Appearance.** *Goldberg RP, Genant HK*

861 **Complications of Catheter Cerebral Arteriography: Analysis of 5,000 Procedures. I. Criteria and Incidence.** *Mani RL, Eisenberg RL, McDonald EJ Jr, Pollock JA, Mani JR*

867 **Complications of Catheter Cerebral Arteriography: Analysis of 5,000 Procedures. II. Relation of Complication Rates to Clinical and Arteriographic Diagnoses.** *Mani RL, Eisenberg RL*

871 **Complications of Catheter Cerebral Arteriography: Analysis of 5,000 Procedures. III. Assessment for Arteries Injected, Contrast Medium Used, Duration of Procedure, and Age of Patient.** *Mani RL, Eisenberg RL*

875 **Coronal Computed Tomography: Indications and Accuracy.** *Mass S, Norman D, Newton TH*

881 **CT Contrast Enhancement in Cerebral Infarction.** *Norton GA, Kishore PRS, Lin J*

CASE REPORTS

887 ***Streptococcus bovis* Septicemia as a Clue to Colon Neoplasms in Two Cases.** *Smith TR, Friedman SN, Adler H*

889 **Bile Leak into a Hepatic Abscess in a Liver Transplant: Demonstration with ^{99m}Tc-Diethyl-Iminodiacetic Acid.** *Klingensmith WC III, Koep LJ, Fritzberg AR*

892 **Legionnaires Disease.** *Reed JC, McLelland R, Nelson P*

895 **Ultrasound Diagnosis of Hydatid Disease (Echinococcosis) in Two Cases.** *Babcock DS, Kaufman L, Cosnow I*

898 **Diffuse Lymphatic Dysplasia with Hepatic Oil Embolism.** *Tatezawa T, Akisada M*

901 **Free-floating Calculi in the Pericardial Cavity.** *Littleton JT, Cady JB*

904 **Focal Perfusion Defect Caused by Sequestration in Two Cases.** *Van Aman ME, Lloyd TV, Johnson JC*

906 **Complications from Intraarterial Lidocaine in Upper Extremity Arteriography.** *Chuang VP, Widrich WC*

907 **Ultrasonic Visualization of a Cervical Cord Cystic Astrocytoma.** *Reid MH*

909 **Huge Laparotomy Pad Granuloma Simulating a Gastric Wall Tumor.** *Carsky EW, Haswell DM*

911 **Enlargement of the Intervertebral Foramina: An Unusual Cause.** *Patel DV, Ferguson L, Schey WL*

914 ***Chlamydia trachomatis:* A Cause of an Infantile Pneumonia Syndrome.** *Stickney RH, Bjelland JC, Capp MP, Harrison RR, Hansen R*

TECHNICAL NOTES

916 **Radiography of LeVeen Type Peritoneovenous Shunts.** *Freiman DB, Ring EJ, Oleaga JA, Rosato EF*

918 **Pathologic Index for Arrangement of Teaching File.** *Daffner RH*

919 **Progress in Radiology: Total Body Opacification.** *Griscom NT*

926 **Editorial: Rare Earth Screens and Silver.** *Wilson RA*

928 **Letters**

931 **Abstracts of Current Literature**

946 **Book Reviews**

950 **News**

929 **ARRS 1979 Meeting Summary**

American Journal of Roentgenology

Vol. 131 **December 1978** **No. 6**

DIAGNOSTIC IMAGING

955 **Prospective Comparison of Ultrasound and Computed Tomography in the Evaluation of Gynecologic Pelvic Masses.** *Walsh JW, Rosenfield AT, Jaffe CC, Schwartz PE, Simeone J, Dembner AG, Taylor KJW*

961 **Sonolucent Areas in the Placenta: Sonographic and Pathologic Correlation.** *Spirt BA, Kagan EH, Rozanski RM*

967 **Analysis of Ultrasonographic Criteria in the Evaluation for Ectopic Pregnancy.** *Brown TW, Filly RM, Laing FC, Barton J*

973 **Uterine Anomalies Associated with Renal Agenesis: Role of Gray Scale Ultrasonography.** *Fried AM, Oliff M, Wilson EA, Wisnant J*

977 **Gray Scale Features of Hematomas: An Ultrasonic Spectrum.** *Wicks JD, Silver TM, Bree RL*

981 **Comparison of Whole Lung Tomography and Computed Tomography for Detecting Pulmonary Nodules.** *Muhm JR, Brown LR, Crowe JK, Sheedy PF II, Hattery RR, Stephens DH*

985 **Radiographic Manifestations of Pulmonary *Mycobacterium kansasii* Infections.** *Christensen EE, Deitz GW, Ahn CH, Chapman JS, Murry RC, Hurst GA*

995 **Identification of Thoracic Isomerism from the Plain Chest Radiography.** *Soto B, Pacifico AD, Souza AS Jr, Bargeron LM Jr, Ermocilla R, Tonkin IL*

1003 **Congenital Pulmonary Atresia: Photographic Subtraction as an Aid in Recognizing Hypoplastic Pulmonary Arteries.** *Fulton RE, Davis GD*

1009 **Radiographic and Echocardiographic Evaluation of Newborns Treated with Indomethacin for Patent Ductus Arteriosus.** *Edwards DK, Higgins CB, Merritt TA, DiSessa TG, Friedman WF*

1015 **Intermittent Bleeding from Minute to Minute in Acute Massive Gastrointestinal Hemorrhage: Arteriographic Demonstration.** *Sos TA, Lee JG, Wixson D, Sniderman KW*

1019 **Protean Manifestations of Mycotic Aneurysms.** *Kaufman SL, White RI Jr, Harrington DP, Barth KH, Siegelman SS*

1027 **Transcatheter Occlusion of the Arterial Supply to Arteriovenous Fistulas with Gianturco Coils.** *Layne TA, Finck EJ, Boswell WD*

1031 **Mammographic Parenchymal Patterns as Risk Indicators for Incident Cancer in a Screening Program: An Extended Analysis.** *Krook PM*

1037 **Radiology of the Jugular Tubercles.** *Osborn AG, Brinton WR, Smith WH*

1041 **Technetium-99m Pertechnetate as an Indicator of Gastric Mucosal Proliferation.** *Pecora DV, Sagar V, Piccone J*

1043 **Drip Infusion Urography with Meglumine Iodamide.** *Robbins AH, Rosenfield AT, Pizzolato NF, Irwin GA, Putman CE, Gerzof SG, Ulreich S*

1047 **Shoulder Arthrography as a Treatment Modality.** *Gilula LA, Schoenecker PL, Murphy WA*

1049 **Association of Diffuse Idiopathic Skeletal Hyperostosis (DISH) and Calcification and Ossification of the Posterior Longitudinal Ligament.** *Resnick D, Guerra J Jr, Robinson CA, Vint VC*

1055 **Intraarticular Methyl Methacrylate: A Complication of Hip Surgery.** *Tailor CC, Murphy WA, Smith EL*

1059 **Postoperative Bony Stenosis of the Lumbar Spinal Canal: Evaluation of 164 Symptomatic Patients with Axial Radiography.** *Quencer RM, Murtagh FR, Post MJD, Rosomoff HL, Stokes NA*

1065 **Diagnostic Oncology Case Studies: Colonic Polyposis and Cancer.** *Contributed by Rao A, Khazin A, Fremland A*

CASE REPORTS

1069 **Pheochromocytoma with Reversible Renal Artery Stenosis.** *Velick WF, Bookstein JJ*

1072 **Embolization for Postbiopsy Renal Arteriovenous Fistula: Effective Occlusion Using Homologous Clot.** *Rosen RJ, Feldman L, Wilson AR*

1074 **Demonstration of Pancreatic Cysts in Adult Polycystic Disease by Computed Tomography and Ultrasound.** *Shirkhoda A, Mittelstaedt CA*

1077 **Pseudomass of the Liver Due to Pleural Effusion and Inversion of the Diaphragm.** *Katzen BT, Choi WS, Friedman MH, Green IJ, Hindle WV, Zellis A*

1079 **Cathartic Colitis.** *Kim SK, Gerle RD, Rozanski R*

1082 **Multinodular Primary Amyloidosis of the Lung: Diagnosis by Needle Biopsy.** *Bierny JP*

1084 **Abdominal Twiddler's Syndrome.** *Rodan BA, Lowe JE, Chen JTT*

1086 **Computed Tomography of Circumcaval Ureter.** *Gefter WB, Arger PH, Mulhern CB, Pollack HM, Wein AJ*

1088 **Periosteal Chondromas of the Anterior Tibial Tubercule: Two Cases.** *Kirchner SG, Pavlov H, Heller RM, Kaye JJ*

1090 **Intraarterial Nitroprusside Treatment for Ergotism.** *Husted JW, Ring EJ, Hirsh LF*

1093 **Ulnar Artery Aneurysms: Angiographic Considerations in Two Cases.** *Latshaw RF, Weidner WA*

TECHNICAL NOTES

1096 **A Transparent Head Support for Magnification Cerebral Angiography.** *Cromwell LD, Moore WE*

1098 **Transurethral Conversion of a Percutaneous Ureteral Stent to an Indwelling Stent.** *Bigongiari LR, Lee KR, Mebust WK, Foret J, Weigel JW*

1101 **Special Article: National Guidelines and Standards for Health Planning: Their Relation to Radiology.** *Evens RG*

1105 **International Cancer Research Workshop on Low Dose Rate Teletherapy.** *Edited by Wilson JF*

1111 **From Earlier Pages.** *Lang EF*

1113 **Editorial: Contrast-Induced Acute Renal Failure.** *Heneghan M*

1116 **Letters**

1119 **Memorials**

1121 **Abstracts of Current Literature**

1128 **Book Reviews**

1133 **News**

1137 **ARRS Meeting Summary**

1143 **Index to Volume 131**

For years we've made it our business to help hospitals control image quality, contain costs and improve patient care. The results speak for themselves.

Imaging Management

DUPONT

REG U.S. PAT. & TM. OFF.

Imaging Management gets results: Better image quality. Tighter cost containment. Improved patient care.

Supplier involvement with hospital radiology departments probably doesn't sound like a terribly novel idea today, but before 1970 it was. That was when DuPont initiated an in-depth Quality Control Program for hospitals. DuPont led the way then, and today DuPont still sets the pace in quality assurance.

Over the years, DuPont's involvement with its customers has grown beyond the original Quality Control Program. This involvement now includes a range of training and consultation services in all areas of radiology management. For the most part, these newer programs have been aimed at improving cost containment and patient care, which have joined image quality as key department goals.

Today, DuPont can offer the hospital radiology department a selection of imaging services unmatched in depth and variety. The challenge now is to apply these programs and services so that they meet the unique needs of each individual department and produce the specific results that the profession demands.

Imaging Management meets today's needs.

Imaging Management is DuPont's answer to this "challenge to produce results." It is a proven process of selecting, implementing and monitoring those radiology programs that will achieve specific departmental goals rapidly and effectively.

Imaging Management follows an orderly procedure of needs analysis, objective setting and program selection, to produce an action plan that is unique for each radiology site. It provides guidelines and assistance during implementation of the plan and concludes with a quantitative measurement of program results. The entire process is conducted as a "team effort" between the radiology department and DuPont, using the best resources of both.

The whole point: To put you in control.

The Imaging Management Concept recognizes the interrelationship of people, products and services in effective radiology administration. It acknowledges the importance of managing these three variables to achieve specific depart-

mental goals. The whole point is to put you in control of your image quality, costs and patient care, and that's exactly what happens.

Imaging Management not only promises better quality and lower costs; it can also result in a more efficient staff, a more efficient department layout and more efficient administrative procedures.

For the patient, it can mean faster exams, less waiting time and lower X-ray dosage.

The results speak.

Imaging Management principles and techniques have produced results like these at hospitals across the country.

Boston City Hospital saved $7,500 in film costs by reducing repeats 18% and minimizing film spoilage. Radiograph quality and department efficiency improved, too.

St. Luke's Hospital Center in New York City reduced their repeat rate from 10% to 4% and realized a noticeable improvement in department efficiency.

Temple University Hospital in Philadelphia saved over $4,000 a month with improved inventory control and fewer repeats.

Baptist Hospital in Miami cut radiation dosage in half in 90% of their general procedure exams.

Our customers can tell you about dozens of similar successes.

It starts with the use of quality Imaging Products

The key to effective Imaging Management is quality: Quality of objectives, quality of programs, quality of results. Equally important is quality of products.

DuPont has the widest choice of quality film/screen combinations available for any diagnostic procedure.

Among our more recent innovations: A new line of Medical Recording Films for computed tomography, ultrasound and nuclear medicine; three new film/screen/cassette combinations especially developed for imaging extremities; a new high-capacity processor and chemical mixer.

And, of course, there's the original DuPont Daylight Film Handling System, which makes it possible to do all film

handling, even the processing, in room light. This important development allows you to use satellite units, including computed tomography, ultrasound and nuclear medicine, that are not tied to the darkroom. Technologists can virtually take the X-ray department to the patient, thereby improving patient care.

These and many other quality consumable and equipment products form the foundation for our long-term involvement with hospitals.

People and services wrap it up.

DuPont Technical Representatives are trained to be responsive to radiology departments' needs, to search out ways to help control costs, improve image quality and patient care. To meet these needs, they call on the finest and most complete resource package in the industry... DuPont's series of Imaging Services, including Quality Control, Computerized Cost Analysis, Training in Budget Administration and Management Principles, Layout Assistance, Resident and Student Education, and a full range of technical programs. Working with your radiology team, our Technical Representatives can help develop managerial and technical skills to new levels of proficiency.

DuPont's new Seminar on Imaging Management offers in-depth training.

Radiology department administrators and their assistants, chief technologists, QC coordinators and other hospital personnel are invited to participate in DuPont's new seminar on Imaging Management, to be held at key locations around the country in the months ahead. The seminar will be conducted in half-day segments or as a week-long training program; you can choose the format that best fits your schedule.

For full information, get to know your DuPont Technical Representative.

Your DuPont "TR" is the direct link to Imaging Management. Let him help you develop and implement a management system that will meet the unique needs of your department to control image quality and costs and improve patient care.

Ask him about the Imaging Management Seminar, too. He has more valuable information to offer and a prospectus folder on the training program. Or write DuPont Company, Room 36673, Wilmington, DE 19898.

Imaging Management.
It puts you in control of image quality, costs and patient care.

DUPONT

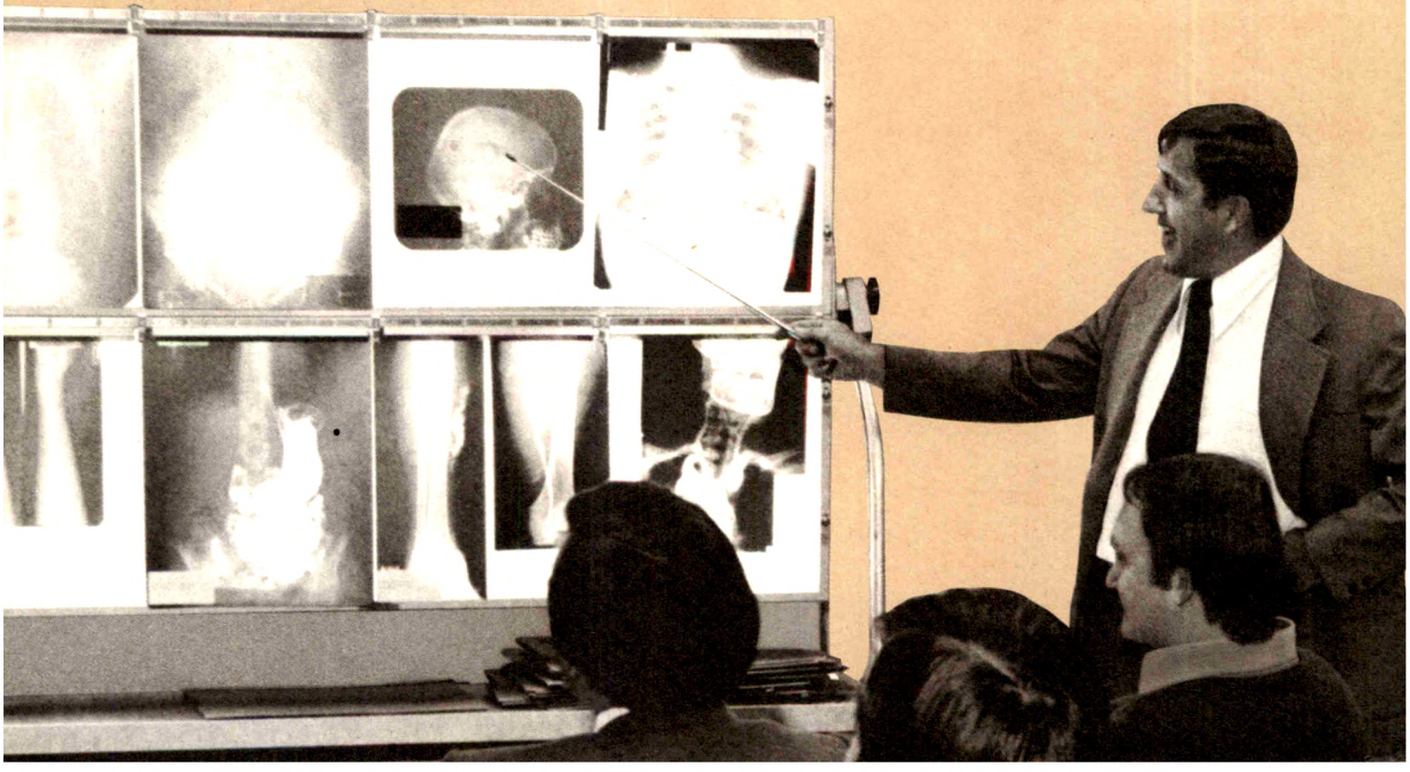

Liquid Polibar with Super XL

A Total System

For double-contrast examination of the colon.

Satisfactory results in the double-contrast examination of the colon require special attention to two aspects of the procedure.

First, the barium sulfate formulation. Our Liquid Polibar (56% w/w) is a bubble-free, non-precipitating uniform suspension formulation ... with proper flow and coating characteristics. No blending required and once routines are established, you can rely on its consistency.

The second concern is with the proper apparatus. The E-Z-EM system is unique in that 1/2" lumen tubing attached to the enema bag is utilized — for freer, more uniform flow. Miller Air Retention Tip, with or without optional cuff completes the system.

A total system for ease of administration and consistently reliable radiological results. For additional literature, write:

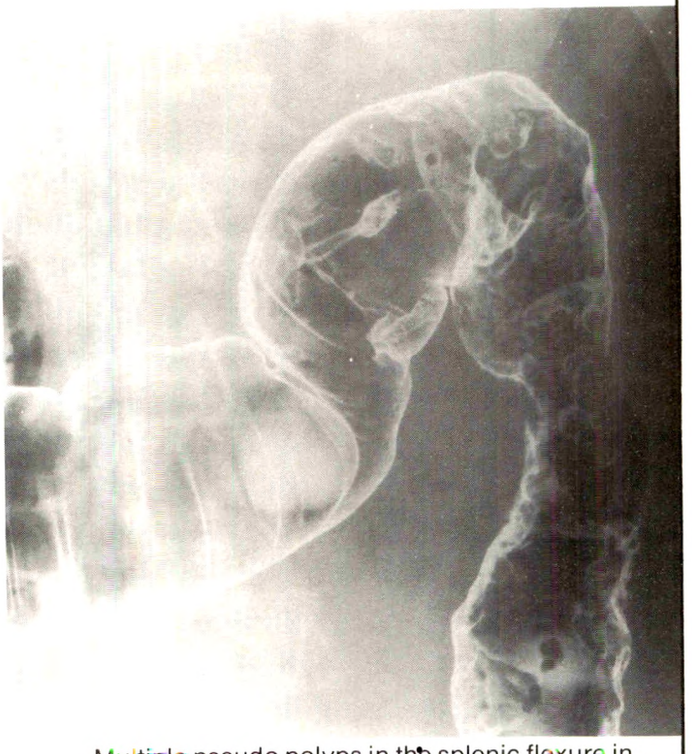

Multiple pseudo polyps in the splenic flexure in longstanding ulcerative colitis.
Film courtesy of Richard Palmer Gold M.D. Columbia Presb. Medical Center N.Y.

E-Z-EM

7 Portland Ave.
Westbury, New York 11590
(516) 333-8230

7/78

SIEMENS

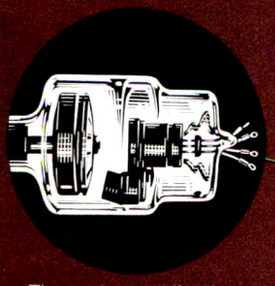

The custom application OPTI-150 CT X-ray tube permits continuous patient scanning at a rate of up to 125 scans/hour.

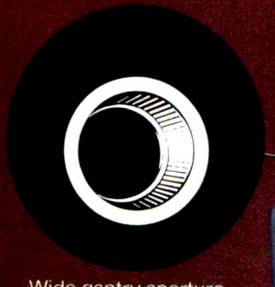

Wide gantry aperture and scan field (both 54 cm. in diameter) facilitate patient handling and positioning.

Exclusive dual-section, flat-top table system with motorized patient conveyor.

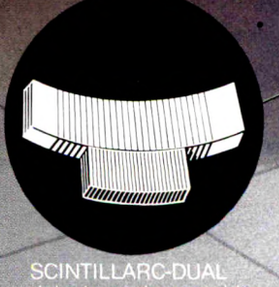

SCINTILLARC-DUAL detector system provides maximized detector utilization with optimized clinical results.

The only CT scanners with instantaneous image reconstruction

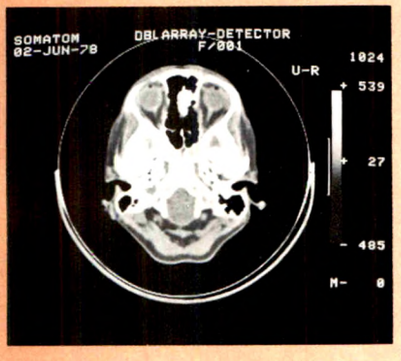

Instantaneous image reconstruction makes the SOMATOM (whole body scanner) and the SIRETOM (head/neck scanner) the most sophisticated computed tomographic systems available today. Upon completion of each scan, the image is immediately available for clinical evaluation. The SOMATOM offers selectable scan times of four and eight seconds while the SIRETOM scan time options are 60, 120 and 180 seconds.

The EVALUSKOP, an independent evaluation console, extends the capability for CT image manipulation and analysis. Programmable and available at the push of a button are window variation, multiple region of interest selection, distance and angle measurement, histogram, magnification, saggital/coronal reconstruction, multiple tomogram displays, tomogram addition and subtraction, and filter manipulation.

Siemens' full line of computed tomographic equipment is designed to fulfill the exacting requirements of CT application. Behind each system definition—X-ray tubes, tables, generators, radiation measurement, and signal processing—is more than 100 years of engineering excellence.

Siemens' world-wide reputation for product support and service is unsurpassed. In the United States alone, Siemens has a technical staff of over 500 trained professionals ready to serve you—should the need arise.

For further information

Please contact your local Siemens Representative or Siemens Corporation, Medical Systems Division, 186 Wood Avenue South, Iselin, New Jersey (201) 494-1000.
In Canada: Siemens Canada Limited, P.O. Box 7300, Pointe Claire 730-P.Q.

Concepts... engineered to radiologic excellence

A Public Service of this magazine & The Advertising Council Ad Council

Your Business can be one, too.

Red Cross needs individual volunteers, and donors of blood and money, by the millions.

But we need even more help. We need the solid support of American Business. And we never needed it more.

If your business is already helping, by organizing blood drives, and by supporting payroll deductions—either directly for the Red Cross, or through the local combined fund drive—the whole community owes you thanks. And we thank you, too.

Last year, with help from our friends, we offered major aid at over 30,000 disasters—from typhoons, to local (but just as devastating) house fires.

We were able to help the elderly with practical programs, we helped veterans by the hundreds of thousands, we taught people by the millions to swim or swim better. And that's just the tip of the iceberg.

Think of America without The American Red Cross.

And you'll know why we need your business as a Red Cross Volunteer. In your community. And all across America. Contact your local Red Cross Chapter to see how your company can become a volunteer.

Red Cross. The Good Neighbor.

The Second Announces A First

dvanced regional learning seminars on radiographic imaging. From the
econd largest producer of photographic products in the world, the Agfa-Gevaert Group.

Introducing

The Image Center

Advanced learning seminars on radiographic imaging.

A unique Resource Center.
Now, Radiology Departments throughout the country will have regional facilities to provide the most up-to-date information available on radiographic imaging: The Image Center. An educational resource where ideas can be exchanged. A resource that offers the opportunity to discuss new systems and techniques with recognized experts. A resource that provides continuing education credits in selected subject areas.

Located throughout the country.
These state-of-the-art centers, located in major cities in the U.S. including Los Angeles, Atlanta, San Francisco, Chicago, Dallas and metropolitan New York, contain classrooms, conference rooms and fully equipped radiographic rooms. Designed specifically for study and practice of new radiographic techniques, The Image Center provides hands-on experience with the latest equipment and imaging technology.

For the Radiologist.
The Image Center is a forum for bringing physicians together to exchange the latest ideas, procedures and information. Speakers who are experts in their field will conduct seminars on relevant topics in medical imaging. Business, government and legal aspects of radiology will be discussed . . . topics not readily available from other sources.

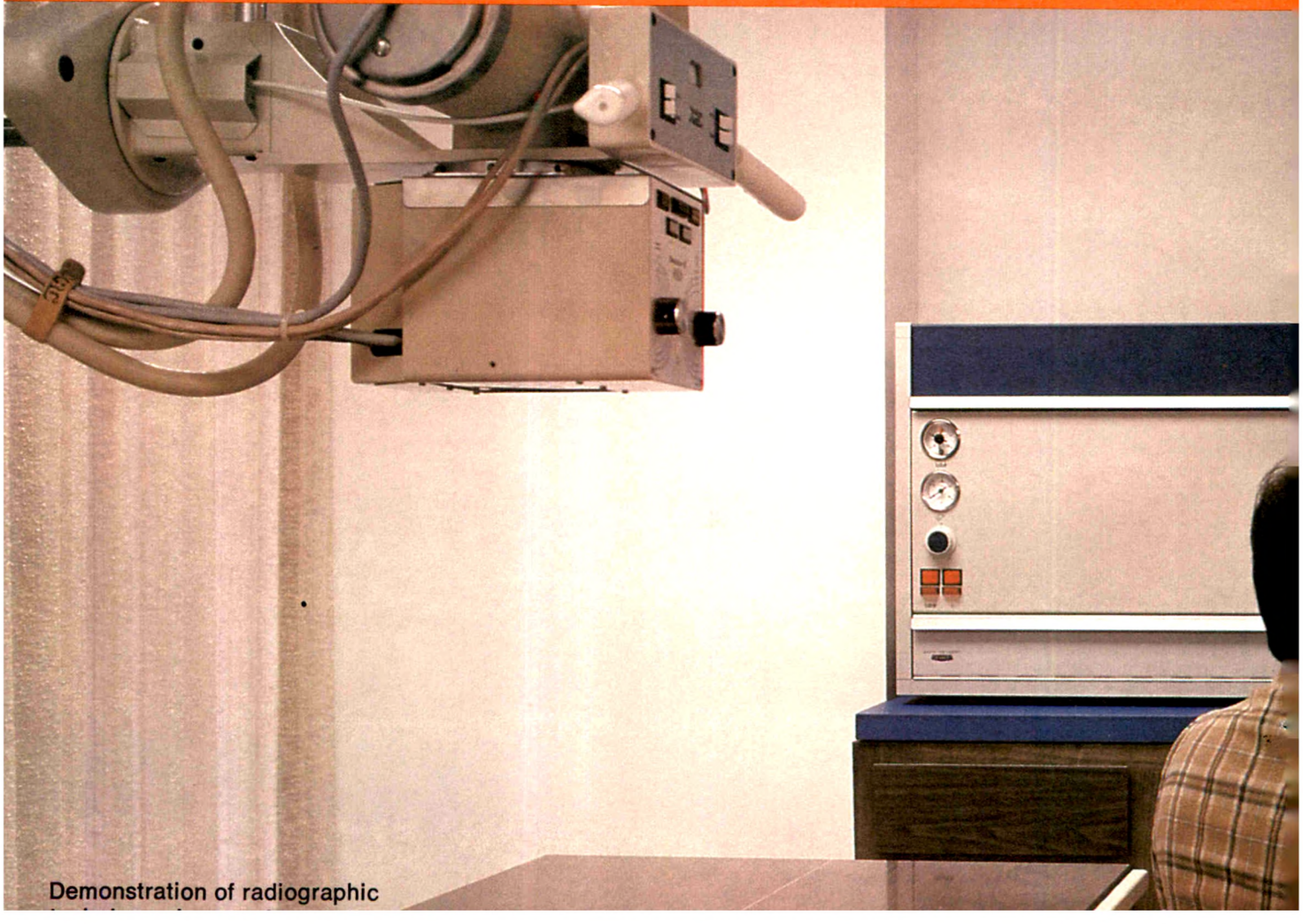

Demonstration of radiographic

AGFA-GEVAERT REX INC.

A subsidiary of Agfa-Gevaert Group, the second largest film maker in the world. White Plains, N.Y. Tel. 914 682-5650

For the Radiologic Technologist.
The Image Center is an educational resource for teaching and keeping technologists up-to-date on current techniques and trends in medical radiography. It is a technical, in-service, educational program with emphasis on key factors affecting diagnostic quality of the finished radiographs. Laboratory sessions will provide the opportunity to use a variety of imaging and processing systems and to discuss related technical problems.

For the Resident.
Whether it's sensitometry, conventional radiography, CRT imaging or ultra-sound, The Image Center offers a broad range of educational seminars. Latest advances in radiographic imaging will be covered and many seminars qualify for Continuing Education credits.

For the Department Administrator.
Special seminars on cost effectiveness, business and financial management workshops are all available at The Image Center.

For the Physicist.
Physicists will receive information directly related to basic aspects of X-ray film and chemistry. Technical seminars will cover relevant R & D subjects and new products under development.

Contact your Agfa-Gevaert Rex representative for more information about scheduled seminars and programs being offered at The Image Center servicing your area.

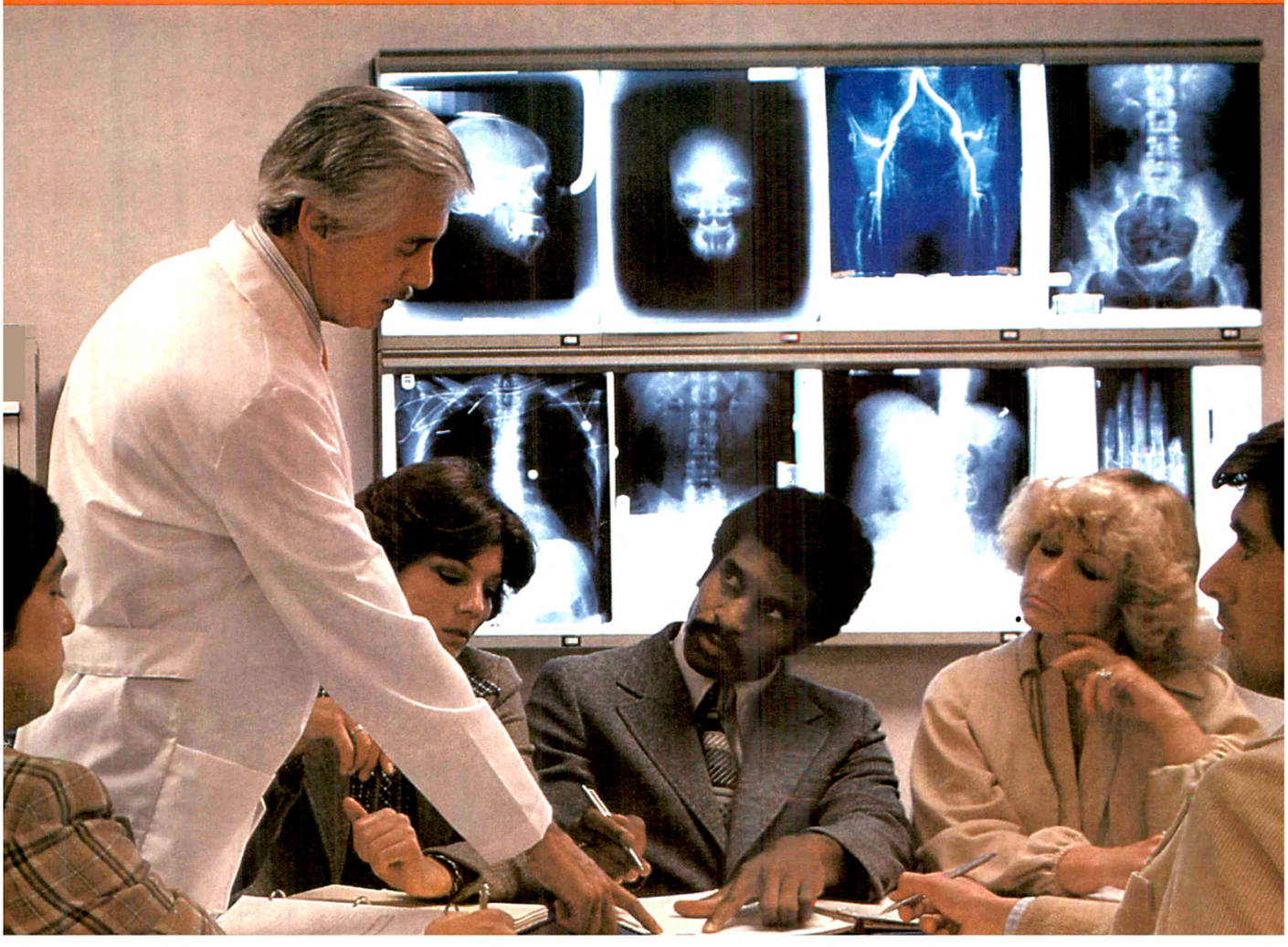

dedicated to progress . . .

The National Conference on Breast Cancer
18th Annual Conference on
Detection and Treatment

Atlanta, Georgia
March 5-8, 1979

The American College of Radiology
6900 Wisconsin Avenue, Chevy Chase, Maryland 20015
(301) 654-6900

CHARLES C THOMAS • PUBLISHER

THE FUNDAMENTALS OF X-RAY AND RADIUM PHYSICS (6th Ed., 2nd Ptg.) *by* **Joseph Selman,** *Tyler Junior College, Tyler, Texas.* This is the text against which all other tomes of similar intent are measured. Now in its Sixth Edition, this classic introduction to x-ray and radium physics has again been revised, rewritten, updated and enlarged to accommodate a constantly changing field. The basic format — proven effective in many classrooms over many years — has been retained. Selected for new or amplified discussions in this edition are such items as focal spot evaluation, modulation transfer function, new types of intensifying screens, the basic phenomena of phosphorous luminescence, direct magnification in small vessel angiography, high kilovoltage radiography, and radiation protection. *'78, 616 pp., 296 il., 29 tables, $18.75*

THE CERVICAL SYNDROME (4th Ed.) *by* **Ruth Jackson,** *Southwestern Medical School of The Univ. of Texas, Dallas. Foreword by* **A. Steindler.** The new edition of this definitive treatise continues to stress the basics: fundamental anatomy, a careful patient history, meticulous examination, and adequate radiography. The anatomy of the cervical spine is presented more clearly and in greater detail than ever; the etiology of responsible factors has been further amplified; symptomatology and clinical findings receive expanded and updated coverage. The section on radiographic examination has been enlarged, with material on cineradiography, panoramic tomography, angiography, myelography and discography. The section on treatment stresses more fully the importance of prevention and updates its reportage of proven therapeutic techniques. *'78, 416 pp., 459 il. (7 in color), $22.50*

TEXTBOOK OF DENTAL RADIOGRAPHY (Rev. 2nd Ptg.) *by* **Olaf E. Langland,** *Louisiana State Univ., New Orleans, and* **Francis H. Sippy,** *Univ. of Iowa, Iowa City.* The science and art of producing dental radiographs of high diagnostic quality is explored in this handsomely illustrated text. X-ray production, requisites of a diagnostic radiograph, radiobiology and radiation hygiene, intra-oral and extra-oral projection techniques, processing procedures, panoramic radiography, and legal aspects of dental radiography are among the topics discussed. A complete glossary of terms and several appendices on radiographic supplies and equipment also are included. ". . . this book is the best [this reviewer has] seen in the field of dental radiography." —*Oral Health. '78, 400 pp. (6 3/4 x 9 3/4), 303 il., $21.75*

ANATOMICO-ROENTGENOGRAPHIC STUDIES OF THE SPINE (3rd Ptg.) *by* **Lee A. Hadley,** *Syracuse Memorial Hospital, Syracuse, New York.* "The work is beautifully illustrated with excellent roentgenograms and photographs. The volume is a tribute to a devoted investigator's experience with the spine, accumulated over 30-odd years. His attempt to coordinate the roentgenographic image with the actual anatomical condition of the structure is successfully achieved." Thus said the *Journal of the American Medical Association* in its review of this book. The broad scope of study in the text is revealed in the contents which include development of the spine, vertebral arteries, posterior spinal articulations with innervation studies, spinal curvatures, infective spondylitis, tumors and tumorous conditions. *'76, 560 pp. (6 3/4 x 9 3/4), 644 il., $22.75*

Orders with remittance sent, on approval, postpaid

301-327 East Lawrence Avenue • Springfield • Illinois • 62717

In just one second we'll show you something in CT imaging no one else can.

PICKER

ONE OF THE CIT COMPANIE

For high-quality CT body scans,

Wishard Memorial Hospital, Indianapolis, IN

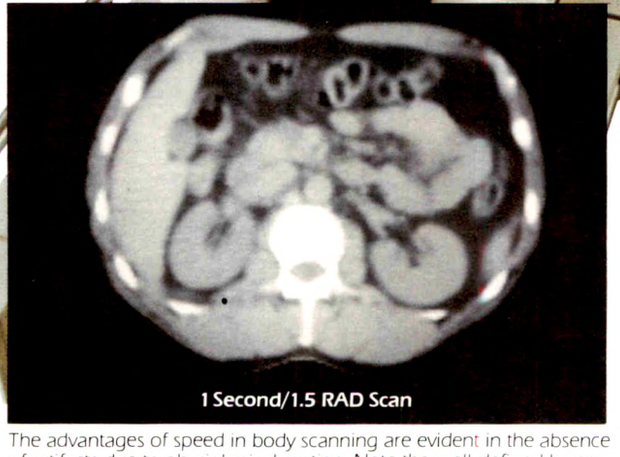

1 Second/1.5 RAD Scan

The advantages of speed in body scanning are evident in the absence of artifacts due to physiological motion. Note the well-defined loops of bowel in the above scan. Other structures seen are liver, gallbladder, left and right kidneys and renal arteries.

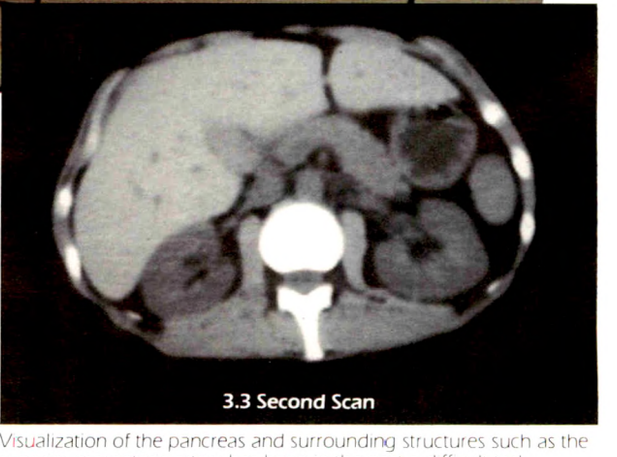

3.3 Second Scan

Visualization of the pancreas and surrounding structures such as the superior mesenteric artery has been in the past a difficult task. Synerview's fast scanning times combined with superb diagnostic image quality have significantly contributed to the evaluation of abdominal disease.

There's only one 1-second

faster is better.

To achieve high-quality body scans, faster is better. Synerview is the fastest scanning CT system presently available. It can routinely perform high-quality scans, as fast as 1 second.

Because of the natural involuntary motions that occur within the human body, fast-scanning capabilities are necessary for clear images in body scans. The faster your CT scanning capabilities, the more you can minimize motion artifacts caused by peristaltic, muscular, respiratory, and cardiovascular actions.

And for CT diagnosis to be effective for uncooperative, unconscious, pediatric or geriatric patients, you need 1-second scanning.

Ready to advance the state-of-the-art for CT. An investment in Synerview is the best way to obtain a high-quality CT scanner and minimize the obsolescence factor. Other manufacturers have reached the limit of their CT capabilities with the technology employed in their present systems. But Synerview, based on the proven Stationary Detector principle, has the potential to advance state-of-the-art for CT. Synerview is ready to expand its capabilities when new technology becomes available.

Because only components of proven dependability were incorporated in the Synerview design, we don't have to offer you a "special warranty."

Synerview performance features. Synerview has features that help make CT operation fast and convenient. Our unique patient transport is one example. It lets you prepare a patient for scanning almost anywhere in the hospital.

The high-contrast resolution of Synerview allows excellent delineation of subtle density differences. In the above head scan, taken through the lateral horns, the caudate nucleus, calcified choroid plexus and pineal gland, note the white and gray differentiation.

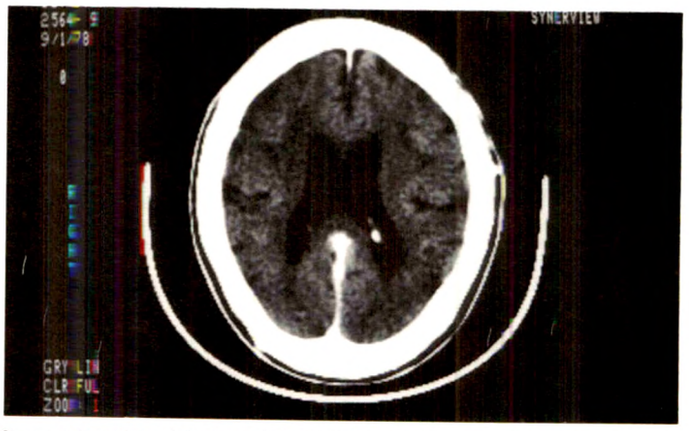

Sharp delineation of the bone/brain interface is demonstrated in the above image. Synerview's exceptional detail allows visualization of white and gray matter and cortical sulci.

And to maximize your patient throughput, Synerview combines fast patient-data entry and scanning selection protocol with processing as fast as 25 seconds.

Superb software capabilities bring added dimensions to your CT operations. Synerview can display sagittal and coronal reconstructions in less than 5 seconds. Our bone correction software is establishing new diagnostic standards. In addition, Synerview's optional therapy treatment planning feature can be supplied either for economical shared use, or for more versatile independent use.

And a field size of 48 cm means Synerview can perform body scans with even your larger patients.

Head to head, there's no one better. We have the latest technology and the images to prove it.

A large portion of any CT caseload involves head scans. It's of particular significance to know that Synerview brings you high-quality head scans in addition to high-quality body scans. It's also important that you can position your patient's head easily with Synerview. You can get the right scan — the first time. And, for accurate Towne's projections, Synerview's ultra-stable gantry can tilt ± 20 degrees.

CT system. Synerview.

PICKER®

Synerview. Developing a fine image.

The Synerview installations pictured are currently in operation and producing optimum diagnostic results. Our various CT systems include the Synerview 120, which utilizes Translate/Rotate geometry, and the Synerview 300 and 600, both of which employ the Stationary Detector method.

Carlisle Hospital, Carlisle, PA

We have the experience and the resources to help you acquire the right CT system for your needs.

Certificate of Need Assistance. Picker CT representatives work with you to help you acquire your Synerview. From acquisition to installation, we can help. And that includes Certificate of Need counseling and room-layout planning.

Financial Assistance. Through our parent CIT Financial Corporation, we can arrange your financing. Our financial arrangements can be as flexible as your financial needs. If and when they change, our arrangements can too.

Training and Installation. We train you on the same Synerview you purchase. So, before operation begins, you are familiar with all the features of the CT system you'll use every day. And installation is usually accomplished in seven to ten days in a prepared room. When you're ready to start full CT operations, so is Synerview.

Service. Your local Picker representative's service engineers undergo rigorous training. Upon completion of this training, each Synerview service engineer is assigned to a system and follows it through the final tests at the factory. The Synerview is then escorted to its installation site, where the installation checkout and performance certification are performed before turnover to you. The service engineer is then assigned to the area to provide swift, professional service. In addition, there is always a team of specialists, based at Picker, to further support your Synerview.

Over 62 years of diagnostic imaging. When you think about computed tomography, it makes sense to think about Picker. Picker's dedication to the total field of diagnostic imaging emerged from a strong X-ray background. That experience and knowledge helped us develop the world's first 1-second CT scanner. Synerview.

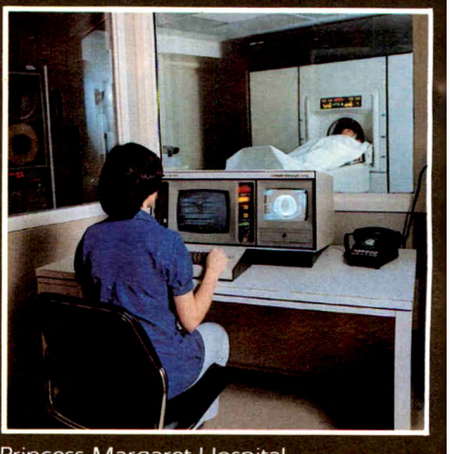

Princess Margaret Hospital, Toronto, Canada

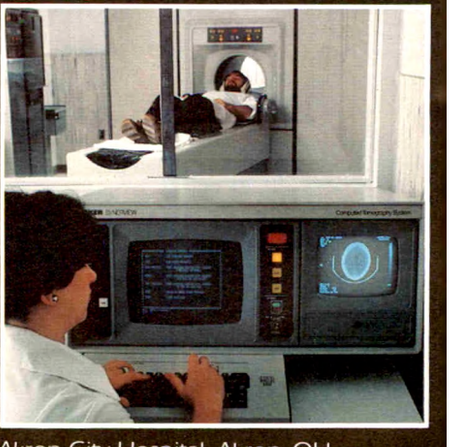

Akron City Hospital, Akron, OH

For a free portfolio of Synerview head and body scans, contact your local Picker representative, or call collect 216/461-9100, CT Marketing, extension 332. Picker Corporation, 595 Miner Road, Cleveland, OH 44143.

PICKER®

ONE OF THE CIT COMPANIES

FISCHER X-RAY introduces... TTC/T Linear Tomographic System

Fulcrum bar is conveniently "parked" when not in use
be removed to convert from tomo

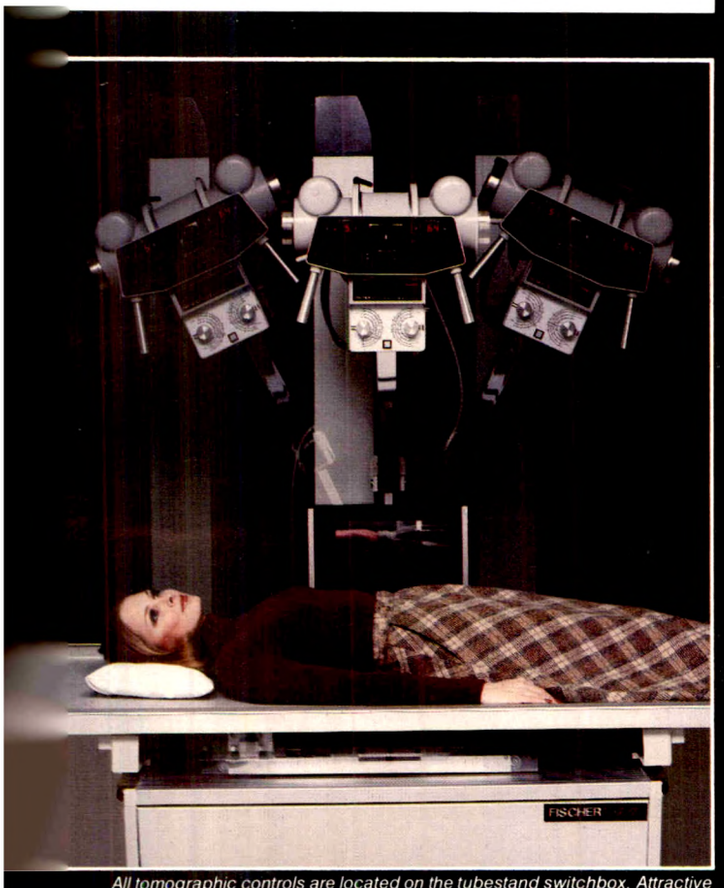

All tomographic controls are located on the tubestand switchbox. Attractive panel features "Light Touch" controls.

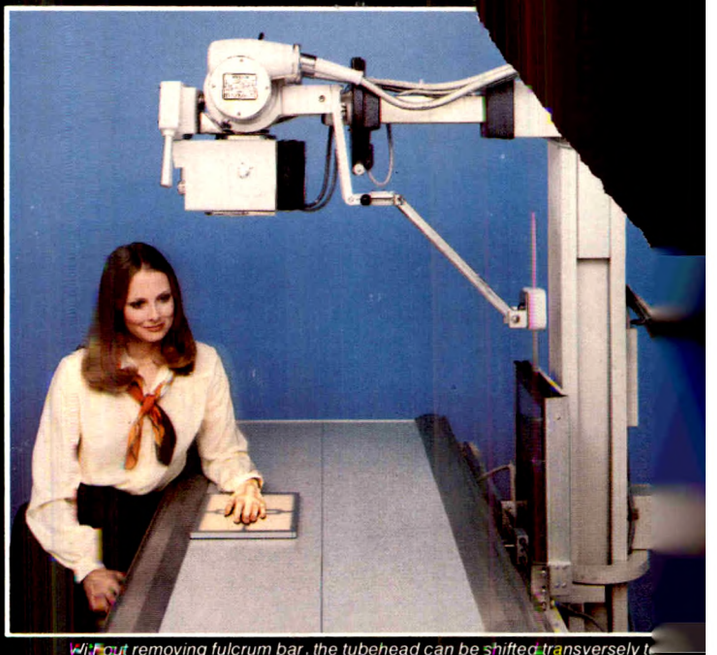

Without removing fulcrum bar, the tubehead can be shifted transversely t
permit radiography of extremities at table's edge

- Precision tomography in seconds
- Exceptional versatility for all radiographic functions
- Available with any Fischer single- or three-phase generator

The Fischer TTC/T System is a state-of-the-art linear tomographic system which will routinely provide sharp tomograms with millimeter accuracy. Tomographic controls are located in the tubehead switchbox, providing exceptionally rapid positioning and selection of variables. Beyond its tomographic capabilities, moreover, the versatile TTC/T System can be utilized for many other types of radiographic examinations without removing the tomographic attachments, greatly extending its usefulness in a busy department.

Write or call for detailed information or the name of your local Fischer X-Ray Representative.

FISCHER® X-RAY

An established manufacturer of radiographic equipment, serving the medical profession since 1910.

many people
u know who have
n cured of cancer?

Almost everybody knows someone who has died
. But the fact is about two million living
ans have been cured. Not only cured but leading
normal lives. Another fact is millions more could h

By getting to the doctor in time.

By availing themselves of the most effective
thods of treatment today.

By advances made through cancer research.
Research made possible with the help of the American Cancer Society.

However, there's much more to be done.
To help save more people, the American Cancer Society needs more money. So, please, give. We want to wipe out cancer in your lifetime.

American Cancer Society

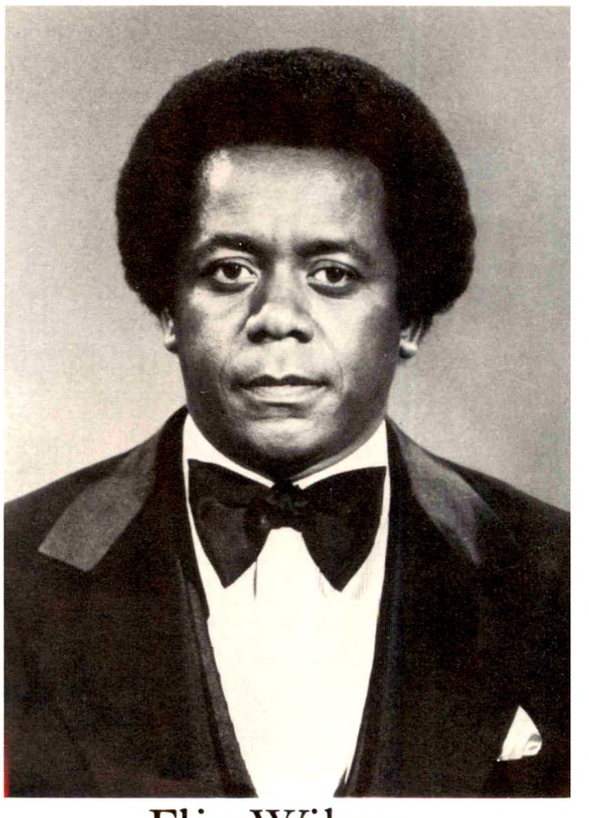

Flip Wilson,
National Crusade Chairman

This space contributed by the publisher as a public service.

Philips Angiography Systems.

TOTAL BODY COVERAGE WITH THE BROADEST RANGE OF EQUIPMENT

. . . from the only company offering all the choices you need!

Poly Diagnost C

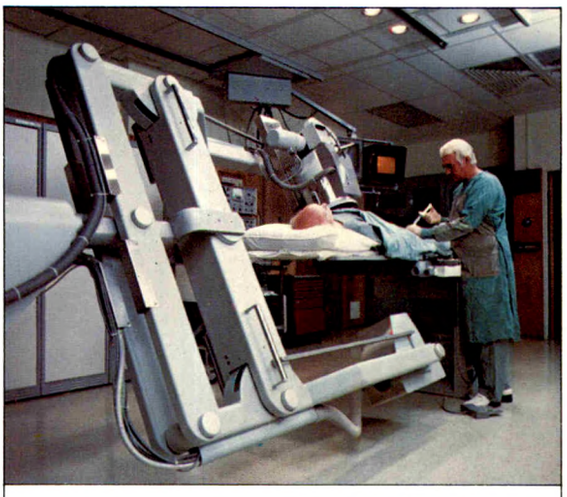

The parallelogram construction of the Poly Diagnost C permits the patient to remain stationary, leaving the physician more relaxed and able to concentrate fully on the procedure. Insuring maximum safety for both patient and operator, the Poly C provides both routine and cranio-caudal views that insure clear, unobstructed views of overlapping vessels. Stenoses which might have been obscured can be detected with a high degree of efficiency and operational ease.

Designed for both the brachial and femoral techniques of cardiac angiography, the Poly C is also successfully used in abdominal and thoracic studies.

Poly Diagnost N

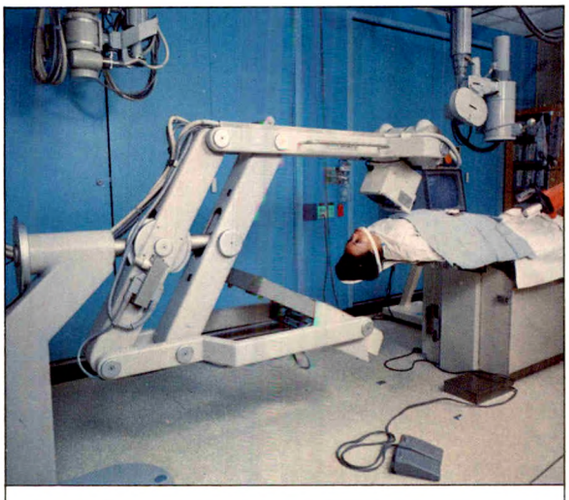

Designed specifically for cerebral angiography at 2:1 magnification, the Poly Diagnost N easily provides views of the patient previously difficult (or impossible) to achieve. The parallelogram construction allows full rotation around the long axis of the body *and* the maximum desirable head-to-foot angulation. The unique construction insures all motions are isocentric and all results are distortion free.

Designed for use in single or bi-plane operation with a Puck rapid film changer, the Poly N lends itself to extensions for more dedicated requirements, such as the latest configuration with a quickly interchangeable image intensifier and a rapid film changer.

PHILIPS MEDICAL SYSTEMS, INC.
710 Bridgeport Avenue, Shelton, Conn. 06484

Philips Angiography Systems.

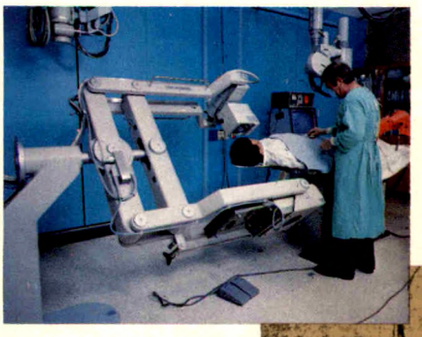

Poly Diagnost N

The first in Philips' family of dedicated cerebral angiography systems with parallelogram construction. For optimum results with isocentric patient positioning for all projections.

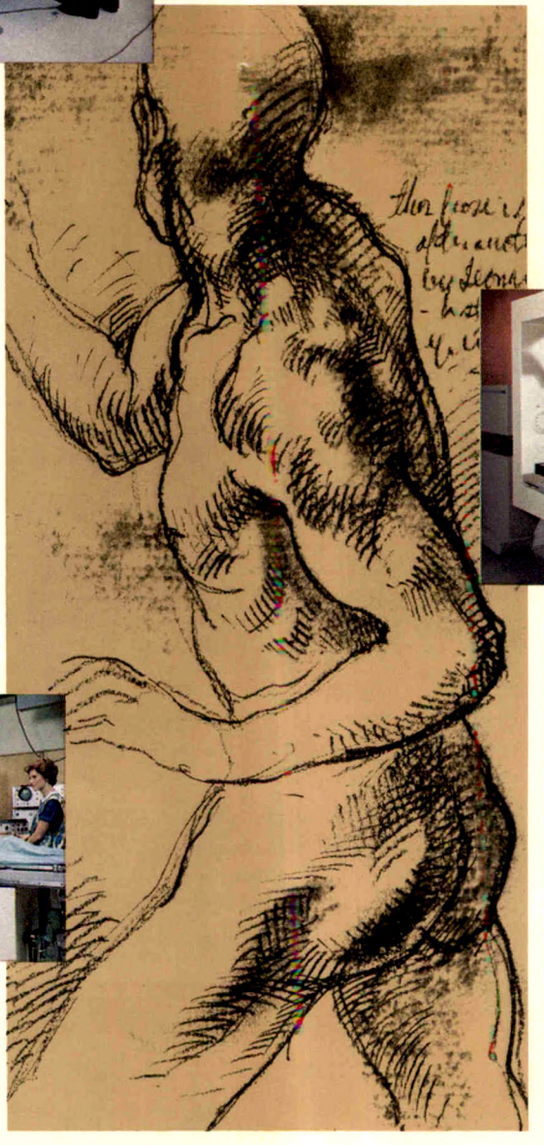

Poly Diagnost UPI

Philips' new universal angiography system for the most flexible filming of cerebral, thoracic, abdominal and peripheral angiography, with full provision for occasional cardiovascular examinations.

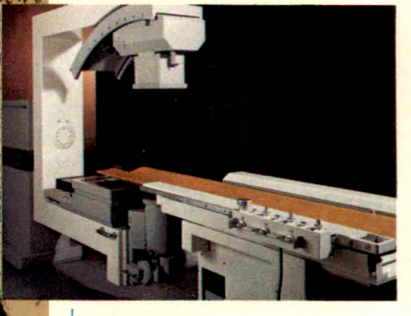

Diagnost C

xtension of the U-arm
ciple first developed by
ips in the Cardio Diagnost,
Poly C is a dedicated
diovascular system.
allelogram construction
ides routine and cranio-
al views without moving
atient, making the Poly C
used for imaging the
and abdominal areas.

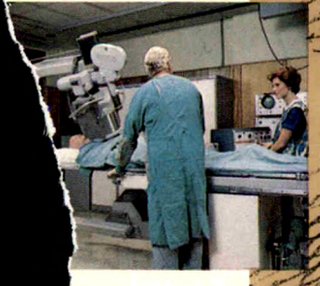

Poly Diagnost UPI

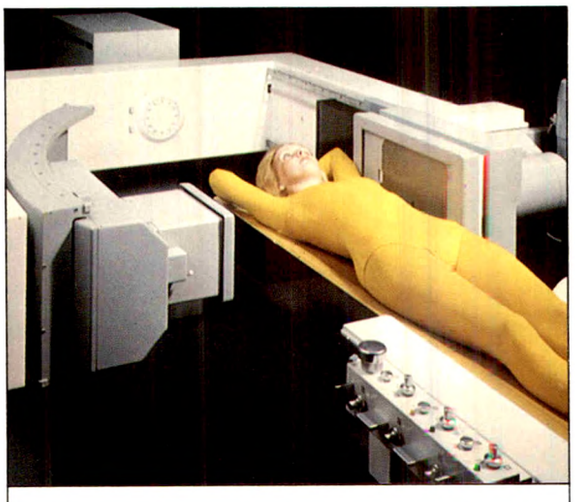

A universal system with revolutionary design, the Poly Diagnost UPI features a rotat ng U-arm that carries the X-ray tube and an image intensifier and rapid film changer which are quickly interchangeable.

A new experience in examination convenience, the Poly UPI is a masterful combination of system features: free choice of oblique, cranio-caudal and caudo-cranio projections; rapid changeover from fluoroscopy to film changer work; automatic control of object-film distance; motorized height adjustment of both table and U-arm, which provides contact and up to 2:1 geometric enlargement; and a unique boating movement that keeps the object centered in the beam while the object-film distance is automatically controlled in every projection. It's the ideal universal system for angiography!

PHILIPS®

A COMPLETE FAMILY OF IMAGE INTENSIFICATION SYSTEMS, X-RAY TUBES AND GENERATORS FOR PHILIPS ANGIOGRAPHIC EQUIPMENT.

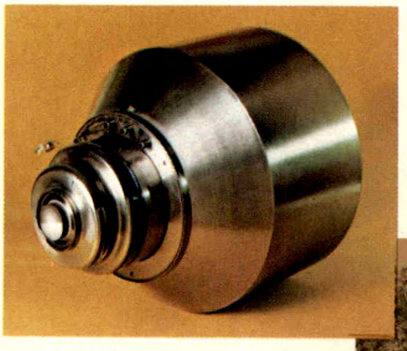

The 14″ Triple-Mode Image Intensifier
Another first from Philips! An amazingly lightweight 14″ image intensifier for highly detailed surveys with outstanding results.

Super Rotalix and Trinodex X-ray Tubes
Preferred for exceptional image quality and reliable performance in sustained operation, Philips' tubes are designed for high loadability and superbly efficient heat dissipation.

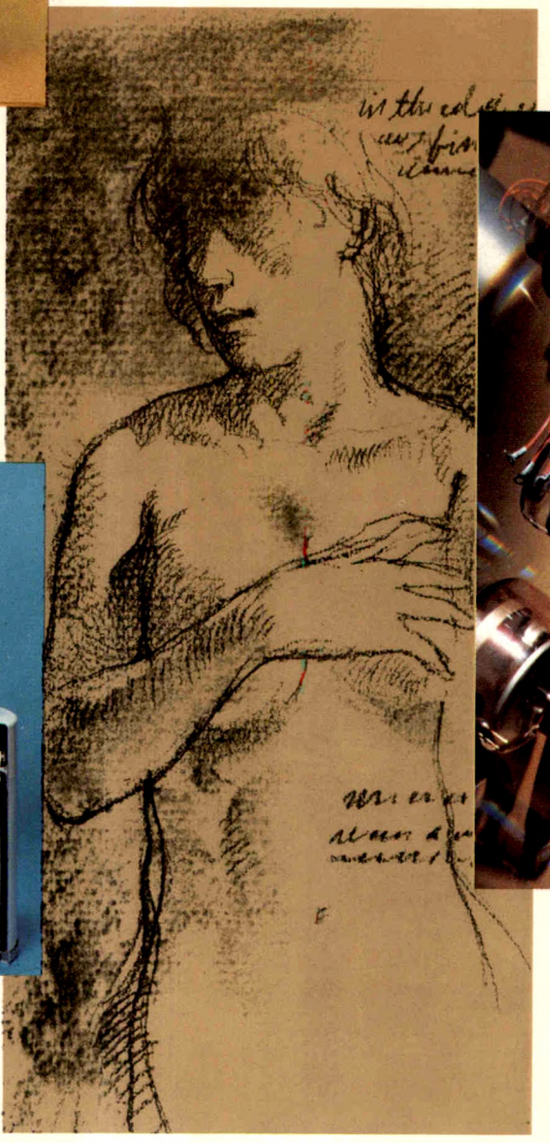

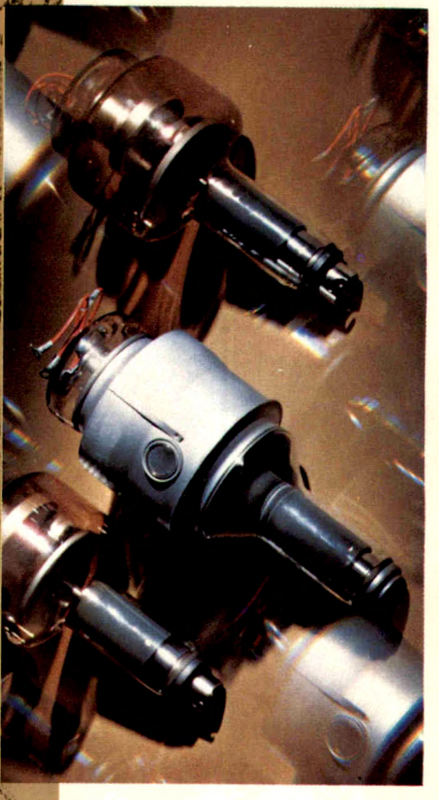

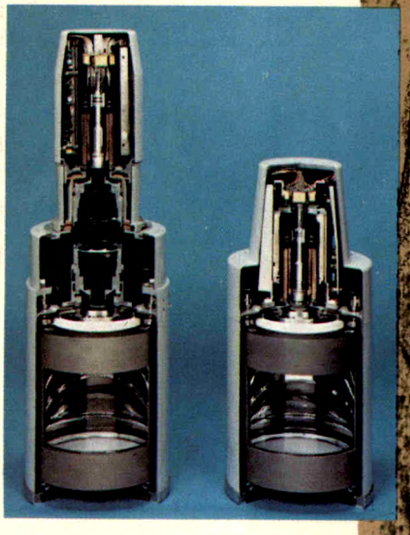

Conventional or Fiber Optic Image Intensifiers
Select from a full range of fields in conventional image intensifiers . . . or Philips' Exclusive Fiber Optic Image Intensification System. Fiber optics provides 30:1 contrast ratio for greater detail, uniform image quality over the entire screen, optimum image transfer and compactness for easy maneuverability.

PHILIPS®
the most reliable family of systems and people in the industry.

A Full Range of Generators
From the very affordable three-phase, high output Classic line, to a full range of Modular Generators, to the computerized Optimus M200, Philips' family of generators combines quality, performance and price for your every examination need.

For Double Contrast Stomachs, Use

E-Z-HD™

High Density with High Fluidity Barium Sulfate for Suspension

NOTE THE ANTRAL POLYP (ARROW) AND THE LACELIKE AREAE GASTRICAE IN THE BODY OF THE STOMACH
Film, courtesy of Robert E. Koehler, M.D. Washington University, Dept. of Radiology, St. Louis, Missouri

Double contrast radiography appears to offer the potential for significant improvements in diagnostic accuracy.

Double contrast studies of the stomach best demonstrate the surface pattern of the stomach (areae gastricae). This leads to improved detection of superfical erosions and ulcers, malignancies, polyps and other benign tumors, and ulcer scars.

E-Z-HD barium sulfate provides the basic ingredient necessary for good double contrast of the stomach.

The higher the density of the barium suspension, the better the coating, E-Z-HD allows for the highest density suspension of any commercial product on the market today: 85% w/w, 250% w/v. E-Z-HD achieves this density while remaining fluid for ease of administration.

- High density
- High fluidity
- Palatable
- Unit dose convenience.

E-Z-HD – The barium for the double contrast examination of the stomach and duodenum.

Optimal Density & Fluidity for the Modern Double Contrast Examination of the Stomach and Duodenum

Refrences:

David W. Gelfand: The Japanese-Style Double Contrast, Examination of the Stomach, Gastrointest Radiol. 1, 7-17 (1976)

Igor Laufer: The Diagnostic Accuracy of Barium Studies of the Stomach and Duodenum – Correlation with Endoscopy, Radiology 115: 569-573, June 1975

Roscoe E. Miller: The Air Contrast Stomach Examination: an overview. Radiology 117: 743-744 Dec. 1975

E-Z-EM

For Further Information Write:

7 Portland Ave.
Westbury, New York 11590
(516) 333-8230

9/77

Simple Cyst?

The wall of a simple cyst is usually demarcated by a very fine margin.

In the following case, the "thick" peripheral margin indicates that the renal mass is not a simple cyst. Its benignity or malignancy must be determined.

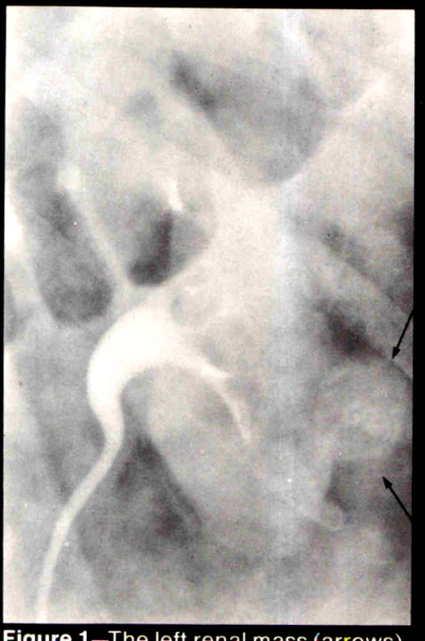

Figure 1—The left renal mass (arrows) is detected on conventional excretory urography, but its detail is not adequately defined.

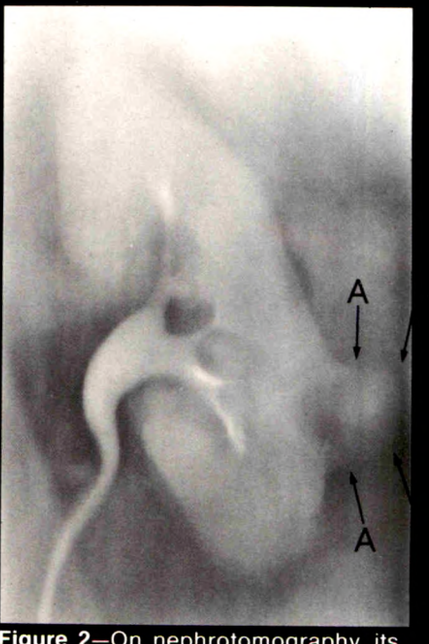

Figure 2—On nephrotomography, its radiographic characteristics are demonstrated:

- relative lucency
- "beak" of adjacent renal parenchyma (A)
- thick peripheral margin (arrows)

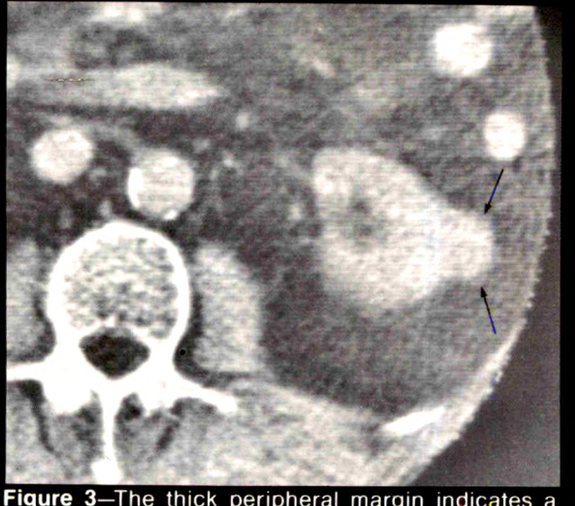

Figure 3—The thick peripheral margin indicates a complex lesion which was further evaluated. On computed tomography, the peripheral mass was demonstrated and its density (25 CT units) determined. It was not enhanced by intravenous contrast.

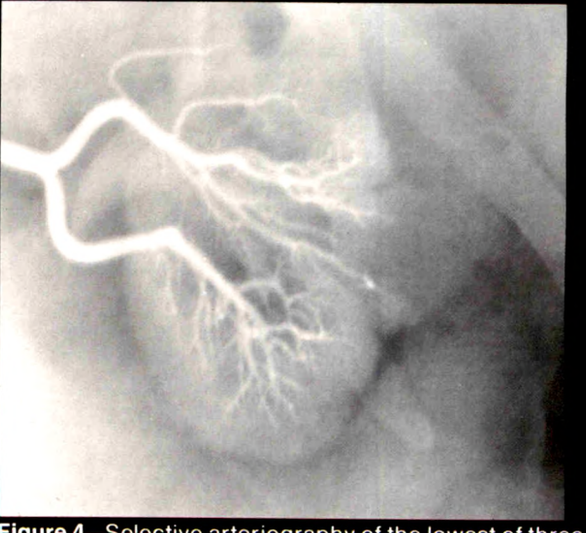

Figure 4—Selective arteriography of the lowest of three renal arteries revealed no neovascularity. Other selective injections confirmed the absence of new vessels.

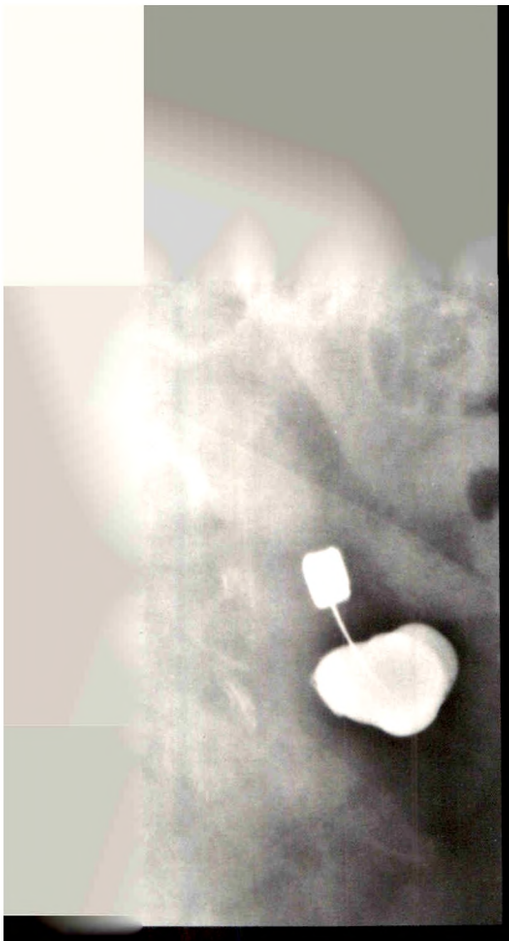

at the time of renal mass puncture. Cytologic examination showed no malignant cells.

Figure 6—Since benignity could not be definitely established, surgery was performed. Pathologic examination revealed a hemorrhagic cyst with no evidence of malignancy.

©Eastman Kodak Company, 1978

Because diagnostic decisions can sometimes depend upon the quality of the diagnostic image, Kodak is committed to providing you with quality films for use in all imaging modalities—radiography, computed tomography, nuclear medicine, ultrasound, and thermography.

For more information on the imaging products which will best meet your needs, ask your Kodak Technical Sales Representative or your x-ray products dealer. Or write: Eastman Kodak Company, Dept. 740-B, Rochester, New York 14650.

Kodak

A commitment to quality

John C. Bierwirth* believes the United States is a sound investment.

So do 93% of the other people employed by Grumman Corporation.

That's the percentage of Grumman employees who are regular investors in the Payroll Savings Plan.

"People understand Savings Bonds," says Mr. Bierwirth. "They really do know that they are as safe an investment as they can possibly make."

An employee who saves regularly is "not just a better employee but a better citizen in his community in every way."

John C. Bierwirth has another reason for believing in U.S. Savings Bonds, one that may not be as readily apparent to the average Savings Bonds subscriber.

"The U. S. Government is the biggest borrower in the world . . . and it needs to have a steady source of funds. Thus, Savings Bonds are important to the stability of the economy because they provide a source of government funds outside the traditional money markets."

Nevertheless, Mr. Bierwirth feels that whether for practical or patriotic reasons, "the Plan sells itself."

To receive a free information kit, about the Payroll Savings Plan, simply mail the coupon.

*Chairman of the Board and Chief Executive Officer Grumman Corporation.

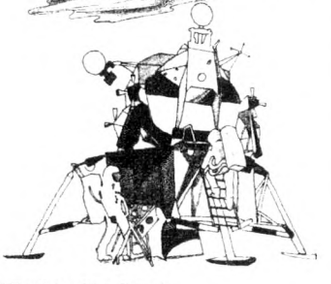

U.S. Department of the Treasury
Director of Sales
U.S. Savings Bonds Division
Washington, D.C. 20226

Yes, send me your free information kit about the Payroll Savings Plan.

Take stock in America.

Buy U.S. Savings Bonds

Name_____ Position_____

Firm_____

Address_____

City_____ State_____ Zip_____

Ad Council A Public Service of This Magazine & The Advertising Council

PROBLEM: Reflux and Migration of Embolic Agents

SOLUTION: MEDI-TECH Occlusion Balloon Catheters

REF: Greenfield, A.J.; Transcatheter Embolization: Complications and Prevention With Balloon Catheters. PROGRAM OF THE AMERICAN ROENTGEN RAY SOCIETY: Seventy-eighth Annual Meeting, September 26-30, 1977, Boston, Mass.

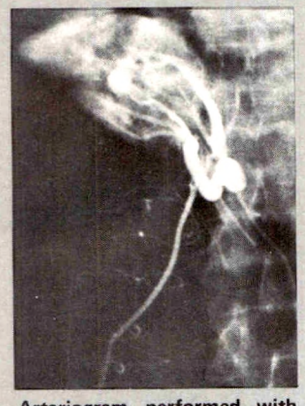

Arteriogram performed with balloon inflated prior to embolization

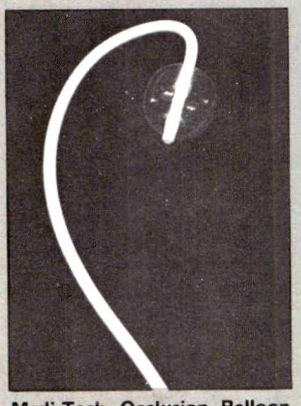

Medi-Tech Occlusion Balloon Catheter OB/7/2/65 (also used in X-Ray at left)

When carrying out therapeutic embolization, the risk that embolic agents will be carried to non-intended locations should be considered.

REF: Woodside, J.; Schwarz, H.; Bergreen, P.: Peripheral Embolization Complicating Bilateral Renal Infarction With Gelfoam. American Journal of Roentgenology: Vol. 126: 1033-1034, 1976.

Gang, D.L.; Dole, K.R.; Adelman, L.S.: Spinal Cord Infarction Following Therapeutic Renal Artery Embolization. JAMA: VOL. 237, No. 26, June, 1977.

Bradley, E.L.; Goldman, M.L.: Gastric Infarction After Therapeutic Embolization. SURGERY: Vol. 79, No. 4, April, 1976.

With the development of the MEDI-TECH Occlusion Balloon Catheters this risk has been significantly reduced.

MEDI-TECH offers the only balloon catheter available today with a polyethylene catheter body. Unlike polyvinyl chloride (PVC) which softens at body temperature, polyethylene retains its torque and holds pre-set curves. This enables selective placement of the balloon either with or against the blood flow.

The smooth tip profile and large I.D. (.038" in the 7F) allow percutaneous introduction by Seldinger Technique over a .035" guide wire.

(For more information fill out the coupon below and mail, or call Toll Free 800-225-3238).
In Massachusetts 617-923-1720.

CATHETERS AVAILABLE

Catalog Number	French	Lumens	Balloon Dia. (mm)	Tip I.D. (.000")	Usable Length (cm)
OB/7/2/65	7	2	12	38	65
OB/7/2/100	7	2	12	38	100
OB/5/2/65	5	2	8.5	27	65
OB/5/2/100	5	2	8.5	27	100

MEDI-TECH
Div. of Cooper Scientific Corporation
372 Main Street • Watertown, Massachusetts 02172

☐ I'd like more information sent
☐ I'd like a representative to call

Name _____ Dept. _____
Hosp. _____
Address _____
City _____ State _____ Zip _____
Phone _____ ( ) Area Code

Remote but not removed.

With our new Galaxy™ II Remote system, you can perform high-quality R&F examinations with the time-saving accuracy and ease of remote control. And yet, you can change easily to tableside operation when being close to your patient is important. A turn of a key fulfills your choice—either remote or classic operating modes.

Remote operation offers maximum patient throughput with minimum operator fatigue in a minimum radiation environment...while you maintain control over every examination.

Understandably certain examinations such as myelography or those involving the uncooperative patient require close patient contact and suggest tableside operation. Then again, for routine GI work with cooperative patients, why not relax at your remote console? The choice is yours for remote or classical operation.

The Flushmount™ imaging concept maximizes spotfilm results with improved patient geometry. And our "mini-cassetteless" Multispot 100 camera eliminates the need to change spotfilm cassettes during the examination. Also, for those who prefer a spotfilmer, a programmed Multiview filmer is available.

Galaxy II Remote.

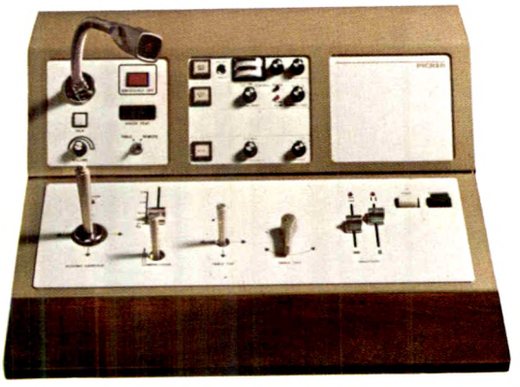

For installation versatility, Picker's Galaxy II Remote console may be desk or pedestal mounted in the control booth. The compact design requires minimal space and features simple operator controls. These are human engineered for quick orientation.

Maximum diagnostic information is achieved with our high-performance, dual-mode televised imaging system. For permanently recorded images, automatic exposure control provides consistent film density...exposure after exposure.

Four-way power top coverage for full patient positioning is provided. The Galaxy II-90 Table is capable of all necessary motions for tableside or remote R&F procedures. The Universal Bucky II features sinusoidal grid drive to give line-free films with X-ray exposures as short as 2 milliseconds.

And like all Picker equipment, this system is backed by our worldwide service organization which has a reputation for top performance.

Galaxy II Remote works hard to make your work easy. For more information contact your local Picker representative, or write Picker Corporation or Picker International, 595 Miner Road, Cleveland, OH 44143.

PICKER®
ONE OF THE CIT COMPANIES

Hanley Space Saver X-Ray and Medical Record Cabinets are installed in most hospitals in America.

Top quality and low price is the reason. It's #1. Regular 5 compartment with doors or open 19½ x 32 x 83. Deluxe Oversize 5 High 23 ¾ x 32 x 88. F.O.B. Factory. **In X-Ray rooms it's the oversize.** Extra depth means easier filing.

AMERICA'S LARGEST DISTRIBUTOR OF X-RAY CABINETS.

HANLEY MEDICAL EQUIPMENT CO.
5614 South Grand X-Ray Division St. Louis, Mo. 63111
Phone 314-351-3359

In reply to advertisers
please mention that you saw
their advertisement in

THE
AMERICAN JOURNAL OF
ROENTGENOLOGY

published monthly for
The American
Roentgen Ray Society
by

CHARLES C THOMAS • PUBLISHER
Springfield, Illinois 62717

STANFORD

X-RAY STEREOSCOPE
CONSULTATION IN 3-D

International usage
for over 30 years
See Your X-Ray Dealer
Manufactured in U.S.A.

SCHNEEMAN ELECTRONICS, Inc.
Grants Pass, Oregon, 97526

Help us to help you.

OSHA—the Occupational Safety and Health Act of 1970—benefits everybody. Employers and employees alike.

Today, Red Cross is helping employers all over the country to meet OSHA standards, by training employees in first aid and hazard recognition practices. The result is that, everywhere, factories and other places of business are safer and healthier. Another side benefit: employees trained in first aid are more valuable employees.

Next time you wonder where "all those dollars you gave to the Red Cross" are going—you might consider this: a lot of them are being plowed right back into your business! For information about First Aid Training call your local Red Cross Chapter.

Red Cross. The Good Neighbor.

DISCOVER MORE WITH CLEAR DEFINITION

new AMIPAQUE® (metrizamide)

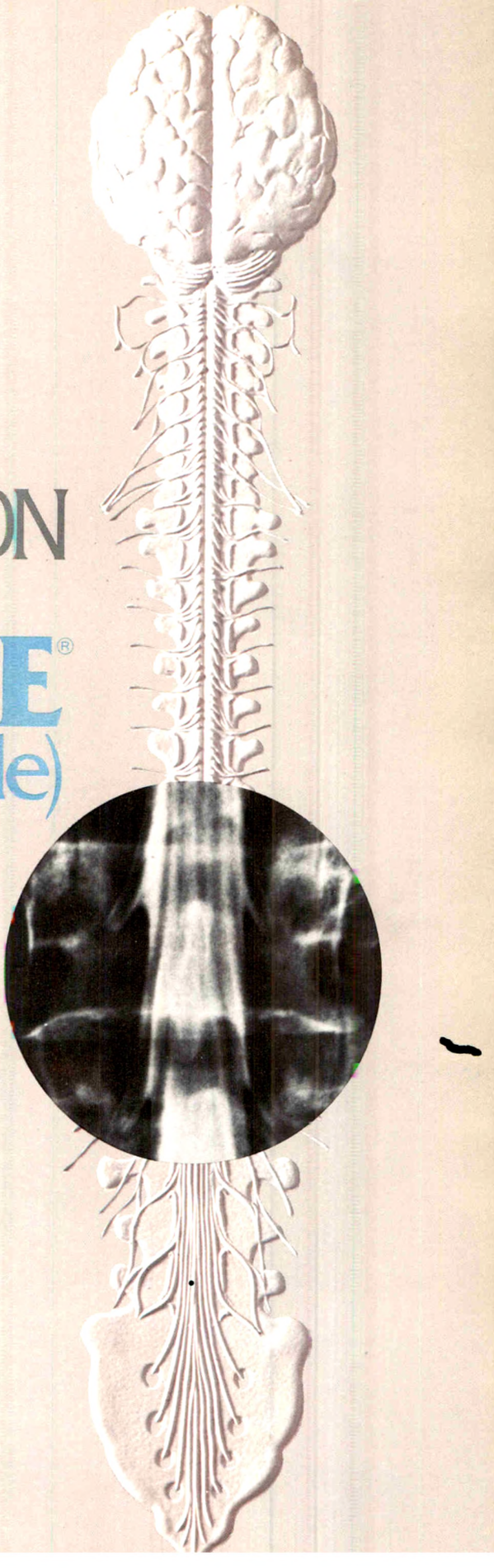

See last page for important product information including warnings, adverse reactions, and prescribing and precautionary recommendations.

COMPARE RADIOGRAPHS

iophendylate

Lumbar myelogram of 27-year-old female (anteroposterior view): Note high-density shadows and failure of contrast medium to adequately fill nerve-root sheaths.

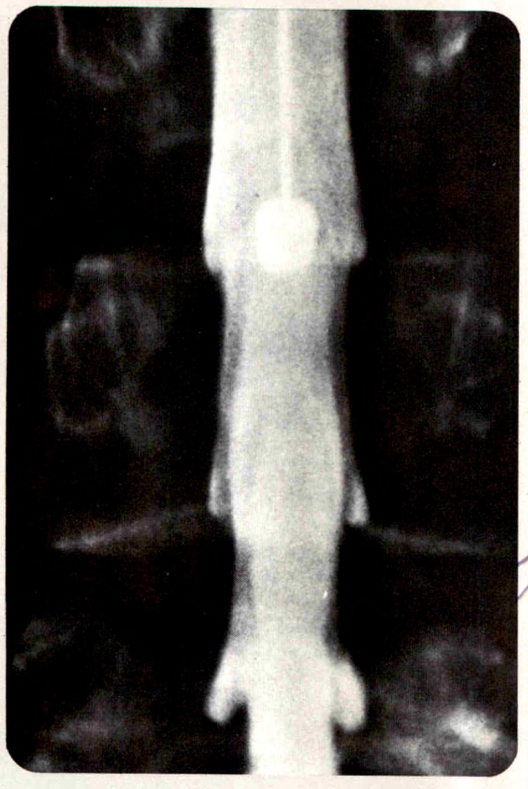

AMIPAQUE (metrizamide)

Lumbar myelogram of 20-year-old male (anteroposterior view): Note graded density of shadows and filling of nerve-root sheaths by the low-viscosity, water-soluble contrast medium.

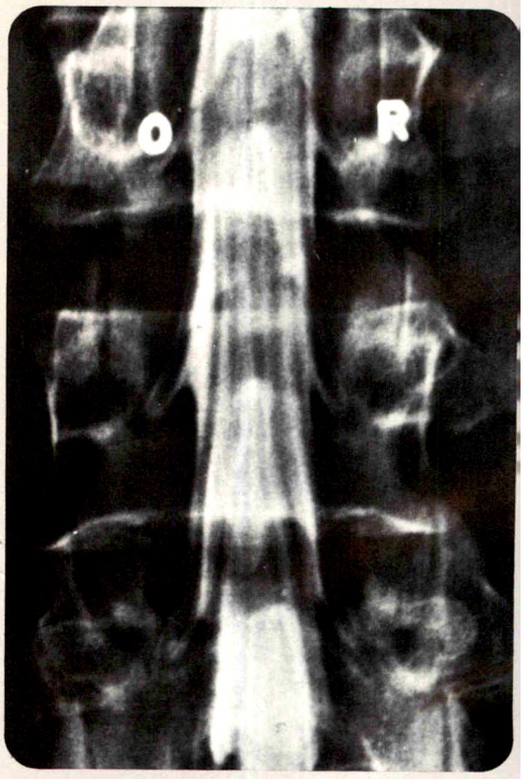

See last page for important product information including warnings, adverse reactions, and prescribing and precautionary recommendations.

CLEARER VISUALIZATION

Water-soluble, low viscosity

- ☐ Miscible with CSF for more uniform distribution around structures in subarachnoid space.[1,2]
- ☐ Flows into and through narrow subarachnoid spaces, fills slender cavities of nerve-root sheaths.[1,3]
- ☐ Usually diffuses around all except total obstructions with a single injection.
- ☐ Radiographic contrast provides nonobscured view of fine details.

Slightly hyperbaric

- ☐ Allows control of contrast distribution during initial phase of radiologic study, if desired.[1,3]

SIMPLIFIED MYELOGRAPHY

Nonionic... does not dissociate in solution

Isotonic with CSF at concentrations most frequently used (170 mgI/ml).

Low viscosity

- ☐ Allows use of narrow-bore needle (22-gauge).
- ☐ Less chance of CSF leakage... less chance of trauma to dura.

Resorbed and excreted mainly via kidneys in 48 hours

- ☐ No need for aspiration or second puncture... lessens potential for neurologic damage.
- ☐ No needle left in place during procedure... facilitates patient manipulation.

PATIENT TOLERANCE

- ☐ In general, the types of adverse reactions following subarachnoid injection of AMIPAQUE are not substantially different from those seen after lumbar puncture alone.
- ☐ The most frequently occurring reactions are headache, nausea, and vomiting.
- ☐ Rarely have reactions been severe or persistent beyond 24 hours.
- ☐ Although metrizamide is relatively safe and, in comparative studies, less toxic than other compounds for these indications, side effects ranging from headache and nausea to epileptic fits, convulsions, slow wave patterns on EEGs, petit mal states, paralysis, and arachnoiditis have occurred with the use of such compounds. Neurologic examinations were performed before and at intervals after the procedures in 1,495 of 1,850 cases. No clinically significant changes were found.

INDICATIONS:

lumbar, thoracic, cervical, and total columnar myelography; and for use in computerized tomography of the intracranial subarachnoid spaces following spinal subarachnoid injection.

new AMIPAQUE® (metrizamide)

More fully investigated before introduction than any other subarachnoid contrast agent

☐ 158 published reports ☐ 5 years in clinical research ☐ 2 years in U.S. medical centers

Description: Metrizamide, 2-[3-Acetamido-2,4,6-triiodo-5-(N-methylacetamido) benzamido]-2-deoxy-D-glucopyranose, is a compound derived from metrizoic acid and glucosamine. It is a nonionic water-soluble contrast medium with a molecular weight of 789 (iodine content: 48.25%). The chemical structure is as follows:

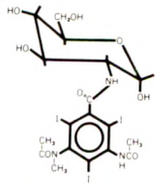

AMIPAQUE (metrizamide) is provided as a sterile, white lyophilized powder. Each 3.75 g/20 ml vial contains 3.75 g metrizamide (1.81 g organically-bound iodine) and 1.2 mg edetate calcium disodium. Each 6.75 g/50 ml vial contains 6.75 g metrizamide (3.26 g organically-bound iodine) and 2.16 mg edetate calcium disodium.

Each 20 ml vial of sterile aqueous diluent contains 0.05 mg/ml sodium bicarbonate in water for injection. pH is adjusted with carbon dioxide, USP, if necessary.

When AMIPAQUE is reconstituted to the lowest recommended concentration (170 mgI/ml) it has a specific gravity of 1.184 at 37°C, is hyperbaric to cerebrospinal fluid, is isotonic with CSF, and has a pH of approximately 7.4.

Clinical Pharmacology: AMIPAQUE is absorbed from cerebrospinal fluid into the bloodstream. Approximately 60 percent of the administered dose is excreted unchanged through the kidneys within 48 hours.

The initial concentration and volume of the medium, in conjunction with appropriate patient manipulation, will determine the extent of the diagnostic contrast that can be achieved. This can be monitored by fluoroscopy.

Following spinal subarachnoid injection, conventional radiography will continue to provide diagnostic contrast for approximately an hour. At 4 to 5 hours contrast is hazy and none is detectable at 24 hours.

Following subarachnoid placement, irrespective of the position the patient has maintained, upward diffusion of AMIPAQUE takes place through the CSF.

After introduction into the lumbar subarachnoid space, computerized tomography (CT) shows CSF contrast enhancement in the thoracic region in about one hour, in the cervical region in about 2 hours, and in the basal cisterns in 3 to 4 hours.

When low doses of AMIPAQUE (see DOSAGE AND ADMINISTRATION) are introduced into the lumbar CSF and moved cephalad under gravity control and examined by CT scanning, they will provide immediate CSF contrast in the basal cisterns. Depending on the specific technique used, the lateral, third, and fourth ventricles may also be visualized. The contrast in this area will markedly diminish at 6 hours and disappear by 24 hours. CSF enhancement will be evident at the cortical sulci and interhemispheric fissures at 6 hours. Between 12 and 24 hours the surfaces of the cerebrum and cerebellum, in contact with the subarachnoid spaces, will develop a "blush" effect on the scan which will normally disappear in 36 to 48 hours. The rate, time, extent of diffusion, and the disappearance or stasis of AMIPAQUE as demonstrated with CT scanning, can be used to detect or infer the presence of CNS abnormalities.

Indications and Usage: AMIPAQUE is indicated for lumbar, thoracic, cervical, and total columnar myelography and for use in computerized tomography of the intracranial subarachnoid spaces following spinal subarachnoid injection.

Contraindications: AMIPAQUE should not be administered to patients with a known hypersensitivity to metrizamide.

Warnings: If grossly bloody CSF is encountered, the possible benefits of a myelographic procedure should be considered in terms of the risk to the patient.

Usage in pregnancy. No teratogenic effects attributable to AMIPAQUE have been observed in reproduction studies in animals. However, before administration of AMIPAQUE to women during pregnancy, the benefit to the patient should be carefully weighed against the possible risk to the fetus.

Until further experience is gained in children younger than 12 years, administration of AMIPAQUE in this age group is not recommended.

Fatal reactions have been associated with the administration of water-soluble contrast media. Although no fatal reactions have been associated with AMIPAQUE, it is of utmost importance that a course of action be carefully planned in advance for the immediate treatment of serious reactions, and that adequate and appropriate facilities and personnel be readily available in case of a severe reaction.

Precautions: Caution is advised in patients with a history of epilepsy, severe cardiovascular disease, chronic alcoholism, multiple sclerosis, or with a history of bronchial asthma or other allergic manifestations.

Before a contrast medium is injected, the patient should be questioned for a history of allergy. Although a history of allergy, including asthma, may imply a greater than usual risk, it does not arbitrarily contraindicate the use of the medium. Premedication with antihistamines to avoid or minimize possible allergic reactions may be considered. No conclusive relationship between severe reactions and antigen-antibody reactions or other manifestations of allergy has been established.

Patients who are receiving anticonvulsants should be maintained on this therapy. Should a seizure occur, intravenous diazepam or sodium phenobarbital is recommended.

Prophylactic anticonvulsant treatment with barbiturates or diazepam orally for 24 to 48 hours should be considered in patients with evidence of inadvertent intracranial entry of a large or concentrated bolus of the contrast medium since there is an increased risk of seizures in such cases.

Any drugs, such as neuroleptics, including phenothiazine derivatives, which lower the seizure threshold should be avoided. These drugs should not be used as premedications. If possible, they should be withdrawn at least 48 hours before the examination and not used for at least 12 hours postprocedure.

In patients with severe renal insufficiency or failure, the drug is excreted by the liver into the bile at a much slower rate. Patients with hepatorenal insufficiency should not be examined unless the possibility of benefit clearly outweighs the additional risk. Reexamination should be delayed for five to seven days.

Adverse Reactions: In general, the adverse reactions following subarachnoid injection of AMIPAQUE are not substantially different from those seen after lumbar puncture alone. The most frequently occurring adverse reactions are headache, nausea, and vomiting. These reactions occur 3 to 8 hours postinjection, almost all occurring within 24 hours. They are usually mild to moderate in degree lasting for a few hours and disappearing within 24 hours. Rarely have the headaches been severe or persisted beyond 24 hours.

Backache, neck stiffness, numbness and paresthesias, leg or sciatic-type pain occurred less frequently, often in the form of a transient exacerbation of preexisting symptomatology. Temperature elevations and dizziness have also been reported.

Rarely, muscle spasm or generalized convulsions have occurred 4 to 8 hours following injection and in some cases were attributed to a history of epilepsy, medication with neuroleptic drugs, or inadvertent overdose. In all cases, treatment with intravenous diazepam or sodium phenobarbital has provided rapid control.

Transient alterations in vital signs may occur, the significance of which is difficult to assess since these parameters may be affected by the procedure or the patient's physical or emotional state.

Other rarely occurring adverse reactions include the following:

Allergy or Idiosyncrasy: chills, pruritus, urticaria, nasal congestion, and dyspnea.

CNS: mild and transitory perceptual aberrations such as hallucinations, depersonalization, anxiety, depression, hyperesthesia, visual and speech disturbances, confusion and disorientation. In addition, malaise, weakness, EEG changes, and meningismus have occurred.

Cardiovascular: chest pain, tachycardia, bradycardia, and arrhythmia.

Other: diarrhea.

Dosage and Administration: The dosage and concentration of AMIPAQUE will depend on the degree and extent of contrast required in the area(s) under examination and on the equipment and technique employed. Concentrations which are approximately isotonic (170 to 190 mgI/ml) are recommended for examination in the lumbar region. For movement of the medium to distant target areas, higher concentrations are recommended to compensate for dilution of AMIPAQUE with CSF.

A total dose of 3000 mg of iodine should not be exceeded.

The recommended usual and maximum doses of AMIPAQUE are summarized in the following table:

DOSAGE TABLE

Procedure	Conc. of Solution (mgI/ml)	Usual Recommended Dose* (ml)	Max. Dose Total (mgI)
Lumbar myelogram	170-190	10-15	2850
Thoracic myelogram	220	12	2640
Cervical myelogram (via lumbar injection)	250-300	10	3000
Cervical myelogram (via lat. cervical inj.)	220	10	2200
Total columnar myelography	250-280	10	2800
CT cisternography (via lumbar inj.)	170-190	4-6	1140

*Refer to RECONSTITUTION TABLE for preparation of Solution.

PATIENT MANAGEMENT

PREPROCEDURE: Anesthesia is not necessary. Premedication sedatives or tranquilizers are usually not needed. The use of neuroleptic drugs, including phenothiazine derivatives, should be avoided and such medication should be discontinued, when possible, 48 hours before the procedure (see PRECAUTIONS). Epileptic patients should be maintained on their anticonvulsant medication.

INSTRUCTIONS FOR PREPARATION OF THE SOLUTION: Contents under vacuum. Use only if vacuum is present as evidenced by diluent being drawn into vial when stopper is punctured.

1. Fill a sterile syringe with the exact volume of diluent as indicated in the following RECONSTITUTION TABLE to obtain the desired iodine concentration. *Examples: a.* For vials containing 3.75 g AMIPAQUE: To obtain 170 mgI/ml, use 8.9 ml of diluent; to obtain 190 mgI/ml, use 7.8 ml of diluent. *b.* For vials containing 6.75 g AMIPAQUE: To obtain 170 mgI/ml, use 16.1 ml of diluent; to obtain 190 mgI/ml, use 14.0 ml of diluent.

RECONSTITUTION TABLE

Conc. of Solution (mgI/ml)	Volume of Diluent to be Added 3.75 g Vial (ml)	6.75 g Vial (ml)
170	8.9	16.1
180	8.3	15.0
190	7.8	14.0
220	6.5	11.7
250	5.5	10.0
260	5.2	9.4
270	5.0	9.0
280	4.7	8.5
290	4.5	8.1
300	4.3	7.8
	The volume of the final solution will equal the volume of the diluent + 1.7 ml	The volume of the final solution will equal the volume of the diluent + 3.1 ml

The volume of the final solution will exceed the amount required to achieve the recommended dosage. For precise volume for injection refer to DOSAGE TABLE.

2. Inject the diluent into the vial, and leave the syringe and needle in place.
3. Gently swirl the vial (without shaking) until its contents are dissolved (approximately 3 to 10 minutes). The solution should be clear and colorless to slightly yellow.

Use immediately after reconstitution (see DOSAGE AND ADMINISTRATION). Discard any unused portion.

As with any lumbar puncture, sterile technique must be employed. The lumbar puncture is usually made between L3 and L4, but if pathology is suspected at this level the interspace immediately above or below may be selected. A lateral cervical puncture may also be used.

POSTPROCEDURE: The lumbar puncture needle may be removed immediately following injection since it is not necessary to remove AMIPAQUE after injection into subarachnoid spaces.

Management of the patient is similar to that used following simple lumbar puncture. Maintaining the patient recumbent in bed with the head raised 15° to 30° for 8 hours may reduce the rate of upward dispersion of the medium. The patient may then remain horizontal for a further 16 hours at the discretion of the physician.

How Supplied: *Kits, each containing:* one-3.75 g/20 ml single-dose vial of AMIPAQUE with 1 vial of diluent (NDC 0024-0044-01); or one-6.75 g/50 ml single-dose vial of AMIPAQUE with 1 vial of diluent (NDC 0024-0046-01).

Combination packs, each containing: five-3.75 g/20 ml single-dose vials of AMIPAQUE with 5 vials of diluent (NDC 0024-0044-12); or five-6.75 g/50 ml single-dose vials of AMIPAQUE with 5 vials of diluent (NDC 0024-0046-12).

Protect vials of AMIPAQUE from light.

References: 1. Grainger RG, Kendall BE, Wylie IG: Lumbar myelography with metrizamide—a new non-ionic contrast medium. *Br J Radiol* 49:996-1003, 1976. **2.** Peeters FLM: Myelography with metrizamide. *Radiol Clin* 46:203-213, 1977. **3.** Hindmarsh T: Myelography with the non-ionic water-soluble contrast medium metrizamide. *Acta Radiol [Diagn] (Stockh)* 16:417-435, 1975.

new **AMIPAQUE®** (metrizamide)

from the originators of the broad line of contrast media

Winthrop Winthrop Laboratories New York, N.Y. 10016

CHARLES C THOMAS · PUBLISHER

RADIOGRAPHY OF INFANTS AND CHILDREN

A Problem Oriented Manual of Radiographic and Fluoroscopic Procedures

Third Edition

Edited by **Donald B. Darling,** *Tufts Univ. School of Medicine, Boston, Massachusetts. Foreword by* **John Caffey.** *(16 Contributors)* The text provides a concise, illustrated description of routine and specialized procedures in diagnostic radiology and computed tomography in the infant and child age group.

Completely new material on conventional and computerized tomography, cardiac catheterization and angiography, and portable radiography is included in this new edition. In addition, the sections on neuroradiologic, peripheral angiographic and specialized pediatric examinations have been extensively rewritten and expanded. Discussions of the special design requirements of pediatric radiography rooms and of radiation protection for both patients and radiologic personnel have also been enlarged and revised. Indeed, the entire text has been updated to authoritatively reflect the present state of the pediatric radiographic art.

A sampling of chapter topics includes: *Pediatric Technology Origins and Development, Equipment and Application, General Radiological Procedures in Infants and Pre-School Children, General Radiographic Procedures in School-Age Children, Neuroradiological Procedures in Infants and Children, and Other Special Procedures.*

A most important feature continues to be a detailed description of procedures and techniques — including projections, positioning and restraints — for each anatomical area of examination. Appendices include a full set of exposure tables and data on equipment, mixtures and supplies.

As Doctor John Caffey states in the Foreword, "Doctor Darling's book should be welcome to all those who are concerned with the problems of satisfactory radiologic examinations of younger patients." *'79, 512 pp. (9 x 12), 1055 il., 48 tables, $60.00*

NEURORADIOLOGY OF SELLAR AND JUXTASELLAR LESIONS

By **K. Francis Lee,** *Thomas Jefferson Univ. Hospital, Philadelphia, Pennsylvania, and* **Shu-Ren Lin,** *Univ. of Rochester School of Medicine and Dentistry, Rochester, New York.* This volume offers the reader precise methods for the neuroradiological evaluation of sellar and juxtasellar lesions. Techniques involving plain skull radiography, conventional and computerized tomography, angiography, conventional and computerized tomography, angiography and polytome encephalography are detailed.

Contents include:

- *Anatomical and Pathological Foundations of Sellar and Juxtasellar Lesions* such as: sella turcica, clivus, optic canal, superior orbital fissure, and basal cisterns
- *Neoplastic Lesions* including: pituitary adenomas, craniopharyngiomas, meningiomas, and gliomas
- *Vascular Lesions* detailing: aneurysms, arteriovenous malformations, carotid-cavernous fistulas, and elongation of the basilar artery
- *Inflammatory Lesions* covering: granulomas, abscesses, parasites, and mucoceles of the sphenoid sinus
- *Developmental Lesions* explaining: basal encephaloceles, tuberous sclerosis, and transventricular coronal connexus
- *Trauma* examining: fractures, foreign bodies, extradural hematomas, and post-traumatic infections
- *Miscellaneous Juxtasellar Lesions* including: ischemic chiasmal syndrome, empty-sella syndrome, and lipoid proteinosis

Neuroradiologists will find this very thorough text to be an invaluable and unfailing source of information on sellar and juxtasellar lesions. *To be Published 1979, 512 pp. (6 3/4 x 9 3/4), 581 il., 13 tables, $73.00*

CLINICAL SIALOGRAPHY

Gordon B. Manashil

Monmouth Medical Center
Long Branch, New Jersey

This concise atlas of salivary gland pathology and its roentgen interpretation has been designed to simplify the diagnostic approach to salivary gland lesions. Methods of identification, cannulation, roentgen study, and illustrative case material are among the topics discussed.

The author reviews and illustrates the anatomy of the parotid and submaxillary glands; the technique of sialography detailing information on necessary supplies and basic contrast agents available for use; and all aspects of the normal sialogram emphasizing the filling phase, post-evacuation phase, duct filling and alveolar filling phases.

The section on tumors provides in-depth coverage of malignant lesions, mucoepidermoid tumors, malignant mixed tumors, adenocarcinomas and squamous cell carcinomas. This is followed by discussions of nonneoplastic lesions, including chronic and acute inflammatory diseases, and several types of trauma.

A delineation of possible pitfalls in roentgen diagnosis and representative case histories complete the book's thorough review of clinical sialography.

Sialography is an easy-to-perform, quickly executed, diagnostic study that is extremely valuable. The mystique of needle placement, injection, and interpretation of this x-ray examination has been exaggerated. The study is indicated in evaluating recurrent pain or swelling in the parotid or submaxillary region, obscure origin of dryness of the mouth and eyes, a mass in the salivary gland or adjacent to it, investigation of calcifications seen on plain radiographs facial palsy of obscure origin, and preoperative evaluation of pathologic processes.

This elucidative text will be helpful in the diagnosis and treatment planning of lesions in the salivary glands. It will prove valuable to radiologists and all other physicians interested in salivary gland disease. *'78, 112 pp. (6 3/4 x 9 3/4), 129 il., 7 tables, $16.75*

Orders with remittance sent, on approval, postpaid

301-327 East Lawrence Avenue • Springfield • Illinois • 62717

New imaging versatility.

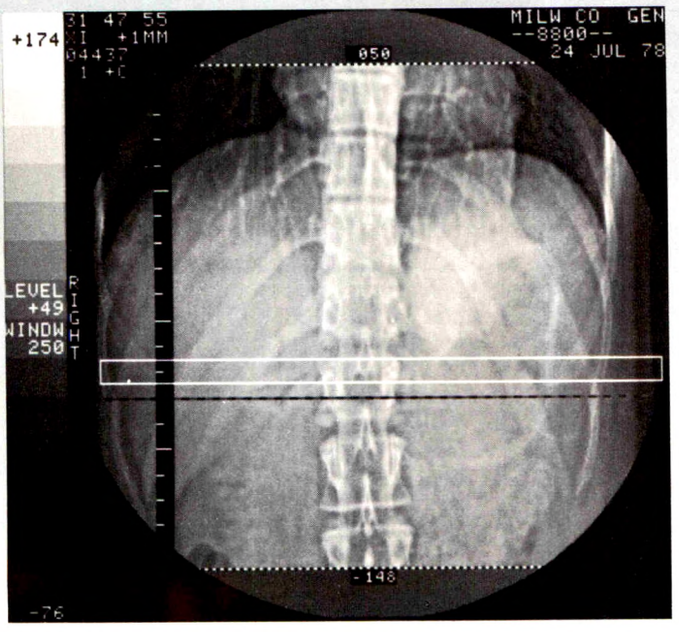

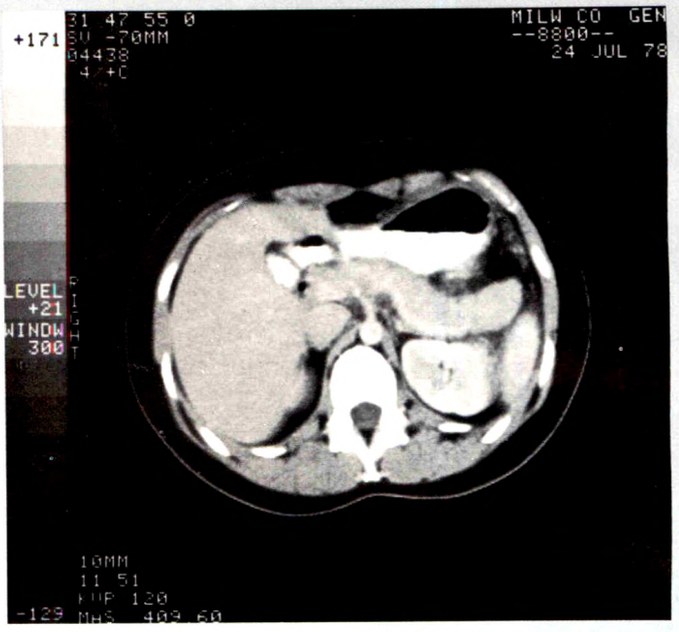

These images demonstrate how ScoutView imaging simplifies pancreatic localization. An axial slice taken at the mid to lower L-1 vertebral level is almost invariably at the takeoff of the superior mesenteric artery from the abdominal aorta, and the body of the pancreas will be included in the same slice.The scan sequence can then be monitored both above and below this level to ensure that the complete pancreas has been studied. Unnecessary slices resulting from attempts to define the level of the pancreas from external landmarks are thus avoided.

The image at the right was taken at the level indicated by the box on the ScoutView image. In this case, the patient has a horizontally oriented pancreas, and the slice taken at this level, following an intravenous bolus injection of 25 cc of Renographin 60, clearly demonstrates the splenic vein and superior mesenteric vein, in addition to the superior mesenteric artery on the posterior surface of the pancreas. Note the obliteration of the spleno-renal angle due to pancreatitis. Gas is present within the distal common bile duct secondary to a previous sphincteroplasty on the ampulla of Vater.

Clinical documentation of ScoutView's usefulness in diagnostic procedures is provided in a new 4-page Medical Systems Report. It's yours for the asking from your GE Medical Systems representative, or write ScoutView, P.O. Box 414 (W-512), Milwaukee, WI 53201.

New operator's console, one part of the ODC package, lets you initiate ScoutView imaging, then position a cursor on the image to select scan locations and plan gantry angulation. The new console also allows set up and control of axial scans, plus viewing of the last slice. When the physician's console is not in use, image analysis can be controlled at the operator's console.

SDC physician's console (far right), standard with CT/T systems, provides complete axial, sagittal and coronal scan image manipulation and analysis capability. With the optional ODC package, this console also displays ScoutView images, which can be analyzed with magnification, angle

You'd expect it from GE.

GE's new Optional Diagnostic Capability package (ODC) offers these key features:

- **New operator's console with image viewing, manipulation and recording capability**
- **Improved, coordinated anatomical reference system utilizing new table electronics**
- **1.5 mm contiguous axial slice capability**
- **ScoutView™ localization imaging—AP/PA, lateral and oblique**
- **Easily installed on existing CT/T 7800 and 8800 systems**

ScoutView localization provides important new benefits for the CT/T operator. The scanner actually generates a radiograph-like image that is used to accurately plan first and last slice locations, plus the exact gantry angulation needed. Each axial scanning procedure is thus tailored precisely to the anatomy of the individual patient, since the ScoutView image and the axial scans share a coordinated anatomical reference system.

A ScoutView procedure is performed in just 5 to 10 seconds, and the image is reconstructed in less than 40 seconds. Dosage is low, varying from 6 mR to 600 mR depending on technic and patient size.

At the operator's console, ScoutView images and the last slice may be viewed without interrupting diagnostic activity at the physician's console. And when the physician's console is not in use, the operator can perform virtually all image manipulation and recording functions at the operator's console.

ScoutView images can also be displayed, manipulated and analyzed at the physician's console. Because of the coordinated reference system, axial scans can be selected for viewing according to their locations on the ScoutView image.

This new package is further evidence of GE's Continuum concept: to provide important options without major systems changes. This cost-saving concept has brought you GE's fast-reconstruct option, X-2 ultra-high resolution detector, and the Independent Diagnostic Console. And now the ODC with ScoutView imaging.

That's just what you'd expect from GE. The best images and best value...now and in the future.

General Electric Medical Systems,
Milwaukee, Toronto, Madrid.

GENERAL ELECTRIC

Here's what Business is doing for America through the United Way.

Through a program of corporate giving, plus contributions from employees, American business is doing its share to insure a better quality of life for all of us, the United Way.

The United Way makes possible the good work of local human service agencies in over 2,300 communities around the United States. The services these agencies provide touch the lives of everyone. And have a positive impact on us all. Often, we take them for granted. And that's a mistake. Because without support, they would have to drastically curtail their services or, very possibly, cease to exist.

Imagine if there were no recreational facilities in our town. No mental health services. No youth organizations, assistance for the aged, child care centers or family counseling services. Imagine if there were none of the thousand and one other services for which the United Way lends financial support. It's unthinkable.

Thanks to your generosity, the United Way and the agencies it helps support will be here when we need them.

Thanks to you . . . it works . . . for ALL OF US.

United Way

Ad Council A Public Service of This Magazine & The Advertising Council

temp · guard™

temperature stabilizer

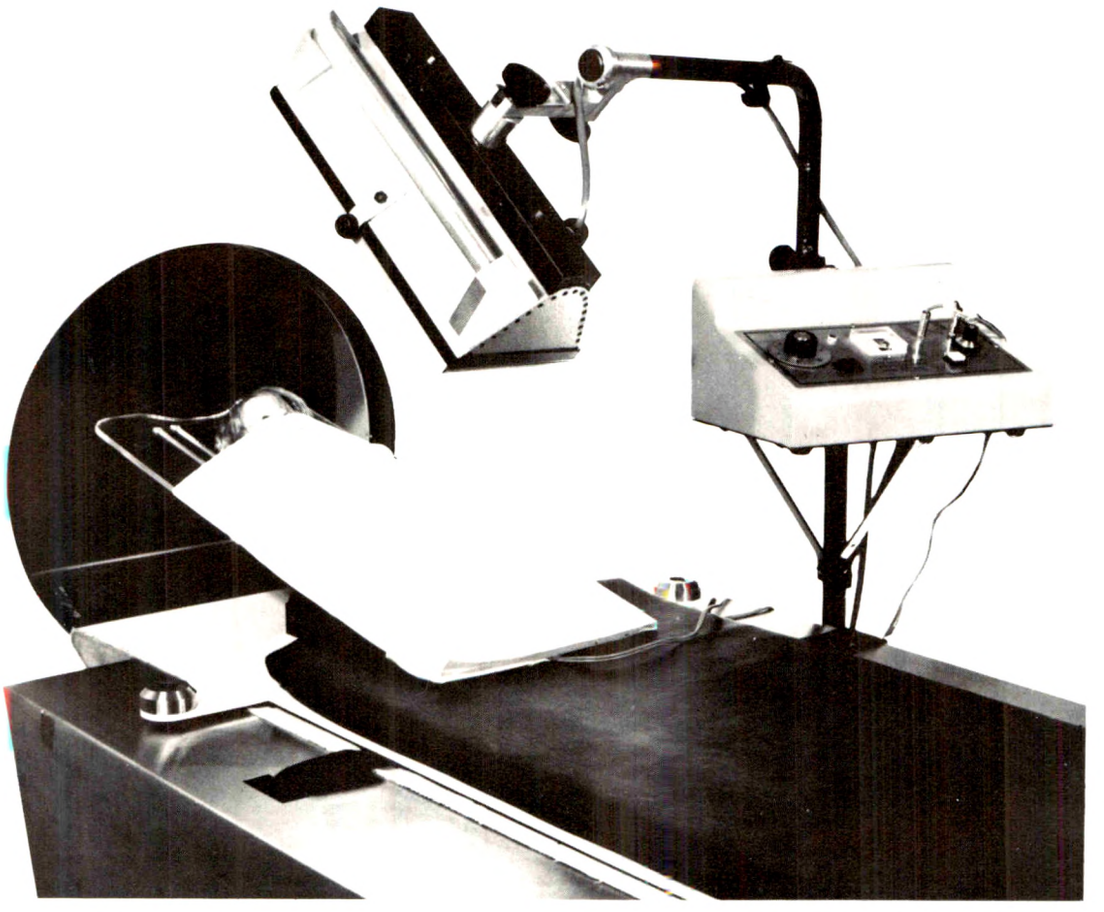

- coverless temperature support system for complete accessibility
- mobile and versatile
- for use in fluroscopy, special procedures, c.t. and ultrasound
- feed back probe which provides accurate temperature control and readout display
- fail safe instrumentation

call direct 716 882-0862

or write

gordon consultants, inc. 361 dewitt st. • buffalo, new york 14213

SIEMENS

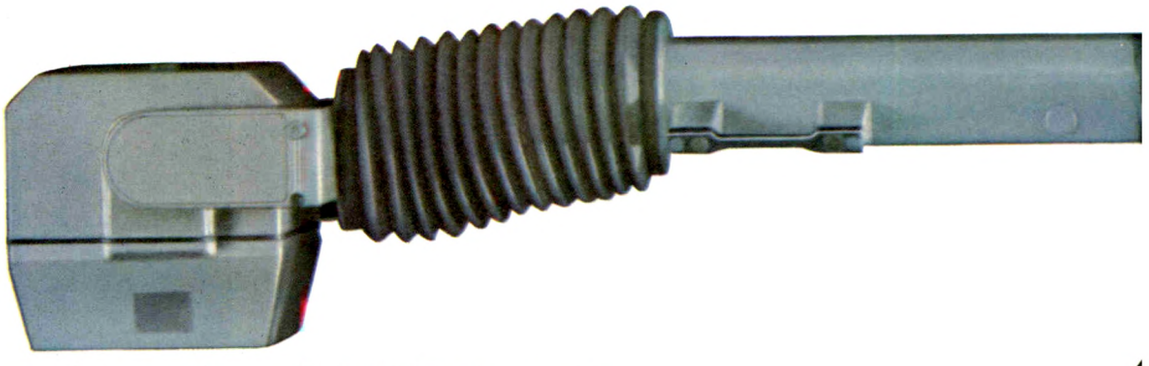

Introducing the MOBIL XR: A revolutionary concept in X-ray systems

Siemens has taken the concept of mobile X-ray systems and redesigned it from top to bottom. The result is total freedom of positioning, exceptional maneuverability, and ease of operation seen only in the MOBIL XR.

Only the MOBIL XR simplifies positioning.
Its innovative flexible extender arm provides a height and distance capability over and above any other mobile X-ray system. Without moving the unit from the foot of the patient's bed, the operator can easily maneuver the X-ray tube housing into any position, including lateral. Typically, at a bed height of 32 inches, the MOBIL XR will allow a 60-inch source-image distance. No other mobile unit can offer this capability.

Only the MOBIL XR has complete computerized organ programming.
By simply activating the push-button controls, the operator can select specific organ programs, reprogram the unit for specialized application techniques, or switch to manual settings. And for functional security, a digital readout displays the Kv, mAs, and battery condition of the unit.

Only the MOBIL XR has a custom-designed cassette tunnel.
It establishes and maintains the proper perpendicular relationship between X-ray tube and film cassette to provide optimum geometric positioning accuracy.

Only the MOBIL XR is easy to clean and keep aseptic.
That's because its design is free of corners, ridges, and hidden surfaces. Bacteria has no place to hide on the smooth fiberglass body of the MOBIL XR.

The Siemens family of mobile X-ray units extends beyond the MOBIL XR to include the KONDIAMOBIL 125 and the SIREMOBIL 2U. All are products of the quality engineering that reflect Siemens' standard of excellence in the field of radiological equipment.

For further information, please contact your local Siemens Representative or Siemens Corporation, Medical Systems Division, 186 Wood Avenue South, Iselin, New Jersey (201) 494-1000. In Canada: Siemens Canada Limited, P.O. Box 7300, Pointe Claire 730-P.Q.

SIR-408

Concepts...
engineered to radiologic excellence

Mental retardation is not a household word.

And we don't want it to become one.

Only you can prevent mental retardation in your family. We'll give you the facts.

Write me . . . at the National Association for Retarded Citizens, P.O. Box 6109, Arlington, Texas 76011

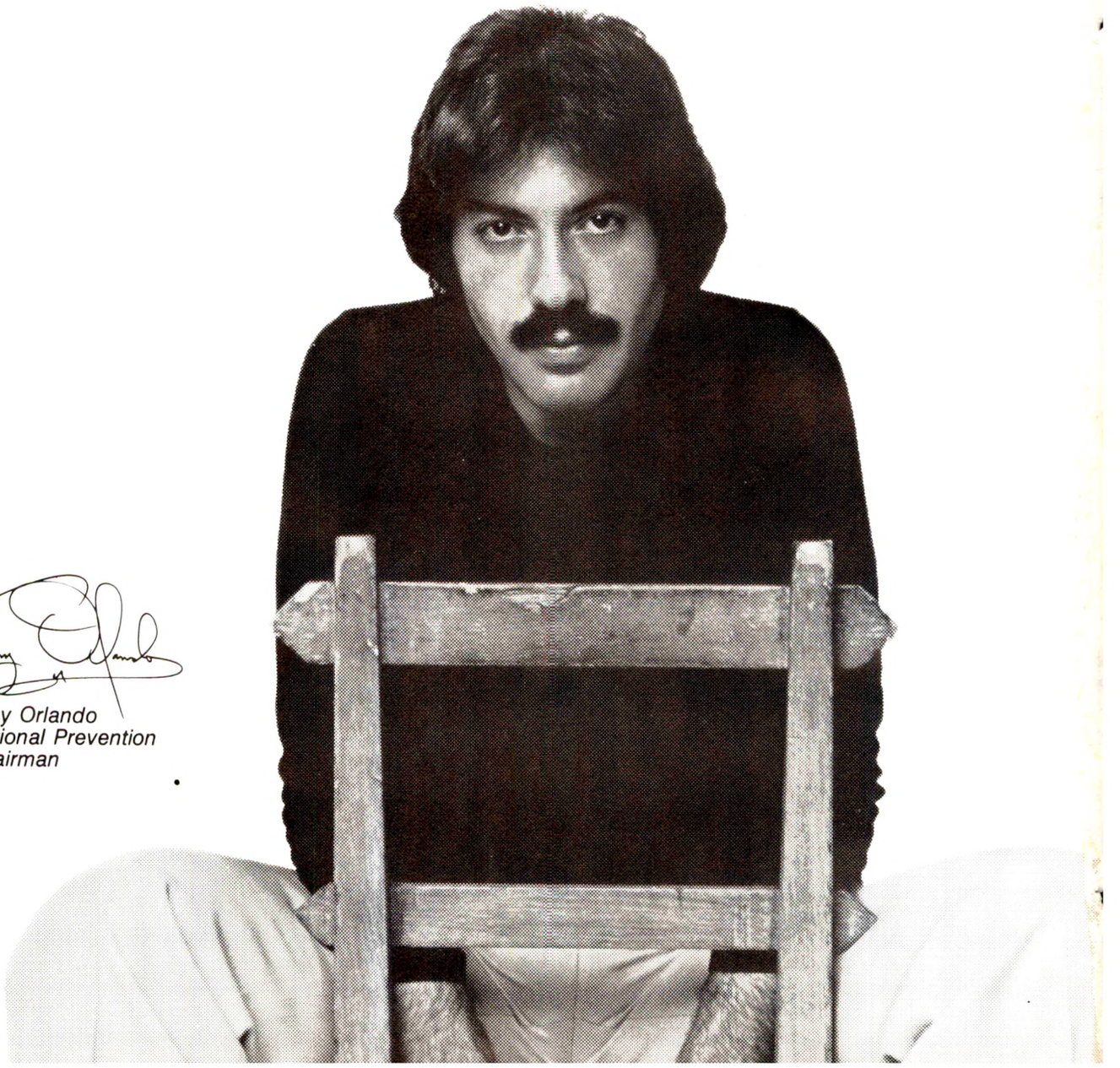

Tony Orlando
National Prevention
Chairman

AJR Index to Advertisers

(In Order of Appearance)

Machlett Laboratories
Ortho Pharmaceutical Corporation
Pfizer, Inc.
The Purdue-Frederick Company
Procter and Gamble
C. B. Fleet
Sybron/Liebel-Flarsheim
Elema-Schonander, Inc.
Radiologic Sciences, Inc.
Dunn Instruments, Inc.

• • •

E. I. Du Pont de Nemours and Company, Inc.
E-Z-EM Company
Siemens Corporation
Agfa-Gevaert Rex, Inc.
American College of Radiology
Charles C Thomas · Publisher
Picker Corporation
H. G. Fischer, Inc.
Philips Corporation
E-Z-EM Company
Eastman Kodak Company
Medi-Tech, Inc.
Picker Corporation
Hanley Medical Equipment Company
Schneeman Electronics, Inc.
Winthrop Laboratories
Charles C Thomas · Publisher
General Electric Company
Gordon Projectors
Siemens Corporation
Charles C Thomas · Publisher
CGR Medical Corporation
Guerbet Laboratory
Lea and Febiger

CHARLES C THOMAS • PUBLISHER

ANATOMICAL EXERCISES IN COMPUTERIZED TOMOGRAPHY BODY SCANNING *by* **Fred C. Shipps,** *Good Samaritan Hospital and Medical Center, Portland, Oregon.* Students of computerized tomography body scanning will find this book most helpful in transferring knowledge of conventional anatomy into a cross-section perspective. The author contends that the highest level of accuracy in identification of anatomical structures is achieved by reading or comparing a *series* of cuts. The illustrations have been simplified to include only those structures that are of major importance in C.T. body scanning. Special attention has been given to the vertical localization of these structures. *'78, 70 pp. (8 1/2 x 11), 186 il. (63 in color), $22.75, spiral (paper)*

XERORADIOGRAPHY: Breast Calcifications *by* **John N. Wolfe,** *Hutzel Hospital, Detroit, Michigan.* Each illustration is accompanied by text which includes history, radiographic observations and thoughts of the interpreter at the time the x-ray report was submitted, presentation of the diagnosis, and discussion of the case. Topics include calcifications associated with malignancies, characteristic tumor calcifications of specific forms of malignancies, calcifications associated with benign conditions, calcifications within lymph nodes, calcifications of the skin and areola, arterial calcifications, pseudocalcifications and specimen radiography. *'77, 184 pp. (8 1/2 x 11), 284 il., 3 tables, $26.00*

XERORADIOGRAPHY: Uncalcified Breast Masses *by* **John N. Wolfe,** *Hutzel Hospital, Detroit, Michigan.* This book presents information and graphic material to assist the radiologist in arriving at a reasonable differential diagnosis when confronted with uncalcified breast masses. The order of presentation proceeds from the obvious malignancies characterized by a mass with a well-developed spiculated margin, through the more subtle circumscribed carcinomas such as the medullary or colloid variety, and finally, to the most difficult, those that do not present a well-defined mass but merely an area of increased density. *'77, 208 pp. (8 1/2 x 11), 307 il., $32.50*

PERCUTANEOUS ANGIOGRAPHY *by* **S. Swamy,** *Michael Reese Medical Center;* **Lewis Irwin Segal,** *Louis A. Weiss Memorial Hospital; and* **S. Mouli,** *Foster-McGaw Medical Center; all of Chicago.* Numerous sketches explain the basic angiographic techniques and present solutions to common technical problems. The first section covers the roles of the patient, the doctor and the equipment in angiography. The second section explores specific angiographic methods and the final portion of the text focuses on patterns. This approach provides a broad logical background which will assist the physician in establishing a proper diagnosis. *'77, 848 pp. (8 1/2 x 11), 1455 il., $80.00*

CORONARY ANGIOGRAPHY (2nd Ptg.) *by* **Harold A. Baltaxe,** *Cornell Medical College, New York City;* **Kurt Amplatz,** *Univ. of Minnesota Medical School, Minneapolis; and* **David C. Levin,** *Cornell Medical College, New York City.* This volume describes gross and radiographic anatomy of the coronary artery tree and provides a description of the diverse pathologic processes involved. The text is not restricted to atherosclerotic coronary artery disease but also deals with congenital anomalies. For those who are organizing a new laboratory devoted to coronary arteriography, there is a section describing equipment and techniques of catheterization. The chapter on complications gives a listing of problems one encounters and their order of frequency, and postoperative complications due to new surgical procedures. *'76, 256 pp., 173 il., $26.00*

Orders with remittance sent, on approval, postpaid

301-327 EAST LAWRENCE
SPRINGFIELD • ILLINOIS • 62717

PULMORAPID™

CGR's new fast vertical chest system for radiography

Pulmorapid is an advanced approach to chest radiography. The system consists of a film exposure cabinet and an integrated tubestand—both floor mounted. So your ambulatory patient always remains standing at the floor level during the examination.

Exposure cabinet and tubestand are electronically interlinked to provide automatic centering of x-ray tube to film. No mechanical linkage. Patient-to-film distance is only 20mm (.787") grid and phototimer pick up chamber included. And there's excellent film-to-screen contact via pneumatic pressure. Two systems are available depending on your choice of film formats—14 x 17" (35cm x 43cm) or 16 x 16" (40cm x 40cm). And both models have a 12 x 12" (30cm x 30cm) image size reduction instantly available for pediatrics.

Pulmorapid is offered with an integrated automatic film processor or with a removable film receiving magazine. With the film processor, you achieve exposed film to dry processed film in only 136 seconds.

The new systems are designed for fast, easy technologist operation. Convenient 100 sheet film packs load quickly in daylight. Film is advanced and keyed automatically by simply inserting the patient's IBM type ID card. A digital film counter, of course, with warning light when film supply reaches five sheets. And there's easy access to intensifying screens for routine cleaning.

Other features include a removable grid—110 line, 10:1 ratio, 72" focus and a U80 three field integrated phototiming pick up chamber.

Pulmorapid. A clean, fast, cost effective system for chest radiography.

Your CGR representative has all the details.

CGR MEDICAL CORPORATION
2519 Wilkens Avenue
Baltimore, Maryland 21223
(301) 233-2300

CGR CANADA LTÉE-LTD.
500 Boulevard de l'Aéroparc
Lachute, Québec, Canada
(514) 562-8806

CGR
13 Square Max Hymans
75741 Paris, France
273-8200

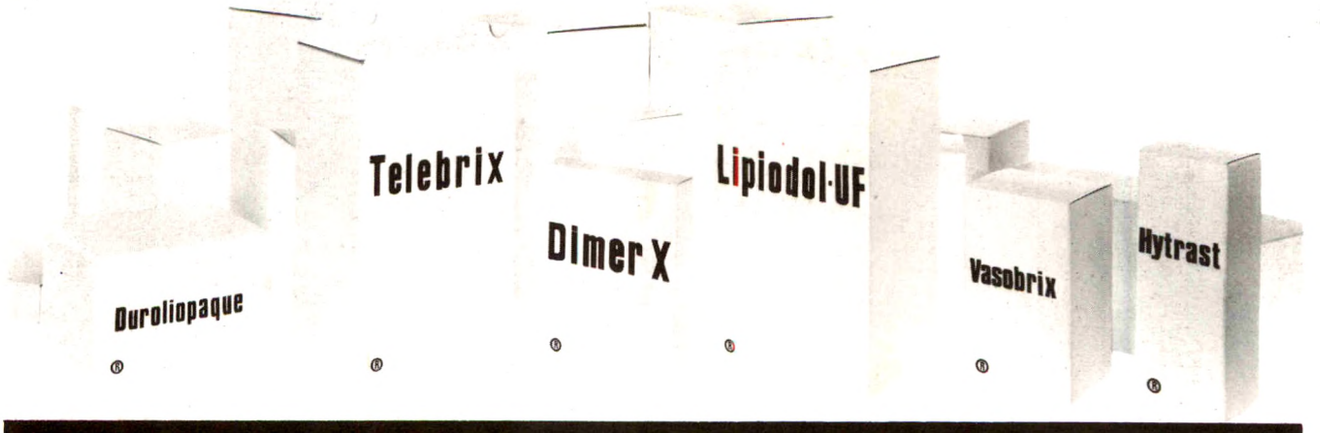

WE MANUFACTURE

contrast

MEDIA

OUR

products

ARE

known

WORLD-WIDE

OUR

name isn't

GUERBET

BETTER CONTRAST MEDIA THROUGH RESEARCH

Laboratoire Guerbet, 16/24, rue Jean-Chaptal
93601 AULNAY-SOUS-BOIS Cedex - FRANCE
Telex : Guerbet 690682

Textbook of Nuclear Medicine: Basic Science

Antonio Fernando Gonçalves Rocha, M. D.

Director, Centro de Medicina Nuclear da Guanabara
Advisor, Comissão Nacional de Energia Nuclear
Rio de Janeiro

John Charles Harbert, M. D.

Associate Professor of Medicine and Radiology
Director, Division of Nuclear Medicine
Georgetown University Hospital, Washington, D.C.

(32 Contributors)

Basic science—a comprehensive treatment of nuclear medicine—is presented in this general textbook which covers every aspect from basic atomic structure and measurement of radioactivity to activation analysis and the newest developments in computerized tomography and ultrasound. This volume reflects the recent technologic advances from many contributing fields such as physics, chemistry, engineering and energy, while retaining all of the important elements which form the basic science of nuclear medicine. It is an international collaboration which brings together contributions from recognized authorities throughout the world.

Representing completely new treatment not found in most standard texts are chapters that the reader will find especially interesting, including labeled carbon breath analysis, *in vitro* neutron activation analysis, ultrasound and computerized tomography. Also included are extensive sections on radiochemistry, radionuclide production and instrumentation. Initially discussing the physical basis of matter and energy, radioactivity, decay processes, and interaction of radiation with matter, the text provides excellent coverage of radiation detector systems, radioactivity and statistical counting, compartmental analysis, biologic effects of radiation, radiation dosimetry and safety, production of radionuclides, radionuclide generator systems, radiopharmaceutical chemistry of technetium and iodine, radiopharmaceutical quality control, and discussion of rectilinear scanners, scintillation cameras, and computer systems.

This highly functional and concise text is intended for use by practicing physicians, students, and residents in nuclear medicine, and as a useful reference for the laboratory scientist with nuclear counting and radioassay problems.

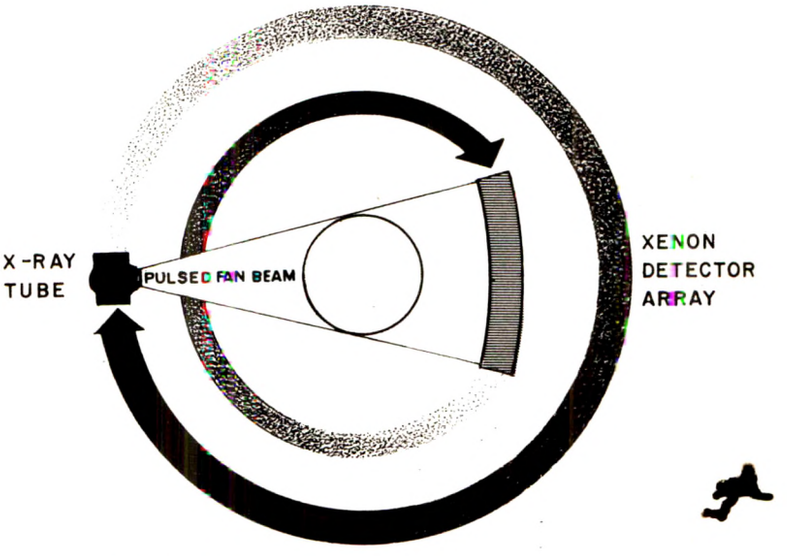

FIG. 17-9. *Third generation pure rotational fan-beam scanning.*

TEXTBOOK OF NUCLEAR MEDICINE: **Basic Science** is designed as one of two volumes which together provide a composite picture and solid grounding of both fundamentals and clinical application of nuclear medicine. The companion volume, edited by Doctors Rocha and Harbert, is entitled **TEXTBOOK OF NUCLEAR MEDICINE: Clinical Applications**, and is available from Lea & Febiger.

412 pages (7 x 10), illustrated, $27.50
Published September, 1978, ISBN: 0-8121-0630-X, L.C. No. 78-17195

Lea & Febiger

600 South Washington Square, Philadelphia, Pennsylvania 19106

American Journal of Roentgenology

Vol. 131 December 1978 No. 6

DIAGNOSTIC IMAGING

955 **Prospective Comparison of Ultrasound and Computed Tomography in the Evaluation of Gynecologic Pelvic Masses.** *Walsh JW, Rosenfield AT, Jaffe CC, Schwartz PE, Simeone J, Dembner AG, Taylor KJW*

961 **Sonolucent Areas in the Placenta: Sonographic and Pathologic Correlation.** *Spirt BA, Kagan EH, Rozanski RM*

967 **Analysis of Ultrasonographic Criteria in the Evaluation for Ectopic Pregnancy.** *Brown TW, Filly RA, Laing FC, Barton J*

973 **Uterine Anomalies Associated with Renal Agenesis: Role of Gray Scale Ultrasonography.** *Fried AM, Oliff M, Wilson EA, Whisnant J*

977 **Gray Scale Features of Hematomas: An Ultrasonic Spectrum.** *Wicks JD, Silver TM, Bree RL*

981 **Comparison of Whole Lung Tomography and Computed Tomography for Detecting Pulmonary Nodules.** *Muhm JR, Brown LR, Crowe JK, Sheedy PF II, Hattery RR, Stephens DH*

985 **Radiographic Manifestations of Pulmonary *Mycobacterium kansasii* Infections.** *Christensen EE, Dietz GW, Ahn CH, Chapman JS, Murry RC, Hurst GA*

995 **Identification of Thoracic Isomerism from the Plain Chest Radiograph.** *Soto B, Pacifico AD, Souza AS Jr, Bargeron LM Jr, Ermocilla R, Tonkin IL*

1003 **Congenital Pulmonary Atresia: Photographic Subtraction as an Aid in Recognizing Hypoplastic Pulmonary Arteries.** *Fulton RE, Davis GD*

1009 **Radiographic and Echocardiographic Evaluation of Newborns Treated with Indomethacin for Patent Ductus Arteriosus.** *Edwards DK, Higgins CB, Merritt TA, DiSessa TG, Friedman WF*

1015 **Intermittent Bleeding from Minute to Minute in Acute Massive Gastrointestinal Hemorrhage: Arteriographic Demonstration.** *Sos TA, Lee JG, Wixson D, Sniderman KW*

1019 **Protean Manifestations of Mycotic Aneurysms.** *Kaufman SL, White RI Jr, Harrington DP, Barth KH, Siegelman SS*

1027 **Transcatheter Occlusion of the Arterial Supply to Arteriovenous Fistulas with Gianturco Coils.** *Layne TA, Finck EJ, Boswell WD*

1031 **Mammographic Parenchymal Patterns as Risk Indicators for Incident Cancer in a Screening Program: An Extended Analysis.** *Krook PM*

1037 **Radiology of the Jugular Tubercles.** *Osborn AG, Brinton WR, Smith WH*

1041 **Technetium-99m Pertechnetate as an Indicator of Gastric Mucosal Proliferation.** *Pecora DV, Sagar V, Piccone J*

1043 **Drip Infusion Urography with Meglumine Iodamide.** *Robbins AH, Rosenfield AT, Pizzolato NF, Irwin GA, Putman CE, Gerzof SG, Ulreich S*

1047 **Shoulder Arthrography as a Treatment Modality.** *Gilula LA, Schoenecker PL, Murphy WA*

1049 **Association of Diffuse Idiopathic Skeletal Hyperostosis (DISH) and Calcification and Ossification of the Posterior Longitudinal Ligament.** *Resnick D, Guerra J Jr, Robinson CA, Vint VC*

1055 **Intraarticular Methyl Methacrylate: A Complication of Hip Surgery.** *Tailor CC, Murphy WA, Smith EL*

1059 **Postoperative Bony Stenosis of the Lumbar Spinal Canal: Evaluation of 164 Symptomatic Patients with Axial Radiography.** *Quencer RM, Murtagh FR, Post MJD, Rosomoff HL, Stokes NA*

1065 **Diagnostic Oncology Case Studies: Colonic Polyposis and Cancer.** *Contributed by Rao A, Khazin A, Fremland A*

CASE REPORTS

1069 **Pheochromocytoma with Reversible Renal Artery Stenosis.** *Velick WF, Bookstein JJ, Talner LB*

1072 **Embolization for Postbiopsy Renal Arteriovenous Fistula: Effective Occlusion Using Homologous Clot.** *Rosen RJ, Feldman L, Wilson AR*

1074 **Demonstration of Pancreatic Cysts in Adult Polycystic Disease by Computed Tomography and Ultrasound.** *Shirkhoda A, Mittelstaedt CA*

1077 **Pseudomass of the Liver Due to Pleural Effusion and Inversion of the Diaphragm.** *Katzen BT, Choi WS, Friedman MH, Green IJ, Hindle WV, Zellis A*

1079 **Cathartic Colitis.** *Kim SK, Gerle RD, Rozanski R*

1082 **Multinodular Primary Amyloidosis of the Lung: Diagnosis by Needle Biopsy.** *Bierny JP*

1084 **Abdominal Twiddler's Syndrome.** *Rodan BA, Lowe JE, Chen JTT*

1086 **Computed Tomography of Circumcaval Ureter.** *Gefter WB, Arger PH, Mulhern CB, Pollack HM, Wein AJ*

1088 **Periosteal Chondromas of the Anterior Tibial Tubercle: Two Cases.** *Kirchner SG, Pavlov H, Heller RM, Kaye JJ*

1090 **Intraarterial Nitroprusside Treatment for Ergotism.** *Husted JW, Ring EJ, Hirsh LF*

1093 **Ulnar Artery Aneurysms: Angiographic Considerations in Two Cases.** *Latshaw RF, Weidner WA*

TECHNICAL NOTES

1096 **A Transparent Head Support for Magnification Cerebral Angiography.** *Cromwell LD, Moore WE*

1098 **Transurethral Conversion of a Percutaneous Ureteral Stent to an Indwelling Stent.** *Bigongiari LR, Lee KR, Mebust WK, Foret J, Weigel JW*

1101 **Special Article: National Guidelines and Standards for Health Planning: Their Relation to Radiology.** *Evens RG*

1105 **International Cancer Research Workshop on Low Dose Rate Teletherapy.** *Edited by Wilson JF*

1111 **From Earlier Pages.** *Lang EF*

1113 **Editorial: Contrast-Induced Acute Renal Failure.** *Heneghan M*

1116 **Letters**

1119 **Memorials**

1121 **Abstracts of Current Literature**

1128 **Book Reviews**

1133 **News**

1137 **ARRS Meeting Summary**

1143 **Index to Volume 131**